

Lecture Notes in Civil Engineering

Tom V. Mathew
Gaurang J. Joshi
Nagendra R. Velaga
Shriniwas Arkatkar *Editors*

Transportation Research

Proceedings of CTRG 2017

 Springer

Lecture Notes in Civil Engineering

Volume 45

Series Editors

Marco di Prisco, Politecnico di Milano, Milano, Italy

Sheng-Hong Chen, School of Water Resources and Hydropower Engineering,
Wuhan University, Wuhan, China

Ioannis Vayas, Institute of Steel Structures, National Technical University of
Athens, Athens, Greece

Sanjay Kumar Shukla, School of Engineering, Edith Cowan University, Joondalup,
WA, Australia

Anuj Sharma, Iowa State University, Ames, IA, USA

Nagesh Kumar, Department of Civil Engineering, Indian Institute of Science
Bangalore, Bangalore, Karnataka, India

Chien Ming Wang, School of Civil Engineering, The University of Queensland,
Brisbane, QLD, Australia

Lecture Notes in Civil Engineering (LNCE) publishes the latest developments in Civil Engineering - quickly, informally and in top quality. Though original research reported in proceedings and post-proceedings represents the core of LNCE, edited volumes of exceptionally high quality and interest may also be considered for publication. Volumes published in LNCE embrace all aspects and subfields of, as well as new challenges in, Civil Engineering. Topics in the series include:

- Construction and Structural Mechanics
- Building Materials
- Concrete, Steel and Timber Structures
- Geotechnical Engineering
- Earthquake Engineering
- Coastal Engineering
- Ocean and Offshore Engineering; Ships and Floating Structures
- Hydraulics, Hydrology and Water Resources Engineering
- Environmental Engineering and Sustainability
- Structural Health and Monitoring
- Surveying and Geographical Information Systems
- Indoor Environments
- Transportation and Traffic
- Risk Analysis
- Safety and Security

To submit a proposal or request further information, please contact the appropriate Springer Editor:

- Mr. Pierpaolo Riva at pierpaolo.riva@springer.com (Europe and Americas);
- Ms. Swati Meherishi at swati.meherishi@springer.com (Asia - except China - and Australia/NZ);
- Ms. Li Shen at li.shen@springer.com (China).

Indexed by Scopus

More information about this series at <http://www.springer.com/series/15087>

Tom V. Mathew · Gaurang J. Joshi ·
Nagendra R. Velaga · Shriniwas Arkatkar
Editors

Transportation Research

Proceedings of CTRG 2017

 Springer

Editors

Tom V. Mathew
Department of Civil Engineering
Indian Institute of Technology Bombay
Mumbai, Maharashtra, India

Gaurang J. Joshi
Department of Civil Engineering
Sardar Vallabhbhai National Institute
of Technology
Surat, Gujarat, India

Nagendra R. Velaga
Department of Civil Engineering
Indian Institute of Technology Bombay
Mumbai, Maharashtra, India

Shriniwas Arkatkar
Department of Civil Engineering
Sardar Vallabhbhai National Institute
of Technology
Surat, Gujarat, India

ISSN 2366-2557 ISSN 2366-2565 (electronic)
Lecture Notes in Civil Engineering
ISBN 978-981-32-9041-9 ISBN 978-981-32-9042-6 (eBook)
<https://doi.org/10.1007/978-981-32-9042-6>

© Springer Nature Singapore Pte Ltd. 2020

This work is subject to copyright. All rights are reserved by the Publisher, whether the whole or part of the material is concerned, specifically the rights of translation, reprinting, reuse of illustrations, recitation, broadcasting, reproduction on microfilms or in any other physical way, and transmission or information storage and retrieval, electronic adaptation, computer software, or by similar or dissimilar methodology now known or hereafter developed.

The use of general descriptive names, registered names, trademarks, service marks, etc. in this publication does not imply, even in the absence of a specific statement, that such names are exempt from the relevant protective laws and regulations and therefore free for general use.

The publisher, the authors and the editors are safe to assume that the advice and information in this book are believed to be true and accurate at the date of publication. Neither the publisher nor the authors or the editors give a warranty, expressed or implied, with respect to the material contained herein or for any errors or omissions that may have been made. The publisher remains neutral with regard to jurisdictional claims in published maps and institutional affiliations.

This Springer imprint is published by the registered company Springer Nature Singapore Pte Ltd. The registered company address is: 152 Beach Road, #21-01/04 Gateway East, Singapore 189721, Singapore

Editorial

Introduction

Ever since the onset of economic reforms in the early 1990s, India has experienced rapid economic growth along with an increase in prosperity and income levels of citizens. However, this economic growth has also resulted in exponential growth of private-vehicle ownership and use (similar to what the USA and Europe have experienced in the early 1950s and late 1960s, respectively), which coupled with the increase in population and other related factors has resulted in transportation problems, namely accidents, congestion and pollution, at a severe level. All this and similar developments have brought home the urgency of recognizing that an efficient transportation system is necessary for increasing productivity and enabling the country to compete effectively in the world market. Adequacy and reliability of transport infrastructure and services are important factors that contribute towards the ability of the country to compete in the field of international trade and attract foreign direct investments. Considering these aspects, the Planning Commission of India in its 11th Five-Year Plan clearly recognizes the necessity to foster the development of the various transport modes in an integrated manner that will lead to the realization of an efficient, sustainable, safe and regionally balanced transportation system, where each mode of transport operates in its field of economy and usefulness, with competitive and non-discriminatory prices that are adequate to support progressive development of transport infrastructure and services. Accordingly, the Planning Commission has earmarked 34% of the total investment in infrastructure, which is 9% of the GDP by 2011–2012, exclusively for transportation infrastructure.

However, all these efforts, made by the government, put the onus on transportation researchers, educators, managers and policymakers across all transport sectors to orient their actions and works towards facilitating the achievement of desired outputs expected from the current and proposed investments by the government and to ultimately harbour the overall growth of the country. This is important to also achieve the vision of sustainable and integrated multi-modal transportation system for the country, as envisaged by the Planning Commission.

Therefore, in December 2011, the Transportation Research Group (TRG) initiated a unique forum within India (First Conference of Transportation Research Group of India—1st CTRG) for professionals across all modes of transport, not only to come together and interchange ideas and knowledge, but also to collate and publish the research literature across all transportation sectors and modes for better intermodal understanding. Since then, the conference is being organized biannually, and CTRG 2017 marked the fourth of its kind.

CTRG 2017

The 4th CTRG was held on December 2017, in the city of Mumbai with the intention to cover a wide spectrum of topics related to transportation of people and freight. The conference was designed to facilitate the contribution of research articles and deliberations along four tracks, namely Sustainable Transport (Track I), Transportation Modes, Planning and Demand Forecast (Track II), Traffic Systems Analysis (Track III) and Highway Materials and Pavement (Track IV). Several interdisciplinary themes were covered in each of this track keeping comprehensiveness of the field of transportation, encompassing economics, financial management, social equity, green technologies, operations research, big data analysis, econometrics and structural mechanics.

Track I: Sustainable Transport

This track deals with the topics related to approach and practices towards achieving sustainability of decisions related to transport system improvement and enhancement. Issues related to economic policy and planning, transport project evaluations in a multi-modal environment, transport impacts, public transport planning and strategies for inclusive mobility including non-motorized transport, socio-economic impacts of transport projects, project financing, project management and smart mobility options are the broad themes expected to be addressed by this track. Research outcomes related to short-, medium- and long-term transport climate-change-resilient policy options and case studies demonstrating a path towards sustainable development goals are covered under this track.

Track II: Transportation Modes, Planning and Demand Forecast

This track covers the topics related to all the transport modes including road transport and focuses on planning and design of transport systems in an integrated fashion. Research papers based on studies related to demand forecast for passenger and freight movements, multi-modal network design, land-use transport integration,

spatial interaction models, travel behaviour choice models, freight network equilibrium models, activity-based models, routing and scheduling, logistics, harbour and fleeting services, container and truck terminal planning, application of planning software, urban rapid transit system operations and management of the urban and regional transport systems are included under this track. This track also deals with the methodologies for planning data collection, compilation, storage, retrieval and dissemination for efficient planning and design of transport systems.

Track III: Traffic Systems Analysis

The topics related to operations and management of traffic systems and multi-class and multi-category users are the main focus of this track. The topics related to human factor analysis, traffic flow behaviour, traffic safety and geometric design improvements, design of traffic facilities, development of the application of intelligent transport systems, travel time reliability for transit operations, corridor and area traffic coordination systems, user-perceived level of service, inclusive design of intersections and transfer stations, efficacy analysis of safety measures and its economics, real-time traffic data collection and analysis and vehicle dynamics are covered under this theme. This track also considers research outcomes based on simulation studies on roadway operations, toll plaza operations, crowd management as well as intercity and urban freight movements.

Track IV: Highway Materials and Pavement

This track deals with the characterization of conventional and non-conventional highway materials, their performance assessment, pavement analysis and design, performance analysis, long-lasting pavements, green highways, porous pavements, composite pavements, pavement response and rehabilitation and pavement maintenance. The topics related to instrumentation of pavement performance evaluation, pavement-deterioration modelling, structural health monitoring, forensic investigations, life-cycle cost analysis, pavement management system, construction methodologies and techniques and highway drainage are also covered in this track.

Acknowledgements

The major financial share of the conference expenses came from our sponsors: Mumbai Metro Rail Corporation Limited (MMRCL), Mumbai Metropolitan Region Development Authority (MMRDA), Transportation Research and Injury Prevention Programme (TRIPP), Citilabs, PTV Group, City and Industrial Development Corporation (CIDCO), Infrastructure Leasing & Financial Services (IL&FS),

Springer, G V Sutaria Constructions, Raj Constructions, Bhavani Constructions and RKC Infrabuilt Pvt. Ltd. We express our sincere gratitude to these agencies for their generous support.

We would like to acknowledge the efforts of authors for submitting and presenting quality papers at CTRG 2017. We specially thank our keynote and invited speakers. We convey our sincere appreciations to our colleagues Dr. K. V. Krishna Rao, Dr. Gopal R. Patil, Dr. Vedagiri P., Dr. Dharamveer Singh and Dr. Avijit Maji at IIT Bombay, who worked along with us at all stages of the conference for its success. We also thank our colleagues from SVNIT, Surat, Dr. Ashish Dhamaniya, Dr. Rakesh Kumar, Dr. Patel Chetankumar Ramanlal and Dr. Amit J. Solanki, who worked along with us for the success of the conference.

The review process of the papers was coordinated by the members of the scientific committee with the help of many renowned researchers. We acknowledge with thanks the contribution of Dr. M. Parida (IIT Roorkee), Dr. Bhargab Maitra (IIT Kharagpur), Dr. S. Velmurugan (CSIR-CRRI) and Dr. A. Veeraragavan (IIT Madras) as conveners of the conference tracks in completing the review process. We would like to thank our research scholars Ayyanna Habal, Anna Charly, Bharat Kumar Pathivada, Chetan Kumar H., Aditya Kumar Das, Remya K. P., Tushar Choudhari, Sharmila Babu and Monalisa Patra for their assistance in scientific committee.

We would like to thank the executive board of the Transportation Research Group of India, consisting of Dr. Ashish Verma (IISc Bangalore), Dr. Akhilesh Maurya (IIT Guwahati), Dr. Vinod Vasudevan (IIT Kanpur), Dr. Partha Chakraborty (IIT Kanpur), Dr. Sudeshna Mitra (IIT Kharagpur), Dr. Rajan Choudhary (IIT Guwahati), Dr. Neelima Chakraborty (CSIR-CRRI), Dr. Prashant Sahu (BITS Pilani), Mr. Rajeev Kumar Sharma (Tech Mahindra, Gurgaon), Mr. Saleh Ahmed Choudhury (ARR&TI, Guwahati) and Dr. S. P. Dutta (IIT Kharagpur) for their support in the conducting of the conference. We thank the members of the conference organizing committee, students of transportation systems engineering and IIT Bombay administration for their valuable assistance in the successful organization of the conference.

Tom V. Mathew
Professor
Mumbai, India

Gaurang J. Joshi
Professor
Surat, India

Nagendra R. Velaga
Associate Professor
Mumbai, India

Shriniwas Arkatkar
Associate Professor
Surat, India

Contents

Sustainable Transport

Comparative Study of Pedestrians’ Movement on Different Types of Pedestrian Sidewalks in Sikkim, Gangtok	3
Arunabha Banerjee and Akhilesh Kumar Maurya	
Real-Time Vehicular Air Quality Monitoring Using Sensing Technology for Chennai	19
P. Partheeban, H. Prasad Raju, Ranganathan Rani Hemamalini and B. Shanthini	
Assessing the Impact of Bus Arrival Rate on the Bus Lane Capacity: A Simulation-Based Approach	29
Anshuman Sharma, Manoranjan Parida, Ch. Ravi Sekhar and Jayvant Choudhary	
A Local level Transit-Oriented Development Typology: Using Two-Step Clustering Technique	39
Prashanth Shekar Lokku, C. S. R. K. Prasad and K. Bala Krishna	
Assessment of Induced Fuzziness in Passenger’s Perspective of Transit Service Quality: A Sustainable Approach for Indian Transit Scenario	51
Suprava Jena, Hetsav Dholawala, Mahabir Panda and P. K. Bhuyan	
Comparative Analysis of Pedestrian Walking Speed on Sidewalk and Carriageway	65
Ninad Gore, Sanjay Dave, Jiten Shah, Manish Jain, Dipak Rathva and Vinay Garg	
Real-World Emissions from Diesel Passenger Cars During Peak and Off-Peak Periods	77
Srinath Mahesh and Gitakrishnan Ramadurai	

Candidate Driving Cycle Construction for Emission Estimation	85
Boski P. Chauhan, Gaurang J. Joshi and Parida Purnima	
Effect of Pedestrian Hybrid Beacon Signal on Operational Performance Measures at the Mid-block Location and Adjacent Signalized Intersection	99
Nutan Teketi and Srinivas S. Pulugurtha	
Preference Contour Model for Traffic Planning and Management of Tourist Place in Andaman and Nicobar Islands	113
Surendran Raji	
Comparative Study of Legal and Illegal On-Street Parking Behaviour in CBD Area—A Case Study of Surat City	125
Dixit Chauhan, Rahul Pitroda, Ninad Gore, Sanjay Dave and Gaurang J. Joshi	
On-Street Parking Demand Assessment in CBD Area Using Different Data Frequency	137
Rahul Pitroda, Dixit Chauhan, Ninad Gore, Sanjay Dave and Gaurang J. Joshi	
Comparative Study of Pedestrian Critical Gap Estimation Methods at Unsignalized Midblock Crosswalks	151
V. S. Vinayaraj, Avinash Chaudhari, Shriniwas Arkatkar, Gaurang J. Joshi and Manoranjan Parida	
Modeling on-Street Parking Scenario and Response to Paid Parking Policy Using Statistical Techniques for CBD Area of Vadodara City	169
Sanjay Dave, Nandan Dawada and Gaurang J. Joshi	
Optimum Point of Intersection Selection in Horizontal Highway Alignment Design: A Comparative Study Using Path Planner Method and Ant Algorithm	185
M. B. Sushma, Sandeepan Roy, M. B. R. Prasad and Avijit Maji	
Studies on Importance and Design Needs for Non-motorized Trips—A Review	201
Anshu Bamney and Rajat Rastogi	
GIS Based Road Connectivity Evaluation Using Graph Theory	213
Cynthia Baby Daniel, S. Saravanan and Samson Mathew	

Transportation Modes, Planning and Demand Forecast

Estimating Modal Shift of Home-Based Work Trips Due to the Development of Kochi Metro and Reduction in Fuel Consumption and Emissions 229

Ardra S. Krishna, Jomy Thomas and P. N. Salini

Analysis of Travel Time Expenditure of School-Going Children 243

M. Manoj, T. M. Rahul, Ashish Verma and Sumit Yadav

Activity-Based Travel Demand Models to Evaluate Transport Policies 253

Pranav Padhye, M. S. Nagakumar, S. Sunil and A. H. Manjunatha Reddy

Financial Feasibility Analysis of Truck Parking Terminal—A Case Study 263

Chitranshu Mathur, Kaja Jadav, Sireesha Bandapalli, Khushbu Raval and Ashish Dhamaniya

Walking and Bicycling to School—Understanding the Impact of Socio-economic Factors and Built Environment 275

Kuldeep Kavta and Bhargav Adhvaryu

The Effects of Mixed Land Use on the Household Travel Behavior: A Case Study of Agartala, Tripura 287

Neetu Choubey, Amitabha Acharjee and P. P. Sarkar

Private University Students’ Mode Choice Behaviour for Travel to University: Analysis in the Context of Dhaka City 299

Sharmin Nasrin

Understanding and Quantifying Delays in Accessing ICD, Nagpur 311

Ashwini Thakare, Amit Kumar, Vishrut Landge and Sumeet Jaiswal

Household Structure and the Travel Pattern of Senior Citizens for Leisure Trips 325

G. Nantha Priya, Samson Mathew and G. Subbaiyan

Traffic Systems Analysis

Application of Queuing Theory to a Toll Plaza-A Case Study 343

Naveen Malipatil, Soumya Iswar Avati, Hosahally Nanjegowda Vinay and S. Sunil

A Hierarchical Modeling Approach to Predict Pedestrian Crash Severity 355

Aafreen Asma Jahangeer, Sai Suresh Anjana and Vivek R. Das

Modelling Operating Speeds for Multilane Divided Highways 367

Gourab Sil, Suresh Nama, Avijit Maji and Akhilesh Kumar Maurya

A New Model to Evaluate Percent-Time-Spent-Following on Two-Lane Highways	377
Vivek	
Analysis of Vehicular Pedestrian Interaction at Urban Undesignated Mid-block Sections	389
Hareshkumar Dahyabhai Golakiya, Manish Patkar and Ashish Dhamaniya	
Study of Effect of On-Street Parking on Traffic Capacity	409
Prashoon Prakash, Ranja Bandyopadhyaya and Sanjeev Sinha	
Travel Time Reliability Measure and Level of Service Criteria for Urban Midblock	419
C. P. Muneera and Krishnamurthy Karuppanagounder	
Modelling Dynamic PCUs Using Occupancy Time Approach at Urban Signalised Intersections Under Mixed Traffic Conditions	429
Pinakin Patel and Ashish Dhamaniya	
Estimating Environmental Benefits of Electronic Toll Collection (ETC)	441
Dipanjnan Nag, Anibrata Roy and Arkopal K. Goswami	
Strategy to Reduce Queuing Time at Toll Plaza	453
Amit Kumar, Ashwini Thakare and Abhay Tawalare	
Estimation of Dynamic Equivalency Factor Under Heterogeneous Traffic Condition on Urban Arterial Road—A Case Study of Porbandar City	465
Yash R. Dasani, Monicaba Vala and Bindiya Patel	
Urban Corridor Travel Time Estimation Modelling Using Fuzzy Logic Technique: A Case Study of Indian Metropolitan City	475
Krishna Saw, Bhimaji K. Katti and Gaurang J. Joshi	
Application of Accident Analysis and Modeling Tool—Pilot Study for Sadashivanagar Area of Bangalore	491
Ankit Rai, Ashish Verma and Sonal Ahuja	
Applicability of Unconventional Intersection Designs Over Pretimed Signalized Intersection Design Along a Coordinated Corridor	503
Ajinkya S. Mane and Srinivas S. Pulugurtha	
Evaluating the Influence of a Freeway Capacity Improvement Project on Travel Time-Based Performance Measures Within Its Vicinity	517
V. S. R. S. Sudheendra Yesantarao and Srinivas S. Pulugurtha	
Assessment of Walkability and Pedestrian Level of Service in Two Cities of Kerala	533
A. Jegan Bharath Kumar and T. Ramakrishnan	

Gap Acceptance Behaviour of Vehicles at Unsignalized Intersection in Urban Area	545
Saurabh Vinchurkar, Manish Jain, Dipak Rathva and Sanjay Dave	
Modelling Queuing of Vehicles at Signalized Intersection	557
Dhaval Parmar, Ninad Gore, Dipak Rathva, Sanjay Dave and Manish Jain	
Development of Consistency Evaluation Criteria for Indian Two-Lane Rural Highways	567
Jacob Anitha, Akkara Jisha and R. Midhun Mohan	
Effect of Shoulder Width on Traffic Flow Parameters on Two-Lane Undivided Roads	579
Pallav Kumar, Joyjeet Chakraborty, Shrinivas Arkatkar and Gaurang J. Joshi	
Estimation of Saturation Flow at Signalized Intersections Under Heterogeneous Traffic Conditions	591
Rakesh Kulakarni, Akhilesh Chepuri, Shrinivas Arkatkar and Gaurang J. Joshi	
Evaluation of Centre Line Marking on Driver Behaviour	607
P. C. Rehna, M. Harikrishna and M. V. L. R. Anjaneyulu	
Critical Appraisal of Traffic Management Strategies for a Mega Religious Procession: Case of NH-58 During Kanwar Yatra, India	621
Hasmeet Kaur and Uttam K. Roy	
Pedestrian Accident Prediction Modelling—A Case Study in Thiruvananthapuram City	637
Ancy Santhosh, Ebin Sam and B. K. Bindhu	
Understanding Driver Behavior at Intersection for Mixed Traffic Conditions Using Questionnaire Survey	647
Ajinkya Ingale, Prasanta Sahu, Rishabh Bajpai, Avijit Maji and Ashoke Sarkar	
Vehicle Category-Wise Service Time Analysis at Tollbooths Under Mixed Traffic Scenario	663
Mahaveer Singh, Yogeshwar V. Navandar and Ashish Dhamaniya	
Evaluation of Traffic Congestion Parameters Under Heterogeneous Traffic Condition: A Case Study on Bhubaneswar City	675
Satya Ranjan Samal and Aditya Kumar Das	
Driver Behavior as Affected by Static Objects: A Naturalistic Driving Approach	685
Bhupali Dutta and Vinod Vasudevan	

Development of a Model for Heterogeneous Traffic Simulation	699
Amit Kumar Das, Manoj Kumar Biswal and Ujjal Chattaraj	
Highway Materials and Pavement	
Resource Mapping of Highway Materials Along with Their Characteristic Properties and Desirability	709
P. N. Salini, B. G. Sreedevi and Sam Ebin	
Understanding Effects of Crushing Mechanism on Aggregate Morphology Using AIMS	725
Bharat Rajan, Dharamveer Singh, Saurabh Maheshwari and Gaurav Garg	
Effect of Gradation of Fine Aggregates on Creep Deformation of Fine Aggregate Mix (FAM) and Asphalt Mix	737
Ambika Kuity and Animesh Das	
Warm Mix Asphalt—A Comprehensive Case Study	747
Atasi Das and Yash Pandey	
The Effect of Using Acid-Modified Mixes on Performance of Asphalt Concrete	757
A. Ramesh, G. Abdul Khader and M. Kumar	
The Effect of Model Uncertainty on the Reliability of Asphalt Pavements	771
Abhishek Mittal and A. K. Swamy	
Investigation on Rutting Performance of Gap-Graded Asphalt Mixtures: Study on Aggregate Gradation.	781
Veena Venudharan and Krishna Prapoorna Biligiri	
Performance Characteristic Evaluation of Asphalt Mixes with Plastic Coated Aggregates	793
Priyadarshini Saha Chowdhury, Sonu Kumar and Dipankar Sarkar	
Effect of Non-uniform Soil Subgrade on Critical Stresses in Concrete Pavement	805
Rameshwar J. Vishwakarma and Ramakant K. Ingle	
Comparative Study on Rheological Properties of Coir Fiber and Coir Powder Modified Bitumen.	819
T. Sreelatha, Bino I. Koshy and Jithin Kurian Andrews	
Calibration of M-E PDG Rutting Model for Indian Conditions	829
Bhanoj Dokku and J. Murali Krishnan	
Development of Fatigue Model for Warm Mix Asphalt Based on Testing Frequency and Post-processing Method	843
K. Lakshmi Roja, A. Padmarekha and J. Murali Krishnan	

Influence of Aggregate Gradation on Laboratory Rutting Performance of Hot-Mix Asphalt Mixtures 857
 B. S. Abhijith, Uma Chakkoth and J. Murali Krishnan

A Study on Permeability Characteristics of Asphalt Pavements 869
 Rajan Choudhary, Vikramkumar R. Yadav, Abhinay Kumar and Anirudh Mathur

Characterization of Colloidal Stability of Blended Bitumen 883
 Uma Chakkoth, K. R. Krishna, M. Ramkumar, P. V. C. Rao, Parag Ravindran and J. Murali Krishnan

An Investigation on Resilient Modulus of Bituminous Mixtures 895
 S. Deepa and J. Murali Krishnan

About the Editors

Tom V. Mathew is Professor in the Department of Civil Engineering in Indian Institute of Technology Bombay, where he specializes in transportation systems engineering. After completing his M.Tech and PhD from Indian Institute of Technology Madras, Chennai, he went on to work as a senior software engineer in the Amada Software International for two years, before joining as faculty in the Department of Civil Engineering, Indian Institute of Technology Bombay, Mumbai in 2001. His current research interests include traffic flow modeling and simulation, traffic signal control systems, transportation network design, intelligent transportation systems, and traffic safety. He has authored more than 70 research papers in reputed journals and conferences and is currently a member of various technical bodies such as the American Society of Civil Engineers, the Indian Society of Technical Education, Indian Roads Congress, Delhi, and the Transport Research Group of India.

Gaurang J. Joshi is an Associate Professor and the Section Head of Transportation Engineering and Planning in the Department of Civil Engineering, Sardar Vallabhbhai National Institute of Technology, Surat. He has done his PhD from V.N. South Gujarat University, Surat. Dr Joshi's research interests include urban transportation planning, urban & regional travel, demand forecasting, traffic flow modeling, traffic regulation & control, designing non-conventional materials for highway pavements, and frameworks for sustainable urban transport systems. He has been a member of various government committees for urban and rural transport and authored more than 80 research papers in reputed journals and conferences.

Nagendra R. Velaga is an Associate Professor in Department of Civil Engineering in Indian Institute of Technology Bombay. After completing his M.Tech in Transportation Systems Engineering from IIT Bombay, he went on to do his Ph.D in Transport Studies from Loughborough University, UK. Dr Velaga's core areas of

expertise are traffic and intelligent transportation systems, transportation accessibility and mobility, and transportation safety. He serves as a reviewer for more than 18 journals and has published more than 90 research papers.

Shriniwas Arkatkar is an Assistant Professor in the Department of Civil Engineering in Sardar Vallabhbhai National Institute of Technology, Surat, where he specializes in Transportation Engineering and Planning. He has done his PhD in transportation Engineering from IIT Madras. His research interest include traffic flow modeling and simulation, traffic operation and management, emerging traffic data collection techniques, transportation systems planning, design and operation, public transportation and sustainable transportation and road safety and simulation. He has published 2 books and more than 100 research papers in reputed journals and conferences.

Sustainable Transport

Comparative Study of Pedestrians' Movement on Different Types of Pedestrian Sidewalks in Sikkim, Gangtok



Arunabha Banerjee and Akhilesh Kumar Maurya

Abstract The paper aims at comparing between movement of pedestrians over an elevated/access-controlled sidewalk, a horizontal at-grade sidewalk and a gradient sidewalk and also analyses the pedestrian flow characteristics such as age, gender and carrying of baggage. The pedestrian data were collected using videography technique at three different types of sidewalks (viz. elevated, at-grade horizontal and gradient) in Gangtok, Sikkim. Basic relationships between speed, flow rate and density were plotted in order to understand the behaviour of pedestrians over the three different facilities. Moreover, in order to compare and understand if a significant difference exists between the various parameters, statistical tests were carried out. It could be visualized that walking speed of pedestrians is highly influenced by the age, gender, location and gradient. The elevated/access-controlled sidewalk is seen to have a higher flow rate in comparison with the gradient and at-grade horizontal sidewalks. The result of the statistical tests which are carried out in order to check whether there is any significant difference between the various pedestrian groups, indicate that a significant difference exists between the pedestrians based on age and gender; while the presence or the absence of baggage and direction of travel does not affect the walking speed significantly. Moreover, the jam density and capacity are also predicted based on Greenshields' model. Results indicate that a greater jam density and higher flow rate are observed for elevated sidewalk in comparison with the gradient and at-grade horizontal sidewalks due to its location.

Keywords Pedestrian · Sidewalk facility · Statistical tests · Greenshields' macroscopic model

A. Banerjee (✉) · A. K. Maurya
Civil Engineering Department, Indian Institute of Technology Guwahati, Guwahati 781039,
Assam, India
e-mail: arunabhabanerjee77@gmail.com

A. K. Maurya
e-mail: maurya@iitg.ernet.in

1 Introduction

Pedestrians who are exposed to their highly challenging surrounding environmental factors have a tendency to shift from their normal walking behaviour to a more testing walking behaviour. Pedestrians tend to change their walking behaviour depending on the type of facility available and how well maintained that facility is for walking. Depending on the condition of the facility and its surrounding, pedestrians have a tendency to change their walking speed. This wide choice of freedom makes them far more vulnerable than motorized traffic. ‘Sidewalk’ or ‘footpath’ (as per Highway Capacity Manual [1]) is the most important facility for pedestrians in India, which occupies the highest volume of pedestrians and is located in proximity and in parallel to roadways. These facilities are either poorly maintained or encroached by vendors or parked vehicles. This ultimately forces the pedestrians using such facilities to shift to the carriageway which hampers their safety. It is thus of utmost importance to create and maintain proper pedestrian facilities in order to make them more adaptable to pedestrians and thus encourage walking. Some of the studies on level sidewalks have been conducted in the different cities of India by various researchers, but a comparative study between pedestrian movements on elevated sidewalk, at-grade horizontal sidewalk and gradient sidewalk has rarely been done in India. The limited number of these studies conducted in India on different types of sidewalk facilities and under different land-use types provides scope and motivation for carrying out research in this particularly less explored area. Next section presents some of the related studies conducted on sidewalk facility across the globe.

2 Literature Review

Various researchers across the globe have made significant studies on movement of pedestrians over sidewalks in order to calculate pedestrian flow characteristics (including pedestrian walking speed, flow and density). Oeding [2] conducted a study on a footpath in Germany and measured fundamental flow parameters. Movement of pedestrians on footways in shopping streets in England was studied by Older [3], and it could be concluded that more efficient use was made by pedestrians of the narrow footway than of the wider ones. Gender and density parameters were observed by Polus et al. [4] to play pivotal part in defining walking speed of pedestrians over sidewalks in Haifa, Israel. A study to examine the characteristics of pedestrians in Singapore was done by Tanaboriboon et al. [5], and it could be concluded that Singaporeans had a slower walking rate than their American counterparts. Lam et al. [6] through a study tried to find out the pedestrian flow characteristics in Hong Kong and saw that the speed–flow–density models developed for Hong Kong were similar to those developed for Singapore for the similar types of facilities. Modelling of pedestrian walking speeds on sidewalks in Edinburgh (UK) was done by Al-Azzawi and Raeside [7], and it was seen that when gradients became steep the walking

was impaired and speeds also declined with age. Parida et al. [8] tried to establish correlation between different physical attributes of sidewalks and satisfaction level of users. An extensive research on flow characteristics on sidewalks in mixed traffic flow condition was done by Laxman et al. [9], and they found free-flow speed to be 80 m/min, which was further influenced by age and gender. Rastogi et al. [10, 11] had worked on the design implications of walking speed for different types of pedestrian facilities on the basis of function and width, and found out that mean speed on sidewalks and wide sidewalks was more than that on precincts, and that different flow characteristics needed to be adopted for facilities under varying widths and operating under varying conditions. Das et al. [12] observed relationships of field data considering conventional and soft computing approach for sidewalk in India. Level of service information based on pedestrian space, flow rate and speed is developed by the Highway Capacity Manual (HCM) [1] and guidelines for pedestrian facilities [13].

The pedestrians who form the major portion of the traffic system have been neglected till date in our country. At present, the pedestrian facilities are provided on makeshift basis, are not properly maintained or are encroached by vendors and parked vehicles which forces the pedestrians to use the carriageway, which ultimately leads to the interaction between pedestrian and vehicular traffic. Thus, it is important to design and maintain the pedestrian facilities rigorously. In India, work has mainly been based on single regime approach and not on multi-regime models due to limited data. A thorough study near maximum flow has not been done, categorization based on pedestrian types (such as commuters, shoppers, disabled person and children) for capacity estimation is rarely done, and capacity values are rarely validated according to actual field conditions. Moreover, cultural differences and geographical characteristics which affect pedestrian speed are not taken into consideration, most of the studies are based on zero gradient, and study on the differently abled persons is not done with due importance. In other developed countries, detailed study has been initiated for long time on capacity and level of service of pedestrian facilities, while in India the study in this field is very limited. As the planning and designing of pedestrian facilities are the needs of the hour, thus the relevance and the importance of this neglected area encourage further detailed study in this particular field. The need for the development of proper guidelines for the development and maintenance of pedestrian facilities as per Indian conditions is very essential and thus requires more detailed analysis in this field.

3 Data Collection and Analysis

This section presents the details of the data collection sites and procedure for data collection. The procedure for data analysis is also presented in this section. The last part of this section presents the main findings of the study.



Fig. 1 Elevated sidewalk at Ranka Stand (near Hamro Bazaar)

3.1 Data Collection Sites

Sidewalks of three different land uses, viz. transport terminal/commercial, residential/commercial and commercial sites, are studied. Elevated sidewalk at Ranka Stand (near Hamro Bazaar) is used as a public transport terminal/commercial location, while the at-grade horizontal sidewalk near Rumtek Taxi Stand is used as a residential/commercial location and the gradient sidewalk near Denzong Cinema is used as a commercial/recreational location. Survey was done using videography technique for both the locations. Data were collected for peak hour on weekdays for approximately three and a half hours. Rectangular trap of 10-m length was selected for all the locations, and the effective width was also measured. In order to prevent disclosure of identity, the faces of the pedestrians were blurred (refer Figs. 1, 2 and 3).

3.2 Data Extraction

After the peak hour data were collected, they were processed in the laboratory to the required parameters like speed, flow, density and area module. Pedestrians were randomly tracked through the entire section, and walking time was noted for each pedestrian over the trap length. Flow (ped/min) was calculated as the number of pedestrians crossing the line nearer to the camera over each minute. Similarly, flow rate (ped/min/m) was calculated by dividing the flow (ped/m) by the effective width of the trap (m). Effective width was calculated after deducting the shy/buffer distance from the total width. Density (ped/m²) was obtained using the deduced speed and

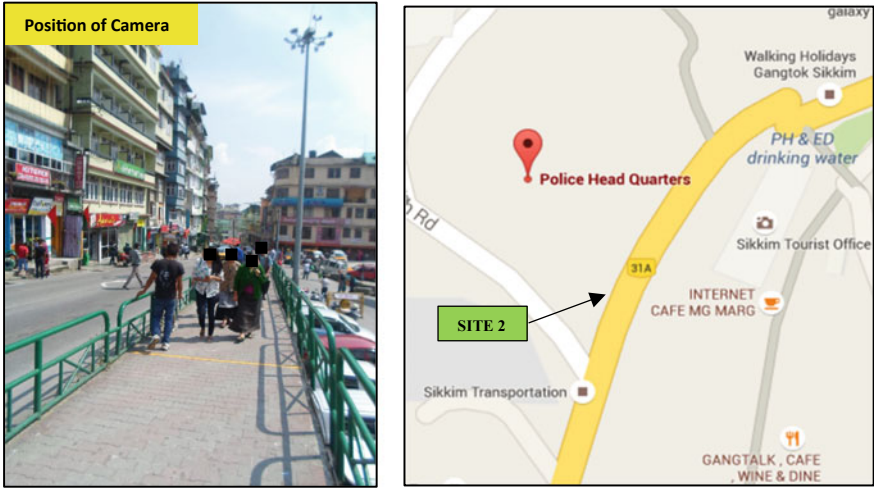


Fig. 2 At-grade horizontal sidewalk near Rumtek Taxi Stand

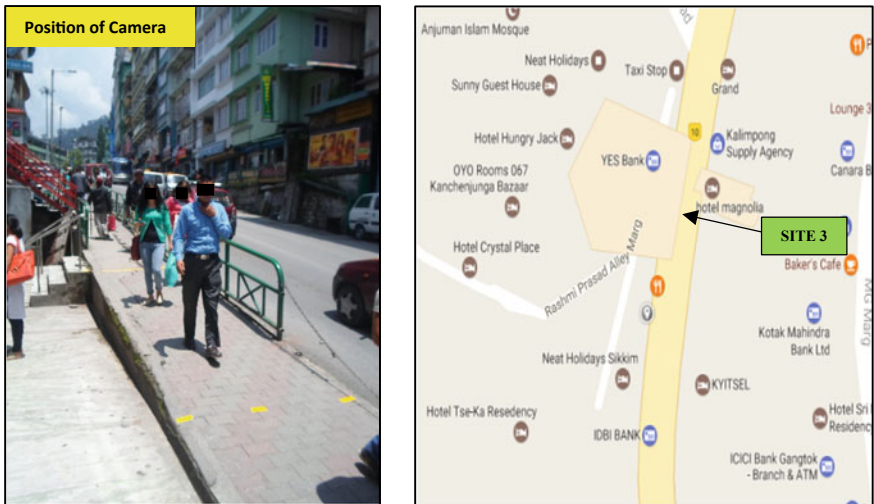


Fig. 3 Gradient sidewalk near Denzong Cinema

flow rate by applying the basic relationship between speed, flow rate and density (i.e. $q = k \times v$), where q , k and v represent flow rate, density and speed, respectively. The pedestrians were categorized based on four input parameters (age, gender, the presence of baggage or not and direction of travel). Age group was divided into three categories like young (<18), adult (18–55) and elderly (>55). Based on the analysis, the various speed–density and speed–flow relationships were analysed.

4 Results of the Study

Collected video data were analysed with the procedure described in the previous section. The data collection details are given in Table 1.

Figures 4, 5, 6, 7, 8, 9, 10, 11 and 12 represent the probability density functions of speed distribution based on gender (male and female), age group (children, adults and elderly), luggage (carrying or not) and direction of movement (towards or away from camera) for all the three sites. x -axis represents the mean speed of pedestrians in m/min, and y -axis shows the relative frequency.

Figures 4, 5, 6, 7, 8, 9, 10, 11 and 12 indicate that all pedestrian categories at site 3 (gradient sidewalk) have a higher accumulation of lower speed in comparison with sites 1 (elevated sidewalk) and 2 (horizontal sidewalk).

Table 2 describes the various statistical parameters for sites 1, 2 and 3 such as mean speed, standard deviation, 15th and 85th percentile speeds, skewness and kurtosis.

From Table 2, it can be seen that male pedestrians have greater mean speed than the female pedestrians for all the three sites. For sites 1 and 2, adult pedestrians have a higher mean speed than child pedestrians, while for site 3 child pedestrians are

Table 1 Data collection details

	Site 1 (elevated sidewalk)	Site 2 (at-grade horizontal sidewalk)	Site 3 (gradient sidewalk)
Date/month of data collection	04.05.2015	04.05.2015	05.05.2015
Duration of data collection (min)	210 (approximately)	200 (approximately)	210 (approximately)
Weather condition	Cloudy	Cloudy	Clear
Tripod altitude	3 m (approximately)		
Sample size	1854	1712	1964
Trap length (m)	10.0	10.0	10.0
Effective width (m)	2.19	2.00	1.44
Gradient (°)	0	0	8.70

Fig. 4 Speed variation among male pedestrians

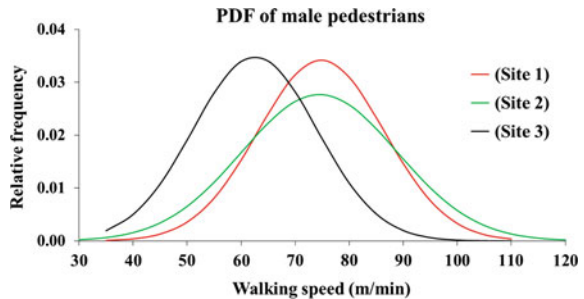


Fig. 5 Speed variation among female pedestrians

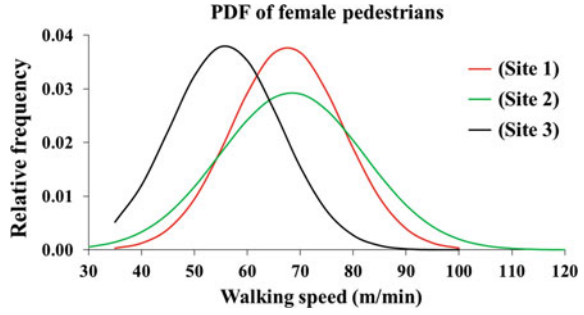


Fig. 6 Speed variation among child pedestrians

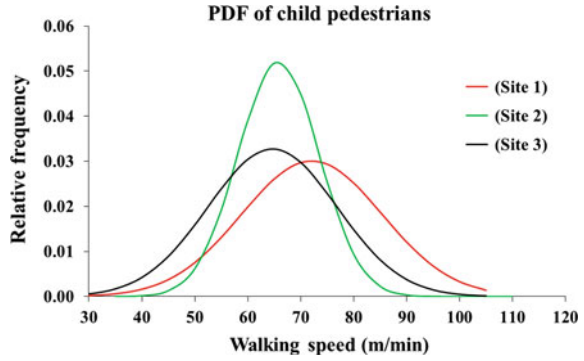


Fig. 7 Speed variation among adult pedestrians

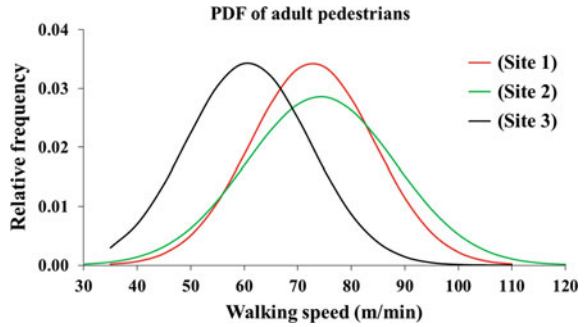


Fig. 8 Speed variation among elderly pedestrians

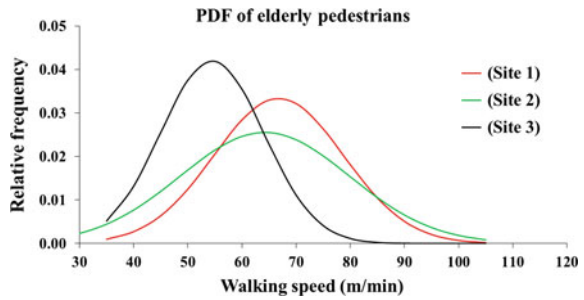


Fig. 9 Speed variation among pedestrians with luggage

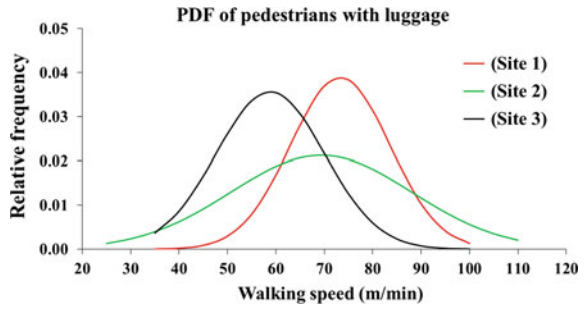


Fig. 10 Speed variation among pedestrians without luggage

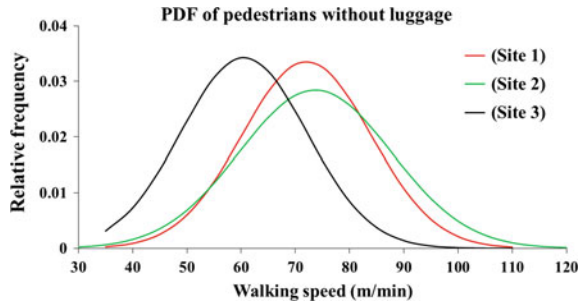


Fig. 11 Speed variation of pedestrians walking towards camera

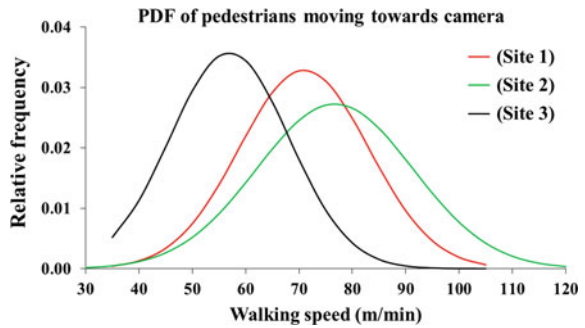


Fig. 12 Speed variation of pedestrians moving away from camera

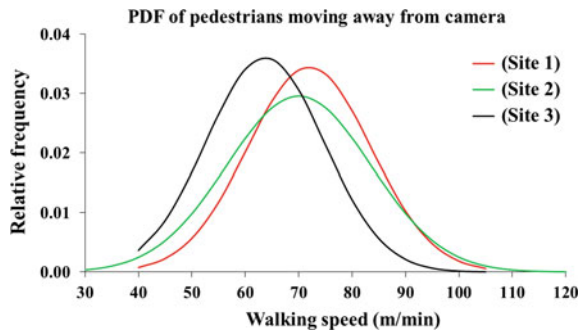


Table 2 Description of statistical parameters

Site	Pedestrian group	Type of pedestrian	Mean speed (m/min)	Standard deviation	Sample size	Fifteenth percentile speed	Eighty-fifth percentile speed	Skewness	Kurtosis
Elevated sidewalk (site 1)	Gender	Male	74.79	11.67	1163	62.41	87.55	0.006	-0.306
		Female	67.57	10.57	681	57.54	77.66	0.274	0.082
	Age	Child	72.08	13.34	82	59.28	86.95	0.362	-0.488
		Adult	72.76	11.64	1617	60.45	85.58	0.136	-0.409
	Luggage	Elderly	66.77	12.01	155	53.07	78.97	-0.002	0.014
		With	73.28	10.29	136	63.15	85.15	-0.063	-0.109
	Direction	Without	72.05	11.89	1718	59.85	84.99	0.154	-0.301
		Towards	70.92	12.15	971	58.21	84.49	0.217	-0.404
At-grade horizontal sidewalk (site 2)	Gender	Away	71.98	11.58	883	60.52	84.67	0.099	-0.167
		Male	74.49	14.41	1390	59.87	89.40	0.022	0.059
	Age	Female	68.41	13.65	322	55.39	82.41	0.321	0.489
		Child	65.83	18.46	62	43.94	85.05	0.239	-0.697
	Luggage	Adult	74.29	13.95	1558	60.12	89.33	0.181	-0.008
		Elderly	64.22	15.71	92	49.57	80.02	-0.144	-0.594
	Direction	With	69.39	18.83	121	49.99	91.24	0.098	-0.557
		Without	73.67	14.03	1591	59.48	87.82	0.129	0.049
	Towards	76.69	14.65	854	61.17	92.17	-0.059	-0.154	
	Away	70.12	13.49	858	57.38	83.71	0.139	0.424	

(continued)

Table 2 (continued)

Site	Pedestrian group	Type of pedestrian	Mean speed (m/min)	Standard deviation	Sample size	Fifteenth percentile speed	Eighty-fifth percentile speed	Skewness	Kurtosis
Gradient sidewalk (site 3)	Gender	Male	62.56	11.47	1329	50.27	74.88	0.293	-0.137
		Female	55.92	10.50	632	45.12	66.70	0.563	0.405
	Age	Child	64.66	12.54	31	55.52	79.01	1.269	1.372
		Adult	60.72	11.62	1825	48.48	73.36	0.344	-0.116
	Luggage	Elderly	54.48	9.55	111	43.07	65.77	0.165	-0.788
		With	58.84	11.23	131	48.15	69.52	0.600	0.204
		Without	60.49	11.64	1833	48.17	73.01	0.347	-0.091
	Direction	Towards	56.95	11.17	962	45.45	68.53	0.577	0.282
		Away	63.67	11.07	1002	52.60	75.66	0.269	-0.057

observed to have a significantly higher speed in comparison with adults; the reason could be that the sample size of child pedestrians of site 3 is significantly lower than the adults. The elderly pedestrians are seen to have a significantly lower speed than child and adult pedestrians for all the locations. Pedestrians with luggage are observed to have higher walking speed than the ones without luggage for site 1, while for sites 2 and 3 the ones without luggage have a greater walking speed than the pedestrians with luggage, and the reason for this could be that gradient and land-use type affect the walking speed of pedestrians who carry luggage. Even though the pedestrian sample size for all the sites is nearly equal, yet the direction of flow does not have any impact on walking speed for site 1 while it does have an impact for sites 2 and 3. The main reason could be that the pedestrians at site 2 who are moving towards the camera are moving towards the commercial hub and are walking at a faster speed, while at site 3 the pedestrians walking towards the camera have to climb a steeper gradient so they have a lower speed.

The skewness and kurtosis values give a measure of the shape of the distribution. Skewness value indicates how asymmetric a distribution is, whereas kurtosis indicates how heavy the tails of distribution are. Moreover, positive skewness value indicates a larger accumulation of lower speeds and higher kurtosis value indicates distinct peak near the mean and heavier tails. From Table 2, it is observed that for site 1 child pedestrians have highest skewness and that female pedestrians have highest kurtosis. For site 2, female pedestrians have the highest skewness and kurtosis. Similarly, it can be seen that maximum skewness and kurtosis value are for child pedestrians of site 3. This indicates that there is larger accumulation of lower mean speed and that there is heavier tail with distinct peak near mean for the female and child pedestrians of sites 2 and 3, respectively, as compared to the other pedestrian groups for the same location.

Statistical tests were conducted in order to check whether there was any significant difference between various pedestrian groups. *t*-test was performed in case of pedestrian gender group and whether they were carrying luggage or not. *t*-test is a statistical hypothesis test which is performed in order to determine whether two sets of data are significantly different from each other or not, and is generally applied when the test statistics follows normal distribution. Similarly, ANOVA test is a statistical test performed for comparing statistical significance for three or more groups, generalizes the *t*-test to more than two groups and was used for comparing age category. Table 3 shows the results of *t*-test for pedestrian gender group for all the four sites as well as with or without luggage for site 1 only. Similarly, Table 4 shows the results of ANOVA test for age group for all the three sites.

Table 3 shows that a significant difference exists between male and female pedestrians for all the sites as *t*-statistical value is more than *t*-critical value. Moreover, it can also be observed that pedestrians with and without luggage and also pedestrian direction for sites 1 and 3 have no significant difference, while at site 2 significant difference exists.

Table 4 shows that *F*-statistical value is greater than *F*-critical value and also *P*-value for both the sites is less than 0.05. This indicates that at 5% significance level, a significant difference exists between the pedestrians based on age category

Table 3 Results of *t*-test for pedestrian gender group and whether they were carrying luggage

Sidewalk	Pedestrian group	<i>t</i> -Statistical value	<i>t</i> -Critical value	Difference
Elevated (site 1)	Gender	13.25	1.96	Significant
	Luggage	1.17	1.96	Not significant
	Direction	1.67	1.96	Not significant
At-grade horizontal (site 2)	Gender	6.81	1.96	Significant
	Luggage	3.14	1.96	Significant
	Direction	9.76	1.96	Significant
Gradient (site 3)	Gender	12.29	1.96	Significant
	Luggage	1.56	1.96	Not significant
	Direction	1.33	1.96	Not significant

Table 4 ANOVA single factor test results for pedestrian age group

Sidewalk	Pedestrian group	<i>F</i> -Statistical value	<i>F</i> -Critical value	<i>P</i> -value
Elevated (site 1)	Age	18.62	3.00	0
At-grade horizontal (site 2)		30.89	3.00	0
Gradient (site 3)		17.18	3.00	0

and that there is a significant difference in walking speed between child, adult and elderly pedestrians for all the three sites.

The correlation between speed and density was -0.39 , -0.42 and -0.56 for sites 1, 2 and 3, respectively. As the values are near -1 , hence this predicts that a strong relationship exists between the two variables and a linear straight line having negative slope can be fitted. Therefore, Greenshields' model was used in describing the speed–density relationship (refer Fig. 13a–c). Further, Greenshields' model is also plotted for speed–flow rate relationship (refer Fig. 14a–c) to predict the capacity for these three locations.

The observation which could be deduced from the predicted relationships is given below:

- i. The free-flow speed for sites 1 and 2 is found to be around 90–95 m/min, while it is approximately 75–80 m/min for site 3.
- ii. The predicted jam densities for the three sites are 2.4, 1.5 and 2.1 ped/m², respectively.
- iii. The predicted maximum flow rates for the three sites are 47, 31 and 37 ped/min/m, respectively.

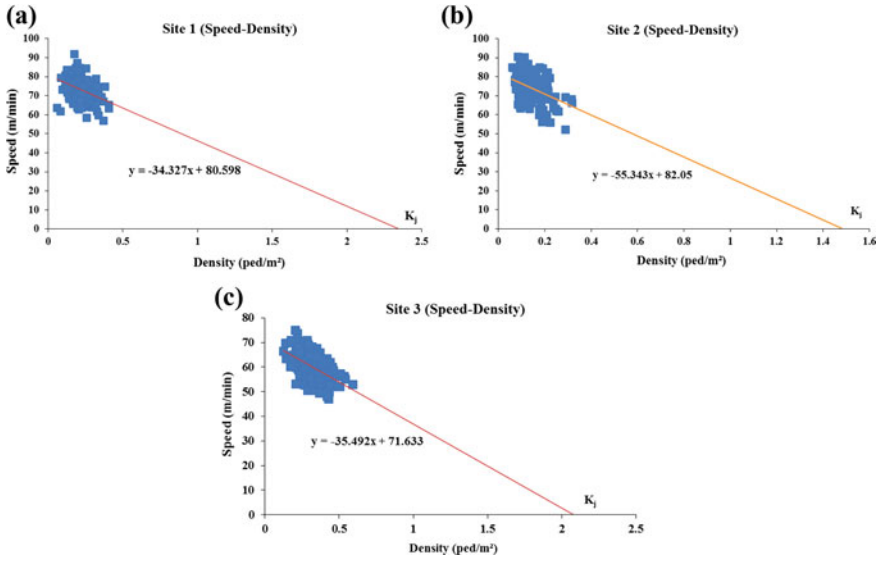


Fig. 13 a, b and c Speed–density relationship for sites 1, 2 and 3

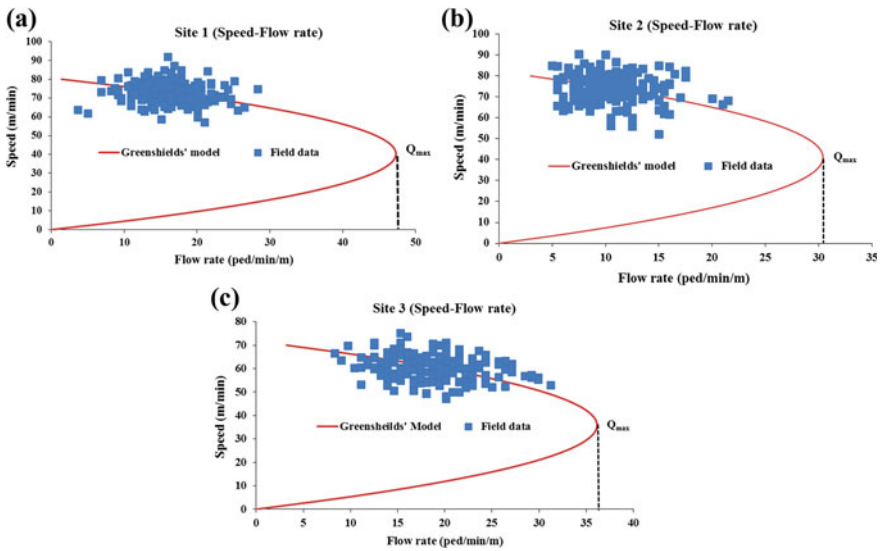


Fig. 14 a, b and c Speed–flow rate relationship for sites 1, 2 and 3

5 Conclusions

After collecting and analysing the data, the following conclusions could be drawn:

- i. Female pedestrians are observed to have lower walking speed than male pedestrians for all the three locations.
- ii. Gender ratio shows that the percentage of male pedestrians for site 1 (62.7%), site 2 (81.2%) and site 3 (67.7%) is considerably higher than their female counterparts.
- iii. The age ratio shows that the percentage of adult pedestrians for site 1 (87.3%), site 2 (91.0%) and site 3 (93.1%) is highest in comparison with child and elderly pedestrians.
- iv. The percentage of pedestrians with luggage is considerably low for site 1 (7.3%), site 2 (7.1%) and site 3 (6.7%) in comparison with the pedestrians without luggage.
- v. The direction of flow has an impact on walking speed even when the proportion of pedestrians is nearly equal in both the directions depending on the type of land use and the presence of gradient.
- vi. It can also be seen that in comparison with sites 1 and 2, site 3 pedestrians have a significantly lower free-flow speed and mean speed, and the steep gradient could be a factor for such an observation.
- vii. The free-flow speed is considerably higher for sidewalk without gradient (sites 1 and 2) in comparison with the sidewalk with gradient (site 3), and thus gradient does impact the pedestrian walking speed.
- viii. It is observed that pedestrian density and speed are linearly related. Speed of pedestrian reduces as density increases. Predicted jam densities for elevated and gradient sidewalks are 2.4, 1.5 and 2.1 ped/m², respectively. The reduction at site 2 may be due to lower density observed during data collection as well as the land-use type.
- ix. It is observed that predicted maximum flow rate was higher for site 1 (47 ped/min/m) in comparison with site 2 (31 ped/min/m) and site 3 (37 ped/min/m). The reason site 3 sidewalk having lower maximum flow rate may be the narrower width (1.44 m) and relatively steep gradient. Moreover, the location of site 1, i.e. public transport cum commercial area, may also attract higher flow rate in comparison with sites 2 and 3, which are residential/commercial and commercial/recreational areas, respectively.

Acknowledgements The authors acknowledge the support received from CSIR-CRRI in collection of data required in developing this paper.

References

1. HCM (2010) Highway capacity manual. Transportation Research Board, Washington, DC
2. Oeding D (1963) Verkehrsbelastung und Dimensionierung von Gehwegen und anderen Anlagen des Fußgängerverkehrs (Traffic volume and dimensioning of footways and other facilities of pedestrian traffic). Straßenbau und Straßenverkehrstechnik, Series number 22. Ministry of Traffic, Bonn
3. Older SJ (1968) Movement of pedestrians on footways in shopping streets. *Traffic Eng Control* 10(4):160–163
4. Polus A, Schofer JL, Ushpiz A (1983) Pedestrian flow and level of service. *J Transp Eng ASCE* 109(1):46–56
5. Tanaboriboon Y, Hwa SS, Chor CH (1986) Pedestrian characteristics study in Singapore. *J Transp Eng ASCE* 112(3):229–235
6. Lam WHK, Morrall JF, Ho H (1995) Pedestrian flow characteristics in Hong Kong. *Transportation research record* 1487, TRB, National Council, Washington, DC, pp 56–62
7. Al-Azzawi M, Raeside R (2007) Modelling pedestrian walking speeds on sidewalks. *J Urban Plan Dev* 133(3):211–219
8. Parida P, Najamuddin, Parida M (2007) Development of qualitative evaluation methodology for sidewalks in Delhi. *ITPI J* 4(3):27–33
9. Laxman KL, Rastogi R, Chandra S (2010) Pedestrian flow characteristics in mixed traffic conditions. *J Urban Plan Dev* 136:23–33 (Special issue: Challenges in transportation planning for Asian cities)
10. Rastogi R, Thaniarasu I, Chandra S (2011) Design implications of walking speed for pedestrian facilities. *J Transp Eng* 137(10):687–696
11. Rastogi R, Ilango T, Chandra S (2013) Pedestrian flow characteristics for different pedestrian facilities and situations. *Eur Transp* 53(6)
12. Das P, Parida M, Katiyar VK (2015) Analysis of interrelationship between pedestrian flow parameters using artificial neural network. *J Mod Transp* 23(4):298–309
13. IRC: 103 (2012) Guidelines for pedestrian facilities. The Indian Roads Congress, New Delhi, India

Real-Time Vehicular Air Quality Monitoring Using Sensing Technology for Chennai



P. Partheeban, H. Prasad Raju, Ranganathan Rani Hemamalini and B. Shanthini

Abstract Air pollution in urban areas is posing a great threat to urbanites all over the world. Various factors which contribute to air pollution are industrial, commercial and domestic activities. Statistics show that among these sources, motorised transportation is the highest contributing air pollution in recent past. Further, it may increase unless any major mitigation measures are planned and implemented. Therefore, assessing quality of the atmospheric air for breathing time to time is very important to control further damage. Currently, to access air quality-related data is limited. To overcome this, authors have designed and developed an air quality monitoring instrument (AQMI) using solid-state gas sensors and GPS module. It was used to measure the air pollution levels at Chennai city in real time and analysed the air pollutants levels in two different periods and suggested mitigation measures. Air quality on four routes in Chennai has been measured in 2013 and 2017 and compared in order to study the impact of air quality due to Vardhah cyclone. Four routes are considered in Chennai, namely Avadi to Tambaram (route 1—R1), Neelankari to T. Nagar (route 2—R2), Avadi to Chennai central (route 3—R3) and Tonakela camp to Redhills bus stand (route 4—R4). It is observed that the air pollution monitored in 2013 on the three routes shows about 60–70% locations having concentrations exceeding Central Pollution Control Board (CPCB) norms and one route has exceeding values at three places. After monitoring air quality in 2017, it was found that at some places, the pollution levels are increased when compared to that of 2013 due to further increase in vehicular traffic as well as Vardhah cyclone. Air quality data obtained using AQMI could serve various applications. Health conscious people could also take advantage of this to navigate through pollution-free areas. Patients with air pollution-related health problems would find data valuable to determine the less polluted routes.

Keywords Vehicular emissions · Air pollution · Health problems · Sampling · Analysis · Gas sensors · Real-time mobile monitoring

P. Partheeban (✉) · R. Rani Hemamalini · B. Shanthini
St. Peter's College of Engineering and Technology, Chennai, India
e-mail: parthi011@yahoo.co.in

H. Prasad Raju
Sree Vidyanyikethan Engineering College, Tirupati, India
e-mail: prasadrāju@gmail.com

© Springer Nature Singapore Pte Ltd. 2020
T. V. Mathew et al. (eds.), *Transportation Research*, Lecture Notes
in Civil Engineering 45, https://doi.org/10.1007/978-981-32-9042-6_2

1 Introduction

Air pollution is a major problem in India, especially in urban areas. In general, air pollution in urban areas is posing a great threat to urbanites all over the world. It is the fifth leading cause of deaths among top 10 killers across the world [1]. The various factors that contribute to air pollution are industrial, commercial and domestic activities. Industrial activities include manufacturing of chemicals, metallurgical and metal processes to make semi-finished and finished goods, electroplating, painting, etc. Commercial and domestic activities include motorised transportation, combustion of fuels for cooking and heating, burning of wastes on roadsides, construction activities, etc. Statistics show that among these sources, motorised transportation is one of the major contributors of air pollution, about 60–70% in urban areas, in the recent past [2]. Further, it may increase unless any major mitigation measures are planned and implemented. Therefore, assessing the quality of the atmospheric air we breathe from time to time is very important to control further damage.

Current pollution measurement methods use expensive equipment at fixed locations or dedicated mobile equipment laboratories. This is a *course-grained system* where the pollution measurements are few and far in-between. The analysis of samples in practice is mass spectroscopy (MS), gas chromatography (GC), Fourier transform infrared instrument (FTIR) method, etc, and provides accurate and selective gas reading, but cumbersome, expensive and time-consuming. It is desirable to have access to real-time measurements, i.e. to be able to quickly analyse and identify alarming levels of pollutants. Currently, access to such data is limited. It is available to a few who are well informed on the subject of pollution. Due to these reasons, researchers started designing cost-effective embedded systems with readily available low-cost solid-state gas sensors having fast response and possibility of real-time data transfer.

Solid-state gas sensors are the type of gas sensors which cause change in electrical resistance by a loss or a gain of surface electrons as a result of adsorbed oxygen reacting with the target gas. Quantitative response is achieved as the magnitude of change in electrical resistance is a direct measure of the concentration of the target gas. In this study, readily available sensors in the market are used to measure air quality. Hence, sensors are not developed specific to this study.

It has been reported that the vehicular emissions contribute carbon monoxide, carbon dioxide and nitrogen oxides to the air pollution [3]. The major contribution to Chennai air pollution load is vehicular sector (71.28%) followed by industrial sector (19.70%) [4]. The objectives of this study are as follows: (i) to design and develop an AQMI using solid-state gas sensors and GPS; (ii) to measure and analyse the air quality data in 2013 and 2017 in Chennai for selected four routes; (iii) to display the measured air pollution levels at Chennai city in real time through a website (www.airpollutioninchennai.com); and (iii) to analyse the air pollutants levels and suggest mitigation measures.

2 Literature Review

Various attempts have been made to employ mobile monitoring systems using sensors in order to obtain *fine-grained* air quality data. In order to bridge the gap between the sampling phase and the analysis phase, researchers introduced monitoring approaches using commodity sensors, which can provide real-time air pollutants' data. An air pollution monitoring study conducted on school bus at University of California along with National Resources Defence Council (NRDC) highlighted the health hazards posed to school children by their exposure to diesel pollutants. The study emphasized the urgent need for mobile monitoring of air quality as the diesel exhaust is known for its carcinogenic character and a cause of respiratory illnesses [5]. Narasimha Murthy et al. [6] have designed a wireless network which consists of end devices with sensors and routers that propagate the network over long distances. Their design is based on ARM7 processor with LPC2378 microcontroller and EZ430RF 2480 ZigBee module to process and communicate the data effectively with low power consumption.

A wireless sensor system for real-time monitoring of toxic environmental volatile organic compounds was developed by Tsow et al. [7]. This system was based on a smart sensor microconverter equipped with a network capable application processor that downloads the pollutants' level to personal computer for further processing. Jung et al. [8] have installed an air pollution geo-sensor network consisting of 24 sensors and 10 routers to monitor several air pollutants. Raja Vara Prasad et al. [9] have formed multi-hop mesh network with the array of pre-calibrated sensors interfacing with the wireless sensors motes and have been developed a lightweight middleware and Web-based interface for online monitoring of the data in the form of charts from anywhere on Internet.

3 Air Quality Monitoring Instrument

Air quality monitoring instrument (AQMI) is designed and developed for mobile monitoring of air quality in real time. It consists of a hardware unit that integrates a single-chip microcontroller (ARM7 processor—LPC2129 is TDMI-S CPU with real-time emulation and embedded trace support), air pollution sensors (CO₂, CO and NO) array, signal sensing conditioners and a GPS module. Its output is connected to a high-end personal computer (PC) with GSM module which acts as Internet connectivity.

The hardware unit gathers air pollutants' (CO₂, CO and NO) concentrations and packs them in a frame with the GPS physical location, time and date. This frame is subsequently uploaded to the GSM modem through RS232 interface and transmitted to the Central Server via wireless network. Central Server is interfaced to Google Maps to display the location of hardware unit. The basic building blocks of AQMI

instrument are shown in Figs. 1 and 2. The list of sensors along with their features used in the AQMI is presented in Table 1.

Website www.airpollutioninchennai.com is designed and developed to display observations, i.e. pollutants' concentrations measured at different locations in real time as shown in Fig. 3. The AQMI measures concentrations of gases such as CO,

Fig. 1 Basic building block diagram of data receiver (ARM-7 module)

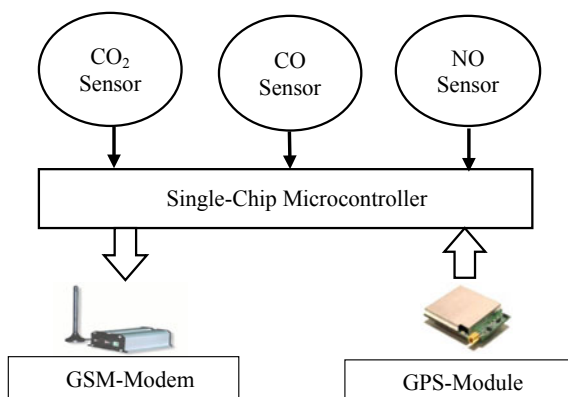


Fig. 2 Basic building block diagram of data network system

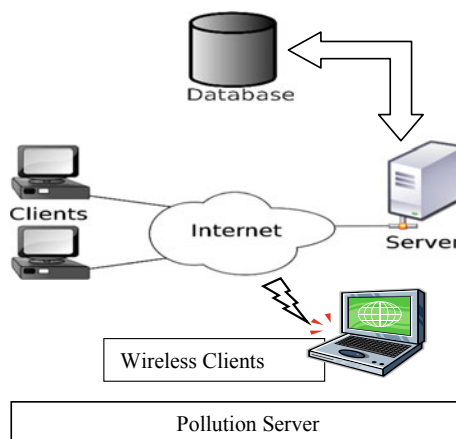


Table 1 Features of the sensors used in the AQMI

Sensor	CO ₂ (ppm)	CO (ppm)	NO (ppm)
Response time (T90) (s)	<120	<60	<45
Operating range (ppm)	350–30,000	0–10,000	0–20
Operating life (years)	>2	>2	>2
Diameter (mm)	20	20	20
Sensitivity	44–72 mV/ppm	1.2–2.4 nA/ppm	400–480 mV/ppb

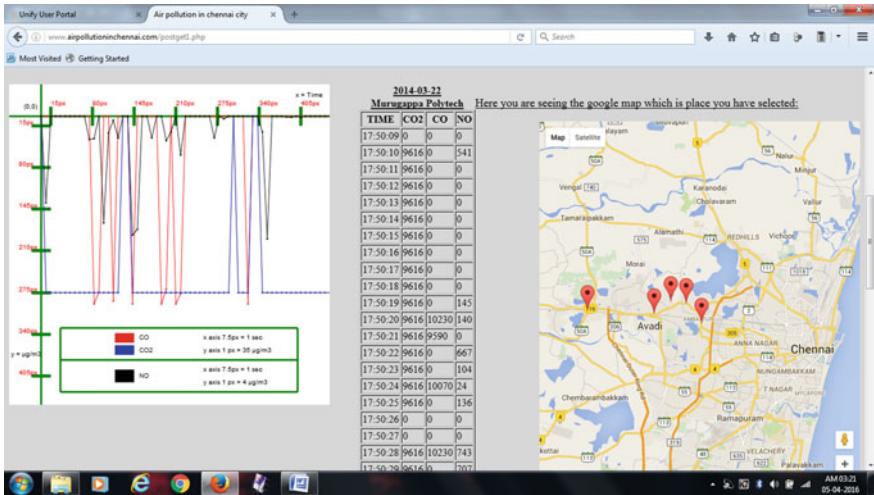


Fig. 3 A sample image of the website

CO₂ and NO and displays on the website in real time. The information displayed consists of hardware location with round red colour pointer on Google Map on the right side. The table consists of pollutants' concentration with time at centre and the date above the table. On the left side, the red, blue and black colour lines are graphical representation of pollutants' concentration CO, CO₂ and NO, respectively.

4 Monitoring of Air Quality Using AQMI and Analysis

First requirement in air quality monitoring is the location of sampling sites, which must be representative of the area under study. From a health perspective, the sampling site must be located in such a way that the collected samples represent true air quality that is actually breathed by the exposed population group. An ideal sampling site would therefore locate on the ground level between 1 and 2 m. In general, special attention has to be given to see that the selected locations have the free flow of air movement. The AQMI instrument's data receiver system is mounted on top of the car (about 1.5 m height from the road surface) while the data network system is kept within the car for data collection and storage.

Four routes are selected for monitoring within and around the Chennai city. Different routes cover different areas such as high and low traffic volumes, domestic, commercial and industrial areas. Routes selected and monitored are Avadi to Tambaram

(route 1—R1), Neelankari to T. Nagar (route 2—R2), Avadi to Chennai central (route 3—R3) and Tonakela camp to Redhills bus stand (route 4—R4) as shown in Fig. 4.

As per the norms of Central Pollution Control Board (CPCB), the limits for pollution levels for CO and NO are ≤ 6 and ≤ 0.035 ppm, respectively. There are no specified limits for CO₂ whose excessive presence in the atmosphere is most responsible for global warming phenomenon. The observed pollution levels of CO and NO are shown for route 1 in Figs. 5 and 6, respectively. The red coloured bar on CO and NO bar charts represents the permissible concentration levels as per the Ambient Air Quality Standards specified by the Central Pollution Control Board.

From the overall study, it has been observed that in all routes except the few places, pollution levels increased at all places in 2017 when compared to 2013 observed noise levels. It can be mainly due to increase in motor vehicles and more traffic on roads. The motor vehicles population in Chennai as on 1 March 2013 were 3,881,850, and

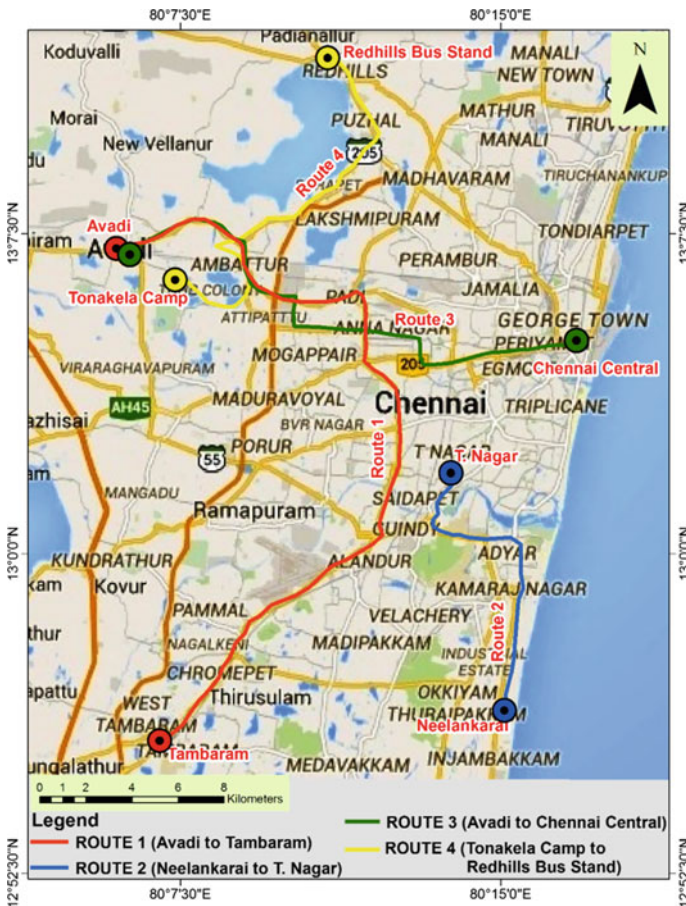


Fig. 4 Four routes in which the pollution levels measured in Chennai city

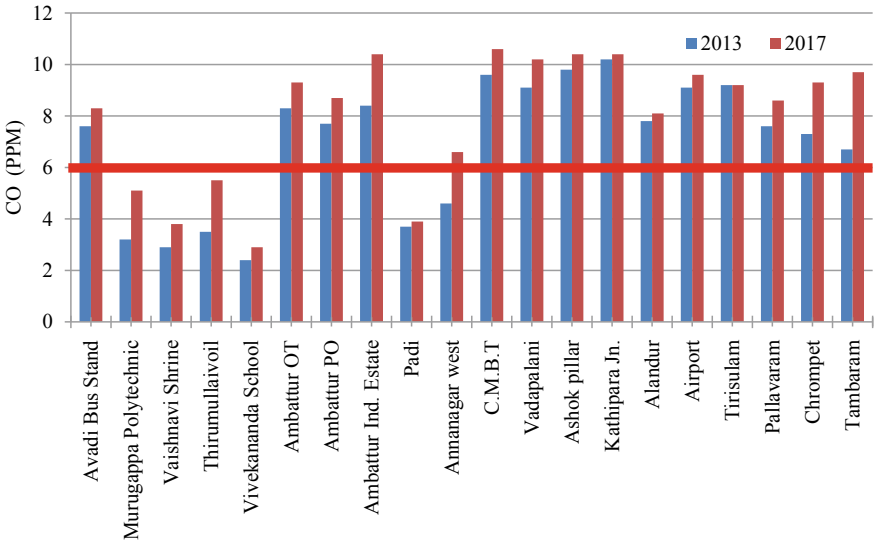


Fig. 5 CO concentrations at various locations on route 1 in 2013 and 2017

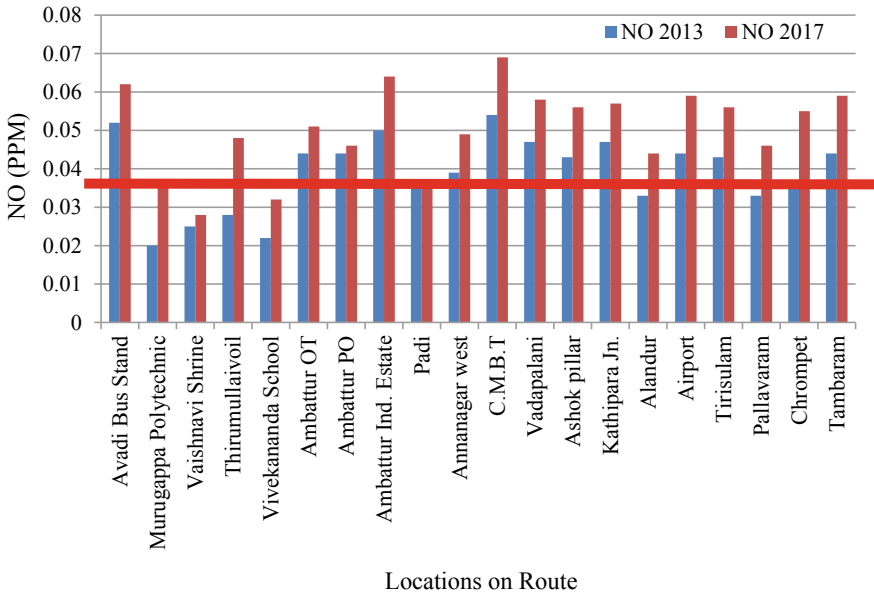


Fig. 6 NO concentrations at various locations on route 1 in 2013 and 2017

it has increased to near about 5,444,777 by March 2017. It clearly shows that the increase in pollution levels is due to increase in number of motorised vehicles that came to ply on the roads.

4.1 Analysis of Air Pollutants Monitored in Four Routes

Routes 1 and 4 together run from south to north, and Route 3 from West to East and route 2 running through another important area on the sidelines of the coast are shown in Fig. 4. It was observed that in 2013, the pollution levels of CO at routes 1, 2 and 3, 60–75% of locations have more than CPCB norms (6 ppm) except in the route 4. Route 4 covers sub-arterial roads (with more residential areas along the road) and a part of National Highway 5 (NH5) in the Chennai Metropolitan Area. It was found that interior roads are having the pollution levels within the norms and along NH5 exceeded. It is the same case when the pollution levels were monitored in 2017 but increased concentrations except two places in the route 1, namely Padi and Trisulum, two places in route 2, namely Gandhi Nagar and Anna University, one place in route 3 namely Vivekananda School and along route 4 more or less remained same at all locations. Increase in air pollution is due to the loss of many trees during Vardhah cyclone in December 2015 and also subsequent increase in motor vehicles' population in Chennai.

In 2013, the observed pollution levels of NO along the routes 1, 2 and 3 were exceeded at about 60–80% of locations except route 4 where only at 3 places on the National Highway (NH) exceeded the CPCB limits (0.035 ppm). In 2017, the monitored values show substantial amount in increase of pollution levels at about 60–85% places more than norms along the routes 1, 2 and 3 except route 4. In the route 4 at four places exceeded the norms including the 3 places that of 2013 year and at all other places, it remained within the limits but increased due to increase in vehicles population. The results obtained using AQMI with solid-state gas sensors are in comparison with the standard methods and robust in obtaining the pollutants' concentration levels which can be made available in real time and can be used for assessing the air quality.

4.2 Suggestions for Mitigation Measures

Our new environments should be 'future proofed' to cope with the demands placed upon the future population, for example innovative schemes to maintain air quality providing traffic-free zones, designing pedestrian-friendly streets, making footpaths usable always (i.e. removal of obstacles immediately, if placed across footpaths by defaulters) which will ensure safety as well to both pedestrians and commuters on vehicles. Design of streets might include special provision for non-motorised

transport for example bicycles, tricycles. In general, civic bodies in all towns and cities should adopt design of environmental friendly streets and sustainable mobility.

In Chennai, currently, many main roads lack proper footpaths, a situation that becomes worse with the monsoon. If footpaths are maintained well, then many people even like to walk for small distances rather than using motor vehicles. To protect air quality, more plants might be planted, and soil protection measures are to be taken to preserve this vital resource for proper growth of plants. Planning and policy might also take account of people's desire for self-sufficiency and provenance which will indirectly helps in maintaining of good quality of air. Contemporary construction and then deconstruction of urban fabric and consumer products will also be key to resource reuse and waste minimization to avoid an urban environmental pollution burden in the future greater than that which we are already dealing with.

5 Conclusions

This paper presents fine-grained real-time mobile monitoring instrument deployable on public transportation infrastructure and personal vehicles. The air pollution level is increased due to the Vardhah cyclone which uprooted many trees in the city in 2015 and also due to simultaneous growth in motor vehicles population. The data shows the pollutant levels and their conformance to local air quality standards. It is worth mentioning that much more work is required to be done to commercialize the instrument. It is necessary to increase the number of plants within and around the city to protect the environment.

The air quality data obtained using such sensing instruments could serve various applications. Individuals using such system may become more knowledgeable about the extent of air pollution and shall be motivated to follow the better driving patterns. It includes not allowing vehicles to be idle for long periods, driving at a speed that generates less air pollution, driving through less polluted areas, keeping vehicles in good condition and following proper maintenance procedures. Health conscious people could also take advantage of this to navigate through pollution-free areas. Patients with air pollution-related health problems would find data valuable to determine the less polluted routes. Apart from these applications, this data could be used for policy making on prevention and control of air pollution through regulatory and legislative means. For example, public health officers and policy-makers could use the data to predict potential health impacts across various areas of city to make decisions on new bus routes formation, sanctions for the establishment of new schools and colleges, etc.

References

1. <http://www.downtoearth.org.in/content/air-pollution-killing-620000-indians-every-year-global-burden-disease-report>. Last accessed 15 Sept 2014
2. Singh SK (2005) Review of urban transportation in India. *J Public Transp* 8(1):79–97
3. Automobile Emissions (2014) An overview. United States Environmental Protection Agency—Office of Mobile Sources. <http://www.epa.gov/otaq/consumer/05-autos.pdf>. Last accessed 04 Nov 2014
4. Development Plan for Chennai Metropolitan Area (2006) Environment and disaster management, chap VI. CMDA special publication. The Chennai Metropolitan Development Authority, Chennai
5. Honicky R, Brewer EA, Paulos E, White R (2008) N-SMARTS: networked suite of mobile atmospheric real-time sensors. In: Proceedings of the second ACM SIGCOMM workshop on networked systems for developing regions (NSDR 2008), ACM, New York, NY, USA, pp 25–30. <http://doi.acm.org/10.1145/1397705.1397713>
6. Narasimha Murthy Y, Sukanya V, Saritha C (2013) Design and development of ZigBee based wireless sensor network for monitoring air pollutants. *Int J Sci Eng Res* 4(3):1–5
7. Tsow F, Forzani E, Rai A, Wang R, Tsui R, Mastroianni S, Knobbe C, Gandolfi AJ, Tao NJ (2009) A wearable and wireless sensor system for real-time monitoring of toxic environmental volatile organic compounds. *IEEE Sens J* 9:1734–1740
8. Jung YJ, Lee YK, Lee DG, Ryu KH, Nittel S (2008) Air pollution monitoring system based on geosensor network. In: IEEE international geoscience remote sensing symposium, vol 3, pp 1370–1373
9. Raja Vara Prasad Y, Baig MS, Mishra RK, Rajalakshmi P, Desai UB, Merchant SN (2011) Real time wireless air pollution monitoring system. *ICTACT J Commun Technol* 2(2):370–375 (Special issue on next generation wireless networks and applications)

Assessing the Impact of Bus Arrival Rate on the Bus Lane Capacity: A Simulation-Based Approach



Anshuman Sharma , Manoranjan Parida , Ch. Ravi Sekhar 
and Jayvant Choudhary

Abstract Bus lane capacity is undoubtedly an essential ingredient in the planning, design and operation of bus corridors. Among the various factors influencing the bus lane capacity, bus arrival rate has been underexplored. Therefore, this study focusses on assessing the impact of eight different arrival rates on bus lane capacity. To achieve this aim, a simulation model is developed, and two simulation experiments were performed. One with fixed dwell time and varying arrival rates, and second with fixed arrival rate and varying dwell time. To compute the capacity, transit capacity and quality of service manual (TCQSM) model is selected. Based on the analysis, as the arrival rate increases, the bus lane capacity increases at the cost of increase in the queue length. Furthermore, for a fixed arrival rate, when the dwell time decreases, the bus lane capacity increases. From the practitioners' and policy makers' viewpoint, the findings of this study highlight the importance of judiciously selecting an arrival rate.

Keywords Arrival rate · Bus lane capacity · TCQSM · BRTS · Dwell time

A. Sharma (✉)

School of Civil Engineering & Built Environment, Science and Engineering Faculty, Queensland University of Technology, 2 George St., Brisbane, QLD 4001, Australia
e-mail: anshuman.sharma@hdr.qut.edu.au

M. Parida

Civil Engineering Department, Indian Institute of Technology Roorkee, Roorkee, India
e-mail: mprdafce@iitr.ac.in

Ch. Ravi Sekhar

Transportation Planning Division, CSIR-Central Road Research Institute, New Delhi, India
e-mail: chalumuri.ravisekhar@gmail.com

J. Choudhary

Department of Civil Engineering, Indian Institute of Technology (Banaras Hindu University) Varanasi, Varanasi, India
e-mail: jayvant05@gmail.com

© Springer Nature Singapore Pte Ltd. 2020

T. V. Mathew et al. (eds.), *Transportation Research*, Lecture Notes in Civil Engineering 45, https://doi.org/10.1007/978-981-32-9042-6_3

1 Introduction

As the demand for transportation is increasing, the needs for sustainable modes become more evident. An efficient bus rapid transit system (BRTS) is a boon for cities, which are ridden with innumerable transportation problems due to increase in traffic density, population explosion, the concentration of economic activities in central business districts and poor urban planning. From the transit user's perspective, BRTS offers enhanced frequencies, increased system reliability and a reduction in travel time and delays. BRTS capacity is a critical factor that impacts bus frequency, system reliability, and lower travel time. Therefore, the success of a BRTS heavily relies on its capacity.

BRTS capacity is dictated by the bus lane capacity and the passenger capacity. It also reflects the interaction between the passenger flow and the bus flow. The bus lane capacity is defined as a maximum number of buses which can utilise the facility in an hour. As per National Academies of Sciences [1], the bus lane capacity is governed by the loading area capacity. In general, firstly, loading area capacity of a bus stop is calculated; secondly, bus stop capacity is calculated depending on the number of loading areas present at the bus stop; thirdly, the first two steps are repeated to evaluate the capacity of all the bus stops present on the bus lane; fourthly, the critical bus stop is identified (the bus stop with the least capacity is termed as the critical bus stop); and finally, the bus lane capacity is calculated which is equal to the critical bus stop's capacity [1]. Hereafter, critical bus stop capacity is referred as bus lane capacity.

In order to calculate the bus lane capacity, various mathematical and simulation models are available in the literature [1–9]. However, it is still unclear which model should be preferred when computing the bus lane capacity. Furthermore, a comprehensive review of these models is missing in the literature. Synthesis of the literature further reveals that most of the research studies focussed on how lane capacity is impacted by the dwell time [10], failure rate [7], signalised intersection [11], etc. Another important factor which impacts the bus lane capacity is bus arrival rate (AR) [12, 13]. Surprisingly, this factor is still underexplored.

Motivated by the aforesaid research needs, the present study first reviews three of the most popular models, reports their features and unfolds their specific limitations. Furthermore, this study aims to investigate the impact of bus arrivals on the bus lane capacity. A comprehensive understanding of ARs will assist the practitioners and policymakers to fix a particular AR or opt for time adaptive ARs with the objective of maximising the bus lane capacity and minimising the queue length at the bus stop. In the present study, nine different ARs are investigated by using a simulation model.

The remaining of the paper is organised as follows. Section 2 reviews the bus lane capacity estimation models. Section 3 describes the methodology and Sect. 4 discusses the results and findings. The conclusions drawn from the study and the future work are presented in Sect. 5.

2 Bus Lane Capacity Estimation Model

Intuitively, before developing a new model or implementing a particular model, it is of utmost importance to evaluate the models and comprehend their pros and cons. Thus, in this section, only three (due to space constraints) but most cited capacity estimation models are reviewed. Table 1 presents different features and limitations of these models. Highly preferred TCQSM model to estimate the lane capacity has two major limitations: (a) ignorance of complex stochastic process noticeable at the bus stop, for example, passenger movements, bus arrival and departure; (b) underprediction of stop capacity values as compared to the field observations. The TCQSM model still can be applied to the bus stops with non-complex passenger–bus interactions. Based on the review, we conjecture that there is a need for developing a reliable, robust and realistic capacity estimation model. In this regard, the important elements which fully specify the bus stop [12] and shall be considered when computing the bus lane capacity are as follows:

- The bus stop area and the platform
- Berth configuration (linear, sawtooth, parallel, etc.)
- Utilisation of berths
- Single or multiple stops
- Character of the stop (mandatory or optional)
- Entry and Exit discipline to the stop area (First In First Out (FIFO) or overtaking allowed)

All these factors impact the passenger–bus interaction.

To investigate the impact of AR on the bus lane capacity, this study adopts TCQSM model to compute the capacity. Importantly, to enhance the applicability of the model and lessen the impact of its limitations, this study focusses on a section of a one-lane busway with one on-line stop constituting single loading area and no traffic signal. This is critical because the primary aim of this study is to comprehend how AR impacts bus lane capacity rather than developing a new model.

There are two important components of TCQSM model, namely the dwell time and the failure rate. The dwell time at a bus stop begins when the bus arrives and stops at the stop, and ends when the bus leaves the stop [14]. As per TCQSM, the dwell time is calculated as the sum of boarding and alighting time, door opening and closing time, and passenger service time. The other component, failure rate is defined as the probability of finding all the loading areas occupied when a bus arrives at the bus stop. In this study, the failure rate is calculated in percentage as total time spent by all the buses in queue divided by 3600 and incorporated using Z , same as TCQSM. Furthermore, as there is no traffic signal, the g/C ratio is equal to 1. Since the bus stop consists of a single birth, N_{e1} is equal to 1. The t_c is assumed to be equal to 10 s.

Table 1 Review of bus lane capacity estimation models

Model	Equation (buses/h)	Model parameters	Limitations
TCQSM model [1]	$\frac{3600(\frac{g}{C})N_{el}f_{tb}}{t_c+t_d(\frac{g}{C})+ZC_Vt_d}$	$\frac{g}{C}$ is green time ratio, t_c is the clearance time (s), t_d is the average dwell time (s), C_V is the coefficient of variation of dwell time and Z is the standard normal variable corresponding to a failure rate	The formulation assumes that ARs of buses as well as passengers are constant for the analysis period [13]. Also, the values of empirical factors (N_{el} , f_{tb} , etc.) are derived from a few case studies. As wide variety of bus operations and passenger–bus interaction exist, the results based on these empirical factors might be misleading. Furthermore, a clear definition of the failure rate is missing. Fernandez and Planzer [13] reported that the TCQSM model under predicts the capacity
IRENE simulation model [12]	$\frac{3600n}{s+t_b}$	n represents the average number of buses that can enter the stop area, s is the bus lane saturation flow (bus/s) and t_b is the average duration for which the last birth is blocked (s)	Limited flexibility to choose bus arrivals and passenger flows. Particularly, only two types of bus arrivals are present, namely fixed and negative exponential
PASSION simulation model [3]	$\frac{3600N_b}{t_c+\sum_{i=1}^{N_b}(t_{pi}+t_{ei})}$	N_b represents the number of buses in the simulation, t_c is the constant clearance time, t_{pi} is the passenger service time of the i th bus (s) and t_{ei} is the extra delay for the i th bus (s)	This model caters for various interactions present at the bus stop. The data required for input and to calibrate make the implementation of this model difficult [14]

3 Methodology

Before detailing the methodology, it is important to define bus ARs. The AR in this study is defined as the rate with which buses will arrive at the bus stop if there is no queue at the bus stop. For example, if the AR is 5 min, then the buses arrive 5 min apart.

3.1 Simulation Model Development

A microscopic single bus lane simulation model is developed in AIMSUN 6.1 [15]. AIMSUN has been successfully used previously for evaluating bus lane capacity [2].

The geometric configuration of the model and a 3-D visualisation are presented in Fig. 1. As follows from the figure, the bus lane constitutes of an on-line bus stop with single loading area. Other features of the simulation model are presented in Table 2.

Simulation 1

In the first simulation, the mean AR is varied from 1 to 5 min with a 30 s increment, and the standard deviation of AR is fixed to 30 s. Bus arrivals are assumed to be normally distributed. For each AR (total eight), the simulation is run for one hour, the dwell time was fixed to 120 s, and the passenger boarding time and the alighting time were fixed to 1.2 and 0.8 min, respectively. The opted dwell time, and boarding and alighting time have been observed on the bus stations of Bhopal BRT corridor [7]. Corresponding to each AR, the failure rate, the number of buses in the queue and the total time in queue (TTQ) were calculated from the simulation, and the capacity is evaluated using TCQSM model.

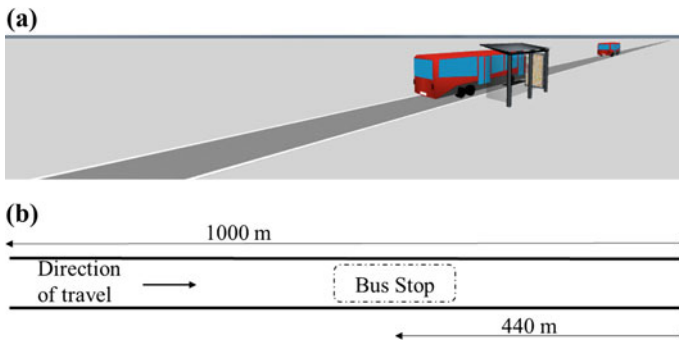


Fig. 1 AIMSUN simulation model. **a** 3-D visualisation of the section near the bus stop; **b** geometric configuration of the bus lane section

Table 2 AIMSUN simulation model characteristics

<i>Schedules</i>	
Initial time	5.00 p.m.
Duration	1 h
Departure times	Interval ^a (Punctual)
Departure distribution	Normal
<i>Bus static features</i>	
Length	12 m
Width	2.5 m
<i>Bus dynamic features</i>	
Mean maximum acceleration	1.00 m/s ²
Mean normal deceleration	2.00 m/s ²
Mean maximum desired speed	90 km/h
<i>Driver behaviour</i>	
Car-following model	Modified Gipps' model
Reaction time	0.8 s
Reaction time at stop	1.3 s

^aInterval governs the AR

The TTQ is defined as the total time spent by all the buses in the queue at the bus stop. The mathematical formulation of TTQ is given by Eq. (1):

$$TTQ = \sum_{i=1}^n t_i \quad (1)$$

where i is the bus number according to their entry in the simulation ($i = 1, 2, 3, \dots, n$), n is the bus number representing the last bus in the simulation, and t_i is the time spent by the i th bus in the queue at the bus stop.

Simulation 2

The second simulation is performed with the objective of inspecting the impact of dwell time on bus lane capacity for a fixed AR. This is to mimic the scenario when an AR is fixed for the buses running on a bus lane and the passenger flow has changed over the months. Four simulation runs are carried out each with a different dwell time value. The dwell times employed are 120, 50, 40, and 30 s, and the fixed AR is 1.5 min. Similar to the simulation 1, the failure rate, the number of buses in the queue, and the TTQ are calculated from the simulation; the capacity is evaluated using TCQSM model. The factors impacting the AR, for example, passenger demand, are out of the scope of this paper and the considered mean AR can be assumed as fixed by the relevant public transit agency after considering all the factors.

4 Results and Discussion

Figure 2 depicts the trajectories of buses for all the eight ARs. Although the trajectory plots have been utilised in traffic flow modelling from decades, these are rarely preferred in demonstrating the bus operations. Evidently, from the figure, the trajectory plots are an effective way to describe where the bus has stopped, the location of the bus stop, the queue at the bus stop, and the total travel time of the bus.

From Fig. 2, it is straightforward to observe that AR of 1 min resulted in long queues. As expected, the queue length decreases as AR decreases (moving from AR 1 min to AR 5 min).

The estimated capacity and other results are presented in Table 3. The largest capacity achieved is 49 buses/h, and this capacity corresponds to the ARs of 1 and 1.5 min. Moreover, for the AR of 1 min, the TTQ is the largest. These two findings are important from the bus scheduling viewpoint. For example, the practitioners can opt for an AR of 1.5 min which leads to a substantial reduction in TTQ without compromising with the bus lane capacity.

Furthermore, we conclude that for a fixed dwell time, there exists an inflection AR interval below and above which the bus lane capacity is constant. For the presented case, the inflection AR interval is 1.5–2.5 min. Therefore, developing on these findings, an appropriate AR can assist in achieving the desired bus lane capacity.

The results of simulation 2 are summarised in Table 4. As follows from the table, for a fixed AR, the TTQ and the failure rate increases if the dwell time increases. The highest bus lane capacity observed is 65 buses/h for a dwell time of 30 s. To

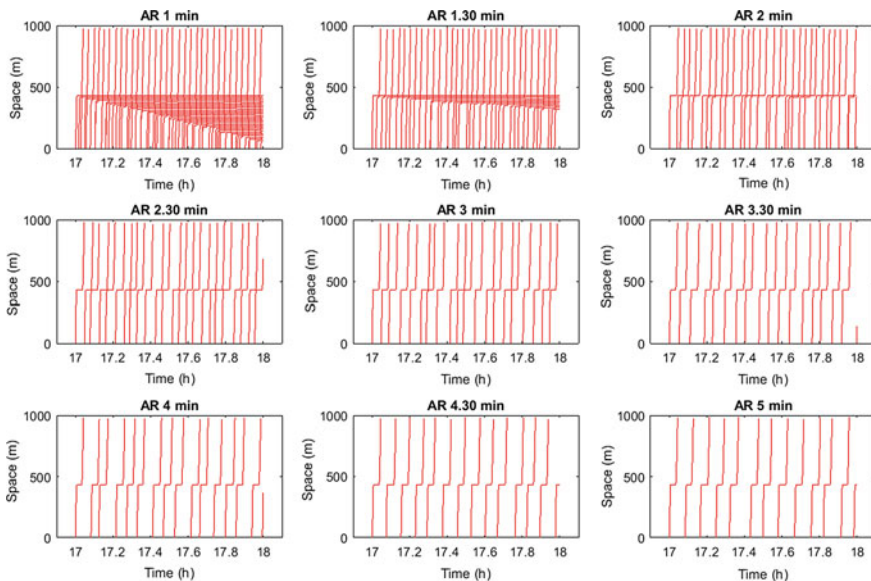


Fig. 2 Space–time variation of the buses during the simulation period corresponding to each AR

Table 3 Simulation 1 results and the bus lane capacity values for each AR

AR (min)	Failure rate (%)	Number of buses in simulation	TTQ (h)	Bus lane capacity (buses/h)
1	>100	60	10	49
1.5	>100	40	3.9	49
2	20	31	0.2	30
2.5	0	24	0.0	25
3	0	20	0.0	25
3.5	0	18	0.0	25
4	0	16	0.0	25
4.5	0	14	0.0	25
5	0	13	0.0	25

Table 4 Simulation 2 results and the bus lane capacity values corresponding to the dwell times

Dwell time (s)	Failure rate (%)	Number of buses in simulation	TTQ (h)	Bus lane capacity (buses/h)
100	>100	60	10	49
50	100	60	2	49
40	19	60	0.2	59
30	12	61	0.1	65

highlight the importance of this simulation, consider a situation where the AR of buses is fixed for a bus lane by taking into account the existing dwell time.

Over the period, if this dwell time increases, the fixed AR will not serve the purpose and will result in lower bus lane capacity values. Thus, before fixing an AR for a bus lane, the changes in dwell time or the dwell time pattern over the months shall be considered.

Above-mentioned findings unfold the need for passenger demand-dependent AR which can ensure a lower TTQ and a higher bus lane capacity.

5 Conclusion and Future Work

This study investigates the impact of AR on bus lane capacity. To achieve this, a simulation model is developed in AIMSUN 6.1, and two simulation experiments are performed. The first simulation experiment attempts to analyse how bus lane capacity changes with a change in bus AR. On the other hand, the focus of the second simulation experiment is to analyse how changes in the passenger flows (reflected by the change in dwell time) impact the bus lane capacity for a fixed AR. The results of the first experiment reveal that for a fixed dwell time at a bus stop,

lower AR (moving from 1 to 5 min) leads to lower delays at the bus stop but at the cost of reducing the bus lane capacity. Moreover, for a fixed AR, if the dwell time increases, bus lane capacity decreases as demonstrated by the results of the second experiment. Based on these findings, a passenger demand-dependent AR can serve the purpose of maximising the bus lane capacity and minimising the delays in the queue. Also, from the practitioners and policymakers viewpoint, a particular AR shall be judiciously selected keeping in mind the possible changes in the dwell time over a long-time period.

Furthermore, estimating bus lane capacity of BRTS is imperative for decision-makers and planners. The main reason is to determine the state beyond which the capacity cannot be increased further without making design changes in the bus lane. This study showcases (by pointing out the limitations of the existing models) the need for reliable, robust and realistic capacity estimation models which are capable of incorporating a wide variety of stochasticity present on the bus lane. For example, stochastic passenger flow, the number of loading areas, bus ARs, etc. From the modelling perspective, simulation models can simulate a wide variety of scenarios and therefore they have an edge over simplified mathematical models. However, the mathematical models present at the core of the simulation packages still require improvements.

Understanding different factors impacting AR and thereby bus lane capacity could provide valuable insights. This is a topic of future research.

Acknowledgements The authors would like to thank Dr. Ashish Bhaskar for his support in developing the simulation model, and anonymous reviewers for insightful and constructive comments.

References

1. National Academies of Sciences E (2013) Transit capacity and quality of service manual, 3rd edn
2. Widanapathirana R, Bunker JM, Bhaskar A (2015) Modelling the BRT station capacity and queuing for all stopping busway operation. *Public Transp* 7:21–38
3. Fernandez R (2001) A new approach to bus stop modelling. *Traffic Eng Control* 42:240–246
4. Szasz PÁ, de Carvalho Montans L, Ferreira EO (1978) COMONOR: ordained bus convoy. *Companhia de Engenharia de Tráfego*
5. Ortiz MÁ, Bocarejo JP (2014) Transmilenio BRT capacity determination using a microsimulation model in VISSIM. Presented at the transportation research board 93rd annual meeting of transportation research board, National Academics, Washington, DC
6. Siddique A, Khan A (2006) Microscopic simulation approach to capacity analysis of bus rapid transit corridors. *J Public Transp* 9
7. Sharma A, Parida M, Sekhar CR, Katheria A (2015) Capacity analysis of Bhopal BRTS using empirical and simulation model. *J East Asia Soc Transp Stud* 11:1575–1593
8. Hsu T-P, Lu C-T (1999) Bus lane capacity—a revised approach. *J East Asia Soc Transp Stud* 3:381–395
9. Gu W, Li Y, Cassidy MJ, Griswold JB (2011) On the capacity of isolated, curbside bus stops. *Transp Res Part B Methodol* 45:714–723

10. Jaiswal S, Bunker J, Ferreira L (2010) Influence of platform walking on BRT station bus dwell time estimation: Australian analysis. *J Transp Eng* 136:1173–1179
11. Gibson J (1996) Effects of a downstream signalised junction on the capacity of a multiple berth bus-stop. Presented at the traffic management and road safety. In: Proceedings of seminar held at the 24th European transport forum, vol P407, Brunel University, England, 2–6 Sept 1996
12. Gibson J, Baeza I, Willumsen L (1989) Bus-stops, congestion and congested bus-stops. *Traffic Eng Control* 30
13. Fernandez R, Planzer R (2002) On the capacity of bus transit systems. *Transp Rev* 22:267–293
14. Reilly J, Aros-Vera F (2013) Estimating capacity of high volume bus rapid transit stations. Presented at the 92nd annual meeting of transportation research board, National Academics, Washington, DC
15. TSS (2010) AIMSUN 6.1 microsimulator and mesosimulator user's manual

A Local level Transit-Oriented Development Typology: Using Two-Step Clustering Technique



Prashanth Shekar Lokku, C. S. R. K. Prasad and K. Bala Krishna

Abstract Transit-oriented development (TOD) is regarded as mixed land uses within the half-mile radius around the transit stations with high-density development, pedestrian-friendly environment and well-connected road network with frequent public transportation system. TOD typology is a way grouping different TODs having a common set of features. The TOD typology will help local practitioners, decision-makers, and officials understand the assets and vulnerabilities, and how each transit station area fits within the regional context. No one-size-fits-all, like different implementation strategies, are needed for different place types. TOD typology offers a strategic planning of transportation combination with land use and enables comparisons and performance assessments within the station classes. The study is based on the wide parameters namely built environmental, network parameters, and different transport centers that help in understanding the TOD area characteristics to the greater extent. The two-step clustering technique is adapted to develop typology of 20 TODs of Hi-tech city and its surrounding area into six clusters. The study will try to make an attempt of recommendations and time-bound implementation strategies for the TOD clusters.

P. S. Lokku (✉) · C. S. R. K. Prasad · K. Bala Krishna
National Institute of Technology Warangal, Warangal, India
e-mail: lps.lokku@gmail.com

C. S. R. K. Prasad
e-mail: csr@nitw.ac.in

K. Bala Krishna
e-mail: kpbkce@gmail.com

Keywords Transit-oriented development · TOD · Clustering technique · Implementation strategies

1 Introduction

1.1 TOD

TOD is a concept of urban planning which deals with transit corridor and its influential area, which has physiognomies of mixed land use, compactness, walking distance, and development focused around public transit area. TOD is usually demarcated as compactness, diverse land use near existing or new transit station that makes provisions of residence, employment, recreation, and civic amenities within walking distance. The impartial of TOD is to maximize travel demand to public transport and assimilate arrangements to encourage transit ridership.

A TOD area characteristically has a center also called node, may be transit station, metro station, tram stop, or bus stop fenced by comparatively high-density development with gradually lower-density development unfold from the center. TODs usually located within a radius of 400–800 m from a transit node, as this is appraised to be an apt scale for pedestrians, thus solving the last mile problem. TOD is the contemporary fast-growing trend in creating livable, vibrant, and sustainable communities. This makes the people to live in pleasant conditions with respect to transport facility such that dependence of private mode can be reduced on mobility grounds [1].

As TOD ensures integration of land use and transport planning and also aims to prosper strategic sustainable urban centers to have healthy and civilized communities with high-density mixed land use development. People will also have open green and public spaces with great access along with transit system connectivity. TOD enhances trips with various purposes say shopping, entertainment, and work. To achieve successful TOD, strategies and policies are to be made at initial stages. For better understanding of TOD and its elements Fig. 1 is presented, which may help to plan, design, and enforcement measures for success story of TOD [2].

1.2 TOD Influence Zone

TOD Influence zone is known to be an area which gets affected by activities are happening because of Transit node (Metro station, MMTS, BRTS, City Bus, or LRT) and new infrastructure developments. As TOD is mainly depending on walkability, it is generally up to a radius of nearly 500–800 m (10–12 min of walk) of the transit node. When the distance between the two successive transit nodes is less than 1 km, then there will be an overlap in the influence area, and it can be identified as a delineated zone (around 500 m) on either side of transit corridor. Center for Transit



Fig. 1 Key components of transit-oriented development. *Source* National TOD Policy Report [2]

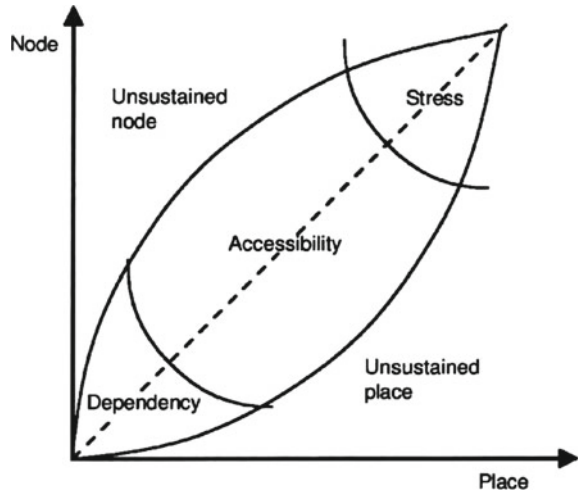
Oriented Development classifies TOD influence area into three categories. First one is core: Up to 200 m, second one is primary walking catchments distance between 200 and 400 m, and third one is secondary walking catchments covers distance between 400 and 800 m [3].

1.3 Balance Between Transit Node and Place

This is an analytical framework to designate transport (node) and urban development (place), characteristics of location, and their relationships. Five typical situations proposed, those are named as balance, stress, dependency, unsustainable nodes, and unsustainable places. A balance situation offers better positive impacts on development. The schematic frame work is shown in Fig. 2. The description of each node–place type in detail as following [4].

- **Balance Condition** is observed to be both node and place are equally have the potential for development.
- **Stress Condition** is observed to be potential for land use development (Strong Node) and transport (Strong Place) are high.

Fig. 2 Node–place relationship. *Source* Bertolini [4]



- **Dependency Condition** is observed to be demand for both node and place are insufficient to generate an autonomous development dynamics.
- **Unsustained Nodes Condition** is observed that where node (transportation facilities) is strong in terms of development than place (urban activities).
- **Unsustained Places Condition** is observed that where place (urban activities) is much more developed than the node (transportation facilities).

1.4 Purpose of TOD Typology

Purpose of TOD typology is to reduce operational and management complication for planners or organizations by permitting the application of standards in operation and development, and ensuring achievements. Typology also provides a framework for understanding what types of implementation strategies are needed in city transit station areas [5]. Each station area has its own set of implementation needs, and the typology offers a basic framework for prioritization and understanding these needs at a glance. Typology provides information of station area's economic potential, and road map of funding and implementation of development activities. Typology enables judgements and performance assessments within the station classes, and realizing successful standards or emphasizing desires for action [6, 7].

1.5 Goals of TOD Typology

The set of goals of the TOD Typology are:

- It should brief the story of transit station communities.
- Identify station areas, which are potentially vulnerable to displacement pressures.

- Identify areas where the production and preservation of affordable housing are needed.
- Understanding of TOD interventions needed for equitable TOD.
- Catalyze TOD in communities where the markets are primed to respond to TOD investments.
- Identify where and what types of infrastructure improvements are needed to support equitable TOD.
- It should specify the investment and return policy on the time scale in the TOD clusters.
- It should brief the clusters of greatest economic potential, and how certain activities can be funded and implemented.

2 Need for the Study

Various aspects such as need, characteristics of TOD, factors driving toward TOD, and key components of TOD are understood. Though TOD concept is not a new one in international context, coming to Indian context proposals are initiating for development/redevelopment in long-term strategies. However, implementation of TOD principles in Indian cities will boost the smart urban areas. The Government of India also started necessary steps for TOD approach implementation in Indian cities and formulated National Transit Oriented Development Policy recently. Thus, it is understood that in nearby TOD concept will enter in Indian cities also. The present study transit-oriented development typology, i.e., clustering of TOD areas based on similarities of characteristics will offer flexibility of understanding on a macro-level and enhance the planning, design, and operational activities. Typology supports the identification of general development potentials and necessary future adoptions [8]. The study tries to give the desired densities, mix of land uses, connectivity levels, and functions of transit system and therefore, the present study TOD typology supports the design of an optimal TOD at a given site. The study will reduce the management complexity for infrastructure companies, town planning authorities by enabling the application of standards in development and operations, and securing consistency of actions across large portfolios and geographic regions.

3 Clustering Technique

The various popular clustering techniques are present like hierarchical agglomerative clustering, *K*-means clustering, fuzzy *C*-means clustering, and two-step clustering technique. In this study, two-step clustering technique is chosen to do the analysis.

3.1 Two-Step Clustering Technique

The SPSS two-step clustering component is a scalable cluster analysis algorithm. It can be handled both continuous and categorical variable, as it needs only one data pass in the process. The analysis is done in two stages. In the first stage of the process, all the data have to be pre-clustered in such a way that it goes into many small sub-clusters. Then, clustering is performed based on the sub-clusters from the pre-cluster stage into the anticipated or pre-defined number of clusters. The SPSS two-step cluster component is used to find the proper number of clusters and the results were gathered from running a simulation, which are steadily accurate and scalable in recital. The simulation also displays that the automatic process of finding the number of clusters mechanism remarkably well and fast. The two-step clustering assures and can evident that a similar group of characteristics are grouped for considering to next level analysis of the study.

4 Study Area

Hi-Tech city, Madhapur area, is one of the leading information technology, engineering, health informatics, and bioinformatics hubs of India situated in Hyderabad, Telangana. Cyber Towers, L&T Infocity, HICC, Mindspace IT Park, Ascendas IT Park, RMZ Futura IT Park, Tech Mahindra Campuses, Microsoft Hyderabad Campus, Facebook Hyderabad, The TCS Deccan Park Campus, IIIT Hyderabad, Hardware Park, etc. offices are in this area. The area has emerged as a symbolic heart of Cosmopolitan Hyderabad. The study area comprises of varieties of transportation facilities, such as city bus, MMTS, and metro rail under construction. Thus, the area has diversity of transit services which enables generation of multiple TODs with variety of nodes in the area. The Hi-tech city and its surrounding area of 45.73 km² is considered for study analysis (Fig. 3).

Figure 4 shows 20 TODs considered for clustering process. In which 13 TODs are falling on metro line, five TODs are of City bus oriented and two are of local MMTS station's one.

5 Indexing and Analysis

Primary and secondary data are collected for this study. Primary data collected from the field are detailed land use and detailed road inventory. Secondary data collected from the Hyderabad Metropolitan Development Authority (HMDA) like population and employment details, etc. Parameters finalized to do analysis are NMT facility indicator (NMTI), floor space index (FSI) [9], land use mix index (MI), open land

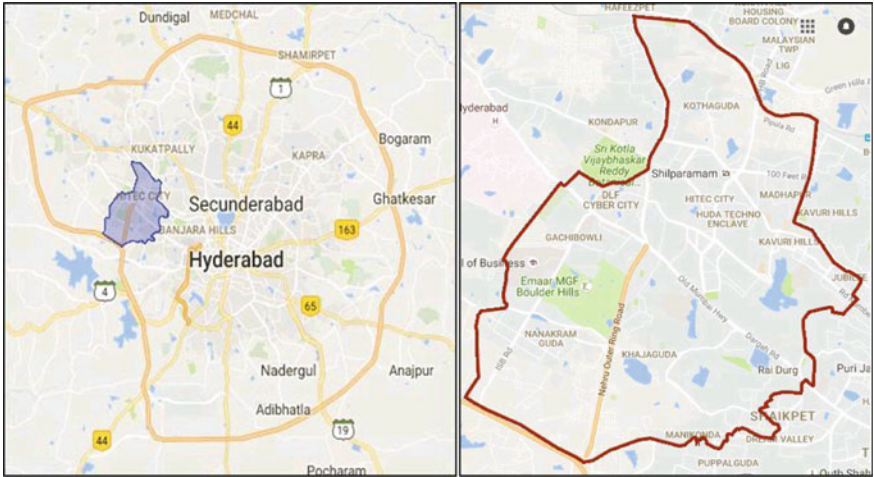


Fig. 3 Hi-Tech city and its surrounding area

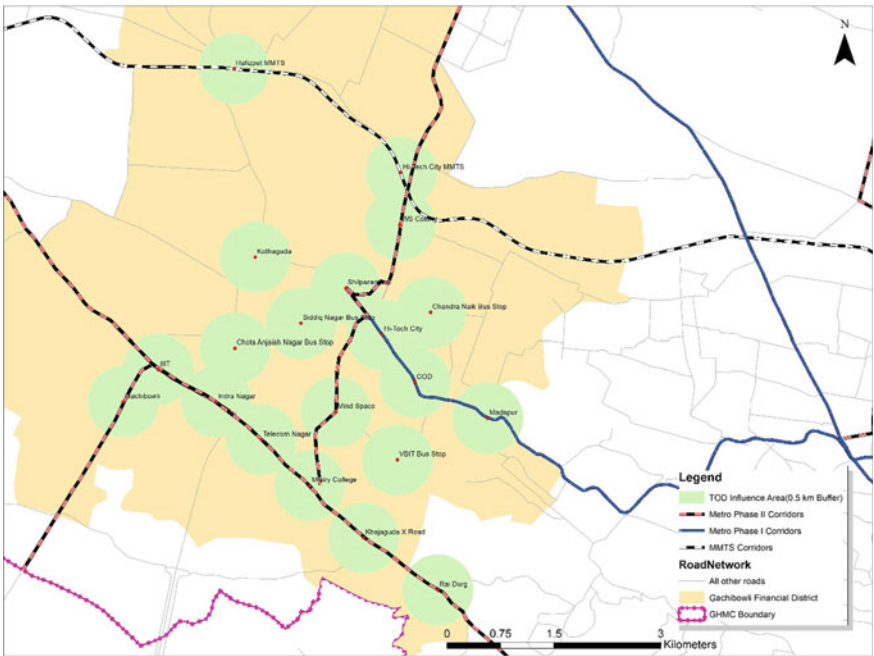


Fig. 4 TODs in study area

Table 1 List of TODs with data

TOD ID	TOD name	NMTI	FSI	MI	OI	TI
1	Madhapur Metro Station	0.08	2.05	0.76	0.38	0.25
2	COD Metro Station	0.00	2.02	0.66	0.27	0.20
3	Hi-Tec City Metro Station	0.25	2.75	0.77	0.39	0.15
4	Shilparamam Metro Station	0.28	2.49	0.76	0.73	0.11
5	WS Colony Metro Station	0.65	1.49	0.67	0.91	0.10
6	Mind Space Metro Station	0.27	3.21	0.49	0.42	0.17
7	Gachibowli Metro Station	0.35	2.02	0.44	0.64	0.12
8	IIIT Metro Station	0.25	2.12	0.73	0.35	0.14
9	Indra Nagar Metro Station	0.00	2.16	0.46	0.34	0.25
10	Telecom Nagar Metro Station	0.10	2.33	0.63	0.48	0.13
11	Mistry College Metro Station	0.05	2.93	0.54	0.40	0.18
12	Khajaguda X Road Metro Station	0.00	1.37	0.47	0.73	0.12
13	Raidurgam Metro Station	0.00	1.29	0.50	0.53	0.09
14	VBIT Bus Stop	0.16	4.65	0.53	0.40	0.10
15	Siddiq Nagar Bus Stop	0.18	2.32	0.60	0.20	0.16
16	Chota Anjaiah Nagar Bus Stop	0.06	2.58	0.59	0.33	0.22
17	Chandra Naik Bus Stop	0.07	2.15	0.60	0.39	0.23
18	Kothaguda Bus Stop	0.04	3.27	0.52	0.41	0.15
19	Hi-Tec City MMTS Station	0.11	1.63	0.56	0.58	0.32
20	Hafeezpet MMTS Station	0.05	1.06	0.49	0.21	0.26

availability index (OI), and transport land index (TI). Table 1 shows the final input data for two-step clustering procedure.

5.1 Indexing

Non-Motorized Transport Index (NMTI) is calculated based on road network inventory survey conducted. The total length of the footpaths and bicycles path available in TOD influence zone is considered and normalized the value to 0–1. The highest value represents more NMT facility exist in that location

Floor Space Index (FSI) is calculated based on the detailed land use survey done. It is the ratio of the total floor area of buildings to the total land area.

Mixed Index (MI) is given by a quantized description of the land use mixing. Land use mix is a heterogeneity index, ranging from 0 to 1, where zero represents the single land use and 1 represents the maximally mixed use. In the present context, six land use types are considered based on the observations from field survey (detailed land use

survey). Those are residential, commercial, office, mixed, public and semi-public, and institutional land uses.

Open land availability Index (OI) Area available with no development is considered to calculate this parameter. And it is normalized to 0–1. The values are from field investigation survey.

Transport land Index (TI) Total length of the road network present in the influence area multiply with the right of way will be the area cover under transportation. The proportion of the transport area to the total TOD area will be the TI. The obtained values are normalized to get an index that is in between 0 and 1.

5.2 Clustering

SPSS software is used for clustering. The output obtained is as given in Table 2. Totally, six numbers of clusters are formed based on given five parameters, in which four clusters are of equal share of having 20% of TODs and two clusters are of 10% each.

Fig. 5 shows that, how each variable is influenced with in the cluster in terms of percentage is presented.

Table 3 shows that final list of clusters along with the list of TODs. A total of six clusters are formed with similar characteristics. This typology data are also used for immediate understanding of lack in design facilities and to set the benchmarks for the future reference.

Table 2 Cluster distribution: Grouping of TODs

Cluster distribution			
Cluster	No. of TODs	% of combined	% of total
1	4	20.00	20.00
2	4	20.00	20.00
3	4	20.00	20.00
4	2	10.00	10.00
5	4	20.00	20.00
6	2	10.00	10.00
Combined	20	100.00	100.00
Total	20		100.00

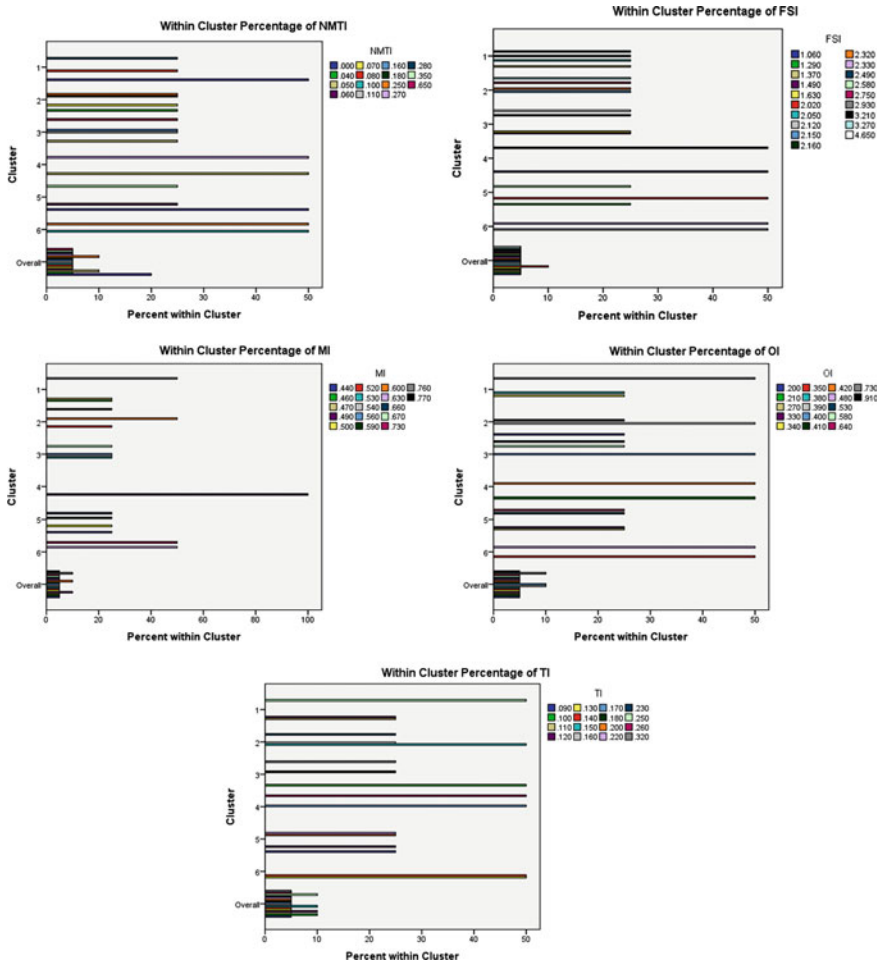


Fig. 5 Showing percentages of each variable within cluster

6 Conclusions

Transit-oriented development typology provides a framework for understanding what types of implementation strategies are needed, and for prioritization and understanding of these needs at a glance. It is observed that there are no specific parameters for deriving typology in an area on universal acceptance. Different authors of different countries considered different parameters for their studies based on the context. However, the more number of relevant parameters results in the completeness of TOD typology.

20 TOD areas are identified on the diversity of transit nodes such as City Bus Stops, Metro Stations, MMTS Stations in Gachibowli Financial District. The success

Table 3 List of TODs with proposed typology

Clusters	TOD ID	TOD name
C-1	1	Madhapur Metro Station
	4	Shilparamam Metro Station
	9	Indra Nagar Metro Station
	12	Khajaguda X Road Metro Station
C-2	3	Hi-Tec City Metro Station
	15	Siddiq Nagar Bus Stop
	17	Chandra Naik Bus Stop
	18	Kothaguda Bus Stop
C-3	5	WS Colony Metro Station
	11	Mistry College Metro Station
	14	VBIT Bus Stop
	19	Hi-Tec City MMTS Station
C-4	6	Mind Space Metro Station
	20	Hafeezpet MMTS Station
C-5	2	COD Metro Station
	7	Gachibowli Metro Station
	13	Raidurgam Metro Station
	16	Chota Anjaiah Nagar Bus Stop
C-6	8	IIT Metro Station
	10	Telecom Nagar Metro Station

of any TOD depends on the balance between node and place. In the present study, parameters of node, built environmental and network parameters are considered. The Hi-tech city and its influence area are rapidly developing areas having compact development, lot of employment, and observed vast vacant land is available in and around. Hence, a proper co-ordination measures result in compact, mixed land use development in a short time.

For deriving the typology, five indices were developed, those are NMT facility indicator (NMTI), floor space index (FSI), land use mix index (MI), open land availability index (OI), and transport land index (TI). Two-step clustering technique is used for clustering of these 20 TODs resulted in formation of six clusters such as C-1, C-2, C-3, C-4, C-5, and C-6.

References

1. Austin M, Belzer D, Sam Z, Lyman A (2010) Performance-based transit-oriented development typology guidebook. Center for TOD, California
2. National Transit Oriented Development Policy (2017) Ministry of Urban Development, New Delhi, 8 May 2017

3. Guidelines and development control norms for MRTS influence zone for TOD: UTTIPEC report 2012, Delhi Development Authority, New Delhi
4. Bertolini L (1999) Spatial development patterns and public transport: the application of an analytical model in the Netherlands. *Plan Pract Res* 14(2):199–210
5. Kamruzzaman M, Baker D, Simon W, Turrell G (2014) Advance transit oriented development typology: case study in Brisbane, Australia. *J Transp Geogr* 34:54–70
6. Transit oriented development best practices handbook 2004. Calgary Land Use Planning and Policy, Calgary
7. Transit oriented development guidelines 2003. Bay Area Rapid Transport, San Francisco
8. Zemp S, Stauffacher M, Lang DJ, Scholz RW (2011) Classifying railway stations for strategic transport and land use planning: context matters! *J Transp Geogr* 19(4):670–679
9. Floor Space Index (FSI) in Indian Cities. <https://www.slideshare.net/GRealtech/floor-space-index-fsi-in-indian-cities>, 3 May 2017

Assessment of Induced Fuzziness in Passenger's Perspective of Transit Service Quality: A Sustainable Approach for Indian Transit Scenario



Suprava Jena, Hetsav Dholawala, Mahabir Panda and P. K. Bhuyan

Abstract Passengers form the most important stake-holding body in public transit services. This study deals with the complexity of assessing transit service quality by identifying attributes affecting passenger's satisfaction. An innovative questionnaire was designed by taking passengers' demographic information and a wide spectrum of attributes related to operating conditions of two bus rapid transit systems (BRTS), i.e., Janmarg (Ahmedabad city) and Sitalink (Surat city) in the state of Gujarat. Total 23 variables are extracted using factor analysis with a Kaiser-Meyer-Olkin (KMO) value of 0.63 to conclude that the sample size is adequate enough for the model. These variables are grouped into six principal components and changed over to fuzzy sets with three membership functions each to map the fuzziness and ambiguity in passengers' perception. The complications of generating $3^6 = 729$ number of fuzzy rules are solved by introducing a hierarchical fuzzy inference system (FIS) with two lower-level FIS and one higher-level FIS. The first lower FIS consists of "accessibility," "service provisions," and "reliability" as fuzzy input variables to get "availability" as an output variable. The second lower FIS contains "safety and security," "fare," and "comfort" as input parameters to produce "comfort and convenience" as an output variable. The resulting fuzzy values are used in higher-level FIS and defuzzified to evaluate the satisfaction level of passengers by max-min composition technique. This method will help in improving existing transit facilities and devising strategies for ensuring sustainability.

Keywords Transit service quality · Perception survey · Factor analysis · Fuzzy inference system · Membership functions

S. Jena (✉) · H. Dholawala · M. Panda · P. K. Bhuyan
Department of Civil Engineering, National Institute of Technology Rourkela, Rourkela 769008, India

e-mail: suprava728@gmail.com

H. Dholawala

e-mail: hetsavddholawala@gmail.com

M. Panda

e-mail: mpanda@nitrrkl.ac.in

P. K. Bhuyan

e-mail: pkbtrans@gmail.com

© Springer Nature Singapore Pte Ltd. 2020

T. V. Mathew et al. (eds.), *Transportation Research*, Lecture Notes in Civil Engineering 45, https://doi.org/10.1007/978-981-32-9042-6_5

1 Introduction

At present, managing the road networks has been dreadfully challenging as demand increases and resources are limited. This often results in unruly traffic growth and congestion in the flow of traffic. If a city is properly planned and organized, public transits can fulfil up to 90% of the mobility requirements generated by private automobiles. This modal shift toward public transit can effectively reduce the use of private vehicles and lead to decongestion of streets, high mobility, time-saving, and better quality of life. However, public transportation systems in India are plagued by congested and overcrowded roadways operating under a chaotic environment. So, there is a bare need for improving the serviceability of public transportation system to reassure the travelers for modal shift, which can exemplify a step toward improving the environment. Many researchers have estimated the service quality offered by public transit system from varying perspectives. However, passengers form the most important stake-holding body in public transit services, and therefore, the complexity of transit service quality should be assessed from its user's perspective. Transit service quality is associated with a wide spectrum of attributes such as spatial coverage, service period, frequency, stop/station access, fare, speed, reliability, on-board comfort, safety, and security. Ensuring sustainability of transit service forms an important aspect, which directly depends upon upholding the existing users and attracting new users. Along with that, the choice of strategies should be made carefully to attain cost-effective implementations. The proposed research focusses on two aspects, such as (i) identifying influential attributes affecting passenger's satisfaction for existing transit services in developing countries and (ii) developing a suitable method for the evaluation of transit service quality, which will help in improving existing facilities and devising strategies for ensuring sustainability.

Some research work has been carried out for the determination of Transit service quality, taking passengers' perceptions of service quality. Morfoulaki et al. [1] studied the relationship between the service quality and the probability of customer being satisfied. Fu and Xin [2] proposed a new service quality index called transit service index (TSI), taking spatial and temporal variations in travel demand of a transit system. Dowling et al. [3] developed a new methodology for transit level of service (LOS) considering the transit to be internally dependent upon other modes of travel and pedestrian LOS. Tyrinopoulos and Antoniou [4] authors demonstrated a well-coordinated transportation environment to be the primary aim of the policy-makers in Athens, followed by other quality attributes. Eboli and Mazzulla evaluated the transit passenger's point of view using choice-based conjoint analysis. This study found frequency, reliability, cleanliness, and bus stop facilities are the influencing attributes affecting passengers' perception [5]. Dell'olio et al. [6] distinguished the perceived quality and the desired quality in public transportation taking different categories of users and potential users. Awasthi et al. [7] developed a hybrid model using SERVQUAL and Fuzzy TOPSIS for evaluating the service quality of urban transportation systems. Khurshid et al. [8] studied the impact of the transit service quality on male and female customers. The study revealed, males are more driving

conscious and females are highly dissatisfied with the waiting time, cleanliness, security, and seating issues. Mahmood and Hine [9] suggested that the individual analysis of both subjective (perception) and objective (performance) quality presents evidence for transit service quality evaluation. Noor et al. [10] identified that overcrowding and safety during night were among the most significant attributes affecting passengers' satisfaction. Pavlína [11] studied the service quality concept with the aim of quantifying factors and identified loyalty as the most important factors influencing passengers' satisfaction in Czech Republic. In this study, the variety of existing approaches has been justified by integrating the complexity of the service quality concept; the imprecision and subjectivity of the attributes used to analyze it; and the heterogeneity of passenger's perception.

2 Study Methodology

Considering different modeling approaches in the past few decades, a variety of deterministic and stochastic models have been employed to assess the service quality of transportation systems. But those customary techniques might not be effective when the inter-dependencies between variables are too complex. In reality, quantitative assessment of passenger's satisfaction is very intricate and difficult to decode as most of their decisions come off with fuzziness, ambiguity, and imprecision. Hence, an attempt was made in this study to assess the transit service quality using fuzzy logic by mapping the ambiguity of traveler's insight. Yet, the motive behind not taking all the responses composed as input parameters for the decision model as there may be a high correlation between each individual statement. Therefore, the data collected from the questionnaire were framed into uncorrelated set of variables using factor analysis.

2.1 Factor Analysis

Factor analysis is used to compress a large data set to smaller subsets of elements. This exploration is used for (i) understanding the arrangements of variables; (ii) building a questionnaire which processes the underlying variable; and (iii) reducing the data set to a more adaptable size to retain more novel information as possible. The factor analysis undertakes that the rankings of the variables are created by some unnoticed and underlying approaches. The basic formula of the factor analysis is explained by Eq. (1) as follows:

$$X_{ji} = \sum_{k=1}^m (\lambda_{jk} F_{ki}) + \varepsilon_{ji}, \quad (1)$$

where $j = 1, 2, \dots, J$; $i = 1, 2, \dots, N$; X_{ji} symbolizes the score of statement j for participant i ; J signifies the number of statements; N signifies the number of observations; F_{ki} implies the k th factor of participant i ; λ_{jk} (also known as loading) indicates the relation of j th variable with k th common factor; and ε_{ji} signifies the associated error. Equation (1) undertakes J statements, N observations and m factors considered in the model. It is required to be summoned up that factor scores (F_{ki}) were not observed. This exploration calculates both factor scores and respective loadings to make best use of the information maintained from original statements.

KMO and Bartlett's test of sphericity is the main aspect in factor analysis. The KMO statistic is used to quantify sampling adequacy for each variable. KMO values greater than 0.8 is measured as good, i.e., the factor analysis is suitable for the variables. Bartlett's test of sphericity is related to the implication of the study to show the validity and correctness of the collected responses to address the problem. The value of Bartlett's test of sphericity < 0.05 is recommended as a suitable value in factor analysis. Another important aspect mentioned in this study is rotated component matrix to decide the total number of factors that should be analyzed, if a variable is linked to more than one factor. Rotation maximizes high item loadings and minimizes low item loadings to produce a simplified solution. In this study, orthogonal varimax rotation technique is used that produces uncorrelated factor structure. To measure the consistency of a questionnaire, reliability analysis (denoted by Cronbach's alpha) is used.

2.2 Fuzzy Inference System

The human brain interprets imprecise and incomplete sensory information j provided by perceptive organs. Fuzzy sets theory provides a systematic calculus to deal with such information linguistically, and it performs numerical computation by using linguistic labels stipulated by membership functions (MF). Moreover, a selection of fuzzy if-then rules forms the key component of a fuzzy inference system (FIS) that can effectively model human expertise in a specific application. Although the fuzzy inference system has a structured knowledge representation in the forms of fuzzy if-then rules, it lacks the adaptability to deal with changing external environments.

Fuzzy Set Theory

In contrast to a classical set, a fuzzy set, as the name implies, is a set without a crisp boundary. That is, the transition from "belong to a set" to "not belong to a set" is gradual, and this smooth transition is characterized by membership functions that give fuzzy sets flexibility in modeling commonly used linguistic expressions. Such imprecisely defined sets or classes play an important role in human thinking, particularly in the domains of pattern recognition, communication of information, and abstraction. As fuzzy sets have smooth boundaries of transition, a belongingness of a particular value to the fuzzy set is represented by a membership function. A

fuzzy set can be explained mathematically; If X is a collection of objects denoted generically by x , then a fuzzy set A in X is defined as a set of ordered pairs:

$$A = [\{x, \mu A(x) | x \in X\}] \quad (2)$$

where $\mu A(x)$ is called the membership function for the fuzzy set A . The MF maps each element of X to a membership grade between 0 and 1.

Fuzzy Reasoning

Fuzzy reasoning, also known as approximate reasoning, is an inference procedure that derives conclusions from a set of fuzzy if-then rules and known facts. The basic rule of inference in traditional two-valued logic is modus ponens, according to which we can infer the truth of a proposition B from the truth of A and the implication $A \rightarrow B$. Premise 1 (fact): x is A , Premise 2 (rule): if x is A then y is B , Consequence (conclusion): y is B . Where A' is close to A and B' is close to B . When A, B, A', B' are fuzzy sets of approximate universes, the foregoing inference procedure is called approximate reasoning or fuzzy reasoning. The fuzzy membership functions for linguistic variables along with these fuzzy if-then rules compose a framework of fuzzy knowledge base of fuzzy expert system. Imposing any values of the variables, knowledge bases can infer a consequence using expert system.

Defuzzification

The fuzzy inference system can take either fuzzy inputs or crisp inputs, but the outputs it produces are almost always fuzzy sets. Sometimes, it is necessary to have a crisp output. Therefore, defuzzification of the fuzzy sets has to be done so as to achieve a crisp output. With crisp inputs and outputs, a fuzzy inference system implements a nonlinear mapping from input to output space. This mapping is accomplished by a number of fuzzy if-then rules, each of which describes the local behavior of the mapping. In particular, the antecedent of a rule defines a fuzzy region in the input space, while the consequent specifies the output in the fuzzy region.

3 Study Area

To achieve the objective of the proposed research, a perception survey was conducted in two urban agglomerations, i.e., Janmarg (Ahmedabad city) and Sitilink (Surat city) in the state of Gujarat, India, to gather required information on passenger's satisfaction about bus rapid transit systems (BRTS). Figure 1 shows BRTS routes of the two studied cities. The selection of the study area is done on such basis that simulates the urban agglomerations and prevalent conditions, i.e., traffic characteristics of the area to the maximum extent. So that the entire spectrum of operating conditions can be modeled. As in this research, the passengers' satisfaction is considered for assessing the quality of service of public transit which operates on prescribed routes

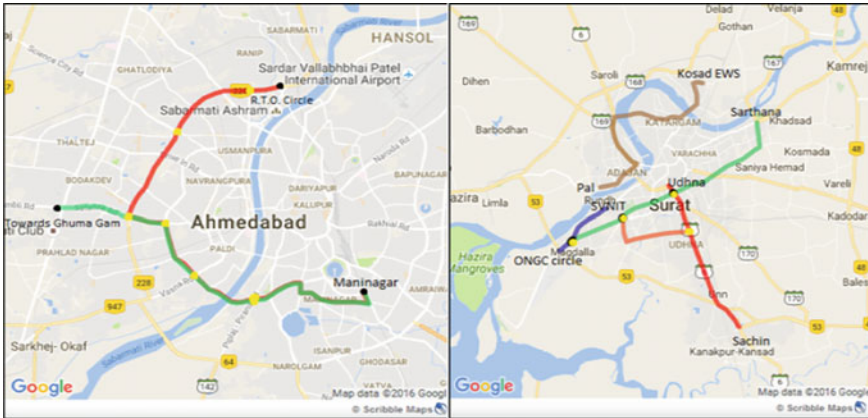


Fig. 1 Map showing study area in Janmarg BRTS and Sitilink BRTS, respectively

and on fixed schedule, e.g., in Janmarg BRT, the routes from Maninagar to Ghuma Gam and from Maninagar to Chandkheda were found to be in utmost demand. Apart from being the most important routes in the network, these routes incorporate most number of transfer points. Hence, it can be assumed that on these transfer points, passengers from the farthest ends of the networks are present.

4 Data Collection

An innovative questionnaire was designed by taking sets of operating conditions of BRTS at bus stops, routes, and at network levels as shown in Table 1. The whole questionnaire was divided into two subsections. The first section was about the respondents' personal profile, e.g., age, gender, purpose of travel, trip origin-destination, etc. The second part consists of 19 quality of service attributes those might have significant influence on passenger's satisfaction level, e.g., mode of access, ease of access, cleanliness, fare structure, service coverage, etc. The survey forms were distributed among the participants at important pick-up bus stops and inside the buses. The participants were asked to rate each service attribute and the overall satisfaction (OS) on a Likert scale ranging from "1" (highly dissatisfied) to "5" (highly satisfied). For better understanding of participants, the technical terminologies were explained in regional languages. Nearly 320 participants were interviewed while waiting at bus stops or traveling by bus. The diversity in demographic and socio-economic variables during data collection from different locations showed a strong potential of data sets to model transit service quality.

Table 1 Synopsis of variables and the measuring units

Variables	Units of measurement			
Gender	Male		Female	
Age	15–25	26–40	41–55	>55
Trip purpose	Work	Business	Education	Recreation
	Likert scales (1–5)			
Accessibility	Walking	Bicycle	Auto	Any Other
Transit frequency	5–10 min	10–30 min	30–60 min	>1 h
Parking provision	Present		Absent	
Transit availability, ease in access, bus stop nearness, in bus time, transfers, fare structure, fare collection, reliability, seating/standing, boarding/alighting, door width, cleanliness, lighting conditions, personnel behavior, comfort, accidents/breakdowns, and safety and security				Likert scales (1–5)
Overall satisfaction	Likert scales (1–5)			

5 Result and Discussion

This section provides a detailed discussion about factor analysis to decide the input variables and application of fuzzy logic for the model development process. The prediction performance of the input parameters was also assessed in terms of several statistical parameters.

5.1 Factor Analysis

Factor analysis was carried out on the 23 statements with varimax rotation (orthogonal). The analysis starts by testing the validity of the data analysis with the help of Kaiser-Meyer-Olkin (KMO) and Bartlett's test of sphericity.

The test is proposed to find out whether all the examined data are adequate to be factored analysis. Factor is suitable if KMO value is greater than 0.60. With the KMO value 0.631 for the collected data, it shows that the data do not have a multi-collinearity problem and the suitable items are appropriate to test its factor analysis. Bartlett's test of sphericity is used to recognize that the correlation among the items is adequate for factor analysis.

The factor analysis is implemented using principal component analysis and varimax rotation with the objective to test the underlying factor structure of the data. Total five items with a factor loading smaller than 0.50 were discarded and items that cross-loaded too. Table 2 contains the rotated factor loadings, which signify both weighted variables and the correlation between the variables and the factor. Firstly, to reduce the multi-collinearity among the input variables, factor analysis was conducted over the collected responses. Total 18 variables were found to be significant,

Table 2 Rotated component matrix

Component	1	2	3	4	5	6	7
Gender	-0.045	-0.620	0.162	0.137	0.103	0.318	-0.232
Trip purpose	-0.062	-0.173	-0.065	0.339	-0.028	0.669	-0.061
Age	-0.129	-0.074	-0.048	0.031	-0.063	-0.685	-0.038
Temporal availability	-0.033	0.622	-0.041	0.106	-0.169	-0.096	-0.221
Spatial availability	0.419	-0.193	0.068	-0.019	0.569	-0.031	-0.230
Ease in access	-0.876	-0.073	0.144	0.023	-0.007	-0.091	-0.001
Mode of access	0.689	-0.179	-0.088	0.035	0.005	0.093	0.123
Parking	-0.015	0.620	0.251	-0.259	0.107	0.155	-0.188
Bus stop nearness	0.897	0.000	-0.108	-0.045	-0.081	-0.037	0.006
In bus time	-0.283	-0.101	0.694	-0.049	0.187	-0.071	0.170
Transfers	-0.097	-0.111	0.479	0.106	-0.051	-0.489	-0.055
Fare structure	-0.027	-0.121	-0.085	0.003	0.570	0.390	0.208
Fare collection	0.010	0.082	0.147	0.297	0.470	-0.012	0.405
Reliability	-0.116	0.407	0.617	-0.038	-0.152	0.110	-0.234
Seating/standing	0.021	-0.107	0.541	0.402	-0.034	-0.106	0.078
Boarding/alighting	-0.011	-0.130	-0.022	0.092	-0.021	0.073	0.769
Door width	0.337	-0.051	0.270	0.203	-0.027	-0.112	0.508
Cleanliness	-0.047	0.132	0.179	0.641	-0.207	0.273	0.076
Lighting conditions	-0.149	0.617	-0.192	0.219	-0.107	0.168	0.024
Personnel behavior	-0.055	-0.070	0.036	0.676	0.282	-0.046	0.057
Comfort	-0.121	-0.279	0.512	-0.045	0.277	0.242	0.352
Accidents/breakdowns	-0.153	-0.098	0.054	0.097	0.615	-0.026	-0.069
Safety and security	0.159	0.068	-0.156	0.517	0.339	0.077	0.252

which were précised into six uncorrelated set of variables such as accessibility, service provisions, reliability, safety and security, fare, and comfort.

5.2 Hierarchical Fuzzy Inference System

The six input variables were changed over to fuzzy sets with “bell” shaped membership function due to simpler formula and computational efficiency. Total six primary input variables taken into consideration for the prediction model and each variable has three descriptors. So, there might be complications in generating $3^6 = 729$ number of fuzzy rules. This rule explosion problem can be solved by introducing a hierarchical fuzzy inference system (FIS), which is subdivided into two lower-level FIS and one higher-level FIS. The two higher-level fuzzy components are (i) availability (AVAL) and (ii) comfort and convenience (CC). These two parameters are further taken as

input variables for mapping them into overall satisfaction observed by transit user. The model is suggested keeping in mind that the customer satisfaction is mapped on the stop levels and route/segment levels and not for entire network. The first lower FIS consists of “accessibility,” “service provisions,” and “reliability” as input variables, which were fuzzified to get “availability” as an output variable. Similarly, “safety and security,” “fare,” and “comfort” were the input parameters for second lower FIS to produce “Comfort and Convenience” as an output variable. The resulting fuzzy values are the input variables for higher-level FIS to evaluate the satisfaction level of passengers. Centroid and max-min composition techniques were used to defuzzify the continuous membership functions for the determination of transit LOS of both the cities.

Construction of Membership Functions

Membership functions are the most important aspect of fuzzy inference system. “Fuzzification from crisp data set to fuzzified data set” and “defuzzification from fuzzified data set to crisp data set” are based entirely upon the parameters of membership function. Fuzzy membership functions include two details to be quantified, i.e., shape of MF and parameters of MF. Each variable is categorized as per human perception and given the linguistic labels such as “Poor,” “Fair,” and “Good” in an ascending order. The shape of MF used here is generalized bell function. Each parameter of “*bellmf*” controls a particular property of the function. The top width, the slope, and the midpoint are controlled by the parameters a , b , and c , respectively. In order to evaluate these parameters, histograms, i.e., graph between frequency and category was drawn and the shape of it proposed bell function to be used as a membership function. The parameters used to construct MF for each variable along with linguistic label are shown in Table 3.

Construction of Membership Functions

The constructed set of fuzzy if-then rules for linguistic variables are based on a framework of fuzzy knowledge base of fuzzy expert system. For example, Premise 1 (fact): If availability is poor and comfort and convenience is poor, Consequence (conclusion): Then overall satisfaction is “ F .” Similarly, all other fuzzy rules are generated by every possible combination of MFs.

Defuzzification

The outputs from fuzzy logic can be of two types: (a) fuzzy set and (b) crisp output. It is often required to have a crisp value at the end of fuzzy analysis. As for our analysis, the aim is to achieve the overall satisfaction of the respondents, we need a crisp output. Therefore, a fuzzy linguistic label that has resulted from the FIS has been defuzzified and converted back to crisp value output. This process is termed as defuzzification. The defuzzification technique used here is “Centroid technique.” Center of gravity also known as centroid method is the commonly used defuzzification strategy for continuous membership functions. Table 4 shows an example of how to obtain LOS category out of the fuzzy analysis. The score corresponding to “AVAL” and “CC” are the defuzzified fuzzy score from lower-level fuzzy logics. These scores are further

Table 3 Fuzzy membership functions parameters

	Variable	Category	MF grades (<i>bellmf</i>)		
			<i>a</i>	<i>b</i>	<i>c</i>
First lower-level FIS	Accessibility	Poor	0.8	3.366	1.201
		Fair	0.57	2.5	2.75
		Good	1.02	3.84	4.555
	Service provision	Poor	2.27	7.32	0.2567
		Fair	0.728	2.5	3.41
		Good	1.27	5.55	5.57
	Reliability	Poor	2.27	7.32	0.2567
		fair	0.728	2.5	3.41
		Good	1.27	5.55	5.57
Second lower-level FIS	Safety and security	Poor	2.27	7.32	0.482
		Fair	0.676	2.5	3.69
		Good	1.27	5.55	5.835
	Fare	Poor	2.27	7.32	0.1509
		Fair	0.818	2.5	3.35
		Good	1.21	4.93	5.441
	Comfort	Poor	2.41	9.45	0.0979
		fair	0.852	4.332	3.36
		Good	1.21	4.618	5.43
Higher-level FIS	Availability	Poor	1.5	6.328	1.12
		Fair	0.8	4.095	3.42
		Good	0.9	3.818	5.13
	Comfort and convenience	Poor	0.9	4.21	1.54
		Fair	0.8	3.97	3.245
		Good	0.9	4.18	4.946

Table 4 Membership grades and defuzzification process

No.	Input		LOS	Max-Min composition
	AVAL	CC		
5	Fair (0.22)	Fair (0.99)	D	Min (0.22,0.99) = 0.22
6	Fair (0.22)	Good (0.008)	C	Min (0.008,0.22) = 0.008
8	Good (0.7519)	Fair (0.99)	B	Min (0.7519, 0.99) = 0.7519
9	Good (0.7519)	Good (0.008)	A	Min (0.008, 0.7519) = 0.008

Max of ($D = 0.22$; $C = 0.008$; $B = 0.7519$; $A = 0.008$) = B

Table 5 Route-wise LOS counts in percentage for in each category

Segment	Route	LOS counts (%)						Total
		<i>F</i>	<i>E</i>	<i>D</i>	<i>C</i>	<i>B</i>	<i>A</i>	
1	Maninagar to Shivaranjani	0	11.5	69.2	19.2	0	0	100
2	Shivaranjani to Maninagar	0	12.5	62.5	12.5	12.5	0	100
3	Maninagar to RTO	0	8.11	83.8	8.11	0	0	100
4	RTO to Maninagar	0	0	71.4	28.6	0	0	100
5	Maninagar to Ghumagam	0	0	92.3	7.69	0	0	100
6	Ghumagam to Maninagar	0	0	66.7	33.3	0	0	100
7	Pal RTO to Kosad	0	16.7	66.7	16.7	0	0	100
8	Kosad to Pal RTO	0	0	100	0	0	0	100
9	Sarthana to Dumas	0	11.1	44.4	44.4	0	0	100
10	Dumas to Sarthana	0	0	80	20	0	0	100
11	Udhna to Sachin	0	0	90	10	0	0	100
12	Sachin to Udhna	0	0	100	0	0	0	100
13	SVNIT to Dumas	0	0	25	75	0	0	100
14	Dumas to SVNIT	0	0	0	100	0	0	100

used to predict the outcome, i.e., overall satisfaction of respondent. The scores were further classified as per the membership grades (α cuts). These membership grades were used to obtain OS values using centroid method. The significant rules were Rule# 5, 6, 8, and 9. Max-min composition resulted into LOS category of *B*. The observed value from the respondent was 4 which largely falls into “*B*” LOS levels. The collected data were classified route-wise as well as direction-wise due to the fact that BRTS have exclusive routes for its bus service as well different segments are provided direction-wise. Hence, the possibility of a single LOS level being dominant over all routes is rather less. The range in which LOS falls majorly as well as the aggregate behavior of respondents is important from the managerial perspective. Table 5 shows 14 entries for seven different routes direction-wise. The total responses were cross-classified between different categories of LOS and different route segments.

6 Conclusion

The proposed research focusses on identifying influential transit service attributes affecting passenger’s satisfaction and developing a suitable method for the evaluation of existing transit service quality to devise strategies for its sustainability. Considering

different modeling approaches in the past few decades, a variety of deterministic and stochastic models have been employed to assess the service quality of transportation systems. But those customary techniques might not be effective, when the interdependencies between variables are too complex. In reality, quantitative assessment of passenger's satisfaction is very intricate and difficult to decode as most of their decisions come off with fuzziness, ambiguity, and imprecision. Hence, fuzzy inference system is applied in this study to assess the transit service quality by mapping the ambiguity of passenger's perception in two bus rapid transit systems (BRTS), i.e., Janmarg (Ahmedabad city) and Sitilink (Surat city) in the state of Gujarat, India.

Factor analysis results in six input variables with a Kaiser-Meyer-Olkin (KMO) value of 0.63, which represents the sample size is adequate enough for the proposed model. The six input variables were changed over to fuzzy sets with "bell"-shaped membership function. Each variable has three descriptors. So, there might be complications in generating $3^6 = 729$ number of fuzzy rules. This rule explosion problem can be solved by introducing a hierarchical fuzzy inference system (FIS), which is subdivided into two lower-level FIS and one higher-level FIS. The resulting fuzzy values from lower-level FIS are the input variables for higher-level FIS to evaluate the satisfaction level of passengers on fourteen routes of the two BRTS "Janmarg" and "Sitilink." These kinds of models have not yet come into attention, which uses linguistic information and real-life problems of passengers about the current state of services. Hence, the proposed method would be more credible than previous models to support the decision-makers for long-term planning and designing transit networks.

References

1. Morfoulaki M, Tyrinopoulos Y, Aifadopolou G (2007) Estimation of satisfied customers in public transport systems: a new methodological approach. *J Transp Res Forum* 46:63–72. <https://doi.org/10.5399/osu/jtrf.46.1.981>
2. Fu L, Xin Y (2007) A new performance index for evaluating transit quality of service. *J Public Transp* 10. <https://doi.org/10.5038/2375-0901.10.3.4>
3. Dowling R, Flannery A, Landis B, Petritsch T, Roupail N, Ryus P (2008) Multimodal level of service for urban streets. *Transp Res Rec J Transp Res Board* 2071:1–7. <https://doi.org/10.3141/2071-01>
4. Tyrinopoulos Y, Antoniou C (2008) Public transit user satisfaction: variability and policy implications. *Transp Policy* 15(4):260–272. <https://doi.org/10.1016/j.tranpol.2008.06.002>
5. Eboli L, Mazzulla G (2009) A new customer satisfaction index for evaluating transit service quality. *J Public Transp* 12(3):21–37. <https://doi.org/10.5038/2375-0901.12.3.2>
6. Dell'Olio L, Ibeas A, Cecin P (2010) Modelling user perception of bus transit quality. *Transp Policy* 17(6):388–397. <https://doi.org/10.1016/j.tranpol.2010.04.006>
7. Awasthi A, Chauhan SS, Omrani H, Panahi A (2011) A hybrid approach based on SERVQUAL and fuzzy TOPSIS for evaluating transportation service quality. *Comput Ind Eng* 61(3):637–646. <https://doi.org/10.1016/j.cie.2011.04.019>
8. Khurshid R, Naeem H, Ejaz S, Mukhtar F, Batool T (2012) Service quality and customer satisfaction in public transport sector of Pakistan: an empirical study. *Int J Econ Manage Sci* 1:24–30

9. Mohamed M, Hine J (2013) Measuring the influence of the perceived bus transit quality on the perceptions of users. In: 13th world conference on transport research, Rio. <https://doi.org/10.1080/03081060.2016.1142224>
10. Noor H, Nasrudin N, Foo J (2014) Determinants of customer satisfaction of service quality: city bus service in Kota Kinabalu, Malaysia. *Procedia Social Behav Sci* 153:595–605. <https://doi.org/10.1016/j.sbspro.2014.10.092>
11. Pavlína P (2015) The factors influencing satisfaction with public city transport: a structural equation modelling approach. *J Compet* 7(4):18–32

Comparative Analysis of Pedestrian Walking Speed on Sidewalk and Carriageway



Ninad Gore, Sanjay Dave, Jiten Shah, Manish Jain, Dipak Rathva and Vinay Garg

Abstract This study aims to analyze the walking speed of the pedestrian on carriageway and sidewalk. In order to support the objective, a busy urban street in the CBD area of Vadodara city, Gujarat, India was considered. Selected study stretch is characterized by odd–even date on-street parking scheme; hence, sidewalk and carriageway on the either side were considered for the investigation of walking speed of pedestrians. Investigation revealed that 25% pedestrian are compelled to move on carriageway due to inadequate space. Empirical observation revealed that the pedestrian flow on no-parking carriageway face (NPCF) is greater than that of parking carriageway face (PCF). The analysis revealed that male pedestrian dominated movement on carriage, while female pedestrian dominated movement on sidewalk. Female pedestrians were observed to be slower by 4–6% than male pedestrians. The study results revealed that the walking speed of male pedestrian was 7–12% lower in evening compared to female for parking sidewalk face (PSF). This reduction in speed can be due to larger share of female pedestrians on sidewalk. Speed reduction on PSF ranged 27–32% with respect to the non-parking sidewalk face (NPSF), while the same for (PCF) observed in the range 10–15% with respect to face (NPCF), which can be attributed to friction owing to parking. The study results showed a reduction of 5–25% in walking speed of pedestrian on carriageway compared to

N. Gore · S. Dave (✉) · M. Jain · D. Rathva · V. Garg
The Maharaja Sayajirao University of Baroda, Vadodara, India
e-mail: smdave-ced@msubaroda.ac.in

N. Gore
e-mail: ninadgore24@gmail.com

M. Jain
e-mail: manish.jain-ced@msubaroda.ac.in

D. Rathva
e-mail: dipakrathwa-ced@msubaroda.ac.in

V. Garg
e-mail: vngarg370@gmail.com

J. Shah
Institute of Infrastructure Technology Research and Management, Ahmedabad, India
e-mail: jitenshah@iitram.ac.in

sidewalk, which may be attributed to safety against vehicular movement. Walking speed of pedestrian on carriageway was analyzed further with respect to the direction of vehicular movement. Observation revealed that male pedestrian against vehicular traffic moved with higher speed as compared to male along the direction of vehicles. However, an opposite trend was observed in females walking on the carriageway.

Keywords Walking speed · Sidewalk · Carriageway · On-street parking · Vehicular movement

1 Introduction

Walking is considered as the most essential and efficient mode of transport, as any trip starts or ends with walking. Therefore, the importance of pedestrian movement cannot be ignored. In India, very less attention has been devoted toward the development of effective and efficient pedestrian facilities in accordance with the pedestrian behavior and their needs. Though pedestrians are considered as the prime users of road, the space allocation for their movement is often neglected, which has subsequently led to degradation in the walking environment. Further, lack of exclusive pedestrian facilities, particularly in CBD area, results in pedestrians walking on the carriageway, creating a constant state of conflict with vehicular traffic. Moreover, encroachment by vendors on the present facilities and on-street parking creates an additional friction for their movement and such scenario prevails across many CBD areas of Indian cities. Since design of any pedestrian facility is standardized with respect to its flow rate and walking speed, it, therefore, becomes fundamental to study their behavior and suggest measures to improve walking environment.

2 Review of Literature

Pedestrian behavior is quite diverse when compared to the vehicle driving behavior as it does not follow lane discipline [1]. A significant number of studies regarding pedestrian flow characteristics on sidewalk exist. Some of the noteworthy contributions along these lines are explained next. Fruin [2], Polus et al. [3], Tarawneh [4], Montufar et al. [5], Finnis, and Walton [6] observed that female pedestrian walks slower than male pedestrians. Further, the authors concluded that age of pedestrian has a substantial effect on walking speed, and it reduces as the age of pedestrian increases. Moreover, it was also observed that the speed of pedestrian is also influenced by the type of pedestrian (i.e., local or outsider).

Tanaboriboon et al. [7] observed that the mean walking speed of the Singaporeans is slower (74 m/min) when compared with the speed of US pedestrians (89 m/min) and concluded that pedestrians in Singapore walk slower as compared to pedestrians in USA. Polus et al. [3], Koushki [8], and Morrall et al. [9] found that the average

walking speed for pedestrian of Israel, Riyadh, and Sri Lanka is 79, 65, and 75 m/min, respectively. Similarly, Kotkar et al. [10] found that the average walking speed for Indian pedestrian is 72 m/min. Dammen and Hoogendoorn [11] concluded that the pedestrian walking speed depends on walkway characteristics such as width, type of facility (i.e., with or without guardrail), and environmental factor. The walking speed of pedestrian is also affected due to the activity performed during walking.

Al-Masaeid et al. [12] and Singh and Jain [13] concluded that different land use such as business area, residential area, and educational area have a pronounced effect on walking speed of the pedestrian. Authors concluded that the surrounding environment is an important factor which affects the walking speed of the pedestrian. Singh and Jain [13] observed that pedestrians walking in commercial areas are faster than those in residential areas. Al-Masaeid et al. [12] developed the pedestrian speed-flow relationship for the central business district (CBD) areas in Irbid, Jordan. Authors suggested to design pedestrian facilities for pedestrian demand to capacity ratio of 0.5. Finnis and Walton [6] observed that the walking speed of pedestrian in indoor walkways is slower than the outdoor walkways. Knoblauch et al. [14] concluded that group size (platoon size) significantly affects pedestrian walking speed. Walking speed is observed to get reduced when walking in group compared to walking alone.

Rastogi et al. [15] found that the pedestrian free-flow speed is high on sidewalks (1.576 m/s) and low on precincts (1.340 m/s). The increase in the width of the facility resulted in increased space available to a pedestrian and as a result higher free-flow speed. Al-Azzawi and Raeside [16] conducted a number of video surveys of the movement of 7535 pedestrians on sidewalks, which were representative of different levels of service. The average walking speed was found to be 50.16 m/min. Advani et al. [17] concluded that the broad reason for walking on the carriageway is 'not-good' footpath. Two broad reasons for walking on the footpath are low space occupancy and high space occupancy. Advani and Nisha [18] observed that usage of the main carriageway by pedestrians is a common site on urban Indian roads. While the quality of footpath is an obvious factor, traffic on the main carriageway also plays an important role in pedestrian's decision to use the carriageway for walking, especially under heterogeneous traffic conditions. Heterogeneous traffic conditions on the sample section have been measured by 'space occupancy', which is based on classified traffic volume count data. Authors observed increased an percentage of walking on carriageway during the medium space occupancy on carriageway compared to low and high space occupancies and the behavioral difference was statistically validated. Further, the authors concluded that the major concerns of safety and comfort are compromised during low space occupancy, while comfort is reduced during high space occupancy.

3 Need of Study

The movement of pedestrian on the carriage is the most common scenario, which prevails across many Indian cities. Review of literature suggested that very few studies are concentrated on pedestrian movement on carriageway, which necessitates to

study pedestrian behavior on carriageway. The present study emphasizes on pedestrian walking speed on carriageway and sidewalk for a case representing CBD area of Vadodara city, India.

4 Study Site and Data

The urban street considered in the CBD area of Vadodara city is characterized by odd–even date on-street parking scheme. Therefore, sidewalk and carriageway encompassing both legal and illegal parked vehicles were considered to investigate pedestrian movement. Videography technique was employed to collect pedestrian data during morning peak hour (10.30–12.30) and evening peak hour (4.30–6.30 pm) covering two days. Pedestrian data were collected by segmenting sidewalk and carriageway to illustrate entry and exit of trap. A trap of 10 m in section was delineated on sidewalk and carriageway. The pedestrian data like flow (ped/min/m) and walking speed (m/sec) were extracted manually for every minute of the recorded video to capture pedestrian movement at microscopic levels. Attributes like gender and direction of pedestrian movement were also considered during data extraction. Pedestrian flow was measured by calculating the number of pedestrian crossing the predefined section. Sampling was assorted, to obtain walking speed of pedestrians. Five pedestrians in each minute in each direction were considered to determine walking speed on both sidewalk and carriageway. The walking speeds were extracted by recording the entry and exit time to cross a predefined trap. A total of 9600 pedestrian records were extracted (Figs. 1 and 2).

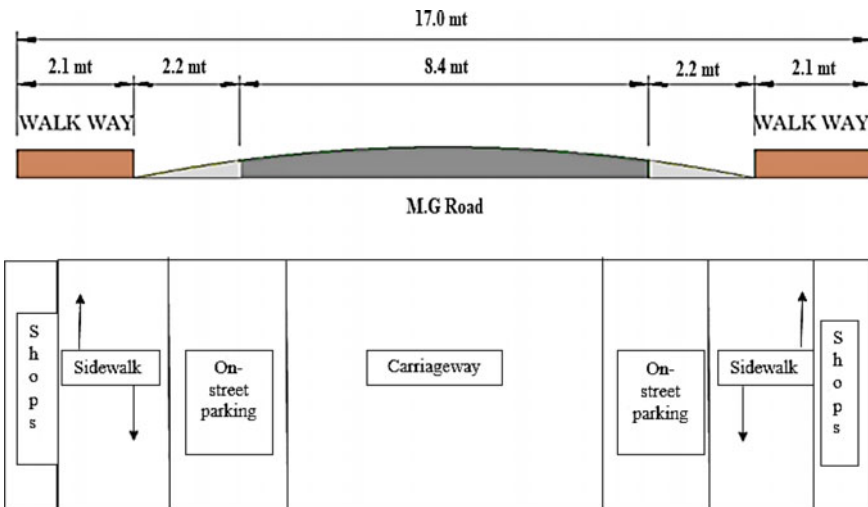


Fig. 1 Cross-sectional and schematic plan of the study site



Fig. 2 Photographs of study site representing a legal parking face b illegal parking face

5 Data Analysis

The sidewalk and carriage corresponding to legal parking face are termed as parking sidewalk face (PSF) and parking carriageway face (PCF), while that conforming illegal parked vehicles is coined as non-parking sidewalk face (NPSF) and non-parking carriageway face (NPCF) respectively. Analysis of data revealed that considerable volume (25%) of pedestrian movement is observed on carriageway. It was further noted that movement on carriageway is greater on NPCF compared to PCF. Empirical observations revealed female-dominated pedestrian movement on sidewalk, while male pedestrians dominated pedestrian movement on carriageway. Therefore, female has greater affinity to walk on sidewalks as compared to male. Figure 3 represents pedestrian volume on a different walkway path and as per on-street parking side.

The walking speed analysis is summarized in Table 1. It could be noted that the speed of pedestrian on PSF and PCF is much lower than speed of pedestrian on NPSF and NPCF for both days. In addition, the speed of pedestrian on sidewalk for

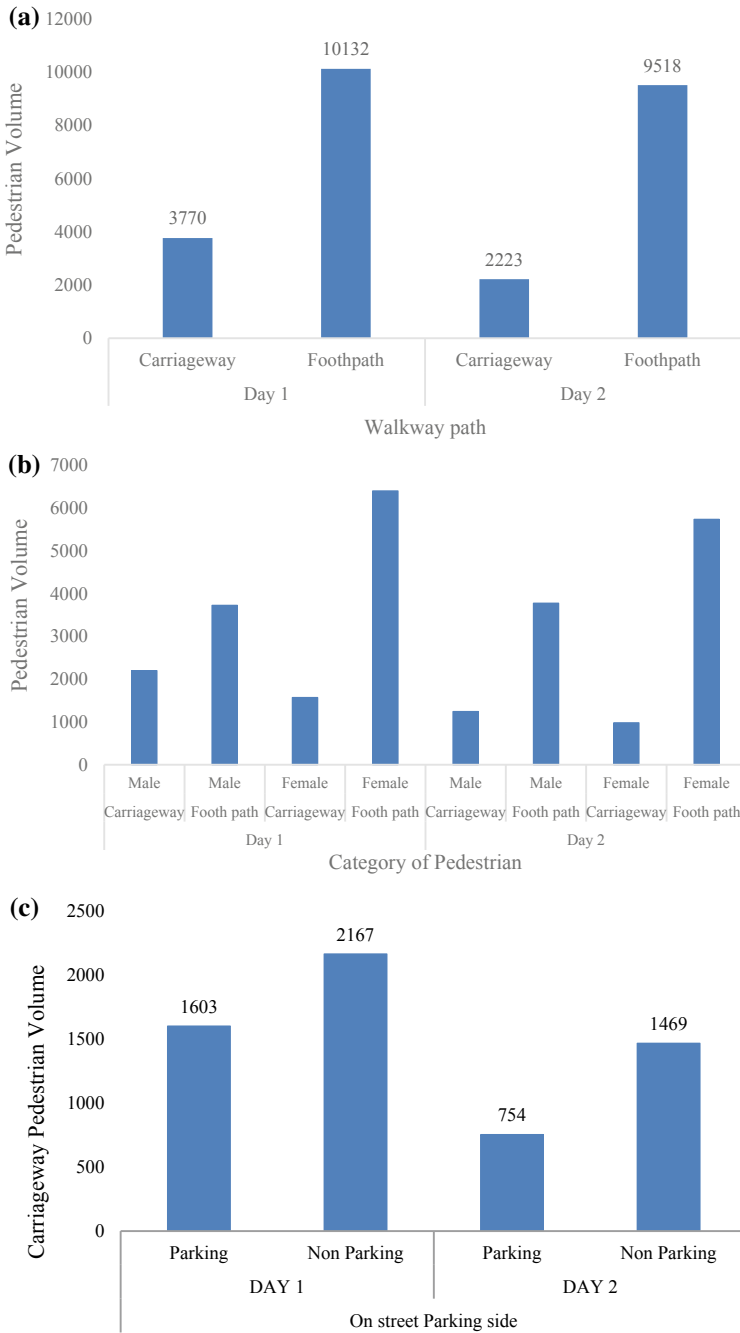


Fig. 3 Pedestrian volume **a** on different walkway path, **b** on walkway path as per gender, and **c** based on on-street parking side

Table 1 Average speed of pedestrian for different walking paths

Walking path	Face	Morning		Evening	
		Speed male (m/min)	Speed female (m/min)	Speed male (m/min)	Speed female (m/min)
Sidewalk	Parking day 1	57.86	54.24	30.04	33.67
	Non-parking day 1	60.05	45.37	49.07	43.97
	Parking day 2	73.627	59.799	48.378	52.427
	Non-parking day 2	58.71	68.86	70.68	68.86
Carriageway	Parking day 1	45.61	34.09	45.59	40.23
	Non-parking day 1	46.22	39.36	55.05	43.97
	Parking day 1	34.69	31.28	56.29	51.39
	non-parking day 1	43.88	38.47	68.18	51.64

both faces is greater than the speed of pedestrian on carriageway. To supplement, males were found to be walk swiftly in morning on PSF, NPSF, PCF, and NPCF, respectively, while females in evening had higher speed compared to males on PSF for both days.

Walking speed of pedestrian on sidewalk and carriageway for both faces was statistically checked at 5% significance for null hypothesis, “no difference in walking speed on sidewalk and carriageway exists.” In addition, speed of males and females on PSF, NPSF, PCF and NPCF, checked statistically. Further, the speed of pedestrian as per time of day was checked statistically. The results of hypothesis testing are summarized in table (Tables 2, 3 and 4).

It can be concluded that the speed of pedestrian on both faces of sidewalk and carriageway significantly varied in morning and evening. In addition, variation in speed between PSF and NPSF and between PCF and NPCF was found significant. An average reduction of 25–32% in speed on PSF is observed with respect to NPSF, while an average reduction of 10–15% in speed on PCF is noted with respect to NPCF. Speed reduction on parking face with respect to non-parking face can be attributed to the presence of parked vehicles. Moreover, it was observed that speed between sidewalk and carriageway varied significantly. An average reduction in range 5–25% in speed on carriageway for both faces with respect to sidewalk was recorded. Reduction in speed on carriageway can be attributed to reduced safety on carriageway. To supplement, speeds of male and female pedestrian varied for both faces of sidewalk and carriageway significantly. It was observed that females walked 4–6% slower compared to male. It was also noted male pedestrian walked 7–12% slower compared to female in evening on PSF for both days. This reduction may be accredited to larger female volume on PSF compared to male, thereby creating female follow regime.

Table 2 Hypothesis testing of walking speed on sidewalk and carriageway

Sidewalk	F-value	p-value	Remark
<i>Parking day 1</i>			
Male (morning–evening)	169.16	0.00	Rejected
Female (morning–evening)	13.72	0.0002	Rejected
Male–female morning	29.54	0.00	Rejected
Male–female evening	17.87	0.00	Rejected
<i>Non-parking day 1</i>			
Male (morning–evening)	38.48	0.00	Rejected
Female (morning–evening)	2.90	0.08	Accepted
Male–female morning	128.83	0.00	Rejected
Male–female evening	6.16	0.013	Rejected
<i>Parking day 2</i>			
Male (morning–evening)	252.30	0.00	Rejected
Female (morning–evening)	9.32	0.0023	Rejected
Male–female morning	65.05	0.00	Rejected
Male–female evening	24.99	0.00	Rejected
<i>Non-parking day2</i>			
Male (morning–evening)	39.61	0.00	Rejected
Female (morning–evening)	0.15	0.99	Accepted
Male–female morning	76.63	0.00	Rejected
Male–female evening	0.0009	0.97	Accepted
Carriageway			
<i>Parking day 1</i>			
Male (morning–evening)	0.0009	0.99	Accepted
Female (morning–evening)	6.55	0.011	Rejected
Male–female morning	15.95	0.0001	Rejected
Male–female evening	10.89	0.0010	Rejected
<i>Non-parking day 1</i>			
Male (morning–evening)	29.31	0.00	Rejected
Female (morning–evening)	5.12	0.024	Rejected
Male–female morning	10.69	0.0012	Rejected
Male–female evening	48.61	0.00	Rejected
<i>Parking day 2</i>			
Male (morning–evening)	37.84	0.00	Rejected
Female (morning–evening)	27.65	0.00	Rejected
Male–female morning	1.33	0.25	Accepted

(continued)

Table 2 (continued)

Sidewalk	<i>F</i> -value	<i>p</i> -value	Remark
Male–female evening	2.45	0.11	Accepted
<i>Non-parking day2</i>			
Male (morning–evening)	151.98	0.00	Rejected
Female (morning–evening)	38.37	0.00	Rejected
Male–female morning	12.65	0.0004	Rejected
Male–female evening	50.32	0.00	Rejected

Note Accepted or rejected in reference to null hypothesis

Table 3 Hypothesis testing result between parking and non-parking faces

Between parking and non-parking faces		<i>t</i> -test (<i>p</i> -value)	Remark
Sidewalk	<i>Day 1</i>		
	Male PSF–NPSF morning	0.01	Rejected
	Male PSF–NPSF evening	0.00	Rejected
	Female PSF–NPSF morning	0.41	Accepted
	Female PSF–NPSF evening	0.00	Rejected
	<i>Day 2</i>		
	Male PSF–NPSF morning	0.00	Rejected
	Male PSF–NPSF evening	0.00	Rejected
	Female PSF–NPSF morning	0.00	Rejected
	Female PSF–NPSF evening	0.00	Rejected
Carriageway	<i>Day 1</i>		
	Male PCF–NPCF morning	0.00	Rejected
	Male PCF–NPCF evening	0.00	Rejected
	Female PCF–NPCF morning	0.01	Rejected
	Female PCF–NPCF evening	0.01	Rejected
	<i>Day 2</i>		
	Male PCF–NPCF morning	0.00	Rejected
	Male PCF–NPCF evening	0.00	Rejected
	Female PCF–NPCF morning	0.01	Rejected
	Female PCF–NPCF evening	0.92	Accepted

Note Accepted or rejected in reference to null hypothesis

Table 4 Hypothesis testing result between sidewalk and carriageway

Between sidewalk and carriageway	<i>t</i> -test (<i>p</i> -value)	Remark
<i>Parking face day 1</i>		
Male (sidewalk and carriageway)	0.00	Rejected
Female (sidewalk and carriageway)	0.00	Rejected
<i>Non-parking face day 1</i>		
Male (sidewalk and carriageway)	0.00	Rejected
Female (sidewalk and carriageway)	0.00	Rejected
<i>Parking face day 2</i>		
Male (sidewalk and carriageway)	0.00	Rejected
Female (sidewalk and carriageway)	0.00	Rejected
<i>Non-parking face day 2</i>		
Male (sidewalk and carriageway)	0.00	Rejected
Female (sidewalk and carriageway)	0.00	Rejected

Note Accepted or rejected in reference to null hypothesis

5.1 Speed Analysis with Respect to Direction of Traffic

Speed of pedestrian on carriageway was analyzed with respect to direction of traffic. The direction of pedestrian movement in the same direction of traffic was considered as up, while pedestrian movement opposite to traffic is termed down. Walking speed is as summarized in table. It could be noted that males for both PCF and NPCF, walked faster in down direction, while an opposite trend was observed in females. Therefore male pedestrian are more confident in walking against vehicular traffic with higher speed as compared to male along direction of vehicles (Table 5).

Table 5 Carriageway speed detail

Day	Face	Morning				Evening			
		Male up	Male down	Female up	Female down	Male up	Male down	Female up	Female down
Day 1	PCF	39	51.96	39.6	28.8	40	52.2	46.2	33.6
	NPCF	42	50.4	41.4	37.2	51.1	59.4	45.6	42.6
Day 2	PCF	33.6	36	30	33	54.5	58.2	49.2	54
	NPCF	40.2	48.6	39.9	37.2	63.2	73.2	55.8	48

Note Speed (m/min)

6 Conclusion

The present study attempts to analyze pedestrian walking speed on sidewalk and carriageway under the influence of on-street parking for case representing CBD area of Vadodara city. The following conclusions are drawn:

1. Pedestrian in Vadodara are slower than pedestrian across different countries. They are nearer to their counterpart Riyadh, Saudi Arabia.
2. Speed of pedestrian in CBD area is lesser than speed reported by other researchers. This differential speed may be due to the difference in commercial activities.
3. Encroachment of facility in CBD area has compelled pedestrian to move on carriageway.
4. The presence of parked vehicles significantly reduced pedestrian speed on PSF and PCF, respectively. Therefore, surrounding environment affects pedestrian speed.
5. Speed of pedestrian reduces on carriageway as compared to sidewalk. Reduction in speed can be attributed to compromise safety when moving on carriageway.

7 Recommendation

In the present study, the speed of pedestrian reduced on both PSF and PCF compared to speed on NPSF and NPCF, respectively. Therefore, the presence of parked vehicles influences pedestrian speed. In addition, practical enforcement issues associated with illegal parking can be regulated by provision of temporary barriers on illegal parking face, which can significantly improve pedestrian environment and may reduce the occupancy of pedestrian movement on carriageway.

References

1. Blue VJ, Adler JL (2001) Cellular automata microsimulation for modelling bi-directional pedestrian walkways. *Transp Res Part B Methodol* 35:293–312
2. Fruin JJ (1971) *Pedestrian planning and design*. Metropolitan Association of Urban Designers and Environmental Planners, New York
3. Polus A, Schofer JL, Ushpiz A (1983) Pedestrian flow and level of service. *ASCE J Transp Eng* 109(1):46–56
4. Tarawneh MS (2001) Evaluation of pedestrian speed in Jordan with investigation of some contributing factors. *J Saf Res* 32:229–236
5. Montufar M, Arango J, Porter M, Nakagawa S (2007) Pedestrians normal walking speed and speed when crossing a street. *Transp Res Rec J Transp Board* 2002:90–97
6. Finnis KK, Walton D (2008) Field observations to determine the influence of population size, location and individual factors on pedestrian walking speeds. *Ergonomics* 51(6):827–842. <https://doi.org/10.1080/00140130701812147>

7. Tanaboriboon Y, Hwa SS, Chor CH (1986) Pedestrian characteristics study in Singapore. *J Transp Eng ASCE* 112(3):229–235
8. Koushki PA (1988) Walking characteristics in Central Riyadh, Saudi Arabia. *J Transp Eng* 114(6):735–744
9. Morrall JF, Ratnayake LL, Seneviratne PN (1991) Comparison of central business district pedestrian characteristics in Canada and Sri Lanka. *Transp Res Rec* 1294:57–61 (Transportation Research Board, Washington DC)
10. Kotkar KL, Rastogi R, Chandra S (2010) Pedestrian flow characteristics in mixed flow condition. *ASCE J Urban Plan Dev* 136(3):22–23
11. Dammen W, Hoogendoorn SP (2003) Experimental research of pedestrian walking behaviour. In: Proceedings of annual meeting of transportation research board, CD-ROM. National Academy Press, Washington. Guidelines for pedestrian, Indian Road Congress-103, 1988
12. Al-Masaeid HR, Al-Suleiman TI, Nelson DC (1993) Pedestrian speed flow relationship for central business areas in developing countries. *Transp Res Rec* 1396:69–74 (National Research Council, Washington, DC)
13. Singh K, Jain PK (2011) Methods of assessing pedestrian level of service. *J Eng Res Stud* 2(1):116–124
14. Knoblauch RL, Pietrucha MT, Nitzburg M (1996) Field studies of pedestrian walking speed and start-up time. In *Transp Res Rec* 538:27–38 (TRB, National Research Council, Washington DC)
15. Rastogi R, Ilango T, Chandra S (2013) Pedestrian flow characteristics for different pedestrian facilities and situations European transport. *Trasporti Europei* 53:1–21
16. Al-Azzawi M, Raeside R (2007) Modeling pedestrian walking speeds on sidewalks. *J Urban Plan Dev* 133(3):211–219
17. Advani M, Parida P, Patnaik S (2015) Why and when pedestrians walk on carriageway in presence of footpath?—a behavioural analysis in mixed traffic scenario of India. In: Urban mobility India conference and expo
18. Advani M, Nisha G (2013) Behavioural analysis of pedestrians for walking on footpath and on carriageway in ‘Space-Sharing’ traffic scenario. *Indian Highw* 41 (Indian Road Congress)

Real-World Emissions from Diesel Passenger Cars During Peak and Off-Peak Periods



Srinath Mahesh and Gitakrishnan Ramadurai

Abstract Emissions from motor vehicles lead to significant adverse effect on air quality of cities, with many cities reporting ambient air concentration of pollutants well beyond the permissible standards. In this paper, we determine the effect of changing driving patterns during peak and off-peak periods on emissions from diesel passenger cars. Second-by-second emissions of CO, CO₂, HC, and NO_x were measured during both peak and off-peak periods using portable emission measurement system (PEMS). It is seen that during peak hour, average speed decreases, percentage time spent in acceleration, deceleration, and idling increases, while time spent in cruising mode decreases significantly. Further, EFs are developed for peak and off-peak periods and compared with the Automotive Research Association of India (ARAI) emission standards. The EFs during peak periods are found to be significantly different from off-peak periods. The results of this study would be useful in accurate quantification of emissions.

Keywords Air quality · Real-world emissions · Diesel cars · Emission factor

1 Introduction

Emission from motor vehicles has become a serious problem in all large cities worldwide leading to higher lung ailments and health costs. Studies indicate that almost 50% of total emissions in a city are contributed by motor vehicles [1–3]. Although tremendous advancements have been achieved in vehicle emission control systems, no improvement in air quality is seen. This is due to the exponential increase in the number of vehicles and vehicle usage (vehicle kilometers travelled) because of urban sprawl. The resulting effects on health and well-being of the citizens have been a matter of debate among policymakers and scientists.

S. Mahesh (✉) · G. Ramadurai
Transportation Engineering Division, Department of Civil Engineering, IIT Madras, Chennai,
India
e-mail: srinath.nda@gmail.com

G. Ramadurai
e-mail: gitakrishnan@iitm.ac.in

© Springer Nature Singapore Pte Ltd. 2020
T. V. Mathew et al. (eds.), *Transportation Research*, Lecture Notes
in Civil Engineering 45, https://doi.org/10.1007/978-981-32-9042-6_7

In India, the number of registered cars grew from 7.05 to 19.23 million between 2001 and 2011 [4]. Similar growth has been observed in other countries [5]. Moreover, the share of diesel vehicles has seen a rising trend, particularly in the last five years, which may be due to the lesser price of diesel as compared to gasoline. There are approximately 1 million registered passenger cars plying in Chennai out of which 40% run on diesel [6]. However, studies indicate that vehicles running on diesel emit a significantly higher amount of pollutants than gasoline vehicles.

Traditionally, tests to quantify emissions from motor vehicles have been laboratory based. However, real-world driving causes sudden changes in speed and acceleration of the vehicles due to inter-vehicle interactions. Further, in congested traffic, vehicles experience stop-and-go conditions which lead to higher fuel consumption and emissions [7]. Laboratory emission tests using standard driving cycles fail to capture these variations in driving leading to unrepresentative test conditions.

Recent advances in instrumentation have led to the development of portable emission measurement systems (PEMS) that are capable of measuring real-world second-by-second emissions of all the major ambient air pollutants. Wyatt et al. [8] recorded on-road emissions from a passenger car using PEMS to quantify the impact of road grade on CO₂ emissions. Yu and Li [9] evaluated emissions of buses near bus stops using PEMS and determined the influence of bus stop characteristics on emissions. Yu et al. [10] used PEMS to determine the effect of passenger load on emissions from buses. In another study, O'Driscoll et al. [11] used PEMS data from 39 diesel passenger cars over a test route consisting of urban and motorway sections. Thus, PEMS-based emission studies are gaining popularity due to their ability to capture real-world emissions.

The main objective of this study is to quantify emissions from diesel passenger cars using real-world measurements. This study attempts to answer the following questions: (1) are emission factors during peak periods different from that during off-peak? If yes, by how much do they differ? and (2) are the emission factors determined using real-world measurements within the permissible standards?

The research includes the following tasks: (a) to collect real-world second-by-second emission data from passenger car using PEMS; (b) to compare the vehicle operating characteristics during peak and off-peak periods; and (c) to develop emission factors from real-world data for peak and off-peak periods.

2 Methodology

2.1 Study Area

The study area consisted of a test route around IIT Madras campus as shown in Fig. 1. It consisted of four main arterial roads having different geometric characteristics with many signalized intersections. This route was chosen as it carries a significant volume of traffic and is representative of arterial roads in Chennai. The total distance of the



Fig. 1 Test route consisting of four main arterial roads

route was approximately 14 km with each emission test starting and ending at the main gate of IIT Madras campus.

2.2 Test Vehicles

Two diesel passenger cars of different manufacturers were used for emission monitoring, both of the same age, and complying with Bharat Stage IV emission standards. Specifications of the test vehicles are shown in Table 1.

2.3 Data Collection

The tests were done on two typical weekdays in July 2015. The peak hour data was collected between 9:00–10:00 a.m. and 6:00–7:00 p.m., while off-peak hour data was

Table 1 Test vehicle specifications

Vehicle type	Chevrolet Spark	Toyota Etios
Mileage (km)	44,205	63,714
Transmission	5 speed, manual	5 speed, manual
Manufacturer	Chevrolet	Toyota
Weight (kg)	840	1020
Max. power (bhp)	57 @ 4000 rpm	67 @ 3800 rpm
Engine displacement (cm ³)	936	1364
Cylinder number	3	3
Catalytic converter	Three-way converter	Three-way converter

collected from 2:00–3:00 p.m. The on-road driving (speed time) data was collected using a GPS, whereas vehicle rpm and flow rate were obtained from an onboard diagnostic (OBD) reader. The second-by-second emissions of CO, CO₂, HC, and NO_x were measured using AVL Ditest 1000 gas analyzer. The probe from the gas analyzer was attached to the tailpipe of the vehicle and the emission data was obtained in a laptop computer.

2.4 Data Analysis

The emission concentration in % vol. or ppm was converted to instantaneous emission rate (g/s) by using the exhaust flow rate as follows:

$$ER_p = P \times FR \times \rho_p \quad (1)$$

where P is the instantaneous concentration of pollutant P (% vol. or ppm), FR is the exhaust volumetric flow rate in L/s, and ρ_p is the density of pollutant in g/L. The emission factor (g/km) was determined by dividing the total emissions by the distance travelled.

3 Results and Discussion

The traffic flow characteristics during off-peak hour (OPH) and peak hour (PH) are shown in Table 2. It is seen that during PH, average speed decreases, percentage time spent in acceleration, deceleration and idling increases, while time spent in cruising mode decreases significantly. This is due to higher congestion during PH leading to frequent stop-and-go conditions as seen from Fig. 2. The speed time plot for OPH has

Table 2 Traffic flow characteristics during OPH and PH

Characteristics	OPH	PH	Difference (PH-OPH)
Distance (km)	13.61	13.61	–
Time (s)	1814	2298	484
Average speed (km/h)	27.01	21.35	–5.66
Idling (%)	10.22	24.50	14.28
Acceleration (%)	19.01	30.94	11.93
Deceleration (%)	14.09	25.67	11.58
Cruising (%)	56.69	18.89	–37.80

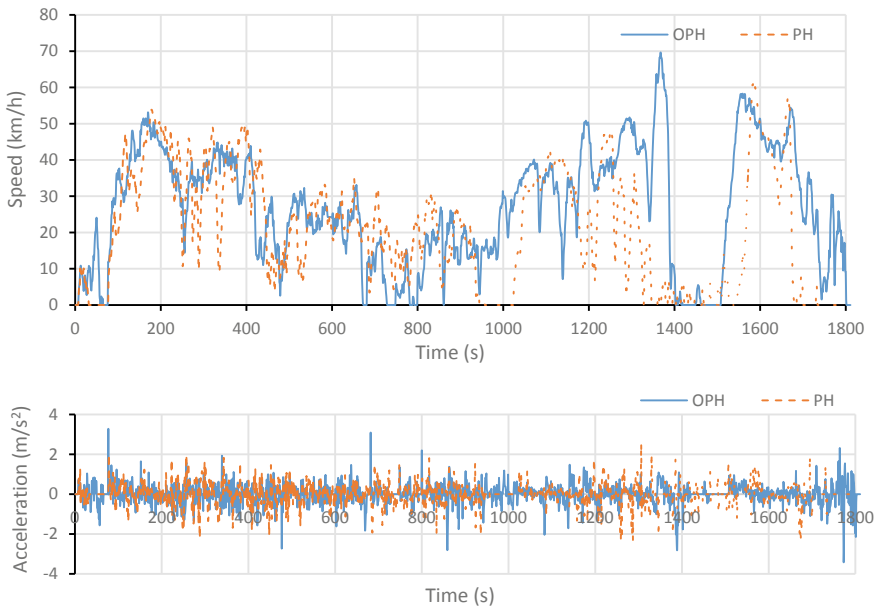


Fig. 2 Speed and acceleration during peak and off-peak periods

higher peaks with fewer stops, whereas the PH plot has larger fluctuations in speed. Moreover, higher magnitudes of acceleration and deceleration are observed in the PH. This leads to higher total emissions during PH for the same distance travelled as seen in Fig. 3. Further, significant variability is seen in the emissions between the two cars, particularly for HC and NO_x emissions.

Table 3 shows the emission factors for the tested vehicles during peak and off-peak periods and compared with ARAI emission standards [12]. The values in bold font indicate EF values above the emission standards. The CO emission factors exceeded permissible standards during PH, whereas they were within limits during

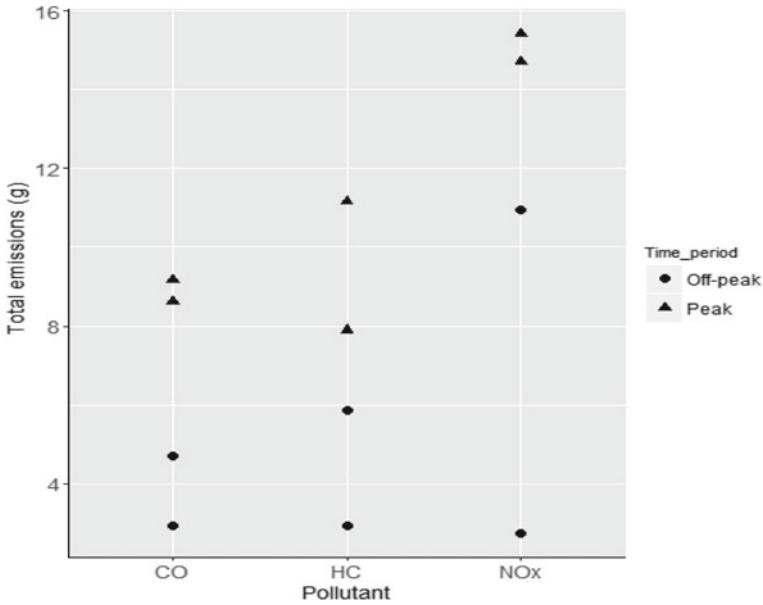


Fig. 3 Total emissions during peak and off-peak periods

Table 3 Emission factors for both cars during peak and off-peak periods

Pollutant	Car 1 (g/km)		Car 2 (g/km)		ARAI emission standard (g/km)
	Peak	Off-peak	Peak	Off-peak	
CO	0.632	0.213	0.673	0.345	0.50
HC	0.580	0.216	0.821	0.431	0.05
NO _x	1.081	0.804	1.132	0.201	0.25
CO ₂	242.970	191.975	489.705	409.104	–

OPH. Similarly, the HC and NO_x emission factors also exceeded permissible limits during PH. Further, the percentage increase in total emissions in PH is shown in Fig. 4. All the pollutants increase considerably during PH, with NO_x emissions increasing by more than 450%. This is due to the increased temperature of the engine as a result of higher idling times during PH, similar to that observed in past studies [13, 14]. Overall, the increase in emission factors during PH may be due to: low-cruising speeds, higher number of stop-and-go events, and unpredictable driving due to congestion during PH.

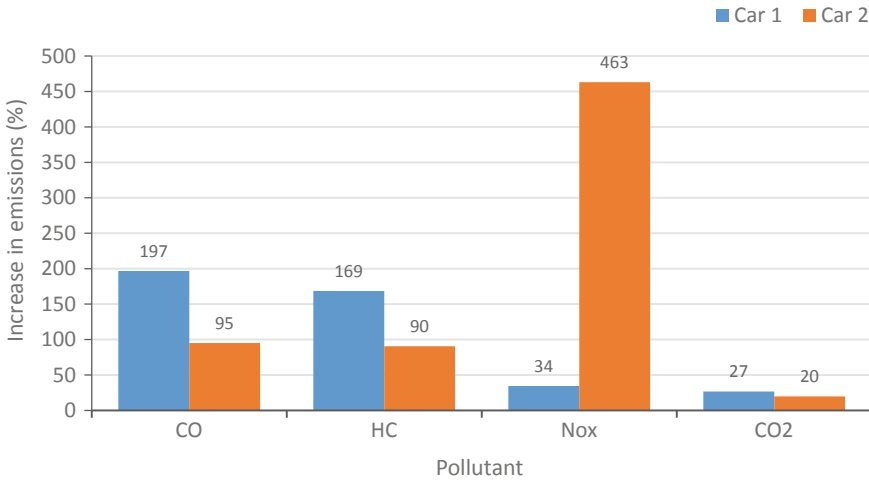


Fig. 4 Percentage increase in total emissions during peak periods w.r.t. off-peak periods

4 Conclusions

Emissions from diesel vehicles have been a subject of immense interest in the recent past. This is due to the deteriorating air quality in cities which is attributed to motor vehicles. In this context, this study aimed to quantify emissions from diesel passenger cars during peak and off-peak periods using onboard emission measurement systems (PEMS). Since most of the past emissions monitoring studies are laboratory based, this study provides unique insights regarding emissions in real-world conditions.

The major findings of the study are as follows. The emissions from the test vehicles were influenced by the traffic characteristics with significantly higher emissions for all the pollutants during peak hour relative to off-peak periods. The measured emission factors exceeded the permissible limits during peak hours. Also, the emission factors were different for the tested vehicles, thereby leading to varying total emissions. The findings suggest that measures to improve the flow of traffic would go a long way in reducing air pollutant emissions from road vehicles.

This study has the following limitations. Firstly, only diesel passenger cars were considered. Emissions from cars using other fuels such as CNG/petrol may also be useful in developing emission inventories. Secondly, only two cars were used in this study, which may not be representative of the entire fleet of cars. Lastly, emissions of particulate matter were not measured due to unavailability of measuring instrument. Addressing these limitations provide scope for future research.

References

1. Gurjar BR, Van Aardenne JA, Lelieveld J, Mohan M (2004) Emission estimates and trends (1990–2000) for megacity Delhi and implications. *Atmos Environ* 38(33):5663–5681
2. Ramachandra TV, Shwetmala, Emissions from India's transport sector: statewise synthesis. *Atmos Environ* 43(34):5510–5517
3. Sahu SK, Beig G, Parkhi NS (2011) Emissions inventory of anthropogenic PM_{2.5} and PM₁₀ in Delhi during commonwealth games 2010. *Atmos Environ* 45(34):6180–6190
4. MoRTH (2016) Road transport year book (2014–2015)
5. Dargay J, Gatley D (1999) Income's effect on car and vehicle ownership, worldwide: 1960–2015. *Transp Res Part A Policy Pract* 33(2):101–138
6. Authority ST (2016) Growth of vehicles. Available: <http://www.tn.gov.in/sta/stat1.html>. Accessed 15 Feb 2017
7. Gokhale S (2012) Impacts of traffic-flows on vehicular-exhaust emissions at traffic junctions. *Transp Res Part D Transp Environ* 17(1):21–27
8. Wyatt DW, Li H, Tate JE (2014) The impact of road grade on carbon dioxide (CO₂) emission of a passenger vehicle in real-world driving. *Transp Res Part D Transp Environ* 32:160–170
9. Yu Q, Li T (2014) Evaluation of bus emissions generated near bus stops. *Atmos Environ* 85:195–203
10. Yu Q, Li T, Li H (2016) Improving urban bus emission and fuel consumption modeling by incorporating passenger load factor for real world driving. *Appl Energy* 161:101–111
11. O'Driscoll R, ApSimon HM, Oxley T, Molden N, Stettler MEJ, Thiagarajah A (2016) A portable emissions measurement system (PEMS) study of NO_x and primary NO₂ emissions from Euro 6 diesel passenger cars and comparison with COPERT emission factors. *Atmos Environ* 145(2):81–91
12. Marathe SR (2013) Emission factors for Indian in use vehicles
13. Fu M, Ge Y, Wang X, Tan J, Yu L, Liang B (2013) NO_x emissions from Euro IV busses with SCR systems associated with urban, suburban and freeway driving patterns. *Sci Total Environ* 452–453:222–226
14. Yao Z, Wu B, Wu Y, Cao X, Jiang X (2015) Comparison of NO_x emissions from China III and China IV in-use diesel trucks based on on-road measurements. *Atmos Environ* 123:1–8

Candidate Driving Cycle Construction for Emission Estimation



Boski P. Chauhan, Gaurang J. Joshi and Parida Purnima

Abstract Transportation emissions are the main contributor to air pollution and create many environmental problems. To control vehicle emission and to achieve air quality, driving cycle is one of the concepts applied for emission estimation. Driving cycle is fundamentally profile of speed of vehicle versus time or distance. The constitution of a driving cycle is directly related to the accuracy of any air quality analysis, so an accurate analysis of the driving cycle is important for emission estimation. In the present study, driving cycle data has been analyzed to generate candidate driving cycle, which is the single representative cycle used for emission estimation and represents the actual driving activity of the study area. This study highlights the micro-trip-based method for construction of the candidate cycle. Micro-trips are grouped and arranged to get the candidate driving cycle. The best candidate cycle is selected on the basis of cycle assessment parameters. Driving cycle data collection has been carried out in urban corridor of Vadodara city, Gujarat. The study corridor composed of four signalized intersections and one rotary intersection. The numbers of candidate cycles have been generated from the collected base data of driving cycle by the micro-trip method. The selection of the best candidate cycle is done by comparing the driving parameters of base data cycles and generated candidate cycles. The candidate cycle has the least value of root-mean-square error is selected as a final representative cycle and used for the emission estimation. A single parameter average speed is taken to estimate emission at a macroscopic level based on emission factors.

Keywords Driving cycle · *K*-means clustering · Micro-trips · Root-mean-square error (RMSE) · Emission factors

B. P. Chauhan (✉) · G. J. Joshi
Civil Engineering Department, Sardar Vallabhbhai National Institute of Technology, Surat
395007, Gujarat, India
e-mail: boski.chauhan@ckpcet.ac.in

G. J. Joshi
e-mail: gjsvnit92@gmail.com

P. Purnima
Planning & Business Development, CSIR-CBRI, Roorkee, Uttarakhand, India
e-mail: punam31@gmail.com

1 Introduction and Background

Rapid urbanization plays a lead role for a remarkable growth of vehicle population. Vehicle population induces transportation-related exhaust emissions, which acts as a principal contributor to air pollution in the city of developing countries. Transportation-related environmental issues become a serious risk to human health while exploring in the area of high traffic congestion. To develop inventories of air quality and for executing strategies of emission control, the driving cycle is the important concept being used for many years [1]. Driving cycle is constructive for the purpose of emission testing and estimation [2]. It is derived from a series of data points denoting the speed of vehicles versus time [3, 4]. It is the plot of driving pattern of a vehicle for a particular route and mostly characterized by driving parameters associated with the speed of vehicles. Driving cycles are the platform between driving conditions and characteristics of discrete vehicle as well as their respective emissions [5]. Development of driving cycle imparts method to interpret the precision of emission measurement from a microscopic level to macroscopic level. Candidate driving cycle is the representative cycle that can be generated from the real-world driving data. To construct candidate driving cycle with the corresponding vehicle test data, different methods have been suggested. Micro-trip-based cycle construction is one of the approaches to create candidate driving cycles. In this method, driving cycles is to be compiled by “micro-trips,” which are defined as the driving activity between adjoining stops, including the leading period of idle. A driving cycle is constructed by compiling representative micro-trips with the goal that the cycle closely matches with the real-world data. The data collection of the driving cycle includes instrumentation, study area selection, and day of the data collection. V-box (Velocity box) is the speed measuring device used for driving cycle data collection [6]. In the present study, speed data survey has been carried out for urban corridor of Vadodara city, Gujarat. Speed survey is conducted on regular weekdays during the peak period of traffic for auto rickshaw mode.

Kamble Sanghpriya et al. [7] developed Pune driving cycle consisting sequence of driving parameters; idle, acceleration, cruise, and deceleration. These parameters are considered as the indication for driving characteristic of the city. Nesamani and Subramanian [8] have discussed driving characteristics of another Indian city called Chennai. The speed characteristics of intra-city buses are collected through Global Positioning System. The results show that the time spent in idle mode is too high which is independent of road type and travel time. Seedam et al. [9] developed an onboard system to record real-world driving pattern of motorcycle mode for Khon Kaen city, Thailand. This system is validated through results of high precision.

Fotouhi and Montazeri-Gh [10] explained the new approach for the development of a driving cycle for Tehran city for car mode. The suburban area is also considered for the clustering the data. *K*-means clustering algorithm is used to cluster data into definite four groups. Salamati et al. [11] compared emissions of roundabout and signalized intersections by macroscopic approach. The emissions have been estimated based on the vehicle specific power considering demand-capacity ratio,

signal timing, and signal progression characteristics as variables. Song et al. [12] developed models for emissions and fuel consumption based on the influence of driving parameters on emission results. The set of mesoscopic vehicle emission and fuel consumption models are generated using real-world vehicle operation and emission data.

2 Objectives of Research

In the present study, driving cycle data called base data has been collected by auto rickshaw mode in Vadodara city. The main focus of this study is to generate candidate driving cycle based on real traffic data which represents the actual traffic condition. Driving cycle is divided into small sections called micro-trips and driving parameters namely average speed, maximum speed, average acceleration, average deceleration, maximum acceleration, maximum deceleration, percentage time spent in acceleration, percentage time spent in deceleration, percentage cruise time, and percentage idle time calculated for base cycle and micro-trips. A code has been developed to segregate micro-trips from base data and parameters have been computed. Further *K*-means clustering algorithm is used to compile micro-trips with similar characteristics, and finally, representative micro-trips have been selected on the basis of the least distance from the cluster center. Selected micro-trips are chained and arranged to get profile of candidate cycle. A number of candidate cycles can be produced from micro-trip. The prime objective of this study is to generate candidate driving cycle which is a representative cycle for the study area and further can be used for emission estimation. Emission is estimated at macro-level-based on the activity of the average speed.

3 Study Corridor and Data Collection

Vadodara is the third largest city in the Gujarat state in India in terms of population and covered area. The vehicle maneuver in the city is directed by 30 main roads and possesses overall 303 km length. The construction of additional roads has not been taken place in the last few years. The vehicular population is increasing at a greater amount with a rising rate of 8–9% per year. The study area comprises considerable vehicle population of 2W, 3W and 4W share 95% in total vehicle composition.

3.1 Study Corridor

Speed data has been collected for the Old Padra road of the city located at central business district. The study corridor has an origin point Akshar chowk from which

the test vehicle is driven to collect real-world data. The end point of the corridor is Genda circle located at 4.3 km distance from origin. The speed fluctuation is observed in the corridor due to the role of intersection and their relative distances. Figure 1 shows the location of intersections in the study corridor. Distance of intersections from origin point is shown in Table 1. Intersections I1, I2, I3, and I5 are signaled intersections whereas I4 is a rotary intersection. I2, I3 and I4, I5 are closely spaced. V-box (Velocity box) is mounted on the test vehicle to capture the speed of specific vehicle on the corridor. Figure 2 shows speed–distance plot of driving cycle in peak hour period for auto rickshaw mode. Vertical bars in figure indicate the location of intersections.

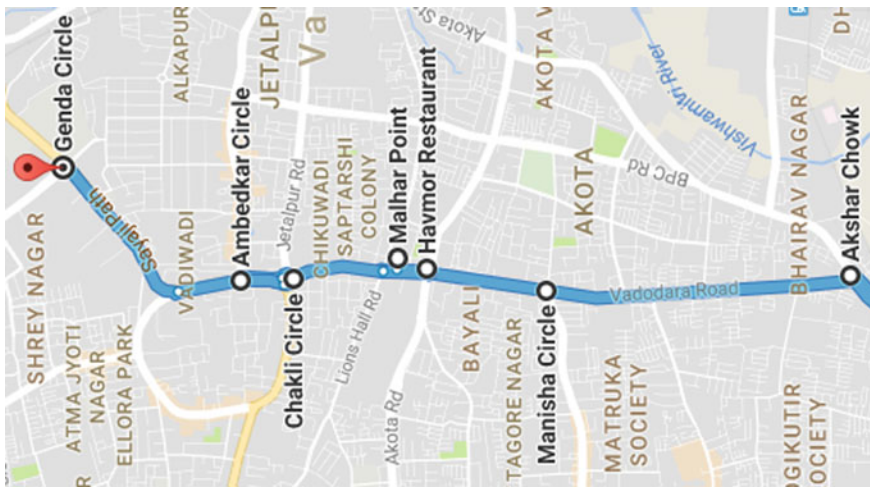


Fig. 1 Location of intersection in study corridor

Table 1 Distance of intersections from the origin point

Corridor	Distance (km)
Akshar chowk (origin point)	0.0
Vasna circle (I1)	1.6
Havmore intersection (I2)	2.2
Malhar point circle (I3)	2.4
Chakli circle (I4)	2.9
Ambedkar circle (I5)	3.2
Genda circle (End point)	4.3

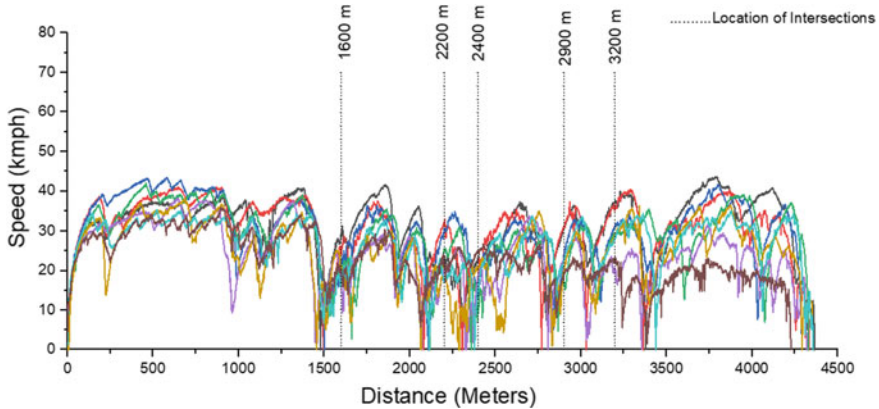


Fig. 2 Driving cycle profile for auto rickshaw mode

4 Data Treatment Methodology

Data collection for driving cycle comprises of GPS system in performance box. The driving cycle is developed from micro-trips. Micro-trips are the stretch of driving cycle between two successive stop conditions of the vehicle. Micro-trips express the existing traffic condition. This methodology considers important driving parameters of speed–time profile, namely acceleration, deceleration, idle, cruise, average speed, maximum speed, maximum acceleration, maximum deceleration, average acceleration, and average deceleration.

4.1 Driving Cycle Development Methodology Based on Micro-trip

Micro-trip is an expedition between two successive time points at which the vehicle is stopped. This section of motion consists of driving activities like acceleration, cruise, idle, and deceleration modes of vehicle. By accordance, a period of idling of vehicle is at the starting and end of a micro-trip. The steps involved in the construction of candidate cycle are data collection, segregation of base data in form of micro-trips, compiling of micro-trips, selecting representative micro-trips, and arranging selected micro-trips in series to get final candidate driving cycle. The vehicle speed with respect to time or distance is recorded on the selected route. Real data is divided into number of micro-trips. Figure 3 shows the methodology in detail for generating the candidate driving cycle. Data has been analyzed by calculating several driving parameters for the base cycle and micro-trips. Driving parameters of candidate driving cycle are also calculated for the selection of the best cycle. Driving parameters comprise the percent time in acceleration, percent time in deceleration, percent time

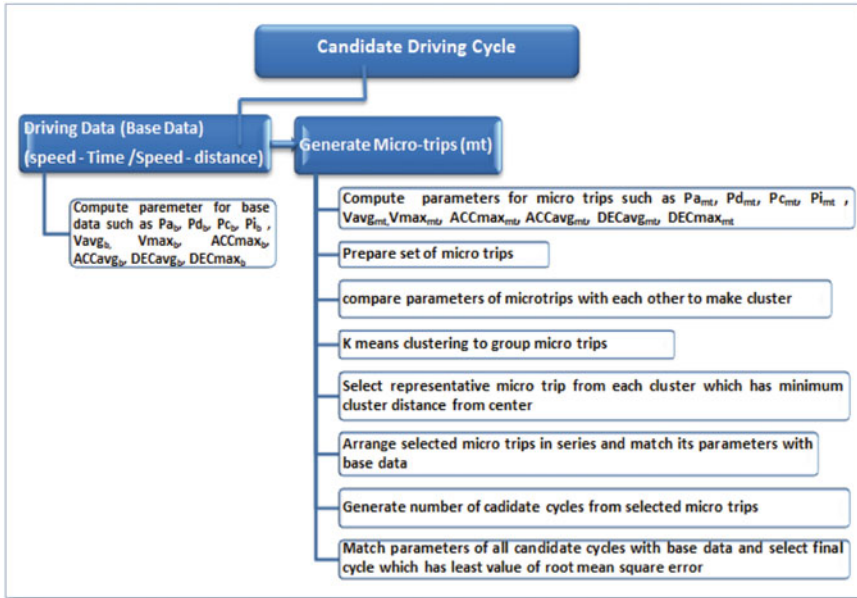


Fig. 3 Candidate driving cycle development methodology

in cruise, percent time in idle, average velocity, maximum speed, average acceleration, maximum acceleration, average deceleration, and maximum deceleration. A total of ten parameters have been taken for the generation of the representative cycle [13]. The following ten parameters are computed for base data and micro-trips data [14, 8].

1. Average speed (V_{avg})—Average speed of entire trips (kmph)
2. Maximum speed (V_{max})—Maximum speed of entire trips (kmph)
3. Average acceleration (Acc_{avg})—Average acceleration of entire trips (m/s^2)
4. Average deceleration (Dec_{avg})—Average deceleration of entire trips (m/s^2)
5. Maximum acceleration (Acc_{max})—Maximum acceleration of entire trips (m/s^2)
6. Maximum deceleration (Dec_{max})—Maximum deceleration of entire trips (m/s^2)
7. Percentage of time spent in acceleration mode (P_a)—Acceleration greater than $0.1 m/s^2$
8. Percentage of time spent in deceleration mode (P_d)—Acceleration less than $-0.1 m/s^2$
9. Percentage of time spent in cruise mode (P_c)—Speed greater than 5 kmph and acceleration -0.1 to $0.1 m/s^2$
10. Percentage of time spent in idle mode (P_i)—Speed less than 5 kmph and acceleration -0.1 to $0.1 m/s^2$

Parameters are calculated for base data and generated micro-trips. The parameters of the first micro-trip are compared with other micro-trips and their groups are

formed. Clustering of micro-trips is done by *K*-means clustering method, and groups of micro-trips are prepared which have similar driving characteristics. The representative micro-trips which have less distance from the cluster center are selected and all selected micro-trips from the respective group are arranged to generate the candidate driving cycle. The procedure is repeated for different clusters of micro-trips, and the number of candidate cycles has been generated. The same parameters are calculated for the candidate cycle and checked with the base data. The candidate driving cycle which has minimum deviation from base data is selected as a final cycle and represents the speed characteristics of study area [15].

Computer program is generated to get micro-trips from base data. Micro-trips are generated from base data even of 0.2 s also. These micro-trips do not serve the purpose as they are not correct description of the data. In the present study, the micro-trips up to 5 s are not considered in the analysis. Figure 4 shows the segregation of micro-trips through programming. Large numbers of micro-trips have been generated, and all driving parameters are calculated for micro-trips. To handle a large amount of data and to generate the candidate cycle, it is necessary to make a cluster of micro-trips which have similar characteristics. Clustering is done on the basis of driving

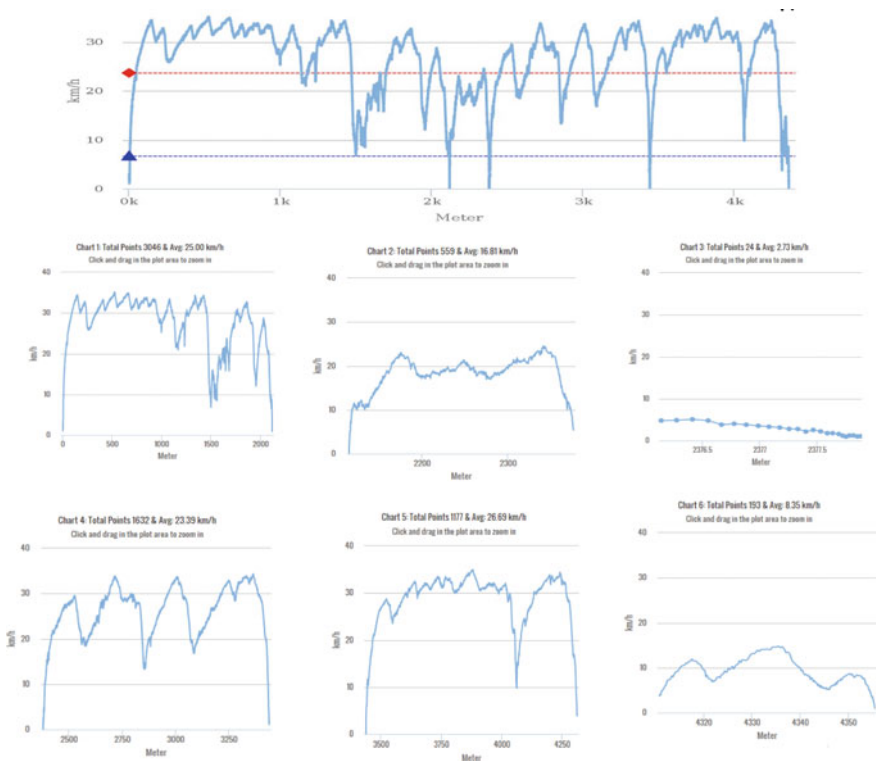


Fig. 4 Generated micro-trips from base cycle

parameters. *K*-means clustering is used to group micro-trips. It can be easily done in SPSS software. In the software, the inbuilt function requires necessary input from user and numbers of clusters have been given to generate groups. *K*-means clustering gives a definite distance of micro-trips from the cluster center, which indicates the parameters of individual micro-trips are closely related to the cluster center. The micro-trips with the least value of the cluster center in each group have been taken for the generation of candidate driving cycle.

4.2 *RMSE (Root-Mean-Square Error) for Selecting Candidate Cycle*

To consider all the criteria for cycle synthesis, the RMSE is introduced for selecting the best driving cycle. It represents the absolute sum of the differences of the selected parameters between the candidate cycle and the target statistics. The root-mean-square error (RMSE) (also called the root-mean-square deviation, RMSD) is a used measure of the difference between values calculated by a model and the values actually observed from real data. The RMSE is defined as the square root of the mean squared error. In the present study, the error has been estimated to select final candidate cycle from number of the generated candidate cycles. Equation 1 shows the difference of value for observed data and calculated data.

$$\text{RMSE} = \sqrt{\frac{\sum_{i=1}^n (X_{\text{obs},i} - X_{\text{model},i})^2}{n}} \quad (1)$$

where X_{obs} is observed values and X_{model} is modeled values.

The smaller RMSE value, the better real-world driving pattern is represented. Therefore, the candidate cycle with the least error will be selected as the most representative driving cycle for the corresponding group.

5 Results and Analysis

As per the methodology discussed earlier, data has been analyzed for auto rickshaw mode. The travel time taken for this corridor varies from 590 to 800 s for one direction of traffic. Total 53 micro-trips are generated from base data and used to generate candidate driving cycles. Figure 5 shows the driving parameters for the base data.

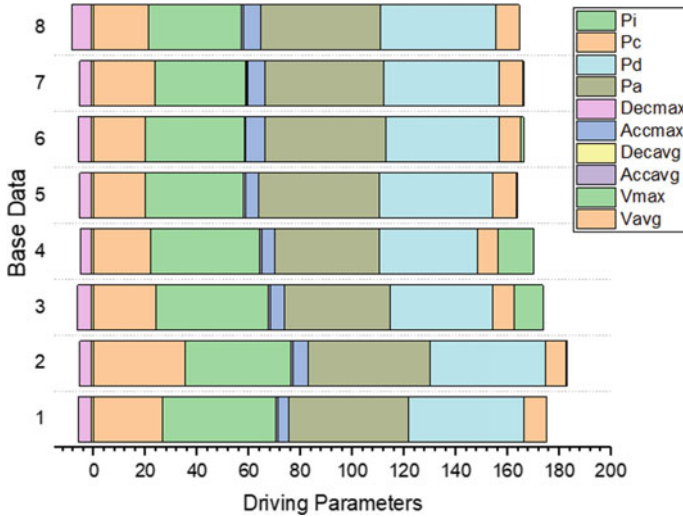


Fig. 5 Driving parameters for base data

5.1 Candidate Driving Cycle

K-means clustering is used to compile micro-trips which have similar characteristics in terms of driving parameters. *K*-means clustering is used to group or classify parameters based on characteristics into *K* number of groups. Micro-trips are grouped according to their parameter characteristics. Figure 6 shows the candidate driving cycle generated after compiling representative micro-trips from each group.

Candidate cycles are generated by arranging the representative micro-trips from each cluster. Each representative micro-trip has the least cluster distance from the center. Numbers of clusters are generated from total micro-trips, and it is matched with the base data. All ten parameters have been calculated for the generated candidate cycles and final candidate cycle selected on the basis of the least root-mean-square error.

Table 2 shows four candidate cycles generated from 53 micro-trips and their parameters are compared with the base cycle. Among all four cycles, cycle-4 has minimum RMSE, which is selected as final candidate cycle and taken for emission estimation.

5.2 Emission Estimation

The generated driving cycles are matched with the base data, and the final cycle has been selected which is used for emission estimation. Final candidate cycle is the representative speed profile for study area [16]. In the present paper, emission

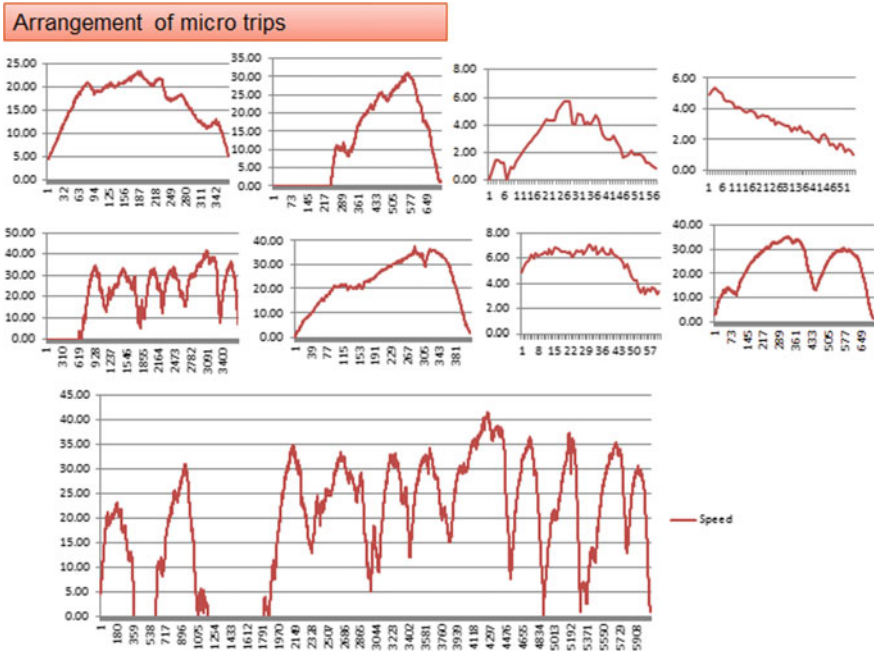


Fig. 6 Generated candidate cycle from representative micro-trips

estimation is done at the macroscopic level. The parameter average speed has been taken for estimation. The measurement of exhaust emissions of vehicles is done by using the following equation [17]. The given equation of emission estimation is useful in macro-level estimation where detailed information is not required. Emission is estimated using Eq. 2 in which average speed is taken as an activity and emission factor is taken according to mode of vehicle and fuel type.

$$E = A * EF \tag{2}$$

where

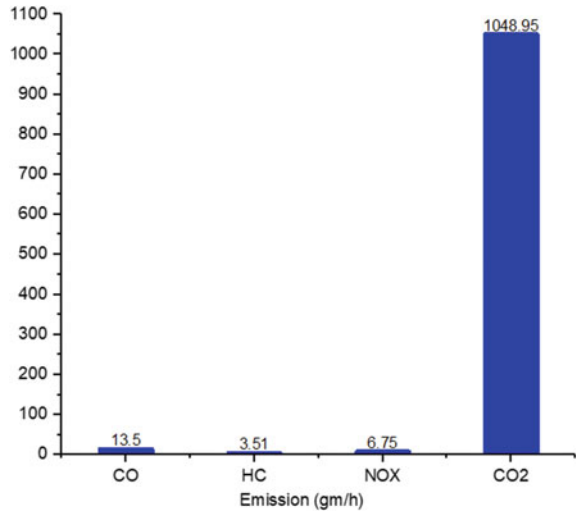
- E* emissions, gm/h,
- A* activity rate, in terms of average speed, kmph
- EF* emission factor, gm/km

The total emission is calculated by using emission factors. In Fig. 7, the emission factor is taken as 1 g/km for CO, 0.26 g/km for HC, 0.5 g/km for NO_x, and 77.7 g/km for CO₂ based on vehicle mode as auto rickshaw and fuel-type CNG [18]. The final emission in terms of g/h is calculated based on average speed as an activity. The average CO emission is 13.5 g/h, HC emission is 3.51 g/h, NO_x emission is 6.75 gm/h, and CO₂ emission is 1048.95 gm/h.

Table 2 Candidate cycle parameters and final candidate cycle

Candidate cycle	V_{avg} (kmph)	V_{max} (kmph)	Acc_{avg} (m/s^2)	Dec_{avg} (m/s^2)	Acc_{max} (m/s^2)	Dec_{max} (m/s^2)	P_a (%)	P_d (%)	P_c (%)	P_1 (%)	RMSE
Candidate cycle-1	13.45	23.48	0.61	- 0.65	1.89	-2.41	31.01	34.13	25.99	8.87	9.99
Candidate cycle-2	12.71	22.37	0.67	- 0.71	2.09	-2.61	33.795	34.73	23.57	8.01	9.39
Candidate cycle-3	14.11	24.49	0.674	- 0.71	2.18	-2.88	34.99	35.72	22.09	7.21	8.33
Candidate cycle-4	13.5	23.21	0.72	- 0.76	2.54	-2.76	35.83	36.38	20.52	7.27	8.25

Fig. 7 Emission estimation



6 Conclusion

The present methodology is based on calculating ten important driving parameters of time–speed profile; the percentage time spent in acceleration, deceleration, idle, and cruise, average and maximum acceleration, average and maximum speed, average, and maximum deceleration. The final driving cycle is constructed by micro-trips method. The driving cycle for Vadodara city is constructed and compared with the collected base data. The generated candidate cycle is compared with the parameters of base data, and the cycle has the least root-mean-square error has been selected as a final representative candidate cycle. The final candidate cycle is used for emission estimation. An average speed is taken as an activity for emission estimation, which estimates emission value at macro-level. The estimated emission does not give the amount of pollutants at different speed fluctuation but gives an average amount of pollutants generated in the study area based on the emission factor. The main focus of the analysis is to highlight the method for candidate driving cycle construction.

References

1. Yu L, Wang Z, Shi Q (2010) PEMS-based approach to developing and evaluating driving cycles for air quality assessment. Report SWUTC/10/169300-1, pp 1–94. <https://static.tti.tamu.edu/swutc.tamu.edu/publications/technicalreports/169300-1.pdf>
2. Kumar Ravindra, Saleh Wafaa, Durai BK, sharma Neeraj (2012) Development of motorcycle driving cycle and estimation of emissions from micro-simulation models. *J Environ Protect* 3:1268–1273
3. Blacksbury V (2009) A reference book of driving cycle for use in measurement of road vehicle emissions. Published Project Report PPR 354. <https://trl.co.uk/reports/PPR354>

4. Sinha S, Kumar R (2013) Driving cycle pattern for cars in medium sized city of India. In: Proceedings of the Eastern Asia Society for Transportation Studies, vol 9
5. Andr M, Rapone M, Joumard R, Inrets-lte R (2006) Analysis of the cars pollutant emissions as regards driving cycles and kinematic parameters. Report INRETS—LTE 0607. <https://hal.archives-ouvertes.fr/hal-00545918/document>
6. Bokare Prashant Shridhar, Maurya Akhilesh Kumar (2013) Study of effect of speed, acceleration and deceleration of small petrol car on its tail pipe emission. *Int J Traffic Transp Eng* 3(4):465–478
7. Kamble Sanghpriya H, Mathew Tom V, Sharma GK (2009) Development of real-world driving cycle: case study of Pune, India. *Transp Res Part D Transp Environ* 14(2):132–140
8. Nesamani KS, Subramanian KP (2011) Development of a driving cycle for intra-city buses in Chennai, India. *Atmos Environ* 45:5469–5476
9. Seedam A, Satiennam T, Radpukdee T, Satiennam W (2015) Development of an onboard system to measure the on-road driving pattern for developing motorcycle driving cycle in Khon Kaen city, Thailand. *IATSS Res* 39:79–85
10. Fotouhi A, Montazeri-Gh M (2013) Tehran driving cycle development using the k-means clustering method. *Scientia Iranica* 20(2):286–29. <https://doi.org/10.1016/j.scient.2013.04.001>
11. Salamati K, Roupail NM, Frey HC, Liu B, Schroeder BJ (2017) Simplified method for comparing emissions in roundabouts and at signalized intersections. *Transp Res Rec J Transp Res Board* 2517:48–60. <https://doi.org/10.3141/2517-06>
12. Song Y, Yao E, Zuo T, Lang Z (2013) Emissions and fuel consumption modeling for evaluating environmental effectiveness of ITS strategies. *Discrete Dyn Nat Soc*. <http://dx.doi.org/10.1155/2013/581945>
13. Tamsanya S, Chungpaibulpattana S, Atthajariyakul S (2006) Development of automobile Bangkok driving cycle for emissions and fuel consumption assessment. In: The second joint international conference on sustainable energy and environment, pp 1-6
14. Brady and O'Mahony (2013) The development of a driving cycle for the greater Dublin area using a large database of driving data with a stochastic and statistical methodology. In: Proceedings of the ITRN2013, Trinity College Dublin, pp 1–24
15. Hung WT, Tong HY, Lee CP, Ha K, Pao LY (2007) Development of a practical driving cycle construction methodology: a case study in Hong Kong. *Transp Res Part D* 12:115–128
16. Jiun-HorngTsai Hung-Lung Chiang, Hsu Yi-Chun, Peng Bo-Jun, Hung Rong-Fang (2005) Development of a local real world driving cycle for motorcycles for emission factor measurements. *Atmos Environ* 39:6631–6641
17. Mathew T (2014) Fuel consumption and emission studies. *Transp Syst Eng*. http://nptel.ac.in/courses/105101008/downloads/cete_43.pdf
18. The Automotive Research Association of India (2008) Air quality monitoring project—Indian clean air programme (ICAP). Project Rep No.: AFL/2006-07/IOCL/Emission Factor Project/FinalRep, ARAI, Pune. http://www.cpcb.nic.in/Emission_Factors_Vehicles.pdf

Effect of Pedestrian Hybrid Beacon Signal on Operational Performance Measures at the Mid-block Location and Adjacent Signalized Intersection



Nutan Teketi and Srinivas S. Pulugurtha

Abstract Pedestrian hybrid beacon (PHB) signals, formerly known as High-intensity Activated crossWalk (HAWK) signals, are used at mid-block crosswalk locations to assist pedestrians safely cross high traffic volume/high-speed/multi-lane roads. The PHB signals help decrease pedestrian crashes and increase their safety. However, interrupting the flow of traffic and bringing vehicles to a complete stop at mid-block crosswalk locations could increase delay and reduce operational performance, in particular, along coordinated signal corridors. The reduction in the operational performance may extend to downstream and upstream intersections, making it overall operationally ineffective. This study focuses on evaluating the effect of PHB signals on operational performance measures at the mid-block crosswalk location as well as the adjacent signalized intersection. VISSIM traffic microsimulation software was used to compute the delay and maximum queue length at three different PHB signal locations and their adjacent signalized intersections in Charlotte, North Carolina. The effect of an increase in pedestrian volume and traffic volume on delay and maximum queue length at each PHB signal location and adjacent signalized intersection was studied. Further, the effect of the distance between a PHB signal location and the nearest signalized intersection on delay and maximum queue length was also studied. The findings indicate that a PHB signal location nearer to a signalized intersection has a significant effect on delay and maximum queue length at the signalized intersection. As the distance of the PHB signal location from the signalized intersection increases, delay decreases. Further, an increase in the pedestrian volume and traffic volume will increase delay and maximum queue length at the PHB signal location and adjacent signalized intersection only up to some extent.

Keywords High-intensity Activated crossWalk (HAWK) · Pedestrian hybrid beacon (PHB) · VISSIM · Delay · Maximum queue length

N. Teketi · S. S. Pulugurtha (✉)
The University of North Carolina at Charlotte, Charlotte, NC 28223-0001, USA
e-mail: sspulugurtha@uncc.edu

N. Teketi
e-mail: nteketi@uncc.edu

1 Introduction

Crosswalks for pedestrians are generally provided at either signalized or unsignalized intersections or at mid-block locations where more pedestrian activity or pedestrian crashes are observed. The crosswalks help the pedestrians to safely cross from one end of the road to the other end of the road. Mid-block crosswalk locations with low vehicular volume are usually provided with pedestrian yield control, while mid-block crosswalk locations with high vehicular volume are provided with High-Intensity Activated crossWalk (HAWK) signal [1] or pedestrian signal. Pedestrian yield controls are installed at a distance from the crosswalk to alert the motorist and yield to the crossing pedestrian. This may result in less safety to the pedestrian when installed on the road with higher traffic volume [2].

HAWK signals, currently referred to as pedestrian hybrid beacon (PHB) signals, are generally provided at mid-block crosswalk locations between two intersections on the major approaches where high vehicular volumes are observed. The head of a PHB signal consists of two red lenses above a single yellow lens. The signal is normally dark until a pedestrian activates the system. When activated by a pedestrian, initially yellow flashing is observed for a few seconds to alert the motorists that the signal has been activated. The flashing yellow is followed by a steady red indication to stop the vehicles and create a gap for pedestrians to cross the road [1]. After the pedestrian walking phase ends, the pedestrian signal indicates flashing don't walk to notify the pedestrians not to begin crossing. During the flashing don't walk phase, PHB signal displays alternating flashing red light to allow motorists to proceed after stopping if pedestrians have cleared the road.

The alternating flashing red light during flashing don't walk phase of pedestrian signal often causes confusion to motorists even after pedestrian clearance. As a result, increasing vehicular delay is observed near the PHB signal locations during peak hours. As PHB signals are typically installed along high traffic volume/high-speed/multi-lane roads, the effect on delay and maximum queue length gets often extended to upstream and downstream intersections.

The effect of a PHB signal installed at a mid-block crosswalk location and adjacent signalized intersection could depend on pedestrian volume and traffic volume along the road. It could also depend on the distance between the mid-block crosswalk location with the PHB signal and the adjacent signalized intersection.

The primary focus of this paper is on evaluating the effect of a PHB signal on delay and maximum queue length at the mid-block crosswalk location and the adjacent signalized intersection.

2 Literature Review

PHB signals were first implemented in Arizona to assist pedestrians safely cross a road in the late 1990s. These signals were proven to be effective in decreasing the number of pedestrian crashes by 69% and total crashes by 29% [2]. A few researchers

focused on delay and behavioral changes that could occur due to the installation of the PHB signals. Arhin and Noel [3] observed that 50–65% of the pedestrians follow the PHB signal. They seem to be ineffective when installed along low traffic volume corridors. Pulugurtha and Self [4] observed that there are no negative consequences, behavioral related, due to the installation of the PHB signal at two out of three PHB study locations considered in their study.

Schroder et al. [5] observed that PHB signals are more effective in reducing delay compared to the normal pedestrian actuated signal. Godavarthy and Russell [6] observed that the PHB signals decrease delay compared to signalized mid-block locations, if motorists understood the operation of the PHB signals. Li and Zhang [7] observed that the installation of the PHB signals reduce pedestrian delay when pedestrian volume and traffic volume are low. They also observed that the PHB signal causes excessive delay for pedestrians at stop-controlled intersection, where traffic volume is typically low.

Literature documents several other efforts on the effectiveness of PHB signals to improve pedestrian safety and reduce pedestrian delay [8–13]. Sandt and Zegeer [14] compared the crashes at mid-block locations and intersections with respect to determining safety treatments for mid-block locations. Fitzpatrick and Park examined the total number of severe vehicle and pedestrian crashes before and after the installation of PHB signals using Empirical Bayes (EB) method. The results obtained from their study showed a 13–29% reduction in all crashes and ~50% reduction in the pedestrian crashes [15]. There could be some negative consequences due to a lack of adequate understanding of the signal operation, sudden stopping of vehicles by motorists, or other reasons. The negative consequences due to the installation of PHB signals could depend on demographic characteristics, socioeconomic characteristics, land use characteristics, and on-network characteristics.

Overall, literature documents that the PHB signals may not be effective at all mid-block crosswalk locations. The operational performance of PHB signals and its effect on adjacent signalized intersections was not investigated in the past. Further, the effect of traffic volume, pedestrian volume, and distance to the adjacent signalized intersection were not examined in the past. This paper focuses to address these limitations and contributes to the body of knowledge. The findings from this research help assess and identify operational conditions under which a PHB signal might be effective.

3 Methodology

The methodology adopted to conduct this research is discussed in this section.

3.1 Study Area

Three mid-block crosswalk locations with PHB signals and their adjacent signalized intersections in the city of Charlotte, North Carolina, USA were selected to evaluate the effect of PHB signals on operational performance. The selected PHB signal locations are:

- I. PHB signal on University City Blvd; 700 ft. from University City Blvd and John Kirk Dr intersection.
- II. PHB signal on N Tryon St; 800 ft. from N Tryon St and East Mallard Creek Church Rd intersection.
- III. PHB signal on JW Clay Blvd; 1300 ft. from N Tryon St and JW Clay Blvd intersection.

3.2 Data Collection

Data required for the analysis is pedestrian volume, traffic volume, geometric characteristics, and signal timing and phasing details of each adjacent signalized intersection. The evening peak hour traffic volume, signal timings, and phasing details of the adjacent signalized intersections were collected from the city of Charlotte Department of Transportation (CDoT). Pedestrian volume data was collected from the field during the evening peak hour using traffic counters. Google Earth was used to capture the geometric characteristics of each selected mid-block crosswalk location and adjacent signalized intersection.

3.3 Model Building

VISSIM microsimulation software was used to develop simulation models for each selected mid-block crosswalk location and the adjacent signalized intersection. The aerial image of study locations was captured using Google Earth and added in VISSIM as a background image to model the existing condition. The background image was scaled to add links and pedestrian crosswalk as per the existing condition. After adding the background image, links were added as per the lane configuration with separate through lanes, left turning lanes, and right turning lanes within the network (extends up to 0.5 miles from the mid-block crosswalk and the adjacent signalized intersection in all directions).

Traffic volume and static routes of vehicles were provided in VISSIM to input patterns of vehicles going through, left, and right in the selected network. Signal controller with actual signal timing and phasing details were designed, and signal heads were placed on each link, at each PHB signal and adjacent signalized intersection.

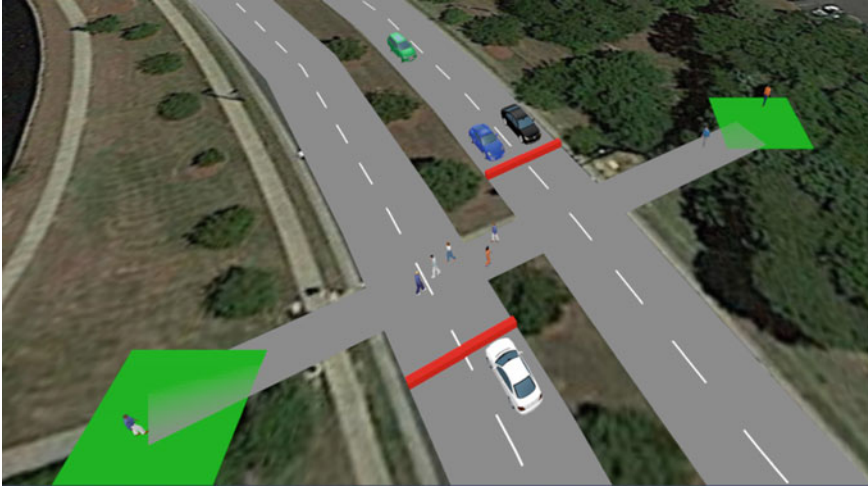


Fig. 1 VISSIM model for JW Clay Blvd PHB signal location

The pedestrian mid-block crosswalks were also added at each PHB signal location. Pedestrian volume inputs in each direction and pedestrian static routes were then specified. The signal controller for pedestrians at each PHB signal location was designed and placed at the mid-block crosswalk location (both directions of crossing). The detectors were placed at the mid-block crosswalk to stop the vehicular traffic when a pedestrian is crossing at each mid-block crosswalk location. Figure 1 represents the model built in VISSIM at PHB signal location on JW Clay Blvd.

Different seed numbers are generally preferred to test and replicate the actual traffic scenario on a road. All the aforementioned models were simulated independently with ten different random seed numbers. The average of ten different random seed numbers were used to estimate the outputs such as traffic flow, delay, and maximum queue length.

3.4 Model Calibration

It is important to calibrate the model developed in VISSIM to mimic existing conditions and yield accurate results. All the three models were calibrated using existing traffic volumes. A simulation time of 3600 s with 900 s intervals was selected for the analysis. The vehicle network performance results in VISSIM give the total number of vehicles that were generated by the model. This total vehicular volume generated by the model was compared with the vehicle input to assess the accuracy of the model.

Table 1 shows the total vehicular volume generated, input volume, and the percentage of traffic volume (Eq. 1) generated at each PHB signal location. The percent-

Table 1 Comparing traffic volumes generated and provided as input

Intersection	Input volume (vehicles)	Volume generated by the model (vehicles)	% of accuracy
University City Blvd and John Kirk Dr	4218	3880	92
N Tryon St and E Mallard Creek Church Rd	4613	4248	91
N Tryon St and JW Clay Blvd	3013	2713	90

age indicates the accuracy and illustrates the replication of real-world road traffic scenario in the simulation environment. Higher percentage of accuracy results in yielding good results, mimicking the real-world scenario.

$$\% \text{Traffic Volume} = \frac{\text{Traffic volume generated by the model}}{\text{Traffic volume input into the model}} \times 100 \quad (1)$$

3.5 Computation of Average Delay and Maximum Queue Length

The average delay and maximum queue length at each PHB signal and adjacent signalized intersection were computed using actual pedestrian volume collected in the field and provided as an input to VISSIM. The pedestrian volume was then increased in 25% increments up to 100%. The average delay and maximum queue length were computed for each scenario and compared with the existing scenario to observe the change in delay and maximum queue length with an increase in pedestrian volume.

The analysis was also done by increasing the traffic volume in 25% increments up to 100%. The average delay and maximum queue length were computed for each scenario and compared with the existing scenario to observe the change in delay and maximum queue length with an increase in traffic volume.

The average delay and maximum queue length were also computed by altering the distance between the PHB signal location and the adjacent signalized intersection. Distances of 500, 1000, and 1500 ft. from the adjacent signalized intersection were considered for simulation and evaluation. The results obtained for each scenario were compared with the existing scenario to observe the change in delay and maximum queue length with the change in distance.

Node function in VISSIM was used to capture the delay and maximum queue length for each scenario. Figure 2 represents the node data collection point at the JW Clay Blvd PHB signal location. Similarly, nodes were placed at each PHB signal and



Fig. 2 Defining nodes at JW Clay Blvd PHB signal location

adjacent signalized intersection. The maximum queue lengths for each simulation and the 85th percentile of maximum queue length were then computed.

3.6 Validation of Model

For the validation of results, field data was collected and compared with the results obtained using VISSIM. Video cameras were used to collect field data during peak hour at each selected PHB signal location and their adjacent signalized intersection. The maximum queue lengths were observed from the video recordings. The average delay was computed using Eq. 2. The correction factor for different free-flow speeds and queuing vehicles was obtained from the Highway Capacity Manual [16].

$$D = TQ + CF * \frac{VS}{V} \quad (2)$$

where

D = Average delay per vehicle (s),

TQ = Time in queue per vehicle (s),

CF = Correction factor to convert stopped delay to control delay,

VS = Number of arriving vehicles stopping, and,

V = Total arriving volume of vehicles.

4 Results

Data was collected in the field at three mid-block crosswalk locations to compute the average delay and maximum queue length for each location. The results from field observations and VISSIM simulations are summarized in Table 2. The computed average delay and maximum queue length at the PHB signal locations are marginally lower than the average delay and maximum queue length observed in the field. They are relatively close without a definite trend at the adjacent signalized intersections. One possible reason for the difference in computed values and field observations could be not considering variation in traffic conditions within the study hour.

The differences between average delays and maximum queue lengths are higher for University City Blvd PHB signal location when compared to the other two PHB signal locations. Higher pedestrian and traffic volume could be the reason for higher differences at the University City Blvd PHB signal location.

Figure 3 depicts the variations in average delay and maximum queue length with an increase in pedestrian volume for all the three PHB signal locations. The average delay at PHB signal location on University City Blvd increased with pedestrian volume (by four times with a 100% increase in pedestrian volume) while the effect was marginal at the adjacent signalized intersection. Similarly, the maximum queue length increased (by two times with a 100% increase in pedestrian volume) while the effect was marginal at the adjacent signalized intersection.

The average delay and maximum queue length increased at the N Tryon St PHB signal location and the adjacent signalized intersection. While the average delay and maximum queue length increased at the JW Clay Blvd PHB signal location and its adjacent signalized intersection, there was no trend or increase in maximum queue length with an increase in pedestrian volume at this location.

Table 2 Delay and maximum queue length—comparison

Location	PHB signal		Adjacent intersection	
	Delay/vehicle (s)	Queue length (vehicles)	Delay/vehicle (s)	Queue length (vehicles)
<i>Field observations</i>				
University City Blvd	9.16	23	24.96	32
N Tryon St	7.04	16	34.64	28
JW Clay Blvd	7.39	6	26.38	11
<i>VISSIM simulations</i>				
University City Blvd	8.00	21	24.32	34
N Tryon St	5.70	15	32.44	26
JW Clay Blvd	6.00	6	27.46	12

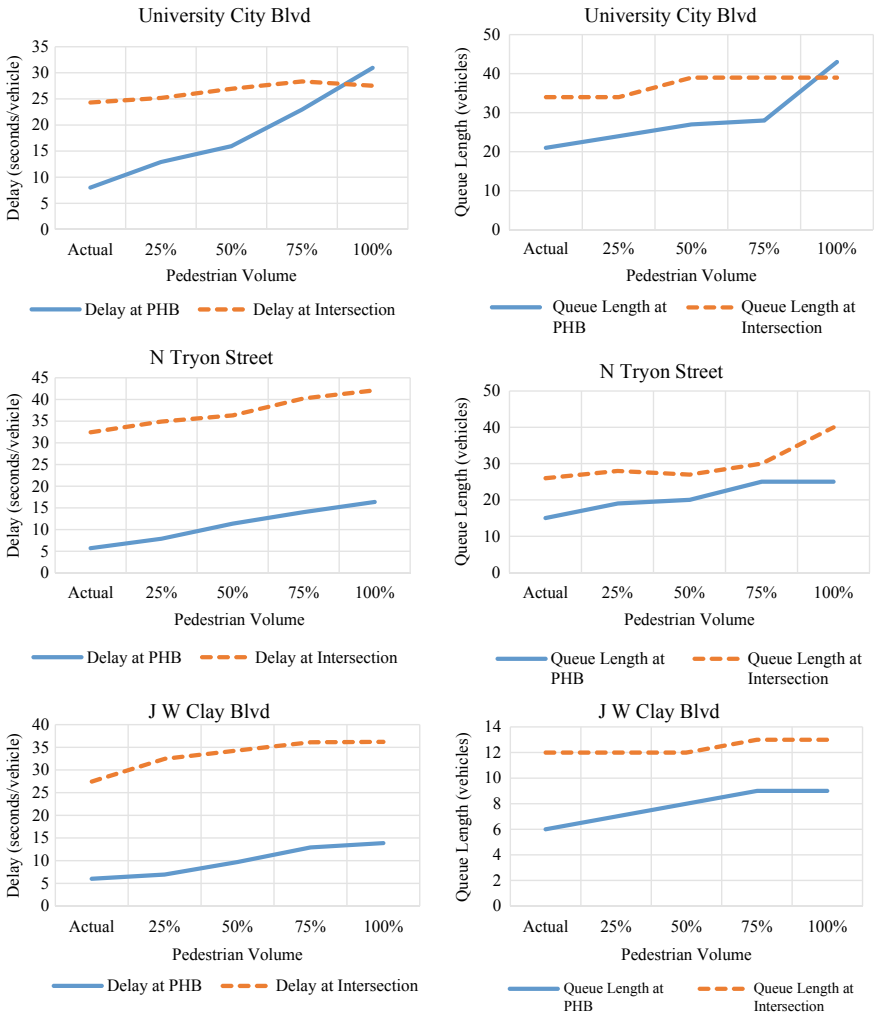


Fig. 3 Average delay and maximum queue length by pedestrian volume

The change in average delay and maximum queue length with an increase in traffic volume is shown in Fig. 4. The average delay and maximum queue length at PHB signal location on University City Blvd increased (by more than three times with a 100% increase in traffic volume), while the average delay at the adjacent signalized intersection reached the maximum when traffic volume was increased by 50% and tend to decrease with further increase in traffic volume. The maximum queue length increased by 1.38 times at the adjacent signalized intersection on University City Blvd when traffic volume was increased by 25% percent, while further increase in traffic volume did not show any increase.

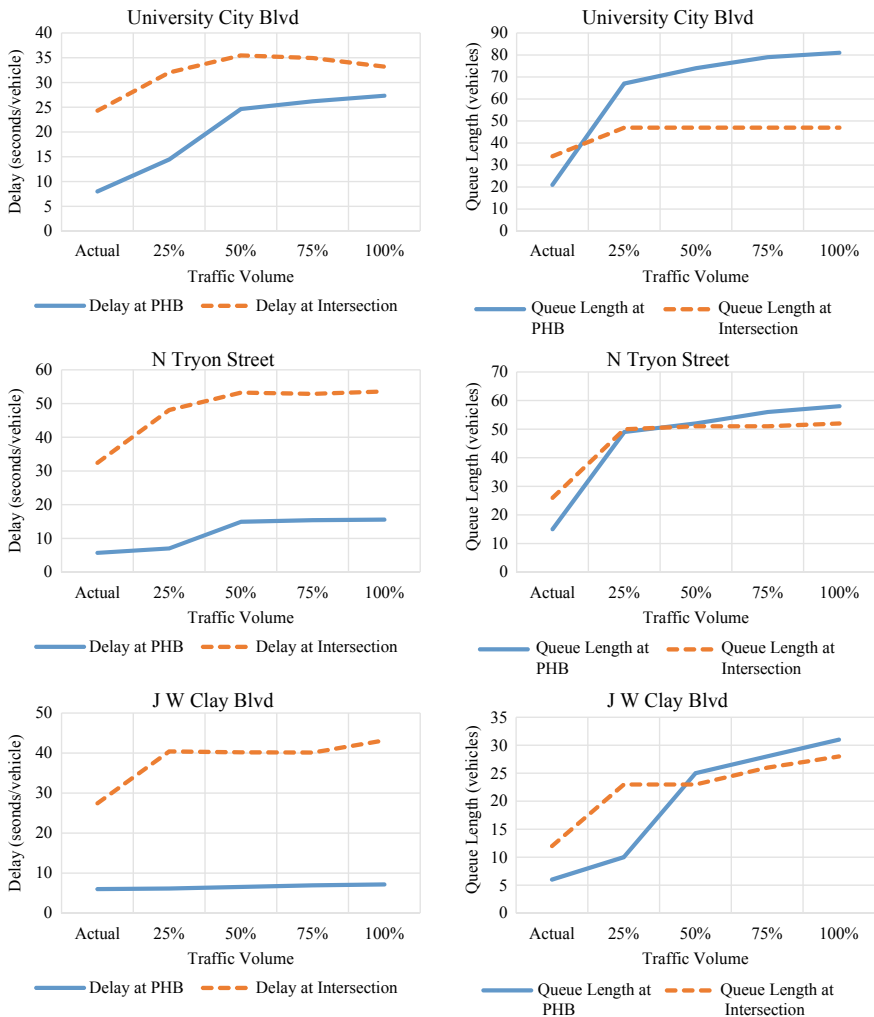


Fig. 4 Average delay and maximum queue length by traffic volume

The average delay and maximum queue length on N Tryon St PHB signal location and its signalized intersection increased up to 50% increment, while there was no trend with further increase in traffic volume. The results obtained from the simulation of the PHB signal location at J W Clay Blvd indicate that there was no increase in the average delay, while maximum queue length increased by five times with a 100% increase in traffic volume. The average delay and maximum queue length on J W Clay signalized intersection have increased up to 25% increase in traffic volume and further increase in traffic volume did not show any trend in increase.

The distance between the PHB signal and its adjacent intersection plays a major role during peak hour where spill over and spill back can be observed. The effect of distance between PHB signal and its adjacent intersection was evaluated by altering the distance. Distances of 500, 1000, and 1500 ft. from the signalized intersection were considered for the analysis. The simulation results with the change in the distance are summarized in Fig. 5. The average delay and maximum queue length at PHB signal location on University City Blvd decreased, while the maximum queue length at its adjacent intersection has increased with an increase in distance. Similarly, a decrease in the average delay and maximum queue length at PHB signal location on N Tryon St and its adjacent intersection was observed. The results obtained from

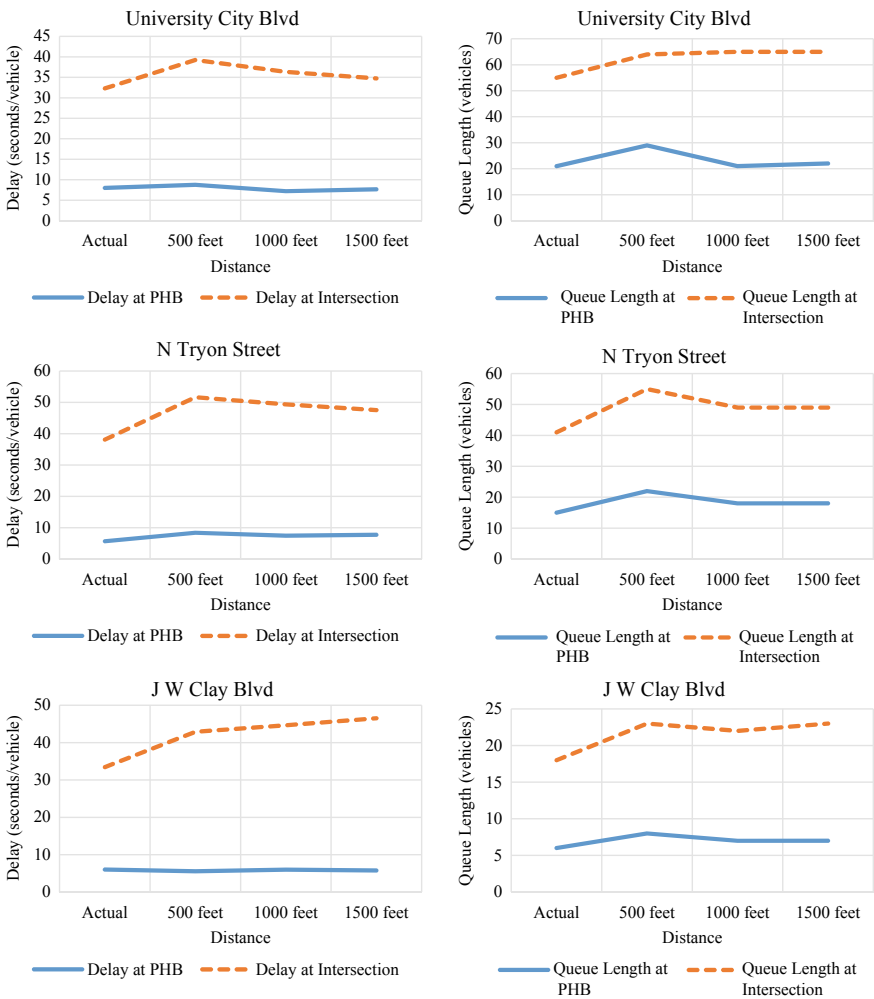


Fig. 5 Average delay and maximum queue length by distance

the simulation of J. W. Clay Blvd PHB signal location indicate that there is not much variation in the average delay and maximum queue length at this PHB signal location, while the change in the average delay and maximum queue length was observed at its adjacent intersection.

5 Conclusions

Three PHB signal locations were selected to evaluate the effect of PHB signal on operational performance at the location and adjacent intersections. The simulation models were validated by comparing vehicular input with the number of vehicles generated by each model. The models were found to be 90% accurate, replicating the existing condition. Delay and the maximum queue length at all the three PHB signal locations and adjacent signalized intersections were compared with the field data.

Delay and maximum queue length increased at one PHB signal location with an increase in pedestrian volume, while the increase at the other two PHB signal locations was only up to a 75% increase in pedestrian volume (26–30 pedestrians/h). Likewise, an increase in pedestrian volume at the PHB signal location influences its adjacent signalized intersection only up to a 75% increase in pedestrian volume (26–30 pedestrians/h). Further, an increase in pedestrian volume at the PHB signal location does not influence the adjacent signalized intersection. Installation of PHB signals at locations with higher pedestrian volume will have a significant effect at, both, PHB signal location and its adjacent intersection.

Delay and maximum queue length at two out of three PHB signal locations and its adjacent signalized intersections increased up to 50% of traffic volume (2049 vehicles/h for PHB signal within 800 ft. and 744 vehicles/h for PHB signal within 1300 ft. from its adjacent intersection) increase. An increase in traffic volume beyond 50% does not influence operational performances. Higher delays and maximum queue length were observed at the University City Blvd PHB signal location and its adjacent signalized intersection. The reason could be that University City Blvd has higher traffic volume and pedestrian volume compared to the other two PHB signal locations. The distance from adjacent signalized intersection could also be the reason for higher delay and maximum queue length at this PHB signal location. The results obtained from hypothetical scenarios also indicate that delay could be lower if the distance between a PHB signal location and the adjacent signalized intersection is higher. Also, the installation of the PHB signal greater than 500 ft. from its adjacent intersection will have a marginal effect on delay and maximum queue length at the PHB signal location and its adjacent intersection compared to PHB signals within 500 ft. Irrespective of pedestrian volume and traffic volume, the distance between the PHB signal location and its adjacent intersection plays a key role on vehicular delay and maximum queue length. It is recommended to install a PHB signal at a distance greater than 500 ft. from its adjacent signalized intersection.

References

1. Federal Highway Administration. <https://www.fhwa.dot.gov/publications/research/safety/10045>
2. Federal Highway Administration. http://safety.fhwa.dot.gov/ped_bike/tools_solve/fhwasa14014
3. District Department of Transportation. <http://www.pedbikeinfo.org/cms/downloads/Final%20Report%20-%20HAWK%20Signal%208-30-2010.pdf>
4. Pulugurtha SS, Self DR (2015) Pedestrian and motorists' actions at pedestrian hybrid beacon sites: findings from a pilot study. *Int J Injury Control Safety Promot* 22(2):143–152
5. Schroeder BJ, Roupail NM, Hughes RG (2008) Toward roundabout accessibility—exploring the operational impact of pedestrian signalization options at modern roundabouts. *J Transp Eng* 134(6):262–271
6. Godavarthy RP, Russell ER Sr, Effectiveness of a HAWK beacon signal at mid-block pedestrian crossings in decreasing unnecessary delay to the drivers. Transportation Research Board 89th Annual Meeting, Washington, DC
7. Li S, Zhang Y (2011) Pedestrian delay and HAWK pedestrian treatment. Transportation Research Board 90th Annual Meeting, Washington, DC
8. Swartz DL (2009) Implementing hybrid (HAWK) pedestrian signals, ITE 2009 Technical conference and exhibit
9. Transportation Research Board. http://onlinepubs.trb.org/onlinepubs/nchrp/nchrp_w91.pdf
10. Shurbutt J, Van Houten R, Turner S, Huitema B (2009) Analysis of effects of LED rectangular rapid-flash beacons on yielding to pedestrians in multilane crosswalks. *Transp Res Rec* 2140:85–95
11. Ullman B, Fitzpatrick K, Trout N (2004) On-street pedestrian surveys of pedestrian crossing treatments. ITE Annual Meeting and Exhibit, Orlando, FL
12. Van Houten R, Ellis R, Marmolejo E (2008) Stutter-flash light-emitting-diode beacons to increase yielding to pedestrians at crosswalks. *Transp Res Rec* 2073:69–78
13. Nassi R, Barton M (2008) New traffic control for an old pedestrian crossing safety problem. *APWA Reporter* 75(6):44–49
14. Sandt L, Zegeer C (2006) Characteristics related to midblock pedestrian—vehicle crashes and potential treatments. *Transp Res Rec* 1982:113–121
15. Fitzpatrick K, Park E (2009) Safety effectiveness of HAWK pedestrian treatment. *Transp Res Rec* 2140:214–223
16. Federal Highway Administration. <https://ops.fhwa.dot.gov/publications/fhwahop08054/sect3.htm>

Preference Contour Model for Traffic Planning and Management of Tourist Place in Andaman and Nicobar Islands



Surendran Raji

Abstract The traffic system, in any tourist intensive place, requiring of static or dynamic seasonal planning needs to be monitored with an effective Management Information System (MIS). Properly designed planning tools help in controlling the growth of traffic population addressing the needs of sustainable development especially in an island atmosphere where land use pattern is governed by tourism-related activities and capacity is restricted due to limited natural resources. Havelock Island, known for its beaches, rich coral reefs, and lush green forest and much sought after tourist destination by all tourists visiting Andaman and Nicobar Islands, is one such tourist destination where concentrated development of tourism-related infrastructures has made network of roads spread across the islands leaving less scope for expansion and posing challenge for overloaded capacity for existing carriageway. The growth of tourism industry for last one decade has been a major contributor to the increased economic activity throughout the islands and also it has created jobs making it a dominant economic activity. The impacts of tourism, on the other side of this growth, are not widely understood therefore still has not become greatest interest or concern. Many people think of tourism in terms of economic impacts, jobs, and taxes; however, the range of impacts includes uncontrolled growth of infrastructure and vehicular population. The local administration imposing restriction of inflow of vehicles to Havelock Island, gave the understanding, for the first time, that tourism development may result in many and complex impacts. A study was carried out for finding the essential features of Havelock tourism business and its related link to vehicular population. The study included a survey of identified roads to various tourist destinations spread across Havelock Island, traffic volume survey during the peak timings, hotel occupancy rate, and inflow of tourists in Havelock Island. The future requirement of traffic facilities and related infrastructure could have been analysed with any of the conventional forecasting tools but it related to a static growth pattern. The off-season inflow was much less as compared to the peak season flow of tourists. But the prevailing methodologies of forecasting were only giving related data for probable increase in traffic and infrastructure facilities but were not

S. Raji (✉)

Civil Engineering Department, Dr. B.R. Ambedkar Institute of Technology, Port Blair, Andaman and Nicobar Islands, India

e-mail: rajipradeepportblair@yahoo.co.in

© Springer Nature Singapore Pte Ltd. 2020

T. V. Mathew et al. (eds.), *Transportation Research*, Lecture Notes in Civil Engineering 45, https://doi.org/10.1007/978-981-32-9042-6_10

113

addressing the ecological sustainability and resource management for livelihood security. This envisaged development of a model applying information and communication technology (ICT) network matrix for Havelock Island as a useful tool in assessing the tourist transport requirement in Havelock. The matrix defined different level of transport facilities as preference contours which would give the user to choose the contour as per their convenience and place of stay in the island and at the same time will allow the authorities to implement facilities which are sustainable and suitable to the fragile island ecology. It will support productivity, sustainability of livelihood through the resource management. The outreach of ICTs in microlevel of societal environment and its direct and indirect use can be linked for creating a wide network of Management Information System (MIS) which can be made convergent for traffic micromanagement and safeguarding inflow of vehicular population. The paper suggests that ICTs can be extensively used in development as they are so multifaceted and easily adaptable with island population having high-literacy rate compared to other areas of the country. The study drew a conclusion of an innovative institutional mechanism to link tourist and transport facility requirement by creating different contours of preferences with suitable ICT intervention and exploring sustainable development framework.

Keywords Parking behaviour · Urban street · Parking enforcement · Percentage repetition of vehicles

1 Introduction

Havelock Island is one of the beautiful inhabited islands in the archipelago of 556 islands, constituting the Union Territory (UT) of Andaman and Nicobar (A & N) Islands. This island attracts tourists from all over the world for its pristine sea beaches and related natural environment. Though, beach attraction in Andaman and Nicobar Islands is not limited to this island but the infrastructure facilities available to cater varying categories of tourist have given Havelock more popularity and rating as compared to other tourist destinations of the UT. The geographical setting of the UT offers beaches, abundance of coral deposits, and dense forests define the geographical setting of these islands but in spite of this, the beaches in Havelock Island has become more popular than other places because of the tourist facility development happened in these locations. This substantiates the fact that tourists visit places for many purposes but the place that accommodates most tourists are large multifunctional entities into which tourists can be effortlessly absorbed and thus become to a large extent economically and physically visible (Gregory Ashworth et al. 2011).

Tourism has been one of the fastest growing industries for Andaman and Nicobar Islands and its contribution to the UT economy with reference to SDP is more than 20%. This is mainly due to tourism service sector facilities and its auxiliary supporting units engaged in economic activities like travel management, transport mode operation, resource management, and related suppliers to feed the tourist industry.

As stated by UNESCO [8], tourism with an annual average growth rate of about 5%, the international travel might nearly double until 2020 compared to 2006. Having experienced a growth of 25% between 1995 and 2005, tourism today accounts for 10% of the world's economic activity and is one of the main generators of employment. Tourism is also a major source of foreign exchange earnings for many developing countries. The report also states that the tourism industry ranks about sixth in international trade after trade in fossil fuels, telecommunications and computer equipment, automotive products, and agriculture.

Further, it is pertinently observed that the entire tourist visiting Port Blair essentially visits Havelock Island. Tourism being a service industry largely depends on human resources at all levels which include accommodation, travel agencies, travel operators, and resource suppliers, etc. The dependency on human resources keeps the quality of tourism service in dynamic mode constantly. The people engaged for various tourism-related services ranges from semi-skilled to highly skilled manpower. Skills learnt at one level allows the vertical economic growth and thereby people shift for finding better scope of business for economic gain. Such shift in activity also leads to the fluctuation in quality and service as mentioned above.

Though increase in tourism has added the economic activity for the local residents of Havelock Island, at the same time propagated the migration of tourism associated skilled people towards this island. In addition to services like hotels and resorts, the transport operations are the most targeted business by entrepreneurs in such tourism-driven island. This has not only resulted in a rise in land values but also has created challenges for hoteliers and congestion for transport operators. The increase in vehicular population lead to the restriction of vehicular flow to Havelock Island since the capacity of existing facility is not able to accommodate the same. The paper is presenting data and measures envisaged for proposing solution for addressing this problem wherein employment opportunities to local youth is not affected and better options are explored for sustainability of business and environment.

2 Study Area Details

Havelock Island is having more than 70% of land used for agriculture. The proportion of agriculture lands in the revenue villages of Havelock Island varies between 67 and 85% as shown in land use map in Fig. 1. In Havelock, the local administration is brought under two-gram panchayats which are distributed to five villages of Govind Nagar, Vijaynagar, Krishnannagar, Shyamnagar, and Radhanagar. An average of about 4% of the revenue lands at Havelock Island is under commercial use. This percentage is the highest, standing at 8% in Vijaynagar, wherein most of the hotels and resorts are newly developed.

The terrain is mild rolling abruptly raising the coast to a height of 30–40 m. In addition to the spread of reserve forests beyond the territories of revenue villages, forests occupy 9% of the land forming part of revenue villages at Havelock (master plan, APWD, [7]). Within the revenue area, forests become the second largest

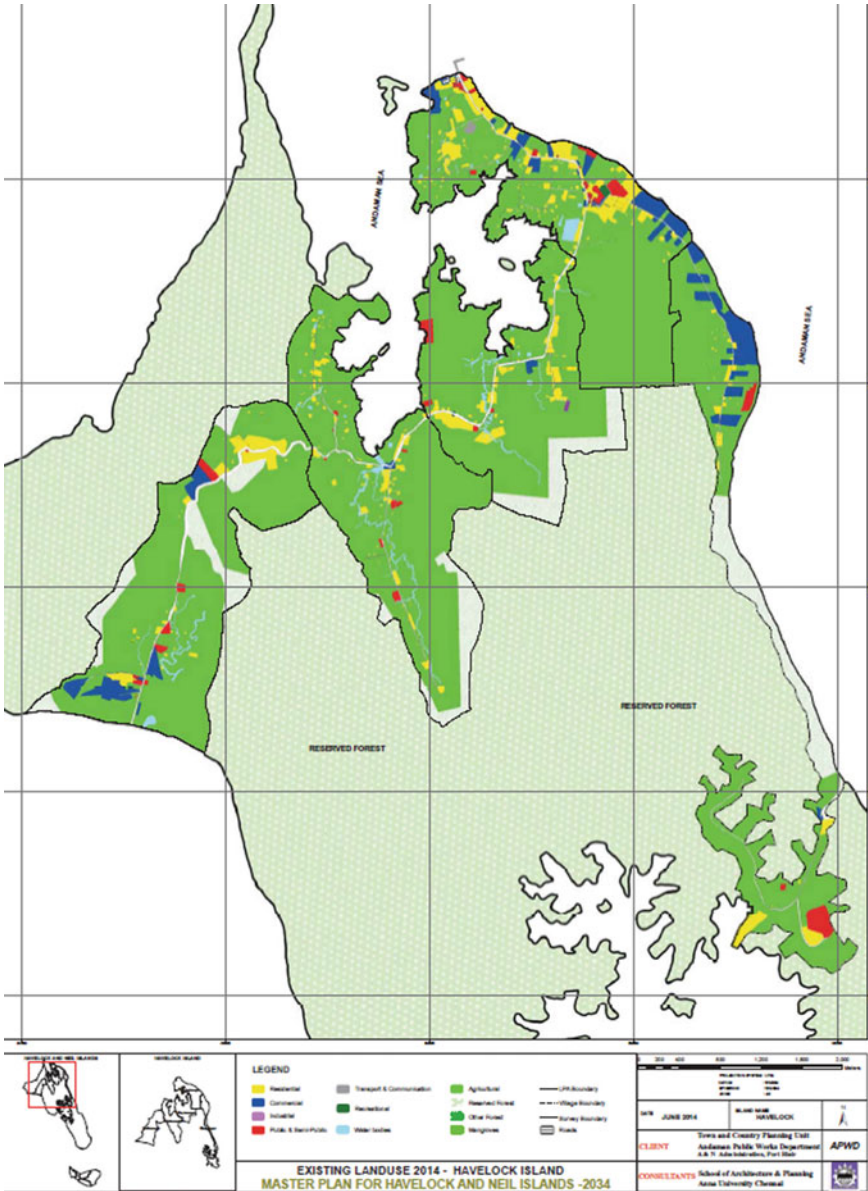


Fig. 1 Land use map for Havelock Island Source APWD

occupant of land. Moreover, in Havelock revenue villages, more than one-third of the forests are grown at Vijayanagar.

The tourist entry point for Havelock Island is at Govindnagar as all the intraisland ferry boats touched at the Jetty located in this village. Hence, the traffic flow originates from here to the destinations situated at Vijayanagar and Radhanagar where places of tourist interests are located. Further, the road network consists of mainly major link roads, as shown in Fig. 2, to villages followed by the small feeder roads and footpath linking them to hotels and beaches. Therefore, roads leading from Jetty area remain loaded with high-volume traffic during the peak hours when, ferry boats, carrying tourists arrive in the forenoon and depart in the evening. Therefore, traffic flow for the roads leading to these destinations was measured for analysis.

Traffic volume surveys were carried out for seven days of a week, during the month of December, considered to be the peak season of tourist inflow, to measure the count from Jetty area to leading destination and converted to passenger car units. Three main stretches of roads connecting Govindnagar to Jetty, Vijaynagar, and Radhanagar, respectively were selected as these roads lead to most of the sought after Hotels and beaches visited by tourists. The observed PCU during the survey is as given in Table 1.

Further being village roads under village administration, the road network carrying such flow of traffic volume is catered by carriageways [IRC 64: 1990] having an average width of 6 m. Figure 3 shows the graphical representation of PCU loads for selected stretches.

Moreover, Havelock Island having a population with more than 6000 people has catered visiting tourist in nearing to 30,000 in numbers. This is as per the statistics obtained from Department of Shipping Services, Andaman and Nicobar Administration, till the year 2015, who operates ferries and issues tickets for the people visiting this much sought after tourist island. It is apparent that the vehicle population also increased exponentially. The rise in vehicle and tourist numbers is shown in Fig. 4. This has added to the problems of infrastructure, natural resources, road capacity, parking, and quality of service.

Further looking into the trend of tourist inflow, it is obvious that in coming year, it will rise substantially. More than arranging provision for infrastructure facility to accommodate the expected increased inflow of tourists, the concerns of its impact have already become evident as the local youth/tour operators have been restricted with permits to move any more vehicles to Havelock roads.

3 Preference Contour Analysis

As stated by Gregory Ashworth and Stephan (2011), the tourist, and indeed the tourism industry avails much of the urban tourism experience in zero-price since markets, monuments, museums, and general atmosphere of the city are either free public space or provided well below cost as a public service. In the case of rural areas like Havelock Island, the cost becomes still lower. On the other hand opposite

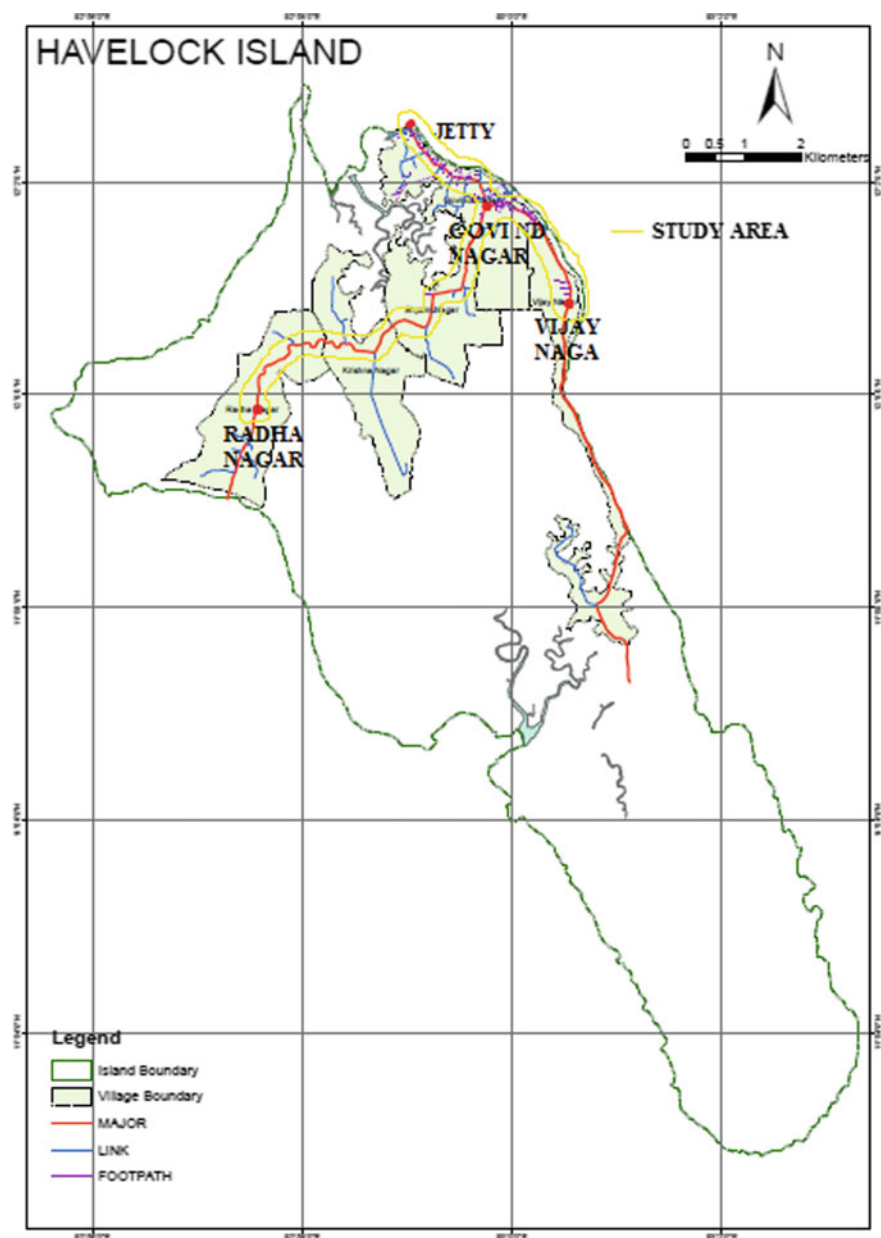


Fig. 2 Road network for Havelock Island. Source APWD

Table 1 PCU observed for high-volume roads

Day	Strech No. 1		Strech No. 2		Strech No. 3	
	Jetty to Govind Nagar	Govind Nagar to Jetty	Govind Nagar to Vijaynagar	Vijaynagar to Govind Nagar	Govind Nagar to Radhanagar	Radhanagar to Govind Nagar
Monday	1428	1363	888	955	715	647
Tuesday	1385	1385	954	868	744	703
Wednesday	1328	1266	863	831	705	700
Thursday	1651	1604	946	887	851	858
Monday	1428	1382	764	870	717	718
Saturday	1465	1406	917	843	931	900
Sunday	1418	1406	884	882	948	927

TRAFFIC VOLUME IN DIFFERENT STRECHES IN PEAK HOURS

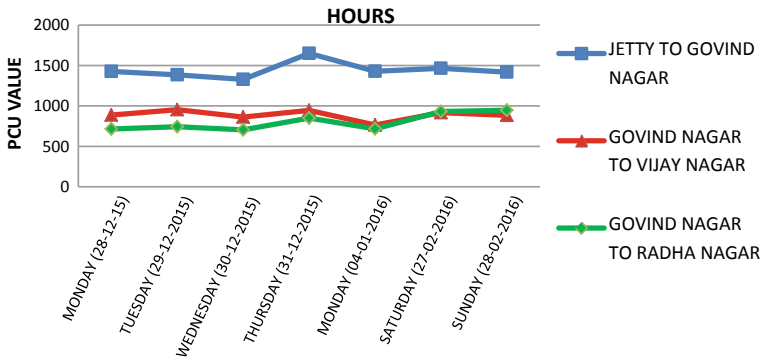


Fig. 3 Graphical representation for PCU Volume

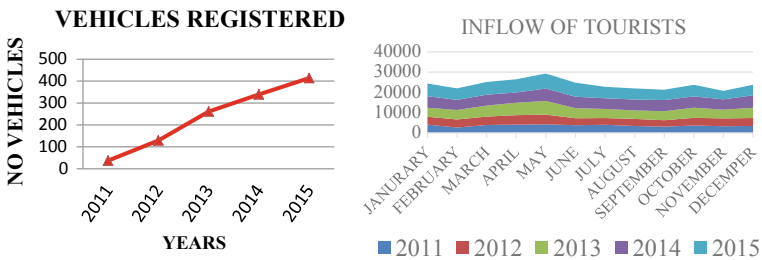


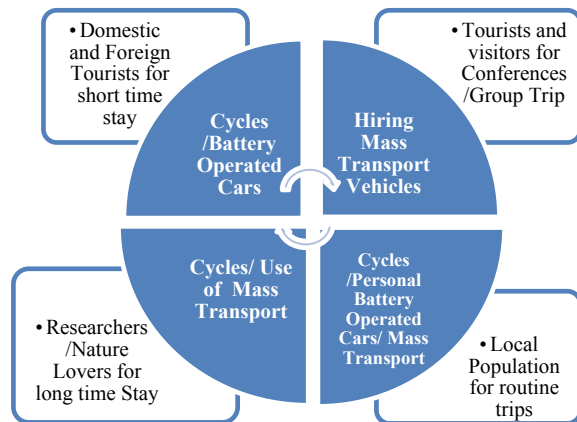
Fig. 4 Graphs showing inflow of vehicles and tourists

to this situation, it is also possible that the local residents may reap benefits from the presence of tourists and tourism services. This includes ‘free-ride’ upon tourism facilities, enjoying an urban atmosphere of animation or just gains psychic profits of pride and self-esteem. The problem is the very familiar one of reconciling public costs with private benefits, in economic terms, gaining internalised benefits from the external facilities, and in spatial terms, balancing costs and benefits at different spatial scale jurisdictions (Haley et al. 2005). Therefore, the internal benefit reaped by the transport facility providers due to the economic activity directly related to inflow of tourists needs to be understood according to the choice opted by visiting tourist using such transport facility. The study attempted for proposing a matrix, as shown in Fig. 5 to explain the types of tourist and their choice of transport facility by creating four levels of preference contour to understand the scope of service expected by visiting tourists.

Further, the matrix can become a suggested MIS for the Preference Contour Model (PCM) where ICT tools can be applied to keep the facility in readiness and to plan and manage the traffic flow to suit economy as well as sustainability concerns of island environment and the much-concerned factor of resource management. Moreover, it has been seen that cities with good public transportation systems, very few tourists hire private transport; however, in places with poor public transport, most tourists will have a higher demand for public transportation systems and hire private transport. Thus, the number of tourist arrivals to such places should be considered as a factor in the design and planning of local mass transportation supply [1]. In order to address the present problem of restriction of vehicles in the islands and to meet the available capacity of Havelock roads, mass transport system needs to be encouraged.

The present system of personal vehicle hiring, which is encouraging the population of sport utility vehicles (SUVs) and cars shall be replaced with compact battery-operated green vehicles suitable for Havelock road capacity. The availability of green energy operated four-wheelers/three-wheelers, with self or driven facility, will also provide employment for local youth. In order to encourage mass transport

Fig. 5 Preference contour matrix



system, the component of intelligent transport system (ITS) such as advanced traveller information system (ATIS) shall be adopted to provide vital information to the users regarding traffic regulation, route and location guidance, hazardous situations and safety advisory, and warning messages. The frequency and route mapping of such mass transport facilities should discourage the use of personal/hired vehicles. Well-laid cycle track alignment to tourist destinations will also discourage use of personal vehicles.

In addition to above, the hire charges of such personalised vehicles should also be kept very high to keep the preference contour of such vehicles for expensive choice. This will simply encourage the travellers to opt the contour offering cycles and mass transport system. Therefore, it envisages the need to revamp the present infrastructure facilities supporting the transportation system in Havelock Island. As adopted in developed countries, the transportation strategies [6] need to be objected as more balanced and sustainable transportation solutions than infrastructure- and capital-intensive activities. Thus, ITS solutions and its related transport facilities will surely divert towards sustainability and futuristic development.

4 MIS for Traffic Planning and Management

The microenterprise occupation in smaller livelihood consists of [3] survivalist and entrepreneurs. Survivalist is drawn into enterprise by the lack of other income generating activities whereas macroenvironment created by the entrepreneurs forms the majority of microenterprises who are directly contributing to the economy. Thus, the restriction of inflow of vehicles to Havelock Island has affected the survivalist category of the microenterprise supporting the tourism industry with road transport services. Therefore, the study attempted to propose the preference contour modal for future traffic planning and management for Havelock Island, as shown in Fig. 6, which can be adopted for other such islands tourism offers livelihood services to the islanders.

The preference contour will not only provide green transport options for tourists/visitors but also will encourage and compel the enterprisers and local population to adopt such eco-friendly measures for the livelihood activities supported by tourist industry. The flow of traffic on Havelock roads can be checked with green energy/eco-friendly/mass transport vehicles and the related auxiliary services, as indicated in Fig. 6, will provide continuous avenues of employment and entrepreneurial activities for local youth. It will also bring the challenges for the local government to give provisions and facilities for ICT education and skills required for implementing such modal for addressing present problem of stagnant growth. Since the integrated transport system (ITS) which applies ICT tools to coordinate transportation systems in a safe and efficient manner, it will give ample scope of skill development and related employment to microenterprise occupants. Further, the flow of vehicles can be checked by phasing out used vehicles according to their utility and requirement.

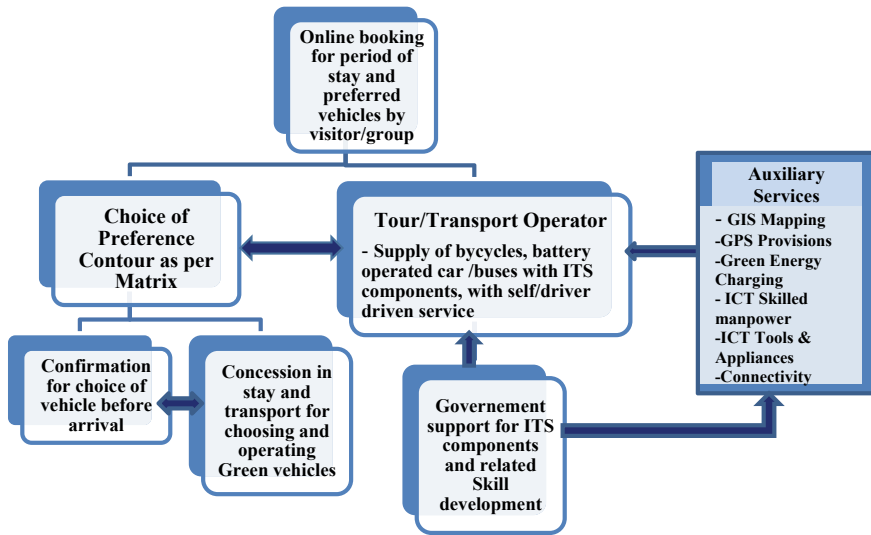


Fig. 6 Preference contour modal for future traffic planning and management

5 Conclusion

The paper was objected to carry out a study to propose the PCM not only to address the present problem of increasing vehicular flow to Havelock Island but also to present a sustainable solution for the livelihood of people who forms the major part of informal sector supporting the tourism economy of the island. The informal sector who is the typical unregistered occupants earning a livelihood with services related to forest, agriculture, fishing, commercial transport, and construction services can also be drawn to ICT usage through proper training as impregnation of mobile phones in all strata of social framework has increased the outreach. Thus, entrepreneurial enterprises may employ skilled manpower and use more IT-related technologies for business gain than survivalist enterprises. This informal sector presently more dependent on livelihood based on transport service interacts more effectively with established local markets so ICT literacy will make them more competent for better livelihood.

The local government and authorities need to modify their policies for adhering to more green practices to assure sustainability and growth. This also asks for facilities and support to develop existing and futuristic ICT and ITS components by training native population to keep a check on migration of people which may affect adversely the capacity of these fragile islands. Thus once successfully implemented on Havelock Island, the same PCM can be adopted for other such tourist intensive islands, according to the local conditions, of this Union Territory. As the present bandwidth for internet facility will not be supportive to implement proposed PCM but with arrival of better internet facilities in future, this PCM model can be effectively tested

to keep a check on the transport-related impact within the threshold to sustain the fragile ecology of island environment.

References

1. Albalate D, Bel G (2010) Tourism and urban public transport: holding demand pressure under supply constraints. *Tour Manag* 31(3):425–433
2. Ashworth G, Page SJ (2010) Urban tourism research: recent progress and current paradoxes. *Tour Manag* 32:2–8
3. Duncombe RA, Heeks RB (2002) Enterprise across the digital divide: information systems and rural micro-enterprise in Botswana. *J Int Dev* 14(1):61–74
4. Gill N, Bharath BD (2013) Identification of optimum path for tourist places using GIS based network analysis: a case study of New Delhi. *Int J Adv Remote Sens GIS Geogr* 1:2–3
5. Kantawateera K, Naipinit A, Promsaka T, Sakolnakorn N, Kroeksakul P (2015) Tourist transportation problems and guidelines for developing the tourism industry in Khon Kaen, Thailand. *Asian Soc Sci* 11(2):2–7
6. Praveen K, Singh, Dhanunjaya R (2005) Advanced traveler information system for Hyderabad city. *IEEE Trans Intell Transp Syst* 6(1):03–05
7. Master Plan for Havelock & Neil islands, Town Planning department, APWD, 2014, pp 1–17
8. UNESCO Report, Sustainable Tourism Development in UNESCO Designated Sites in South-Eastern Europe, 2007, pp 02–14

Comparative Study of Legal and Illegal On-Street Parking Behaviour in CBD Area—A Case Study of Surat City



Dixit Chauhan, Rahul Pitroda, Ninad Gore, Sanjay Dave
and Gaurang J. Joshi

Abstract The sharp contradiction between the rapidly growing number of vehicles and limited on-street parking space has resulted in the phenomenon of “difficult and disorderly parking”, which has adverse impacts on performance of urban roads. Propensity towards usage of private vehicles coupled with ineffective public transport has led to unmanageable demand for parking, especially in CBD with observance of illegal parking every day. In order to formulate enforcement measures to reduce occupancy of illegal parking, it becomes imperative to investigate behavioural aspects associated with illegal parking. To comprehend this objective, two busy urban streets in CBD area of Surat city were selected for comparative assessment of legal and illegal parking demand. Preliminary, on-street parking inventory was carried out by licence plate method at 1 h interval during business hours to determine peak parking hours. The survey observed dominancy of two wheel-motorized vehicles on both sides for both roads, and hence all analyses were carried out in terms of two wheel-motorized vehicles. Microscopic parking inventory was then carried for both legal and illegal parking demands at 10 min data monitoring interval using licence plate survey method during peak parking hours. Statistical check on demand accumulation revealed significant difference in legal and illegal parking demand. To probe further, microscopic behavioural analysis was carried by obtaining percentage repetition of parked vehicles (PRPVs) between two successive sets of observations for different data monitoring intervals. Paired *t*-test at 5% significance level between

D. Chauhan · R. Pitroda · N. Gore · S. Dave (✉)
The Maharaja Sayajirao University of Baroda, Vadodara, India
e-mail: smdave-ced@msubaroda.ac.in

D. Chauhan
e-mail: chauhandixit@yahoo.com

R. Pitroda
e-mail: pitrodarahul@yahoo.com

N. Gore
e-mail: ninadgore24@gmail.com

G. J. Joshi
Sardar Vallabhbhai National Institute of Technology (SVNIT), Surat 395007, Gujarat, India
e-mail: gjsvnit92@gmail.com

legal and illegal PRV values for different data monitoring intervals revealed isotropic behaviour between legal and illegal parking regimes. Further, efficient utilization of the available parking space in terms of turnover in 2 W per hour was analysed for each data frequency which indicated high value for high data frequency and vice versa. However, efficiency in terms of turnover was varying for both the demands with poor value for illegal parking. Research suggests that illegal problem in Surat city is a behavioural problem, and henceforth, stringent enforcement measures need to be formulated to reduce its occupancy.

Keywords Central business district (CBD) · On street · Illegal parking · Legal parking

1 Introduction

Apart from other developing countries, India is one of the fastest growing countries in the world. With increase in population and income, the numbers of parked vehicles are also increasing, leading to parking problems in most of the metropolitan cities. The problem becomes more acute in the developing countries like India, particularly in CBD area of metropolitan city. The on-street parking reduces the flow speed and creates congestion on the street, particularly in the CBD area. Congestion leads to loss of time as well as cost. Insufficient space in the CBD area, less off-street parking facilities, dense development, high land value, etc., force the users to park their vehicles on street. To regulate this on-street parking, it required to address the on-street parking demand. The usual practice of local bodies to manage the demand adopts odd–even date free-of-cost on-street parking scheme on the corridors of high demand. Due to high attraction trip rate and lack of available space after applying odd–even date free-of-cost on-street parking policy, visitors are sometimes compelled to park their vehicles on illegal side. Understanding parking behaviour is an effective way to analyse the effects of parking policy measures. Therefore, for effective and efficient regulation of on-street parking demand, it becomes imperative to study legal and illegal parking behaviour.

2 Review of the Literature

The demand for parking spaces is brought about by the necessity (in the motorized culture) to utilize the road transport infrastructure at particular destination. Every vehicle trip requires parking at its destination, and so it considers parking facilities as integrated component of the roadway system. The understanding of parking demand is critical to the findings associated with parking studies. Most literature refers to parking demand as the observable parking occupancy of a defined parking facility. Apart from that, some of the literature reported is discussed in the follow-

ing section. Chimba and Onyango [1] studied three land-use types like downtown area dominated by offices, commercial shopping centre and beach park. The study conducted a continuous parking survey of licence plate numbers for at least 3 h and recorded at every 5 min interval. Using statistical power analysis method, the authors concluded that, to detect all possible optimal parking characteristics and cost-efficient surveying, licence plates should be monitored at intervals less than every 30 min for downtown and 60 min for beach parks. The main likely factors that affect the preference of the choice of parking location are security, available parking space, comfortability and closeness of parking place to the destination [2]. The factors that affect the illegal parking are lack of national policy, deficiency in local regulations, rapid economic growth, inadequate provision of parking infrastructure and bad social habits. Accordingly, the effective parking policy and regulation, better education and advanced strategies are more helpful in solving the problem [3]. Axhausen and Polak [4] evaluated the costs that appear when on-street illegal parking is detected in Barcelona, New York. For that, the authors formulated the different types of journey cost and accordingly formulated the cost for illegal parking. The author observed the reduction in illegal parking which gives higher road capacity and greater traffic fluidity. Mohammed [5] has done parking survey on five main locations where legal and illegal parking was observed in Jeddah. He segmented the observation in three time periods which are morning peak, afternoon peak and evening peak in weekday and weekend, and result shows that illegal parking is common in selected stretch in Jeddah. Cheng and Miaomiaoa [6] formulated the parking generation model considering different factors, such as the average turnover rate, parking place occupancy, service level, parking fees and growth rate of automobiles. Moreover, the capacity of road network is applied to rectify the short-term parking demand forecast and model was applied in Beijing Road CCD in China. Hilvert et al. [7] concluded based on stated and revealed preference data that price in terms of both the overall parking cost and the hourly fee is the dominant factor in parking-related decisions. Das and Ahmed [8] made the parking demand estimation model and calculated the parking level of service for two CBD area of Kolkata. Illegal parking, according to [9], occupied the spaces of roads and caused imbalanced demand of garage parking and roadside parking. The prevalence of illegal parking was mainly due to parking supply shortage and lack of parking information. Besides, the improper urban planning also contributed to this problem. Review of the above literature suggested that very few studies are concentrated on assessment of illegal on-street parking behaviour, especially in developing countries, which thereby propagates the need to study on-street parking behaviour.

3 Study Site and Data

The selected study stretches are located in the oldest central business district of Surat city in the state of Gujarat, India. Surat is regarded as the fourth fastest developing city of India, a bustling metropolitan, and is one of the most important cities on industrial

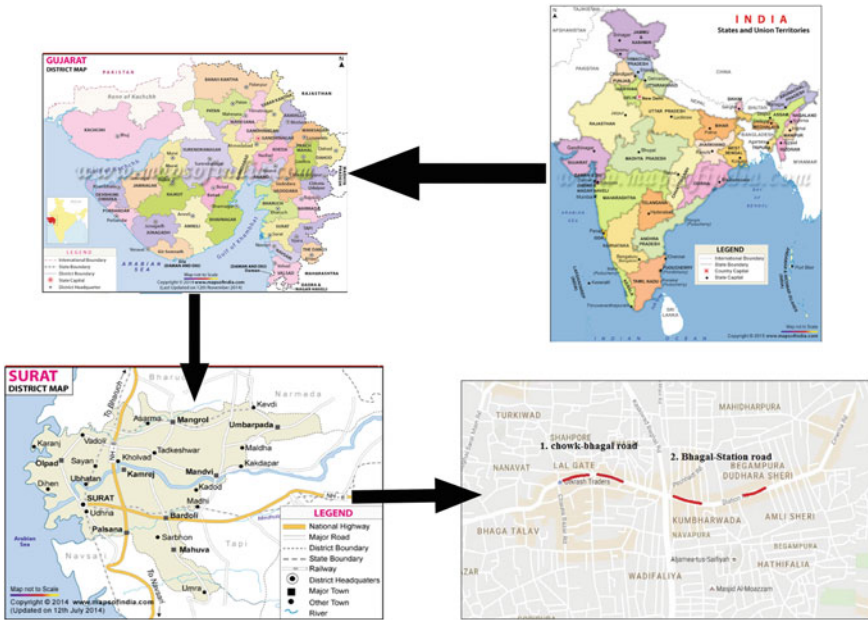


Fig. 1 Location of study area in Surat city

map of the country with dominance of diamond polishing and textile industries. The city has a population of 4.4 million (2011) and has observed an extortionate growth in personalized vehicles, due to addition of average 109,000 motorized two-wheelers (2-Ws) and 22,000 cars every year. Exorbitant vehicular growth coupled with inefficient public transport has developed proclivity towards usage of personalized vehicles, restricting the mode share of public transportation below 5% (Fig. 1).

3.1 On-Street Parking Scenario

The selected stretches comprise of mixed land use essentially commercial at ground level and residential houses at the upper levels. Substantial concentration and proximity of various commercial activities attract a lot of shoppers from all parts of the city, which generates unmanageable parking demand. Saturated on-street parking spaces are predominately observed, though developed off-street parking facilities are provided. On-street parking is not monitored by traffic police, which has resulted in chaotic parking by cars and motorized two-wheelers. Further, the on-street parking demand spills over the available supply, which interludes smooth flow through traffic. Parking permission on both the selected streets is regulated by *odd-even date free-of-cost on-street parking scheme*. Illegal parking is a common phenomenon which is observed throughout the business hours. Irregular towing of vehicles is a

Table 1 Road inventory detail

Detail of road	Chowk Bazar Road (SR1)	Bhagal-Station road (SR2)
Type of road	Undivided	Undivided
Right of way	16.5–18.5	17.5–24.5
Width of carriageway	9.5–11.5	14.5–20.5
Width of parking space	2 m (each side)	2 m (each side)
Width of footpath	1.5 m	1.5 m

sole enforcement measure adopted by local police to curb illegal parking. For both study sites, right angle parking for 2-Ws and kerb-side parallel parking for cars and 3W (auto-rickshaw an IPT mode of transport) are permitted. Road inventory details of subject roads are summarized in Table 1.

3.2 Methodology of Data Collection

The methodology for data collection of on-street parking demand becomes crucial as duration of parking varies with different vehicles. Parking inventory survey was carried out using licence plate method for period of 12 h at 1 h interval to determine peak parking hours. Thereafter, microscopic parking inventory was carried out at the 10 min data monitoring interval using licence plate survey method during peak parking hours for three days, to account for variation in parking demand. Parking survey traps of different lengths were considered along the street to exemplify parking demand of the entire street and to accommodate temporal variations in demand due to variation of commercial activities. Individual bays were not demarcated on the study site, and hence a number of bays were calculated as per guidelines given in [10].

4 Data Analysis

Preliminary observation revealed heterogeneity in parking demand with dominance of 2-Ws followed by car and 3W. Some light commercial vehicles parked on-street were included in 3W category.

In Figs. 2 and 3, it can be noted that maximum parking demand accumulation was observed during 4–7 pm for both the subject roads. Further investigation was performed by collecting parking demand data at 10 min frequency using licence plate method during peak parking hours for three days to account variation in parking demand. Since parking demand had dominance of 2-Ws, it was found appropriate

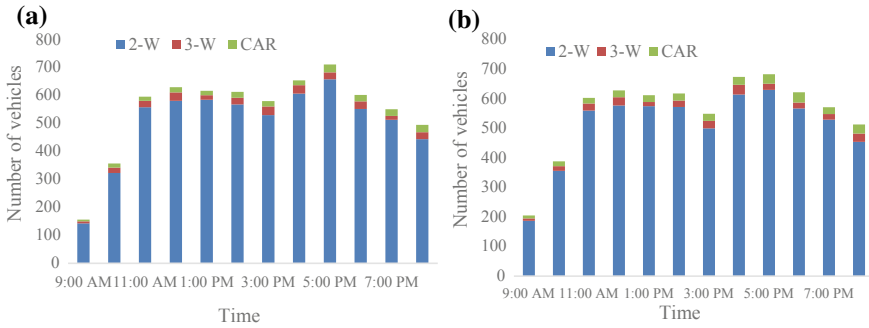


Fig. 2 Parking accumulation for 12 h interval for SR1. **a** Legal side and **b** illegal side

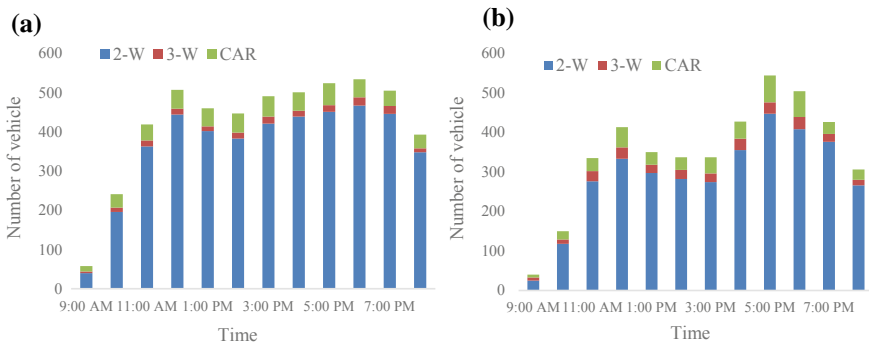


Fig. 3 Parking accumulation for 12 h interval for SR2. **a** Legal side and **b** illegal side

to convert recorded parking demand into equivalent two-wheeler (E2W) demand. Therefore, to normalize, cars and auto-rickshaws were converted into equivalent 2-W space (E2WS), where one car was considered as four 2-Ws while one auto-rickshaw was considered as two 2-Ws [10].

Parking demand accumulation for selected streets for the data collection period is represented in Fig. 4. Legal parking demand is represented in the form of bar chart, while the line plot signifies illegal parking demand. From Fig. 4, it can be observed that temporal fluctuation in legal and illegal parking demand followed a uniform trend within the day for both subject roads of the city, but varied significantly among days. In addition, legal and illegal parking had similar occupancy for the entire data collection period for 3 h, which was checked statistically for different data monitoring intervals using two-tail paired *t*-test at 10% significance level for null hypothesis “no difference in legal and illegal parking demand exists”. Alternate hypothesis was assumed as “significant difference exists in legal and illegal parking demand”. The null hypothesis was rejected for every data monitoring interval in reference to *p* value. Therefore, though having marginal difference in occupancy, there exist statistically two parking demand regimes (Table 2).

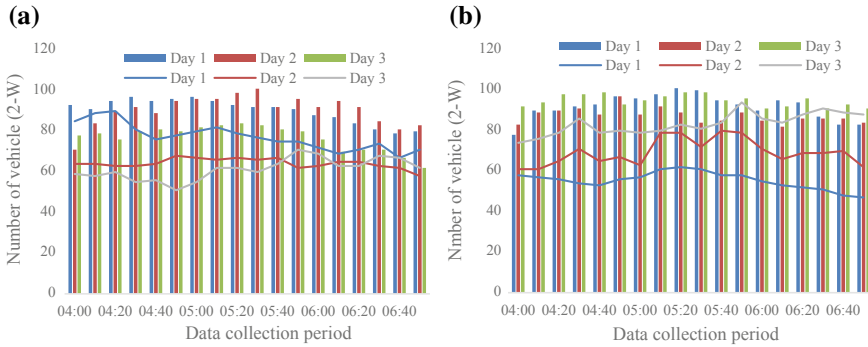


Fig. 4 Parking demand accumulation of legal and illegal side during peak hours for **a** SR1 and **b** SR2

Table 2 Hypothesis testing result between legal and illegal sides for both roads

Road name		Chowk Bazar Road		Bhagal-Station road	
Day	Frequency	<i>p</i> value	Remarks	<i>p</i> value	Remarks
Day 1	10 min	0.038	Rejected	0.020	Rejected
	20 min	0.011	Rejected	0.001	Rejected
	30 min	0.004	Rejected	0.018	Rejected
	40 min	0.035	Rejected	0.011	Rejected
	50 min	0.025	Rejected	0.020	Rejected
	60 min	0.366	Accepted	0.003	Rejected
Day 2	10 min	0.000	Rejected	0.000	Rejected
	20 min	0.004	Rejected	0.002	Rejected
	30 min	0.013	Rejected	0.004	Rejected
	40 min	0.027	Rejected	0.008	Rejected
	50 min	0.047	Rejected	0.027	Rejected
	60 min	0.065	Rejected	0.017	Rejected
Day 3	10 min	0.003	Rejected	0.097	Rejected
	20 min	0.004	Rejected	0.019	Rejected
	30 min	0.017	Rejected	0.093	Rejected
	40 min	0.074	Rejected	0.023	Rejected
	50 min	0.028	Rejected	0.005	Rejected
	60 min	0.016	Rejected	0.026	Rejected

Note Accepted or rejected in reference to null hypothesis

4.1 Percentage Repetition of Parked Vehicles

Behaviour of parkers on legal and illegal side was investigated further by obtaining percentage repetition of vehicles (PRVs) between two successive sets of observations for different data monitoring intervals. Figures 5 and 6 represent PRV of legal and illegal parking regimes for a different data monitoring for both subject roads. *Solid line plot represents PRV of legal parking demand, while dotted line plot signifies PRV of illegal parking demand.*

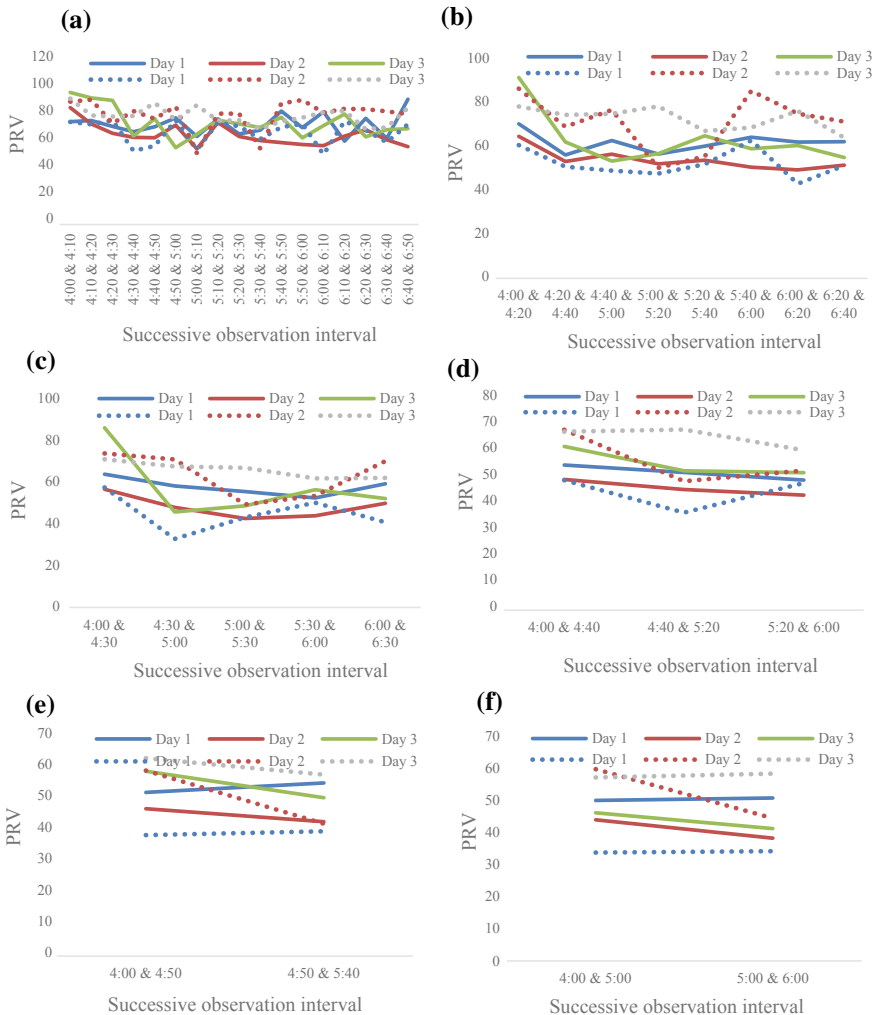


Fig. 5 PRV for different frequency intervals for legal and illegal side for SR1. **a** 10 min, **b** 20 min, **c** 30 min, **d** 40 min, **e** 50 min, **f** 60 min

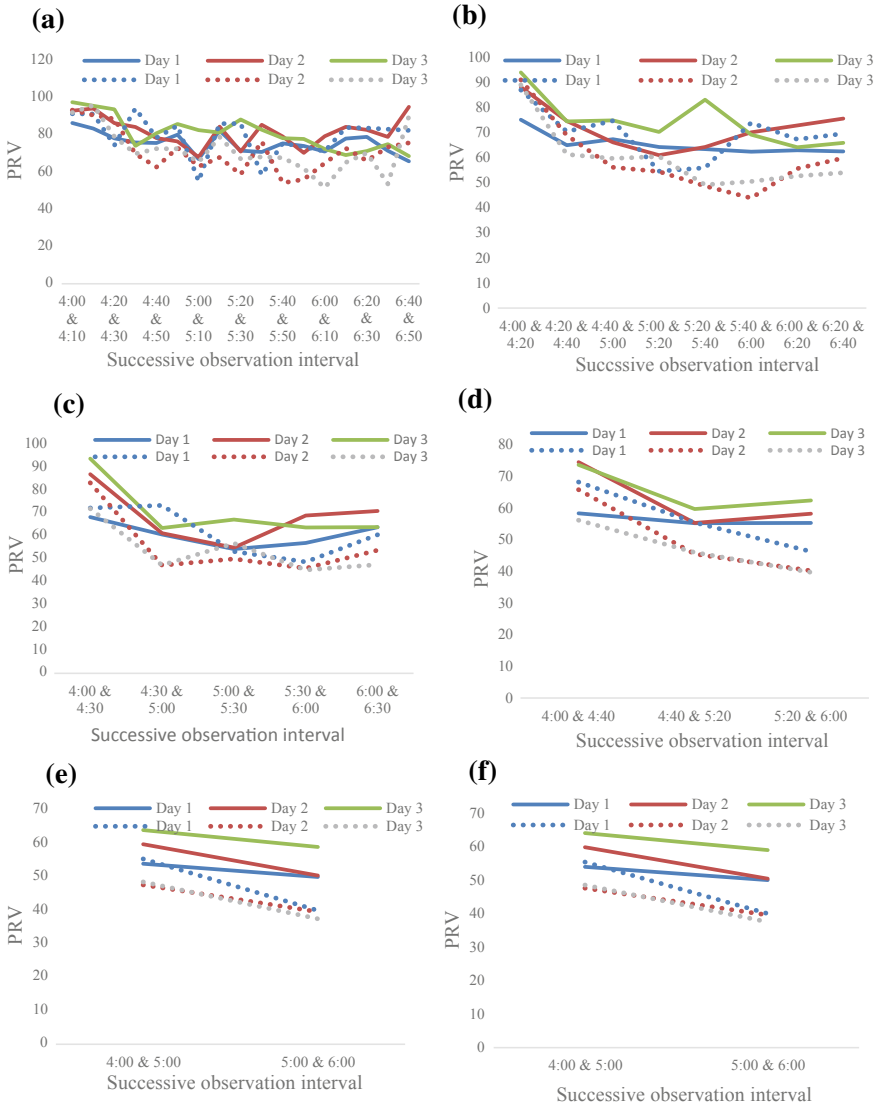


Fig. 6 PRV for different frequency intervals on legal and illegal side for SR2. **a** 10 min, **b** 20 min, **c** 30 min, **d** 40 min, **e** 50 min, **f** 60 min

It can be observed that percentage repetition of vehicles (PRVs) for legal and illegal regimes followed a decreasing trend as the monitoring interval increases, which can be attributed decrease in recorded demand, for both the streets. In addition, greater inconsistency for higher frequency (10–30 min) and stabilization in PRV was observed after 30 min data monitoring interval. Variation in PRV is consistent for legal parking demand when compared to illegal parking demand, which is reflected from Figs. 5 and 6. Further, it could be observed that PRV for legal and illegal parking at different data monitoring intervals for all three days of both subject roads followed a consistent trend indicating uniform parking behaviour. PRV values between legal and illegal regimes were checked statistically to signify parking behaviour using two-tail paired *t*-test at 10% significance for null hypothesis “no difference in percentage repetition of vehicles between legal and illegal regimes exists”. Alternate hypothesis was assumed as “significant difference in PRV between legal and illegal parking regimes exists”. From Table 3, it can be concluded percentage repetition of vehicle (PRV) had statistical similarity between legal and illegal regimes, indicating behavioural analogy between the two.

Table 3 Hypothesis testing result between legal and illegal sides for both streets

Road name		Chowk Bazar Road		Bhagal-Station road	
Day	Frequency	<i>p</i> value	Remarks	<i>p</i> value	Remarks
Day 1	10 min	0.210	Accepted	0.230	Accepted
	20 min	0.289	Accepted	0.154	Accepted
	30 min	0.254	Accepted	0.218	Accepted
	40 min	0.374	Accepted	0.311	Accepted
	50 min	0.998	Accepted	0.720	Accepted
	60 min	0.358	Accepted	0.302	Accepted
Day 2	10 min	0.111	Accepted	0.091	Accepted
	20 min	0.064	Accepted	0.144	Accepted
	30 min	0.314	Accepted	0.356	Accepted
	40 min	0.113	Accepted	0.551	Accepted
	50 min	0.366	Accepted	0.321	Accepted
	60 min	0.086	Accepted	0.179	Accepted
Day 3	10 min	0.067	Accepted	0.097	Accepted
	20 min	0.124	Accepted	0.194	Accepted
	30 min	0.244	Accepted	0.932	Accepted
	40 min	0.168	Accepted	0.238	Accepted
	50 min	0.923	Accepted	0.504	Accepted
	60 min	0.252	Accepted	0.268	Accepted

Note Accepted or rejected in reference to null hypothesis

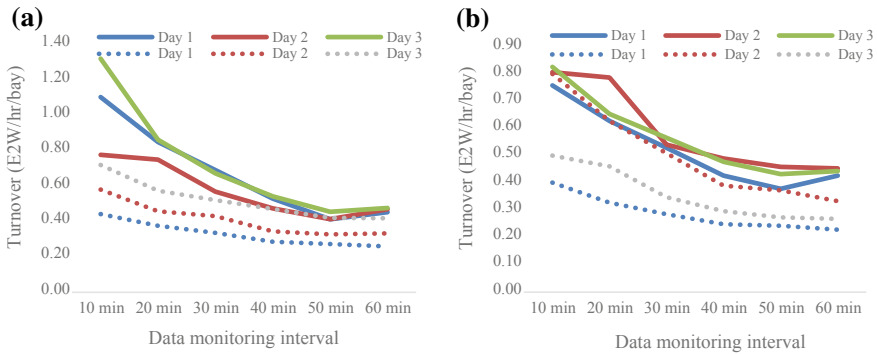


Fig. 7 Turnover for different frequency intervals on legal and illegal side for a SR1, b SR2

4.2 Parking Efficiency

Efficiency of parking space in terms of turnover was evaluated for further investigation. As the observed demand was converted into equivalent two-wheelers, turnover was calculated in terms of E2W/h/bay. Figure 7 represents turnover for subject roads at different data monitoring intervals. Here, solid line plot represents legal parking demand, while dotted line plot signifies illegal parking demand. It can be noted that turnover decreased as the data monitoring interval increases. This can be attributed to data leakage of short-term parked vehicles at higher monitoring interval.

From the above figure, it can be noted that legal-side demand is much more efficient compared to illegal-side demand. This can be attributed to purpose orientation parking occupancy on illegal side. Moreover, SR1 was observed to be efficient compared to SR2.

5 Conclusion and Discussion

Disproportionate use of personalized vehicles for commuting has created severe shortage of legal parking facilities particularly in CBD areas of fast-growing metropolitan cities in India. High concentration and proximity of different commercial activities attract a lot number of shoppers, which generates unmanageable parking demand. Social reluctance towards on-street parking regulations leads to observance of daily illegal parking demand. The present study emphasizes on analysis of legal and illegal parking demand behaviour for busy urban streets of Surat city. Statistical analysis revealed that legal and illegal parking demand varied significantly though having marginal difference in occupancy. Therefore, both illegal and legal parking regimes were independently analysed. Microscopic analysis of parking demand behaviour was accomplished by extracting percentage repetition of vehicles (PRVs) between two successive sets of observation for different data monitoring inter-

vals and revealed consistent trend for legal and illegal parking regimes. Therefore, behavioural analogy exists between legal and illegal parking regimes. Turnover analysis revealed that illegal parking remained occupied for longer duration as compared to legal parking which needs to be addressed by stringent enforcement measures.

6 Recommendation

1. On-street parking inventory should be carried out at 10 min data frequency to microscopically access on-street parking demand.
2. On-street parking should be assessed in equivalent two-wheeler space (E2WS) instead of equivalent car space (ECS) where demand is dominated by motorized two-wheelers.
3. The study proposes to charge on-street parking space based on efficiency rather than land cost as recommended by NUTP (2014).
4. The study recommends that stringent illegal parking enforcement in the form of photographs of illegally parked vehicles may be implemented in order to reduce illegal parking occupancy.

References

1. Chimba D, Onyango M (2012) Optimization of short-term “on-street park-pay” license plate surveying. *J Infrastruct Syst* 18(1):194–201
2. Teknomo K, Kazunori H (1997) Parking behavior in central business district a study case of Surabaya, Indonesia. *East J* 2:551–570
3. Spililpoulou C, Antoniou C (2012) Analysis of illegal parking behavior in Greece. *Procedia-Soc Behav Sci* 48(2012):1622–1631
4. Axhausen KW, Polak JW (1991) Choice of parking: stated preference approach. *Transportation* 18(1):59–81
5. Mohammed A (2016) Analysis of illegal parking behavior in Jeddah. *Curr Urban Stud* 4:393–408
6. Cheng T, Miaomiaoa T (2012) The model of parking demand forecast for the urban CCD. *Energy Procedia* 16:1393–1400
7. Hilvert O, Toledo T, Bekhor S (2012) Framework and model for parking decisions. *Transp Res Rec* 2319:30–38
8. Das D, Ahmed M (2017) On-street parking demand estimation model: a case study of Kolkata. *Indian J Sci Technol* 10(12)
9. Zhang Q (2006) Car parking problem in big cities in China: a case study on Shanghai. Tongji University, Master
10. Guidelines for parking facilities in urban areas, Indian Road Congress, Special Provision, IRC SP-12 2015

On-Street Parking Demand Assessment in CBD Area Using Different Data Frequency



Rahul Pitroda, Dixit Chauhan, Ninad Gore, Sanjay Dave
and Gaurang J. Joshi

Abstract In many Indian cities, CBD areas are characterized by high demand for on-street parking, which has often led parking space problems, especially during peak hours and special events. Lack of data for on-street parking demand and absence of unambiguous on-street parking policy result in business as usual condition for parking on major streets of CBD area. To analyze on-street parking demand and optimize the survey interval for which parking survey should be carried in CBD area, two busy urban streets of Rajkot city, Gujarat, India were considered. Selected streets have two different land-use types, namely medical and commercial. On-street parking inventory survey was carried out by license plate method 1 h interval during business hours for a normal working day to determine peak parking hours. Microscopic parking investigation was further carried out during peak parking hours by collecting demand data at 10 min data monitoring interval for four normal working days and weekends. Uniform patterns of parking were observed throw out the survey period of frequency at 10 min, however, variation in demand observed among the day. Data monitoring interval had a significant effect on observed demand. To probe further, the percentage of unique parked vehicles was extracted from the observed demand for different data monitoring interval. Analysis of PUPV revealed that PUPV followed a progressively increasing trend as monitoring interval increases. Further, a consistent trend was observed for all survey day for both subject land use. Consistency of PUPV in the form (C.V) was observed for 30 min data monitoring interval for both subject

R. Pitroda · D. Chauhan · N. Gore · S. Dave (✉)
The Maharaja Sayajirao University of Baroda, Vadodara, India
e-mail: smdave-ced@msubaroda.ac.in

R. Pitroda
e-mail: pitrodarahul@yahoo.com

D. Chauhan
e-mail: chauhandixit@yahoo.com

N. Gore
e-mail: ninadgore24@gmail.com

G. J. Joshi
Sardar Vallabhbhai National Institute of Technology (SVNIT), Surat 395007, Gujarat, India
e-mail: gjsvnit92@gmail.com

land-use types. Microscopic behavioral analysis carried by obtaining percentage repetition of parked vehicles (PRPV) between two successive sets of observations for different data monitoring intervals revealed that PRV followed a decaying trend with data monitoring interval. Statistical analysis on PRV values between different data monitoring intervals revealed similar behavior post-20 min data monitoring interval. Turnover analysis revealed a decaying trend with data monitoring interval. Turnover was observed to be consistent at 30 min data monitoring interval. In the context to consistent PUPV and consistent turnover, the study proposes to evaluate parking utilization and parking efficiency at 30 min data monitoring interval in CBD areas of developing countries. In addition, based on the statistical result on PRV, the study proposes to provide 20 min as free parking duration.

Keywords CBD · On-street parking · Demand assessment · Percentage of unique parked vehicles · Percentage repetition of parked vehicles · Turnover

1 Introduction

The rapid rate of motorization in amalgamation with urbanization has resulted in a significant increase in traffic demand and consequently increased saturation of the road network. One of the major problems associated with an increase in the traffic is the acute shortage of parking space, especially in urban centers [1]. The burgeoning gap between available parking space and increased demand for on-street parking makes the problem more acute, especially in developing countries. This therefore has ensued the phenomenon of disorganized and problematic parking [2, 3]. Effectively managing on-street parking is an ongoing battle especially for large central cities as they face competing and contradictory objectives along with an ever-increasing demand for space [4]. The parking demand in the core area of the walled city is a prominent problem for the second-order metropolis of India. Limitation of space and high attraction due to commercial activity makes the problem more acute and needs to be addressed particularly in the context of free on-street parking policy. The usual practice of local bodies to manage the demand is to adopt odd and even date on-street parking scheme on the corridors of high demand. The lack of on-street parking policy and unavailability of parking demand data are the major issues, which needs to be addressed for solving the parking problem. Hence, appropriate methodology to assess the on-street parking demand needs to be formulated to frame on-street parking policy for its effective management.

2 Review of Literature

From Indian context, very limited literature is available for the assessment of on-street parking demand. Work reported by some researchers in this area is discussed in this section. Chimba and Onyango [5] studied three different land-use types like

downtown area, shopping center, and beach park. The study conducted a continuous parking survey of license plate numbers for at least 3 h, recorded at every 5 min interval. The analysis found that, to detect all possible optimal parking characteristics and cost-efficient surveying, license plates should be monitored at intervals less than every 30 min for downtown and 60 min for beach parks. Huayan et al. [6] performed a parking survey study on the campus of the Beijing University of Aeronautics and Astronautics. The study analyzed demand at different times of day by collecting inflow and outflow data to the university campus at the main university entrance and exit. Parking duration for each vehicle was obtained by subtracting entry time from exit time. The study performed a simple parking demand, duration, and turnover analysis. Tong et al. [7] presented a method based on the cluster analysis, to construct aggregate parking accumulation profiles at car parks to increase the efficiency of survey data collected. The authors stated that the accumulation profiles can assist transport professionals in the decision process and validate parking demand models. Millard-Ball et al. [8] have applied theoretical models calibrated with parking sensor data from the SFpark pricing program in San Francisco and found that parking pricing significantly impacts the number of city blocks cruised. Levy et al. [9] using a simulation model demonstrated how an occupancy rate above 92–93% results with a sharp increase in cruising time, which depends on spatial dynamics. However, parking occupancy level may not reflect the overall parking utilization level as the same occupancy might correspond to different parking circulation (e.g., number of cars using a parking place throughout the day). Wong et al. [10] assumed that the parking activity associated with individual land-use variables has a unique parking accumulation profile, and surveys were conducted to determine these profiles. The results of these surveys have been used to develop parking demand models in Hong Kong. Chen et al. [11] studied parking characteristics like parking indexes, parking saturation, peak parking ratio, parking turnover rate, and parking duration for different land-use types and different parking facilities in Shanghai. The authors observed that market areas and food- and drink-oriented areas exhibited high parking saturation. However, in business and office-oriented areas, the total parking space supply is sufficient to meet current parking demands.

3 Need and Objectives of the Study

Review of available literature revealed that very few studies are concentrated upon assessment of on-street parking in developing countries like India. Hence, the present study is an attempt to develop a methodology to assess on-street parking demand. With this motivation, the objectives of the present study have been formulated to assess on-street parking demand for two land-use types representing CBD area of Rajkot city.

4 Study Area and Data

4.1 Study Area

Rajkot has a strong manufacturing economic base, with a market that extends beyond not only the state of Gujarat, but also across the national boundaries. In its early history, Rajkot was organized around the textile mills. More recently, the city economy has shifted to small and medium industries dominated by foundries, manufacture of oil engine, machine tools, engineering and automobile works, castor oil processing, gold and silver jewelery, handicrafts, ready-made ladies garment, spices, medicines, and wall clocks. The major modes of transport in Rajkot are motorized two-wheeler (2-W) and auto-rickshaw (an IPT mode of transport). Rajkot city has witnessed an extraordinary vehicular growth during the past five years, with the registration of average 241 motorized two-wheelers (M2-W) and 24 cars per day, which generates significant demand for parking. This exorbitant vehicular growth has subsequently increased demand of parking, particularly in the area of high attractions like CBD located in the old walled city. Therefore, for the present study, two busy streets with diverse different land-use patterns in CBD area were selected as shown in Fig. 1.

Sir Lakhajiraj Road (RR1): This road carries major traffic volume of city. It inhibits high commercial activities due to the location of jewelery, footwear, ready-made garment, and cosmetics shops in the vicinity, which has a high potential for trip attraction during business hours. It allows the on-street parking on either side of the carriageway with *odd-even date parking scheme*. **Vidyanagar main Road (RR2)** another popular road of the city area in Rajkot having dominance medical shops and hospitals. High on-street parking demand of visitors is observed during the morning peak hours. Parking is permitted on both the sides of this road. The road inventory details of both the roads are presented in Table 1.

Figure 2 represents chaotic parking in Rajkot city. On both streets, it was observed that no demarcations of parking bays were made for the vehicles. During the business hours, both the streets observed high on-street parking demand, however, limited availability of on-street parking space thereby resulted in double parking as well as

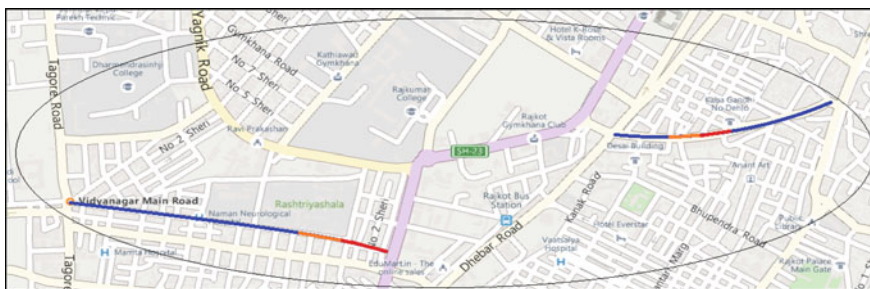


Fig. 1 Location of study area in Rajkot city

Table 1 Road inventory details

Detail of road	Sir Lakhajiraj Road (RR1)	Vidyanagar Main Road (RR2)
Length of the street	600 m	748 m
Effective curb length for parking	558 m	700 m
Right of way	17 m	17 m
Width of carriage way	11 m	9 m
Width of parking space	1.5 m (each side)	1 m (each side)
Width of sidewalk	1.5 m	0
Maximum no. of parking bays	650 as per IRC bay size for two-wheeler (0.85 × 2.5 m)	823 as per IRC bay size for two-wheeler (0.85 × 2.5 m)
Land-use type	Commercial	Medical

**Fig. 2** Current on-street parking situation within study sites

illegal parking. Such chaotic parking reduces the carriageway width, which hindered a smooth flow of through traffic, apart from congestion problems. Encroachment by the street hawkers in the parking space is commonly observed, which also restricts the available parking stretch of carriageway.

4.2 Data Collection Methodology

Primarily, parking inventory using license plate was carried out on both subject roads at 1 h interval for 12 h (8 am–8 pm) during business hours on a normal working day, to determine peak parking hours. Thereafter, microscopic assessment of parking demand was carried out during peak parking hours by collecting demand data at 10 min monitoring interval during September–October 2016 for four days covering normal working day and weekend using license plate method in order to account the variation in parking demand over the days. Parking survey traps of different lengths were considered at different locations along the entire street to capture variation in

parking demand due to the discrepancy in activity types and to exemplify parking characteristics of the entire street. Individual bays were not demarcated on the study site, and hence, a number of bays were calculated as per guidelines given in [12].

5 Data Analysis

Analysis of parking inventory revealed that peak parking demand varied for both land-use patterns and is conclusive from Fig. 3. Furthermore, empirical observation revealed heterogeneity in parking demand with the dominance of motorized two-wheeler.

From Fig. 3, it can be noted that maximum parking accumulation was observed 5–8 pm for road serving commercial land use while 9 am–12 noon for the road serving hospital land use reflecting the influence of land-use type. Since parking demand was observed to be dominated by motorized two-wheelers (2-Ws), it was found appropriate to convert demand in terms of equivalent 2-W (E2W) demand. Therefore, one car was considered as four 2-Ws, while one 3-W (auto-rickshaw) was considered as two 2-Ws [12]. Figure 4 represents parking demand accumulation during peak hours at monitoring interval of 10 min.

5.1 Observed Demand and Percentage of Unique Parked Vehicles

Observed parking demand was extracted for different data monitoring interval (10–60 min). From this observed demand, unique vehicles and their respective percentage were extracted for each data monitoring interval for both subject roads as summarized in Tables 2 and 3. Here unique vehicles are distinct (non-repetitive

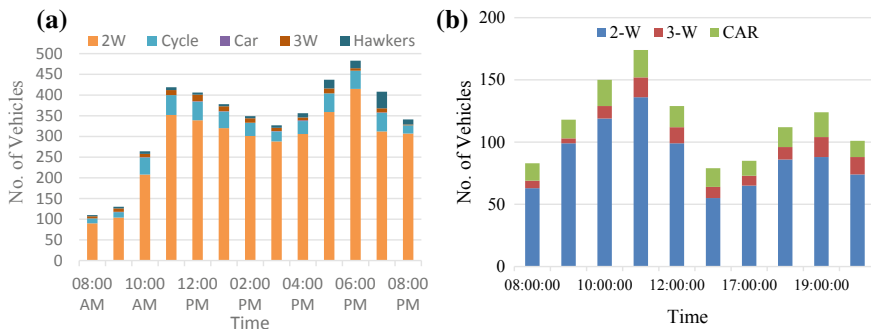


Fig. 3 Parking accumulation for 12 h interval. a RR1, b RR2

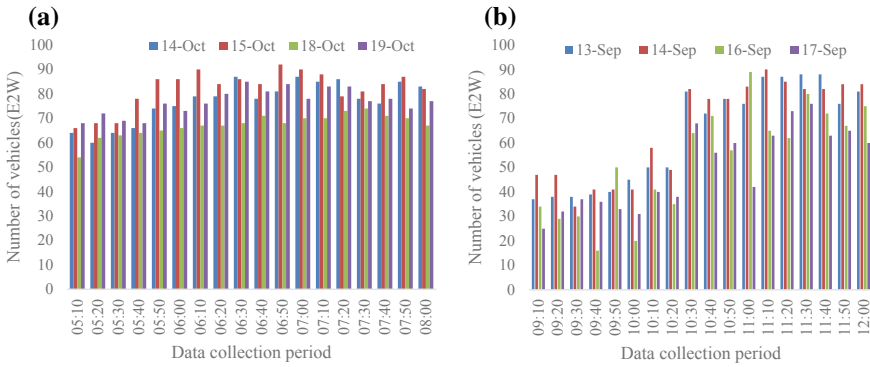


Fig. 4 Parking demand accumulation during peak hours for **a** RR1 (commercial), **b** RR2 (medical land use)

Table 2 Observed parking demand for different data monitoring interval

Road name/data monitoring interval	Survey date	10 min	20 min	30 min	40 min	50 min	60 min
RR1 (commercial land use)	14th October	1387	697	448	395	296	228
	15th October	1479	744	490	413	328	244
	18th October	1210	599	397	327	259	191
	19th October	1382	692	454	386	303	227
RR2 (medical land use)	13th September	821	409	255	230	109	117
	14th September	913	446	295	181	119	141
	16th September	857	415	266	257	126	113
	17th September	935	468	302	206	142	135

Table 3 Percentage of unique parked vehicles for different data monitoring interval

Road name/data monitoring interval	Survey date	10 min	20 min	30 min	40 min	50 min	60 min
Sir Lakhajiraj road (commercial land use)	14th October	21	31	43	36	40	57
	15th October	23	38	43	43	44	61
	18th October	25	38	48	45	49	70
	19th October	21	32	41	38	43	58
Vidhyanagar main road (hospital land use)	13th September	19	34	40	47	60	57
	14th September	19	36	44	55	64	51
	16th September	20	38	46	45	62	56
	17th September	19	35	44	59	59	53

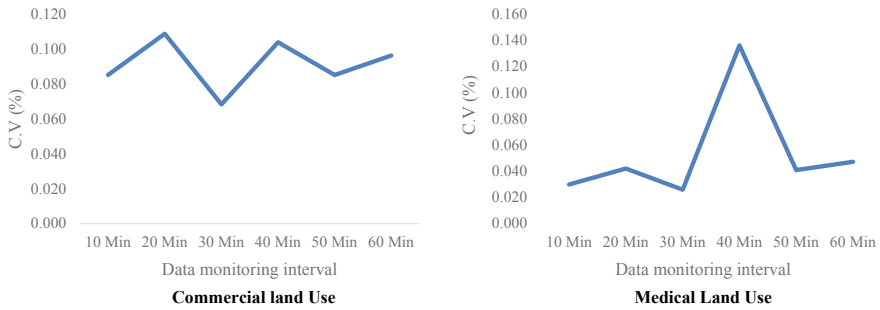


Fig. 5 Coefficient of variation for unique vehicle

vehicles) which used a given parking space. In simple words, unique vehicles do not account for repetitive vehicles.

From Table 2, it can be noted that monitoring interval has a significant effect on observed demand. Observed demand followed a decreasing trend as data monitoring interval decreases. Higher demand at smaller monitoring interval (10–30 min) can be attributed to observance of the same vehicle throughout the data collection period. However, the percentage of unique parked vehicles (PUPV) followed an increasing trend as monitoring interval increases. A consistent trend was observed for all survey days of both subject roads. To probe further, consistency of PUPV in terms of coefficient of variation was obtained for different data monitoring interval as shown in Fig. 5.

From Fig. 5, consistency of parking demand (lowest value of C.V) is observed at 30 min frequency for both land uses. Therefore, on-street parking inventory should be carried out at 30 min in CBD areas.

5.2 Percentage Repetition of Parked Vehicles (PRV)

Microscopic demand assessment analysis was carried out by obtaining percentage repetition of vehicles (PRV) between two sets for successive observations for different data monitoring interval for subject land-use patterns. It can be observed that for 10 min data monitoring interval PRV nearly had values of 100%, and therefore, it was found appropriate to collect data at every 10 min monitoring interval (Figs. 6, 7, 8, 9, 10 and 11).

It could be observed that percentage repetition of the parked vehicle for different data monitoring intervals followed a decreasing trend as monitoring interval increases. This can be attributed to the data leakage of parked vehicles at higher monitoring interval (40–60 min). Percentage repetition of parked vehicles followed a consistent trend after 40 min frequency, indicating uniform parking behavior of long-term parkers. Statistical check using one-way ANOVA was carried out for rep-

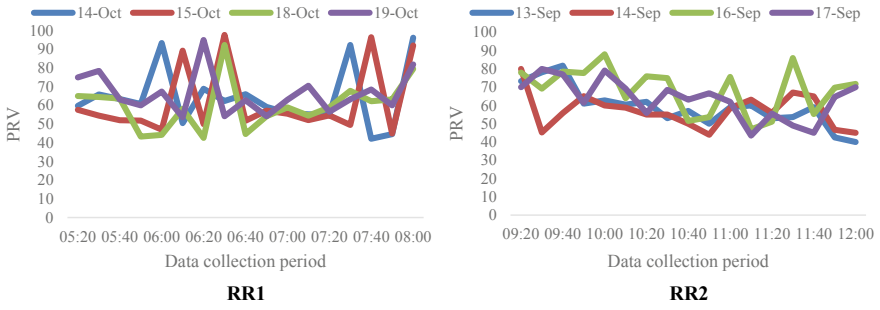


Fig. 6 Percentage repetition of vehicle during 10 min for 3 h

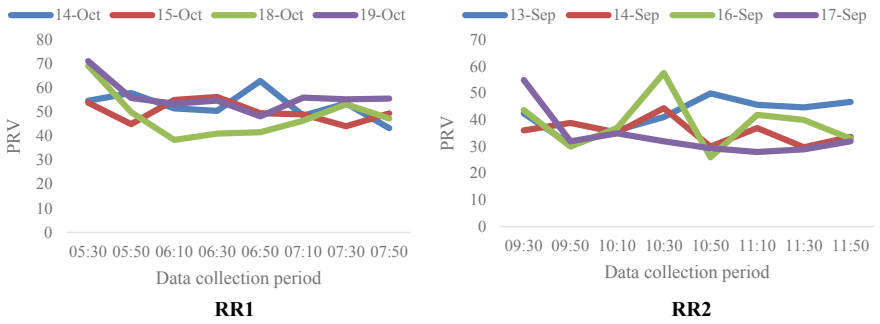


Fig. 7 Percentage repetition of vehicle during 20 min for 3 h

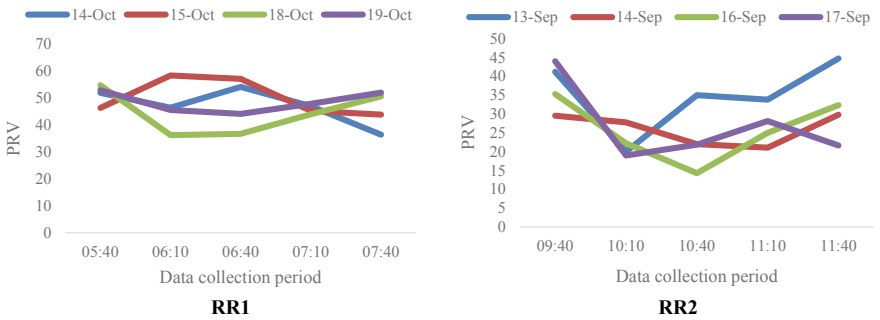


Fig. 8 Percentage repetition of vehicle during 30 min for 3 h

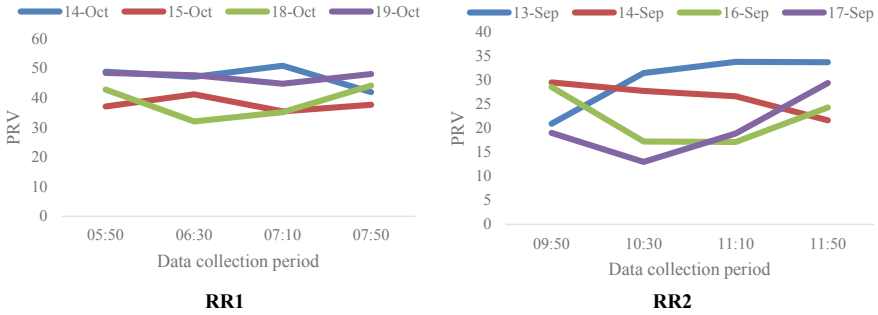


Fig. 9 Percentage repetition of vehicle during 40 min for 3 h

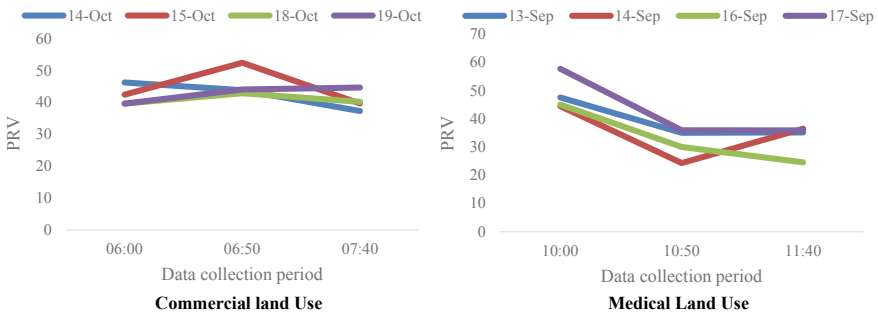


Fig. 10 Percentage repetition of vehicle during 50 min for 3 h

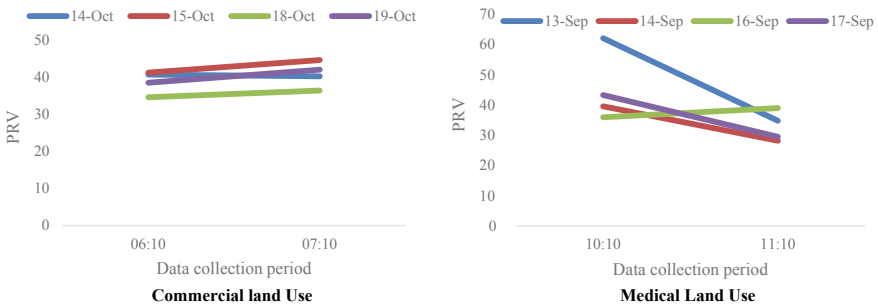


Fig. 11 Percentage repetition of vehicle during 60 min for 3 h

etition of the parked vehicle between different data monitoring interval for both land-use type. Results are shown in Tables 4 and 5.

Ho: The percentage repetition of the parked vehicle is statistically similar for different data frequency.

Table 4 ANOVA test result

RR1 (commercial land use)					
Time interval	Survey date	<i>F</i>	<i>p</i> -value	<i>F</i> _{critical}	Remarks
10, 20, 30 min	14th October	3.091	0.050	3.354	Rejected
	15th October	4.272	0.024	3.354	Rejected
	18th October	4.806	0.016	3.354	Rejected
	19th October	8.331	0.001	3.354	Rejected
40, 50, 60 min	14th October	1.952	0.222	5.143	Accepted
	15th October	2.347	0.176	5.143	Accepted
	18th October	1.243	0.333	5.143	Accepted
	19th October	7.701	0.065	5.143	Accepted

Table 5 ANOVA test result

RR2 (medical land use)					
Time interval	Survey date	<i>F</i>	<i>p</i> -value	<i>F</i> _{critical}	Remarks
10, 20, 30 min	13th September	4.802	0.017	3.354	Rejected
	14th September	4.282	0.034	3.354	Rejected
	16th September	6.528	0.004	3.354	Rejected
	17th September	1.456	0.250	3.354	Rejected
40, 50, 60 min	13th September	0.688	0.538	5.143	Accepted
	14th September	0.799	0.492	5.143	Accepted
	16th September	1.062	0.402	5.143	Accepted
	17th September	0.624	0.567	5.143	Accepted

In reference to *p*-value, it can be concluded that significant difference exists in percentage repetition of parked vehicles between 10 and 30 min data monitoring interval, and hence, monitoring intervals of 10, 20, and 30 min were considered for further microscopic analysis. To scrutinize further, difference of repetition between different frequency intervals, *t*-test was carried out at 5% significance for null hypothesis; “no difference in variation for percentage repetition of vehicles between different frequency intervals exists.” Results are summarized in Table 6.

From Table 6, it can be concluded that parking behaviour becomes consistent after 20 min data monitoring interval. Henceforth, significant variation in demand behaviour exists till 20 min; therefore, the threshold time limit for free on-street parking may be recommended up to 20 min for both land uses. Further examination was carried out by calculating the efficiency of space.

Table 6 Hypothesis testing results

Time interval	RR1 (commercial land use)			RR2 (medical land use)		
	Date	<i>p</i> -value (t-test)	Remarks	Date	<i>p</i> -value (t-test)	Remarks
10 min–20 min	14th October	0.049	Rejected	13th September	0.042	Rejected
	15th October	0.095	Accepted	14th September	0.038	Rejected
	18th October	0.038	Rejected	16th September	0.040	Rejected
	19th October	0.028	Rejected	17th September	0.311	Accepted
20 min–30 min	14th October	0.879	Accepted	13th September	0.974	Accepted
	15th October	0.935	Accepted	14th September	0.211	Accepted
	18th October	0.452	Accepted	16th September	0.180	Accepted
	19th October	0.032	Rejected	17th September	0.523	Accepted

5.3 Turnover

Turnover, which symbolizes the efficiency of space, was calculated from unique vehicles for different data monitoring interval for both subject land-use types. Figure 12 represents turnover for different data monitoring intervals.

It can be observed that turnover followed a decaying trend as data monitoring interval increases. A consistent trend was observed for both subject land-use types. Furthermore, it can be observed from the figure that a consistent turnover values are

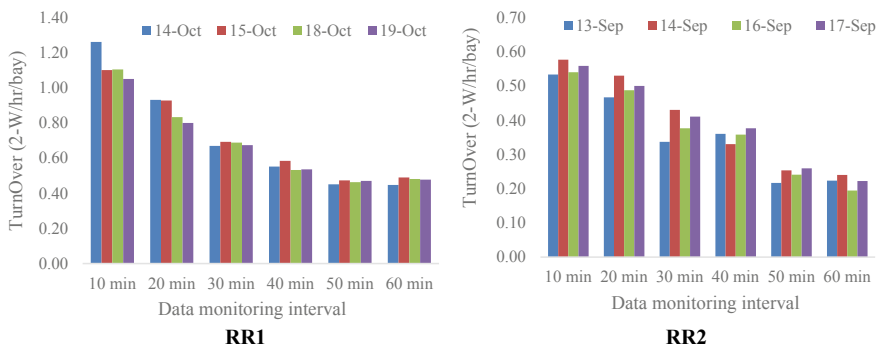


Fig. 12 Turn over for different data monitoring intervals

observed for 30 min data monitoring interval for both subject land-use types, further supporting the observations of Fig. 6. Therefore, on-street parking utilization and efficiency should be carried out at 30 min data monitoring interval.

6 Conclusion

The present attempts to analyze on-street parking demand for a case representing CBD area of Rajkot city. Two diverse land-use types were considered for the assessment of on-street parking demand. The following conclusion is drawn from the study:

1. On-street parking inventory should be carried out at 10 min data monitoring interval for comprehensive assessment on-street parking demand.
2. The on-street parking should be accessed in terms of E2W where demand is dominated by 2-Ws.
3. Consistency of PUPV and turnover was observed for 30 min data monitoring interval, and therefore, on-street parking utilization and efficiency should be evaluated at 30 min data monitoring interval.
4. In the context to statistical results on PRV for different data monitoring intervals, maximum time-free on-street parking should be restricted to 20 min.
5. The study proposes to formulate paid on-street parking policy in accordance with efficiency (turnover) of parking space rather based on land cost as advocated by NUTP 2014.

Acknowledgements The authors extend a deep sense of gratitude toward Municipal Corporation of Rajkot city, for granting permission to carry out parking inventory. The authors are immensely thankful to those helped in parking survey.

References

1. Stockholms stad (2013a) Mobility strategy: parking plan, Mars 2013 (in Swedish). Available at: www.stockholm.se/trafikkontoret. Accessed July 2014
2. Rastogi R (2006) Preference of vehicle parker's in Kota city—a stated preference study. *Indian Highways* 34(3):45–59
3. Barter P (2011) Parking policy for developing countries. Asian Bank Development Report. Asian Development Bank, Mandaluyong City
4. De Cerreno A (2004) Dynamics of on-street parking in large central cities. *Transp Res Rec: J Transp Res Board* 1898:130–137
5. Chimba D, Onyango M (2012) Optimization of short-term on-street park-pay license plate surveying. *J Infrastruct Syst* 18(1):194–201
6. Huayan S, Wenji L, Haijun H (2007) Empirical study of parking problems on University Campus. *J Transp Syst Eng Inf Technol* 7(2):135–140
7. Tong CO, Wong SC, Leung BSY (2004) Estimation of parking accumulation profiles from survey data. *Transportation* 31:183–202

8. Millard-Ball A, Weinberger RR, Hampshire RC (2014) Is the curb 80% full or 20% empty? Assessing the impacts of San Francisco's parking pricing experiment. *Transp Res Part A Policy Pract* 63:76–92
9. Levy N, Martens K, Benenson I (2013) Exploring cruising using agent-based and analytical models of parking. *Transp A Transp Sci* 9(9):773–797
10. Wong SC, Tong CO, Lam WCH, Fung RYC (2000) Development of parking demand models in Hong Kong. *J Urban Plann Dev* 55–74. [https://doi.org/10.1061/\(ASCE\)0733-9488\(2000\)126:2\(55\)](https://doi.org/10.1061/(ASCE)0733-9488(2000)126:2(55))
11. Chen Q, Wang Y, Pan S (2015) Characteristics of parking in Central Shanghai, China. *J Urban Plann Dev* [https://doi.org/10.1061/\(asce\)up.1943-5444.0000293](https://doi.org/10.1061/(asce)up.1943-5444.0000293)
12. Guidelines for parking facilities in urban areas, Indian Road Congress, Special Provision, IRC SP-12 2015

Comparative Study of Pedestrian Critical Gap Estimation Methods at Unsignalized Midblock Crosswalks



V. S. Vinayaraj, Avinash Chaudhari, Shriniwas Arkatkar, Gaurang J. Joshi and Manoranjan Parida

Abstract This study determines critical gaps using different methods like Raff's, maximum likelihood (MLM), root-mean-square (RMS), probability equilibrium (PEM), and logit. These are then compared to single out the most appropriate one. Five locations in the western part of India are studied, selected based on type of land use, number of lanes, and carriage-way width. Video cameras were used to capture the mixed-traffic flow and pedestrian crossing movements simultaneously. The results also conclude that logit method is the most appropriate one for estimating critical gap, as it considers the effect of pedestrian behaviour and vehicular characteristics concurrently. The critical gap values vary considerably when pedestrian characteristics are considered. The results are expected to provide inputs for framing design parameters for pedestrian crossing facilities, thereby enhancing pedestrian safety.

Keywords Critical gap · Midblock · MLM · Logit method · Pedestrian behaviour · Vehicular characteristics

V. S. Vinayaraj · A. Chaudhari · S. Arkatkar (✉) · G. J. Joshi
Civil Engineering Department, Sardar Vallabhbhai National Institute of Technology (SVNIT),
Surat, Gujarat 395007, India
e-mail: sarkatkar@gmail.com

V. S. Vinayaraj
e-mail: vinayaraj4u@gmail.com

A. Chaudhari
e-mail: avinashchaudhari17@yahoo.com

G. J. Joshi
e-mail: gjsvnit92@gmail.com

M. Parida
Department of Civil Engineering, Indian Institute of Technology Roorkee, Roorkee, UK 247667,
India
e-mail: mparida@gmail.com

1 Introduction

Midblock crosswalks act as connectors between adjoining activities based on a particular landuse type. At midblocks, under unsignalized conditions, there are higher chances of conflicts between the crossing pedestrians and approaching vehicles. Researchers [1] have reported that significant number of pedestrian fatalities is observed at midblock locations. Consequently, crossing at midblocks turn out to be a serious hazard to pedestrians, particularly under heterogeneous traffic conditions. Critical gap is one of the most important parameters in gap acceptance process and hence determining the safety as well as investigating the accident-risk analysis of pedestrians. One of the ways of studying pedestrian crossing behaviour is to estimate critical gap, using accepted/rejected gaps by the pedestrians, which also may indicative of safety levels prevailing at pedestrian facilities. As per [2], the minimum time gap (seconds) for a pedestrian to attempt crossing the road is the critical gap. However, pedestrians may resort to crossing the road with a time gap less than the critical gap indicating different behavioural features, such as increase in speed, crossing path change condition, rolling behaviour, increase in the number of attempts, and pedestrian group behaviour. The critical gap is affected by several factors such as age, gender, and also other induced factors, and it plays a major role from the safety point of view at unsignalized midblock crosswalk. Furthermore, driver-yielding behaviour also affects the pedestrian's accepted gap size, particularly under mixed-traffic conditions.

The background of the research is examined for the comprehensive review of existing literature related to various approaches, which were adopted for the assessment of the critical gap and its applicability in heterogeneous traffic conditions. The pedestrian crossing behaviour can be studied with the help of gap acceptance theory: [3, 4]. Several methods are available for the determination of critical gap and most of these methods assume drivers to be consistent and homogeneous. Some of the earlier research studies have explored critical gap was estimated by different methods like Raff's method [5, 6]. Ashworth [7] estimated critical gap using major stream traffic flow, standard deviation of accepted gap, and mean value of accepted gap. Tian et al. [8] used maximum likelihood method (MLM) for estimation of driver's critical gap, logit as well as probit models [4–9] found in his study that most of the crossing cases involving elderly pedestrians accept more time gap. Rastogi et al. [10] also carried out studies in pedestrian crossing speed, and he mentioned that crossing speed of a male pedestrian is comparable with that of a female pedestrian irrespective of the road type and land use. Kadali and Vedagiri [11] investigated that the pedestrian behavioural characteristics like the rolling gap, driver-yielding behaviour, and frequency of attempts play an important role in pedestrian uncontrolled midblock road crossing. The results [12] concluded that number of lanes, vehicular volume, and pedestrian characteristics have a great significance on the pedestrian accepted gap values. Pedestrian walking speed depends on the individual characteristics such as age, direction, gender, luggage condition [5, 12–14] and varies with the prevailing conditions such as environmental and traffic flow [15]. Decrease in critical gap is

witnessed due to smaller gaps available in traffic stream at higher volume of traffic [12]. Pawar and Patil [16] also stated that the values of critical gap are higher in developed countries than for Indian condition due to the aggressive driver behaviour. Wu [17], Kadali and Vedagiri [18], Chandra and Kumar [19], Fitpatrick [20], Troutbeck [21], Wu [22], Cassidy et al. [23], IRC [24], Kumar and Parida [25], Troutbeck [26], Chaudhari [27] proposed probability equilibrium method (PEM), which is based on the equilibrium of probability between rejected and accepted gaps, established macroscopically using the cumulative distribution of rejected and accepted gaps. Kadali and Vedagiri [18] used different techniques for estimation of critical gap method, and the result revealed that there is a significant difference in critical gap values estimated with-and-without considering pedestrian behavioural characteristics. Limited studies are available related to the effect of human factors on critical gap, which has a significant effect on pedestrian safety. Furthermore, it is also evident that critical gap analysis-related studies at unsignalized midblock crosswalk, particularly under heterogeneous traffic scenario, are very few. Hence, it is worth studying, the appropriateness of critical gap estimation methods, while explaining the effect of human factors on size of critical gaps at unsignalized midblock sections. The objective of the study is to compare and select the most suitable method from the selected methods such as Raff's, MLM, RMS, PEM, and logit methods for pedestrian critical gap estimation at unsignalized midblock crosswalks under mixed traffic conditions. The paper is organized in five sections. An overview of critical gap and gap acceptance behaviour at midblock section is given in Sect. 1 and followed by literature review related to gap acceptance. Section 2 describes the selection of study area and methodology of data collection. Section 3 presents the analysis of critical gap. Critical gap estimation method and results are presented in Section 4, followed by conclusions in Sect. 5.

2 Study Area and Data Collection Methodology

In order to verify the influence of physical characteristics of the facility, geometry, and cultural diversity of folks, study sites were selected at five different locations in the western part of India, namely, (i) Varachha in Surat, (ii) Astodia in Ahmadabad, (iii) Bandra, (iv) Vile parle, and (v) Vakola in Mumbai. Locations for data collection were selected on the basis of type of land use, number of lanes (four-lane divided, six-lane divided, and eight-lane divided), carriage width of the road and pedestrian behavioural characteristics with wide range of available gaps as shown in Fig. 1. Video graphic surveys were carried out from 8:00 am to 6:00 pm using two high-resolution video cameras, mounted on a nearby high-rise building, which captured the mixed traffic flow as well as pedestrian crossing movement at selected sections simultaneously. The recorded video data was extracted from Avidemux video editor software and the parameters like pedestrian flow, vehicular characteristics (vehicle speed, type of vehicle), demographic composition of pedestrians (based on age), crossing movement, and vehicular gap accepted by the pedestrians were obtained



Fig. 1 Schematic photographs of selected study locations

Table 1 Details of study locations with traffic flow data

S. no.	Study sites	Classification of road	Total road width	Pedestrian volume (Ped/h)	Traffic volume (PCU/h)	Average traffic speed (Kmph)
1	Varachha, Surat (commercial)	Six-lane divided	9.6	1235	3554	24.75
2	Astodia (Ahmedabad) (Mixed land use)	Four-lane divided	6.7	610	4612	27.5
3	Bandra Mumbai (commercial)	Four-lane divided	6.6	711	2674	24
4	Vile parle Mumbai Rail transit terminal	Four-lane divided	6.4	818	3432	18.84
5	Vakola, Mumbai Rail transit terminal	Eight-lane divided	12.8	980	4174	38.34

and analysed. Analysis based on vehicle composition showed that the mode share of car is dominant in Bandra, Vakola, Varachha and Vile parle whereas, in Astodia, two-wheelers are found to be prevalent. The proportion of non-motorized (cycle) vehicles at the selected midblock section was found to be relatively very low. Moreover, dynamic PCU values of Chandra's (2003) [19] were used to convert traffic volume into pcu/hr. Table 1 depict that details of the study locations and traffic flow data.

3 Analysis of Critical Gaps

Critical gap is one of the most important parameters influencing the gap acceptance process of pedestrians crossing the road. Pedestrian critical gap is defined as the average minimum time gap between approaching vehicles allowing the pedestrian to cross the road safely and measured in seconds (s). The critical gap is the parameter which cannot be measured in field, but it is generally measured in terms of accepted and rejected gap. The estimation of critical gap is also a crucial process, when applied to heterogeneous conditions like India, because of lack of lane discipline. Several methods are available for the determination of critical gap, and most of these methods assume drivers to be consistent and homogeneous. A consistent driver will accept all gaps, which are more than his critical gap and will reject all other gaps which are less

than his critical gap. The critical gap value was calculated from the field observed accepted and rejected gap data of five study locations in India using Raff’s method, maximum likelihood method (MLM), root-mean-square method (RMS), probability of equilibrium method (PEM), and logit method.

4 Critical Gap (CG) Estimation Methods and Results

4.1 Raff Method

In order to find the critical gap by using Raff’s method, the critical gap is estimated by utilizing an empirical distribution function of accepted gaps $F_a(t)$ and rejected gaps $F_r(t)$ and the relationship is shown in Eq. (1)

$$F_a(t) = 1 - F_r(t) \tag{1}$$

This method is commonly used for estimating the critical gap due to its simplicity. The cumulative distribution of accepted gap, $F_a(t)$ is plotted on the same graph with the reverse cumulative distribution of rejected gaps, $1 - F_r(t)$. The point where the two curves intersect (Accepted and rejected) is termed as critical gap: [20–6]. Figure 2 indicates the critical gap value as 3.5 s. Based on this aforementioned procedure, average critical gap results were estimated at different study sites, having different pedestrian, vehicular and traffic characteristics, results of which are shown in Table 2. It can be observed that critical gap value varies between gender and among different age groups.

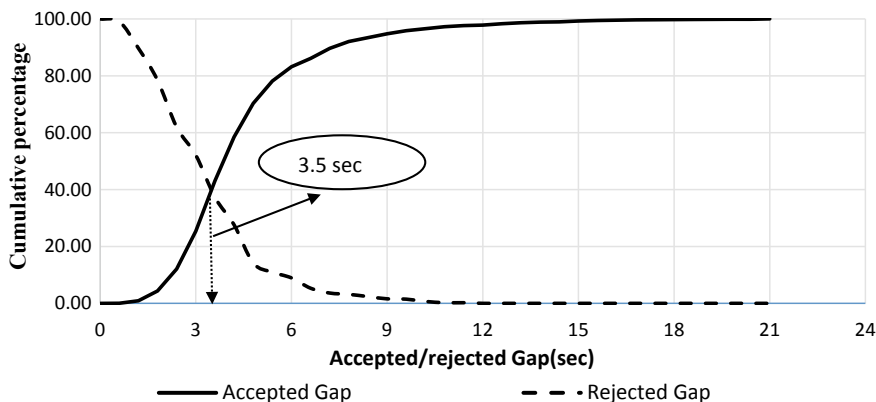


Fig. 2 Critical gap estimation by Raff method

Table 2 Estimation of pedestrian critical gap results by Raff’s method

Demographic characteristics	Category	Pedestrian critical gap (s)				
		L1	L2	L3	L4	L5
Combined		4.4	2.23	6.1	3.5	5.2
Gender	Male	4.15	2	6.0	3.3	5.1
	Female	4.40	2.22	6.9	3.6	5.3
Children(<15 age)	Male	4.5	2.1	5	3.6	5.2
	Female	4.4	2.24	5.4	3.8	5.7
Younger(15–30)	Male	3.5	2.02	5.1	2.9	4.5
	Female	4.2	2.2	5.6	3.2	4.8
Middle (31–50)	Male	3.9	2.12	5.5	3.6	5.0
	Female	4.5	2.3	6	4	5.5
Elder (>50)	Male	4.8	2.12	6.5	3	5.1
	Female	5.0	2.28	7.2	3.4	5.8
Group behaviour	Group size one	4.47	2.09	4.72	3.01	4.8
	Group size two	5.06	2.1	5.03	3.5	5.3
	Group size three	5.19	2.14	5.37	3.8	5.57

Note Location no., L1: Varachha; L2: Ahmadabad; L3: Vakola; L4: Bandra; L5: Vile parle

4.2 Maximum Likelihood Method (MLM)

Troutbeck [20] developed a model for estimating critical gap based on the maximum likelihood method. This model assumes the log-normal distribution of accepted and maximum rejected gaps; the maximum rejected gap and the corresponding accepted gap of each vehicle are treated pair-wise. For a specific scenario, pedestrian i observed one accepted gap (a_d) and one corresponding to the maximum rejected gap (r_d). The maximum rejected gap is the largest value of all rejected gaps. It is assumed that each and every pedestrian will reject gap value, which is smaller than critical gap and accept greater than or equal to critical gap. The likelihood function is defined as the probability that the critical gap distribution lies between the observed distribution of the maximum rejected gaps and the accepted gaps. The MLM then calculates the probability of the critical gap being between the largest rejected gap (r_d) and accepted gap (a_d). The likelihood Eq. (2) is given below.

$$L^* = \prod_n^{d=1} (F_d(a_d) - F_r(r_d)) \tag{2}$$

The parameters of distribution function of the critical gaps, the mean μ and variance σ^2 are obtained by maximizing the likelihood function. After getting the values of mean (μ) and standard deviation (σ) (Iteration by solver tool pack) following, Eq. (3) is used to estimate the critical gap values.

Table 3 Estimation of pedestrian critical gap results by MLM method

Demographic characteristics	Category	Pedestrian critical gap (s)				
		L1	L2	L3	L4	L5
Combined one		4.0	2.34	4.75	3.84	4.23
Gender	Male	3.7	2.3	4.63	3.71	4.21
	Female	4.04	2.43	4.82	4.09	4.25
Children (<15 Age)	Male	3	2.23	4.39	4.03	4.24
	Female	3.4	2.57	4.75	4.32	4.34
Younger (15–30)	Male	3.6	2.33	4.68	3.02	4.42
	Female	3.9	2.57	4.87	3.59	4.61
Middle (30–50)	Male	3.7	2.33	4.73	3.91	3.92
	Female	4	2.57	4.79	4.28	4.07
Elder (>50)	Male	3.8	2.5	4.73	4.01	4.02
	Female	4.1	2.48	4.89	4.1	4.13
Group behaviour	Group size one	3.6	2.36	4.66	3.38	4.13
	Group size two	3.9	2.3	4.72	3.42	4.21
	Group size three	4.2	2.3	4.99	4.61	4.35

Note Location no, L1: Varachha; L2: Ahmadabad; L3: Vakola; L4: Bandra; L5: Vile parle

$$t_c = e^{\mu+0.5\sigma^2} \tag{3}$$

where

t_c Critical gap (CG)

μ Mean of accepted and maximum rejected gaps

σ Standard deviation of accepted and maximum rejected gaps

Based on the above procedure, CG values were calculated and are shown in Table 3.

4.3 Root-Mean-Square Method (RMS)

The root-mean-square (abbreviated RMS) also known as the quadratic mean in statistics. It is defined as the square root of the mean of the squares of a sample. The RMS value of a set of values is the square root of the arithmetic mean of the squares of the values or the square of the function that defines the continuous variable. In the present study, estimation of critical gap has been done by minimizing the objective function shown in Eq. (4) (sum of the root-mean-square function values for each dataset) by adjusting the critical gap value, which is giving arbitrarily. Since this is an iterative process, it necessitates the use of Solver tool of excel. Critical gap results were calculated based on the aforementioned procedure for all selected sites with

Table 4 Estimation of pedestrian critical gap results by RMS method

Demographic characteristics	Category	Pedestrian critical gap (s)				
		L1	L2	L3	L4	L5
Combined one		4.01	2.24	4.67	3.28	3.98
Gender	Male	3.6	2.18	4.63	3.1	3.99
	Female	4.0	2.35	4.75	3.63	4.04
Children (<15 Age)	Male	3.1	2.14	4.24	3.55	3.99
	Female	3.5	2.35	4.72	3.59	4.27
Younger (15–30)	Male	3.4	2.1	4.5	2.15	4.2
	Female	3.8	2.32	4.6	3.09	4.25
Middle (31–50)	Male	3.6	2.25	4.48	3.59	3.81
	Female	4.0	2.45	4.54	3.73	3.92
Elder (>50)	Male	3.7	2.31	4.67	3.59	3.84
	Female	4.0	2.32	4.76	3.80	3.96
Group behaviour	Group size one	3.6	2.22	4.49	2.82	3.89
	Group size two	4.1	2.2	4.65	3.0	3.95
	Group size three	4.5	2.2	4.89	3.27	4.17

Note Location no., L1: Varachha; L2: Ahmadabad; L3: Vakola; L4: Bandra; L5: Vile parle

demographic characteristics and group behaviour as shown in Table (4).

$$RMS = \sum_{i=1}^n \sqrt{\frac{(t_{ai} - t_c)^2 + (t_c - t_{ri})^2}{2}} \tag{4}$$

where

- t_{ai} Accepted gap of individual vehicle i
- t_{ri} Rejected gap of individual vehicle i
- t_c Critical gap value.

4.4 Probability Equilibrium Method (PEM)

A novel approach for the estimation of critical gap at unsignalized intersection is developed by Wu [17]. This method is purely based on the background of probability equilibrium between the rejected and accepted gaps.

The equilibrium is proven macroscopically using the cumulative distribution of the rejected and accepted gaps. The model generates directly the probability distribution function of the critical gaps. This model can take into account all relevant gaps not only the maximum rejected gaps as is the case of the Trout beck model (1992) and

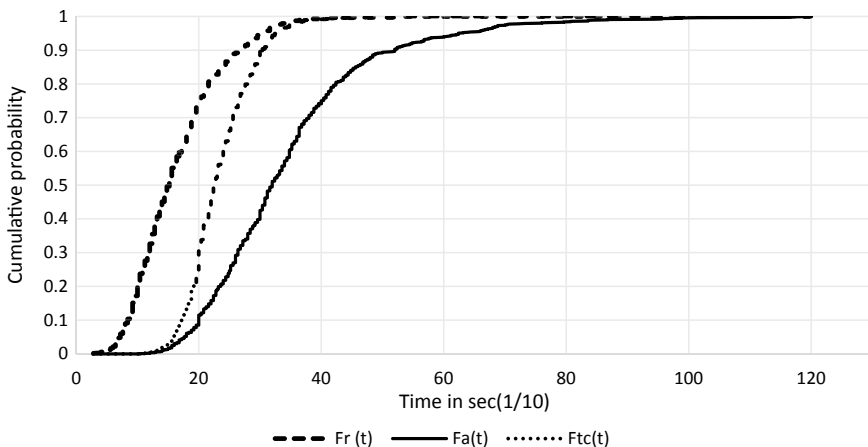


Fig. 3 Cumulative probability distribution of probability equilibrium method

yields the empirical PDF of the critical gaps directly. Imperative aspect of PEM method is that the user does not need to assume a distribution type for the critical gaps and that the method does not involve an iterative process. The critical gaps $F_t(t)$ always lies between the CDFs of the rejected, $F_r(t)$ and accepted, $F_a(t)$ gaps [17–22]: are presented in Fig. 3. The CDF of critical gaps, $F_t(t)$, is calculated using Eq. (5). Table 5 depicts estimated pedestrian critical gap results, which were found at selected locations in different cities.

$$F_t(t) = 1 - \frac{1 - F_r(t)}{F_a(t) + 1 - F_r(t)} \tag{5}$$

4.5 Logit Model

The decision-making process of a pedestrian to cross the road can be identified by binary logistic (BL) technique. Decision-making process of pedestrian based on vehicular gaps (accepted or rejected) gaps is modelled using discrete choice theory [11]. The utility equation for gap acceptance is obtained by considering gap size as the independent variable and the acceptance or rejection (choice) of the gap as the predictor variable. The probability of selecting an alternative (accept/reject) is based on a linear combination function (utility function) and is expressed as:

$$U_i = \alpha_i + \beta_{i1} X_1 + \beta_{i2} X_2 + \beta_{i3} X_3 + \beta_{i4} X_4 + \beta_{i5} X_5 \dots + \beta_{in} X_n \tag{6}$$

where

Table 5 Estimation of pedestrian critical gap results by PEM method

Demographic characteristics	Category	Pedestrian critical gap (s)				
		L1	L2	L3	L4	L5
Combined one		4.0	2.34	4.87	3.88	3.9
Gender	Male	3.6	2.29	4.85	3.74	3.81
	Female	3.9	2.46	4.98	4.13	4.12
Children (< 15 Age)	Male	2.9	2.34	4.46	4.08	3.81
	Female	3.3	2.56	4.64	4.44	4.04
Younger (15–30)	Male	3.4	2.26	4.79	3.2	3.64
	Female	3.7	2.43	4.91	3.65	3.93
Middle (31–50)	Male	3.6	2.32	4.79	3.92	3.93
	Female	3.7	2.58	4.90	4.27	3.97
Elder (>50)	Male	3.7	2.39	4.80	3.96	4.03
	Female	3.9	2.45	4.94	4.13	4.16
Group behaviour	Group size one	3.6	2.32	4.77	3.33	3.82
	Group size two	4.1	2.31	4.83	3.45	4.01
	Group size three	4.4	2.30	5.11	4.65	4.20

Note Location no., L1: Varachha; L2: Ahmadabad; L3: Vakola; L4: Bandra; L5: Vile parle

- U_i the utility of choosing the alternative i ;
- i number of alternatives (for binary logit model it has taken as two (accept/reject);
- X_1, X_2, \dots, X_n variable that influence the pedestrian decision;
- n number of independent variables;
- α constant;
- β coefficients of corresponding variables.

The probability of a pedestrian accepting the ‘ i ’th available gap and crossing the road is given by Eqs. (6) and (7) [16, 23]. The probability of choosing alternative ‘ i ’ is then calculated using the following function:

$$P(i) = 1/[1 + \exp(Ui)] \tag{7}$$

This model is calibrated with the help of SPSS software platform. Using logit model, critical gap is estimated, using gap size as independent variable and response variable is pedestrian decision based on acceptance/rejection of a given gap. The probability of acceptance or rejection of a gap is predicted by this model and the critical gap is estimated as the gap for which the probability of acceptance is 0.50. The cumulative probability plot presented in Fig. 4 represents the probability of acceptance for the observed gaps. The 50th percentile of gaps representing the critical gap for pedestrians is observed as 4.3 s. The critical gap value is calculated based on utility equation and critical gap results are indicated in Table 6.

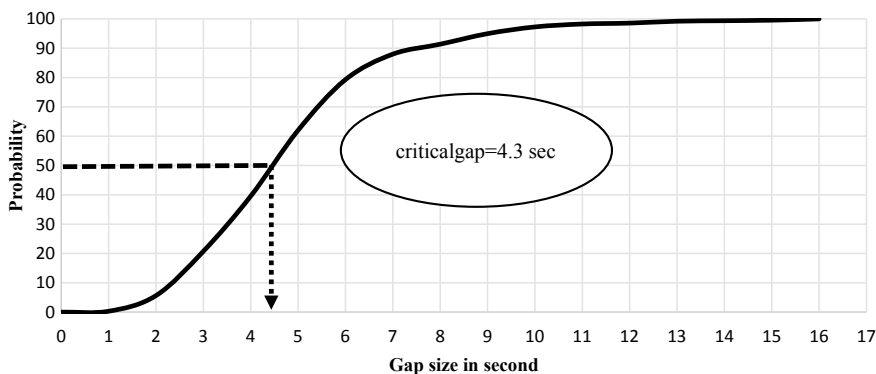


Fig. 4 Critical gap estimation by logit method

5 Comparison of CG Results by Different Methods

Tables 2, 3, 4, 5 and 6 suggest that the critical gap value is a function of a number of factors related to roadway geometry, individual pedestrian (demographic) characteristics and behaviour, vehicular and traffic characteristics. The pedestrians were classified into four groups as young (age 15–30), middle age (31–50 years), and old age (more than 50), and children (age <15) as perceived through video data. Young male pedestrians with low critical gap value 2.02 s, indicates a very risky crossing manoeuvres existing in the mixed traffic condition or it shows highly aggressive behaviour of pedestrians because of high waiting time. In general, older pedestrians were found accepting larger gaps as compared to pedestrians in other age groups. This might be the effect of their age-related crossing capabilities as well as their higher safety consciousness. For group behaviour, if the platoon size increases accepted gap value will increase in all study locations. For all study sites, it is confirmed that the critical gaps accepted by male pedestrian are significantly lesser than female pedestrian, thereby indicating the risk-taking behaviour of male pedestrian. Critical gap value of each individual pedestrian was found out when the pedestrians use behavioural tactics such as rolling behaviour (pedestrian rolls over the small available vehicular gaps), speed and path change conditions while crossing the road. This might be decreasing the critical gap. From Tables 2, 3, 4, 5, and 6, it can be seen that wide range of estimated critical gap values using different methods and the suitable selection of critical gap value influences the usefulness of the pedestrian design facilities. MLM and PEM also have more or less similar values for all study sites. However, MLM assumes the log-normal distribution of accepted and maximum rejected gaps, whereas PEM does not need to assume any distribution type for the critical gaps and that the method does not involve an iterative process. But, Raff's method is the oldest empirically deterministic method, which is used widely due to its simplicity and the critical gaps used by this method is quite less as compared to other methods. This method at Ahmedabad gives critical gap of young male

Table 6 Estimation of pedestrian critical gap results by logit method

Locations	Accepted/rejected gaps	Utility equations	Critical gap (s)	<i>Cd</i> (Nagelkerke R^2)
Vakola	3276	$U = -10.41 + 1.22 * V_{gap} - 0.052 * G_{psize} - 0.105 * Age - 0.52 * Av + 5.347 * Frq - 0.010 * V_{speed}$	5.5	0.88
Varachha	14,578	$U = -4.021 + 0.374 * V_{gap} - 0.031 * V_{speed} + 4.957 * Frq - 0.088 * G_{psize} + 0.030 * Av + 0.083 * Age$	4.1	0.78
Vile parle	7524	$U = -10.96 + 0.611 * V_{gap} - 0.004 * V_{speed} + 7.57 * Frq + 0.236 * G_{psize} + 0.055 * Av - 0.045 * Age + 0.248 * Gender$	4.2	0.87
Bandra	3378	$U = -21.80 + 2.658 * V_{gap} + 1.053 * Gender - 1.165 * G_{psize} + 0.056 * V_{speed} + 12.58 * Frq + 5.861 * G_{aptype} + 0.201 * Av$	3.7	0.90
Ahmedabad	9286	$U = -7.550 + 2.31 * V_{gap} + 7.247 * C_{spc} - 0.083 * Av + 1.887 * Frq + 0.327 * Gender - 0.064 * G_{psize} + 0.010 * V_{speed} - 0.420 * G_{aptype}$	2.1	0.84

Where: V_{gap} : vehicular gap; G_{p} size: Pedestrian Group size; Age: Age of pedestrian; Av : Area of vehicle; Frq : Frequency of attempt; V_{speed} : Vehicular speed; Gender: Pedestrian; Gap type: Gender; C_{spc} : pedestrian path change condition: Gap type: Near gap or far gap

Note Significance at 95% confidence interval with P -value < 0.05; Coefficient of determination (Cd)

pedestrians about 2.02 s, which is quite low value. This signifies that young pedestrians' acceptance behaviour is highly risky and hence, they ignore safety, while crossing the roads with smaller gaps (rolling behaviour of pedestrian). Moreover, proportion of two-wheelers was very high at that particular location, which may be one of the main reasons for obtaining lesser critical gap value compare with other four-lane sections. Tables 2, 3, 4, 5, and 6 show that for mega-city, such as Mumbai, the critical gap across four-lane divided road (3.6–4.32 s), which is found to be lower than eight-lane divided road (5.1 s) in same city. This may be attributed to the rolling gap acceptance behaviour in the case of eight-lane divided road (wider roads). Rolling gap here is considered as the sum of smaller gaps accepted, while crossing roadway width (number of lanes) in stages. However, in a metropolitan city like Surat having six-lane divided urban road, the critical gap is found to be between 3 and 4.1 s, which is significantly less than or near to the four-lane divided multilane road (3.6–4.32). This reflects the forceful crossing behaviour in Surat. This implies how human factors play a significant role in the gap acceptance behaviour. The detailed analysis of gap acceptance attributing human factors such as gender and age groups is summarized in Table 6. From Table 6, it depicts that the calculated critical gap by logit method is highly influenced by pedestrian behaviour (pedestrian speed as well as path change condition, rolling behaviour, frequency of attempts, and group size), traffic (type of gap, waiting time, and available gap) and vehicle characteristics (vehicle speed, type of vehicle, and area of vehicle). The critical gaps estimated by logit method results in higher values than the Raff's as well as MLM, PEM, and RMS method. In logit method, each rejected gap situation is considered and behaviour of pedestrian with all rejected gap values can represent the actual condition of the field comprehensively.

The variability in critical gap results can be classified (i) row wise: that is, across different locations of crosswalks for given attribute of pedestrian using a given method, (ii) column wise: that is, for a given location of crosswalk across different attributes of pedestrian using a given method, and (iii) row wise and column wise as mentioned in (i) and (ii) for different methods. The critical gap estimated by different methods is compared with each other based on the coefficient of variation (C_v). It measures the relative variability of two or more data sets. This variability is quantified using coefficient of variation (C_v), which was found to vary across locations which are higher than the variation of C_v for different attributes within a given location. Across the locations, MLM method returned the least variation in C_v (around 23%). The variation of C_v for different methods in comparison to MLM were found to be in the range of, 35% for Raff's method; 30% for logit method; 25% for RMS method; and 24% for PEM method). This indicates that maximum variation is observed with Raff's method, which is a deterministic empirical method. MLM, PEM, and RMS are probabilistic methods and are in the range of 23–25%, hence exhibit almost same performance. Logit method considers individual demographic, traffic and vehicular characteristics; it gives variation of about 30%. This value lies in between other probabilistic and deterministic methods. The reasons for this variation can be the variation in attributes like land use, road width, traffic volume, pedestrian demographic and individual characteristics. The variation due to land use is found to

be in the range of 5–14%. The maximum variation (14%) is observed for crosswalk at Vile parle, due to nearby rail transit terminal station, indicating additional influencing variable such as, fluctuating demand of transit passengers using crosswalk over time. The minimum variation (5%) is observed for crosswalk at Ahmedabad having mixed land use. This variation may be less also due to higher traffic volume during data collection, where critical gap is 2 s. Crosswalk with nearby commercial land use, however depicts variation of about 10%, which may also be attributed to side friction and other recreational activities.

6 Conclusions

The study has explored the details of the analysis of pedestrian critical gap using different methods. Five critical gap methods were studied as: Raff method, MLM, RMS, PEM, and Logit method. The critical gap values estimated using Raff's method and RMS have little difference, and this minor difference is evident only to a particular location. While comparing MLM and PEM, it was found that the critical gap values are relatively closer. This is because of the probabilistic approach taken in both the methods. Moreover, these methods were very accurate and robust. Troutbeck [26] compared the ability of MLM and PEM to predict the mean and standard deviation of critical gap and claimed MLM to be superior to PEM. But, in this study, the results by both the methods were not found to be significantly different based on t-test ($P < 0.05$, at 95% confidence interval) and ANOVA ($P > 0.05$, at 95% confidence interval). The reasons for the variation of critical gap across locations can be the difference in land use patterns, road characteristics, and pedestrian behaviour, and the variation within a location can be attributed to pedestrian behavioural changes alone. From CV analysis, MLM shows the least value, which shows that this is the best method to find the critical gap at unsignalized midblock sections, when pedestrian or behavioural characteristics are not considered.

The study results also concluded that logit method is the most appropriate one for the estimation of critical gap, as it considers the effect of pedestrian behavioural and vehicular characteristics. Moreover, it gives the actual representation of pedestrian street crossing behaviour at crosswalk under mixed traffic conditions. Critical gap value of each individual pedestrian was found out, when the pedestrians use behavioural tactics such as rolling behaviour, speed and path change conditions, while crossing the road. These aspects may decrease the critical gap value significantly in comparison to the one adopted in HCM [2] and other developed countries. The study results also concluded that the individual characteristics of pedestrians (gender and age) and group size are meaningfully contributing to the critical gaps. Wherein the female pedestrians have higher critical gap values as compared to the male pedestrian and the elders have higher critical gaps than other age groups (young and middle pedestrian groups) in all the study sites. The study results concluded that pedestrian group behaviour has higher critical gap than the single pedestrian and younger male pedestrians have critical gap value which was very low because of

their aggressive nature. Moreover, when the waiting time increased due to heavy traffic flow, pedestrians exceeded their tolerable limit and crossed the street without considering conflicting vehicles. Pedestrian rolling gap makes pedestrians to accept small vehicular gaps instead of long waiting time (exceeding the tolerable limit). It was also established that discrete pedestrian characteristics like gender and age affect critical gap significantly. In the pedestrian crossing analysis, the minimum gap value is less than the critical gap value, which indicates that the pedestrian gap acceptance behaviour is highly risky and show high degrees of disregard to safety. In this study, it is revealed that the geographical characteristics and city characteristics play a significant role in the crossing behaviour of pedestrian. The results of the present study are expected to be useful in realizing the need of having a relook at design parameters for pedestrian crossing facilities, thereby improving the existing facilities to enhance pedestrian safety. In this study, pedestrians' age was obtained by visual analysis from the video, which may slightly contradict the actual age of pedestrians. Moreover, the pedestrians' personal characteristics were not included in this model. In a nutshell, this study highlights the significance of pedestrian behavioural characteristics in critical gap analysis which is important in the context of developing countries, where the behavioural characteristics are frequently used. Moreover, results presented in this research work are expected to be useful for researchers as well as practitioners mostly in Asian countries having similar nature of traffic conditions and compliance behaviours from pedestrians.

Acknowledgements This study is part of a project sponsored by planning commission of India entitled 'Development of Indo-HCM'. The authors are grateful to Central Road Research Institute Delhi for their support and funding provided by them.

References

1. Mohan D, Tsimhoni O, Sivak M, Flannagan MJ (2009) Road Safety in India: Challenges and Opportunities. University of Michigan, USA
2. Highway Capacity Manual (2010) Transportation Research Board, Washington, DC
3. DiPietro M, King L (1970) Pedestrian gap-acceptance. Highway Res Rec 308:80–91
4. Oxley J, Fildes B, Ihsen E, Charlton J, Days R (2005) Crossing roads safely: an experimental study of age differences in gap selection by pedestrians. *Accid Anal Prev* 37:962–971
5. Brilon W, Koenig R, Troutbeck RJ (1999) Useful estimation procedures for critical gaps. *Transp Res Part A* 33:161–186
6. Raff MS, Hart JW (1950) A volume warrant for urban stop signs, eno foundation for highway traffic control. Saugatuck, Connecticut
7. Ashworth R (1970) The analysis and interpretation of gap acceptance data. *Transport Sci* 4(3):270–280
8. Tian Z, Vandehey M, Robinson BW, Kittelson W, Kyte M, Troutbeck R, Brilon W, Wu N (1999) Implementing the maximum likelihood methodology to measure a driver's critical gap. *Transport Res Part A Pol Pract* 33(3):187–197
9. Hamed MM (2001) Analysis of pedestrians' behavior at pedestrian crossings. *Saf Sci* 38(1):63–82

10. Rastogi R, Chandra S, Vamsheedhar J, Das VR (2011) Parametric study of pedestrian speeds at midblock crossings. *J Urban Plann Dev*. [http://dx.doi.org/10.1061/\(ASCE\)UP.19435444.0000083](http://dx.doi.org/10.1061/(ASCE)UP.19435444.0000083). 137(4):381–389
11. Kadali BR, Vedagiri P (2015) Modelling pedestrian road crossing behavior under mixed traffic condition. *Eur Trans* 55(3):1–17
12. Chandra S, Rastogi R, Das VR (2014) Descriptive and parametric analysis of pedestrian gap acceptance in mixed traffic conditions. *KSCE J Civil Eng* 18(1):284–293
13. Tanaboriboon Y, Guyano JA (1991) Analysis of pedestrian movements in Bangkok. *Transportation* 40 research record 1294, TRB, Washington, D.C., pp 52–56
14. Laxman KK, Rastogi R, Chandra S (2010) Pedestrian flow characteristics in mixed traffic conditions. *J Urban Plann Dev ASCE* 136:23–33
15. Chandra S, Bharti AK (2013) Speed distribution curves for pedestrians during walking and crossing. In: Conference of Transportation Research Group of India (2nd CTRG) procedia—social and behavioral sciences 104:660–667
16. Pawar S, Patil (2014) Pedestrian temporal and spatial gap acceptance at Mid-block Street crossing in developing world. In: 95th annual transportation research board meeting, Washington D.C
17. Wu N (2006) A new model for estimating critical gap and its distribution at un-signalized intersections based on the equilibrium of probabilities. In: Proceeding of the 5th international symposium on highway capacity and quality of service. Yokohama, Japan, 25–29 July, Transportation Research Board of the National Academies, Washington, D.C
18. Kadali BR, Vedagiri P (2016) Analysis of critical gap based on pedestrian behaviour during peak traffic hours at unprotected midblock crosswalks. *Asian Trans Stud* 4(1):261–277
19. Chandra S, Kumar U (2003) Effect of lane width on capacity under mixed traffic conditions in India. *J Transport Eng ASCE* 129:155–160
20. Fitpatrick K (1991) Gaps accepted at stop-controlled intersections. *Transport Res Rec J Transport Res Board* 1303:103–112
21. Troutbeck RJ (1992) Estimating the critical acceptance gap from traffic movements, Queensland University of Technology
22. Wu N (2012) Equilibrium of probabilities for estimating distribution function of critical gaps at un-signalized intersections. *Transport Res Rec J Transport Res Board* 2286:49–55
23. Cassidy MJ, Madanat SM, Wang M-H, Yang F (1995) Un-signalized intersection capacity and level of service: revisiting critical gap. Preprint 950138, Transportation Research Board, Annual meeting
24. IRC: 103 (2012) Guidelines for pedestrian facilities, Indian road congress (IRC) New Delhi, India
25. Kumar P, Parida M (2011) Vulnerable road users in multimodal transport system for Delhi. *Journeys, LTA* 6:38–47
26. Troutbeck RJ (2014) Estimating the mean critical gap. In: 93rd annual meeting of Transportation Research Board, CD-ROM
27. Chaudhari A, Shah J, Arkatkar S, Joshi G, Parida M (2016) Examining effect of individual characteristics on walking speed at un-signalized mid-block crossings. In: 95rd annual meeting of Transportation Research Board, CD-ROM (2016)

Modeling on-Street Parking Scenario and Response to Paid Parking Policy Using Statistical Techniques for CBD Area of Vadodara City



Sanjay Dave, Nandan Dawada and Gaurang J. Joshi

Abstract On-street parking is most popular among personal vehicle users, and it has become one of the major problems for CBD area of all metropolitan cities of India. Various ill effects such as accidents, congestion, reduction in carriage width, and air pollution has been caused due to on-street parking. To manage on-street parking demand, it is necessary to assess existing demand and formulate appropriate policy measures. National Urban Transport Policy [11] has given guidelines for managing on-street parking in urban areas. It clearly emphasizes on pricing of parking facilities to reflect actual land cost. However, due to poor social acceptability and lack of political will, the local government refrains from adopting paid on-street parking measures and prefers to offer free parking with odd–even date scheme. This results in spillover of parking demand, illegal, and chaotic parking behavior particularly in CBD areas where there is high a concentration of commercial activities. In the present study, two streets in CBD area of Vadodara city were selected for on-street parking demand assessment and response to proposed parking policy measures. Parking inventory using license plate method was carried out at 1 h monitoring interval for 12 h to determine peak parking hours which were observed as 5–8 PM. Further microscopic parking inventory was carried out at 10 min monitoring interval during observed evening peak parking hours on normal working day to determine parking characteristics like parking duration and turnover. Average parking duration of 40 min was observed with poor value of turnover (0.5–0.8). The parking survey observed dominance of motorized two-wheelers (M2-w) with uniform demand throughout the peak parking period. Further, the study conducted field survey of on-street vehicle parkers using stated preference method to collect responses for two proposed parking policies namely, “space restraint paid parking policy” and paid parking with “vehicle certifi-

S. Dave (✉)

The Maharaja Sayajirao University of Baroda, Vadodara, India
e-mail: smdave-ced@msubaroda.ac.in

N. Dawada

Vadodara Institute of Engineering, Vadodara, India
e-mail: nandandawda@gmail.com

G. J. Joshi

Sardar Vallabhbhai Patel National Institute of Technology(Surat), Surat, India
e-mail: gjsvnit92@gmail.com

© Springer Nature Singapore Pte Ltd. 2020

T. V. Mathew et al. (eds.), *Transportation Research*, Lecture Notes
in Civil Engineering 45, https://doi.org/10.1007/978-981-32-9042-6_14

169

cate policy (VPC).” Space restraint policy offers utilization of available on-street parking space on priority basis as per guide lines of NUTP 2014, while VPC permits use of only one vehicle per household and shop to use on-street parking space at subsidized parking charge. Response to both policies was modeled using multinomial logistic regression in SPSS software. It was observed that socioeconomic variable like household income and travel attributes like trip length, trip frequency, parking duration, searching time for parking and walking time from parking to destination significantly influenced the response of vehicle users. The study provides insight into on-street parking demand scenario in CBD area and assesses response to proposed paid on-street parking policies.

Keywords On-street parking · NUTP · CBD area · Multinomial logistic regression

1 Introduction

The rapid rate of motorization in amalgamation with urbanization has resulted in a significant increase in traffic demand and consequently increased saturation of the road network. One of the major problems associated with an increase of traffic is the acute shortage of parking space, especially in urban centers. [1]. Each vehicle making a trip needs a parking space at its origin and destination, regardless of the parameters defining the trip [2]. Parking is a critical and central element of urban transportation planning and research [3–6]. The parking demand in the core area of walled city is a prominent problem for second order metropolis of India. Burgeoning gap between available parking space and increased demand for on-street parking makes the problem more acute and therefore needs to be addressed particularly in context of free on-street parking policy. The usual practice of local bodies to manage the demand by formulating odd and even date on-street parking scheme on the corridors of high demand. The lack of on-street parking data and concrete on-street parking policy results in unmanageable on-street parking scenario. Parking pricing policy a measure for efficient management of existing demand has a strong impact not only on the operation of the parking subsystem but also on the entire transportation system and the city in general. Traditional parking policies have been focusing on providing supply to meet the demand, which has dented the use of public transport and non-motorized transport. However, paradigm shift in parking policy as demand management tool focuses on effective management of existing supply to meet ever-increasing demand has proved to be a thrust for establishing effective and balanced urban transportation system. Travel policy, revenue, and sustainability of urban transport can be affected by parking policies [7]. Rational formulation of on-street parking policies requires comprehensive investigation of on-street parking demand and factors governing on-street parking decisions. Ottosson et al. [8] examined how pricing affected parking indexes, such as parking turnover rate, parking duration, and parking accumulation, using automatic transaction data from parking pay stations in Seattle. Cats et al. [9] proposed a survey methodology to empiri-

cally measure the impacts of on-street parking policies based on automated parking transaction data. Authors compared the average and maximum parking occupancy levels, throughput, parking duration and total fare collection for before and after the introduction of a new parking scheme for visitors to Stockholm inner city and Sweden. The results indicated that the policy fulfilled its objective to increase the ease of finding a vacant parking place in the central areas and even resulted in underutilized parking spaces. [10] concluded based on stated and revealed preference data that price both in terms of the overall parking cost as well as the hourly fee-is the dominant factor in parking-related decisions.

2 Need and Objectives of Study

Review of available literature revealed very few studies are reported on on-street parking policy formulation in Indian context. Moreover, in Indian context, ministry of urban housing affairs (MOUHA) has formulated National Urban Transport Policy [11] which recommends guiding principles to effectively manage insatiable parking demand by pricing, which should reflect length of stay and market value of occupied land. Apart from regulating the existing demand, parking policies are also geared toward revenue generations, which can be further used to efficiently manage existing demand for parking. Parking policies, especially in Indian cities, are often compromised due to social hostility and political creates chaotic unacceptability, which situation especially in CBD areas. Therefore, with such intricacy, it becomes inevitable to assess on-street parking demand and accordingly formulate on-street parking policies. With this stimulus, the objectives of the present study have been formulated to assess on-street parking demand. The study is further poised toward modeling responses to two proposed on-street parking policies. In light of the framed objectives, the scope of the study is strictly limited to commercial land-use, as they are predominant in CBD areas of Indian cities.

3 Study Area

Vadodara is the 20th largest populated city of India with an area of 159.95 km² and population of 1.82 million (2014) and is the cultural capital of the state of Gujarat. Every year an average 8500 new motorized two-wheelers (2-w), and 19,000 new cars are registered. This addition of vehicles has consequently generated high demand for parking space, particularly in congested CBD area having high commercial attraction for shopping throughout the business hours.

3.1 Study Site and on-Street Parking Scenario

Two study sites were considered to assess existing on-street parking demand. Responses to two formulated parking policies namely, “space restraint paid on-street parking policy” and paid “vehicle parking certificate” were collected for these study sites. Selected street had mixed land use pattern essentially comprising of commercial at ground level followed by residential at next level. Garment shops, crockery and footwear’s dominate the commercial structure and thereby attract a lot number of shoppers resulting into high demand for on-street parking. Saturated on-street parking spaces are predominantly observed throughout the business hours though developed off-street parking facilities are provided. On-street parking is not monitored by paring warden or traffic police, which has resulted in chaotic scenario for both the subject sites. On-street parking permission for the survey sites is regulated by “odd-even date free on-street parking scheme”. Right angle parking for 2-ws and parallel parking for cars and 3-ws is permitted (Three-wheeler is an IPT mode of transport). Road inventory detail of the survey sites is summarized in Table 1. Figure 1 represents photographs of study location.

4 Data Collection

Since the study is oriented toward assessing on-street parking demand and modeling responses to paid on-street parking policy, the data collection for the present study was divided into two sections:

- (a) On-street parking demand assessment
- (b) Stated preference survey

For on-street parking demand assessment, parking data was collected at monitoring interval of 10–60 min using license plate survey during peak parking hours for both survey sites.

For modeling responses to two formulated parking policies namely, “space restraint paid parking policy and “paid vehicle parking certificate policy (VPC)”

Table 1 Road inventory detail

Detail of road	Vinoba Bhawe	M.G road
Length of the street	920 m	350 m
Right of way	8.6–14 m	18 m
Width of carriage way	6.6–12 m	8.4 m
Width of parking space	2.0 m (each side)	2.0 m (each side)
Width of sidewalk	2.1 m(each side)	2.1 m(each side)
Number of commercial shops	397	241



Fig. 1 On-street parking scenario at study location

face-to-face interview of 410 respondents was carried out during normal working hours for weekdays and weekends using structured questionnaire survey during the time of parking and unparking of the vehicle. Space restraint policy offers the utilization of available on-street parking space on a priority basis as per guidelines of NUTP 2014. Under the concept of space restraint policy parking spaces will be first reserved for the non- motorized transport vehicles, emergency vehicles, and public transport vehicles, then after if space will be left it shall be allocated to the private vehicle users. VPC permits use of only one vehicle per household and shop to use on-street parking space at subsidized parking charge. Vehicle parking certificate (VPC) specifies that in every house one vehicle will be given free parking certificate, i.e., means no charges shall be introduced for that vehicle if used in the city. However, if the vehicle without parking certificate has been used than the market parking charges will be applied. The response was collected for three basic parameters, i.e., socioeconomic status, travel attributes, and parking policy response to model their behavior. The questionnaire format consisted of 11 variables, 3 of which were mode abstract (not affecting trip-making decision) like gender, origin, and destination. Eight were mode specific (affecting trip-making decision) such as household income, travel time, trip length, purpose of trip, frequency of visiting CBD area, parking duration of the vehi-

Table 2 Proposed parking charge

Duration (h)	On-street parking charge (in terms of rupees)		Duration (h)	Off-street parking charge (fixed charges applied)	
	Two-wheelers	Four-wheelers		Two-wheeler	Four-wheeler
0–1	05	20	0–1	5	20
1–2	10	40	0–2	5	20
2–4	10 Rs/h	20 Rs/h	2–4	10	20
>4	15 Rs/h	30 Rs/h	>4	10	30

cle, searching time for the parking space, and walking time from the parking to the destination in the CBD.

The response to the space restraint policy was collected for the proposed parking charge reflecting the land cost as shown in the following Table 2. The respondent was offered graded parking charge for on-street as per the parking duration and fixed parking charge for off-street parking.

The above parking charges were proposed by considering as per the “land cost” published by the land revenue department of the government of Gujarat. The graded parking charges proposed according to parking duration were based on the key principle suggested by NUTP 2014. The choices against the proposed space restraint policy offered to the respondent were:

1. Continue to arrive by private mode and ready to pay prescribed parking charge;
2. Shift to off street parking with less parking charge;
3. Shift to another mode of transport;
4. Change the destination where free parking is available;

Similarly, for VPC policy, the choices offered to the respondent were:

1. Will use all vehicles as using now and ready to pay proposed parking charge;
2. Will make limited use of non VPC vehicle and pay market parking charges;
3. Will use only VPC vehicle for all trips to paid parking and use other mode for other trips;
4. Will use non VPC vehicle with fixed monthly budget of parking fees;

5 Data Analysis

The data analysis is bifurcated in two segments: (a) on-street parking demand assessment (b) modeling responses to formulated on-street parking policy.

5.1 On-Street Parking Demand Assessment

Figure 1 represents the on-street parking demand accumulation for two days for both survey sites. Empirical observation revealed heterogeneity in on-street parking demand with dominance of motorized two-wheelers (M-2W) and therefore observed demand was converted into two-wheeler demand according to factors given in [11]. Here VR 1 and VR 2 represent M.G road and Vinoba Bhave road.

From Fig. 2, it can be noted, maximum parking demand accumulation was observed during 5–8 pm for Vadodara (Fig. 3a–b).

It can be observed that parking demand followed a consistent trend within the day for entire data collection period but varied significantly between days. A similar trend was observed for both survey sites. The on-street parking demand was further accesses by obtaining parking duration and turnover for different data monitoring interval. Parking duration was extracted for smallest data monitoring interval i.e.,

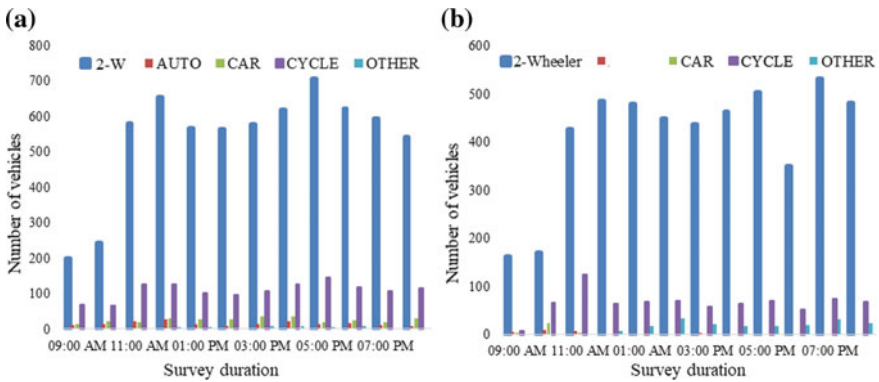


Fig. 2 Parking demand accumulation during 12 h for a VR 1 b VR 2

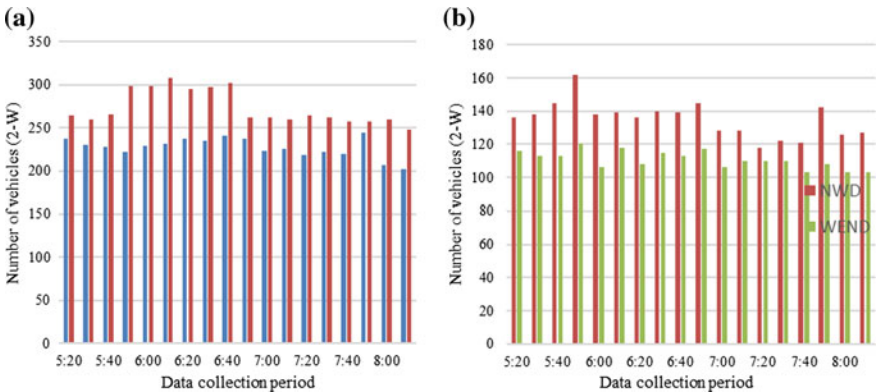


Fig. 3 Parking demand accumulation during peak hours for a VR 1 b VR 2

10 min, to portray actual parking scenario. Parking duration for both the study sites is represented in Fig. 4.

It can be observed that nearly 60–75% demand had parking duration of 40 min and therefore was considered as average parking duration. Turnover which represents efficiency of space was calculated for different data monitoring interval and is presented in Fig. 5.

It can be observed that, turnover followed a decreasing trend with increase in data monitoring interval. At average parking duration (40 min), turnover had the value in the range 0.5–0.8, indicating poor efficiency of the space majorly. Therefore, to promote short-term parkers and improve efficiency of the space, it becomes absolutely necessary to formulate on-street parking policies and model their responses.

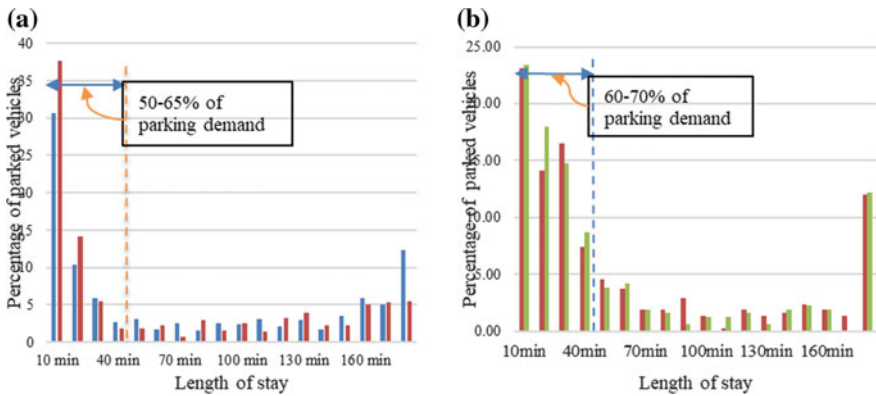


Fig. 4 Parking duration for a VR 1 and b VR 2

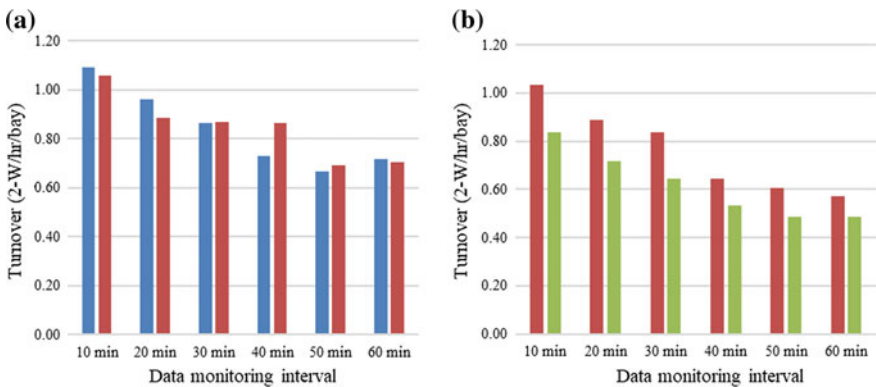


Fig. 5 Turnover for different data monitoring interval for a VR 1 and b VR 2

6 Modeling on-Street Parking Responses

The descriptive analysis of the collected response for the policy measure is as shown in Table 3.

7 Multinomial Logit Model

Multinomial logistic regression model developed for visitors responding to space restraint parking policy and vehicle parking policy in the study area. The model was developed using SPSS 22.0 software. Here, as per the requirement of the software, parking space on legal side is not available was considered as reference category. Reference category was decided upon the maximum number of responses obtained for a particular reason for illegal parking. Therefore, for the present case parking on legal side is not available was the most preferred choice among respondents and hence was considered as reference category. Results of multinomial logit regression for space restraint and VPC parking policies are summarized in Tables 4 and 5.

From the above-mentioned two models, it can be concluded that socioeconomic as well as parking attributes influences the behavior of the people toward the parking policy. The most dominating factors which affects the both the policies is monthly income.

8 Finding and Conclusion

The present study attempts to analyze on-street parking demand and model responses to two proposed on-street parking policies formulated under the guidelines of NUTP for a case representing CBD area of Vadodara. The major finding from the study is summarized below:

- Average parking duration of 40 min is observed with poor turnover for the study area.
- Result of descriptive statistics reveals that respondents have shown positive response to paid on-street parking policies and about 50% commuters are ready to pay for the on-street parking facility.
- Paid on-street parking policy does not cause any negative effect on economic activity of the CBD area as poor response to cancelation of trip and change of destination area was observed in field survey.
- Willingness to pay prescribed parking charges in response to both the parking policies indicates auto dependency of commuters and the demand of parking space may remain inelastic for short-term parkers as observed in multinomial models.

Table 3 Descriptive analysis of variables

Socioeconomic characteristics				
Gender	Male		Female	
	83%		17%	
Household income	<20,000	20,000–30,000	30,000–40,000	>40,000
	32%	20%	17%	31%
Age group	18–20	21–35	36–49	50–70
	10%	44%	33%	13%
<i>Travel attributes</i>				
Purpose of trip	Work	Shopping	Education	Others
	54%	33%	5%	8%
Trip length	<3 km	3–7 km	7–11 km	>11 km
	25%	53%	15%	7%
Frequency	Daily	Weekly	Monthly	Occasionally
	46%	29%	9%	16%
<i>Parking attributes</i>				
Searching time	Immediately	0–2 min	2–5 min	>5 min
	29%	24%	24%	23%
Walking time	2–5 min	5–10 min		>10 min
	66%	24%		10%
Parking duration	<½ h	½–1 h	1–2 h	>2 h
	31%	17%	21%	31%
Response to space restraint policy	Continue to arrive		43%	
	Shift to off street parking		28%	
	Shift to another mode		12%	
	Change the destination		16%	
Response to vehicle parking certificate policy	Will use all vehicles as using now and ready to pay		37%	
	Will make limited use of non VPC vehicle and pay market parking charges		29%	
	Will use only VPC vehicle for all trips to paid parking and use other mode for other trip		32%	
	Will use non VPC vehicle with fixed monthly budget of parking fees		2%	

Table 4 Multinomial model of space restraint policy

Parameter estimates		B	Std. error	Wald	Df	Sig.	Exp(B)	90% Confidence interval for exp(B)	
								Lower bound	Upper bound
Shift to off-street parking	Intercept	-1.816	0.722	6.330	1	0.012			
	Income <20,000	0.581	0.300	3.763	1	0.052	1.789	1.092	2.929
	Purpose of trip	0.875	0.466	3.534	1	0.060	2.400	1.116	5.161
	Duration 1/2-1 h	-0.710	0.397	3.199	1	0.074	0.492	0.256	0.945
	Frequency weekly	0.734	0.391	3.521	1	0.061	2.084	1.095	3.965
	Monthly	1.000	0.498	4.034	1	0.045	2.718	1.198	6.163
Shift to another mode	Intercept	2.504	2000.626	0.000	1	0.999			
	Income <20,000	1.601	0.450	12.681	1	0.000	4.958	2.367	10.385
	20,000-30,000	1.396	0.483	8.364	1	0.004	4.039	1.826	8.934
	30,000-40,000	1.251	0.482	6.733	1	0.009	3.494	1.581	7.722
	Duration 1/2-2 h	-0.846	0.544	2.422	1	0.120	0.429	0.175	1.049
	1-2 h	-0.923	0.522	3.128	1	0.077	0.398	0.169	0.937
Change destination	Searching time 0-2 min	1.170	0.523	5.004	1	0.025	3.222	1.363	7.615
	2-5 min	0.923	0.495	3.472	1	0.062	2.516	1.114	5.682
	Income <20,000	2.242	0.423	28.083	1	0.000	9.415	4.694	18.885
	20,000-30,000	1.275	0.471	7.320	1	0.007	3.580	1.649	7.775

(continued)

Table 4 (continued)

Parameter estimates		B	Std. error	Wald	Df	Sig.	Exp(B)	90% Confidence interval for exp(B)	
Preference for paid parking ^a								Lower bound	Upper bound
	Purpose work	1.401	0.630	4.947	1	0.026	4.061	1.441	11.449
	Frequency daily	-1.976	0.470	17.646	1	0.000	0.139	0.064	0.301
	Searching time immediately	1.079	0.483	4.986	1	0.026	2.941	1.329	6.512
	0-2 min	0.899	0.496	3.290	1	0.070	2.457	1.087	5.552
^a The reference category is: continue to arrive and pay									
Chi-square		200.424							
-2 Log likelihood		992.694							
R-square Cox and Senell		0.331							
R-square Nagelkerke		0.357							
R-square Mc Fadden		0.153							
Model classification		48.7%							

Table 5 Multinomial model of VPC policy

Parameter estimates		B	Std. error	Wald	Df	Sig.	Exp(B)	90% confidence interval for exp(B)	
Response for paid parking ^a								Lower bound	Upper bound
Will make limited use of non-VPC vehicle and pay parking charge	Intercept	-2.0493	0.764	10.654	1	0.001			
	Below 20,000	0.862	0.308	7.801	1	0.005	2.367	1.425	3.931
	Between 20,000 and 30,000	0.861	0.356	5.853	1	0.016	2.365	1.317	4.247
	Between 30,000 and 40,000	1.323	0.344	14.816	1	0.000	3.754	2.133	6.608
Will use only VPC vehicle for all trips to paid parking and use other mode for other trips	Intercept	-3.775	0.806	21.961	1	0.000			
	Income <20,000	1.666	0.312	28.446	1	0.000	5.291	3.165	8.844
	Between 20,000 and 30,000	1.370	0.352	15.102	1	0.000	3.933	2.203	7.023
	Between 30,000 and 40,000	1.157	0.376	9.459	1	0.002	3.181	1.713	5.907
	Trip Length <3 km	1.163	0.559	4.320	1	0.038	3.198	1.275	8.026
	3-6 km	0.920	0.528	3.043	1	0.081	2.510	1.054	5.979
	Purpose of trip work	0.892	0.502	3.159	1	0.076	2.441	1.069	5.574
	Walking time 2-5 min	0.914	0.442	4.276	1	0.039	2.495	1.206	5.164

(continued)

Table 5 (continued)

Parameter estimates		B	Std. error	Wald	Df	Sig.	Exp(B)	90% confidence interval for exp(B)		
Response for paid parking ^a								Lower bound	Upper bound	
Will use non VPC vehicle with fixed monthly budget of Rs. _____ parking fees	Walking time 5–10 min	1.145	0.456	6.317	1	0.012	3.144	1.486	6.654	
	Frequency monthly	0.879	0.496	3.147	1	0.076	2.409	1.066	5.444	
	Intercept	38.421	2.389	258.579	1	0.000				
	Income 20,000–30,000 Rs	1.991	0.686	8.431	1	0.004	7.323	2.371	22.622	
	Walking time 2–5 min	-45.230	0.996	2062.167	1	0.000	2.27E-20	4.418E-21	1.170E-19	
	Walking time 5–10 min	-45.456	1.010	2027.406	1	0.000	1.815E-21	3.450E-21	9.551E-20	
	Frequency	2.085	1.066	3.823	1	0.051	8.045	1.392	46.482	
	<i>^aThe reference category is: will use all vehicles as using now and ready to pay parking charge</i>									
	Chi-square				118.612					
-2 Log likelihood				956.640						
R-square Cox and Senell				0.212						
R-square Nagelkerke				0.234						
R-square Mc Fadden				0.101						
Model classification				50.5%						

- Significance of household monthly income in formulation of both the multinomial models and their coefficients reveals that lower and middle-income group parkers are likely to be more sensitive toward paid parking policy.
- Travel attributes like frequency of trip, trip length, parking duration, and purpose of trip were the most significant variables governing the response to paid parking policies.

References

1. Stockholmsstad (2013) Mobility strategy: parking plan mars 2013 (in Swedish). Available at www.stockholm.se/trafikkontoret. Accessed July 2014
2. Spililpoulou C, Antoniou C (2012) Analysis of illegal parking behavior in Greece. *Proc Soc Behav Sci* 48:1622–1631
3. Davis A, Pijanowski B, Robinson K, Engel B (2010) The environmental and economic costs of sprawling parking lots in the United States. *Land Use Policy* 27(2):255–261
4. Khodaii A, Aflaki E, Moradkhani A (2010) Modeling the effect of parking fare on personal car use. *Scientia Iranica—Trans Civil Eng* 17(3):209–216
5. Shoup DC (2006) The price of parking on great streets, planetizen, 29 Mar 2006. Available from <http://www.planetizen.com/node/19150S>. Accessed 20 June 2011
6. Barata E, Cruz L, Ferreira JP (2011) Parking at UC campus: problems and solutions. *Cities* 28:406–413. <https://doi.org/10.1016/j.cities.2011.04.001>
7. Rye T, Hunton K, Ison, Kocak N (2008) The role of market research and consultation in developing parking policy. *Transp Policy* 15(6):387–394
8. Ottosson DB, Chen C, Wang T, Lin H (2013) The sensitivity of on-street parking demand in response to price changes: a case study in seattle, WA. *Transp Policy* 25:222–232
9. Cats O, Zhang C, Nissan A (2016) Survey methodology for measuring parking occupancy: Impacts of an on-street parking pricing scheme in an urban center. *Transp Policy* 47:55–63. <https://doi.org/10.1016/j.tranpol.2015.12.008>
10. (2015) Guidelines for parking facilities in urban areas, Indian Road Congress, Special Provision, IRC SP-12 2015
11. National Urban Transport Policy (2014) MOUHA

Optimum Point of Intersection Selection in Horizontal Highway Alignment Design: A Comparative Study Using Path Planner Method and Ant Algorithm



M. B. Sushma, Sandeepan Roy, M. B. R. Prasad and Avijit Maji

Abstract This paper proposes the application of the path planner method (PPM) for optimizing horizontal alignment. The method operates on the principle of rapidly exploring random tree (RRT) [1, 2] and is capable in efficiently searching non-convex high dimension space. In this method, the entire search space is explored by the randomly generated point of intersections (PIs) which are connected to develop a tree-like path by expanding from start to end point, iteratively. These paths would meet the highway geometric guidelines and minimize associated cost. The potential sets of PIs are connected to generate the tangent sections, thus in developing an alignment. The alignment is checked for encroachment towards restricted areas and any violation leads to further refinement of the PI locations. Various researchers have extensively used artificial intelligence (AI) based heuristics algorithms for optimization of horizontal alignment. The proposed PPM is compared with one such algorithm, i.e. the ant algorithm (AA). Further, the suitability of the PPM in optimizing the horizontal alignment is reviewed. The efficiency of both the methods is verified through two case studies, one being a hypothetical and another using a real topographical map of a place in Gujarat, India.

Keywords Horizontal highway alignment · Path planner method · Ant algorithm · Highway geometric design · Alignment optimization

M. B. Sushma (✉) · S. Roy · M. B. R. Prasad · A. Maji
Department of Civil Engineering, Indian Institute of Technology Bombay, Mumbai 400 076, India
e-mail: prustysushma618@gmail.com

S. Roy
e-mail: sandeepanroy1991@gmail.com

M. B. R. Prasad
e-mail: balurajendramadanu@gmail.com

A. Maji
e-mail: avijit.maji@gmail.com

1 Introduction

Highway alignment design aims to connect two desired end locations at the minimum possible cost. It has two components: vertical and horizontal alignment. The vertical alignment consists of gradients and vertical curves, whereas the horizontal alignment is composed of three elements: tangent section, circular curve and transition curve. In a plain terrain, the horizontal alignment ensures fulfilment of the obligatory point requirements, i.e. passing through the control areas and avoiding restricted or prohibited areas. To ensure the safety of a highway, it is required to meet the geometric guidelines as well. Hence, the overall objective of an optimal horizontal alignment would be to satisfy the highway geometric design guidelines, compliance with the obligatory point requirements while minimizing the associated alignment cost. These costs include length-dependent cost, right-of-way cost, environmental impact cost and penalty cost for violating the obligatory points. Practising engineers design the horizontal alignment manually based on experience and engineering judgement. Hence, this process does not guarantee an optimal solution. Numerous feasible alignments could exist between two destinations thus, making the design process complex. Various studies have, thus, developed computer-aided optimization models to overcome this limitation in horizontal alignment design. These heuristics (such as genetic algorithm (GA), Tabu Search, artificial neural network, simulated annealing and ant algorithm (AA)) have established their applicability for numerous complex real-life problems. These heuristic-based methods are particularly considered more appropriate in application than the classical optimization, particularly, when the study area becomes large and complex with a number of parameters involved (such as cost components, design parameters, etc.). These models generate the PIs on orthogonal planes, placed at a regular interval between the two desired points. These PIs are connected using suitable tangent and curve sections, to generate the horizontal alignment. In essence, the PIs are confined to the location and number of orthogonal planes, in these models. Hence, only the PIs located on the orthogonal sections can be used for generating the highway alignment. Selecting PIs in such a way would negatively impact the generated horizontal highway alignment by affecting its precision. This may in turn result in a local optimal or near-optimal solution.

This study presents the path planner method (PPM), an optimization model that overcomes the above-mentioned limitation. The PPM generates intermediate PIs without any such location-based constraints, therefore, improving the precision of the generated highway alignment. PPM develops an alignment by exploring the entire study area, subject to the objectives and guidelines essential for the design of an optimal horizontal alignment for highways. In addition, a brief explanation of the application of the ant algorithm (AA) in highway alignment design is also provided in this study. A comparison is then made between both the PPM and AA using two case studies, one being a hypothetical case scenario and other being a real-world case. This comparison is primarily done to check the efficiency and quality of the solution generated by both these methods. This study uses a geographic information

system (GIS)-based map database, where the end points of the alignment are defined. The decision variables in this optimization problem formulation are the locations of a set of randomly generated points in the study area.

2 Horizontal Highway Alignment Optimization Models

Horizontal highway alignment consists of linear segments (tangents) which are joined with curves. Curve sections ensure a smooth change in directions while avoiding obstructions. Typically, circular curves are used for highways. To prevent the vehicle from lateral skid and maintain the centrifugal force, appropriate curvature and superelevation are provided along the length of the curve sections. These values are based on design speed and side friction requirements. The highway alignment optimization problem formulation consists of cost minimization (or maximization benefit) as an objective function with various geometric design guideline-based constraints. The problem is solved by developing mathematical search models that are used to solve for an optimized solution.

Various automated computer-aided methods have been developed in the last few decades that optimized highway alignment design by minimizing the total highway alignment cost. These works can be broadly classified based on the type of the methods used for formulating and solving the optimization problem vis-a-vis calculus of variation, dynamic programming, network optimization, neighbourhood search heuristic with MIP, genetic algorithms and particle swarm algorithm. Howard et al. [3] assumed the cost function between the two desired points to be continuous in nature, to develop optimum curvature principle (OCP) using the calculus of variations. However, assuming a continuous cost function might not be suitable for real-world application. Network optimization model was used by Parker [4] to solve the highway alignment optimization problem, where the costs at the individual link of the networks were added to estimate the total cost of the alignment. This was solved by network optimization model. The result would supposedly be a highway network with an optimized total cost, however, not guaranteeing the optimality of each link in the network. Mondal et al. [5] developed a mixed integer problem formulation and optimized the horizontal alignment along specific corridors. The model used a black-box heuristic approach to improve the horizontal alignment by adjusting the PIs of an existing base alignment. Limiting the search space to corridors along the alignment length alone might not guarantee the optimality of the result. The model proposed by Jha [6, 7], Jha and Schonfeld [8] and Jong et al. [9], and adopted by Kang et al. [10], formulated a nonlinear mixed integer problem for optimizing the highway alignment that was solved using a genetic algorithm. Shafahi and Mehdi [11] similarly formulated a nonlinear mixed integer problem that was solved using particle swarm algorithm. These works consider intermediate PIs along predefined orthogonal planes which confined the location and number of PIs thus, likely impacting the generated horizontal highway alignment negatively. The relevant methods and corresponding notable studies are detailed in Table 1.

Table 1 Optimization models for design of horizontal alignment

Methods	References
Calculus of variation	Howard et al. [3], Thomson and Sykes [12], Shaw and Howard [13] and Wan [14]
Network optimization	Parker [4], Turner and Miles [15], Trietsch [16], Athanassoulis and Calogero [17]
Dynamic programming	Nicholson et al. [18] and Hogan [19]
MIP and derivative-free optimization	Mondal et al. [5]
Genetic algorithms	Jong et al. [9], Jha [6, 7], Jha and Schonfeld [8], Kang and Jha [9], Maji and Jha [20, 21], Tat [22]
Particle swarm algorithm	Shafahi and Mehdi [11]

3 Horizontal Alignment Cost

Horizontal alignment cost is mainly comprised of length-dependent and location-dependent costs. Length-dependent cost components include construction cost which varies directly with the total length of the alignment. The length-dependent cost mainly depends on the nature of construction and maintenance of an alignment which are represented using unit length costs, respectively. As mentioned earlier, total alignment length includes the length of tangential and curve sections. So, the total length of the alignment can be formulated as shown in Eq. (1) [6–10]. If length-dependent cost is formulated considering the construction cost only, then it can be evaluated by using Eq. (2):

$$L = \sum_{i=0}^{N-1} \sqrt{(x_i^T - x_{i+1}^C)^2 + (y_i^T - y_{i+1}^C)^2} + \sum_{j=1}^{NC} R_j \Delta_j \tag{1}$$

$$C_{LN} = L \times ULC \tag{2}$$

where

- L Total alignment length
- (x_i^C, y_i^C) Coordinate at intersection of i th tangent and following circular curve
- (x_i^T, y_i^T) Coordinate at intersection of i th tangent and previous circular curve
- N Total number of PIs
- Δ_j Intersection angle of j th circular curve along the alignment
- R_j Radius of curvature of j th circular curve along the alignment
- NC Total number of curve sections
- C_{LN} Total length-dependent cost
- ULC Construction cost per unit length

The location-dependent costs consist of all the direct and indirect costs incurred during the acquisition of the land for building the highway. These costs include right-of-way cost for the highway and impact on environmentally sensitive land features

like wetlands, marshes and forest. Right-of-way cost is modelled by estimating the cost for all the fractions of land parcels through which the alignment passes. Then, the total right-of-way cost can be modelled as the product of the unit cost and the fraction of the area acquired from the land parcel, as shown in Eq. (3). Impact on environmentally sensitive land features is modelled by estimating all the fractions of the environmentally sensitive land parcels through which the alignment passes. This research work is limited to the optimization of total alignment cost expressed in monetary values. Multiplying a high penalty cost with the impacted area converts it into monetary terms as shown in Eq. (4). Equation 5 shows the mathematical formulation for the estimation of the total location-dependent cost [21].

$$C_R = \sum_{i=1}^{APL} C_{LPi} \times a_i \tag{3}$$

$$C_{EN} = \sum_{j=1}^{EPL} P \times a_j \tag{4}$$

$$C_{LO} = C_R + C_{EN} \tag{5}$$

where

- C_{LO} Total location-dependent cost
- C_R Right-of-way cost
- C_{LPi} Unit cost of i th land parcel
- APL Total number of land parcels
- a_i Fractional area of i th land parcel acquired for the highway alignment
- C_{EN} Environmental impact expressed in monetary terms
- EPL Total number of environmentally sensitive land parcels
- P High penalty cost
- a_j Fractional area of j th environmentally land parcel acquired for the highway alignment

4 Objective

A well-planned highway alignment can save resources during the design stage. The overall length of the alignment directly affects this process as a longer alignment increases the overall cost of the highway. This additional expenditure can be avoided by optimizing the length of the alignment. Conversely, alignment length is directly dependent on the number and location of tangent and curve sections, which are determined based on the location of the PIs. In essence, selecting PIs at appropriate locations and fitting suitable curves affects the length and associated cost of the alignment and thus, the design process considerably. Similarly, avoiding environmentally

sensitive land decreases the negative impact of the highway on the local environment. An appropriate horizontal alignment should, thus, minimize this negative impact on the environment as well. Hence, the overall objective of this study is to minimize the sum of the total length-dependent and location-dependent cost where the decision variables are the locations of a set of PIs in the study area. Therefore, mathematically it can be represented as shown in Eq. (6)

$$\text{Minimize } C_{HA} = C_{LN} + C_{LO} \quad (6)$$

where

- C_{HA} Total alignment cost
- C_{LN} Total length-dependent cost
- C_{LO} Total location-dependent cost

5 Path Planner Method (PPM)

This study presents a holistic method known as PPM to develop the optimal horizontal alignment. The model initiates by developing the PIs in the study area and then approaches to develop a good piecewise linear segment by selecting the optimal PIs that minimizes the alignment cost. The selection of the PIs for the generation of horizontal highway alignment is mainly based on three parameters. Firstly, step size defines the distance between any two subsequent PIs. It is selected depending on the number of the sensitive area located within the considered study area and their density as well as the minimum tangent length. It is also vital to select the proper step size range; as long straight section may generate driving fatigue. Secondly, the point population (i.e. the possible PIs) is iteratively generated in the entire study area and is utilized for the development of the horizontal alignment. Lastly, the number of iteration helps to obtain an optimal solution. The value of these parameters depends on the characteristics of the study area, such as the number of sensitive areas and their density compared to the considered study area. Hence, for the development of the optimal alignment, it is very important to select these parameters appropriately [23].

5.1 Methodology

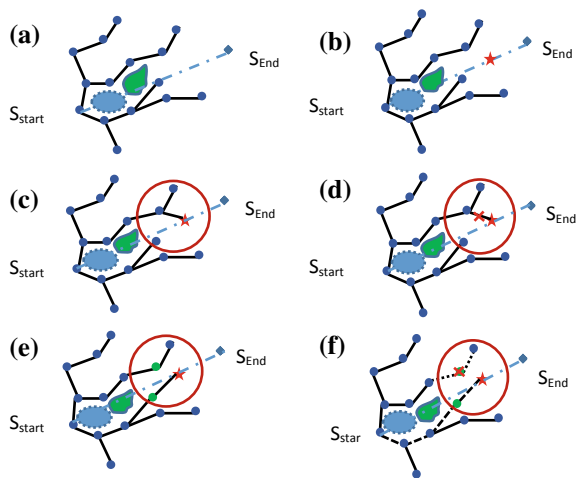
Development of an optimal horizontal alignment depends on the location of the PIs. These PIs are positioned along the centreline of the alignment and are implemented on the ground to develop an alignment. The PPM helps to determine the location of the PIs, by satisfying the constraints. The process initiates a tree-like path that propagates iteratively from one desired location to the other. While propagating, the

method uses the random points generated by discrepancy sampling technique in the study area. These points are connected to create piecewise linear segments which are the candidates for possible horizontal alignment. Dispersion δ of a set R of finite points is defined in Eq. (7).

$$\delta(R, \emptyset) = \sup_{y \in Y} \min_{r \in R} \emptyset(y, r) \tag{7}$$

where Y is the search space and \emptyset is a metric on Y . In essence, the dispersion can be considered as the radius of the largest empty ball (under γ) in the space [23]. The study area is explored using Voronoi diagram-based exploration [24]. The PPM initiates the tree from the start point, S_{start} , and is incremented to the end point, S_{end} , by connecting the random point population within the study area. The connected points are the candidate potential PIs of the horizontal alignment. Any new connection between the established point on the tree and the newly generated random point, S_{rand} , is established, only if the new connection satisfies the design constraints of the alignment and the obligatory point requirements and also possesses the minimum cost from the generated path connecting to the start point, S_{start} . The method deletes the points from the tree if it does not propagate towards the end point. These deleted points are regenerated in the locations that lead the tree to the end point. This process reduces the memory allocation space and enhances the efficiency of the method. With each iteration, the method explores the entire tree for more feasible connections, and it reconnects for the refinement of the alignment. In this way, the study area is explored by connecting all the possible potential PIs; hence, the path is progressed towards the end location. The process continues until it satisfies the termination criteria, i.e. if there is no change in the cost of the alignment over a significant number of iterations. The generation of the PIs in the PPM can be visualized from Fig. 1 [23].

Fig. 1 Generation of PIs in PPM Source Maji [23]



6 Ant Algorithm

Ant algorithm (AA) was first developed by Dorigo [25]. The inspiring source for the algorithm is ants' foraging behaviour, i.e. the indirect communication between the ants by means of chemical pheromone trails. In this, pheromone trail following behaviour of ants, each ant perceives pheromone concentrations in its local environment and selects the direction with the highest pheromone concentration. This behaviour emerges into finding the best alternative. AA has shown efficiency in solving discrete optimization problems. However, the use of AA for solving continuous optimization problems is still under investigation. Hence, AA is widely considered as a local search optimization algorithm. This basic reason also makes the algorithm work faster with less computation time to reach near-optimal solutions. Some of the problems for which ACO has yielded reasonably promising results include the travel salesman problem, job shop scheduling, quadratic assignment problem and vehicle routing problem [25]. Samanta and Jha [26] solved the highway optimization problem by using ant algorithm and compared its performance with a genetic algorithm (GA). For highway optimization problem, the number of PIs is randomly generated on equally spaced orthogonal sections placed between a start point and end point [6–9]. AA is applied for each of the orthogonal sections. Each ant starts moving from the starting point to each of the PIs generated on the orthogonal sections. The pheromone levels associated with each of the PIs decides which PI gets selected by the AA. The PI which minimizes the total cost is selected by the influence of the pheromone levels. The entire process is shown in Fig. 2. The probability distribution that controls the selection of PIs is given as in Eq. (8) where $p_i(a, b)$ = probability of ant i moving from PI a to PI b

$$p_i(a, b) = \begin{cases} \frac{[\tau(a,b)]^\gamma [\eta(a,b)]^\gamma}{\sum_{c \notin N_i} [\tau(a,c)]^\gamma [\eta(a,c)]^\gamma} & \text{if } b \notin N_i \\ 0 & \text{otherwise} \end{cases} \quad (8)$$

The pheromone trail is updated based on the total cost. The local trail update formula is given as in Eq. (9)

$$(a, b) = (1 - \beta) \cdot \tau(a, b) + \beta \cdot \tau_0 \quad (9)$$

where

$$\begin{aligned} \tau_0 &= \text{Parameter} \\ \beta, \gamma &= \text{parameters that control trail versus visibility} \end{aligned}$$

The visibility is basically an inverse function of the total length of the alignment for a particular iteration. Similarly, the ant moves probabilistically from one PI to another based on the intensity of the pheromone with respect to the corresponding link. This process is then repeated for n number of ants, which gives the minimal cost path for that particular iteration. After each iteration, the pheromone intensity

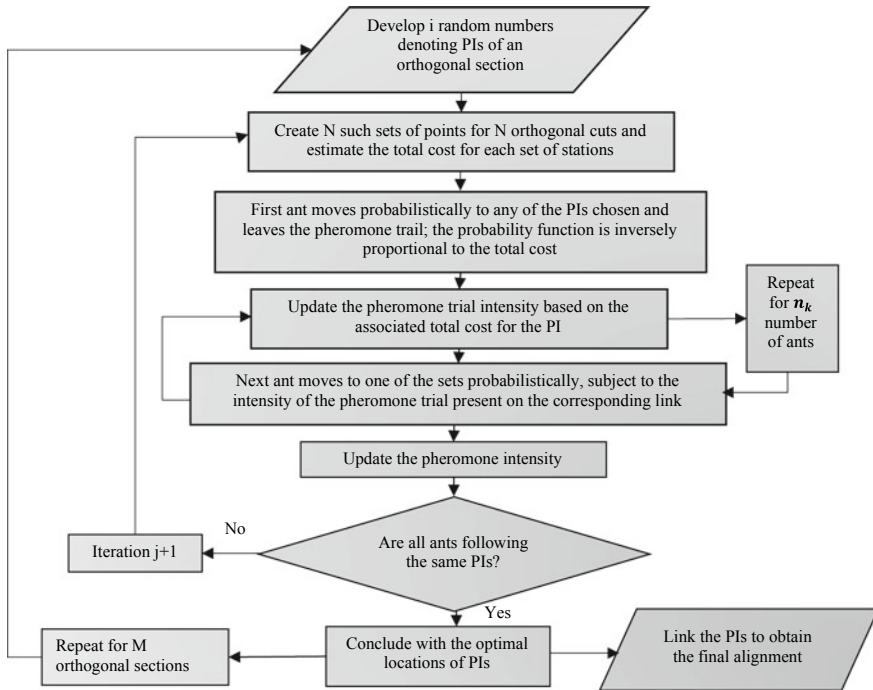


Fig. 2 Flow chart for highway alignment optimization with ant algorithm

is updated globally by Eq. (10),

$$\varphi(a, b) = (1 - \beta) \cdot \varphi(a, b) + \beta \cdot \Delta\varphi(a, b) \tag{10}$$

where $\Delta\varphi(a, b)$ is the inverse of the least cost. The above process is repeated for j number of iterations or until the solution converges. The entire above process is then repeated for remaining orthogonal sections.

7 Case Studies

Comparative performance analysis of PPM and ACO method on horizontal highway alignment problem was done using two case studies. The first case study considered a hypothetical scenario, whereas the second considered a real-world scenario. Length-dependent cost was considered as the objective function for both case studies.

7.1 Case 1

A hypothetical scenario with ideal conditions, i.e. without any environmentally affected land parcels such as wetland area, forest area and agricultural area, was selected for this study. In this experiment, the length considered between the start point and the end point is of about 5.6 km. The objective of this problem is to generate a minimum length alignment between the two given points using PPM and ant algorithm. No geometric constraints such as minimum tangential section and minimum curve length were considered in this problem. After applying the two optimization methods, an optimal set of points are obtained, which represent the PIs of the alignment between the start and the end points. The input values and other relevant parameters for the horizontal highway alignment problem are shown in Table 2.

For the above given numerical example, the optimal PIs with PPM and ant algorithm are shown in Fig. 3. From these figures, it can be observed that the alignment formed by both the optimization methods using the same number of random population and iterations differ. PPM generates a proper straight line between the start and the end point, as a straight line is considered as the shortest distance between any two points, when there are no obstacles, shown in Fig. 3b, whereas the alignment generated by AA is not a straight line as of PPM, shown in Fig. 3a. From the results, it can be concluded that PPM generates minimum cost alignment compared to the alignment generated by ant algorithm.

Table 2 Input parameters for PPM and ant algorithm for case 1

Input parameters	PPM	Ant algorithm
Coordinates	Start point: [10, 10] and end point: [50, 50]	
Factors controlling the trail (β)	–	0.1
Factors controlling visibility (γ)	–	2.0
Rate of pheromone evaporation	–	$\tau = 0.5$
Number of population	50	$n_k = 50$
Number of iterations	500	500

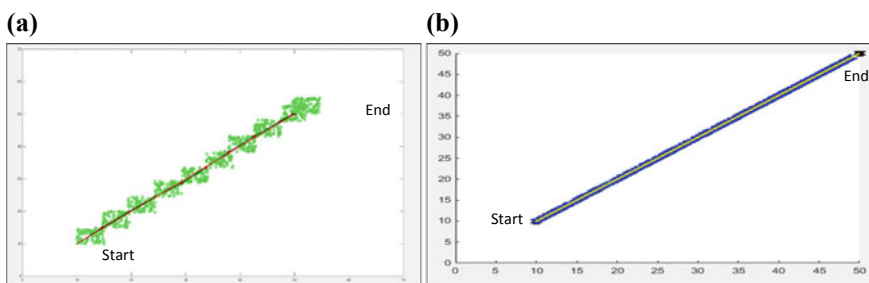


Fig. 3 Path generated using **a** AA and **b** PPM

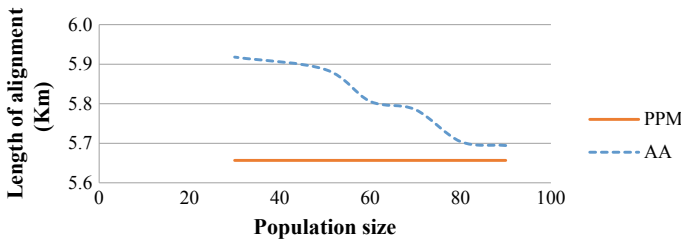


Fig. 4 Trends of formation of the highway alignment by PPM and AA

The values of the objective function over successive random population for 500 iterations are represented in Fig. 4, which give an idea of the formation of the alignment by the two algorithms for the highway alignment problem.

7.2 Case 2

A real field study is conducted between the two cities, Gadhvana ($21^{\circ}31'12''N$, $69^{\circ}58'33.6''E$) and Bantiya ($21^{\circ}32'24''N$, $70^{\circ}17'27.6''E$) in Gujarat, India. The Euclidean distance between the two selected cities is 31 km approximately. In this study, Gadhvana is considered as the origin and Bantiya as the destination of the alignment. The study area was identified with 919 sensitive land parcels. The land parcels represented by forest and wetlands are identified in the selected study area. These areas are represented together as environmentally sensitive regions. Any impact on these land parcels is considered as environmental impact, during the alignment optimization process. The alignment should not pass through these land parcels. These land parcels are extracted in a shapefile which is being read in MATLAB 2014b. The total area of these sensitive land parcels is about 31% of the total study area. Based on this the step size should be in the range of 550–850 m. The alignment is considered for a two-lane two-way highway. Table 3 shows the input design parameters for the problem. Table 4 shows the input parameters for the PPM and AA.

Table 3 Input design parameters for the problem

	Parameters	Values
Design parameters	Road width	10 m (2 lanes, with each 3.75 m and shoulder 2.5 m)
	Design speed	100 km/h
Cost parameters	Price of road construction per m	\$150
	Land acquisition cost (Gujarat) m^2	\$2.48
	Price of impact area per m^2	\$80

Table 4 Input parameters for PPM and AA for case 2

Input parameters	PPM	Ant algorithm
Coordinates	Start point: 21°31'12"N, 69°58'33.6"E End point: 21°32'24"N, 70°17'27.6"E	
Factors controlling the trail (β)	–	0.1
Factors controlling visibility (γ)	–	2.0
Rate of pheromone evaporation	–	$\tau = 0.5$
Number of population	4000	$n_k = 4000$
Number of iterations	420,000	420,000

The alignment generated by PPM and AA is shown in Fig. 5. Table 5 shows the results for the alignment generated by both PPM and AA. From the results, it can be observed that the PPM gives a more optimal alignment. The alignment generated by PPM has lesser alignment cost, lower environmental impact and lower total length. However, the time taken for computation is significantly different with AA giving the result much faster than PPM.

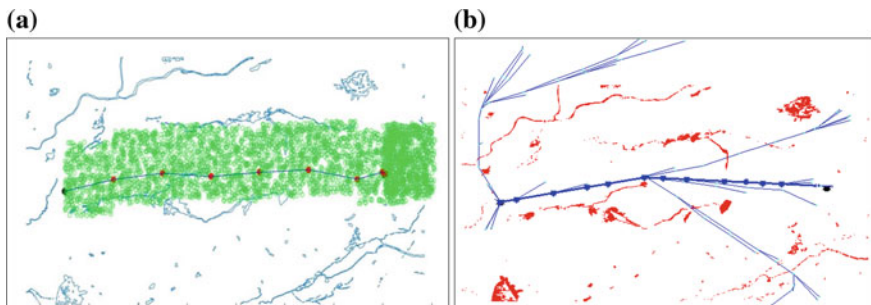


Fig. 5 Optimal path obtained by **a** ant algorithm and **b** path planner method

Table 5 Objective values of the obtained horizontal alignment

Parameters	Alignment generated by AA	Alignment generated by PPM
Length of road	34.2 km	33.4 km
Environmental impact	3315.932,446 m ²	0 m ²
Total cost of road	6.28 \$ million	5.67 \$ million
Total time taken	8 h	8 h

8 Summary

This research presents an optimization method that generates the PIs without constraining it to any orthogonal sections, while the generation of the PIs the model satisfies the geometric code requirements for the minimum tangent length section and as well as minimizes the alignment length and environmental impact cost. The objective function is formulated to deal with length- and location-dependent costs. Using this function, in addition to avoiding high-cost areas, the solution produced has also minimum length.

The paper also provides a brief idea about the ant algorithm and does a comparative test between the ant algorithm and the PPM. The results obtained by the two optimization problem are discussed in Table 6. It shows that the results obtained by both the algorithms are reasonably close, although discretization of the search space was necessary for the ant algorithm, where the search space was divided into regular intervals. As the problem size considered here is relatively small, computation time with the algorithms is insignificant. But, it needs to be considered that the PPM uses a probabilistic search method, so sometimes the intermediate solutions enter into the

Table 6 Comparison between PPM and Ant algorithm

	Path planner method	Ant algorithm
Type of search space	The method works for continuous search space	It is suitable for discrete search space [26]. However, some ant algorithms have been developed for the continuous search space. But very less problems are solved for continuous search space
Population	Points are generated incrementally over the entire search space	An initial population needs to be generated over the equally spaced orthogonal planes
Flexibility of PIs	PIs are not constrained by any parameters and can be generated all over the search space	PIs are constrained by the orthogonal places, which are formed in an equidistant between the start and the end point
Termination criteria	Maximum number of iteration has reached	Maximum number of iteration has reached and also when all the ant's convergences to a single solution
Computation time	More (for dense areas)	Less
Transition rule	Uses the cost function to select the next node. The method checks the cost of the neighbour node as well as the cost of the node initial state. The node possessing the minimum cost is then selected	Uses the probabilistic transition rule to select the next node from the set of feasible neighbourhood nodes
Optimality of solution	Global solution	May be local or global solution

infeasible spaces while searching for an optimal path. This increases the computation time (which may be significant for larger problem sizes) as the computations are to be performed for both the infeasible and feasible areas.

For ant colony optimization method, however, the computations are performed only for the feasible spaces as it uses deterministic rules that require the approximate feasible solution space to be specified a priori through discretization. The flexibility in generating discrete PIs at a random location helps the proposed method to efficiently explore the entire search space and increases the possibility of obtaining an optimal horizontal alignment. This method has the capability of steering the PIs away from the boundaries of restricted or prohibited areas and closer to the control points. Overall, it does not get trapped to local optimum solutions due to the discrete infeasible regions.

In future, this research can be extended several directions. In this paper, only the generation of PIs is discussed. An appropriate curve fitting methodology can be added to get a realistic horizontal alignment. This method can be extended to incorporate the development of the vertical alignment also. In future, this research is worth in investigating for three-dimensional alignment.

References

1. Adiyatov O, Varol HA (2013) Rapidly-exploring random tree based memory efficient motion planning. In: *Mechatronics and Automation (ICMA)*, IEEE international conference, 2013, pp 354–359
2. LaValle SM, Kuffner JJ (2000) Rapidly-exploring random trees: progress and prospects
3. Howard BE, Bramnick Z, Shaw JF (1969) Optimum curvature principle in highway routing, pp 236–241
4. Parker NA (1977) Rural highway route corridor selection. *Transport Plann Technol* 3(4):247–256
5. Mondal S, Lucet Y, Hare W (2015) Optimizing horizontal alignment of roads in a specified corridor. *Comput Oper Res* 64:130–138
6. Jha MK (2002) Optimizing highway networks: a GA and swarm intelligence based approach. In: *Computing in Civil Engineering*, 2002, pp 76–89. ASCE
7. Jha MK (2003) Criteria-based decision support system for selecting highway alignments. *J Transport Eng* 129(1):33–41
8. Jha MK, Schonfeld P (2000) Integrating genetic algorithms and geographic information system to optimize highway alignments. *J Transport Res Board* 1719(1):233–240
9. Jong JC, Jha MK, Schonfeld P (2000) Preliminary highway design with genetic algorithms and geographic information systems. *Comput Aided Civil Infrastruct Eng* 15(4):261–271
10. Kang MW, Jha MK et al (2012) Applicability of highway alignment optimization models. *Transport Res Part C Emer Technol* 21(1):257–286
11. Shafahi Y, Bagherian M (2013) A customized particle swarm method to solve highway alignment optimization problem. *Comput Aided Civil Infrastruct Eng* 28(1):52–67
12. Thomson NR, Sykes JF (1988) Route selection through a dynamic ice field using the maximum principle. *Transport Res Part B Methodol* 22(5):339–356
13. Shaw JF, Howard BE (1982) Expressway route optimization by OCP. *J Transport Eng* 108(TE3)
14. Wan F (1995) *Introduction to the calculus of variations and its applications*. CRC Press
15. Turner AK, Miles RD (1971) The GCARS system: a computer-assisted method of regional route location. No 348

16. Trietsch D (1987) A family of methods for preliminary highway alignment. *Transport Sci* 21(1):17–25
17. Athanassoulis GC, Calogero V (1973) Optimal location of a new highway from A to B—a computer technique for route planning. In: PTRC seminar proceedings on cost models and optimization in highway, 1973
18. Nicholson AJ, Elms DG, Williman AA (1976) Variational approach to optimal route location. *Highway Engineer* 23(3)
19. Hogan JD (1973) Experience with OPTLOC optimum location of highways by computer. In: PTRC seminar proceedings on cost models and optimization in highways (session L10), London, 1973
20. Maji A, Jha MK (2009) Multi-objective highway alignment optimization using a genetic algorithm. *J Adv Transport* 43(4):481–504
21. Maji A, Jha MK (2011) A Multiobjective analysis of impacted area of environmentally preserved land and alignment cost for sustainable highway infrastructure design. *Proc Soc Behav Sci* 20:966–972
22. Tat CW, Tao F (2003) Using GIS and genetic algorithm in highway alignment optimization. In: *Proceedings of the intelligent transportation systems, 2003 IEEE*, vol 2, pp 1563–1567, 2003
23. Maji A (2017) Optimization of horizontal highway alignment using Path Planner Method (PPM). *Urban Transport 2017*, 5–7 Sept 2017, Rome, Italy
24. Gold CM (1991) Problems with handling spatial data—the Voronoi approach. *Canadian Inst Surv Mapp J* 45:65–80
25. Dorigo M, Caro GD, Gambardella LM (1999) Ant algorithms for discrete optimization. *Artif Life* 5(2):137–172
26. Samanta S, Jha MK (2012) Applicability of genetic and ant algorithms in highway alignment and rail transit station location optimization. *Int J Oper Res Inf Syst (IJORIS)* 3(1):13–36

Studies on Importance and Design Needs for Non-motorized Trips—A Review



Anshu Bamney and Rajat Rastogi

Abstract Increased pollution, congestion, traffic jams, higher travel cost, travel distance, travel time, accidents, and dependence on imported oil, etc., are the major problems that the countries in the world are facing today. Non-motorized transport or active transport is one of the measures to conquer such problems. The trips conducted by non-motorized modes are important because these are a very flexible solution to accessibility, especially where the resources are scarce. These are capable of generating employment and poverty alleviation. In addition to this, the total cost of non-motorized traffic infrastructure along with operating costs is 4–8 times cheaper than that needed for motorized vehicles. Studying these trips will help planners to understand the needs of non-motorized trip makers. By knowing this, one can design facilities and policies for the use of non-motorized vehicles. This paper aims to present information about the modal share of non-motorized trips, importance of these trips in present scenario, factors affecting non-motorized vehicles, and policies and design needs which can help in increasing the modal share of non-motorized trips.

Keywords Non-motorized vehicles · Non-motorized trips · Modal share · Policy · Design needs

1 Introduction

The most vexing transportation-related problems that the world is facing due to increase in motorization are increase in pollution, congestion, traffic jams, travel cost, travel distance, travel time, accidents, and dependence on fossil fuel. Increasing the share of non-motorized vehicles (NMVs) in trip making can partly reduce these. These are generally used for short-distance trips, using bicycle, bullock cart, hand

A. Bamney (✉)

Department of Civil Engineering, Rewa Engineering College, Rewa 486001, India
e-mail: anshubamne19@gmail.com

R. Rastogi

Department of Civil Engineering, Indian Institute of Technology Roorkee, Roorkee 247667, India
e-mail: rajatfce@iitr.ac.in

© Springer Nature Singapore Pte Ltd. 2020

T. V. Mathew et al. (eds.), *Transportation Research*, Lecture Notes
in Civil Engineering 45, https://doi.org/10.1007/978-981-32-9042-6_16

201

cart, pedicabs, etc. Various other manual or electric variants are also available. These modes can be used as a tool of employment generation and poverty alleviation. Irrespective of merits and demerits of their use, in most of the developing countries, more than 60% of the non-motorized trips (NMTs) are under 3 km and in some well-planned German cities, it is as high as 80% [1]. In the same light, the acceptable cycling distance for Delhi, Tiruchirappalli, and Mumbai are reported as 5100, 5200, and 2724 m [2]. For Indonesia and China, this distance is found to be 3300 and 6000 m.

In most of the countries, the share of NMTs in terms of total kilometers traveled is small, but in terms of number of trips, it is substantial. These trips are generally conducted for going to school or college or for transporting goods and services for short to medium distances of 3–10 km. Another study [3] suggests that the share of bicycling and walking is not affected by average trip length. It was reported [4] that NMTs account for 40–60% in major Asian cities and in African cities this proportion is even higher. Furthermore, it was reported [5] that Indian cities have substantial trips using bicycles. Its use varies from 7 to 15% in large cities to 13–21% in medium and small cities. Its high ownership, low cost, and easy use make it a desirable mode of transport for students and low-income workers. Most of the medium and large cities have 35–65% households owning one or more cycles, whereas, in the smaller cities, it varies between 33 and 48%. Along with this in Indian megacities (population more than 8 million), trip share of NMT (walking or bicycling) is 30% [6]. High percentage of people in urban cities lives in slums, e.g., Mumbai 41.3%, Kolkata 29.6%, and Chennai 28.5% (census 2011). These people cannot afford motorized modes for their daily travel. The main mode of travel for them is either walking or cycling. Another study [7] reported that the share of NMVs varied between 33 and 51% in Roorkee, a class I city in India. Share of cycle-rickshaw varied between 6 and 21% and that of cycle varied between 27 and 30%. Their use was influenced by the type of development on roadsides and the type of areas. 33% share of NMVs was observed in new development and 51% in densely populated areas. Another study [8] for the same city reported NMV share between 72.5 and 15.5%, and proportion of bicycles between 59 and 11%. Bicycle volume at some locations of the city was found to be nearly 50% of the total traffic during peak hour.

The above discussion clearly tells us that at world level and in the developing country like India, the share of NMTs is relatively quite high. Timely and adequate size of NMV facilities needs to be provided for their safe and smooth movement. Different countries have different codes for provision of NMV facilities, namely The Geometric Design of Pedestrian, Cycle and Equestrian Routes (UK), Registration and Classification of paths (Denmark), Dutch CROW, American Association of State Highway and Transportation Officials (AASHTO) Guide for Bikeway Facilities, and Urban Bikeway Design Guide by National Association of City Transportation Officials (NACTO), USA. The Indian Road Congress Code IRC: 11 1962 on recommended practice for the design and layout of cycle tracks is very old, limited and gives only few information regarding design of cycle track. It has not been revised for a long time. It also does not talk about flow characteristics. The scenario has

changed over the years. The design needs for different NMVs are different and need upgradation in the light of new information.

This study was carried out with an objective to understand the factors that influence the NMTs and to compile the information on design needs for NMVs so that an increase in the modal share of NMVs in short trips can be ensured. The following subsections present the associated information in sequential form.

2 Importance of Non-motorized Trips

The importance of NMVs is discussed before outlining the factors that influence the design needs for such trips.

It was reported by [9] that NMTs provide flexible solution to accessibility, especially where the resources are scarce. They are flexible as well as affordable. Flexibility ensures the door-to-door transport of persons and goods and improves travel time and provides route options. For poor people, NMVs provide access to employment, social services, educational activities, and household chores. Affordability is a function of purchase price in relation to the income. An economic study [10] concluded that bicycle infrastructure, compared to motorized traffic lane, provides savings on infrastructure and trip costs (35% of the total annual cost of bicycle infrastructure). The total cost (infrastructure and operating costs) for motorized traffic is 4–8 times higher than for bicycles. In addition to this, the contribution of NMTs in total kilometers traveled is found to be small though it is substantial in terms of total numbers of trips [11]. It is true for less developed countries with low-income households and developed countries with high-income households.

Apart from these, the NMTs are environment-friendly [1]. Bicyclists and pedestrians are most efficient users of scarce road space and helps in combating congestion. NMTs are economically vital and reduce country's dependence on imported oil and improve accessibility for poor and social cohesion. These are capable of reducing premature deaths due to traffic accidents. The improvement in bicycle and walking facilities in Bogota (1997) reduced death rate from 2 to 3 people per day to 1–2 people per day.

3 Factors Influencing Non-motorized Trips

There are many socioeconomic, demographic, built environment, and travel factors that affect NMTs. The following paragraphs explain each of them.

A study was conducted in Mumbai [12] and Bhopal [13] India. The persons with better socioeconomic background were found least interested to use walk or bicycle as their mode of transport for all types of trips. Similar findings were observed in Bandung, Indonesia [14], and India [15]. NMVs were found to be the main mode of travel for low-income group, women, and students. People with a higher household income

were found to travel more and rely on cars, probably because of lower sensitivity to travel cost [16, 17]. Occupation level is also an important factor [12, 18]. People belonging to higher occupation level were found reluctant to use NMVs. Moreover, education level was also found influencing NMTs indirectly [16, 19]. Respondents with education level as graduation or more tend to have longer commuting Vehicle Miles Traveled (VMT) compared to those who graduated only high school. This was probably because they might not be getting suitable job in nearby location. Increase in age has a negative effect on NMV usage [18, 19]. As the age of people increases, they tend to drive more, may be due to work- and family-related travel needs. However, older people eventually drive less after they reach certain age. Furthermore, gender also influences NMTs [10, 18]. Males were more interested in using NMVs for trips as compared to females. On the contrary, women in Sweden were found more willing to use travel modes that have a positive impact on environment (i.e., reducing car usage) [20, 21].

Along with socioeconomic and demographic factors, built environment also plays an important role in increasing and decreasing the share of NMVs. New Urbanism (in the USA) and Compact City (in Europe) are the two approaches that focus on creating diverse, compact, and transit-oriented neighborhoods for pleasant, comfortable, and safe environment for pedestrians and bicyclists. It was found that density, land use, diversity, and pedestrian-oriented designs generally reduce trip rates and encourage non-motorized travel in statistically significant ways [22]. Further, population and job densities are found positively influencing non-motorized travel [23, 24]. Higher population density at origin encouraged the use of NMVs and public transit for work trips, while higher population density at destination matters for both work and non-work trips [24]. Higher job density at the origin was insignificant for both work and non-work trips while higher job density at the destination promotes the use of biking, walking, and mass transit for work trips but not for non-work trips. Walking was found most strongly related to land use diversity, intersection density, and the number of destinations within walking distance [25]. A study conducted in four geographical areas (Seattle, Virginia, Baltimore and Washington) [19] found that residential density and entropy (the extent of land use mix) were negatively correlated with VMT in all the areas. It was also observed that average block size distance from CBD positively influenced VMT. Since land-use mix provides walkable access to destinations, it decreases the percentage of private motorized trips. Along with these factors, topography and weather were found influencing NMT [18]. Topographic features like sloping hills and hilly terrain negatively impacted these trips. A study in Santander, Spain, found weather to be the most influential variable for bicycle use [26]. Bicyclists need a safe environment which is free from risks.

Apart from these factors, higher job housing balance (around 1) is found to decrease motorized vehicle usage and increase the share of NMVs and public transit [22, 27, 28]. It was found that urban mobility behavior can be affected by NMV facilities and street patterns. Higher proportion of intersections per road kilometer reduces VKT per household [29]. Higher connectivity can increase walking and bicycling, and VMT can be decreased by connected road networks [30, 31]. Moreover, walkable communities reduce driving and increase the share of NMVs [32]. A study in

Raleigh-Durham, North Carolina, found that length of sidewalk is an effective factor in reducing miles traveled per person. VMT can also be increased by increasing bicycle lane density [34, 35].

In addition to this, the NMV infrastructure and facilities also play an important role in influencing NMTs. Following factors were found affecting the bicycle service quality [36]—effective width of outside through lane, pavement condition index, traffic volume, traffic speed, roadside commercial activities, interruptions by unauthorized stoppages of intermittent public transits, vehicular ingress–egress to on-street parking area, and frequency of driveways carrying a high volume of traffic. The study also advocated for the minimization of bicycle–vehicle interaction and prohibition of road side vending activities, illegal on-street parking activities, and unauthorized stoppages of intermittent public transits in order to improve the share of NMVs. Another study [37] found commuter safety as an important issue and suggested the need to segregate cycle lanes and signals at intersections. It was highlighted that the perception of an individual toward a particular mode, attitudes, social norms, and habits plays an important role in increasing its share. In a study, six intersection attributes, namely road width per direction, peak hour traffic volume, pavement condition index, average stopped time delay incurred by bicyclists, land use pattern, and on-street parking turn-over were found to have a significant influence on the bicyclist’s perceived satisfaction levels under heterogeneous traffic flow condition [38]. It was observed that along with objective variables like, socio-economic and household characteristics, mode availability and trip characteristics, certain latent variables like lifestyle, safety and comfort, awareness, direct disadvantages, subjective norms, individual capabilities, and non-commuting cycling habit also play a significant role in influencing NMTs [39]. Another study [40] found that perceived benefits, physical barriers, safety hazards, social barriers, and road condition significantly influence bicycle mode choice. In addition to this, marketing campaign for bicycle usage and a good urban landscape planning and design is necessary to attract people to use more bicycles [39, 40].

4 Design Needs for Non-motorized Trips

In order to encourage NMV trips and reduce the share of MVs, certain policies and designs are adopted across the world. These are discussed in the following paragraphs.

Separation of the bicycle track, on routes where bicycle traffic is more, is suggested to solve the problem on road sections, but it cannot solve the problem at intersections. At intersections, bicyclists need to be made visible to other road users. It can be done by making available enough road space to the cyclists. Ensuring prevention of bicycle theft is considered to be an effective tool to promote wider use of the bicycle [10]. It may also help in inducing shift from motorized modes. Another factor is the positioning or appropriately locating the guarded parking lots with respect to the

major destinations. This will ease out the use of bicycle. It may be associated with reasonable parking prices.

Certain policies which are in use to make bicycle available to urban poor and to increase the share of NMVs are:

1. Credit and savings schemes, which gave good results in Eldoret (Kenya).
2. Bicycle sale-on-credit-program.
3. Bicycle lease contract, which was welcomed in Morogoro (Tanzania).
4. Promotional bicycle sales to women and children entering secondary school.
5. A premium policy to pay monthly 20 USD by local Government of Belgium to those employees, who use NM mode to come to work. It was successful.

Certain measures related to facilities, network, and regulation which were found improving the share of NMVs in trips are [1]:

1. Traffic crossing signals: A separate phase in signal should be provided to allow pedestrians and other NMVs to cross the road safely (quite uncommon in developing countries).
2. Pedestrian- and Traffic-calming facilities: Slowing down of traffic speeds, through speed restrictions and physical infrastructure changes like neckdowns at intersections, restructuring roads to meander around trees and planters and medians. Need to cross at uncontrolled intersections shall be reduced or eliminated. Raising pedestrian ways at intersections sends a signal to drivers that they are on space designed for pedestrians. Pedestrian facilities shall be physically protected from infiltration by motor vehicles.
3. Designated lanes for NMV: Physically and non-physically separating NMV lanes give bicyclists a greater sense of entitlement to the road.
4. Cycle routes and signs: Simple to understand and direct bicycle routes and proper signage can help in cutting down the bicycle traffic from arterials, secondary and tertiary roads. It will help bicyclists to know more about bicycle-friendly roads.
5. Road network: Road network for cyclists and pedestrians should be designed in such a way that the detour factor should be as less as possible. Detour factor represents the unease of travel. It is the ratio of total distance traveled by user to the straightline distance of the destination from origin.
6. Regulations for cycle-rickshaw: To fight against congestion problem, it is advised to divide the city in green zone, amber zone, and red zone. Green zone represents no restriction on number of rickshaws allowed to operate, amber zone represents some restriction, and red zone represents that cycle-rickshaws are not allowed at all.

Design needs and policies to improve the use of NMVs for trips are suggested below [2]

1. Walk policy: A sidewalk of minimum 1.5 m width, with viable separation, so as to accommodate pedestrians and persons with disability.
2. Pedestrianize intersection: The design of intersection should be clear, and street crossings should be removed by slip lanes, medians, and bulb outs. The geometry of intersection should prioritize the movement of NM modes and pedestrians.

3. Signal placement: Signals should be placed at optimum visibility during critical movements. Box span, mast arm, and corner pole signals should be preferred.
4. Illumination: Crossing areas, walking areas, and sidewalks should be illuminated so that pedestrians remain within clear visibility to the vehicle drivers.
5. Simplify midblock crossing: Safety of the pedestrians who cross more than one lane can be achieved by constructing median in the center of the carriageway.
6. Schools: Geometry of roadway should be such that it improves the flow of pedestrians and bicyclists. This can be achieved by raised crossing, diverter and roundabout, and by appropriate layout of on-street parking.
7. Eliminate reversing of vehicles: Many accidents take place when cars and other vehicles are reversed from parking places. In order to reduce this hazardous interaction, walking should be minimized in parking areas. Some measures that can reduce such accidents are “U” pattern drop-offs, long throat driveways lined with sidewalks, and segregated walking space between parking lots.
8. Combining walk with transit: Providing access to the transit stations on foot, about 500 m is considered as acceptable walking distance to transit which takes about 5–10 min. Transit stations should be easy to reach by walk and stops should be shaded, visible, and have comfortable arrangement for sitting and waiting.
9. Certain policies, like employee commuter subsidies which include breakfast and bath at office, time relaxation in office hours, monetary benefits for owning and operating bicycles, etc., and other policies like bike-on-transit which includes several systems like bike-and-ride, bike-on-rail, bike-on-ferries, and bike-on-vanpool can increase the number of cyclists on road. Provision of better parking facility at transit stations and integration of bicycles with public transport is helpful in increasing NMTs.
10. Bike-on transit system: Bike-on-Bus system in the USA has led to an increase in bicycle share between 17 and 68% in different transportation districts of the country.
11. Support to bicycle manufacturing industry: This is one of the key policies for high bicycle share in a country. Chinese government is the best example of it.

Various other researchers [41, 42] have also suggested measures to improve share of NMTs. These are improved sidewalks, crosswalks, paths, bicycle lanes, and network; public bicycle system (automated bicycle renting systems for short trips); increase in road and path connectivity, with special non-motorized shortcuts; traffic calming; traffic speed reductions, vehicle restrictions and road space reallocation, safety education, law enforcement and encouragement programs; bicycle parking; bicycle integration in transit systems; addressing security concerns of pedestrians and cyclists, congestion pricing; vehicle parking policies; and fuel taxes. It was observed in a study that when parking costs were increased by 10%, vehicle trips reduced by 1–3% [43]. Another study states that Vehicle Quota System (VQS) policy applied in Singapore in 1990 was a successful one and reduced annual growth rate of MVs to 3% [44]. Park and ride facilities also encouraged people to shift from private motorized vehicles to public transit [45]. Yet these facilities are criticized because they

occupy land and encourage people to use private motorized vehicles to reach at least transit stations [46].

Various measures have been taken in most European cities to promote NMV use. Priority is given to NMVs on certain streets and intersections by designing green phases at traffic lights. Some one-way streets have been converted into two-way streets for exclusive use of non-motorized users. Moreover, NMVs are exempted from many turn restrictions [47]. Some European cities have dedicated car-parking space to non-motorized lanes and non-motorized parking. Bike storage points are also provided at public-private interchanges. Additional measures are taken to increase the cost of traveling by motorized vehicles. In order to increase the number of trips by NMVs, the highest negative utility (travel time, cost, and bad weather) of the bicycle lanes should be decreased [26]. Renting of the NMVs and making available public bicycle docking stations throughout the city will facilitate bicycle users and increase bicycle usage. Bicycle paths and routes shall be introduced to make traveling more comfortable and safe throughout the city. Private car penalization policy must be introduced which increases the cost of travel by private vehicle to city center and make motorized vehicle trips unattractive. The introduction of congestion pricing in the city center affects the motorized population, except bicycle users. This method has been effective in increasing the number of NMV trips in many cities like Milan, London, and Singapore.

5 Research Gaps

Transportation planners and engineers are trying their best to attain the sustainable transportation system, and NMVs are a crucial part of it. The above discussion highlights that there are many socioeconomic, demographic, built environment, and physical factors that affect NMV usage. Furthermore, there are certain infrastructural and policy provisions (Vehicle Quota System, Bike-on transit, segregated NMV lane, etc.) that can encourage NMV usage and decrease MV usage. Along with this, there are certain factors that are latent, e.g., habit, user perception regarding NMV, etc., influence NMVs. Such latent factors need to be identified for developing countries, and suitable policies should be developed accordingly which can increase the share of NMVs. In addition to this, many studies reported user perception as a highly important factor. The analysis of user's perception regarding NMV usage needs to be done across various user profiles such as age, gender, income, occupation, and education level. Lastly, in Indian context, the compatibility of roadways for bicycle use under heterogeneous traffic condition is less studied. This needs to be explored more.

6 Conclusions

There is a need to study NMTs, especially in developing countries because the resources are scarce. If the developing countries continue to consume resources at its present pace, then the future generation will face the bad consequences. There is a lack of data related to NMVs traveling on NMV lanes. This also creates problem in knowing whether we are designing facilities correctly or not. There is a need to find the latent variables that affect NMV usage in developing countries. Cities in many developing countries have as high as 60% share of the NMTs, and in Indian megacities, this share is 30%. Therefore, importance and design needs of NMVs have to be studied. Acceptable cycling distances are dependent on the size of the city. In terms of space and population, these are city-specific and found varying between 5200 and 2724 m. Modal share of NMTs is dependent on the area density and type of development in the city. The demographic characteristics (age, gender, and ethnicity) of users play an important role in the use of non-motorized modes. Their expectation of facilities for NMV trips should be known. It has been found that the persons with better socioeconomic background, higher occupation, and education level were reluctant to use NMVs. It was also found that students, low income group and women were major NMV users. With the increase in residential and job density, land use mix, detour factor, number of intersections per kilometer and diversity and decrease in distance to CBD, the VMT decreases. This leads to an increased share of NMVs and public transport. Moreover, road patterns, facility design, and bicycle lane density also affect NMV share. The environmental factors, like rain, heat, snow, and topographic features like mountains and slopes affect bicycle trips in a negative way. The availability of facilities like cycle tracks, cycle lanes, bicycle-docking stations, bike-on transit system, bicycle-renting system, separate traffic signals, employee commuter subsidies, and proper signal placement are important to increase the modal share of NMTs.

Many guidelines are available in many countries, but they are area-specific. These guidelines cannot be directly applied in any other city or country. The government should also introduce NMV-oriented and vehicle-restrictive policies to increase the modal share of NMTs. At the same time, government should not introduce automobile-oriented policies, as this will lead to an increased share of motorized vehicles on road. The increase in the share of these vehicles would obviously decrease the share of non-motorized vehicles. Therefore, to increase the share of NMVs, it is important to clearly identify the factors which may influence the use of NMVs in local settings and then to pick the policies and possible design changes which may be needed to motivate the road users to use NMVs.

References

1. Hook W (2003) Preserving and expanding the role of non-motorized transport, sustainable transport: a sourcebook for policy makers in developing cities, module 3d. Transport and Mobility Group, GTZ, Eschborn, Germany
2. Rastogi R (2011) Promotion of non-motorized modes as a sustainable transportation option: Policy and Planning issues. *Curr Sci* 100(9):1340–1348
3. Pai M (2009) Integrated transport indicators in India. Embarq, Washington DC
4. Gwilliam KM (2002) Cities on the move: a World Bank urban transport strategy review. The World Bank, Washington D.C
5. Tiwari G, Jain H (2008) Bicycles in urban India in position papers on bicycling in Asia. Interface for cycling expertise, pp 3–20
6. Tiwari G (2011) Key mobility challenges in Indian cities. Discussion paper, international transport forum. Leipzig, Germany
7. Khadaiya P (2014) Flow characteristics of non-motorized traffic, Masters' thesis. Department of Civil Engineering, IIT Roorkee, India
8. Bhargav R (2009) Bicycle movements in a class-I city, Masters' thesis. Department of Civil Engineering, IIT Roorkee, India
9. Guitink P, Holste S, Lepo J (1994) Non-motorized transport: confronting poverty through affordable mobility. Transport No. UT-4
10. Servaas M (2000) The significance of Non-motorized transport for developing countries, strategies for policy development. The World Bank, Washington DC
11. Rietveld P (2001) Biking and walking: the position of non-motorized transport modes in transport systems. Tinbergen Institute Discussion Paper, Amsterdam, The Netherlands
12. Rastogi R (2010) Willingness to shift to walking and bicycling to access suburban rail: case study of Mumbai India. *J Urban Plann Dev* 136(1):3–10. [https://doi.org/10.1061/\(asce\)0733-9488\(2010\)136:1\(3\)](https://doi.org/10.1061/(asce)0733-9488(2010)136:1(3))
13. Bamney A, Rastogi R (2016) Willingness to use non-motorized vehicle for trips in urban areas. Transportation planning and implementation methodologies for developing countries, Indian Institute of Technology Bombay, India
14. Joewono TB, Kubota H (2005) The characteristics of paratransit and non-motorized transport in Bandung, Indonesia. *J Eastern Asia Soc Transp Stud* 6:262–277. <https://doi.org/10.11175/easts.6.262>
15. Deb S (2014) National transport report moving India to 2032. Delhi, India
16. Hong J, Qing Shen Q, Zhang L (2014) How do built-environment factors affect travel behavior? a spatial analysis at different geographic scales. *Transportation* 41(3):419–440. <https://doi.org/10.1007/s11116-013-9462-9>
17. Dieleman FM, Dijst M, Burghout G (2002) Urban form and travel behaviour: micro-level household attributes and residential context. *Urban Stud* 39(3):507–527. <https://doi.org/10.1080/00420980220112801>
18. Bhat CR, Guo JY, Sardesai R (2005) A report on non-motorized travel in San Francisco Bay Area. Department of Civil Engineering, The University of Texas at Austin, USA
19. Zhang L, Hong J, Nasri A, Shen Q (2012) How built environment affects travel behavior: A comparative analysis of the connections between land use and vehicle miles traveled in US cities. *J Transp Land Use* 5(3):40–52. <https://doi.org/10.5198/jtlu.v5i3.266>
20. Polk M (2003) Are women potentially more accommodating than men to a sustainable transportation system in Sweden? *Transp Res Part D: Transp Environ* 8(2):75–95. [https://doi.org/10.1016/s1361-9209\(02\)00034-2](https://doi.org/10.1016/s1361-9209(02)00034-2)
21. Polk M (2004) The influence of gender on daily car use and on willingness to reduce car use in Sweden. *J Transp Geography* 12(3):185–195. <https://doi.org/10.1016/j.trf.2006.09.004>
22. Cervero R, Kockelman K (1997) Travel demand and the 3Ds: density, diversity, and design. *Transp Res Part D* 2(3):199–219. [https://doi.org/10.1016/s1361-9209\(97\)00009-6](https://doi.org/10.1016/s1361-9209(97)00009-6)
23. Ewing R, Cervero R (2001) Travel and the built environment: a synthesis. *Transp Res Rec* 1780:87–114. <https://doi.org/10.3141/1780-10>

24. Zhang M (2004) The role of land use in travel mode choice—evidence from Boston and Hong Kong. *J Am Plann Assoc* 70(3):344–360. <https://doi.org/10.1080/01944360408976383>
25. Ewing R, Cervero R (2010) Travel and the built environment: a meta-analysis. *J Am Plann Assoc* 76(3):265–294. <https://doi.org/10.1080/01944361003766766>
26. Olio DL, Ibeas A, Bordagaray M, Ortuzar JD (2014) Modeling the effects of pro bicycle infrastructure and policies toward sustainable urban mobility. *J Urban Plann Dev* 140(2):04014001. 1. [https://doi.org/10.1061/\(asce\)up.1943-5444.0000190](https://doi.org/10.1061/(asce)up.1943-5444.0000190)
27. Ewing R, Deanna M, Li S (1996) Land use impacts on trip generation rates. *Transp Res Rec* 1518:1–6. <https://doi.org/10.3141/1518-01>
28. Kuzmyak R, Baber C, Savory D (2006) Use of a walk opportunities index to quantify local accessibility. *Transp Res Rec* 1977:145–153. <https://doi.org/10.3141/1518-01>
29. Pushkar A O, Hollingworth BJ, Miller EJ (2000) A multivariate regression model for estimating greenhouse gas emissions from alternative neighborhood designs. In: 79th annual meeting of the Transportation Research Board, Washington DC
30. Dill J (2004) Measuring network connectivity for walking and biking. In: 83rd annual meeting of the Transportation Research Board, Washington DC
31. Kulash W, Anglin J, Marks D (1990) Traditional neighborhood development: will the traffic work? In: 11th annual pedestrian conference, Bellevue WA
32. Handy S, Mokhtarian P (2005) Which comes first: the neighborhood or the walking access. *Access Magazine* 1(26)
33. Fan Y (2007) The built environment, activity space, and time allocation: an activity-based framework for modeling the land use and travel connection. Doctoral dissertation, Department of Civil Engineering, University of North Carolina
34. Bhat CR, Eluru N (2009) A Copula-based approach to accommodate residential self-selection effects in travel behavior modeling. *Transp Res Part B* 43(7):749–765. <https://doi.org/10.1016/j.trb.2009.02.001>
35. Bhat CR, Sen S, Eluru N (2009) The impact of demographics, built environment attributes, vehicle characteristics, and gasoline prices on household vehicle holdings and use. *Transp Res Part B* 43(1):1–18. <https://doi.org/10.1016/j.trb.2008.06.009>
36. Beura SK, Chellapilla H, Bhuyan PK (2017) Urban road segment level of service based on bicycle users' perception under mixed traffic conditions. *J Mod Transp* 25(2):90–105. <https://doi.org/10.1007/s40534-017-0127-9>
37. Verma M, Rahul TM, Reddy PV, Verma A (2016) The factors influencing bicycling in the Bangalore city. *Transp Res Part A: Policy Pract* 89:29–40. <https://doi.org/10.1016/j.tra.2016.04.006>
38. Beura SK, Kumar NK, Bhuyan PK (2017) Level of service for bicycle through movement at signalized intersections operating under heterogeneous traffic flow conditions. *Transp Dev Econ*. 3(21). <https://doi.org/10.1007/s40890-017-0051-z>
39. Muñoz B, Monzon A, López E (2016) Transition to a cyclable city: latent variables affecting bicycle commuting. *Transp Res Part A: Policy Pract* 84:4–17. <https://doi.org/10.1016/j.tra.2015.10.006>
40. Majumdar BB, Mitra S (2015) Identification of factors influencing bicycling in small sized cities: a case study of Kharagpur, India. *Case Stud Transp Policy* 3(3):331–346. <https://doi.org/10.1016/j.cstp.2014.09.002>
41. Litman T (2010) Quantifying the benefits of nonmotorised transportation for achieving mobility management objectives. Victoria Transport Policy Institute, Victoria, Canada
42. Victoria Transport Policy Institute. <http://www.vtpi.org/tm/tm25.htm>
43. Vaca E, Kuzmyak JR (2005) Traveler response to transportation system changes. Chapter 13- Parking pricing and fees. Transit Cooperative Research Program, USA
44. Han SS (2010) Managing motorization in sustainable transport planning: the Singapore experience. *J Transp Geogr* 18(2):314–321. <https://doi.org/10.1016/j.jtrangeo.2009.06.010>
45. Noel E (1988) Park-and-ride: alive, well and expanding in the United States. *J Urban Plann Dev* 114(1):2–13. [https://doi.org/10.1061/\(asce\)0733-9488\(1988\)114:1\(2\)](https://doi.org/10.1061/(asce)0733-9488(1988)114:1(2))

46. Parkhurst G (2001) Can car-bus interchange policies make a contribution to sustainability? In: Proceedings of 13th annual TRICS conference, London, UK
47. Yazid MM, Ismail R, Atiq R (2011) The use of Non-motorized for sustainable transportation in Malaysia. Proc Eng 20:125–134. <https://doi.org/10.1016/j.proeng.2011.11.147>

GIS Based Road Connectivity Evaluation Using Graph Theory



Cynthia Baby Daniel, S. Saravanan and Samson Mathew

Abstract The topological structure of road network is a significant factor that shapes the city. Evaluation of the road network is therefore an important aspect of urban transportation planning. Connectivity refers to the density of connections within a transport network. Increased connectivity tends to increased accessibility and mobility of the road network. Recent advancement in geographic information system (GIS) has enhanced the understanding of the topographical properties of road networks. The aim of this paper is to analyse the connectivity of the road network of 36 wards of Thiruvananthapuram district of Kerala based on graph theory. Connectivity indices are computed using the Network Analyst extension of ArcGIS. The different parameters include cyclomatic number, alpha index, beta index, gamma index, eta index, network density, intersection density, completeness, etc. Statistical analysis is carried out to find the relationship that exists between these parameters. The road pattern was also identified based on these indices. The variations of the network parameters at two spatial levels were also determined. The study aims to evaluate the effectiveness of the road network in terms of connectivity and coverage that in turn highlights its accessibility. Accessibility of the wards via road network was computed using Shimbel index.

Keywords Road connectivity · Graph theory · GIS · Accessibility · Shimbel index

C. B. Daniel (✉) · S. Saravanan · S. Mathew
Department of Civil Engineering, National Institute of Technology Tiruchirappalli,
Tiruchirappalli, India
e-mail: cynthiababydaniel@gmail.com

S. Saravanan
e-mail: ssaravanan@nitt.edu

S. Mathew
e-mail: sams@nitt.edu

1 Introduction

Transportation networks in its simplest form can be represented as a topological map or graph to understand the characteristics more easily. The connectivity of a network may be defined as the degree of completeness of the links between nodes. Kanksy [1] studied the structure of transportation networks and developed various descriptive indices such as alpha, beta, gamma, indices and cyclomatic number for measuring the connectivity of networks. Network length, intersection density and network density are parameters which quantify the coverage of the road network [2]. Alpha, beta and gamma indices can be used to evaluate the circularity of the road network [3]. The importance of geographic information system (GIS) in the field of town planning was explored by computing the connectivity levels of road network in Aurangabad City [4]. Road connectivity evaluation based on graph theory indices was done to find the spatial variation of road network development in the district of Cooch Behar district of West Bengal and to determine the spatial imbalance in the area [5]. Graph theory provides a basis for the identification of the network pattern [6, 7]. Shimmel index reflects the relative accessibility of nodes, and it can be used to determine the centrality of settlements and other points of interest [8, 9]. The relationship between connectivity and tourist patronage was assessed, and also, the road accessibility of hotels was determined using Shimmel index for Kongi district [10]. Most of the past studies concentrate just on the determination of connectivity, and the spatial variation at different levels is not explored. The boundary roads play a role in this variation.

The aim of this paper is to analyse the connectivity and coverage of the road network based on graph theory using GIS. The study also aims at computing the centrality of the wards. The pattern of the road network is also analysed from the measures computed. The road network of 36 wards of Thiruvananthapuram Corporation is selected for the study. Thiruvananthapuram is the capital and the largest city of the Indian state of Kerala. It is the most populated city in Kerala.

2 Network Parameters

A graph is a symbolic representation of a network and its connectivity. A directed graph $G = (N, A)$ consists of a set N of nodes or vertices and a set A of arcs or edges whose elements are ordered pairs of distinct nodes [11]. A road network can be considered as a directed graph where vertices (v) correspond to the junctions or street intersections and the edges (e) as road segments between them. The different network parameters [12] are discussed below:

Cyclomatic number (μ) is the number of additional edges required to form a closed path or circuit.

$$\mu = e - v + 1 \quad (1)$$

Alpha index (α) or meshedness coefficient is a measure of connectivity which evaluates the number of cycles in comparison with the maximum number of cycles. The higher the alpha index, the more a network is connected. Trees and simple networks will have alpha value of 0.

$$\alpha = \frac{e - v + 1}{2v - 5} \quad (2)$$

Beta index (β) measures the level of connectivity in a graph and is expressed by the relationship between the number of links over the number of nodes. Trees and simple networks have beta value of less than one.

$$\beta = \frac{e}{v} \quad (3)$$

Gamma index (γ) is a measure of connectivity that considers the relationship between the number of observed links and the number of possible links. The value of gamma is between 0 and 1 where a value of 1 indicates a completely connected network and would be extremely unlikely in reality.

$$\gamma = \frac{e}{3(v - 2)} \quad (4)$$

Eta index (η) is the average length (L) of network per link.

$$\eta = \frac{L}{e} \quad (5)$$

Grid tree pattern (GTP) is a measure for identifying the pattern of the network, varying from 0 in case of tree pattern to 1 in case of grid pattern [13].

$$\text{GTP} = \frac{e - v + 1}{(\sqrt{v} - 1)^2} \quad (6)$$

Network density is the total length of the network per area of each zone. It is expressed in km/sq km. Intersection density is the number of junctions per area of each zone expressed in junctions/sq km. The total length of the network, the network density and the intersection density are indicators of coverage of the network.

Network density differs from the completeness measure in that it provides a measure of the size of the actual network in comparison to the size of the urban area. Completeness (ρ) does not account for the urban area size and looks at the connectivity of the network using basic principles of graph theory. The network density can be considered to be a measure of the network intensity, while the completeness is a measure of the efficiency in network connectivity. It can be expressed in percentage. A network is said to be 100% complete if all nodes in a network are directly linked to all other nodes [14].

$$\rho = \frac{e}{v^2 - v} \quad (7)$$

The road pattern that exists in the area can also be analysed using the relationship existing between nodes and links.

Shimbel index (S_i) in its basic form indicates the number of arcs needed to connect any node with all the other nodes in the network by the shortest path [15]. The Shimbel distance matrix holds the shortest paths between the nodes of the network. The summation of rows or columns represents the Shimbel distance for each node. A smaller value indicates that the node is more accessible. Simple Shimbel index takes into account the number of edges only and not the distance between them. By giving weights to edges, i.e. considering the road length and modifying the equation such that the node with greater value corresponds to the one with greater centrality/accessibility, the Shimbel index can be calculated as follows:

$$S_i = \frac{\sum \sum d_{ij}}{\sum d_{ij}} \quad (8)$$

where S_i is the Shimbel index for node i , and d_{ij} is the distance between nodes i and j . It is a dimensionless quantity.

3 Methodology

Road network of the study area is obtained from National Transportation Planning and Research Centre (NATPAC), Thiruvananthapuram. Road network of each of the ward is extracted by overlaying the ward boundary over the road network. The road network is projected to Universal Transverse Mercator (UTM) coordinate system so as to compute the length of road segments. The network is made free from all the topological errors. The road network created as shapefile is first converted into network data set so as to be used in Network Analyst. The road network has to be topologically correct so as to convert it into a network data set. Network data sets are created from source features, which can include simple features (lines and points) and turns, and store the connectivity of the source features. The count of nodes and edges is obtained from the network data set in order to compute the above-

mentioned indices. Connectivity indices are computed using the Network Analyst extension of ArcGIS. The different parameters include cyclomatic number, alpha index, beta index, gamma index, eta index, network density, intersection density, GTP, completeness, etc. These indices give us an overview of the connectivity and coverage of the road network of the area.

In order to find the Shimbel index, a 36×36 matrix was constructed with the centroids of 36 wards representing the origins and destinations. The distance of each ward to every other ward was computed and tabulated to form the matrix.

Population densities of the wards were calculated from Census of India 2011 as the ratio of population to the area of the zone considered.

4 Analysis and Results

The population density map and the network density of the study area were prepared using ArcGIS 10.2. as shown in Figs. 1 and 2, respectively. It clearly shows that the wards with greater population density have greater network density.

The descriptive statistics of the connectivity indices were computed using SPSS 16 as shown in Table 1. Network pattern classification based on gamma index established by [16] reveals that the network analysed in this study has a spinal pattern. The GTP value also ranges from 0.02 to 0.49 which reveals a tree or spinal pattern of the network. Alpha index also confirms the same.

The descriptive statistics of the coverage indices computed using SPSS 16 as shown in Table 2. Network density was greatest for Vazhuthacaud and Thycaud. Njandoorkonam had the least value of network density. Thycaud had the greatest intersection density while it was least for Njandoorkonam.

The correlation matrix of the connectivity indices was computed using SPSS 16 in order to find out the association between the connectivity indices and network density as shown in Table 3. The correlation was computed 0.05 level of significance.

Eta index showed a negative correlation with network density with a Pearson correlation coefficient of 0.83. GTP had a correlation coefficient of 0.98 with alpha index and 1 with gamma index and 0.87 with beta index. Alpha index and gamma index showed a correlation coefficient of 0.99 when tested for 0.05 level of significance. Alpha, beta and gamma indices show high degree of correlation almost near to 1 implying that either of the parameters can be used as an indicator of connectivity. Regression model developed based on the correlated parameters is as below:

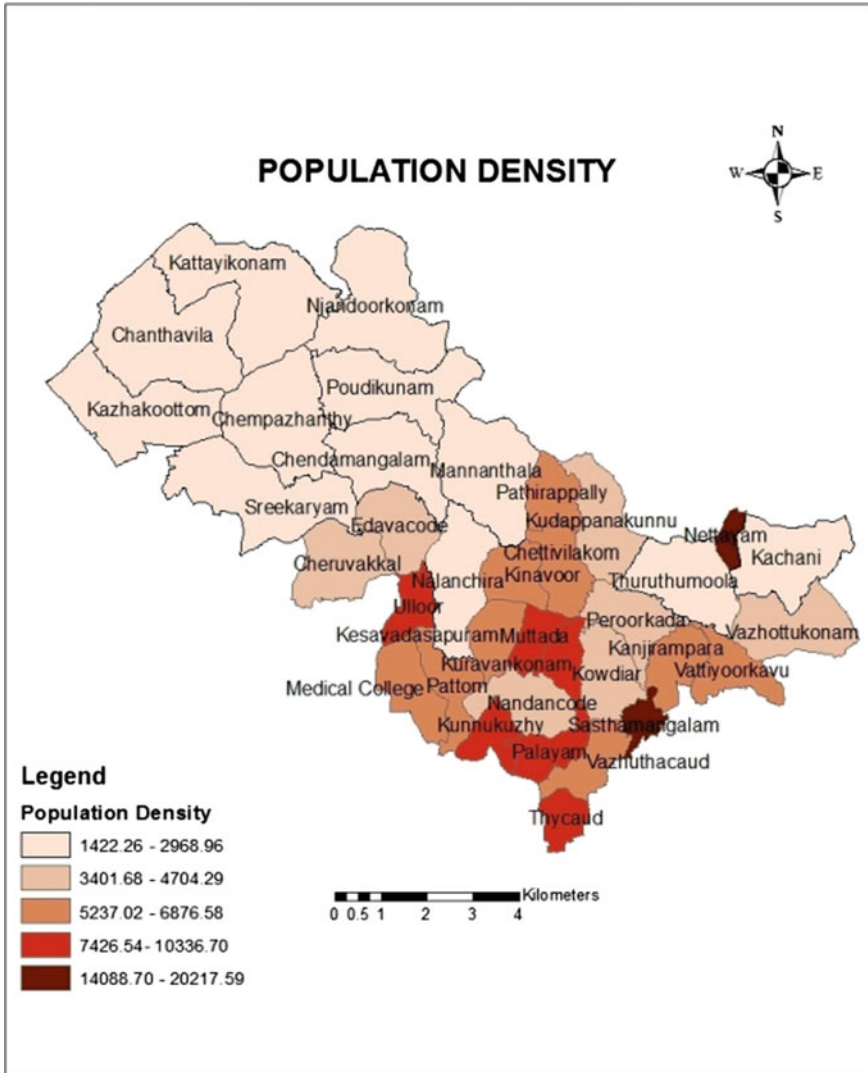


Fig. 1 Population density

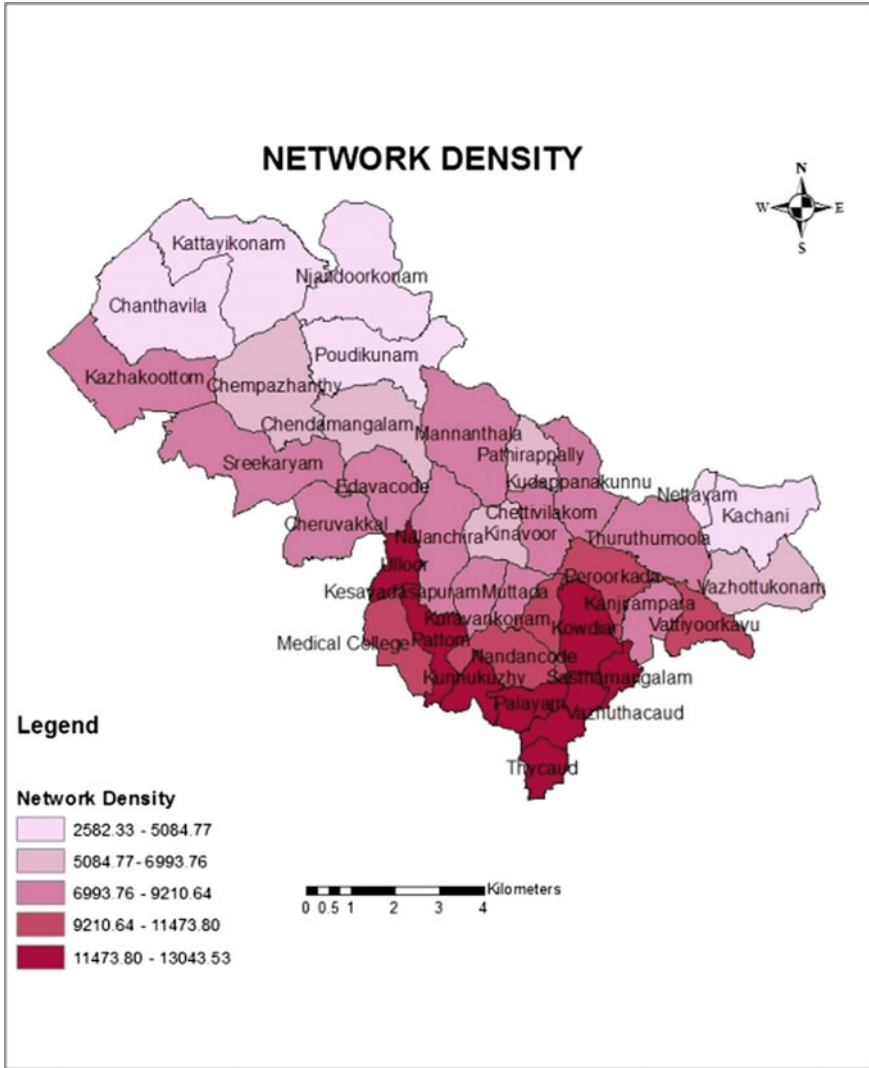


Fig. 2 Network density

Table 1 Descriptive statistics of connectivity indices

	Minimum	Maximum	Mean	Std. deviation
Alpha index	0.01	0.16	0.05	0.04
Beta index	1.01	1.31	1.08	0.06
Gamma index	0.34	0.47	0.37	0.03
Eta index	0.10	0.43	0.17	0.07
Grid tree pattern	0.02	0.49	0.12	0.10
Completeness	0.00	0.11	0.01	0.02

Table 2 Descriptive statistics of coverage indices

	Minimum	Maximum	Mean	Standard deviation
Network density	2.58	13.04	8.69	2.83
Intersection density	5.65	110.34	56.02	29.07

$$\text{Network density} = 14.419 - 33.238 \eta \text{ with } R^2 = 0.7$$

$$\text{GTP} = 2.623 + 7.535 \alpha - 1.536 \beta - 3.270 \gamma \text{ with } R^2 = 1$$

This reaffirms the fact that the structure of the road network is dependent on alpha, beta and gamma index. Figure 3 shows the comparison of the parameters in two scales, i.e. when the road network of the 36 wards was considered together and when each ward was considered separately. Alpha, beta, gamma indices developed by [1] do not consider the weight and quality of the network; i.e., it does not differentiate between a one-way and two-way. However, these parameters can be used to compare the networks at different scales and at different phases of development to give an insight into the improvement in road infrastructure over a period of time [17].

Table 3 Correlation matrix of indices

	Alpha index	Beta index	Gamma index	Eta index	Grid tree pattern	Completeness	Network density
Alpha index	Pearson correlation	0.95	0.99	-0.21	0.98	0.50	0.19
	Sig. (2-tailed)						
Beta index	Pearson correlation	0.95	0.88	-0.32	0.87	0.19	0.35
	Sig. (2-tailed)						
Gamma index	Pearson correlation	0.00	1.00	-0.14	1.00	0.63	0.09
	Sig. (2-tailed)						
Eta index	Pearson correlation	0.00	-0.14	0.41	0.00	0.00	0.58
	Sig. (2-tailed)						-0.83
Grid tree pattern	Pearson correlation	0.21	0.41	1.00	0.37	0.14	0.00
	Sig. (2-tailed)						
Completeness	Pearson correlation	0.98	1.00	-0.15	1.00	0.65	0.09
	Sig. (2-tailed)						
Network density	Pearson correlation	0.00	0.63	0.25	0.65	1.00	-0.39
	Sig. (2-tailed)						
	Pearson correlation	0.00	0.09	-0.83	0.09	-0.39	1.00
	Sig. (2-tailed)						
		0.28	0.58	0.00	0.59	0.02	

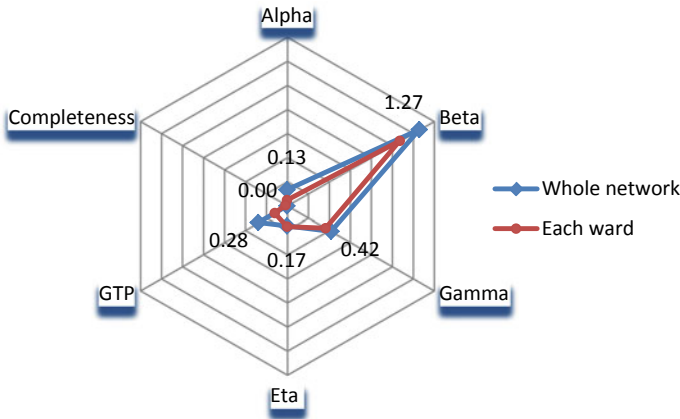


Fig. 3 Radar diagram showing the variation of connectivity indices at different scales

When the road networks of the 36 wards considered together, connectivity was on a higher side than when each of the wards was considered separately. Alpha index had a value of 0.13, beta 1.2, gamma 0.42 and eta 0.17 when the indices were computed considering the study area as a whole. This shows that at a larger scale, the network shows greater connectivity. This can be by virtue of the “edge effect” of the boundary roads of each zone.

Table 4 shows the sample distance matrix created for the 36 wards. The Shimbel index calculated as per Eq. (8) is also shown. The distances are expressed in kilometres.

Map shown in Fig. 4 gives the variation of Shimbel index in the 36 wards.

Table 4 Sample distance matrix for the calculation of Shimbel index

Ward no	Ward name	Kazhakkootam	Chanthavila	Kattaikonam	Sreekaryam	Cheruvakkal	Ulloor	Edavacode	Chendamangalam	Chempazhanthy	Powdikonam	Vattiyoor kavu	Shimbel index
1	Kazhakkootam	0.0	2.6	4.7	5.8	8.1	9.4	8.4	7.6	4.3	6.9	18.1	22.0
2	Chanthavila	2.6	0.0	2.3	6.1	8.4	9.7	8.6	7.6	4.3	6.5	18.2	21.9
3	Kattaikonam	4.7	2.3	0.0	6.1	8.0	9.3	8.2	6.7	3.7	5.6	17.5	22.9
4	Sreekaryam	5.8	6.1	6.1	0.0	3.4	4.7	3.6	4.5	3.6	5.9	13.3	31.2
5	Cheruvakkal	8.1	8.4	8.0	3.4	0.0	2.5	2.0	3.3	4.7	4.7	11.3	37.7
6	Ulloor	9.4	9.7	9.3	4.7	2.5	0.0	2.3	4.1	6.1	5.6	9.2	45.6
7	Edavacode	8.4	8.6	8.2	3.6	2.0	2.3	0.0	2.7	5.0	4.2	10.5	40.3
8	Chendamangalam	7.6	7.6	6.7	4.5	3.3	4.1	2.7	0.0	3.6	1.9	11.6	38.0
9	Chempazhanthy	4.3	4.3	3.7	3.6	4.7	6.1	5.0	3.6	0.0	3.4	14.2	30.1
10	Powdikonam	6.9	6.5	5.6	5.9	4.7	5.6	4.2	1.9	3.4	0.0	12.3	34.1
...
36	Vattiyoor kavu	18.1	18.2	17.5	13.3	11.3	9.2	10.5	11.6	14.2	12.3	0.0	33.2

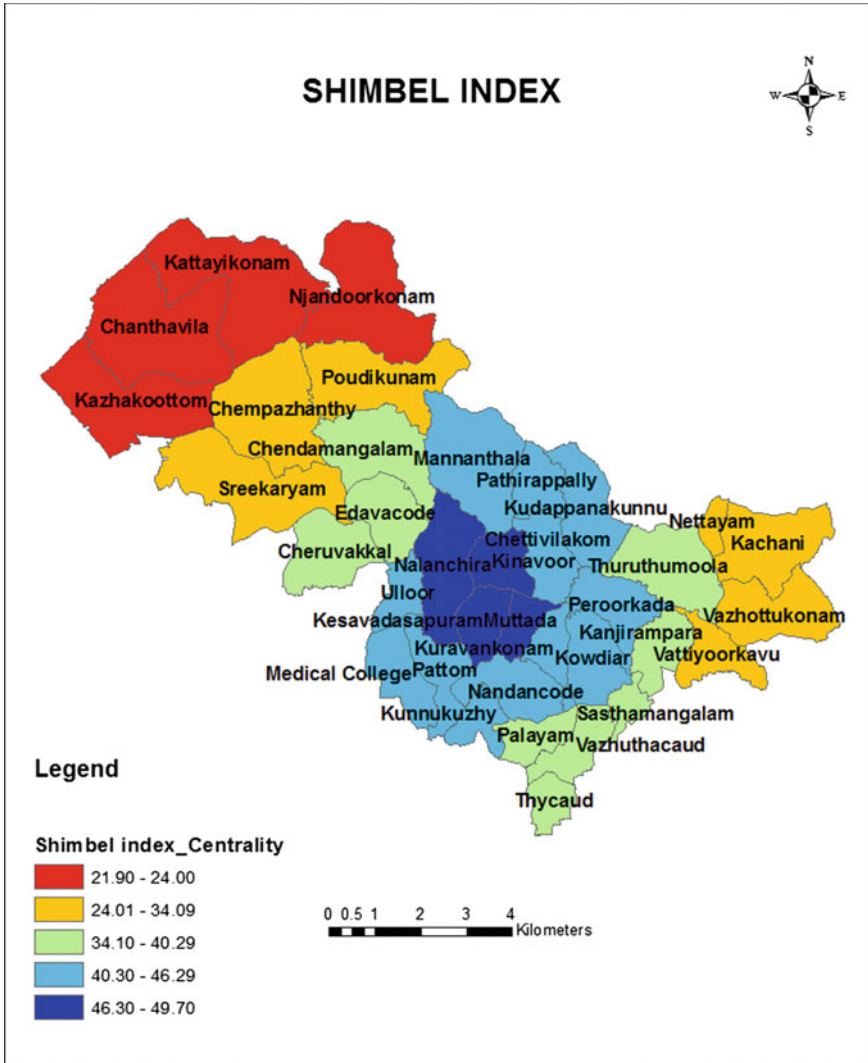


Fig. 4 Shimbel index

The wards with greater value of Shimbel index are expected to have better accessibility. From the analysis, it was found that Muttada, Kesavadasapuram, Nalanchira and Kinavoor wards had greater accessibility/centrality.

5 Conclusion

Road networks play an important role in the economic growth of a country. This study aims to evaluate the effectiveness of the road network in terms of connectivity and coverage which in turn highlights its accessibility. The quantitative assessment of connectivity of road network provides a better understanding of the road structure and helps the urban planners to propose new routes to enhance accessibility and coverage. GIS proves to be an efficient tool for analysing the structure of the road network. Graph theory provides a basis for identifying the spatial pattern of the road network in a primary level, thus proving to be a good method for pattern recognition of roads. The road network considered in this study has a spinal structure based on the indices calculated. The graph theory-based parameters overlook the weightage based on the type of road or its hierarchy. The accessibility of each ward via roads was also computed, and the wards with better accessibility/centrality were determined using Shimbel index. One of the limitations of this study is that geometric centres were chosen as the nodes for computing the Shimbel index. Central business districts or nodes with more human activity could lead to better results in terms of travel demand.

References

1. Kansky KJ (1963) Structure of transportation networks: relationships between network geometry and regional characteristics. University of Chicago Press, Chicago
2. Sreelekha MG, Krishnamurthy K, Anjaneyulu MVL (2014) Assessment of topological pattern of urban road transport system of Calicut city. *Transp Res Proc* 17:253–262
3. Liu Z, Zhao S (2015) Characteristics of road network forms in historic districts of Japan. *Front Archit Res* 4:296–307
4. Nagne AD, Vibhute AD, Gawali BW, Mehrotra SC (2013) Spatial analysis of transportation network for town planning of Aurangabad city by using geographic information system. *Int J Sci Eng Res* 4:2588–2594
5. Sarkar D (2013) Structural analysis of existing road networks of Cooch Behar district, West Bengal, India: a transport geographical appraisal. *Ethiopian J Environ Stud Manage* 6(1):74–81
6. Xie F, Levinson D (2007) Measuring the structure of road networks. *Geog Anal* 39:336–356
7. Quium ASMA, Hoque SAMA (2002) The completeness and vulnerability of road network in Bangladesh. *Eng Concerns Flood* 59–76
8. Istrate MI (2015) Assessment of settlements' centrality in Botoşani county using Shimbel index. *J Community Positive Pract* 15(3):57–69
9. Modinpuroju A, Prasad CSRK (2016) Planning and evaluation of rural road network connectivity using GIS. *Geo-China*, pp. 83–90
10. Olawale TN, Adesina KI (2013) An assessment of the relationship between road network connectivity and tourists' patronage in Lokoja Metropolis, Kogi State. *J Nat Sci Res* 3(9):1–11
11. Ahuja RK, Magnanti TL, Orlin JB (1993) Network flows: theory, algorithms and applications. Prentice Hall, New Jersey
12. The geography of transport system. <https://people.hofstra.edu/geotrans/eng/methods/ch1m3en.html>
13. Sreelekha MG, Krishnamurthy K, Anjaneyulu MVL (2016) Interaction between road network connectivity and spatial pattern. *Procedia Technol* 24:131–139
14. Parthasarathi P (2014) Network structure and metropolitan mobility. *J Transp Landuse* 7(2):153–170

15. Oni AO, Akindele DB, Akinjare O (2014) Graph-theoretic approach to resolving the accessibility and site selection issues in planning and development. *Mediterr J Soc Sci* 5(8):11–20
16. Taaffe EJ, Gauthier HL (1973) *Geography of transportation*. Prentice Hall, New Jersey, USA
17. Cesar D, Lugo I (2013) Structure and dynamics of transportation networks: models, methods and applications. In: *The Sage handbook of transport studies*. Sage, pp 347–364

Transportation Modes, Planning and Demand Forecast

Estimating Modal Shift of Home-Based Work Trips Due to the Development of Kochi Metro and Reduction in Fuel Consumption and Emissions



Ardra S. Krishna, Jomy Thomas and P. N. Salini

Abstract Kochi, the commercial hub of Kerala, is already experiencing urban growth pressures. The city is most congested during peak hours, in which home-based work trips and school trips are the main contributors. For the upcoming years, the travel demand is expected to shoot-up. Road-based public transport, cannot meet this demand. So government introduced a light metro system in the city. As this is the first metro rail system in Kerala, attitude of the people towards this new development is ambiguous. This work aims to study the commuter's mode-choice behaviour towards the metro rail System. A questionnaire survey was conducted to collect data on the current mode used by the commuters, travel details and the socio-economic characteristics of commuters, which are the major factors influencing the mode choice. A willingness to shift survey was also included in the questionnaire to know the preference of shift to metro. Stated preference (SP) approach was used in the study to frame different scenarios. Binary logit models are developed to examine the overall probable shifts of work trips from the presently used mode to metro. Separate binary logit models are developed to study the shift from two-wheeler and bus users to metro. From this study, a set of influencing factors, with reliable and predictable data base, to explain the variation in modal shift behaviour has been identified. Overall and mode-wise probable shift from existing mode to metro, possible reduction in the vehicle emission and percentage fuel cost savings have been estimated. Elasticity analyses on travel time and travel cost of metro were also done.

Keywords Stated preference · Revealed preference · Mode shift · Binary choice models · Elasticity analysis

A. S. Krishna (✉) · P. N. Salini
National Transportation Planning and Research Centre, Thiruvananthapuram, Kerala, India
e-mail: krishnardra@gmail.com

P. N. Salini
e-mail: salini.jayaprakash@gmail.com

J. Thomas
Rajiv Gandhi Institute of Technology, Kottayam, Kerala, India
e-mail: jomy@rit.ac.in

1 Introduction

Rapid urbanization and intense commercial developments in the recent past have resulted in steep rise in travel demand, putting Kochi's transport infrastructure to stress. Similar to other fast-developing metropolitan cities, Kochi has proposed metro as a sustainable measure to improve travel structure and to reduce congestion of ground transportation. As this is the first metro rail project in Kerala, the changes in travel characteristics brought by the metro are unpredictable and ambiguous. Moreover, travellers' mode-choice behaviour may differ after the introduction of such a high-speed alternative. Thus, this study attempts to assess the modal shift of work trips from the existing transportation modes to metro. The work mainly focusses on the commuters and their home-based work trips since they are the major contributors of peak hour traffic congestion. The study uses stated preference and revealed preference data which are collected from the commuters using a questionnaire survey conducted at the metro corridor. Using binary logit models, separate utility functions have been developed for the existing mode and metro mode. The probable modal shift of home-based work trips, from the existing mode to metro and mode-wise probable shift have been estimated. An elasticity analysis has also been done for studying the effect of variation of travel time and metro fare on mode share. These findings will be useful and valuable for the policy improvements and decision-making. The possible reduction in the vehicle emission and the percentage fuel cost savings were also estimated.

2 Objectives

The study attempts to analyse the travel characteristics of commuters in the metro corridor and to develop certain binary choice models for the 'existing mode' and 'metro mode'. The major objectives of this study are:

- To develop specific utility equations for the alternatives which are capable of predicting the probable mode share.
- To estimate the overall probable shift of work trips from the existing mode to metro using a binary mode-choice modelling technique.
- To estimate the probable shift of work trips to metro from different mode users using a binary logit mode-choice modelling technique.
- To study the elasticity of attributes like metro fare and travel time in mode choice using scenario analysis.
- To estimate the possible emission reductions and savings in fuel consumption.

3 Methodology

Methodology of the work starts with the selection of the study area. The study areas selected are the corridor between Aluva and Petta (25.6 kms) and the Kochi metro corridor (shown in Fig. 1) [1]. The stretch includes 22 metro stations. By adopting area sampling, 11 stations among the 22 were chosen in an alternative fashion. Respondents were chosen randomly from these areas and interviewed. The survey was conducted at the premises of sample stations to get the details of the socio-economic characteristics of the trip maker, their trip-related characteristics, mode-specific characteristics, etc. A stated preference experiment was also included in the questionnaire to understand their willingness to shift to metro.



Fig. 1 Study area—metro corridor

Table 1 Attributes and attribute levels selected

Attributes	Attributes levels		
	Fare	X	1.5X
Headway (min)	5	7	10
Feeder service	Yes	No	
Parking facility	Yes	No	

The study tries to examine respondents’ preferences towards four attributes. The attribute lists selected are shown in Table 1. Here the attributes fare and headway have three levels, the other two attributes, i.e. feeder service and parking facility, have two levels. With these attributes and attribute levels, 36 scenarios were generated (32×22) after considering all possible combinations among attributes and their levels. This is known as a complete factorial design. It is impractical to use a complete factorial design unless the experiment involves a very small number of attributes or levels; therefore, using fractional factorial experimental design, subsets of sample (scenarios) were selected logically. The attribute ‘feeder service’ was eliminated for the respondents residing or working nearer (up to 200 m) to the metro stations as the feeder service is not mandatory for them and with the rest three attribute scenarios were framed, i.e. $3^2 \times 2^1 = 18$ scenarios. Eliminating all irrelevant ones, the scenarios were cut short to 50 (i.e. $32 + 18 = 50$ scenarios). The entire scenario sets were split into subsets and were included in different questionnaire sheets so that task of facing all scenarios was reduced to 4 or 5 for each individual. Therefore, by interviewing 250 respondents, we get 1045 stated preference responses.

4 Data Collection and Analysis

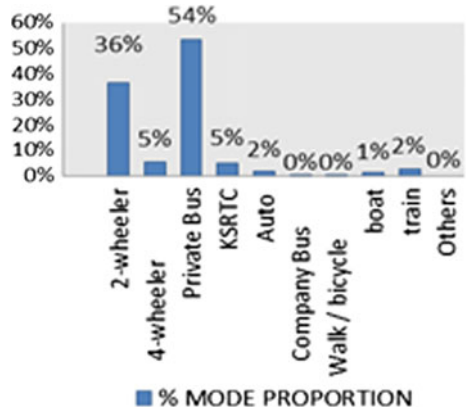
For the field survey, participants were chosen randomly from the selected sample areas, and a questionnaire survey was conducted at their work centres or residences. Of all respondents, 55% were male and the remaining, female. Most of the respondents fell in the age group of 17–30 (Fig. 2).

By analysing the data collected, it was found that on an average, the distance travelled by a commuter for his or her work trip is 13 km. The major mode used by the commuters in metro corridor is the city private bus (Fig. 3). The average travel

Fig. 2 Percentage composition of work trip distance



Fig. 3 Percentage mode share of commuters for work trip



cost spent by the commuters for their work trip (one side travel) is Rs. 24. The major concern the commuters pointed out was about the accessibility to metro. Many of them were willing to shift if feeder services are made available. Other finding from the survey was the people residing or working in the CBD or within certain radius from metro stations are ready to shift their work trips completely to metro, whereas the people coming from the Fort Kochi, Mattancherry, Kakkanad, etc. (faraway places), have last-mile connectivity problems. They have straight buses or boat facilities for their work trips which are more comfortable, convenient and accessible than the metro mode and stated that they are not ready to change their modes.

5 Model Development

As the study is concerned with estimation of the probable shift of commuters from the present mode to proposed metro, the number of possible alternatives is two. Hence, the mode-choice model selected for the study is binary logit model. The choice sets here are the ‘present mode’ and ‘metro’ between which an individual is supposed to choose. Three different binary logit models were developed for different categories of samples.

5.1 Binary Logit Model to Predict the Overall Shift from Present Mode to Metro

The study surveyed 250 individuals; the questionnaire given to each of the respondents contained four or five SP scenarios. This gives a total of 1045 data sets, out of which 75% of observations were used for generating models to predict the overall shift, whereas rest of the data were used for model validation. Travel cost, comfort,

nearness (or distance to access the mode) and feeder service are the independent variables considered for the model formulation. The following utility equations were obtained:

$$\begin{aligned}
 U(\text{PRESENTMODE}) &= -0.58888 - 0.01418 * \text{TC} + 0.25781 * \text{COMFORT} \\
 &\quad - 0.50687 * \text{NEARNESS} + 0.34486 * \text{FEEDER} \\
 U(\text{METRO}) &= -0.01418 * \text{TC} + 0.25781 * \text{COMFORT} \\
 &\quad - 0.50687 * \text{NEARNESS} + 0.34486 * \text{FEEDER}
 \end{aligned}$$

All the abbreviations used for variables in the three models are explained below:

U(PRESENTMODE) = utility value of presently using mode, U(METRO) = utility value of proposed metro mode, TC = travel cost, COMFORT = comfort of the mode, NEARNESS = distance to access the mode, FEEDER = a separate bus service to carry people to nearest metro station is available or not, A_PRESEN = mode-specific constant for ‘present mode’, TT = travel time, HEADWAY = time headway for the modes, PRE_WOR1 = mode-specific parameter work trip distance, PARKING = parking facilities available or not, PRE_AGE1 = mode-specific parameter age of a person and PRE_INC1 = mode-specific parameter household income [2].

By analysing the binary logit model, it is found that the choice of the mode mainly depends on the comfort of travel and nearness to access the mode. The estimate values of these parameters (Table 2) show greater significance at 99 and 95% as indicated by Wald’s statistic. All the coefficients of variable used in the model have logically correct signs.

LL ratio test = 171.5742

Pseudo-R square $\rho^2 = 0.2$

Adjusted pseudo-R square $\rho^2 = 0.1547$

To determine the overall statistical significance of the model, the log-likelihood function of the base model and estimated model was compared. When the calculated $-2LL$ value is compared to χ^2 statistic, the value exceeded the critical chi-square value. Therefore, the null hypothesis that the specified model is no better than the base comparison model was rejected [3]. This calibrated model was used to predict the modal shift, and the value of log-likelihood calculated. With the holdout 25% observations, a separate model was calibrated and the log-likelihood was estimated.

Table 2 Estimated model parameters (Model 1)

Choice	Coefficient	Standard error	Z	P value
TC	-0.01418	0.00690	-2.05	0.0399
COMFORT	0.25781	0.09391	2.75	0.0060
NEARNESS	-0.50687	0.05057	-10.02	0.0000
FEEDER	0.34486	0.13843	2.49	0.0127
A_PRESEN	-0.58888	0.25269	-2.33	0.0198

Table 3 Validation results for the model

Description	Model calibrated with 75% data	Model calibrated with 25% data
Initial log-likelihood	-543.248	-177.353
Final log-likelihood	-457.461	-134.305
Likelihood ratio test	171.542	86.09638
Likelihood ratio index ρ^2	0.16	0.24
Estimated LL (with holdout data)		-134.305
Calculated LL (model applied to holdout data)		-144.094

Next, the model initially calibrated with the 75% data was applied to the holdout sample, and the log-likelihood was calculated. Then, the two values of log-likelihood (estimated LL and calculated LL) were compared to their closeness as shown in Table 3. From Table 3, two log-likelihood values are fairly close to each other, thus proving the validity of the model [4].

5.2 Binary Logit Model to Predict the Shift from the Bus Users to Metro

As per the survey, city private buses are the major carriers of commuters. To know the shift from bus users, a separate binary logit model was developed. The model was formulated with bus users’ data set, i.e. with a total data set of 573 observations, and a binary logit model was calibrated and validated. Out of the different trials, travel time, nearness (or distance to access the mode), feeder service, headway of mode and work trip distance were found to be significant.

$$\begin{aligned}
 U(\text{PRESENTMODE}) &= -2.43592 + 0.03827 * \text{PRE_WOR1} - 0.01477 * \text{TT} \\
 &\quad - 0.69893 * \text{NEARNESS} + 0.90817 * \text{FEEDER} \\
 &\quad - 0.21658 * \text{HEADWAY} \\
 U(\text{METRO}) &= -0.01477 * \text{TT} - 0.69893 * \text{NEARNESS} + 0.90817 \\
 &\quad * \text{FEEDER} - 0.21658 * \text{HEADWAY}
 \end{aligned}$$

The estimate values of all parameters except travel time show greater significance at 99% as indicated by Wald’s statistic and show logically correct relationship. Travel time has lesser significance of 90% but still acceptable and has logically correct sign. Time headway is an important factor for the bus users for their modal choice. People are equally willing to choose both the modes if the time headway is less; it can be seen that the coefficient of headway is negative. As the distance to bus stop or metro

Table 4 Estimated model parameters (Model 2)

Choice	Coefficient	Standard error	Z	P value
TT	-0.01477	0.00790	-1.87	0.0615
NEARNESS/DIST	-0.69893	0.08037	-8.70	0.0000
FEEDER	0.90817	0.25484	3.56	0.0004
HEADWAY	-0.21658	0.05628	-3.85	0.0001
A_PRESEN	-2.43592	0.48101	-5.06	0.0000
PRE_WOR1	0.03827	0.01413	2.71	0.0068

Table 5 Validation results for the model

Description	Model calibrated with 75% data	Model calibrated with 25% data
Initial log-likelihood	-293.568	-95.2651
Final log-likelihood	-229.334	-73.7223
Likelihood ratio test	128.46756	43.08556
Likelihood ratio index ρ^2	0.219	0.226
Estimated LL		-73.7223
Calculated LL		-75.9646

station is less, the more chance to select the mode. People are positive towards feeder service facility, as the coefficient for the same is positive (Table 4).

Pseudo-R square $\rho^2 = 0.2$

Adjusted pseudo-R square $\rho^2 = 0.215048$

The likelihood ratio test gave a value 293.568 which when compared with the table of χ^2 value for five degrees of freedom at $\alpha = 0.05$ was decently greater. The pseudo-R2 statistic associated with choice models is estimated and found to be acceptable. Calibrated model was used to predict the modal shift, and the value of log-likelihood was calculated. The validation procedure adopted for the three models was the same. The two values of log-likelihood were compared to their closeness as shown in Table 5. From Table 5, two log-likelihood values are fairly close to each other, thus proving the validity of the model.

5.3 Binary Logit Model to Predict the Shift from the Two-Wheeler Users to Metro

Among the sample, the second commonly used mode among the commuters in the study area is the two-wheelers. The mode-choice decision of two-wheeler users is very crucial in a city; it can bring a noticeable change in the trend of transport scenario of Kochi. Out of the 360 data sets obtained from the two-wheeler users, 75% were used for calibration and 25% for validation. Travel time, comfort, nearness, parking

and work trip distance were found as the influencing factors in modal selection. The following utility equations were defined in NLOGIT:

$$\begin{aligned}
 U(\text{PRESENTMODE}) &= 0.22688 - 0.12873 * \text{PRE_WOR1} - 0.08784 * \text{TT} \\
 &\quad - 0.92352 * \text{NEARNESS} + 1.61697 * \text{PARKING} \\
 &\quad + 0.63268 * \text{COMFORT} \\
 U(\text{METRO}) &= -0.08784 * \text{TT} - 0.92352 * \text{NEARNESS} \\
 &\quad + 1.61697 * \text{PARKING} + 0.63268 * \text{COMFORT}
 \end{aligned}$$

Pseudo-R square $\rho^2 = 0.3$

Adjusted pseudo-R square $\rho^2 = 0.342919$

All the coefficients of variable have logically correct signs and show 99% significance. Two-wheeler users face the problem of climate and bad weather more badly; this may be the reason of the greater significance in comfort for travel. If metro stations are nearer to home or workplaces, then chances of selecting the metro mode are more. Travel time is another important factor. For two-wheeler users, a variable on parking facilities gains more weightage. The mode-specific attribute work trip distance has greater significance (Table 6).

Calibrated model was used to predict the modal shift, and the value of log-likelihood was calculated. The model was validated, and the two values of log-likelihood were compared to their closeness. From Table 7, two log-likelihood values are fairly close to each other, thus proving the validity of the model.

Table 6 Estimated model parameters (Model 3)

Choice	Coefficient	Standard error	Z	P value
TT	-0.08784	0.02127	-4.13	0.0000
NEARNESS/DIST	-0.92352	0.12837	-7.19	0.0000
PARKING	1.61697	0.36104	4.48	0.0000
COMFORT	0.63268	0.17739	3.57	0.0004
A_PRESEN	0.22688	0.60430	0.38	0.7073
PRE_WOR1	-0.12873	0.02966	-4.34	0.0000

Table 7 Validation results for the model

Description	Model calibrated with 75% data	Model calibrated with 25% data
Initial log-likelihood	-179.4919	-53.1758
Final log-likelihood	-117.3764	-42.87259
Likelihood ratio test	124.23104	20.60642
Likelihood ratio index ρ^2	0.35	0.19
Estimated LL		-42.87259
Calculated LL		-48.13320

5.4 Elasticity and Scenario Analysis

Elasticity analysis is useful for studying the effect of variation of attributes on mode share. On the basis of changing the attributes fare and travel time, elasticity analysis is done [5].

Figures 4 and 5 show the elasticity effects of metro fare on the two alternative modes. The different scenarios tried were

1. For the responses against metro fare = X,
2. Metro fare = 1.5X,
3. Metro fare = 2X, where X = the present travel cost.

The elasticity has been checked by keeping all other parameters remain the same, and the metro fare has been changed from X to 1.5 times X and again for 2 times X. The probability of metro being selected as the daily work trip mode decreased as the fare increased, and the variation is depicted in the graph shown (Fig. 4). There is a variation of 6 and 5% probability when the fare changed to 1.5X and 2X, respectively. The cross-elastic effect of metro fare on present mode caused an increase in the probability of mode choice. The probability of modal selection showed an increase from 58 to 64% and then to 69% at X, 1.5X and 2X fare scenarios, respectively, i.e. an increase of 6 and 5%, respectively (Fig. 5).

An attempt was done to check the travel time elasticity among the bus users. Figures 6 and 7 show the elasticity effects of travel time reduction of metro on

Fig. 4 Direct elastic effect of metro fare on metro mode share

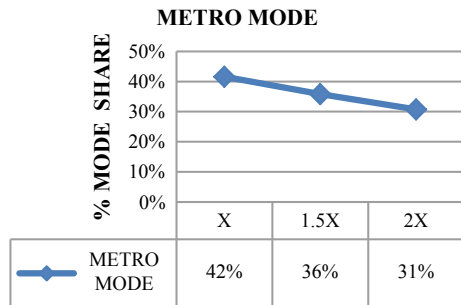


Fig. 5 Cross-elastic effect of metro fare on present mode share

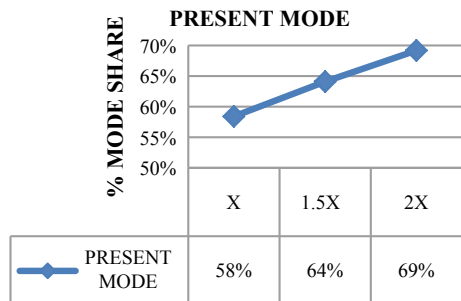


Fig. 6 Direct elastic effect of travel time on metro mode share

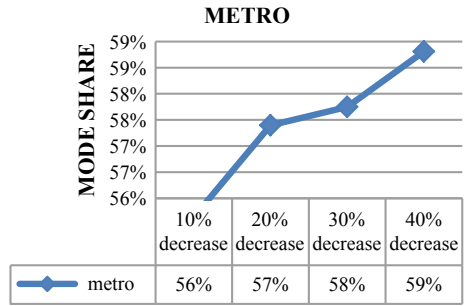
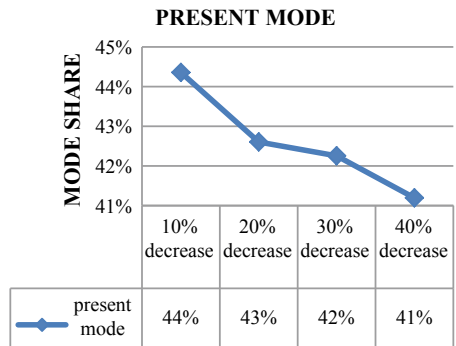


Fig. 7 Cross-elastic effect of travel time on present mode share



the two alternative modes. The different scenarios considered are when there is a decrease in travel time of metro of 10, 20, 30 and 40%, respectively.

Figure 6 shows the direct elasticity, i.e. showing the effect of variation travel time of metro on the mode choice of same mode. All other parameters remain the same; a 10% decrease in the travel time of metro causes an increase of 1% probable mode share towards it. Similarly by checking the various scenarios at 20, 30 and 40%, the mode share is changed from 56 to 57%, 58 and 59%, respectively. The cross-elastic effect of travel time reduction of metro in the present mode causes decrease in the mode share. From Fig. 7, a decrease in 10, 20, 30 and 40% of travel time causes decrease in mode share from 44 to 43%, 42 and 41%, respectively.

5.5 Fuel Savings and Emission Analysis

Fuel efficiency is a major parameter which influences the vehicle emissions causing pollution. By calculating the total trip length (in vehicle kilometres) of the different mode users for their work trip and adopting values for average mileage for different vehicle types, the fuel consumed by the sample of vehicles for their daily trip length was estimated. The fuel efficiency details for the sample data are shown in Table 8.

Table 8 Fuel efficiency details

Mode	Two-wheeler	Car	Auto	Total
Daily trip length (km)	4179	769	52	5000
Mileage (km/litre)	40	20	15	
Fuel consumption (litres)	104.5	2.6	51.3	158.34

Table 9 Pollutant emission coefficients for different modes

Pollutants	Emission coefficients		
	Two-wheeler	Auto-rickshaw	Car
CO	1.65	1.37	0.84
HC	0.61	2.53	0.12
NO _x	0.27	0.2	0.09
CO ₂	24.97	62.41	172.95
PM	0.035	0.045	0.002

Analysing the sample with an assumption that 90% of cars use petrol and the remaining diesel, the total fuel cost per day estimated was 10,556.73 and Rs. 3,293,700.81 annually.

Calculating the fuel cost consumption for the share of switching vehicles, it was estimated that there could be a possible savings in fuel consumption which further amounts to an economy in fuel savings of Rs. 3419 per day, i.e. Rs. 10.67 lakhs per year [6].

Analysis was done with the collected sample to estimate the possible reduction in vehicle emission. Table 9 gives the pollutant emission coefficients considered for each mode.

The emission for the existing scenario and the possible reduction in pollution along the metro corridor due to modal shift were also calculated using the collected sample. Figure 8 explains the pollutant emissions (in grams) for the ‘existing’ and ‘after-shift’ scenarios. It is seen that there is positive reduction in all the pollutants. The overall percentage reduction of each pollutant is illustrated in Table 10. There is about 32% reduction of CO and NO_x, 32% of HC and PM and also 33% of CO₂.

6 Summary and Conclusions

The study used binary logit models to estimate the average probability of shift of commuters from the currently used mode to metro on introduction of metro rail system. The study found that travel cost, comfort, availability of feeder service and nearness affected the modal shift behaviour. Model developed to study the overall shift from all modes of transport in Kochi showed that the average probability of shift is 52%.

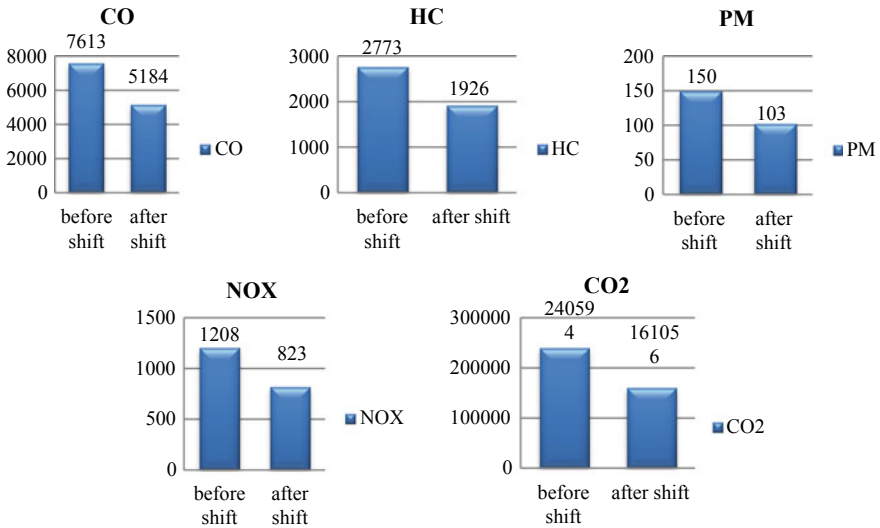


Fig. 8 Pollutant emission (in grams) for ‘existing’ and ‘after-shift’ scenarios

Table 10 Percentage reduction in vehicle emission

Pollutants	2w (%)	Car (%)	Emission g (%)
CO	32	35	32
HC	32	35	31
NO _x	32	35	32
CO ₂	32	35	33
PM	32	35	31

To study the shifting behaviour of commuters using bus, separate logit model was developed. The influencing parameters were travel time, nearness, feeder service, time headway of mode and work trip distance. The probable shift estimated was 57%.

The model to predict the probable shift of commuters from two-wheeler mode to metro mode showed an excellent fit. The study found that travel time, comfort, nearness, parking and work trip distance were the influencing variables. From the study, the average probability of two-wheeler commuters in shifting their work trips to metro mode is 38%.

Elasticity of metro fare was checked against the mode share of two alternatives. The direct elastic effect showed a decrease of 6 and 5% probability in modal shift as the metro fare changed to 1.5X and 2X, respectively. Elasticity of travel time is analysed among the public transport bus users. The result showed that the mode share of metro showed an increase from 56 to 57%, 58 and 59% at different changing scenarios of metro travel time reduction at 10, 20, 30 and 40%, respectively.

Analysis on the fuel efficiency and pollutant emission for the 'existing' and 'after-shift' scenarios was done with the collected sample. The results shows that there could be a possible savings in fuel consumption which further amounts to an economy in fuel savings of Rs. 3419 per day, i.e. Rs. 10.67 lakhs per year as an impact of the predicted scenario. Also there could be a positive reduction in pollutant emissions (i.e. about 31–33%) for the predicted scenario.

Acknowledgements The authors express their sincere gratitude to principal and professors of Civil Engineering Department, Rajiv Gandhi Institute of Technology, Kottayam, for their valuable guidance, suggestions and continuous encouragement throughout the course of the work. The authors express their sincere thanks also to the director and scientists of National Transportation Planning and Research Centre (KSCSTE-NATPAC) for providing necessary facilities and assistance in doing the work.

References

1. DMRCL (2011, Aug) Detailed project report Kochi metro
2. Greene W (2008) LIMDEP/NLOGIT econometrics software and user manual
3. Hensher DA, Rose JM, Greene WH (2005) Applied choice analysis-a primer. Cambridge University Press, US
4. Vedagiri P, Arasan VT (2009) Estimating modal shift of car travelers to bus on introduction of bus priority system. *J Transp Syst Eng Inf Technol* 9(6):120–129
5. Regmi MB, Hanaoka S (2012) Assessment of modal shift and emissions along a freight transport corridor between Laos and Thailand. *Int J Sustainable Transp* 9:192–202
6. Valuing air quality impacts of transportation: a review of literature. School of Urban Development Faculty of Built Environment and Engineering, Queensland University of Technology (QUT), Brisbane, Australia, 2006

Analysis of Travel Time Expenditure of School-Going Children



M. Manoj, T. M. Rahul, Ashish Verma and Sumit Yadav

Abstract Travel behaviour of school-going children has been a topic of scientific discourse. School trips hold a significant share of peak-hour trips in many Indian cities and are considered a major contributor to congestion. Commute mode choice, time-of-day of trip departure, time use, intra-household interaction with regard to chauffeuring, etc., are some of the topics on children's travel behaviour that have seen significant development over the past decades. However, relatively less research has been undertaken on children's travel time expenditure. This research contributes to the domain of travel time analysis. The present study hypothesizes that school-going children (usually) have a travel time bound associated with their school commute. The revealed travel time can be considered as a function of this bound. Stochastic frontier modelling, alternatively production frontier concept, is considered for investigating the travel time expenditure. This approach allows for investigating the unobserved bound using the revealed travel time and several explanatory variables. The econometric model is estimated using the household travel survey data for Bangalore city for the year 2010. The statistically significant empirical model for the conditional mean indicates that the concept of travel time bound holds for the data set. Parameter estimates suggest that male students have a higher bound compared with females, an observation aligning with conventional wisdom. Furthermore, students travelling on motorized modes are observed to have a higher time bound compared with non-motorized mode users. This might be an indication of the unreliability associated with the travel time on motorized vehicles during congested times when most school

M. Manoj (✉) · S. Yadav
Indian Institute of Technology Delhi, New Delhi 110016, India
e-mail: manojm@civil.iitd.ac.in

S. Yadav
e-mail: ce1140391@civil.iitd.ac.in

T. M. Rahul
Amrita School of Engineering, Amritanagar, Coimbatore 641112, India
e-mail: tm.rahul@gmail.com

A. Verma
Indian Institute of Science Bangalore, Bangalore 560012, India
e-mail: ashishv@civil.iisc.ernet.in

trips happen. Planning implications of the research findings are also discussed in the chapter.

Keywords School children · Travel time · Frontier modelling · Policy · India

1 Introduction

Children's travel behaviour receives less attention in transportation planning for Indian cities. School-commute holds a reasonable share of peak period trips in most of the Indian cities [1] and to a large extent add to the congestion on roads in and around school locations. International literature has shown a substantial interest in understanding the influence of children's activity-travel patterns on various behavioural aspects including vehicle ownership and long-term mobility decisions [2], intra-household interaction [3], mode choice [4] and activity allocation [5]. Substantial research has been undertaken to incorporate children's activity-travel patterns in advanced travel demand modelling systems [6, 7]. The important differences between children's and adults' travel behaviour are visible in terms of daily activity participation features, time allocation behaviour between weekdays and weekends, spatial distribution of out-home activities, joint activity participation decisions and frequencies and spatial and temporal constraints shaping (in-home and out-of-home) day-to-day activities [8].

Though research on children's activity-travel behaviour has progressed substantially by revealing interesting insights from developed countries, much less progress has been made in developing countries like India. The present study contributes to the literature on children's time-use behaviour by investigating the commute travel time allocation decisions of school children in a megacity in India. The present study assumes that school-going children usually have a travel time bound for their school commute, and this bound shapes their revealed travel time, which is equal to or less than the maximum time limit (bound). The objective of this research is to investigate this bound if exists. To the authors' knowledge, no other studies have contributed in this direction from a developing country's perspective.

The rest of the chapter is organized as follows. Next section presents a brief review of the time-use behaviour of school-going children. Following this, the data and the statistical modelling methodology adopted for the current research are explained. Subsequently, empirical model estimation results are described, and planning implications of the research are highlighted. Final section summarizes the current research and concludes the article.

2 Review of Related Works

The literature review presented here is undertaken under two main headings: children's travel behaviour and time budget studies. The following sections briefly discuss the articles whose findings are relevant for the research presented in the article.

2.1 *Children's Travel Behaviour*

The distinguishable feature of children's travel behaviour is they spend nearly 7 h a day (on weekdays) at school and that forms a constraint on time use [9]. However, on weekends, as is the case with work-related travel, the time-use constraints are relatively absent for children [8]. Further, children's activity participation and travel are also influenced by their age group [10].

Modelling the choice of a travel mode to school has been one of the areas on children's activity-travel behaviour that has received increased attention in travel behaviour literature. Various demographic factors including age, gender, etc. of children and household attributes such as household vehicle availability are observed to influence the mode choice of school commuting children in the USA [5, 11]. The class/grades in which the students study [12, 13] and intra-household interaction [3] also influence the school-commute mode choice of children. Further, the health status of children was found to shape their recreational activities and travel [14, 15], and gender of a child was observed to influence the '*with whom dimension*' of household interaction [8]. Though significant research has been undertaken on several dimensions characterizing activity-travel behaviour, very little knowledge exists about the travel time bound concerning (school) commute of children.

2.2 *Travel Time Budget*

Mokhtarian et al., in an empirical study, noted the positive utility associated with travel and enhanced the notion of derived demand philosophy [16]. However, this positive utility was found to exist only for a specific range of travel time [17]. Subsequently, Mokhtarian and Chen modelled the travel time expenditure using multiple data sources [18]. The authors explained the travel time expenditure using the socio-demographic (age, gender, etc.) and land use variables and elicited the changing nature of the travel time budget. Banerjee et al. explored the concept of travel time frontier to model the travel time bound [19] defined by Mokhtarian and Salomon [16], and according to them, the unobserved frontier influenced the observed travel time of individuals. In the present research, the travel time expenditure is explored using the concept of travel time frontier introduced by Banerjee et al. [19].

3 Data and Methods

3.1 Data Source

The research presented in the article is based on the study conducted on a secondary household travel survey data for the city of Bangalore in India. Bangalore's current population is nearly 9 million. Past travel behaviour data of Bangalore indicates that school trips contribute reasonably to the peak-hour trip demand [1].

The study utilizes the household travel behaviour data for Bangalore for the year 2009. The survey was funded by the Bangalore Metropolitan Region Development Authority (BMRDA). As is common for any household travel survey data, the survey captured a respondent's household socio-demographics, personal socio-demographics and travel behaviour information for a weekday. The sample size was 2% of the total size of households in the study area, and the sample was found to be a representative of socio-demographic trends in the study area in terms of household size (4.2 in sample and 4 in census) and male to female ratio (1.1 in sample and 1.09 in census) [20].

A subsample of the data comprising only of school trips is utilized for the current analysis. This data set was developed from the main database based on the information regarding the trip purpose, age and educational status.

3.2 Modelling Method

The present paper uses the stochastic production frontier approach to explore the travel time for school-commute trips. Aigner et al. [21] proposed the alternative formulation of stochastic production frontier models with the error part partitioned into two components. Travel behaviour research has utilized this approach for explaining the travel time budget of individuals [19]. The following discussion about the modelling approach is mostly based on Banerjee et al. [19].

Travel time frontier represents the maximum amount of time an individual is willing to allocate for travelling [19]. Revealed travel time is either equal to less than that bound. Stochastic frontier modelling approach helps investigating the bound. If t_i is the observed travel time and F_i represents the unobserved frontier for t_i , then,

$$T_i = F_i - \delta_i \quad (1)$$

where,

$$T_i = \ln(t_i)$$

δ_i = non-negative random term.

Here, the natural logarithm of revealed travel time is taken to adjust the skewness in the distribution of t_i . The stochastic frontier model then can be represented as [19, 21]:

$$F_i = \beta' x_i + v_i \tag{2}$$

This further implies that

$$T_i = \beta' x_i + v_i - \delta_i = \beta' x_i + \varepsilon_i \tag{3}$$

In matrix form, β is a coefficient matrix, and X_i is a vector of explanatory variables; v_i ranges between $-\infty$ to $+\infty$. The term, $\beta' x_i + v_i$, in Eq. (3) is the location of the frontier. If v_i follows normal distribution and δ_i a half-normal distribution [19, 21], then the derived distribution of ε_i is:

$$h(\varepsilon_i) = \frac{2}{\sqrt{2\pi}} \sigma_\delta \left\{ 1 - \phi\left(\frac{\varepsilon_i \lambda}{\sigma}\right) \right\} \exp\left[-\frac{\varepsilon_i^2}{2\sigma^2}\right]; \quad -\infty < \varepsilon_i < \infty \tag{4}$$

Here,

$$\sigma^2 = \text{var}(v_i + \delta_i) = \sigma_\delta^2 + \sigma_v^2; \quad \lambda = \sigma_\delta / \sigma_v \tag{5}$$

The parameters of the model are estimated by maximizing the log-likelihood function in Eq. (6)

$$LL = \sum_{i=1}^n \ln[h(\varepsilon_i)] \tag{6}$$

' τ ' the ratio between the (expected) reveal travel time and the expected travel time frontier and can be found using the expression in Eq. (7) [19].

$$\tau = \frac{\text{Exp}(t_i)}{\text{Exp}(\text{TTF})} = 2 \exp\left(\frac{\sigma_\delta^2}{2}\right) [1 - \phi(\sigma_\delta)] \tag{7}$$

4 Empirical Results

Travel behaviour information of 1293 school-going children is utilized for the analysis. Table 1 presents a brief summary of the socio-demographic and travel behaviour information of the sample. Table 1, in alignment with the expectations, indicates that a significant number of children belong to the age band 5–12 years. Further, the sample statistics show about 60% of respondents being males, and about 80% of

Table 1 Summary of main variables

<i>Age</i>	
Up to 5	3.5
5–12 years	37.4
12–18 years	45.8
Above 18 years	13.3
<i>Gender</i>	
Male	58.9
Female	41.1
<i>Education</i>	
Primary	21.7
Up to HSC	72.3
Travel time (avg.) [min]	18.4
Above HSC	6
<i>Mode</i>	
Walking	55.9
Bicycle	4.8
Motorized two-wheeler	1.2
Auto-rickshaw	5.8
Car	12.6
Bus (public)	15.7
Bus (others)	3.7
Others	0.3
<i>No. of cars</i>	
None	89.8
One	9.8
More	0.4
<i>No. of two-wheelers</i>	
None	36.8
One	56.2
More	7
<i>No. of vehicles (any)</i>	
None	31.8
One	52.3
Two	14.7
More	1.2
<i>Household income</i>	
Below 4000	33.5
4000–15,000	64.4

(continued)

Table 1 (continued)

Above 15,000	2.1
<i>No. of household earners</i>	
One	86.8
Two	9.9
More	3.3
Sample size	1293

respondents being at or above '10 + 2' level with respect to their completed degree. Travel patterns suggest that about 56% of students commute on foot and nearly 20% by bus. Surprisingly, about 13% of students in the sample had travelled by car and their proportion is nearly equal to the students who can legally drive (age ≥ 18 years). Nearly 65% of students in the sample have at least one motorized two-wheeler in their home. Approximately, the same per cent of students has at least one or two vehicles (any type) at home. Household income distribution suggests that 65% of students belongs to the middle-income group households. Finally, the table also indicates that nearly 87% of students come from one-worker households.

The model estimation results are shown in Table 2. Age of the respondent has a weak but significant association with the unobserved travel time bound. The association is intuitive: older students allocate more time for travelling than younger ones. Effect of gender suggests that males tend to have larger frontier than females; an

Table 2 Model estimation results

Variable	Coefficient	p-value
Age	0.003	0.018
Gender (male)	0.764	0.015
Educational level (up to HSC)	-0.096	0.002
Above HSC	0.062	0.000
Mode (motorized vehicles)	0.806	0.000
Vehicle ownership (any)	0.069	0.001
Income (4k-15k)	0.136	0.000
High income >15k	0.497	0.000
More earners in household	0.015	0.000
Constant	1.771	0.000
σ^2	0.441	
λ	1.031	
σ_v	0.462	
σ_δ	0.477	
X^2 (df)	758.60 (9)	
Sample size	1293	
τ	0.733	

interesting finding has given the active age group and gender-related restrictions in Indian societies. Compared to the individuals who are below the higher secondary education level, students above this grade are observed to allocate more time for travel. This might be suggesting that individuals in higher grades are allocating time for other activities like coaching, tuition, etc. which may help them in their studies. An interesting finding with respect to the commute mode choice is the broader frontier for motorized mode users (bus, car, etc.) compared with non-motorized users. This might be a reflection of uncertainty due to congestion in most of the roads in the city during peak hours. Household vehicle ownership is associated with a larger bound; this finding aligns with the case of commutes in the USA [19].

The model shows an increase in travel time bound as individuals move from low income to higher income households. There is a clear distinction between low- and medium-income households and between medium- and high-income households as implied by the model. Finally, as the number of earners in a household increases the frontier also broadens. Even though unapparent, this might be a reflection of the shouldering of household activities by children in multi-earner households. Further research is needed to verify this assertion.

Finally, Table 2 also shows that the ratio, τ , between the expected value of observed travel time to the expected value of the unobserved frontier is 0.733. This indicates that the students are spending (on average) about three-fourth of the time that they are willing to allocate for travel. To put in other words, the unobserved frontier of the populace under investigation is about 1.4 times their actual travel time. The value of τ also suggests that if the school-commute constraints are relieved, the travel of children can expand up to the bound observed in the study.

4.1 Planning Implications

The research findings have important planning and policy implications, particularly in the context of the study area. Bangalore has been actively considering road infrastructure improvement and rapid transit systems for improving the travel time of commuters. In case of reduction in congestion, motorized mode users can release some time for other activities and travel which would eventually contribute to induced-travel demand. As evident from the literature, releasing of commute constraints can influence children's activity participation and travel. Hence, policy makers may include the possibility of induced travel due to children's activity participation in upcoming transport plans. The study also hints that with the increase in vehicle ownership there would be an increase in the travel time bound.

5 Summary and Conclusions

This research contributed to the domain of travel time analysis. The present study assumed that school-going children usually have travel time bound for their school commute. The revealed travel time is influenced by this bound and it is equal to or

less than that. Stochastic frontier modelling, following production frontier concept, was considered for the present research. This approach allows for modelling the unobserved bound using several independent variables. The research utilized the commute travel information of school-going children from a household travel survey conducted in Bangalore city in 2009. The important findings of the research include the following.

- i. Compared with individuals having an educational status below or up to higher secondary level, students having an educational status above higher secondary level are observed to allocate more time for travel.
- ii. Motorized mode users have a broader frontier than non-motorized mode users.
- iii. Male students tend to have larger bound than female students.
- iv. The ratio between the expected value of observed travel time to the expected value of the unobserved frontier is 0.733.

Overall, the present study indicates that the concept of travel time frontier or budget applies to school-going children. The present research can be expanded to further dimensions. A comparative analysis of travel time frontiers of children across small and large Indian cities could be one avenue for research. Further, travel behaviour research would also be benefitted by models, the error components of which would follow distributions other than normal and half normal.

References

1. Karnataka Urban Infrastructure Development and Finance Corporation (KUIDFC) (2007) Comprehensive Traffic and Transport Plan for Bangalore, Final Report
2. Paleti R, Bhat C, Pendyala R (2013) Integrated model of residential location, work location, vehicle ownership, and commute tour characteristics. *Transp Res Rec* 2382:162–172
3. Ermagun A, Levinson D (2016) Intra-household bargaining for school trip accompaniment of children: a group decision approach. *Transp Res Part A Policy Pract* 94:222–234
4. Bhat CR (1997) Work travel mode choice and number of nonwork commute stops. *Transp Res Part B* 31(1):41–54
5. Yarlagaadda AK, Srinivasan S (2008) Modeling children's school travel mode and parental escort decisions. *Transportation* 35(2):201–218
6. Copperman R, Bhat CR (2010, Jan) Children's activity-travel patterns and implications for activity-based travel demand modeling. In: Compendium of papers CD-ROM, transportation research board 89th annual meeting, Washington DC
7. Pinjari A, Eluru N, Srinivasan S, Guo JY, Copperman R, Sener IN, Bhat CR (2008, Jan) Cemdap: modeling and microsimulation frameworks, software development, and verification. In: Proceedings of the transportation research board 87th annual meeting, Washington DC
8. Copperman R, Bhat CR (2007) An analysis of the determinants of children's weekend activity participation. *Transportation* 34(1):67–87
9. Hofferth SL, Sandberg JF (2001) How American children spend their time. *J Marriage Family* 63:295–308
10. Yathindra K (2009) Exploratory analysis of children's travel patterns using time-use and trip-based surveys. Masters thesis, University of Florida
11. Nasar JL, Holloman C, Abdulkarim D (2015) Street characteristics to encourage children to walk. *Transp Res Part A Policy Pract* 72:62–70

12. O'Brian C, Gilbert R (2003) Kids on the move in Halton and Peel: final report. Report prepared for The Center for Sustainable Transport
13. Stefan KJ, Hunt JD (2006) Age-based analysis of children in Calgary, Canada. In: 85th annual meeting of the transportation research board, Washington, DC
14. Clifton KJ (2003) Independent mobility among teenagers: an exploration of travel to afterschool activities. *Transp Res Rec* 1854:74–80
15. Weston LM (2005) What helps and what hinders the independent travel of non-driving teens. Ph.D. dissertation, The University of Texas at Austin
16. Mokhtarian PL, Salomon I, Redmond LS (2001) Understanding the demand for travel: it's not purely 'derived'. *Innovation Eur J Soc Sci Res* 4(4):355–380
17. Mokhtarian PL, Salomon I (2001) How derived is the demand for travel? Some conceptual and measurement considerations. *Transp Res Part A Policy Pract* 35(8):695–719
18. Mokhtarian PL, Chen C (2004) TTB or not TTB that is the question: a review and analysis of the empirical literature on travel time (and money) budgets. *Transp Res Part A Policy Pract* 38(9):643–675
19. Banerjee A, Ye X, Pendyala RM (2007) Understanding travel time expenditures around the world: exploring the notion of a travel time frontier. *Transportation* 34(1):51–65
20. Census of India (2011) Figures at a glance—Karnataka (in CD-Rom)
21. Aigner D, Lovell CK, Schmidt P (1977) Formulation and estimation of stochastic frontier production function models. *J Econom* 6(1):21–37

Activity-Based Travel Demand Models to Evaluate Transport Policies



Pranav Padhye, M. S. Nagakumar, S. Sunil and A. H. Manjunatha Reddy

Abstract Transportation planning plays a critical role in shaping the economic health and quality of life of the general public. A good deal of the demand for transport is concentrated on a few hours of a day, at particular section of urban areas where congestion takes place during specific peak periods. Hence, modelling of this travel demand from the transportation point of view is necessary. There are two basic approaches to this travel demand modelling—traditional four-stage travel demand modelling and activity-based travel demand modelling. According to transport department data of Bangalore city collected in 2012, there are 41.86 lakh of two-wheelers, 11.8 lakh of cars and 5.91 lakh of transport vehicles. The share is 69% of two-wheelers, 22% of LMVs, 5% of HTVs and 4% of other vehicles. From the earlier research, it has been found that the activity-based modelling is more efficient to evaluate the transport policies than traditional four-step modelling particularly for the cities like Bangalore having a large amount of vehicle population. Here, an attempt has been made to develop the activity-based travel demand models for the selected zone of Bangalore city. Bangalore city has been divided into three major areas and further into 47 zones. The data has been collected through individual person survey considering certain parameters which are influential to develop person tours. This collected data is then analysed through SPSS software, and models are developed considering the several parameters such as age, gender, monthly income, distance of travel, daily travel cost and vehicle ownership. Simultaneously, the zonal public transport policies have been studied to understand the norms regarding the transport such as quality of transport, pricing, financing and parking facilities. The results obtained in the form of models are compared with the traditional models

P. Padhye · M. S. Nagakumar · S. Sunil (✉)

Department of Civil Engineering, RV College of Engineering, Bengaluru 560059, India
e-mail: sunils@rvce.edu.in

P. Padhye

e-mail: pranavpadhye4@gmail.com

M. S. Nagakumar

e-mail: nagakumar@rvce.edu.in

A. H. M. Reddy

Department of Biotechnology, RV College of Engineering, Bengaluru 560059, India
e-mail: ahmanjunatha@rvce.edu.in

© Springer Nature Singapore Pte Ltd. 2020

T. V. Mathew et al. (eds.), *Transportation Research*, Lecture Notes
in Civil Engineering 45, https://doi.org/10.1007/978-981-32-9042-6_20

and are used to evaluate the public transport policies. Also, the factors influencing the trips of each individual have been studied and the effects of those factors are analysed. The results obtained are found satisfactory in terms of R^2 value and other testing parameters. Transport policies are selected, and models are linked to the policies to evaluate them. Study concludes with the effective linking of the models to the policies which will help the authorities to bring it into play.

1 Introduction

The world including transport is changing fast. Emerging countries are becoming more significant in the world stage, but they suffer serious transport problems as well. Transport modelling supports planning and has an important role in the process of transportation. The models developed are tested for the goodness of fit, and the model validation is being carried out. These models give the suitability of the transport system which is currently in use; also, the modifications are to be done in it. This process is called as evaluation in broad sense. Travel demand models are the powerful tools for efficient transportation planning within the city. Though all the models have certain advantages and disadvantages, they are being successfully used all over the world. Many attempts have been done for different cities in the world to do the transportation planning [1].

The scope of the present study is to develop the activity-based travel demand models which will be useful in evaluating the transport policies. For this reason, RV College of Engineering, Bangalore, is selected as the study area and data is collection performed. The data is collected from each of the staff members, non-technical staff and many students. The sample size is 213 individual samples. The study also includes the detailed study of transport policies of Bangalore city to understand the public transport scenario. Collected data is fed into the SPSS software to develop the travel demand models for trip generation and modal split. The developed models are then analysed to find out the most influential parameters for making travel patterns of the people. These models are also used to evaluate the transport policies of Bangalore city. According to the transport department data of Bangalore city collected in 2012, there are 41.86 lakh of two-wheelers, 11.8 lakh of cars and 5.91 lakh of transport vehicles. The share is 69% of two-wheelers, 22% of LMVs, 5% of HTVs and 4% of other vehicles [2]. The study conducted by Pulugurta et al. [3] concludes giving the superiority of fuzzy logic in modelling travel demand. It is also successfully demonstrated in simulating several public transportation policies most efficiently. Lekshmi et al. [4] state that transportation planning plays an important role in improving public transportation system. The paper concludes that the method can serve as a basis for predicting the number of tours so that land use plans can be formulated. In the study carried out by Manoj et al. [5], an attempt is made to model the activity-travel behaviour of non-workers for the city of Bangalore in India. The results found satisfactory after testing for goodness of fit. The study concludes stating that this is the first attempt made by the authors to use activity-based models

for any Indian city. In the study carried out by Yagi and Mohammadian [6], a comprehensive activity-based modelling system using utility maximization approach has been developed by providing precise estimates which will work as the best inputs for evaluation of unlike transportation policy situations. The paper concludes that the new models established in the study will help to an enhanced understanding of urban travel behaviour and progress of the travel demand forecasting methodology.

2 Methodology

Comparative study has been carried out in between household survey process and workplace survey process. After the study, it is found that workplace survey is suitable and samples to be collected are discrete. The workplace which satisfies the requirements is selected.

In this study, workplace or individual interview survey is performed which gives discrete data of the population. Questionnaire may be of same type, also variables to be collected are same, and there is a variety of samples. As per the requirements of the B. P. R., the minimum sampling size should be 10% of total population in case of individual or discrete survey. In the current project work, the sample size collected is 213 out of 720 samples. It is approximately 30% which fulfils the B. P. R. requirement. Among the collected 213 samples, there are 132 samples of teaching staff and 81 samples of non-teaching staff. Standard questionnaire survey format is used for the data collection process. The sheet containing format is distributed among the teaching staff of all the departments of RV College of Engineering. For the data collection of non-teaching staff, a common questionnaire sheet is prepared and interview had been taken of each individual peon, foreman, laboratory assistant, clerk, programmer and other. Figure 1 shows the standard questionnaire survey format. The variables include profession, monthly income, purpose of trip, origin and destination, distance of travel, travel time, daily travel cost, travel mode, vehicle ownership, number of owned vehicles in the family, gender, age and household size.

Origin and Destination Survey has been carried out at the centroids of the four zones by Household Interview Survey.

3 Primary Data Analysis

Primary data analysis includes understanding the travel mode use scenario of the working staff of RV College of Engineering. Analysing the collected data, it is found that there are seven variables which are most influencing on the mode choice behaviour of the staff as tabulated in Table 1. These seven variables are age, gender, activity in the trip, income, distance of travel, daily travel cost and vehicle ownership. This analysis provides the information about how the individual variable affects the choice of the mode of transport of the staff.

R. V. College of Engineering, Bangalore

Data Collection and Survey for the M. Tech (Highway Technology) Dissertation Work

Title of the Dissertation Thesis – Activity-based Travel Demand Modelling to Evaluate Transport Policies

Name of Guide – Prof. Dr. M. S. Nagakumar Conducted by – Pranav R. Padhye (M. Tech SE – CHT)

Date:- _____ **Sex:-** Male/Female

Age:- _____ Years **Number of Person in Family:-** _____

Questionnaire:

1. Profession -	2. Monthly Income (Rs) –
3. Purpose of Trip –	
4. Origin of Trip (House Location) -	5. Destination of Trip -
6. Distance of Travel (Km) -	
7. Travel Time (min) Home to Work –	Work to Home –
8. No. of Home-based Other Trips/Week (Shopping/Recreational) -	
9. Travel Mode – Bus / Metro / Owned Car / Two Wheeler / Rickshaw / College Bus / Other	
10. Daily Travel Cost (Rs) -	11. Vehicle Ownership – Yes / No
12. Number of Owned Vehicle in Family:- Two Wheelers - _____ Four Wheelers - _____	

Fig. 1 Standard questionnaire survey format

Table 1 Share of mode of transport

Different modes used	Modes in nos.	Percentage
No. of person using owned car	57	26.76
No. of person using owned bike	79	37.08
No. of person using bus	31	14.55
No. of person using rickshaw	13	6.10
No. of person using college bus	21	9.85
No. of person using other modes of transport	12	5.63
Total	213	100

Figure 2 shows the total share of mode of transport of all the working staff of RV College of Engineering. Above is the general analysis of mode choice behaviour of the people. Then, the variable-wise analysis has been carried out. The analysis gives certain inferences such as age and income as increased people are preferring owned car than owned bike or bus. Gender-wise distribution is balanced for mode of travel. It is observed that teachers are more interested in using owned car and owned bike rather than availing public transport.

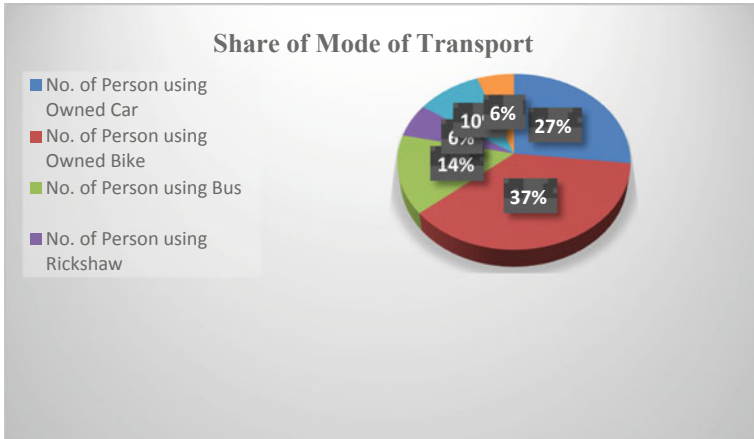


Fig. 2 Share of mode of transport

3.1 Trip Generation Analysis

For the activity-based approach of trip generation, the following trips are considered.

1. Home to work and work to home (HWH)
2. Home to work and work to home with one stop (H + W)
3. Tour with sub-tour and back to home (T + H).

The following models are developed for activity-based approach.

1.
$$TG_{(HWH)} = 1.986 + 0.329(A) - 0.011(G) + 0.789(MI) + 0.001(AT) - 8.307E - 0.005(DT) + 9.100(TM) + 2.325(DTC) + 0.008(VO) \quad R^2 = 0.719$$
2.
$$TG_{(H+W)} = 1.237 + 0.011(A) - 0.143(G) + 1.239(MI) - 0.724(AT) - 0.001(DT) + 0.99(TM) + 0.001(DTC) - 0.322(VO) + 0.88(OT) \quad R^2 = 0.788$$
3.
$$TG_{(T+H)} = -0.097 + 0.029(A) + 0.418(G) + 7.311(MI) + 0.139(AT) + 0.010(DT) - 0.09(TM) + 0.003(DTC) - 0.028(VO) + 1.233(ST) \quad R^2 = 0.863$$

The above variables are also tested for multi-co-linearity and VIF. From the regression analysis, obtained the VIF value of each explanatory variable less than 10 and tolerance value greater than 0.1. It can be concluded that there is non-co-linearity between them. When VIF is greater than 10 and tolerance value is less than 0.1, then there is no practical difference in co-linearity.

3.2 Modal Split Analysis

“Utility maximization approach” is used for modal split analysis, and with the help of IBM SPSS software package, multinomial logistic regression analysis has been

Table 2 Model fitting information and pseudo-R-square for MNL analysis of seven variables

Model fitting information				
Model	Model fitting criteria	Likelihood ratio tests		
	-2 log likelihood	Chi-square	df	Sig.
Intercept only	665.526			
Final	24.957	640.569	900	1.000
Pseudo-R-square				
Cox and Snell		0.951		
Nagelkerke		0.994		
McFadden		0.963		

carried out for modal split model development. Equations show the modal split models formed from the obtained coefficients considering seven variables. Owned bike is the most preferred mode; it is considered as base for analysis.

1. $U_{(OB)} = 0$
2. $U_{(OC)} = -1.592 + 3.223(A) + 1.517(G) + 6.211(MI) + 2.661(AT) + 1.266(DT) - 11.018(DTC) + 1.226(VO)$
3. $U_{(B)} = 3.098 + 1.657(A) + 1.887(G) + 10.099(MI) - 0.276(AT) + 0.237(DT) - 9.529(DTC) + 2.004(VO)$
4. $U_{(CB)} = 0.507 + 1.17(A) + 1.006(G) + 0.227(MI) + 0.210(AT) - 2.662(DT) - 1.832(DTC) + 0.847(VO)$
5. $U_{(R)} = -4.603 + 4.503(A) + 1.562(G) + 17.706(MI) - 0.387(AT) + 3.488(DT) - 21.552(DTC) + 1.252(VO)$
6. $U_{(O)} = -24.307 + 12.241(A) + 1.577(G) + 10.171(MI) + 3.509(AT) - 7.053(DT) - 4.505(DTC) + 1.796(VO)$

Table 2 gives the model fitting information and pseudo-R-square for MNL analysis of seven variables.

3.3 Trip Distribution Analysis

Household survey data gives the origins and destinations of the trips being produced within the zones. Later, trip matrix is produced; this matrix is followed by the distributed matrix of trips by one of the methods. In the current project work, trip generation is carried out for the RV College of Engineering only. But the trips producing here are observed, and it is got to know that people are coming here from various areas of Bangalore city. The four zones are, namely, Kengeri, Kengeri Satellite Town, RR Nagar and Vijaynagar and are surveyed. Zonal household survey has been carried out to know the origin and destination of the trips. Two hundred and

twenty-one households were surveyed to obtain the necessary data from all the four zones. From the collected data, one general origin and destination matrix was formed to know the interzonal trips. Then, various other trip matrices were formed to distribute the trips according to mode of transport. Trip distribution has been done by “growth factor method”. This growth factor is calculated with the help of observed and predicted values of trips. Then, the growth factor is calculated as follows:

$$E = \text{Predicted Trips} / \text{Observed Trips}$$

where

‘E’ is the growth factor for that particular mode of transport. Observed values of trips are obtained from survey data, and predicted values are obtained from IBM SPSS 20 trip generation analysis.

3.4 Trip Assignment Analysis

Trip assignment is also done with the help of the trip distribution matrices. “All or nothing assignment” technique is used here which predominantly assumes only time and sometimes cost of travel as the influencing parameter on the trip-making behaviour. All interzonal trips have been assigned.

3.5 Economic Evaluation (Value of Travel Time Savings)

Cost-benefit analysis has been done for all interzonal routes to find out the most convenient mode of travel as shown in Table 3. This has been done based on the trip assignment carried out. This analysis will definitely be helpful in evaluating the public transport policies.

For the bus as the mode of travel, stopping time at the bus stops is considered as delay which is 4 min. and is added to the total travel time. The route is free from signalized intersection. Hence, no signalized delays are considered. The ratio for bus is lesser in the entire considered mode for the travel between these zones. Hence, bus is the most suitable mode of transport.

Table 3 Cost-benefit analysis for zone 2 and zone 4

Origin	Destination	Route	Distance (km)	Travel mode	Travel time (min)	Cost (Rs.)	Cost–time ratio
Kengeri Satellite Town/ Vijaynagar	Vijaynagar/ Kengeri Satellite Town	Old Outer Ring Road	9.9	Owned car	33	41.25	1.25
				Owned bike	22	18.56	0.84
				Bus	33	19	0.57
				Rickshaw	30	24.75	0.825

4 Transport Policy Evaluation

Figure 3 shows the flow diagram for the policy evaluation.

Transport policies can be evaluated directly from the collected data with the manual interpretation which is carried out earlier. Software analysis can be carried out directly after the data collection and manual data interpretation. Then, the models are developed and these models are linked to transport policies. The selected public transport policies for evaluation are

1. Improvement of Frequency

The models applicable to this policy are given below.

$$U_{(B)} = 3.098 + 1.657(A) + 1.887(G) + 10.099(MI) - 0.276(AT) + 0.237(DT) - 9.529(DTC) + 2.004(VO)$$

$$U_{(R)} = -4.603 + 4.503(A) + 1.562(G) + 17.706(MI) - 0.387(AT) + 3.488(DT) - 21.552(DTC) + 1.252(VO)$$

From the considered variables in the models, it is observed that daily travel cost (DTC) and vehicle ownership (VO) are the only influential parameters for the evaluation of this policy. More weightage of vehicle ownership variable for bus shows that bus frequency should be improved compared to rickshaws.

2. Comfort Index

Comfort index policy is primarily concerned with the modes such as owned car, bus and rickshaws. The models applicable to the comfort index are shown below.

$$U_{(OC)} = -1.592 + 3.223(A) + 1.517(G) + 6.211(MI) + 2.661(AT) + 1.266(DT) - 11.018(DTC) + 1.226(VO)$$

$$U_{(B)} = 3.098 + 1.657(A) + 1.887(G) + 10.099(MI) - 0.276(AT) + 0.237(DT) - 9.529(DTC) + 2.004(VO)$$

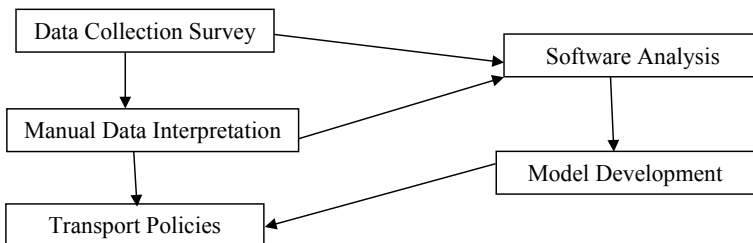


Fig. 3 Flow diagram for policy evaluation

$$U_{(R)} = -4.603 + 4.503(A) + 1.562(G) - 17.706(MI) - 0.387(AT) + 3.488(DT) - 21.552(DTC) + 1.252(VO)$$

From the comfort index point of view, the affecting variables are age (A), distance of travel (DT) and vehicle ownership (VO). Considering age as the parameter, travel mode rickshaw is offering more comfort as the supporting weightage is more. Distance of travel and vehicle ownership also give more comfort for rickshaw as the mode of travel. If monthly income is considered as an affecting parameter, then it is found that rickshaw is negatively correlated with and its weightage is highly negative which shows that bus is most comfortable from income point of view.

3. Fuel Prices

Fuel prices are changing at each and every moment. There should be a systematic way to evaluate these policies from the developed modal split models. Fuel is consumed by all the vehicles. Hence, all the modes of travel are considered to compare the weightage of parameters.

$$U_{(OC)} = -1.592 + 3.223(A) + 1.517(G) + 6.211(MI) + 2.661(AT) + 1.266(DT) - 11.018(DTC) + 1.226(VO)$$

$$U_{(B)} = 3.098 + 1.657(A) + 1.887(G) + 10.099(MI) - 0.276(AT) + 0.237(DT) - 9.529(DTC) + 2.004(VO)$$

$$U_{(CB)} = 0.507 + 1.17(A) + 1.006(G) + 0.227(MI) + 0.210(AT) - 2.662(DT) - 1.832(DTC) + 0.847(VO)$$

$$U_{(R)} = -4.603 + 4.503(A) + 1.562(G) - 17.706(MI) - 0.387(AT) + 3.488(DT) - 21.552(DTC) + 1.252(VO)$$

Among the above seven variables, the most affecting variables on the fuel prices are monthly income (MI), distance of travel (DT) and daily travel cost (DTC). From the observed weightage, it can be found that change in the fuel prices will affect more in the utility of rickshaws than other three of the above modes. Utility of college bus will not get affected much due to variation in the fuel prices. Distance of travel is also affected much for rickshaws if fuel prices vary. More fuel cost will force the consumer to spend more amounts on daily travel cost. Owned car is found to be most unsuitable from this point of view.

5 Conclusions

The following conclusions are drawn out of this study.

1. From the primary data analysis, it is found that preference of modal choices of the public is increasing from public transport, i.e. bus to private transport, i.e. owned car as per the increase in age, income, professions, travel distance and daily travel cost.
2. The R^2 values found from the trip generation models using activity-based approach are 0.520, 0.786 and 0.841 which are more significant than the R^2 values found from the traditional approach of trip generation modelling. This shows that the variables used for the activity-based models are fitting the data.
3. The observed VIF values of explanatory variables are less than 10 and greater than 0.1 which helps in detecting the overall collinearity problem that does not involve in the intercept and indicates non-collinearity between them.
4. McFadden R^2 values in modal split analysis are found to be 0.963, 0.374 and 0.927 for the 7, 5 and 4 variables, respectively. It shows that the higher value obtained from modal split analysis of 7 variables, i.e. 0.963, fits the data and considered hypotheses are proved.
5. From the analysis of value of travel time savings, it is found that the ratio of cost to time is less for the bus among the other modes of transport, which shows bus as the suitable and economical mode of transport within the cities.
6. Zonal public transport policies have been studied, and the models are linked to the policies for evaluation. It is found that distance of travel and vehicle ownership are the most influencing independent variables on the evaluated transport policies and much concentration should be given to these parameters while designing an effective transportation system.

References

1. de Dios Ortuzar J, Willumsen LG (2014) Modelling transport, 4th edn. Wiley, London
2. Padhye P (2017) Activity based travel demand models to evaluate transport policies. M.Tech dissertation thesis to be submitted to VTU, Belagavi
3. Pulugurta S, Madhu E, Kayitha R (2015) Fuzzy logic based travel demand model to simulate public transport policies. J Urban Plann Dev, ASCE, 44-1-44-11
4. Amruta Lekshmi GR, Landge VS, Sanjay Kumar VS (2014) Activity based travel demand modelling for Thiruvananthapuram urban area. In: Proceedings of 11th TPMDC conference, Dec 2014. Elsevier, Amsterdam, pp 498-505
5. Manoj M, Verma A (2013) Analysis and modelling of activity-travel behaviour of non-workers from a city of developing country, India. Procedia Soc Behav Sci 104:621-629. Elsevier
6. Yagi S, Mohammadian A (2006) An activity based model of travel demand in the Jakarta metropolitan area. J Adv Technol Transp, ASCE, 683-688

Financial Feasibility Analysis of Truck Parking Terminal—A Case Study



Chitranshu Mathur, Kaja Jadav, Sireesha Bandapalli, Khushbu Raval and Ashish Dhamaniya

Abstract To circumvent the problem of haphazard movement of trucks in the Kandla port area, it becomes important to plan the parking terminal to satisfy the desired demand for parking of all goods-carrying vehicles under the influence of the port. This will result in time and cost savings for all the associated transport agencies. In lieu of that the vehicle may charge an entry fee to meet out the construction and maintenance cost. The study is taken up to access the financial feasibility of the project for the concession period of 10 years. Hence, a financial analysis is carried out to determine the viability of the idea. The objective of such a study was to ensure that a project is worth investment or not. The financial evaluation of the project is carried out considering three growth scenarios: normal, optimistic, and pessimistic with three levels of occupancy (100, 80, and 70%). Three patterns of parking charges are also considered for providing useful tool to the policy makers for implementing the project.

Keywords Parking · Traffic · Feasibility · Public–private partnership · Break-even point

C. Mathur · K. Jadav · S. Bandapalli · K. Raval · A. Dhamaniya (✉)
Civil Engineering Department, Sardar Vallabhbhai National Institute of Technology, Surat
395007, India
e-mail: adhamaniya@gmail.com

C. Mathur
e-mail: chitranshu12@gmail.com

K. Jadav
e-mail: kajalj834@gmail.com

S. Bandapalli
e-mail: bandapallisireesha@gmail.com

K. Raval
e-mail: khushburaval42@gmail.com

1 Introduction

Kandla port in Gujarat handles more than 210 lakh MT commodity annually through road network, which results in extensive trucking activity. Further, based on historical trend of traffic growth, traffic volume is expected to grow substantially in the upcoming time with the increase in economic activities in the vicinity. The present parking shortfall is evidenced by the many trucks parked along shoulders near rest areas, for refreshments, and at other roadside locations. This issue has a colossal adverse effect on safety and causes travel time delays of through traffic. As of now, there is no provision of formal parking facility with all mandatory rules and regulations and all necessary service facilities at port area/within KPT premises. Currently, Minister of Road Transport and Highways (MoRTH), Government of India lays strong emphasis to plan and accommodate the efficient movement and parking facilities of all goods-carrying vehicles under the influence of the port. This will eventually result in time and cost savings for all the associated transport agencies. Before implementing the truck parking terminal project, feasibility of centralized truck parking considering all the relevant technical, locational, and financial aspects along with the implementation strategies are necessary to assess.

Financial analysis (also referred to as financial statement analysis or accounting analysis or analysis of finance) refers to an assessment of the viability, stability, and profitability of a business, sub-business, or project. It is performed by professionals, who prepare reports using ratios, that make use of information taken from financial statements and other reports. These reports are usually presented to top management as one of their pedestals in making business decisions.

Financial analysis may be determined if a business will:

- Continue or discontinue its main operation or part of its business;
- Make or purchase certain materials in the manufacture of its product;
- Acquire or rent/lease certain machineries and equipment in the production of its goods;
- Issue stocks or negotiate for a bank loan to increase its working capital;
- Make decisions regarding investing or lending capital;
- Make other decisions that allow management to make an informed selection on various alternatives in the conduct of its business.

Costs considered for financial analysis are:

1.1 Construction Cost (Fixed Cost)

The construction cost considered for financial analysis is as given in benefit–cost analysis (clause).

1.2 Maintenance Cost (Variable Cost)

Maintenance cost and its escalation for every year as per 5% inflation rate and discounting that cost by 12% p.a. discount rate (as per IRC SP-30).

Maintenance cost (Variable cost) of pavement is considered as 50,000 Rs/year for 1 km of road 7 m wide (IRC: SP 30) by considering that maintenance cost for parking pavement is calculated.

$$\text{Maintenance cost for pavement per year} = 50,000 * (\text{Area of parking pavement (m}^2\text{)}) / (1000 * 7)$$

Total cost = fixed cost (Construction Cost) + Variable cost (Maintenance Cost)

2 Methodology

The main aim of this study is to determine the break-even point (BEP) and the net present value (NPV). To accomplish this, the benefits or the revenue generated from parking of trucks and trailers according to the duration of parking segregated as short-term (1 h), medium-term (3 h), and long-term (5 h) needs to be determined. Two approaches are undertaken to carry out the financial analysis of the project, viz.

2.1 Based on 16% of Construction Cost Benefit as Desired by KPT

As per KPT, benefit of 16% of total construction cost is desired. The revenue is calculated by assuming certain parking cost for different traffic growth and parking occupancy conditions. Net present value (NPV) is determined taking into consideration of inflation rate as 5% and discount rate as 12% and accordingly the parking cost is adjusted so as to obtain NPV equal to the value that obtained by 16% of total construction cost.

2.2 Based on Assumed Rates of User Charges

The revenue as per BOT is calculated as Net Revenue = (Total revenue – annuity). Annuity to be paid annually = $\frac{r(1+r)^n}{(1+r)^n - 1} \times \text{Present benefit}$ where r = rate per period and n = no of years. This revenue is used for the determination of BEP.

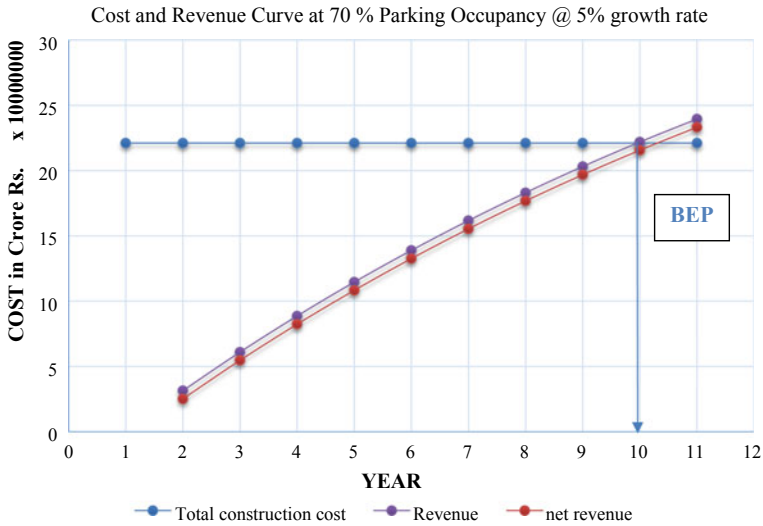


Fig. 1 BEP for 70% parking occupancy @ 5% growth rate

The methodology adopted for the same is as per Fig. 1.

The parking prices are changed annually assuming the parking price growth rate as 5%. In the next stage, the parking price changes phase-wise, i.e., from the construction period to horizon period, three phases were considered and each phase consists of 3 years each. The parking price within the phase is kept constant. The last case considered is that the parking price is kept constant throughout the horizon period for all the parking occupancies and for all the traffic growth rates.

3 Financial Analysis of Truck Terminal Parking

Case-I Based on a benefit of 16% of total construction cost and maintenance cost as desired by Kandla Port Trust

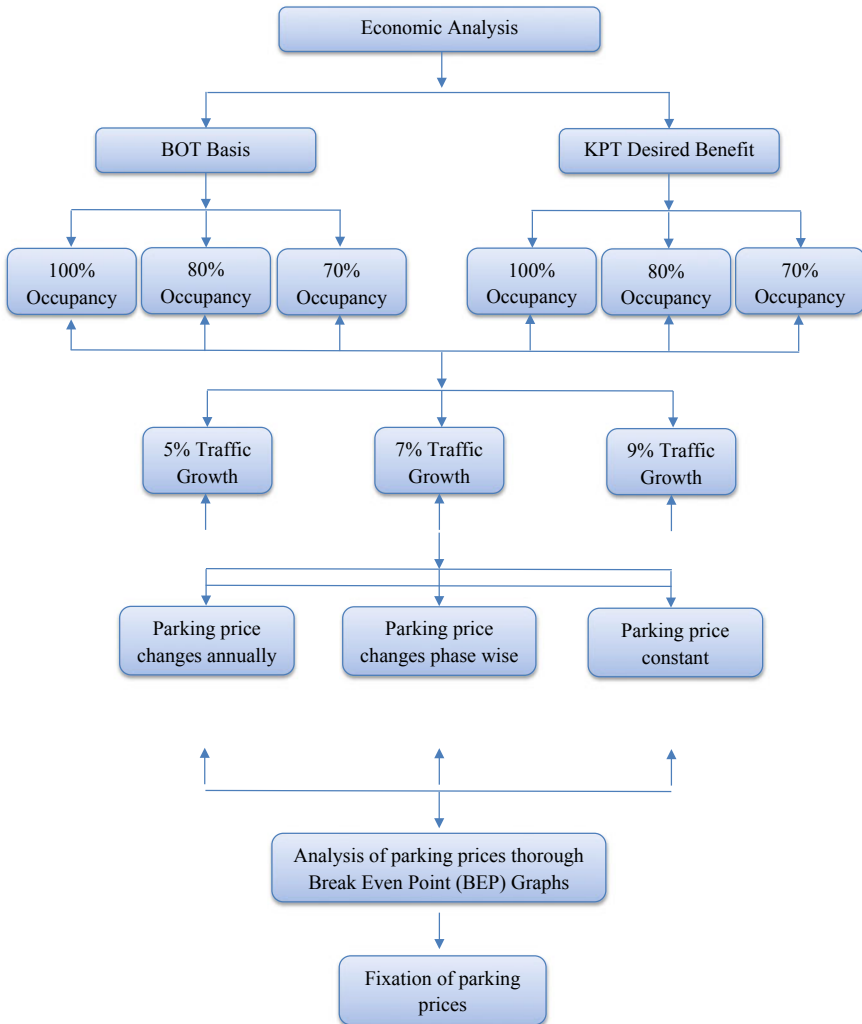
$$\begin{aligned} &\text{Total construction + maintenance cost (discounted cost)} \\ &= 22 \text{ cr. for 7 and 5\% growth rate} \end{aligned}$$

$$\text{Total construction + maintenance cost (discounted cost)} = 23 \text{ cr. for 9\% growth rate}$$

$$\begin{aligned} \text{Total benefit desired by KPT} &= 16\% \text{ of total construction} \\ &+ \text{maintenance cost (discounted cost)} \\ &= 3.54 \text{ cr. (for 5 and 7\%)} \text{ and } 3.63 \text{ cr. (for 9\%)} \end{aligned}$$

To opt the desired benefit parking prices was fixed such that a benefit of 3.54 cr. for 5 and 7% traffic growth rate and 3.63 cr. for 9% traffic growth rate can be achieved. Revenue calculated from the traffic in parking facility is calculated by their staying period and type of the vehicle.

Analysis for financial evaluation at 5% growth rate for 70% parking occupancy is shown in Table 1. Similar analysis is carried out for all the cases and net present values are calculated (Table 2).



These parking charges are fulfilling the criterion for the worst case which is parking price constant (case-III) for 70% parking occupancy @ 5% growth rate.

Case-II based on analysis done for built operate and transfer (BOT) basis

Table 1 Analysis for financial evaluation @ 5% growth rate for 70% occupancy

Sl. no.	Year	Cost of construction (outflow)	Discounted construction cost	Maintenance coat (outflow)	Discounted maintenance cost	Total discounted cost	Revenue (inflow)	Discounted revenue	Net benefit (NPV)
		Col. 1	Col. 2 = (Col. 1/1.12 ⁿ)	Col. 3	Col. 4 = (Col. 3/1.12 ⁿ)	Col. 5 = Col. 2 + Col. 4	Col. 6	Col. 7 = (Col. 6/1.12 ⁿ)	Col. 8 = Col. 5 - Col. 7
1	2016-17	16.22	16.22	0.000		16.217	0.000	0.000	-16.217
2	2017-18			0.061	0.054	0.054	3.799	3.392	3.338
3	2018-19			0.064	0.051	0.051	3.989	3.180	3.129
4	2019-20	4.39	3.12	0.067	0.048	3.169	4.188	2.981	-0.188
5	2020-21			0.070	0.045	0.045	4.398	2.795	2.750
6	2021-22			0.074	0.042	0.042	4.617	2.620	2.578
7	2022-23	4.68	2.37	0.077	0.039	2.409	4.848	2.456	0.047
8	2023-24			0.081	0.037	0.037	5.091	2.303	2.266
9	2024-25			0.085	0.034	0.034	5.345	2.159	2.124
10	2025-26			0.090	0.032	0.032	5.613	2.024	1.992
11	2026-27			0.094	0.030	0.030	5.893	1.897	1.867
			22		0.412	22			Total NPV = 3.686

Table 2 Parking charges for all possible cases as per KPT desired benefit

Sr. no.	Retention time (h)	Year	Parking prices at very first year and last year of parking facilities (INR)								
			Trucks			Tailors			Tankers		
			<1 h	3 h	>5 h	<1 h	3 h	>5 h	<1 h	3 h	>5 h
1	Case-I Parking price annually changes	2017-18	25	30	35	30	35	40	30	35	40
		2026-27	39	54	70	47	62	78	47	62	62
2	Case-II Parking price changes phase-wise	2017-18	25	30	35	30	35	40	30	35	40
		2026-27	43	51	60	51	60	68	51	60	60
3	Case-III Parking price constant	2017-18	25	35	45	40	50	60	40	50	60

Discounted construction cost and maintenance cost of the project is same as in case-I and revenue calculation has been done based on the assumed parking price.

Annuity to be paid annually is calculated as given in IRC: SP-30:

$$\text{Annuity to be paid annually} = \frac{r(1+r)^n}{(1+r)^n - 1} * \text{Present benefit}$$

where,

r = Rate per period and n = No. of years.

Annuity calculated from above formula is found to be 63 lakhs Rs. per year for the period of 10 year. Calculation of net revenue as (total revenue-annuity) has been calculated as shown in Table 3. Accordingly, net revenue for all the cases has been calculated.

Break-even point (BEP) has been calculated from graphical representation for one case as shown in Fig. 1. Accordingly, for all the cases, BEP has been found.

Parking prices which has been fixed to get BEP before the completion of project is as shown in Table 4 (Fig. 2).

4 Conclusion

The financial evaluation of the project is carried out considering three growth scenarios: normal, optimistic, and pessimistic with three levels of occupancy (100, 80, and 70%). Three patterns of parking charges are also considered for providing useful tool to the policymakers for implementing the project. The proposed project of Truck Terminal at Kandla Port is found to be feasible financially with positive NPV for all the possible scenario and implementation options. For all the possible options, the worst cases of 70% occupancy @ 5% of growth rate it is found to be satisfactory. The project can be implemented on PPP basis either on the basis of lease or concession.

Table 3 Analysis for financial evaluation @ 9% growth rate for 70% occupancy (constant price)

Sr. no.	Year	Cost of construction (outflow)	Discounted construction cost	Maintenance cost (outflow)	Discounted maintenance cost	Total discounted cost	Total cumulative cost (construction + maintenance cost)	Revenue (inflow)	Cumulative revenue	Discounted revenue	Discounted cumulative revenue	Net benefit (NPV)	Amnity	Net revenue = revenue discounted (inflow) – Amnity
		Col. 1	Col. 2 = (Col. 2/1,12 ⁿ)	Col. 3	Col. 4 = (Col. 3/1,12 ⁿ)	Col. 5 = (Col. 2 + Col. 4)	Col. 6 = Col. 1 + Col. 3	Col. 6	Col. 7	Col. 8 = (Col. 6/1,12 ⁿ)	Col. 9 = (Col. 7/1,12 ⁿ)	Col. 10	Col. 11	Col. 12 = Col. 8 – Col. 11
1	2016–17	16.22	16.22	0.0000	0	16.217	16.22	0	0	0	0	-16.217	0	0
2	2017–18			0.0606	0.054	0.054	16.28	3.09	3.098	2.77	2.77	2.712	0.63	2.14
3	2018–19			0.0636	0.051	0.051	16.34	3.54	6.64	2.83	5.59	2.774	0.63	6.01
4	2019–20	4.39	3.12	0.0668	0.048	3.169	19.53	4.05	10.69	2.89	8.48	-0.284	0.63	10.07
5	2020–21			0.0701	0.045	0.045	19.60	4.63	15.33	2.95	11.42	2.902	0.63	14.70
6	2021–22			0.0736	0.042	0.042	19.67	5.30	20.63	3.01	14.43	2.968	0.63	20.01
7	2022–23	4.68	2.37	0.0773	0.039	2.409	22.12	6.06	26.70	3.07	17.51	0.665	0.63	26.07
8	2023–24			0.0812	0.037	0.037	22.20	6.94	33.64	3.14	20.65	3.103	0.63	33.01
9	2024–25			0.0852	0.034	0.034	22.29	7.93	41.58	3.21	23.85	3.172	0.63	40.95
10	2025–26			0.0895	0.032	0.032	22.38	9.08	50.66	3.28	27.13	3.243	0.63	50.04
11	2026–27			0.0940	0.030	0.030	22.47	10.38	61.05	3.35	30.47	3.315	0.63	60.43
												Total NPV (cr.) = 8		

Table 4 Parking charges for possible cases as per BOT
 Parking prices at very first year of opening of parking facilities (INR)

Sr. no.	Retention time (h)	Years	Trucks			Tailors			Tankers				
			<1 h	3 h	>5 h	<1 h	3 h	>5 h	<1 h	3 h	>5 h		
1	Case-I Parking price annually changes	2017-18	20	30	40	30	40	50	30	40	50	30	40
		2026-27	31	47	62	47	62	78	47	62	78	47	62
2	Case-II Parking price changes	2017-18	20	30	35	30	35	40	30	35	40	30	35
		2026-27	34	51	60	51	60	68	51	60	68	51	60
3	Case-III Parking price constant	2017-18	30	40	45	35	40	50	35	40	50	35	50

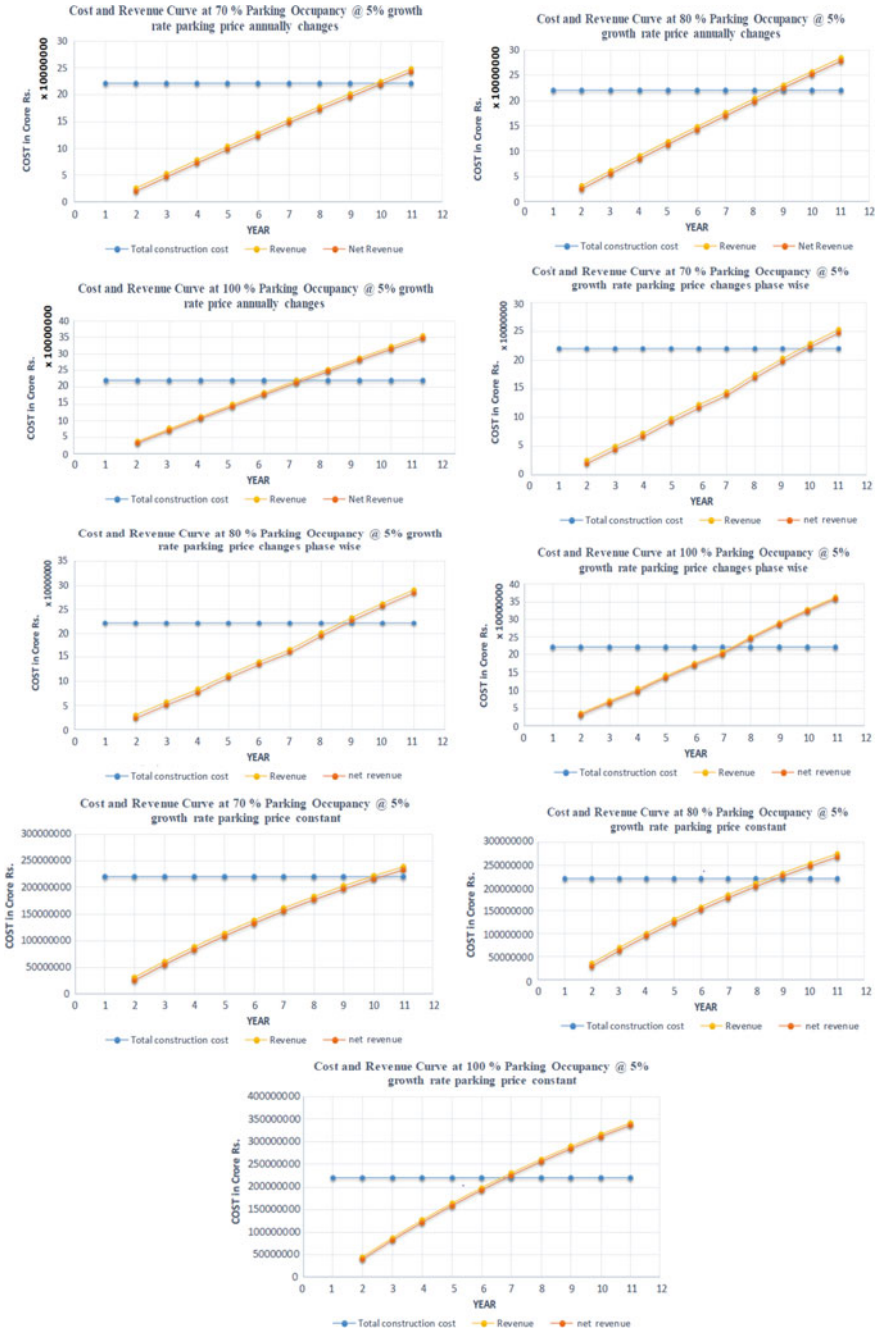


Fig. 2 Graphs for BEP of all cases, i.e., for parking price changing annually, phase-wise and as constant

References

1. IRC SP: 30: Manual on economic evaluation of highway projects in India
2. Schedule of Rates (2016) Kandla Port Trust
3. Dutta BN. Estimation and costing in civil engineering. UBS Publishers

Walking and Bicycling to School—Understanding the Impact of Socio-economic Factors and Built Environment



Kuldeep Kavta and Bhargav Adhvaryu

Abstract Unlike western countries, there has been very limited research related to mode choice for school children in India. The sharp decline in the use of non-motorized transport (NMT) in developed countries has been the motivation behind such studies. The hypothesis of the same trend in India cities was tested in this study. The results were quite alarming as it showed a fall of 46% in NMT use for the school trip. The paper explores mode choice literature on for school-going children and also the studies relating NMT use with the health. Investigation of mode choice for school children in India was carried out based on two major perspectives namely socio-economic attributes of the parents and built environment. Survey of 526 parents was carried out from different primary schools in the study area and a multinomial logit (MNL) model was developed. The factors like vehicular ownership, school distance, education level of parents, type of school, and standard of child proved significant for the mode choice of children in this model. The analysis for the effect of built environment factors and its effect on NMT use was separately conducted. The results of this analysis showed that 54% parents did not feel safe to send their children to school by walk or cycle and the primary reasons stated were “long distance to school” and “crime and safety”. Since long distance proved to be a major factor for creating a disutility for NMT mode, a binary logit analysis was done to find the probability of NMT use. The result shows that the breakeven distance is 2.3 km, at which the probability of usage of motorized vehicle and non-motorized vehicle becomes the same. The paper concludes with the recommendations based on the result of the study and future prospects of work that can be done.

Keywords Multinomial logit model · Mode choice · Non-motorized transportation · School children mobility

K. Kavta (✉)
Indian Institute of Technology Kharagpur, Kharagpur, India
e-mail: kavta.kuldeep@gmail.com

B. Adhvaryu
CEPT University, Ahmedabad, India
e-mail: bhargav@cantab.net

1 Introduction

Mode choice for school-going children has been widely researched in the developed countries [1–3]. The need for these types of studies was instigating not just from transportation perspective, but also because of economic and social issues occurring because of the decline in walking and cycling. Most importantly the seriousness of this decline of NMT modes in school-going children was discussed from the health perspective. Walking and cycling for short trips are considered to be a very important form of physical exercise for improving the health and keeping obesity in check [4, 5]. McMillan [6] argues that while mode choice among children is obviously a transport issue, it is also the health issue. Therefore, associated health and social benefits must also be kept in mind while discussing the use of NMT as a mode for transport for school children. Bearing in mind the socio-economic implications along with the transportation perspective of reduced NMT share, it becomes necessary to check if the same problem is happening in India. If the hypothesis of reduction in the NMT share in Indian cities is accepted, then it is of utmost importance to understand the reasons. Understanding of the causes and relationships of such variables will be helpful in devising solutions for sustainable mobility in the Indian context.

2 Literature Review

The study requires the identification of variables to be used in the analysis for understanding the relationships between the variables and the mode choice. Most of the research has been considering the trip characteristics, built environment and socio-economic aspects in mode choice studies. Black et al. [7] state that the choice of travel mode for the school trip is an integral part of the household decision-making process. Continuing on the same lines, Seraj et al. [8] suggest that the attitudes and perceptions of parents towards walking and bicycling play a crucial role in deciding which travel modes children use. Considering the direction in which the recent literature points out, it becomes a new area to study the role of parent's socio-economic characteristics on a child's mode choice apart from other traditional attributes. This new dimension of study becomes even more interesting when the context of the study becomes specific to Indian cities. Indian cities are very different from other cities in developing countries due to its dense mix built up spatial property, transportation systems and the trip characteristics. Along with the differences in physical character, the social demographic economic aspects of the people in Indian cities differ significantly in comparison with people in developed countries. These differences in the aspects and the intricacies among them make the study of child mode choice to school in India considerably unique.

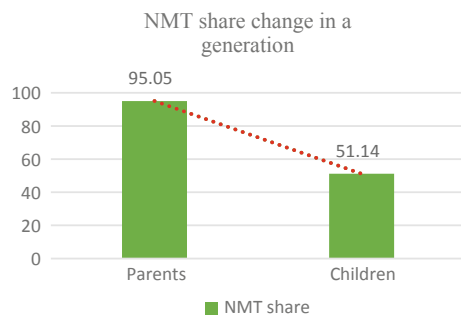
A general observation in Indian cities is that a few decades back most of the children walk or cycled to school. Walking and cycling gave the opportunity to explore the surrounding environment along with health benefits. Rapid urbanization in the

last few decades resulted in urban sprawl (mainly resulting from households preferring peri-urban areas for housing) which consequently increased the motor vehicles and made the lifestyle oriented to private vehicles like cars and two wheelers. This has affected the scenario in two ways—firstly, the distance to school on average has increased and secondly, higher intensity of vehicles has increased the probability of accidents. This gets worse as most cities do not have proper footpaths and crossings for safe movement. It is argued that traffic congestion will worsen and more children will be chauffeured by parents [7, 9, 10]. School trips have become more dependent on parents due to the change in the cities owing to rapid urbanization in the last decade. Apart from the increase in dependency of child on parent, the changes in the built environment due to urbanization are also an area to understand and intervene. The results by Shokoohi et al. [11] reveal that parents and children with negative perceptions of neighbourhood safety tend to use motor vehicles or to escort their children while walking to and from school. With this background, it becomes necessary to check whether the rapid urbanization has reduced the use of NMT for school trips over the years or is it unchanged?

3 The Change in a Generation

As discussed in the preceding section, it is important to check whether the tendency of decrease in NMT use is prevalent in India as it is in the case of developed countries. The result of the study gave a clear alarming indication about the current trends. When compared, the NMT use 25–30 years ago and now the results confirmed the drastic decrease. The share of cycling and walking when parents used to go to school was 95.05%, and now it has reduced to 51.14%. So, an overall decrease of NMT use is 46.2% in a generation, i.e., in a period of around 25–30 years (Fig. 1). If we compare the scenario in USA, walking and bicycling represented 87% of all trips to school of less than one mile in 1969 and the automobile accounted for only 7% of trips. Conversely, by 2001, 36% of trips to school less than one mile were automobile trips, while the percentage of walk/bike trips had dropped to 55% [12]. So in a period of around 30 years, Indian cities saw a decline of 46.2%, while in the same duration

Fig. 1 NMT share change in a generation



USA saw a decline of 58.62%. Similar trends were seen in Britain where the increase in car use was at the cost of walking and cycling [9]. Although in percentage terms it looks that the decline is less in India than USA but in absolute terms, it will be much higher due to the large population in India. The decline in the NMT share is obtained from our sample and this value cannot be extrapolated directly to the entire country since many other factors need to be taken into account while predicting for the entire population. But, this value can be taken as a starting point to understand the shift and can be taken as a base for estimating for the population which is not in the scope of this study.

The decrease in NMT is a serious problem because as discussed earlier mode for the child is not just a transport problem, but it is directly related to health. The evidence clearly shows that lack of physical activity can lead to a number of adverse health conditions including obesity [13]. Also, the decrease from NMT mode must have shifted to the motorized mode which has many economic and social implications like congestion, cost, environmental pollution, etc. Thus, it becomes important for transport professionals to look into the problem, analyse it and give policy recommendations to improve the scenario. Understanding the factors that influence the mode choice of school-going children can help us to improve the modal share implementation.

4 Mode Choice Modelling

The objective of this analysis is not to obtain the future predictions of modal share; it is solely meant for understanding the influential factors so that a preliminary understanding can be developed from it for doing improvement in the existing situation.

4.1 Study Area and Data Collection

The study area selected for this analysis is Anand city in Gujarat. It lies between two metropolitan cities Ahmedabad and Vadodara and is well known as a knowledge hub in the state. The Anand metropolitan area has a population of 2.8 lakh as per 2011 Census of India and it encompasses the fast-growing belt of Anand-Vidyanagar-Karamsad burgeoning with economic activities. The study area has around 50 primary schools ranging from government schools to high-end private schools. The urban pattern and the socio-economic characteristics of the city could be considered similar to many Indian cities.

The data was collected from the parents of the school-going children, and the survey form was designed in local language for giving a better understanding to the parents. The survey form had three parts: first part contained the details of parents, the second part about the details of child and school and the third part about the built environment. A total of 526 samples were collected from 30 schools in the

region using proportionate stratified sampling. The schools are divided into two strata (government and private) and sampled based on the proportion of school in each stratum. The scope of the study was limited to primary schools having children aged below 15 years.

4.2 Model Formation

From the discussions in the literature review section the two dimensions namely “parent’s socio-economic” and “built environment” needs to be examined when it comes to mode choice for school-going children. Socio-economic characteristics like income, vehicular ownership, age, gender, number of children, income, education level, and number of children have been used in similar studies. Along with socio-economic characteristics, the variables related to the child were also included in mode choice modelling. These variables included the age of the child, type of school, standard and school timing. The variable “type of school” and “school timing” was considered to be related to child for model simplicity purpose. The analysis of impact of the built environment was not included in mode choice modelling and was done separately. All the variables were taken as an input to the mode choice model, and finally, the model was derived based on the significance (CI = 95%).

In this case, the regressand (outcome variable) is unordered and nominal namely NMT (non-motorized transportation, i.e., walking/cycling), private vehicle and public transport. For the probabilistic modelling of such unordered nominal regressand, multinomial logit model is extensively used [14]. McFadden developed the multinomial logit (MNL) model to explain choices made among alternatives when the nature of the choice is probabilistic [15]. The model is based on principal of utility maximization where utility is given as $U_{nj} = V_{nj} + E_{nj}$ where V_{nj} is deterministic part and E_{nj} is probabilistic part. The probability of choosing a mode j is given by the equation below:

$$\Pr(j) = \frac{\exp(V_j)}{\sum \exp(V_i)}$$

V_j = Utility of mode j

V_i = Utility of all modes, i from 1 to n where n is total number of mode.

The statistical modelling part was done using the SPSS software.

4.3 Model Fitting Information and Likelihood Tests

See Table 1.

Pseudo R -square

The presence of a relationship between the dependent variable and a combination of independent variables is based on the statistical significance of the final model chi-square in Table 1. The null hypothesis that there is no relationship between independent and dependent variables was rejected. The alternative hypothesis, i.e. a relationship between the independent variables and the dependent variable was accepted. The pseudo *R*-square values show a decent fit of the overall model. Variable like home to school distance (C HS DIS in km), school type (C STYP; 0 = public, 1 = private), vehicular ownership (V OWN; 0 = no, 1 = yes), parents' education level (P EDU; 1 = primary, 2 = higher secondary, 3 = graduate), and child's standard (grade) (C STD; 1 = 1-2, 2 = 3-5, 3 = 6-8) proved to be significant to the mode choice of school-going children. The significance test of the variable is at 95% confidence interval (Table 2).

4.4 Simple Descriptive Statistics

The charts give a brief idea about the data collected (Fig. 2). The graphs depict the mode choice of school-going children with respect to the factors that have proved to be significant at 95% confidence level in the multinomial logit model. The detailed interpretation of the data is done in the later part of the paper, but these descriptive data gives the broader idea about the mode choice. Few direct interpretations can be made from the data to understand the preference of choices for different groups. For example, a clear dominance of motorized transport in the private schools as compared to the government schools was observed. Higher educated parents seem to prefer sending their children to school in motorized vehicles in comparison to NMT.

Table 1 Model fitting

Model	Model fitting criteria	Likelihood ratio tests		
	-2 log likelihood	Chi-square	df	Significance
Intercept only	692.988	0	0	
Final	458.595	234.392	14	0.000
C HS DIS	502.249	43.654	2	0.000
C STYP	491.142	32.547	2	0.000
V OWN	504.939	46.343	2	0.000
P EDU	473.421	14.825	4	0.005
C STD	481.557	22.962	4	0.000

Table 2 Pseudo *R*-square

Cox and Snell	0.360
Nagelkerke	0.418

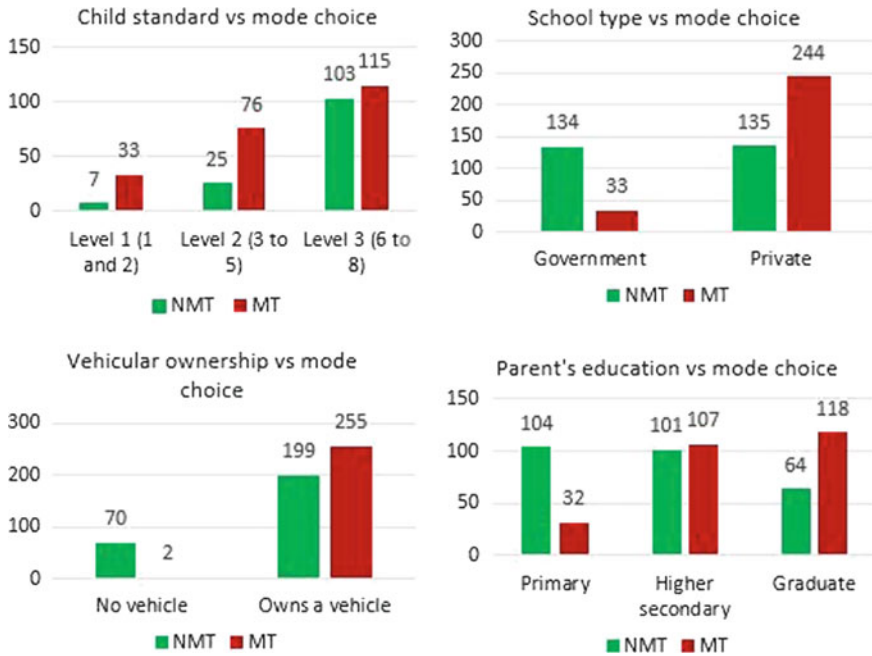


Fig. 2 Simple descriptive statistics

An intuitive higher share of motorized vehicles in the families that own a car or two wheeler was seen as compared to the families that do not own a vehicle. But almost nil share of motorized transportation (MT) in the families that do not own cars and two-wheelers gives impression that these families prefer to send their children by NMT rather than motorized public transport if given a choice between these two modes. The detailed explanation is discussed in the subsequent section.

4.5 Parameter Estimates and Results

As shown in Table 3, β is the coefficient of the variables included in the model. It helps to understand the nature of relationship between the dependent and the independent variable. The negative sign of β for home to school distance shows that the increase in home to school distance results in decrease of the odds of choosing NMT $\text{Exp}(\beta) = 0.762$ which means that increase in the home to school distance decreases the odds of choosing NMT in comparison to private vehicles. With the increase in distance from home to school by 1 km, the odds of choosing private vehicle increases by a factor 1.3 times while odds of choosing NMT reduces by a factor of 0.762. Children in government school go to school majorly using NMT modes as compared to children in private schools. The probability of choosing NMT

Table 3 Parameter estimate

Mode	Variable	β	Exp(β)
NMT	Intercept	1.311	
	C HS DIS	-0.272	0.762
	C STYP = 0	2.087	8.060
	C STYP = 1	0 ^b	
	V OWN = 0	21.511	2,198,823,882
	V OWN = 1	0 ^b	
	P EDU = 1	1.230	3.420
	P EDU = 2	0.313	1.368
	P EDU = 3	0 ^b	
	C STD = 1	-1.400	0.247
	C STD = 2	-1.207	0.299
	C STD = 3	0 ^b	
	Public transport	Intercept	0.603
C HS DIS		0.066	1.068
C STYP = 0		0.930	2.535
C STYP = 1		0 ^b	
V OWN = 0		18.450	102,940,441.0
V OWN = 1		0 ^b	
P EDU = 1		0.188	1.207
P EDU = 2		0.223	1.250
P EDU = 3		0 ^b	
C STD = 1		-0.252	0.777
C STD = 2		-0.318	0.728
C STD = 3		0 ^b	

^bIndicates the base level

in government school children is roughly eight times higher than private school children. This can be directly related to the income level of parents whose children go in government school to the income level of parents whose kids go in private schools. Vehicular ownership has a significant impact on mode choice of school-going children. If parents do not own a vehicle, then log odds of choosing NMT are very high. Also, a particular behaviour is observed here that if a family does not own vehicle, then odds of choosing NMT are higher than choosing public transport. The reason could be that families who do not own a vehicle are unable to afford public transport (which includes van, auto rickshaw, city bus, and school bus). The second reason might be that public transport does not seem to be a safer option due to deterrents like overcrowding or accidents.

As parents' education level increases from primary to graduate level, the odds of choosing NMT for their child decreases. The likelihood of choosing NMT over

private transport decreases with increase in education level from primary education to graduate level education. Parents with education level up to secondary school prefer using public transport over private for their children. If parent's education level is secondary, likelihood of choosing public transport for their children will be 1.25 times of choosing private, while for primary-level education, it will be 1.207 times of the same. Higher standard children use public transport more than lower standard with reference to private mode. Lower standard children use private modes more than public transport that is they are escorted on private vehicles by parents. Also, the reason of sending the higher standard student to school by public transport may be that parents feel that child is mature enough to use public transport.

5 Analysis Related to Built Environment

As discussed earlier, the impact of the built environment on mode choice of school-going children is of utmost importance to understand the rapid change in built environment and subsequently the decreasing from the NMT share. Before beginning this analysis, a generic question was asked about parents' perception for sending their child to school on cycle or walking. Out of 526 responses, 46% felt that it was safe to send their children to school by NMT while 54% felt unsafe. The next question that was asked to them was regarding the built environment factors that make them feel unsafe. Total five factors namely—unavailability of footpaths, unavailability of dedicated cycle lanes, long distance, crime/accidents, and others were given to respondents, out of which two factors “accident/crimes” and “long distance to school” turned to be most significant. Out of 283 people that felt unsafe to send their children to school by cycle or walk 38% felt long distance responsible for their fear and 63% felt accidents and crime as the responsible factor.

Since parents considered “long distance to school” as a factor for feeling unsafe to send their children on cycle or walk to school, it is intriguing to identify the distance at which confidence is regained in NMT mode so that a good share of NMT can be achieved. In order to find this breakeven distance for the NMT use, a binary logit analysis was applied and probability of using NMT was found with respect to distance of the school. The graph shows the home to school distance and probabilities of using NMT (Fig. 3). It was found that after a distance of around 2.3 km, mode shift occurs from NMT to motorized mode. This is useful for planner when doing neighbourhood/local area planning.

6 Recommendations and Conclusion

The principal objective of the study was to understand the effect of socio-economic characteristics of parents and characteristics of the built environment on mode choice of school-going children. The literature review in the study established the need to

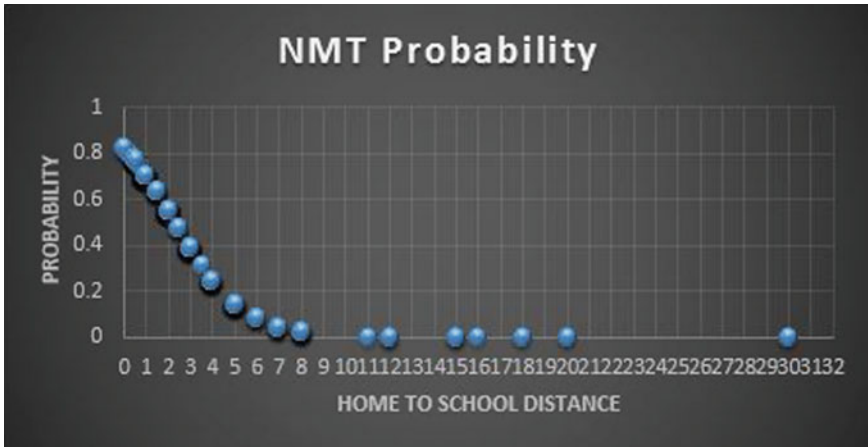


Fig. 3 NMT probability

view NMT not merely as a transport mode since walking and bicycling to school has many other positive externalities attached to it such as health. After understanding the importance of NMT, the study proceeds with a generational analysis to detect if there is a fall in the share of NMT for going to school over the years. The result of this analysis was alarming as a sharp fall of 46.3% was detected over change in a generation, i.e. in time duration of around 25–30 years. Similar trends were also seen in developed countries like USA in the last decade. In order to identify the influential factors related to parents and child that affected mode choice, a multinomial logit model was developed. The result and interpretation of the mode choice modelling can help to form a base for further research on school-going children especially in developing countries like India. Apart from developing a mode choice model, a study on built environment was carried out for understanding the influence of built environment on mode choice, where the perception of parents towards the safety at using NMT as a mode for their children was analysed. The negative attitude towards NMT use was mainly attributed to factors like “long distance to school” and “crime or accidents”. The long distance to school was also an influential factor in the multinomial logit model, so in order to find the breakeven distance and the probability of NMT use, a binary logit model was developed. The result of this model showed that there was a shift to motorized mode from non-motorized modes when the distance to school is beyond 2.3 km. This result can be used to in making local area plans. It is recommended to develop a detailed concept of neighbourhood schools that serve the population of the particular neighbourhood based on breakeven distance. This concept was briefly discussed by Ewing et al. [16]. Also to neutralize the negative perception because of safety issues, a programme in like ‘Safe route to schools’ [17] should be developed in the Indian context.

References

1. McDonald NC (2008) Household interactions and children's school travel: the effect of parental work patterns on walking and biking to school. *J Transp Geogr* 16(5):324–331. <https://doi.org/10.1016/j.jtrangeo.2008.01.002>
2. McMillan TE (2007) The relative influence of urban form on a child's travel mode to school. *Transp Res Part A Policy Pract* 41(1):69–79. <https://doi.org/10.1016/j.tra.2006.05.011>
3. Pucher J, Dijkstra L (2003) Promoting safe walking and cycling to improve public health walking and cycling: the MOST sustainable transport modes. *Am J Public Health* 93(9):1509–1516. <https://doi.org/10.1016/j.yjmed.2009.07.028>
4. Lee C, Zhu X, Yoon J, Varni JW (2013) Beyond distance: children's school travel mode choice. *Ann Behav Med* 45(suppl_1). <https://doi.org/10.1007/s12160-012-9432-z>
5. Saelens BE, Sallis JF, Frank LD (2003) Environmental correlates of walking and cycling: findings from the transportation, urban design, and planning literatures. *Ann Behav Med* 25(2):80–91. https://doi.org/10.1207/S15324796ABM2502_03
6. McMillan TE (2005) Urban form and a child's trip to school: the current literature and a framework for future research. *J Plan Lit* 19(4):440–456. <https://doi.org/10.1177/0885412204274173>
7. Black C, Collins A, Snell M (2001) Encouraging walking: the case of journey-to school trips in compact urban areas. *Urban Stud* 38(7):1121–1141
8. Seraj S, Sidharthan R, Bhat C, Pendyala R, Goulias K (2012) Parental attitudes toward children walking and bicycling to school: multivariate ordered response analysis. *Transp Res Rec* 2323:46–55
9. Mackett RL (2013) Children's travel behaviour and its health implications. *Transp Policy* 26:66–72. <https://doi.org/10.1016/j.tranpol.2012.01.002>
10. Wen LM, Fry D, Rissel C, Dirkis H, Balafas A, Merom D (2008) Factors associated with children being driven to school: implications for walk to school programs. *Health Educ Res* 23(2):325–334. <https://doi.org/10.1093/her/cym043>
11. Shokoohi R, Hanif NR, Dali M (2012) Influence of the socio-economic factors on children's school travel. *Procedia Soc Behav Sci* 50(July):135–147. <https://doi.org/10.1016/j.sbspro.2012.08.022>
12. McDonald N (2005) Getting to school: the impact of free transit on low income and minority students. In: Annual meeting of the transportation research board
13. Department of Health, Physical Activity, Health Improvement and Protection (2004) At least five a week—evidence on the impact of physical activity and its relationship to health. *Nutr Bull* 29:350–352. <https://doi.org/10.1111/j.1467-3010.2004.00455.x>
14. Gujarati DN (2004) Basic econometric. New York. <https://doi.org/10.1126/science.1186874>
15. Mcfadden D (1980) Econometric models for probabilistic choice among products. *J Bus* 53(3):S13–S29
16. Ewing R, Schroerer W, Greene W (2004) School location and student travel: analysis of factors affecting mode choice. *Transp Res Rec* 1895(1):55–63. <https://doi.org/10.3141/1895-08>
17. Safe Route to School (n.d.) Retrieved 12 May 2017, from <http://www.saferoutesinfo.org/>

The Effects of Mixed Land Use on the Household Travel Behavior: A Case Study of Agartala, Tripura



Neetu Choubey, Amitabha Acharjee and P. P. Sarkar

Abstract In today's time, there is a growing concern over managing the traffic on Indian roads. From smaller two or three-tier cities to big metropolitan cities, the traffic problem is prevalent. It is especially becoming more challenging day by day as there has been a vast shift of interest of people from public transit or non-motorized modes to private automobiles; the reason of this momentous change could be urbanization, economic growth of the country or the ease in the affordability of vehicle by an individual, nowadays. Recently, this concern has grabbed many researchers' attention. From the pool of many possibilities, one solution could be to discourage the use of private automobiles through imposing some restrictions or providing such kind of neighborhood where a person feels constrained to use the private vehicle. There are plenty of studies available which have analyzed the correlation between land use parameters and trip length before; nonetheless, due to the peculiarity of land use development and mixed traffic conditions in India, it is not viable to implement those procedures without inculcating India's characteristics. Through this study, we are making our best efforts, while keeping the Indian traits in mind, to find the impact of the built environment on the travel behavior of the people. Agartala capital of Tripura, a city in the northeastern part of India, has been selected for this case study. Models have been prepared with slightly modified indices, which encompass the anomaly of Indian land use development, for studying the effect of land use parameter in explaining the variability of trip length as well as the behavioral mode choice. The correlations unfolded through these models were found to be significant and could be used for planning of efficient urban transportation system. The modified indices, to no small extent, were satisfactory in explaining the pattern of the household travel behavior based on their neighborhood development.

N. Choubey (✉) · A. Acharjee · P. P. Sarkar
National Institute of Technology Agartala, Agartala, Tripura, India
e-mail: Neetuchoubey1@gmail.com

A. Acharjee
e-mail: amitabhaacharjee1990@gmail.com

P. P. Sarkar
e-mail: ps_sarkar@yahoo.co.in

Keywords Land use · Trip length · Mode choice · Travel behavior · Mixed land use indices · Regression modeling

1 Introduction

The effects of the automobiles on everyday life have been a controversy. While the introduction of this system, on one hand, has given us an immense comfort in mobility, on the other hand, it is also one of the pivotal reasons behind the disconnection in community or social isolation, rise in obesity, the generation of air and noise pollution, urban spread out and overall urban decay. Due to urbanization, the increase in automobiles usage is inevitable. In India, from small cities to big metro cities like Delhi and Kolkata are facing traffic-related problems such as congestion, jams, and lack of infrastructure for parking. The increase in usage of automotives is an integral part of the development and therefore difficult to mitigate; nevertheless, with the proper planning, this can be channelized toward a better outcome for the society. Out of all the automobiles usage, use of private automotives is most prevalent and has a big contribution toward the cons side of automation. Increase in private automobile ownership leads to traffic congestion, which again leads to an increase in the demand of the transportation pathways and also overall affects the balance between number of vehicle and road length.

There are studies that support the fact that transport infrastructure influences the urban development trends and residential location choices; in addition to that, suggestions have also been made on the fact that changing land use influences the trip lengths, travel time, destinations, and modes to be chosen. This proves that travel patterns and land use are closely intertwined and the models used to solve transportation planning issues need to be incorporated with land use models in order to support the conclusion drawn. Frank and Pivo [1] have used the data from the 1989 Puget Sound Transportation Panel and inferred that urban density and land use mix both influence mode choice for both work and shopping trips after controlling for household type. They have used entropy index to describe the evenness of the distribution of built square footage, among seven land use categories. It was found that the increase in land use mix increases the use of transit and walk mode. They have also suggested that using both the land use parameters, at origin and destination tracts, give better result rather considering only at the origin.

According to a report by the Ministry of Urban Development, Government of India (2008) share of private transport is 57% in 2007 which is predicted to go up to 71% by 2031 [2]. To draw the attention of people toward the other side of the spectrum of vehicle usage, there is an obvious need to revolutionize the transit system of the country; however, just improvisation of public transport won't be of much help unless we discourage the use of private automobiles. Various parameters have been unfolded through this study of that have an influence on the travel behavior of an individual household, the critical ones being, and socioeconomic factors such as age, gender, income, and education qualification. Another important factor which

unfurled while studying about factors influencing travel behavior hence making this study noteworthy is the neighborhood built environment or surrounding locality.

2 Study Area and Data Collection

Agartala, the capital of Tripura, is situated along $23^{\circ}45' - 23^{\circ}55'$ N latitude and $91^{\circ}15' - 91^{\circ}20'$ E longitude. The city of Agartala has an altitude of 12.8 m and the central portion of the city is shaped like a saucer. Agartala Municipal Corporation or AMC is the municipal body which governs and maintains the city of Agartala. AMC is divided into four zones named East, South, Central, and North zones. Each zone is subdivided into wards which are 49 in number.

In this study, the land use has been broadly divided into five categories of land uses, i.e., residential, commercial (shops, theaters, etc.) service (offices, banks, etc.), educational (schools, institutes, etc.), and social welfare (temple, orphanage, etc.). Travel data, in the form of travel diary, have been collected through a household survey conducted in the study area during January–March 2017. Sample size, in terms of households, is about 1% of the total number of households of the study area. Socioeconomic and demographic data like age, gender, educational qualification, family size, vehicle ownership, driving license holding status, and income have also been collected. The sample was found to be representing the overall travel pattern of Agartala residents. In the collected sample, 28% of the trips are non-motorized and more or less a similar figure was conveyed in a report of Ministry of Urban Development, Government of India. Statistics of sample data are given in Table 1. The modal split of the collected data is shown in Fig. 1.

Land under forest, ponds, lakes, barren land, and agriculture have been ignored. A digitalized map was created based on the above-mentioned varied land uses of the whole city with the help of GPS instrument. The latitudes and longitudes of the building, all over the study area, being used for various purposes were collected using a GPS instrument (Handheld Trimble JUNO-SB). The ground floor purpose of the building has been selected as the type of building. The dimensions of the building or an area have been taken either by tapes or simply eye estimations. Google Earth data have been used while categorizing the residential building. ARCGIS software, version 10.2, has been chosen for the land use analysis. All the data had been put in ARCGIS with the help of MS Excel. Different shape files were created for different types of buildings falling under above-mentioned land use categories based on the dimension collected, on the georeferenced images of the study area which were taken from Google Earth.

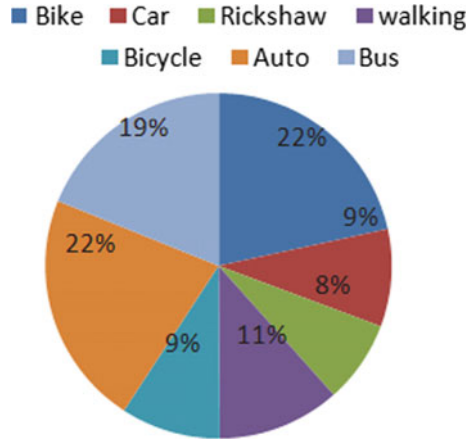
Table 1 Summary of socio-demographic data obtained from the sample

Socioeconomic Characteristic	Value (in %)
<i>Gender</i>	
Male	66.6
Female	33.4
<i>% of individual in the age category</i>	
Below 20	4
20–35	42.9
35–60	43.8
>60	9.3
<i>% of household having driving license</i>	
Having	45.5
Not having	54.5
<i>Vehicle ownership</i>	
Car ownership	12.4
MTW ownership	49.5
Bicycle ownership	22.9
<i>Monthly household income</i>	
0–2000 Rs.	3.1
2001–5000 Rs.	4.0
5001–10,000 Rs.	12.2
10,001–15,000 Rs.	4.7
15,001–20,000 Rs.	10.7
20,001–30,000 Rs.	10.9
30,001–40,000 Rs.	10.5
40,001–50,000 Rs.	14.1
50,001–70,000 Rs.	9.1
70,001–90,000 Rs.	10.3
90,001–150,000 Rs.	5.9
>150,001 Rs.	4.5

3 Mixed Land Use Analysis in the Study Area

For the land use development analysis, three indices, viz. entropy, dissimilarity, and mix-type have been chosen. These indices have been modified to embrace the peculiarity of the study area.

Fig. 1 Modal composition of sample



3.1 Entropy Index

The entropy index is a measure of land use mix which takes into account the relative percentage of two or more land use types within an area calculated using Equation one. The use of term “entropy” references an analogy to statistical mechanics, in which two bodies of a fluid will naturally mix and become integrated over time. The entropy measure was first used by Cervero [3].

$$\text{Entropy} = \sum j P_j \frac{\ln(P_j)}{\ln(j)} \tag{1}$$

where P_j is the percentage of the land use corresponding to the j th type land use. j is the total number of land use considered in the study area.

Entropy index is calculated for an individual household. 256 household data have been collected from the various parts of the study area and a buffer of 1000 m was created around each and every surveyed household, as shown in Fig. 2.

Limitations of Entropy Index

With the advantage of its simplicity, entropy index has some limitations too. Since it incorporates only proportion of different land uses without any biasness toward type of land use, it fails to differentiate if there is any change in the type of land use. For example, if the type of land purposes changes, with a proportion being the same, which eventually directly or indirectly affect the trip behavior of the area overall; nonetheless, the entropy index will still give the same value hence, failing to address this change in land use development.

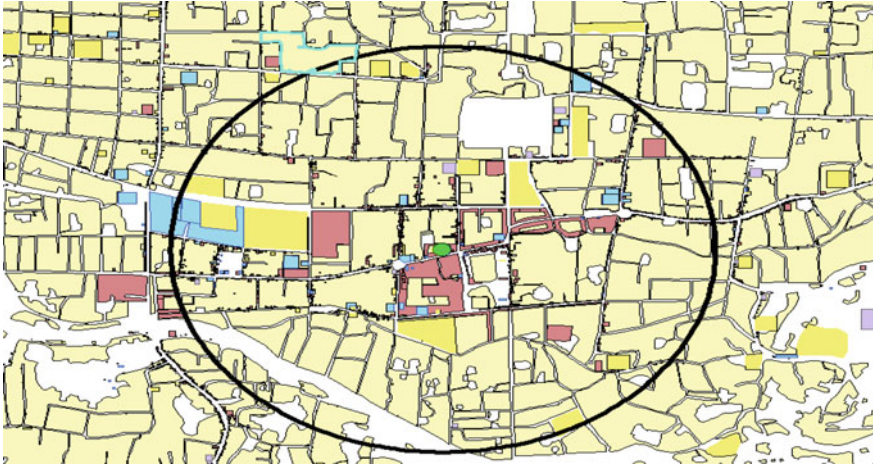


Fig. 2 A 1000 m buffer around a household

3.2 Dissimilarity Index

The dissimilarity index (DI) was used to compute the dissimilarity among the grid cells, by creating a grid cell size of 100 m. According to Cervero and Kockelman [4], the dissimilarity index is calculated based on the points awarded to each actively developed cell surrounding the considered cell based on the variation of its land use from the selected one. In a similar way, each cell was considered and all the surrounding cell is awarded a value of 1 or 0 based on the its land use variation from the subjected cell. The average of these point accumulations, across all the active cells in an area, is the dissimilarity index for that grid zone. The equation used for the calculation of DI is shown as in Eq. (2).

$$\text{Dissimilarity Index} = \sum_k \frac{1}{k} \sum_i^8 \frac{X_{ik}}{8} \quad (2)$$

where k is number of actively developed grid cells in a census tract or municipal ward.

$X_{ik} = 1$ if land use category of neighborhood differs from the grid cell.

Else, $X_{ik} = 0$.

A census grid of 1000×1000 m was created on the whole study area, and these tracts were further divided in the cell size of 100×100 m as shown in Fig. 3. The land use of a 100×100 m cell was decided on the basis of the majority of land use area covering that particular grid cell.

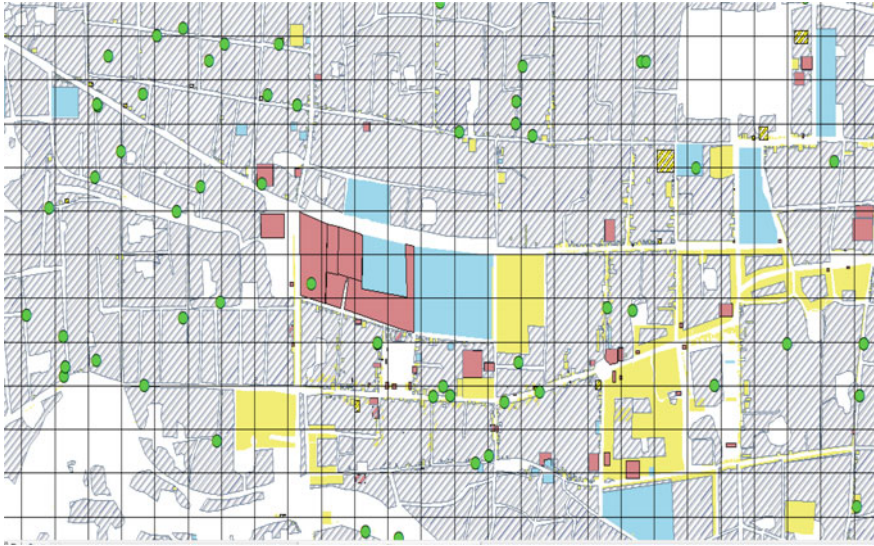


Fig. 3 Grid pattern for conventional dissimilarity index

3.3 Modified Dissimilarity Index

The dissimilarity index has slightly been modified to include the peculiarities found in the study area. Instead of finding out dissimilarity for the whole study area, DI was calculated for sampled household separately. A 2000×2000 of square buffer (1000 m around the household) was created around each and every single household and was further divided into 100×100 m cell as shown in Fig. 4.

Limitations of Dissimilarity Index

Even the dissimilarity index is unable to inculcate the type of land use mix. For example, the points awarded to each actively developed cell play a major role in the calculation of dissimilarity index (DI) for a given region of land. Points were awarded based on the comparisons of the land uses of the eight neighboring cells with that of the subject/central cell. Let's take two different grid cells for the calculation of DI, one having three commercial, three services, and two residential land uses out of eight neighboring cells and another one has six commercial land uses and two residential land uses out of eight neighboring cells. According to the DI formula, the points awarded to the central cell for both the cases would be same, i.e., $6/8$, but the behavior of from the transportation point of view could be entirely different. Hence this way, this index fails to recognize the variation among the grid cells.

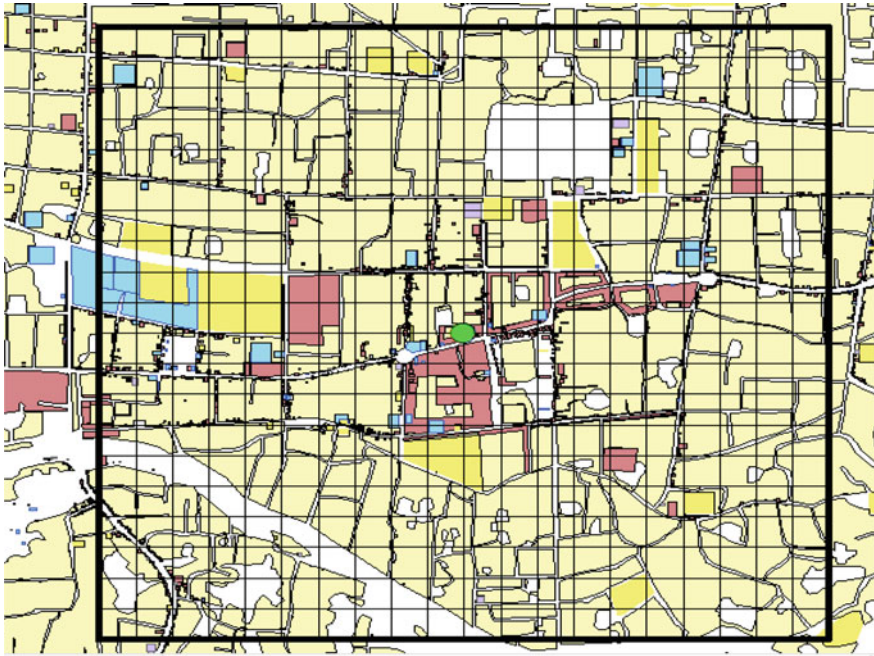


Fig. 4 Grid pattern for modified dissimilarity index

3.4 Mix-Type Index

To overcome the limitations of the dissimilarity index, a new index, known as mix-type index has been introduced. Mix-type index measure allots points to each of the actively developed cells based on the mix of the land uses in the surrounding cells.

$$\text{Mix-Type Index} = \frac{1}{k} \sum_k \frac{X_k}{\text{Number of distinct land uses in the study area}} \quad (3)$$

where X_k = Number of distinct land uses observed in the surrounding cells, including k .

k = Number of actively developed cells in a tract.

The calculation of mix-type index is similar to dissimilarity index the only change in the allocation of value to X_k . Conventional as well as modified mix-type index has been calculated in a similar way as dissimilarity index has been calculated.

With reference to above example taken for explaining DI index, the intensity of mixing is more in the first case as there are three types of land uses present in the eight adjoining cells. On the other hand, in the second case of, only two distinct land uses can be seen in the eight adjoining cells. Using the proposed index for Case 1, the points allotted to the central cell are $3/5$ (three types of land uses present and

five types of major land uses considered in this study) and the points allotted in the case; and for Case 2, it is 2/5. It can be said that the new index is able to incorporate the extent of land use mix and also information about the differences in the land use around the central cell.

4 Effects of Compact Development on Household Travel Behavior

To study the effects of mixed land use on the travel behavior of an individual household, various travel-related data were gathered. In total, 256 household data were collected from the various parts of the study area from a diversified range of household backgrounds. The socioeconomic factors have some influence on the travel behavior of an individual household like mode choice, trip length, and number of trips [5]. To get the knowledge of the trip behavior of a household, travel data have been collected from these surveyed households such as trip length, duration, purpose of the trip, and chosen mode. To find the relationship between various calculated indices and trip behavior of an individual household, a base model was prepared considering socioeconomic factors like gender, age, and household income, and travel behavior of a person by considering trip length of an individual as a variable. Regression modeling has been done among the dependent and independent variables. After the preparation of the base model, an index was added one by one and its correlation with the trip length was observed carefully. The indices were not taken all at a time, as they have a high correlation among them and it wouldn't be meaningful to add all of them together. The subsequent model was compared with the base model to get an idea about the effects of land use on the travel behavior of a household and to what extent these indices are feasible to explain the distinctiveness in the traveling patterns of a house.

5 Result and Discussions

This section analyses the modeling part of this case study. Under this heading, the impacts of built-up environment on travel behavior have been studied, and the relationship between them has been discussed here. The correlations among the various indices were also examined, and the significance of them on explaining the trip behavior of a household is debated. A simple regression model was prepared by considering socioeconomic data, various calculated indices and trip length as a proxy to vehicle miles travelled (VMT).

The correlation matrix was also found out for the indices calculated, i.e., entropy, dissimilarity, modified dissimilarity, mix-type, and modified mix-type indices. The calculated indices are household indices and hence a measure of built-up environment

Table 2 Correlation matrix for mixed land use parameter

	Modified DI	Mixed type	Normal DI	Entropy	Modified mixed type
Modified DI	1				
Mixed type	0.270163035	1			
Normal DI	0.260495135	0.803876122	1		
Entropy	0.568601506	0.613843171	0.649341477	1	
Modified mixed type	0.661645596	0.587518462	0.558283803	0.826704778	1

around the 1000 m radius of the household. These indices calculation, considering household as unit analysis, played an important role while establishing a relationship with travel behavior of a household. The correlation among them is shown in Table 2.

A regression analysis has been done to find out the influence of mixed land use on the travel behavior. For the base model, trip length is taken as a dependent variable and socioeconomic factors like age, vehicle ownership (car and bike ownership, taken separately), household income, number of working adults, and type of employment are considered as independent variables for the analysis. Due to the correlation between the indices, calculated indices values were added one by one, in the subsequent models, to study the influence of the built-up environment on the trip length. The significance of *t* value was taken as 1.65, and all the considered variables were found to be significant as shown in Table 3.

As it is evident from Table 3, the mixed land use parameters have a strong influence on the trip length. The modification in mixed land use is the best in explaining the oddness of the travel behavior of various household according to the neighborhood characteristics of that particular household.

Socioeconomic data that were considered for this study was successful in explaining the trip behavior of the respective households. Data like age, vehicle ownership, and household income found to be significant when it came to explain the trip length of person trips. Trip length has a positive link with household income, motorized two-wheeler ownership, and license ownership; however, it was found out that, the trip length has a negative correlation with the age of the person making a trip. This is self-explanatory, since old people tend to travel lesser distance as compared to young or working adults.

On the other hand, when the calculated indices were included in the regression model, each index found out to have a strong association with the trip length. The possible explanation behind this strapping relationship could be that the calculated indices were calculated by taking household as unit analysis. Almost every index has shown a negative relationship with the trip length. As the densification of land use increases, trip length decreases appreciably, which proves the point of this study. Among all the calculated land use parameters, modified mix-type index was found to be most significant in explaining the travel behavior of a household. Modified mix-type land use overcomes the important limitation, which dissimilarity fails to

Table 3 Model for trip length

Socio economic parameters	Base model with socioeconomic variables only	Model with land use parameters				
		Entropy	Normal DI	Modified DI	Mixed type	Modified mixed type
Constant	4.16	4.37	5.52	3.03	5.43	5.73
Age	-6.25	-6.32	-5.96	-6.27	-6.36	-6.44
Bike ownership	2.53	2.73	2.81	2.43	2.66	2.98
Car ownership	-1.76	-1.77	-1.74	-1.68	-1.73	-1.89
Household income	1.80	1.92	2.67	1.68	2.46	2.38
Number of working adults	2.4	2.39	2.87	2.34	2.89	2.58
Type of employment	-2.75	-2.77	-2.49	-2.78	-2.34	-2.69
Land use parameter	-	-4.23	-5.67	-0.51	-2.93	-4.1
Adj (R^2)	0.07	0.081	0.12	0.07	0.09	0.09

address, i.e., the intensity of land use mix in a census tract; the modification in the implementation, that is rather than taking for the whole city under the census tract, a tract of 100×100 m has been made around 1000 m side of a household individually, played a key role in its apparent explanation of the trip behavior of the individual households.

Another index that was quite convincing while explaining the unusualness of the trip behavior was dissimilarity index. A 100×100 m of grid cell was sufficient enough to high add in the density of mixed land use that is quite prevalent in the Agartala city. There is a whooping around 58% increase in the adjusted R value as compared to the considered base model.

6 Conclusions

Through this study, an effort has been made to elucidate the relationship that holds by built environment of the surrounding environment with the travel behavior of that particular household. The case study has been done on the Agartala city, a fast-growing city, in a disorganized way, at the northeastern part of India. The study

has emphasized the need of planning for a developing country like India. Agartala represents a perfect picture of developing India, as it has densely built-up environment with a need of better public transportation facilities. The conventional indices which give just a right depiction of the developed countries like USA and Canada fail to include the particularity of developing countries like India. Therefore, with the slight modification, these indices have been implemented and found to be significant while explaining the travel behavior of the Agartala city. This study showed that household-based land use measures were convincing enough when it comes to encompass mixed land use development effects on trip length and how socioeconomic factors like age, vehicle ownership, type of employment, and number of employees in a household governs the trip behavior of a household. The conclusion drawn from this study can be used for:

- The better planning of the cities which are developing at a similar pace like Agartala, these results can be used to provide facilities of transit system.
- The relationship between land use and trip length can be used to design the road network for smart cities to discourage the use of private automobiles.
- The factors governing trip length, established through this study, can be further investigated to mitigate the vehicle emissions by developing a community which encourages a shorter trip length.

Acknowledgements I would like to acknowledge AICTE with gratitude and appreciation for providing financial support for travel data collection as a part of the project “The Effects of Mixed Land Use on the Household Travel Behavior: A case study of Agartala, Tripura,” numbered 8023/BOR/RID/RPS-250.

References

1. Frank L, Pivo G (1994) The impacts of mixed use and density on the utilization of three modes of travel: the single occupant vehicle, transit, and walking. *Transp Res Rec* 1466:44–52
2. Sarkar PP, Chunchu M (2016) Quantification and analysis of land-use effects on travel behaviour in smaller Indian cities: case study of Agartala. *American Society of Civil Engineers, Agartala*
3. Cervero R (1989) *America’s suburban centres: the land use transportation link*. Unwin Hyman, London
4. Cervero R, Kockelman K (1997) Travel demand and the 3Ds: density, diversity, and design. *Transp Res Part D Transp Environ* 2(3):199–219
5. Sun X, Wilmot CG, Kasturi T (1998) Household travel, household characteristics, and land use: an empirical study from the 1994 Portland activity-based travel survey. *Transp Res Rec: J Transp Res Board* 1617(1):10–17
6. Ewing R, Cervero R (2010) Travel and the built environment: a meta-analysis. *J Am Plan Assoc* 76(3):265–294
7. Maat K, Wee VB, Stead D (2005) Land use and travel behaviour: expected effects from the perspective of utility theory and activity-based theories. *Environ Plann B Plann Des* 32(1):33–46
8. Ewing R et al (2010) Traffic generated by mixed-use developments—six-region study using consistent built environmental measures. *J Urban Plann Dev*
9. Song Y, Knaap JG (2004) Measuring urban form. *J Am Plan Assoc*

Private University Students' Mode Choice Behaviour for Travel to University: Analysis in the Context of Dhaka City



Sharmin Nasrin

Abstract Dhaka, the capital city of Bangladesh, is facing tremendous pressure in meeting the traffic demand of its inhabitants. In Dhaka among other trips, significant percentages of trips comprise education trips. A paper-pencil-based survey has been conducted by the University of Asia Pacific students in Dhaka from May 2016 to July 2016. The result from exploratory analysis and multinomial logit model revealed that cost, comfort, time and availability are the main factors for choosing different modes for private university students' education trip. Results showed that the magnitude of the coefficient of attribute comfort is significantly higher compared to travel cost and travel time. The result from this paper can be used by policymakers and government agencies to provide strategies that support in a more cost-effective and comfortable journey to the university.

Keywords Multinomial logit model · Bangladesh · University student · Travel behaviour · Transport planning

1 Introduction

Dhaka, the capital city of Bangladesh, is experiencing severe traffic congestion. According to the Revised Strategic Transport Plan in Dhaka, about 6,000,000 trips are education trip per day [1]. This number comprises all education trips such as primary, secondary, higher secondary, graduate and post-graduate trips. According to the World Bank data, Dhaka has about 54 private universities with about 90,000 students and 1500 tertiary colleges with about 800,000 students. Therefore, it can be assumed that private university and tertiary college students generate a significant number of trips. Most of the public universities have transport facility for non-resident students and accommodation facility within the university campus for resident students. However, private universities usually not only lack in accommodation facility, but also most of them do not have any transport facility as well. This paper explores significant factors for private university students' education trip to the university.

S. Nasrin (✉)
University of Asia Pacific, Dhaka, Bangladesh
e-mail: snasrin@uap-bd.edu

© Springer Nature Singapore Pte Ltd. 2020
T. V. Mathew et al. (eds.), *Transportation Research*, Lecture Notes
in Civil Engineering 45, https://doi.org/10.1007/978-981-32-9042-6_24

Results from this paper can be used by policymakers and researchers as a platform to conduct more detailed study.

The prime research question that will be answered by this research is: What are the significant factors for private university students to choose different modes for travel to their university? Both exploratory analysis and multinomial logit (MNL) choice model are the methodological approaches adopted by this research. The model was calibrated with the survey data collected on a private university student in Dhaka.

2 Literature Review

Several studies have been discussed the important deterministic of students' mode choice decision. Guzman and Diaz analysed students' mode choice behaviour for the students of Ateneo De Manila University and Miriam College in Philippines [2]. Their analysis found that travel time, travel cost and convenience are the key determinants of students' mode choice. Similarly, the mode choice model calibrated on students at the Texas A&M University showed that travel time and travel cost were key attributes for students' mode choice decision [3]. A multinomial logit model developed by Whalen for students at the McMaster University in Hamilton, Canada, found that the travel time coefficients for private auto and bicycle were positive, indicating that students tend to enjoy longer trips by these modes [4]. Volosin in her thesis analysed students' travel behaviour at Arizona State University, USA. She used the multinomial logit model. Her analysis found that those students' travel patterns vary substantially from those of the rest of the population [5].

Das et al. in his research did a descriptive analysis on the travel behaviour of university students at VIT University in Tamil Nadu and found that many factors influence mode choice of students like travel time, travel cost, age, gender, distance, vehicle and licence ownership [6]. Among these factors, travel time, travel cost and vehicle ownership played a major role in the travel patterns of off-campus residents.

Abiola and Ayodeji developed a mode choice model for a typical Nigeria university using Federal University of Agriculture, Abeokuta. Results showed that location, waiting time at the bus stop, number of trips, the cost to school and time to the bus stop are the significant variables [7].

Danaf et al. investigated differences between the mode choice patterns of students of the American University of Beirut (AUB) and the general population of the Greater Beirut Area. Results from the discrete choice model showed that students at AUB put a higher value on travel time compared to the general population [8].

Yasmin et al. investigated mode choice factors for public university students in Dhaka, considering Dhaka University as their case study. Their analysis found that five modes such as university bus, public bus, private auto, auto rickshaw and rickshaw are prominent mode choice of the students of University of Dhaka [9]. The outcomes of these the analysis indicate that about 68% students choose university bus as their primary mode. One of the most surprising and interesting findings is that there is no rationality between distance, in-vehicle travel time and cost in Dhaka city.

This nullifies the usual interrelationship between distance, time and travel cost, making cost much higher and acquiring more travel time compared to distance traverse. This could probably be because of severe traffic congestion in Dhaka city.

Therefore, from the literature review, it is found that travel time is the dominant factor for students to choose modes even in a different country setting. Only one research was found on public university students' mode choice decision based in Dhaka. However, as stated earlier, private and public university students' travel behaviour varies. This is mainly because of the availability of bus and accommodation facilities to the public university students in Dhaka. Unfortunately, none of the research found specifically for private university students in Bangladesh. This paper will overcome that research deficiency by exploring travel survey data and understanding the result from the mode choice model.

3 Survey Design

3.1 Overview of Survey

Survey for this research was conducted at the University of Asia Pacific (UAP) in Dhaka. Respondents of the survey were the full-time student of the UAP. The reason for choosing this university as a study area is because it is situated at Dhaka's central position and students from diverse background are admitted into this university.

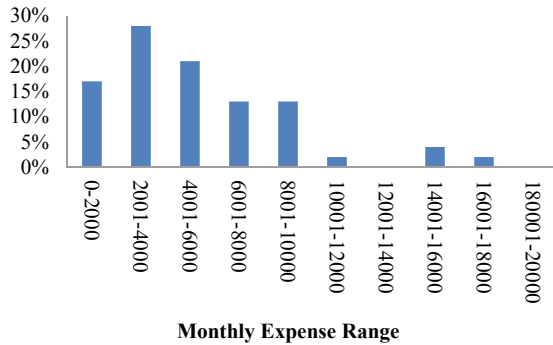
The survey was divided into two parts; first part contained limited demographic questions such as age, monthly expense (includes transport cost) and gender, and second part contained questions on their actual mode used for the trip to the university.

3.2 Survey Design and Implementation Strategy

The main objective of the survey was find out (1) the current travel behaviour of private university students for their trip to university and (2) problems students facing while travelling to their university.

Due to students' busy class schedule, face-to-face survey method during their class break has been adopted for this survey. The questionnaire was prepared in English. As students have an adequate English background, it was not difficult for the respondent to understand the questionnaire. The main risk associated with this survey was students' missed class. However, this risk has been handled by conducting the survey on break time. All data collected was stored safely in the computer and as hard copy format as well.

Fig. 1 Percentage of respondents' monthly expense range



4 Exploratory Analyses of Survey Data

4.1 Demographic Characteristics

Among the respondents, 81.7% represents male students and 18.3% female students. According to the World Bank data, the female share of private university student is only 23% of total students. Therefore, the percentages of male and female share in survey data are compatible with the World Bank data.

Figure 1 illustrates the students' monthly expense range. Figure 1 shows most of the students spend 2000–4000 BDT in a month. A very insignificant percentage of students spend more than 10,000 BDT in a month.

4.2 Relationship of Modal Share with Gender and Monthly Expense

From the survey data, it can be said that respondents use six types of modes for travelling to university; these are bus, laguna (omnibus), rickshaw, car, bicycle and walk. Figure 2 illustrates the modal share of the respondents. From the figure, it can be seen that even though the bus has the maximum percentage of mode share, about half of the respondents who use the bus are not satisfied with it.

Figure 3 illustrates the influence of monthly expense on different modes. Figure 3 revealed that there is no significant influence on students' mode choice decision and monthly expense. However, students who are in low monthly expense range do not use expensive modes such as rickshaw and car.

Figure 4 illustrates the influence of gender difference on mode choice decision of students. Figure 4 showed that except car, none of the modes is gender specific. This can be justifiable as car is the most comfortable mode among the modes students use. From the observation, it is known that female road users, in general, are the significantly vulnerable group of road users. Therefore, female respondents who can

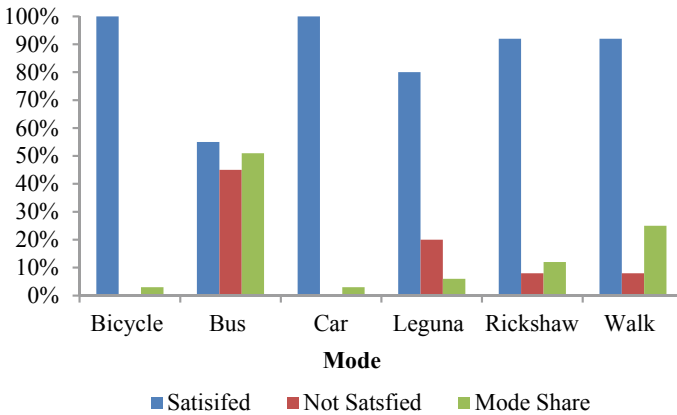


Fig. 2 Percentage of mode share with their satisfaction and dissatisfaction percentages

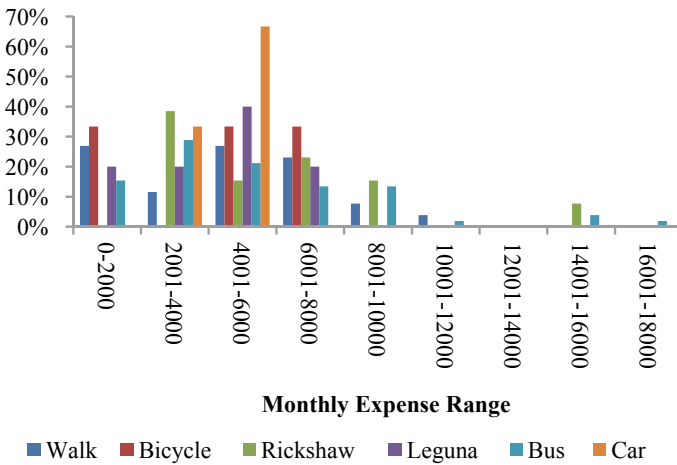


Fig. 3 Students' monthly expense range and mode share

afford have more tendencies to choose a car for travelling to the university. However, it can be also said that in private universities, female students are predominantly from higher-income families who own a car and can use that for their education trip.

Figure 4 also showed that among the total females, a significant percentage of females are using bus for their education trip. None of the female respondents uses the bicycle for education trip. This is completely justifiable in Bangladesh's socio-economic context, where bicycle use is very rare among female road users. Due to conservative society in Bangladesh usually, female riding a bicycle is not widely accepted. Significant percentages of female respondents walk to their university. This is mainly because most of the students live near their university. Therefore, travelling

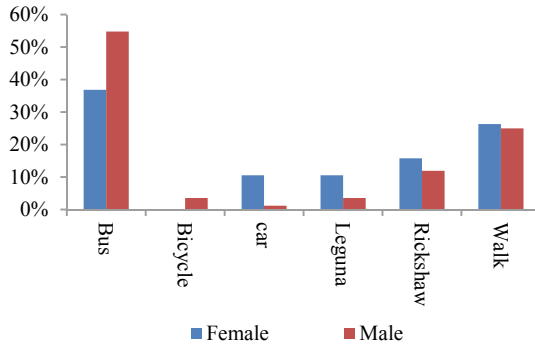


Fig. 4 Percentage of male and female student modal share

to the university by walk not only reduces their monthly expense for transport but also gives them the opportunity to get relief from standing in Dhaka’s severe traffic congestion.

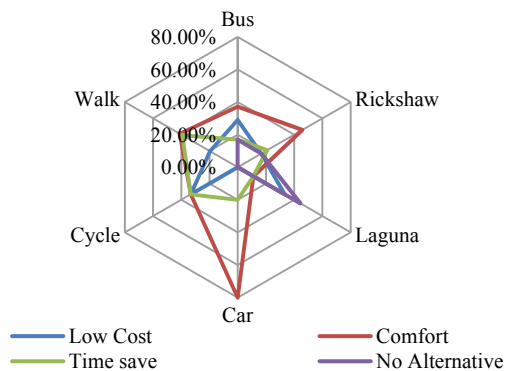
5 Factors to Choose Different Modes

From the exploratory analysis, some factors have been found that play the roles for private university students to choose any mode. Those factors are low cost, comfort, time-saving and no available alternatives.

Figure 5 illustrates the percentages of respondents for choosing different modes according to different factors. Among the bus users, maximum percentages chose bus because they think the bus is comfortable compared to other available modes.

In Dhaka, rickshaw and cycle riding are sometimes not comfortable to the users due to severe bad road condition. Because of the lack of law and order, some students do not feel safe while travelling to their university by rickshaw as well.

Fig. 5 Percentages of respondents various mode choices according to specific factors



A significant percentage of respondents also chose bus for its low cost compared to other modes. In Dhaka, bus fare is comparatively low than other modes such as rickshaw and leguna.

In many instances, travelling by leguna is significantly cumbersome due to its fare rate being higher than bus for the same route distance. Moreover, small-sized leguna does not provide any comfort and during traffic congestion; it is of no use. Rather, rickshaw is more usable to avoid jam as it can use alternate routes and also more comfortable than laguna. Compared to other modes, walking saves travel time more, and its comfort level is also satisfactory than other modes except bus. Its cost factor is also mentionable as it needs no fare. Car and cycle users do not show any significant influence for any factor as their response rate is low in the survey.

6 Overview of Multinomial Logit (MNL) Choice Model

6.1 Model Choice Set

Due to the insignificant percentage of mode share for mode choice model calibration, leguna and bicycle have been merged with rickshaw and walk, respectively. Therefore, for model calibration bus, rickshaw, car and walk are used as modal choices.

6.2 Significant Attributes

As previously discussed, the significant attributes for students to choose different modes are cost, time, comfort and unavailability of any alternative other than their chosen modes. Due to time constraint comfort and unavailability of any alternative, other than their chosen modes were merged into single attribute stating that as comfort factor.

Social demographic factors, such as age, education, gender and monthly expense, do not influence students' decision to choose different modes. The surveyed students are particularly tertiary private university students of the same age and same educational qualifications. Exploratory analysis showed that there is no significant relationship with students' mode choice and their monthly expense. However, gender has a significant influence on students' decision to choose car.

Due to the unavailability of any other model data, Google Map was used to calculate expected travel time and travel cost of un-chosen modes based on respondents' stated work location and home location. Based on the assumption that they would take the shortest possible route, distance travelled by each respondent was calculated using the MapInfo geographic information software.

With different combinations of attributes (i.e. age, gender, expense, distance travelled, waiting time, in-vehicle time, access time to bus stop, total travel cost, total

Table 1 Attributes used in the calibrated MNL model

Attributes	Description of attribute	Variable state	Coded value	Attributes' notation
Total cost for trip	Total money (in BDT) students spent for trip			tc
Total time spent for trip	Total time spent by any vehicle or by walk			tt
Comfort for trip	Students are satisfied with their chosen mode	Comfortable	0	c
		Uncomfortable	1	
Gender		Male	1	g
		Female	0	
Constant	Constant for rickshaw, car and walk are ASCRIC, ASCCAR, ASCWALK respectively			

time, cost for access mode and comfort), several models were tried. After several tries, the most significant attributes found are listed in Table 1. Utility functions for bus, rickshaw, walk and car are provided with Eqs. (1), (2), (3) and (4), respectively.

$$U_{(bus)} = \beta_1 * tc + \beta_2 * tt \tag{1}$$

$$U_{(ric)} = ascric + \beta_1 * tc + \beta_2 * tt + \beta_3 * c + \beta_4 * g \tag{2}$$

$$U_{(walk)} = ascwalk + \beta_2 * tt + \beta_3 * c \tag{3}$$

$$U_{(car)} = asccar + \beta_2 * tt + \beta_3 * c + \beta_4 * g \tag{4}$$

where $U_{(bus)}$, $U_{(ric)}$, $U_{(walk)}$ and $U_{(car)}$ are utilities of bus, rickshaw, walk and car. β_1 , β_2 , β_3 and β_4 are coefficients for associate attributes.

6.3 Discussion on Estimated Coefficients

A wide range of qualitative and dependent variable models can be estimated with the “LIMDEP” software [10]. Due to this capability, in the current study, LIMDEP was used for model calibration. The performances of various trial models calibrated in LIMDEP software were assessed based on their statistical significance, predictive ability and logical reasoning. According to Ortúzar and Willumsen, an attribute will be significant when its student’s t statistic is sufficiently large, typically greater than

Table 2 Result for model calibrated with survey data

Mode	Attribute	Coefficient	Std. err.	T statistics	P value
Considering all modes	Total cost	-0.008913	0.461E-02	-1.960	<0.01
	Total time	-0.008798	0.413E-02	-2.130	<0.01
Rickshaw, car	Gender	-0.763432	0.540	-1.500	<0.01
Rickshaw, car and walk	Comfort	-1.839859	0.559	-3.289	<0.01

Log likelihood function of base model = -113, log likelihood function of estimated model = -99, -2LL = 14, critical $\chi^2 = 2.167$ (seven degrees of freedom), pseudo $R^2 = 0.13$, $N = 104$

1.96 at a 95% confidence level [11]. Table 2 presents the estimation result for the best-calibrated model.

With the log likelihood ratio test (-2LL), overall significance of the calibrated model was conducted. According to Almasri and Alraee for a model to be statistically significant, -2LL value should be more than critical χ^2 value at 95% confidence level [12]. From the model result, it was found that at 95% confidence level, critical χ^2 value is 2.167, which is less than -2LL value of 14. Therefore, the model is significant.

As the bus mode share was the highest, this was used as the reference mode in the calibrated model. The best model was calibrated with generic travel cost and travel time as the results from model calibrated with mode specific travel cost and travel time were insignificant. This may be because the sample size is not significantly high. The estimated result showed that the coefficients of generic travel cost and travel time are significant (*t* statistics, for these coefficients, are greater than 1.96). Results show that as total cost and total time for travel have expected negative signs, the increasing value of these attributes will reduce the utility of the respective mode.

According to exploratory analysis, gender difference has an impact on students' modal share. However, adding gender attribute in the utility function of bus estimated fixed parameters. This may be because it is not their gender identity that led female respondents for the decision to choose or not to choose bus, but because of their locality. Adding gender attribute in the utility function of car and rickshaw estimated slightly less significant coefficient. This may be because of less car and rickshaw sample for model calibration. Model result estimated the negative coefficient for gender attribute for rickshaw and car modes. Therefore, it can be said that females have more tendency to choose rickshaw and car compared to male respondents.

Comfort attribute turns out insignificant for bus and significant for rickshaw, car and walk. For rickshaw, car and walk, the coefficients of the dummies that represent comfort are negative. This is justifiable as comfort has been coded as 0 and discomfort coded as 1. Therefore, it represents that with the increased comfort, students will tend to choose these modes.

7 Elasticity Values of Different Attributes

Elasticity value can measure the response to the change of attributes. A direct elasticity measures the percentage change in the probability of choosing a particular alternative for the change of attributes for that respective alternative. Cross-elasticity measures the change of probability for other available alternatives for the change of those attributes. This section discusses the effect of change of different attributes on students’ mode choice decision. The elasticity of attributes can be calculated with Eq. (5).

$$\text{Elasticity} = \frac{\text{Percent Change in Probability}}{\text{Percent Change in Attribute}} \tag{5}$$

7.1 Elasticity of Cost

Table 3 lists elasticity values of travel cost for all modes. The values in bold and italic are direct elasticity for that respective mode. All modes are relatively inelastic to travel cost as elasticity values are less than 1.

7.2 Elasticity of Total Time

Table 4 lists elasticity values of travel time for all modes (bold and italic values

Table 3 Elasticity values of travel cost

Mode	Bus	Rickshaw
Bus	<i>-0.088</i>	0.167
Ric.	0.073	<i>-0.384</i>
Walk	0.089	0.198
Car	0.242	0.291

Table 4 Elasticity values of travel time

Mode	Bus	Rickshaw	Walk	Car
Bus	<i>-0.296</i>	0.188	0.161	0.017
Rickshaw	0.255	<i>-0.423</i>	0.144	0.011
Walk	0.286	0.201	<i>-0.744</i>	0.008
Car	0.760	0.377	0.226	<i>-0.691</i>

Table 5 Elasticity values of comfort

Mode	Rickshaw	Walk	Car
Bus	0.080	0.055	0.008
Rickshaw	<i>-0.136</i>	0.012	0.001
Walk	0.021	<i>-0.180</i>	0.002
Car	0.021	0.015	<i>-0.240</i>

represent direct elasticity for that respective mode). All modes are relatively inelastic to total time, as elasticity values of total time for all modes are less than 1. However, the magnitude of elasticity values of total time is more compared to the elasticity values of travel cost. Therefore, it can be assumed that students are more elastic to travel time than travel cost.

7.3 Elasticity of Comfort

Table 5 lists elasticities of comfort for all modes (bold and italic values represent direct elasticity for that respective mode). Elasticity value showed all modes are relatively inelastic to comfort. As previously stated as the comfortable state had been coded as 0, negative value implies increasing comfort of the respective mode will increase the share of that mode.

8 Conclusions and Recommendations

Model result and exploratory analysis revealed that significant factors for private university students to choose different modes are travel cost, travel time and comfort. However, comfort has comparatively more significance than travel cost and travel time for rickshaw, walk and car.

The result from this paper can be used by policymakers and government agencies to provide policies, such as subsidised bus rapid transit for students or student only bus. Improvement of the walking facility also would be beneficial for students. One of the limitations of this research is the small sample size. However, small sample size provides the effects of attributes except calculating the significantly small effect of attributes. Further research with a big sample size is recommended to understand the significantly small effect of attributes.

References

1. Japan International Cooperation Agency (JICA) and Dhaka Transport Coordination Authority (DTC) (2015) The project on the revision and updating of the strategic transport plan for Dhaka. Almec Corporation, Oriental Consultants Global, Katahira & Engineers International
2. Guzman MPD, Diaz CE (2005) Analysis of mode choice behavior of students in exclusive schools in metro Manila: the case of Ateneo de Manila University & Miriam College. In: Eastern Asia society for transportation studies
3. Maneesh M et al (2007) Examination of student travel mode choice. In: 86th annual meeting of the transportation research board, Washington DC
4. Whalen KE (2011) Travel preferences and choices of university students and the role of active travel. In: School of geography and earth sciences. McMaster University, Canada, p 88
5. Volosin SE (2014) A study of university student travel behavior. In: Civil engineering. Arizona State University, Arizona, pp 1–196
6. Das R et al (2016) Analysis of university students travel behaviour: en route to sustainable campus. *Indian J Sci Technol* 9(30)
7. Abiola OS, Ayodeji JD (2012) Travel demand model for a typical Nigeria University. *Int J Civ Environ Eng IJCEE-IJENS* 12(3):89–99
8. Danaf M, Abou-Zeid M, Kaysi I (2014) Modeling travel choices of students at a private, urban university: insights and policy implications. *Case Stud Transp Policy* 2(3):142–152
9. Yasmin F, Basu N, Palash AR (2006) A study on mode choice behaviour of public university students—case study of University of Dhaka. In: Urban and regional planning (BURP), Dhaka
10. Greene WH (1998) LIMDEP (Version 7.0) [Econometric software]
11. Ortúzar JDD, Willumsen LG (2011) Modelling transport, 4th edn. Wiley, Chichester, UK
12. Almasri E, Alraee S (2013) Factors affecting mode choice of work trips in developing cities—Gaza as a case study. *J Transp Technol* 3:247–259

Understanding and Quantifying Delays in Accessing ICD, Nagpur



Ashwini Thakare, Amit Kumar, Vishrut Landge and Sumeet Jaiswal

Abstract Industrial development and deployment depend on the eases and efficiency of transport network and support it receives for their logistic and mobility needs. Particularly, relevant is the speed with which industries can transport its raw materials and its finished products. In today's world of high globalization, any delay in the transportation can be very expensive for industries in terms of their competitiveness and profitability. Therefore, industries are putting greater weights to the availability of good quality transport connectivity. Nagpur, in its quest to host quality industries and thereby developing as the industrial power hub, has its own Inland Container Depot (ICD) to support its manufacturing and service industries. However, no specific study trying to quantify the efficiency and effectiveness of the transport connectivity between ICD and its customers has been done. This study is an attempt to develop an understanding of how containers move from ICD to their place of distribution. The paper conceptualized the potential solution to minimize the delay. For this study, we are developing the geographical spread (origin and destination) pattern for ICD, Nagpur. The paper also tried to develop a route profile for firms using the services of ICD, Nagpur. We are using a vehicular tracking system to identify the possible delays. The study used questionnaires, interviews, GIS, observation techniques, and reviews in order to bring out the results of the study as expected. The results of the study will quantify the factors responsible for delays in the journey from a particular route. Depending upon the intensity of the problem, the particular solution will be obtained to improve the efficiency of the existing transport system. Quantification of factors responsible for overall delays helps the transport planner to provide options to choose the best route available to avoid the possible delays due to inefficiencies of the road network. Our study emphasizes on optimal utilization of roads and fleet management which in turn helps in reducing congestion and queue length (which happens due to the entry of container vehicle in traffic stream), results in lesser fuel consumption, lesser emission of greenhouse gases and also results in

A. Thakare (✉) · A. Kumar · V. Landge
Department of Civil Engineering, Visvesvaraya National Institute of Technology, Nagpur 440010,
India
e-mail: thakreashu10@gmail.com

S. Jaiswal
Department of Civil Engineering, Marathwada Institute of Technology, Aurangabad 431028, India

lesser transportation cost. The paper concludes with a discussion on the need of having an effective connectivity to fully explore the economic potential of existing ICD and surrounding industries.

Keywords Delay · Logistics · Transportation

1 Introduction

Freight transport plays a vital role in the economic development of the country. Freight transport includes a transfer of products and goods in bulk from place of their origin to the place of their distribution. Time is very crucial in this journey as the delay in a timely delivery of products and goods costs a lot in terms of money. For on-time delivery of products, the transport system must be efficient and effective not only in planning stage but also in designing and maintenance stage.

However, the lack of studies concerning the nature and scale of freight task leads improper freight management leading to delays in freight delivery which further attracts problems in terms of loss of money, inventory, and the relationship between seller, distributor, and buyers.

Out of all available modes of freight transport, road transport has a market share of 70%. Considering the unique location of Nagpur of being in the center of India and also the winter capital of Maharashtra, it caters to major industrial needs and facilities for industries in the Vidarbha region. However, lack of planning and infrastructural development leads to a considerable reduction in speeds of the vehicle carrying freight from Inland Container Depot, Nagpur to its various clients. When it comes to the development of the transport system, the government rules are slightly focused toward intercity development of highways. While in case of intra-city development even though heavy vehicles are considered by converting them into equivalent passenger car unit, the problems faced by the driver of freight vehicle are different from that of people driving standard four wheeler vehicle which is car.

This is because driving heavy vehicle is slightly different from driving normal (two-wheeler/four-wheeler) vehicle because of its physical variance (in terms of size, width, and height) compared to other vehicles moving on the road. In case of mixed traffic conditions, the entry of heavy vehicle causes the problem to the rest of the vehicles in traffic stream in terms of congestion; while on the other hand, the problem of reduction in speed of heavy vehicle due to the entry of other vehicles takes place.

2 Literature Support

Literature search to understand travel pattern of heavy-duty vehicles moving from ICD, Nagpur has not resulted in any success. This resulted in designing the project using the fundamentals of travel survey.

2.1 Travel Survey Methodology

In Australia, Inbakaran and Kroen [1] investigate various method implemented for travel survey exercise and data collection. They classified the survey methods into two broad groups—the first group was called traditional approaches involving methods such as face-to-face interviews, self-administered surveys, and telephone surveys. The second group was called new approaches involving methods such as Internet surveys, survey using technologies like GPS devices, and mobile phones. However, each survey method has issues with response rate, coding, quality of data, and cost of running the survey.

2.2 Travel Survey Questionnaire

The questions selected for preparing questionnaire were simple and easy to understand but at the same time important enough to extract necessary information about the factors responsible for causing overall delays from driver's point of view.

3 Study Area

The ICD at Nagpur is located behind Narendra Nagar near the Ajni Marshaling Yard of Central Railway. It is linked by rail to the east–west and north–south trunk rail routes making it possible to run trains from and to all the parts of the country (Fig. 1).

4 Data Collection

Because of lack of proper approach to study the travel behavior of heavy-duty vehicular movement, the combination of various method studied in the past was used to get specific information needed to quantify the factors responsible for causing overall delays in trip from ICD, Nagpur to various destinations.

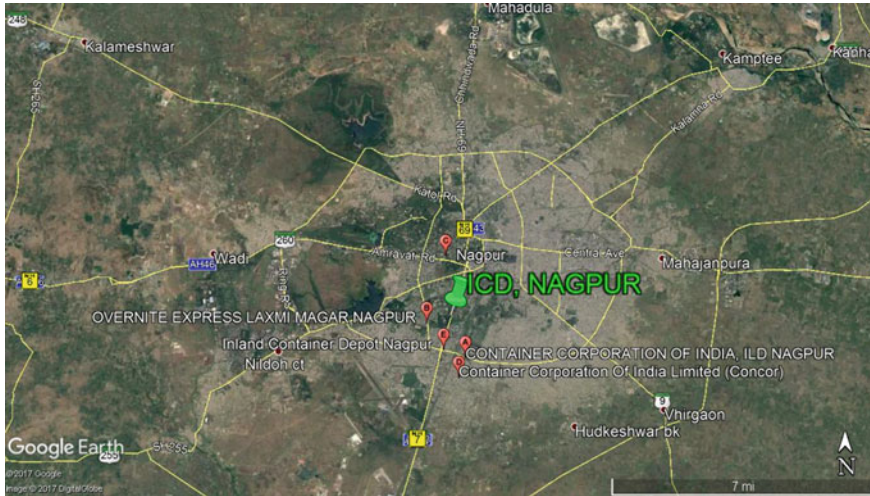


Fig. 1 ICD Nagpur. *Source* Google Earth

4.1 *Survey Methodology*

To study the factors responsible for delays in overall journey of heavy-duty vehicle moving from ICD, Nagpur to various destinations it is necessary to study the problem from user's point of view. So the survey method adopted includes the personal interview approach as well as preparation of travel survey questionnaire [1–3]. In personal interview approach, the questions were asked to drivers as well as other road users and the company owners (where the product is being delivered) regarding their views on factors causing delays in the journey. The questions were asked in such a way that they will provide necessary information about various factors causing overall delays.

4.2 *Survey Questionnaire*

The questionnaire was prepared in two languages which are English (as shown in Table 1) and Hindi to minimize linguistic problems. The question numbers are restricted to 22 as respondent should not get bored with too many questions. The first three questions give personal information of the driver. The next three questions give information regarding vehicle condition. Further, information regarding travel route and road condition with problems faced by heavy-duty vehicles in mixed traffic conditions was covered.

Table 1 Questionnaire survey table

1	May I know your name?
2	What is your age?
3	How much is your experience of driving?
4	Do you work for CONCOR only or any private firm?
5	What is your frequency of travel?
6	How old is your vehicle?
8	Vehicle load-carrying capacity?
9	Do you face any problems because of your vehicle?
10	Which routes you follow?
11	Are there any alternate routes?
12	Is there any route restriction from NMC?
13	Do you think road conditions are up to the mark?
14	Do you face any problem due to bad road condition?
15	Are you satisfied with the available turning radius during your travel?
16	How much the signal stoppage affects your journey?
17	What kind of problems you face due to mixed traffic?
18	What’s your average and maximum possible speed?
19	Do you face problems due to change in weather conditions?
20	How many road accidents you faced or you eye witnessed?
21	Do you think accident cause delays and up to what extent?
22	What are the other problems you face which cause delays?

4.3 Video Graphical Data Collection

To know the live traffic on route, road environment, pavement condition, surface characteristics, encroachment, on-street parking, roadside hindrance, any ongoing construction activities, variation in road width, highway structures, possible stoppage and many more factors which affect the journey of test vehicle when test truck is taking the trip from ICD to destination factory/industry, video graphical data collection is done using mobile phone. To record the video of the route, we fixed the device on truck’s windscreen so that it will remain stable and record all the possible information without any error.

4.4 Photographical Data Collection

This method is primarily a research tool; it is useful in studies of interrelationship of several factors such as spacing, speeds, lane usage, acceleration rates, merging and crossing maneuvers, and delays at intersections [4]. This method is applicable

to a short test section only. Using this technique, we clicked the photographs of roadside constructional activities, road deterioration, road width reduction, highway structures, gas station, roadside parked vehicles, road accidents, and intersections.

4.5 GPS-Based Data Collection

Transportation planners and engineers across the country still employ the manual or stopwatch method using a test car in obtaining travel time and delay data. This method is labor-intensive and is prone to human errors. Ritz and Regidor [5] in their paper demonstrated a more efficient method using GPS tools for travel time and delay surveys.

Mauricio et al. [6] presented their obtained data through time–distance, speed–distance, and distance–speed diagrams and used GIS to illustrate the study routes only. However, this initial research did not come up with an established methodology that could easily be applied for future travel time and delay studies.

Most GPS-based studies on travel time data collection cover two important components namely the hardware and software part of the system. The hardware consists of the GPS device, laptop, and or other equipment mounted on a test vehicle that can collect and store traffic conditions by monitoring the location and speed of the test vehicle. On the other hand, the software part refers to the data processing procedures and tools that can be used for post-processing or real-time monitoring of traffic data. Some good examples that developed GPS-based travel time collection system are GPS–GIS integrated system for travel time surveys are GISTT [7] and GPS-Trek [8, 9].

4.5.1 Selection of GPS Unit

For the data collection, we searched for a GPS app which can give us accurate information like the route followed, distance versus speed graph, distance versus time graph, maximum, average, and minimum speed throughout the journey. After extensive research, we found **GPS speedometer** by **gpxscan.com** which enables us to share the information on other devices, and it records all the desired information mentioned above [10].

5 Data Analysis

Figure 2 shows the speed versus journey graph of various trips from ICD, Nagpur. From overall ten trips to various locations from ICD, it can be observed that not a single journey speed reaches to its specified limit which is set at 40 kmph by Nagpur Municipal Corporation.

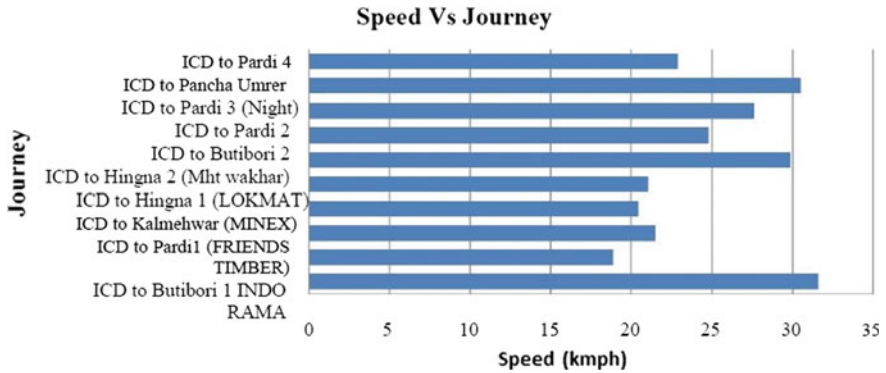


Fig. 2 Speed versus journey

From the graph, it can be seen that maximum speed reduction occurs in the trip from ICD to Pardi.

5.1 Analysis of Distance Versus Speed Graph

On analyzing the characteristics of distance versus speed and distance versus time graphs obtained from ‘GPS speedometer’ application, it is observed that there are considerable variations of speed with respect to time and distance. The sudden brakes are applied by the driver if he incurred obstruction on the road. Also the brakes are applied on signalized intersection during the red time. When the brakes are applied at a particular location, the speed may reduce or it may reach zero; i.e., the vehicle becomes stationary. The reduction in speed can be analyzed with the help of downward limb of distance versus speed graph. Sharp downward inclining limb shows a sudden drop of speed or possibility of sudden application of brakes. While the gradually downward inclining limb shows the gradual application of brakes. Similar is the case with acceleration, it will achieve after application of brakes to start the journey again.

5.2 Analysis of Distance Versus Journey Time Graph

The distance versus journey time graph helps to predict the possible distance where there is a reduction of speed along the journey. The exact time at which reduction in speed occurred at particular location can be analyzed with the help of distance versus time graph as the limb where the slope of the graph flattens.

5.3 Analysis from Video Recording

The exact reason behind the reduction of speed of the heavy vehicle at a particular location at a particular time can be seen from the video-recording recorded during journey on respective study routes.

Various reasons for speed reduction along the particular study route are mentioned below.

Also, the general findings from the various points of views are also discussed.

5.4 Analysis from Questionnaire Responses

From the questionnaire responses, we came to know about the past behavior of road and traffic environment from the perspective of truck drivers. We also found the information regarding alternate routes to a particular journey and why they choose particular route over other alternative routes available. Some of the findings from their responses regarding alternate routes are as follows:

- (i) Traffic congestion: Many drivers reported that they do not follow particular route because of the traffic congestion problem. Traffic congestion is the leading cause of speed reduction, especially when time sensitivity of delivery of goods is critical.
- (ii) Poor road quality: Some drivers respond that they avoid driving on a particular route because of poor road condition. On such roads, chances of road mishaps are more.
- (iii) Roadside obstructions: Avoiding a particular route because obstruction caused by electric wires on roadside is one of the neglected but peculiar issue of concern to drivers of heavy vehicles.
- (iv) Height of heavy vehicle is greater than that of normal four wheeler vehicle. So while driving in the areas where there is the problem of electric wire network alongside road, driving heavy vehicle is difficult. Possibility of wires getting stuck with the truck may cause reduction of speed.

5.5 Analysis of Factors Responsible for Delays on Study Routes

Delay identification is a complex process where there is a contribution of various factors for causing overall journey delay. For analysis purpose, we have to see the interaction of these various factors. However, it is not possible to mention all these factors in a single table. So, to make analysis procedure easier list of problems related to various major factors causing delays are listed in Table 2.

Table 2 Factors causing delays

Factors responsible	Related to	Problem description
Roads	Road geometry	Rough road surface
		Road width reduction
		Horizontal curvature/vertical curvature
		Grade separation
		Absence of road marking
		Taking U-turn/waiting to take U-turn
		Delays to heavy vehicle while merging from minor to major road
	Roadside environment	Objects next to the road
		Setback
		Road accident
		Poor road sign legibility
		Roadside construction work
		Roadside parked vehicles
Traffic congestion		Delays on intersection (signalized/unsignalized)
		Entry of slow moving vehicle
		Merging of another vehicle into traffic stream ahead of the test vehicle
		Waiting for green signal
Driver		Age/experience
Temporary factors		Distraction and overload
		Night/day
Weather condition		Summer
		Winter
		Rainy
Procedural		Weighing by third party
		Toll plaza
		Diesel filling
Vehicle		Recently manufactured
		Old

5.5.1 Analysis of Trip from ICD, Nagpur to Pardi

From overall ten trips from ICD, Nagpur to various destinations, major delay occurred in trip to Pardi. So the trip from ICD to Pardi is taken under consideration for analyzing the delay problem.

To develop macro-level understanding of trips originating from ICD, Nagpur and viewing the particular route followed by the truck driver (can be seen from map prepared in ARC GIS software) refer Fig. 3.

The data obtained from ‘GPS Speedometer’ application is used to formulate the graph showing information regarding the speed of the vehicle at any time along the journey. The graph obtained for the journey from ICD, Nagpur to Pardi can be seen in Fig. 4.

The sudden reduction of speed can be seen in the graph with the help of downward peaks of speed. The reduced speed to particular values is marked on the trough depressions of the graph. Locations, where sudden reduction of speed occurred, is analyzed with the help of video recording and the responses from travel survey.

The various factors responsible for the overall delay for the trip from ICD, Nagpur to Pardi can be compared with the help of following pie chart in Fig. 5.

From the figure, it is concluded that for causing overall delay for heavy-duty vehicle to travel from ICD, Nagpur to Pardi the factors traffic and road-related factors contribute majorly. On further analysis, the various traffic-related and road-related factors responsible for delays and their total contribution to the problem for the trip from ICD, Nagpur to Pardi can be seen with the help of Figs. 6 and 7.

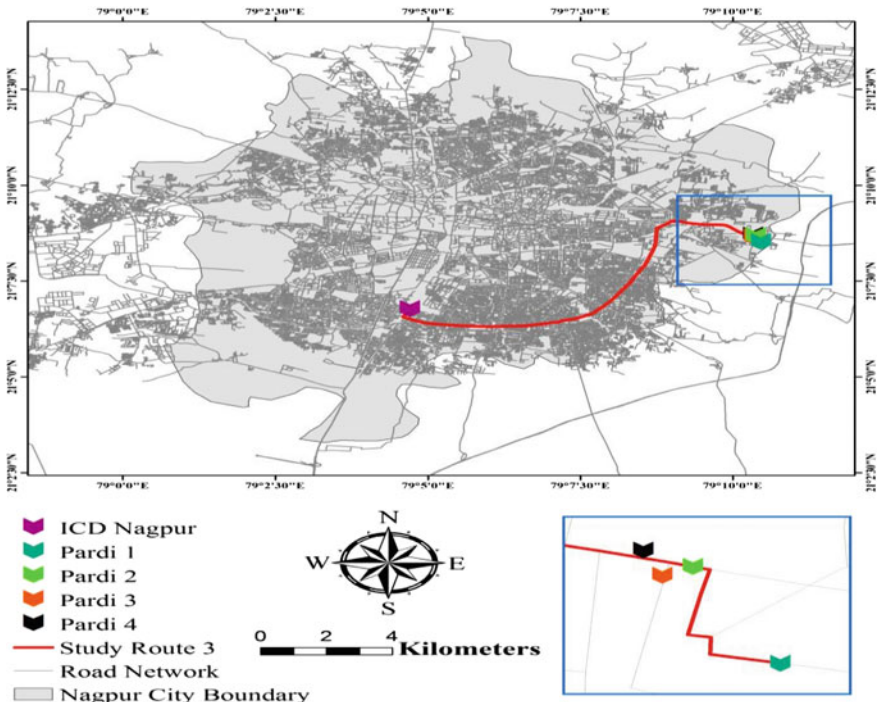


Fig. 3 Route map from ICD, Nagpur to Pardi

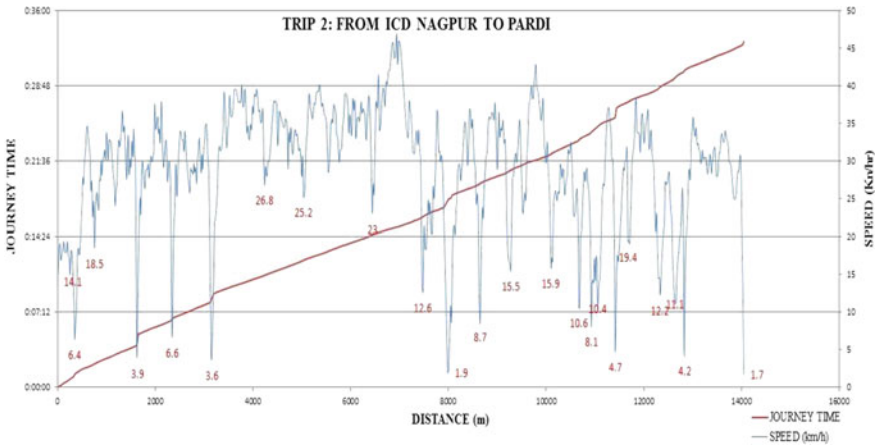


Fig. 4 Time versus distance versus speed graph

Contribution of various factors responsible for overall delay

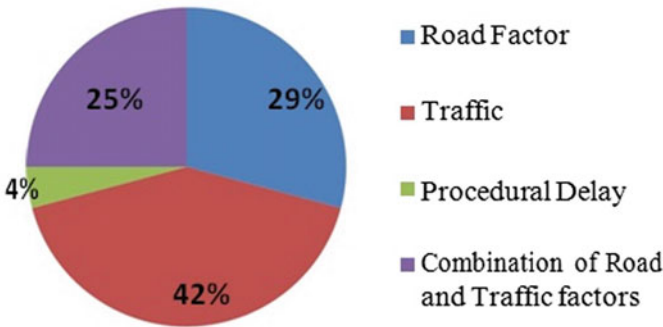


Fig. 5 Contribution of various factors responsible for overall delay

Traffic related problems from ICD to Pardi

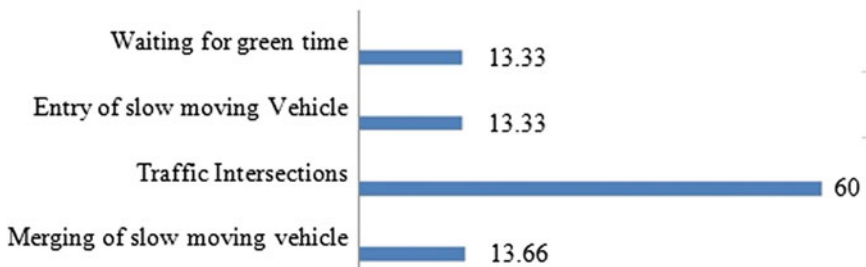


Fig. 6 Traffic-related problems from ICD to Pardi

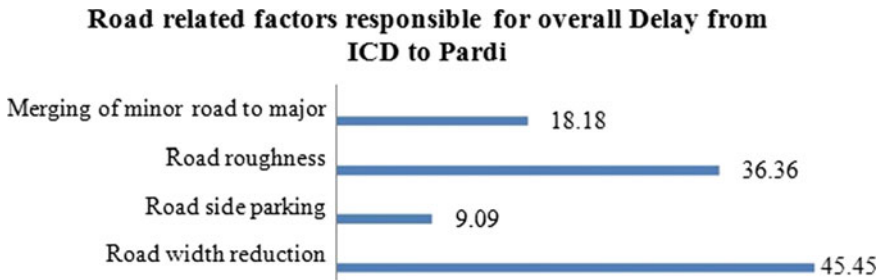


Fig. 7 Road-related problems from ICD to Pardi

To improve the existing situation for the particular study route, the problems related to traffic condition and roads are being addressed here. The traffic engineers can segregate heavy-duty traffic from normal lightweight traffic to reduce the delays. At the same time, the pavement designer can improve the road geometrics and overall road quality to reduce the overall delays.

6 Conclusion

The graphs can be analyzed by the researchers concerning to particular factor responsible for delay. The characteristics of graphs can be analyzed by pavement engineer to improve the road geometric conditions. Also, the city planners and traffic managers can make use of these graph characteristics for identifying the probable spots where there is a chance of reduction in speed with the help of which they can plan better transport environment. Also, the speed characteristics of different heavy vehicles can be analyzed by mechanical engineers for improving the brakes efficiency of the vehicle.

From the practice perspective, the main contribution of this research is the development of a more refined approach for identifying various factors responsible for delays in freight movement.

6.1 Implications of This Research

Though this research used a particular inland container depot as its case study, the findings of this research may be applied to any ICDs. The results from this research have applications both for researches and practices contributing to regional and national economy. With the improvement of transportation, the on-time delivery of time-sensitive goods would be possible which will further improve supply chain management. Hence, from a practical application perspective, the new methodology for identifying and estimating delayed delivery time along the journey can help trans-

port planners in improving scheduling and in turn could greatly enhance the travel time reliability.

6.2 Future Scope

This study was actually more complicated than what we initially thought because the authorities of ICD Nagpur were quite reluctant and at the same time were unaware of what we were planning to do. So the quality time was wasted in discussion with the officials than having data collection. For conducting such type of research in future, the authorities must be participative in the research. Also because of time constraint, we were unable to add the requisite amount of samples. However, more number of samples will be helpful for model making which will quantify the complexity of various factors involved in overall delay.

References

1. Inbakaran C, Kroen A (2011) Travel surveys—review of international survey methods
2. Richardson A, Ampt E, Meyburg A (1995) Survey method for transport planning. In: Australasian transport research forum 2011 proceedings, Adelaide, Australia, 28–30 Sept 2011. Eucalyptus Press, Melbourne
3. Jaiswal S et al (2016) Understanding travel behaviour of employees of an industrial area—Aurangabad case study. In: 12th transportation planning and implementation methodologies for developing countries
4. Mathew TV (2016) Measurement along a Length of Road. NPTEL, https://www.civil.iitb.ac.in/tvm/nptel/523_TrDensity/web/web.html. Accessed 15 Oct 2016
5. Ritz RJ, Regidor JR (2011) A study on travel time and delay survey and traffic data analysis and visualization methodology. Proc East Asia Soc Transp Stud 8
6. Mauricio IC, Santos RC, Regidor JR, Tiglaio NC (2003) Travel time and delay analysis using GIS and GPS. In: 5th Eastern Asia society for transportation studies conference
7. Byon YJ, Shalaby A, Abdulhai B (2006) Travel time collection and traffic monitoring via GPS technologies. In: 2006 IEEE intelligent transportation systems conference, Toronto, Canada, 17–20 Sept 2006
8. Li S, Zhu K, Van Gelder BHW, Nagle J, Tuttle C (2002) Improving efficiency of INDOT traffic data collection using GPS devices. Report No. FHWA/IN/JTRP-2002/19. U.S. Department of Transportation Federal Highway Administration and Indiana Department of Transportation
9. Li S, Zhu K, Van Gelder BHW, Nagle J, Tuttle C (2002) Reconsideration of sample size requirements for field traffic data collection using GPS devices. In: Transportation research board 2002 annual meeting CD-ROM
10. GPS Speedometer (Version:3.7.46) (2016) Google Android Play Store. gpxscan.com

Household Structure and the Travel Pattern of Senior Citizens for Leisure Trips



G. Nantha Priya, Samson Mathew and G. Subbaiyan

Abstract The travel patterns of the senior citizens are significantly influenced by social and cultural norms. Household structure also has an important bearing on the travel pattern of senior citizens. The specific household structure and the number of co-residents have huge implications on their travel outcomes. This investigative paper is an attempt to analyse the trips undertaken by senior citizens for leisure activities. The aim of the study is to examine the travel mode choice and length of the leisure trips made by senior citizens, based on household structure. The household questionnaire survey method is adopted for data collection. The gathered data is analysed using Statistical Package for the Social Sciences (SPSS) and NLOGIT 5 software. The variables analysed for the study include income, employment and education grouped under socio-economic variables; age, household size and gender grouped under socio-demographic variables; driving licence, shared rides, activity, frequency of travel, time of travel, mode, trip length, travel cost and travel time grouped under travel characteristics. Decision trees are developed to analyse the trip length. Choice modelling, i.e. multinomial logit (MNL) model, is adopted to find the travel mode preference of senior citizens for leisure trips.

Keywords Senior citizens · Household structure · Decision trees · Choice modelling · Multinomial logit

1 Introduction

The changing demographic profile of a rapid ageing population who enjoy extended life expectancy is presently witnessed all over the world due to low fertility and

G. N. Priya (✉) · S. Mathew

Department of Civil Engineering, National Institute of Technology, Tiruchirappalli, India
e-mail: gnanthapriya@gmail.com

S. Mathew
e-mail: sams@nitt.edu

G. Subbaiyan
Department of Architecture, National Institute of Technology, Tiruchirappalli, India
e-mail: subbaiah@nitt.edu

© Springer Nature Singapore Pte Ltd. 2020

T. V. Mathew et al. (eds.), *Transportation Research*, Lecture Notes
in Civil Engineering 45, https://doi.org/10.1007/978-981-32-9042-6_26

significant improvements to diet, lifestyle and hygiene. This rapid increase in the proportion of the senior population has tremendous implications on transportation planning. The transport needs of senior citizens are diverse and tend to change over a period of time as the process of ageing has a direct bearing on capacity to drive. The household structure has a significant influence on the travel pattern of senior citizens since the manner in which leisure time is spent depends, by and large, on the family structure. The importance of household structure on travel pattern in an urban area can be determined by a comparative analysis of different people from varying socio-economic and cultural backgrounds. The demarcated study area is Tiruchirappalli City Corporation in Tamil Nadu. The population of senior citizens in the Tiruchirappalli City Corporation of Tamil Nadu state is 98,356 as per 2011 census, which is 13.46% of the total population. Three categories of household structure are analysed: retiree household (retired people with no adult children or grandchildren), adult family (retired people with their adult children, but no grandchildren) and extended family (retired people with their adult children and grandchildren).

2 Literature Review

Family roles tend to influence leisure decisions through the course of life and across social contexts. Family composition (e.g. the number of children, adults and senior citizens within the family group) may provide different opportunities for leisure participation [1]. Earlier researchers have demonstrated the usefulness of using the family life cycle to describe the leisure participation of individuals and families [2, 3]. The impact of the family circle on leisure activities as well as the correlation between the presence/absence of children/grandchildren and leisure activities has been documented by earlier studies [4–7]. A comprehensive literature study has been undertaken to fully explore the influence of family structure on the travel mode preference and length of trips made by senior citizens.

2.1 *Mode Choice and Family Structure*

The significance of the travel behaviour and mode choice of senior citizens in transportation planning and policy has so far been given scant importance; a majority of studies on travel behaviour and mode choice are focused on the working-age population. Some studies have found that age is a major factor influencing non-home activity, travel behaviour and travel mode choice of senior citizens. For instance, it was found that the senior citizens aged 60 and above tend to have fewer non-home activities compared with other age groups [8]. It was observed that as age increased the travel time spent for non-home activities decreased. However, age was found to be positively associated with travel time, although overall non-home activities were negatively associated with age [9].

Senior citizens preferred to make recreational and shopping trips during non-peak hours [10]. It was found that the travel time for leisure activities was influenced by the choice of travel mode [11]. As the household size increases, senior citizens tend to opt for shared rides and public transport [12]. Senior citizens belonging to small households with either one or two members prefer the convenience of travelling by using their own vehicles, often self-driving.

2.2 Trip Length and Family Structure

Information about the distance a person travels is a good indicator of the quality of life enjoyed and is useful in the framing an appropriate transportation planning policy. It provides an indirect measure of mobility and freedom to move around the built-up environment. In contrast to the studies on distance travelled related to gender and urban structure, there has been limited research that focuses on the length of trips made by senior citizens. The travel behaviour of senior citizens is significantly different from other segments of the population. In general, age has a negative effect on distance travelled. The distance travelled by the senior citizens decreases as they grow older. Reports have found that older people tend to have shorter commute distances than young people [13]. It should be emphasized that commute distance is of limited use when trying to understand the behaviour of the senior citizen since the journey to work is less prevalent among this group. Distance and frequency of trips made for recreational purposes show a downward trend after the age of 80 [10]. Physical, economic and social environments influence the health, household income, work status and driving licence ownership and car ownership of the senior citizen, and these are the variables that have been reported to positively impact the trip length [10]. The relevance of modality can be inferred from the challenges posed by driving cessation or lack of access to private and public vehicles [14]. The individual and built environment relationships are particularly pertinent in the case of senior citizens [15]. The current ageing-in-place trend also has some impact on the length of trips made to access services [16–18]. Existing literature on the relationship between task division by household members and related activity–travel patterns place a strong emphasis on the travel behaviour of the seniors. The findings suggest that due to role specification and task allocation within the household for different activities with different intensity (frequency and duration), it is evident that the family structure influences the travel pattern of the seniors. The aim of the current paper is to analyse the travel mode choice and length of leisure trips made by senior citizens, based on household structure.

2.3 Research Design

Leisure trips include social visits, recreational sojourns, religious trips, restaurant visits and trips to gyms or fitness centres. The travel modes covered under the analysis are bus, Intermediate Para Transit (IPT), car, two-wheeler, cycle and by walk. Three categories of household structure are analysed. Chi-square Automatic Interaction Detector (CHAID) analysis is done to explore the heterogeneity in trip length to access leisure activity. Choice modelling, i.e. MNL, is adopted to find the travel mode preference of senior citizens for leisure trips.

3 Data Collection

This exploratory paper analyses the travel pattern of the senior citizens for various leisure activities. The target group chosen is senior citizens in the age group of 60 years and above, the criterion being that they must be able to make at least one trip once a month. The study area is divided into four zones which includes Srirangam with 15 wards, Ariyamangalam with 18 wards, Ponmalai with 17 wards and Abieseekapuram with 15 wards. A home interview survey is conducted to collect the secondary data. The questionnaire has three parts: household information, personal information and travel diary. A total of 10,081 households are considered for the survey. Among them, households with senior citizens are segregated for further analysis. The response proportion of senior citizens is found to be 18%. This study used all possible precautions to ensure the confidentiality, anonymity and privacy of the data and the participants involved. People were informed details of the research and also that the participation in the survey is purely voluntary. The home interview survey was conducted after getting consent from those who wished to respond on their own and out of their interest.

3.1 Methods

Preliminary analysis is done using the data collected through questionnaire survey. The travel demand for leisure trips is estimated based on the length of leisure trips and the mode preference of the senior citizens to access leisure activities. The length of the trip made by the respondent is estimated using CHAID analysis and the travel mode preference by using multinomial logit model. SPSS package is used to calculate the regression, and CHAID analysis and NLOGIT 5 are used for modelling the mode preference.

3.1.1 CHAID Analysis

The length of trips made for leisure activities is calculated using CHAID analysis. Chi-square Automatic Interaction Detector is a method that uses chi-square statistics to identify optimal splits. It is an analysis that determines how variables best combine to explain the outcome for a given dependent variable. CHAID analysis can be used to analyse nominal, ordinal and continuous data, and hence, it is used to model trip length. In CHAID analysis, if the dependent variable is continuous, the F test is used and if the dependent variable is categorical, the chi-square test is used. Each pair of predictor categories is assessed to determine the least significant value with respect to the dependent variable. Due to these steps of merging, a Bonferroni adjusted p -value is calculated for the merged cross tabulation.

3.1.2 Multinomial Logit Model

The multinomial logit model is used for analysing the travel mode choice of the senior citizens to access various leisure activities. It is the most preferred and widely used model in discrete choice analysis. Logit model development consists of formulating model specifications and estimating numerical values of the parameters for the various attributes specified in each utility function by fitting the models to the observed choice data. The coefficient of the logit model is estimated by the method of maximum likelihood estimation. The general expression for the probability of choosing an alternative ' i ' ($i = 1, 2 \dots j$) from a set of j alternatives is:

$$\Pr(i) = \frac{\exp(V_i)}{\sum_{j=1}^j \exp(V_j)} \quad (1)$$

where $\Pr(i)$ is the probability of the decision-maker choosing alternative i and V_j is the systematic component of the utility of alternative j .

4 Preliminary Analysis

The profile of the respondents is given in Table 1. The overall profile shows a more or less uniform pattern of the respondents in the study area for all categories. Female respondents are seen to be more, from all types of families. People falling under the 'Below SSLC' and 'Plus two' categories are comparatively more than other categories.

Homemakers and retired group senior citizens are noted to be more compared to other categories. The number of people falling into the extended category of self-employed seniors is larger than other categories of people. The number of morning trips is more compared to the evening. The homemaker category has more members

Table 1 Respondent detail

Variable	Particulars	Percentage of trips		
		Retiree family	Adult family	Extended family
Gender	Male	34	36	38
	Female	66	64	62
Education	Below SSLC	81	88	85
	Plus two	15	10	13
	Graduate	1	1	1
	Postgraduate	1	1	0
	Professionals	1	0	0
Travel time	5:00 a.m. to 8:00 a.m.	17	26	25
	8:00 a.m. to 11:00 a.m.	49	39	39
	11:00 a.m. to 2:00 p.m.	11	7	7
	2:00 p.m. to 5:00 p.m.	17	20	22
	5:00 p.m. to 8:00 p.m.	7	8	7
Mode	Bus	14	21	18
	IPT	1	1	1
	Car	2	3	6
	Two-wheeler	13	15	18
	Cycle	5	6	4
	Walk	65	54	55
Monthly income	No income	62	58	57
	<Rs 10,000	32	36	33
	Rs 10,000–Rs 25,000	4	4	8
	Rs 25,000–Rs 50,000	1	1	1
	>Rs 50,000	1	0	1

which consequently leads to an increase in the number of senior citizens falling under ‘No income’ category, it is seen that senior citizens are to a great extent dependent on their family members. Walking is the predominant mode of travel. Bus and two-wheelers are observed to share more or less equal percentage of trips. Most senior citizens do not possess a valid driving licence, and hence, it can be inferred that walking and public transport would be their preferred alternate mode of travel. ‘No income’ category is found to be more in all types of families. Comparatively, the retiree family type is seen to have a maximum number of people falling under the ‘No income’ category. This implies that the younger generations are upwardly mobile and readily move to greener pastures whereas senior citizens dislike change of any kind, are reluctant to move to new locales and prefer to reside in familiar places. There are an insignificant number of senior citizens earning more than Rs. 50,000.

5 Model Development—Trip Length

5.1 Trip Length—Retiree Family

The tree table for trip length of retiree family is shown in Table 2. The average distance travelled by the senior citizen in this category is 1.5 km. The primary influencing variable is the possession of a valid driving licence. A majority of senior citizens do not possess a valid driving licence. The next influencing variable is the distance from the residence to the bus stop. If the distance between the residence and the bus stop is more, the length of any trip made for leisure activity correspondingly tends to increase. Hence, the percentage of leisure trips will decrease with an increase in the distance between the residence and bus stop, particularly for the retiree category families. The travel frequency is the next influencing variable.

Figure 1 shows the decision tree for finding the length of trips made by retiree families to access leisure activities. The figure shows that a majority of senior citizens do not possess a valid driving license. On analysing the next influencing factor, which is the distance from the residence to the bus stop, 81% of the respondents without a valid driving license are found to be influenced by this factor. The number of leisure trips is maximum if the distance from the residence to the bus stop is less than 1 km. Even when the distance between the residence and bus stop is short, the frequency of travel is less. The preference for long-distance trips becomes negative if the distance from the residence to bus stop is more. In summation, retiree families, consisting only of couples aged 60 years and above, do not prefer to travel longer distances for leisure trips when they do not hold a valid driving licence, particularly when the distance from their residence to the bus stop is more.

5.2 Trip Length—Adult Family

The trip length of the adult family is shown in Table 3. The average distance travelled by the senior citizens in an adult family is 2.6 km. Figure 2 shows the length of trips taken by the senior citizens in an adult family. The prime factor influencing the trip length is the travel time. A study of the structure of the adult family reveals that the household responsibility of the seniors in this category is more compared to other family structures. This fact is corroborated by Fig. 2 where it is seen that travel time is the main influencing factor for accessing leisure activities. The travel cost is the next influencing factor. Hence, for senior citizen dwelling in an adult family, travel time and travel costs are the primary influencing factors that have a bearing on access to leisure activities.

Table 2 Tree table—Trip length retiree family

Node	Mean (km)	Percent	Predicted mean (km)	Parent node	Independent variable	Split values
0	2.1	100	1.5			
1	2.0	81	1.4	0	Driving licence	No
2	2.6	19	1.9	0	Driving licence	Yes
3	0.3	10	0.3	1	DistHB ^a	≤0.42
4	0.5	9	0.5	1	DistHB ^a	(0.42, 0.5]
5	0.6	6	0.6	1	DistHB ^a	(0.5, 0.7]
6	0.8	5	0.8	1	DistHB ^a	(0.7, 0.9]
7	1.0	20	1.0	1	DistHB ^a	(0.9, 1]
8	1.5	5	1.5	1	DistHB ^a	(1, 1.8]
9	2.3	10	2.3	1	DistHB ^a	(1.8, 3.22]
10	4.4	8	4.5	1	DistHB ^a	(3.22, 5]
11	8.3	7	9.2	1	DistHB ^a	>5
12	0.4	2	0.4	2	DistHB ^a	≤0.42
13	0.5	2	0.5	2	DistHB ^a	(0.42, 0.5]
14	0.6	1	0.6	2	DistHB ^a	(0.5, 0.7]
15	0.8	2	0.8	2	DistHB ^a	(0.7, 0.9]
16	1.0	4	1.0	2	DistHB ^a	(0.9, 1]
17	1.5	1	1.5	2	DistHB ^a	(1, 1.8]
18	2.3	3	2.3	2	DistHB ^a	(1.8, 3.2]
19	4.5	2	4.5	2	DistHB ^a	(3.2, 5]
20	9.3	2	9.7	2	DistHB ^a	>5
21	0.4	2	0.4	3	Travel frequency	≤Once in a month
22	0.4	6	0.4	3	Travel frequency	(Once in a month, Once in two week]
23	0.3	2	0.3	3	Travel frequency	(Once in two week, Once in a week]
24	0.3	1	0.3	3	Travel frequency	>Once in a week
25	0.6	2	0.6	5	Travel time	≤5
26	0.6	4	0.6	5	Travel time	>5
27	0.8	1	0.8	6	Hour of travel	≤5:00 a.m. to 8:00 a.m.

(continued)

Table 2 (continued)

Node	Mean (km)	Percent	Predicted mean (km)	Parent node	Independent variable	Split values
28	0.8	3	0.8	6	Hour of travel	(5:00 a.m. to 8:00 a.m., 11:00 a.m. to 2:00 p.m.]
29	0.8	1	0.8	6	Hour of travel	> 11:00 a.m. to 2:00 p.m.
30	1.5	1	1.5	8	Age	≤61
31	1.5	1	1.5	8	Age	(61, 62]
32	1.5	1	1.5	8	Age	(62, 63]
33	1.5	0	1.5	8	Age	(63, 64]
34	1.5	1	1.5	8	Age	(64, 65]
35	1.5	1	1.5	8	Age	(65, 68]
36	1.5	0	1.5	8	Age	>68
37	2.2	5	2.1	9	Travel cost	≤0
38	2.5	4	2.5	9	Travel cost	(0, 4]
39	2.8	1	2.9	9	Travel cost	(4, 6]
40	2.4	1	2.4	9	Travel cost	>6

^aDistance from residence to bus stop

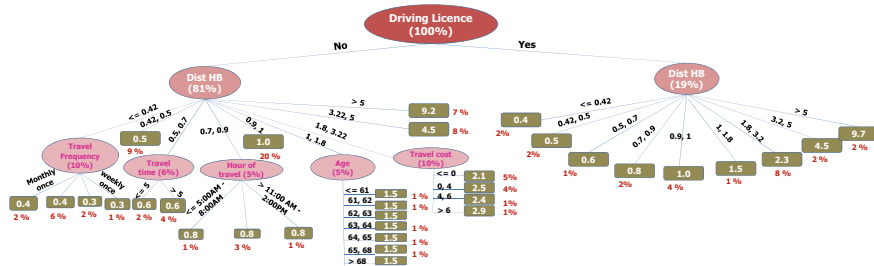


Fig. 1 Decision tree—Trip length—Retiree family

5.3 Trip Length—Extended Family

The length of trips made by the extended family is given in Table 4. Figure 3 shows the decision tree for analysing the length of trips made by extended families to access leisure activities. The influencing variables are travel time, travel frequency, mode of travel, travel cost, distance from residence to bus stop and income. The average distance travelled by the senior citizen in this category is 2.7 km. The primary influencing variable is the travel time. Only a minimum percentage of people (10%) in this category travel for longer durations trips. The next influencing variable is the

Table 3 Tree table—Trip length adult family

Node	Mean (km)	Percent	Predicted mean (km)	Parent node	Independent variable	Split values
0	2.6	100	2.6			
1	0.7	20	0.7	0	Travel time	≤6
2	1.4	36	1.4	0	Travel time	(6, 10]
3	2.9	22	2.9	0	Travel time	(10, 15]
4	4.3	13	4.3	0	Travel time	(15, 23]
5	7.6	10	7.6	0	Travel time	>23
6	0.6	17	0.6	1	Travel time	≤67
7	1.0	3	1.0	1	Travel time	>67
8	0.9	28	0.9	2	Travel cost	≤0
9	2.5	5	2.5	2	Travel cost	(0, 3]
10	4.6	3	4.6	2	Travel cost	>3
11	1.8	9	1.8	3	Travel cost	≤0
12	2.4	3	2.4	3	Travel cost	(0, 3]
13	3.2	3	3.2	3	Travel cost	(3, 4]
14	4.7	6	4.7	3	Travel cost	>4
15	2.4	4	2.4	4	Travel cost	≤0
16	3.6	2	3.6	4	Travel cost	(0, 3]
17	5.0	4	5.0	4	Travel cost	(3, 6]
18	6.5	3	6.5	4	Travel cost	>6
19	4.4	3	4.4	5	Travel cost	≤4
20	9.0	7	9.0	5	Travel cost	>4
21	0.6	14	0.6	6	Driving licence	No
22	0.4	3	0.4	6	Driving licence	Yes

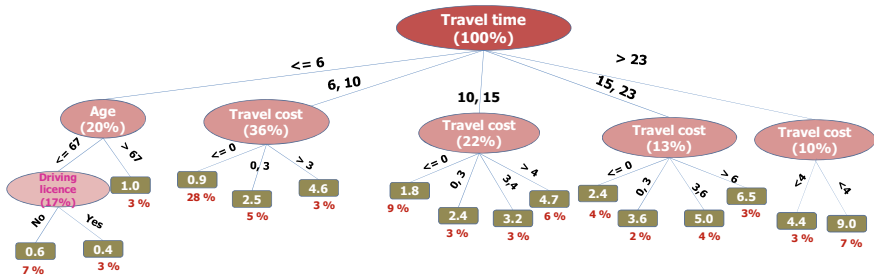


Fig. 2 Decision tree—Trip length—Adult family

Table 4 Tree table—Trip length extended family

Node	Mean (km)	Percent	Predicted mean (km)	Parent node	Independent variable	Split values
0	2.7	100	2.7			
1	0.6	21	0.6	0	Travel time	≤5
2	1.2	34	1.2	0	Travel time	(5, 10]
3	2.7	19	2.7	0	Travel time	(10, 15]
4	4.7	18	4.7	0	Travel time	(15, 25]
5	9.0	10	9.0	0	Travel time	>25
6	0.8	3	0.8	1	Travel freq	≤Once in a month
7	0.4	10	0.4	1	Travel freq	(Once in a month, once in two wk]
8	0.8	7	0.8	1	Travel freq	>Once in two wk
9	0.9	25	0.9	2	Mode	Walk
10	2.0	6	2.0	2	Mode	Two-wheeler; cycle; car; IPT
11	3.0	2	3.0	2	Mode	Bus
12	1.6	8	1.6	3	Travel cost	≤2
13	2.1	3	2.1	3	Travel cost	(2, 3]
14	3.7	4	3.7	3	Travel cost	(3, 5]
15	4.3	4	4.3	3	Travel cost	>5
16	2.0	4	2.0	4	Travel cost	≤0
17	4.3	4	4.3	4	Travel cost	(0, 5]
18	5.8	6	5.8	4	Travel cost	(5, 9]
19	6.6	3	6.6	4	Travel cost	>9
20	4.7	3	4.7	5	Travel cost	≤5
21	8.4	2	8.4	5	Travel cost	(5, 9]
22	11.9	5	11.9	5	Travel cost	>9
23	0.5	4	0.5	8	DistHB*	≤0.58
24	1.1	3	1.1	8	DistHB*	>0.58
25	0.6	7	0.6	9	DistHB*	≤0.5
26	0.9	18	0.9	9	DistHB*	>0.5
27	1.2	2	1.2	10	Travel cost	≤2
28	2.5	3	2.5	10	Travel cost	>2

(continued)

Table 4 (continued)

Node	Mean (km)	Percent	Predicted mean (km)	Parent node	Independent variable	Split values
29	2.9	2	2.9	14	Mode	Two-wheeler; car
30	4.4	2	4.4	14	Mode	Bus
31	4.1	2	4.1	15	Gender	≤male
32	4.6	2	4.6	15	Gender	>male

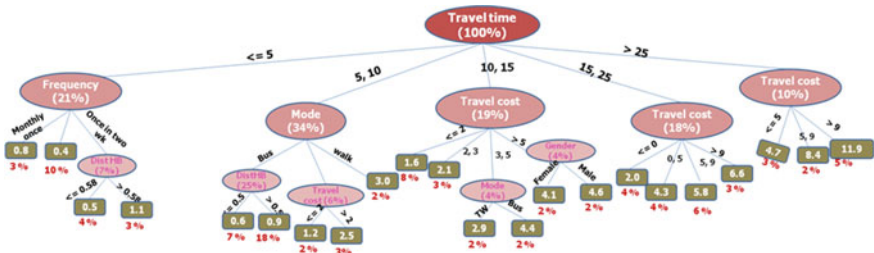


Fig. 3 Decision tree—Trip length—Extended family

mode of travel. The senior citizens in this category prefer to travel by bus for longer trip lengths, and the mean trip length is 3 km. For shorter distances, the preferred mode of travel is on foot. Bus is the preferred travel mode for short distances between the residence and bus stop. Hence, for seniors residing in an extended family, the number of trips is more if the home to bus stop distance is within 1 km and the preferred mode of travel is by bus, provided the travel time is less than 10 min.

6 Multinomial Logit Model—Choice of Mode

The multinomial logit model is used to analyse the available choice of travel modes and preference. The exploratory variables are employment, education, time of travel, income, shared ride and gender. The travel modes considered for the analysis are bus, Intermediate Para Transit (IPT), car, two-wheeler, cycle and on foot.

6.1 Mode Choice—Retiree Family

The travel mode choice of the senior citizens in a retiree family is shown in Table 5. IPT and car are not preferred due to the higher travel cost involved. The most frequent

Table 5 Parameter estimate—MNL model—Retiree family

Variables	Bus	IPT	Car	Two-wheeler	Cycle	Walk
Constant	-3.243					
Travel cost		-0.082	-0.111			
Travel time	0.434	-0.262	0.116		-0.328	
Travel frequency			-0.906	-1.20		0.323
Income			1.458			-2.568
Age	-0.098	-.070	-0.217	-0.154		
Hour of travel						-2.543
Travel distance	-0.890					

mode of travel is on foot. The car is preferred by people falling under the high-income category and walking is preferred by those under the low-income category.

6.2 Mode Choice—Extended Family

The mode choice model for the senior citizen living in the extended family is given in Table 6. Walking is not preferred for long trips. People belonging to low-income category prefer the bus and two-wheeler for leisure trips. Bus and IPT are preferred by the seniors without a driving licence.

Table 6 Parameter estimate MNL model—Extended family

Variables	Bus	IPT	Car	Two-wheeler	Cycle	Walk
Constant	-3.99					
Travel cost	-0.518	1.563	-0.023	0.459		
Travel distance	0.420	0.033				-1.572
Travel time	0.578	0.860	0.985			
Employment	-0.686			-1.15		-0.364
Household size		1.35	3.175	0.922	0.568	
Travel frequency	-0.819		-0.876			
Driving licence	2.44	1.952	-2.41	-1.406	0.540	
Working hours					-1.22	
Gender		1.31	3.665			1.421

Table 7 Parameter estimate MNL—Adult family

Variables	Bus	IPT	Car	Two-wheeler	Cycle	Walk
Constant	-0.525					
Travel distance				2.395	0.512	
Travel cost	-0.921	-0.393	-0.098	-0.098		
Travel time	0.403	2.533	1.182	1.182	-0.177	0.512
Income		1.12247	1.077			
Age			-0.163	-.283	-0.283	
Employment	-1.059	-1.009	-0.865	-1.914		-0.546
Education	-0.681	-1.651				
Household size				1.675	-0.556	

6.3 Mode Choice—Adult Family

The travel mode preference of the senior citizens residing in the adult family is given in Table 7. For commuting longer distances, the two-wheeler is preferred while the cycle is preferred for shorter distances. Car and IPT are preferred by people under the high-income category. Educated people do not prefer to travel by bus and IPT.

7 Results and Discussion

The steadily increasing ageing population in Indian urban areas has necessitated the reliable estimation of the travel patterns of senior citizens. An attempt has been made in this research study to estimate the travel pattern of senior citizens accessing leisure activities, based on the family size, the study area being Trichy City Corporation, which is a medium-sized city. CHAID model is developed to find the trip length, and MNL is developed to determine the travel mode preferences of senior citizens for leisure trips. Three types of families are analysed: adult, extended and retiree families. The proportion of senior citizens living in an adult family is more compared to other family groups. The length of trips made by senior citizens living in a retiree family is less compared to other categories of families. Driving licence is the most influencing variable for the retiree family category, and travel time is an influencing variable for the other family groups. The length of trips made by the senior citizens of the adult family is shorter, usually less than one km, and it is constrained by the travel time and travel cost. Possession of driving licence is the predominant factor influencing the length of trips made by the senior residents of the retiree family. Distance from home to bus stop is the succeeding level parameter influencing the length of trips undertaken by senior citizens of the retiree family. The frequency of trips is more if the residence to bus stop distance is minimum. Travel time is the predominant variable for extended family type. The succeeding hierarchical variables that influence length

of trips made by the senior residents of the extended family are travel mode and travel cost. Bus is preferred if the distance between the residence and the bus stop is minimum. The trip length is more when higher travel cost is involved. Trip length increases with increase in travel time. Walking is the most preferred mode of travel by all the three categories of senior citizens. Retiree family seniors take the maximum number of trips, with walk mode preferred for short trips and short distances. The senior residents of the extended family take a minimum number of leisure trips with longer trip lengths. IPT is the least preferred mode of travel by the senior citizens of all three family groups. After walking, the next preferred modes of travel are two-wheeler and bus.

8 Conclusion

This paper adopts a holistic approach to analyse the travel pattern of senior citizens based on the family structure. Two models are developed to analyse the trip length and travel mode preference of the senior citizens for leisure activities. Adult family and extended family share their household responsibilities; hence, the frequency of trips and trip length is less compared to retiree family. The number of senior citizens in possession of a driving licence is less, and hence, senior citizens depend on public transport and walking for their leisure trips. The interactions of family members and the household activities decide the travel behaviour of the senior citizens since they are largely dependent on their family members for their livelihood. This research can be further extended to analyse the neighbourhood interaction to give a complete urban morphology about the travel pattern of the senior citizens for leisure activities.

Acknowledgements The authors gratefully acknowledge the research funding from Centre for Excellence in Transportation Engineering (CETransE) NIT Tiruchirappalli, a Centre of Excellence funded by the Ministry of Human Resources Development, Government of India.

References

1. Osgood NJ, Howe CZ (1984) Psychological aspects of leisure: a life cycle development perspective. *Soc Leisure* 7:175–196
2. Kelly JR (1974) Socialization toward leisure: a developmental approach. *J Leisure Res* 6:181–193
3. Kelly JR (1978) Family leisure in three communities. *J Leisure Res* 10:47–60
4. Bollman SR, Moxley VM, Elliot NC (1975) Family -and community activities of rural non-farm families and children. *J Leisure Res* 7:53–62
5. Buchanan T, Christensen JE, Burdge RI (1981) Social groups and the meanings of outdoor recreation. *J Leisure Res* 13:254–266
6. Burch WR (1964) Two concepts for guiding recreation management decisions. *J Forest* 62:707–712

7. Burch WR, Wegner WO (1967) The social characteristics of participants in three styles of family camping. USDA Forest Service, Pacific Northwest Forest and Range Experiment Station, Portland, OR
8. Kuppam A, Pendyala R (2001) A structural equations analysis of commuters' activity and travel patterns. *Transportation* 28:33–54
9. Lu X, Pas E (1999) Socio-demographics, activity participation and travel behaviour. *Transp Res* 33A:1–18
10. Steed JL, Bhat CR (2000) On modeling departure-time choice for home-based social/recreational and shopping trips. *Transp Res Rec J Transp Res Board* (1706):152–159. TRB, National Research Council, Washington, D.C
11. Lanzendorf M (2002) Mobility styles and travel behaviour: application of a lifestyle approach to leisure travel. *Trans Res Rec J Transp Res Board* (1807): 163–173. TRB, National Research Council, Washington, D.C
12. Sungyop Kim, Gudmundur Ulfarsson F (2015) Activity space of older and working-age adults in the puget sound region. *Wash J Transp Res Board* 2494:37–44
13. Rouwendal J, Rietveld P (1994) Changes in commuting distances of Dutch households. *Urban Stud* 31:1545–1557
14. Páez AP, Scott DM, Potoglou D, Kanaroglou P, Newbold KB (2007) Elderly mobility: demographic and spatial analysis of trip making in the Hamilton CMA. *Can Urban Stud* 44:123–146
15. Rodriguez DA, Targa F, Aytur SA (2006) Transport implications of urban containment policies: a study of the largest twenty-five US metropolitan areas. *Urban Stud* 10:1879–1897
16. Blanchard J, Golant S, Moody H, Anthony B, Heumann L (2004) Ageing in place: a look beyond these four walls. *Gerontologist* 44:104–114
17. Harlow K, Garcia C (2002) Ageing in place: neighborhood characteristics, experiences and quality of life. *Gerontologist* 42:236–246
18. Lloyd L (2000) Making ageing in place work. *Housing Stud* 15:652–654

Traffic Systems Analysis

Application of Queuing Theory to a Toll Plaza-A Case Study



Naveen Malipatil, Soumya Iswar Avati, Hosahally Nanjegowda Vinay and S. Sunil

Abstract Queuing areas are the junctions involving vehicles waiting in lines and are characterized by an arrival pattern, a service facility arranged in a particular manner and service time. Since the maximum capacity of roads and service facility (i.e. number of booths in case of tolls) are fixed for certain period (i.e. design period), it is necessary to measure the efficiency of a facility. In case of toll booths on highways/freeways which are attractors of vehicles from different origin presumes the flow to be continuous and the vehicle inter-arrival random, adding to this is variability in demand and service (service time in toll booths), poses a problem in optimizing the service facility. In the present study, an existing toll plaza on a 4-lane divided highway having two-way movement (N–S and S–N) is evaluated based on queuing theory. Parameters like traffic volume, space-mean speed and time headway are expressed in 1 h intervals. The vehicle arrival patterns on both directions are postulated to be Poisson distributed and the observed data were fitted to the Poisson distribution. In case of N–S movement, observed frequency and theoretical frequency are found out to be equal indicating the postulated Poisson distribution to be the true population distribution. The use of chi-square test as an index of the goodness of fit for significance level 5% with 10° of freedom justifies the postulated Poisson distribution can be used for future analysis of vehicle arrivals in the respective direction. Finally, the utilization factor indicates a single booth in N–S direction to be under steady-state condition during the study period.

N. Malipatil · S. I. Avati · S. Sunil (✉)

Department of Civil Engineering, Rashtreeya Vidyalyaya College of Engineering,
Bengaluru, India

e-mail: sunils@rvce.edu.in

N. Malipatil

e-mail: naveenpatil87922@gmail.com

S. I. Avati

e-mail: soumya.avati@gmail.com

H. N. Vinay

Department of Civil Engineering, Adichunchanagiri Institute of Technology, Chikkamagalur,
India

e-mail: vinay.hn28@gmail.com

© Springer Nature Singapore Pte Ltd. 2020

T. V. Mathew et al. (eds.), *Transportation Research*, Lecture Notes
in Civil Engineering 45, https://doi.org/10.1007/978-981-32-9042-6_27

Keywords Queuing theory · Observed and theoretical frequency · Chi-square test · Significance level · Poisson distribution · Utilization factor

1 Introduction

One of the major issues in traffic analysis is the analysis of delay. Delay may be seen in a traffic system where in the demand exceeds the capacity. If the delay results in formation of waiting line, such delays are called as queuing delays. Queuing delays are analysed by queuing theory. The fundamental idea of the theory is that delay in a traffic system is caused by an interruption in the flow pattern as mentioned by Drew [1]. Queuing is characterized by an arrival pattern, a queue discipline and a service facility providing service to the demand. A queuing system can be described by elements like arrival rate, queue discipline, number and arrangement of service facility and service rate. Elements like arrival patterns and service pattern are analysed based on assumptions.

The objective of the present work is as follows: (1) to choose a toll plaza on a highway facility to examine the applicability of the queuing method; (2) to collect the road inventory of the queuing system; (3) to record the traffic volume at mid-block section away from the queuing area as per Indian roads congress guidelines; (4) to present the space-mean speed of vehicles at the entry point of the queuing area and very near to the booth indicating the retardation in speed of vehicles; (5) to measure the random arrival rate of vehicles towards the toll plaza; (6) to measure the service rate of a single booth; and (7) to analyse the arrival rate follows Poisson distribution and to see goodness of fit using chi-square test and finally to check whether the system is in steady-state condition using utilization factor. All the data are collected manually. The paper does not focus on any gap in the study. Rather, the paper examines the applicability of queuing theory for a toll plaza. Young Taeson et al. [2] in their study questioned the assumption of steady-state in the analysis of the queuing system under stochastic method. They have presented a simulation-based methodology for evaluating the appropriateness of the steady-state assumption on a two-lane highway work zone. They have finally concluded that it is not always reasonable to assume steady-state tendency of a highway queuing system prior to exploiting stochastic queuing technique. Woo and Hoel [3], have worked a methodology for evaluating the capacity and level of service (LOS) for toll plazas. The LOS for the selected four toll plazas in Virginia was defined on the criterion of average density, which is highly correlated with volume to capacity ratios. Ceballos and Curtis [4], have shown that the simple analytical models can be used for an initial understanding of the queuing system but warn that good judgement must be employed while using the analytical models, as their results may differ significantly from real-life plaza operation. According to them, simulation should be used for advance planning, design, operation and management of toll and exit plaza facilities. Anokye et al [5], have shown that queuing theory can be applied in modelling the vehicular traffic flow and minimize vehicular traffic in order to reduce delays on roads of Kumasi-Ashanti

region. They have suggested that the use of public transport by the government of Ghana would help in reducing congestion on the roads, which in turn boost the productivity. Vandaele et al [6], have shown that queuing models can be applied in assessing the traffic flow parameters compared to traditional empirical methods, which lack in terms of predictive power and the possibility of sensitivity analysis. They believe that speeds have a significant influence on vehicle emissions, and models can be effectively used to assess the environmental impact of road traffic. Cottrell [7] developed a three-regime model for identifying daily queuing period based on annual average daily traffic (AADT), and capacity (C) ratio (AADT/C) for Das and Levinson [8] applied queuing analytical technique to a freeway section in the city of Minneapolis, USA, to develop a new approach for validating densities and speeds on freeway sections. The selected site for the study can be traversed on Indian National Highway (NH-75) near Kirasave (chainage-119.0 km) from Bengaluru towards Mangaluru. The selected road is a divided four-lane National Highway. The site has been selected to explore the applicability of queuing theory a toll plaza.

2 Road Inventory

Road inventory data basically consist of data necessary to identify the project under evaluation. This consists of the geometric details of the project which are collected visually walking along the entire stretch. All of these data will remain constant until the pavement undergoes maintenance which is shown in Tables 1 and 2.

2.1 Traffic Volume

In the present study, the traffic count census is done on four consecutive days in both directions in accordance with Indian Roads Congress (IRC) standard on non-urban roads [9]. To take into account the randomness, the traffic volume study was carried out for duration of one hour on each day. The results are shown in Table 3.

Table 1 Details of pavement geometrics before toll plaza

SL. No	Parameters	Collected data
1	Type of pavement	Flexible pavement
2	Divided/undivided	Divided
3	Number of lanes	Four
4	Width of pavement (m)	9
5	Median width (m)	2.5
6	Shoulder width (m)	1.5
7	Type of shoulder	Earthen

Table 2 Details of queuing area

SL.NO	Parameters	Collected data
1	Type of pavement	Rigid
2	Width of pavement (one side)	30 m
3	Length of pavement on arrival side	250 m
4	Length of pavement on merging side	250 m
5	Number of toll booth on one side	5
6	Length of each toll booth	2.4 m
7	Width of each toll booth	1.9 m
8	Width between toll booths	3.6 m
9	Type of merging	Leftmost merging

Table 3 Details of traffic flow in both the directions

SL no	Direction	Time, hrs	Traffic flow, vehicles/hour	Average traffic flow, vehicles/hour
1	N-S	4:00 to 5:00	396	375
		5:00 to 6:00	518	
		9:00 to 10:00	321	
		10:00 to 11:00	262	
2	S-N	4:00 to 5:00	297	345
		5:00 to 6:00	311	
		9:00 to 10:00	354	
		10:00 to 11:00	417	

2.2 Space-mean Speed

The speed of arriving vehicles towards the toll plaza on both directions (N-S and S-N) was analysed on two designated location, one near to the booth (near speed breaker) and another location where in pavement changes from flexible to rigid (i.e. entrance of queuing area) towards the plaza. The speed data of vehicles were collected manually using the below equation. The values obtained in the field are given in Table 4.

$$\text{Space-mean speed} = \frac{\text{Distance in metres}}{\text{Average time taken in seconds}}$$

$$V_s = \frac{3.6 * d * n}{\sum ti} \tag{1}$$

Table 4 Details of space-mean speed of vehicles

Duration, hours	Direction	Average time, sec	Distance, m	Number of vehicles	Average velocity, km/h	Remark
4	N-S	0.80	10	453	20.38	Near booth
4	S-N	0.96	10	366	13.72	
4	N-S	0.63	10	598	34.17	Away from booth
4	S-N	0.76	10	556	26.33	

2.3 Time Headway

Time headway (h) or simply headway is the time counted between the passages of the fronts of two vehicles at a specified point. It is measured in seconds. Time headway is necessary to know the inter-arrival rate among the vehicles which is needed for the analysis of arrival pattern in a queuing system. In the present study, the average headway on particular days was found out manually by using a stopwatch at the designated location. The headway details collected included different class of vehicles. The arrival rate, which can be interpreted as the inverse of headway, on those respective days is presented in Table 5. The data reveal that vehicle arrival patterns are randomly distributed.

2.4 Arrival Rate

In a queuing system, it is necessary to define the distribution of arrivals. Generally, the arrival pattern has been defined around three types of distributions, namely binomial, Poisson and negative binomial. Gerlough’s [10] analytical work discusses in detail the application of the Poisson distribution in highway traffic. Some of the uses open to the traffic engineer are shown to include the analysis of arrival rates at a given point by Drew [1]. In the present study, vehicle arrivals are assumed to be Poisson distributed. Field data were collected for each of 120–30 s intervals for five consecutive days. The summarized vehicle arrival rate for the study period is shown in Table 6.

Table 5 Details of headway of vehicles in both directions

Direction	Time duration (1 h)	Average headway $h_{avg} = hi/nt$ (s)	Arrival rate $q = 1/h_{avg}$ (v/h)
N-S	Day 1	20.6	174
	Day 2	21.5	167
S-N	Day 1	25.3	142
	Day 2	17.1	210

Table 6 Details of vehicle arrivals

Sl. no	Directions	Observed vehicles	Duration in hours	Average arrival rate, (v/h)
1	N-S	1991	5	398.2
2	S-N	2327	5	465.4

When the number of events becomes very large, the binomial distribution approaches the Poisson distribution as a limit and is expressed as in Eq. 2.

$$P(x) = \frac{e^{-m}m^x}{x!} \tag{2}$$

The fitting of the Poisson distribution to the collected field data for each direction is presented in Tables 7 and 8. The theoretical frequency for the postulate Poisson’s distribution is obtained from Eq. 3.

m = average number of vehicle arrivals per 30 s interval

$$m = \frac{1991}{600} = 3.32, (N - S)$$

$$m = \frac{2327}{600} = 3.88, (S - N)$$

So the Poisson distribution for the north–south direction (N–S) will be of the form

$$P(x) = \frac{e^{-3.32} \cdot (3.32)^x}{x!}$$

The Poisson distribution for the south–north direction (S–N) will be of the form

$$P(x) = \frac{e^{-3.88} \cdot (3.88)^x}{x!}$$

The theoretical frequency = total intervals observed $\cdot P(x)$

$$F = 600 \cdot P(x) \tag{3}$$

2.5 Service Rate

The service rate depends upon the type of operation involved in providing service to the customers. Generally, cash collecting service takes more time than the automatic way of collection. Service rate denotes the rate at which vehicles are being served

Table 7 Details of observed frequency from north–south direction

Number of vehicles arriving for every 30 s	Observed frequency					Total number of vehicles	Probability $P(X) = \frac{e^{-3.32} \cdot 3.32^X}{X!}$	Theoretical frequency $F = 600 P(X)$
	Day 1	Day 2	Day 3	Day 4	Day 5			
0	6	7	8	2	4	27	0	21.6
1	11	10	21	13	10	65	0.122	72.0
2	21	22	22	32	31	128	0.2	120
3	19	16	23	35	34	127	0.22	132
4	24	20	24	20	24	112	0.182	109.2
5	18	19	7	9	12	65	0.121	72.6
6	13	15	5	6	4	43	0.067	40.2
7	3	5	8	3	0	19	0.032	19.2
8	2	2	2	0	1	7	0.013	7.8
9	2	2	0	0	0	4	0.005	3.0
10	0	1	0	0	0	1	0.002	1.2
11	0	1	0	0	0	1	0.0005	0.3
12	1	0	0	0	0	1	0.00013	0.08
Above 12	0	0	0	0	0	0	0.00013	0.82
Total	600					1991	1.000	600

Table 8 Details of observed frequency from south–north direction

Number of vehicles arriving for every 30 s	Observed frequency					Total number of vehicles	Probability $P(X) = e^{-3.88} \cdot 3.88^X / X!$	Theoretical frequency $F = 600 \cdot P(x)$
	Day 1	Day 2	Day 3	Day 4	Day 5			
0	2	0	12	12	12	38	0.021	13.0
1	6	2	14	18	15	55	0.078	47.0
2	8	7	25	40	30	110	0.151	91.0
3	14	11	27	22	23	97	0.196	118.0
4	15	16	20	16	20	87	0.190	114.0
5	21	20	10	4	15	70	0.148	89.0
6	16	18	8	6	3	51	0.096	58.0
7	12	15	4	1	1	33	0.053	32.0
8	13	12	0	0	1	26	0.026	16.0
9	6	11	0	0	0	17	0.011	7.0
10	6	5	0	1	0	12	0.0044	3.0
11	1	2	0	0	0	3	0.0016	1.0
12	0	1	0	0	0	1	0.0005	0.3
Above 12	0	0	0	0	0	0	0.00016	0.7
Total	600					2327	1.000	590

in a system. But the problem with manual service facility is variation in service rate and to predict the average service rate is difficult. In the present study, the average service time of a single toll booth with first-in-first-out queue discipline was found out to be 8 s. The service rate of the booth is found out to be 450 vehicles/h.

3 Analysis of Field Data

The delay and waiting time of drivers in toll plaza depend on service time and arrival rate. The quick service time and a number of toll booths can reduce the time taken by vehicles in queue. The wasted time can be calculated and minimized by analysis of the observed data, by calculating the wasted time the performance of the servers can be analysed and also the delay in overall travel time can be found. In the present work, chi-square test is used as an index of goodness of fit. The test with a significance level of 5% was carried out to check the randomness of the data as Poisson distributed. The vehicle arrival's field data were tested for the two decisions taken from Gerlough's analytical findings [10]:

- a. It is not very likely that the true distribution (of which the observed data constitute a sample) is in fact identical with the postulated distribution.
- b. The true distribution (of which the observed data constitute a sample) could be identical with the postulated distribution as shown in Table 9.

The critical value for the significance test at 5% level with 8°, 9° and 10° of freedom was obtained from the chi-square table-III of appendix-A [11], and the data are presented in Table 10.

3.1 Utilization Factor

The solution to a queuing problem entails the assessment of a system's performance, which in turn is described by a set of measures of performance [12]. In the present study, a term called utilization factor is used to quantify the traffic intensity handled by the queuing system. Utilization factor is defined as the ratio of the mean arrival rate per unit time to the mean service rate per unit time. If the utilization factor of the queuing system works out to be less than unity, indicating the system to be in a steady-state condition.

$$\text{Utilization factor}(\rho) = \frac{\text{mean arrival rate } (\lambda)}{\text{mean service rate } (\mu)} < 1.0 \quad (1)$$

A single booth of the toll plaza having first-in-first-out (FIFO) queue discipline on both directions was analysed for the steady-state condition using utilization factor. The recorded value indicates that the single booth on N-S direction is under steady-

Table 9 Details of chi-square value for the vehicle arrivals for every 30 s

Vehicles arrivals for every 30 s	Observed frequency, f	Theoretical frequency, F	f^2/F	Statistical value	Chi-square test value $\chi^2 = \sum f^2/F - n$
0	27	21.6	33.75	Mean = 1.028 Variance = 8.932	617.3 - 600 = 17.3
1	65	72.0	58.68		
2	128	120	136.5		
3	127	132	122.19		
4	112	109.2	114.87		
5	65	72.6	58.20		
6	43	40.2	46.0		
7	19	19.2	18.80		
8	7	7.8	6.28		
9	4	3.0	5.33		
10	1	1.2	0.83		
11	1	0.3	3.33		
12	1	0.08	12.5		
Above 12	0	0.82	0.0		
Total	600	600	617.3		

Table 10 Details of significance level for both directions

Directions	Significance level	Degrees of freedom	Critical value	Computed value	Remarks
N-S	5%	8	15.51	17.3	Poisson rejected
		9	16.92		Poisson rejected
		10	18.31		Poisson accepted

Table 11 Details of traffic intensity of single booth in both directions

Direction	Mean arrival rate (λ) V/h	Mean service rate (μ) V/h	Utilization factor (ρ)
N-S	398.2	450	0.884
S-N	465.4	450	1.034

state condition, but the booth on S–N direction is not under a steady-state condition as shown in Table 11.

4 Discussions

Highway facilities providing service to the vehicles have got systems arranged in a specific manner (e.g. toll booth) at designated locations on the highway. At the entry point and exit point of those systems, vehicles have to wait and proceed in order to be served. Such systems in turn create waiting lines of vehicles called as queue length. Such queuing systems which tend to form queue of vehicles have to be analysed using queuing theory. Most of the highway systems that are analysed based on queuing methods, assume the system to be operating under the steady-state condition which is seldom in nature.

In the present study, a toll plaza located on National Highway (NH-75) was evaluated based on queuing theory over different time interval. Since it is a general practice in the traffic engineering profession to analyse traffic systems on hourly basis, the same approach was adopted for the present study. Parameters like traffic volume, space-mean speed, time headway, arrival rate and service rate are expressed in 1-hr intervals. The results of traffic volume and time headway recorded on different days ascertain that vehicle's count is highly random on hourly basis. The arrival rate was postulated to be Poisson distributed. Field data were recorded for each of 120–30 s interval for five consecutive days on both directions and the fitting of the Poisson distribution to the observed data on both directions has been presented. In case of vehicles on north–south (N–S) direction, there is a high degree of agreement between the total observed and theoretical frequencies, so the postulated theoretical (Poisson) distribution is in fact the true population distribution based on mere inspection. In case of south–north (S–N) direction, there is very less degree of agreement between the total observed and theoretical frequencies indicating that the postulated theoretical (Poisson) distribution does not reflect the true population distribution. Further, the vehicle arrival data on north–south direction were tested for goodness of fit using the chi-square (χ^2) test with a significance level of 5% (0.05) and 3° of freedom (8, 9, 10). Since the computed value ($\chi^2 = 17.3$) exceeded the critical value for degrees of freedom 8 and 9 indicating the postulated Poisson distribution to be incorrect, but for the same significance level (5%) with 10° of freedom the computed value ($\chi^2 = 17.3$) is less than the critical value indicating the postulated Poisson distribution can be used for analysis of vehicle arrival. Finally, a single booth of the toll plaza having first-in-first-out (FIFO) queue discipline on both directions was analysed for the steady-state condition using the utilization factor. The booth on the N–S direction is found to be under steady-state condition whereas the booth on S–N direction is not under steady-state condition. In brief, the findings from the study are the assumptions made in vehicle arrivals, service rate and about the steady-state system generally made in queuing methods applied to highway facilities call for attention.

5 Conclusions

The existing toll plazas located on highway systems can be analysed using queuing theory to estimate the distribution characteristics like arrival rate and service rate. But these characteristics are analysed using different probabilistic distribution to ascertain the true population from the sampled population. From the present study, the following conclusions can be drawn, and in case of arrival rate in N–S direction there is a high degree of agreement between the observed frequency and theoretical frequency, indicating the postulated Poisson distribution to be the true population distribution. Thus, the Poisson distribution can be considered for analysing the queuing systems.

References

1. Drew DR (1968) Traffic flow theory and control. McGraw-Hill, New York
2. Son YT, Cassidy MJ, Modanat SM (1995) Evaluating steady-state assumption for highway queueing system. *J Transp Eng ASCE* 121(2):182–190
3. Woo TH, Hoel LA (1991) Toll plaza capacity and level of service, transportation research record. 1320:119–127
4. Ceballos G, Curtis O (2004) Queue analysis at toll and parking exit plazas: a comparison between multi-server queuing models and traffic simulation. Institute of Transportation Engineers, Annual Meeting, FL
5. Anokye M, Abdul-Aziz AR, Annin K, Oduro FT (2013) Application of queuing theory to vehicular traffic at signalized intersection in Kumasi-Ashanti region, Ghana. *Am Int J Contemp Res* 3(7):23–29
6. Vandaele Nico, Van Woensel Tom, Verbruggen Aviel (2000) A queueing based traffic flow model. *Transp Res–D Transp Environ* 5:121–135
7. Cottrell WD (2001) Empirical freeway queuing duration model. *J Transp Eng ASCE* 127(1):13–20
8. Das S, Levinson D. Queuing and statistical analysis of freeway Bottleneck formation. *J Transp Eng ASCE*. 130:787–795
9. Traffic Census on Non-Urban Roads, IRC: 9-1972, Indian Roads Congress, New Delhi
10. Gerlough DL (1955) Use of poisson distribution in highway traffic, in “poisson and traffic,” the Eno foundation for highway traffic control, Conn, Saugatuck
11. Montgomery DC, Runger GC (2003) Applied statistics and probability for engineers, 3rd edn. Wiley, New York
12. Papacostas CS, Prevedouros PO (2011) Transportation engineering and planning, 3rd edn. Pearson Education, NJ

A Hierarchical Modeling Approach to Predict Pedestrian Crash Severity



Aafreen Asma Jahangeer, Sai Suresh Anjana and Vivek R. Das

Abstract The crashes involving pedestrians are increasing at an alarming rate over the years in urban Bangalore. The past year witnessed 1592 crashes in urban Bangalore out of which 338 pedestrians were killed and 1254 were injured. The gravity of the problem requires immediate attention of road safety experts, engineers, and other stakeholders who are directly or indirectly involved in traffic safety. Hence, an in-depth analysis of this problem is required to draw out sound and reliable engineering countermeasures that will address the safety issues of pedestrians and improve the safety performance of roadways. For this, data was collected from Bangalore City Traffic Police, and it was found that the maximum number of pedestrian vehicle collisions occurs in the Bangalore–Chennai Highway, which is our study location. This study mainly focuses on identifying the factors contributing to the severity of pedestrian crashes in urban mid-blocks. From the literature review, it was identified that pedestrian crashes are associated with characteristics of pedestrian, location, land use, environment, and crash. For modeling vehicle–pedestrian crashes, the review of the literature shows that different regression techniques such as logit and probit models are widely used. Crash patterns may vary across locations, and this variation is not accounted in the traditional models. The traditional models cannot accommodate the array of variables at multiple levels like regional, site, crash, and driver–vehicle unit level. To increase the accuracy of model prediction, a hierarchical modeling approach is considered in the present study. This study considers traffic, geometric, and environmental variables and identifies their association with vehicle–pedestrian crashes.

Keywords Pedestrian–vehicle crash severity modeling · Pedestrian safety study · Hierarchical modeling · Traffic safety

A. A. Jahangeer · S. S. Anjana (✉) · V. R. Das
Department of Construction Technology Management and Highway Technology, Dayananda Sagar College of Engineering, Bengaluru 560078, India
e-mail: anjana.sai.09@gmail.com

A. A. Jahangeer
e-mail: aafreenjahangeer@gmail.com

V. R. Das
e-mail: vivekdurgadath@gmail.com

1 Introduction

Of all the systems that people have to deal with on a daily basis, road transport is the most complex and the most dangerous. Road traffic injuries are one of the leading causes of death in the world. The drastic increase in number of vehicle registered in India along with the population growth with each passing year causes an increase in fatalities in road traffic crashes. In India alone, road crashes account for the highest fatality rate reaching to almost peak of 15–20 times than that of developed nations. Moreover, poor roads, ill-maintained vehicles, rash and negligent driving, intake of intoxicants (alcohol/drugs) by driver/victims, poor sense of traffic rules, etc., lead to increased involvement of people in road traffic crashes. Motor vehicle–pedestrian crash is a significant public health concern.

Road traffic injury is considered to be the leading cause of death among young people. More than one-fifth of people killed on roads around the world are pedestrians [1]. An estimate prepared by World Health Organization (WHO), on worldwide share of pedestrian deaths among all traffic deaths during the year 2010, shows that 22% of the victims were pedestrians. According to a report published by the National Crime Records Bureau (NCRB) in India, during the year 2014, 28,118 pedestrian fatalities were reported out of which 25,444 pedestrians were the victims and 2,674 pedestrians were the offenders. The percentage share of pedestrian death in India is 4.7% of total road traffic deaths [2]. In Karnataka, 551 pedestrians were killed in 2014 among which 255 were from Bangalore. Pedestrian deaths and injuries are preventable but still do not attract the attention it deserves. Bangalore is one of the worst Indian cities for pedestrians, according to a study conducted by the city police in coordination with the National Institute of Mental Health and Neurosciences. The city scored 0.63 on a walkability index that measured pedestrian facilities, footpaths, and other amenities. By comparison, Chandigarh scored 0.91 and Delhi 0.87. Nearly half of those who die on Bangalore's roads are not motorists, but pedestrians. Of the 771 road-related deaths reported across the city in the year (2013), 382 victims were pedestrians [3, 4]. Statistics of injury-only-accidents are no different; a large chunk involves pedestrians. The percentage share of pedestrians killed in India during the year 2013 was 9.1% of total road users, which declined to 8.8% in 2014, which then further increased to 9.5% in the year 2015.

The gravity of the problem requires immediate attention of road safety experts, engineers, and other stakeholders who are directly or indirectly involved in traffic safety. Hence, an in-depth analysis of this problem is required to draw out sound and reliable engineering countermeasures that will address the safety issues of pedestrians and improve the safety performance of roadways. This study mainly focuses on identifying the factors contributing to the severity of pedestrian crashes in urban mid-blocks.

2 Literature Review

Comprehensive exploration and analysis of the factors that influence the probability of pedestrian crash occurrence and severity levels are important for improving pedestrian safety. Many studies have tried to find the impact of different factors on pedestrian crashes. Most of them use quantitative methods of analysis and focus on developed countries. The mainly used methods are logistic binomial regression [5, 6] and ordered response model [7, 8].

Many studies have shown that the pedestrian crash severity increases with pedestrian age [9–11]. Season was also found to affect the crash severity adversely. Some studies suggest that severe crashes were found to occur when the road surface was wet [12], whereas certain other studies [8, 11] suggest that adverse weather conditions lower the probability of a fatality. Daylight conditions have also been found to affect the pedestrian crash severity. Lack of proper lighting at night time is found to increase the crash severity [12, 13]. Pedestrian gender also shows a relationship with pedestrian crash severity. Most studies [14–16] suggest that males are more vulnerable to severe crashes as men tend to engage in more risky behaviors. Pedestrian injury severity increased with increase in vehicle size [7, 13] as thorax injuries are more common when a bigger vehicle is involved in the crash compared to car.

3 Study Area

Bangalore is the fifth most populous urban agglomeration and third most populous city in India. It is also the 18th most populous city in the world. This study stretch is a 25-km 6-lane 2-way mid-block section in Hosur road, consisting of both service road and main road. Even though a flyover is also present in this stretch, since pedestrians are not permitted on the flyover, it is not considered for this study. The main road is a six-lane divided carriageway, with three lanes in each direction, separated by a median of height 0.30 m. Two service roads are present on either side of the main roads. The service roads are single carriageway roads with no median. The width of the main road varies from 10 to 11 m throughout the study area, and width of service road ranges from 6 to 7 m on both service roads. Mixed land use was observed in the section, with majority of the sections with commercial land use. There are covered drains on the main road which is being used as sidewalk by the pedestrians. The service roads have no sidewalks, and people can be found walking on the carriageway due to lack of walking space. The service roads are separated from the main road by a railing throughout the stretch which opens only at junctions or other very few designated areas. In most of the cases, the presence of these railings and lack of proper opening for pedestrian passage leads to jaywalking which can prove to be dangerous for the pedestrian.

4 Data Collection

The data collection consists of two stages, i.e., preliminary data collection and secondary data collection. Primary data consisting of road inventory data, peak hour traffic volume, spot speed in a section, and peak hour pedestrian volume was collected by conducting field surveys. The secondary data which includes the crash severity over the past 3 years was collected from the traffic FIR Center, Shivajinagar, Bengaluru. The variables obtained from the primary data such as road width, presence of median, presence of subway, presence of bus stop, and presence of sidewalk were obtained from the road inventory survey, and the other variables such as peak hour traffic volume and peak hour pedestrian volume were obtained from other hourly counts. Spot speed study was also done on all sections. The variables obtained from the secondary data are age and gender of the pedestrian involved in the crash, type of the vehicle involved in the crash, time and date of crash, location of crash, climate, severity of the crash, location and action of the pedestrian during the time of crash and if the crash was hit and run. This study makes use of data from 2013 to 2016, under the assumption that the section under scrutiny has not undergone major changes during that period. Table 1 presents the summary of the crash data collected, and Table 2 shows the summary statistics of the collected data.

5 Database Preparation

The study area was divided into 30 sections, each of equal length. The data collected from the police station was compared with the landmarks of the sections to find the section in which the crash occurred. In this dataset, any crash that occurred within 20 m of any intersection is considered as an intersection crash and then removed. All other crashes are mid-block crashes and are considered. The data was filtered to get rid of all outliers and other missing data. The explanatory factors considered in this study are season, daylight, day of week, gender, hit and run, presence of median, presence of bus stop, presence of subway, presence of sidewalk, type of pedestrian movement, vehicle involved, location of pedestrian during the time of crash, age of the pedestrian, and number of lanes. The variables are given ordinal or nominal values as shown in Table 3.

5.1 Response and Explanatory Variables

The dependent variable or the response variable in this study is pedestrian injury severity. The severity level of pedestrian vehicle collision was classified into three groups, namely minor injury, grievous, and fatal, based on IRC 53:2012. As per this code, minor injury can be defined as crashes where the victim does not require

Table 1 Distribution of pedestrian crash severity over the study period

Factor	Severity			Total	
	Minor	Grievous	Fatal	Number of crashes	Crashes (%)
<i>Age of pedestrian</i>					
Below 19 years	0	9	0	9	7.76
19–55 years	7	62	22	91	78.45
Above 55 years	0	10	6	16	13.79
<i>Pedestrian gender</i>					
Female	2	19	6	27	23.27
Male	5	62	22	89	76.73
<i>Season</i>					
Winter	2	13	4	19	16.38
Pre-monsoon, post-monsoon	3	41	12	56	48.28
Monsoon	2	27	12	41	35.34
<i>Daylight</i>					
Day	5	46	20	71	61.21
Dawn, dusk	1	16	3	20	17.24
Night with streetlight	1	19	5	25	21.55
<i>Day of week</i>					
Weekend	1	16	9	26	22.41
Weekday	6	65	19	90	77.59
<i>Vehicle involved</i>					
Two wheeler	4	35	8	47	40.52
Three wheeler	1	8	0	9	7.76
Car	1	20	3	24	20.69
Lorry, bus	1	18	17	36	31.03
<i>Pedestrian movement</i>					
Others	2	12	5	19	16.38
Standing near carriageway	0	3	0	3	2.59
Walking along the road	0	2	2	4	3.45
Crossing the road	5	64	21	90	77.58
<i>Pedestrian location</i>					
Others	2	14	6	22	18.97
Edge of carriageway	0	4	14	18	15.52
Near pedestrian crossing	0	13	3	16	13.79
In the road	5	50	5	60	51.72
<i>Hit and run</i>					
Not hit and run	6	53	19	78	67.24
Hit and run	1	28	9	38	32.76

Table 2 Summary statistics of collected data

Factor	Minimum	Maximum	Mean	Standard deviation
Pedestrian volume	26	752	134	168
Traffic volume	778	7397	3182	1968
Spot speed	17.11	49.56	30.49	10.82
Road width	5.9	24.4	13.68	7.54
Median width	1.1	4.67	3.29	0.9

hospitalization; i.e., only first-aid is required. A crash victim who suffered fractures, concussions, internal lesions, crushing, severe cuts and lacerations, severe general shock requiring medical treatment, and any other serious lesions requiring detention in hospital is called as a grievously injured person. A crash in which one or more persons were killed is known as a fatal crash.

5.2 Site Characteristics

The site characteristics include presence of median, subway, bus stop, sidewalk, and number of lanes. Median is present throughout the stretch of main road and absent throughout the stretch of service road. Bus stops are present in eight sections of the main road. Most portions of the NH-7 highway are separated from the service road using fence. However, gaps in the structural barriers were observed in some areas so as to provide access for pedestrians. This poses a threat to the pedestrians who gets access to walking on the main road with high-speed traffic.

5.3 Crash Characteristics

Type of vehicle involved, pedestrian location at the time of crash, pedestrian movement at time of crash, and hit and run are the crash characteristics considered in this study. Based on the literature [6, 9], pedestrian injury severity increases as the frontal area and weight of the colliding vehicle increases. Crash severity will be higher when the crash occurred is hit and run, as the much-needed medical attention is delayed. Pedestrian location and movement also play an important role in crash severity. Pedestrians can be located anywhere at the time of crash such as the edge of carriageway, near pedestrian crossing, or in the road. Any other location such as the pedestrian being near the bus stop during the occurrence of the crash is considered under the group 'others.' Similarly, the pedestrian movement at the time of crash is also classified into standing near the carriageway, walking along the road, or crossing the road. All other pedestrian movements are taken under the category 'others.'

Table 3 Coding of variables

Variable	Coding	Type of variable
<i>Dependant variable</i>		
Severity	1: Minor 2: Grievous 3: Fatal	Ordinal
<i>Independent variables</i>		
<i>Site characteristics</i>		
Presence of median	1: No 2: Yes	Ordinal
Presence of bus stop	1: No 2: Yes	Nominal
Presence of sidewalk	1: Yes 2: No	Ordinal
Number of lanes	1: Two lane 2: Three lane	Ordinal
Type of road	1: Service road 2: Main road	Ordinal
<i>Crash characteristics</i>		
Type of vehicle involved	1: Motor cycle 2: Auto rickshaw 3: Car 4: Goods Lorry, Truck, Tractor	Ordinal
Pedestrian location at the time of crash	1: Others 2: Edge of carriageway 3: Near pedestrian crossing 4: In the road	Ordinal
Hit and run	1: No 2: Yes	Ordinal
Pedestrian movement	1: Others 2: Standing near carriageway 3: Walking along carriageway 4: Crossing the road	Ordinal
<i>Pedestrian characteristics</i>		
Pedestrian age	1: 19–55 years 2: Up to 18 years 3: Above 55 years	Ordinal
Gender	1: Female 2: Male	Nominal
<i>Environmental characteristics</i>		
Season	1: Winter 2: Pre-monsoon, post-monsoon 3: Monsoon	Ordinal
Daylight	1: Day 2: Dawn, dusk 3: Night with street light	Ordinal
Day of week	1: Weekend 2: Weekday	Nominal

5.4 Pedestrian Characteristics

Pedestrian age and gender are the pedestrian characteristics used in this study. Though certain studies show that females have higher risks of being severely injured, some others show that males are at a higher risk [6, 9]. Due to this reason, no rank has been assigned for pedestrian gender. In case of pedestrian age, seniors are at a higher risk due to their brittle bones. If a crash of the same intensity affects an adult and a senior, the chances and rate of recovery is much higher for the adult than the senior. Injury severity of children is followed by those of seniors. Pedestrian age has been classified into three groups, i.e., children (up to 18 years), adults (19–55 years), and seniors (above 55 years).

5.5 Environmental Characteristics

Season, daylight, and day of week are the environmental factors in this study. Crash severity is higher during monsoon because the visibility reduces and road surface becomes wet. Even though the drivers are usually cautious during this period, crashes, if any, will have a high severity. Classification of season is done according to the classification provided by Meteorological Department of India. They have classified seasons into winter (January to February), pre-monsoon (March to May), southwest monsoon (June to September), and post-monsoon (October to December). Similarly crash severity tends to be least during the daytime and high during the nighttime due to better visibility compared to the night. Moreover, at night, the crash severity will be high owing to the very low traffic count which usually leads the driver to drive/ride on unreasonably high speeds. At dawn, the traffic conditions are similar to night and the daylight will just start appearing. The traffic condition at dusk is similar to daytime, but the daylight reduces. Daylight has been classified into four categories such as dawn, day, dusk, and night with street light.

6 Crash Data Analysis and Modeling

Various studies have made use of various statistical approaches to analyze pedestrian crash injury severity. Binary models, ordinary discrete models, and unordered multinomial discrete models are three main statistical techniques that have been used to study pedestrian crash severity levels.

The statistical modeling framework employed in this study to determine the possible factors influencing pedestrian vehicle crash severity was the hierarchical linear mixed model. A generalized linear mixed model (GLMM) is an extension to the generalized linear model in which the linear predictor contains random effects in addition to fixed effects. Mixed models are ones with both fixed and random effects. A given

effect may be both fixed and random if it contributes to both the intercept and the covariance structure for the model. The choice of this type of model was influenced by the polytomous nature of the response variable. Multinomial logit has been used extensively for the analysis of crash severity and is preferred over the ordinal logit model. In this study, multinomial distribution with cumulative logit as link function was used. Statistical Package for the Social Sciences (SPSS) was used for modeling. The major capabilities that differentiate mixed models from traditional models are that mixed models handle correlated data and unequal variances. It also handles more complex situations in which experimental units are nested in a hierarchy.

7 Results

Modeling was done using the input data, and the results were obtained to 87.1% accuracy. This means that model predicts the severity of the crash accurately 87.1% of the time. All the grievous crashes are predicted as grievous, whereas for fatal crashes, the percentage accuracy reduces to 71.4%; i.e., in 28.6% of the cases, the fatal crashes will not be predicted as fatal crashes, instead as grievous. This occurs due to the small size of data. The factors influencing crash severity in this section were found to be the following: presence of median, traffic volume, road width, pedestrian volume, and presence of bus stop. Traffic volume and pedestrian volume showed an inverse relationship with pedestrian vehicle crash severity, whereas increase in road width increased the crash severity. The presence of median decreased the crash severity, and the presence of bus stop increased the crash severity. Season, daylight, vehicle involved, and pedestrian location are the other factors that influence pedestrian vehicle crash severity. Pedestrian gender, day of week, hit and run crash, presence of sidewalk, movement of the pedestrian at the time of crash, and age of the pedestrian have shown to have no specific effects on the pedestrian vehicle crash severity. Table 4 shows the coefficients and significance of fixed and random effect factors present in the model. In the absence of impact speed data, spot speed was considered as a variable, but it was later removed from the model due to an unseemly result.

8 Conclusion

From the model, it can be seen that the presence of median, presence of bus stop, traffic volume, pedestrian volume, road width, season, daylight, vehicle involved in the crash, and pedestrian location are the factors that influence pedestrian crash severity. The crash severity is less during winter and high during monsoon. This can be due to the low visibility conditions and wet road surface. Even though the drivers tend to be cautious during such weather conditions, any crashes occurring during this period tend to have severe consequences. Similarly, the severity of the crashes increases from day to night, owing to the low daylight conditions and poor

Table 4 Values of fixed and random effect values in model

Fixed effect coefficient			
Model term	Coefficient	<i>t</i>	Significance
Intercept	-4.608	-1.889	0.0376
Presence of median	-2.907	-1.445	0.1510
Peak hour traffic volume	-0.001	-1.951	0.0542
Width of road	0.229	0.418	0.0677
Peak hour pedestrian volume	-0.000	-0.185	0.8530
Presence of bus stop	0.243	0.315	0.7530
<i>Random effect coefficient</i>			
Model term	Estimate	Z	Significance
Season	0.071	0.125	0.301
Daylight	0.190	0.281	0.779
Vehicle involved	0.262	0.470	0.638
Pedestrian location	1.020	1.348	0.178

visibility at night. The crash severity also increases with the absence of median and the presence of bus stop. Similarly, crash severity reduces with increase in traffic volume and pedestrian volume. When the traffic volume increases, the road will be congested, and this will facilitate easy movement of pedestrians. When the pedestrian volume is high, the drivers will watch out for any pedestrian coming in their way. Moreover, the observed crossing pattern adopted in this road by pedestrians is to maneuver the road in platoons, which again reduces crash frequency and severity. The crash severity is found to increase with increase in road width and vehicle size. Wider the road, more severe will be the crash. Similarly, larger the vehicle, more severe will the crash. It was also found that the crash severity was high when the pedestrian was in the road, and less when the pedestrian was located at the edge of carriageway at the time of crash.

Since the most important factors resulting in a severe injury crash have been identified, measures can be adopted to reduce such crashes and their severity. Crashes associated with environmental conditions like wet weather can be reduced to an extent by providing adequate camber and road surface treatments to drain surface water effectively. Under poor lighting conditions, pedestrians should be encouraged to wear retroreflective clothing for better visibility. Roads with high pedestrian activity should have adequate lighting facilities. The presence of median and wider roads encourages motorist to adopt higher speeds, and at such highways, pedestrian activities should be controlled. At-grade uncontrolled pedestrian crossings can be replaced by pelican crossings for better compliance by motorists.

One major step toward achieving pedestrian safety is to provide adequate pedestrian facilities and infrastructure. Sign boards are barely present in this stretch of the road. Since there are a lot of crossing movements occurring in this stretch, proper

crossing facility should be provided. Even though pedestrian subways are constructed in few places, it is not fully operational. Lack of proper lighting raises safety concern, as people especially female pedestrians fear using poor lit facilities, which results in them resorting to unsafe crossing practices such as jaywalking. Therefore, providing proper lighting in all such facilities is also an important factor. Pelican signals can also be installed in areas where there is higher number of pedestrian traffic. This can facilitate easier and safe pedestrian movement. Properly paved and demarcated sidewalks should be present on the service road, as currently there is no sidewalk and this result in a tendency to walk beyond the shoulder and on the road. Another most important task includes educating drivers and other road users on road safety and the importance of giving way to vulnerable road users, more importantly pedestrians. Enforcement methods such as installing speed cameras and CCTV cameras should be implemented along with warning and a heavy fine to punish the defaulters.

References

1. Department of Violence and Injury Prevention and Disability (2009) Global status report on road safety. World Health Organization, Switzerland. http://apps.who.int/iris/bitstream/10665/44122/1/9789241563840_eng.pdf
2. National Crime Record Bureau (2014) Accident deaths and suicides in India 2014. Ministry of Home Affairs, New Delhi. <http://ncrb.nic.in/StatPublications/ADSI/ADSI2014/adsi-2014%20full%20report.pdf>
3. Ministry of Road Transport and Highways (2015) Road accidents in India 2015. MORTH, Transport Research Wing, New Delhi. <http://pibphoto.nic.in/documents/rlink/2016/jun/p20166905.pdf>
4. Ministry of Road Transport and Highways (2013) Road accidents in India 2013. MORTH, Transport Research Wing, New Delhi. <http://revista.dgt.es/images/informe-accidentes-India-2013.pdf>
5. Sze N, Wong S (2007) Diagnostic analysis of the logistic model for pedestrian injury severity in traffic crashes. *Crash Anal Prevent* 39:1267–1278. <http://www.sciencedirect.com/science/article/pii/S0001457507000590>
6. Roudsari SD, Mock CN, Kaufman R, Grossman D, HenaryBY, Crandall J (2004) Pedestrian crashes: higher injury severity and mortality rate for light truck vehicles compared with passenger vehicles. *Injury Prevent* 10:154–158. <http://injuryprevention.bmj.com/content/10/3/154>
7. Kim JK, Ulfarsson GF, Shankar VN, Kim S (2008) Age and pedestrian injury severity in motor-vehicle crashes: a heteroskedastic logit analysis. *Accid Anal Prevent* 40:1695–1702. <https://www.ncbi.nlm.nih.gov/pubmed/18760098>
8. Kim JK, Ulfarsson GF, Shankar VN, Mannering FL (2010) A note on modeling pedestrian-injury severity in motor-vehicle crashes with mixed logit model. *Accid Anal Prevent* 42:1751–1758. <http://www.sciencedirect.com/science/article/pii/S0001457510001326>
9. Martin J, Lardy A, Laumon B (2011) Pedestrian injury patterns according to car and casualty characteristics in France. In: *Annals of advances in automotive medicine/annual scientific conference*, vol 55. Association for the advancement of automotive medicine. <https://trid.trb.org/view.aspx?id=1122625>
10. Oh C, Kang YS, Youn Y, Konosu A (2008) Development of probabilistic pedestrian fatality model for characterizing pedestrian vehicle collisions. *Int J Autom Technol* 9(2):191–196. <http://ijat.jatsxml.org/journal/view.php?number=502>

11. Verzosa N, Miles R (2016) Severity of road crashes involving pedestrians in Metro Manila, Philippines. *Accid Anal Prevent* 94:216–226. <http://www.sciencedirect.com/science/article/pii/S0001457516302020>
12. Gyimah RA, Aidoo EN, Akaateba MA, Appiah SK (2016) The effect of natural and built environmental characteristics on pedestrian vehicle crash severity in Ghana. *Int J Inj Control and Saf Promotion*, pp 1–10. <http://www.tandfonline.com/doi/abs/10.1080/17457300.2016.1232274>
13. Martin A (2006) Factors affecting pedestrian safety: a literature review. TRL Limited, Wokingham, Berks. <https://trl.co.uk/reports/PPR241>
14. Pour AT, Moridpour S, Tay R (2016) Modeling pedestrian crash severity at mid-blocks. *Transportmetrica A: Transp Sci* 13(3):273–297. <http://www.tandfonline.com/doi/abs/10.1080/23249935.2016.1256355>
15. Wang X, Chen M (2012). Safety analysis on urban arterials considering operational conditions in Shanghai. In: International symposium on safety science and technology, *procedia engineering*, vol 45, pp 836–840. <https://www.infona.pl/resource/bwmeta1.element.elsevier-d24a66c6-b507-322e-8bb5-9594b5e0fdfe>
16. Kim M, Kho SY, Kim DK (2017) Hierarchical ordered model for injury severity of pedestrian crashes in South Korea. *J Saf Res* 61:33–40. <http://www.sciencedirect.com/science/article/pii/S0022437516301220>

Modelling Operating Speeds for Multilane Divided Highways



Gourab Sil, Suresh Nama, Avijit Maji and Akhilesh Kumar Maurya

Abstract Different geometric parameters (e.g., radius, curve length and preceding tangent length) affects vehicle speed in horizontal curve. Inconsistency in driver's speed selection may lead to unsafe situation at horizontal curve. The differences between operating speed of successive elements and deviation with design speed of single element have been used as a measure to evaluate geometric design consistency and safety. Researchers have studied speed behaviour considering strong lane discipline to predict preferred vehicle operating speed in two lane highways. However, studies considering weak lane discipline to predict operating speed for multi-lane divided highways are limited. Therefore, in this study, passenger car and heavy vehicle speed data at the starting and centre of ten horizontal curves in a four-lane divided highway are collected. The 85th percentile speeds at eight sites are analysed to develop a linear speed prediction model. Curve length is found to be the only explanatory variable in the model developed for location at the starting of a curve. Whereas, radius is found as the explanatory variable to predict speed at centre of the curve. The developed models are validated at two different sites. Statistical analysis shows that *I*-value is lesser than 0.2, which confirms the acceptability of the proposed model.

Keywords Operating speed · Horizontal curve · Speed prediction model · Multilane divided highway

G. Sil (✉) · A. Maji
Department of Civil Engineering, Indian Institute of Technology Bombay, Powai, Mumbai,
Maharashtra 400076, India
e-mail: silgourab@gmail.com

A. Maji
e-mail: avijit.maji@gmail.com

S. Nama · A. K. Maurya
Department of Civil Engineering, Indian Institute of Technology Guwahati, Guwahati, Assam
781039, India
e-mail: nsureshce@gmail.com

A. K. Maurya
e-mail: akmaurya@gmail.com

1 Introduction

Horizontal curves are considered as one of the critical geometric elements for highway safety [1]. Crash rate in horizontal curve is higher than straight section. Most of these crashes in horizontal curves are single-vehicle crash [1]. Fatality due to single vehicle crash at horizontal curve is the highest. It has been reported that vehicle, driver and roadway geometry as influencing factors for these crashes. Driver's perception about road geometry plays a very important role in driving. Their perception is affected by highway geometry, road-side conditions and vehicles within their vicinity. In absence of other vehicles, drivers choose vehicle speed based on their perception of geometry. This is perceived speed or free flow speed. While approaching a horizontal curve, drivers may not get sufficient time to slow down from higher speed to a lower speed. This happens when the change in highway geometry does not meet driver's perception. It can make the vehicle unstable and cause road or lane departure crash such as road runoff crash. Operating speed has been extensively used by researchers to evaluate safety of road and is relatively easy to measure in real time conditions. Highway sections that facilitate drivers in travelling almost at uniform vehicle operating speed have been considered as consistent. The difference in operating speed between successive highway sections has been used as a measure to evaluate geometric design consistency. Similarly deviation of operating speed from design speed of an element has been considered as a consistency measure. Thus, present study considered operating speed as a surrogate measure for safety evaluation of horizontal curves.

At present, National Highway Authority of India (NHAI) maintains 100,087 km of National Highways (NH). Out of this, about 22,900 km is already developed and 25,000 km is being developed as a multi-lane divided facility. Most of these highways are four-lane divided and are essentially used by both fast and slow moving vehicles. Due to heavy load, commercial vehicles run slower compare to passenger cars. Moreover, weak lane discipline with no right of way segregation for slow and fast moving vehicles prevails. Slow and fast moving vehicles share same carriageway. These traffic characteristics influence driving perception. This driving perception can reflect during uninfluenced driving conditions. Hence, there is a need to study driver behavior at horizontal curves for multilane divided highways.

This study aims to understand the perceive speed behavior at the starting and center of horizontal curves. The 85th percentile speed of vehicles has been analyzed for several highway geometric parameters in these locations. The obtained speed values are further examined to identify the influencing geometric parameters. In the process, the effects of different geometric elements on operating speed of vehicle are studied. Study sites containing 10 horizontal curves on the National Highway 3 (NH-3) connecting Gonde and Vadape in Maharashtra have been chosen in the present study. These sites are chosen considering the variation in horizontal curve radius (R), deflection angle (Δ), length of curve (CL), gradient (G) and preceding tangent length (PTL). Whereas, in selected study sites carriageway width (CW), shoulder width (SW), and superelevation (e) do not have any variation. The values of CW ,

SW , e are 7, 3 m and 5%, respectively. Apart from geometric data, vehicle speed data is essential for this study. The speed data includes speed at entry and center of a curved section. In the preliminary study, it has been observed that only passenger cars and heavy vehicles predominantly use the selected survey sites. Again, it has been identified that speed of passenger cars and sports utility vehicles/multi utility vehicles are not significantly different. Hence, vehicles representing passenger cars and heavy vehicles are considered in this study. Filtering and smoothing techniques have been conducted to eliminate the outlier data and only error free speed data are used for further analysis. The primary geometric data (i.e., radius, length of curve etc.) are extracted from the plan and profile drawings provided by Mumbai Nashik Expressway Limited. The vehicle speed data have been collected using video recording technique. To find the accuracy of the geometric data obtained from the plan and profile drawings a cross verification has been carried out in the field using the Laser Distance Meter. So far no discrepancy has been found.

Operating speed prediction models are developed using the collected speed data. The speed prediction models are represented by multi linear regression equations, which is developed using collected speed data at entry and center point of the horizontal curves with geometric variation. The regression analysis has been performed separately for passenger car and heavy vehicle speed data to find out the effect geometric variables on vehicle speed at the entry and center of the horizontal curve. The operating speed model presented in this paper could be used as surrogate safety evaluation of horizontal curves. The present findings can help in identifying the unsafe horizontal curve section in four-lane divided highways. This study overcomes the limitation of availability of speed consistency evaluation tool in four-lane divided highways under weak-lane discipline.

2 Literature Review

Curve radius affects vehicle's preferred speed significantly [2–4]. Vehicles are safe when the preferred speed is similar in consecutive geometric elements and equal to or less than the design speed of the curve. Therefore, poor judgment in speed selection while entering a horizontal curve may make vehicle out of control and lead to single vehicle crash.

Horizontal curves on highway are prone to crash and most of these crashes are single vehicle in nature [1]. Crash rate on horizontal curve is dominant compare to other geometric elements such as tangent [1]. It has been found that fatality rate due to single vehicle crash in horizontal curve is much higher than tangents in highway [1, 5–7]. Moreover, in India it has been reported that one third of the total fatalities occurred in horizontal curves on National Highways [8]. Therefore, safety at horizontal curves has been considered as major concern [1, 6].

Consistent operating speed in consecutive geometric elements (e.g. tangent to curve and curve to curve) and operating speed consistent with design speed of horizontal curve reduces rate of single vehicle crash significantly [9]. Researchers have

Table 1 Geometric design consistency evaluation criteria [2]

Design safety	Criteria I (kmph)	Criteria II (kmph)
Good	$ V_{85} - V_d \leq 10$	$ V_{85i} - V_{85i+1} \leq 10$
Fair	$10 < V_{85} - V_d \leq 20$	$10 < V_{85i} - V_{85i+1} \leq 20$
Poor	$ V_{85} - V_d > 20$	$ V_{85i} - V_{85i+1} > 20$

Where; Criteria I = Difference between design speed and operating speed of a section

Criteria II = Difference between operating speeds of consecutive elements

V_{85} = 85th percentile speed or operating speed, V_d = Design speed

used speed as surrogate parameter to evaluate consistency and safety [2, 3, 10, 11]. Safety and consistency evaluation of consecutive elements (tangent to curve and curve to curve) can be done using absolute operating speed difference [2–4]. Whereas, only curve section can be evaluated using difference in design speed and operation speed of the curve [2–4]. Lamm et al. [2] proposed some consistency and safety evaluation criteria, which is presented in Table 1. Therefore, to evaluate safety and consistency, estimation of operating speed at the curve is essential.

Researchers developed models to predict operating speed of horizontal curves [5, 12–15]. Generally, operating speed prediction models are developed to estimate the free flow speed for various horizontal curve geometry. Researches have studied vehicle’s speed behaviour at different locations of horizontal curves in two-lane highways and proposed speed prediction models. Very limited models is found for four-lane highways [16, 17]. An extensive review of earlier works reveal that most of the proposed models are developed considering lane discipline [5, 12–16]. Whereas, model developed considering weak lane discipline is limited [17]. Jacob and Anjaneyulu [11] proposed speed prediction models for heterogeneous traffic in two-lane highway in India. Researchers [18, 19] have studied speed behaviour at horizontal curve in four lane highways too. However, these studies are limited to reflect true free flow speed considering weak lane discipline in proposed model. Hence, speed prediction models considering weak lane discipline in four-lane divided highways is limited.

Hence, there is a need to study speed behavior at four-lane divided highways considering weak lane discipline conditions. This would help to understand the speed characteristics of Indian drivers in horizontal curves. Further, analyzing the vehicle free flow speed for weak lane discipline can help to identify the critical aspect of traffic safety in horizontal curves. Therefore, the objective of present study is development of speed prediction models at starting and centre of four-lane divided horizontal curves in weak lane discipline.

Table 2 Descriptive statistics of study sites

	R (m)	Δ ($^{\circ}$)	PTL (m)	CL (m)	G (%)
Mean	285	55	233	267	-0.007
Max	430	114	500	523	4.29
Min	90	23	100	100	-4.26

3 Study Sites

Four-lane divided highway is a type of multi-lane divided facility. Ten horizontal curves on National Highway-3 (NH-3) in India are selected in this study. These sites are located between Mumbai and Nashik of Maharashtra, India. Eight horizontal curve sites are selected for model development and remaining two for model validation. At these locations the highway has four-lane divided cross section with 7 m carriageway width (CW). About three meter wide shoulder is available on the far side of the cross section and the surface layer is of asphaltic concrete. Superelevation of all these sites is limited to 5%. All the sites are free from influence of intersections or median openings. Sites are also checked for absence of any side friction due to on-street parking, illegal contraflow movements, bus bays etc. Proper vantage points are identified to install cameras hiding from direct view of drivers. Survey is conducted in very low traffic volume in good pavement and weather conditions. The descriptive statistics of geometric variables of the study sites are given in Table 2.

4 Data Details

Geometric data of all sites are obtained from plan and profile drawings provided by National Highways Authority of India (NHAI) and Mumbai Nasik Expressway Limited (MNEL). The obtained information is cross-checked at the site using surveying equipment. In all ten locations the geometric data available in plan and profile drawings matched with the site data. Speed data is collected using video recording technique simultaneously at starting and centre of curve for about three hours. This helps in tracking the free flow vehicle. A trap length of 15 m is marked at these locations for vehicle speed data collection. The video camera is installed in such a way that the trap lines are visible without any obstruction. Only the vehicles satisfying free flow conditions proposed by Sil et al. [17] as presented below are considered for analysis.

Condition A: Maintaining a threshold headway of 5 s between the subject vehicle and its lead vehicles at the observation stations; and

Condition B: No passing movement between the observation stations.

In laboratory the recorded video is played frame by frame on big screen in order to extract speed data. Recorded videos have the time accuracy of 0.04 s. Total travel



Fig. 1 Car tire touching the first and second line of trap length

time to traverse the 15 m trap length are noted. Suppose the time when the front tire of a car touches the first line of the trap is t_1 and the time when it touches the second line of the trap is t_2 (see Fig. 1). Therefore, travel time is $(t_2 - t_1)$. Hence the speed of the car can be estimated using Eq. 1

$$V = \frac{15 \times 3.6}{t_2 - t_1} \quad (1)$$

where,

t_1 Time in sec when front tire touched first line of the trap (Fig. 1)

V Speed, kmph

t_2 Time in sec when front tire touched second line of the trap (Fig. 1).

5 Model Development

Before going for model development all the data are reviewed for normal distribution. For this purpose the Shapiro-Wilk test is conducted at 95% confidence interval. The test results indicates p -values are more than 0.05. Therefore, from the test results it can be conclude that the speed data of all sites are normally distributed. These data set can be used for developing the speed prediction model by regression analysis. To develop the model, operating speed or 85th percentile speed are estimated from the field data at starting and centre of circular curve of selected eight horizontal curves. A correlation analysis is conducted for all the available influencing variables, which are R , Δ , PTL , CL , G . Hence, the Spearman's rho correlation analysis is selected for the purpose. Results are shown in Table 3. No, correlation has been observed between the variables. Therefore, all the variables are selected for regression analysis. Also, two transformed form of R has been used in regression analysis. The reason is to get the better form of R , which gives more significance to the model.

A stepwise regression analysis is performed to develop the operating speed (i.e., 85th percentile speed) prediction models at PC and CC of horizontal curves. The

Table 3 Spearman’s rho correlation coefficients

	<i>R</i>	Δ	<i>PTL</i>	<i>CL</i>	<i>G</i>
<i>R</i>	1.00	-0.05	-0.42	0.63	0.12
Δ	-0.05	1.00	0.02	0.69	0.15
<i>PTL</i>	-0.42	0.02	1.00	-0.31	-0.53
<i>CL</i>	0.63	0.69	-0.31	1.00	0.22
<i>G</i>	0.12	0.15	-0.53	0.22	1.00

Table 4 Developed models

No.	Model	R^2_{Adjust}	<i>p</i> -values	Beta value
1	$V_{85Car_SC} = 84.73 + 0.02 CL$	0.75	<0.05	0.89
2	$V_{85Car_CC} = 61.07 + 1.68\sqrt{R}$	0.87		0.94
3	$V_{85HV_SC} = 64.93 + 0.02CL$	0.49		0.75
4	$V_{85HV_CC} = 72 - \frac{566.67}{R}$	0.70		0.86

developed model and its corresponding adjusted R^2 values are shown in Table 4. The *p*-values in Table 4 indicates the significance of the predictors in the models. Whereas, other eliminated influencing variables have *p*-value more than 0.05, which confirms their insignificant contribution to the model and not included as predictor. Beta value in Table 4 describes the sensitivity of the predictors. It indicates that passenger car models are highly sensitive to predictor than *HVs*. Regression analysis shows that transformed form of radius i.e. square root of radius and inverse of radius contributes significantly in model no. 2 and 4, respectively. The developed speed prediction model at starting of the circular curve (*SC*) implies that passenger cars and heavy vehicles speed increases with curve length (Ref. Model no. 1 and 3). Whereas, at centre of curve (*CC*) speed increases with radius.

6 Model Validation

In order to test the significance level of the developed models, a statistical validation is conducted. For this purpose, method suggested by Esposito et al. [20] and Dell’ Acqua [21] has been used. “*I*” value has been calculated using Eq. (2). Authors suggested that if “*I*” value is less than 0.2, then the prediction model can be considered as good.

I (constant) value = Root mean square error (*RMSE*) divided by the mean predicted operating speed

$$I = \frac{RMSE}{\sum_{i=1}^n \frac{(Predicted V_{85})_i}{n}} \tag{2}$$

where; i = site number, n = total number of study sites, $RMSE = \sqrt{\frac{\sum_{i=1}^n D_i^2}{n}}$, $D_i = (\text{Observed } V_{85} - \text{Predicted } V_{85})$.

Remaining two sites having the geometric features similar to sites adopted for model development, are selected for the validation. The obtained I value is lower than 0.2 for all the models. Therefore, it can be concluded that developed speed prediction model is statistically significant in predicting operating speed at starting and centre of horizontal curve in four lane divided highway. Also, the adjusted R^2 -value for models (1)–(4) confirms the goodness of fit of the model developed.

7 Conclusion

Operating speed prediction models at starting and centre of horizontal curve are proposed in this paper. These models are developed considering weak lane discipline conditions in four-lane divided highway. Which overcomes the limitation of availability of models in these conditions. Moreover, this study proposed separate models for passenger car and heavy vehicles.

The models developed in this paper for weak lane discipline appear to be useful for many applications such as the detection of unsafe horizontal curve locations, evaluation and design of single and successive elements of horizontal curves, estimation of operating speed reduction due to road geometry, and the predictions of operating speed. Thus this research may suggest a point of reference to engineers in adjusting or designing four-lane divided highways, placing of low cost safety measures, and value-addition in-vehicle warning system.

References

1. Torbic DJ, Harwood DW, Gilmore DK, Pfefer R, Neuman TR, Slack KL, Hardy KK (2004) NCHRP report 500. Volume 7: a guide for reducing collisions on horizontal curves. HRB, National Research Council, Washington, D.C
2. Lamm R, Psarianos B, Chourieri EM, Soilemezoglou, G. (1995) A practical safety approach to highway geometric design. International Case Studies: Germany, Greece, Lebanon and the United States. International Symposium on Highway Geometric Design, 9:1–9:14
3. Lamm R, Choueiri EM, Mailaender T (1990) Comparison of operating speed on dry and wet pavement of two lane rural highways. Transp Res Rec 1280:199–207. Transportation Research Board, Washington, D.C.
4. Gibreel GM, Easa SM, Hassan Y, El-Dimeery IA (1999) State of the art of highway geometric design consistency. J Transp Eng 125:305–313
5. Glennon JC, Neuman TR, Leisch JE (1985) Safety and operational considerations for design of rural curves. Report FHWA/RD-86/035. FHWA, U.S. Department of Transportation
6. Fitzsimmons EJ, Souleyrette RR, Nambisan SS (2012) Measuring horizontal curve vehicle trajectories and speed profiles: pneumatic road tube and video methods. J Transp Eng 139(3):255–265

7. Campbell JL, Richard CM, Graham J (2008) NCHRP Report 600B: human factors guidelines for roadway systems. HRB, National Research Council, Washington, D.C
8. Road accidents in India. Ministry of road transport and highways (2015) Transport research wing, New Delhi, India
9. Dell'Acqua G, Busiello M, Russo F (2013) Safety data analysis to evaluate highway alignment consistency. In *Transportation research record: journal of the Transportation Research Board*, No. 2349, Transportation Research Board of the National Academies, Washington, D.C., pp 121–128
10. Hassan Y, Sarhan M (2011) Modeling operating speed: synthesis report. Chapter 1: introduction. *Transportation research E-circular*, (E-C151)
11. Jacob A, Anjaneyulu MVL (2013) Operating speed of different classes of vehicles at horizontal curves on two-lane rural highways. *J Transp Eng* 139(3):287–294
12. Abdul-Mawjoud AA, Sofia GG (2008) Development of models for predicting speed on horizontal curves for two-lane rural highways. *Arab J Sci Eng* 33(2):365
13. Bennett CR (1994) A speed prediction model for rural two-lane highways. Ph.D. Dissertation, University of Auckland, New Zealand
14. Misaghi P, Hassan Y (2005) Modeling operating speed and speed differential on two-lane rural roads. *J Transp Eng* 131(6):408–418
15. Lamm R, Choueiri EM (1987) Recommendations for evaluating horizontal design consistency based on investigations in the state of New York. *Transp Res Rec* 1122, Transportation Research Board, Washington, D.C., pp 68–78
16. Gong H, Stamatidis N (2008) Operating speed prediction models for horizontal curves on rural four-lane highways. In *transportation research record: journal of the Transportation Research Board*, No. 2075, Transportation Research Board of the National Academies, Washington, D.C., pp 1–7
17. Sil G, Maji A, Nama S, Maurya AK (2019) Operating speed prediction model as a tool for consistency based geometric design of four-lane divided highways. *Transport* 34(4):425–436
18. Nama S, Maurya AK, Maji A, Edara P, Sahu PK (2016) Vehicle speed characteristics and alignment design consistency for mountainous roads. *Transport Dev Econ* 2(2):1–11
19. Maji A, Sil G, Tyagi A (2018) The 85th and 98th percentile speed prediction models of car, light and heavy commercial vehicles for four-lane divided rural highways. *J Transport Eng Part A: Syst* 144(5)
20. Esposito T, Mauro R, Russo F, Dell'Acqua G (2011) Speed prediction models for sustainable road safety management. *Procedia-Soc Behav Sci* 20:568–576
21. Dell'Acqua G, Russo F, Mauro R (2013) Validation procedure for predictive functions of driver behavior on two-lane rural roads. *Eur Transp Trasporti Europei* 53:1–13

A New Model to Evaluate Percent-Time-Spent-Following on Two-Lane Highways



Vivek

Abstract This paper presents the evaluation of percent-time-spent-following (PTSF), one of the key service measures as indicated by Highway Capacity Manual (HCM) to assess level of service (LOS) under heterogeneous traffic conditions for two-lane highway. The PTSF is defined as “the average percentage of travel time that vehicles must travel in platoons behind slower vehicles because of their inability to pass.” Two-lane highway flow is very different from that of single-lane highways mainly because vehicles oppose traffic in the opposite lane, and as a result, they may be subjected to delaying because of their inability to pass slow-moving vehicles. Detecting from the existing studies, it is declared that measuring PTSF directly in the field is quite tedious. However, Highway Capacity Manual put forward some logical stratagem to evaluate PTSF with the 3 s surrogate measure which overestimated the field results. Because of this difficulty, the evaluation of PTSF has been based on methodical procedure which uses equations obtained from simulations and field examination at given location based on substitute measure, the percent of vehicles traveling with headway less than 3 s. In this study queuing analogy is employed to measure PTSF by measuring the headways inside and outside platoons on the two-lane highways of Himachal (India). In this analysis, middle or average range will be that where number of headways inside and outside the platoon will be equal. The difference in range of PTSF grows as volume increases. The range of PTSF measured is lesser than that accorded in the HCM. The main difference for the range of PTSF between the current study and HCM is that using queuing analogy LOS “A” has a PTSF value less than 16% while for HCM it is 35%. This study also propounds a new method of estimating PTSF which can be used as a powerful tool to provide rational idea of various measures for LOS that would otherwise be very hard to estimate.

Keywords Level of service · Percent-time-spent-following · HCM · Platoon formation · Queuing analogy · Two-lane highway

Vivek (✉)

Department of Civil Engineering, Jawaharlal Nehru Government Engineering College,
Sundernagar, Himachal Pradesh, India
e-mail: vivak.k12@gmail.com

1 Introduction

The HCM implemented the study of percent-time-spent-following (PTSF) for two-lane highways to evaluate the level of service [1]. The Highway Capacity Manuals HCM 2000 and HCM 2010 use percent-time-spent-following (PTSF) to allocate LOS for two-lane highway [1, 2]. HCM estimates PTSF by analytical procedures using simulation with 3 s surrogate measure. The findings from the literature review reveal that HCM results mostly overestimate the indicator [3–7]. The movement of traffic in India is heterogeneous in nature with different sizes and different operational characteristics. Vehicles usually get retarded their speed because of their impotence to pass slow-moving vehicles. In this situation, vehicles enlarge interactions among themselves in the same and in the opposite lane. These interactions become greater in size with the increase in traffic flow in both directions. A platoon genesis until a fast-moving vehicle overtakes a slow-moving vehicle until not exposed to danger or risk. In the current study, queuing analogy is used to generate a new range of PTSF in mixed-type traffic condition. There are mainly three parameters, namely flow, traffic intensity, and “freedom of flow,” introduced using queuing model. The current study propounds that weighted average gives more appropriate results when traffic mix involves a relatively large proportion of heavy vehicles, among which most of vehicles are slow-moving vehicles.

2 Background

The utilization of PTSF values as service measures for two-lane highways by HCM is under criticism from various studies. It is not due to its inadequacy to be used as a service measure; it is because it is difficult to be measured directly in the field. It is due to the fact that it is very complex to find the data related to fast-moving vehicles that follow slow-moving vehicles. It requires complicated and expensive equipment for direct measurements. Another method to calculate PTSF is using simulation. One of the major drawbacks of using simulation is that it requires assumptions regarding traffic behavior and driver passing maneuvers [3]. Further, the two approaches used by the HCM for obtaining PTSF were confirmed to produce inconsistent results as compared to the values obtained in the field; analytical procedures overestimate PTSF [8–12]. Heavy reliance on traffic simulation in developing HCM procedures has been blamed as the key cause of the difficulty for direct field measurement of PTSF [13]. Researcher observed and recorded overestimation of PTSF for all values of flow rates [14] except MHCM model where differences in driver following behavior were considered as dominant parameter. An alternative method prescribed by the current study closer to reality for field measurement of PTSF is given. In this study, queuing analogy is employed to measure PTSF by evaluating the headways inside and outside platoons for the two-way highways of Himachal Pradesh, India. The 3 s surrogate measure is to be used for field measurement of PTSF. The simple count of headways

inside and outside the platoons through videography is used to analyze important parameters studied in the present study. By using simple count of headways inside and outside the platoons, new estimate range of PTSF was determined. It is assumed that each platoon acts as a one-server queuing system, in which “service time” is determined by the time interval spent by the fast vehicle in the first position just behind the delayed vehicle. M/M/1 queuing model was used to analyze the traffic pattern, and the same model was used to analyze the interaction and traffic growth. Further, it was assumed that M/M/1 queuing model has Poisson ratio and having input with parameter λ e designated as exponential service μ and customers are served in FIFO/FCFS basis. Using M/M/1 queuing model, the current study elaborates a theory-based queuing relationship so that flow characteristics such as speed, flow, traffic density, PTSF, and freedom of flow can be easily estimated on the two-lane highways. The current study focused on reviewing the range of PTSF for different ranges of LOS.

3 Collection of Field Data

During the data collection, it was observed that the density of queues was more at morning peak from 8:00 a.m to 11:00 a.m and at the evening from 4:30 p.m to 8:00 p.m. All the traffic data was recorded during the morning peak traffic hours. It is pertinent here to mention that data was collected on the rural two-lane two-way highways of Himachal Pradesh (India).

These traffic data was collected on 10 one-way sections of different highways which are straight, level, and free from other capacity restrictions. During the data collection, the pavement was dry and fair weather condition was observed. On each highway segment, video recording technique was used to collect data for a period of one hour during the peak hour period on week days.

Videography is done by a portable camera placed at an appropriate height which can cover the stretch of 18 m, and road users are unaware of the data collection so that the actual behavior of the drivers can be captured. A stretch mark of 18 m was marked over the road section using suitable marker which is in this case of lime powder. Data is then analyzed using Avidemux software which has a precision up to 4 decimals of a second, using which time headways and other important parameters are obtained. The number of headway inside and outside of platoon were calculated and given in Table 1.

4 Results and Discussions

The data on various characteristics, namely traffic volume, traffic intensity, average speed of vehicles, number of headways inside and outside the platoons, and platoon formation, is analyzed, PTSF was calculated, and its new range for various levels of

Table 1 Number of headway inside and outside the platoons

Road	One-way hourly volume (Vph)	Speed of vehicles (kmph)	Headways inside platoons	Headways outside platoons	No of vehicles inside platoons	No of vehicles inside platoons
Pungh (North)	191	64.23	61	134	1.40	2.84
Pungh (South)	171	63.79	44	126	1.26	3.10
Hamirpur(North)	522	53.05	237	285	2.14	2.12
Hamirpur(South)	620	53.409	319	284	2.34	2.09
Nagrota–Ranital (North)	330	51	159	162	2.1	2.20
Nagrota–Ranital (South)	265	42.6	186	168	2.47	2.31
<i>Mandi</i>						
Road (North)	98	62.8	17	81	1.125	5.01
<i>Mandi</i>						
Road (South)	119	63.81	23	95	1.2	4.69
<i>Bilaspur</i>						
Road (North)	1219	46.40	801	416	3.45	1.76
<i>Bilaspur</i>						
Road (South)	1272	40.95	899	370	3.81	1.59

service was determined to check the performance of a highway facility. The values of percent-time-spent-following obtained in this study are validated on four highway sections by using weighted approach method. This current study also compares the results obtained with the values given in HCM 2000 and HCM 2010 and further also is compared with Polus and Cohen study.

5 Calculation of Headways

In this current study, time headway is calculated by considering the fact that platoon only considered if it is formed by less than 3 s. This indicated the 3 s surrogate measure that is taken for the formation of platoons. Data is calculated and shown in Table 1 for measuring the number of headways inside and outside the platoons, and also, the average speed of vehicles is measured as given in Table 1. Using M/M/1 model of queuing theory, different parameters, namely level of service and intensity of traffic, were calculated. These parameters are calculated by simple measuring of vehicles inside and outside the platoons as per queuing analogy.

6 Estimation of Flow Characteristics

The first characteristic flow which was related to density and is a main indicator of driving attributes was calculated. The second parameter is “traffic intensity” measures the quality of flow. The third important parameter is a measure of “freedom of flow” which measured as ratio between free travel time when driving between platoons and the delay time of the second vehicle moving behind the delaying vehicle when searching for safe overtaking distance.

6.1 Relationship Between Speed and Flow

The relationship between speed and flow for the two-lane, two-way highways is given in Fig. 1. It was assumed that during the collection of data there was continuous flow of traffic and there was no breakdown condition. The trend of speed and flow relationship was shown in Fig. 1. It was observed from Fig. 1 that the maximum speed of vehicles was maintained at very low traffic flow and the speed decreases steadily as the traffic flow increases. It was further assumed that higher levels of interaction between vehicle traveling in same and in opposing direction on two-lane highways result in some distracted point from the straight line.

Linear equation obtained for speed and flow relationship is given as,

$$y = -0.019x + 67.15 \text{ and } R^2 = 0.8083.$$

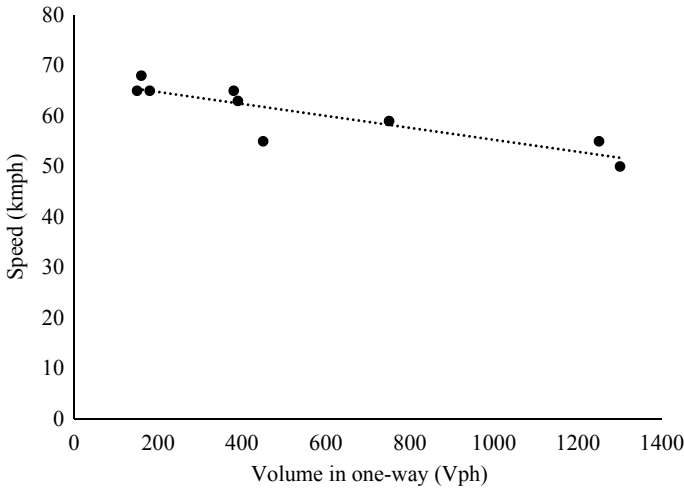


Fig. 1 Speed versus one-way volume on rural two-lane, two-way highway

The R^2 value shows that the trend is significant and therefore the model is also significant.

6.2 Relationship Between Traffic Intensity and Volume

The relationship between traffic intensity and one-way volume is expressed graphically in Fig. 2. The equation obtained is given as,

$$y = 0.235 \ln(x) - 0.86 \text{ and } R^2 = 0.83$$

This relationship shows that queue does not grow sharply at high volumes of traffic, and we see that curve is going to be asymptotic to 0.7 which is less than 1. This may be attributed to the facts that it is difficult to pass or overtake as less passing gaps are accessible and thus vehicles are not having power to leave one queue and join another.

6.3 Relationship Between Freedom of Flow and Flow

One of the important parameters, namely freedom of flow, is also calculated using queuing theory which is also used to assign level of service for a two-lane highway. It is designated by symbol η . Essentially, η is the ratio between the time of undisturbed driving (the driver has no pressure from other adjacent drivers) and the time span in

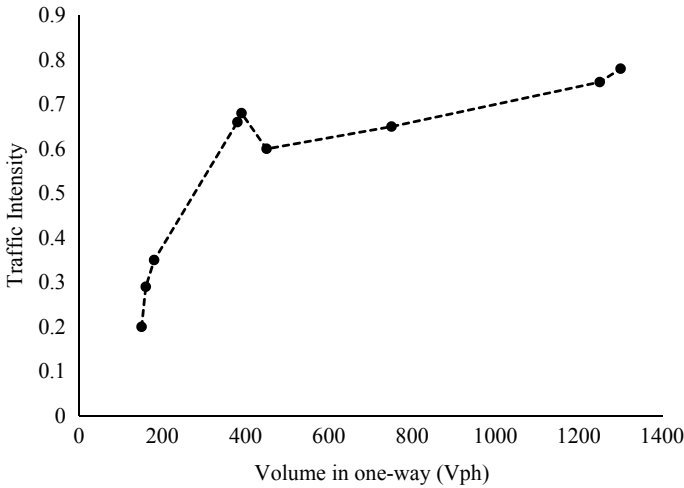


Fig. 2 Traffic intensity versus one-way flow on rural two-lane, two-way highways

which the driver tries to overtake the slower vehicle. Mathematically,

$$\eta = \frac{N_0}{\rho}$$

where N_0 = number of headways inside platoon
and ρ = traffic intensity

The hyperbolic relationship between freedom of flow and the two-way flow is presented in Fig. 3. It can be observed that the change in freedom of flow is less with higher values of the flow. The bigger the value of freedom of flow, the more is the LOS because it represents that the free travel time between platoons is more than the time needed to wait until an appropriate passing gap appears in the opposite flow. The range of freedom of flow obtained for different LOS is given in Table 2.

These are the values obtained by the two-lane two-way highways study in the state of Himachal Pradesh (India). The variables according to which the freedom of flow η is calculated are constructed on both the directions: the rate at which vehicles approach the queue in the representing the main direction, and the mean time in the first position, which conditioned largely on the critical passing gap and the number of vehicles in the opposite direction.

7 Estimation of PTSF

The flow obtained and PTSF calculated are given in Table 2. PTSF is calculated using queuing theory. It was suggested that the “official” empirical model (National

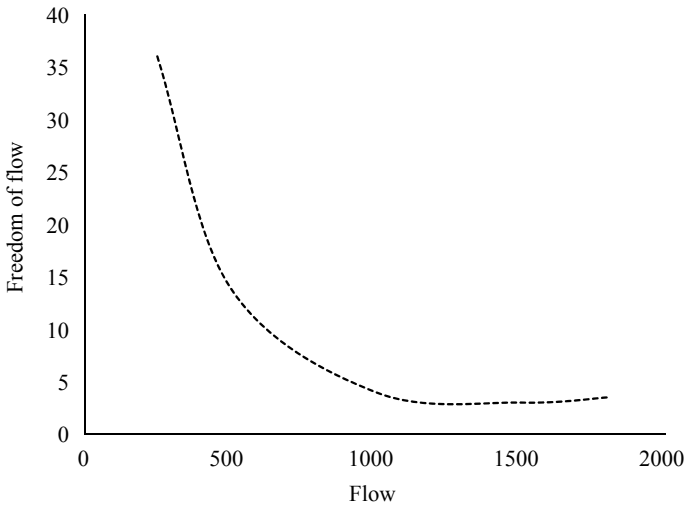


Fig. 3 Relationship between freedom of flow and traffic flow on two-lane, two-way highways

Table 2 Range of freedom of flow obtained for different LOS

S. no	Level of service	Freedom-of-flow thresholds
1	A	≥ 34
2	B	13.5–34
3	C	7–13.5
4	D	3–7
5	E	3–2
6	F	≤ 2

Academy of Sciences 2000) has been over predicting PTSF, and perhaps, this is the reason that the related HCM (National Academy of Sciences 2000) thresholds have been relatively high for a given level (Table 3).

PTSF is unquestionably a right measure to evaluate LOS and majority suitable for economic measuring of delay costs, because it makes a calculation of the time lost in platoons that can be converted to monetary values.

As the flow of traffic increases, platoon formation began to form. Thus, the condition is induced when slower vehicles will slow down the speed of vehicles moving behind them. Thus, the mean time spent by vehicles inside the platoon increases leading to an increase in PTSF. But the rate at which PTSF increases is higher in the beginning and becomes lower as the traffic flow increases beyond a certain limit. As mentioned previously, Highway Capacity Manuals 2000 and 2010 have procedure which is very complicated to assess the LOS for two-lane highway and also overestimated the range of percent-time-spent-following for the two-lane, two-way

Table 3 PTSF evaluated and flow on the two-lane, two-way highways

S. no.	Highway	One-way hourly volume	Traffic flow	PTSF (%)
1	Pungh (North)	191	418	31.89
2	Pungh (South)	171	370	27
3	Hamirpur(North)	522	788	47
4	Hamirpur(South)	620	936	53.7
5	Nagrota–Ranital (North)	330	512	49
6	Nagrota–Ranital (South)	265	570	53.3
7	Mandi road (North)	98	143	18.3
8	Mandi road (South)	119	173	20.49
9	Bilaspur road (North)	1219	1840	67.5
10	Bilaspur road (South)	1272	1935	78.5

highways. As per the current study, PTSF was calculated and is compared with PTSF recommended by HCM given in Table 4.

It was evident from Table 4 that percent-time-spent-following calculated from this study is lesser than that of percent-time-spent-following calculated from HCM values for different ranges of level of service. It was observed from the literature that also HCM 2000 and HCM 2010 overestimated the values of PTSF for level of service and also the range of PTSF given by HCM is not valid in the mixed Indian traffic conditions in the state of Himachal Pradesh of India. As a result, there is great loss of money if the evaluation of two-lane highway was monitored by the range of PTSF for different LOS as given by HCM. For operational analysis, proper planning, and preliminary design analysis, use of default values is generally required, since few details are available at this stage of consideration. PTSF is mostly a perfect measure to assess LOS and especially as per economic point of view.

Table 4 Proposed PTSF thresholds for level of service on two-lane highways

S. no	Level of service	Proposed PTSF thresholds (%)	HCM PTSF thresholds for Class 1 highways (%)
1	A	≤16	≤35
2	B	16–33	>35–50
3	C	33–50	>50–65
4	D	50–67	>65–80
5	E	67–84	>80
6	F	>84	—

8 Results Comparison

The range of PTSF obtained through this study is compared with that given in HCM 2010 and with the study done by Polus and Cohen as given in Table 5. It was observed from Table 5 that PTSF values are low in both the present study and PTSF recommended by Polus and Cohen study. The PTSF calculated in the current study through weighted approach method is given in Table 6. It was observed and concluded from the above study that the present study is very helpful and can be effectively used in the heterogeneous traffic condition to assess LOS. Freedom of flow value and flow values for different LOS were given in Table 7.

Table 5 Range of PTSF proposed by different studies

S. no	Level of service	Proposed PTSF thresholds (%)	HCM PTSF thresholds for class 1 highways (%)	PTSF thresholds as proposed by Polus and Cohen study (%)
1	A	≤16	≤35	0–15
2	B	16–33	>35–50	15–30
3	C	33–50	>50–65	30–45
4	D	50–67	>65–80	45–60
5	E	67–84	>80	60–75
6	F	>84	—	75–100

Table 6 Ranges of PTSF using weighted approach method and queuing theory

S. no	Highway	PTSF (%)	PTSF using Queuing theory (%)
1	Bilaspur road (North)	62.45	67.5
2	Bilaspur road (North)	53.66	78.5
3	Hamirpur (N)	45.7	47
4	Hamirpur (S)	50.44	53.7

Table 7 Freedom of flow value and flow values for different LOS

Level of service	Current study		Polus and Cohen study	
	Freedom of flow	Flow value	Freedom of flow	Flow value
<i>A</i>	≥ 34	0–150	≥ 16.5	0–300
<i>B</i>	13.5–34	150–350	7.1–16.5	300–700
<i>C</i>	7–13.5	350–700	4.1–7.5	700–1200
<i>D</i>	3–7	700–1500	2.8–4.1	120–1800
<i>E</i>	3–2	1500–3000	1.8–2.8	1800–2700
<i>F</i>	≤ 2	>3000	≤ 1.8	≥ 2700

References

1. TRB (2000) Highway capacity manual, 4th edn. National Research Council, Washington, D.C.
2. TRB (2010) Highway capacity manual, 5th edn. National Research Council, Washington, D.C.
3. Polus A, Cohen M (2011) Estimating percent-time-spent-following on two-lane rural highways. *Transp Res Part C: Emerg Technol* 19(6):1319–1325
4. Al-Kaisy A, Durbin C (2007) Estimating percent time spent following on two-lane highways: field evaluation of new methodologies, in presented at the Transportation Research Board 86th annual meeting, 21–25 Jan. Transportation Research Board, Washington, D.C.
5. Dixon MP, Sarepali SSK, Young, KA (2002) Field evaluation of highway capacity manual 2000 analysis procedures for two-lane highways. *Transportation Research Record* 1802:125–132. Transportation Research Board. National Research Council, Washington, D.C.
6. Harwood DW et al (2003) Two-lane road analysis methodology in the highway capacity manual. In NCHRP Project 20-7(160) Washington, D.C
7. Luttinen RT (2001) Capacity and level of service on finnish two-lane highways, in helsinki 2001, finnish road administration, Traffic and Road Engineering, Finnra reports 18/2001, Helsinki, Finland
8. Polus A, Cohen M (2009) Theoretical and empirical relationships for the quality of flow and for a new level of service on two-lane highways. *J Transp Eng ASCE* 135(6):380–385
9. Rozenshtein S, Polus A, Cohen M (2012) Models for estimating drivers following on two-lane rural highways. *Transp Res Rec* 2286(1):68–75. *Journal of the Transportation Research Board*
10. Saha P, Pal M, Sarkar A (2012) Study on percent time spent following, in advances in civil engineering and building materials, CRC Press. 899–902
11. Van A, Van Niekerk CA (2007) South African highway capacity research, in TRB Workshop 153. South African National Roads Agency, Limited
12. Al-Kaisy A, Karjala S (2008) Indicators of performance on two lane rural highways: empirical investigation. *Transp Res Rec* 2071(1):87–97. Transportation Research Board, National Research Council. Washington, D.C.
13. MOWM (2011) Malaysian highway capacity manual. Highway Planning Unit, Ministry of Works, Malaysia
14. Othman CP (2004) Drivers's car following headway on single carriageway roads. *Jurnal Keju-ruteraan Awam* 16(2):15–27. Universiti Teknologi Malaysia

Analysis of Vehicular Pedestrian Interaction at Urban Undesignated Mid-block Sections



Hareshkumar Dahyabhai Golakiya, Manish Patkar and Ashish Dhamaniya

Abstract In the present study, the interaction between vehicle and pedestrian crossing at the undesignated mid-block location is assessed. The traffic survey is conducted at thirteen urban mid-block sections in three heavily populated and fast-growing cities of India. To study the interaction between vehicle and pedestrian, speed of vehicles has taken a prime variable and the effect of pedestrian crossing on vehicle speed has been assessed. The speed reduction in individual category of vehicles due to pedestrian crossings has been determined. Considering the fact that speed is linearly related to density, speed models are generated for section without side friction (base section) and with pedestrian crossing (friction sections) for six-lane urban arterials. The result shows that for the given traffic volume and proportion of traffic mix speed at friction section significantly reduces as compared to the base section. The study is useful for the designer for designing traffic facility as HCM keeps mum in such a traffic condition.

Keywords Pedestrian · Speed · Mid-block · Interaction · Base section · Friction section

1 Introduction

Traffic rules violation or following the traffic rules partially are common phenomenon found in developing countries which mostly leads towards unsafe traffic operation. If all the traffic rules are followed strictly by road users, theoretically there will not be any road crash. However, many other reasons are also there like the failure of the vehicle operating system, carelessness of the driver, use of alcohol, etc. But most of

H. D. Golakiya · M. Patkar · A. Dhamaniya (✉)
Civil Engineering Department, Sardar Vallabhbhai National Institute of Technology, Surat
395007, India
e-mail: adhamaniya@gmail.com

H. D. Golakiya
e-mail: hdgolakiya@yahoo.co.in

M. Patkar
e-mail: manish.patkar@gmail.com

© Springer Nature Singapore Pte Ltd. 2020
T. V. Mathew et al. (eds.), *Transportation Research*, Lecture Notes
in Civil Engineering 45, https://doi.org/10.1007/978-981-32-9042-6_31

such collisions can be avoided by following traffic rules and become more cautioner. In all over the world, accidents rate is there in more or less proportion in different countries. In developing countries, such accident rate is higher. In a country like India, due to high population, economical constrains, lack of awareness of traffic rules and lack of traffic rule enforcement, in spite of the existence of good traffic rules, accident rate could not control even in recent time. Globally, the picture is more or less the same. More than 1.2 million people die each year on the world's roads, making road traffic injuries a leading cause of death. Most of these deaths are in low- and middle-income countries where rapid economic growth has been accompanied by increased motorization and road traffic injuries. Data suggest that the road traffic deaths and injuries in low- and middle-income countries are estimated to cause economic losses of up to 5% of GDP. Wide-reaching, an estimated 3% of GDP is lost to road traffic deaths and injuries. The road infrastructure is mainly constructed with the needs of motorists in mind, although the report indicates that 49% of all road traffic deaths occur among pedestrians, cyclists and motorcyclists. Globally, road traffic crashes are a leading cause of death among young people, and the main cause of death among those aged 15–29 years (WHO) [1]. The analysis of road accident data 2016 for India reveals that about 1,317 accidents and 413 deaths take place every day on Indian roads which further translates into 55 accidents and loss of 17 lives on an average every hour in India. About 46.3% of all persons killed in road accidents are in the 18–35 years age group during the year 2016. Among all death, the death rate of pedestrians is 10.5% in the road crash in India in the year 2016 [2]. These statistics of accident data indicates that still something is missing in our road and traffic infrastructure design and this is very high time to think in this direction. In most of the traffic facilities in urban roads, particularly in developing countries the design is biased towards motorized vehicles. Pedestrians and non-motorized vehicles have not given due weightage, even in metropolitan cities. Walking and crossing facilities for pedestrians are very limited in urban areas. If the walking path is provided for pedestrian, then it is occupied by vendors and unauthorized parking or other such activities. Moreover, such facilities are not continuous in nature. Due to such an existing scenario, pedestrians have no option left than using the regular traffic lane. Pedestrian crossing facilities are also very less, and the frequency of such facilities is very less, due to which pedestrians choose to cross the road at their convenient place mostly at mid-block. Hence, mid-block crossing put the pedestrians at very high risk of collision with regular traffic, additionally it also affects and disturbs the regular traffic. Pedestrians use force gap to cross the road and as a result vehicle driver has to either change the path or slow down the vehicle which negatively affects the speed of the interacting vehicle or other vehicles present in the traffic stream. The study aims to analyse such interaction of pedestrians with the vehicle at mid-block pedestrian crossing locations in various cities of India.

2 Literature Review

Many researchers have attempted modelling of speed in homogeneous as well as in mixed traffic conditions. Most of the work has been carried out on homogeneous traffic conditions. A few works have been reported in mixed traffic condition. The initiation of research in this direction was done by Greenshields [3] who developed the linear relationship between speed and density. Al-Ghamdi [4] analysed spot speed data like mean, variance and 85th percentile, at urban roadway sections in Riyadh. Shankar and Mannering [5] generated a structural model which relates mean speed and speed deviations by lane. Dixon et al. [6] found that Highway Capacity Manual rule-of-thumb free-flow estimation technique based on posted speed limit does not adequately estimate free-flow speed for the higher speed limit condition. Najjar et al. [7] used ANNs to develop models to predict V85 from roadway characteristics on two-lane rural Kansas highways. The comparison of ANN models with regression-based models for prediction of operating speed was carried out by McFadden et al. [8], and the results of the study reveal that the predictive powers of ANN models were comparable with regression models. Donnell et al. [9] developed a speed prediction models using regression and simulation on field data to predict 85th percentile truck operating speed at the horizontal curve with the effect of length and grade of approach tangent, horizontal curve radius, length and grade of tangent. Figueroa Medina and Tarko [10] developed models to predict user-selected percentile free-flow speeds on two-lane rural and four-lane rural and suburban. Koshy and Arasan [11] used a simulation approach to study the influence of bus stops on the traffic flow in heterogeneous traffic flow. Dey et al. [12] suggested the mathematical equations for the speed with a unimodal or a bimodal speed distribution curve. Perco [13] developed a prediction equation to estimate the powered two-wheeler (PTW) speeds starting from passenger car operating for urban streets by studying speed distribution of PTW and passenger car. In addition to this, very few researches have been carried out to quantify the effect of pedestrian crossing on traffic characteristics. Bak and Kiec [14] studied the influence of three types of mid-block pedestrian crossings like Zebra crossings, crossings with refuge median islands, and signalized crosswalks on roadway capacity by the VISSIM simulation model. Dhamaniya and Chandra [15] analysed the effect of pedestrians crossing at undesignated places on urban roads. They found there is no influence on capacity when pedestrian cross flow is less than 200 pedestrians per hour, but the capacity was reduced by 30% when pedestrian cross flow is increased to 1,360 pedestrians per hour. Kadali et al. [16] analysed the effect of pedestrian crossing on the vehicular flow characteristics at mid-block sections in mixed traffic conditions. These researchers have made an attempt to model speed in homogeneous and mixed traffic condition without the effect of any side friction. A few researchers attempted to analyse the effect on pedestrian crossing on traffic characteristics like speed and capacity, but much more research is required to quantify the effect pedestrian crossing on speed and other traffic characteristics. The present study is in direction of fulfilling this gap and presented models to predict speed for various categories of vehicles in the presence and absence of crossing pedestrian.

3 Research Methodology

Speed is an important traffic parameter for traffic operation, safety, comfort and level of service. Along with traffic speed, traffic density, traffic composition and traffic flow also play their role in traffic operations. Generally, traffic speed can also be affected by road geometry and environmental condition, but for the observation time these parameters remain unchanged. In such case, the traffic speed is mainly governed by above-listed traffic characteristics. Additionally, the traffic operation is affected by relative interaction between vehicles available in the stream, their proportion in traffic stream along with the traffic density. When these traffic characteristics remain constant, then manoeuvrability of particular type of vehicle, its size, shape area occupied and acceleration–deceleration characteristics play an important role. Out of all these characteristics, manoeuvrability is a very important factor affecting the speed of vehicle. In the traffic stream, if the traffic flow and accordingly traffic density is very less, then each category of vehicle will travel with the desired speed according to driver's and vehicle's characteristic, which is termed as free-flow speed but when the flow increases due to relative interaction between available category of vehicles and their density the speed of vehicles as well as stream speed will reduce. In the study, the stream speed of various categories of vehicles is modelled as the function of free-flow speed and density of other category of vehicle. Pedestrians are generally crossing the road mostly at mid-block, in doing so vehicles are forced to reduce their speed or change the path. In both conditions, the speed of vehicle is reduced. So, at friction section along with the above-listed parameters, stream speed is also affected by the pedestrian cross flow. It is quite obvious that stream speed reduced with increase in pedestrian cross flow. So, this effect of a pedestrian crossing on speed is also modelled in the study.

3.1 Data Collection

To evaluate the effect of crossing pedestrians on the speed of vehicles at the urban road, the data was collected from thirteen different 6-lane mid-block locations, with and without the effect of pedestrian cross flow in highly populated cities of India namely, New Delhi, Jaipur, Chandigarh, Noida and Surat. Video-graphic survey was conducted at five friction sections in three cities of India, namely Noida, Jaipur and Surat and at eight base sections at New Delhi, Chandigarh and Jaipur. Figure 1 shows the images of the base and friction sections of study locations. A mid-block section having about 500 m length was selected with uniform traffic flow condition with no access point on base section; however, on friction section pedestrian cross flow was observed which affect the regular traffic flow. A longitudinal trap of 60 m was marked in the middle of the selected mid-block section to obtain traffic characteristics like flow and speed. Data were collected through video camera at each section on a typical

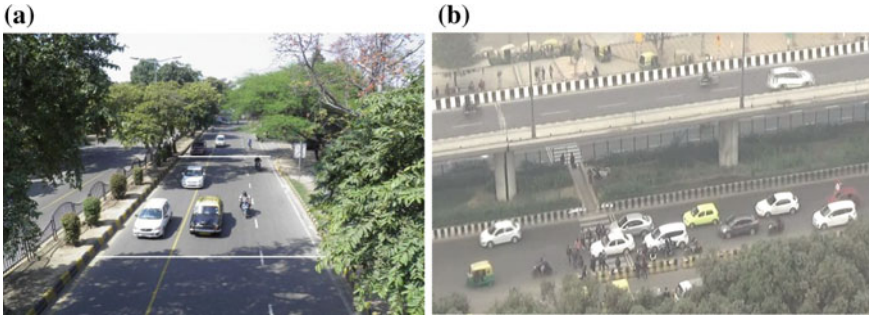


Fig. 1 Study location images **a** base section **b** friction section

weekday during 6:00 AM to 6:00 PM. The video camera was mounted on the stand and placed at a vantage point so as to cover the entire length of the trap.

Base section locations were free from the effect of intersection, gradient, curvature and side frictions like bus stop, parked vehicles, curvature, gradient, pedestrian movement. For selection of friction section, the criteria was that it should be free from the effect of gradient, curvature and side frictions other than pedestrian cross flow. On the selected friction sections, the significant variations of pedestrian cross flow were observed. All the vehicles in the stream were divided into five categories.

3.2 Data Extraction

The recorded film was replayed on large screen computer in the laboratory to extract the desired information. The entry and exit time of the vehicle in the trap were noted down using the software Avidemux 2.6 which converts the one-second video into 25 frames. The classified volume count was also recorded. Initially, for every one-minute traffic volume count was observed and later converted into five minute classified volume count. On friction section with addition to speed and volume count, pedestrian cross flow is also observed and recorded. Table 1 shows the vehicle composition at thirteen study locations.

4 Development of Mathematical Model

The average speed for one-minute period for a particular category of vehicle was extracted using the time taken by vehicle to pass the 60 m trap length. The time was measured by the accuracy of 40 m s. Number of vehicles pass the trap for the same one-minute duration was observed accurately for the classified category of vehicle. For friction section, the number of pedestrian crosses the road is counted accurately

Table 1 Composition of different categories of vehicles at study locations

Section no.	Types of section	Vehicular composition (%)				
		Two wheeler (2W)	Three wheeler (3W)	Small car (SC)	Big car (BC)	Heavy vehicles (HV)
1	Base section	33.40	20.60	38.30	5.10	2.60
2		28.11	10.43	51.50	5.96	4.00
3		31.43	17.74	30.35	10.66	9.82
4		31.47	20.30	31.27	12.59	4.36
5		33.72	15.43	30.12	10.38	10.35
6		29.61	12.70	46.50	7.55	3.64
7		57.50	10.48	26.50	4.00	1.52
8		53.27	8.00	32.80	3.65	2.28
9	Friction section	33.75	21.22	33.54	7.58	3.90
10		56.08	10.92	21.17	10.59	1.24
11		58.19	7.96	18.77	10.69	4.39
12		60.33	8.96	19.11	7.39	3.91
13		23.23	12.94	38.31	16.46	9.06

for one-minute time stamp. One-minute traffic data converted into five minutes traffic data. As it is difficult to measure density in the field, it is projected as the number of vehicles of a each category passed in every five minute count period divided by the average speed. The proposed mathematical form of the model for the base section without the effect of pedestrian crossing is given in Eq. (1).

$$V_i = a_0 - a_1 \left(\frac{n_{2W}}{V_{2W}} \right) - a_2 \left(\frac{n_{3W}}{V_{3W}} \right) - a_3 \left(\frac{n_{SC}}{V_{SC}} \right) - a_4 \left(\frac{n_{BC}}{V_{BC}} \right) - a_5 \left(\frac{n_{HV}}{V_{HV}} \right) \quad (1)$$

where ‘V’ is the speed in m/s of various categories of vehicle. ‘n’ is the number of vehicle passed the section per second (vps), 2W, 3W, SC, BC and HV are different categories of vehicle as per Table 1. a_0 is regression coefficient which represents free-flow speed for any of the category of the vehicle, and a_1, a_2, a_3, a_4, a_5 are regression coefficients, which represents the impact of density of particular category of vehicle on free-flow speed of i th category of vehicle.

In the friction section, the speed of vehicle is also affected by pedestrian cross flow. Number of pedestrian crossing per second is worked out from pedestrian crossing data along with other traffic characteristics used in the friction section model. The mathematical model proposed for friction section by considering the effect of pedestrian cross flow on the speed of vehicle is shown below.

$$\begin{aligned}
 V_i = & a_0 - a_1 \left(\frac{n_{2W}}{V_{2W}} \right) - a_2 \left(\frac{n_{3W}}{V_{3W}} \right) - a_3 \left(\frac{n_{SC}}{V_{SC}} \right) \\
 & - a_4 \left(\frac{n_{BC}}{V_{BC}} \right) - a_5 \left(\frac{n_{HV}}{V_{HV}} \right) - a_6 (N_{ped})
 \end{aligned}
 \tag{2}$$

where N_{ped} is the number of pedestrian crossing per second, a_6 is the regression constant for pedestrian cross flow showing the effect of pedestrian cross flow on the speed of vehicle. Speed of a vehicle type is influenced to different extents by the vehicles of different categories, and their proportion is stream and therefore coefficients a_0 to a_5 are estimated to be significantly different when the speed of individual type of vehicle is modelled. Regression constants a_0 to a_5 are estimated from field data and given as below. The values given in parentheses are the student ‘t’ test coefficients.

$$\begin{aligned}
 V_{2W} = & 16.35 - 42.83 \left(\frac{n_{2W}}{V_{2W}} \right) - 45.98 \left(\frac{n_{3W}}{V_{3W}} \right) \\
 & (146.09) \quad (25.98) \quad (10.66) \\
 & - 26.90 \left(\frac{n_{SC}}{V_{SC}} \right) - 38.29 \left(\frac{n_{BC}}{V_{BC}} \right) - 24.39 \left(\frac{n_{HV}}{V_{HV}} \right) \\
 & (20.02) \quad (4.99) \quad (3.75) \quad R^2 = 0.836
 \end{aligned}
 \tag{3}$$

$$\begin{aligned}
 V_{3W} = & 13.92 - 35.16 \left(\frac{n_{2W}}{V_{2W}} \right) - 53.29 \left(\frac{n_{3W}}{V_{3W}} \right) \\
 & (141.16) \quad (25.14) \quad (14.00) \\
 & - 22.67 \left(\frac{n_{SC}}{V_{SC}} \right) - 11.29 \left(\frac{n_{BC}}{V_{BC}} \right) - 45.01 \left(\frac{n_{HV}}{V_{HV}} \right) \\
 & (17.75) \quad (4.06) \quad (3.88) \quad R^2 = 0.825
 \end{aligned}
 \tag{4}$$

$$\begin{aligned}
 V_{SC} = & 16.96 - 33.16 \left(\frac{n_{2W}}{V_{2W}} \right) - 52.44 \left(\frac{n_{3W}}{V_{3W}} \right) \\
 & (202.30) \quad (25.51) \quad (17.11) \\
 & - 43.80 \left(\frac{n_{SC}}{V_{SC}} \right) - 35.93 \left(\frac{n_{BC}}{V_{BC}} \right) - 62.05 \left(\frac{n_{HV}}{V_{HV}} \right) \\
 & (37.48) \quad (9.11) \quad (4.93) \quad R^2 = 0.915
 \end{aligned}
 \tag{5}$$

$$\begin{aligned}
 V_{BC} = & 17.36 - 47.34 \left(\frac{n_{2W}}{V_{2W}} \right) - 62.65 \left(\frac{n_{3W}}{V_{3W}} \right) \\
 & (109.62) \quad (17.68) \quad (10.98) \\
 & - 30.21 \left(\frac{n_{SC}}{V_{SC}} \right) - 77.98 \left(\frac{n_{BC}}{V_{BC}} \right) - 81.01 \left(\frac{n_{HV}}{V_{HV}} \right) \\
 & (15.74) \quad (6.90) \quad (5.36) \quad R^2 = 0.874
 \end{aligned}
 \tag{6}$$

$$\begin{aligned}
 V_{HV} = & 13.50 - 37.70 \left(\frac{n_{2W}}{V_{2W}} \right) - 41.74 \left(\frac{n_{3W}}{V_{3W}} \right) \\
 & (82.96) \quad (14.22) \quad (6.96) \\
 & - 15.98 \left(\frac{n_{SC}}{V_{SC}} \right) - 27.51 \left(\frac{n_{BC}}{V_{BC}} \right) - 151.68 \left(\frac{n_{HV}}{V_{HV}} \right) \\
 & (9.64) \quad (3.80) \quad (8.00) \quad R^2 = 0.745 \quad (7)
 \end{aligned}$$

In case of friction section, the speed of any category of vehicle is also affected by pedestrian cross flow along with the density of other vehicles in the traffic stream. From field data when the pedestrian cross flow is also available, the regression coefficients a_1 to a_6 were estimated. The a_0 represents the free-flow speed of particular category of vehicle, which is measured when vehicle and pedestrian volume is vary less (vehicle volume less than 1,000 veh/h/lane as per HCM 2010) remain unchanged in case of friction section. Mathematical models developed using the regression analysis of empirical data are given in Eqs. (8)–(12).

$$\begin{aligned}
 V_{2W} = & 16.35 - 74.07 \left(\frac{n_{2W}}{V_{2W}} \right) - 21.20 \left(\frac{n_{3W}}{V_{3W}} \right) - 19.66 \left(\frac{n_{SC}}{V_{SC}} \right) \\
 & (23.90) \quad (2.81) \quad (2.33) \\
 & - 53.30 \left(\frac{n_{BC}}{V_{BC}} \right) - 61.32 \left(\frac{n_{HV}}{V_{HV}} \right) - 6.76 N_{ped} \\
 & (3.15) \quad (12.97) \quad (6.10) \quad R^2 = 0.972 \quad (8)
 \end{aligned}$$

$$\begin{aligned}
 V_{3W} = & 13.92 - 41.84 \left(\frac{n_{2W}}{V_{2W}} \right) - 44.19 \left(\frac{n_{3W}}{V_{3W}} \right) - 13.44 \left(\frac{n_{SC}}{V_{SC}} \right) \\
 & (19.24) \quad (5.21) \quad (2.27) \\
 & - 94.90 \left(\frac{n_{BC}}{V_{BC}} \right) - 152.80 \left(\frac{n_{HV}}{V_{HV}} \right) - 2.08 N_{ped} \\
 & (7.49) \quad (10.13) \quad (2.81) \quad R^2 = 0.988 \quad (9)
 \end{aligned}$$

$$\begin{aligned}
 V_{SC} = & 16.96 - 66.64 \left(\frac{n_{2W}}{V_{2W}} \right) - 12.18 \left(\frac{n_{3W}}{V_{3W}} \right) - 63.40 \left(\frac{n_{SC}}{V_{SC}} \right) \\
 & (17.68) \quad (2.49) \quad (6.17) \\
 & - 75.20 \left(\frac{n_{BC}}{V_{BC}} \right) - 129.45 \left(\frac{n_{HV}}{V_{HV}} \right) - 5.65 N_{ped} \\
 & (3.65) \quad (22.51) \quad (4.19) \quad R^2 = 0.971 \quad (10)
 \end{aligned}$$

$$\begin{aligned}
 V_{BC} = & 17.36 - 45.34 \left(\frac{n_{2W}}{V_{2W}} \right) - 19.21 \left(\frac{n_{3W}}{V_{3W}} \right) - 37.76 \left(\frac{n_{SC}}{V_{SC}} \right) \\
 & (19.04) \quad (2.02) \quad (5.59)
 \end{aligned}$$

$$\begin{aligned}
 & - 291.30 \left(\frac{n_{BC}}{V_{BC}} \right) - 101.80 \left(\frac{n_{HV}}{V_{HV}} \right) - 5.85 N_{ped} \\
 & \qquad (20.66) \qquad (6.97) \qquad (7.21) \qquad R^2 = 0.993 \qquad (11)
 \end{aligned}$$

$$\begin{aligned}
 V_{HV} = & 13.50 - 22.99 \left(\frac{n_{2W}}{V_{2W}} \right) - 19.20 \left(\frac{n_{3W}}{V_{3W}} \right) - 39.98 \left(\frac{n_{SC}}{V_{SC}} \right) \\
 & \qquad (6.95) \qquad (2.51) \qquad (4.35) \\
 & - 103.20 \left(\frac{n_{BC}}{V_{BC}} \right) - 356.80 \left(\frac{n_{HV}}{V_{HV}} \right) - 0.47 N_{ped} \\
 & \qquad (5.25) \qquad (17.90) \qquad (0.42) \qquad R^2 = 0.975 \qquad (12)
 \end{aligned}$$

In the above equations, ‘t’ value of all coefficients except coefficient for pedestrian cross flow in case of heavy vehicle is more than 1.96, which shows that all coefficients are significant at 95% level of confidence except pedestrian coefficient for heavy vehicle speed. Signs of all the coefficients are negative which shows as the density of any category of vehicle increase speed decrease from free-flow speed. In all model equation, value of R^2 is appreciably high which indicates the model is more compatible for predicting speed. As the speed parameter is on both sides of the model equation, it can be solved by the iteration process. A small program was written in MATLAB software to solve these simultaneous equations.

The coefficient of pedestrian cross flow found significantly affects the speed of all categories of vehicles except heavy vehicle. The proportion of heavy vehicles was less than 5% at most of the section. According to the field data in most of the cases while pedestrian crossing the road, it is found that pedestrian rejects appreciably large gap when the heavy vehicle is present on the way. Due to such behaviour of pedestrian keeping safety in mind in case of heavy vehicle, the speed of heavy vehicle is not affected significantly by pedestrian cross flow. But in case of all other vehicle, the speed of vehicle is significantly affected by pedestrian cross flow.

5 Sensitivity Analysis

The speed of any category of vehicle in mixed traffic condition is affected by traffic flow and traffic composition at that instant of time. It is quite obvious that at increase of traffic flow, the speed of any category of vehicle will reduce. As the traffic volume increases, the freedom to select desire speed will reduce as a result of the interaction between vehicles present in the stream increase. In case of friction section in addition to traffic flow and traffic proportion, the speed of any category of vehicle significantly affected by the pedestrian cross flow. As the pedestrian cross flow increases, the speed gets decrease. The variation of speed has been plotted with traffic flow keeping pedestrian cross flow constant. Moreover, keeping the vehicular flow constant, the variation of speed has also been studied with varying pedestrian cross flow.

5.1 Base Section

Figure 2 shows the variation in speed of five different categories of vehicle with variation in traffic flow keeping traffic proportion constant. The variation in speed has been quantified by solving the simultaneous equation by varying the traffic flow from 500 to 3500 veh/h in steps of 500 veh/h. The proportion of traffic stream kept constant during solving the simultaneous equations as 40, 20, 20, 13 and 7% for 2W, 3W, SC, BC and HV, respectively. From the figure, it can be observed that the speed for all five categories of vehicles is decreasing as traffic flow increases, but the variation in speed for different categories of vehicles is different. The reduction in speed observed for a small-sized vehicle like 2W and 3W is less, while the reduction of speed with traffic flow is more for larger-sized vehicles like BC and HV. As traffic flow increases in the traffic stream, the density also increases and the interaction between the vehicles present in the traffic stream also get an increase. The smaller vehicles require less area and have better manoeuvrability, so they can be able to maintain their speed or reduction in speed is less and they create the poorer operating condition for other larger-sized vehicles. Whereas in case of vehicle with larger area requirement and lesser manoeuvrability, the reduction in speed is significant.

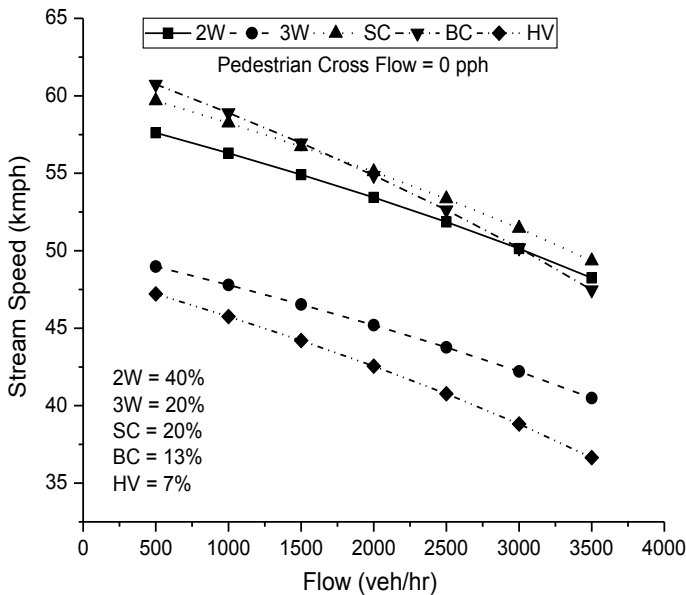


Fig. 2 Speed variation of different categories of vehicles with traffic flow at base sections

5.2 Friction Section

Figure 3 shows the speed variation with traffic flow in case of friction section. Pedestrian cross flow 750 ped/h has been taken to get the speed fluctuations. As per the observation of the plot, it can be seen that the speed range in case of friction section is considerably low as compared to the base section, i.e. pedestrian cross flow has a significant effect on the speed of each category of vehicle and ultimately on stream speed. The variation in speed for the individual category of vehicles is also considerably more than that at base section. In friction section, also the same trend has been observed for heavy vehicles as the base section. The speed of heavy vehicles with larger area requirement and less manoeuvrability reduced significantly more than vehicles having a smaller area and more manoeuvrability. Figures 4, 5, 6, 7 and 8 show comparison of speed variation with traffic flow for different categories of vehicles for base section and friction section. From graphs, it can be detected that reduction of speed in case of friction section is appreciably more than base section in case of each category of vehicles. Moreover, the variation observed in case of base section follows a linear trend while in case of friction section up to some point the trend is linear but after that point (mostly observed at 2000 veh/h) the variation in speed follows curve path and rapid reduction in speed is observed. If vehicular flow increased, it leads to breakdown in steady vehicular flow and will result into traffic congestion.

The percentage reduction in speed observe is different depending upon its manoeuvrability and size, in addition to this characteristic of driver and drivers' yielding

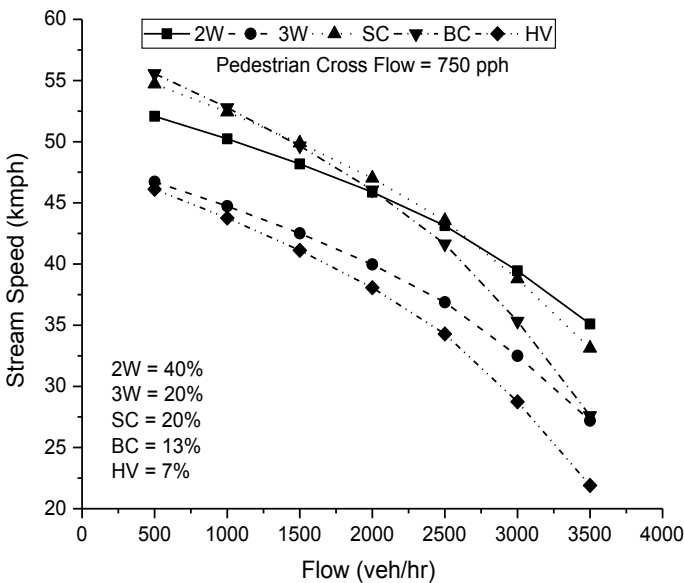


Fig. 3 Speed variation of different categories of vehicles with traffic flow at friction sections

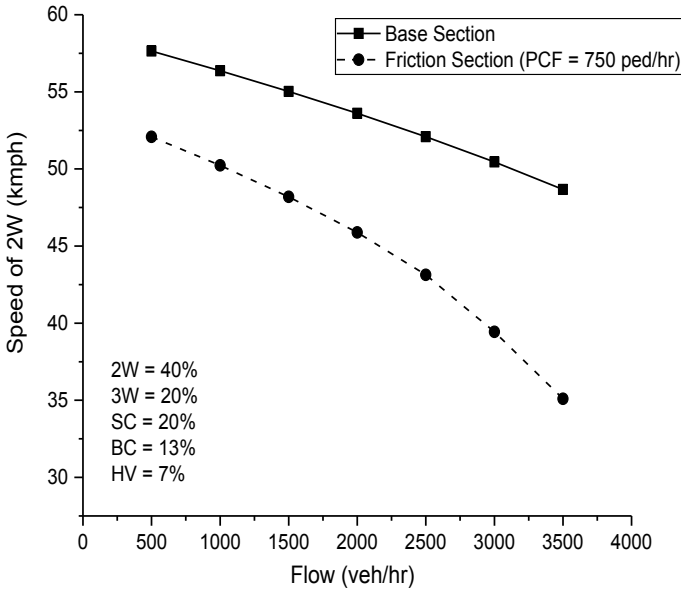


Fig. 4 Comparison of speed variation of two wheelers with traffic flow for base section and friction section

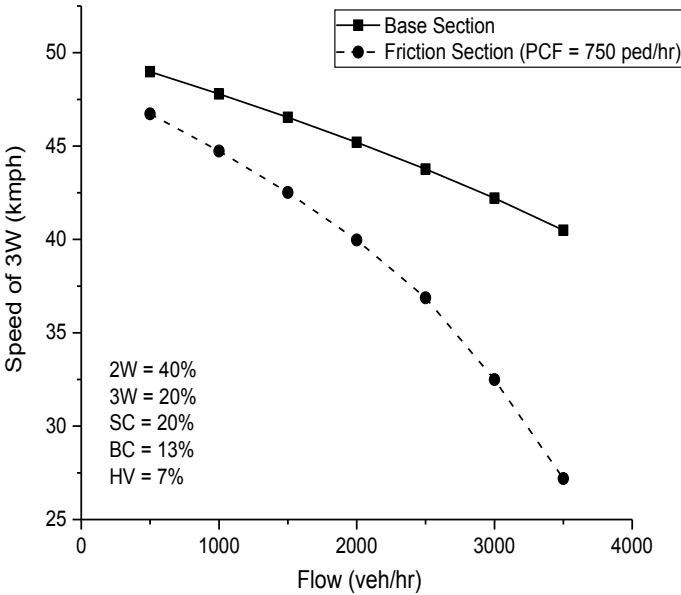


Fig. 5 Comparison of speed variation of three wheelers with traffic flow for base section and friction section

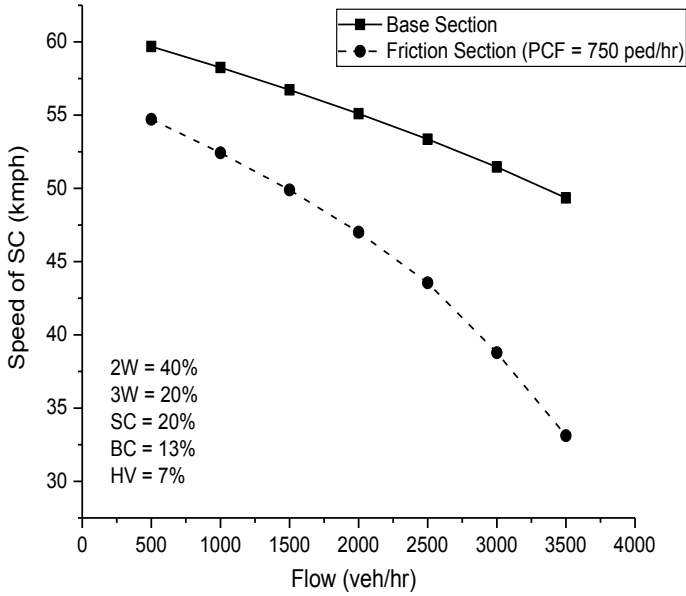


Fig. 6 Comparison of speed variation of small cars with traffic flow for base section and friction section

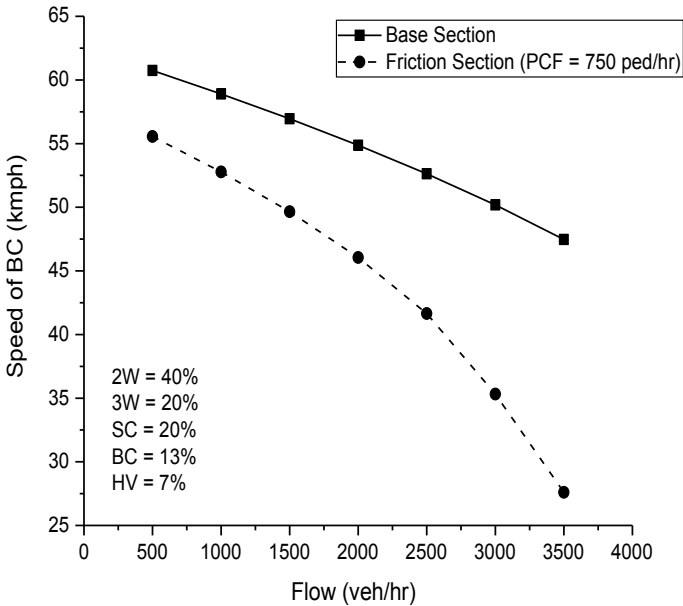


Fig. 7 Comparison of speed variation of big cars with traffic flow for base section and friction section

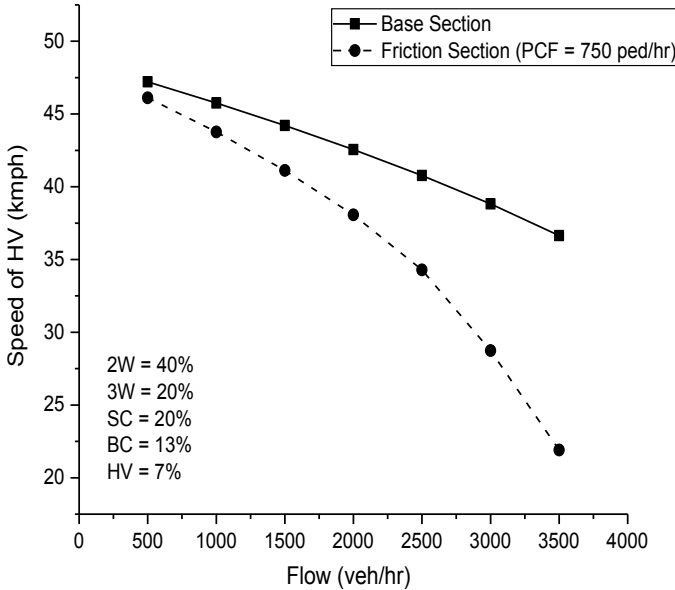


Fig. 8 Comparison of speed variation of heavy vehicles with traffic flow for base section and friction section

behaviour to pedestrian which are also equally important. Two wheeler with lesser area requirement and good manoeuvrability could maintain the higher operating speed, so percentage reduction in speed is least in case of two wheeler. On the other side, heavy vehicle with higher area requirement and lesser manoeuvrability is having higher reduction in speed. The same picture is reflected in Fig. 9. Highest reduction in speed is found in case of heavy vehicles followed by big car, small car, three wheeler, and least reduction is observed in case of two wheeler. So, the results show variation in a reduction in speed varies according to vehicle size due to manoeuvrability characteristics.

Figure 10 shows the impact of pedestrian cross flow on speed of different categories of vehicle at constant flow level. The speed variation of all five categories at varying pedestrian cross flow has been studied. It can be observed that as pedestrian cross flow increases, the speed of all category decreases. The reduction in speed is more significant in case of 2W, BC and SC. In case of HV and 3W, speed variation is not as high as other vehicles as pedestrians avoid to cross the road in the presence of heavy vehicles. Free-flow speed of 2W, BC and SC is more as compared to 3W and HV. So, for the safe operation of such high-speed vehicles in the presence of pedestrian cross flow, it is mandatory to reduce speed for controlling vehicle and to give way to pedestrians accepting force gap. As a result of that, speed reduction is more in case of 2W, BC and SC. The free-flow speed of 3W and HV is less so less reduction in speed is required for safe operation during pedestrian crossing. Figure 11 shows the percentage reduction in speed at different pedestrian cross flow levels. Due to

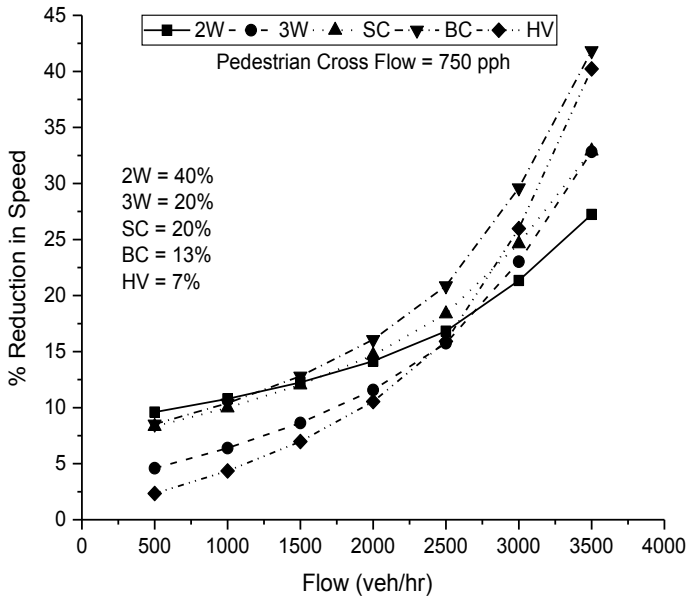


Fig. 9 Speed reduction of different categories of vehicles with traffic flow for friction section

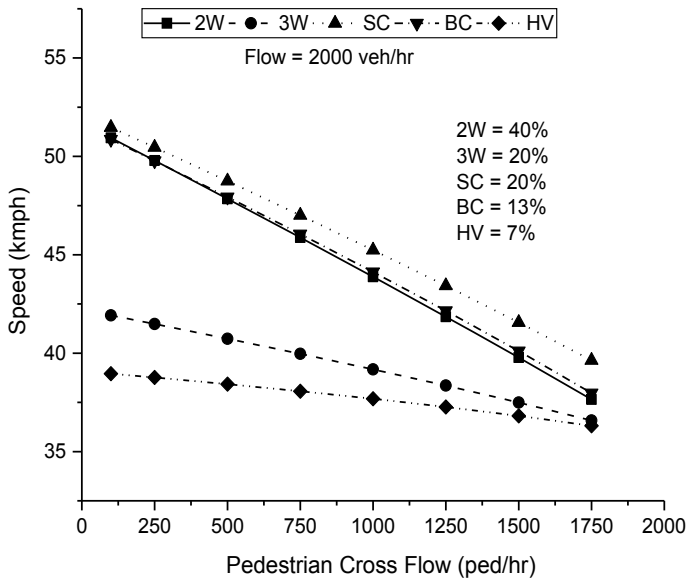


Fig. 10 Variation of speed of different categories of vehicles with pedestrian cross flow

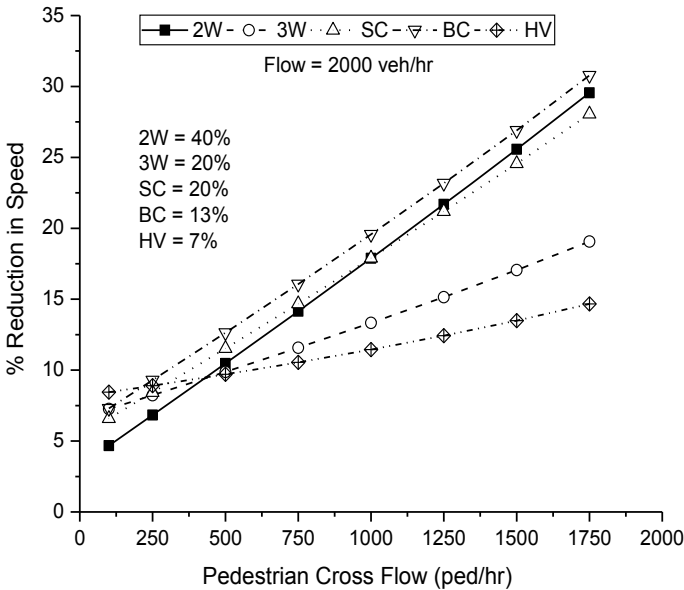


Fig. 11 Percentage reduction in speed of different categories of vehicles with pedestrian cross flow

pedestrian cross flow, the speed of various categories reduces significantly. Reduction in the speed of 2W, SC and BC is above 30% when pedestrian cross flow is 1750 ped/h; whereas, it is 16% in HV and 21.21% in case of 3W.

6 Model Validation

To evaluate the accuracy of the models developed in the present study, field data are collected at one more base section at New Delhi and one friction section at Jaipur. From five min, classified volume count and average speed of all categories of the vehicle were extracted from a video. Using the data simultaneous equations solved to work out the predicted speed for each category of vehicle. The observed speed at filed and predicted speed using model developed was plotted as shown in Figs. 12 and 13 for the base section and friction section, respectively. From the figure, it can be seen that all the points derived from observed and predicted value lie on 45° line, so it can be said the model can predict the speed for various categories of vehicles accurately. Moreover, *t*-test was carried out to at 5% significant level with 54° of freedom for base section and 67° of freedom at friction section to check statistical validation. From the result of the test, it showed that *t*-statistics value as 1.73 for base section and 1.19 for friction section, which is less than *t*-critical value 2.00 at 5% significant level. Hence, statistically there is no significant difference between the predicted and the observed speeds.

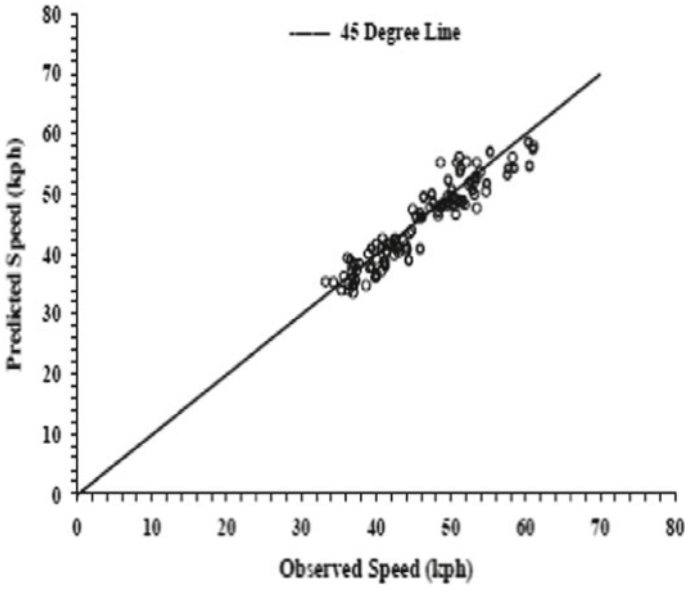


Fig. 12 Comparison between predicted speed and observed speed at base sections

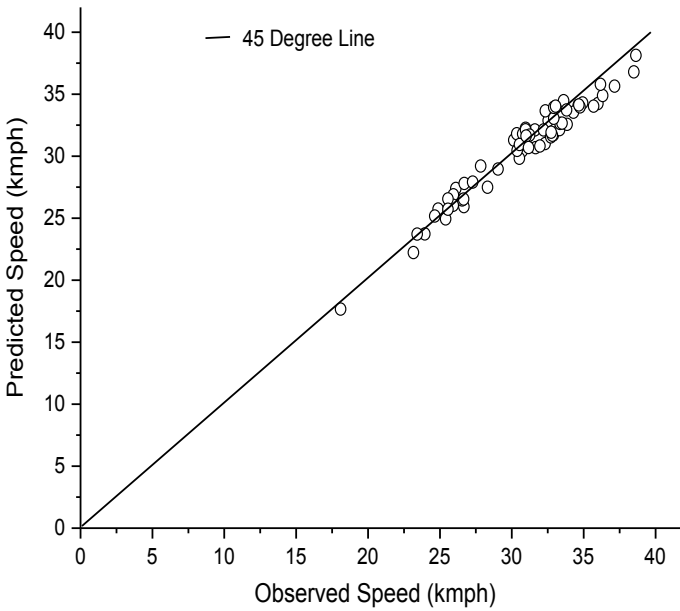


Fig. 13 Comparison between predicted speed and observed speed at friction sections

7 Conclusion

The present study proposed models for speed prediction for different categories of vehicles at six-lane urban arteries with and without the effect of pedestrian cross flow. Interaction between vehicles and pedestrian at urban mid-block section has been evaluated by considering speed as a prime variable. The speed at urban arteries depends on the composition and flow of vehicles. So, the base section model has been developed for predicting speed using composition and flow of vehicles. On a friction section in addition to vehicle composition and flow of vehicle, pedestrian cross flow is a major parameter which has been incorporated in speed prediction model. As the models having simultaneous equations for speed, a small programme has been written in MATLAB to solve the equations. The model can be used to predict the speed at the base or friction section by knowing the vehicle composition and flow and pedestrian cross flow at any section, as it is easy to measure in the field. Besides this, sensitivity analysis has been carried out which shows that at a base section increase in vehicle flow the speed reduction is more in case of heavy vehicles as compared to smaller vehicles. The effect of pedestrian cross flow has also been studied. The effect of pedestrian cross flow on speed of different categories of vehicles has been shown graphically. At increment in a pedestrian cross flow by keeping the vehicular flow constant, the speed of smaller vehicles affected more as pedestrian try to cross the road by accepting force gap. In case of heavy vehicles, pedestrians wait until it passes the section, so speed of heavy vehicles is not so affected as smaller vehicles. Speed reduction is higher in case of the vehicle with higher free-flow speed like 2W, BC and SC to control the vehicle when pedestrian is crossing as compared to vehicle with less free-flow speed like 3W and HV. Both the models have been also validated using a statistical test. The present study will be exceptionally helpful for design engineers to obtain the speed on six-lane urban arterial location with or without pedestrian cross flow without conducting any video-graphic survey and tedious data extraction process.

Acknowledgements Authors would like to thank Department of Science and Technology (DST), of the Ministry of Science and Technology, Government of India that subsidizes the research project entitled "Traffic and pedestrian movement analysis at undesignated pedestrian crossings on urban mid-block sections" (File No. YSS/2014/000760).

References

1. World Health Organization http://www.who.int/violence_injury_prevention/road_safety_status/2015/en/
2. Study on road accidents in India 2015, Ministry of Road Transport and Highways (MoRTH), Government of India
3. Greenshields BD (1935) A study of traffic capacity. In: 14 annual meeting of the highway research board proceedings

4. Al-Ghamdi A (1998) Spot speed analysis on urban roads in Riyadh. *Transp Res Rec* 1635(1):162–170
5. Shankar V, Mannering F (1998) Modeling the endogeneity of lane-mean speeds and lane-speed deviations: a structural equations approach. *Transp Res Part A Policy Pract* 32(5):311–322
6. Dixon BKK, Sarasua WA, Daniel J, Mazur GD (1999) Posted and free-flow speeds for rural multilane highways in Georgia. *J Transp Eng* 125(6):275–283
7. Najjar Y, Stokes R, Russell E (2000) Setting speed limits on Kansas two-lane highways: neuronet approach. *Trans Res Rec* 1708(1):20–27
8. McFadden J, Yang W-T, Durrans S (2001) Application of artificial neural networks to predict speeds on two-lane rural highways. *Transp Res Rec* 1751(1):9–17
9. Donnell E, Ni Y, Adolini M, Elefteriadou L (2001) Speed prediction models for trucks on two-lane rural highways. *Trans Res Rec* 1751(1):44–55
10. Figueroa Medina, Tarko AP (2004) Reconciling speed limits with design speeds. Joint Transportation Research Program, U.S. Department of Transportation
11. Koshy RZ, Arasan VT (2005) Influence of bus stops on flow characteristics of mixed traffic. *J Transp Eng* 131(8):640–643
12. Dey PP, Chandra S, Gangopadhaya S (2006) Speed distribution curves under mixed traffic conditions. *J Transp Eng* 132(6):475–481
13. Perco P (2008) Comparison between powered two-wheeler and passenger car free-flow speeds in urban areas. *Transp Res Rec J Transp Res Board* 2074:77–84. <https://doi.org/10.3141/2074-10>
14. Bak R, Kiec M (2012) Influence of midblock pedestrian crossings on urban street capacity. *Trans Res Rec J Trans Res Board* 2316:76–83. <https://doi.org/10.3141/2316-09>
15. Dhamaniya A, Chandra S (2014) Influence of undesignated pedestrian crossings on midblock capacity of urban roads. *Trans Res Rec* 137–144
16. Raghuram Kadali B, Chiranjeevi T, Rajesh R (2015) Effect of pedestrians un-signalized mid-block crossing on vehicular speed. *Int J Traffic Transp Eng* 5(2):170–183

Study of Effect of On-Street Parking on Traffic Capacity



Prashoon Prakash, Ranja Bandyopadhyaya and Sanjeev Sinha

Abstract On-street parking is common in Indian cities and allows individuals to park close to their destination. This reduces the capacity of the through travel lanes of roads. The parking manoeuvre of vehicles moving in or moving out of the parking areas causes delay to through traffic along the roads. When parking lot is partially filled, vehicles slowing down to search for adequate parking gap also cause reduction in the capacity of the through lane. Many researchers studied the effect of parallel and angle on-street parking on various traffic flow parameters and delays of through traffic caused by entrance and departure manoeuvres of on-street parking. Limited research has been done to study the effect of different level of parking (percentage of parking length filled by parked vehicles) on traffic capacity. The present work attempts to study the effect of different levels of on-street parking on traffic capacity of four-lane divided urban roads for two Indian cities Patna and Bhubaneswar. It can be observed that for both cities, traffic capacity in PCU has decreasing trend with increasing parking occupancy level, but when the parking space is nearly occupied the capacity again has an increasing trend. It could also be observed that traffic capacities for similar parking levels vary for both the cities, which can be attributed to the difference in traffic composition. The PCU measure taken for unifying the traffic composition may not be adequate for studying traffic flow characteristics of the region.

Keywords Traffic capacity · Parking occupancy · Greenshields' model · Curve enveloping technique

P. Prakash (✉) · R. Bandyopadhyaya · S. Sinha
Department of Civil Engineering, National Institute of Technology Patna, Ashok Rajpath, Patna
800005, Bihar, India
e-mail: meet2prashoon@gmail.com

R. Bandyopadhyaya
e-mail: ranja@nitp.ac.in

S. Sinha
e-mail: sanjeev@nitp.ac.in

1 Introduction

On-street parking is common in many crowded mid-sized cities of the world. This is encouraged as it provides convenient access to destinations and no proper parking infrastructure building is required. Riggs [1] analysed how parking reforms, traveller information system and incentive affect an increase in the use of public transit and non-motorised modes. On-street parking mainly is of two types, namely parallel parking and angle parking. Yousif and Purnawan [2] analysed the delays caused by entrance and departure on-street parking manoeuvres and differentiated between parallel and angle on-street parking. In many cities in India, two-wheeler and four-wheeler are parked in random order according to the space available to the driver. Yousif and Purnawan [3] showed that the design of on-street parking layouts strongly affects driver parking and un-parking behaviour.

On-street parking reduces the capacity of the through travel lanes of roads. AASHTO [4] also confirms that on-street parking reduces capacity and interferes with the free flow of adjacent traffic. Eliminating curb parking can increase the capacity of four- to six-lane (curb-to-curb) arterials by 50–80%. The parking manoeuvre of vehicles moving in or moving out of the parking areas causes delay to through traffic along the roads. Chick [5] used the number of lanes and the number of parking manoeuvres per hour as the variables to represent the capacity reduction caused by on-street parking. When parking lot is partially filled, vehicles slowing down to search for adequate parking gap also cause reduction in capacity of the through lane. Valleley [6] established a relationship between the number of parked vehicles and the reduction in street width and capacity. Thompson and Richardson [7] proposed a model which represents the parking search behaviour of motorist and a relationship was developed for estimating the utility of a car park incorporating access, waiting, direct and egress cost components. Henser and King [8] investigate the role of parking pricing and supply by time to drive and park in the central business district (CBD).

Roadside parking is an ordinary parking mode, and vehicles pulling in and out of parking areas will disturb the normal running of dynamic traffic. Marshall et al. [9] gave a broad assessment related to on-street parking, ranging from parking demand to less researched topic such as land use and the impact on vehicle speed, which produce negative impact on road capacity. Klappenecker et al. [10] have discussed on the problem of predicting the available parking spaces in parking lots. The parking lot is modelled by a continuous-time Markov chain, following Caliskan, Barthels, Scheuermann and Mauve. Portilla et al. [11] applied an $M/M/\infty$ queuing model to quantify the influence of badly parked vehicles and on-street parking manoeuvres on average link journey times. Tam and Lam [12] proposed a model to examine whether existing road network and parking supply are capable of accommodating future zonal car ownership growth. But the relationship has not been developed because of the lack of an explicit model. Based on a two-way multi-lane road, the disturbance on dynamic traffic by vehicles parked roadside and also by vehicles pulling in and

out of parking spaces used by means of formula deduction from free flow speed and traffic volume study established the relationship between traffic capacity and on-street parking.

2 Objectives

The objective of the present work is to study the effect of different levels of on-street parking on traffic capacity of four-lane divided urban roads. Two different mid-sized Indian cities are chosen for the study to assess whether the effect on capacity is independent of changes in traffic characteristics.

3 Methodology

The work attempts to study the effect of on-street parking on traffic capacity. The overall methodology of the work is given in Fig. 1.

Two-hour video graphic survey in peak hours (10:00 AM–12:00 AM) is conducted in four stretches of Bhubaneswar, viz. Acharya Vihar, Patia Road, Samanta Vihar and near Nalco Square, and three stretches of Patna, viz. Fraser road east, Fraser road west and Doctor colony Kankarbagh. The parking level and speed and flow are extracted from the video and analysed in 5 min window. From speed–flow data, traffic capacity is determined at different levels of parking by the use of Greenshields’ model of traffic flow. Comparison is done between percentage parked vehicles and traffic capacity of all the sections of Bhubaneswar and Patna.

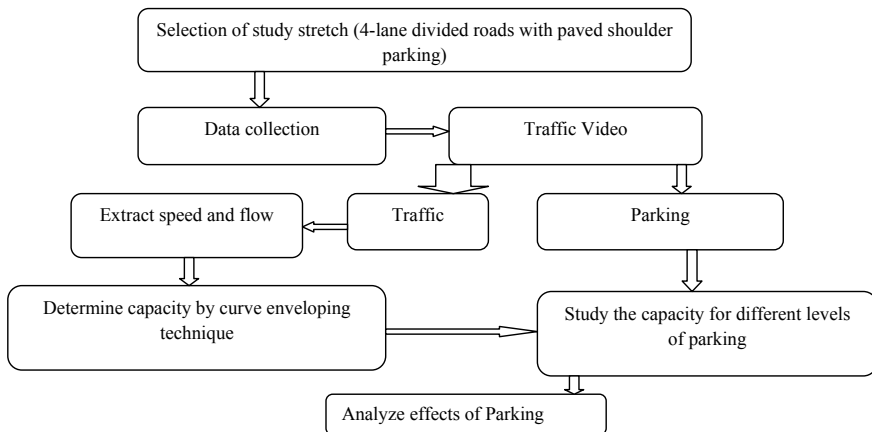


Fig. 1 Methodology

4 Data

Two types of data are used for the study. The first is the speed–flow data from which the capacity of segments is decided. The second is the % parking present in the segment; both the data are collected by video recording at all four stretches of Bhubaneswar, viz. Acharya Vihar, Patia Road, Samanta Vihar and near Nalco Square, and three stretches of Patna, viz. Fraser road east, Fraser road west and Doctor colony Kankarbagh.

Data was collected near are Mid block section should be free from the effect of intersection and bus stops. The length of the section is minimum of 30 m for precise measurement and shall sustain mixed traffic flow. The width of the on-street parking should be a minimum of 2.5 m as required for the study. The actual length of section is, however, dependent on the height of the camera, and it ranged from 30 to 60 m. The traffic of pedestrians is completely neglected. Road will be a four-lane two-way road with proper demarcation, and there shall be no intermingling of traffic from opposite direction. After selecting the appropriate site for data collection, the video camera is required to be mounted at the roof of the building near the site or any other elevated place from where road can be viewed clearly and recording was done. Traffic video is taken for four different locations in Bhubaneswar and three different locations in Patna. Details of all the sections of cities Bhubaneswar and Patna are shown in Table 1.

The traffic flow video recoded traffic flow in the trap length of 30 m and the roadside parking scenario within the trap length. The traffic flow and speed are

Table 1 Detail of all section in cities Bhubaneswar and Patna

Name of section	Time of duration (10:00 AM–12:00 AM)	Length of section	Width of each lane (m)	Width of paved shoulder	Width of total road for vehicle to move (m)
Acharya Vihar Road	10:00 AM–12:00 AM	30	3.5	3.3	10.3
Patia Road	10:00 AM–12:00 AM	30	3.5	3.3	10.3
Samanta Vihar Road	10:00 AM–12:00 AM	30	3.5	3.4	10.4
Near Nalco Square	10:00 AM–12:00 AM	30	3.5	3.4	10.4
Fraser Road East	10:00 AM–12:00 AM	30	3.5	3	10
Fraser Road West	10:00 AM–12:00 AM	30	3.5	3.4	10.4
Doctor Colony Kankarbagh	10:00 AM–12:00 AM	30	3.5	3.4	10.4



Fig. 2 Parked vehicle in Bhubaneswar and Patna, respectively

extracted from the traffic video manually. The traffic flow is taken as the five-minute flow of different categories of vehicles. The space mean speed of individual vehicles is calculated using the entry and exit time within the study trap. The five-minute traffic flow is converted to hourly flow. The vehicle mix on the road of Patna and Bhubaneswar varies as shown in Fig. 2.

Parking data is extracted for each of the trap locations studied for the same five-minute duration. The parking data is classified into different percentage parking levels or percentage occupancy levels in intervals of 10%.

5 Results and Discussion

The traffic flow, speed and level of parking are obtained from the traffic video. For each section, the speed and flow data are segregated for different levels of parking. The capacity of the road section for each particular level of parking is obtained by using considering liner Greenshields' model of traffic flow. The speed and corresponding flow values obtained from the traffic video for a particular level of parking are plotted. An enveloping parabola is drawn to include all the points. The maximum flow indicated by the enveloping parabola is taken as the traffic capacity for that section for the particular level of parking.

The procedure is illustrated using Fig. 3. Here, the speed and corresponding flow values are plotted for Acharya Vihar Road section in city Bhubaneswar when on-street parking varies between 70 and 80%.

From Fig. 3, it can be observed that the traffic capacity indicated by the enveloping parabola is 2706 PCU/hour/2lane. In similar way, traffic capacity for each section for different observed levels of on-street parking is calculated. Table 2 summarises the calculated capacities for various on-street parking levels for different sections of the city of Bhubaneswar. It can be observed that the traffic capacity in PCU has an overall decreasing trend with increasing parking occupancy level. But, when the parking space is nearly occupied the capacity again has an increasing trend.

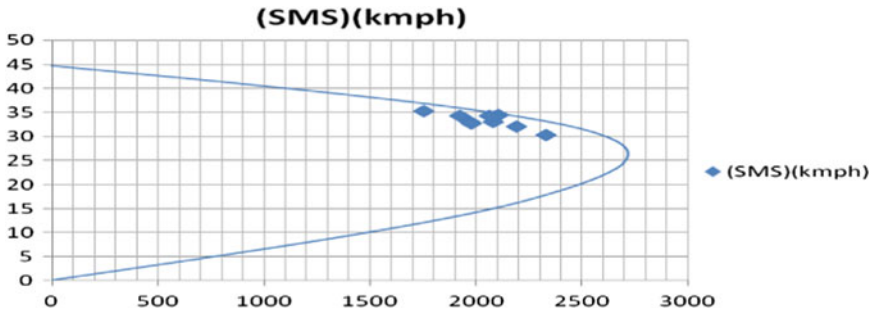


Fig. 3 Speed–flow relationship (% occupancy 70–80)

Table 2 Traffic capacity and parking level for Bhubaneswar city

Name of section	Occupancy level	Average occupancy	Traffic capacity (PCU/hour/2lane)
Acharya Vihar Road	70–80	75	2706
Acharya Vihar Road	80–90	85	2170
Patia Road	70–80	75	2678
Patia Road	80–90	85	2412
Samanta Vihar Road	60–70	65	1736
Near Nalco Square	40–50	45	2848
Near Nalco Square	50–60	55	2451

Table 3 summarises the calculated capacities for various on-street parking levels for different sections of the city of Patna. It can be observed that for the city of Patna, the overall capacity values are lesser than the city of Bhubaneswar. But, similar observation of decreasing trend for initial increase of parking level and increase of capacity when the parking is nearly full can be made that for the city of Patna.

Table 3 Traffic capacity and parking level for Patna city

Name of section	Occupancy level	Average occupancy	Traffic capacity (PCU/hour/2lane)
Fraser Road East	70–80	75	1704
Fraser Road East	80–90	85	1476
Fraser Road West	80–90	85	2826
Fraser Road West	90–100	95	2491
Doctor Colony Kankarbagh	20–30	25	2104
Doctor Colony Kankarbagh	30–40	35	1886

The effect of on-street parking on traffic capacity for the two cities though has similar trend but varies in overall capacity values. This may be due to difference in their traffic composition and driving behaviour. To study the effect of on-street parking on traffic capacity in detail, the traffic capacity and on-street parking for the two cities are analysed in the two subsections below.

5.1 Percentage Occupancy and Capacity for Bhubaneswar

To analyse the effect on the percentage of shoulder space occupied by on-street parking on traffic capacity, the traffic capacity is plotted for average parking value as specified in Table 2.

Initially, a linear co-relation is taken. It can be observed that the linear co-relation does not fit the trend well. A polynomial co-relation which shows the decreasing trend for traffic capacities with initial increase in shoulder space occupied by parked vehicle and then an increasing trend can capture the scenario more appropriately (Fig. 4).

This may be due to the fact that when the availability of parking space decreases, initially the vehicles slow to search for parking space. When the decrease in space is more, the vehicles from a distance can observe that no parking is available and do not slow down affecting the overall capacity of the stream. Also, the overall decrease in trend with space occupancy of shoulder with parked vehicle may be attributed to the effect of unavailability of shoulder for the driver driving in the mainstream.

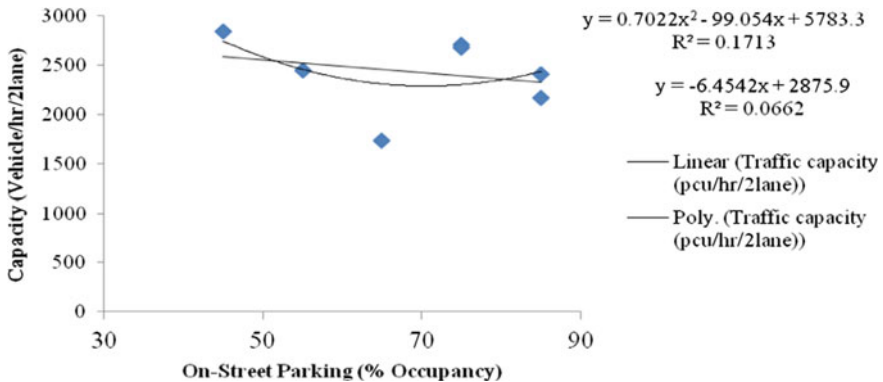


Fig. 4 Capacity and on-street parking for Bhubaneswar

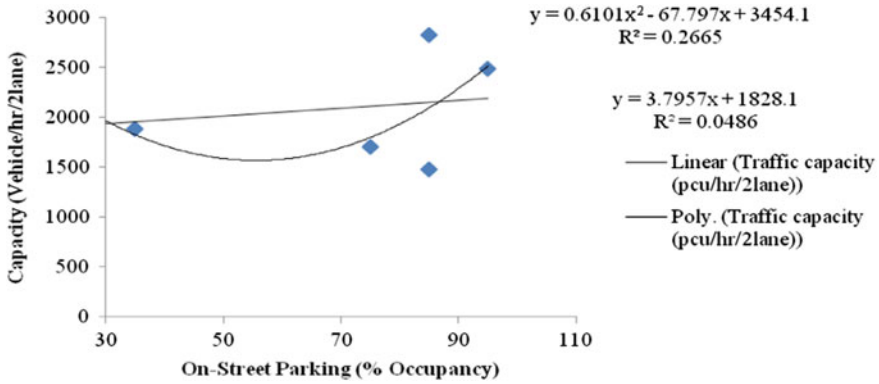


Fig. 5 Capacity and on-street parking for Patna

5.2 Percentage Occupancy and Capacity for Patna

To analyse the effect on percentage of shoulder space occupied by on-street parking on traffic capacity, the traffic capacity is plotted for average parking value as specified in Table 3.

The linear trend is not significant as observed in case of the city Bhubaneswar. Similar decreasing trend is observed for increasing in occupancy of shoulder with parked vehicle for lower to medium occupancy levels. For high occupancy level, the trend is reversed (Fig. 5).

When comparing the effect of on-street parking on traffic capacity for the two cities, it can be observed that the overall traffic capacities for the city of Patna are lower for each occupancy level. This may be attributed to the difference in traffic composition in the two cities. The PCU measure taken for unifying the traffic composition may not be adequate for studying traffic flow characteristics of the region.

6 Conclusions

While studying the effect of traffic capacity on the level or percentage shoulder space occupied by on-street parked vehicles, the effects are studied individually for the two cities considered. This is due to the fact that the traffic composition and the driver characteristics vary significantly in the two cities. The trends of effect of on-street parking level on traffic capacities are similar for two cities, but their capacity values differ significantly. The following are the major conclusions that could be drawn from the present work.

1. It can be observed that the traffic capacity in PCU has an overall decreasing trend with increasing parking occupancy level for both cities Bhubaneswar and

Patna. But, when the parking space is nearly occupied the capacity again has an increasing trend.

2. It can be observed that for the city of Patna, the overall capacity values are lesser than the city of Bhubaneswar at the same parking occupancy levels. This is mainly due to different traffic composition and driving behaviour.
3. The PCU measure taken for unifying the traffic composition may not be adequate for studying traffic flow characteristics of the region.

References

1. Riggs W (2014) Dealing with the parking issue on an urban campus UK: the case of UC Berkeley. *Case Stud Transp Policy* 2(3):168–176
2. Yousif S, Purnawan (1999) A study into on-street parking: effects on traffic congestion. *Traffic Eng Control* 40(9):424–427
3. Yousif S, Purnawan (2004) Traffic operations at on-street parking facilities. *Proc Inst Civ Eng Transp* 157(3):189–194
4. AASHTO (1994) Standard specifications for structural supports for highway signs luminaires and traffic signals. AASHTO, Washington DC
5. Chick C (1996) *On-street parking: a guide to practice*. Landon Publishing, London
6. Valleley M (1997) *Parking perspectives: a source book for the development of parking policy*. Landon Publishing, Landon
7. Thompson RG, Richardson AJ (1998) A parking search model. *Transp Res Part A Policy Pract* 32(3):159–170
8. Hensher DA, King J (2001) Parking demand and responsiveness to supply, pricing and location in the Sydney central business district. *Transp Res Part A Policy Pract* 35(3):177–196
9. Marshall WE, Garrick NW, Hansen G (2008) Reassessing on-street parking. *Transp Res Rec* 2046:45–52
10. Klappenecker A, Lee H, Welch JL (2014) Finding available parking spaces made easy. *Ad Hoc Netw* 12:243–249
11. Portilla AI, Orena BA, Berodia JL, Diaz FJ (2009) Using M/M/∞ queueing model in on-street parking maneuvers. *J Transp Eng* 135(8):527–535
12. Tam ML, Lam WHK (2000) Maximum car ownership under constraints of road capacity and parking space. *Transp Res Part A Policy Pract* 34(3):145–170

Travel Time Reliability Measure and Level of Service Criteria for Urban Midblock



C. P. Muneera and Krishnamurthy Karuppanagounder

Abstract The study reported here aimed to quantify the travel time reliability of urban midblock under heterogeneous traffic condition. Travel time index is taken into account for the measure of reliability for urban midblock. Geometric data, traffic volume count, and travel time data of seven urban midblock in Kerala, India forms the database for this study. Statistical evaluation of travel time index of each midblock is calculated for reliability estimation. A model was developed and validated for travel time index with traffic flow rate to predict the travel time reliability. The exponential model gave an accurate prediction on travel time reliability with traffic flow rate. This work also concentrates on proposing level of service criteria using travel time reliability measure. Hence, these new criteria can be used for travel time reliability prediction and also act as a basis to assess the level of service criteria for urban midblock under heterogeneous traffic condition.

Keywords Travel time · Travel time index · Travel time reliability · Speed ratio · Level of service · Regression model

1 Introduction

Travel time reliability is a useful indicator which estimates the quality of the traffic flow in the transportation system and is also a key input to the transport planning and traffic management purposes. Travel time reliability is referred as the level of inconsistency in terms of trip, mode, and route in the transportation system [1]. Travel time reliability is an effective indicator which can be used for congestion quantification. FHWA [2] defines that the travel time reliability is the measure of consistency or dependability in travel time. High variation of reliability in travel time indicates the reduction in the performance of the roadway. Prior information on

C. P. Muneera (✉) · K. Karuppanagounder
Department of Civil Engineering, National Institute of Technology Calicut, Calicut 673601,
Kerala, India
e-mail: muneeranit@gmail.com

K. Karuppanagounder
e-mail: kk@nitc.ac.in

© Springer Nature Singapore Pte Ltd. 2020
T. V. Mathew et al. (eds.), *Transportation Research*, Lecture Notes
in Civil Engineering 45, https://doi.org/10.1007/978-981-32-9042-6_33

the variation of the travel time from the normal condition in the roadway helps the passengers to schedule their travel time and choice of route for traveling in advance.

Travel time reliability concepts have been introduced by Asakura and Kashiwadani [3] based on the probability of trip for a given time interval. The perusal of literature reveals that measure of travel time reliability is mainly categorized into two groups, namely mathematical measurements and statistical measurements. Mathematical measurements are based on systematic approaches by using user equilibrium (UE) principle [4, 5]. Reliability measure is developed in the category of statistical measurements, which uses travel time distribution perceived by the road users in the roadway. The statistical measure mainly uses the mean, standard deviation, and variance of travel time for the quantification of travel time reliability. The statistical parameters communicate in a simple way which can easily understand for both highway engineers and road users. Therefore, statistical measure is considered for this study.

Level of service (LOS) is a quantitative measure that represents quality service of traffic in the transportation system (HCM 2010) [6]. The traditional way of evaluating the performance of urban links is based on the level of service criteria and its volume capacity ratio. Highway capacity manual defines six levels of service to define the quality of traffic facilities in the transportation system. Basically, HCM uses fundamental measures such as volume to capacity (v/c) ratio, speed, and density. These measures do not capture the reliability in travel time of individual drivers. Thus, the finding of the earlier studies which differ from the quantification of the level of service criteria considering the reliability measure under heterogeneous traffic condition forms the motivation of the present study.

The primary objective of this study is to evaluate the travel time reliability of an urban midblock for a better understanding of the operational efficiency of the system. In this study, a methodology is presented to predict travel time reliability considering traffic flow rate. Lastly, this research work proposes level of service criteria for urban midblock using travel time reliability measure. This research work contributes to proposing level of service measures using travel time reliability measure, under heterogeneous traffic conditions.

2 Measurements of Travel Time Reliability and Level of Service on Urban Roads

Literature from the past reveals that several indicators are used as the statistical measure of travel time reliability such as variability percentages in travel time, travel time index, buffer index, and planning time index. Lomax et al. [1] propose reliability measures using variability in percentages such as 5, 10 and 15%. 95th percentile uses the travel time reliability measurements as indices in the form of buffer index and planning time index [7–9]. This paper examines travel time reliability with a statistical measure namely travel time Index. Travel time index (TTI) compares travel time in

the peak period to travel time during free flow or posted limited speed conditions [10]. The range of travel time index varies from one to any positive number. Travel time index 1.8 points out that travel time during that specific period is 80% longer than free flow period. Travel time represents the average travel time that spends on the roadway. As the travel time index increases, the duration of travel time and reliable disorder of that stretch increases. Travel time index can be mathematically represented as in Eq. (1).

$$\text{Travel time index} = \frac{\text{Average travel time}}{\text{Free flow travel time}} \quad (1)$$

State-of-the-art related to the level of service criteria under heterogeneous traffic condition revealed that the speed ratio has a significant role in the formulation of fixing criteria for the level of service [11]. Therefore, this study considers the speed ratio along with travel time reliability measure for the level of service criteria for urban midblock. The speed ratio is the ratio between mean travel speeds to the mean free flow speed of that midblock. The speed ratio is varying from zero and one, the higher the speed ratio value indicates the best quality. Speed ratio can be mathematically expressed as in Eq. (2).

$$\text{Speed ratio} = \text{Actual mean speed of a trip} / \text{Mean free flow speed} \quad (2)$$

Traffic flow, the fundamental measure of the traffic system is chosen for the influencing factor for the travel time reliability prediction and level of service criteria has done based on the speed ratio. For urban road with heterogeneous traffic conditions, a new methodology has proposed for level of service criteria using travel time reliability indicator. For the above-stated purposes, study stretches were selected in the heterogeneous traffic scenario.

3 Study Area

The study stretches for data collection were selected from Calicut and Ernakulam cities in Kerala, India. Calicut city is the third largest city in Kerala. It is situated on the west coast of India at a latitude of 11° 15' 0"N and a longitude of 75° 46' 0"E. The city of Ernakulam is located in the southwestern India at latitude of 9° 59' 0"N and a longitude of 76° 17' 0"E and it is in the central part of Kerala. Ernakulam is the commercial capital city of Kerala, and it has the highest revenue collection. Eight single carriageways, operating at different traffic volume under heterogeneous traffic conditions, are having a length varying from 208.6 to 799.29 m and carriageway width of 6.1–10.22 m has considered for this study.

4 Data Description

To study the travel time reliability and to develop level of service criteria of the urban link, basically, three types of data are required. The first one was the road geometry data. Geometric data such as length of road stretches and carriageway width were collected manually from the site. The second one was travel time data, and the other one was traffic count data. Traffic parameters including traffic volume count and travel time data were collected through video graphic survey. The data were collected from 7.30 AM to 6.00 PM in each link in a normal day to capture the variation in the traffic flow. Free flow travel time data collected separately during the early morning when the traffic flow was very less.

The license plate matching technique was used to measure the travel time for the link. For this, video cameras are placed at the entry and exit location of the study area. Collecting vehicle license plate numbers for the entry point and exit point through the video and computing their time difference at exit and entry point gives the travel time for each vehicle. The travel time variation was collected for each study link and the minimum and maximum value in the travel time of the study stretches are depicted in Fig. 1. The variation of the average travel time of the study links ranges from 1 to 545 s. A commercial center is located near Link7 and construction of a new transportation facility (metro) near the link increases the average travel time abnormally.

The speed of the vehicle is obtained by dividing the length of the midblock to the time taken by the vehicles along the stretches. Actual mean speed and free flow speed for the vehicles during the day along the study stretches were calculated separately to speed ratio was calculated for each stretches.

Traffic volume data are observed from a camera that is fitted to the entry point of the link. The Data were collected from 7.30 AM to 6.00 PM in each link to capture variation in the traffic flow and database is aggregated for each 5 min interval and converted to PCU by using IRC: 86-1983 [12]. The variation in the traffic flows of each stretch is depicted in Fig. 2. The maximum flow, 952 PCU/h/m, is observed in Link7.

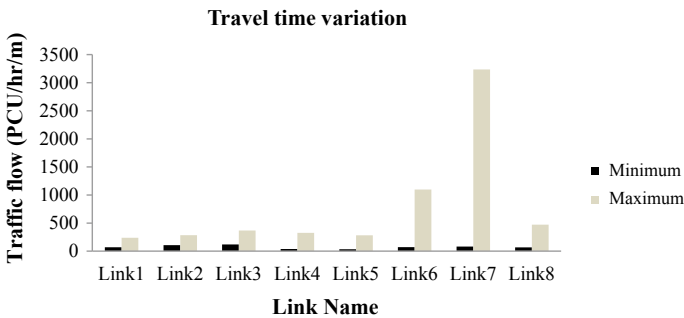


Fig. 1 Travel time variation along the study stretches

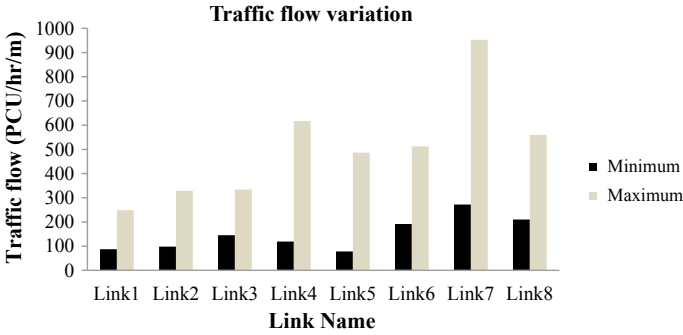


Fig. 2 Variation of travel time along the study stretches

5 Reliability Measure of Urban Midblock

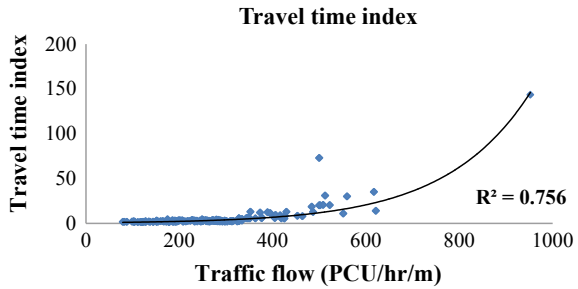
Travel time index for each study stretches was calculated for measuring the reliability of urban midblock. Statistical variation in the travel time index was estimated and presented in Table 1.

Link5 shows a minimum planning time index and Link7 shows maximum planning time index among the study stretches. To know the variation of travel time index with traffic flow, a scatter plot was developed and predicted in Fig. 3. The result from the plot indicates that travel time index is highly correlated with traffic flow. The trend explains that when more vehicles use the road at same e time, the average travel time of the vehicles increases and thus leads to an increase in the value of travel time index. This necessitates for the model development for travel time index using traffic flow rate.

Table 1 Summary statistics for travel time index

Road name	Minimum	Maximum	Mean	Standard deviation
Link1	1.27	4.35	2.36	0.69
Link2	1.52	4.07	2.39	0.59
Link3	1.55	4.8	2.59	0.83
Link4	1.51	6.9	2.93	1.25
Link5	1.12	12.56	4.53	2.56
Link6	2.02	30.88	14.73	9.46
Link7	3.61	143.56	31.51	37.04
Link8	1.91	30	10.74	6.61

Fig. 3 Variation of travel time index with traffic flow



6 Model Development

Models were developed for travel time reliability by taking travel time indices as the dependent variable and traffic flow rate as an independent variable. A total of 400 data is taken for modeling of the travel time reliability. From the data set available, two-third data used for the model prediction and the remaining one-third data were used for model validation. Regression models were developed for the performance prediction of the links. From the different model form tried, nonlinear regression provides the best prediction and it is selected as the final model. The model form for predicting the travel time index on the traffic flow rate is given in Eq. (3).

$$\text{Travel time indices} = a * e^{b * V} \tag{3}$$

where a and b were estimated for different indices and shown in Table 2. In this model, V is the traffic volume in PCU/h/m width of the road. The estimated parameters are significant at 95% confident intervals.

Travel time index shows an exponential growth with traffic flow rate in the urban single carriageway. The coefficient of determination, R^2 , explains that 82% of total variation in travel time index is explained by the relationship between travel time index and traffic flow rate. The standard error predicts that the parameters taken for modeling are significant. Travel time index gives an idea about the extra travel time taken with respect to free flow travel time for traveling in the study stretches. Therefore, as the traffic volume increases, the travel becomes unreliable to road users. The model predicts the travel time index for different traffic volume of urban

Table 2 Model for travel time index

Sl. no.	Indices	Model	R^2	Standard error		RMSE	
				Constant	Coefficient of flow	CD	VD
1	Travel time index	$0.363e^{0.008v}$	0.825	0.041	0.001	1.695	1.521

Note CD Calibration Data set and VD Validation Data set

Table 3 Prediction of travel time reliability

Sl. no.	Indices	Traffic flow rate PCU/h/m				
		150	250	350	450	550
1	Travel time index	1.32	2.95	6.57	14.63	32.58

midblock. Hence, travel time index model helps to predict the average travel time that has to spend on an urban link.

7 Model Application

This study gives an illustration of how the developed models in this study can be used to predict the travel time reliability of urban midblock. For the illustration, traffic flow is taken from 150 to 550 PCU/h/m width of the roadway. Table 3 shows the predicted values of the travel time indices over wide traffic volume ranges.

The result of the evaluation shows that as the traffic volume increases, passengers allocate more travel time for their trip. For example, at a traffic flow rate of 250 PCU/h/m, the travel time index is 2.95, which implies that passengers should plan to allocate a travel time 2.95 times that of free flow travel time in order to ensure of on-time arrival. Therefore, the reliability of travel time along the road stretches decreases with the traffic flow rate increases.

8 Level of Service Criteria Developments

In order to assess the level of service (LOS) criteria, a model was developed considering travel time index as a dependent variable and speed ratio as the independent variable. The speed ratio is the ratio of mean speed and free flow speed. An IRC 106-1990 guideline provides the level of service criteria, which is a qualitative measure that describes the operational condition of the traffic stream under heterogeneous traffic conditions [13]. The model form for travel time index for assessing level of service criteria is expressed in Eq. (4).

$$TTI = 1/a + b * SR \tag{4}$$

where TTI is the travel time index, *a* and *b* are estimated coefficients, and SR is the speed ratio. Statistical parameters for evaluating travel time index model is given in Table 4.

Considering *R*² value from the table, regression models are seen fairly good prediction. Standard errors of the coefficients are significant at percentage confident intervals. Travel time index for different speed ratios, recommended in IRC 106-

Table 4 Travel time reliability model with speed ratio

Sl. no.	Indices	Model	R^2	Standard error		RMSE	
				Constant	Coefficient of flow	CD	VD
1	Travel time index	$1/0.027 + 0.99SR$	0.94	0.009	0.02	1.79	1.62

Note CD Calibration Data set and VD Validation Data set

Table 5 Prediction of travel time reliability

Criteria	A	B	C	D	E	F
Mean speed	0.9 Vf	0.7 Vf	0.5 Vf	0.4 Vf	0.33 Vf	<0.33 Vf
Travel time index	1–1.08	1.08–1.38	1.38–1.91	1.91–2.36	2.36–2.82	>2.82

1990 was found out and level of service criteria was developed from the obtained model. Therefore, maximum and a minimum level of service criteria for each mid-block were calculated and presented in Table 5.

9 Conclusions

This study focuses on the estimation of travel time reliability of urban single carriageway under heterogeneous traffic condition using the statistical measure of travel time reliability and travel time index. Eight single carriageways, operating with considerable variation in traffic flow, were selected for this study. Total travel time, traffic volume count, and geometric data were collected and used for the analysis. The model was developed to assess the travel time reliability in urban midblock using observed traffic flow rate. The developed model helps to predict the travel time reliability under considerable variation of traffic flow. The level of service criteria has developed based on speed ratio values and travel time index under the same traffic conditions. The following conclusions have been obtained.

1. Travel time index, a statistical measure of travel time reliability shows a positive exponential growth with traffic flow rate. This study predicts allocation of travel time for the passengers for on-time arrival at different traffic flow rate on urban single under heterogeneous traffic condition. As the travel time index increases, the reliability in the travel time in the traffic system decreases, since road users have to spend more time on the roadway.
2. Level of service criteria proposed for urban single carriageway using travel time reliability measure under the same traffic condition using the speed ratio as the dependent variable. The result forms the study indicates that the level of service criteria A is satisfied when the value of travel time index is from 1 to 1.08 and F

reached when the value is greater than 2.82. This method gives a new research direction to propose a level of service criteria using travel time parameters.

This study demonstrates the usefulness to evaluate the travel time reliability for urban midblock. The scope of the study is limited to the heterogeneous urban single carriageway with observed traffic flow rate. This study will be useful to the field engineers for traffic management purposes and for transport planners for the regional transport planning.

Acknowledgements The authors sincerely thank the support received from the Centre for Transportation Research, Department of Civil Engineering, National Institute of Technology Calicut, a Centre of Excellence setup under FAST Scheme of MHRD, Govt. of India.

References

1. Lomax T, Schrank D, Turner S, Margiotta R (2003) Selecting travel reliability measures. Texas Transportation Institute, College Station, TX
2. FHWA Report (2006) Travel time reliability: making it there on time, all the time. In: Web proceedings of the Eastern Asia society for transportation studies, vol 9. US Department of Transportation, Federal Highway Administration, 2013 document from Jan 2006
3. Asakura Y, Kashiwadani M (1991) Road network reliability caused by daily fluctuation of traffic flow. In: 19th PTRC summer annual meeting, proceedings seminar G, pp 73–84
4. Chen A, Ji Z, Recker W (2003) Effect of route choice models on estimation of travel time reliability under demand and supply variations. In: The network reliability of transport. Proceedings of the 1st international symposium on transportation network reliability (INSTR), Pergamon, pp 93–117
5. Lee S, Moon B, Asakura Y (2000) Reliability analysis calculation on large scale transport networks. In: Reliability of transport networks. Research Studies Press, pp 203–216
6. National Research Council Transportation Research Board (2000) HCM 2000, Highway capacity manual
7. Chalumari RS, Chandra S, Bharati AK (2013) Performance evaluation of urban arterial in Delhi using travel time reliability. In: Proceeding of the Eastern Asia society for transportation studies, vol 9
8. Higatani A, Kitazawa T, Tanabe J, Suga Y, Sekhar R, Asakura Y (2009) Empirical analysis of travel time reliability measures in Hanshin expressway network. *J Intell Transp Syst* 13(1):28–38
9. Lyman K, Bertini R (2008) Using travel time reliability measures to improve regional transportation planning and operations. *Transp Res Rec J Transp Res Board* 2046
10. Texas Transportation Institute and Cambridge Systems, Inc. Travel time reliability: making it there on time, all the time. FHWA Office of Operations, US Department of Transportation http://ops.fhwa.dot.gov/publications/tt_reliability
11. Bhuyan PK, Krishna Rao KV (2011) Defining level of service criteria of urban streets in Indian context. *Eur Transp* 49:38–52
12. Indian Road Congress (1983) Geometric design standards for urban roads in plains. IRC code for practice, vol 83, New Delhi
13. Indian Road Congress (1990) Guidelines of capacity of urban roads in plain areas. Indian Road Congress, IRC code for practice, New Delhi

Modelling Dynamic PCUs Using Occupancy Time Approach at Urban Signalised Intersections Under Mixed Traffic Conditions



Pinakin Patel and Ashish Dhamaniya

Abstract At signalised intersections, the mixed traffic flow is converted to corresponding car flow using a passenger car unit. Earlier studies showed that PCU value is not static but depends on the interaction of vehicles for a particular traffic stream. This study suggests a methodology to find the PCU value at urban signalised intersections based on the PCU value obtained by time occupancy method during the saturation condition with varying interaction between the vehicles. For the analysis, traffic data have been collected with the help of videography at Ahmedabad and Surat, Gujarat. Traffic flow discharge and clearance time of different vehicular categories have been extracted from the video during the saturated green time. The variation in PCU values with respect to traffic composition and discharge rate is carried out in this study. Regression-based PCU models are developed to estimate the PCUs for different category of vehicles considering the traffic flow and compositions. Further, a stream equivalency factor has been developed to convert the heterogeneous traffic into homogeneous traffic without making use of PCU values.

Keywords Passenger car units · Mixed traffic · Signalised intersection

1 Introduction

The signal system is provided in urban area to manage the adverse movements of pedestrian and vehicles. The passenger car unit (PCU) values play an important role to convert different static and dynamic behaviour of mixed flow into homogenous equivalent flow for the capacity estimation of signalised junctions. The traffic and roadway factors are affecting on a PCU value of particular vehicle category. For the exact derivation of PCU values, it is essential to study precisely the influence of traffic and roadway factors on vehicular movement.

P. Patel (✉) · A. Dhamaniya
Department of Civil Engineering, Sardar Vallabhbhai National Institute of Technology, Surat
395007, India
e-mail: pnpatel123@gmail.com

A. Dhamaniya
e-mail: adhamaniya@gmail.com

© Springer Nature Singapore Pte Ltd. 2020
T. V. Mathew et al. (eds.), *Transportation Research*, Lecture Notes
in Civil Engineering 45, https://doi.org/10.1007/978-981-32-9042-6_34

To represent the buses and trucks in a traffic stream to an equivalent passenger car unit, the concept of PCU was introduced in 1965 by the US Highway Capacity Manual [1]. IRC SP: 41 [2] had recommended static PCU values for each category of vehicles. There are different methods used for the derivation of PCUs. Branston and Van Zuylen [3] suggested a method to estimate PCUs using regression technique. In regression method, saturated green time is considered as depending variable on number of different class of the vehicles approaching stop line. The similar approach was used by Arasan and Jagadeesh [4], Minh and Sano [5]. The statistical technique of headway ratio process has developed by Vien et al. [6] for finding the PCU values at signalised intersection in Malaysian traffic conditions. The concept of area occupancy is incorporated by Arasan and Dhivya [7] for finding the PCU on urban roads. The derived PCU values of homogenous traffic are not suitable for heterogeneous traffic, where the traffic is composed of different vehicles categories, static and dynamic characteristics and absence of lane discipline. Hence, the suitable method is developed incorporating mixed traffic attributes for the PCU estimations. Chandra and Kumar [8] proposed a method to estimates the PCU of different vehicles category considering speed and area occupancy ratio. In the present study, the speed ratio is replaced by the clearance time ratio for each movement. The present method measures the occupied time taken by a vehicle for the deriving PCUs which includes delay indirectly, which is performance assessment parameter for categorising level of service as per US Highway Capacity Manual (HCM-2010). The objective of this research is to estimate PCU for different category of vehicles under different level of interaction of mixed traffic during saturated green time at the signalised intersections. The mathematical models are developed considering mixed traffic flow behaviour to estimate the PCUs for each vehicular category.

2 Methodology

2.1 Time Occupancy Method

The small car is considered as a standard vehicle for the determination of PCU values. The idea of dynamic PCU was developed by Chandra and Kumar [8] considering the several traffic and flow characteristics. The clearance time between the stop lines is taken as time occupancy. The variable clearing-time includes the effect of several roadway geometry and traffic aspects disturbing the movement of a vehicle in a given intersection [9]. The PCU for a vehicle can be determined using Eq. (1).

$$PCU_m = \frac{\left(\frac{T_m}{T_c}\right)}{\left(\frac{A_c}{A_m}\right)} \quad (1)$$

where PCU_m = passenger car unit for the subject vehicle 'm' in the traffic; A_c/A_m = space ratio of the standard car (in m^2) to the subject vehicle 'm' (in m^2); T_m/T_c = clearing time ratio of subject vehicle 'm' (in seconds) to standard car (in seconds); The classification of vehicle is done based on their physical size. The physical dimensions for two-wheelers (2W), three-wheelers (3W), light commercial vehicles (LCV), heavy commercial vehicles (HCV), standard car (CS) and big car (CB) were measured in the field and found as 1.2, 4.48, 9.50, 24.54, 5.36 and 8.11 m^2 , respectively [9].

2.2 PCU Models

The PCU models are developed based on the statistical significance of identified sensitive parameters. The models are validated for field conditions. Based on the data collected, PCU models have been developed for various modes considering the effect of compositions of mixed traffic through regression approach. The standard model is given in Eq. (2).

$$Y = 1 + a_1 P_{cb} + a_2 P_{3w} + a_3 P_{2w} + a_4 P_{lcv} + a_5 P_{hcv} + 1/N \quad (2)$$

where Y = PCUs of different modes; P_{2w} = % share of 2W; P_{3w} = % share of 3W; P_{cb} = % share of CB; P_{lcv} = % share of LCV; P_{hcv} = % share of HCV in the traffic stream; and N = flow rate in vehicles/seconds.

3 Data Collection

The study is performed at three important urban signalised junctions of Ahmedabad and Surat, India. The particular intersections satisfy the norms of base conditions for signalised intersections. The lane formation varies from 2 to 4 lanes. The left-turning traffic is using separate lane without interrupting to through traffic. The camera is placed at vantage points to capture various aspect of mixed traffic behaviour by recording traffic movement at approaches. The queue formation and discharge patterns are extracted from the video using manual technique. In Webster's method [10], analysis period was fixed as 5 s at the signalised intersection. The numbers of each category of vehicles and time occupied by each vehicle category vehicles from one stop line to another stop line for straight moving and right-turning traffic during each 5 s of the effective green phase is extracted and later on used for the estimation of PCUs. This process is used for every cycle. The total of 75 cycles from five approaches is considered for analysis. The maximum traffic flow is detected on the particular approaches. Tables 1 and 2 summaries the statistics of data collected at signalised intersections.

Table 1 Observed intersection details

Intersection	Study approaches	Width (m)	Green time (s)	Cycle time (s)	Right turn (%)	Saturation flow (veh/h)
I-01	01	14	44	110	0	15,588
	02	7.2	17	146	0	9000
I-02	03	10.5	35	110	5	13,212
	04	10.5	41	115	20	15,804
I-03	05	10.5	35	125	31.78	10,770

Table 2 Observed traffic at approaches of junctions

Intersection	Study approaches	Composition (%)					
		2W	Auto/3W	Small car	Big car	LCV	HCV
I-01	01	63.24	18.62	5.20	9.42	1.23	1.21
	02	79.40	10.10	5.30	4.10	1.10	0.00
I-02	03	58.76	30.03	3.56	4.31	2.30	1.04
	04	72.92	14.98	4.10	3.80	1.10	0.49
I-03	05	63.78	16.36	9.12	9.28	1.06	0.41

4 Data Analysis

The variation in traffic characteristics and physical size are able to explain in PCU for a vehicle type. From the time occupancy data, higher the occupancy time of a particular category of vehicle with respect to standard car implicates higher value of delay and results in higher PCU. Whereas, lower occupancy time of vehicles having lesser physical dimension than small car implies lower value of delay and results in lower value of PCU. Figure 1 shows the extraction of time occupancy data using the software Avidemux-2.6.

The calculated PCU values using Eq. (1) for the different intersections are tested for their variance using the analysis of variance (ANOVA) at 5% level of significance. The results are shown in Table 3 which indicates that there is no variation in PCU values for different movements and intersection for the particular vehicle category.

Figures 2 and 3 show the box—whisker and normal plots for different vehicle categories.

From Fig. 2, it is clear that the decrease in physical size of vehicle will require less time to clear the junction compared to larger-size vehicle which have better manoeuvrability and low PCU values.

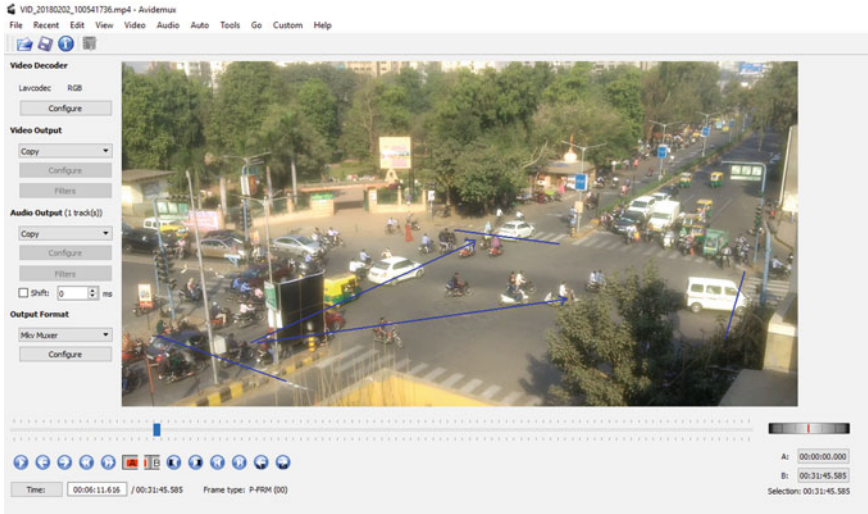


Fig. 1 Snapshot for extraction of time occupancy data

Table 3 Data of PCUs calculated for different vehicle classes

Type of vehicle	I-01	I-02	I-03	<i>p</i> -value	<i>F</i>	<i>F</i> critical	<i>F</i> < <i>F</i> _{critical}	Standard deviation	Average PCU
2W	0.22	0.18	0.20	0.7726	0.3730	2.6373	Yes	0.04	0.20
3W	0.68	0.69	0.71	0.1479	1.8379	2.7318	Yes	0.13	0.69
Small car	1	1	1	–	–	–	–	–	1.00
Big car	1.52	1.51	1.46	0.9708	0.0800	2.6407	Yes	0.27	1.51
LCV	1.97	1.93	2.14	0.1751	1.7171	2.7862	Yes	0.44	2.02
HCV	5.93	5.09	5.81	–	–	–	–	1.24	–

5 Developments of PCU Models

Mathematical models based on regression method were developed to allow easy and fast estimation of PCU values for the prevailing traffic conditions. The proposed regression models are shown in Eqs. (3)–(5). The *t*-values of model are significant at 95% level of confidence. Values in parenthesis show *t*-statistics and *R*²-values. The proportion of LCV and HCV is very less, so that is not considered for the development of mathematical models.

$$PCU_{2W} = 1 - 0.0075P_{2W} - 0.0077P_{3W} - 0.0063P_{cb} - 2.14/N \quad (R^2 = 0.98)$$

$$(57.11) \quad (21.10) \quad (17.98) \quad (6.58) \quad (3)$$

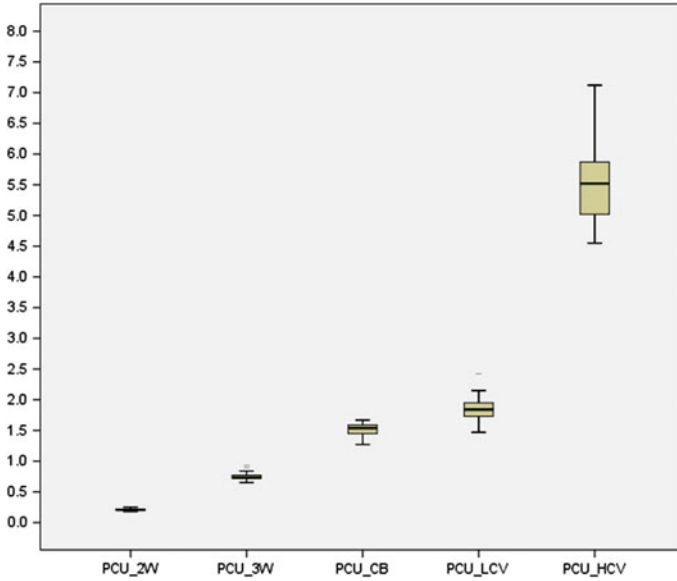


Fig. 2 Box plot of PCU

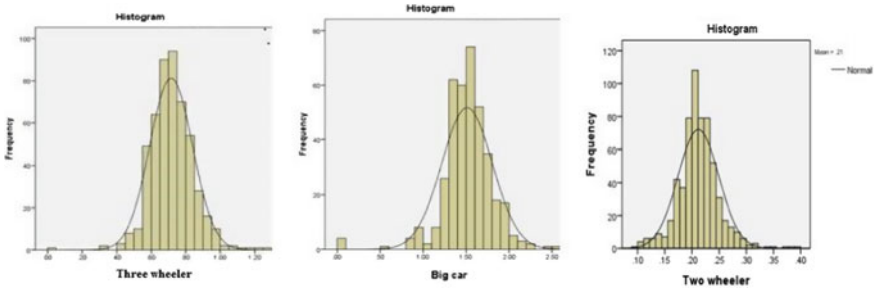


Fig. 3 Variation of PCU values with histogram plots of normal distribution

$$PCU_{3W} = 1 - 0.001P_{2W} - 0.0035P_{3W} - 0.0046P_{cb} - 0.92/N \quad (R^2 = 0.88) \tag{4}$$

(4.90) (4.01) (7.59) (2.7)

$$PCU_{cb} = 1 + 0.0047P_{2W} + 0.0044P_{3W} + 0.00577P_{cb} + 1.52/N \quad (R^2 = 0.91) \tag{5}$$

(3.79) (3.17) (5.83) (3.19)

where PCU_{2W} = PCU of motorised 2W, PCU_{3W} = PCU of motorised 3W, PCU_{cb} = PCU of CB, P_{2W} = Composition of 2W for a particular interval, P_{3W} = Composition of 3W for a particular interval, P_{cb} = Composition of CB for a particular interval and N = Total number of vehicles per 5 s.

Table 4 Significance test of PCUs at 5% level of significance

Type of vehicle	<i>t</i> -value	<i>t</i> -critical	<i>p</i> -value
2W	1.37	2.03	0.088
3W/auto	0.125	2.04	0.450
Big car	1.18	2.05	0.123

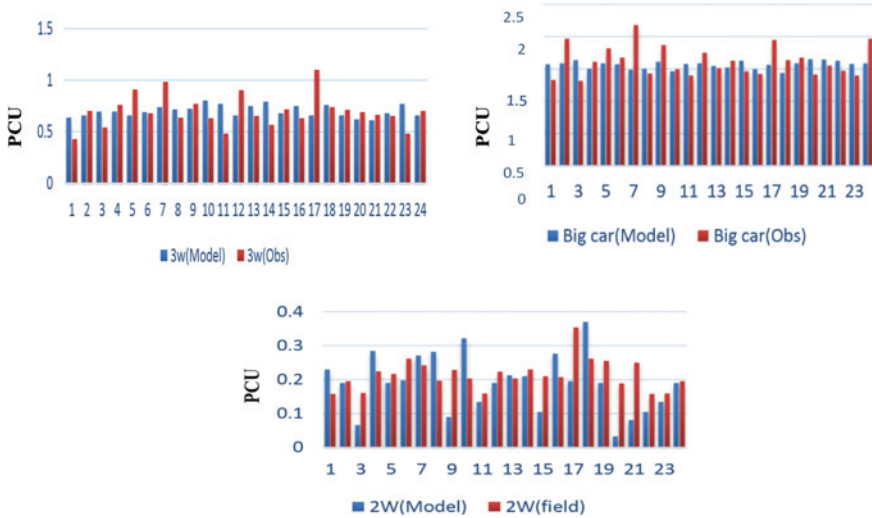


Fig. 4 Comparison of PCUs from model and observed/field

Developed models for PCU are validated for a different intersection by taking representative samples to observe the feasibility of the model having different traffic composition and geometrical characteristics. To check the likely change in variance of observed and model PCU values of 2W, 3W and CB statistically, paired *t*-test was done by equating the variance in PCU values for all the vehicle categories at 5% level of significance. It has been observed that variation in variance and PCU values is not significantly different in both the cases for the representative category of vehicles as *t*-statistics value is less than *t*-critical value and *p*-value also suggests the comprehensibility of the model. Test results are given in Table 4.

Figure 4 shows the comparisons of field and model PCUs. The variation observed is very less between field measured and model PCUs.

5.1 Variations of PCUs

The effect of discharge rate on PCUs is studied from the developed models of PCUs for different traffic volume and for a predefined composition of traffic. Figure 5 shows

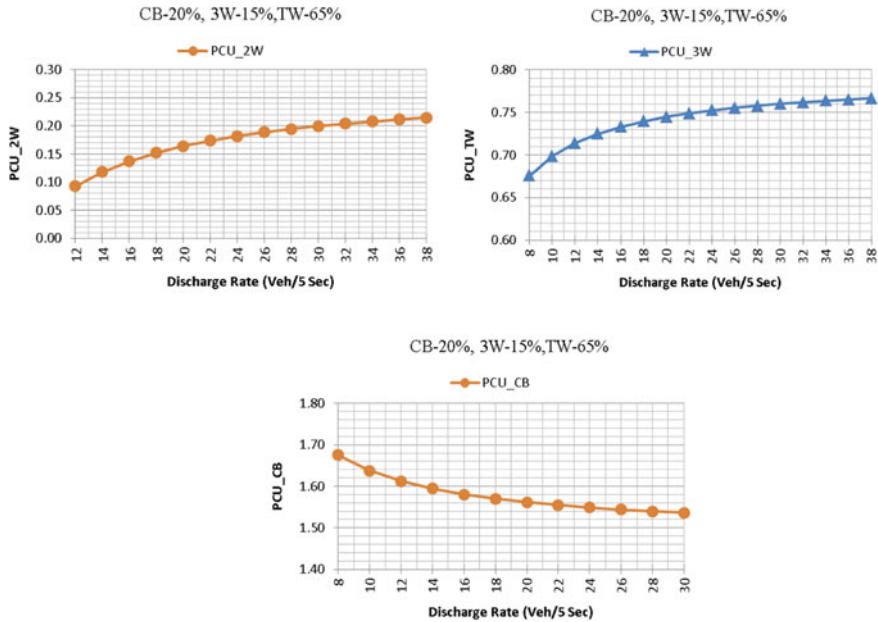


Fig. 5 Variation PCU with discharge rate for 2W, 3W and CB

the variation of PCU for different category of vehicles with the respective discharge rate.

From Fig. 5, it has been seen that the PCU of vehicles smaller than the reference vehicle increases with increase in discharge rate, whereas the PCU of vehicles larger than the reference vehicle decreases with increase in discharge rate. It is observed that, when the composition of small-size vehicles are high in the traffic stream, in that case, the tendency of small-size vehicle is to travel towards edge lane of roadway in a group of platoon and create poorer operating condition among themselves which, in turn, increases in average occupancy time and results in more PCU, but the scenario becomes opposite for big cars, and therefore, with less speed differential invariably reduces the PCU at the signalised intersections. The slope of graphs is flat, so less variation in PCUs with the discharge rate.

The proportion of two categories of vehicles is kept constant and the other two categories are varied in a contemporary manner. Figure 6 shows the various graphs of variation in PCU with their own vehicle proportion at the various saturation flow level of 7200, 14,400, and 21,600 veh/h which was observed in the field. It has been seen that the PCU of motorised two-wheeler and three-wheelers goes on decreasing with increase in their own proportions. PCU values for big cars showed a different trend. There is increase in dynamic PCU values with increase in particular vehicles proportion. At an intersection, it is also observed that small-size vehicles like 2W and 3W have more manoeuvrability and they can accept the gaps between the large-size vehicles and able to passage in any space accessible between big-size vehicles and

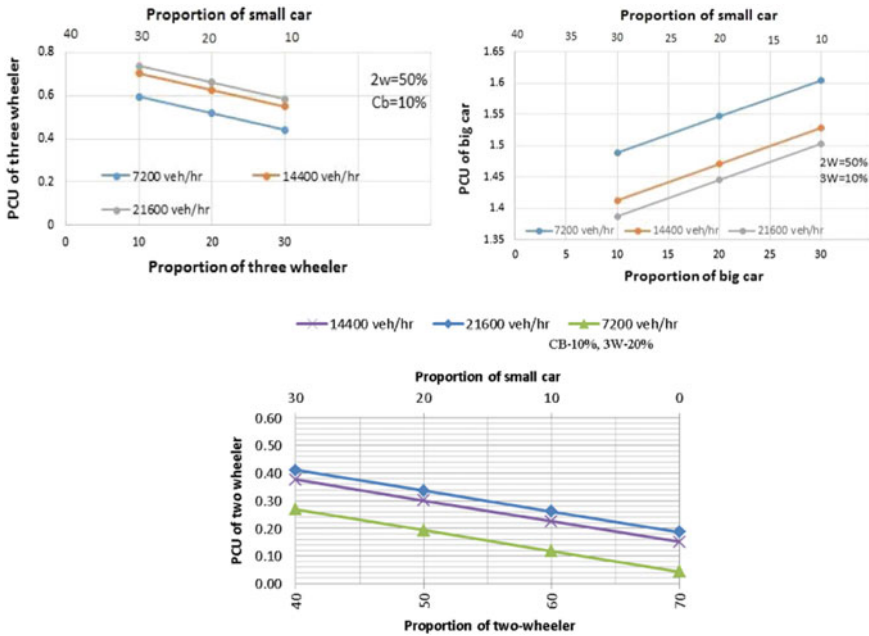


Fig. 6 Variation in PCU of 3W, CB and 2W with their proportions

thus they are minimum affected, but they make poorer operative conditions for other vehicles [11, 12]. The variation in PCU values during the saturation time is mainly due to the composition effect and their interaction among the vehicles. Increase or decrease in PCU values is attributed to speed of reference and subject vehicles during the discharging operations.

6 Stream Equivalency Factor

A stream equivalency factor has been suggested by Dhamaniya and Chandra [13] to convert mixed traffic flow to equivalent car flow. The derived stream equivalency factor (k) is for the stream conversion. The same concept is used by Patel and Dhamaniya [14] at signalised junction and derived the equivalency factor. It is flow ratio between PCUs and vehicles. In the current study, the estimated average PCU values from Table 3 are used for developing the stream equivalency factor (Fig. 7).

The linear regression model is developed to estimate the k -value by adopting the influence of heterogeneous traffic on k . The relation is given in Eq. (6).

$$k = 1 + 0.3793 \times \frac{1}{N} + 0.005 \times C_{CB} - 0.0032 \times C_{3W}$$

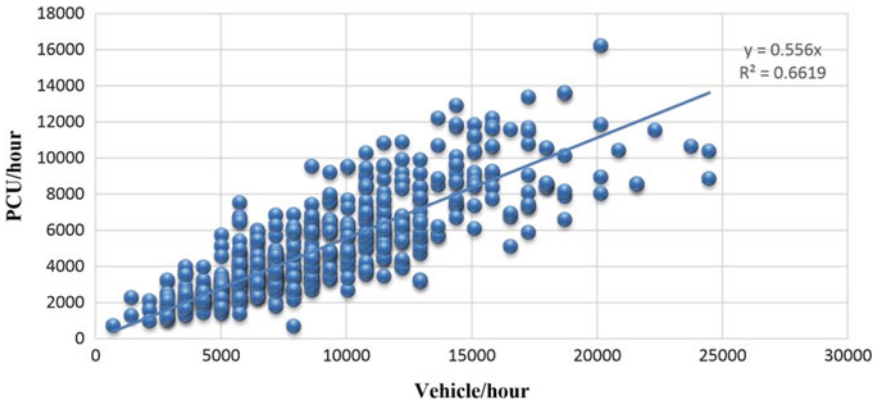


Fig. 7 Stream equivalency factor

$$- 0.0078 \times C_{2W} + 0.0479 \times C_{HCV} + 0.0081 \times C_{LCV},$$

$$R^2 = 0.96 \tag{6}$$

where N average of vehicles, C_{CB} , C_{3W} , C_{2W} , C_{HCV} and C_{LCV} are the average share of CB, 3W, 2W, HCV and LCV, respectively, for each 5 s. The R^2 -value and t -value indicate good strength significant at the 95% level of confidence. The coefficients' signs are also logical for smaller-size and large-size vehicles.

7 Conclusions

The passenger car equivalent is most crucial parameter to address the mixed traffic condition mainly comprised of different static and dynamic characteristics of vehicles and absence of lane-disciplined driving. The several techniques are suggested by the researcher for PCU estimation and obtained values may vary to certain range. Still, all the approaches limit to a specific set of PCU value for different traffic environments. The current study explains the dynamic nature of PCU value in urban signalised junction. The PCU values are derived by new technique of occupancy time. Meanwhile, the occupancy time of a vehicle is influenced by the composition and flow rate on a stream, a set of equations is developed considering the above factors. Variation of PCU is denoted graphically for different discharge rate and traffic composition. PCU of two wheelers and three wheelers decreases with increase in its own due to their small size and higher manoeuvrability. Similarly, PCU of big car increases with increase in its own composition because of its lesser gap accepting behaviour. This study provides a methodology for estimation of dynamic PCU factors during the saturated green time. The equations are developed for PCU

and stream equivalency for the different compositions level to predict PCUs and stream equivalent factors at signalised junctions under mixed traffic flow.

References

1. Highway Research Board (1965) Highway capacity manual. Special rep. 87, Washington, DC
2. Indian Roads Congress (IRC) (1994) Guidelines for design of at-grade intersections in rural and urban areas. IRC special publication no 41, New Delhi
3. Branston D, Van Zuylen H (1978) The estimation of saturation flow, effective green time and passenger car equivalents at traffic signals by multiple linear regression. *Transp Res* 12
4. Arasan TV, Jagadish K (1995) Effect of heterogeneity of traffic on delay at signalized intersections. *J Transp Eng* 121(5):397–404. [https://doi.org/10.1061/\(ASCE\)0733-947X\(1995\)121:5\(397\)](https://doi.org/10.1061/(ASCE)0733-947X(1995)121:5(397))
5. Minh CC, Sano K (2003) Analysis of motorcycle effects to saturation flow rate at signalized intersection in developing countries. *J East Asia Soc Transp Stud* 5:1211–1222
6. Vien LL, Ibrahim W, Mohd AF (2008) Effect of motorcycles travel behaviour on saturation flow rates at signalised intersections in Malaysia. In: 23rd ARRB conference, Adelaide, Australia
7. Arasan VT, Dhivya G (2010) Methodology for determination of concentration of heterogeneous traffic. *J Transp Syst Eng Inf Technol* 10(4):50–61
8. Chandra S, Kumar U (2003) Effect of lane width on capacity under mixed traffic conditions in India. *J Transp Eng* 129(2):155–160. [https://doi.org/10.1061/\(ASCE\)0733-947X\(2003\)129:2\(155\)](https://doi.org/10.1061/(ASCE)0733-947X(2003)129:2(155))
9. Mathew S, Dhamaniya A, Arkatkar S, Joshi G (2016) Time occupancy as measure of PCU at four legged roundabouts. *Transp Lett* 1–12. <https://doi.org/10.1080/19427867.2016.1154685>
10. Webster FV, Cobbe BM (1966) Traffic signals. Road research technical paper no 56. Her Majesty's Stationery Office, London
11. Preethi P, Ashalatha R (2016) Estimation of dynamic PCU using area occupancy concept at signalized intersections. In: International conference on transportation and development. ASCE, pp 825–837. <https://doi.org/10.1061/9780784479926.075>
12. Dhamaniya A, Chandra S (2016) Conceptual approach for estimating dynamic PCU on urban arterial roads using simultaneous equations. In: 95th annual meeting of transportation research board, Washington, DC
13. Dhamaniya A, Chandra S (2013) Concept of stream equivalency factor for heterogeneous traffic on urban arterial roads. *J Transp Eng* 139(11):1117–1123. [https://doi.org/10.1061/\(ASCE\)TE.1943-5436.0000581](https://doi.org/10.1061/(ASCE)TE.1943-5436.0000581)
14. Patel P, Dhamaniya A (2019) Stream equivalency factor for mixed traffic at urban signalized intersections. *Transp Res Procedia* 37:362–368

Estimating Environmental Benefits of Electronic Toll Collection (ETC)



Dipanjnan Nag , Anibrata Roy and Arkopal K. Goswami

Abstract Toll plazas across India have been deploying electronic toll collection (ETC) systems since 2010. As they are at a relatively early stage of implementation, the demonstrated benefits of reduced delay and emissions, when compared to manual toll collection (MTC), may not be evident immediately. This paper develops a planning-level methodology to demonstrate the benefit ETC toll booths may have on reducing emissions. Existing levels of CO₂, CO, and NO_x were calculated while vehicles were idling in the queue, while they moved slowly in the queue toward the toll booth counter, as well as while they were at the toll booth counter. Subsequently, several scenarios of ETC usage were simulated, based on the arrival rates of vehicles and service time at the toll booth counter, and emissions were estimated. It was observed that a 42, 22, and 64% reduction in CO₂, CO, and NO_x emissions, respectively, can be achieved during a 24-h period when the current usage of ETC lanes is doubled and service rate of 700 veh/h is achieved in the ETC lane.

Keywords Electronic toll collection · Environmental impacts · Emission factors · Queuing theory

1 Background

Highways and expressways enhance the mobility of motorized vehicles. Ironically however, constructed on these modern roads, which are increasingly being financed under various public–private partnership (PPP) models, are toll plazas that collect tolls, and in turn impede the very mobility, for which the roads are designed. In India, as of 2015, approximately 8,700 km of toll roads are being built using the

D. Nag · A. Roy · A. K. Goswami (✉)
Ranbir & Chitra Gupta School of Infrastructure Design & Management, Indian Institute of Technology Kharagpur, Kharagpur 721302, India
e-mail: akgoswami@iitkgp.ac.in

D. Nag
e-mail: el.diablo.diablo78@gmail.com

A. Roy
e-mail: way2aniroy@gmail.com

© Springer Nature Singapore Pte Ltd. 2020
T. V. Mathew et al. (eds.), *Transportation Research*, Lecture Notes
in Civil Engineering 45, https://doi.org/10.1007/978-981-32-9042-6_35

BOT (Toll) mechanism whereas approximately 8,300 km are being built using BOT (Annuity) model. Apart from introducing travel delays, such toll plazas are increasingly becoming environmental hot spots, where vehicles emit gases like HC, CO₂, and NO_x which is formed due to incomplete burning of fossil fuels. A study estimates that such travel delays, along with other factors, are costing India's freight industry an estimated Rs. 60,000 crore per year [1]. Other studies have shown that upper respiratory tract diseases among toll plaza workers are higher than those of other people due to vehicular emissions at toll plazas [2]. These issues have arisen because of various factors that include an increase in the volume of vehicles passing through the toll plaza, toll plaza geometry, and also the slow service rate of manual toll collection.

To counter this situation, automatic toll collection techniques were introduced that include smart cards, credit cards, and coin machines. More recently, electronic toll collection (ETC) has been introduced in various toll plazas, with a vision to eventually move toward all-electronic tolling (AET) and open road tolling (ORT). Norway was the first nation in the world to implement ETC. In the year 1987, separate subscription lanes were opened in the city of Alesund in the western part of Norway that offered electronic fee collection (EFC). The three major urban toll ring systems in Bergen, Oslo, and Trondheim are "open" tolling systems where drivers pay a fixed amount when passing the toll station, regardless of the distance travelled [3]. In the USA, ETC lanes are in operation since the 1990s. In 2015, 35 of the 50 US states have at least one tolled highway, bridge or tunnel, and 37 million transponders are being used to electronically collect toll [4].

There are several documented benefits of an ETC system worldwide. In comparison with manual toll collection lanes that can process 350 veh/h, ETC lanes can process 1,200 veh/h [5]. In addition, ETC lanes provide other benefits that include savings due to the reduction in fuel consumption, reduced travel time, and manpower cost reduction [6]. One study done at the Carquinez Bridge in the San Francisco Bay area found that ETC saved about 40% on the fuel consumption over a 10-year assessment period. Data from five toll facilities in five states of USA has shown that ETC provides cost savings of \$135,000 per lane in annual operating and maintenance costs compared with manual toll booths [7]. In a study carried out in Taiwan, analysts determined that between the years 2013 and 2019, as the usage of the ETC lanes increased there was a significant decrease in the overall service time at the toll plaza [8].

Compared to the developed nations, ETC usage in India began only in 2010. A committee under the chairmanship of Shri Nandan Nilekani recommended passive radio-frequency identification (RFID) as the appropriate ETC technology for India [9]. Currently, out of the 324 toll plazas in the country, 240 toll plazas have deployed ETC systems [9]. At such a relatively early stage of implementation, toll agencies may face several hurdles that make it difficult for them to realize the true benefits of ETC systems. Such hurdles may include determining the exact number of ETC lanes at the toll plaza, acquisition of land to build new ETC toll booths, the cost of upgrading existing manual toll booths to an ETC booth, willingness of the users to enroll in the ETC scheme, and price of the in-vehicle transponder unit. Due to such

reasons, deployment of ETCs usually gets deferred, and as a result, the realization of their benefits is delayed as well. This paper looks into one such aspect, i.e., achieving the benefit of reduced emissions through optimal usage of an ETC lane.

2 Methodology

Data was collected at the toll on National Highway (NH) 6 along the Kolkata–Mumbai route at the Dhulagarh Toll Plaza. Video data was recorded at the toll plaza for a 24-h period. Based on the video footage, the following data was extracted:

- Arrival at queue (AQ)—Time stamped when vehicle joins at back of the queue;
- Arrival at counter (AC)—Time stamped when vehicle reaches at the toll booth counter;
- Departure from counter (DC)—Time stamped when the vehicle leaves the toll booth counter.

Based on these three data elements, the following were calculated:

- Service time (S_T)—Time elapsed between vehicle arriving and exiting toll booth counter

$$S_T = DC - AC \tag{1}$$

- Queue time (Q_T)—Time elapsed between vehicle joining at back of the queue and vehicle existing toll booth counter

$$Q_T = AC - AQ \tag{2}$$

- Inter-arrival time (IA_T)—Time elapsed between two subsequent vehicles, i.e., n and $(n + 1)$, joining the back of the queue.

$$IA_T = AQ_{n+1} - AQ_n \tag{3}$$

2.1 Emissions Due to Manual Toll Collection

Total existing emission levels of a particular pollutant (E_{PT}) were measured by utilizing queuing theory rather than direct field measurements. E_{PT} was broken down into two components:

$$\sum_1^3 E_{PT} = \sum_1^3 E_{PQ} + \sum_1^3 E_{PS} \tag{4}$$

where

E_{PT} = pollutant total emission (i.e. CO₂, CO, or NO_x);

E_{PQ} = pollutant emission while the vehicle is moving in queue;

E_{PS} = pollutant emission while the vehicle is receiving service at toll booth counter.

The emissions, while the vehicle is moving in the queue, in turn, depend upon the emission rate of the particular pollutant and the position of the vehicle in the queue:

$$E_{PQ} = Q_L \times QR_{CO_2} \quad (5)$$

where

Q_L = Queue length

QR_{CO_2} = Rate of CO₂ emissions while moving in the queue

Queue length was determined by observing the position of the vehicle when it joins the back of the queue, and subsequently, adding up the lengths of the vehicles ahead of it. For ease of the calculation, the various types of vehicles were converted into either a standard truck of length 12 m or a compact midsize sedan of length 4 m. The rate of emissions of a particular pollutant was derived from secondary sources.

Finally, the emissions due to idling at the toll booth counter while paying toll depends upon the service time and the pollutant's idling emission rate for the vehicle:

$$E_{PS} = S_T \times IR_{CO_2} \quad (6)$$

where

S_T = Service time, as determined earlier (in s)

IR_{CO_2} = Rate of CO₂ emissions while idling at toll booth counter (in g/s).

As earlier, the rate of emissions of a particular pollutant was derived from secondary sources.

2.2 Emissions Due to Electronic Toll Collection

Five scenarios of ETC usage were simulated using the existing queuing metrics of inter-arrival time and service time. The criterion of minimizing system delay was used in simulating ETC usage. Both, inter-arrival and service times, the ETC lanes were simulated using the exponential probability distribution. Service rates of existing ETC toll booths from across the world were taken as benchmarks. The methodology to calculate the emissions was similar to the one employed in the previous section.

The following assumptions were made in the study:

- a. The traffic flow is constant in a short period.
- b. A two-server system is simulated; 1 MTC and 1 dedicated ETC lane.

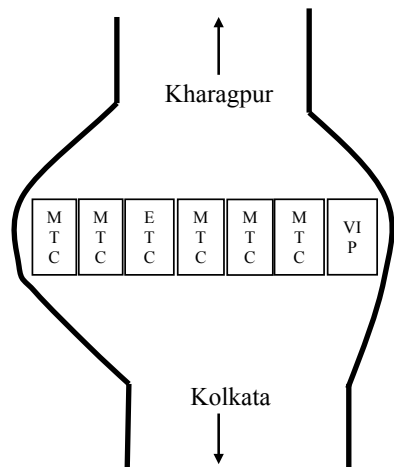
- c. A vehicle using the ETC lane will not encounter a queue, and its service time is exponentially distributed.
- d. The merging areas prior to and after the toll plaza are not considered in this study for delay or emission calculations.
- e. The arrival rate for the simulated ETC lanes is calculated using Little’s Law.
- f. The idling emission of vehicles was found to be 4636 g/h (1.29 g/s) of CO₂, 20 g/h (0.0055 g/s) of CO and 86 g/h (0.024 g/s) of NO_x [10].

3 Data Collection

The toll plaza consisted of 13 lanes, 6 in each direction, with a 7th reversible VIP Lane. One out of the six lanes in each direction is being used as a dedicated ETC lane. The geometry of the toll plaza is such that it widens up more toward the lane 1 and lane 2, as is shown in Figure 1. 24-h data was collected on February 21, 2017, that constituted a total of 2,446 vehicles. All the vehicles were sub grouped under two broad categories of trucks and midsize compact sedans. The percentages of trucks were 57% and for midsize sedans were 43%. The mean service time for a 24-h day was 21 s, whereas the mean queue time was 68 s.

Data collected at the MTC lane revealed that the average arrival rate (average inter-arrival time 24 s) of vehicles was 150 veh/h, whereas the average service rate was 300 veh/h (average service time 12 s). At the same time, in the ETC lane, vehicles are arriving at an average rate of 2.58 veh/h (average inter-arrival time 16 min 14 s), and the average service rate at the toll booth counter was 29.75 veh/h (average service time 121 s).

Fig. 1 Toll plaza sketch plan on NH-6



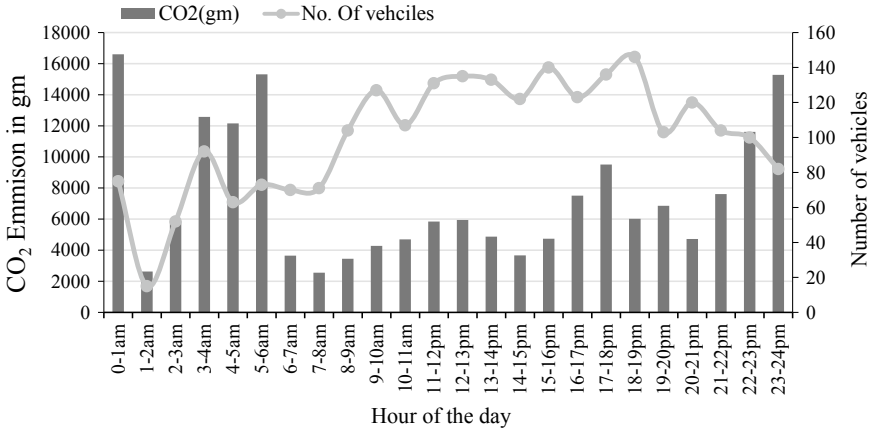


Fig. 2 CO₂ emission in MTC lane

The average system delay was found to be 57 s. A comparison of the MTC and ETC lanes indicates that the ETC lanes are not yet being utilized, possibly due to lack of awareness among the drivers since it was inaugurated recently in May 2016. During conversations with the authorities, it was mentioned that currently only 290 RFID transponders were registered with the users.

4 Data Analysis

4.1 Emissions in MTC Lane

During the 24-h study period, the total CO₂ emissions were 177 kg, total NO_x emissions were 51 kg, and the total CO emission was 72 kg. The hourly variations in emissions during the study period are shown in Figs. 2, 3, and 4. It was observed that CO₂ and CO emissions were not strongly correlated to the number of vehicles, whereas NO_x emissions had a strong correlation.

4.2 Emissions in ETC Lane

It was further noted that the number of vehicles using ETC was very less compared to MTC, where the ratio was 30:1. The interrelationship between the speed and emission factor of pollutant caused by the vehicles is explained by Matthew [11]. The study assumed that approximately 70 m prior to the toll plaza, the drivers decide

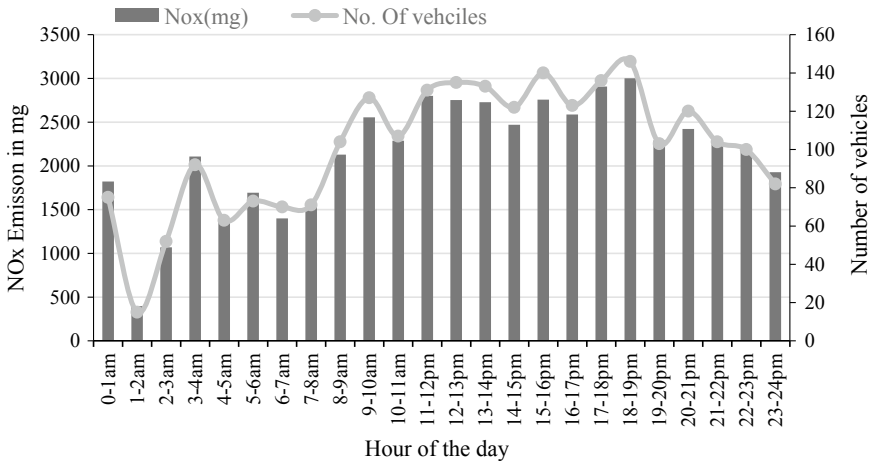


Fig. 3 NO_x emission in MTC lane

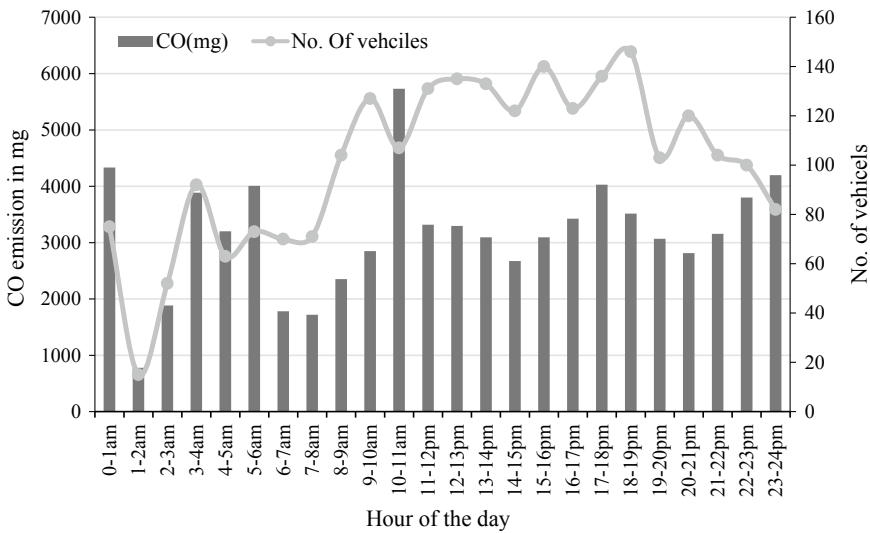
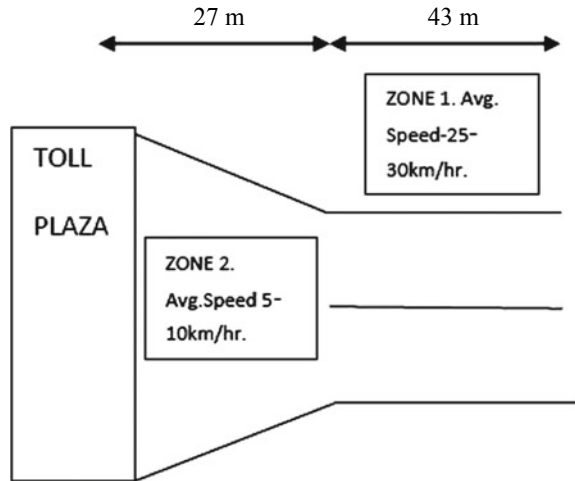


Fig. 4 CO emission in MTC lane

which lane he/she must opt to reach the counter in a minimum time based on the queue length and the number of vehicles [12].

As per Fig. 5, this length of 70 m is divided into two zones, the first one of 43 m and the second of 27 m. When the vehicle is in Zone 1 they travel at a speed of around 25–30 km/h. As such, the emission is estimated for the distance it has travelled. When the vehicle reaches Zone 2 and enters the ETC lane to pay toll electronically, the speed of the vehicle is approximately 5–10 km/h. As such, the

Fig. 5 Zones in toll plaza



emission in Zone 2 is calculated separately. The total emission in ETC lanes can be found out by adding the emission at Zone 1 and Zone 2. Emission of NO_x at zone 1 at an observed speed of 25–30 km/h was found to be in the range of 1100–1800 mg/m, whereas at Zone 2 at an observed speed of 5–10 km/h is found to be in the range of 900–700 g/m [11]. Similarly, for CO_2 , the emission at Zone 1 is found to be in the range of 0.198–0.222 g/m, and the emission at Zone 2 is found to be in the range of 0.1–0.11 mg/m [11]. Again referring to the same secondary source, for CO, the emission at zone 1 is found to be in the range of 0.001–0.019 g/m, and at Zone 2 was 0.001–0.019 g/m [11].

4.3 Use Rate of ETC Versus Reduction in Emission

As explained in the earlier sections, the use rate of ETC as compared to MTC was found to be low, it is assumed that in the near future, drivers would be more aware and use rate may increase; thus, it is of importance to see if there is any benefit if the use rate of ETC increases in term of environmental benefits. Four different cases were simulated where the ETC use rate has been progressively increased in concurrence with a base case where all the cars are driving through the MTC lane.

Base Case The total number of vehicles observed in the toll plaza was 2,446. In the base case, we consider the total NO_x emission from vehicles is due to the use of MTC lanes only. This has already been determined and shown in the previous section to be 51,487 mg.

Case 1 Next, the ETC-enabled vehicles were increased in the proportion of 30:1 (which is the existing condition). The ETC use rate is 3.27%. For this rate, the emis-

sion of NO_x of vehicles is 49,648 mg. And the pollution for ETC-enabled vehicles due to NO_x is 3.3 mg. There is a consequent reduction of NO_x emissions of 3.57%.

Case 2 The new proportion used was 25.6:5. The ETC use rate is 16.35%. For this rate, the pollution due to 2,046 vehicles due to NO_x is 42,891 mg. And the pollution for ETC-enabled vehicles due to NO_x is 17 mg.

Similarly, cases 3 and 4 were developed for 50 and 100% ETC usage rate along with the similar set of analysis for were done for CO_2 and CO (Figs. 6, 7 and 8).

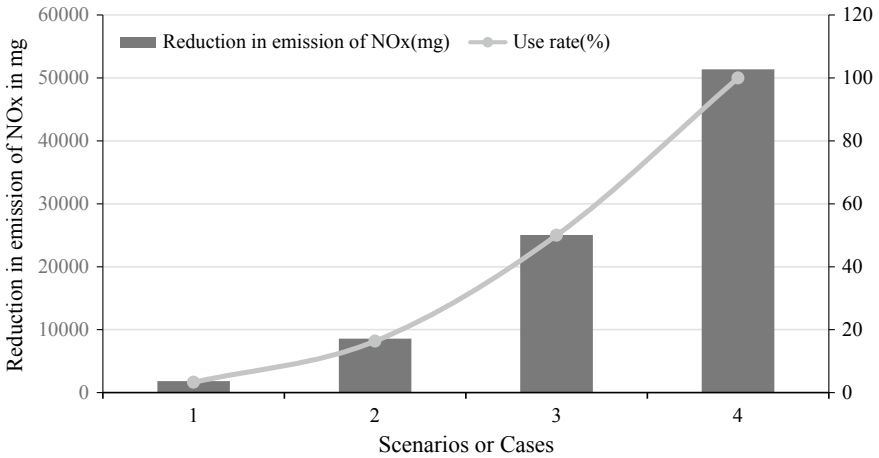


Fig. 6 NO_x emission reduction—ETC usage scenarios

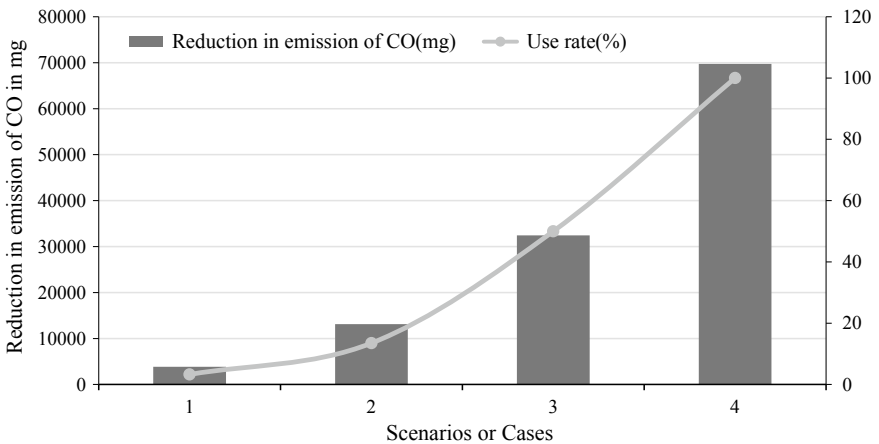


Fig. 7 CO_2 emission reduction—ETC usage scenarios

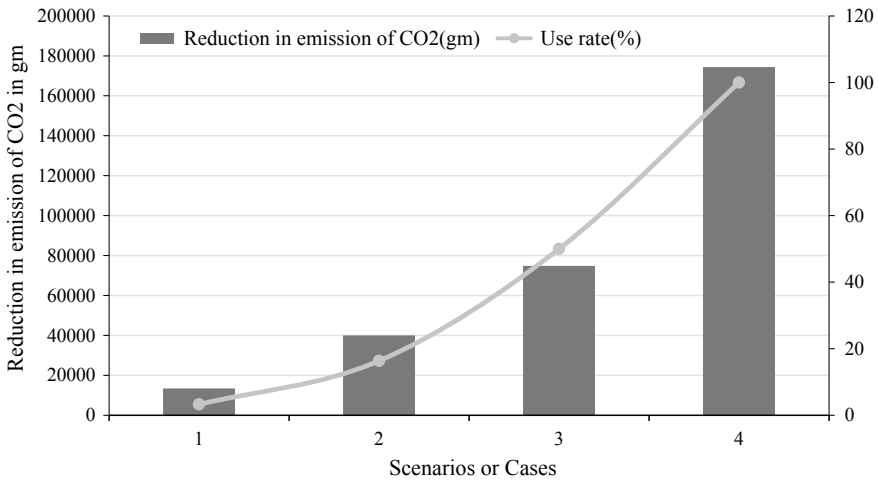


Fig. 8 CO emission reduction—ETC usage scenarios

4.4 Findings and Discussion

It is thus evident from the analysis that as the usage of the ETC lanes are increased there is a reduction in the emissions of NO_x , CO, and CO_2 , if the usage rate of ETC be even increased to 50%, there is a reduction in the emission of these pollutants by 42, 22, and 64%, respectively. Presently for the simulation of the queuing model for estimating the optimum delay of 57 s of the overall toll plaza had used a service rate of 700 veh/h for the ETC lane, however, international literatures on ETC lanes suggest that service rate at ETC lanes could go up to 1200 veh/h [13] for “no-stopping/drive through” ETC lanes. Even if the “no-stopping” ETC lanes are not feasible for ETC lanes in India at present, the possibility to increase the service rate of ETC lanes more than 700 veh/h would further decrease the emission of pollutants.

5 Conclusion

The present contribution and the significance of the results lie in the fact that the ETC technologies are still in a very nascent stage and could be enhanced even further to achieve the goal of a smaller delay to its users and lower impact to the environment. In this research, the study site so selected had a very recent introduction to the ETC technologies. Comparing the base case (from the analysis section) where no ETC lane was available in the toll plaza to the case where there is a 30:1 ratio of ETC usage, considerable reduction in the emission was seen for NO_x (4%), CO (19%) and CO_2 (8%). Thus, it is advocated that the ETC usage should be increased by the concerned authorities by making its user aware of its benefits.

6 Future Work

The study demonstrated a planning-level methodology to determine the environmental benefits of ETC toll collection systems. Their study is to be further strengthened by validating the results of existing emissions by conducting on-field emission measurements. Furthermore, decelerating and accelerating zones have to be taken into consideration to further fine-tune the emission measurements. In addition, data from several other toll booths can be collected to strengthen the findings.

Acknowledgements We would like to express our sincere gratitude to Mr. Ashutosh Gautam (Chief General Manager, Tech) of National Highways Authority of India (NHAI), Regional Office Kolkata. Also, we convey our profound gratitude to Mr. S Mukherjee (Manager, Tech) of NHAI, RO Kolkata. In addition, we would like to thank Mr. Ravi Mishra (Toll Manager) at the Dhulagarh Toll Plaza. Finally, we thank IT Officers Mr. Subrata Pal and Pallab Mallick for their help, without which we could not have completed the project successfully. Last but not the least, we express our heartfelt thanks to many students of RCGSIDM, IIT Kharagpur who helped us to complete our project successfully. A very special mention to research scholar Mr. Kuldeep Kavta, whose efforts toward compiling and structuring this paper, is well appreciated.

References

1. Mitra S (2014) Operational efficiency of freight transportation by road in India. Technical report, Transport Corporation of India & Indian Institute of Management Calcutta
2. Huang ZN, Pan JC, Wu YJ, Huang CY (2006) Investigation on health effect of indoor air pollution in the toll-gates. *J Occup Health Emerg Res* 24:43–44. <https://doi.org/10.3390/ijerph14010037>
3. Waersted K (2005) Urban tolling in Norway—practical experiences, social and environmental impacts and plans for future systems. In: PIARC seminar on road pricing with emphasis on financing, regulation and equity. <https://www.piarc.org/ressources/documents/281,2.1-Waersted-0405C11.pdf>
4. International Bridge, Tunnel & Turnpike Association (IBTTA) https://ibtta.org/sites/default/files/documents/MAF/2015_FactsInBrief_Final.pdf
5. Persad K, Walton CM, Wang Z, Hussain S, Robertson C (2007) Electronic vehicle identification: industry standards, performance, and privacy issues. Technical report, Texas Department of Transportation, Austin. http://ctr.utexas.edu/wp-content/uploads/pubs/0_5217_P2.pdf
6. Saffarzadeh M, Rezaee-Arjroody A (2009) Cost-benefit analysis of electronic toll collection (ETC) system in Iranian freeways (case study : Tehran-Qom freeway). In: 16th ITS world congress and exhibition on intelligent transport systems and services. Transportation research international documentation
7. Hensher DA (1991) Electronic toll collection. *Trans Res Part A Gen* 25:9–16
8. Tseng PH, Lin DY, Chien S (2014) Investigating the impact of highway electronic toll collection to the external cost: a case study in Taiwan. *J Technol Forecast Soc Change* 86:265–272. <https://doi.org/10.1016/j.techfore.2013.10.019>
9. National Highway Authority of India (NHAI) (2011) Electronic toll collection. Technical report, Apex Committee for ETC Implementation, New Delhi
10. Khan BMS, Clark NN, Thompson GJ, Wayne WS, Gautam MD, Lyons W, Hawelti D (2006) Idle emissions from heavy-duty diesel vehicles: review and recent data. *J Air Waste Manag Assoc* 56:1404–1419

11. Mathew TV (2014) Fuel consumption and emission studies. In: Transportation systems engineering. IIT Bombay, Mumbai, pp 1–25
12. Indian Roads Congress (2014) Four-laning of highways through public private partnership. IRC special publication no 84, New Delhi

Strategy to Reduce Queuing Time at Toll Plaza



Amit Kumar, Ashwini Thakare and Abhay Tawalare

Abstract It is observed that many of the toll plazas across India face congestion or long queues on one (major flow) side only, during some particular peak timing in a day or on weekend or during festival season. Long queues have been noticed during these particular timing on one (major flow) side while other (minor flow) side remains congestion-free most of the time. Thus, the lanes on the other side generally remain unused in such situations. This paper attempts to provide a solution to the above-discussed problem at toll plaza to reduce queue length/queue time on the problematic side. The paper presents the results of the reversible lane concept for collection of toll by optimizing the toll servers according to the demand from a particular side, resulting in optimization of queue length/queue time. The case study methodology is used to validate the proposed optimization strategy. The real-time data was collected from one of the toll plaza on National Highway 6. The analysis was performed using simulation and M/M/1 queue model. Simulation was adopted in the analysis to get a real-world situation by considering randomness in the field data. This model calculates the present and future values of parameters like average queue length, average waiting time of a customer, total time spent in the system, traffic handling capacity of each server and toll plaza. The result showed that the implementation of the reversible lane concept for toll collection reduces congestion from the problematic side and optimizes the queuing length/queuing time. Since the queue length will be reduced, people will not avoid the toll plaza because of longer queuing time, and the revenue generation will not be affected. Also, the vehicle will stand idle for less period of time, and the fuel consumption and vehicular emission will be lowered.

Keywords Queue model · Simulation · Queue length

A. Kumar (✉) · A. Thakare · A. Tawalare (✉)
Department of Civil Engineering, Visvesvaraya National Institute of Technology,
Nagpur 440010, India
e-mail: amitalgarh@gmail.com

A. Tawalare
e-mail: abhaytawalare@civ.vnit.ac.in

A. Thakare
e-mail: thakreashu10@gmail.com

1 Introduction

As we all know that most of the services are not utilized to its full extent, we always try to get maximum output and benefit from a service. That can be achieved by proper planning, analyzing the service again and again and with proper management or by other means. Same is the case with toll plaza service. Toll plazas are designed to handle the traffic flow on present assumptions but over the time due to economic reasons, new trend patterns and new policies or due to some other factors, the present capacity of toll plaza is not sufficient to cater the traffic smoothly, and congestion and long queues are observed at toll plaza in future. Due to the presence of long queues at toll plaza section, people get panicked either they do not pay the toll and fight with the operator of the toll plaza or they choose other alternative way to avoid congestion and toll, which in turn affects the revenue generation. Due to congestion and waiting in the queues, there is wasting of time, fuel, and money, and it also has environmental and health issues too.

Although many methods have been proposed to address the queuing problem at toll plaza including (ETC) electronic toll collection and advance transportation management system, each system comes with a significant monetary and operating cost and with different constraints. We consider the reversible toll collection as one of the cost-effective methods to increase the capacity of the existing toll plaza. The principle of reversible toll collection is to configure the toll servers of toll plaza to match available capacity to the traffic demand. These reversible toll servers are particularly effective because they take advantage of the unused capacity in the minor flow direction side to increase the capacity in the major flow direction, thereby eliminating the need to construct additional toll servers. This method is most effective when highly unbalanced directional flows are present, such as those that occur during some particular daily peak period, on weekend, and during festival season. In Indian condition, traffic is heterogeneous and huge randomness is present. So, for each and every different situation, we have to provide different solutions, so that each service is utilized to its maximum or to its optimal extent. Therefore, optimization is must needed.

2 Literature Study

The importance of reversible or convertible facilities on highways has been addressed in synthesis 340 of NCHRP on Convertible Roadways and Lanes by Transportation Research Board [1]. This synthesis addresses the requirement for an expanded dimension of understanding with respect to convertible and reversible lane use. The synthesis reports the verifiable improvement of reversible lanes, applications for different requirements, exercises gained from the past usage, expenses and advantages related with their utilization, and different procedures and fruitful practices that have been created.

Highway performance gets reduced due to the formation of long vehicular queues amid a congested period. Numerous non-transportation fields, for example, the activities of modern plants, warehouses, shops, administration situated ventures, phone systems, and PC systems should likewise give genuine thought to the issue of queuing. In 1909, Erlang gives ideas about queuing theory in his research paper “the theory of probabilities and telephone conversations” [2]. His spearheading work invigorated numerous authors to build up an assortment of queuing models incorporating various arrival nature, various service time distributions. Queuing hypothesis is the numerical investigation of waiting queues.

In queuing theory, a model is constructed so that queue lengths and waiting time can be predicted. Mannering et al. [3], they discussed the queuing theory in their book. In this queuing theory is discussed with the help of queuing models. Queuing models are regularly distinguished by three alphanumeric notations. The primary esteem demonstrates the arrival rate supposition, the second esteem gives the take off presumption, and the third esteem shows the number of take off channels. For traffic landing and flight presumptions, the uniform, deterministic appropriation is meant as D and the exponential dissemination is meant M. In view of this, following kind of models are created D/D/1, M/D/1, M/M/1, and M/M/N queuing. M/M/1 queuing model that accepts one take off station and exponentially dispersed arrival and take off times are appropriate in some rush hour traffic applications. For instance, exponentially dispersed take off examples may be a sensible assumption at a toll plaza, where some landing drivers have the right toll and can be handled rapidly and others do not have the right toll, creating a distribution of takeoffs about some mean take off rate. With the help of this model, we can find the average length of queue in vehicles, average waiting time, and average time spent in the system.

Sztrik [4] also discussed queuing theory in his book. He explained various queue models using Kendall’s notation A/B/m/K/n/D. Edie [5] had done work in toll design, who considers traffic delays at tollbooths of homogenous booths and homogenous vehicles. At the point when a circumstance is influenced by arbitrary factors usually hard to get close from conditions that can be utilized for valuation. Simulation is a general method for assessing factual proportions of a perplexing framework. Therefore, to consider the randomness present in the traffic flow, simulation analysis is considered for analysis of toll plaza problem.

Shanmugasundaram and Punitha [6], “Over viewing the tollgate system in Salem”, this paper shows the results of the simulation model which has been used in this study, and the analysis of simulation gives two sorts of perceptions. One is the executives can without much of a stretch discovers which framework is occupied and which framework is perfect. The other one is to examine the numerical investigation of the toll server to accomplish increasingly productive execution. In this, they determined the line length, the client holding up time, and normal administration times in toll entryway. It exhibited the fundamental thoughts for a recreation-based way to deal with mathematical information. The numerical examination demonstrates the plausibility of the framework. Shanmugasundaram and Banumathi [7], in this paper, they analyzed the queuing problem of Southern Railway using the Monte Carlo simulation technique. The principle point of this paper is the future conduct of Southern

Railway and how to diminish the queue length and system length, queue time and system time which is compared to the analytical method. Aradhya and Kallurkar [8], in this paper, they optimize the length of the queue as well as the waiting period of the pilgrims at Shri Vitthal Rukmini Mandir, Pandharpur.

Kim [9], in this article, a discrete-event simulation technique is utilized to examine the affectability of toll booth execution for various kinds of traffic stream. Two traffic patterns, deterministic and probabilistic traffic stream, are considered. The assessed future traffic for the toll bridge is utilized to consider the distinction between the two traffic designs.

3 Data Collection

Traffic flow data including vehicular arrival time and service time at toll plaza section was collected for Nagpur to Amravati side and for Amravati to Nagpur side on Gondhkhairi toll plaza, km 20-NH6, Nagpur to Amravati NH6. Traffic data was collected on peak days before Diwali festival from 29th October 2016 to 30th October 2016 for 48 h. For this, CCTV footage was collected from the operator (M/S Atlanta Infra Assets Ltd) under the guidance of NHAI. The required data is generated from the CCTV footage. For each side of traffic, there are four toll servers; one is ETC enabled and the other three do manual collection only. Since ETC users are very few, so most of the transaction is through the manual collection only. At this toll plaza, every user is free to choose any lane to pay toll, because ETC lane toll server also collects toll manually. So for the simplicity of the analysis, we considered same behavior of each server. So, the service time of each server is considered same. During the peak period, each server gets almost equal traffic volume. So for the simplicity of the analysis, we considered homogeneity in toll booths and homogeneity in vehicle arrival and vehicle departure, i.e., at any point of time equal numbers of vehicles will be waiting for service at each server on a particular side.

The Gondhkhairi toll plaza will face directional congestion during morning peak period (8:00–10:30 a.m.) on Nagpur to Amravati side and Amravati to Nagpur side will remain congestion-free during this period. And during the evening peak period (5:30–8:00 p.m.), Amravati to Nagpur side will face congestion and Nagpur to Amravati side will remain congestion-free. From the CCTV footage, we get the vehicular arrival rate (λ) (Table 1).

Table 1 Vehicular arrival table

Sr no.	Side	Timing	λ (veh/h)
1	Nagpur to Amravati	8:00–10:30 a.m.	436
2	Amravati to Nagpur	8:00–10:30 a.m.	260
3	Nagpur to Amravati	5:30–8:30 p.m.	448
4	Amravati to Nagpur	5:30–8:30 p.m.	280

Table 2 Service time distribution table

Sr. no.	Service time (s)	No. of vehicles	Probability	Cumulative probability	Tag no.
1	15	2294	0.274	0.274	0–273
2	25	2956	0.353	0.627	274–626
3	35	1398	0.167	0.794	627–793
4	45	996	0.119	0.913	794–912
5	55	302	0.036	0.949	913–948
6	65	242	0.029	0.978	949–977
7	75	184	0.022	1	978–999
Total		8372			

Since toll is collected manually through cash, card payment or by other means of payment each vehicle gets different service time because some drivers have exact cash and some do not have so service time varies customer to customer. Since we are considering homogeneity in departure time for the analysis, we require a simulated average service time which considers randomness in data and gives a representation of the real-time situation. Vehicular departure rate (μ) will be generated through the following simulation as shown in Tables 2 and 3 to get realistic values by considering randomness in the field data [10].

4 Assumptions

- System is homogenous for a particular side/direction of traffic flow.
- Every approaching vehicle is free to choose any toll server.
- At any point of time, equal numbers of vehicles will be waiting for service at each server on particular side, i.e., queue length and waiting time are same behind every server on particular side/direction.
- All type of vehicles will be considered as one vehicle unit.
- System has an infinite capacity to handle the queues.
- First Come First Serve (FCFS) queue discipline is followed.

5 Optimization of Queue Length and Toll Servers

We consider the reversible toll collection as one of the cost-effective methods to increase the capacity of the existing toll plaza. The principle of reversible toll collection is to configure the toll servers of toll plaza to match available capacity to the traffic demand. These reversible toll servers are particularly effective because they

Table 3 Calculation simulation table

Sr. no.	1	2	3	4	5	6	7	8	9	n	Average
Random no.	830	569	410	50	136	714	679	251	444	82	
Service time (s)	45	25	25	15	15	35	35	15	25	15	29.82

take advantage of the unused capacity in the minor flow direction side to increase the capacity in the major flow direction, thereby eliminating the need to construct additional toll servers.

Right now at Gondhkhairi toll plaza, there are total eight toll servers, four toll servers for each side as shown in Fig. 1. We are suggesting for this particular toll plaza if we make the middle two toll servers reversible so that they can operate for both the directions according to the demand of capacity as shown in Figs. 2 and 3. In that case for major flow side, $4 + 1 = 5$ toll server will be available during peak period, and for minor flow side $4 - 1 = 3$ toll server will be available. By doing so, we will be able to optimize the toll server capacity and queue length.

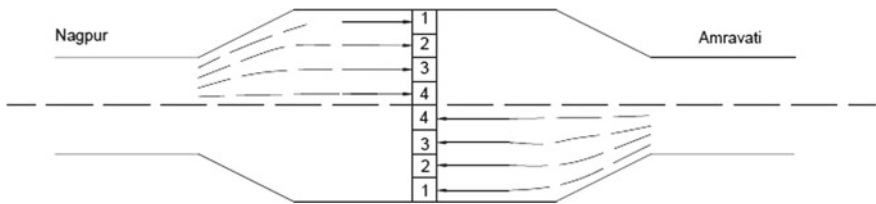


Fig. 1 Present configuration of Gondhkhairi toll plaza

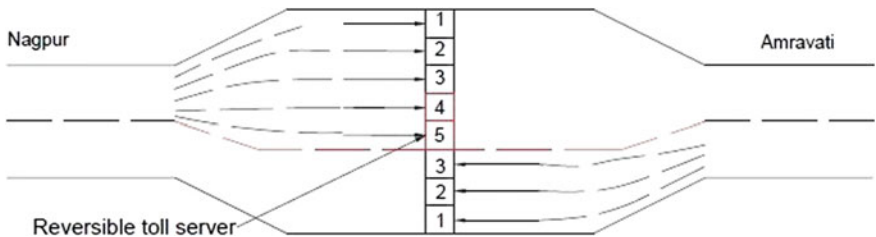


Fig. 2 Proposed configuration of Gondhkhairi toll plaza (morning peak period)

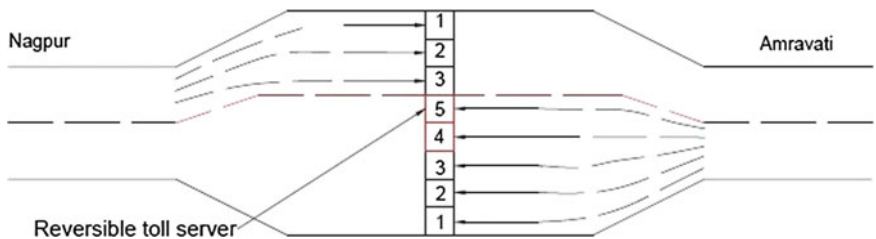


Fig. 3 Proposed configuration of Gondhkhairi toll plaza (evening peak period)

6 Model Analysis

For the analysis purpose, M/M/1/∞*/∞/ FCFS model is adopted. Here, first M stands for exponentially distributed arrival, second M stands for exponentially distributed departure, 1 is the departure channel, ∞* is system queue capacity, ∞ size of the population of the jobs to be served, and FCFS is the queue discipline. Under standard M/M/1 assumptions at toll booth following queuing equation can be applied (assuming $\rho < 1$):

$$\text{Average length of waiting queue in vehicle } (Q) = \frac{\rho^2}{(1 - \rho)}$$

$$\text{Average length of vehicle queue in system } (Q_s) = \frac{\rho}{1 - \rho}$$

$$\text{Average waiting time in queue, in unit time per vehicle } (W) = \frac{\lambda}{\mu(\mu - \lambda)}$$

$$\text{Average time spent in the system, in unit time per vehicle } (T) = \frac{1}{\mu - \lambda}$$

where $(\rho) = \frac{\lambda}{\mu}$ (Traffic intensity, unit less)

(λ) = average arrival rate in vehicles per unit time, and

(μ) = average departure rate in vehicles per unit time.

6.1 Calculations for Morning Peak Period (8:00–10:30 a.m.)

Case 1—When a number of toll servers are equal for both sides, ($N = 4$).

(a) *Nagpur to Amravati side*

Total vehicular arrival rate for four servers from Table 1 = 436 veh/h.

So, vehicular arrival rate for single server $(\lambda) = 109 \text{ veh/h} = 1.816 \text{ veh/min}$.

From Table 3, average service time = 29.82 s.

So, vehicular departure rate $(\mu) = 2.012 \text{ veh/min}$.

Since simulated average service time is taken for all the servers equally, the vehicular departure rate will remain the same 2.012 veh/min for the rest of the calculations.

$\rho = 0.90 < 1$, we can use M/M/1 queue model.

Using equations of M/M/1 queue model, we get the following results:

Average length of waiting queue in vehicle $(Q) = 8.36 \text{ veh}$

Average length of vehicle queue in system $(Q_s) = 9.26 \text{ veh}$

Average waiting time in queue, in unit time per vehicle $(W) = 4.60 \text{ min/veh}$

Average time spent in the system, in unit time per vehicle $(T) = 5.10 \text{ min/veh}$.

(b) Amravati to Nagpur side

Total vehicular arrival rate for four servers = 260 veh/h.

So, vehicular arrival rate for single server (λ) = 65 veh/h = 1.083 veh/min.

Vehicular departure rate (μ) = 2.012 veh/min.

$\rho = 0.538 < 1$, we can use M/M/1 queue model.

Average length of waiting queue in vehicle (Q) = 0.63 veh

Average length of vehicle queue in system (Q_s) = 1.16 veh

Average waiting time in queue, in unit time per vehicle (W) = 0.58 min/veh

Average time spent in the system, in unit time per vehicle (T) = 1.08 min/veh.

Case 2—After implementation of reversible toll server lanes.**(c) Nagpur to Amravati side (Number of servers = 4 + 1 = 5)**

Total vehicular arrival rate for five servers = 436 veh/h.

So, vehicular arrival rate for single server (λ) = 87.2 veh/h = 1.453 veh/min.

Vehicular departure rate (μ) = 2.012 veh/min.

$\rho = 0.722 < 1$, we can use M/M/1 queue model.

Average length of waiting queue in vehicle (Q) = 1.88 veh

Average length of vehicle queue in system (Q_s) = 2.60 veh

Average waiting time in queue, in unit time per vehicle (W) = 1.29 min/veh

Average time spent in the system, in unit time per vehicle (T) = 1.78 min/veh.

(d) Amravati to Nagpur side (Number of servers = 4 - 1 = 3)

Total vehicular arrival rate for four servers = 260 veh/h.

So, vehicular arrival rate for single server (λ) = 86.66 veh/h = 1.444 veh/min.

Average service time = 29.82 s.

So vehicular departure rate (μ) = 2.012 veh/min.

$\rho = 0.717 < 1$, we can use M/M/1 queue model.

Average length of waiting queue in vehicle (Q) = 1.82 veh

Average length of vehicle queue in system (Q_s) = 2.54 veh

Average waiting time in queue, in unit time per vehicle (W) = 1.26 min/veh

Average time spent in the system, in unit time per vehicle (T) = 1.76 min/veh.

6.2 Calculations for Evening Peak Period (5:30–8:30 a.m.)

In the similar way, all the calculations were done for the following traffic data for evening peak period and results were shown in Table 4.

Table 4 Results

Sr no.	Parameters	Mrmg. peak period (8:00–10:30 a.m.)						Evng. peak period (5:30–8:30 p.m.)					
		Present ($N = 4$)			Proposed ($N = 4 \pm 1$)			Present ($N = 4$)			Proposed ($N = 4 \pm 1$)		
		Ngp to Amv	Amv to Ngp	Ngp to Amv	Amv to Ngp	Ngp to Amv	Amv to Ngp	Amv to Ngp	Ngp to Amv	Amv to Ngp	Ngp to Amv	Amv to Ngp	Ngp to Amv
1	Q (veh)	8.36	0.63	1.88	1.82	11.85	2.13	0.80	2.58	11.85	2.13	0.80	2.58
2	Q_s (veh)	9.26	1.16	2.60	2.54	12.78	2.87	1.38	3.35	12.78	2.87	1.38	3.35
3	W (min per veh)	4.60	0.58	1.29	1.26	6.35	1.43	0.68	1.67	6.35	1.43	0.68	1.67
4	T (min per veh)	5.10	1.08	1.78	1.76	6.85	1.93	1.18	2.16	6.85	1.93	1.18	2.16
5	$\rho = U$	0.9	0.538	0.722	0.717	0.927	0.742	0.58	0.77	0.927	0.742	0.58	0.77

Case 1—When a number of toll servers are equal for both sides, ($N=4$).**(a) Amravati to Nagpur side**

Total vehicular arrival rate for four servers = 448 veh/h.

So, vehicular arrival rate for single server (λ) = 112 veh/h = 1.866 veh/min.

Vehicular departure rate (μ) = 2.012 veh/min.

(b) Nagpur to Amravati side

Total vehicular arrival rate for four servers = 280 veh/h.

So, vehicular arrival rate for single server (λ) = 70 veh/h = 1.166 veh/min.

Vehicular departure rate (μ) = 2.012 veh/min.

Case 2—After implementation of reversible toll server lanes.**(c) Amravati to Nagpur side (Number of servers = $4 + 1 = 5$)**

Total vehicular arrival rate for five servers = 448 veh/h.

So, vehicular arrival rate for single server (λ) = 89.6 veh/h = 1.493 veh/min.

Vehicular departure rate (μ) = 2.012 veh/min.

(d) Nagpur to Amravati side (Number of servers = $4 - 1 = 3$)

Total vehicular arrival rate for four servers = 280 veh/h.

So, vehicular arrival rate for single server (λ) = 93.33 veh/h = 1.55 veh/min.

Vehicular departure rate (μ) = 2.012 veh/min.

7 Results and Discussion

From the above results, it is clearly observed that queue length and waiting time are minimized to a great extent on problematic major flow direction due to increment in available servers, and there is a little increase in the queue length and waiting time on minor flow direction due to reduction of available servers; by doing so, we will be able to increase the efficiency of toll plaza. This also optimizes the utilization of toll servers. In the present situation, if a commuter is using the service of toll plaza, Nagpur to Amravati side during morning peak period while going toward Amravati from Nagpur, he has to face an average queue length of 8.36 vehicles and waiting of 4.60 min. In case, if he is returning back from Amravati side to Nagpur during evening peak period again, he has to face an average queue length of 11.85 vehicles and waiting of 6.35 min. In total, he has to face an average of 20.21 vehicles queue length and waiting time of 10.95 min.

If we adopt the reversible toll lane concept, in that case this reduces to four vehicles queue length and waiting time 2.72 min. And at the same time for minor flow direction, the customer will face queue of 4.4 vehicles instead of 1.43 vehicles in total and waiting time of 2.93 min instead of 1.26 min in total. So in the proposed scenario, queue length and waiting time will be almost equal on both sides instead of long queues on one particular side.

8 Conclusion

From the analysis, it is clear that at any toll plaza if the directional flow is unbalanced during some periods, reversible toll lane system is an effective solution to reduce the queue length and waiting time from major flow direction, and it increases the efficiency and overall capacity of the toll plaza. These reversible toll servers are particularly effective because they take advantage of the unused capacity in the minor flow direction side to increase the capacity in the major flow direction, thereby eliminating the need to construct additional toll servers. This system is more beneficial where there is existence of highly unbalanced directional flow and where there is a restriction to increase the number of servers like at tunnels, bridges, etc. For the Indian scenario where people are not adopting electronic toll collection (ETC), this concept can be useful to increase the efficiency and capacity of toll plazas. The transitional operation of reversible toll server and lanes requires some changes in configuration in toll plaza system. For the smooth transition of reversible toll server and lanes, lane use control signals, overhead changeable lane use signals, pavement marking, and portable devices such as movable barrier, cones, pedestals, tubes, etc., are required. Due to time constraints, the analysis was done on one toll plaza only, and we understand that the result of one toll plaza cannot be generalized; we need to study this for a significant number of toll plazas to give the generalized result. We hope that in our next paper we will take more number of toll plazas and also categorize the vehicles. Further study is needed in effective implementation of the reversible toll collection system, and cost-benefit analysis is also needed.

References

1. National Cooperative Highway Research Program (NCHRP) (2004) Synthesis 340. A synthesis of highway practice on convertible roadways and lanes. Transportation Research Board
2. Erlang AK (1909) The theory of probabilities of telephone conversations. *Nyt Jindsskrift Math B* 20:33–39
3. Mannering F, Kilareski W, Washburn S (2009) Principles of highway engineering and traffic analysis. Wiley
4. Sztrik J (2012) Basic queuing theory
5. Edie LC (1954) Traffic delays at toll booths. *J Oper Res Soc Am* 2:107–138
6. Shanmugasundaram S, Punitha S (2014) A simulation study on toll gate system in M/M/1 queuing models. *IOSR J Math* 10(3), Ver. VI
7. Shanmugasundaram S, Banumathi P (2016) A simulation study on M/M/C queuing models. *Int J Res Math Math Sci* 2(2)
8. Aradhya A, Kallurkar S (2014) Application of queuing theory to reduce waiting period of pilgrim. *Int J Innov Res Sci Eng Technol* 3(10)
9. Kim BJ (2011) Conceptualization of traffic flow for designing toll plaza configuration: a case study using simulation with estimated traffic volume. *Int J Ind Eng* 18(1):51–57
10. Gentle JE (2003) Random number generation and monte carlo methods. Springer

Estimation of Dynamic Equivalency Factor Under Heterogeneous Traffic Condition on Urban Arterial Road—A Case Study of Porbandar City



Yash R. Dasani, Monicaba Vala and Bindiya Patel

Abstract This paper presents the concept of “Dynamic Equivalency Factor” (DEF) for the urban arterial roads under heterogeneous traffic condition, and it reflects that the PCU (Passenger Car Unit) is not a static factor as assumed. The parameters considered for the estimation of DEF are (1) average speed of the vehicle, (2) traffic composition, (3) time headway, and (4) roadway width. The traffic data was collected from three urban roads of Porbandar City, and it was collected at the mid-block section as of the following roads: (1) M.G Road, (2) S.V.P Road and (3) Chhaya Road. The mid-block section was kept of 30 M and traffic data was collected. The following road selected varies in road widths as two lanes divided and two lanes undivided and having different traffic composition. The sections were such selected that it was free from parked vehicles, bus stop, effects of the intersection, curvatures, etc. The DEF was obtained by the following methods (1) multiple regression method, (2) headway method, (3) Chandra’s method and (4) homogenization coefficient method. The traffic data was collected using videography technique for morning 8 a.m.–8 p.m. from which the morning peak hours 8:30–11:30 and evening peak hours 5–8 was concluded for the roads by the study of traffic volume. The peak hour traffic was used to calculate the DEF values and efforts were made to suggest the best realizable DEF value.

Keywords Dynamic equivalency factor · PCU · Traffic volume · IRC 106-1990 · Heterogeneous traffic

1 Introduction

The Passenger Car Unit values are estimated to simplify the estimation of the capacity of the road as in context to Indian roadway conditions there is a large variation in the vehicular characteristics on the roadway, and hence, it becomes difficult to estimate the roadway capacity with such variation. For this, the IRC (Indian Road Congress) has suggested the PCU values which gives a factor to convert the heterogeneous

Y. R. Dasani (✉) · M. Vala · B. Patel
Marwadi Education Foundation Group of Institution, Rajkot, India
e-mail: yashdasani83@gmail.com

© Springer Nature Singapore Pte Ltd. 2020
T. V. Mathew et al. (eds.), *Transportation Research*, Lecture Notes
in Civil Engineering 45, https://doi.org/10.1007/978-981-32-9042-6_37

traffic stream to the homogeneous traffic stream and car is used as the basic unit to convert the different classes of the vehicles. The PCU values suggested in IRC is adopted for roads in India. As all of the roads in India vary greatly in its geometric conditions, traffic conditions, etc., it becomes very necessary to incorporate such numerous dynamic factors which vary greatly from place to place in India. As the traffic in India is greatly growing with an ample amount of increase day to day, so the efforts to consider numerous dynamic factors affecting the PCU values are to be considered to provide a more economical environment in the road design and provide a safe environment of the roadway. DEF values calculated in this paper are an effort towards considering the effects of varying factors such as traffic volume, traffic speed, roadway width and average time headway for various kind of vehicles, and the values are estimated using four most commonly developed methods as Satish Chandra's method, homogenization coefficient method, multiple regression method and headway method and all the values of DEF are compared to the IRC values and the variations in the values are checked to suggest the best reliable method considering the effects of all possible factors considered affecting the DEF values.

2 Literature Review

- (2.1) From paper [1], we can state that the PCU values change with the change in road width and traffic volume. PCU value increases for the wider lane widths. Higher PCU values were found for bus, LCV, trailers and for 2W and auto-rickshaw it was lower than the standardized values by IRC.
- (2.2) In study [2], it was found that the PCU for a vehicle increases with increasing lane width. It was found that PCU values for motorcycle, auto-rickshaw, from all sections are smaller than the values given in IRC, and for truck, trailer and LCV were found higher than the value given in IRC 64-1990. Satish Chandra and Kumar's method was used. Speed and volume relation was developed.
- (2.3) In study [3], it was found that the PCU values for different vehicle categories increase with the increase of carriageway width and horizontal curve radius. The relationship was clearly observed in the case of heavy vehicles. The light vehicles had a small size with respect to the lane width, and therefore, the increase in lane width (or carriageway width) was not an important factor that increases PCU.
- (2.4) The increase of the traffic flow kept the PCE values constant without any changes, and in some cases, it decreased by 1 in case of trucks. No certain co-relation was found between PCE and traffic flow levels in case of highways and arterials. Total percentage of truck traffic affects the PCE value by 1–5 in some cases [4].
- (2.5) In study [5], it was found that the PCU value for a vehicle type varies with traffic volume and composition on the road. It was also affected by the type of road as well. Carriageway width also affects the PCU value for all types of vehicles. Chandra's method was used. Car value varies from 1.46 to 1.59 for

- two-lane roads, 1.23 to 1.55 for intermediate roads and 1.58 for single-lane roads.
- (2.6) In study [6], it was found that homogenization coefficient method gives higher PCU values for smaller vehicles as 2W, 3W compared to Chandra's method. Chandra's Method gives higher PCU values for larger vehicles as bus, LCV, truck and MAV compared to homogenization coefficient method. The PCU value obtained was $2W = 0.58$, $3W = 1.14$, $LCV = 1.97$, $Car = 1.00$, $Bus = 5.04$, $Truck = 2.64$, $MAV = 4.85$.
 - (2.7) In study [7], it was found that the PCU value of each vehicle is not a constant but varies with several factors such as the proportion of other classes, level of service and volume to capacity. In this study, the average value of speed and time headway was taken. PCU value obtained was $Car = 1.00$, $Motorcycle = 0.6$, $Van = 1.58$, $Small Lorry = 1.92$, $Big lorry = 2.58$, $Bus = 2.33$.
 - (2.8) The PCU values were found to be reduced with the addition in traffic flows at low traffic flow levels and at high traffic flows the PCU values increased with the addition of traffic flows for larger vehicles than the car. And in case of vehicles smaller than the car the above cases inverses at low traffic level PCU values increases with addition of traffic flow and at high traffic flows level the PCU value reduced with addition of the traffic flows. PCU values were not being affected for lengths more than 1600 m [8].
 - (2.9) The direct co-relation of MDM (modified density method) was with the average speed of the traffic. The HCM (homogenization coefficient method) was identified to be in direct relation with an average speed of the traffic and vehicle type. The THM (time headway method) was in direct relation with the average speed of the vehicle and the time gap between two passing vehicles [9].
 - (2.10) In study [10], it was found that, for Indian mixed traffic conditions, DCU (Dynamic Car Unit) is appropriate for converting vehicle flow into equivalent term. It was found that the variation in DCU was observed at different flow rate level enhances classification of DCU based on the flow rate variation. It was concluded that compare to IRC PCU values, DCU values are more appropriate and reliable. DCU Value of $2W = 0.44$, DCU Value of $3W = 0.70$, DCU Value of $Truck = 3.85$ and DCU Value of $Bus = 5.85$ were found in this study.

3 Data Collection

For the determination of DEF value classified traffic volume, average speed, headway, road width of all the different type of vehicles and roads are measured. Videography technique was used to collect 12 h traffic data. Classified volume, average speed and average headway are counted manually from the video data extraction. From the 12 h

data, the peak hours were known the DEF values were considered for peak hours only rest non-peak hours were omitted for the study.

4 Methods for Estimation of DEF Values

The methods used for the study are as under:

(4.1) Chandra's method

This method is the modification of homogenization coefficient method in which the length of the vehicle is considered for the PCU calculation while in here the length of vehicle is replaced by the projected area of the vehicle. The PCU value is determined by using the following equation:

$$PCU = V_c/V_i \div A_c/A_i \quad (1)$$

where V_c and V_i are speeds of car and vehicle i , respectively, and A_c and A_i are their projected rectangular area.

(4.2) Homogenization coefficient method

This method is mainly adopted by the developed countries where homogeneous traffic conditions persist and lane discipline is followed. The DEF value is determined by:

$$PCU = L_i/V_i \div L_c/V_c \quad (2)$$

where L and V are the length and speed of a vehicle; suffix i indicates a vehicle type and c indicates the car.

(4.3) Multiple regression method

Under this method, the DEF values are determined by expressing the speed-flow relationship in the form of multiple regression equation taking the speed of cars as the dependent variable and volume of different categories of vehicles as the independent variables. The ratio of the regression coefficients of different categories of traffic to the regression coefficient of the car will give an estimate of PCU factors. The speed of the car is regressed against the volumes of different types of vehicles as shown below:

$$V_1 = A_0 + A_1 \cdot Q_1 + A_2 \cdot Q_2 + A_3 \cdot Q_3 + \dots + A_n \cdot Q_n \quad (3)$$

where V_1 = Speed of cars, Q_1 = Flow of cars, Q_2, Q_3, \dots, Q_n = Flow of vehicle type 2, 3, ..., n , A_1, A_2, \dots, A_n = Regression coefficients and A_0 = Constant. The DEF of vehicle type n is given by: $DEF = A_n/A_1$.

(4.4) Headway method

PCU values are determined by taking ratio of mean headways for any vehicle type to mean headways for car mathematically:

$$PCU(x - x) = h(x - x) / h(c - c) \tag{4}$$

where $PCU(x - x) = PCU$ factor for any vehicle type x , $h(x - x) =$ Average headway for any vehicle type $(x - x)$, $h(c - c) =$ Average headway for car following car $(c - c)$.

5 Data Analysis

5.1 Chhaya Road

- A. Chandra’s method (Table 1, Fig. 1)
- B. Homogenization coefficient method (Table 2, Fig. 2)
- C. Multiple regression method (Table 3, Fig. 3)
- D. Headway method (Table 4, Fig. 4)

Table 1 DEF by Chandra’s method (Chhaya Road)

Type of vehicles	Towards Panch Hatdi	Towards Chhaya Area
2W	0.196775	0.206285
3W	0.801155	0.812645
Car	1.000000	1.000000
Bus	9.221080	10.017800
Truck	6.332940	5.951140
LCV	2.017750	2.124140
MAV	9.548255	9.985620

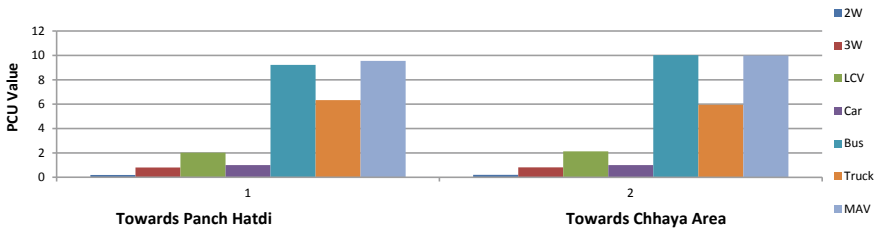


Fig. 1 DEF by Chandra’s method

Table 2 DEF by homogenization coefficient method (Chhaya Road)

Type of vehicles	Towards Panch Hatdi	Towards Chhaya Area
2W	0.441831	0.463176
3W	0.824536	0.836360
Car	1.000000	1.000000
Bus	5.110110	5.551650
Truck	3.317810	3.429990
LCV	1.453650	1.530300
MAV	5.478720	5.755140

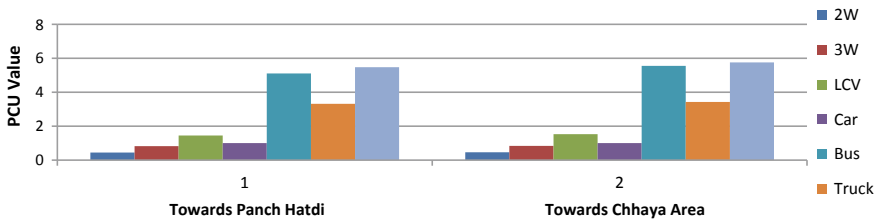


Fig. 2 DEF by homogenization coefficient method

Table 3 DEF by multiple regression method (Chhaya Road)

Type of vehicles	Towards Panch Hatdi	Towards Chhaya Area
2W	0.119115	0.201433
3W	0.765785	0.394273
Car	1.000000	1.000000
Bus	2.713550	3.382520
Truck	6.741280	4.641950
LCV	1.092980	1.402610
MAV	7.415680	5.287200

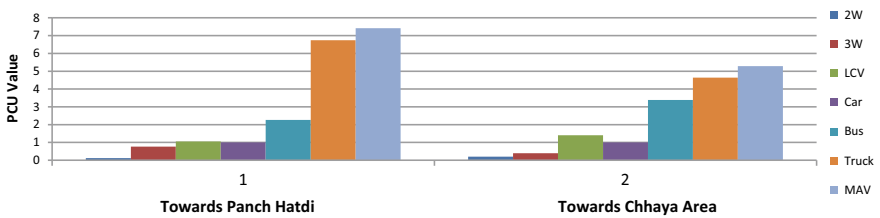


Fig. 3 DEF by multiple regression method

Table 4 DEF by headway method (Chhaya Road)

Type of vehicles	Towards Panch Hatdi	Towards Chhaya Area
2W	0.044101	0.101377
3W	0.137177	0.258023
Car	1.000000	1.000000
Bus	21.798000	31.726000
Truck	3.307100	9.174200
LCV	1.20300	2.546700
MAV	33.200000	33.967000

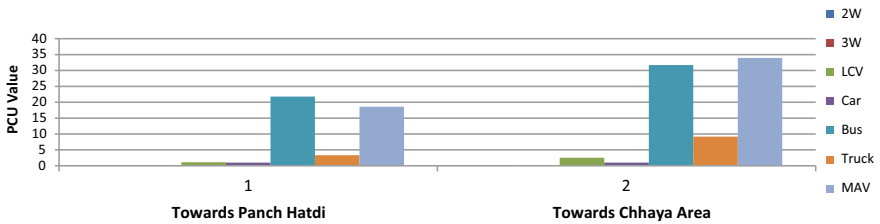


Fig. 4 DEF by headway method

5.2 M.G Road

- A. Chandra’s method (Table 5)
- B. Homogenization coefficient method (Table 6)
- C. Multiple regression method (Table 7)
- D. Headway method (Table 8)

Table 5 DEF by Chandra’s method (M.G Road)

Type of vehicles	Towards Sudama Chowk	Towards Kamla Baugh
2W	0.22919	0.23137
3W	0.89305	0.94464
Car	1.0000	1.000000
Bus	6.58090	6.71481
Truck	4.1134	4.10883
LCV	2.05312	2.23417
MAV	6.198261	7.402943

Table 6 DEF by homogenization coefficient method (M.G Road)

Type of vehicles	Towards Sudama Chowk	Towards Kamla Baugh
2W	0.514627	0.519504
3W	0.919118	0.972218
Car	1.0000	1.000000
Bus	3.6699	3.7211
Truck	2.37073	2.36810
LCV	1.47912	1.60685
MAV	3.57233	4.26664

Table 7 DEF by multiple regression method (M.G Road)

Type of vehicles	Towards Sudama Chowk	Towards Kamla Baugh
2W	0.49695	0.26494
3W	1.36675	0.96615
Car	1.0000	1.000000
Bus	5.5729	6.45711
Truck	5.9623	6.45916
LCV	2.247	2.535
MAV	7.78045	7.34132

Table 8 DEF by headway method (M.G Road)

Type of vehicles	Towards Sudama Chowk	Towards Kamla Baugh
2W	0.2285699	0.2265729
3W	0.82037	0.64391
Car	1.0000	1.000000
Bus	25.926	6.72069
Truck	10.147	9.32117
LCV	1.4065	1.2968
MAV	39.457	33.7705

5.3 S.V.P Road

- A. Chandra’s method (Table 9)
- B. Homogenization coefficient method (Table 10)
- C. Multiple regression method (Table 11)
- D. Headway method (Table 12)

Table 9 DEF by Chandra's method (S.V.P Road)

Type of vehicles	Towards Shitla Chowk	Towards Kadiya Plot
2W	0.219461	0.218591
3W	0.8896855	0.900504
Car	1.0000	1.000000
Bus	6.277764	6.11891
Truck	3.922092	3.875039
LCV	1.988036	2.072548
MAV	6.5472565	6.553182

Table 10 DEF by homogenization coefficient method (S.V.P Road)

Type of vehicles	Towards Shitla Chowk	Towards Kadiya Plot
2W	0.492764115	0.49081166
3W	0.916	0.927
Car	1.0000	1.000000
Bus	3.47899	3.39096
Truck	2	2
LCV	1.432241	1.49312
MAV	3.7735	3.7769

Table 11 DEF by multiple regression method (S.V.P Road)

Type of vehicles	Towards Shitla Chowk	Towards Kadiya Plot
2W	0.4556449	0.5243851
3W	1.179191	1.921314
Car	1.0000	1.000000
Bus	2.93873	3.3717
Truck	2.14587	3.7135
LCV	1.795	2.275
MAV	7.9761	6.8875

Table 12 DEF by headway method (S.V.P Road)

Type of vehicles	Towards Shitla Chowk	Towards Kadiya Plot
2W	0.35988162	0.3216458
3W	1.0907	1.2262
Car	1.0000	1.000000
Bus	20.6715	25.527
Truck	6.213248	6.449534
LCV	2.160392	1.38149
MAV	24.19362	30.60

6 Conclusions

- Headway method gives higher DEF values for truck, bus and MAV and lower DEF values for 2W and 3W than IRC standards.
- Multiple linear regression method gives higher DEF values for truck, bus and MAV and lower PCU values for 2W and 3W and DEF of LCV is nearly the same to that of IRC PCU standards.
- Homogenization coefficient method gives DEF values for all classes of the vehicle nearly the same with a little amount of variation to IRC PCU values.
- Chandra's method gives lower DEF values for 2W and 3W and higher DEF values for LCV, bus, truck, MAV than IRC standards.
- Chandra's method can be suggested as the best reliable method as it considers the projected area of vehicle rather than only longitudinal length used in homogenization coefficient method.
- The Headway method yield much more higher values of DEF is it is directly dependent on time headway of vehicles.

References

1. Khanorkar AR, Ghodmare SD (2014) Development of PCU value of vehicle under mix nature traffic condition in cities on congested highways. *Int J Eng Comput Sci* 6109–6113
2. Khanorkar AR, Ghodmare SD, Khode BV (2014) Impact of lane width of road on passenger car unit capacity under mix traffic condition in cities on congested highways. *Int J Eng Res Appl* 180–184
3. Shalkamy A, Said D, Radwan L (2015) Influence of carriageway width and horizontal curve radius on passenger car unit values of two-lane two-way rural roads. *Civ Environ Res*
4. Elefteriadou L, Torbic D, Webster N (n.d.) Development of passenger car equivalent for free-ways, two lane highways, and arterials. *Transp Res Rec*
5. Mardani MN, Chandra S, Ghosh I (2015) Passenger car unit of vehicles on undivided intercity roads in India. *Procedia Comput Sci* 52:926–931
6. Patel MB, Jadeja BN, Vala MM (2016) Determination of dynamic PCU's of different types of passenger vehicles on urban road: a case study of Rajkot City. *Int J Sci Res Dev*
7. Anand S, Sekhar SV, Karim MR (1999) Development of passenger car unit (PCU) values for Malaysia. *J East Asia Soc Transp Stud*
8. Arkatkar SS, Arasan VT (2012) Micro-simulation study of vehicular interactions on upgrades of intercity roads under heterogeneous traffic conditions in India. *Eur Transp*
9. Swetha D (2016) Estimation of passenger car unit for heterogeneous traffic in Visakhapatnam. *Int J Eng Sci Res*
10. Reddy V, Patel CR (n.d.) Dynamic equivalency factor of mixed traffic stream for urban arterial mid blocks. Indian Institute of Technology, Bombay

Urban Corridor Travel Time Estimation Modelling Using Fuzzy Logic Technique: A Case Study of Indian Metropolitan City



Krishna Saw, Bhimaji K. Katti and Gaurang J. Joshi

Abstract Traffic and transport planning in fast-growing metropolitan cities in India is the most challenging task for the Urban Transport Planner, in view of the faster traffic and transport demand growth observed in recent time. The main transport corridors in urban area are heavily loaded and facing severe traffic problems. Increase in travel time is one of the significant issues. The Level of Service is decreasing, and vehicular delays are intolerable during peak periods. Situations call for in-depth analysis of travel time with respect to heterogeneous traffic plying on urban corridors and other associated attributes with travel time variations and development of an appropriate model for travel time estimation. As the travel time attributes assessment is part of the human decision process, a soft technique fuzzy logic approach has been advocated for developing the model. The model incorporates roadside friction prevailing on roadside haphazard parking as well as pedestrian encroachment at a number of spots along the corridor in addition to the traffic intensity. Intersection factor in terms of impact on speed is another important parameter initiated in the present study.

Keywords Fuzzy logic · Intersection factor · Roadside friction · Travel time · Travel time attributes

1 Introduction

The achievement of fast and reliable travel time on the urban road network is one of the important objectives of a transport planner/trip maker in an urban transport system. However, the quality of movement on corridors is observed as degrading day by day with an increase in vehicle population, pedestrian interruption and haphazard kerb parking in the absence of proper infrastructure facilities and enforcement. Eventually, it results in traffic congestion, longer and variable travel time. These contribute to the

K. Saw (✉)
RITES Ltd., Gurgaon 122001, Haryana, India
e-mail: kriscivil_10@yahoo.com

B. K. Katti · G. J. Joshi
Civil Engineering Department, SVNIT, Surat 395007, India

© Springer Nature Singapore Pte Ltd. 2020
T. V. Mathew et al. (eds.), *Transportation Research*, Lecture Notes
in Civil Engineering 45, https://doi.org/10.1007/978-981-32-9042-6_38

anxiety, stress and waste of time of the commuters. There are a number of attributes which influence travel time and vary with respect to space and time [1]. Therefore, it is necessary to examine various attributes of travel time in recurrent conditions for their role in the estimation of travel time which useful in urban traffic control and management. Most of the studies have not given due weightage to the roadside traffic interruptions and the presence of intersections. The present study attempts to incorporate these very factors in travel time estimation modelling.

As the qualitative judgment of travel time attributes is embedded in uncertainty, fuzzy logic soft computing technique is employed in the proposed model to deal with vague and imprecise information. With this background, an important urban traffic corridor of Surat city of Gujarat state in India has been selected for the study purpose.

2 Travel Time: Research Overview

Travel time on urban corridors is mainly influenced by physical features of the corridors such as with road width, geometry, intersection controls and varied traffic characteristics in terms of traffic flow and density under heterogeneous conditions. Roadside friction as a recurring factor has to bear on travel time. Some of these attributes and their impact are dealt with in traffic congestion modelling by speedograph approach [2]. Vlahogianni [3] studied the relationship between travel speed, traffic volume and traffic composition in urban arterials of Greece and found that strongest relations between speed and volume. Influence of traffic volume, road accidents and weather condition is touched by Shekhar et al. [4] for urban corridors in non-recurrent situations. Wang et al. [5] recognize lane widths and number of traffic streams in their study. Jenelius and Koutsopoulos [6] covered both signalized and un-signalized intersections in the study “travel time of urban road using Probe Vehicle Data in Stockholm, Sweden”. They found that delay at the un-signalized intersection is shorter than the signalized intersection. Accident, extreme weather conditions and certain instantaneous events occurring due to procession and breakdown of the vehicles, etc., are non-recurring factors. Impact of extreme weather conditions on speed profiles was considered by Chakrabarty et al. [7] in their study carried in Delhi. However, it is hardly found the necessary focus on the roadside friction in terms of haphazard parking and pedestrian disturbances for developing travel time estimation model. Various techniques were adopted for developing travel time estimation modelling in past. Sisiopiku et al. [8], Zhang and He [9], Fils [10] employed multiple-linear regression approach for travel time estimation modelling for its simplicity. Shekhar et al. [4] formulated a regression model using road traffic volume collected through loop detector. Saw et al. [11] developed multiple-linear regression travel time estimation model based on travel time data collected from Probe Vehicle and mixed mode traffic volume from videography, whereas Yang [12] adopted data mining technique. Skabardonis and Geroliminis [13] and Bhaskar et al. [14] attempted analytical methods to estimate the travel time for arterial road based

on kinematic wave theory using data of loop detectors. Dharia and Adeli [15], Jiang and Zhang [16] and Lee [17] applied artificial neural network (ANN) in travel time modelling. Time series data analysis approach was proposed for travel time model development by Yang [18] and Hu and Ho [19]. They found that the accuracy of the time series model is influenced by the outliers of the historical time series data. Khoei et al. [20] applied the seasonal auto-regressive integrated moving average (SARIMA) approach for modelling of travel time based on Bluetooth data. Liu et al. [21] and Hu and Ho [19] employed simulation technique for travel time estimation considering link cruising time and intersection delays. However, uncertainty prevails on account of subjective and qualitative assessment of travel time attributes, the traditional models are not effective in the estimation of travel time. Therefore, the use of fuzzy logic advocated by Zadeh [22] to address the uncertainty in database bears importance in developing travel time estimation model.

3 Travel Time Factors

Main factors affecting the travel time across the city corridors are:

- (a) **Physical Features:** Number of lanes, lane width, number and configuration of intersections are main attributes. The lane width and number of lanes play a vital role in mixed traffic flow behaviour, as it does involve passing and lane changing phenomenon. The intersection configuration and control system, on the other hand, are equally important as they act as sinks and bulging spots of traffic interruption.
- (b) **Traffic Volume:** It is one of the important factors in assessment in traffic quality as it has a significant impact on the traffic delay and density.
- (c) **Mixed Traffic:** It influences significantly on vehicular movement mechanism due to inter-modal vehicular interactions.
- (d) **Roadside Friction:** The parameters considered here are:
 - **Pedestrian disturbance:** pedestrian encroachment on carriageway interrupts the traffic flow in terms of reducing speed and capacity.
 - **Kerb parking:** the haphazard parking at the kerbside at riders' convenient leads to a reduction in effective road width and so the capacity.

Moreover, roadside land use development often encourages into haphazard kerb parking of mixed modes and pedestrian's activities related to roadside shopping, etc.

4 Study Area and Field Studies

4.1 Corridor Location

Pilot surveys were conducted on the number of stretches on city corridors to have the traffic characteristics and traffic variations with reference to travel time to meet the research requirements. Finally, Udhana–Sachin Corridor, a length of 5.8 km situated in south zone of Surat, has been selected. Surat is a fast-developing industrial city in Gujarat state having nearly 50 lakh population to date. This is a one of the main traffic corridors and connects the southern side of the city to the central business. The corridor has six lanes inclusive of two lanes of bus rapid transit system (BRTS) at the centre and two lanes available for the mixed traffic flow on either side. Figure 1a provides the location diagram of the study corridor and classified volume count (CVC) locations, whereas schematic diagram of study segments, along with configurations of the intersection, is shown in Fig. 1b. C₃, C₄ and C₅ are the major intersections in Segment I. Intersections in other segments are minor in nature. The study corridor has been separated in three segments, each of nearly 2 km, for study purpose. Heavy commercial activities dominate adjacent to Segment I with the

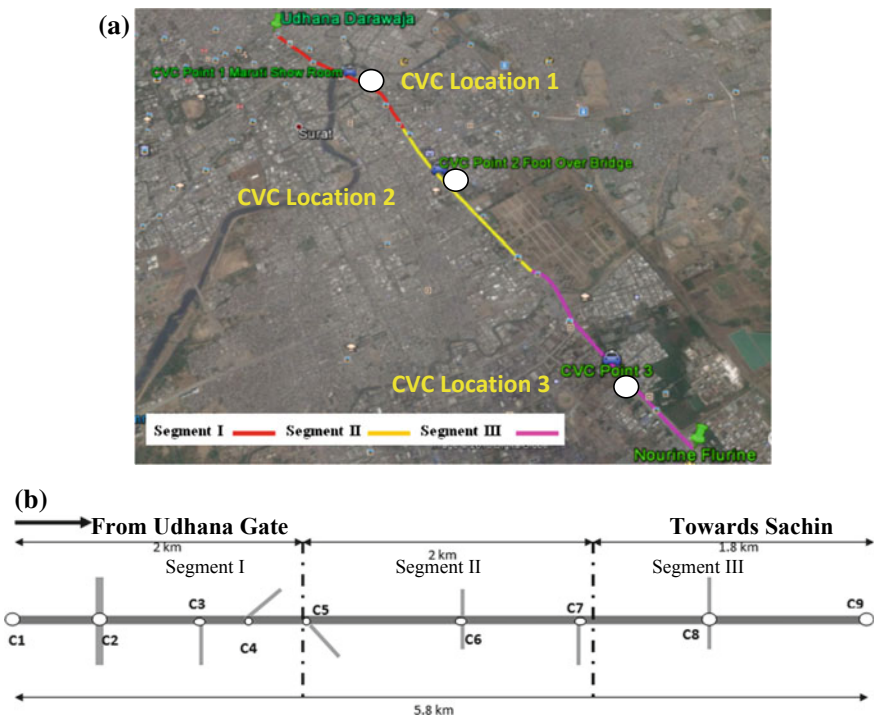


Fig. 1 a Study corridor. b Schematic diagram of study segments

dense residential area behind, whereas manufacturing medium as well as commercial activities industries are marked along Segments II and III.

All intersections on Corridor are un-signalized. Inter-spacing (m) of intersections of the study corridor is as under

C ₁ to C ₂	C ₂ to C ₃	C ₃ to C ₄	C ₄ to C ₅	C ₅ to C ₆	C ₆ to C ₇	C ₇ to C ₈	C ₈ to C ₉
600	700	300	400	1000	800	900	1100

4.2 Field Studies

To note the necessary traffic characteristics, the field studies are conducted as under:

- Traffic volume and composition survey
- Roadside friction survey (RSF)
- Speed profile survey.

All surveys are conducted simultaneously for morning and evening peak and off-peak periods based on eight-hour pilot surveys.

4.2.1 Traffic Volume and Composition Survey

One of the fundamental measures of traffic characteristics on road is traffic volume in a given time period. Videography technique is employed in the present study to capture the mixed traffic flow at the identified midway locations (CVC 1, 2, 3) in each segment as shown in Fig. 1a. Videography recording is carried out segment-wise for both morning and evening peak and off-peak periods simultaneously at the three locations of the corridors along with other surveys. The cameras captured both up and down flows covering around 150 m stretches of moving traffic. The mode-wise volume is counted at an interval of 5 min. Vehicles are classified as Two-Wheelers (2Ws), Auto-Rickshaws (3Ws), Cars (4Ws) and Commercial Vehicles (CVs). CVs include light commercial vehicles (LCV), trucks and buses.

4.2.2 Roadside Friction Survey (RSF)

Haphazard kerb parking and pedestrian interruptions prevail along the corridor. The pedestrian encroachment on the road as well as crossing pedestrian is part of the pedestrian interruption. These two very factors have been considered as part of RSF attributes. RSF has a significant influence on traffic flow and eventually on traffic capacity. Three trained enumerators are employed to note the RSF in terms of ratings

1–5 in qualitative expression, where 1 is for lowest and 5 for highest RSF during speed profile survey. The ratings are based on visual assessment of quantitative situations with the support of five typical photographs provided to represent five sets of RSF. The ratings assigned by the enumerators are averaged normalized to 0–1 scale. Chinguma [23] measured RSF in three levels of low, medium and high in his study.

4.2.3 Speed Profile Survey

Speed profile survey in the present study is conducted using GPS laden Probe Vehicle of 3Ws, being the dominated mode of transport. The main benefit of GPS laden Probe Vehicle-based speed survey is that it provides second-to-second speed and data are saved automatically. The speed profiles are collected for morning and evening periods covering both peak and off-peak. The sample size in such type of GPS laden Probe Vehicle survey results in lower volume as compared with the licence plate method but has the merit of second-to-second speed particulars. In this study a total of 14 runs in each direction have been carried out over a length of 5.8 km covering peak and off-peak periods. Overall 84 samples form with both up and down three segments movement together. Moreover, speed profiles of Probe Vehicle largely reflect on movements of vehicle platoon at certain sections during the peak traffic flow as shown in Fig. 2.



Fig. 2 Platoon flow behaviour

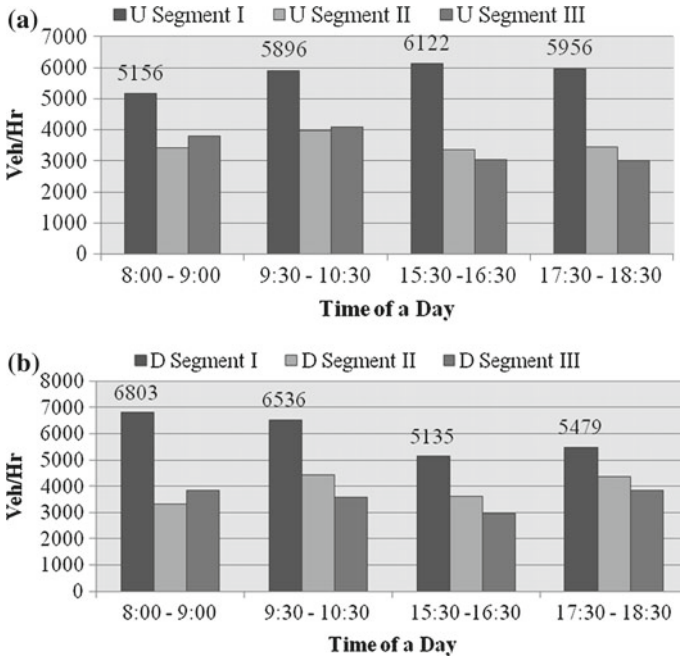


Fig. 3 a Traffic volume (upward). b Traffic volume (downward)

5 Data Analysis

5.1 Traffic Volume

Hourly traffic volume analysis of both directions has been carried out and it is found that the traffic pattern in both directions, i.e. up (Udhana to Sachin) and down (Sachin to Udhana) is almost same. Figures 3a and b provide segment-wise traffic variations, Segment I has high hourly traffic flow compared with the other two Segments. Traffic variation can be noticed for peak and off-peak periods.

5.2 Traffic Composition

The mixed traffic in India comprises of 2Ws, 3Ws, 4Ws and CVs. It is an important attribute of traffic characteristics for its significant impact on travel impedance. Table 1 provides share of each mode on segment basis. The domination of 2Ws is evident on corridor to the extent of 53–62%, followed by 3Ws 28%. Slightly higher share of 2Ws is observed in Segment I, whereas Segments II and III having higher share of 4Ws and CVs. Traffic composition plays a vital role in traffic movement, but

Table 1 Traffic composition (%)

Mode	Up direction			Down direction		
	Segment I	Segment II	Segment III	Segment I	Segment II	Segment III
2W	60	53	53	62	59	56
3W	27	28	28	27	34	31
Car	9	13	13	8	12	12
CV	4	6	6	5	7	5

Table 2 Roadside friction

	Up direction			Down direction		
	Segment I	Segment II	Segment III	Segment I	Segment II	Segment III
Min	0.6	0.47	0.33	0.53	0.50	0.33
Max	1	0.77	0.63	0.90	0.70	0.63
Avg.	0.79	0.61	0.44	0.74	0.59	0.45
Std. dev	0.112	0.086	0.076	0.11	0.07	0.08

very few studies have accounted for mixed traffic in travel time. The mixed traffic is converted into passenger car unit (PCU) by referring to equivalent PCU factors specified by IRC 106-1990 [24] for urban mid-block sections in the development of a model to reflect on the likely impact of traffic composition.

5.3 Roadside Friction (RSF)

As discussed earlier, the ratings observed by the three trained enumerators along the roadsides during the Probe Vehicle Surveys are averaged and normalized on 0–1 scale for analysis purpose, i.e. larger the value higher the RSF. RSF in Segment I varies from high to very high and it varies from medium to high in Segment II, whereas in Segment III it varies low to medium in both directions depending upon the peak and off-peak period conditions. Statistical observations of the RSF are summarized in Table 2. The average value of RSF varies from 0.44 to 0.79.

5.4 Intersection Factor (IF)

As discussed earlier, the study corridor has a number of intersections. Intersection type and configurations, control system and level of crossing traffic matter on the degree of impedance for main traffic flow and accordingly main traffic speeds are dropped [6]. This fact has been reasonably addressed here by introducing Intersection

Factor (IF) defined as average segment speed to drop-down speed at the intersection. If a more number of intersections are there in the segment, the cumulative effect is to be considered as a segment intersection factor and it is

$$\text{Intersection Factor of Segment (IF}_s) = \sum_{i=1}^n \left(\frac{\text{Average segment speed}}{\text{Drop down speed at intersection } i} \right)$$

where, n —Numbers of intersections in the segment.

The drop-down speeds are observed from the speedo-graphs obtained in V-Box survey. A drop-down speed is the reduced speed of the Probe Vehicle at the intersection. The statistical observations of the IF for the Segments for both up and down directions are shown in Table 3.

It is observed that Segment I bears higher IF due to the presence of three major intersections followed by Segment II and Segment III which consist of minor and few number of intersections. For illustration, a speed profile of a trip is provided in Fig. 4. The speed-drop with respect to average speed can be noted at intersections C_2, C_3, C_4, C_5 at 600, 1300, 1600 and 2000 m, respectively, for the Segment I at 17:45–18:00 h.

Table 3 Intersection factor (IF)

	Up direction			Down direction		
	Segment I	Segment II	Segment III	Segment I	Segment II	Segment III
Min	7.64	2.89	1.19	10.27	3.90	1.44
Max	38.68	18.41	28.52	35.19	17.6	7.5
Avg.	18.49	8.62	7.33	25.44	11.74	4.87
Std. dev.	10.15	5.89	11.33	8.17	5.16	1.72

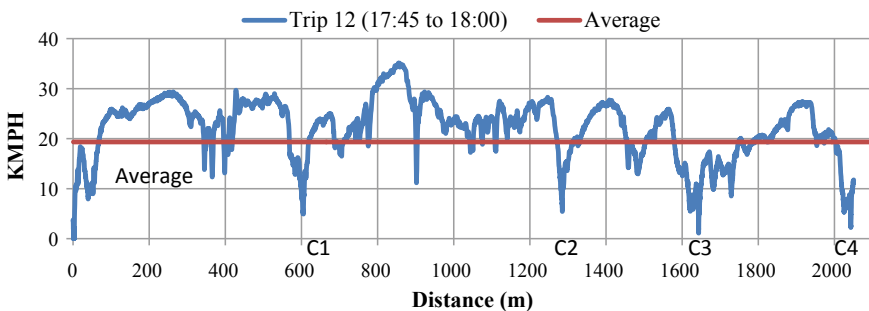


Fig. 4 Space–speed profile of Segment I (17:45–18:00 h)

5.5 Travel Time Studies

Observed travel time (min/km) is noted for both directions on segment basis obtained through Probe Vehicle as shown in Fig. 5. Other statistical observations are summarized in Table 4. Higher travel time is noted in Segment I due to higher traffic flow, RSF and IF. Observed travel time/km of Segment II and Segment III in both directions is almost the same due to similar traffic characteristics and roadside interruptions as discussed earlier. Similar is the pattern of standard deviation for these segments.

6 Development Fuzzy Rule-based Travel Time Model (FRB-TTM)

Development and operation of fuzzy rule-based travel time model (FRB-TTM) comprises of three stages namely fuzzification, fuzzy inference system (FIS) and defuzzification as under.

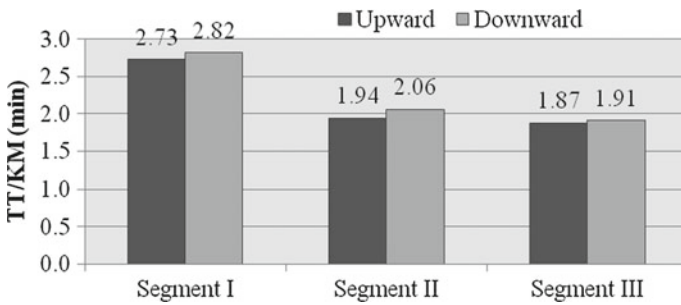
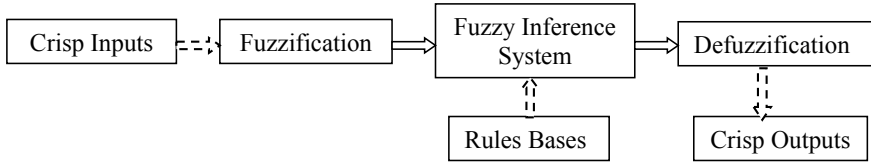


Fig. 5 Observed travel time

Table 4 Travel time statistics (min/km)

	Upward			Downward		
	Segment I	Segment II	Segment III	Segment I	Segment II	Segment III
Min	2.18	1.77	1.67	2.34	1.68	1.67
Max	3.24	2.19	2.15	3.41	2.22	2.15
Avg.	2.73	1.94	1.87	2.82	2.06	1.91
Std. dev.	0.32	0.12	0.18	0.29	0.17	0.14



6.1 Fuzzification

Fuzzification is an important step in the fuzzy logic theory, which converts crisp inputs into fuzzy sets. The main inputs of the model segment-wise are:

- Traffic volume in PCU/hr (000)
- Roadside friction (RSF) and
- Intersection factor (IF).

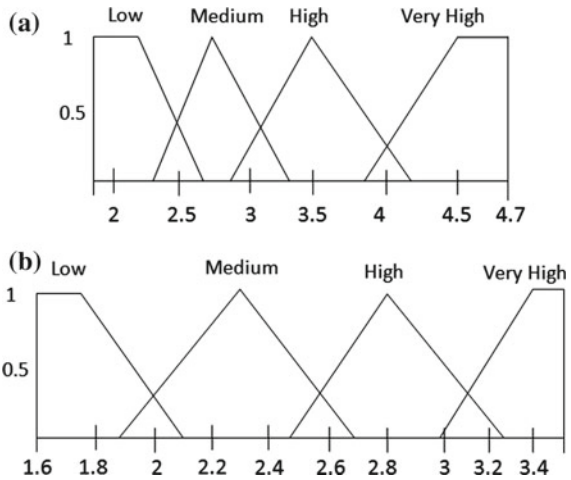
And the model output variable is travel time/km (min).

Categorization of variables in linguistic terms, the membership shape adopted and input ranges for particular input level, etc. are as shown in Table 5. Here, triangular and trapezoidal membership functions (MFs) are preferred for their simplicity. Their ranges and overlapping, etc. are based on a trial basis. Four levels of input are

Table 5 Range of variable used in FRB-TTM

Variable	No. of MFs	Linguistic variable	Type of MF	Fuzzy no.
PCU	4	Low	Trapezoidal	[1.9 1.9 2.15 2.64]
		Medium	Triangular	[2.32 2.81 3.38]
		High	Triangular	[2.96 3.53 4.12]
		Very high	Trapezoidal	[3.83 4.44 4.7 4.7]
RSF	4	Low	Trapezoidal	[0.25 0.25 0.28 0.42]
		Medium	Triangular	[0.350.48 0.63]
		High	Triangular	[0.56 0.71 0.84]
		Very high	Trapezoidal	[0.76 0.92 1.0 1.0]
IF	4	Low	Trapezoidal	[1 1 3.5 10.85]
		Medium	Triangular	[6.73 14.1 22.5]
		High	Triangular	[17.66 25.7 33.5]
		Very high	Trapezoidal	[29.01 37.4 40 40]
TT/km	4	Low	Trapezoidal	[1.6 1.6 1.80 2.13]
		Medium	Triangular	[1.91 2.27 2.71]
		High	Triangular	[2.45 2.86 3.27]
		Very high	Trapezoidal	[2.99 3.31 3.5 3.5]

Fig. 6 **a** MFs for PCU.
b MFs for travel time



considered from low intensity to very high intensity for all the three inputs and output.

Figures 6a and b indicate the MFs particulars for traffic variable and travel time output, respectively, for illustration purpose.

6.2 Fuzzy Inference System

Fuzzy inference system is a process of mapping of input and output. In this study, fuzzy inference system addresses the above-said inputs and output and follows Mamdani fuzzy inference system for the development of the model.

Fuzzy rule-based system is generated with reference to inputs and the output. The number of MFs of input variables is decisive in deciding number of “IF-THEN” rules. Here, a total 64 “IF-THEN” rules ($4 * 4 * 4$) were framed. Some rules are mentioned below for illustration purpose.

IF <PCU/h is low> and <RSF is low> and <IF is low> **THEN** <TT is low>.

IF <PCU/h is medium> and <RSF is medium> and <IF is High> **THEN** <TT is medium>.

IF <PCU/h is high> and <RSF is high> and <IF is high> **THEN** <TT is high>.

IF <PCU/h is Very high> and <RSF is Very high> and <IF is medium> **THEN** <TT is high>.

IF <PCU/h is Very high> and <RSF is Very high> and <IF is Very high> **THEN** <TT is very high>.

The antecedents which are the first part of the rule provide fuzzy set input, whereas the second part of **THEN** are consequents to represent the output for the rules framed.

6.3 Defuzzification

Defuzzification is the process of generating a quantifiable output in fuzzy logic for which generally centroid method is adopted to obtain the crisp outputs. This method builds the resultant MFs by taking the algebraic sum of outputs from each of the contributing fuzzy sets. The typical output value of travel time/km (2.58), for the considered inputs, is as shown in MATLAB snapshot (Fig. 7).

Surface plots for predicted travel time/km in min by the developed model are shown in Fig. 8.

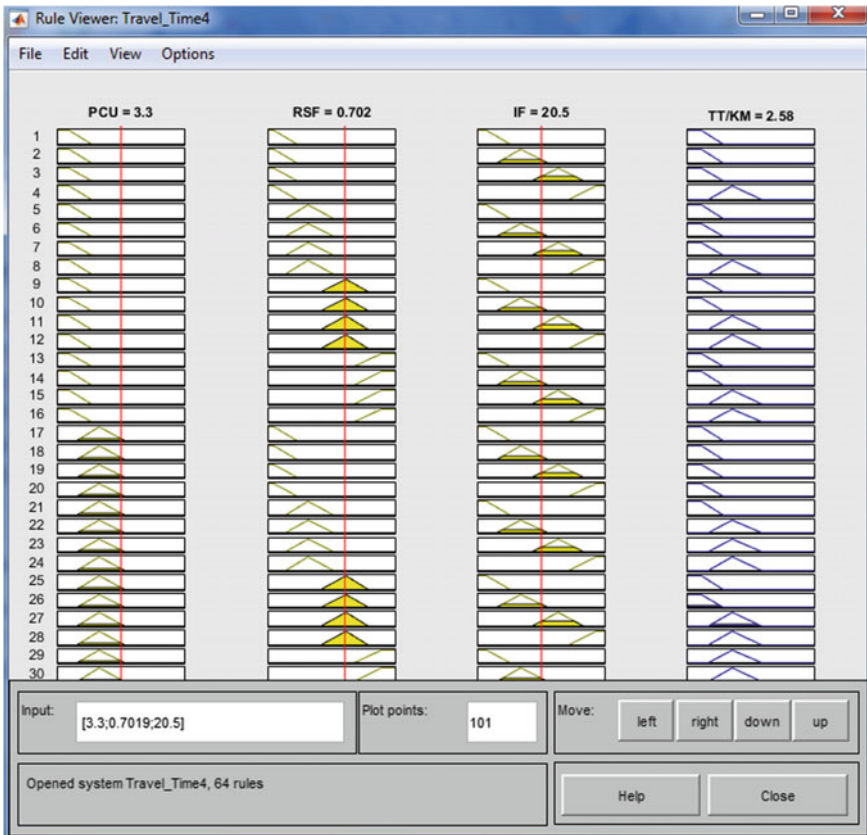


Fig. 7 Typical MATLAB snapshot of rule viewer window

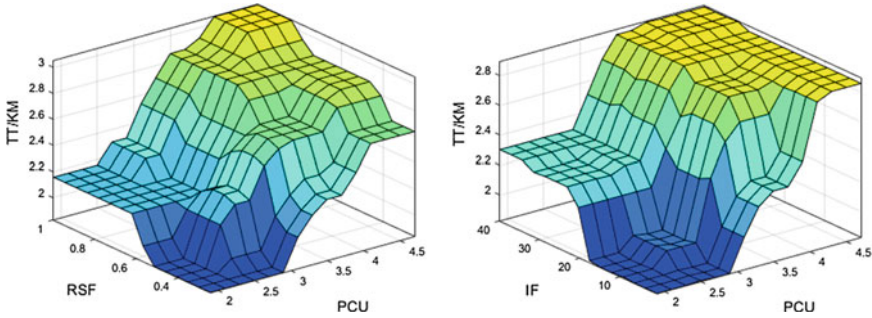
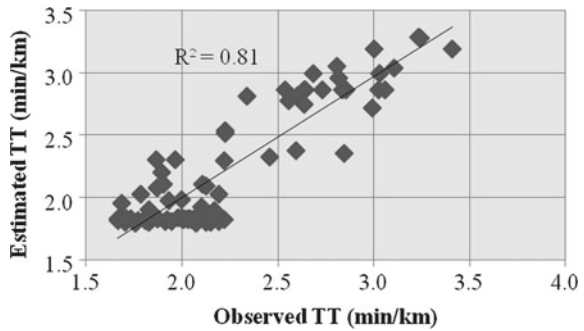


Fig. 8 Surface plots for predicted travel time

Fig. 9 Observed and estimated travel time



6.4 Measurement of Model Effectiveness and Validation

The estimated values using fuzzy logic are then compared against the observed values as shown in Fig. 9 indicating good agreement between them with R^2 as 0.81. Moreover, the model estimated values for the typical situation are verified with observed one and are found to be in order. Root-mean-square error (RMSE) value of 0.21 min (9.6%) of the model output is quite satisfactory.

7 Conclusion

Higher urbanization rate observed in the metropolitan cities in India has resulted in significant growth in urban traffic and travel system. Eventually, this has a considerable impact on urban road network traffic leading to substantial degradation in traffic quality which is reflecting an increase in travel time. However, it is equally important to understand the associated parameters of travel time closely for their likely impacts. The study carried out in this regard on an important city corridor reveals the role of roadside friction (RSF) and intersection factors (IF) apart from the varying traffic

volume and composition under mixed traffic environment. RSF accounts both haphazard kerb parking and as well as pedestrians' disturbances prevail in a sub-arterial situation. The probe vehicle technique suits better to cover the speed profile across the study corridor along with qualitative observations of RSF in a trip. Looking at the uncertainty component in attributes observations, fuzzy rule-based travel time model (FRB-TTM) is found more suitable in estimating the travel times. The model finds wide application in measuring the traffic flow status and provides the base for improvement measures as part of traffic control and management of urban corridors.

References

1. Lin HE, Zito R, Taylor MAP (2005) A review of travel-time prediction in transport and logistics. *Proc East Asia Soc Transp Stud* 5:1433–1448
2. Das AK, Saw K, Katti BK (2016) Traffic congestion modelling under mixed traffic conditions through fuzzy logic approach: an Indian case study of arterial road. In: 12th international on TPMDC, IIT Bombay, 19–21 Dec 2016
3. Vlahogianni EI (2006) Some empirical relations between travel speed, traffic volume and traffic composition in urban arterials. *IATSS Res* 31(1):110–119
4. Shekhar RC, Iryo T, Asakura Y (2012) Analysis of travel-time variation over multiple sections of Hanshin expressway in Japan. *Curr Sci* 102(11)
5. Wang D, Fu F, Luo X, Jin S, Ma D (2016) Travel time estimation method for urban road based on traffic stream directions. *Transportmetrica A Transp Sci*
6. Jenelius E, Koutsopoulos HN (2013) Travel time estimation for urban road networks using low frequency probe vehicle data. *Transp Res Part B Methodol* 53:64–81
7. Chakrabarty N, Gupta K, Kumar R, Singh G (2014) Effect of extreme weather conditions on speed profiles of drivers: a case study in Delhi, India. *Int J Res Appl Sci Eng Technol* 2(IX)
8. Sisiopiku VP, Roupail NM, Santiago A (1994) Analysis of correlation between arterial travel time and detector data from simulation and field studies. *Transp Res Rec* 1457(1994):166–173
9. Zhang M, He JC (1998) Estimating arterial travel time using loop data. Public Policy Center, University of Iowa
10. Fils PB (2012) Modeling travel time and reliability on urban arterials for recurrent conditions. University of South Florida
11. Saw K, Katti BK, Joshi GJ (2018) Travel time estimation modelling under heterogeneous traffic: a case study of urban traffic corridor in Surat, India. *Period Polytech Transp Eng*. <https://doi.org/10.3311/PPtr.10847>
12. Yang X (2011) Car travel time estimation near a bus stop with non-motorized vehicles. *Int J Comput Intell Syst* 4(6)
13. Skabardonis A, Geroliminis N (2005) Real-time monitoring and control on signalized arterials. *J Intell Transp Syst* 12(2):64–74
14. Bhaskar A, Chung E, Kuwahara M, de Mouzon O, Dumont AG (2007) Urban network travel time estimation from stop-line loop detector data and signal controller data. *WIT Trans Built Environ* 96
15. Dharia A, Adeli H (2003) Neural network model for rapid forecasting of freeway link travel time. *Eng Appl Artif Intell* 607–613
16. Jiang G, Zhang R (2001) Travel-time prediction for urban arterial road: a case on China. In: *Proceeding of the IEE international conference on vehicle electronics, Tottari*, pp 255–260
17. Lee Y (2009) Freeway travel time forecast using artificial neural networks with cluster method. In: *Proceeding of 12th international conference on information fusion, Seattle*, pp 331–338
18. Yang JS (2005) A study of travel time modeling via time series analysis. In: *Proceedings of the IEEE conference on control applications, Toronto, Canada*

19. Hu T-Y, Ho W-M (2010) Travel time prediction for urban networks: the comparisons of simulation-based and time-series models. In: Proceedings of 17th ITS world congress, Busan
20. Khoei AM, Bhaskar A, Chung E (2013) Travel time prediction on signalised urban arterials by applying SARIMA modelling on bluetooth data. In: 36th Australasian transport research forum (ATRF), Brisbane
21. Liu H, van Zuylen HJ, van Lint H, Chen Y, Zhang K (2006) Prediction of urban travel times with intersection delays. In: Proceedings of the 8th international IEEE conference on intelligent transportation systems, Vienna, Austria
22. Zadeh LA (1975) Concept of a linguistic variable and its application to approximate reasoning—I. *Inf Sci* 8:199–249
23. Chinguma LM (2007) Analysis of side friction impacts on urban road links: case study Dar-es-Salaam. PhD thesis, School of Architecture and the Built Environment, Royal Institute of Technology Stockholm, Sweden
24. IRC: 106-1990 (1990) Guidelines for capacity of urban roads in plain areas. The Indian Road Congress, New Delhi

Application of Accident Analysis and Modeling Tool—Pilot Study for Sadashivanagar Area of Bangalore



Ankit Rai, Ashish Verma and Sonal Ahuja

Abstract Along with industrial and infrastructural development, advancement in socioeconomic conditions of the people is creating additional burden on roads by increasing the number of vehicles. While this extent of progress has led to various advantages, road accidents have also become one of the main causes of concerns due to both, life and economic losses. The WHO has predicted that road accidents will be one of the biggest killers in India by 2020. This calls for assessment of these accidents by identifying and analyzing the causes that are responsible for their occurrence, and recommending various remedial measures to mitigate the accidents. This study aims to look at this problem by utilizing an accident analysis and modeling tool to arrive upon the comprehensive understanding of accidents and formulation of remedial measures. The study demonstrates the application of VISUM Safety tool and measures its effectiveness using statistical methods. The tool presents the accident data in a way that helps in analyzing and understanding the data, by bringing the otherwise concealed factors to the fore, through its visual graphics. The data was collected for different road stretches in the Sadashivanagar region of Bangalore, which is one of the major black spot locations of the city. The accident prediction models are based on these data points collected from this whole region across junctions and road links. It is envisaged that the study will help propose effective course of action that needs to be adopted by the transportation planners in designing a safer road-user environment. As tabular and statistical representation takes viewers longer to comprehend and read due to their structure, tool-generated reports would be of great significance when presented to local governing authorities. It can be referred to identify factors affecting road safety in relation to ‘black spot’ identification and network safety analysis. The concluding statements in the form of vivid and self-explanatory visual

A. Rai (✉) · A. Verma

Department of Civil Engineering, Indian Institute of Science, Bangalore 560012, India
e-mail: anktrai89@gmail.com

A. Verma

e-mail: ashishv@civil.iisc.ernet.in

S. Ahuja

PTV MENA Region DMCC, #1601, Fortune Tower, Dubai 309012, UAE
e-mail: sonal.ahuja@ptvgroup.com

© Springer Nature Singapore Pte Ltd. 2020

T. V. Mathew et al. (eds.), *Transportation Research*, Lecture Notes
in Civil Engineering 45, https://doi.org/10.1007/978-981-32-9042-6_39

graphics would certainly have an upper hand on tabular and statistical representation and will help the viewer connect the dots effortlessly.

Keywords Accident analysis · Blackspot identification · Accident modelling · Road safety tool

1 Introduction

Road accidents are one of the major causes of unnatural deaths in India. On an average, 16 people were killed in road accidents every hour and 387 every day in the year 2014. This was a rise of 2.9% from previous year. Based on 2014 report of National Crime Bureau, 450,898 cases of road accidents took place that year resulting in 141,526 fatalities and injuring 477,731. These are disturbing numbers. Further, WHO has predicted that road accidents will be one of the biggest killers in India by the year 2020. There is increasing demand for assessing these accidents through identifying and analyzing the causal factors that are responsible for their occurrence, and also to propose corrective measures to mitigate these accidents. VISUM Safety is one such tool which visualizes the accident data in a way that helps in analyzing and understanding the accident data by bringing the otherwise concealed factors to the fore through its visual graphics. It is now an integral part of transportation plans to focus on the road-user safety aspects for the present as well as for the changing scenario of the traffic flow. The work in this paper would focus on predominant causal factors by using statistical techniques and then incorporate it into the model to make the tool's predictions as accurate as possible. VISUM Safety tool is used for analyzing crash data. With this tool, it is possible to integrate the safety aspects into transport planning from the very beginning. Crash data can be imported and analyzed, and effective long-term strategies can be developed. VISUM Safety aids us in various assignments with the following capacity:

- It visualizes crash data and identifies black spots and high-risk sections. It visualizes crash using clear and easy-to-understand heat maps.
- Detailed information about each individual crash allows analysts to find similarities and contributing factors to draw conclusion about crashes and develop, plan and optimize effective and cost-effective mitigation measures.
- Filter accident according to their characteristics, and compare development across different time periods.
- Crash prediction model and generation of interactive statistics and road safety reports.

It works in tandem with a platform named Vistad. It is an optimal platform for collection, validation and analysis of accident data. It allows filtering of accidents both geographically and according to numerous attributes such as involved parties, age, sex or degree of injury. Figures can be compared, and historical comparative statistics can be performed to trace the development of accident figures. It was found desirable to support or validate the conclusions of the tool with other sources. The

safety tool would be validated by developing an accident prediction model that would depict the effect of some of the major causal factors for accident on urban roads. The tool's accident prediction model (APM) encompassed the crucial variables such as traffic volume, traffic speed, accident rate and link length to predict the accidents on various road segments.

2 Literature Review

Since the 1940s, researchers turned the wheel of study on road accidents by incorporating statistics to discern the factors that encompass the fatalities. Smeed's law [1] was the first relation to exist linking annual road deaths to number of registered vehicles and population together, representing the traffic congestion. Andreassen [2] did not concede with Smeed and presented slightly varying relation in 1995 using the same variables. Ponnaluri [3] developed seven models embracing variants of Smeed and Andresson models and applied to Indian data. He used 19 years' (1991–2009) road-related data collected across 29 states and tested for the fitness of Smeed and Andreassen models in Indian scenario. Further, he checked for time invariance and state-wise specificity. The results showed that though the estimations of Smeed's model were consistent with actual data, generalized models deviated more than the state-variant models. Abdel-Aty and Radwan [4] used negative binomial model to check relation of accidents with factors like annual average daily traffic, degree of horizontal curvature, lane, shoulder and median widths, type of road and the section's length. Their work illustrated relative influence of the variables on young, middle and old-aged vehicle users. The paper also shows the difference in mentalities of female and male drivers and the situations where each group is prone to accidents.

Relating geometric and traffic conditions to accident frequencies not only lets one to understand quantitatively the major causes of accidents but also helps to create prediction models to foreknow the number of accidents that could occur in the future. Many studies have been done to understand the relation between the likelihood of catastrophes in a region at a particular time to the characteristics of road apart from the obvious influence of the victim's mental state or response. Goyal et al. [5] tried to create a generalized accident prediction model for national highways of India based on AADT and road conditions. They analyzed the accident data of eleven years (2000–2010) on a particular section of national highway NH-77. The paper presented a linear equation, with 0.89 R^2 value, measuring the accidents per km per year from AADT and road and shoulder condition rank. The parameters signify that the number of accidents increased with increase in AADT but have the chance of decreasing with improvement in road and shoulder conditions. An interesting point was drawn in the study that the definition of accident frequency changes the way results can be interpreted. For example, the accident rate in terms of the number of accidents per km-year increased with traffic volume but the accident per million-vehicle kilometer-year (MVKY) decreased with increase in traffic volume during the same study period. Comparable models were developed recently by [6, 7] using

multiple linear regression. The studies were conducted in the states of Ahmedabad and Bangalore, respectively. Both approached by considering all the possible road and traffic characteristic variables that might influence frequency of accidents and later eliminating the less prominent factors and interdependency of each variable through the correlation matrix. Bhat et al. [6] suggested a model with 0.99 adjusted R^2 verified with accident data of a road stretch in Ahmedabad barring 155 accidents in the year of study. They propounded that out of all variables taken into consideration during the study, width of carriageway, width at approach of minor crossing and exits, average speed of the traffic stream, percentage of auto rickshaws, buses and cars affect the frequency of accidents the most. Similarly, results of [7] show that road condition, carriageway width, shoulder type, percentage of trucks in traffic stream and land use have considerable impact on occurrence of accidents.

3 Methodology

Accident data was first obtained from the authorities, and aspects of data quality were first looked at. Within the overarching goal of accident analysis and accident prediction model, this study adopts two methods to arrive at the potential solution. One method exploits the use of VISUM Safety tool, and the other adopts statistical methods. In the tool approach, data is first imported onto the tool interface and visualized to examine and understand thematically represented accident clusters and density maps. Trends and patterns in accidents, if any, could be detected here, and it helps in black spot management as well as network safety management when looking at an aggregate level. Figure 1 reflects the methodological framework of the study.

4 Safety Tool Approach

In this method, the Safety tool's interface is used to analyze the accident data. Data is first fed into the Vistad and then imported to VISUM Safety interface to further investigate the data attributes and arrive upon the accident prediction model. In the further section, the Safety tool's working model and steps involved in the analysis are explained.

4.1 Working with Accidents

The accidents are first called into the VISUM Safety graphical user interface (GUI). Accidents were saved in a '.csv' file format and then called into the tool. While the accident data file is being imported, the allocation parameters need to be fed before

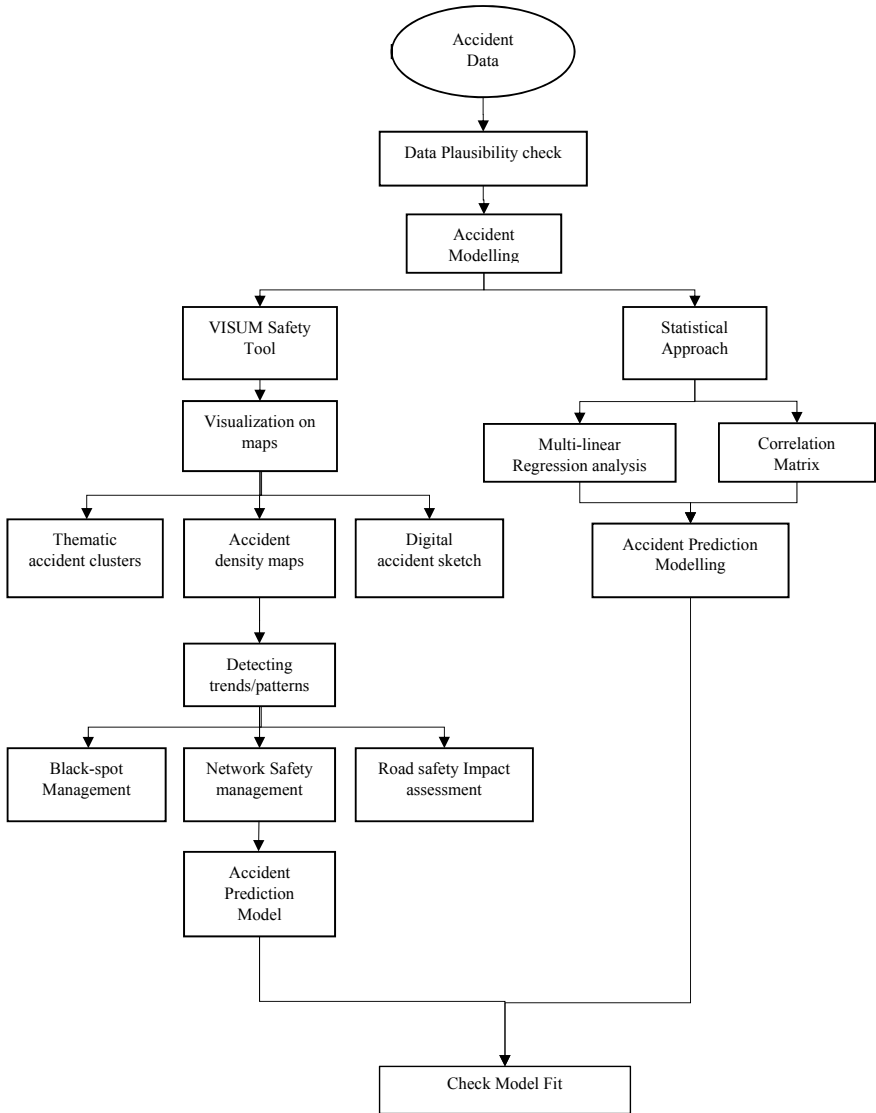


Fig. 1 Study of framework

moving further. The allocation could depend upon the link density or the number of nodes in study area (Fig. 2).

The imported accidents appear on the GUI as per the graphical parameters assigned to the type of accident and category of vehicles involved. Here in this case (Fig. 3, left), we see the imported accidents for the Sadashivanagar region of Bangalore.

Though to have a comprehensive understanding of geo-spatial attributes of accident, it is important to turn on the OpenStreetMap (OSM) plug-in available within the tool. The data then appears to be visually more appealing (Fig. 3, right).

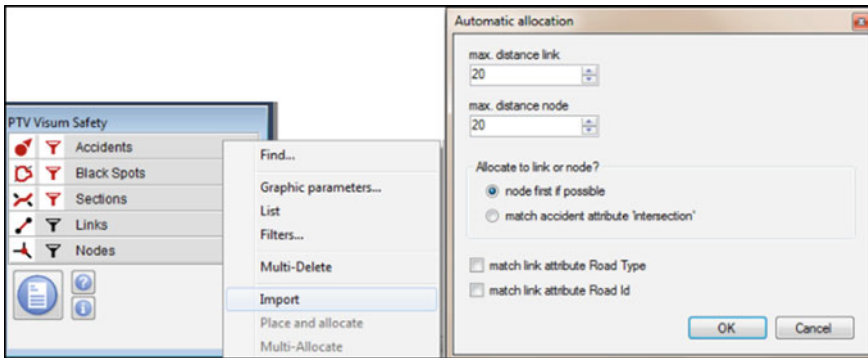


Fig. 2 Importing accidents



Fig. 3 Imported accidents in OSM background

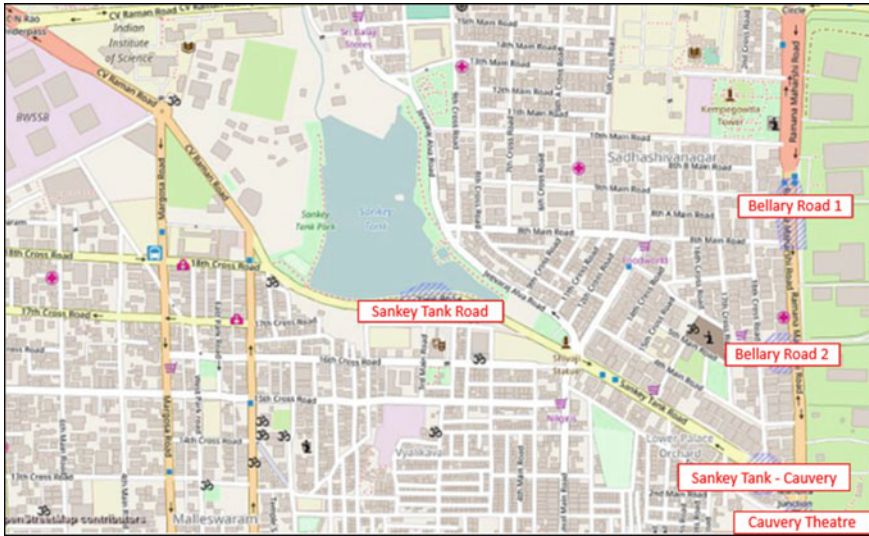


Fig. 4 Black spot locations

4.2 Assigning Black Spots

The tool helps in assigning or calling a region a black spot, provided it satisfies attributes like radius and the number of accidents for a region. These attributes were defined at the time of creating a black spot. Figure 4 shows the black spots defined for the study area and labeled based on their spatial identity (location or road name). Black spots could also be defined and visualized to represent the number of accidents that has taken place, like in Fig. 5. In this case, we see that the road stretch from Mekhri Circle to Cauvery Theatre Junction has two black spots accounting for a total of 11 accidents.

4.3 Tool’s Accident Prediction Model

The main objective of performing accident prediction model was to develop simple, practical accident models which could predict the expected number of accidents on urban roads as accurately as possible. The model can be used to identify factors affecting black spots and inform local road authorities in taking up network safety analysis. The accident prediction model is based on data from 89 data points across junctions and road links falling within the jurisdiction of Sadashivanagar Police Station. The road and traffic characteristics were manually recorded by enumerators. The APM of Safety tool takes into account traffic volume, link length and accident rate. Modeling accidents for junctions is a complicated exercise when compared to

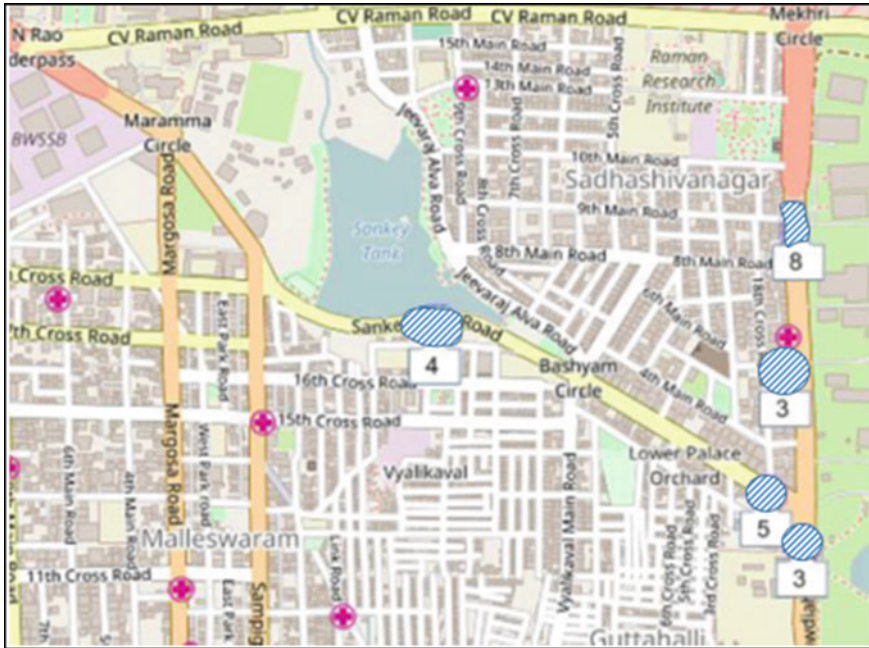


Fig. 5 Black spots by the number of accidents

road links as the links have more uniform accident pattern when compared to the junctions. Also, there is lack of adequate explanatory variables for junctions (Figs. 6 and 7).

The main objective of this study was to develop an accident prediction model based on empirical data, which would forecast the expected number of accidents on road links in the region, as closely as possible. Furthermore, the models were to be used to identify factors affecting safety, i.e., road geometry, traffic characteristics,

```
ACC RATE
[if([SAFETY_LINK_APM_TYPE]=0, 0,
[if([SAFETY_LINK_APM_TYPE]=70 & [NUMLANES]<=2, 0.46,
[if([SAFETY_LINK_APM_TYPE]=70 & [NUMLANES]>2, 0.55,
[if([SAFETY_LINK_APM_TYPE]=60 & [NUMLANES]=1, 0.48,
[if([SAFETY_LINK_APM_TYPE]=60 & [NUMLANES]>1, 0.57,
[if([SAFETY_LINK_APM_TYPE]=50, 0.53,
[if([SAFETY_LINK_APM_TYPE]=40, 0.78, If([SAFETY_LINK_APM_TYPE]=20 &
[SAFETY_LINK_SEPARATED] | [SAFETY_LINK_APM_BACKLANES]=0), 2.69, If
[SAFETY_LINK_APM_TYPE]=30 & ([SAFETY_LINK_SEPARATED]
[SAFETY_LINK_APM_BACKLANES]=0), 1.85, If([SAFETY_LINK_APM_TYPE]=20, 5.1, If
[SAFETY_LINK_APM_TYPE]=30, 3.49, If([SAFETY_LINK_APM_TYPE]=10 &
[SAFETY_LINK_CALMED], 1.5, If([SAFETY_LINK_APM_TYPE]=10, 3, 0)))))))))))]
```

Fig. 6 Defining accident rate



Fig. 7 Accident density prediction for various links

land use, etc. Field visits were carried out by enumerators to collect data on junction and road link geometry.

5 Statistical Approach

In this approach, regression technique was adopted to arrive upon the accident prediction model. Firstly, a correlation matrix was developed to look for variables which are the predominant causal factors for the dependent variable, viz. accident density. While developing the model, two problems were given attention so that the model is as accurate as possible. Firstly, overfitting was avoided as adding too many independent variables may account for more variance, but do not add much to the model. Secondly, independent variables with high multi-collinearity were ignored.

For the model, potential causal variables were generated and relation between these independent variables and dependent variable was checked using scatterplots and correlations. Scatterplots are just for visual examination, and then we go ahead and run correlation to get objective measure of the relationships. Relation among the independent variables was also checked using scatterplots and correlations. Simple linear regression was then conducted for each independent variable–dependent variable pair. Non-redundant variables were then used in the analysis to find the best fit model, and this best fit model was then further used to make predictions about the dependent variable (Table 1).

From the observed regression output, the accident density model equation can be formulated as below:

Table 1 Model output

Variable	Coefficients	P value
Intercept	-2.76	0.03
Volume	0.002	0.04
Speed	0.044	0.08
Number of approaches	0.191	0.09

$$(Y) = (-2.76) + (0.002 * \text{Link Volume}) + (0.044 * \text{Link Speed}) + (0.191 * \text{Number of approaches})$$

The goodness of fit of the model and adjusted R^2 value of 0.73 suggest that the independent variables selected explain the model to a good extent. Thus, from this statistical model’s standpoint, the accuracy of accident prediction model of VISUM Safety tool can be looked at. In order to do that, prediction models of both the approaches were compared and its results are discussed in the next section.

5.1 Model Comparison

The statistical model output and the tool output were compared to check for significance of difference. T test was done on the output of both approaches.

The predicted accident densities of both, the tool approach and statistical approach, are listed in Table 2 for all link types. As seen in Table 3 in T test results, it is seen that the difference of mean value between both approaches is not significant for a 95% C.I. and thus, from statistical approach’s standpoint, safety tool’s prediction model can be called validated.

Table 2 Comparison of predicted accident density

Link type	VISUM safety tool	Statistical method
1	0	2
2	1.8	1.96
3	3.6	3.18
4	5.3	3.7
5	7.1	7.29
6	8.9	7.67
7	10	8.05

Table 3 T stat for model comparison

T value	Critical t	Result
0.214	2.17	Insignificant

6 Summary and Conclusion

The purpose of the work was to develop an accident prediction model which could describe the expected number of accidents on road links in the region as accurately and practicably as possible. The objective was met by identifying factors which affect safety on the road links by the use of explanatory variables in the model. Predominant variables in the model were those describing the motor vehicle traffic flow and the traffic speed. Also, explanatory variables in the junction models did not improve the ‘percentage explained’ value considerably. A hindrance in safety analysis for this dataset is the relatively small number of observed accidents in the data, which may be problematic for statistical studies. Efforts will be made to augment the data which would then aid in drawing patterns and give the model, leeway to introduce more causal factors. For the region, generalized linear modeling techniques were used to relate accident densities to those predicted by the VISUM Safety tool. It was seen that the two methods highly complement each other in predicting accident densities.

7 Further Research Work

Variables like two-wheeler (TW) composition or involvement of TW could be added to see the variance in severity. More combinations could be brought in and tested in Biogeme tool which allows flexible operations for logit model. Ordered logit model can be adopted to predict the probability of a particular type of accident severity. Variables describing flow characteristics of vulnerable road users (cyclist and pedestrians) can also be included in some of the models.

References

1. Smeed RJ (1949) Some statistical aspects of road safety research. *J R Stat Soc Ser A (Gen)* 112(1):1–34
2. Andreassen DC (1985) Linking deaths with vehicles and population. *Traffic Eng Control* 26(11):547–549
3. Ponnaluri RV (2012) Modeling road traffic fatalities in India: Smeed’s law, time invariance and regional specificity. *IATSS Res* 36(1):75–82
4. Abdel-Aty MA, Radwan AE (2000) Modeling traffic accident occurrence and involvement. *Accid Anal Prev* 32(5):633–642
5. Goyal P, Joshi S, Kamplimath H, Prajapati D (2016) Accident prediction modeling of a major road of Ahmedabad
6. Bhat P, Hebbani L, Rama VA, Kolhar P (1968) Accident prediction modelling for an urban road of Bangalore. *Int J Res Eng Technol*. eISSN 2319-1163
7. Laufer J (2014) Network management and the forecast of accident blackspot locations. In: ARRB conference (No. 4.4), Sydney, New South Wales, Australia, 26 Oct 2014

Applicability of Unconventional Intersection Designs Over Pretimed Signalized Intersection Design Along a Coordinated Corridor



Ajinkya S. Mane and Srinivas S. Pulugurtha

Abstract The focus of this research is on evaluating the performance of three unconventional intersection designs [Michigan U-turn (MUT), superstreet, and continuous green T-intersection (CGT)] over existing pretimed signalized intersection design along Highway 49 in the city of Charlotte, North Carolina, USA. MUT and superstreet intersection designs eliminate the left turns from side streets and replaces them with a combination of right-turn and U-turn movement. However, in the case of CGT, a separate continuous lane is provided for the through movement at one of the approaches of the intersection. Ten signalized intersections were identified along the selected study corridor. A base model was developed using Synchro/SimTraffic traffic simulation software and validated by comparing traffic volumes (provided as input vs. simulated) and through visual audits. Underperforming intersections were identified along the study corridor and were replaced with the aforementioned unconventional intersection designs. Performance measures, such as the total vehicle delay, the total delay per vehicle, and the total number of stops, were computed and compared with the existing condition. The results obtained indicate that the selected unconventional designs are not applicable at all considered intersections. The use of unconventional intersection designs could reduce the average delay per vehicle at the corridor level. However, the use of unconventional intersection designs could result in an increase in the total number of stops at the corridor level. The findings and recommendations from this research help practitioners assess the applicability of the selected unconventional intersection designs over the conventional pretimed signalized intersection design.

Keywords Conventional intersection · Unconventional intersection · Operational performance · Synchro/SimTraffic

A. S. Mane · S. S. Pulugurtha (✉)
The University of North Carolina at Charlotte, Charlotte, NC 28223-0001, USA
e-mail: sspulugurtha@uncc.edu

A. S. Mane
e-mail: amane@uncc.edu

1 Introduction

Conventional signalized intersection designs work efficiently at the corridor level when designed meticulously with geometric and traffic signal demeanor. Nonetheless, the performance of a signalized intersection decreases due to an increase in traffic volume and associated delay. The increase in delay, along with fuel consumption, emissions and, possibly the number of crashes, could be attributed to problems at the entire intersection, certain traffic movements at the intersection, or adjacent intersections. The use of unconventional intersection designs [MUT, superstreet, CGT, bow tie, jughandle, etc.] as an alternative to the traditional pretimed signalized intersection design may reduce the delay and associated problems at the corridor level.

MUT intersection design performs better than a conventional intersection by reducing travel time, delay, and crashes and by increasing the speed at the isolated intersection/along the corridor. Hashim et al. [1] compared MUT intersection with conventional three-legged intersections. Their results indicate that MUT is efficient up to 1250 vehicles/hour/approach for three-legged intersections. Najaf and Pulugurtha [2] observed that unsignalized and signalized MUT intersection performs better when compared to pretimed conventional intersection. The corridor considered in their study has three intersections (two three-legged intersections and one four-legged intersection). Similar findings were observed by other researchers [3–11], in which the operational and safety effects of MUT intersection were compared with the conventional intersection design.

Studies [2, 6, 9, 10, 12, 13] suggest that superstreet intersection design improves the operational performance by increasing capacity as well as by reducing travel time and delay. In most of these studies, conventional intersections were upgraded to superstreet design. However, in the study by Haley et al. [14], existing superstreet intersections were replaced and compared with equivalent conventional intersections. They observed that superstreet design outperformed the conventional intersection at every selected location.

CGT, also referred to as Florida T-intersection, has been implemented in Florida for several decades. Jarem [15] concluded that CGT can reduce total delay per vehicle and total fuel consumption when compared to the conventional T-intersection. Likewise, researchers in the past [16, 17] have observed that operational and safety performance of CGT is better when compared to a conventional T-intersection.

El Esawey and Sayed [18] provided an in-depth literature review on unconventional intersection studies. Overall, researchers have extensively worked on the applicability of unconventional intersection designs at isolated locations/at the corridor level. They have defined the corridor by selecting a maximum of five conventional intersections, which were replaced and then compared with unconventional intersections. In addition, in practice, it is not feasible to propose and implement unconventional intersection designs at every intersection along an existing corridor. None of the studies have evaluated the operational performance of the corridor after implementing unconventional intersections only at selected or underperforming intersections.

The applicability of different unconventional intersection designs among themselves has also not been performed widely either. Further, researching on the applicability of unconventional intersection designs along an existing pretimed coordinated corridor may provide vital insights and assist practitioners in decision making. Therefore, the focus of this research is to identify underperforming intersections along a pretimed coordinated corridor and to check the effectiveness of unconventional intersection designs at these intersections. The findings and recommendations will help practitioners assess the applicability of unconventional intersection designs over the conventional pretimed coordinated signalized intersection design.

2 Methodology

Synchro/SimTraffic traffic simulation software was used to simulate the pretimed coordinated arterial corridor and to check the applicability of unconventional intersection designs along the corridor. The methodology adopted includes the following steps.

1. Build and calibrate the study corridor using Synchro/SimTraffic.
2. Identify underperforming signalized intersections along the corridor.
3. Convert the underperforming signalized intersections to unconventional intersection designs.
4. Compare the system performance of conventional and unconventional intersection designs at intersection and corridor level.

Each step is explained next in detail.

2.1 *Build and Calibrate the Study Corridor Using Synchro/SimTraffic*

Highway 49 in the city of Charlotte, North Carolina, USA was selected as the study corridor. Highway 49 is a four-lane divided arterial road. Ten signalized intersections were identified along the selected study corridor. Six signalized intersections are four-legged intersections and four signalized intersections are T-intersections.

Network characteristics such as lane configuration, storage length, speed limit, and the width of all lanes at each selected signalized intersection were captured using Google Earth. Traffic characteristics such as traffic volume, pedestrian volume, signal timings, and phasing pattern were collected from the city of Charlotte Department of Transportation (CDoT). The traffic data obtained from CDoT was collected in the months of February and March of the year 2014. The evening peak period (4:15–5:15 p.m.) was considered for model development, as congestion levels were higher during this period than the morning peak period. A base model was developed and calibrated using Synchro/SimTraffic (Fig. 1). The base model was

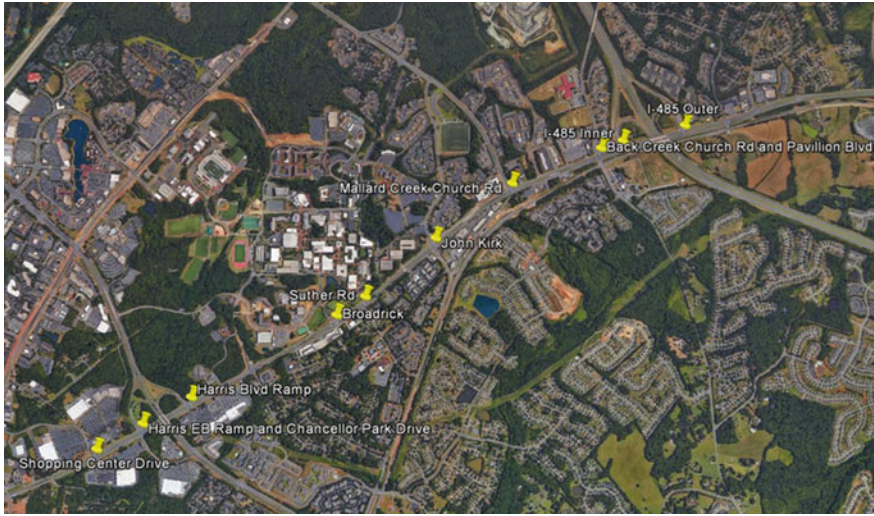


Fig. 1 Study corridor—Highway 49

validated using traffic volume data. The actual traffic volumes provided as input were compared with the simulated traffic volume to check the accuracy of the base model in predicting existing traffic condition. This was also complemented through visual audits.

2.2 Identify Underperforming Signalized Intersections Along the Corridor

The level of service (LOS) for each signalized intersection was obtained from the calibrated and validated Synchro model. Firstly, the calibrated model was simulated in SimTraffic traffic simulation tool using five different random seed numbers. Secondly, the total vehicle delay, the total delay per vehicle, and the total number of stops, for each signalized intersection, were obtained from the simulation outputs to quantify the LOS. The Highway Capacity Manual (2010) guidelines were used to determine the LOS for each signalized intersection. The underperforming signalized intersections may increase the delay along the pretimed coordinated corridor. Therefore, signalized intersections whose LOS is ‘D’ or worse were selected to check the effectiveness of unconventional intersection designs and improve the overall system performance along the corridor. At some intersections, the application of unconventional intersection design may not be possible, since existing signalized intersections were placed very close to each other.

2.3 Convert the Underperforming Signalized Intersections to Unconventional Intersection Designs

The identified underperforming signalized intersections were replaced with MUT, superstreet, and CGT. Each unconventional intersection design is explained next in detail.

Median U-Turn Intersection or Michigan U-Turn (MUT)

In this design, left-turning traffic from the minor street must take a right turn at the intersection, followed by a median crossover on the major street. Also, direct left-turning traffic from the major street is directed to take a U-turn at the downstream directional crossover (Fig. 2a). The crossover is typically a protected signalized intersection. According to the Federal Highway Administration (FHWA) [19], directional crossover is placed at 500–650 feet downstream from the main signalized intersection. According to FHWA [20], a single left-turning lane is provided when left-turning volume is more than 100 vehicles. On the other hand, dual left-turning lanes are provided if left-turning traffic volume is more than 300 vehicles per hour. The recommended cycle length for MUT intersection is 60–120 s. In this study, optimal cycle lengths were computed and were in the range of 60–120 s. Total split for each phase was allocated by the proportion of vehicles from each approach. In this study, traffic signals were designed as per the guidelines provided by the North Car-

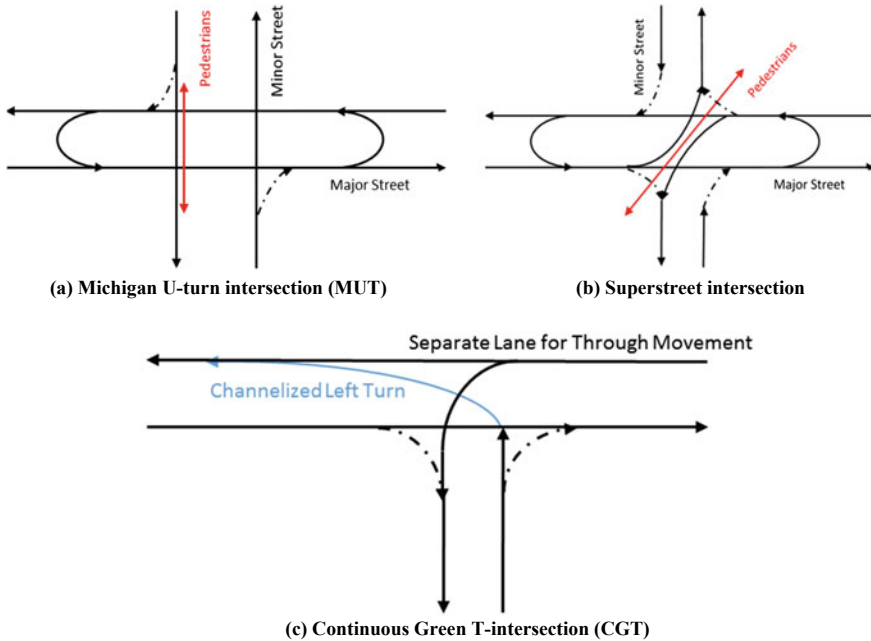


Fig. 2 Selected unconventional intersection designs

olina Department of Transportation (NCDOT) in their traffic signal design manual [21].

Restricted U-Turn/Superstreet/J-Turn Intersection

Superstreet intersection is the modified version of MUT intersection. In this design, through traffic movement and left-turning movement from the minor street are restricted (Fig. 2b). Left turn and through traffic from the minor street have to take U-turn at the directional crossover, which is provided at the median crossover on the major street. Typical distance of directional crossover for U-turn is 400 and 800 feet for stop-controlled and signal-controlled intersections, respectively [22]. However, direct left-turn movement and through movement are possible from the main intersection. For better traffic coordination along the corridor, the same cycle length is recommended for both the major traffic directions. This also helps pedestrians to cross the intersection in a single-cycle length. In this study, traffic signals were designed as per NCDOT traffic signal design manual guidelines [21].

Continuous Green T-Intersection (CGT Intersection)/Florida T-Intersection

CGT is provided to relieve congestion on the main highway. In this design, a separate continuous lane is provided for through movement at one of the approaches of the intersection. Channelized left-turn lanes are provided to merge to the continuous lane (Fig. 2c). In this study, two T-intersections were selected for CGT.

Other unconventional intersection designs such as reverse jughandle, forward jughandle, and bow tie are not suitable for testing and evaluation along the selected corridor, and were, therefore, not explored in this study.

2.4 Compare the Performance of Conventional and Unconventional Intersection Designs at Intersection and Corridor Level

Each proposed unconventional intersection design was compared with the existing condition in Synchro. Existing conventional intersection and proposed unconventional intersection designs at Mallard Creek Church Rd are presented as an example in Fig. 3. The total vehicle delay, total delay per vehicle (includes control delay), and the total number of stops were compared to check the operational performance of the unconventional intersection design with the existing intersection design and at corridor level.

3 Results

The results obtained from modeling are discussed in this section.

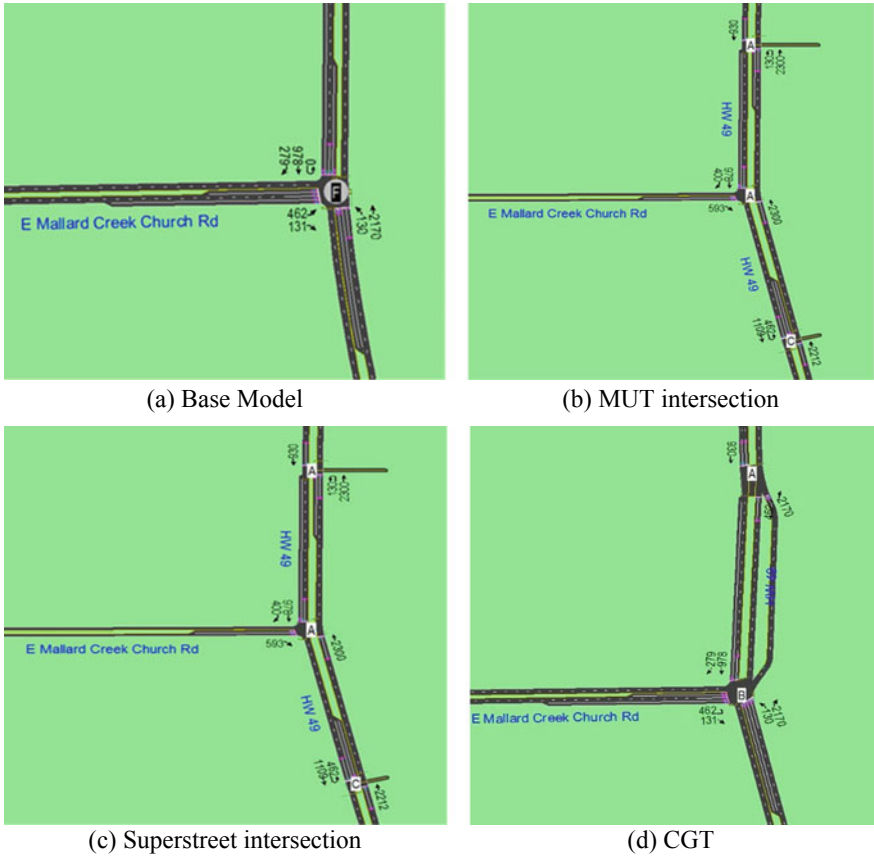


Fig. 3 Comparison of conventional and unconventional intersection designs

3.1 Simulation Model and Validations

In this study, each modeling scenario was simulated using five different random seed numbers and the average of output values obtained are presented as the results. Firstly, the calibrated base model was validated by comparing actual and simulated traffic volumes. On Highway 49, major traffic movement is along the northbound and southbound directions. Therefore, the calibrated base model was validated by comparing traffic volumes for both northbound and southbound directions. The errors in traffic volume were observed to be lower than 10% in both the directions. This indicates that the calibrated base model reasonably replicates the existing traffic condition along the corridor.

3.2 Comparison of Existing Signalized Intersection and Unconventional Intersections

The operational performance of the existing and proposed unconventional intersection was compared using total vehicle delay, total delay per vehicle, and the total number of stops obtained from SimTraffic. Per Synchro/SimTraffic traffic simulation software user guide [23], the total delay is equal to total travel time minus the travel time for the vehicle with no other vehicles or traffic control devices. Further, the total delay per vehicle is equal to the total delay divided by the number of vehicles. This is nothing but the delay incurred due to traffic control devices. The LOS was determined by comparing the computed total delay per vehicle with LOS criteria in HCM 2010.

3.3 LOS for Existing Signalized Intersections

The computed total vehicle delay and the total delay per vehicle are summarized in Tables 1 and 2, respectively. Using the HCM 2010 guidelines, the LOS for all the ten signalized intersections were determined and summarized in Table 3. The results obtained indicate that LOS for seven out of ten signalized intersections were critical

Table 1 Total vehicle delay (h)—comparison

Signalized intersection	Base model	MUT			Superstreet			CGT
		U/S	At	D/S	U/S	At	D/S	
I-485 Outer	23.3	–	22.7	–	–	20.4	–	22.2
I-485 Inner	55.9	–	58.8	–	–	43.0	–	48.1
Pavilion Rd	116.6	–	118.2	–	–	101.9	–	76.6
<i>Mallard Creek Church Rd (T-intersection)</i>	86.0	29.2	23.9	27.1	13.0	14.6	–	83.6
<i>John Kirk Dr</i>	95	21.6	48.9	15.4	54.8	55.3	6.5	100
<i>Suther Rd (T-intersection)</i>	82.7	–	11.5	3.7	–	21.6	19.6	88.3
<i>Broadrick Rd</i>	61.1	7.7	13.5	–	13.4	20.1	–	60.4
<i>E W T Harris Blvd Ramp</i>	109.9	22.4	32.9	26.5	10.7	41.3	112.5	94.9
<i>Chancellor Park Dr</i>	78.2	53.8	61.3	33.6	50.8	39.8	24.0	77.8
Shopping Center Dr	36.5	–	104.5	–	–	95.6	–	33.7

Table 2 Total delay per vehicle (s)—comparison

Signalized intersection	Base model	MUT			Superstreet			CGT
		U/S	At	D/S	U/S	At	D/S	
I-485 Outer	24.0	–	23.5	–	–	20.9	–	23.8
I-485 Inner	54.1	–	57	–	–	40.8	–	48.3
Pavilion Rd	96.6	–	97.5	–	–	80.7	–	66.2
<i>Mallard Creek Church Rd (T-intersection)</i>	82.6	30.5	20.2	27.6	13.6	12.6	–	83.2
<i>John Kirk Dr</i>	86.9	23.3	34.8	17.1	59.7	40.6	7.3	90.4
<i>Suther Rd (T-intersection)</i>	106.4	–	14.2	5.3	–	25.7	25.8	110.7
<i>Broadrick Rd</i>	71.9	8.8	13.8	–	15.9	20.4	–	70.7
<i>E W T Harris Blvd Ramp</i>	103.5	24.1	31.6	31.9	12.1	38.3	141.0	89.1
<i>Chancellor Park Dr</i>	68.7	56.2	49.2	34.6	53.1	33.9	26.5	67.8
Shopping Center Dr	35.8	–	106.4	–	–	98.3	–	32.8

Table 3 LOS—comparison

Signalized intersection	Base model	MUT			Superstreet			CGT
		U/S	At	D/S	U/S	At	D/S	
I-485 Outer	C	–	C	–	–	C	–	C
I-485 Inner	D	–	E	–	–	D	–	D
Pavilion Rd	F	–	F	–	–	F	–	E
<i>Mallard Creek Church Rd</i>	F	C	C	C	B	B	–	F
<i>John Kirk Dr</i>	F	C	C	B	E	D	A	F
<i>Suther Rd (T-intersection)</i>	F	–	B	A	–	C	C	F
<i>Broadrick Rd</i>	E	A	B	–	B	C	–	E
<i>E W T Harris Blvd Ramp</i>	F	C	C	C	B	D	F	F
<i>Chancellor Park Dr</i>	E	E	D	C	D	C	C	E
Shopping Center Dr	D	–	F	–	–	F	–	C

(LOS is 'D' or worse), and appropriate measures should be taken to improve the operational performance along the corridor.

3.4 *Unconventional Intersections*

MUT design was considered for six signalized intersections along the existing corridor. MUT was not considered at Pavilion Rd intersection since the spacing between the upstream intersection (I-485 Inner) and Pavilion Rd intersection is ~450 feet. Further, the distance between Broadrick Rd intersection and Suther Rd intersection is ~600 feet. Therefore, MUT intersection was proposed by considering Broadrick Rd intersection and Suther Rd intersection together as one intersection. In other words, a total of five MUT intersections were proposed at six different locations along the corridor.

Overall, MUT design was considered at Mallard Creek Church Rd, John Kirk Dr, Broadrick Rd, E W T Harris Blvd Ramp, and Chancellor Park Dr intersections along the study corridor. All the six intersections are highlighted in italics in Table 1. Traffic volumes from the base model were adjusted and allocated at appropriate downstream and upstream crossovers and at the main intersection. The LOS for Mallard Creek Church Rd, John Kirk Dr, and E W T Harris Blvd Ramp improved from LOS 'F' to stable flow condition (LOS 'C'). The LOS for Suther Rd and Broadrick Rd improved from LOS 'F' and LOS 'E' to LOS 'B.' The LOS for Chancellor Park Dr improved from LOS 'E' to LOS 'D.' LOS for all the proposed median U-turn crossovers at upstream and downstream locations of respective intersections were in the range of LOS 'A' to LOS 'C' (acceptable range), except at the median U-turn crossover located at the upstream of Chancellor Park Dr intersection, where LOS 'E' was observed. This may be due to the short distance between the Shopping Center Dr and Chancellor Park Dr (~500 feet). Therefore, it is not recommended to implement MUT intersection at Chancellor Park Dr with upstream median U-turn crossover between Shopping Center Dr and Chancellor Park Dr intersections.

The suitability of superstreet intersection design was examined at all the selected MUT intersections. Suther Rd intersection was considered as the upstream median U-turn crossover, for superstreet intersection design at Broadrick Rd intersection, as they are located (~600 feet) very close to each other. Further, traffic volume from the base model was adjusted and allocated at appropriate downstream and upstream crossovers and at the main intersection. The results obtained from SimTraffic indicate that LOS for the proposed superstreet intersections at Mallard Creek Church Rd, Suther Rd, Broadrick Rd, and Chancellor Park Dr intersections were better than the existing condition (Table 3). The LOS for John Kirk Dr and Chancellor Park Dr improved from jammed traffic condition (LOS 'F') or at capacity (LOS 'E') to unstable traffic flow condition (LOS 'D'). Further, acceptable LOS was observed for the majority of the median U-turn crossovers. However, the median U-turn crossovers at the upstream of John Kirk Dr and at the downstream of E W T Harris Blvd Ramp intersections were observed to be underperforming (LOS 'E' and LOS 'F', respectively).

The study corridor has two underperforming T-intersections: Mallard Creek Church Rd and Suther Rd intersections. CGT was proposed at these two intersections. At both the intersections, continuous green phase/separated continuous lane was provided in the northbound direction. In addition, a separate pedestrian signal phase was provided due to the high pedestrian traffic movement (186 pedestrians per hour) to cross Highway 49 at Suther Rd intersection. The results obtained indicate that the LOS for Mallard Creek Church Rd and Suther Rd intersection did not improve at both the intersections.

In addition, the total number of stops for each unconventional design was obtained from SimTraffic and was compared with the base model outputs (Table 4). According to Synchro/SimTraffic traffic simulation software user guide, the total number of stops is defined as a count of vehicle stops when vehicle’s speed drops below ~7 miles/h (10 feet/s). The total number of stops for the majority of the MUT intersections dropped within the range of 14–53% when compared to the respective base model intersections. However, the total number of stops for MUT intersection at Chancellor Park Dr intersection increased by ~43% when compared to the existing condition. The effect of MUT intersection at Mallard Creek Church Rd and Chancellor Dr was observed at nearby conventional intersections (Pavilion Rd and Shopping Center Dr intersections) in terms of increase in the total number of stops.

On the other hand, in case of superstreet intersection design, the total number of stops decreased in the range of ~5–67% for most of the intersections, when compared to the existing condition; except at John Kirk Dr and Chancellor Park Rd intersections where the total number of stops increased by ~53 and ~46%, respectively. Moreover,

Table 4 # stops—comparison

Signalized intersection	Base model	MUT			Superstreet			CGT
		U/S	At	D/S	U/S	At	D/S	
I-485 Outer	1584	–	1538	–	–	1565	–	1522
I-485 Inner	2469	–	2523	–	–	2262	–	2259
Pavilion Rd	4489	–	4780	–	–	4167	–	3399
<i>Mallard Creek Church Rd (T-intersection)</i>	3562	1492	1657	1490	852	1169	–	2867
<i>John Kirk Dr</i>	3263	1287	2780	1257	2589	4986	580	3369
<i>Suther Rd (T-intersection)</i>	2037	–	932	246	–	1241	1202	2219
<i>Broadrick Rd</i>	2312	798	1583	–	963	2047	–	2307
<i>E W T Harris Blvd Ramp</i>	4533	1596	2544	930	1017	4285	2125	4193
<i>Chancellor Park Dr</i>	2279	2787	3281	2875	2618	3329	2040	2172
<i>Shopping Center Dr</i>	2188	–	2702	–	–	2534	–	2090

Table 5 Operational performance of selected corridor

Parameters	Base model	MUT	Superstreet	CGT
Total delay (h)	748.6	741.0	762.4	748.2
Total delay/vehicle (s)	259.1	231.8	246.2	259.2
Total # stops	28,716	39,078	41,571	28,053
Northbound travel time (s)	824	1162	1291	660
Southbound travel time (s)	1183	824	963	1269

in case of CGT intersections, the total number of stops decreased at Mallard Creek Church Rd (~20%) intersection but increased at Suther Rd intersection (~9%) when compared to the existing condition.

In general, delays and total number of stops were lower at MUT intersections when compared to the respective superstreet intersections.

Overall, in terms of delays, the operational performance of the MUT intersection design was observed to be better when compared with the existing conventional intersection design. In the case of MUT intersection design, the total vehicle delay and the total delay per vehicle along the corridor decreased by ~1% and ~10%, respectively, when compared with the existing conventional intersection design (Table 5). In the case of superstreet intersection design, the total vehicle delay increased by ~2% while the total delay per vehicle decreased by ~5% along the corridor when compared to the existing conventional intersection design. However, in the case of CGT intersection design, the total vehicle delay, the total delay per vehicle, and the total number of stops were similar to the results obtained from the existing conventional intersection design. Among the three unconventional intersection designs, the operational performance of MUT intersection is better than superstreet and CGT. Further, the total number of stops along the corridor for MUT and superstreet intersections increased by ~36% and ~45%, respectively, when compared with the existing condition (Table 5). Moreover, in terms of travel time, for the northbound direction, travel time for MUT and superstreet along the corridor increased but decreased for the southbound direction. However, in case CGT intersection design, the travel time was decreased in the northbound direction, but decreased in the southbound direction.

4 Conclusions

The pretimed coordinated system is efficient when signalized intersections are closely spaced. However, a poorly coordinated system results in increased delay and queuing of vehicles at signalized intersections. On the other hand, unconventional intersection designs help eliminate the left-turning movement from minor streets and reduce the number of conflicting points at the signalized intersection. Eliminating the left turns at signalized intersections helps reduce the number of crashes and improve safety. Therefore, to improve the operational performance at underperform-

ing intersections, unconventional intersection designs such as MUT, superstreet, and CGT were evaluated along a selected corridor in this research.

LOS for most of the underperforming intersections improved when compared with the respective conventional intersection design. The total vehicle delay and total delay per vehicle decreased after the implementation of unconventional intersection designs at the majority of the underperforming conventional signalized intersections. Moreover, the total number of stops decreased at majority of the unconventional intersections when compared to the underperforming conventional signalized intersections. The superstreet design is, however, not suitable at John Kirk Dr and E W T Harris Blvd Ramp intersections if decisions are based on the LOS at the corresponding median U-turn crossovers and the total number of stops. The MUT design is particularly not suitable at Chancellor Park Dr intersection based on the LOS at the corresponding median U-turn intersection and the total number of stops. Further, not much difference in travel times (by considering the sum of travel times in the northbound and the southbound directions) was observed along the study corridor after implementing unconventional intersection designs at underperforming conventional signalized intersections. In comparison, among the three unconventional intersection designs, the operational performance of MUT intersection design was observed to be better than superstreet and CGT intersection designs.

Continuous green phase for through movement is not a pragmatic solution due to the high pedestrian movement at Suther Rd intersection. This should be supplemented with a pedestrian overpass or underpass (expensive). Therefore, the application of unconventional intersection designs should be carefully assessed by checking the geometric, traffic, and pedestrian characteristics at the underperforming as well as at the upstream and downstream intersections.

In this study, the effect of each unconventional intersection design was checked independently. Further, using a combination of unconventional intersection designs may increase the operational performance at the corridor level. Also, it is necessary to evaluate the performance of unconventional intersection designs during special events (commencement, football games, etc.) since the use of median crossovers will be higher resulting in increased delays and longer queue lengths. Likewise, their suitability should be modeled and tested under various heterogeneous traffic condition scenarios.

Acknowledgements The authors sincerely thank the staff of the city of Charlotte Department of Transportation (CDOT) for their help with traffic volume and signal timing data.

References

1. Hashim IH, Ragab M, Asar GM (2017) Evaluation of operational and environmental performance of median U-turn design using microsimulation. *Int J Traffic Transp Eng* 7(1):37–51
2. Najaf P, Pulugurtha SS (2014) Efficiency and safety evaluation of unconventional intersections. In: 8th national congress on civil engineering, Noshirvani University of Technology, Babol, Iran, 7–8 May 2014
3. Federal Highway Administration (2007) <https://www.fhwa.dot.gov/publications/research/safety/07033/07033.pdf>
4. Jagannathan R (2007) Synthesis of the median U-turn intersection treatment, safety, and operational benefits. In: 3rd urban street symposium, Washington, DC
5. Zhao J, Ma W, Head KL, Yang X (2014) Optimal intersection operation with median U-turn: a lane based approach. *Transp Res Rec* 2439:77–82
6. Federal Highway Administration (2010) <https://www.fhwa.dot.gov/publications/research/safety/09060/09060.pdf>
7. Henderson SM, Stamatiadis N (2001) Use of median U-turns to improve traffic flow along urban arterials. *J Transp Res Forum* 40(2):137–145
8. Coates A, Ping Y, Koganti S, Du Y (2012) Maximizing intersection capacity through unconventional geometric design of two-phase intersections. *Transp Res Rec* 2309:30–38
9. Reid J, Hummer J (1999) Analyzing system travel time in arterial corridors with unconventional designs using microscopic simulation. *Transp Res Rec* 1678:208–215
10. Reid J, Hummer J (2001) Travel time comparisons between seven unconventional arterial intersection designs. *Transp Res Rec* 1751:56–66
11. Bared JG, Kaisar EI (2002) Median U-turn design as an alternative treatment for left turns at signalized intersections. *J Inst Transp Eng* 72(2):50–54
12. Hummer JE (1998) Unconventional left turn alternatives for urban and suburban arterials: part one. *J Inst Transp Eng* 68(9):26–29
13. Kim T, Edara PK, Bared JG (2007) Operational and safety performance of a nontraditional intersection design: the superstreet. In: 86th annual meeting of the transportation research board, Washington, DC
14. Haley R, Ott S, Hummer J, Foyle R, Cunningham C, Schroeder B (2011) Operational effects of signalized superstreets in North Carolina. *Transp Res Rec* 2223:72–79
15. Jarem ES (2004) Safety and operational characteristics of continuous green through lanes at signalized intersections in Florida. In: Institute of transportation engineers annual meeting and exhibit, Orlando, FL
16. Litsas S, Rakha H (2013) Evaluation of continuous green T-intersections on isolated undersaturated four-lane highways. *Transp Res Rec* 2348:19–29
17. Wood J, Donnell ET (2016) Safety evaluation of continuous green T-intersections: a propensity scores-genetic matching-potential outcomes approach. *Accid Anal Prev J* 93:1–13
18. El Esawey M, Sayed T (2013) Analysis of unconventional arterial intersection designs (UAIDs): state-of-the-art methodologies and future research directions. *J Transp A Transp Sci* 9(10):860–895
19. Federal Highway Administration (2014) https://safety.fhwa.dot.gov/intersection/alter_design/pdf/fhwas14069_mut_infoguide.pdf
20. Federal Highway Administration (2004) <https://www.fhwa.dot.gov/publications/research/safety/04091/04091.pdf>
21. North Carolina Department of Transportation (2004) <https://connect.ncdot.gov/resources/safety/its%20and%20signals%20resources/its%20and%20signals%20unit%20design%20manual.pdf>
22. Federal Highway Administration (2014) https://safety.fhwa.dot.gov/intersection/alter_design/pdf/fhwas14070_rcut_infoguide.pdf
23. Trafficware (2014) Synchro Studio 9: user guide. Trafficware Inc., Albany, CA

Evaluating the Influence of a Freeway Capacity Improvement Project on Travel Time-Based Performance Measures Within Its Vicinity



V. S. R. S. Sudheendra Yesantaroo and Srinivas S. Pulugurtha

Abstract The focus of this research is on examining changes in travel time and related measures during the construction period and after increasing the capacity of a freeway corridor by comparing it with before the construction of the capacity improvement project in an urban area. Along with the freeway, the arterial streets connecting the freeway were also analyzed to assess changes within the vicinity of the project site. Further, the efficiency of the capacity improvement project in reducing congestion is evaluated by the time-of-the-day and day-of-the-week, during peak and off-peak periods on Wednesday, Friday, and Sunday. The findings indicate that travel times increased on the connecting arterial streets due to the migration of traffic from the freeway during the construction period. Also, at times, it appears that the travel time has decreased on the freeway due to the people choosing alternate routes rather than traveling through the construction zone. After the construction, there is a considerable amount of congestion even though the freeway travel time has decreased significantly. This could be due to the induced travel demand resulting in an increase in the travel time. The variations seem to marginally differ by the time-of-the-day and day-of-the-week. It is a general perception that an increase in capacity decreases travel times. However, a slight increase in travel time is observed on most of the links in the considered transportation network. Nonetheless, though there is an increase in buffer time, freeway expansion is very lucrative as a higher number of vehicles pass through a corridor with a marginal increase in travel time.

Keywords Freeway · Capacity · Travel time · Performance measure · Arterial street

V. S. R. S. Sudheendra Yesantaroo · S. S. Pulugurtha (✉)
The University of North Carolina at Charlotte, Charlotte, NC 28223-0001, USA
e-mail: sspulugurtha@unc.edu

V. S. R. S. Sudheendra Yesantaroo
e-mail: vyesanta@unc.edu

1 Introduction

Urban areas worldwide are growing rapidly every year, primarily the ones which serve as a commercial hub for their respective region. Congestion in such urban areas is unavoidable due to the growth (e.g., a considerable increase in population every year). It is important to build new roads or expand the capacity of existing roads to reduce congestion, cater the growing demand, and improve the efficiency of the transportation system.

Increasing capacity of an existing road may or may not have a positive influence on transportation system performance. The influence could be different during the construction period and after the construction is complete when compared to before the construction period. The influence could also vary spatially and may decrease as the distance from the capacity improvement project site decreases. Further, the influence could also extend to roads that are within its vicinity. Furthermore, the influence could also vary by the time-of-the-day and day-of-the-week. However, research on the influence of a capacity improvement project has been limited in the past due to the lack of available data. The possibility of capturing dynamic and continuous travel time and/or speed data, in recent years, makes such an effort a feasibility today. Therefore, this research focuses on examining changes in travel time and related measures during the construction period and after increasing the capacity of a freeway corridor by comparing it with before the construction of the capacity improvement project in an urban area. Along with the freeway, the arterial streets connecting the freeway were also analyzed to assess changes within the vicinity of the capacity improvement project site. The measures considered and compared include the average travel time (TT_{Avg}), 95th percentile travel time (TT_{95} or planning time, PT), buffer time (BT), and buffer time index (BTI).

2 Literature Review

Induced travel demand needs to be taken into consideration when roads are expanded or when capacity is increased. As per this phenomenon, more of a good is consumed as supply increases. In the present context, vehicular volume increases as the number of lanes or capacity of a road is increased.

Hansen and Yuanlin [1] analyzed 18 years of data from 14 Californian metropolitan areas. They found that every 10% increase in lane miles was associated with a 9% increase in vehicle miles traveled for 4 years after road expansion. The Surface Transportation Policy Project [2] for 70 United States metropolitan areas over a 15-year period concluded areas that spent heavily on road capacity projects managed no good in easing traffic congestion than areas that did not spend heavily on road capacity projects. Similar studies were conducted by Fulton et al. [3] and Noland and Cowart [4] to attain the data and trace out the influence of an increase in lane miles on an increase in vehicle miles traveled. Cervero and Mark [5] have analyzed

the induced travel demand using political, environmental, and demographic features and developed vehicle miles traveled model and lane miles model. Their study also exhibited a strong direct relationship between road investment and travel demand.

Goodwin [6] found that proportional savings in travel time were related to a proportional increase in traffic. Their study states that many road proposals have not been effective in the United States due to induced demand. One reason could be that many studies have failed to extract a proper relation to account for road capacity improvements and traffic growth [7–11].

Some researchers discussed the rebound theory with respect to fuel efficiency. Greening et al. [12] stated that an increase in fuel efficiency reduces fuel cost per unit of utilization, which induces more utilization than normal. This is same as induced demand, where people tend to drive more and consume more fuel than normal.

DeCorla-Souza and Cohen [8] and Cohen [10] studied on how road capacity improvements affected travel time or speed. They observed a direct relation between road capacity improvement and travel time. Noland and Lem [13] stated that stronger fuel efficiency standards for new cars can increase the number of miles traveled for each gallon consumed. Higher road capacity can decrease the fuel consumed, in turn, decreasing the cost of the travel and the time taken to reach the destination.

Some researchers focused on operational performance effects associated with work zones. Haseman et al. [14] studied on travel delay at work zones using Bluetooth probes. Khattak et al. [15] studied the relation between work zones and injury as well as non-injury crashes in work zones. Dharia and Adeli [16] developed a neuro-fuzzy logic model to estimate the capacity of a freeway work zone.

Overall, the past studies focused on the effect of road capacity improvement on vehicle miles traveled. Some of them focused on the effect of a road capacity improvement project on operational performance measures. However, not many researchers have analyzed the effect of a road capacity improvement project on links within its vicinity. Further, not many studies focused on temporal variations or different travel time-related measures. This paper focuses on a comprehensive evaluation to understand the effect of a road capacity improvement project on travel time on the freeway as well as connecting arterial streets during the construction period and after the expansion of freeway.

3 Study Area and Data

For evaluating the influence of a freeway capacity improvement project on travel time-based performance measures within its vicinity, a 15-mile stretch along I-85 from W T Harris Blvd at Exit 45 to Kannapolis at Exit 60 in the Charlotte region, North Carolina, United States, was considered as the study area. The study area considered also includes the connecting arterial streets within its vicinity (1 mile). The 1-mile vicinity was considered to exclude the effect of other local traffic and network features that could actually skew the data.

The travel time data was collected at Traffic Message Channel (TMC) level, also referred to as link in this paper. The year 2010 was taken into consideration to compare the travel time variations during the construction period (2012) and after the expansion of the freeway section (2014).

4 Methodology

Raw travel time for every minute, for each link, was obtained from HERE. HERE is a mapping data company that captures location, road network, and traffic patterns. Each TMC or link is not of a definite length. They are defined based on geometric and traffic control characteristics (examples, entry or exit ramps, signalized intersection, etc.). The raw travel time data file had TMC code, time stamp, reference speed, and travel time in minutes.

Weekdays (Wednesday and Friday) and a weekend day (Sunday) were considered for analysis and assessment. Typical weekday patterns are observed on Wednesday, while unusual weekday patterns may be observed on Friday. Four different time periods were taken into consideration for analysis. They are the morning peak period (7:30–9:30 a.m.), afternoon off-peak period (12:30–2:30 p.m.), evening peak period (5:00–7:00 p.m.), and night off-peak period (9–11:00 p.m.). In general, the traffic volume would be high during peak hours but by considering the off-peak hours one can get an idea on the effect of a capacity improvement project during low traffic volume hours.

NTILE function was used in Microsoft Structured Query Language (SQL) to sort the data for the required time periods on required days and compute TT_{95} , TT_{Avg} , BT, and BTI. TT_{95} indicates that the travel time is going to be not more than the 95th percentile travel time 19 out of 20 times. NTILE function distributes the rows in an ordered partition, into a specified number of groups. This ordered partition helps in computing the TT_{95} . The formulae to compute BT and BTI are:

$$BT = TT_{95} - TT_{Avg} \quad (1)$$

where TT_{95} is the 95th percentile travel time, and TT_{Avg} is the average travel time.

$$BTI = (TT_{95} - TT_{Avg})/TT_{Avg} \quad (2)$$

Two different percentages (measures) were computed to compare the travel time measured before, during, and after the construction. They are:

$$\frac{TT_{Avg} \text{ during construction} - TT_{Avg} \text{ before construction}}{TT_{Avg} \text{ before construction}} \times 100 \quad (3)$$

$$\frac{TT_{Avg} \text{ after construction} - TT_{Avg} \text{ before construction}}{TT_{Avg} \text{ before construction}} \times 100 \quad (4)$$

In Eqs. (3) and (4), the TT_{Avg} can be substituted by BT or BTI to compute the percent change in BT and BTI, respectively.

The computed percentage differences are assigned to their respective links along with the starting latitudes–longitudes and ending latitudes–longitudes and were overlaid on the street network shapefile. The travel time measures were color-coded based on the difference in the percentage of travel times.

The level of service (LOS) was not considered in this study due to the diverse nature of the considered network (basic freeway sections, ramps, weaving sections, arterial streets with different speed limits, etc.). Further, the geometric characteristics vary along the study corridor with capacity improvement project.

5 Results

Table 1 shows the change in average travel time (TT_{Avg}), buffer time (BT), and buffer time index (BTI) before the construction, during the construction, and after the construction for both the freeways and arterial streets within the vicinity of the project site. The italic values in the table are associated with travel times for the freeway links whereas the non-italic values are for the connecting arterial streets. It can be observed from the table that the travel time has increased during the construction period while it has decreased after the construction period when compared to before the construction period. A decrease in travel time measures during the construction period was observed on some links. This might be due to the migration of traffic to alternate routes. Likewise, an increase in travel time after the construction was complete was observed on some links, might be due to the induced travel demand.

5.1 *Effect of Capacity Improvement Project During the Construction Period*

Geospatial maps were generated to examine the change in the travel time measures in the study area. The maps depicting BT show an increase of 50% in BT during the construction period. However, the maps depicting BTI show an increase of 25%, indicating that the section is 25% more unreliable compared to before the construction period. The links on freeways have seen a 50% increase in BT during the morning peak period on Wednesday and Friday, which might be due to the closure of one of the lanes for construction. However, the BT has decreased on the freeway links on Sunday during the morning peak period. The decrease in BT on the freeway links might be associated with the low traffic volume during weekends. The sample geospatial map depicting BT for Wednesday morning peak period is shown in Fig. 1.

There was a 25% increase in BTI during the Wednesday and Friday morning peak period. The increase in BTI during the morning peak period on Wednesday and

Table 1 Variation in travel time measures before, during, and after construction

TMC	Average TT				95th percentile				BT			BTI		
	BC	DC	AC	DC	BC	DC	AC	DC	BC	DC	AC	BC	DC	AC
	125+04647	0.80	0.78	0.70	0.84	0.77	0.84	0.75	0.03	0.06	0.05	3.93	7.17	6.78
125+04648	1.85	1.98	1.72	2.07	1.97	2.07	1.82	0.12	0.09	0.10	6.65	4.71	5.92	
125+04649	0.83	0.92	0.79	0.94	0.89	0.94	0.85	0.06	0.02	0.06	6.85	2.17	7.03	
125+04650	1.96	2.00	1.91	2.11	2.08	2.11	2.05	0.12	0.11	0.14	6.12	5.30	7.18	
125+09632	1.69	1.58	1.93	1.73	1.73	1.73	2.52	0.04	0.15	0.59	2.45	9.24	30.23	
125+09633	2.85	2.75	3.17	3.08	2.91	3.08	3.99	0.06	0.33	0.82	2.28	12.13	25.88	
125+09634	2.11	2.01	2.28	2.43	2.15	2.43	3.14	0.04	0.42	0.86	1.75	21.00	37.42	
125+10218	1.27	1.38	1.19	1.43	1.34	1.43	1.28	0.07	0.05	0.09	5.76	3.61	7.35	
125+12235	2.96	3.08	2.88	3.66	2.99	3.66	3.55	0.03	0.58	0.67	0.85	18.72	23.15	
125+12237	1.66	1.66	1.82	1.88	1.71	1.88	2.24	0.05	0.22	0.42	3.09	13.34	23.20	
125+12244	3.35	3.30	3.75	3.62	3.62	3.62	4.98	0.27	0.32	1.23	8.18	9.75	32.70	
125+12245	1.44	1.50	1.69	1.80	1.50	1.80	2.25	0.06	0.30	0.56	4.09	20.34	33.30	
125+12246	3.45	3.46	3.90	3.69	3.59	3.69	5.62	0.14	0.23	1.72	4.19	6.63	44.14	
125+12292	1.72	1.65	1.70	1.74	1.74	1.74	1.89	0.02	0.09	0.19	1.24	5.26	11.16	
125+12293	0.89	0.87	1.00	0.96	0.93	0.96	1.54	0.04	0.09	0.54	3.99	10.53	54.06	
125+12295	2.01	1.80	2.05	2.13	2.20	2.13	2.87	0.19	0.33	0.82	9.21	18.49	40.16	
125-04646	0.58	0.86	0.67	1.41	0.61	1.41	0.95	0.03	0.55	0.28	6.01	64.88	41.64	
125-04647	1.84	4.04	1.59	8.51	2.35	8.51	1.68	0.51	4.47	0.09	27.69	110.60	5.88	
125-04648	1.52	2.49	1.19	6.82	2.82	6.82	1.26	1.30	4.33	0.07	85.43	173.70	6.23	
125-04649	2.03	2.11	1.97	2.18	2.18	2.18	2.07	0.15	0.07	0.10	7.63	3.13	5.01	

(continued)

Table 1 (continued)

TMC	Average TT						95th percentile						BT			BTI																																																																																																																																																																																																																																						
	BC	DC	AC	BC	DC	AC	BC	DC	AC	BC	DC	BC	DC	AC	BC	DC	AC																																																																																																																																																																																																																																					
	125-09631	1.63	1.62	2.27	1.63	1.85	2.92	0.00	0.23	0.65	0.22	14.21	28.53	125-09632	2.76	2.63	3.14	2.91	2.83	4.14	0.15	0.20	1.00	5.43	7.64	31.82	125-09633	2.44	2.36	2.84	2.53	2.87	4.39	0.09	0.51	1.55	3.71	21.60	54.48	125-10218	0.85	1.01	0.71	1.66	2.49	0.75	0.81	1.48	0.04	96.19	147.03	6.22	125-12234	2.89	2.97	2.98	2.96	3.41	3.63	0.07	0.44	0.65	2.49	14.74	21.99	125-12236	1.80	1.89	2.09	1.88	2.77	2.91	0.08	0.88	0.82	4.26	46.75	39.29	125-12243	3.31	3.23	4.46	3.42	3.52	7.48	0.11	0.29	3.02	3.32	9.01	67.86	125-12244	1.42	1.55	1.79	1.51	2.09	2.37	0.09	0.54	0.58	6.03	34.85	32.06	125-12245	3.66	3.64	4.41	4.30	4.30	6.45	0.64	0.66	2.04	17.42	18.00	46.29	125-12291	1.50	1.47	1.72	1.56	1.60	2.00	0.06	0.13	0.28	4.11	8.79	16.35	125-12292	0.94	0.88	1.37	0.93	1.02	1.81	-0.01	0.14	0.44	-0.74	15.48	32.42	125-12294	2.06	1.83	2.20	2.08	2.08	2.78	0.02	0.25	0.58	1.02	13.50	26.63	125N04647	0.65	1.46	0.66	0.70	2.95	0.74	0.05	1.49	0.08	8.14	102.03	12.78	125N04648	0.64	1.29	0.46	1.19	3.57	0.49	0.55	2.28	0.03	85.94	177.79	5.63	125N04649	0.46	0.52	0.40	0.65	0.78	0.43	0.19	0.26	0.03	42.64	50.29	7.21	125N04650	0.73	0.73	0.71	0.80	0.76	0.76	0.07	0.03	0.05	9.03	3.79	7.02	125N10218	0.76	1.05	0.57	1.73	3.63	0.60	0.97	2.58	0.03	126.25	245.01	4.75	125N12234	0.02	0.02	0.02	0.02	0.04	0.02	0.00	0.02	0.00	0.00	85.68	0.63	125N12244	0.08	0.09	0.10	0.10	0.16	0.16	0.02	0.07	0.06	22.48	84.31

(continued)

Table 1 (continued)

TMC	Average TT			95th percentile			BT			BTI		
	BC	DC	AC	BC	DC	AC	BC	DC	AC	BC	DC	AC
125P04647	0.57	0.58	0.51	0.58	0.60	0.55	0.01	0.02	0.04	0.89	4.06	7.84
125P04648	0.40	0.43	0.37	0.42	0.45	0.40	0.02	0.02	0.03	5.86	5.42	6.86
125P04649	0.45	0.50	0.44	0.50	0.51	0.47	0.05	0.01	0.03	10.77	1.81	7.86
125P04650	0.71	0.70	0.69	0.76	0.74	0.74	0.05	0.04	0.05	7.41	5.58	7.11
125P09633	0.27	0.27	0.31	0.27	0.41	0.41	0.00	0.14	0.10	1.54	52.25	32.72
125P10218	0.57	0.62	0.55	0.61	0.64	0.61	0.04	0.02	0.06	6.90	2.40	10.89
125P12235	0.31	0.30	0.29	0.34	0.44	0.42	0.03	0.14	0.13	10.46	48.05	46.26
125P12244	0.10	0.11	0.10	0.11	0.18	0.19	0.01	0.07	0.09	7.53	69.42	83.74
125P12293	0.29	0.27	0.32	0.31	0.32	0.51	0.02	0.05	0.19	6.12	17.64	57.37

Note BC, DC, and AC are before the construction period, during the construction period, and after the construction period

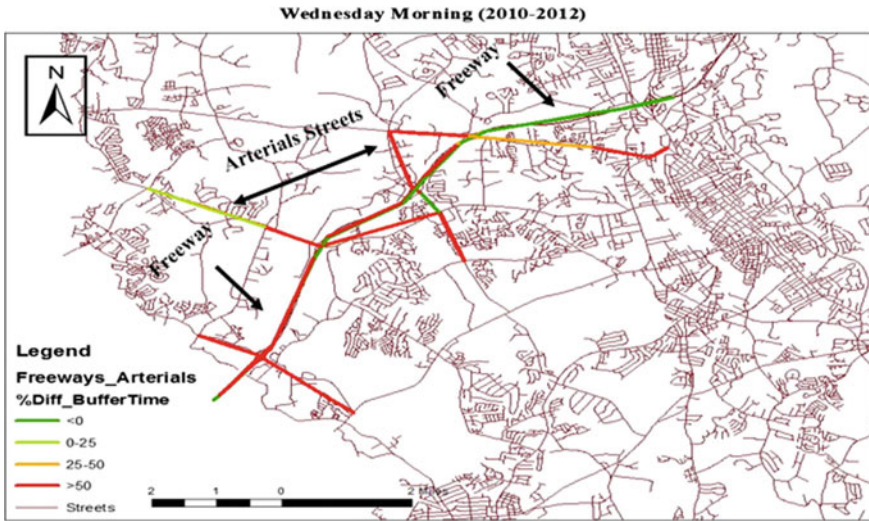


Fig. 1 BT—Wednesday morning peak period—construction period

Friday might be due to the decrease in capacity of the freeway, as one of the lanes is closed for construction. Furthermore, speed limits are generally reduced during the construction period. This could result in an increase in BTI.

Additionally, the morning peak period generally has a high flow of traffic volume on the freeway. Conversely, when Sunday morning peak period was considered, it was observed that some of the sections had a 25% increase in BTI while some of the sections had a decrease in BTI. The 25% increase in BTI indicates that the route is 25% unreliable. The sample geospatial map depicting BTI for Wednesday morning peak period is shown in Fig. 2.

On the other hand, arterial streets showed an increase in BT during the weekday morning peak periods, variably up to 50%. The increase in BT on the arterial streets might be due to the migration of traffic from the freeway (under construction). On the other hand, the arterial streets observed a 25% increase in BTI during all the selected morning peak periods. This indicates that the arterial streets are 25% more unreliable during morning peak periods when compared to before the construction period.

5.2 Effect of Capacity Improvement Project After the Construction Period

A decrease in BT was observed on freeway links after the construction is completed during morning peak periods on Wednesday and Friday. The decrease in BT might be due to an increase in capacity of the freeway. However, fluctuations in BT were

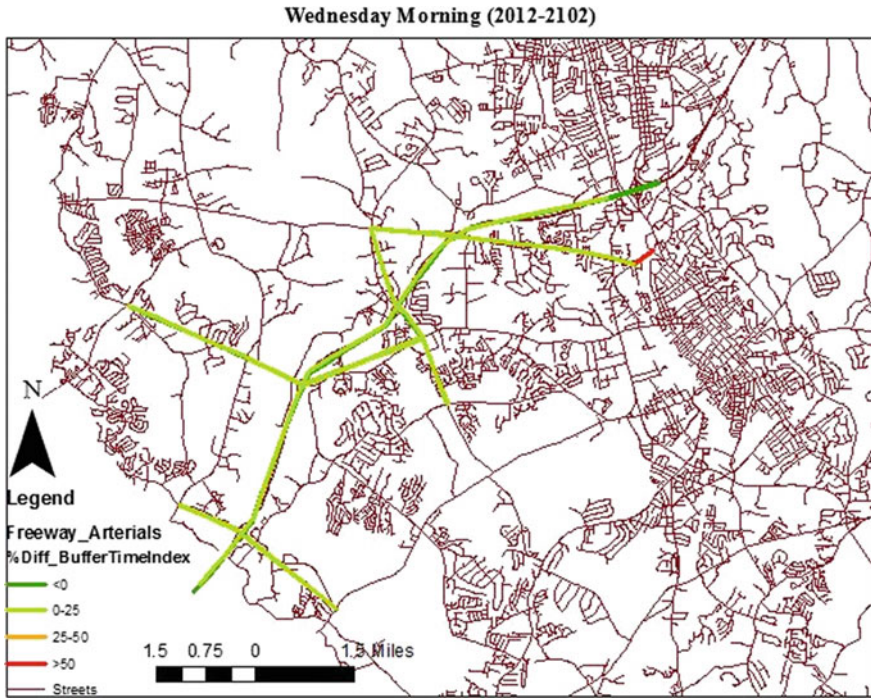


Fig. 2 BTI—Wednesday morning peak period—construction period

observed during the morning peak period on Sunday, which might be due to the induced travel demand. The variations in BT are shown in Fig. 3.

A decrease in BTI was observed during the morning peak period on Wednesday and Friday. The decrease in BTI might be due to the increase in capacity of the freeway, making the route more reliable when compared to travel times of the freeway prior to the construction. Even though the BT has shown fluctuation during the morning peak period on Sunday, it was observed that the route has become more reliable than before the construction of capacity improvement project. The variations in BTI are shown in Fig. 4.

There was an increase in BT by 50% on selected arterial street links on Wednesday and Friday during morning peak periods, after the completion of the capacity improvement project. The increase might be due to the induced travel demand. Similar results were observed on Sunday during the morning peak period.

The BTI increased by 25% on the selected arterial streets, on all the three selected days, during the morning peak period. The increase in the BTI might be due to the induced travel demand.

Along with geospatial maps, scatter plots were developed for selected times of the day and days of the week. The differences were computed by comparing during the construction period and after the completion of the capacity improvement project with before the construction period. Travel time measures compared include TT_{Avg} ,

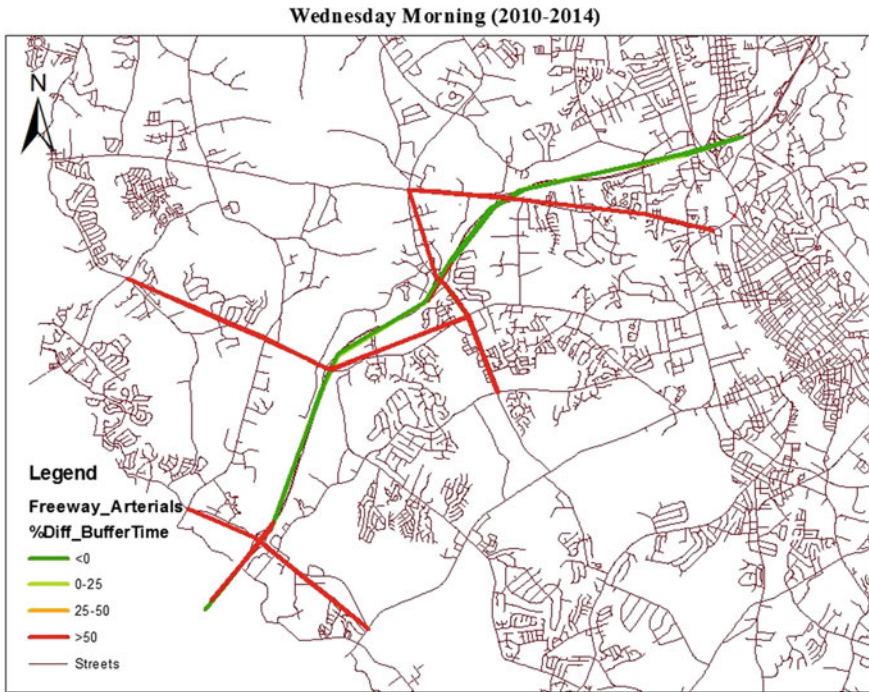


Fig. 3 BT—Wednesday morning peak period after the construction period

TT₉₅, BT, and BTI. The plots provide an idea as to how travel time has changed when approaching the construction zone and leaving the construction zone. Also, the plots represent the change in travel time from Exit 45 to Exit 60 on I-85, in both directions. The northbound section is from W T Harris Blvd (Exit 45) toward Kannapolis (Exit 60), while the southbound section is from Kannapolis (Exit 60) toward W T Harris Blvd (Exit 45). As an example, the scatter plot (Fig. 5) developed for Wednesday morning peak period is discussed next.

During Wednesday morning peak period, it was observed that there was an increase in travel time prior to approaching the construction zone in the northbound direction. This might be due to the bottleneck formation. The bottleneck might be due to the lane closure at the construction zone. After the construction zone, it can be observed that there was a slight increase in travel time as Exit 45 and Exit 46 has a lane configuration of four lanes, whereas the lane configuration after crossing the recently constructed zone is only two lanes. Also, a significant increase in travel time was observed in the northbound direction of the road rather than in the southbound direction due to the directional hourly traffic volume split. There was a significant increase in the TT₉₅. The BT did not follow a trend, possibly due to different link lengths. However, all the BTs in the construction zone were observed to be greater than 0, which shows that there was an increase in BT. There were fluctuations in BT, in both the directions, even after the completion of the capacity improvement project.

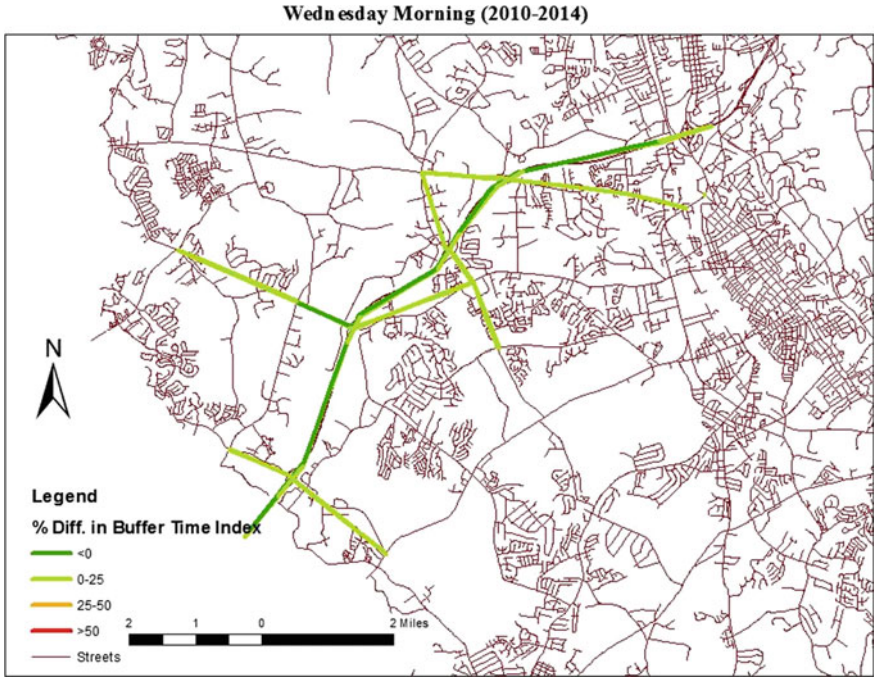


Fig. 4 BTI—Wednesday morning peak period after the construction period

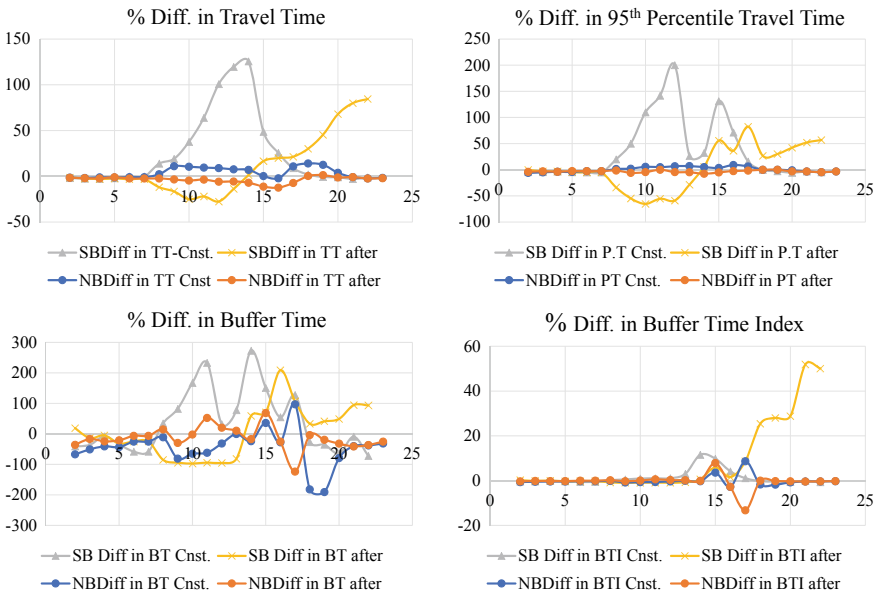


Fig. 5 Wednesday morning peak period—results

The increase in BT after the completion of the capacity improvement project might be due to the induced travel demand. The BTI shows that the extra BT was about 1.2 times the actual BT in the construction zone. It increased after the completion of the capacity improvement project, possibly due to the induced travel demand.

6 Conclusions

There is a general misconception that travel time decreases significantly with the freeway expansion. It encourages people to use the road more than before, resulting in induced travel demand. In this paper, the surrounding arterial streets and the freeway were evaluated during and after the construction of a capacity improvement project by comparing with before the construction period.

The travel time increases due to the decrease in speed and capacity when a freeway is under construction. However, there might be a decrease in travel time as people tend to migrate to other routes. Moreover, during the construction period, there are high chances that the connecting arterials might get congested or become unreliable. It is because there is a normal tendency of avoiding construction zone and using other routes.

The results obtained from this research indicate that during the construction period, the travel time increases as the distance from the construction zone decreases. Similarly, as travelers leave the construction zone, the travel time again decreases unless affected by other geometric factors such as lane configuration. The travel time performance measures do vary by the time-of-the-day and day-of-the-week.

It is recommended that state departments of transportation and local agencies analyze the capacities of the connecting arterials when a freeway capacity improvement project is planned, as these arterial streets get congested due to traveler's tendency to avoid the construction zone.

When a freeway section capacity is increased, the arterial streets connecting the freeway should also be modified accordingly to handle the traffic generated due to induced travel demand. Failing to do so might lead to congestion on arterial streets, which in turn might reduce the reliability and performance of the entire network. The average travel time increases with an increase in traffic volume. The increase in traffic volume on the arterial streets also supplements the increase in travel times and congestion on the network. From the results obtained from this research, arterial streets get congested even after the expansion due to the induced travel demand. Therefore, the expansion of freeways or increase in the capacity of freeways might not improve the travel time significantly. However, a more number of vehicles pass through the stretch at the same time. Moreover, arterial streets suffer the most during the construction period, by handling the migrating traffic and after the expansion by handling the induced travel demand. Therefore, before any freeway expansion, it is recommended to proactively plan and address possible negative effects on arterial streets (either signal timing or capacity).

Only one capacity improvement project was considered in this research. The influence on system performance could depend on the type of project. The influence area could also depend on the type of project. Considering data for multiple constructions projects, other travel time performance measures, and larger influence area as well as conducting advanced statistical analysis to identify critical factors merit further investigation.

Acknowledgements This paper is prepared based on information collected for a research project funded by the United States Department of Transportation—Office of the Assistant Secretary for Research and Technology (USDOT/OST-R) University Transportation Centers Program (Grant # 69A3551747127).

Disclaimer This paper is disseminated in the interest of information exchange. The views, opinions, findings, and conclusions reflected in this paper are the responsibility of the authors only and do not represent the official policy or position of the USDOT/OST-R, or any other State, or the University of North Carolina at Charlotte or other entity. The authors are responsible for the facts and the accuracy of the data presented herein. This paper does not constitute a standard, specification, or regulation.

References

1. Hansen M, Yuanlin H (1997) Road supply and traffic in California urban areas. *Transp Res Part A Policy Pract* 31(3):205–218
2. Texas Transportation Institute Study (1998). <http://www2.johnabbott.qc.ca/~geoscience/temp/TheCity/MISC/analysis.htm>
3. Fulton LM, Noland RB, Meszler DJ, Thomas JV (2000) A statistical analysis of induced travel effects in the US mid-Atlantic region. *J Transp Stat* 3(1):1–14
4. Noland RB, Cowart WA (2000) Analysis of metropolitan highway capacity and the growth in vehicle miles of travel. *J Transp* 27(4):363–390
5. Cervero R, Mark H (2002) Induced travel demand and induced road investment: a simultaneous equation analysis. *J Transp Econ Policy* 36(3):469–490
6. Goodwin PB (1996) Empirical evidence on induced traffic. *J Transp* 23(1):35–54
7. Hill P (1996) What is induced traffic? *J Transp* 23:5–16
8. DeCorla-Souza P, Cohen H (1999) Estimating induced travel for evaluation of metropolitan highway expansion. *J Transp* 26(3):249–262
9. Cervero R (2002) Induced travel demand: research design, empirical evidence, and normative policies. *J Plan Lit* 17(1):3–20
10. Cohen H (2002) The induced demand effect: evidence from national data. In: *Working together to address induced demand*. Washington, DC, Eno Transportation Foundation, pp 39–43
11. Pickrell D (1999) Transportation and land use. In: *The international encyclopedia of geography*, Wiley
12. Greening LA, Greene DL, Difiglio C (2000) Energy efficiency and consumption—the rebound effect—a survey. *Energy Policy* 28(6):389–401
13. Noland RB, Lem LL (2002) A review of the evidence for induced travel and changes in transportation and environmental policy in the US and the UK. *J Transp Res Part D Transp Environ* 7(1):1–26
14. Haseman R, Wasson J, Bullock D (2010) Real-time measurement of travel time delay in work zones and evaluation metrics using bluetooth probe tracking. *Transp Res Rec* 2169:40–53

15. Khattak AJ, Schofer JL, Koppelman FS (1993) Commuters' enroute diversion and return decisions: analysis and implications for advanced traveler information systems. *J Transp Res Part A Policy Pract* 27(2):101–111
16. Dharia A, Adeli H (2003) Neural network model for rapid forecasting of freeway link travel time. *Eng Appl Artif Intell J* 16(7):607–613

Assessment of Walkability and Pedestrian Level of Service in Two Cities of Kerala



A. Jegan Bharath Kumar and T. Ramakrishnan

Abstract Pedestrian becomes most vulnerable victim in most of the road accidents. The provision of facilities to the pedestrian has been altered due to the widening of roads as the traffic is getting increased. Walking and living circumstances in an area forms walkability. It is how supportive an environment is in the circumstances of people who live, walk, shop, visit and spend time in an area. It can be networked to the building quality, urban planning and connectivity, security and desirability for infrastructure accessibility. Walkability is a vital parameter in sustainable urban transport system. It indicates the environment for walking of people. Few factors influencing walkability are high-quality footpaths, traffic, road conditions, land-use pattern, building accessibility and safety. The study focusses to assess, review and quantify existing pedestrian facilities and infrastructure in selected road corridors in two cities. This would lead to understand the present state of walkability in each corridor so that pedestrian level of service (LOS) could be enhanced so as to improve the walkability in each corridor.

Keywords Pedestrian · Walkability · Pedestrian LOS · Factor analysis · Regression

1 Introduction

Walkability is the measure of overall walking and living conditions in an area. It is the extent to which the built environment is friendly to the presence of people walking, living, shopping, visiting, enjoying or spending time in an area. It can be linked to the quality of built environment, the urban form and connectivity, safety and desirability to walk and accessibility of infrastructure. This study aims at comparing the walkability index of two major cities in Kerala, India, reviewing the level of

A. Jegan Bharath Kumar (✉) · T. Ramakrishnan
National Transportation Planning and Research Centre (NATPAC), Thiruvananthapuram 695004,
Kerala, India
e-mail: jegancivil@gmail.com

T. Ramakrishnan
e-mail: ramjeevi@yahoo.co.uk

© Springer Nature Singapore Pte Ltd. 2020
T. V. Mathew et al. (eds.), *Transportation Research*, Lecture Notes
in Civil Engineering 45, https://doi.org/10.1007/978-981-32-9042-6_42

facilities provided for the pedestrian and formulating remedial measures that would bring improvement to the index. The scope of study is constraint to selected road corridors in major cities in Kerala where the pedestrian volume is high. The main objectives are:

- To assess, review and quantify existing pedestrian facilities and infrastructure in selected road corridors in two cities of Kerala.
- To understand and compare current state of walkability in the cities.
- To identify the standards in the existing walking environment and to work on the areas of improvement for better walkability.
- To determine the pedestrians' preference and aspects to improve walkability.
- To formulate strategies to enhance better accessibility, convenient and safe walking environment.

2 Methodology

The methodology of the study includes:

- Identification of road stretches in the major cities in Kerala
- Collection of primary data such as road inventory and pedestrian volume
- Determination of walkability index for the road corridors in both the cities
- Evaluation of pedestrian LOS parameters comprising of physical and user characteristics in each corridor among the pedestrian
- Determination of significant parameter from the pedestrian overall satisfaction score for pedestrian LOS through statistical approach
- Development of statistical model for the two cities with two scenarios one being the corridors with fully available footpath and another being the corridors with partially available footpath.

The two important cities in Kerala, Thiruvananthapuram and Ernakulam, are selected. About 22 corridors in Thiruvananthapuram and 19 corridors in Ernakulam were selected as study corridors. These corridors are selected on the fact that in these corridors, the pedestrian volume is considered to be high (Tables 1 and 2).

3 Pedestrian Level of Service

Pedestrian LOS indicates the environmental qualities of a pedestrian space and serves as a guide for development of standards for pedestrian facilities. Ten parameters affect service quality of pedestrian footpath out of which six are concerned with physical characteristics of the walkway facility like footpath width, surface, obstruction, encroachment, potential of vehicular conflict and continuity. Pedestrian volume, security, comfort and walking environment are the three user factors. To improve the

Table 1 List of road corridors in Ernakulam

Sl. no.	Road stretch	Length (km)
1	Banerji Road (High Court Junction–Kaloor)	2.1
2	Hospital Road (Hospital Jn–KPCC Jn/Ground Jn)	0.56
3	Durbar Hall Road (BTH–Jose Jn)	0.57
4	Church Landing Road (Fine Arts–Pallimukku Jn)	0.5
5	Sahodaran Ayyappan Road (Pallimukku Jn–Vytilla Jn)	3.5
6	Marine Drive Road: Fine Arts–High Court Jn	2.59
7	Mahatma Gandhi Road (Madhava Pharmacy Jn–Ravipuram Jn)	3.12
8	Chittoor Road (Kacheripadi Jn–Valanjabalam Jn)	2.6
9	Veekshanam Road (MG Road–Railway Line)	0.63
10	Pullepady Road (Pullepady Jn–Pullepady ROB)	0.4
11	Rajaji Road (MG Road–Ambedkar Stadium)	0.4
12	Convent Road (Market Road–MG Road)	0.4
13	Amman Kovil Road (MG Road–KSRTC Bus Terminal)	0.46
14	South Railway Station Road (Jose Jn–Railway Station)	0.46
15	Broadway (Banerji Road–Park Avenue Road)	0.9
16	Market Road (Banerji Road–Hospital Road)	1.6
17	TD Road (Banerji Road–Hospital Road)	1.55
18	Madhavan Nair Road (St. George Church Jn–Ravipuram Jn)	0.74
19	Ravipuram Road (Valanjabalam Jn–Ravipuram Jn)	0.75

pedestrian LOS, pedestrian overall satisfaction was extracted from the pedestrian opinion survey against each parameter that is responsible to enhance the level of service. The rating that was given by frequent pedestrians travelling in the road corridor was taken into consideration. The determination of pedestrian overall satisfaction was based on the rating provided by the pedestrian upon the ten parameters that was explained previously which have more influence over pedestrian LOS. The pedestrian overall satisfaction for the selected road corridors in the two cities has been modelled in two scenarios, firstly for the road corridors having fully available footpath and the other being the road stretches with partially available footpath.

4 Data Collection

4.1 Road Inventory

A detailed inventory of existing road network was carried out to obtain information like road length, cross sections, hierarchical pattern of roads, surface condition, intersections, street furniture, parking area, bus bays, etc.

Table 2 List of road corridors in Thiruvananthapuram

Sl. no.	Road stretch	Length (km)
1	MG road (LMS–Manacaud)	3.694
2	War Memorial to Kochulloor via PMG	5.179
3	Over Bridge to Karamana via Thampanoor	2.579
4	Thampanoor Fly-over to Kaudiar via Mettukkada	4.283
5	Thampanoor to Chaka via General Hospital	5.639
6	Kaudiar to Ulloor via Pattom	5.095
7	Killipalam to Eanchakkal via Attakulangara	2.717
8	Killipalam to East Fort via Chalai	1.00
9	Nalumukku to Over Bridge via Uppidamoodu	2.029
10	Uppidamoodu to Churakaatu Palayam via Sreekanandeswaram	1.885
11	Vanchiyoor (Nalumukkurd) to General Hospital	1.060
12	Pattoor to Vanchiyoor	0.497
13	Pulimoodu to Uppidamoodu	0.931
14	Ayurveda College to Old GPO	0.388
15	Ayurveda College to Chettikulangara	0.266
16	Pallimukku to Medical College via Kumarapuram	3.183
17	Kesavadasapuram to Nalanchira	1.740
18	Palayam to DPI via Women's college	1.676
19	Public Library to Kanakakunnu via Nandavanam	0.718
20	Valiyathura to Kochuveli Railway Station	7.912
21	Kumarichanda to Thiruvallam NH bypass	1.172
22	Manacaud to Attukkal	1.291

4.2 Pedestrian Volume

Pedestrian traffic survey was performed at important areas where the lateral and crossing movements of pedestrians take place frequently.

4.3 Pedestrian Opinion Survey

To improve the pedestrian facilities in selected road corridors in two cities and thereby improving the walkability, pedestrian opinion survey was performed to enhance pedestrian LOS in the selected stretches.

A questionnaire was structured to review and improve the pedestrian facilities, thereby comprising details regarding pedestrian characteristics and perception regarding the pedestrian facility. The survey was conducted in 23 corridors in Thiru-

<p>Evaluation of Pedestrian Facilities</p> <p>Location:</p> <p>Road Stretch:</p> <p>Pedestrian Characteristics:</p> <p>1. Gender: Male/Female</p> <p>2. Age: (1) <10 (2)11-20 (3)21-30 (4)31-40 (5)41-50 (6) 51-60 (7)61-75 (8)75+</p> <p>3. Profession: (1) Student (2) Self Employed (3) Business (4) Service (5) Unemployed (6) Housewife (7) Retired (8) Others</p> <p>4. Income per Month: (1) <5K (2) 5K-10K (3) 10K-20K (4) 20K-30K (5) 30-50K (6) >50K</p> <p>5. Trip Purpose: (1) Work (2) Education (3) Shopping (4) Change of Mode (5) Back home (6) Walker (7) Others</p> <p>6. Walk Trip Distance (in m):</p> <p>7. Frequency: (1) Daily (2) Weekly (3) Monthly (4) Occasionally (5) Many trips per day</p> <p>8. Foot Path: (1) Available (2) Not Available (3) Partially Available</p> <p>9. If Available: (1) Walking on footpath (2) Carriageway (3) Both</p> <p>10. Reason for not walking on footpath: (1) Encroachment (2) Footpath surface (3) Safety(4) Environment (5) Comfort (6) Continuity</p>

Fig. 1 Questionnaire for opinion survey

vananthapuram and 19 corridors in Ernakulam. A sample of 100 numbers in each corridor was recorded. About 2300 samples were collected in Thiruvananthapuram, and 1900 samples were collected in Ernakulam. The questionnaire was designed in such a manner that the pedestrian needs to rate each of the ten parameters in Likert scale of 1–5 which varies from satisfactory, very good, good and poor as given in Fig. 1.

5 Determination of Walkability Index

Walkability measures how friendly a region is for people to walk. Walking audit is one way to assess and measure walkability. To determine the walkability of a road or neighbourhood, the number of people walking, lingering and engaging in optional activities within a space subjected to be counted. For different regions, the idea of optional activities may vary. In any event, a walking area is characterized in terms of quality, completeness and health especially by presence of children, senior citizens, people with disabilities, etc.

The study commissioned by the Ministry of Urban Development (MOUD) in India has used walkability index [1]. The index depends on footpath availability and pedestrian facility rating. Availability with quality footpaths, obstructions, maintenance, lighting, crime security, safety of crossing safety and other qualitative elements were assessed in their perception by pedestrians. The primary purpose of index was to compare different sections of roads with various walkability parameters and to inform policymakers, development agencies and other stakeholders of results to improve walkability. Walkability Index (WI) is calculated as given in Eq. (1).

Table 3 Walkability index of roads in Ernakulam

Sl. no.	Road stretch	Walkability index (%)
1	Banerji Road (High Court Junction–Kaloor)	49
2	Hospital Road (Hospital Jn–KPCC Jn/Ground Jn)	54
3	Durbar Hall Road (BTH–Jose Jn)	50
4	Church Landing Road (Fine Arts–Pallimukku Jn)	39
5	Sahodaran Ayyappan Road (Pallimukku Jn–Vytila Jn)	40
6	Marine Drive Road: Fine Arts–High Court Jn	64
7	Mahatma Gandhi Road (Madhava Pharmacy Jn–Ravipuram Jn)	56
8	Chittoor Road (Kacheripadi Jn–Valanjabalam Jn)	40
9	Veekshanam Road (MG Road–Railway Line)	52
10	Pullepady Road (Pullepady Jn–Pullepady ROB)	52
11	Rajaji Road (MG Road–Ambedkar Stadium)	56
12	Convent Road (Market Road–MG Road)	27
13	Amman Kovil Road (MG Road–KSRTC Bus Terminal)	30
14	South Railway Station Road (Jose Jn–Railway Station)	56
15	Broadway (Banerji Road–Park Avenue Road)	36
16	Market Road (Banerji Road–Hospital Road)	40
17	TD Road (Banerji Road–Hospital Road)	46
18	Madhavan Nair Road (St. George Church Jn–Ravipuram Jn)	29
19	Ravipuram Road (Valanjabalam Jn–Ravipuram Jn)	46

$$WI = [(W1 \times \text{Availability of footpath}) + (W2 \times \text{Pedestrian facility rating})] \quad (1)$$

where $W1$ and $W2$ = Assumed weightages (50% for both in this case).

Availability of footpath = (Footpath length/Length of roads in the city) \times (Average available width of footpath/Standard width as per IRC).

Pedestrian facility Rating = Score based on pedestrian facility opinion survey. The calculated walkability index of selected road corridors in two cities is given below which was adopted from the past studies done by NATPAC [2, 3] and is shown in Table 3 (Table 4).

6 Statistical Analysis

Pedestrian opinion survey was structured to assess the existing pedestrian facilities available in the selected road corridor. In order to improve the pedestrian LOS, pedestrian overall satisfaction was extracted from the pedestrian opinion survey against the each parameter that is responsible to enhance the level of service. The rating that

Table 4 Walkability index of roads in Thiruvananthapuram

Sl. no.	Road stretch	Walkability index (%)
1	MG road (LMS–Manacaud)	68
2	War Memorial to Kochulloor via PMG	58
3	Over Bridge to Karamana via Thampanoor	64
4	Thampanoor Fly-over to Kaudiar via Mettukkada	51
5	Thampanoor to Chaka via General Hospital	60
6	Kaudiar to Ulloor via Pattom	68
7	Killipalam to Eanchakkal via Attakulangara	43
8	Killipalam to East Fort via Chalai	23
9	Nalumukku to Over Bridge via Uppidamoodu	38
10	Uppidamoodu to Churakaatu Palayam via Sreekandeswaram	44
11	Vanchiyoor (Nalumukkur) to General Hospital	46
12	Pattoor to Vanchiyoor	86
13	Pulimoodu to Uppilamoodu	44
14	Ayurveda College to Old GPO	32
15	Ayurveda College to Chettikulangara	54
16	Pallimukku to Medical College via Kumarapuram	32
17	Kesavadasapuram to Nalanchira	72
18	Palayam to DPI via Women's college	45
19	Public Library to Kanakakunnu via Nandavanam	74
20	Valiyathura to Kochuveli Railway Station	41
21	Kumarichanda to Thiruvallam NH bypass	17
22	Manacaud to Attukkal	25

was given by the frequent pedestrians travelling in the road corridor was taken into consideration. The determination of pedestrian overall satisfaction based on rating provided by the pedestrian upon the ten parameters that was explained previously which have more influence over the pedestrian LOS.

The parameters influencing the pedestrian LOS were adopted from the IRC 103 [4]. Among the ten parameters, the parameter which has more significant in the selected stretch has been extracted from the pedestrian opinion survey using factor analysis method by Statistical Program for Social Sciences (SPSS) tool. From these analyses, the significant parameters have been chosen from the ten parameters, and with those significant parameters, linear regression model has been developed. The pedestrian overall satisfaction for the selected road corridors in the two cities has been modelled in two scenarios, firstly for the road corridors having footpath and the second for the road stretches without footpath.

6.1 Factor Analysis

Factor analysis (FA), a statistical procedure, reduces a large set of variables into a smaller set of variables. It establishes dimensions among measured variables and latent variables allowing formation and refinement of theory. It also constructs validity evidence of self-reporting scales. FA involved with questions of validity. Factor analysis is the heart of the measurement of psychological constructs. Exploratory factor analysis (EFA), a complex statistical approach taken in the analysis, is in fact sequential and linear, involving many options. Therefore, developing a protocol or decision pathway is crucial in potential oversights. The process of conducting an EFA involves three stages, i.e. extraction, rotation and interpretation [5, 6].

Descriptive Statistics

In descriptive statistics, the means for each of the items appear to be reasonable as each of the items measured on five-point Likert scale, and no values are over 5 and below 1. The standard deviations are similar, and there are no outliers for any of the items (Table 5).

Correlation Matrix

The correlation matrix has been found for both conditions in Trivandrum and Ernakulam. It lists the variable names down the first column and across the first row. The diagonal of a correlation matrix always consists of ones. This is because the correlations between each variable and itself and a variable is always perfectly correlated with itself.

KMO and Bartlett’s Test

It measures the strength of the relationship with the variables. KMO measures the sampling adequacy. Bartlett tests the null hypothesis that the correlation matrix is an identity matrix. Factor analysis will be useful if the value is close to 1.0, whereas if the value is less than 0.50, the usefulness is quiet less.

Table 5 Descriptive statistics for road corridors with partially available footpath in Trivandrum

Variable	Mean	Std. deviation	Analysis <i>N</i>
FPS	2.86	1.456	391
FPW	3.01	1.204	391
OBS	2.58	1.136	391
ENC	2.88	1.230	391
PVC	2.13	1.137	391
CONT	2.40	1.123	391
PEDVOL	3.42	1.208	391
SSEC	3.05	1.191	391
COM	2.14	1.252	391
WE	2.40	1.226	391

It was found that the KMO values for both the cases in Trivandrum and Ernakulam were close to 1 as shown in Table 6.

Communalities

Table 7 represents the proportion of variance of each item that is explained by the factors. It shows how much variance in the variables has been accounted by extracted factors. Similarly, the same has been found for all the sections with partially and fully available footpath for Trivandrum and Ernakulam.

Component Extraction

Eigenvalues have been found out for all the sections in Trivandrum and Ernakulam. Initial eigenvalues for first three factors are meaningful as they have eigenvalues >1. Factors 1, 2 and 3 explain 29.95, 11.7 and 11.05% of the variance, respectively—a cumulative total of 52%. Component extraction has been done for all the sections with partially and fully available footpath for Trivandrum and Ernakulam. A sample done for sections having partially available footpath in Trivandrum is shown in Table 8.

Table 6 KMO and Bartlett’s test for Trivandrum and Ernakulam study areas

City	Condition of road corridor	Kaiser–Meyer–Olkin measure of sampling adequacy	Bartlett’s test of sphericity		
			Approx. χ^2	df	Sig.
Trivandrum	Footpath fully available	0.865	1569.601	45	0.000
	Footpath partially available	0.861	2049.647	45	0.000
Ernakulam	Footpath fully available	0.746	562.450	45	0.000
	Footpath partially available	0.771	1264.059	45	0.000

Table 7 Communalities for road corridors with partially available footpath in Trivandrum

Variable	Initial	Extraction
FPS	0.715	0.772
FPW	0.654	0.652
OBS	0.526	0.520
ENC	0.219	0.110
PVC	0.591	0.579
CONT	0.604	0.587
PEDVOL	0.480	0.999
SSEC	0.464	0.446
COM	0.543	0.461
WE	0.536	0.473

Table 8 Component extraction for road corridors with partially available footpath in Trivandrum

Sl. no.	Initial eigenvalues			Extraction sums of squared loadings			Rotation sums of squared loadings
	Total	% of variance	Cumulative (%)	Total	% of variance	Cumulative (%)	
1	5.020	50.200	50.200	2.308	23.082	23.082	1.710
2	1.372	13.717	63.917	3.290	32.903	55.985	4.496
3	0.809	8.090	72.008				
4	0.763	7.635	79.643				
5	0.500	4.997	84.640				
6	0.416	4.160	88.800				
7	0.352	3.516	92.316				
8	0.321	3.206	95.522				
9	0.250	2.497	98.019				
10	0.198	1.981	100.000				

7 Linear Regression

For development of the model, the significant parameters have been selected from factor analysis done for two scenarios. Those significant parameters were taken as independent variables with respect to the eigenvalue it has got. Though we have already set the eigenvalue limit as 1, the value of the parameters which have got value above 1 would be chosen as more significant parameter. But here the selection have been made in such a way that those values which have score less than 1 also been chosen as per engineering judgement.

Pedestrian overall satisfactions have been taken as dependent variable in the model. It was arrived from the response of the pedestrian on the ten parameters given in Likert scale (ratings) ranging from 1 to 5. The average of all the response for all ten parameters has been taken as the pedestrian overall satisfaction. The model was developed to formulate linear regression for overall satisfaction of the pedestrian with respect to the ten parameters. In case of road corridors with partially available footpath parameters such as footpath surface, width, encroachment, pedestrian vehicle conflict and obstructions are considered as independent variable over the dependent variable pedestrian overall satisfaction. In case of road corridors with footpath fully scenario available parameters such as footpath surface, width, encroachment and obstructions were taken as independent variable over the dependent variable pedestrian overall satisfaction.

For making things simple, the variables were used in the analysis as notations that are: POS—pedestrian overall satisfaction, FPS—footpath surface, FPW—footpath width, OBS—obstructions, ENC—encroachment, PVC—potential for vehicle con-

Table 9 Models developed for Trivandrum and Ernakulam

City	Scenarios	Model developed	R ²
Trivandrum	Footpath fully available	POS = 7.504 + 2.874 FPS + 1.229 FPW + 1.399 OBS + 1.968 ENC	0.781
	Footpath partially available	POS = 3.473 + 0.099 FPS + 3.059 FPW + 1.863 OBS + 1.473 ENC + 2.667 PVC	0.859
Ernakulam	Footpath fully available	POS = 8.906 + 2.239 FPS + 0.159 FPW + 1.860 OBS + 1.387 ENC	0.634
	Footpath partially available	POS = 6.433 + 1.301 FPS + 1.582 FPW + 1.164 OBS + 1.147 ENC + 1.665 PVC	0.627

flict, CONT—continuity, PEDVOL—pedestrian volume, SSEC—safety and security, COM—comfort and WE—walk environment. The models developed for the two conditions are given in Table 9.

8 Conclusion

The road stretches in the two cities, namely Thiruvananthapuram and Ernakulam, were identified where the pedestrian volume was quite high. Walkability index was arrived from the parameters, pedestrian volume, road characteristics and primary pedestrian opinion surveys. The following are the findings from the study and the recommendations. In Thiruvananthapuram study area, Pattoor to Vanchiyoor stretch marked the highest walkability index with 86% while the Kumarichanda to Thiruvallam (NH Bypass road) marked the low score with 17%. In Ernakulam study area, Marine drive road from fine arts to High Court Junction marked the highest walkability index with 64% while the Convent road starting from market area stretch to MG road stretch marked the lowest walkability index with 27%. After determination of walkability index for the road stretches in respective cities, two scenarios have been set out: one being the road corridors with footpath facility and another being the road corridors with partial footpath facility. In order to improve the walkability score in the respective road stretches, a qualitative approach was formulated. In accordance with IRC, ten parameters adopted to improve the pedestrian LOS pertaining to the footpath facilities. The qualitative improvement of pedestrian facility was entrusted from the pedestrian opinion survey from them arriving the pedestrian overall satisfaction. From factor analysis, significant parameters were found among the ten parameters for two scenarios in two cities. It was found that parameters such as footpath surface, footpath width, obstructions, encroachment and potential for vehicle conflict had more significant in case of road corridors with partial footpath facility, whereas parameters such as footpath surface, footpath width, obstructions and encroachment have more significant in case of road corridors with footpath facil-

ity for both the cities. Linear regression equations have been developed for both the scenarios considering those significant parameters as predictors and pedestrian overall satisfactions as the dependent variable. Hence, models are developed for both the cities for two scenarios. From the statistical analysis and towards the development of model, we convey that the walkability index in the eight stretches in Thiruvananthapuram and seven stretches in Ernakulam can be enhanced by increasing the footpath width, improving the surface, removing the obstructions and encroachments in the following road corridors in the two cities. And also by increasing the footpath width, improving the surface, removing the obstructions and encroachments, reducing the potential for vehicle conflicts, walkability index in the seven stretches in Thiruvananthapuram and three stretches in Ernakulam can be improved.

Acknowledgements The authors would like to thank the Director, National Transportation Planning & Research Centre (NATPAC) for the support for the study and providing technical reports for the study.

References

1. Ministry of Urban Development (2008) Traffic & transportation policies and strategies in urban areas in India
2. NATPAC (2014) Pedestrian and bicycle friendly urban transport for Thiruvananthapuram
3. NATPAC (2015) Pedestrian and bicycle friendly urban transport for Ernakulam
4. The Indian Road Congress (2012) Guidelines for pedestrian facilities, IRC no 103. The Indian Road Congress, New Delhi
5. Boduszek D (1989) Explanatory factor analysis in SPSS. University of Huddersfield, United Kingdom
6. Williams B (2012) Exploratory factor analysis: a five step guide for novices.

Gap Acceptance Behaviour of Vehicles at Unsignalized Intersection in Urban Area



Saurabh Vinchurkar, Manish Jain, Dipak Rathva and Sanjay Dave

Abstract Gap acceptance is an important component in microscopic traffic characteristic, which is used in the determination of capacity and delay of the individual movements of vehicles at an uncontrolled intersection. This concept is based on defining the extent drivers will be able to utilize a gap of a particular duration. Most of the studies related to critical gap estimation have been carried out in developed countries where traffic is homogeneous and rules of priorities as well as lane disciplines are followed. However, in developing countries like India, where heterogeneous traffic condition exists, priority rules are less honoured which consequently creates conflicts on intersections. In this paper, an attempt is made to analyse gap acceptance behaviour of motorized two-wheelers (MTW) and cars as these are the dominating vehicles at the selected study location, which is an unsignalized T-intersection. Data was collected for six hours of duration by videography consisting of two hours of duration each for morning, afternoon and evening time. In the study, the straight going flow was considered as a major stream and the other as a minor stream. In this study, three different methodologies are used to determine critical gap assuming independence between the arrival time of minor stream vehicles and the ones of the major stream vehicles. The critical gap for minor to major manoeuvre was calculated for MTW and cars. It was observed that gap acceptance showed variation between various methods. Two methods show nearly the same time while other shows less time of gap acceptance. The gap acceptance of MTW is significantly less than the car, which indicates there is a considerable effect of size and manoeuvrability of vehicles on gap acceptance. Also, there is variation in morning and evening period gap acceptance behaviour; morning gap acceptance is significantly more than evening time,

S. Vinchurkar · M. Jain · D. Rathva · S. Dave (✉)
The Maharaja Sayajirao University of Baroda, Vadodara, India
e-mail: smdave-ced@msubaroda.ac.in

S. Vinchurkar
e-mail: saurabhgotce@gmail.com

M. Jain
e-mail: manish.jain-ced@msubaroda.ac.in

D. Rathva
e-mail: dipakrathva-ced@msubaroda.ac.in

which may be due urgency of vehicle users to reach their destination on account of tiredness and exhaustion.

Keywords Gap acceptance · Critical gap · Raff's method · Accepted gaps · Motorized two-wheelers (MTW) · Two-way stop control (TWSC) intersection

1 Introduction

Unsignalized intersections give no positive indication or control to the driver; due to this, driver is not attentive when to leave the intersection. The driver alone must decide when it is safe to enter the intersection. The driver looks for a safe opportunity or “gap” in the traffic to enter the intersection. This technique is described as gap acceptance. At unsignalized intersections, a driver also has to respect the priority of other drivers. There are other vehicles also which have priority over the driver trying to enter the traffic stream, henceforth the driver must yield to these drivers. The gap acceptance commonly used in the analysis of unsignalized intersections is based on the concept of defining the extent drivers will be able to utilize a gap of particular size or duration. In a developing country like India motorized two-wheeler (MTW) is a predominate mode of travel. Manoeuvrability of MTW is effortless compared to car and heavy vehicles because of its physical dimension. In India, lane behaviour is not observed along with other parameters like speed variation, lane marking, etc., due to which gap acceptance becomes more complex.

2 Concept of Critical Gap

To safely execute the desired movement at conflicting traffic stream on approaching the intersection, a minor street driver has to assess whether a gap is large enough or not. A driver generally rejects all the gaps that are less than his/her critical gap and accepts the rest. Thus, the critical gap is a judgment threshold to whether a minor stream vehicle can enter major stream means a critical gap specifies the least value of gap that is acceptable to a driver [1]. Vehicular characteristics and acceleration rate affect the critical gap [2]. Raff introduced the concept of critical lag which refers to the size of the lag that has the property that number of accepted lags shorter than it is equal to the number of rejected lags longer than it [3]. The most accurate estimation of the mean and standard deviation of critical gap can be obtained by MLM, though it is complicated [4, 5]. HCM 2000 [6] has recommended MLM method for estimating the critical gaps. Moreover, a macroscopic method based on the equilibrium of probabilities between the rejected and accepted gaps is developed by Wu [7]. The statistical probability that a driver will accept a gap has been focused by most models of gap acceptance behaviour [8]. Further, traffic characteristics and intersection design, may to some extent, can be determined by statistical models,

but cannot help for decision making by understanding the cognitive aspects of gap acceptance [9–12]. Even models that do address individual decision processes lack specificity. A model was proposed whereby drivers assess whether the perceived risk of accepting the gap is greater than the perceived loss of time incurred by rejecting it but other situational variables or individual differences for the potential influence do not elaborate by this model [13]. As the speed of oncoming vehicles increases, the probability of driver acceptance of a gap for a given duration increases analysed by Logit model [14]. The possibilities to possess enough gap between vehicles of the upper prioritized streams to cross the conflict spaces securely decide the capacity and service times at minor streets of uncontrolled intersections [15]. Critical gap is affected by the vehicle type, light vehicles, merging from the inner lane to the far lane have smaller critical gaps than heavy vehicles [16]. Driver’s gender, age and conflicting vehicle type, etc., also influence gap acceptance behaviour [17]. To integrate the clearing behaviour of the driver, consider clearing time; defined as the time taken by a lower priority vehicle from the instant, it moves from its stopped position to the instant its tail end reaches the end of the conflict area [18]. The accepted gap by drivers follows the lognormal distribution and probability of accepting gap are higher for young MTW driver [19].

3 Study Area

Present study includes the data collection at unsignalized T-intersection of Vadodara city in the state of Gujarat. The intersection has a small roundabout, which is a common feature as in Indian context to provide a place to mounted statues of renowned persons. The intersection selected for data collection has the following features:

- It is a T-intersection with straight road 15.4 m wide divided and other road to be 25 m wide divided (Fig. 1a) with even and uniform pavement condition, respectively.

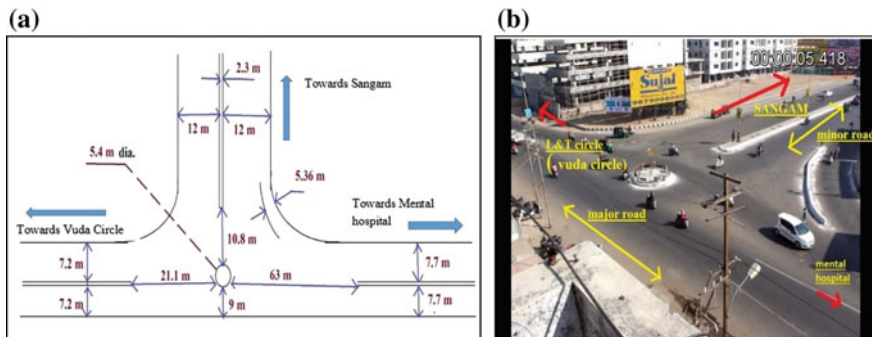


Fig. 1 a Geometric dimension of intersection b camera view of intersection

- Intersection exhibits sizable quantum of traffic on each leg to capture a sufficient number of accepted and rejected gaps.
- Intersection has a negligible proportion of non-motorized traffic (NMT) on all the three arms of the intersection.

4 Data Collection and Extraction

Video graphic data of intersection was collected from the rooftop of a nearby building (Fig. 1). Location of the camera was kept such that the conflict area was properly recorded while taking video. The videography was done for two hours each in morning (9 am–11 am), afternoon (2 pm–4 pm) and evening (5 pm–7 pm) a period of total six hours. Vehicles in the traffic stream have been categorized into MTW, cars, three wheelers, light commercial vehicles and heavy commercial vehicles (comprising of both bus/truck), although for study purpose the subject vehicles selected are only MTW and car as they form a majority traffic composition. The straight moving traffic flow from Mental hospital to Vuda circle is considered as a major stream, while the right moving traffic stream from Sangam is considered as a minor stream.

Gap extraction was carried out from videos categorized in two types of movements.

1. Turning from minor to major traffic manoeuvre (Merging Traffic).
2. Turning from major to minor traffic manoeuvre (Crossing Traffic).

In minor to major movements, the traffic stream from Sangam after crossing major road traffic from Vuda circle would slow down or stop to merge into the major stream. The starting time at which the subject vehicle from the minor stream has just a chance of merging behind leading major stream vehicle has just went ahead is noted. Then after the end time at which the following vehicle's front bumper just reaches the same exact location is noted, so the difference between these two noted times gives us the gap; hence, the accepted gaps are those when the subject vehicle merges while rejected gaps are those when merging does not take place. This same type of extraction is done for the major to minor manoeuvre to cross the road. In this study, time was measured up to the accuracy of 1/10th of a second (Table 1).

5 Estimations Critical Gap by Various Methods

5.1 Raff's Method

The critical lag L is the size lag, which has the property that the number of accepted lags shorter than L is the same as the number of rejected lags longer than L (Raff and Hart). So, the cross point between the number of curves of accepted gaps and

Table 1 Sample data collection

Subject vehicle	Leading vehicle	Following vehicle	Rear time of leading vehicle (min:s.ms)	Front time of following vehicle (min:s.ms)	Gap (front time follow-ing-rear time leading) (min:s.ms)	Observation (accepted/or rejected)
Car	Car	Car	09:31.0	09:33.6	00:02.5	R
MTW	Car	MTW	09:46.8	09:49.4	00:02.6	A

rejected gaps used to the derived critical gap. Raff’s method is expressed in the below expression [3].

$$1 - F(t) = F_a(t) \tag{1}$$

where t is headway of major stream, $F_a(t)$ is the cumulative probability of accepted gap. $F_r(t)$ is the cumulative probability of rejected gap.

The flow rate of major road has a prominent influence on critical gap value. Many countries are using this method widely owing to its simplicity and practicality.

5.2 Logit Method

Logit model is a weighted linear regression model with a mathematical form as shown in the equation below:

$$P(i) = \frac{1}{1 + e^{U_i}} \tag{2}$$

$$U_i = \beta_0 + \beta_1 X_1 + \beta_2 X_2 + \beta_3 X_3 + \dots + \beta_n X_n \tag{3}$$

where U_i is the probability of accepting a gap of size i , and β_i are regression coefficients.

The 50% probability of acceptance of the gap size is plotted on the chart to see the critical time. To verify the influence of different independent attributes in the critical headway, such as the waiting time, avg. speed, etc., this technique is regularly accustomed. In this formulation, a driver who accepts a gap smaller than one previously rejected cannot be outlined as “inconsistent”, since the other independent variables will make a case for that behaviour. Therefore, not only the maximum gap is rejected by each driver, all gaps ought to be evaluated [3].

5.3 Probability Equilibrium Method

An alternative to MLM a probability equilibrium method (PEM) was introduced by Wu [7], which has no complex calculation and can be carried out using a simple spreadsheet. Unlike MLM, this method is free from any inherent assumptions and is capable of including inconsistent drivers and the drivers who have not rejected any gaps. The method can be applied even for smaller sample sizes. The cumulative probabilities of the accepted (F_a) and rejected (F_r) gaps are calculated and used to calculate the probability distribution function of critical gaps using the equation

$$F_{tc}(t) = \frac{F_a(t)}{F_a(t) + 1 - F_r(t)} = 1 - \frac{1 - F_r(t)}{F_a(t) + 1 - F_r(t)} \tag{4}$$

6 Analysis of Data and Results

The accepted gaps and rejected gaps are extracted for the subject vehicles (MTW and car) and critical gaps were estimated by Raff’s method, Logit method and PEM method for morning, afternoon and evening, respectively.

The variation in accepted gaps for MTW and cars for different manoeuvres and along different duration of the day was checked statistically using one way ANOVA at 95% confidence interval. The null hypothesis is considered as no variation in accepted gaps for different duration day, i.e. morning, afternoon and evening for MTW and cars both separately. The results are shown in Table 2.

The results of ANOVA analysis revealed that in case of minor to major merging behaviour, MTW and cars both showed statistically no difference in gap acceptance. However, for crossing manoeuvre, MTW showed statistically significant difference while cars showed a statistically non-significant difference in gap acceptance.

In addition, the variation in accepted gaps between MTW and cars for different manoeuvres and different duration of the day was checked statistically using one way ANOVA at 95% confidence interval for null hypothesis, no variation in accepted gaps between MTW and cars for different duration day. The results are shown in Table 3.

Table 2 Statistical check for MTW and cars for different manoeuvres and along the different duration

Type of manoeuvres	Subject vehicle	F-value	P-value	F critical	Remarks
Minor to major (merging)	MTW	2.044	0.13	3.02	Accepted
	Cars	2.144	0.15	3.02	Accepted
Major to minor (crossing)	MTW	6.176	0.00	3.03	Rejected
	Cars	1.782	0.17	3.09	Accepted

Table 3 Statistical check between MTW and cars for different manoeuvres and along different duration

Type of manoeuvres	Time of the day	F-value	P-value	F critical	Remarks
Minor to major (merging)	Morning	10.67	0.00	3.90	Rejected
	Afternoon	10.67	0.00	3.90	Rejected
	Evening	3.86	0.05	3.91	Rejected
Major to minor (crossing)	Morning	5.21	0.02	3.94	Rejected
	Afternoon	1.22	0.27	3.92	Accepted
	Evening	0.67	0.41	3.93	Accepted

The table shows that in case of minor to major merging behaviour, results between MTW and cars show a statistically significant difference in gap acceptance behaviour along different duration of day. However, for crossing manoeuvre, MTW and cars showed statistically significant difference during morning time, but the non-significant difference in gap acceptance during afternoon and evening time duration. This may be due to driver who is more cautions to cross the traffic compared to merge the traffic stream.

6.1 Analysis by Raff’s Method

As per the method, gap acceptance and rejected gap for MTW with respect to cumulative frequency for whole day data are plotted, and the critical gap is determined as represented in Fig. 2. Similar graphs for determining critical gaps were plotted for car, and their results are shown in Tables 4 and 5.

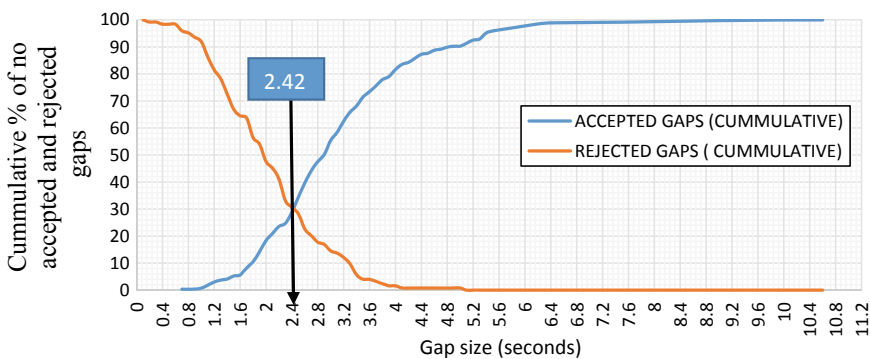


Fig. 2 Critical gap for MTW considering combined duration for minor to major manoeuvre

Table 4 Critical gaps for minor to major manoeuvre by Raff’s method in seconds

Subject vehicle	Morning	Afternoon	Evening	Combined
MTW	2.46	2.57	2.25	2.42
Cars	2.7	2.88	2.39	2.47

Table 5 Critical gaps for major to minor manoeuvre by Raff’s method in seconds

Subject vehicle	Morning	Afternoon	Evening	Combined
MTW	2.73	3.2	2.52	2.42
Cars	3.36	2.55	2.89	3

6.2 Analysis by Logit Method

Logit model for critical gap is developed using the gap size as the independent variable and the driver’s decision of acceptance/rejection of a gap as the response variable as shown in Fig. 3. The model predicts the probability of acceptance/rejection of a gap, and the critical gap is the gap for which the probability of acceptance is 0.5. Similar graphs for determining critical gaps were plotted for car, and their results are shown in Tables 6 and 7.

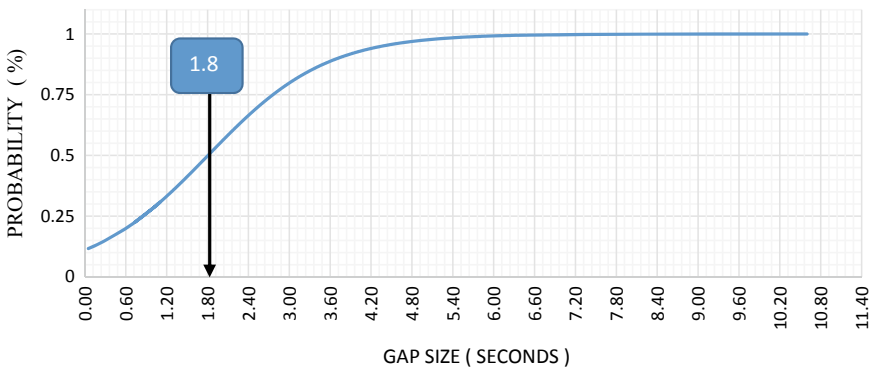


Fig. 3 Critical gap for MTW considering combined duration for minor to major movements

Table 6 Critical gaps for minor to major manoeuvre by Logit method in seconds

Subject vehicle	Morning	Afternoon	Evening	Combined
MTW	2	1.4	1.8	1.8
Cars	2.4	–	2.41	2.4

Table 7 Critical gaps for major to minor manoeuvre by Logit method in seconds

Subject vehicle	Morning	Afternoon	Evening	Combined
MTW	2.5	2.4	2.5	2.6
Cars	2.5	2.4	2.7	2.3

6.3 Analysis by Probability Equilibrium Method (PEM)

The observed CDFs of accepted gaps $F_a(t)$, rejected gaps $F_r(t)$ and the critical gaps $F_c(t)$ are presented in Fig. 4 for MTW for combined duration, where CDF of critical gap represents critical gap for each pair of accepted and rejected gap pairs. Similar graphs for determining critical gaps were plotted, and their results are shown in Tables 8 and 9.

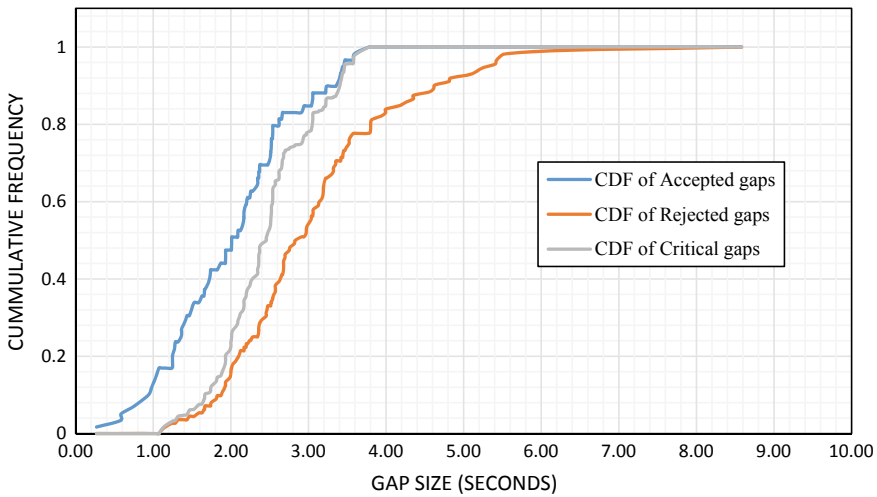


Fig. 4 Cumulative distribution plots for MTW by probability equilibrium method (PEM) for a combined duration

Table 8 Critical gaps for minor to major manoeuvre PEM method in seconds

Subject vehicle	Morning	Afternoon	Evening	Combined
MTW	2.44	2.69	2.24	2.45
Cars	2.8	3.8	2.43	2.86

Table 9 Critical gaps for major to minor manoeuvre PEM method in seconds

Subject vehicle	Morning	Afternoon	Evening	Combined
MTW	2.84	3.5	2.61	2.9
Cars	3.3	2.6	3.32	3.08

7 Comparison of Critical Gaps

In Raff's critical gap for minor to major manoeuvre, it was 2.42 s for MTW and 2.47 s for cars during whole survey period. However, gap acceptance showed variation between morning and evening period.

Results showed a critical gap of 2.46 s for MTW and 2.7 s for the car during morning peak hours. During afternoon, the results showed a critical gap of 2.57 s for MTW and 2.88 s for cars. Moreover, during evening peak hours, it was 2.25 s for MTW and 2.39 s for cars, respectively. While for major to minor manoeuvre in morning duration, critical gap for MTW was 2.73 s and for car it was 3.36 s. Same trend existed in evening and for combined duration, but in afternoon, the critical gap for MTW was more than that of car.

In Logit method for minor to major manoeuvre, MTW followed same trend as that of Raff's method with least critical gap during evening and larger during day duration. Further, the critical gap calculated is higher for car when compared with MTW in morning, evening and combined duration. However, this method was unable to estimate critical gap for car in afternoon, while for major to minor movements MTW and car showed almost same value.

According to probability equilibrium method (PEM) for a minor to the major manoeuvres, critical gap for MTW was minimum and for cars, it was maximum. This trend existed for the morning, afternoon and combined duration. Nevertheless, for major to minor manoeuvre, in morning duration, MTW had higher value and car showed the maximum value of critical gap. In afternoon duration, MTW had a maximum value of critical gap, while car had the least value. For the combined duration, least value of critical gap was for MTW and car had the maximum value of critical gap.

8 Discussion and Conclusion

This study involved initiating research on uncontrolled T-intersections in the urban area of an Indian city. This paper discusses several techniques for the estimation of a critical gap at TWSC intersections. Analysis indicates that gap acceptance varies for different categories of vehicles and varies with different duration of the day. The study reveals that as the day progresses, the gap acceptance behaviour of drivers does not change statistically for both categories of studied vehicles except for MTW for crossing manoeuvre. However, among the vehicles, gap acceptance behaviour

statistically varies throughout the day for merging traffic but shows no change for crossing manoeuvre. This indicates that MTW and cars are equally accepting the risks of crossing manoeuvre as compared to the merging manoeuvre.

MTW has the lowest value of critical gap during morning peak hours, and cars have a higher critical gap as compared to MTW. However, this trend was different during an off-peak hour, which may be due to less vehicular flow and larger size of gap available for most of the time in afternoon for both minor to major and major to minor manoeuvre.

For minor to major manoeuvre, the critical gap by Raff's and PEM methods is nearly same, while Logit method estimated somewhat lesser value of critical gaps. However, for major to minor manoeuvre, the estimated critical gaps by all three methods are nearly the same. The study also observed that during evening time, drivers of both categories of vehicles showed lower gap acceptance behaviour which may be due urgency of vehicle users because of tiredness of whole day work and impatience to reach their destination.

References

1. Guo R-j, Wang X-j, Wang W-X (2014) Estimation of critical gap based on Raff's definition. *J Comput Intell Neurosci* 2014
2. Khan A, Joshi GJ, Arkatkar SS (2014) Mixed traffic gap acceptance behaviour at four legged rotary intersection. M.Tech. dissertation submitted to SVNIT Surat
3. Brilon W, Konig R, Troutbeck R (1997) Useful estimation procedures for critical gaps. In: Proceedings of the 3rd international symposium on intersections without traffic signals, Portland Oregon, USA, 21–23 July 1997, pp 71–87
4. Miller AJ (1972) Nine estimators of gap-acceptance parameters. *J Traffic Flow Transp*:215–235
5. Troutbeck RJ (1992) Estimating the critical acceptance gap from traffic movements. Physical infrastructure centre research report 92-5. Queensland University of Technology, Brisbane, Australia
6. HCM (1994, 2000) Highway capacity manual. Transportation Research Board, National Research Council, Washington DC
7. Wu N (2006) A new model for estimating critical gap and its distribution at un-signalized intersections based on the equilibrium of probabilities. In: Proceedings of the 5th international symposium on highway capacity and quality of services. Japan Society of Traffic Engineers, Yokohama, 25–29 July 2006
8. Ashton WD (1971) Gap-acceptance problems at a traffic intersection. *J Roy Stat Soc Ser C Appl Stat* 20(2):130–138
9. Ashworth R (1970) The analysis and interpretation of gap acceptance data. *Transp Sci* 4(3):270–280
10. Mahmassani H, Sheffi Y (1981) Using gap sequences to estimate gap acceptance functions. *Transp Res Part B Methodol* 15(3):143–148
11. Radwan AE, Sinha KC (1980) Gap acceptance and delay at stop controlled intersections on multi-lane divided highways. *ITE J Inst Transp Eng* 50(3):38–44.
12. Storr PA, Cooper DF, McDowell MRC (1980) Analysis of gap acceptance in a complex traffic manoeuvre. *Eur J Oper Res* 5:94–101
13. Harwood DW, Mason JM, Brydia RE (1999) Design policies for sight distance at stop-controlled intersections based on gap acceptance. *Transp Res Part A* 33:199–216

14. Davis GA, Swenson T (2004) Field study of gap acceptance by left-turning drivers. TRR 1899, Transportation Research Board, National Research Council, Washington DC, pp 71–75
15. Pollatschek MA, Polus A, Livneh M (2002) A decision model for gap acceptance and capacity at intersections. *Transp Res Part B Methodol* 36(7):649–663
16. Amin HJ, Maurya AK (2015) A review of critical gap estimation approaches at uncontrolled intersection. *J Transp Lit* 09
17. Kusumaa A, Koutsopoulos HN (2011) Critical gap analysis of dual lane roundabouts. *Procedia Soc Behav Sci* 16:709–717
18. Ashalatha, Chandra S (2011) Critical gap through clearing behaviour of drivers at un-signalised intersections. *KSCE J Civ Eng* 15(8):1424–1434
19. Patil GR, Sangole JP (2016) Behaviour of two-wheelers at limited priority uncontrolled T-intersections. *J Int Assoc Traffic Saf* 40(1):7–18

Modelling Queuing of Vehicles at Signalized Intersection



Dhaval Parmar, Ninad Gore, Dipak Rathva, Sanjay Dave and Manish Jain

Abstract The present study emphasizes on the determination of the queue length at the signalized intersection by manually collected data and modelling queue length for a busy urban signalized intersection under heterogeneous traffic conditions of Vadodara city, Gujarat, India. Major approaches and one of the minor approaches have an identical width. Flow share of 65% was observed on major approaches. Flow composition on major approaches was characterized by the presence of heavy vehicles; whereas, the same was absent on minor approaches. Moreover, red time of both major and minor approaches was articulated according to flow share. Each lane has a minimum two-lane width but the queue length was not respective to lane discipline. Queue length was measured manually for two hours in the evening peak for three days by graduating medians at 1 m interval. In addition, queue length and its composition were recorded simultaneously until the last second of red time for each lane. Observations revealed that the average queue length varied from 71.47 to 110.64 m on the major approach while it varied from 46 to 55 m on the minor approach, respectively. Further, queue length for one of the major and one of the minor approaches exceeded the cross traffic opening and hence hindered the free movement of cross traffic. Queue composition was dominated by motorized two-wheelers followed by cars and motorized three-wheeler (auto-rickshaws). It was also noted that though queue length was similar, the total PCU value per cycle varied on one of the major approaches. This may be attributed to the presence of heavy vehicles in queue composition resulting into the large gap between vehicles, reducing its local

D. Parmar · N. Gore · D. Rathva · S. Dave (✉) · M. Jain
The Maharaja Sayajirao University of Baroda, Vadodara, India
e-mail: smdave-ced@msubaroda.ac.in

D. Parmar
e-mail: dhaval.parmar76333@gmail.com

N. Gore
e-mail: ninadgore24@gmail.com

D. Rathva
e-mail: dipakrathva-ced@msubaroda.ac.in

M. Jain
e-mail: manish.jain-ced@msubaroda.ac.in

density, and thus reflecting driver behaviour. It was also observed that queue length was dependent upon its composition and associated red time. Multi-linear regression analysis was used to model queue length with respect to its composition, associated red time and width of the road. Further, the queue model for three legs of identical width was statistically validated against queue model of one remaining leg to examine the effect of road width using F -test and was found insignificant. Predicted queue length values were also checked with observed queue length values using t -statistics and t -test analysis, which shows there is no significant difference between two data sets. Mean absolute percentage error (MAPE) was estimated around 14%, indicating fair acceptance of developed queue model.

Keywords Signalized intersection · Queue length · Queue model

1 Introduction

Numerous halt because of jamming and at crossings is a common scenario witnessed for the urban traffic in developing countries like India which in turns results into the accompanying interruptions and pollution. In addition during peak hours, signalized intersection's costs upsurge in holdup for organizing the vehicular movement to achieve safety. The performance evaluation of the signalized intersection can be referred by considering the stretch of the queue and resulting interruptions. The performance and efficiency of the whole road network mainly depend upon the correct planning of the signalized intersection. Since the initiation of this facility, transportation planning mainly focuses on the performance level of the signalized intersection. It has long been observed that the estimation of the queue length at signalized intersections is a significant factor for the effective management and control of traffic. The stretch of the queue for each cycle of red time is the prime element for the assessment of the signalized intersections along with the count of the vehicle's interruption which supports the assessment of effectiveness of the signalized intersections. So, queue length and count of the vehicle's interruption, so-called measures of effectiveness, are the important parameters employed for the assessment of the level of service offered to the users and also from the operational point of view for the aspects like fuel consumption and associated air pollution.

2 Review of Literature

The collection of the field data about number of vehicles in the queue at any instant of time is quite difficult rather it can be determined from the traffic flow data. The approach of using traffic flow for queue length measurement is having certain constraints though it is simple and effective. There are very few researches on queue length in India. The intersection clearing speed for motorized two-wheeler (MTW),

auto rickshaw (three-wheeler-IPT mode of transport) and car obtained from the field observations, the acceleration characteristics of vehicles are investigated. In the outcome demonstrations, there exists the linear relationship between the acceleration of vehicles in the queue and release of vehicles at the green signal [1].

The field data about the clearing speed for two-wheeler, three-wheeler and car at the intersection was collected. Intersection clearing speed of the vehicles in the queue for the various formation of queue was also determined. For the evaluation of the performance of the intersection, the number of vehicles is obtained from the advance and stop bar detectors along with the signal information. The number of vehicles in queue was counted over an analysis period of every 10 s [2]. A simple model of a single server queue is developed in which the control decisions are based on the queue occupancy [3]. The outcome shows the vehicles with larger dimension reduce the saturation flow at the intersection [4]. Queue length at the intersection is estimated by shockwave theory [4]. The simple approach is adopted for the measurement of queue length at signalized intersection by measuring queue length as per the time interval even when the long queue is observed at the junction [5]. The parameters like flow, occupancy, cycle length and detector setback are utilized for queue length determination. The algorithm is based upon the two baseline occupancies corresponding to the relative position of the queue with respect to the location of detector. Traffic simulation is used to evaluate the outcomes of the algorithm and also compared to field observations. The real-time estimation of queue length as per the lane depends upon the detector and the signal information from a set of upstream and downstream detectors [6]. The performance of the proposed method is appropriate for the calibration set and for five different validation sets with 100, 200 and 300 m upstream detectors. The long queue estimation models are proposed by using short vehicle traces obtained from mobile sensors, which consist of two major steps: trajectory reconstruction and delay-based queue length estimation [7]. The model for estimation of queue length at the signalized intersection is developed using RFID detector [8]. The queue lengths and their distribution are obtained by calculating Markov chains [9]. From the distribution, the percentiles of queue lengths can be determined. For stationary traffic conditions, the formula can be derived using regression technique while for non-stationary traffic conditions, the so-called transition techniques can be adopted to derive the formula.

3 Study Area and Data

The selected study site constitutes a part of old NH-8, running through the heart of the city. Akota-Dandia Bazar intersection is characterized by two major approaches named as Rajmahal and Kothi and two minor approaches named as Akota and Dandia bazar. Major approaches and one of the minor approaches have identical width. Intersection has divided carriage way. Queue length was measured manually for two hours in evening peak for three days by graduating medians at 1 m interval.



Fig. 1 Location of the study area

Table 1 Road inventory detail and signal timings

Road	Width (m)	Lane	Red time (s)	Green time (s)	Amber time (s)
RajMahal	11.5	Four lane divided	128	67	3
Kothi	16	Four lane divided	105	90	3
Dandia Bazar	6.5	Two lane divided	163	32	3
Akota	23	Six lane divided	163	32	3

Road inventory details and signal times were noted. Composition of vehicles was calculated. Figure 1 shows the location of the study site.

Road inventory details and signal timings are summarized (Table 1).

4 Data Analysis

Data analysis revealed that major approaches share 65% of the total traffic, while 35% was shared by minor approaches. It was also observed that MTW dominated the flow, followed by car and 3-W for all approaches for all days. It was also observed

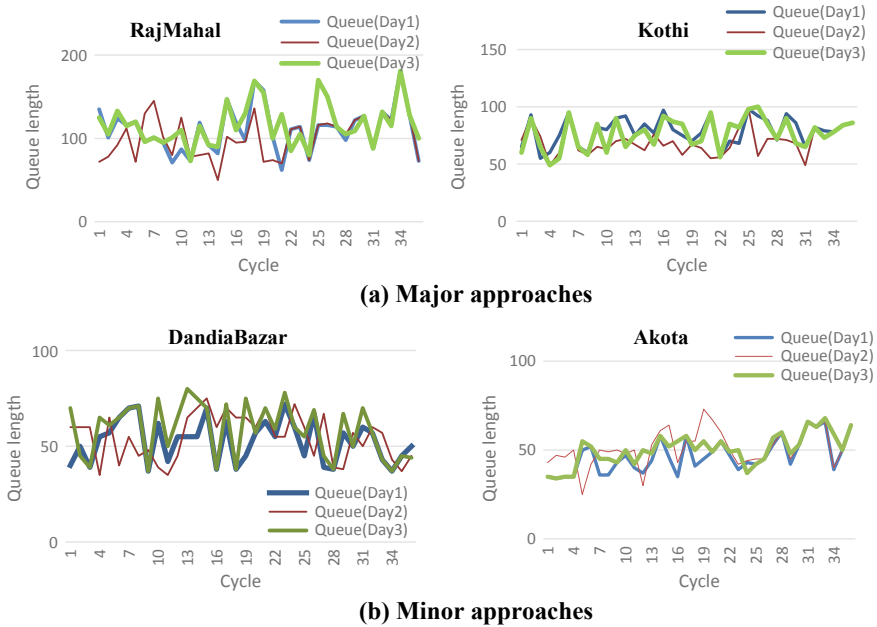


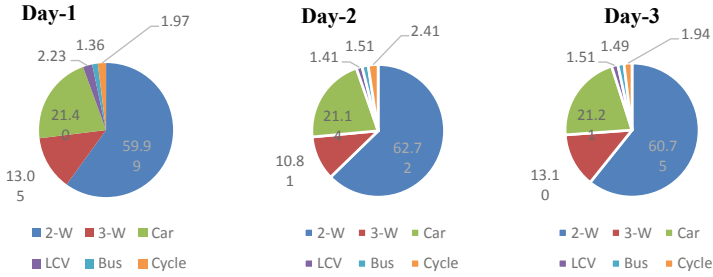
Fig. 2 Variation in queue length for major and minor approaches

that the queue on one of the major and minor approaches exceeded the cross traffic opening and hindered its free movement. Observations revealed that the queue length on major approaches ranged in 68–114 m while for minor approaches it ranged in 46–55 m. In addition, variation in queue length for all approaches for all days was nearly consistent which is reflected in Fig. 2. Further, analysis revealed that MTW dominated the queue composition for all approaches (Fig. 3).

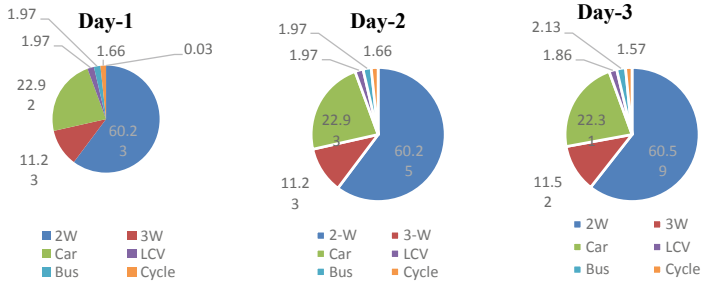
4.1 Effect of Heavy Vehicles

Analysis of data revealed that, for identical queue length, the composition (PCU/Cycle) varies. To probe further, the effect of heavy vehicles for similar queue length was signified. Queue length, encompassing one-sigma limits was considered as queues having similar queue length. Similar queue length was further bifurcated in terms of presence and absence of heavy vehicles. ANOVA test was carried out at 10% significance for null hypothesis; heavy vehicles do not affect queue composition (PCU/Cycle) for identical queue length (Table 2).

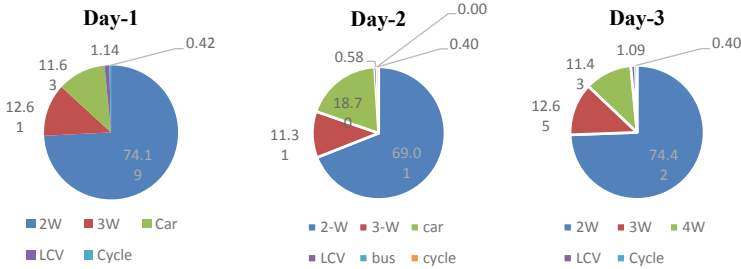
Therefore, in reference to *p*-value for one-way ANOVA, null hypothesis is rejected. Therefore, it can be concluded that for similar queue length, presence of heavy vehicles affects queue composition (PCU/Cycle).



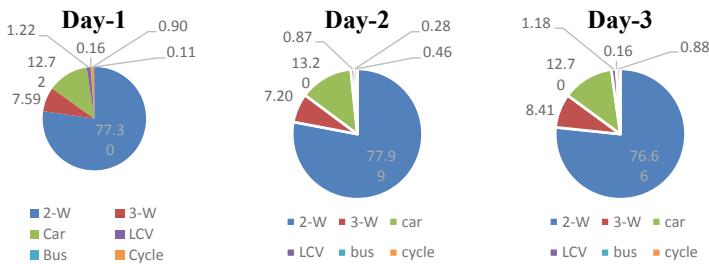
(a) Rajmahal Road (Major Approach)



(b) Kothi Road (Major approach)



(c) Dandia Bazar Road (Minor Approach)



(d) Akota Road (Minor approach)

Fig. 3 a–d Queue composition for major and minor approaches

Table 2 ANOVA test results

Variable	F	p-value	$F_{critical}$	Remark
With and without the presence of heavy vehicles	6.13	0.01	3.97	Rejected

4.2 Modelling of Queue

Pearson correlation test was carried out at 95% confidence interval to signify correlation between queue length and composition in terms of PCU/cycle. PCU values were adopted as per mentioned in [8]. Linear regression approach was adopted to model the relation between queue composition and queue length. Two models based on width were formulated to investigate the effect of width of road on queue length. Model summary is presented in Tables 3 and 4.

The predicted values of both models were checked statistically using *f*-test at 95% confidence interval for the null hypothesis, no significant difference between predicted queue length values exists and was found insignificant. Therefore, it is concluded that the width of road does not hold any effect on queue length. Therefore, three-leg model can be generalized. Further, the model was validated for remaining one-leg. *T*-test and χ^2 tests were also carried out. Further, accuracy of the model in form of MAPE is also calculated. Results are tabulated (Table 5).

As *p*-value obtained for *t*-test and χ^2 test are greater than 0.05, it indicates statistical similarity in estimated and observed speed. As per Lewis scale of measurement of accuracy given by Ban et al. [9], MAPE and RMSE values obtained are fairly low; therefore, the model is robust and fairly adoptable.

Table 3 Summary of three-leg model

Equation	<i>t</i> -Stat	<i>p</i> -value	<i>R</i>	Pearson correlation test (<i>p</i> -value)	R^2
$Y = 0.748 X_1 - 0.1078 X_2$	39.88	0.00	0.98	0.000	0.97
	-6.573	0.000			

Table 4 Summary of one-leg model

Equation	<i>t</i> -Stat	<i>p</i> -value	<i>R</i>	Pearson correlation test (<i>p</i> -value)	R^2
$Y = 0.348 X_1 + 0.109 X_2$	4.95647	0.0	0.97	0.000	0.96
	3.95	0.008			

where *Y* = queue length in PCU, X_1 = red phase time in second, X_2 = road width in metre

Table 5 Statistical checks

Between observed and estimated queue length	
p -value f -test	0.80
T	0.72
p -value t -test (2-tailed)	0.46
t_{cri}	1.95
p -value (χ^2 test)	1.00
MAPE (%)	14.14
RMSE (%)	10.13

5 Conclusions

From the study, it was observed that the arrival of mixed vehicles and PCU adopted plays a major role in the various formation of queue. Though queue length was similar, the total PCU value per cycle varied on one of the major approaches. This may be attributed to the presence of heavy vehicles in queue composition resulting into the large gap between vehicles. MAPE values indicated that the model formulated is robust and can be generalized. The signal timing could be designed as per the queue length formation and its dissipation. This approach of signal design helps to save time of the user, to reduce the fuel consumption and so associated air pollution. This may also be used for the proper control and management of traffic at the junction. The study provides a better understanding of the performance of signalized intersection and design of short-term planning measures like lane prioritization for heavy vehicle for smooth and efficient movement of traffic.

References

1. Anusha Lelitha SP, Vanajakshi D, Sharma A (2013) A simple method for estimation of queue length. Digital Commons University of Nebraska—Lincoln Civil Engineering Faculty Publications
2. Dey PP, Nandal S, Kalyan R (2013) Queue discharge characteristics at signalized intersections under mixed traffic conditions. *Eur Transp* 8(55). ISSN 1825-3997
3. Jagannathan K, Modiano E, Zheng L (2011) On the role of queue length information in network control. *J IEEE Trans Inf Theory* 57(9):5884–5896
4. Evans L, Rothery RW (1981) Influence of vehicle size and performance on intersection saturation flow. In: Proceedings from 8th international symposium on transportation and traffic theory. University of Toronto Press, Toronto, Ontario, pp 193–222
5. Liu HX, Wu X, Ma W, Hu H (2009) Real-time queue length estimation for congested signalized intersections. *Transp Res Part C* 17:412–427
6. Chang J, Talas M, Muthuswamy S (2012) A simple methodology to estimate queue lengths at signalized intersections using detector data. Resubmitted to Transportation Research Board for possible publication in the Transportation Research Record
7. Lee S, Wong SC, Li YC (2015) Real-time estimation of lane-based queue lengths at isolated signalized junctions. *Transp Res Part C Emerg Technol* 56

8. Wu A, Yang X (2013) Real-time queue length estimation of signalized intersections based on RFID data. In: Proceeding of 13th COTA international conference of transportation professionals (CICTP 2013)
9. Ban XJ, Hao P, Sun Z (2011) Real time queue length estimation for signalized intersections using travel times from mobile sensors. *Transp Res Part C Emerg Technol* 19(6)

Development of Consistency Evaluation Criteria for Indian Two-Lane Rural Highways



Jacob Anitha, Akkara Jisha and R. Midhun Mohan

Abstract Maintaining consistency in the design of highway geometry is an effective method in controlling road crashes from the highway-engineer's point of view. Among the various methods available to measure the consistency of geometry, viz., operating speed, driver workload, alignment index, and vehicle stability, alignment index is a method that is highly suitable for a developing country like India where financial resource is always a concern. It is an index used for quantifying how well the alignment features such as radius, curve length, and rate of change of gradient are coordinated with the overall alignment of the highway section. The particular measure does not require any additional data collection rather than the plan and profile of the highway. Had any criteria exist, with minimum investment, it will be possible to evaluate the consistency and subsequently safety. This paper develops a procedure for evaluating two-lane rural highway consistency and safety for Indian road conditions through alignment index. Highway geometry and crash data were made use of, and it was found that average radius and average curve length can be considered as the good alignment indices. Based on the crash data, criteria were developed for evaluating Indian two-lane rural highways. By using the criteria proposed in the work, planners, designers, and road safety auditors can evaluate the geometric design of a highway section as consistent or not. The output of the work further assists in selection of a plan/design among various alternatives, prioritization of rehabilitation works and in implementation of road safety management measures.

Keywords Highway geometric design · Consistency evaluation · Alignment index · Safety evaluation criteria · Rural highway

J. Anitha (✉) · A. Jisha · R. Midhun Mohan
Jyothi Engineering College, Cheruthuruthy, Thrissur, Kerala, India
e-mail: anithajacob@jecc.ac.in

A. Jisha
e-mail: jishaakkara@jecc.ac.in

R. Midhun Mohan
e-mail: midhunmohanr@jecc.ac.in

1 Introduction

The goal of transportation is generally stated as the safe and efficient movement of people and goods. Thus, safety is of prime concern in the design of a roadway. To achieve this goal, designers use many tools and techniques. One technique used to improve safety on roadways is to ensure the consistency of the design. A consistent road should not violate the expectations of motorists or inhibit the ability of motorists to control their vehicle safely. Instead, such a roadway should ensure that drivers could operate safely at their desired speed along the entire alignment.

Design consistency implies that the design or geometry of a road does not violate either the expectation of the motorist or the ability of the motorist to guide and control a vehicle in a safe manner [1]. An inconsistency in design can be defined as a geometric feature or combination of adjacent features that have such unexpectedly high driver workload that motorists may be surprised and possibly drive in an unsafe manner.

The most common measures that were considered useful in evaluating the consistency of geometric alignments were identified as:

- (1) Operating speed
- (2) Vehicle stability
- (3) Driver workload
- (4) Alignment indices

Among the above, this paper focus on alignment-indices-based evaluation of two-lane rural highways [1]. Alignment indices are some quantitative measures of the general characteristic of a roadway segment's alignment. Such indices have several conceptual advantages for use in design consistency evaluation [2, 3]. Inconsistency is identified when there is

- Large increase or decrease in the values of alignment indices for successive roadway segments.
- High rate of change in alignment indices over some length of roadway.
- Large difference between the individual feature and the average value of the alignment index.

For each of these indicators, the amount of change in the index value can be determined and any significant change in this value from that of some threshold limits indicates inconsistency.

An average of the geometry parameters along a roadway segment can indicate the general character of the road. An individual feature that has a value dissimilar to that of the average of the roadway can possibly indicate that there is some inconsistency between that feature and the general alignment of the roadway. This inconsistency may lead to unsafe driving environment for the road users [3]. Researchers have studied the effect of many of these indices on number of crashes [1, 3]. Various alignment indices used in literature are given in Table 1.

This study has two objectives. The first objective is to identify the simple indices that can quantify the geometric design consistency based on the available plan and

Table 1 Alignment indices for consistency evaluation of a section with *i* segments

<i>Horizontal alignment indices</i>	<i>Vertical alignment indices</i>
<p>1. Curvature change rate—CCR (deg/km) $= \Sigma \Delta i / \Sigma Li$ where Δ = deflection angle L = length of section</p>	<p>1. Vertical CCR—VCCR (deg/km) = $\Sigma Ai / \Sigma Li$ where A = absolute difference in grades L = length of section</p>
<p>2. Degree of curvature—DC (deg/km) = $\Sigma (DC) i / \Sigma Li$ where DC = degree of curvature L = length of section</p>	<p>2. Average rate of vertical curvature—V AVG K (km/%) $[\Sigma L / A] / n$ where L = length of section A = algebraic difference in grades (%) n = number of vertical curves</p>
<p>3. Curve length: Roadway length (CL:RL) $= \Sigma (CL) i / \Sigma Li$ where CL = curve length (m) L = length of section</p>	<p>3. Average gradient—VAVGG (m/km) $\Sigma \Delta E i / \Sigma Li$ where ΔE = change in elevation L = length of section</p>
<p>4. Average radius—AVGR (m) = $\Sigma Ri / n$ where R = radius of curve (m) n = number of curves within section</p>	<p><i>Composite alignment indices</i> Combination CCR—COMBO (deg/km) $\Sigma \Delta i / \Sigma Li + \Sigma Ai / \Sigma Li$, where Δ = deflection angle (deg) A = absolute difference in grades (deg) L = length of section (km)</p>
<p>5. Average tangent—AVGT (m) $\Sigma (TL) i / n$ where TL = tangent length (m) n = number of tangents within section</p>	

profile. As a second objective, the threshold values of these indices are to be estimated based on the observed crash history. This will help to formulate criteria for evaluating highway sections based on their alignment.

2 Methodology

2.1 Data Collection and Processing

The study stretch that has been selected is 47 km of the State Highway from Palakkad Town to Guruvayur of Thrissur District in Kerala (Fig. 1).

The data collected include geometric data and crash data. Plan of the highway stretch was developed using a GPS survey, and a total station survey was carried out at necessary sites to capture gradient. The stretch comprised of horizontal curves as well as combination of horizontal and vertical curves. But as the number of samples of latter data was insufficient for analysis, the scope of the study was restricted to horizontal alignment alone. A curve with $\pm 2\%$ gradient was taken as a horizontal curve. The geometric data set comprised of 46 sections.

A handheld GPS unit was used for continuously logging the road coordinates by walking over the entire road stretch. The data from GPS was converted to Excel

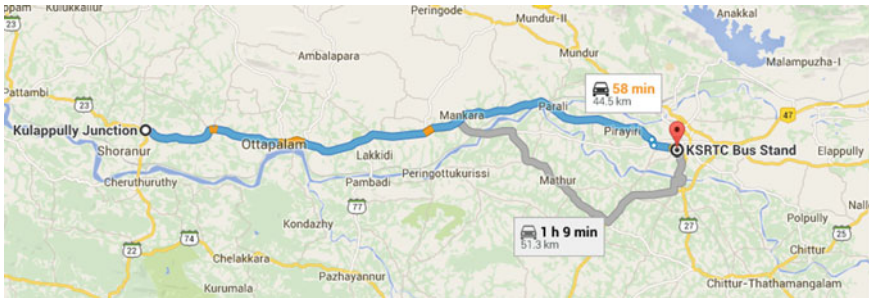


Fig. 1 Study stretch from Palakkad to Kulappully

format and then drawn using AutoCAD software. In order to check the gradient of the alignment, total station survey was conducted. AutoCAD and Microstation software were made use of to retrieve horizontal and vertical alignment characteristics. The variables retrieved after data collection include chainage, radius of curve, length of curve, deflection angle, degree of curvature, gradient and tangent length.

Crash data were collected from the First Information Report of Kerala Police Records with due permission from the concerned heads of Police. Data from 2013 January to 2015 December were manually collected and recorded in a predefined format. The data include the type of crash, type of vehicles involved, severity of crash—property damage only (IPC 279)/minor crash (IPC 337)/major crash (IPC 338)/fatal crash (IPC 304A), place of occurrence, location of spot, number of person involved, age and sex of driver, and address of the complainer for further verification about the crash spot and cause. As the objective of the study is to understand the effect of highway alignment on crashes, irrelevant crash cases such as drunken driving and crashes with cattle were not considered. The data were analyzed to know temporal, vehiclewise, and other characteristics of crash data.

Crash database consists of crashes of different severity levels like minor or non-grievous, major or grievous, and fatal or crashes involving death. In order to evaluate sections based on crash occurrence and severity, it was decided to scale crashes based on the level of severity, ranging from non-grievous to fatal. Each level of severity is given adequate weights and weighted sum of crashes is taken as the equivalent property damage only crash (EPDO). Based on the unpublished research work carried out by Anitha [4], weights of 1, 4, 12 were assigned to property damage only crashes, injury crashes, and fatal crashes, respectively. The weights were arrived at based on the analysis done on the insurance claims offered by insurance companies for different severity level crashes.

2.2 *Development of Alignment Indices*

The information retrieved from plan and profile of the road centerline was utilized to develop alignment indices. The study stretch was divided into one-kilometre sections. Various indices of the section were determined by taking the average of the individual features in the section. The indices developed are Average Radius of section AR_S , Average Tangent Length of section ATL_S , Average Degree of Curvature ADC_S , Average Deflection Angle ADA_S , Average Curvature Change Rate of the section $ACCR_S$, Curve Length: Roadway Length $ACL_S:RL$, Average Radius to Overall Average Radius $AR_S:OAR$, and Average Tangent Length to Overall Average Tangent Length $ATL_S:OATL$. The summary statistics of these alignment indices are given in Table 2.

2.3 *Preliminary Analysis*

A preliminary analysis was done in order to study and explore the data available. Initially, scatter plots between various geometric alignment indices and type of crash were drawn. Figure 2 shows the scatter plot of EPDO against AR_S and $ACCR_S$. Though the sample size is less to define a solemn trend, an eyeball observation shows that with an increase in average radius, number of crashes is decreasing. Also, it can be found that crashes increase with increase in curvature change rate, reaches a maximum, and then decreases. This is in line with the results from various studies that crashes are less on sections with low curvature and sections with high circuitry [5]. Only sections having unexpected curves in generally straight highways come across with more crashes.

A two-way correlation study was done to understand if there is any significant correlation existing between the variables. The variables that are found to be significant with different types of crashes are given in Table 3.

2.4 *Development of Regression Models*

Regression analysis was carried out to quantify the effect of alignment on crashes. Purpose of the analysis is to predict the number of crashes, if the alignment indices for the highway section are known. The dependent variables were the crash-related variables, and the independent variables were the alignment indices. The entire data was divided into two sets, randomly. The first data set contained 30 samples and was used for calibrating the models. Models were calibrated at 95% confidence level. The second data set containing 16 samples was used for model validation. Validation was done by finding the percentage root mean square error (PRMSE) values.

Tables 4 and 5 give the regression models developed for major crashes and EPDO

Table 2 Summary statistics of alignment indices

	ARs	AR _s /OAR	ATL _s	ATL _s /OATL	ACL _s	ACCR _s	ACL _s /RL	ADC _s	ADAs
AVG	313.83	1.05	736.54	0.93	158.90	0.79	0.00	23.40	27.52
MIN	42.75	0.13	0.00	0.00	0.00	0.00	0.00	0.00	0.00
MAX	1205.63	4.05	1763.50	2.23	786.00	1.96	0.02	144.59	93.00
SD	289.07	0.97	582.26	0.74	206.67	0.59	0.00	27.40	26.30

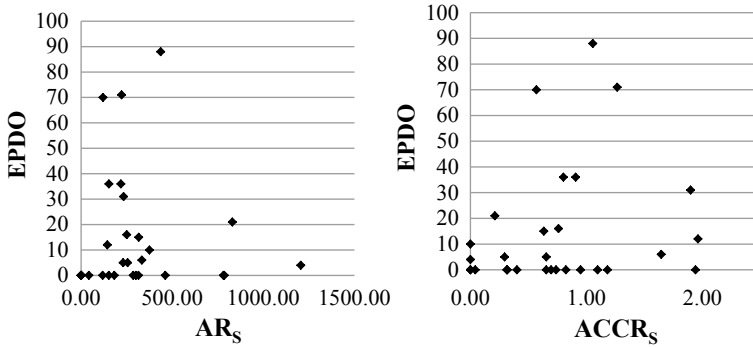


Fig. 2 Scatterplots of alignment indices AR_s and ACCR_s

Table 3 List of significant variables after correlation analysis

Type of crash	Significant variables
Minor crash (MINA)	No significant variables
Major crash (MAJA)	ACL _s , ADC _s , ADA _s
Fatal crash (FATA)	ADA _s , ACCR _s
Total crash (TOTA)	ACL _s , ACL _s :RL
EPDO	ACL _s , ACL _s :ATL _s , ACL _s :RL, ACCR _s

Table 4 Safety evaluation models for major crashes

Sl. no.	Model	R ²	PRMSE
1	$Y = 0.69 + 0.007292 * ACL_s - 0.00102 * AR_s$	0.27	59.8
2	$Y = 1.11 + 0.007138 * ACL_s - 0.00087 * ATL_s$	0.30	50.51

Table 5 Safety evaluation models for EPDO

Sl. no.	Model	R ²	PRMSE
1	$Y = 0.46 + 2376.92 * ACL_{s/RL} + 9.90 * ACCR_s$	0.21	47.2
2	$Y = 0.46 + 0.05 * ACL_s + 9.90 * ACCR_s$	0.21	53.8

crashes, respectively. The *t*-statistic of the model coefficients and constants were checked to verify whether the coefficients are significantly different from zero. No good models could be developed for minor crashes and total crashes. Also, sample size for fatal crashes was not sufficient, hence, no models were developed for such type of crashes.

In all the models, crashes are found to increase with increase in curve length. As the average radius increases, major crashes are found to decrease. With increase in curve length, major crashes as well as equivalent crashes are found to increase. Also,

it is found that with increase in average tangent length of the section, major crashes are found to decrease. With increase in the circuitry of the highway, EPDO values are found to increase.

The models developed could explain only 30% of variability, which means there are variables other than geometry that could cause crashes. Had more variables added to the data set, better coefficient of determination could be obtained; but, the model may become more expensive and complex. Nevertheless, the prime objective of the study is to quantify the consistency of geometry rather than prediction of crashes.

2.5 Development of Safety Evaluation Criteria

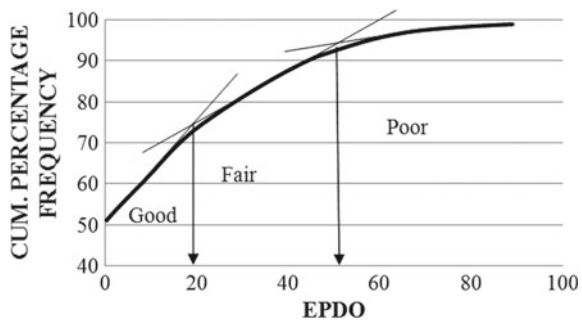
Criteria for evaluating the consistency of a highway were developed based on alignment index and EPDO. Following methodology was adopted for arriving at the criteria. Firstly, a cumulative frequency distribution diagram was prepared for EPDO values (Fig. 3). The locations where a change in the slope of the distribution occurs is identified. The values corresponding to those significant changes in the percentile distribution of EPDO (20 and 50) are selected as the threshold values for classification.

From Fig. 3, highway sections are classified as Good, Fair, and Poor based on their EPDO values. If the EPDO value is less than 20, the highway section can be considered as Good. If the EPDO value is between 20 and 50, the section can be considered as Fairly safe and if the EPDO exceeds 50, then the section can be considered as unsafe or Poor in safety.

Secondly, a safety-consistency grid was prepared as shown in Fig. 4. Each study site will occupy a cell in the matrix based on its alignment index and EPDO value. A tally system was adopted to mark the distribution. The matrix was visually observed to identify the presence of clusters if any. Figure 4 shows the evaluation grid for EPDO versus Average curve length of the section ACL_s .

It can be seen from Fig. 4 that as curve length is increasing, EPDO values are also increasing. With increase in curve length, drivers are subjected to the centrifugal forces for longer distance and difficulties in maneuvering the vehicle get extended.

Fig. 3 Cumulative distribution diagram of EPDO



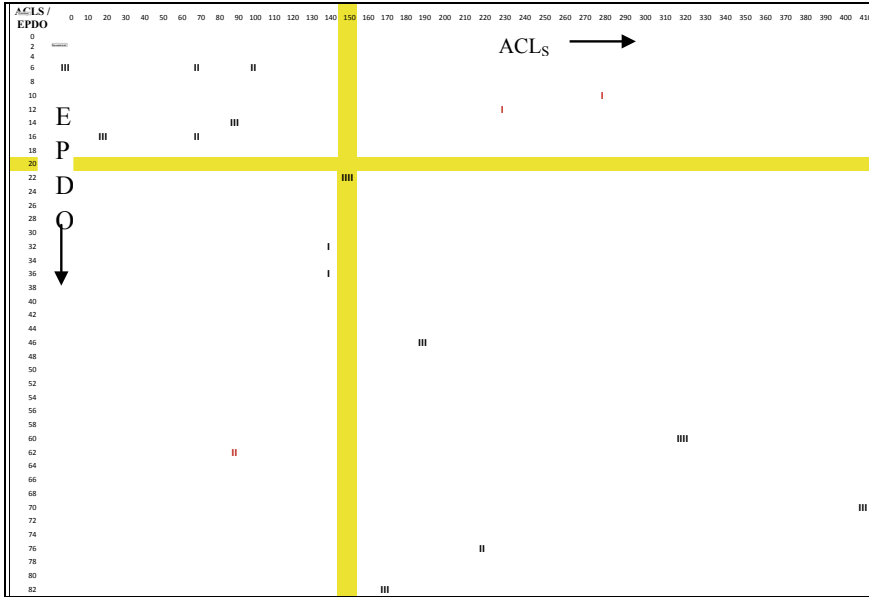


Fig. 4 Safety evaluation grid—EPDO versus ACL_S

The various groups or clusters identified by different clustering trials were tested statistically to select the most logical and representative consistency levels. Analysis of variance test was done to estimate whether significant difference exists on the mean EPDO values of different groups. The classification which gives maximum variance between the groups and minimum variance within the groups was selected as the threshold value for that consistency measure. For example, EPDO crash values are in the unsafe zone when ACL_S values are more than 150 m. Hence, a design can be evaluated as consistent if its ACL_S is less than 150 m. The presence of some outliers in the consistent and inconsistent region is not unexpected which clearly indicates the complexity of crash analysis and the possibility for multiple reasons behind them.

Similar grids were developed for various alignment indices and promising indices were found as AR_S and ACL_S . The consistency evaluation criteria developed based on these indices are given in Table 6.

As per the criteria, sections of highway with average radius less than 200 m or sections with average length of curve more than 150 m are having inconsistent geometry. The criteria developed in the study can be made use of, for evaluating

Table 6 Consistency evaluation criteria

Criteria	Consistent	Inconsistent
1	$AR_S > 200$ m	$AR_S < 200$ m
2	$ACL_S < 150$ m	$ACL_S > 150$ m

and classifying the highway sections as of consistent or inconsistent design based on safety.

3 Conclusions

Highway safety is a major concern of the day. As safety in highways is correlated to geometry of the road, designing the roadway as per the expectation of the users is a challenge for highway engineers and designers. The present work is an illustration of a methodology for developing geometric design consistency evaluation criteria based on highway safety. As per the study, geometry of a highway, new or existing can be evaluated with the help of their alignment indices such as Average Radius and Average Curve Length of the section. Threshold values of these indices are determined and can be used to classify the sections as consistent or inconsistent. As this method requires only the information about the geometry of highway alignment, it will become a handy tool for designers, planners, and road safety auditors for the evaluation of roads at the expense of minimum resources.

4 Future Scope

The present work is done based on limited data of horizontal curves on a state highway. The work can be strengthened by including more samples so that better models and reliable design guideline can be evolved. Also, the work can be extended to incorporate vertical alignment as well.

Acknowledgements Authors acknowledge Jyothi Engineering College, Cheruthuruthy, for giving the opportunity and facilities to conduct such a project work. Special acknowledgement to Prof. Anjaneyulu M. V. L. R., NIT Calicut, Ms. Dhanya T. V. and Mr. Uppaiah Bonagiri, former PG Students of NITC for giving the metadata for the project. Authors also acknowledge the Kerala Police department for permitting us to make use of the crash data of their FIR database.

References

1. Fitzpatrick K, Wooldridge MD, Tsimhoni O, Collins JM, Green P, Bauer KM, Parma KD, Koppa R, Harwood DW, Anderson IB, Krammes RA, Poggioli B (2000) Alternative design consistency rating methods for two-lane rural highways. Technical report, Federal Highway of Administration, FHWA-RD-99-172. US Department of Transportation, Washington DC
2. Hassan Y, Sayed T, Taberner V (2001) Establishing practical approach for design consistency evaluation. *J Transp Eng* 127(4)
3. Anderson IB, Bauer KM, Harwood DW, Fitzpatrick K (1999) Relationship to safety of geometric design consistency measures for rural two-lane highways. *Transp Res Rec Transp Res Board* 1658:43–51

4. Anitha J (2013) Geometric design consistency and safety of two-lane rural highway. Unpublished work for the award of PhD
5. Bhatnagar YS (1994) Observations on the use of chevron alignment markers. In: Proceedings of 17th Australian Road Research Board Ltd (ARRB) conference, vol 17, issue 5, pp 65–81

Effect of Shoulder Width on Traffic Flow Parameters on Two-Lane Undivided Roads



Pallav Kumar, Joyjeet Chakraborty, Shriniwas Arkatkar
and Gaurang J. Joshi

Abstract Traffic flow on two-lane undivided facility is very different from other roadway facilities. In case of two-lane undivided highways, after a certain increase in traffic volume, the overtaking maneuver decreases considerably due to the presence of oncoming vehicles. Also, with further increase in traffic flow, it may result in platoon formation. Two-lane undivided road is a very common facility in both urban and rural settings in India, where such kind of facility can cater to the significant proportion of traffic of that area. Despite this fact, the research available on operation of these types of facilities is very limited. Moreover, very little empirical-based research has been conducted about traffic flow characteristics on two-lane undivided roadway, especially for Class III type facilities (HCM 2010) under Indian conditions. In the present study, three study sections with features like Class III facilities are considered for analysis. Geometric feature of the roadway has 7-m carriageway with additional paved shoulder having varying width. These paved shoulders were also utilized by the vehicles during heavy-flow conditions. For Section 1, formation width was observed as 10.5 m (7-m carriageway and 1.75-m paved shoulder on each side); Section 2, it is 9.7 m (7-m carriageway and 1.35-m paved shoulder on each side); whereas in Section 3, it is observed as 9.5 m (7-m carriageway and 1.25-m paved shoulder on each side). Speed distribution is analyzed for the three study sections for different vehicle categories. It shows reduction in speeds of vehicle with decreasing shoulder widths. Further, to convert heterogeneous traffic in terms of vehicles/hour to PCU/hour, dynamic PCU concept is used. Thereafter, Speed–flow relationships are developed using Greenshields model for the study sections. The capacity of the three study

P. Kumar

Civil Engineering Department, Muzaffarpur Institute of Technology, Muzaffarpur 842003, India
e-mail: pallav318@gmail.com

J. Chakraborty · S. Arkatkar (✉) · G. J. Joshi

Civil Engineering Department, Sardar Vallabhbhai National Institute of Technology Surat, Surat
395007, Gujarat, India
e-mail: sarkatkar@gmail.com

J. Chakraborty

e-mail: joyjeet2222@gmail.com

G. J. Joshi

e-mail: gjsvnit92@gmail.com

© Springer Nature Singapore Pte Ltd. 2020

T. V. Mathew et al. (eds.), *Transportation Research, Lecture Notes*
in Civil Engineering 45, https://doi.org/10.1007/978-981-32-9042-6_46

sections—Bardoli (1st Section), Bardoli (2nd Section), and Olpad are found to be 3400, 2950, and 2800 PCU/h for both directions of movement. Considering Section 1 as standard basic section, the reduction in capacity of Section 2, and Section 3 were found to be 13.2 and 17.6%, respectively, due to the reduction in shoulder width. Finally, level of service analysis is done for the study sections using Percent of Free-Flow Speed (PFFS) as measure of performance (HCM 2010). The results of this study may be useful for studying.

Keywords Two lane undivided road · Heterogeneous traffic · Shoulder width · Level of service

1 Background

Two-lane undivided roadways contribute toward the major proportion of road network in India. However, the research pertaining to such roadway facilities under heterogeneous traffic context in India is limited. Some of the literatures relevant to the study on two-lane undivided facilities are given here. Chandra and Kumar [1] studied the effect of lane width on capacity under mixed traffic conditions in India. For this purpose, data were collected at ten sections of two-lane roads in different parts of India. Further, in another attempt, Chandra [2] analyzed the data collected at more than 40 sections of two-lane roads in India. The study analyzed the impact of various parameters such as: gradient, lane width, shoulder width, traffic composition, directional split, slow-moving vehicles and pavement surface conditions, on capacity of two-lane roads under mixed traffic conditions. Further, analysis resulted in the development of adjustment factors for just-mentioned different parameters. Using these adjustment factors, a systematic approach for estimating the capacity of a two-lane road under mixed traffic conditions is provided. The analysis inferred that there is an increment in PCU of a vehicle type increases linearly with increasing carriageway width. The capacity was found to be second-degree polynomial function of carriageway width. Dey et al. [3] further made an observed that the capacity of a two-lane road decreases as the proportion of three-wheeler, tractor, or heavy vehicle increases in the traffic stream. Bang et al. [4] employed a single linear model with an aim to estimate the capacity of rural roads. Sarana et al. [5] used linear and quadratic forms for developing speed–volume relationships on urban roads in India. Both, linear and quadratic forms could represent only the expected trend between the two variables (speed and volume) and not the capacity of the road. Dey et al. [3] used a simulation technique to estimate the capacity of a two-lane road by developing a speed–volume relationship. Hoban [6] summarized that a linear speed–volume relationship can be used in most of the cases to represent speed–volume relationships, but the slopes of the speed–volume relationships appeared to vary with several factors.

Based on the review of literatures, it is found that two-lane roadway has different characteristics considering the abutting land use through which it passes and the

purpose for which it is designed. The classes of two-lane undivided highway based on HCM [7] are:

Class I: Motorists expect to travel at high speeds, major intercity routes, primary connectors of major traffic generators, daily commuter routes.

Class II: Access routes to class I facilities scenic or recreational routes, or passing through rugged terrain, usually serve relatively short trips.

Class III: Serve moderately developed areas often have reduced speed limits reflecting higher activity level.

Based on the characteristics of different classes of road explained by HCM [7] for two-lane highways, the roadway sections considered for study purpose belongs to Class III facilities. Hence, it can be assumed that the present study is conducted on Class III of two-lane undivided roads under Indian conditions.

With this background, the present study is conducted with the primary objective of analyzing the effect on traffic flow parameters due to change in shoulder width on two-lane undivided roads. The sub-objectives of the study are: (i) to study speed distribution pattern on the two-lane undivided roadway with different shoulder width; (ii) to calculate the dynamic PCU values using speed–area ratio method; (iii) to develop capacity estimates based on change in shoulder width on two-lane undivided highway; (iv) to demarcate level of service boundaries using PFFS as measure for such roadways.

2 Study Site and Data Collection

The data were collected by video-filming technique and recording was done for 8 h during morning/evening hours on a typical weekday, as shown in Fig. 1. Figure 1a, c, e shows the photograph taken from the vantage point at the study locations, where video cameras were installed. Figure 1b, d, f shows the plan of the respective study sections. All the study sections in the present study are located on the outskirts of Surat city, Gujarat. The study sections are named based on the name of location where traffic data was collected. The study sections are named as: Bardoli (1st Section), Bardoli (2nd Section), and Olpad Section.

The study sections selected for the present study are having different widths of paved shoulder, which is quite clear from the plan of study sections, shown in Fig. 1. There was no other variable like potholes, pedestrians, and intersection nearby, which may disturb the traffic flow on the roadway. For the study sections, eight hours of data collected were collected using videography under different flow conditions. The collected video of traffic flow was used for extracting entry and exit time stamp using Avidemux software, as shown in Fig. 2.

The software can measure time at an accuracy of one-hundredth of second. Time stamp can be entered in Microsoft Excel manually, by stopping playback and navigating forward and backward to obtain the actual time stamp when the vehicle enters and exits the trap length. The extracted data is used in the calculation of various

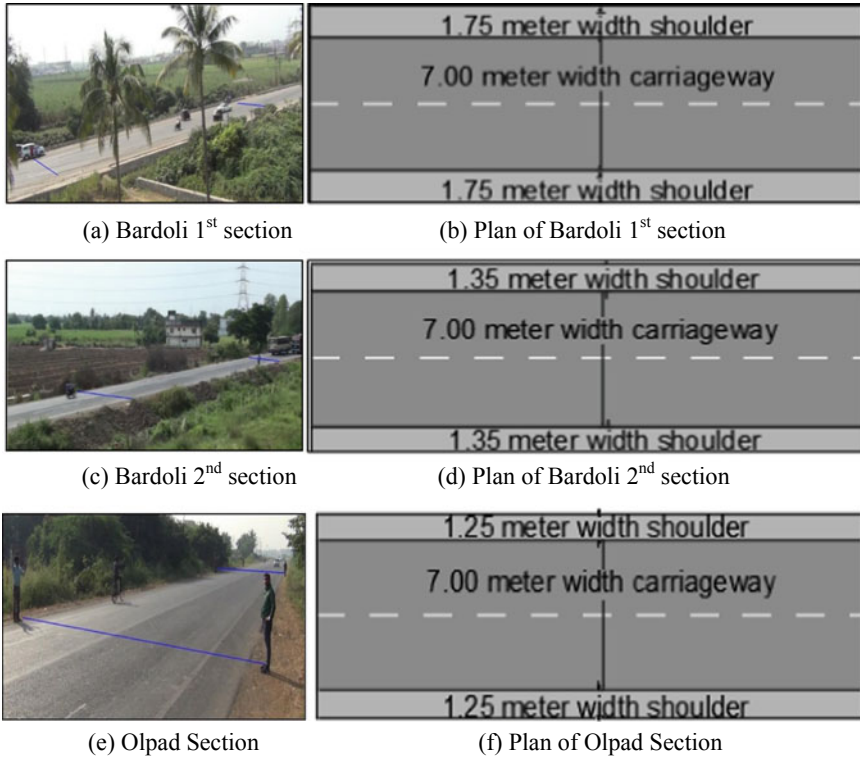


Fig. 1 Study sections and plan



Fig. 2 Data extraction in Avidemux software

traffic parameters such as traffic flow, speed, and density, using the different formula given in Microsoft Excel.

3 Traffic Composition on Study Sections

Traffic composition on selected study sections is shown in Fig. 3. From Fig. 3, it is found that two-wheeler has the highest percentage in the traffic stream of all the three sections, followed by cars (small cars and big cars). Truck, LCV, and bus are also present in a significant proportion over the study sections. It shows that the study sections are showing similar trend in terms of different vehicle composition. However, two-wheeler has the highest proportion in case of Olpad section. The proportion of cars ranges from 30 to 33% for the study sections.

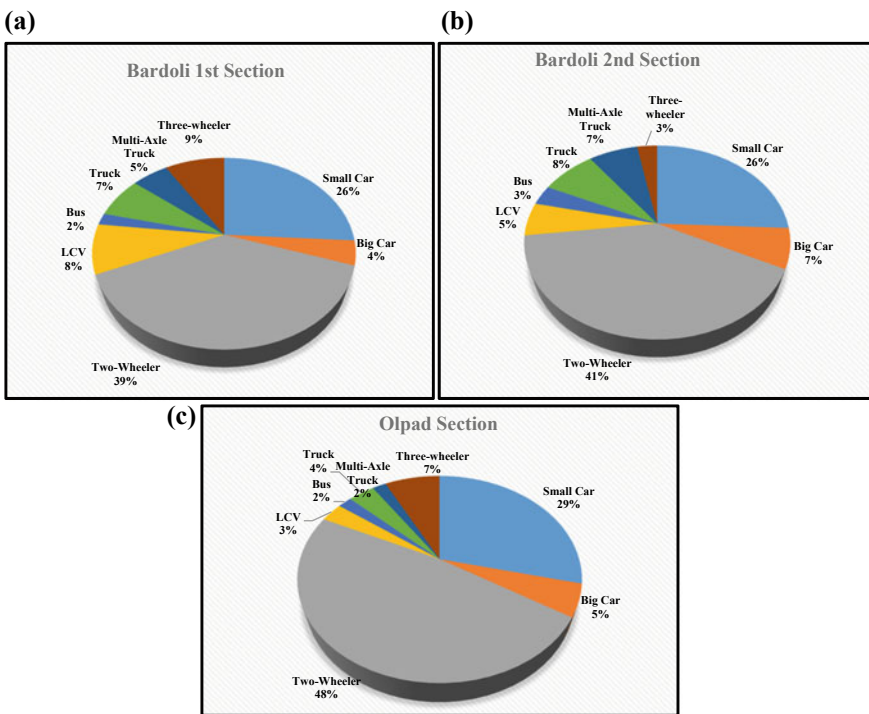


Fig. 3 Traffic composition on a Bardoli section 1, b Bardoli section 2, and c Olpad section

4 Speed Distribution

Speed is a fundamental measure of performance of a given roadway facility. An understanding regarding the speed characteristics is of great importance in traffic engineering. It indicates the quality of service experienced by the road users. Moreover, it helps in further studies related to geometric design, traffic regulation, and level of service. For the present study case also, speed distribution study is carried out for different vehicle categories on the three study sections in the present study, as shown in Fig. 4.

From the figures, it is quite clear that there is slight increment in speed distribution pattern for different vehicle categories with increasing shoulder widths. This is due to the increase in degree of space with increasing shoulder width.

5 PCU Calculations

PCUs are calculated using speed–area ratio method [8], which takes into account heterogeneity in vehicular static characteristics (based on vehicle area) and dynamic characteristics (considering average speed of vehicle type) in its equation.

$$PCU_i = \frac{V_c/V_i}{A_c/A_i} \quad (1)$$

where

PCU_i: PCU of the subject vehicle *i*, V_c : Average speed of cars in the traffic stream, V_i : Average speed of subject vehicles *i*, A_c : Projected rectangular area of a car as reference vehicle and A_i : Projected rectangular area of the vehicle type *i*.

The area of different categories of vehicles were found as shown in Table 1; whereas the mean PCU values obtained for different flow levels using speed–area ratio method are shown in Table 2, for each vehicle categories. From Table 2, there is found to be marginal reduction in PCU values of big car, two-wheeler, and auto with decrease in roadway width. However, the decrements in PCU values are slightly higher for heavy vehicle such as bus, truck, and multi-axle truck. This shows that heavy vehicles create more impedance to the traffic stream with the increase in roadway width.

6 Macroscopic Speed–Flow Relationships

The relationships between macroscopic traffic flow parameters are helpful in planning, design, and operation of a roadway facility. In the present study, speed–flow relationship has been established using linear speed–density assumption proposed

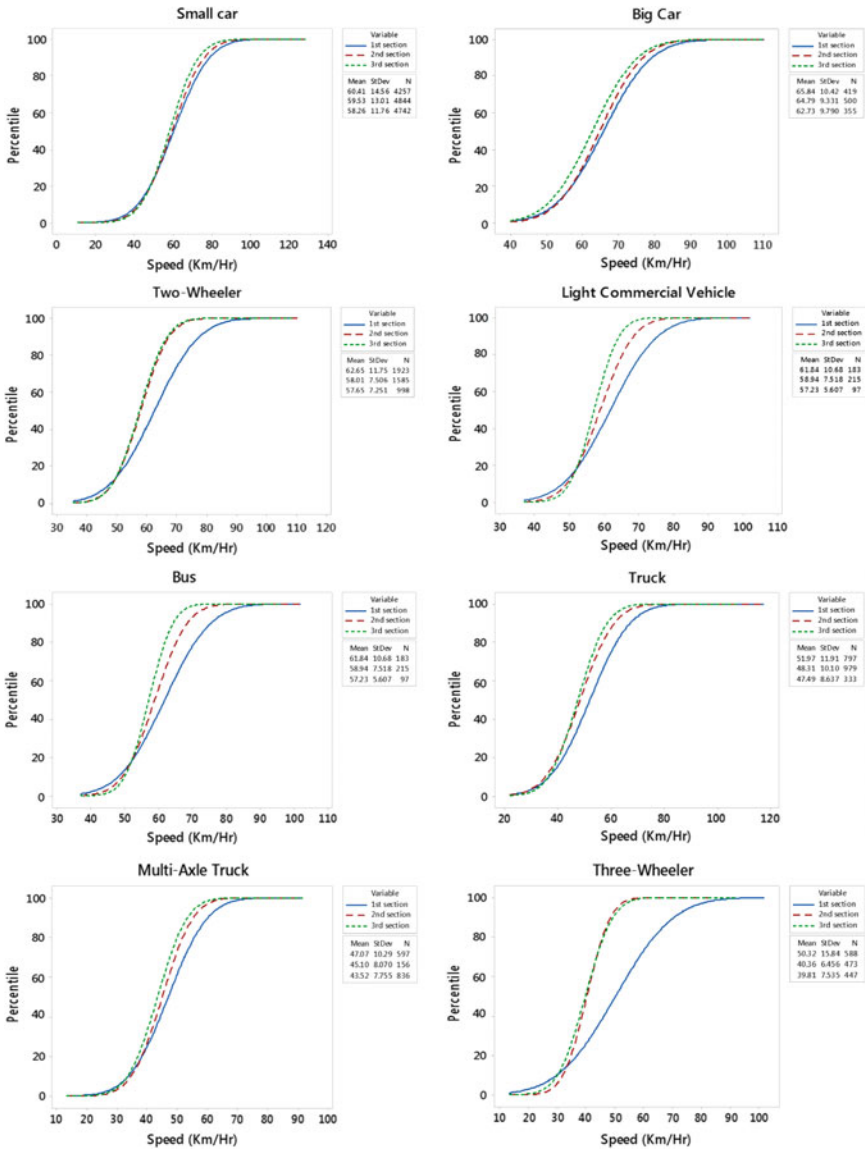


Fig. 4 Speed distribution curve for different vehicle categories on three study sections (first section—Bardoli first section; second section—Bardoli second section; third section—Olpad road)

Table 1 Rectangular area of different categories of vehicles

Vehicle type	Rectangular area of vehicle (m ²)
Small car	5.36
Big car	8.11
Two-wheeler	1.2
LCV	12.81
Bus	24.54
Single axle truck	16.28
Multi-axle truck	17.63
Auto	4.48

Table 2 Mean PCUs of each vehicle category for different sections

Study sections	SC	BC	Two-wheeler	LCV	Bus	Truck	Multi-axle Truck	Auto
Bardoli first section	1	1.47	0.24	3.45	5.62	3.85	4.67	1.32
Bardoli second section	1	1.42	0.23	2.80	4.91	3.71	4.31	1.29
Olpad road	1	1.38	0.21	2.53	4.81	3.48	3.98	1.26

SC Small Car, BC Big Car

by Greenshields [9], as shown in Fig. 5. The relationship is established for three study sections under consideration in the present study. The estimated capacity for the study sections is also marked in Fig. 5.

Table 3 shows the capacity values for different formation widths on the three study sections. It is quite evident that there is a significant reduction in the capacity of two-lane undivided facility with reduction in carriageway width. From the trend, it

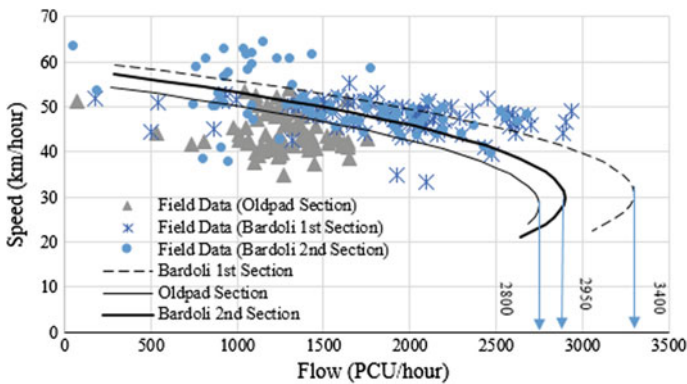


Fig. 5 Speed versus flow curve on the study sections

Table 3 Effect of different shoulder widths on capacity and free-flow speed

Study area identification	Capacity	Free flow speed	Formation width (m)
Bardoli first section	3400	62	7 m + 1.75 shoulder on each side
Bardoli second section	2950	60	7 m + 1.35 shoulder on each side
Olpad section	2800	56	7 m + 1.25 shoulder on each side

is also observed that there is a gradual reduction in stream speed with the decreasing shoulder width.

7 LOS Thresholds for Study Sections

HCM (2010) categorized two-lane highways into three classes. The study sections considered in the present study is having the characteristics of Class III highways. For Class III highways, high speeds are not expected. As the length of Class III segments is generally limited, passing restrictions are also not a major concern. In such cases, drivers would like to make steady progress at or near the speed limit. Therefore, on these highways, Percent of Free-Flow Speed (PFFS) is used to define LOS. Based on the PFFS values shown in HCM (2010), level of service boundaries are demarcated for the three study sections considered in the present study, as shown in Fig. 6.

Table 4 shows the PFFS values given in HCM (2010) [4] and respective speed ranges for each level of service on the study sections. The speed range was defined for the study sections by multiplying the different PFFS values with the free-flow speed on each of the study sections, for different levels of services. The reflected range of speed in Table 4 for two-lane roadway with varying shoulder width may be useful for operational analysis on similar type of facilities. The study can be further extended to roadway with even higher variation in shoulder width. More locations may be further added to relate capacity with shoulder width using empirical data or simulation model, which is in future scope of the work.

8 Conclusion

The present study is carried out to study the effect of shoulder width on traffic flow parameters on two-lane undivided roadways. The roadway with shoulder width of 1.25, 1.35, and 1.75 m are selected for analysis purpose. Based on the characteristics of the land-use and purposes served by the two-lane undivided roadways, such type of roadways belongs to Class III of two-lane highways, as per HCM 2010. From

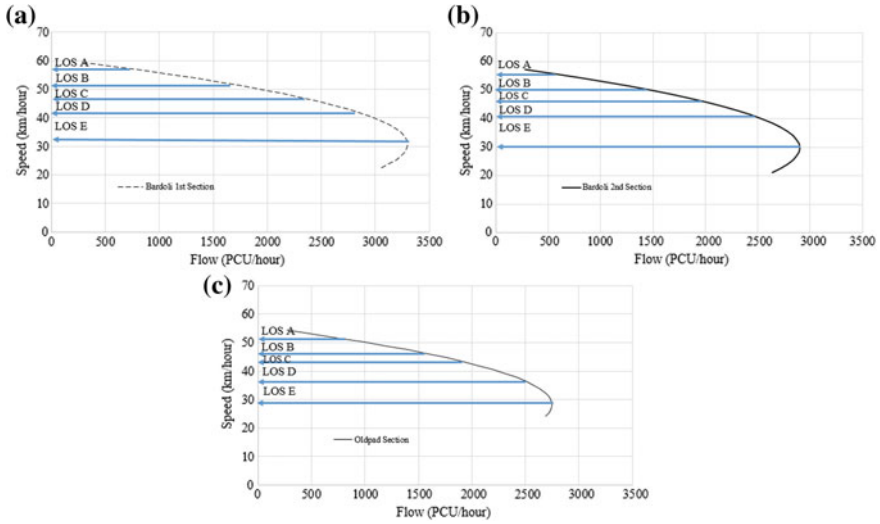


Fig. 6 Level of service demarcation for study sections **a** Bardoli first section, **b** Bardoli second section, **c** Olpad road

Table 4 Level of service for two-lane roads on study sections

Level of service	PFFS (HCM 2010) (%)	Bardoli first section speed range (km/h)	Bardoli second section speed range (km/h)	Olpad road speed range (km/h)
LOS A	>91.7	>57	>55	>51
LOS B	83.3–91.7	>51–57	>50–55	>47–51
LOS C	75.0–83.3	>47–51	>47–50	>42–47
LOS D	66.7–75.0	>41–47	>40–45	>37–42
LOS E	≤66.7	≤41	≤40	≤37

the speed distribution studies, it is found that there is marginal increase in speed of different vehicle categories with increase in shoulder width on the study sections. It is also found that there is an increase in PCU values estimated for the three study sections with increase in carriageway widths. The capacity of the three study sections, Bardoli (1st Section), Bardoli (2nd Section), and Olpad Section are found to be 3400, 2950, and 2800 PCU/h for both directions of movement. The trend of speed–flow relationship also shows the reduction in stream speed with decreasing shoulder widths. Percentage reduction in stream speed under free-flow condition is found to be 3 and 9.6% with decreasing shoulder width, when compared to study section having 1.75-m shoulder on each side. Level of service analysis is also done for the three study sections based on the PFFS as performance measure. The results from the present study may be useful in analyzing the effect of shoulder width on

roadway capacity and level of service on two-lane undivided roads under Indian conditions. However, level of service analysis based on the different parameters for traffic conditions prevailing on similar roadway facilities is also there in future scope of the work.

References

1. Chandra S, Kumar U (2003) Effect of lane width on capacity under mixed traffic conditions in India. *J Transp Eng ASCE* 129:155–160
2. Chandra S (2004) Capacity estimation procedure for two lane roads under mixed traffic conditions. *Indian Roads Congr J* 165:139–170
3. Dey PP, Chandra S, Gangopadhyay S (2008) Simulation of mixed traffic flow on two-lane roads. *J Transp Eng ASCE* 134:361–369
4. Bang KL, Carlsson A, Palgunadi (1995) Development of speed-flow relationship for Indonesia rural roads using empirical data and simulation. *Transp Res Rec* 1484:24–32 (Transportation Research Board, Washington DC)
5. Sarana AC, Jain PK, Chandra G (1989) Capacity of urban roads—a case study of Delhi and Bombay. *Highw Res Bull* 48:1–38 (Indian Roads Congress)
6. Hoban CJ (1987) Evaluating traffic capacity and improvements to road geometry. The World Bank technical paper no 74, Washington DC
7. Transportation Research Board (2010) Highway capacity manual, Washington DC
8. Chandra S, Sikdar PK (2000) Factors affecting PCU in mixed traffic situations on urban roads. *Road Transp Res* 9(3):40–50
9. Greenshields BD (1935) A study of traffic capacity. In: Highway research board, proceedings, vol 14

Estimation of Saturation Flow at Signalized Intersections Under Heterogeneous Traffic Conditions



Rakesh Kulakarni, Akhilesh Chepuri, Shriniwas Arkatkar
and Gaurang J. Joshi

Abstract This research aims to develop a simulation-based methodology in the estimation of saturation flow at signalized intersections under heterogeneous traffic conditions in India. Field surveys have been carried out particularly during peak periods at two signalized intersections, namely Vijay Char Rasta intersection situated in Ahmedabad and Rangila Park intersection situated in Surat. Videographic technique is employed to capture the data at macro- and microlevel. The videographic approach provides the queue building, moving, and queue dissipation at microlevel. The field data pertains to traffic volume, compositions, turning movements, headway, cycle time, and phasing at the approach. The survey also concentrates on noting the queue length of each approach. Apart from videographic survey, road inventory survey and spot speed surveys are also carried out in order to use this data in VISSIM 7.0 for the development of network and defining speed distributions. The present work mainly focused on the development of PCUs, dynamic saturation flows, VISSIM modeling and validation, regression modeling and validation, and sensitivity analysis. Passenger car unit for each vehicle category is calculated by two methods—headway method and optimization method. Saturation flow is estimated with the help of PCU values estimated by different methods, and these values are compared. TRL method is adopted in the estimation of saturation flow. A 5-s interval is considered in this method. Nearly, 8842 VPH is the saturation flow against to 5460 PCU of headway method and 5071 PCU of optimization method for 3 lane approach of Vijay Char Rasta intersection. Saturation flow is almost double in terms of mixed traffic. Therefore, saturation flow cannot be static in present study but is dynamic. Dynamic saturation flow values are provided for varied composition and approach widths.

R. Kulakarni · A. Chepuri · S. Arkatkar (✉) · G. J. Joshi
Civil Engineering Department, Sardar Vallabhbhai National Institute of Technology Surat, Surat
395007, Gujarat, India
e-mail: sarkatkar@gmail.com

R. Kulakarni
e-mail: rakesh.kulakarni@gmail.com

A. Chepuri
e-mail: akhileshchepuri@gmail.com

G. J. Joshi
e-mail: gjsvnit92@gmail.com

© Springer Nature Singapore Pte Ltd. 2020
T. V. Mathew et al. (eds.), *Transportation Research*, Lecture Notes
in Civil Engineering 45, https://doi.org/10.1007/978-981-32-9042-6_47

Base network is created in VISSIM 7.0. Model is calibrated as per Indian driving behavior for both Vijay Char Rasta and Rangila Park. Average queue length is considered for validating the model. Sensitivity analysis is carried out after validating the simulation model. It is observed that change in road width is having significant effect on saturation flow when compared to change in turning movements. Regression analysis is carried out for developing multilinear regression saturation flow model (MLR–SFM). The model is developed between saturation flow and proportion of 2W, 3W, small car, big car, and road width. 65–35 combination is observed to be best fitted combination in developing and validating the model. Similar to the observations in VISSIM modeling, it is observed that change in road width is having a significant effect on saturation flow when compared to change in traffic compositions.

Keywords Saturation flow · Signalized intersection · Heterogenous traffic · Micro simulation

1 Background

Urbanization is the physical growth of urban areas as a result of global economy. It is closely linked to modernization, industrialization, and the sociological process of rationalization. Urbanization is an index of transformation from traditional rural economies to modern industrial one. It is a long-term process. Urbanization is a natural expansion of an existing population, namely the proportion of total population or area in urban localities or areas (cities and towns), or the increase of this proportion over time. It can thus represent a level of urban population relative to total population of the area, or the rate at which the urban proportion is increasing. The urbanization impact has been felt in all urban sectors. It is more so in transportation sector. The transport demand growth in vehicle population and traffic has been observed in a significant way.

Most of the metropolitan cities in India possess diversified traffic characteristics. The characteristics of traffic flow include speed of vehicles, their concentration, and density of flow, and these are governed by a variety of factors attributable to road features, the vehicle performance characteristics, and road-user behavior. Most of the Indian cities comprise of heterogeneous traffic composition, with two-wheeler and four-wheeler as the leading percentages. Heterogeneity not only exists in terms of vehicles but also in case of road users and pedestrians. Deficiency in lanewise discipline is observed compared to the cities of western countries.

Intersections are an important part of an urban roadway network, and they have a significant effect on the operation and performance of the traffic system. Frequently intersecting urban road links lead to conflicts between opposite flow of traffic, thereby causing delay and accident. They are normally major bottlenecks to smooth flow of traffic and a major place for conflicts. Thus, operation of intersection is critical in Indian urban context where the heterogeneous traffic conditions prevail. Signalization of intersection is done to provide an effective movement of the vehicular traffic,

thereby enhancing higher safety to users as well as pedestrians. Signalized intersections are indispensable when due importance is to be given to vehicular flows of all approaches meeting at the intersection. The present research project focuses on mixed traffic behavior at the signalized urban intersection approaches.

Saturation flow is an important input parameter in the design of cycle time for traffic signals. It is the flow that can be accommodated by the lane group assuming that the green phase was displayed 100% of time. The characteristics of heterogeneous traffic are significantly different from homogeneous traffic in terms of lane discipline, driver behavior, and vehicle compositions. Due to heterogeneity of traffic, it is unlikely to use the HCM model directly because it has been developed for a homogeneous traffic conditions. Heterogeneous traffic has varying types of vehicles: two-wheelers, motorized and non-motorized three-wheelers, cars, buses, trucks, bicycles, and miscellaneous types; out of them, two-wheelers are the major mode of transportation in most of the developing countries like India. Due to these high compositions of two-wheelers, the urban traffic behavior is greatly different from developed nations. Minh and Sano [1] analyzed the effect of motorcycles on saturation flow rate in Hanoi and Bangkok. They suggested that the effect of motorcycles is significant and should be taken into account in geometry design and operation of signalized intersections. Anusha et al. [2] studied the effect of two-wheelers on saturation flow at signalized intersection in Bangalore, India. They modified HCM equation by introducing an adjustment factor for two-wheelers and concluded that the saturation flow estimated using calibrated HCM model is closer to field values. Arasan and Jagadeesh [3] estimated the PCU for different categories of vehicles using the multiple linear regression models considering the saturated green time against the number of each category of vehicles crossing the stop line, during the green time. Vien et al. [4] studied the effect of the motorcycles' travel behavior on saturation flow rates at signalized intersections in Malaysia. They divided motorcyclists traveling through an intersection into within the flow (follow a first-in-first-out rule, travel either in front of or behind other vehicles) and outside the flow (do not follow the first-in-first-out rule). They compared the saturation flow rates observed at sites based on motorcycle inside the flow and saturation flow rates estimated using the Malaysia Highway Capacity Manual (2006) based on total volume of motorcycle and concluded that motorcycles inside flow should be considered in the estimation of saturation flow rates.

The various factors like vehicle types, approach width, traffic mix, driver behavior, and roadside activity can influence traffic behavior and in turn the saturation flow rates. A number of studies have been done to model the effects of heterogeneous traffic on saturation flow at signalized intersection. The equation suggested by the Indian Roads Congress (IRC) to estimate saturation flow is $S = 525 * (w)$, PCUs per hour, where $w =$ width. It is valid for width from 5.5 to 18 m. Arasan and Vedagiri [5] studied the influence on saturation flow due to road width by using simulation technique. They found a positive effect on saturation flow with the width of an approach. Patil et al. [6] studied the influence of area type in the PCU values and estimated that the PCU for two-wheeler ranges from 0.09 to 1.23, three-wheeler from 0.23 to 6.14 and that of bus from 1.02 to 3.78. Praveen and Arasan [7] have

derived the vehicle equivalency factors for urban roads in India. It was found that under heterogeneous traffic conditions, for a given roadway and traffic composition, the PCU value of vehicles varies significantly with change in traffic volume. Mathew and Radhakrishnan [8] developed a saturation flow model per lane width using the different traffic parameters, by developing PCUs using optimization technique. They validated the proposed model with saturation flows collected from different locations in India.

Estimation of saturation flow requires a common platform, and this is accomplished by passenger car units. As the significant portion of the traffic in developed nations comprises of passenger cars, it has been taken as the vehicular traffic unit for the purpose of design and analysis which is widely known as “passenger car unit” (PCU). But, in the heterogeneous traffic conditions, drivers do not usually follow lane discipline and can occupy any lateral position on the road. Because of these significant differences in characteristics between the heterogeneous and homogeneous traffic, the research results based on the homogeneous situation are unlikely to give reliable results if applied in the heterogeneous traffic conditions.

2 Study Section and Methodology

Base signalized intersection is an intersection where saturation flow is measured in ideal conditions. So, selection of such intersection plays a vital role in estimating the base saturation flow rate (s_0), which is later applied for other intersections for finding saturation flow by considering other adjustment factors. Present study accompanied at two four-legged intersections, namely Vijay Char Rasta (VCR) intersection in Ahmedabad and Rangila Park intersection in Surat, western part of India. Both the intersections consist of a pre-timed signal (four-phase) with VCR total cycle time of 142 s in the morning and 167 s in the evening and RP total cycle time of 125 s which are operated during the peak hours.

The methodology in the present research study broadly includes the identification of relevant intersections, data collection and extraction of traffic composition, headway and turning movements, and microscopic simulation. Data extraction is carried out through the moviemaker software from the video-recorded files of traffic movement at the study intersection. Thus, extracted values are analyzed using the statistical and frequency distributions. Traffic composition, headway, and turning movements are analyzed to find PCU values and estimate saturation flow. This data is also used in developing regression model. Simulation technique is employed to analyze and compare the results by performing sensitivity analysis. The developed model is validated by using the queue length results. Regression model is developed in order to apply it to other intersection and know the effect of the developed model. The developed model is validated by comparing the observed and expected saturation flow results.

3 Data Collection

Data collection for the present study includes the collection of the data related to traffic volume, turning movements, headway, cycle time, phase, queue length, road geometry, and spot speed of vehicles. Videographic, road inventory, and spot speed surveys are carried out to capture the required traffic characteristics. A total of eight hours of videographic data was initially collected for one weekday covering both morning and evening peak hours. Videographic survey was done on March 20, 2015, for Rangila Park intersection, Surat city, on April 6, 2015, for Vijay Char Rasta, Ahmedabad city (Fig. 1). All the four cameras were placed on the high-raised buildings, each camera covering the respective major and minor approach traffic. Cameras were placed in such a way that they cover the complete queue length formed in each of the individual approach.

Road inventory survey has been carried out during the free flow conditions causing minimum obstruction to the traffic movement and reducing the risk for the surveyors. This data has been used in building a VISSIM 7.0 model and also in developing MLR model for estimation of saturation flow. Spot speed survey is performed using radar guns on all approaches of intersection in both the scenarios. This survey is carried out on same day simultaneously for the duration of one hour to capture the spot speeds of all types of vehicle categories for every 5-min interval.



Fig. 1 Aerial view of Vijay Char Rasta, Ahmedabad

Table 1 Statistics of traffic composition

Intersection	% TW	% 3W	% Small car	% Big car	% HGV
Vijay Char Rasta	60.63	14.88	16.50	7.25	0.56
Rangila Park	57.75	15.23	16.30	10.29	0.43

3.1 Data Extraction and Processing

Data extraction is carried out manually using moviemaker software from video file to evaluate the traffic flow characteristics like turning movements, vehicle composition, headway, and cycle time. Extracted data is processed using Excel and Statistical Practice for Social Science (SPSS) tools for calculating percentiles and frequencies of different variables involved in the present study. Stop line present in each approach is considered as the reference point in the data extraction. Headway is measured as the time gap between former and latter vehicle.

3.2 Analysis of the Extracted Data

3.2.1 Classified Vehicle Count

Classified vehicle count (CVC) is carried out by counting the vehicles for every 5-s interval of green time. Five vehicle classes two-wheeler, three-wheeler, small car, big car, and heavy goods vehicle (HGV) are considered and compositions are calculated (Table 1). Auto rickshaw and light commercial vehicle (LCV), are considered together as three-wheeler, bus, and truck, are considered together as HGV. Vehicles that are discharging from the queue and passing the stop line are taken into consideration in each interval. Flow between 0 and 5 s is considered in 5-s interval. Flow between 5 and 10 s is considered in 10-s interval and so on. This is done for morning one hour and evening one hour for VCR intersection and RP intersection. Extracted data is entered into the Microsoft excel simultaneously. This data is given as volume input in the VISSIM 7.0 model.

3.2.2 Turning Movement Count

Turning movement count (TMC) is carried out for every 5-s interval for all the three directions' traffic. TMC was done for one hour in the morning and evening both the intersections. Moviemaker and KM player tools were used in the extraction of TMC. This data is used in calculating the relative flows of each approach and are given as input in VISSIM 7.0 model (Fig. 2).

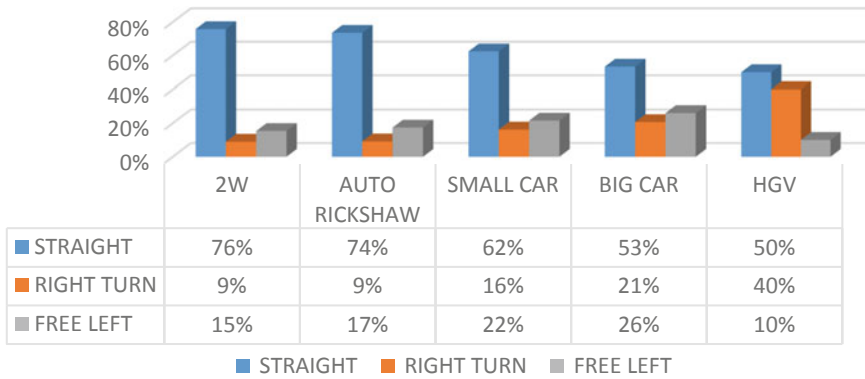


Fig. 2 Directional proportion for Vijay Char Rasta intersection

3.2.3 Spot Speed Data

The parameters like minimum, maximum, 15th, 50th, 85th, and 95th percentile speeds for each vehicular category are calculated. This data has been used further for developing the desired speed distributions in the VISSIM model for simulation purpose. These speed distributions are developed separately for each of the vehicular categories considered in the present study. It is observed that car has maximum speed followed by motorized two-wheelers.

3.2.4 Time Headway

Time taken by successive vehicles to cross the stop line is considered as time headway. Each vehicle category was assigned a number. The time at which each vehicle was crossing the stop line was noted down. Headway is measured as the time gap between former and latter vehicle.

4 Measurement of PCU and Saturation Flow

Flow is normally measured in PCU/h. So, estimation of PCU has more significance. Two methods are adopted in estimation of PCU, viz., headway method and optimization method.

4.1 Headway Method

This method is used for finding the PCUs for various vehicle categories such as two-wheeler, three-wheeler, small car, big car, and HGV. Each vehicular category was assigned a particular number like small car 1, big car 2, three-wheeler 3, and two-wheeler as 4. Time headway was calculated for one hour in the morning as well as evening for all the approaches of Vijay Char Rasta, Ahmedabad, and Rangila Park, Surat. Based on the obtained time headways, respective PCUs are estimated. Time headway is calculated as follows.

$$\text{Time Headway}(h) = T_{\text{follower}} - T_{\text{leader}} \tag{1}$$

PCU values of different types of vehicle are determined by keeping small car as a standard vehicle. Width of the vehicles is also considered along with average time headway in calculation of PCU. Headway ratio and width ratio together comprises to area ratio. Following table shows the width considered in PCU estimation (Table 2).

$$\text{PCU} = \left(\frac{h_i}{h_c}\right) * \left(\frac{w_i}{w_c}\right) \tag{2}$$

where h_i = average time headway of i th vehicle, h_c = average time headway of standard vehicle (small car), w_i = width of the i th vehicle, w_c = width of the standard vehicle (small car).

The obtained average time headway and PCU values for all the intersections by headway method are represented in Table 3.

Table 2 Vehicular dimensions

Vehicle type	Overall dimension (m)		Area (m ²)
	Length	Width	
Motorized two-wheelers	1.87	0.64	1.20
Motorized three-wheelers	2.60	1.40	3.64
Small car	3.72	1.44	5.36
Big car	4.58	1.77	8.11
Buses	10.3	2.5	25.75
Light commercial vehicles	5.00	1.9	9.50
Truck	7.20	2.5	18.0

Table 3 Average headway and PCU values by headway method

Study section	Two-wheeler		Three-wheeler		Small car		Big car		HGV	
	Avg. head-way	PCU	Avg. head-way	PCU	Avg. head-way	PCU	Avg. head-way	PCU	Avg. head-way	PCU
Vijay Char Rasta, Ahmedabad	0.38	0.39	0.45	0.86	0.51	1.00	0.50	1.19	0.65	1.98
Rangila Park, Surat	0.72	0.30	0.77	0.71	1.03	1.00	1.05	1.22	0.80	1.40

4.2 Optimization Technique

This is the method proposed by IIT-Bombay for field measurement of saturation flow. Analysis is carried out in three steps for measurement of saturation flow.

- **Determination of Saturation Green Time**

For measuring the saturation flow, discharge pattern of vehicles in each interval is considered in the analysis. It is observed that most of the times, discharge pattern in the first interval is having low flow values due to start up loss time. It is assumed that saturation flow starts from the second interval. This step determines the saturation period by comparing the flow values obtained in each interval. Analysis of saturation period is found using the ANOVA test. Mean and spread of flow values in consecutive interval are compared to find the flow values which are representing similar dataset. From the test, if samples are found to be statistically equivalent, it means that saturation flow is continuing. The test is carried over all the pairs and saturated green time is found. The saturation period may vary depending on the green time and flow at each approach.

- **Determination of PCU Value**

Initially for calculation of flow values, IRC-suggested PCU values are used. These PCU values are initial PCU values used for optimization. Now onwards, the flow values observed in saturation green time are only used for analysis. By using the appropriate PCU values, the spread of flow values can be reduced. PCU values are the decision variables, and sum of the standard deviations of flow values observed in the saturated green is objective function which is to be minimized. Constraints will be the minimum and maximum values of PCU values for different vehicle classes. These flow values are normalized before optimization using the standard score method to eliminate the effect of absolute value of flow on the sum of standard deviations of flow values in saturated green time.

$$\text{Normalized value} = \frac{X - \mu}{\sigma} \tag{3}$$

where

- X Observed flow value using initial PCU
- σ Standard deviation of all the flow values observed in saturated green time
- μ Mean of all the flow values observed in saturated green time

These flow values are normalized before optimization using the standard score method to eliminate the effect of absolute value of flow on the sum of standard deviations of flow values in saturated green time. Evolutionary algorithm is used for optimization as the problem is nonlinear. Hence, flow values of heterogeneous traffic are adjusted to as homogeneous as possible by changing the PCU values. Table 4 represents the PCU values derived from optimization method.

• **Determination of Saturation Flow**

This step determines the saturation flow by minimizing the error between the assumed saturation flow and observed discharge in saturated green time. Optimization is used to minimize the average error, i.e., average difference between assumed saturation flow and observed flow values in saturated green time. To eliminate the outliers, data in the range of ± 5 of assumed saturation flow is used to calculate average error. Optimization with evolutionary algorithm is used for the minimization of average error. Saturation flow is the decision variable and average error is the objective function which is to be minimized. Constraints will be kept minimum and maximum value a saturation flow can take will be the output of optimization. Saturation flow shall be greater than minimum flow observed in saturated period, and it shall be less than maximum flow observed in saturation period.

The following Table 5 shows the comparison of saturation flow using headway method and optimization method. From Table 5, it can be inferred that saturation flow values obtained by headway method are satisfactory for almost all the approaches

Table 4 PCU values from optimization method

Intersection	Two-wheeler	Three-wheeler	Small car	Big car	HGV
Vijay Char Rasta, Ahmedabad	0.39	1.01	1	1.40	1.40
Rangila Park, Surat	0.34	0.94	1	1.18	1.4

Table 5 Comparison of saturation flow using headway method and optimization method

Intersection	Average saturation flow		Average saturation flow (headway)		Average saturation flow (optimization)	
	veh/h	veh/h/l	PCU/h	PCU/h/l	PCU/h	PCU/h/l
Vijay Char Rasta, Ahmedabad	8620	3434	5272	2105	5849	2310
Rangila Park, Surat	5550	2775	3792	1896	4094	2047

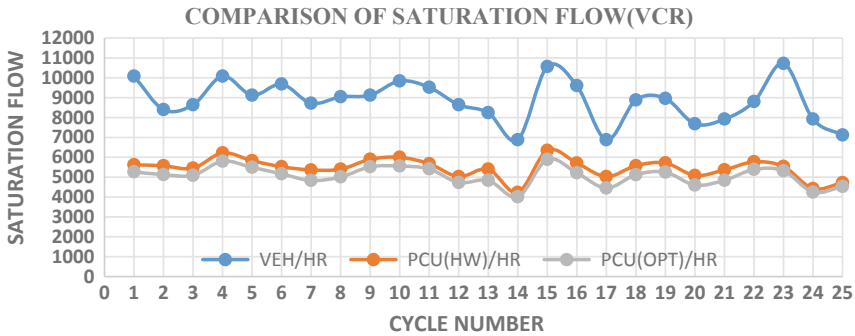


Fig. 3 Comparison of saturation flow

when compared to optimization method. Mathew and Radhakrishnan [8] suggested saturation flow for heterogeneous traffic as 1925 PCU/lane; Arasan and Vedagiri [5] suggested it as 2196 PCU/lane and obtained results for the present study are coinciding with the results of the various literature studies.

Saturation flow is estimated in PCU/h by using the PCU values obtained from two methods. These values are compared in the following Fig. 3.

5 Development of VISSIM Model and Saturation Flow Model

The model is developed based on the conditions related to signals in VISSIM 7.0. The simulation model is validated using the queue length for various approaches, which is a derived parameter. The saturation flow prediction model is developed for the primary data set using multilinear regression technique. The independent variables considered are width of the approach and proportion of vehicular categories. The developed model has been validated using the secondary data set.

5.1 VISSIM Modeling

The model is developed as per the existing network of Vijay Char Rasta as shown in Fig. 4. Traffic surveys which include volume count, turning movements, signal timing, and vehicular speeds are carried out at the specified location and are given as input for the base network file. Figure 5 shows the phasing details of Vijay Char Rasta.

Signal groups in the simulation model are designed and assigned to a particular turning movement according to the field conditions. Queue counters were placed just behind the signal heads to record the total number of vehicles present in the queue.

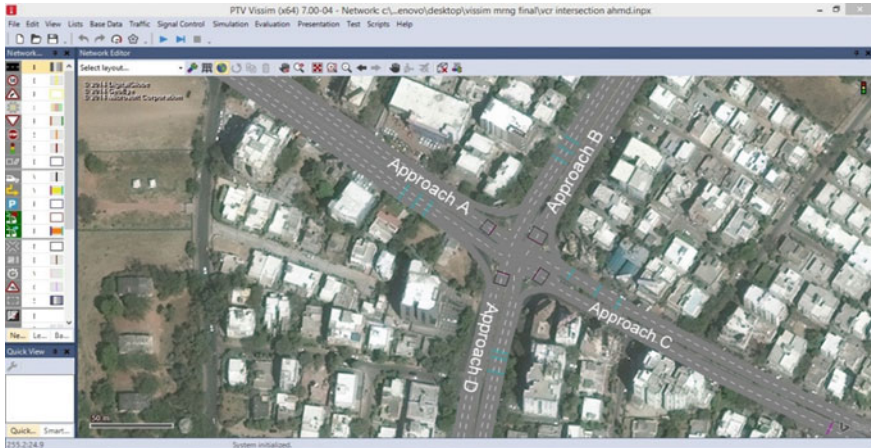


Fig. 4 Screenshot of VISSIM model

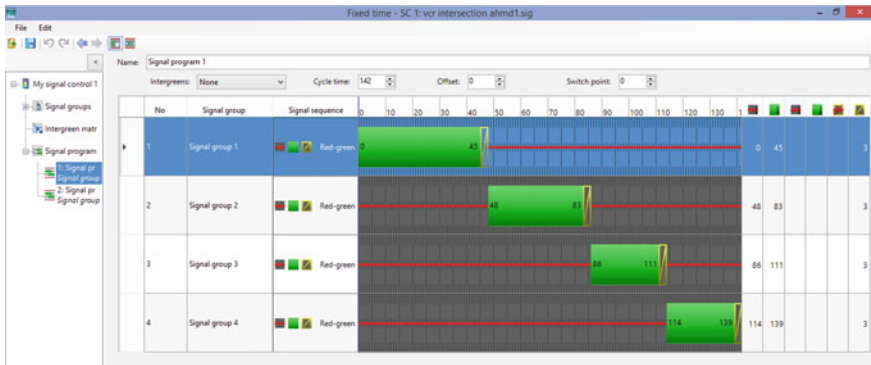


Fig. 5 Phasing details of Vijay Char Rasta

Average queue length is considered for validation. Individual nodes are placed for each approach in the model to obtain the results of headway and number vehicle released for each cycle. The Indian driving behavior is added in VISSIM 7.0 manually since it is heterogeneous in nature. Car following model of Wiedemann 74 is used in the analysis.

5.2 Calibration of VISSIM Model

The calibration process includes the modification of default vehicular geometrical and mechanical parameters. The default values are in accordance with the vehicular

Table 6 Validation results of Vijay Char Rasta

Approach	Queue counter	Average queue length (m) in field	Average queue length (m) in simulation	MAPE
A	1	147.64	260.42	9.13
B	2	57.12	52.59	7.93
C	3	38.84	42.70	9.94
D	4	32.44	29.70	8.45

characteristics in European countries. The 2D/3D models of the vehicular categories are collected from the various sources, and these models are used in the network. It also includes the modification of the default parameters of a car following model in VISSIM 7.0. It is basically a trial and error process and is carried out until the field conditions are observed to be simulated in the model. The conflict areas are defined at the intersection areas and are set according to the field observations. One-hour data is given as input for the base model. Model has been run for 4500 s, out of which first 900 s are considered as buffer time. Buffer time is provided in order to consider the effect of cumulative vehicles during the starting period of evaluation of results.

5.3 Validation of VISSIM Model

The simulation results are considered for the 3600 s of the run after the buffer time. The average queue length data collected for the different approaches has been used as validation parameter. Similar average queue length results for each approach are observed from the calibrated VISSIM model using the queue counters. Field and VISSIM simulated queue lengths for each approach are compared in an hour for minimum possible error. The trial and error method is carried until the errors of field measured, and simulated travel time is observed to be less than 10%. Sensitivity analysis has also been carried out. Table 6 shows the validation results.

5.4 Saturation Flow Prediction Model

The regression analysis is performed in order to develop saturation flow model (SFM). In this analysis, saturation flow in PCU/h is considered as dependent variable and proportion of vehicles and effective approach width are considered as independent variables. The data set corresponding to the first five seconds of each cycle is not considered for the development of the model. This is attributed to the reason that the start-up loss time is accounted in an indirect way. Data sets of both the locations are considered for developing regression model. Attempts are made to develop and validate the model with different combinations (80–20, 75–25, 70–30 and 65–35)

Table 7 Significance test of variables

	Coefficients	Standard error	<i>t</i> Stat	<i>P</i> -value
Intercept	0.00	#N/A	#N/A	#N/A
Two-wheeler	-4249.94	991.5655	-4.28609	3.47E-05
Three-wheeler	-2558.44	1186.739	-2.15586	0.032894
Small car	-3954.60	1408.325	-2.80801	0.005736
Big car	4921.98	1033.104	4.764259	4.89E-06
Width	905.24	81.54211	11.10148	1.14E-20

to develop regression model for saturation flow. 65–35 combination yielded good results, i.e., 65% of the total data is used for developing the SFM and 35% of the total data is used for validation. The SFM is developed by using the data obtained from headway method.

Normality test for the dependent variable (saturation flow) is performed. The significance of the various independent variables is also tested statistically. Following table shows the significance test of variables (Table 7).

From the table, it can be observed that all the independent variables are significant as the *t* statistic values are less than critical value (1.96) at 95% confidence interval and also the significance test is satisfied in the case of *p* test as the *p* statistic values are less than 0.05 at the 95% confidence interval. The following MLR model is obtained from the regression technique in MS excel.

$$S = -4249.94t_w - 2558.44a - 3954.60sc + 4921.98bc + 905.24w \quad (R^2 = 0.97)$$

where *S* = saturation flow in PCU/h, *t_w* = proportion of two-wheelers, *a* = proportion of three-wheelers, *sc* = proportion of small cars, *bc* = proportion of big cars, *w* = effective approach width.

The model developed has been validated using the 35% data set and satisfactory results are obtained. The mean absolute percentage error (MAPE) is observed as 12.45%. The above equation shows the negative relation between 2W, 3W, small car, and saturation flow, and it shows positive relation between big car, width, and saturation flow.

6 Summary and Conclusions

In the present study, PCU is estimated by two methods: headway method and optimization method. It is observed that PCU values which are estimated by headway method are yielding good results. TRL method is considered in the estimation of saturation flow. Saturation flow is estimated in PCU/h by using the PCU values obtained by above two methods. The obtained results are coinciding with the results of the various literature studies. For sensitivity analysis, microscopic simulation using VIS-

SIM 7.0 has been carried out. In validation of VISSIM model, average queue length from field is considered. It can be inferred from present study that change in width has more effect on saturation flow when compared to change in turning movements. Saturation flow model has been developed from multilinear regression analysis by considering the data sets of the intersections and validated for 65–35 combination.

Sensitivity analysis is carried out for SFM developed by regression analysis. In developing the model, proportion of 2W, 3W, small car, big car, and road width are considered along with saturation flow. The developed model shows negative relationship between 2W and saturation flow. Similar relation is observed in the case of 3W and small cars, whereas model shows positive relation of saturation flow with big car and road width. It is also observed that road width is very sensitive parameter in measurement of saturation flow. Hence, it can be inferred from present study that change in width has more effect on saturation flow in both the models.

References

1. Minh CC, Sano K (2003) Analysis of motorcycle effects to saturation flow rate at signalised intersection in developing countries. *J East Asia Soc Transp Stud* 5:1211–1222
2. Anusha CS, Verma A, Kavitha G (2013) Effect of 2w on saturation flow at signalized intersections in developing countries. *J Transp Eng* 139(5)
3. Arasan VT, Jagadeesh K (1995) Effect of heterogeneity of traffic on delay at signalized intersections. *J Transp Eng* 121(5):397–404. [http://dx.doi.org/10.1061/\(ASCE\)0733-947X\(1995\)121:5\(397\)](http://dx.doi.org/10.1061/(ASCE)0733-947X(1995)121:5(397))
4. Vien LL, Wan Ibrahim WH, Mohd AF (2008) Effect of motorcycles travel behaviour on saturation flow rates at signalized intersections in Malaysia. In: 23rd ARRB conference—research partnering with practitioners, Adelaide, Australia, pp 1–11
5. Arasan VT, Vedagiri P (2006) Estimation of saturation flow of heterogeneous traffic using computer micro simulation. In: Proceedings 20th European conference on modelling and simulation
6. Patil GR, Krishna Rao KV, Xu N (2007) Saturation flow estimation at signalized intersections in developing countries. In: 86th transportation research board annual meeting, Washington DC, 07-1570
7. Praveen PS, Arasan VT (2013) Influence of traffic mix on PCU value of vehicles under heterogeneous traffic conditions. *Int J Traffic Transp Engineering* 3(3):302–330. [http://dx.doi.org/10.7708/ijtte.2013.3\(3\).07](http://dx.doi.org/10.7708/ijtte.2013.3(3).07)
8. Mathew TV, Radhakrishnan P (2010) Calibration of micro simulation models for non lane-based heterogeneous traffic at signalized intersections. *J Urban Plan Dev* 136(1):59–66

Evaluation of Centre Line Marking on Driver Behaviour



P. C. Rehna , M. Harikrishna  and M. V. L. R. Anjaneyulu 

Abstract Road crashes are one of the main topics of discussion in the field of transportation nowadays. Studies have proved that driver behaviour is a contributing factor in over 90% of road crashes. As a result, it is required to identify how the driver behaviour varies with safety improvement measures to reduce crash rate. One of the safety improvement measures is delineation of paths for vehicle movement using road markings. The effect of centre line marking on drivers is investigated by studying the position of vehicles on two-lane two-way highways, both at straight sections and at horizontal curves, using a before-and-after study. Data was analysed using tools like traffic distribution analysis, conflict energy distribution, scatter plot analysis and ANOVA test. From traffic distribution plots, it is found that at most of the locations, vehicles that move through the centre of the carriageway shifted their path towards their own lanes after centre line marking was drawn. A linear trend is observed between speed and lateral position of the vehicles. The significance of each vehicle type with respect to speed and lateral position at particular lateral position ranges and speed ranges respectively were also analysed, and in most of the cases, it was found significant. Finally, model was developed for estimation of lateral position of vehicles. The data and analysis results can be used for road safety analysis, identification of improvement measures, as an input into the microscopic traffic simulation models and for developing local logics aimed at advanced driving assistance modelling (ADAM).

Keywords Driver behaviour · Lateral position · Longitudinal position

P. C. Rehna (✉) · M. Harikrishna · M. V. L. R. Anjaneyulu
Department of Civil Engineering, National Institute of Technology Calicut, Kozhikode, India
e-mail: rehnapc@gmail.com

M. Harikrishna
e-mail: harikrishna@nitc.ac.in

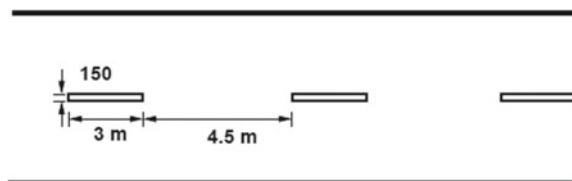
M. V. L. R. Anjaneyulu
e-mail: mvlr@nitc.ac.in

1 Introduction

The road safety situation in India is compromised to a great extent due to the rapid growth of motor vehicles and the inadequate capacity of roads to cope up with the increase in traffic demand. “Fault of drivers, defects in motor vehicles, defect in road conditions, environmental conditions, faults of pedestrians and poor lighting are the main causes of crashes to take place. Drivers’ fault has been revealed as the single most responsible factor for road crashes, killings and injuries on all roads in the country over a long period of time. Drivers’ fault accounted for 77.1% of total road accidents during 2015 as against 78.8% during 2014” [1]. Since drivers having varied physical, mental and emotional characteristics use the roads, the fault of the driver, as pointed out by MoRTH (2015), could be one of the reasons for traffic-related injuries and fatalities. Hence, a study of road user behaviour is essential to improve safety on the roads. Moreover, a study on adherence of road users to traffic rules and regulations, especially with respect to road markings, is the need of the hour.

Road markings are used to guide the traffic and for traffic control on a highway. They help to reinforce the function of traffic signs. Traffic markings help in delineation of traffic path and thereby serve as a psychological barrier of drivers. They ensure the safe movement of traffic and harmonious flow of traffic on a highway. Markings that are placed longitudinally along the direction of traffic on the highway surface are called as longitudinal markings. They serve to indicate the position of the driver on the highway. Many kinds of longitudinal markings are used, among which centre line marking serves to separate the opposing streams of traffic. If the road width is less than 5 m and if it has more than four lanes, no centre line is usually provided. Centre line could be double solid line, single solid line, double broken line or single broken line depending on the requirements of the road and the traffic. When the number of lane is less than four on urban road, the centre line may be single broken line of 3 m long and 150 mm wide segments. The broken lines are placed at intervals of 4.5 m as shown in Fig. 1. However, the intervals shall be reduced to 3 m on curves and near intersections. When there are two traffic lanes on undivided urban roads in each direction, a single solid line of 150 mm wide or double solid line of 100 mm wide can be used as centre line marking which is separated by a space of 100 mm [2]. Figure 1 depicts a centre line marking for a two-lane road, as prescribed by IRC-35(2015). Driver behaviour associated with proper positioning of the vehicle by drivers, with respect to centre line markings, can significantly influence road safety.

Fig. 1 Centre line marking for a two-lane road



In the early research works, driver behaviour classifications were based on the objective experimental data from actual driving experiments or driving simulators. Ogle et al. [3] correlated speeding behaviour to crash rates using vehicle GPS coordinates and speeds in Atlanta (Georgia). With prior knowledge of posted speed limit and deviation from legal speeds, unsafe driving behaviour was shown. The effect of speed on the crash rates was established from this correlation of driving records and amount of safe driving. Different aberrant driving behaviours (violations, errors and lapses) committed by drivers in Finland, Sweden, Greece and Turkey were studied by Warner et al. [4]. Different countries showed different problems with regard to aberrant driving behaviours from the study; this should be considered when promoting traffic safety interventions. In India, lateral position of the vehicle is an important factor of driver behaviour since lane discipline is not followed by vehicles on Indian roads.

Kanagaraj et al. [5] showed that the drivers do not strictly follow their leader in a substantial fraction of the observations and it was also inferred that statistically significant differences among the various vehicle types in travel speeds, accelerations, distance keeping and selection of lateral positions on the highway. Mahapatra and Mauryathe [6] showed that except at lower speeds (speed between 2 and 4 m/s), an inverse relationship exists between the speed and the lateral characteristics. It studied the lateral movement characteristics of the vehicle with respect to speed. Hallmark et al. [7] studied about the endogenous relationship between the speed and the lateral position of vehicles on curves and it showed that vehicles at higher speeds had greater odds of near lane crossings. Stodart and Donell [8] studied the behaviour of speed and lateral position of vehicle in controlled driving conditions at night. The radius of horizontal curve and curve direction showed larger association with the change in vehicle lane position and the restrictive nature of the geometry of the roadway did not show any significant variation. Anil [9] conducted a study in which the principle of conflict probability was used. For a road section, three points were selected and their conflict probabilities were plotted. It was observed that when all the three sets of cumulative frequency pairs intersect nearly at the midpoints of the road section, the improvement needed to raise the cumulative frequency curve is the centre line carriageway marking.

The review of literature on lateral characteristics of vehicles revealed that change in lateral position depends on various traffic parameters, road condition, as well as, the geometrics of the road. Most of the studies conducted were limited to analysis of the lateral movement of vehicle on curves. Studies related to vehicle's lateral characteristics on straight road with mixed and non-lane disciplined traffic were less. Hence, it is necessary to analyse the lateral movement behaviour of vehicles in a traffic stream for formulating an accurate simulation model. The present study aims to evaluate the influence of centre line marking on driver behaviour using the lateral position of the vehicles on the carriageway in a mixed traffic condition on Indian roads. It includes a study on the behaviour of different vehicle types and to quantify the effect of various factors such as traffic volume, traffic speed on lateral position of vehicles at straight stretches and at horizontal curves at free-flow conditions.

2 Methodology Adopted for the Study

Four straight sections and three curved sections were selected in a stretch of NH-17, National Highway in Kerala, India, from Kannur to Kozhikode, and MDR 55, Major District Road, in the state of Kerala, India, from Kattampalley to Munderimotta. Video cameras were used to record the vehicle flow and this was analysed to track the trajectories of vehicles. Vehicle movements are tracked using video camera for 6–8 hours, till 2000 freely moving vehicles are captured on an average, without centre line marking and then with centre line marking. Lateral position was measured before centre line was marked and after the centre line was marked, so as to determine whether any change in drivers' lateral position choice behaviour has occurred. A period of about one month to six weeks was given for the drivers to get accustomed to the road marking after the centre line was drawn. The video recording was used to extract the speed and lateral position of vehicles. Classified vehicle volume count was taken at different locations on both sides of the study stretches. The other measurements taken for this study were the width of the carriageway, the length and radius of the road stretch taken under consideration.

The distribution of lateral position before and after the centre line marking is needed to judge whether any changes have occurred in the driver behaviour. For identifying the lateral position of the vehicles, a grid was overlapped using video analysis software 'Kinovea'. The grids were adjusted in such a way that each grid forms a square of size 50 cm and this was done by adjusting the grid formed using 'Kinovea', with the chalk marking made at the field during data collection. The front left wheel of the vehicle was observed to find the placement of the vehicle. For two-wheelers, the front wheel and for auto-rickshaw, the back left wheel were observed for data collection. These were converted to real-world dimensions with the help of Excel spreadsheets' formula feature. This was labour intensive but was able to provide useful data, especially in a situation where vehicles drift off the road to the left on straight roads and towards the centre line on approaches to curves, where speed measurements could also be taken since they have an effect on vehicle position. From the video recorded, vehicle type and speed were obtained using a software called 'Traffic Data Extractor' created by IIT Bombay. Only freely flowing vehicles were considered for the study. Different statistical tools were used to understand how the various factors are influencing lateral position of the vehicles and how the lateral position in turn affects safety. Linear regression models were developed to model the distance of the vehicle from the edge of the road.

3 Data Analysis and Results

This section discusses the analysis of the collected data and compares at the same location before and after the centre line was marked. Analysis was done using conflict probability, scatter plot analysis, ANOVA test and sensitivity test.

3.1 Conflict Probability

A concept which will be useful to study the traffic distribution across the pavement is the concept of conflict energy. In a two-lane two-way road, the traffic from either direction can use any portion of the pavement, thereby increasing the conflict probability. Taking into account the head-on and bump-in type of collisions that are likely to occur in a strip of pavement, the conflict energy is calculated using the formula given as Eq. (1).

$$CE_i = m_1 u_1^2 + m(u_1 + u_2)^2 \tag{1}$$

where,

- CE_i conflict energy at the i th segment across the section
- m_1 a quantity proportional to volume of traffic in the i th segment in one direction
- m a quantity proportional to minimum of the volumes at the i th segment in two different directions
- u_1 and u_2 speeds of traffic in the two directions at chosen segment.

These values can be obtained across different segments in a particular section in two different directions separately. The cumulative frequency of these energies in two different directions when plotted across a road section has many useful applications. Such a cumulative distribution plot will intersect at nearly the midpoint in the case the distributions are not skewed. Higher the percentage at which this intersection takes place, greater the probability that most of the traffic in each direction is confined to its lane of movement. This work intends to make use of these concepts at selected locations to assess the extent of when a centre line is present.

Conflict energy distribution plots were drawn for all the locations and for each vehicle type. Some of the plots of impact energy and probability distribution at different sites before and after the centre line was marked are shown in Figs. 2, 3, 4 and 5, with a view to compare each other and to recommend improvement measures if required.

Fig. 2 Cumulative energy frequency distribution (Car)

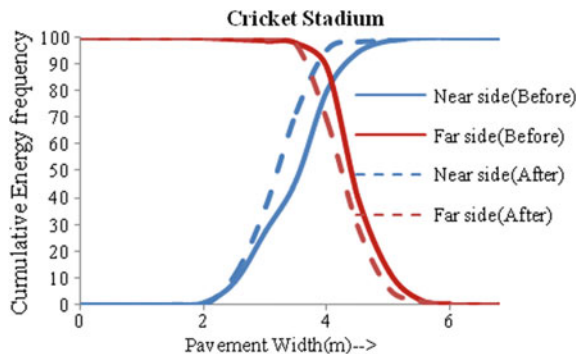


Fig. 3 Cumulative energy frequency distribution (LCV)

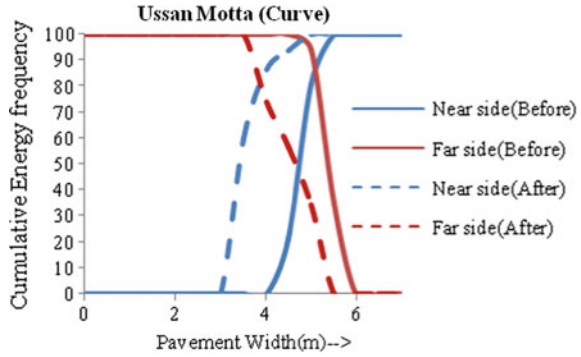


Fig. 4 Cumulative energy frequency distribution (Bus)

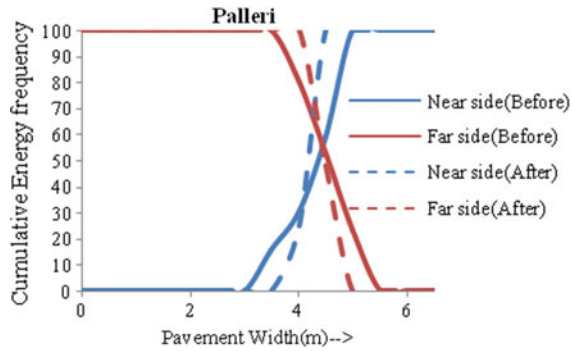


Fig. 5 Cumulative energy frequency distribution (Two-wheelers)

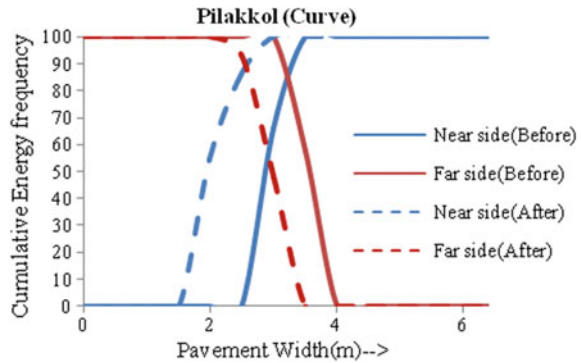


Figure 2 shows that the percentage of vehicles confining to their own lanes travel is found to be 84% in before study and 86% in after study. But its conflict area has reduced in the after study plot. It is observed that cumulative impact energy in each direction approximately intersects at 3.8 m from the edge of the pavement, and 0.4 m shifted away from the centre of the carriageway. Figure 3 shows that percentage of vehicles confining to their own lanes travel is found to be 86% in before study

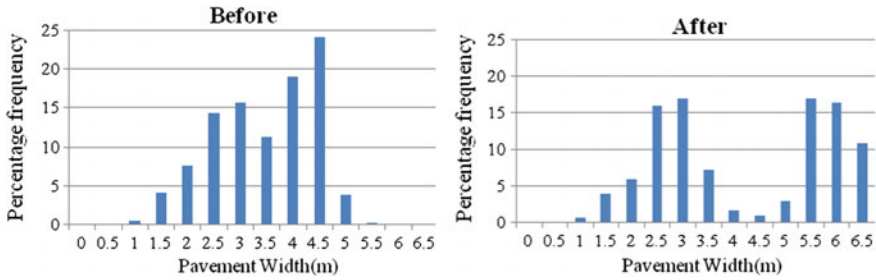


Fig. 6 Percentage frequency distribution

and it reduced to 82% in after study and its conflict area has not reduced in the after study plot. But it is observed that it has shifted more towards the centre of the carriageway (0.3 m from centre of carriageway) and cumulative impact energy in each direction approximately intersects at 3.8 m from the edge of the pavement. Similarly, variations at two other locations are also shown in Figs. 4 and 5. From these figures, it is observed that all the vehicles are showing a variation with and without centre line marking. Among all the vehicle types, two-wheelers and LCV have shifted the point of intersection more towards the centre of the carriageway, indicating that almost all two-wheelers and LCV followed the lane discipline after centre line marking is drawn.

3.2 Traffic Distribution

Figure 6 shows the traffic distribution across the pavement width before and after the centre line marking is drawn respectively at Beach road. From the two plots, it is observed that percentage of vehicles moving through the centre of the carriageway in the after study plot has reduced or shifted towards the sides compared to before study. Similarly, at other locations, vehicles shifted towards the edge after centre line marking was drawn.

3.3 Scatter Plot Analysis

Here, position of the left wheel from the edge of the carriageway width was compared with the speed of the vehicles moving in both the directions (indicated as near side and far side with respect to the camera used for data collection in the legend). The speeds of the vehicles were grouped into intervals of 5 kmph and the vehicles which are moving at a particular speed were grouped into the corresponding speed group.

A linear trend is observed in the relation between speed and position of all categories of vehicles. This implies that as the speed of the vehicle increases, the vehicles

move towards the centre line. Figures 7 and 8 show that vehicles have shifted towards their own lane after centre line was marked, i.e. they move within 2.5 m from the edge of the carriageway. Then, a sampling duration of five minutes was selected and change in position with respect to change in volume and speed was analysed.

Figure 9 shows that in the before study, vehicles moved randomly, but after the centre line marking was drawn, the vehicles appeared to move within their respective

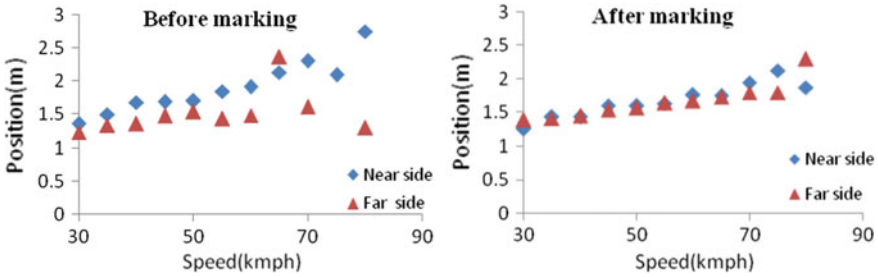


Fig. 7 Position versus speed (Car)

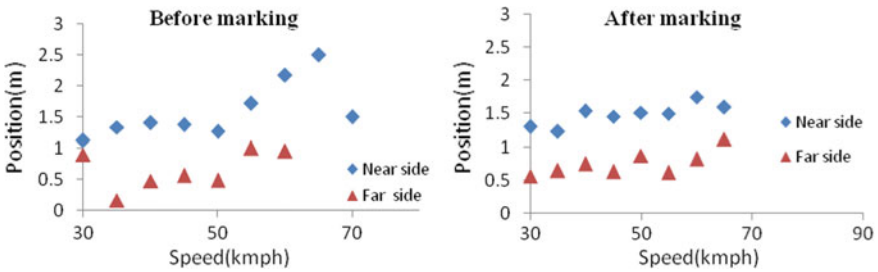


Fig. 8 Position versus speed (Heavy vehicles)

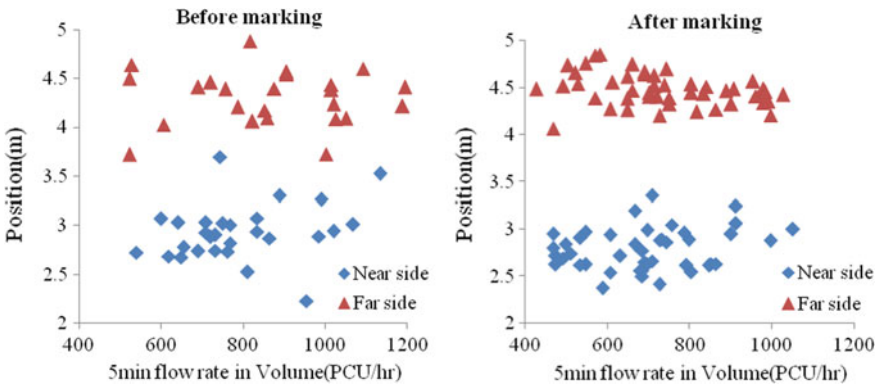


Fig. 9 Position versus volume

lanes and a linear trend was shown between the parameters, i.e. as the volume in the same direction increased, the vehicles moved towards the centre line.

3.4 ANOVA Test

Lateral position of the vehicle could vary with the speed. In order to find out whether the lateral position of different vehicles is significantly different or not, at a particular speed limit, ANOVA test was conducted on the lateral position of different class of vehicles. It was observed that lateral position values of different vehicles are significantly different as the p -value obtained is less than 0.05 and 'F calculated' value is more than 'F critical' in almost all the cases ($F(4.96) = 136.78$, p -value < 0.05). Similarly, in order to find out whether the speeds of different vehicles are significantly different or not, at a particular lateral position limit, ANOVA test was conducted on the lateral position of different class of vehicles. It was found that the speeds of different vehicle types are significantly different, as the p -value obtained is less than 0.05 and 'F calculated' value is more than 'F critical' ($F(4.113) = 25.95$, p -value < 0.05).

3.5 Modelling

The lateral position of the vehicles is observed to vary with different traffic and geometric parameters. In order to predict the position of the vehicle along the width of the carriageway, a mixed non-linear regression model was developed considering speed (v), vehicle type (vt), lane (l) and geometric parameters such as carriageway width (w), roadside feature (sf), presence of centre line (cl). In addition to these variables, some transformations of the variables were also considered in the modelling, namely inverse of radius (ir). The variable 'Lane' indicates the lane in which the vehicle was moving, whether it was 'outer lane' or 'inner lane'. Centre line is the variable used to indicate whether the centre line marking is present or not. As the name indicates, roadside feature is the feature present on the sides of the road. The coding used for the categorical variables is given in Table 1.

The data pertaining to all vehicle types is combined to get a model applicable for any vehicle type. Out of 51,684 samples, calibration was done with 66% of data and remaining was used for validation. This model is used to estimate the lateral position of the centre of the vehicle from the edge of the carriageway, for any straight or horizontal curve, if the geometric details of the location are known and for a particular speed value. It gives an R^2 value of 0.282, indicating that model explains 28.2% of the variability of the dependent variable. Here, all the variables are found significant and are obeying with the sign conventions. Its statistics are provided in Table 2.

Width and inverse of radius of the road stretch are showing a polynomial relation with the dependent variable. As the speed of the vehicle increases, vehicles move

Table 1 Categorical variables coding

Lane	Outer lane	0
	Inner lane	1
Presence of centre line	Present	0
	Absent	1
Roadside features	Barren land	1
	Smaller walls	2
	Pedestrian walkway	3
	Walls	4
	Parked vehicles	5
	Open drainage	6
	Building	7

towards centre of the carriageway, indicated by the positive sign of the coefficient. Similar is the case when centre line is absent and when the vehicle is moving in the inner lane of a curve, vehicles try to move towards centre of the carriageway, indicated by the positive sign of the coefficient. In the case of roadside features, coding is given in the increasing order of interference. As the interference increases, the vehicles move towards the centre of the road, increasing the dependent variable. For example, if the available options are “smaller walls” and “pedestrian walkway” with coding values 2 and 3, respectively. The vehicles will move towards the smaller walls compared to pedestrian walkway, so the dependent variable decreases, indicated by a negative sign of the coefficient.

A number of applications are possible using the models generated for all the vehicles in the above section. They are

(i) Used to specify speed limit regulations

Base condition is that the road is 7 m wide straight National Highway with centre line marking, having barren land on both the sides. The minimum speed value is selected among all the vehicle type at which the vehicle crosses the centre line, as the speed limit in that stretch. The speed limit was identified as 80 kmph for the given base condition.

(ii) The radius of horizontal curves can also be checked for safety

Base condition is that the road is 7 m wide National Highway with centre line marking having barren land on both the sides and with vehicles moving with a speed of 60 kmph. The maximum radius value is selected among all the vehicle type at which the vehicle crosses the centre line, as the safe radius in that stretch. It was identified that the safe radius should be 320 m for the given base condition.

Table 2 Model statistics

Parameter	Parameter estimates										RMSE calibration	RMSE validation
	ν	w^2	w	ir^2	ir	cl	sf	l	vt			
Constant	-312.61	0.005	-7.6	98.003	4,680,224.3	-29,022.79	0.649	-0.316	0.555	0.077	0.804	0.789

(iii) Used to design the width of the carriageway

Base condition is that the road is a straight National Highway with centre line marking having barren land on both the sides and vehicles are moving with a speed of 60 kmph. The minimum carriageway width value is selected among all the vehicle type at which the vehicle crosses the centre line, as the carriageway width in that stretch. The safe carriageway width was identified to be 7 m for the given base condition.

4 Conclusions

In the study, from the percentage traffic distribution plot, it was inferred that vehicles moving through the centre of the carriageway shifted their path towards their own lanes after centre line marking was drawn, at most of the locations. From scatter plot analysis, it is observed that as the speed of the vehicle increases, the vehicles tend to move towards the centre line showing a linear trend. Significant variation was not observed between averaged position of the vehicles with respect to change in volume and averaged position of the vehicles with respect to change in speed. From the ANOVA test results, it was inferred that the lateral position of different vehicles is significantly different from each other at different speed ranges. It was also inferred that the speeds of different vehicles are significantly different from each other at different lateral positions. Hence, it can be concluded that centre line marking has an effect on the driver behaviour in choosing the position of the vehicle while plying on road. By giving proper maintenance to centre line markings, the head-on collision can be reduced.

Linear multiple regression model is formulated to predict the position opted by the driver of the vehicle along the width of the carriageway. Using sensitivity test, the most significant variables influencing the choice of lateral position for a driver were found to be the inverse of the radius of the curve and width of the carriageway. The developed models can be used to specify speed limit regulations. Similarly, the radius of horizontal curves can also be checked for safety using the developed models. The models can also be used to design the width of the carriageway.

References

1. Transport Research Wing, Ministry of Road Transport and Highways (2015) Road Accidents in India 2015. Ministry of Road Transport and Highways, Government of India, New Delhi
2. Kadyali DL (1987) Traffic engineering and transportation planning. Khanna Publishers, New Delhi
3. Ogle J, Guensler R, Bachman W, Koutsak M, Wolf J (2002) Accuracy of global positioning system for determining driver performance parameters. *Transp Res Rec J Transp Res Board* (1818):12–24
4. Warner HW, Özkan T, Lajunen T, Tzamalouka G (2011) Cross-cultural comparison of drivers' tendency to commit different aberrant driving behaviours. *Transp Res Part F Traffic Psychol Behav* 14(5):390–399

5. Kanagaraj V, Asaithambi G, Toledo T, Lee TC (2015) Trajectory data and flow characteristics of mixed traffic. *Transp Res Rec J Transp Res Board* (2491):1–11
6. Mahapatra G, Maurya AK (2013) Study of vehicles lateral movement in non lane discipline traffic stream on a straight road. *Procedia Soc Behav Sci* 104:352–359
7. Hallmark SL, Hawkins N, Smadi O (2013) Relationship between speed and lateral position on curves. In: 16th international conference road safety on four continents. Beijing, China
8. Stodart BP, Donnell ET (2008) Speed and lateral vehicle position models from controlled night-time driving experiment. *J Transp Eng* 134(11):439–449
9. Anil B (1989) Exploration in the use of entropy and conflict probability concepts for site improvement at black spots, Masters' thesis, Department of Civil Engineering, NIT Calicut

Critical Appraisal of Traffic Management Strategies for a Mega Religious Procession: Case of NH-58 During Kanwar Yatra, India



Hasmeet Kaur and Uttam K. Roy

Abstract Many countries have cultural and religious processions in the name of carnivals, parades, special events, etc. These countries have special event plans prepared to avoid disruption in the life of local people while the management strategies in India are quite informal. Kanwar Yatra in India is an annual religious procession. It has duration of 15 days during which all the major roads and highways get choked in North India. The traffic management strategies prepared by traffic police and local administrative bodies are never obeyed by the procession participants. This paper attempts to understand the cause of disobedience of those traffic rules and to propose alternate strategies. The procession starts at Haridwar and disperses to different cities. Since the procession is more concentrated near Haridwar which is the origin city for this procession, NH-58 from Haridwar to Delhi was taken up as a study area. Such special events also boost the economy of the hosting states so the problem needs to be addressed from the perspective of all stakeholders like procession participants, local people, shopkeepers, etc. The various surveys conducted are: (a) origin-destination survey, (b) ethnographic survey and (c) interviews for public opinion. Secondary data like number of visitors during the procession in the past few years were also taken from Kumbh Mela Office, Haridwar. The objective is to bring out a comprehensive diagnosis of the problem followed by some policy level recommendations. If the problem of one national highway can be solved then later on a similar study for other highways can be carried out as well. Largely, it will serve the government authorities to manage the event, earn revenue and build an image of the state or country. The study helps in formulating a macro-level policy/guideline for the region around NH-58. The state/local authorities under the influence area of NH-58 should make micro-level traffic management strategies keeping the larger picture (regional level guidelines) in mind. The micro-level studies like a particular

H. Kaur (✉)

Centre for Transportation Systems, Indian Institute of Technology
Roorkee, Roorkee 247667, India
e-mail: hasmeet90@yahoo.in

U. K. Roy

Department of Architecture and Planning, Indian Institute of Technology
Roorkee, Roorkee 247667, India
e-mail: ukroyfap@iitr.ac.in

© Springer Nature Singapore Pte Ltd. 2020

T. V. Mathew et al. (eds.), *Transportation Research*, Lecture Notes
in Civil Engineering 45, https://doi.org/10.1007/978-981-32-9042-6_49

621

junction or pedestrian flow study in a narrow congested lane are beyond the scope of this paper.

Keywords NH-58 · Kanwar yatra · Religious processions · Ethnographic study · Traffic management · Route choice parameters

1 Introduction

Many countries have cultural and religious processions in the name of carnivals, parades, yatras, etc. These are known as special events in the USA, mega events in Europe and mass gatherings in Saudi Arabia. These countries have special event plans prepared to avoid disruption in the life of local people. Kanwar Yatra is an annual religious procession of India which has duration of 15 days. It usually starts in the mid of July. It starts from Haridwar from where the participants fill Gangajal (holy water of River Ganga) in two containers carry it to a Shiva temple (in Meerut/Bagpat/near their home) where they perform Jalabhishek (sacred act of bathing Lord Shiva's idol with holy water). All the major roads and national highways are choked in many cities across states in North India due to this procession. NH-58 from Haridwar to Delhi experiences one of the worst roadblocks.

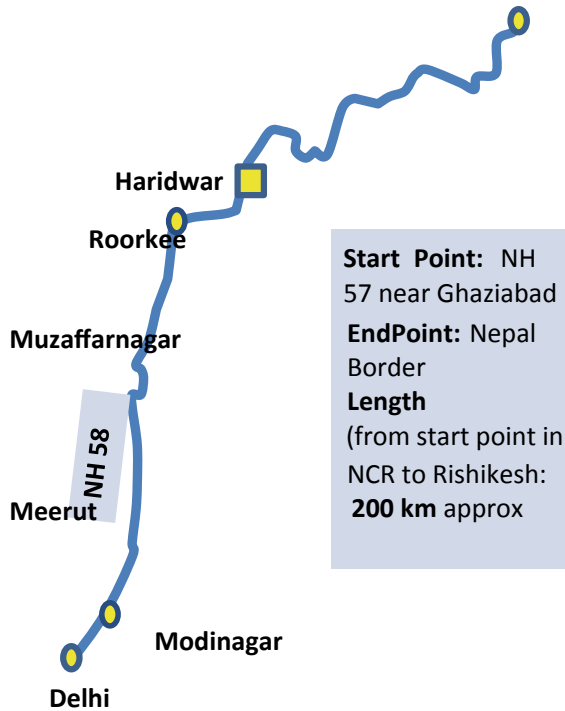
1.1 Area of Study

The route taken up for study is NH-58 from Haridwar to Delhi for a length of about 200 km (refer Fig. 1). The area chosen was so because the maximum pressure of Kanwar Yatra is experienced on NH-58. NH-58 is two-laned from Haridwar to Manglaur and is four-laned from Manglaur to Delhi. So, both the scenarios were covered.

1.2 Need for Diagnosing Traffic Issues During Kanwar Yatra

1. **Mega Scale:** In 2013, 1.95 crores people participated in this procession making it the biggest procession of the world.
2. **Short Duration and Cost Limitation:** Low-cost measures are needed as they will be used only for 15 days.
3. **The Nature of Procession:** The nature of the procession is religious; the proposals given should be acceptable as per religious sentiments of the community.
4. **Too many stakeholders:** The stakeholders involved have contradictory interests, finding a common ground is difficult like local residents versus procession participants.

Fig. 1 Study area NH-58 from Delhi to Haridwar
 Source ICONOS Imagery



5. **Nationwide Phenomenon:** If the traffic during processions in India is managed successfully, those guidelines can be applied to other processions like Ganpati Visarjan in Maharashtra, Gangasagar Mela and Durga Pooja in West Bengal, etc.

1.3 Objective of Study

- To understand the parameters of route choice by participants.
- To give guidelines for better traffic management strategies for religious and other processions in India.

1.4 Scope of Work

The study has the following scope of work:

- To identify the travel pattern of procession participants
- To identify the issues at management, planning and decision-making level

- To conduct a public opinion survey to understand the cause of disobedience of existing traffic management strategies and route choice parameters considered by the procession participants
- To give guidelines at a policy level to propose an alternate route.

The scope of the study is at a regional scale. It is to be noted that solutions for Dak Kanwar and solutions/routing plans for city scale are out of the scope of this study.

2 Methodology

2.1 Secondary Data

The secondary data required for the study was (a) number of participants of procession in the past 5 years (from Kumbh Mela Office, Haridwar), (b) annual growth rate of procession participants (derived from the above data) and (c) existing traffic management strategies for NH-58 (from traffic police/control room, Haridwar).

2.2 Primary Data

The primary data was collected by filling questionnaires. A combined questionnaire was prepared for OD survey and user satisfaction survey. The collected through primary survey is given below.

1. Demographic, socio-economic profile, travel behaviour, OD data of procession participants
2. Problems faced by procession participants
3. Parameters of route choice of procession participants
4. Problems faced by traffic police in implementation of existing traffic management strategies
5. Problems from city dweller's perspective.

The number of questionnaires filled from procession participants was 655, samples taken from participants of Dak Kanwar were 150, so a total of 800 samples were taken. Since the total number of procession participants that visited in the year 2014 was 2.60 crores, the sample of 800 questionnaire forms just 0.03% of total visitors (*kanwariyas*). (Dak Kanwar is a procession that takes place on last two days of Kanwar Yatra which is conducted on two-wheelers and four-wheelers). The sample size was small due to resource constraints as it had to be completed within 15 days with meagre manpower and financial resources and was an academic exercise. But the sample size is sufficiently representative to prepare macro-level policy guidelines.

The following surveys were conducted for the study.

1. OD survey of procession participants
2. Public opinion survey of stakeholders
3. Ethnographic/observatory survey of procession participants.

Origin-Destination Survey of Procession Participants

The origin destination survey was done to understand the dispersal of people to different destinations through different routes. The OD survey was mainly done at Haridwar and Roorkee for 10 days from 10:00 a.m. to 9:00 p.m. and at Muzaffarnagar from 1:00 p.m. to 5:00 p.m. for 1 day. Total 800 people with different socio-economic background were covered to understand the pattern of travel.

Roorkee, the nearest town to Haridwar city was the city where people are least dispersed to different routes towards different cities. Talking to people at or near Har ki Pauri in Haridwar was impossible due to excessive crowd so the maximum number of OD samples was taken from Roorkee.

Public Opinion Survey

This survey was conducted to understand the cause of disobedience of traffic management strategies and the parameters for choosing the route for procession, the problems faced by them and their expectations from the government. This survey was conducted at Haridwar, Roorkee and Muzaffarnagar such that the problems with traffic management strategies for two-laned as well as four-laned road can be understood. In the interview, the parameters that affected the route choice of Kanwar Yatris were marked.

Ethnographic Study/Observatory Survey

Since it is a religious procession, there were certain things people would do as per their faith like would only choose walking as a mode, would take bath after every meal, would not complain about their problems so such things had to be observed silently without letting them know that they were being observed. Certain beliefs, conventional measures had to be understood to be able to give proposals that would be acceptable to them as per their faith. For that informal discussions and silent observation, while walking with them or while sitting on a roadside dhaba, etc. was required. This was done at Haridwar from 12:00 p.m. to 7:00 p.m. for 1 day, at Muzaffarnagar from 1:00 p.m. to 6:00 p.m. for 1 day and at Roorkee from 9:00 a.m. to 1:00 p.m., 1:00 p.m. to 6:00 p.m. and 6:00 p.m. to 10:00 p.m. on 3 different days.

Interview Details for Other Stakeholders

A number of shopkeepers questioned were 15, number of street vendors questioned were 14, number of police personnel questioned were 30, number of local residents questioned were 10 (apart from shopkeepers and police personnel). Though the questions to be asked from local people, shopkeepers and vendors were already prepared but they were asked in an informal way. The following table shows the list of police personnel questioned at different locations.

3 Discussion

3.1 Origin-Destination Survey Results

The devotees reach Haridwar on public transport like bus or train of which 68% come by bus (refer Fig. 2). From there after taking Gangajal, they walk back to a Shiva temple. There are two popular Shiva temples in Meerut and Baghpat cities called Augurnath temple and Pura Mahadev, respectively. 28% of devotees prefer to perform Jalabhishek in these cities while majority of people (72%) take Gangajal to their hometowns, to a Shiva temple in their hometown (Fig. 3).

Origin-Destination Data Analysis

The origin-destination survey revealed that the source of procession was common, which is Haridwar. From there, if the states are considered as different traffic zones, it was revealed that the maximum traffic was going to Delhi (48%) followed by Uttar Pradesh (43%) and then Haryana (9%). Figure 4 shows the percentage of participants going to different states. Figure 5 shows the desire line diagram of OD of procession participants.

Fig. 2 Pie chart for percentage share of mode choice by participants of Kanwar Yatra from City of Origin to Haridwar *Source* OD Survey, July 2014

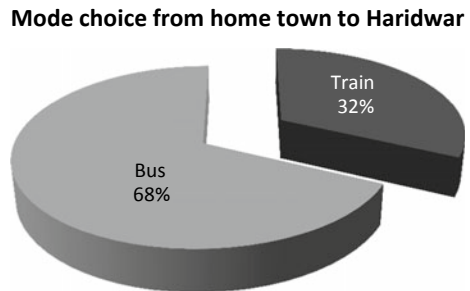


Fig. 3 Pie chart for preferred city for *Jalabhishek* by participants of Kanwar Yatra *Source* OD Survey, July 2014

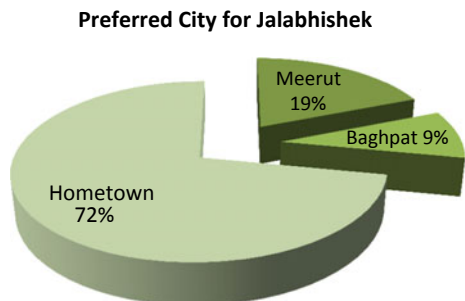


Table 1 Priority wise list of parameters of choosing route preference by procession participants

Sr. No.	Parameter of route choice	Percentage of responses
1.	Shorter route	60
2.	Avoiding dead area and snakes, woods or forest	20
3.	Food, tea, eatables, water tap nearby, (hanger for jhula kanwar), medical facilities at low cost	15
4.	Shade in narrower lanes	4
5.	shops around (for HIG <1% people)	1

Source Primary Survey, July 2014

participants. The priorities are given based on the percentage of responses received for that parameter (Table 1).

The term jhula kanwar in point 3 refers to a kanwar (2 containers tied at the ends of a road) which the devotees/procession participants do not place on ground during their halt, so they need a place at lodging/eating camps to hang it. 94% of the Kanwar Yatris carried Jhula Kanwar. Thus, a facility for it can be an important roadside facility.

The cause of procession participants not following the designated route of Canal Road is that they presume Canal Road to be longer than NH-58. The procession participants used Canal Road only from Haridwar to Roorkee due to presence of food camps at frequent intervals (say 1 at every 2–3 kms). The roads outside the main city are avoided by them due to fears of theft, snakes, etc.

4.2 Results from Interview of Other Stakeholders and Ethnographic Study

Local Residents Perspective:

The problems faced by local residents are listed in Table 2.

The shopkeeper of formal shops complained of losing clientele during Kanwar Mela days as the participants of the procession never prefer formal shops (except 1% of people who had the willingness to spend).

Table 2 Problems from local people's perspective

Other stakeholders	Issues	Response percentage
Local residents	Daily routine trips disrupted	100
Shopkeepers	Shopkeepers along road loose clientele	100
Auto/cycle-rickshaw drivers	Auto-rickshaw and cycle-rickshaw drivers change profession for 15 days	100

Cycle-rickshaw and auto-rickshaw drivers lose job for at least 15 days especially in cities where no traffic zones are declared (e.g. Haridwar). These people go for street vending for 15 days. Thus, they need to incorporate in design as they can add to the convenience of visitors. Also, the other street vendors agreed that their daily income doubles during Kanwar Yatra thus it can be seen as a potential.

This information was retrieved through informal discussions with the vendors at Har ki Pauri in Haridwar (from where the procession starts), the vendors in zero traffic area (near Kotwali Chowk in Haridwar) were interviewed.

Perspective of Participants of the Procession

As per the analysis of demographic and socio-economic data of sample of people interviewed, 30% were females. There were no changing rooms or toilets along the road. The socio-economic situation along with their public opinion survey results shows that they do not prefer buying from shops on the way(as 62% of them had monthly income <Rs. 20,000), they take the roads that go through the city to avoid dead areas as they will be unsafe. They prefer more economical facilities for lodging and eating like street vendors, camps by government/NGO’s.

Problems from Perspective of Traffic Police and Administration:

The planning is done by a team that includes Police Personnel, Senior Superintendent of Police (SSP) and District Magistrate (DM) of the district in the meeting. There is a team of Police Personnel headed by an officer called Mela Adhikari at the Kumbh Mela Office popularly known as Central Control Room (CCR). It is located at Haridwar near Har ki Pauri. Their knowledge is based on their experience of Kumbh Mela as well as Kanwar Yatra. They are the authority that takes counts of total number of participants of Kanwar Yatra and report it every year to the D.M of District Haridwar but are not aware of traffic management guidelines as per IRC.

They try to use low-cost measures like creating a speed breaker using mud as shown in Fig. 6, but they are not aware of the standard dimensions of a speed breaker which is 3.7 m wide and 0.1 m height [1]. Thus, the speed breakers on NH-58 seen were 0.5–0.7 m in width and about 0.1 m in height. These should have their surface

Fig. 6 Temporary speed breaker created on NH-58 in Muzaffarnagar. *Source* Author, July 2014, Muzaffarnagar



rounded at 17 m radius which is not possible with humps when made of mud. For the ease of heavy vehicles, the humps should be supported by 1.5-m-long ramp on both sides.

5 Guidelines Derived from the Study for a Mega Religious Procession

5.1 Identification of Alternate Routes Based on Route Choice Parameters

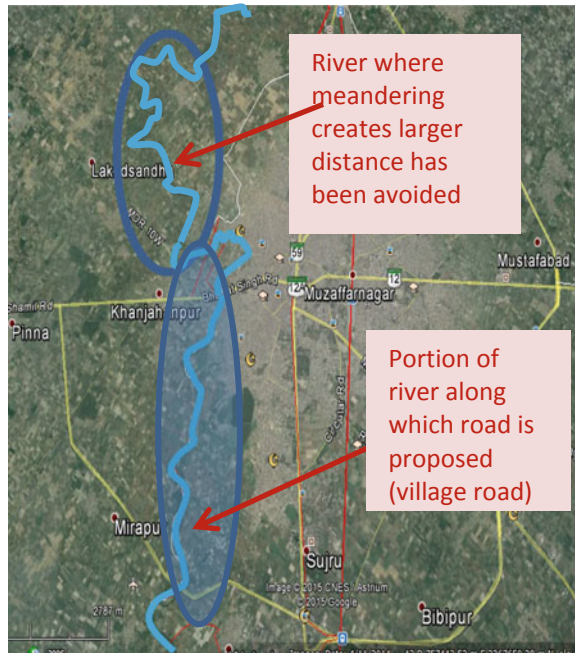
Based on the survey results, the alternate route options were considered for processions. The choice of alternative routes was made based on the following factors:

1. Shortest route which was the most important route choice parameter (for 60% respondents), followed by safety of route (for 20% respondents).
2. The stakeholders' relationship observed was such that <1% participants of the procession were depending on shops in the city; they moved through the city as it seemed safer.
3. The ethnographic factors like giving some space to hang jhula kanwars and frequent availability of taps could make the route more inviting if incorporated in street infrastructure.
4. Providing space for food camps along the proposed route was necessary as 99% participants of procession were dependent on the food, medicine and resting camps along the route.

Following considerations should be made while choosing an alternate route:

- Procession should not be allowed in the inner city roads.
- If it goes through a city, it should be controlled to a particular road which is not a major road.
- Commercial areas should not be assigned for procession.
- Roadside infrastructure like toilets, drinking water fountains, eating/lodging facilities or camps, etc. needed.
- Shortest route should be encouraged; this is the most important parameter as per the public opinion survey.
- Space should be allocated for street vendors.
- Leaving 1.5-m-width space on the shoulder for use by street vendors [2] and camps that are a preferred source of eating and lodging service for the participants of the procession. It will bring required activity spots along the road so that the route does not become a dead route/area. It will also inculcate the "eyes on street" concept.
- Aesthetic elements like a route along an existing river can be used as an advantage (if it will continue to be the shortest route) as shown in Fig. 7.
- Beautification of roads by means of shady trees can be done to make the route more inviting.

Fig. 7 Route along River Kali Nadi with less meandering is selected and the other is rejected in Muzaffarnagar city. *Source* ICONOS Imagery



- Wayfinding and route maps should be installed to guide the procession participants.
- A unifying urban design for the whole new route proposed is necessary.
- Directional signage's at all major junctions.

5.2 Infrastructure Needed to Make the Roads More Inviting

The infrastructure shortlisted below is chosen based on the ethnographic/observatory survey.

- Two-portable toilets at every 800 m (1 for male and 1 for females) [3]. For Example, portable toilets used during Kumbh Mela, 2013 and ones at Kutch in Gujarat along sea [4].
- Drinking water fountains at every 500 m [3].
- Street lights at every 30 m in a staggered pattern.
- Some arrangement to sit alongside canal, river and small river tributary along the route.
- Eating/lodging camps (preferably at 3.5 km) or designated space for street vendors at every 3.5 km. Both can also be allowed but at least one of the two should be there.

The reason for choosing 3.5 km as a standard is that a pedestrian covers 1200 m in 15 min, 2400 m in 30 min and 3600 m in 1.5 h. Considering 1.5 h of walk as

feasible before a person needs a snack break or rest. Since the distance covered is 3600 m in that time frame (on an average) thus three, there should be a camp at a minimum distance of 3.6 km.

- Every eating/lodging camp should have portable bathrooms nearby as the people in procession take bath after eating and before touching the holy water.
- Dustbins near every camp/designated space for vendors.

5.3 Assigning the Alternate Route: An Example from NH-58 Section as Per the Guidelines Above

The roads parallel to the existing routes chosen are the shortest possible routes available. On NH-58, a section from Manglaur to Muzaffarnagar is shown in Fig. 8. There is no parallel road to this section. So, the village roads closest to the highway have been joined and developed as an alternative. The village roads identified can be strengthened or converted to pucca roads such that they can serve the villages even after the procession to improve their connectivity and accessibility. The length of that route should be as close to that of existing road. The table below shows the comparison of these routes (Fig. 9 and Tables 3, 4).

Fig. 8 Nearest roads parallel to NH 58 identified on ICOMOS imagery. Source ICONOS Imagery

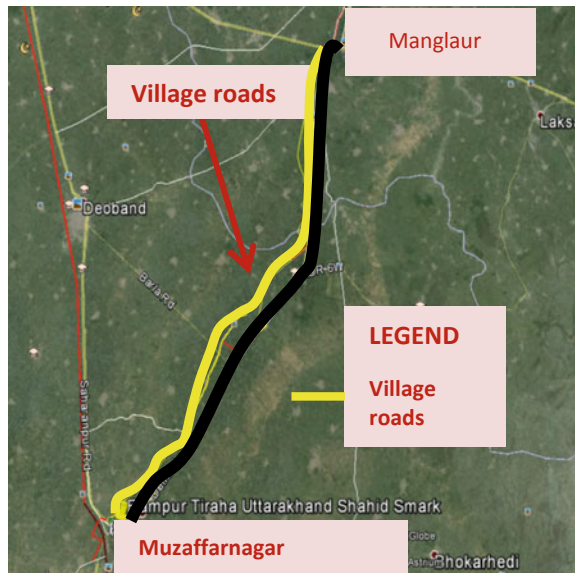


Fig. 9 Comparison o three alternate routes available.
 Source ICONOS Imagery

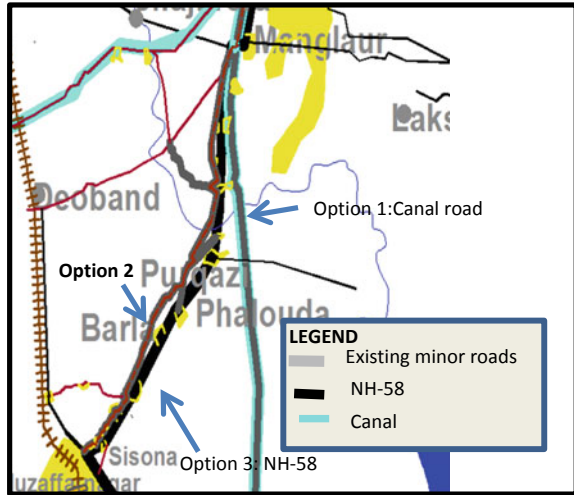


Table 3 Details of road lengths in route option 2 for Manglaur to Muzaffarnagar

Available road stretches	Distance (km)	After use	Modifications required
MDR	0.76	Vehicular road	Widening
Existing village road	9.9	Vehicular road	Widening and metalling
New village road	1.1	Vehicular road	Construction
Existing village road	8.26	Vehicular road	Widening and metalling
New road (along canal)	1	Vehicular road	Construction
Existing village road	16.96	Vehicular road	Widening and metalling
Total length	42.4		

5.4 Guidelines for Administration and Decision-Making

- ULB’s to consider the parameters of route choice like shortest distance and safety discovered in public opinion survey results while making traffic management plans for religious processions.
- Less than 1% of participants use the shops in the cities they pass through.

Table 4 Comparison of route options for Manglaur to Muzaffarnagar

Route options	Distance (km)	After use	Modifications required
Option 1: Canal road	47.6	Vehicular road	Widening and beautification
Option 2: Combination of roads	42.1	- do-	Widening and metalling
Option 3: NH-58 stretch	44	- do-	Widening to 4 lane

- Street design to include components keeping religious sentiments of procession participants in mind like some components where jhula kanwar can be hanged, the frequency of taps is important as the participants of the procession take bath after meal.
- Space allocated for roadside camps can make the routes lively and safe.
- Mobile applications showing the route dedicated for these routes can make the initiative a part of smart city theme.
- After use or long-term use of roads needs to be considered as mentioned in Table 6. The cost-benefit analysis should be done for all the options of alternate routes.
- The alternate routes can be made more inviting by considering the results of ethnographic survey as it is a religious procession.
- The traffic management components used should have dimensions, colour and material for components like speed breakers, barricades, etc. as per IRC Guidelines.
- Projections for expected visitors to estimate the infrastructure required are necessary.
- Research on developing portable toilets with minimal harmful environmental impact (like those developed IIT Kanpur team for Kumbh Mela in 2013 [4]) is required.
- Transportation planners to be involved by ULB's, while making special event plans.

6 Way Ahead

The parameters and their weightage discussed in this paper can be used to develop a mathematical model which can be used in four-stage modelling softwares.

The results of this paper can be checked by a stated preference survey to see if the alternative routes proposed in this paper are preferred over NH-58 by the procession participants.

Similar studies can be done for the processions in other regions in India and a common policy guideline for special events in India can be prepared.

7 Conclusion

- This paper brings out the behavioural aspects of the participants of a religious procession in India.
- The purpose of the paper is to understand the cause of disobedience/failure of the existing traffic management strategies of the world's largest procession.
- The surveys conducted for the study were public opinion survey, OD Survey of participants of the procession and ethnographic/observatory survey.
- Public opinion survey gave the priority wise parameters of route choice of participants of the procession. The main parameters of route choice are short distance and safety of routes which were not being fulfilled by the existing alternate routes proposed by traffic police and local administration.
- The public opinion survey of other stakeholders like shopkeepers and procession participants revealed that <1% of procession participants were dependent on roadside shops for food, medicines, etc.
- The ethnographic/observatory survey helped to discover the additional roadside infrastructure that can make the routes more inviting.
- To avoid the traffic congestion, alternate short routes need to be created.
- Some roads parallel to existing routes taken up by the procession participants can be used for the special event.
- The alternate route should have a uniform urban design, more roadside infrastructure and should be aesthetically more inviting than the usual route.
- Existing traffic management measures should be as per the IRC Codes for traffic management components.
- The transportation planners/engineers should be involved at micro-level planning and decision-making for specific special events. The studies on temporary roadside infrastructure like mobile toilets, etc. can be encouraged to improve the convenience of the participants of special events in India.
- The parameters discovered can be used for creating a mathematical model. Based on the results, the government policy guidelines can be prepared for preparation of a "Special Event Planning Guidelines".

References

1. IRC (1994) Guidelines on low cost traffic management techniques for urban areas IRC Special Publication, No. 43, Indian Roads Congress, New Delhi

2. Bhattacharjee A (2009) Implementation and systemic change with UTTIPEC street design guidelines, unified traffic and transportation infrastructure (Planning and Engineering) Centre. Delhi Development Authority, India
3. National Building Code (2005) National Building Code 2005. Bureau of Indian Standards, New Delhi
4. Can Faith Heal, Down to Earth (2013). <http://www.downtoearth.org.in/content/can-faith-heal>
5. Manchester City Council (2009) open space and recreational needs assessment. Manchester City Council, Manchester
6. Pedestrian Studies, Transportation Systems Engineering. http://nptel.ac.in/courses/105101008/downloads/cete_47.pdf

Pedestrian Accident Prediction Modelling—A Case Study in Thiruvananthapuram City



Ancy Santhosh, Ebin Sam and B. K. Bindhu

Abstract Pedestrians are the most neglected road users and witness an alarming accident rate each year. In India, annually, around one-third of road accidents involve pedestrians as victims. The pedestrian accident-prone urban road stretch along National Highway 66 in Thiruvananthapuram City was selected as the study stretch. In this paper, a statistical model for predicting the number of pedestrian accidents and their severity levels such as grievous, minor and fatal injury was developed for urban midblock sections. Poisson regression models were found to be the most suitable model to fit the data. Several factors such as number of bus stops, speed of vehicles, traffic volume, pedestrian volume along footpath and crosswalk, side roads, signalized crossings and the quality of crossings were found to considerably affect the pedestrian accidents. This paper helps to provide an insight into the hazardous conditions to pedestrians in urban areas and also proposes recommendations for enhancing the safety of the pedestrians.

Keywords Pedestrian · Safety · Accident prediction models · Thiruvananthapuram

1 Introduction

Road safety is one of the most important issues faced by our country with alarming accident rates. The problem of the accident is very severe in highway transportation, especially in India due to the intricate flow pattern of vehicles and the presence of heterogeneous traffic along with pedestrians. Everyone has different preferences considering transportation, but the one that is common for all road users is that everyone is a pedestrian at some stage of a trip chain. When vehicles have a collision

A. Santhosh · B. K. Bindhu
Rajiv Gandhi Institute of Technology, Kottayam, India
e-mail: ancy.santhosh04@gmail.com

B. K. Bindhu
e-mail: bindhu@rit.ac.in

E. Sam (✉)
National Transportation Planning and Research Centre (NATPAC), Thiruvananthapuram, India
e-mail: ebin.natpac@gmail.com

© Springer Nature Singapore Pte Ltd. 2020
T. V. Mathew et al. (eds.), *Transportation Research*, Lecture Notes
in Civil Engineering 45, https://doi.org/10.1007/978-981-32-9042-6_50

with pedestrians, there is a high risk for serious injury or death. When it comes to pedestrians, children have a high risk of injury from traffic accidents due to their size, incapability to judge the distance, and speed of vehicles and inexperience with traffic rules. Road accidents are well thought-out to be the third major cause of deaths in Kerala. According to the Home Ministry of Kerala, the state has nearly three per cent of India's population, but it has documented about 10% of the country's road traffic accidents. Between the years 2009 and 2014, nearly 23,800 people were killed due to accidents in Kerala. Nearly 40% of the people involved in accidents are pedestrians.

It becomes the responsibility of traffic engineers to provide safe traffic arrangements to all road users and guarantee their safety. Road accidents cannot be completely prevented but by appropriate traffic engineering methods, the accident rate can be decreased to a great extent. Hence, systematic studies of traffic accidents are to be carried out in most accident-prone regions. A proper examination of the origin of the accidents will help in proposing suitable remedial measures for improving the traffic conditions. Since pedestrians are the most susceptible among road users and pedestrian involved accidents have significant share, it becomes a necessity to analyse the pedestrian traffic accidents and to identify the unsafe conditions to pedestrians at various road sections in Kerala.

2 Scope and Objectives

The scope of this research is limited to a road stretch on National Highway 66, in Thiruvananthapuram.

The main objectives of this study are:

- To identify road stretch in Thiruvananthapuram City having an utmost number of pedestrian accidents.
- To identify roadway and traffic parameters affecting the safety of pedestrians in the selected road stretch.
- To develop suitable models for predicting pedestrian accidents at a particular road section.
- To propose recommendations for increasing pedestrian safety on the selected road stretch.

3 Earlier Studies on Pedestrian Accidents

Satiennam and Tanaboriboon [1] analysed the pedestrian accidents and conditions of pedestrians in the municipality of Khon Kaen in Thailand. In this research, Arc View GIS spatial analyst was used to spot high pedestrian accident locations. The most desirable model developed was the combination of the number of hospitals located

within the radius of 100 m, number of lanes and number of schools located within the radius of 150 m in the exponential function.

Poisson regression models were formulated by Wedagama et al. [2] to find out pedestrian accidents by focusing on the age groups and the prevailing spatial patterns of urban land use in the Newcastle city centre. They recognized that the accident casualties were higher on adult pedestrians when compared to children and older pedestrians.

Obeng and Salifu [3] conducted a study to develop a pedestrian accident prediction model for the trunk roads in Ghana. Four study roads were selected which was subdivided into identical sections of 161 road links. Generalized linear model was used for developing models. Their findings indicated that the factors affecting pedestrian accidents were the daily pedestrian flow variables and the total kilometres driven, which collectively explained 80% of the variation in the pedestrian accident data.

Abojaradeh [4] conducted a study to evaluate pedestrian safety in the pedestrian bridges of the Amman area. Records from ten pedestrian bridges were composed and analysed. It was finalized that the presence of pedestrian bridges has a positive impact on reducing the number of pedestrian deaths. The main factors that influenced the usage of pedestrian bridges were the width of the crossway, posted speed limit and the presence of the median barrier.

Haghighatpour and Moayedfar [5] conducted a study to find out the pedestrian accident prediction model at intersections and to decide the most influential factors. The three main models including linear regression, Poisson regression, and negative binomial regressions with distinct variables had been determined for 20 signalized intersections in Tehran. It was found out that the maximum number of pedestrian accidents was related to the presence of bus stops near to the intersections, and it increased 17.13% of pedestrian accidents.

4 Methodology

The methodology taken up for this study is given below:

- Collection of pedestrian-accident-related information of Thiruvananthapuram City
- Identification of study stretch
- Primary data collection from field studies
- Formulation of accident prediction models
- Model validation and testing of models
- Analysis of results and proposal of pedestrian safety enhancement strategies.

The accident data of Thiruvananthapuram City, which includes the urban and rural regions, during the year 2010–2014 were collected from the State Crime Records Bureau (SCRB), Pattom. The road stretch along NH-66 which has recorded the maximum number of pedestrian accidents was selected for the study. In order to identify the study stretch, the NH-66 starting from Kadampattukonam to Kaliakkavilai, a total

distance of 80.7 km and the NH-66 Bypass starting from Kazhakkottam to Kovalam of distance 24.7 km was considered. It has been found that even though NH-66 passing through the city has fairly better pedestrian facilities, a greater percentage of pedestrian accidents occur along this stretch. It has been found that urban road section from Ulloor to Karamana has recorded the highest pedestrian accidents per km length. Hence, the study stretch was selected as starting from Ulloor to Karamana along NH-66 and having a total length of 9.5 km. The study stretch was further divided into 19 sections of 500 m each. The accident details of the study area are specified in Table 1.

The primary data collected include the road inventory, inventory of pedestrian walking and crossing facilities, inventory of roadside features, traffic and pedestrian volume, speed of vehicles and adjoining predominant land use. The inventory data that included nearly 40 variables were collected for every 100 m along the study stretch from Ulloor to Karamana from field surveys.

A detailed survey of road inventory was carried out in order to determine the road geometric parameters like number of lanes, roadway width, type of shoulder, shoulder width, type of median, width and height of median. The geometric data was taken for every 100 m and averaged for a section. The features of footpath like width

Table 1 Pedestrian accident data of study stretch

Section code	Chainage	Total pedestrian accidents	Fatal injury	Grievous injury	Minor injury
1	0–500	9	1	4	4
2	500–1000	1	1	0	0
3	1000–1500	6	0	4	2
4	1500–2000	3	0	3	0
5	2000–2500	11	0	11	0
6	2500–3000	13	1	10	2
7	3000–3500	5	0	5	0
8	3500–4000	0	0	0	0
9	4000–4500	9	0	7	2
10	4500–5000	29	0	24	5
11	5000–5500	6	0	5	1
12	5500–6000	16	0	13	3
13	6000–6500	6	0	6	0
14	6500–7000	42	6	22	14
15	7000–7500	5	1	2	2
16	7500–8000	1	0	1	0
17	8000–8500	7	0	6	1
18	8500–9000	11	2	5	4
19	9000–9500	29	2	23	4

and height of footpath, type of footpath and length of guard rails were measured for each section of the study stretch. The data collected also include crossings classified as signalized and unsignalized, with and without refuge, poor and adequate, etc. The crossings were considered as adequate based on three conditions such as the presence of suitable sign boards, clear markings and visibility of the pedestrian waiting to go across the road. The access roads are classified as minor, intermediate and major based on their width. The number of bus stops, schools, hospitals, religious establishments and alcohol sales establishments along the roadside was recorded. A study indicated that pedestrian casualties were related to the number of hospitals and schools located within a radius of 100 and 150 m [6]. Traffic volume has been found to be an important factor affecting accidents [7]. Classified volume count was taken at all major junctions, and peak-hour traffic in terms of PCU was calculated. Pedestrian volume count along the footpath and along the crossing at peak hour was taken at major crosswalk locations. The average speed of vehicles passing through a particular section was found out by conducting moving car observer method.

5 Analysis and Modelling

A statistical model portrays how different variables are related in terms of mathematical equations. Several accident prediction models were used to assess pedestrian risk from police crash data [8]. Different generalized linear models were developed in SPSS 20 software to identify the best relationship among variables. Correlation analysis and scatter plots were obtained to identify the distribution of the data set. The results signify that the relation between the variables and pedestrian accidents is nonlinear.

5.1 Development of Prediction Models

The pedestrian accident prediction models were developed using the total number of pedestrian accidents at each 500 m sections as the dependent variable. Since there were a large number of independent variables, it was not desirable to include all the variables in the model. Hence, several steps were used to lessen the number of variables [9]. In order to identify the factors influencing the severity of pedestrian accidents, models were also developed for grievous injury, minor injury, and fatal injury. From the 19 sections identified as the study area, randomly selected 13 sections were kept for modelling, whereas the remaining sections were reserved for validation. After validation and selection of the best fit model, final models were developed using all the sections.

Among the generalized linear models developed using SPSS software, poisson regression model provided a better fit. The best model was preferred as the one having the least Akaike Information Criterion (AIC) value [10]. The models were

said to be valid only if all the parameters used in the model were significant at 5% level of significance. The final models which satisfied all the statistical tests are specified in Table 2.

5.2 Model Validation

Validation in regression analysis is the process of identifying whether the model represents the actual system. It helps in estimating the sturdiness of the model. In this study, the model for predicting total pedestrian accidents as well as their severity is validated using the Chi-Square test for goodness of fit. R^2 values were also obtained in order to verify the robustness of the model and were in accordance with Chatterjee et al. [11]. The results are specified in Table 3. The obtained values of Chi-square are less than the statistical table value for five degrees of freedom at 5% significance level. The R^2 values are greater than 0.85 which indicates the goodness of fit between the observed and predicted values.

6 Strategies for Improving Pedestrian Safety

A sensitivity analysis was carried out in order to quantify the variation of number of crashes with the causative factors. Based on the site study, models developed and sensitivity analyses, the effect of various accident causative factors and recommendations for improving pedestrian safety in urban areas are summarized.

Pedestrian safety near to bus stops must be enhanced through the scientific design of bus bay, bus shelter, optimizing number of bus stops, etc. The total accidents and grievous accidents can be reduced by 2.13 and 3.63%, respectively, when the number of bus stops per 500 m decreases by 5%.

Suitable traffic calming measures near pedestrian crossing locations must be adopted to control speeding vehicles. Traffic rules must be strictly enforced so that drivers yield to pedestrians at zebra crossings. A 5% decrease in speed will result in 20% reduction in total pedestrian accidents.

Traffic volume must be controlled during peak hours by exploring alternate route options and through ITS applications such as advanced traveller information system. Congestion pricing and effective utilization of public transit system will help in reducing private vehicles. A 5% decrease in traffic volume during peak hour in terms of PCU will result in 11% decrease in total pedestrian accidents and 12.2% reduction in grievous injury accidents.

A decrease in the number of intermediate side roads should be ensured, especially in section 14, or suitable traffic calming measures must be adopted at the junctions. It is to be ensured that U-turn should not be allowed where pedestrian crossings are provided and vice versa. Signalized pedestrian crossing such as pelican and puffin crossings should be installed at all locations. Such crossings should be integrated

Table 2 Pedestrian accident prediction models developed

Accident type	Model
Total accidents	$TOA = e^{(-5.530 + 0.304NOB + 0.193S + 0.000608PCUph - 0.268NCQA + 0.000133PVF)}$
Grievous accidents	$GI = e^{(-1.924 + 0.525NOB + 0.000679PCUph + 0.232ISR)}$
Minor accidents	$MI = e^{(-7.099 + 0.299S + 0.000348PVC - 0.348NCQA)}$
Fatal accidents	$FI = e^{(-17.308 + 0.695S - 0.989NSC)}$
Combined fatal and grievous injury accidents	$FGI = e^{(-2.652 + 0.408 * NOB + 0.146 * S + 0.172 * NOZU + 0.000084 * PVF)}$

The parameters mentioned in the model are:

TOA total number of pedestrian accidents, *GI* number of grievous injury accidents, *MI* number of minor injury accidents, *FI* number of fatal injury accidents, *FGI* number of combined fatal and grievous injury accidents, *NOB* bus stop density/500 m, *S* speed of vehicles in km/h, *PCUph* total number of vehicles in PCU/hr, *NCQA* number of crossings whose quality is adequate, *PVF* peak hour Lateral Pedestrian volume, *ISR* intermediate side roads, *PVC* pedestrian cross volume, *NSC* number of signalized crossing, *NOZU* number of pedestrian crossings where U-turn is possible

Table 3 Model validation results

Model	Chi-square value	R^2 value
Total pedestrian accidents	2.1289	0.959
Grievous injury accidents	5.57122	0.898
Minor injury accidents	7.07301	0.869
Fatal injury accidents	4.70373	0.898
Combined fatal and grievous injury accidents	8.24273	0.846

with signals installed in nearby intersections to prevent queuing. Clear markings, adequate sign boards and proper visibility must be maintained at all designated pedestrian crossing locations.

The width of footpath must be increased in those areas having high pedestrian volume. The footpath along the road stretch from Palayam to Thampanoor must be widened to accommodate high pedestrian volume. Overpasses or underpasses must be provided in areas having high pedestrian crossing and traffic volume, especially in Thampanoor where there is a large number of pedestrians crossing this road at all times of the day owing to the presence of transit terminals, both railway station and bus station opposite each other. Area-wide pedestrian mobility management will enhance accessibility, mobility as well as the safety of pedestrians. Traffic rules equally apply to pedestrians as well and should be strictly enforced. It should be made obligatory that all pedestrians use the footpath and the crosswalks.

7 Conclusions

Models were developed for predicting total pedestrian accidents and severity levels—grievous, minor and fatal. It was found that Poisson regression models are found to be the best fitting. Validation of the models proved that it could be further used for predicting pedestrian accidents in urban midblock sections. Bus stop density, vehicle speed, peak-hour traffic volume and pedestrian volume, density of access roads, signalized crossings and quality of crossings proved to be significant factors. Proper accomplishment of the recommended strategies will help in reducing pedestrian accidents.

References

1. Satiennam T, Tanaboriboon Y (2003) A study on pedestrian accidents and investigation of pedestrian's unsafe conditions in Khon Kaen municipality, Thailand. *J Eastern Asia Soc Transp Stud* 5:95–110
2. Wedagama DMP, Bird R, Dissanayakea D (2008) The influence of urban land use on pedestrians casualties. *IATSS Res* 32(1):62–73

3. Obeng DA, Salifu M (2013) Modelling risk factors of pedestrian accidents on trunk roads in Ghana. *Int Refereed J Eng Sci* 2(5):55–64
4. Abojaradeh M (2013) Evaluation of pedestrian bridges and pedestrian safety in Jordan. *Civil Environ Res* 3(1):66–78
5. Haghighatpour PJ, Moayedfar R (2014) Pedestrian crash prediction models and validation of effective factors on their safety (Case Study: Tehran signalized intersections). *Open J Civil Eng* 4:240–254
6. Satiennam T, Tanaboriboon Y (2003) A study on pedestrian accidents and investigation of pedestrian's unsafe conditions in Khon Kaen Municipality, Thailand. *J Eastern Asia Soc Transp Stud* 5:95–110
7. Karlaftis MG, Golias I (2002) Effect of road geometry and traffic volumes on rural roadway accident rates. *Accid Anal Prev* 34(3):357–365
8. Turner SA, Roozenburg AP, Francis T (2006) Predicting accident rates for cyclists and pedestrians. Report 289, Land Transport New Zealand Research, New Zealand
9. Schneider RJ, Diogenes MC, Arnold LS, Attaset V, Griswold J, Ragland DR (2009) Association between roadway intersection characteristics and pedestrian crash risk in Alameda County, California. *Transp Res Rec J Transp Res Board* 2198:41–51
10. Pour MH, Prasetyo J, Yahaya AS, Ghadiri SMR (2012) Modelling vehicle pedestrian crashes with excess zero along Malaysia federal roads. *Soc Behav Sci* 53:1218–1227
11. Chatterjee A, Wegmann FJ, Fortey NJ, Everett JD (2001) Incorporating safety and security issues in urban transportation planning. *Transp Res Rec J TRB* 1777:75–83

Understanding Driver Behavior at Intersection for Mixed Traffic Conditions Using Questionnaire Survey



Ajinkya Ingale, Prasanta Sahu, Rishabh Bajpai, Avijit Maji and Ashoke Sarkar

Abstract Intersection is a critical location for drivers due to the increase in a number of accidents at conflict points. Besides instrumental error and defective road design, driver behavior is the major cause of such crashes. Driving comprises of the various driving tasks which govern the driver behavior. This study attempted to assess the driver's decision-making behavior at intersections. A questionnaire survey of 770 drivers was conducted in Jaipur city to understand the driver's behavior and tasks at the intersections. The questionnaire dealt with driver's behavior at the signal, dilemma zone analysis, and driver comprehension about the signage. Based on the analysis, it was found that factors like education, age, gender, driving experience, frequency, and income level influence the driver behavior at the intersection. Standard statistical tests were used to analyze the association of driver demographic characteristics with the driver behavior at intersections. Understanding the Indian driver behavior at intersection can aid the development of a better design to accommodate driver expectations while navigating an intersection in mixed traffic condition.

Keywords Driving task · Intersection · Perception-decision-action · Road marking · Traffic sign

A. Ingale · R. Bajpai · A. Sarkar
Birla Institute of Technology and Science Pilani, Pilani 333031, Rajasthan, India
e-mail: ingaleajinkya@yahoo.com

R. Bajpai
e-mail: bajpai.rishabh12@gmail.com

A. Sarkar
e-mail: asarkarbits@gmail.com

P. Sahu (✉)
Birla Institute of Technology and Science Pilani, Hyderabad 500078, Telangana, India
e-mail: prasantsahu222@gmail.com

A. Maji
Indian Institute of Technology Bombay, Mumbai 400076, Maharashtra, India
e-mail: avijit.maji@gmail.com

1 Introduction

Motorization is at its peak by touching the global count of registered vehicles to 1.2 billion globally due to the advancement in technology. The rate of motorization is also showing an increasing trend in India and China with a growth rate of more than 8.5% [1, 2]. The traffic conditions are changing due to the increasing number of vehicles with improved capacities adding to greater mobility. Though the speed is increased, safety concerns are also increased, especially due to driver behavior and mix traffic conditions. According to a global status report on road safety 2015, the total number of fatal road accidents reached 1.25 million making an average of 3287 deaths per day. Besides this, there is a fearing statistics of injuries count of additional 20–50 million drivers in 2015. The statistics in India is also terrifying, as the country stands second highest in the road accident deaths with 11 deaths per 1 lakh population [3]. Among the crashes, it was observed that fifty percent of serious collision occur at the intersection, thus making intersection a critical location for driving [4, 5]. Therefore, this paper focuses on the concerns related to intersection.

There are several potential causes of such crashes, which include improper weather conditions, instrumental error, defective road design, etc., but among them driving behavior is one of the major causes. Drivers complete the driving process by perceiving the situation, deciding on how best to respond to the situation, given the driver's knowledge, and reacting to the situation. Driving is a complex process consisting of control, guidance, and navigation of vehicles [6–8]. For example, yawing of the steering wheel or applying brakes may result in a situation where the vehicle responds for turn change. These driving tasks depend on traffic conditions (density, vehicle mix), geometric conditions, environmental conditions, and other conditions like type of road, road furniture, markings, and traffic controlling measures. This perception-decision-action (PDA) of the driving task is assisted by a traffic signal, marking, and signage for efficient movement across road segments [5, 9]. The related driving tasks play a vital role in guiding and controlling vehicles. Roadway segments like intersections require the processing of more driving tasks than any other type.

Traversing or driving through an intersection is the most complex task. The intersection involves four critical driving states. These states are: (1) vehicles are turning left, (2) turning right, (3) going straight, and (4) stopping safely without any conflict [5, 6]. The intersection becomes a critical location due to the misinterpretation of the sign, cross and rear-end conflicts, vehicle interaction with road furniture, all governed by human behavior. For successful navigation, the driver is expected to recognize and accept the available information, to process and to take a proper action. The driving becomes complex because the driver has to perform a number of mentioned tasks below within a stipulated small time. As it requires more number of tasks, the greater is the possibility of human errors resulting in crashes. The errors that drivers commit which lead to accidents are usually due to lack of knowledge or misinterpretation or missing some additional information about the traffic condition ahead.

The major concern at the intersection is traffic signal phasing, pointing toward the dilemma zone area, where the drivers are left with the confusion whether to stop

or proceed at the intersection before stop line when the signal phase turns amber [8]. Major cross conflicts occur due to improper decision take in the dilemma zone. Researchers also studied that besides the traffic signal phasing, visibility and vehicles ahead also affect the driving task at the intersection and adding safety concern critically [10]. Many studies inferred that the presence of lead vehicle changes driving behavior [10, 11]. The visibility at intersection adds to the better perception of the traffic phasing leading to lesser conflicts [11, 12]. Another major concern is about the knowledge and awareness about the traffic signs to the drivers. The traffic signs convey the information through pictorial format or in words, which helps the driver in guiding and navigating vehicle [13]. The traffic signs are supposed to be effective if there is an appropriate change in the driving style of drivers [14]. The change in the driving style is due to many factors such as age, experience, type of vehicle used, and the frequency of vehicle usage [13–16]. Other major concerns are the inconsistent geometric layouts, weak lane discipline, driving behavior and improper location, and improper knowledge of signage which violates the driver's expectancy and may lead to accidents. Thus, to understand the driver's expectancy, understanding and analyzing the driver behavior will be helpful. Thus, to enhance safety while driving, there is a need to capture, understand, and analyze the driving behavior. Though, the prediction of driving behavior can be stochastic rather than being deterministic [17, 18]. This study attempts to investigate the behavior of Indian drivers at 4-legged intersections on an urban road network.

Capturing the behavioral data is a complicated task. Researchers have a keen interest in getting accurate behavioral data so that their behavioral model can be made reliable. Researchers used the driving simulator for collection of driving behavior data [9, 19, 20]. The change of speed characteristics as well as lateral position change depending upon lane width, shoulder width or the presence of external features like trees, guard rails, road marking, signage, etc. can be captured with the help of driving simulator [20]. The effect of signal ahead sign was studied with the help of driving simulator, and it was found that the greater the speed of the vehicle the lesser is the possibility of the vehicle to stop [19]. Studies were also used to collect the dilemma zone condition, and based on the model developed, it was used to design the dilemma zone [9]. Besides simulator, videographic data can provide information about the lateral position, and speed gun will give the spot speed at the desired location. Data can also be collected with the help of instrumented vehicles (IV) along with different sensors [21]. Along with speed and general kinematics of vehicle, psychophysical interaction of driver like fatigue can be found with the help of IVs [22]. Studies also focused on the interaction of driver with external factors like a traffic signal, signage, environmental condition, vehicles around, etc. which indicated the change in behavior according to change in space and time [17]. Data was also collected using static evaluation method where the drivers were shown images or videos of real world as well as simulator and were asked about their desired speed selection for different external conditions [20].

The above mentioned studies indicated that more accurate behavioural data collection is associated with huge cost. In order to cover a large area with minimal cost, questionnaire survey is the best alternative. There are various kinds of ques-

tionnaire survey like telephonic survey, web-based survey, paper-based survey, etc. This study deals with the use of paper-based questionnaire survey for understanding driver behavior. There had been many studies which involved the use of a questionnaire survey in the prediction of accident. Manchester Driver Behavior Questionnaire is a popular tool involved in such kind of analysis where errors, violations, slips, and lapses are the major factors influencing the accidents. The study indicated an aggressive violation as the prime factor involved in crashes [23]. To study the driver behavior and the self-assessment for their involvement in crashes, telephonic questionnaire survey technique was utilized. Paper-based questionnaire survey can also be an alternative for capturing error, violation, and self-assessment [24, 25]. Questionnaire survey is used in capturing various factors like demographic information, driver's information and license type, duration of driving and driving exposure, traffic violation, involvement in crash, visual ability, driving skills, psychological factors, mood, trip and vehicle characteristics, and other external factors, which generally govern the speed selection and driver behavior [24, 26, 27].

In brief, this study focuses on the understanding of driver decision-making behavior at 4-legged signalized intersections using a questionnaire survey. The questionnaire survey will reveal behavior at dilemma zone, traffic signal understanding and check the correct perception about the signage. Therefore, the first objective of the study is to analyze and interpret the driver's decision-making behavior and safety-related attitudes at the intersection. The driver's decision-making process depends on the perception made by the individual regarding signage and signal, especially related to dilemma zone, thus forming the second objective of the study to understand driver's perception of signal and signage.

2 Methodology

This study dealt with the analysis of driver behavior using a questionnaire survey. The methodology for the analysis consists of four steps. These steps are: (1) identification of locations within the study area to conduct the survey; (2) development of questionnaire; (3) data collection from sample participants; and (4) statistical analysis of the driver data.

2.1 *Identification of Locations for Survey*

The study considered Jaipur city as a study area to find the drivers, who had experience of driving in urban signalized intersections. In order to avoid and rush of vehicles, the study was conducted in parking lots, taxi and auto stands, and other recreation activities park, where people can spare 3–4 min in responding the questions.

2.2 Questionnaire Development

The driver behavior and tasks at the intersection can be analyzed by surveying drivers for their decision-making behavior, their perception regarding the controlling measures like traffic signal, marking and signage, and implementation of knowledge acquired by them. The questionnaire was mainly designed to know about the speed characteristics and the driver's perception of the commonly used signage and also about the dilemma zone at signalized intersection. The basic criteria to be taken into consideration are ease of language and less questions, and there should not be any confusion in the questions.

The questionnaire focused on five parts: demographics, general driving behavior, behavior at intersection and dilemma zone, perception about signal and signage, and the level of driver assistantship required. All the five sections made 33 questions together. A pilot survey was conducted in Jaipur city to check the kind of response and ambiguous questions. It was observed that people are facing some difficulty in understanding the concept of driver assistantship, and also, some questions were found to be ambiguous to the drivers. Hence, the questions were simplified, and the number of questions was reduced from 33 to 22.

The modified questionnaire mainly consisted of four major parts. The first part took care of the demographic characteristics of the driver. Previous study has shown the change in driving characteristics with the change in parameters like age, sex, education, and income level. Vehicle ownership was also considered in order to check the behavioral difference with the ownership. The second part consisted of questions about general driving characteristics about the type of vehicle, speed of vehicle the driver prefers, and the frequency of travel. It also takes care of the lane choice behavior which further helps in understanding the driver behavior in a better way. The third part consists of the questions related to driver's behavior at intersection and dilemma zone. It provided information about the driver's usual tendency to behave during the amber time. The fourth part checks the knowledge of driver about the signage. The sample drivers were shown some images of some common signage like speed limit, give way, crossroad, no entry, no U-turn, and pedestrian crossing. Thus, it helped in checking the awareness of signage among drivers. The survey reveals key information about the choice of speed, speed regulation, and perception ability of drivers which provides an important input in designing intersections for safety and mobility.

2.3 Data Collection from Sample Participants

A total of 770 participants were interviewed in urban areas of Jaipur city and were usually questioned in parking lots. The selection of drivers was random, but it was ensured that the age of the drivers is more than 18, which was the official eligibility age to obtain the driving license. 95% (731 drivers) of the total sample number were holding a driving license, while 5% (39 drivers) were not holding it and were neglected for the purpose of analysis. All types of vehicle classes, like two-wheeler,

three-wheelers, car and trucks, were considered for the questionnaire survey. The drivers were explained about the project and assured about the confidentiality of their responses to avoid biasness of the data.

2.4 Statistical Analysis of Driver Data

To analyze the driver behavior, researchers have used various types of statistical tools to predict the driver behavior and aid their driving process. Statistical tests like *F*-test, Cronbach's alpha coefficient, significant factor analysis, ANOVA, multivariate linear regression, CHAID (Chi-square Automatic Integrated Detector) to analyze the psychometric parameters of driver, for self-assessment of drivers, prediction of accidents, and to check the awareness of the traffic signage among the drivers [9, 17, 18, 24–29].

This paper deals with descriptive analysis of the data collected, reliability analysis of the variables and the chi-square test. The descriptive analysis represents the brief statistics that summarize the dataset. It gives the basic idea about the population surveyed with the frequency of the response of different questions. To measure a latent variable, the consistency of the variables is checked with internal consistency reliability test. The internal consistency reliability test is interpreted with the help of Cronbach's alpha coefficient, whose value lies between 0 and 1. It measures the interrelatedness of a sample of test items, amount of error in measurement and is also used to confirm the homogeneity of the items. The Cronbach's alpha coefficient can be given the following formula:

$$\alpha = \frac{k \times c'}{v' + (k-1)c'}$$

where k = number of items, c' = average of all covariance between items, and v' = average variance of each item.

The association between the driving behavior and the demographic variables needs to be inspected in order to understand driver behavior. The chi-square test of independence serves the purpose when both the variables are categorical and the sample collection is random. To find the significant relation, the frequencies of the observed and expected are compared to check the null hypothesis. It is expected that 90 drivers with income level of 2–4 lakh will stop at the intersection, while it was observed that 94 drivers do the same. Such comparison will be done for each income level and can be applied in the following formula:

$$\Sigma X_i^2 = \sum (O_i - E_i)^2 / E_i$$

where O_i = Observed value of two variables; E_i = Expected value of two variable; and X_i^2 = Chi-square test value.

3 Descriptive Analysis

The dataset was represented in terms of descriptive statistics. The socio-demographic data is summarized in Table 1. Indian driver population is mainly dominated by men by sharing 80.71% of the total number of drivers. The education level of the driver population showed that the majority of drivers were either 12th or graduates forming together 85.49% of the complete sample size. The age group distribution was decided according to WHO standards [30–33], grouping them into the age groups as 18–24, 25–44, and 45–64. Drivers of age group 25–44 have a major proportion, as they are

Table 1 Socio-demographic factors

Socio-demographic factors		Frequency	Percentage
Gender	Male	590	80.71
	Female	141	19.29
Education level	10th	60	8.21
	12th	267	36.52
	Graduation	358	48.97
	Post-graduation	46	6.30
Age	18–24	175	23.94
	25–44	472	64.57
	45–64	84	11.49
Income level	Below 2 lakhs	140	19.15
	2–4 lakhs	213	29.14
	4–6 lakhs	157	21.48
	6–8 lakhs	174	23.80
	Above 8 lakhs	47	6.43
Vehicle type	Two-wheeler	348	47.61
	Three-wheeler	32	4.38
	Car	339	46.37
	Truck	12	1.64
Driving frequency	5–7 days/week	447	61.15
	2–5 days/week	228	31.20
	Once/week	50	6.84
	Once/month	2	0.27
	Rarely	4	0.54
Vehicle ownership	Owned	507	69.35
	Someone else	74	10.13
	Parents	150	20.52
Traffic plate color	White	639	87.41
	Yellow	92	12.59

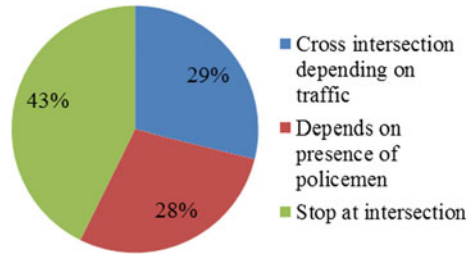
making 65% of total drivers. This may be due to the fact that age group of 25–44 consists of mostly working population, and they are using the vehicles to reach their respective working place. The age group of 18–25 has a major proportion of students and non-license holders. The age group of 45–64 showed the least number of women population drivers.

Out of 731 participants, 75% participants reported their income between 2 to 8 lakhs, while only 6.5% reported income higher than 8 lakhs. The class of vehicle preferred by the population was motorcycle and cars. The questionnaire also tried to capture the vehicle ownership data, and it came to in notice that 69% of the population owned the vehicle. The student class was found to use the vehicle owned by their parents. Number of commercial drivers is 92 (13%), and almost half of these drivers are driving the vehicle owned by others or by the company. Participants were asked to mention the number of days they are driving in a week. From the questionnaire, it was observed that 446 participants (61%) drive 5–7 days per week and 31% drive 2–5 days per week. In this sample, 75% drivers are having the experience between 1 to 15 years. For men, the distribution is fairly uniform, and 52.4% women are having the experience between 1 to 5 years. Only 8 (0.01% to total drivers) women are found to have the driving experience of more than 15 years, compared to 184 (25% of total drivers) men. Men are having the average driving experience of 13.41 years, which is more than double of that of women which is 6.6 years. Average driving experience is 4.09 years, 12.44 years, and 26.78 years for the age group of 18–24, 25–44, and 45–64, respectively.

The distance traveled in a week was also recorded, as it was easier for driver to memorize it. The women drivers travel on average 120.21 km per week, which is only the two-fifths of the distance traveled by men. All women are driving below 400 km per week, and this reflects the fact that women are making short trips relative to men, as 92 men are driving more than 400 km in a week. It is also observed that commercial vehicle drivers drive much more (average 942.43 km/week) than non-commercial drivers (average 165.615 km/week), which is also expected as they drive most of the time in a day. The above information is useful to understand the socioeconomic characteristics of the participants and formed the basis of reduction in data used in statistical analysis.

The questionnaire also focused to capture the driver's general response to traffic operations at signalized intersection. Participants were asked about the change in the speed while approaching an intersection. About 99% of the participants gave the answer in positive way. It meant that they change their speed when approaching an intersection. The driver behavior at the red traffic signal was enquired and the response showed that 57% participants agree to violate the red traffic signal rule (Fig. 1) and the main concern of 28% (172 males and 36 females) of them was the presence of policemen, indicating the absence of policemen will allow them to violate the signal. It was observed that 65 females (46% of female) and 247 males (41.9% of male), stop their vehicle if the signal turns red, while 36 (25%) females and 172 (29.2%) males, decide depending upon the presence of policemen, whether to stop or not, and for 40 (29%) females and 171 (28.9%) males (Fig. 2), the traffic around them is the criteria to take action at the time of red traffic signal. Also, 75%

Fig. 1 Behavior at red light

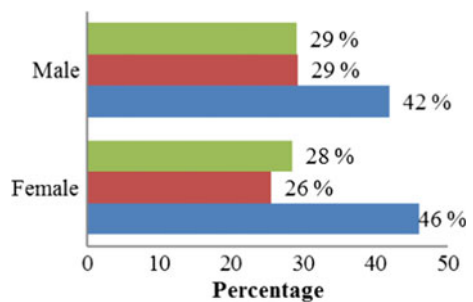


(69 out of 92) of the drivers of the commercial vehicles stop their vehicle when red traffic light appears, and the proportion for the non-commercial drivers is 38% (243 out of 639) for the same. This indicates that the commercial drivers understand the traffic rules better than the non-commercial drivers.

The questionnaire also observed the driver’s behavior during dilemma zone. There was a poor understanding of the amber light and only 35% drivers stop their vehicle at the intersection, and this reveals that 65% drivers are creating the situation of collisions. The amber time creates a sort of confusion, and it can be depicted with 48% of the drivers find it difficult during the green to yellow transition.

Regarding the sufficiency of amber time, 52% of the drivers found the amber time as adequate. Thus, many of them are found to be violating the red signal. About 44% of the drivers usually find themselves ending up running in the red light in which the proportion of female getting caught in amber to red transition is more than men. The perception of traffic signs is a vital part in the guidance and navigation of vehicle. The drivers were assessed for their perception of six traffic signs, and the results are as shown in Fig. 3. It was observed that pedestrian crossing sign was predicted correctly by the majority of the drivers, while give way was percept correctly by very few participants.

Fig. 2 Response to red traffic light



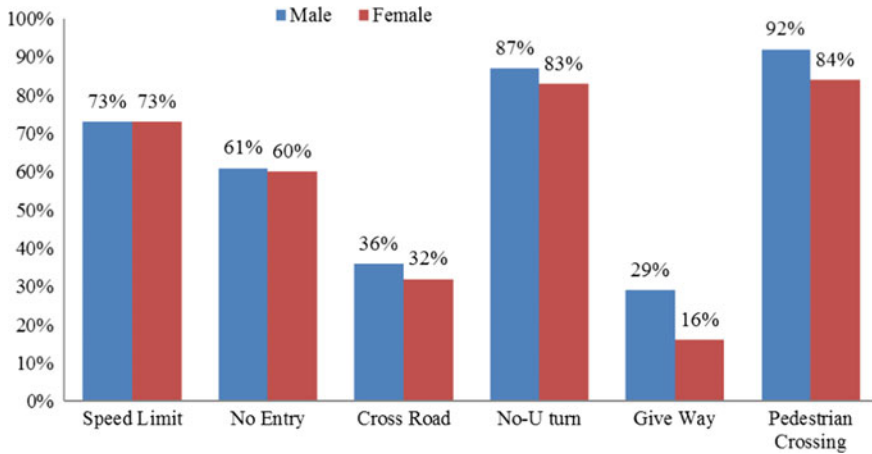


Fig. 3 Perception of traffic signs by drivers

4 Results and Discussion

This study used two statistical analyses such as reliability analysis and chi-square test, which basically gave the internal consistency in measurement and the association of different socio-demographic variables on the behavior of driver at signalized intersection.

4.1 Reliability Analysis

The primary focus of this study is to understand the driving behavior and their safety attributes at the intersection. The safety concerns cannot be measured directly and can only be interpreted with the help of certain questions defining the purpose. Cronbach’s alpha coefficient found in this study is 0.57 with 19 items. There are many studies which suggest the alpha value within a range of 0.5–0.75 can be considered as good for measuring the internal consistency of the items [29, 34]. Thus, it can be inferred that the variables are internally consistent and can be used for the studies.

4.2 Chi-Square Test

The significance value obtained by performing the chi-square test gives us an idea about the influence of independent variables on dependent variables. The cells highlighted with green show us the p value < 0.05 , which indicates that the particular variable influence the dependent variable. The independent variables like education

Table 2 Association of variables and driver behavior

	Education	Gender	Age	Vehicle type	Driving frequency	Income level	Vehicle Ownership
Behaviour at Red light	✓	*	*	✓	*	*	*
Closeness to front vehicle at stop condition	*	✓	✓	*	✓	*	*
Closeness to front vehicle in motion	*	✓	✓	*	✓	✓	*
Speedometer Check	✓	*	✓	*	✓	✓	*
Perception about Yellow light	*	*	✓	✓	*	*	*
Confusion at amber green transition	✓	✓	✓	✓	✓	✓	*
Reason for getting caught in red light	*	*	*	✓	*	*	*
Frequency of getting caught in red	*	*	✓	✓	✓	✓	*
Adequacy of amber time	*	*	✓	✓	✓	✓	*
Observation of road marking and signage	*	✓	✓	✓	✓	✓	*

level, gender, age, vehicle type, frequency of driving the vehicle, income level, and vehicle ownership have been considered in this study, and the significant association are highlighted in green (Table 2). The chi-square test of independence is used to test the null hypothesis of the sample. Some of the inferences made after the test are given as follows.

4.2.1 Behavior at Red Light

The behavior at red light was portrayed in three situations, namely the presence of policemen, crossing intersection depending on traffic, and stopping at the intersection. All the above-mentioned variables were compared, and only education level ($p = 0.045 < 0.05$) and vehicle type ($p = 0.041 < 0.05$) were considered as variables influencing the behavior at red light. The low educated people stop at red light (48% of people with low education) than highly educated people (39% of people with high education). This indicates the less fear of law for high educated people. Similarly in the case of vehicle type, it shows that with the change of vehicle, the behavior of driver at red light changes. The truck drivers (50%) are more conscious ($p = 0.012 < 0.05$) about the red light signal than the three-wheelers (15%). A supplementary question with three-wheeler drivers revealed that in order to earn more money and to get more passengers, they try to escape the red light.

4.2.2 Driver's Visibility and Perception About Safe Distance

There were two conditions which were considered for driver's safe distance perception, one at stop and one in motion. Variables like age, gender, and frequency of driving were giving a significant influence on the safe distance perception, while an additional variable income level also influenced the perception when the vehicle is in motion. In the first case, more males (49%) stop more close to the vehicle ahead ($p < 0.05$) than females (42%). The adult age people take their vehicle close to the bumper more often than the young and middle age people. In the second case, it was observed that men keep more safe distance than females (46% of males as compared to 34% of females). With consideration of age group, the vulnerable age group of 18–24 ($p < 0.05$, 36%) drove close to the vehicle than the adult age people (48%). It was observed that with the increase in experience, the safe distance between the vehicles started increasing ($p < 0.05$). The test also indicated that with the increase in income level, the drivers are more prone to driving closely ($p < 0.05$). There was not much significant difference in education, vehicle type, and its ownership.

4.2.3 Check of Speedometer While Driving

More than 75% drivers check their speedometers while driving, and all variables, except gender, type of vehicle, and its ownership, showed a significant difference in their habit of speedometer check. About 79% of graduates check their speedometers, while 82% of postgraduates check their speedometers ($p < 0.05$). It was observed that with an increase in age, the habit of speedometer checking is more, indicating ignorance of speed check by youth age ($p < 0.002$). The people with more driving frequency check their speed more often as compared to that of less driving frequency ($p < 0.05$). People either with very high-income level or very low-income level check their speedometer more frequently ($p = 0.005 < 0.05$).

4.2.4 Meaning of Amber Traffic Light and Its Adequacy

The correct perception of yellow light lied around 35%, and there was a significant difference in age and vehicle type to percept the same, while there was difference observed in age, vehicle type and frequency of driving, and income level in case of sufficiency of amber time phasing. The yellow light perception was correct with the increase in age, indicating a more number of young people facing the dilemma zone condition, while vehicle type also showed a significant variation. The younger age people ($p < 0.05$, 65%) felt less adequacy of amber light duration as compared to older people (33%). It was also found that car users did not find the amber time to be adequate as compared to all other vehicle users ($p < 0.05$). Drivers who drive regularly felt the amber time adequate as compared to drivers who drive less frequent ($p < 0.005$).

4.2.5 Frequency of Red Light Violation

The young age people are found to be more involved in red light violation ($p < 0.05$) than the other age groups. Depending on type of vehicle, cars (16%) and trucks (16%) are more involved in red light violation, and it was usually due to lesser yellow time or getting stuck due to the presence of other vehicles. The violation also depends on frequency of driving the vehicle, lesser the frequency, more are the chances if red light violation ($p < 0.05$). The frequency of violation also depends on the people from different income group. There was no significant difference found in education, gender, and vehicle ownership in the red light violations.

4.2.6 Observation of Road Signs

All the variables had a significant difference in the observation of sign, except that of education and vehicle ownership. It has been observed that males are more ignorant to signage than females ($p < 0.05$), while with respect to age, young people are more ignorant than older people. Twenty-three percent of motorcycle owners hardly pay attention to signs as compared to vehicles like truck and car (8 and 9% respectively). The drivers with less frequency of driving are more cautious to signs than regular commuters (16% of less frequently driving drivers to observe the signs always as compared to 1% of regular drivers).

4.2.7 Reason for Violation of Red Light

It seems to be very difficult to accept the null hypothesis in this case, and all the variables except vehicle type seem to be significant. Lack of attention and less yellow time had been found to be affecting cars and motorcycles.

5 Conclusion

This study involved the investigation of Indian driver behavior at the intersection with respect to dilemma zone, speed characteristics, and perception about the traffic signal. The driver questionnaire survey is a tool utilized to cover a large population with less amount of cost involved to collect data related to driver behavior during driving task. The present study analyzed the confusion level at dilemma zone and driver behavior at traffic signal. The analysis suggested that 57% of the drivers are red light violators, which can be controlled with certain traffic measures to reduce crash risk induced due to it. In regard to driver perception about the amber light, we found that only 35% of the drivers know the meaning of the amber signal clearly indicates that there is a significant amount of ambiguity among the drivers regarding the traffic signal, which results in around 48% of the driver population to face the

dilemma. The study was able to capture 5% of the non-driving license holders which add to the risk on the road.

The study was also identified some demographic variables which majorly affect the driver behavior at intersection. From the study, the need for more awareness about the traffic signage was also felt. Limited number of drivers could able to perceive correctly 'give way' sign. The chi-square test revealed about the association of different variables with different behavior at the intersection. This study is a part of our ongoing research on analyzing driver behavior while completing the driving task at intersections; more researches are currently underway. The major challenge lies in incorporating the human aspects in the design of intersections. Understanding the Indian driver behavior at the intersection can aid the development of a better design to accommodate driver expectations while navigating an intersection in mixed traffic condition.

References

1. Sperling D, Gordon D (2008) Two billion cars transforming a culture. *TR News*, 259. Nov–Dec 2008
2. Sousanis J (2011) World vehicle population tops 1 billion units. *Ward Auto World*. 15 Aug 2011
3. Debu C (2016) Road accidents in India. <http://www.mapsofindia.com/my-india/government/road-accidents-in-india>, June 2016
4. <https://www.nhtsa.gov/research-data/national-center-statistics-and-analysis-ncsa>
5. Dash DK (2014) Traffic junctions account for half of road deaths in India. <http://timesofindia.indiatimes.com/india/Traffic-junctions-account-for-half-of-road-deaths-in-India/articleshow/40956759.cms>, 27 Aug 2014
6. Sagberg F (2003) Influencing driver behaviour and safety by road system improvements. Institute of Transport Economics, TØI report 648/2003. Oslo
7. <https://www.murcotts.edu.au/resources/driver-behaviour-training/driver-behaviour>
8. Horberry T, García-Fernández P, Ventsislavova-Petrova P, Castro C (2014) Psychological road audits: background, development and initial findings. *Ergon Aust* 6:1
9. Machiani SG (2014) Modeling driver behaviour at signalized intersections: decision dynamics, human learning, and safety measures of real-time control systems. Blacksburg, Virginia, 4 Dec 2014
10. Rittger L, Schmidt G, Maag C, Kiesel A (2015) Driving behavior at traffic light intersections. *Cogn Technol Work* 17(4):593–605
11. Bass P, Charlton SG (2005) Influencing driver behavior through road marking. In: *The New Zealand Road markers federation conference*, Christchurch, 17–19 Aug 2005
12. Liu Y, Ozguner U (2007) Human driver model and driver decision making for intersection driving. In: *Proceedings of the 2007 IEEE intelligent vehicles symposium Istanbul, Turkey*, 13–15 June 2007
13. Kaul R, Baumann M (2013) Cognitive load while approaching signalized intersections measured by pupil dilation. *Tagung experimental arbeitender Psychologen*, Vienna
14. Caird JK, Chisholm SL, Lockhart J (2008) Do in-vehicle advanced signs enhance older and younger drivers intersection performance? *Driving Simulation and eye movement results*. *Int J Hum Comput Stud* 66(3):132–144
15. Jamson SL, Tate FN, Jamson AH (2005) Evaluating the effects of bilingual traffic signs on driver performance and safety. *Economics* 48(15):1734–1748

16. Kline TJB, Ghali Laura MG, Kline DW, Brown S (1990) Visibility distance of highway signs among young, middle-aged, and older observers: icons are better than text. *Hum Factors J Hum Factors Ergon Soc* 32:609–619
17. Xi Z, Levinson D (2006) Modeling pipeline driving behaviors: a Hidden Markov Model approach. *Transp Res Rec* 1980
18. Li J, He Q, Zhou H, Guan Y, Dai W (2016) Modeling driver behavior near intersections in hidden markov model. *Int J Environ Res Public Health*
19. Yan X, Radwan E, Guo D, Richards S (2009) Impact of signal ahead pavement marking on driver behavior at signalized intersections. *Transp Res Part F* 12(1):50–67
20. Fitzpatrick CD (2014) The effect of roadside elements on driver behavior and run-off-the-road crash severity, Masters Theses 1911, University of Massachusetts Amherst, Feb 2014
21. Bifulco GN, Galante F, Pariota L, Spina MR, Del Gais P (2014) Data collection for traffic and drivers' behaviour studies: a large-scale survey. *Procedia Soc Behav Sci* 111:721–730
22. Karali S, Gyi DE, Mansfield NJ (2016) Driving a better driving experience: a questionnaire survey of older compared with younger drivers. *Ergonomics* 60(4):535–540
23. Darren W, James F, Jeremy D (2006) Utilizing the driver behavior questionnaire in an organizational fleet setting: are modifications required. *J Australas Coll Road Saf* 17(2):31–38
24. Shi J, Bai Y, Ying X, Atchley P (2010) Aberrant driving behaviors: a study of drivers in Beijing. *Accid Anal Prev* 42(4):1031–1040
25. Harrison WA Psychometric and Rasch analysis of the driver behaviour questionnaire (DBQ): implications for its use as an evaluation tool with novice drivers. Eastern Professional Services Pty Ltd., Melbourne, Victoria, Australia. <https://warrenharrison.files.wordpress.com/2012/06/free-access-to-psychometric-and-rasch-analysis-of-the-dbq.pdf>
26. Harrison W (2009) Reliability of the driver behaviour questionnaire in a sample of novice drivers. In: 2009 Australasian road safety research, policing and education conference, 10–13 Nov 2009
27. Quimby A, Maycock G, Palmer C, Buttress S (1999) The factors that influence a driver's choice of speed—A questionnaire study. *TRL report* 325
28. af Wählberg A, Dorn L, Kline T (2011) The Manchester driver behaviour questionnaire as a predictor of road traffic accidents. *Theoret Issues Ergon Sci* 12(1):66–86
29. Halit AH (2014) The Validity and reliability test for career intervention program questionnaire (CIPQ). *Int J Soc Sci* 19:2305–4557
30. <http://economics.times.indiatimes.com/news/politics-and-nation/india-has-worlds-largest-youth-population-un-report/articleshow/45190294.cms?intenttarget=no>
31. Sodikin Munawar A, Setiadji BH (2016) Drivers' comprehension of the traffic signs. *Int J Sci Res (IJSR)* 5(2):2319–7064
32. <http://www.dailymail.co.uk/health/article-2430573/An-adult-18-Not-Adolescence-ends-25-prevent-young-people-getting-inferiority-complex.html>
33. Profile of Youth in India, Analysis of NFHS-3 Data. https://en.wikipedia.org/wiki/Middle_age
34. Streiner DL (2003) Starting at the beginning: an introduction to coefficient alpha and internal consistency. *J Pers Assess* 80(1):99–103

Vehicle Category-Wise Service Time Analysis at Tollbooths Under Mixed Traffic Scenario



Mahaveer Singh, Yogeshwar V. Navandar and Ashish Dhamaniya

Abstract The present work carried out to study the relationship between service time and toll rate under mixed traffic condition. Data used for the present study collected from five different toll plazas located on the northern and western part of India. Field observation shows that there is a variation in service time from 2.52 to 63.44 s. This variation in service time may be due to mixed traffic condition, drivers and tollbooth operator's personal attributes, and varying toll rate for different vehicle classes. Service time variation with respect to toll rate studied in the present study. The result shows that the polynomial relationship exists between service time and toll rate. This may be due to service time increases as the toll rate increases up to stable condition then it will start to decrease. It may happen due to toll amount in terms of fifty or hundred required less exchange amount consequently less service time. The study may be useful for toll plaza management and planners to decide toll rate and optimum service time of the vehicle to increase the efficiency of the tollbooth.

Keywords Tollbooth · Toll plaza · Service time · Toll rate · Mixed traffic

1 Introduction

India is a developing country, growth rate and population rate increase exponentially, and due to this, there is an immense requirement of road infrastructure. Due to lack of government funding and higher requirement of road infrastructure, most of the highway projects awarded on public–private partnership (PPP) basis. In PPP projects, private players design, construct, and maintain a particular highway. They will be

M. Singh · Y. V. Navandar · A. Dhamaniya (✉)

Department of Civil Engineering, Sardar Vallabhbhai National Institute of Technology, Surat 395007, India

e-mail: adhamaniya@gmail.com

M. Singh

e-mail: mahaveersingh0107@gmail.com

Y. V. Navandar

e-mail: yogeshwaryog@rediffmail.com

© Springer Nature Singapore Pte Ltd. 2020

T. V. Mathew et al. (eds.), *Transportation Research*, Lecture Notes in Civil Engineering 45, https://doi.org/10.1007/978-981-32-9042-6_52



Fig. 1 Mixed traffic at GTP, MTP, and GFTP

entitled to collect taxes in the form of toll against their investment. In India, most of the toll plaza is having a manual type collection system. On manual collection according to vehicle class and their rate, cash is received by the tollbooth operator. The length of time required to collect this toll at tollbooth is known as service time. Service time depends on many factors such as vehicle class, toll rate, driver, and tollbooth operator's personal attributes [1–3]. Toll rate per kilometer for different type of vehicles has been prescribed for public funded projects in National Highways Fee (Determination of Rates and Collection) Rules [4]. These rates were decided based on saving in vehicle operating costs, damage caused by different type of vehicles, acceptability, and willingness of users to pay. This rate revised based on wholesale price index (WPI) annually in the month of April. Due to this, toll rate varies for all vehicle categories based on road length by the respective undertaking agencies. In India, heterogeneous traffic condition presents and the same is observed at the toll plaza (Fig. 1). Dedicated lanes provided according to vehicle class, but no one follows prescribed rules. Due to varying toll rate and mixed traffic condition, service time variation observed in a different vehicle category. There is limited research available on service time varies according to toll rate in mixed traffic condition. Hence, the present work is carried out to find the effect of the toll rate on service time at tollbooths in mixed traffic condition.

2 Literature Review

According to the study of Woo and Hoel, the service time was found to decrease as the volume at tollbooth increases which might be due to the pressure on the toll collectors to process on the faster rate at the time of queue [3]. Pursula suggested the average service time values from their study as 3.8 (s), 7.5, 10, and 20 s for E-ZPass, token only, token and manual and manual only, respectively [5]. Klodzinski and Al-Deek

and Gordon reported from their study that the service time is the most prominent parameter for calibration of the simulation models [1, 6]. Oliveira and Cybis analyzed the influence of service time on the toll plaza operations and thus reported that the service time mainly depending upon the number of coins processed by the toll collecting attendant [7]. Operational characteristics and capacity estimation were carried out by various researchers using the microscopic simulation model such as TPSIM [1, 8], PARAMICS [9], SHAKER [10], GENTOPS [11], and VISSIM [12, 13].

The Indian Roads Congress (IRC-SP:84:2014) specified a capacity of 240 vehicle/hour for semi-automatic toll lane while considering the maximum service time of 10 s per vehicle at peak flow condition irrespective of the vehicle type [14]. However, IRC is not able to specify the particular vehicle category-wise service time values.

The review of the literature presented above reveals that different researchers have studied processing time (service time), capacity, and simulation studies on toll plaza. There is limited research available on the service time analysis in a mixed traffic condition. Hence, the present work is carried out to find the effect of the toll rate on service time at tollbooths in mixed traffic condition.

3 Research Methodology

Field data on 30-min classified traffic volume count and service time was collected from five different toll plazas located in India. Toll rate amount is depended upon vehicle class, whereas service time is random stochastic variable. The statistical analysis is carried out considering the toll rate as an independent variable and service time as a dependent variable to study the effect of toll rate on the service time. This equation shows the relationship between service time and toll rates. Best fit line for data set is polynomial second order. Second-degree polynomial equation with two roots was derived with one root positive and the other negative. The form of equation considers in the present study as shown in Eq. (1).

$$Y = C + AX + BX^2 \quad (1)$$

where

Y = Average service time, X = Toll rate, C = Constant, and A and B = Quadratic function parameter.

4 Data Collection

To analyze the variation in service time at toll plaza, field observations were collected from five different toll plaza over northern and western regions of India to capture the diversity in drivers' and the tollbooth operators' behavior. Out of the five locations,

Table 1 Study locations and survey details

Sr. No.	Name of toll plaza	City	State	Date and day	Timing	Number of lane
1	Ghoti toll plaza (GTP)	Nasik	Maharashtra	9/3/2016 to 12/3/2016 (Thursday to Sunday)	9 AM to 12.30 PM and 3 PM to 6.30 PM	6
2	Gurgaon-Faridabad toll plaza (GFTP)	New Delhi	Delhi	24/5/2016 (Tuesday)		7
3	Kerki toll plaza (KTP)	New Delhi	Delhi	26/5/2016 (Thursday)		4
4	Mulund toll plaza (MTP)	Mumbai	Maharashtra	27/9/2016 (Tuesday)		6
5	Dahisar toll plaza (DTP)	Mumbai	Maharashtra	29/9/2016 (Thursday)		2

Mulund and Dahisar toll plaza were located in the western region that is economic capital city Mumbai, another one Ghoti toll plaza was also located in the western region near Nasik (Maharashtra) and remaining two toll plazas, namely Gurgaon-Faridabad and Kerki toll plaza, were located in the national capital region (NCR). The details about the selected toll plazas and traffic survey schedule are given in Table 1.

Data was extracted for 25 number of lanes across different five toll plazas, by rewinding the film on a large screen monitor in the laboratory. Avidemux 2.6 software was used for the convenience and for enhancing the accuracy of extracted data. At the time of extraction, the time was noted up to two decimals of seconds (s) for precision. In the spreadsheet, data like lane number, vehicle class, their entry and exit time at the tollbooth (exactly at the toll window for the transaction) entered. Service time is calculated by subtracting exit and entry time of the vehicle at a particular tollbooth. All vehicles in traffic at the tollbooth were divided into seven classes, and the horizontally projected length for different category of vehicles is mentioned in Table 2.

5 Analysis of Field Data

The extracted data was used to calculate the traffic volume passing per hour and also the traffic composition to check its effect on service time. The field observations showed that the car-only traffic was allowed in lane 1, lane 2, and lane 4 which thus

Table 2 Vehicle class and their sizes

Sr. No.	Vehicle class	Vehicle included	Length (m)
1	Small car (SC)	Car	3.72
2	Big car (BC)	Big utility vehicle	4.58
3	Large commercial vehicle (LCV)	Light motor vehicle	5.00
4	Bus	Standard bus	10.30
5	Heavy commercial vehicle (HCV)	2–3 axel truck	7.20
6	Multi-axel vehicle (MAV)	4–6 axel truck	11.70
7	Trailer	More than 7 axel truck	15.60

shows a higher proportion of car. But due to drivers’ behavior of joining shorter queue, the mixed traffic conditions occur in dedicated lane also. Thus, in car-only lane the other class of vehicles was also present. In case of Gurgaon-Faridabad toll plaza (GFTP), the small car (SC) and big car (BC) share was about 88% which shows the prevailing homogeneous condition. In the case of Kerki, Mulund, and Dahisar toll plaza, mixed traffic was observed in all lanes. The proportional share of the different categories of vehicles at the tollbooth is as shown in Table 3.

5.1 Service Time Analysis

Seven vehicle classes have been considered in the present study as shown in Table 2. It has been observed that service time is varying largely across different vehicle class and also for the same vehicle class. In ordered to capture this variation in service time, the frequency and distribution graph was plotted with the extracted data as shown in Figs. 2 and 3. Service times obtained showed that the mean service time for the small car was 10.83 s, whereas for HCV and trailer, they were 27.68 and 30.92 s, respectively. The minimum and maximum service times for bus are observed to be 4.12 and 49.4 s, respectively. The field observation shows that the service time of a vehicle at tollbooth is not a constant value but varies in a wide range as shown in Table 4. IRC (SP: 84) specified service time to be not more than 10 s irrespective of the vehicle class and payment method adopted [14]. The field observation value shows that under mixed traffic condition, the service time of a vehicle at the tollbooth is more than that provided by IRC [14]. This variation may be due to the mixed condition of traffic, the varying toll rate for different vehicle classes, and the random arrival of vehicles at tollbooth. Further, the exact change of toll amount given by the driver and efficiency of the driver may also lead to an effect on this variation of service time. Table 4 includes vehicle category-wise descriptive statistics such as total number of samples, mean, maximum and minimum service time values, standard deviation skewness, etc. It may be observed from Fig. 2 and Table 4 that the number of a small car (SC) sample was highest followed by big car (BC) and the remaining vehicle classes.

Table 3 Traffic composition observed in field

Sr No.	Location and Lane Number	Composition (in percent)						
		SC	BC	LCV	Bus	HCV	MAV	Trailer
<i>Ghoti toll plaza</i>								
1	Lane No.1	42.44	27.73	6.72	2.94	17.65	0.42	2.10
2	Lane No.2	31.51	26.03	7.31	3.20	22.37	1.83	7.76
3	Lane No.3	40.69	15.86	10.34	3.45	22.07	4.14	3.45
4	Lane No.4	62.26	32.08	3.30	N.P.*	0.94	0.47	0.94
5	Lane No.5	41.28	25.74	7.59	2.49	9.96	7.59	5.34
6	Lane No.6	41.02	25.03	9.14	3.16	9.58	7.07	5.01
<i>Gurgaon-Faridabad toll plaza</i>								
7	Lane No.1	52.05	23.84	15.50	0.40	7.28	0.40	0.53
8	Lane No.2	69.72	23.51	4.98	N.P.*	1.79	N.P.*	N.P.*
9	Lane No.3	75.42	14.41	7.63	0.28	2.26	N.P.*	N.P.*
10	Lane No.4	82.88	9.91	1.80	N.P.*	3.60	0.45	1.35
11	Lane No.5	44.27	9.75	15.63	1.39	27.40	0.93	0.62
12	Lane No.6	81.90	15.01	2.82	0.27	N.P.*	N.P.*	N.P.*
13	Lane No.7	76.56	12.86	2.40	N.P.*	2.76	5.41	N.P.*
<i>Kerki toll plaza</i>								
9	Lane No.1	48.91	26.21	9.48	4.03	6.45	1.81	3.83
10	Lane No.2	36.84	22.93	19.17	3.76	10.53	3.38	3.38
11	Lane No.3	48.54	19.09	15.21	1.29	10.03	1.94	3.88
12	Lane No.4	48.21	21.50	14.01	0.33	9.77	3.26	2.93
<i>Dahisar toll plaza</i>								
13.	Lane No.1	29.13	7.17	20.35	18.15	14.05	9.66	1.46
14.	Lane No.2	16.75	12.32	25.12	13.79	19.70	9.85	2.46
<i>Mulund toll plaza</i>								
15.	Lane No.1	50.69	7.63	11.61	13.78	9.88	4.42	1.99
16	Lane No.2	38.66	8.90	17.39	7.51	19.47	4.45	3.62
17	Lane No. 3	32.45	5.96	15.23	11.92	6.62	16.56	11.26
18	Lane No. 4	37.66	9.05	16.78	5.92	21.38	4.93	4.28
19	Lane No. 5	51.36	7.41	11.93	14.29	8.14	5.16	1.81
20	Lane No. 6	50.08	7.82	11.31	13.31	11.48	3.83	2.16

N.P.* Not present in the traffic mix

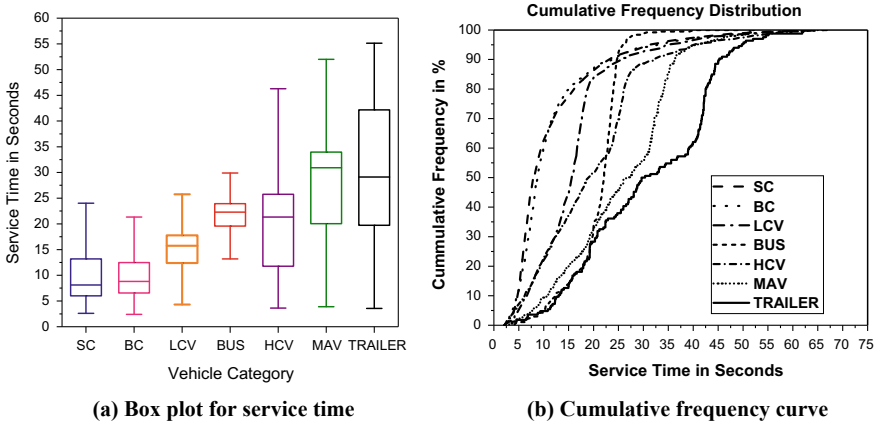


Fig. 2 Service time variation for all vehicle classes

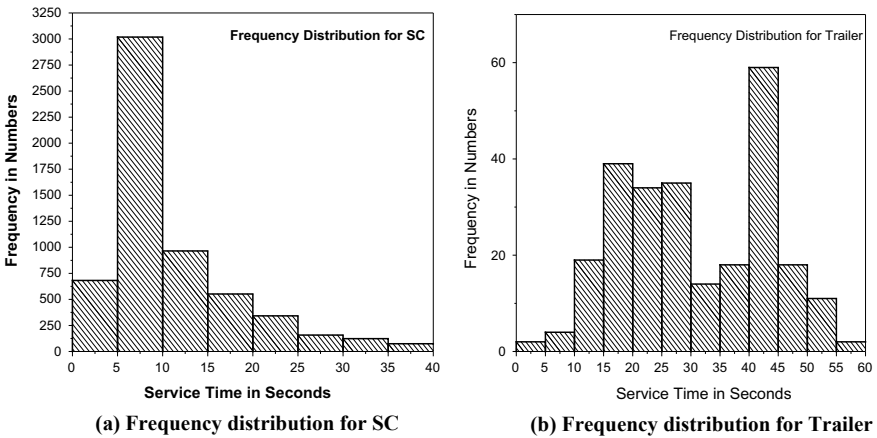


Fig. 3 Frequency distribution curve

Table 4 Statistical analysis of collected service time data

Vehicle class	Sample size	Mean of service time (s)	Minimum (s)	Maximum (s)	Standard deviation	Skewness
SC	5913	10.83	2.4	39.96	7.18	1.669
BC	1665	10.70	2.6	39.96	6.69	1.852
LCV	960	16.19	3.6	56.68	8.20	2.058
BUS	555	21.15	4.12	49.4	5.34	-0.052
HCV	1144	27.68	3.64	59.48	10.72	0.877
MAV	538	27.68	3.88	56.16	10.42	-0.152
Trailer	255	30.92	3.56	55.12	12.51	-0.008

Table 5 includes toll rate-wise descriptive statistics for service time at a tollbooth such as service time, standard deviation and number of observation. The minimum, average, and maximum service time for 59 Rs. toll rate is 3.2, 12.4, and 59.48 s, respectively. The field observation showed that as the toll rate increases, average service time required for a vehicle also increases. This increment of service time is not linear. It shows second-order polynomial relationship is best fitted as shown in Fig. 5. This can be explained on the basis of toll rate as increases at certain level service time also increases but afterward this increment is low and it may be reduced after some stage. This may be because the stable situation arises. Figure 4 shows that service time variation with respect to toll rate. A single set of toll value is a large variation in service time observed. Graph shows as toll rate increases, service time also increases. It may be due to transaction time increases for exchanging toll amount. The graph also shows that at 100 Rs. toll rate, low service time required as compared to service time for higher toll values. This may be due to in the case of 100 Rs. if driver gives 100 Rs., then there is no requirement of exchange. In this type of condition, service time reduces significantly same as shown in Fig. 4.

The present work is carried out to find relationship between service time and toll rate under mixed traffic condition. Recorded film was replayed in laboratory and service time extracted for different vehicle categories for every 30-min count period. In the present study, 30-min count has been considered in order to capture all vehicles and their interaction in a count period. There are total 732 data points each of 30-min count period which was extracted from field data used to develop Eq. (2). The results show that there is a second-degree polynomial relationship between toll

Table 5 Statistical analysis of toll rate and service time

Toll rate in Rs.	Average service time	Minimum service time	Maximum service time	Standard deviation	Number of samples
20	6.36	2.52	40.00	1.55	2711
30	7.80	2.60	39.96	0.58	1376
35	7.44	2.40	39.96	2.35	1725
45	8.45	4.12	40.60	1.45	547
59	12.40	3.20	59.48	1.27	771
65	15.80	6.52	33.68	1.41	579
77	18.6	2.60	39.96	1.51	530
87	22.88	2.12	56.16	1.54	512
90	23.55	5.12	56.96	1.24	903
100	7.68	2.08	10.00	1.51	556
115	28.60	8.84	56.68	3.88	224
270	32.24	19.52	63.44	3.97	196
300	36.86	6.52	42.12	5.26	15
345	42.10	6.12	58.76	4.75	223
555	46.32	7.80	56.16	7.14	162

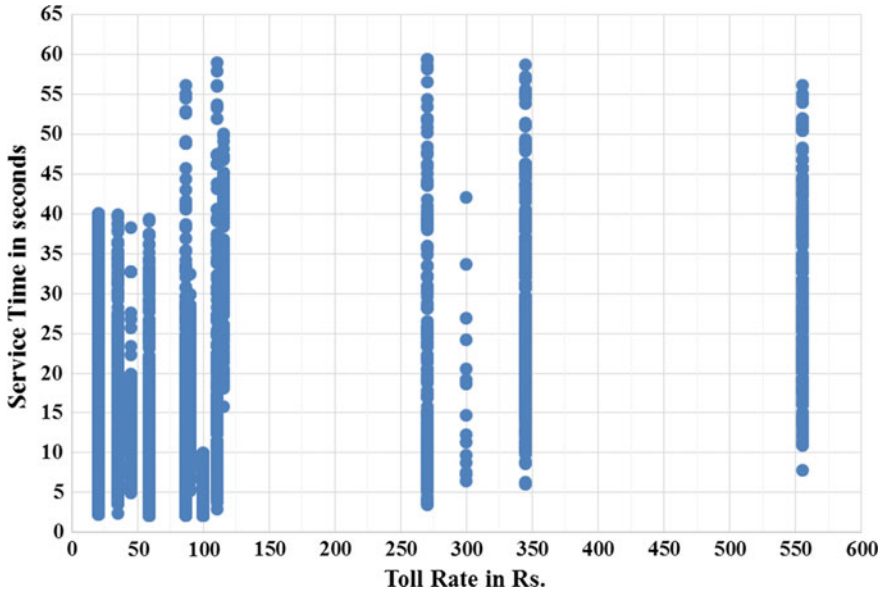


Fig. 4 Service time variation with respect to toll rate

rate and service time (Fig. 5). This relationship may be due to toll rate transaction and exchange, which require more time for the tollbooth operator. This relationship is varied in the form of a polynomial with respect to the increase in toll rates. The toll rate variation observed in the field from 20 to 555 Rs. depending upon the vehicle category and location. Service time increases with increase in the toll rate up to a

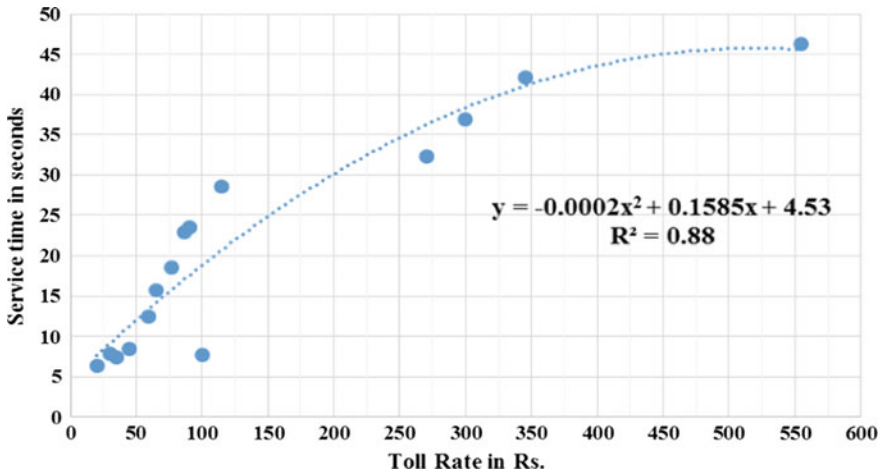


Fig. 5 Toll rate and service time relationship

certain point and once stable condition reach means a transaction in terms of multiple of 50 or 100 then the rate of increment reduces, thus forming a quadratic relation. Polynomial equation a quartic function is defined by a polynomial of even degree. Polynomial function $A \neq 0$ that equation called is quartic equation. Quartic function of A is -0.0002 value which shows it after reaching a particular point service time value start to decrease. Toll rate increases up to certain value, but service time does not increase after reaching stable condition. The model developed shows good reliability, with R^2 value of 0.88. The relationship between service time and toll rate obtained as shown in Eq. (2)

$$\text{Service Time} = 4.53 + 0.1585(\text{Toll Rate}) - 0.0002(\text{Toll Rate})^2 \quad (R^2 = 0.88) \quad (2)$$

6 Model Validation

In order to check the accuracy of the developed service time model in the present study, 20% field data kept aside before the analysis. The field observed values compared with model predicted service time value for different toll rates. There are total 1048 field observations used for model validation. The minimum absolute percentage error (MAPE) value obtained as 7.44%. Hence, there is no significant difference between two sets of service time. It is concluded that there is good agreement between field observed values and model predicted values.

7 Conclusion

Service time analysis plays a significant role in the performance evaluation of toll plaza. There is only limited study done previously in the Indian mixed traffic condition at tollbooth which gives the relationship between toll rate and service time. Hence, the present work is carried out to find the relationship between service time and toll rate variation. The results show that there is a second-order polynomial relationship existing between toll rate and service time. The polynomial model developed shows a good relationship with R^2 value of 0.88. This polynomial relationship may be due to higher toll rate transaction and exchange which requires more time for tollbooth operator but after certain amount the service time should not show much variation. This may be due to the minimum time is required by the tollbooth operator for the necessary money exchange process up to only specific toll value but once toll rate in multiples of 50 or 100 then reduces the service time due to exact exchange amount. The study shows that the average service time for some type of vehicles is more than the service time as per the guideline given in IRC-SP 84 [14]. This shows the necessity of reducing service time at toll plaza based on toll rate. The present work is

useful to the management for optimizing capacity and efficiency of the toll plaza. The model is also useful for estimating the probable service time required for a particular class of vehicle according to their toll rate. This prediction of service time is also useful for toll plaza designing purpose. Also, the result may give some insight for ongoing research on performance evaluation of toll plazas in a mixed traffic scenario.

References

1. Klodzinski J, Al-Deek H (2002) New methodology for evaluating a toll plaza's level of service. *ITE J* 27(2):34–43
2. Zarrillo M, Radwan A, Dowd J (2002) Toll network capacity calculator: operations management and assessment tool for toll network operators. *Transp Res Rec J Transp Res Board* 1781
3. Woo T, Hoel L (1991) Toll plaza capacity and level of service. *Transp Res Rec J Transp Res Board* 1320:119–127
4. Guidelines for Investment in Road sector (2012) Ministry of Road Transport and Highways, Government of India
5. Pursula M (1999) Simulation of traffic system: an overview. *J Geogr Inf Decis Anal* 3(1):1–8
6. Gordan E (1997) Evaluation of the potential benefits to traffic operations at a toll plaza with express ETC lanes, M. Tech. thesis, University of Central Florida, Orlando, Florida
7. Oliveira ML, Cybis HB (2006) An artificial neural network model for evaluating workers performance at tollbooths. In: 1st international symposium on freeway and tollway, operations, Athens, Greece
8. Klodzinski J, Al-Deek H, Radwan A (1988) Evaluation of vehicle emissions at an electronic toll collection plaza. In: Proceeding 77th annual meeting of the transportation research board, Washington D.C.
9. Nezamuddin N, Al-Deek H (2008) Developing microscopic toll plaza and toll road corridor model with PARAMICS. *Transp Res Rec J Transp Res Board* 100–110
10. Zarrillo M, Radwan A (2009) Methodology SHAKER and the capacity analysis of five toll plazas. *J Transp Eng ASCE* 135(3):83–93
11. Aycin M (2006) Simple methodology for evaluating toll plaza operations. *Transp Res Rec J Transp Res Board* 1988:91–101
12. Niu X, Zhang R (2014) The study of new toll station based on VISSM. In: Safe, smart and sustainable multimodal transportation system, ASCE, pp 3372–3379
13. Chakroborty P, Gill R, Chakroborty P (2016) Analysing queuing at toll plazas using a coupled, multiple-queue, queuing system model: application to toll plaza design. *Transp Plan Technol* 39(7):675–692
14. Indian Road Congress (2014) Manual of specification and standards for four laning of highways through public private partnership, IRC code of practice, SP: 84, New Delhi, India

Evaluation of Traffic Congestion Parameters Under Heterogeneous Traffic Condition: A Case Study on Bhubaneswar City



Satya Ranjan Samal and Aditya Kumar Das

Abstract The present study is attempted to explore and evaluate the feasibility of modeling technique for the prediction of congestion indices under heterogeneous traffic conditions at Bhubaneswar city near Patia region. Congestion prediction is attempted under heterogeneous traffic conditions in order to determine their feasibility under the Indian traffic scenario and proposes suggestions of implementing congestion solutions. Two urban road stretches of Patia region of Bhubaneswar city was considered as study area. Survey was conducted for morning peak hours considered from 8:00 a.m. to 11:00 a.m. by video graphic survey. Similarly, survey was conducted for evening peak hours considered from 5:00 p.m. to 7:00 p.m. By synchronizing videos, traffic volume and travel time was obtained which were required for the measure of congestion indices. The average travel time was calculated. Buffer time index, travel time index, and planning time index were estimated. Congestion indices for each direction and each road were evaluated from above parameters. Impact of lane discipline on different congestion indices is analyzed. Formulation of buffer index, travel time index, and planning time index are done to evaluate the various impacts on traffic conditions using nonlinear regression modeling. Average travel time and 95th percentile travel time of different category of vehicles were calculated for each section of road network system for the direction of traffic without considering the lane behavior. Effect of lane discipline on congestion indices of road system was studied. The prime focus of the study relies on congestion indices in terms of travel time reliability measures to find the operational efficiency of urban road network in Bhubaneswar city.

Keywords Traffic congestion · Traffic volume · Travel time · Buffer index · Travel time index · Planning time index · Lane discipline

S. R. Samal (✉)

Kalinga Institute of Industrial Technology University, Bhubaneswar 754012, India
e-mail: satya_papuna@yahoo.com

A. K. Das

Indian Institute of Technology Bombay, Powai, Mumbai 400076, India
e-mail: kumaradityanitr@gmail.com

1 Introduction

The rapid increase in vehicular traffic has imposed a burden on transportation infrastructure. This leads the drivers to experience undesirable delays which ultimately lead to traffic congestion. Traffic congestion refers to the extra delay and vehicle operating costs caused due to the interactions among vehicles on a roadway as traffic volumes approach a road's capacity. Traffic congestion reduces the efficiency of traffic operation, thereby increasing the cost incurred by road users leading them to frustration. Traffic congestion has an adverse impact on both the speed of travel and on their liability of travel conditions. It is the latter that may be of greatest concern to individuals and businesses. Thus, congestion management policies should keep track of travel reliability indicators. Billions of hours are wasted each year due to inefficient traffic management leading to traffic congestion. According to a leading newspaper (Times of India) in a developing country like India, traffic congestion costs 1.5 crore INR annually in just 4 top-tier cities. Traffic congestion not only hinders the mobility, but also pollutes the air, wastes fuel, and hampers economic growth. Non-motorized vehicles also have an important impact on traffic congestion. Traffic congestion is one of the most critical transportation issues which is being faced nowadays, and it is predicted to only get worse during the coming years. Travel time has been a critical measure used to evaluate congestion indices.

Travel time has always been the most important measure associated with effectiveness of the transportation system. Travel time can vary during the day or between days. During peak hours, the travel time can increase significantly as compared to regular hours. Most of the researchers in the past have evaluated the congestion indices in terms of travel time reliability. A reference has been made to travel time index, planning time index, and buffer index in the literature out of which most of the researchers consider buffer index as a measure of congestion. However, in Indian traffic scenario the absence of lane discipline is a major cause for undesirable traffic delays which further leads to traffic congestion. Therefore, for traffic scenario in developing countries, the absence of lane discipline can be considered as a major factor for the cause of congestion. Yet, no work is reported for the measure of congestion indices with consideration of lane changing behavior under Indian traffic conditions. Furthermore, non-motorized vehicles play an important role in urban transportation and their influence on traffic congestion cannot be disregarded. Therefore, the present study aims to select suitable congestion indices based on the study for urban road congestion in developing countries. Further, the study also attempts to develop and validate a model for the travel time reliability measures of selected roads in different cities across India and to recommend possible solutions to the existing traffic congestion.

1.1 Objectives of the Study

- To select appropriate congestion indices based on the study for urban road congestion;
- To develop the model and to validate travel time reliability measures of selected road in Bhubaneswar city;
- To recommend possible solutions to traffic congestion in Bhubaneswar city.

2 Techniques to Measure Travel Time

2.1 Congestion Indices

Congestion indices are an important parameter to know the mobility and operational efficiency of the exiting road network system. Congestion indices are a measure of roadway service quality in transportation network and efficiency. Different congestion indices are

- Travel time index (TTI);
- Buffer index (BI);
- Planning time index (PTI).

95th Percentile Travel Time

The 95th percentile travel time ensures the user is only late 1 out of every 20 trips, in other words, out of 100 travel times on a given corridor, the 95th longest.

Travel Time Index (TTI)

The average amount of time it takes to travel during peak hours compared to off peak hours computed as average travel time divided by off peak travel time.

$$\text{Travel time Index} = \frac{\text{Mean Travel time}}{\text{off peak travel time}} \tag{1}$$

Buffer Index (BI)

The extra time that travelers add to travel to make sure that they are on time most of the time, computed as the difference between the 95th percentile travel time and the average travel time, divided by the average travel time.

$$\text{Buffer Index} = \frac{\text{95th percentile travel time} - \text{Mean Travel time}}{\text{Mean travel time}} \tag{2}$$

Planning Time Index (PTI)

The total time needed to plan for an on-time arrival 95% of the time, computed as 95th percentile travel time divided by off-peak travel time

$$\text{Planning time Index} = \frac{\text{95th percentile travel time}}{\text{off peak travel time}} \quad (3)$$

3 Methodology

The methodology adopted in this study comprises the following steps as follows.

STEP 1 Study of congestion indices and travel time reliability measures

- Detail study about travel time and congestion measures;
- Selection of appropriate congestion indices under Indian traffic condition;
- Selection of urban road network in Bhubaneswar city.

STEP 2 Development of plan and collection of data

- Find techniques for collecting data.
- Develop a schedule plan for collecting data.
- Collect data of traffic volume, travel time, etc.

STEP 3 Calculation of travel time reliability measure parameters

- Estimation of average travel time;
- Estimation of 95th percentile travel time.

STEP 4 Calculation of buffer index

- Evaluation of buffer index for each road;
- Impact of non-motorized vehicle on buffer index is analyzed.

STEP 5 Calculation of travel time index

- Evaluation of travel time index for each road;
- Impact of non-motorized vehicle on travel time index is analyzed.

STEP 6 Calculation of planning time index

- Evaluation of planning time index for each road;
- Impact of non-motorized vehicle on planning time index is analyzed.

STEP 7 Development of model and validation

- Development of travel time model using parameters affecting traffic congestion;
- Validation of model on selected road in Bhubaneswar city.



Fig. 1 Data collection location **a** and **b** Patia–Infocity road **c** and **d** Jaydev Vihar–Nandankanan road

4 Data Collection and Analysis

Data collection and its analysis are the basic steps in any study. Most studies of traffic-related problems begin with the data collection from selected roadway networks, which gives an overview of the collection of the traffic data followed by its analysis. The data collection primarily involves traffic volume, travel time, travel time measurement for urban road sections in Bhubaneswar city. Two locations were selected as: road-1: Patia–Infocity road, and road-2: Jaydev Vihar–Nandankanan road (Fig. 1). The details about road considered for this study were presented in (Tables 1 and 2).

5 Travel Time Modeling

The aim of this study is to develop a model that predicts travel time in terms of traffic parameters obtained from video graphic survey. From the travel time, we can predict the congestion level of road. Congestion can be evaluated in terms of travel time reliability measures. The important parameters that influence travel time include speed, distance, and volume. Models are generally used for the predictive purpose.

Table 1 Recommended PCU factors for various vehicle types in urban roads

Sl. No.	Vehicle type	Equivalent PCU factors Percentage composition of vehicle type in traffic stream	
		5%	10% and above
1	Two-wheeler, motor cycle, or Scooter	0.5	0.75
2	Passenger car, pick-up van	1.0	1.0
3	Auto rickshaws	1.2	2.0
4	Light commercial vehicle	1.4	2.0
5	Truck or bus	2.2	3.7
6	Agricultural tractor trailer	4.0	5.0
7	Cycle	0.4	0.5
8	Cycle rickshaw	1.5	2.0
9	Horse-drawn vehicle	1.5	2.0
10	Hand cart	2.0	3.0

Source IRC 106: 1990

Table 2 Particulars of the selected roads

Sl. No.	Name of the road	Class of road	Lane characteristics
1.	Patia–Infocity road	Arterial	6 lane divided
2.	Jaydev Vihar–Nandankanan road	Arterial	6 lane divided

Validation of model requires comparing the travel time estimated by the model to observed travel time on the roadway.

5.1 Modeling Approach

A regression model expresses a dependent variable as a function of one or more independent variables, generally in the form

$$Y = a + b_1x_1 + b_2x_2 + \dots + e \tag{4}$$

The line that expresses the relationship between the dependent variable, called *Y* which is dependent upon independent variables such as $x_1, x_2 \dots$

5.2 Model Parameters

The travel time model depends on different parameters. One of the most important parameter is speed. Distance is another important variable for determination of travel time, since an increase in the length of the segment will obviously increase the vehicle travel time. From the theoretical point of view, vehicle travel time should be proportional to distance divided by speed. Apart from these parameters, another parameter volume influences the travel time. Peak hour volume is included in the modeling process.

5.3 Model Estimation

Travel time is a continuous variable, so the first modeling formulation used was a linear regression with travel time considered as the dependent variable. Speed, distance, and volume were included in the model as independent variables.

Travel Time Model

$$TT = 18.933 - (1.15 * X1) + (0.34 * X2) + (0.005 * X3) \quad (5)$$

where

- TT* Average travel time in seconds
- X1* Speed in kmph
- X2* Length in meter
- X3* Volume in PCU/h.

Based on data such as volume of traffic flow, speed of the vehicles and distance traveled by vehicle model were estimated. Length gives positive effect to travel time. The reason behind this if the length of the section is increased obviously, there is an increase in vehicle travel time. Speed of vehicle has negative influence on travel time. When speed of vehicle increase, travel time of vehicle will reduce. Volume has the positive influence on travel time model. Increase in volume will obviously cause the congestion at the peak hour traffic.

5.4 Model Validation

The validation process establishes the credibility of the model by demonstrating its ability to replicate actual traffic patterns. Validation of the model requires comparing travel time estimated by the model to observed travel time on the roadway. Validation is typically an iterative process linked to calibration. If the analyst finds that the model output and the independent data are in acceptable limit, the model can be considered and validated (Fig. 2 and Table 3).

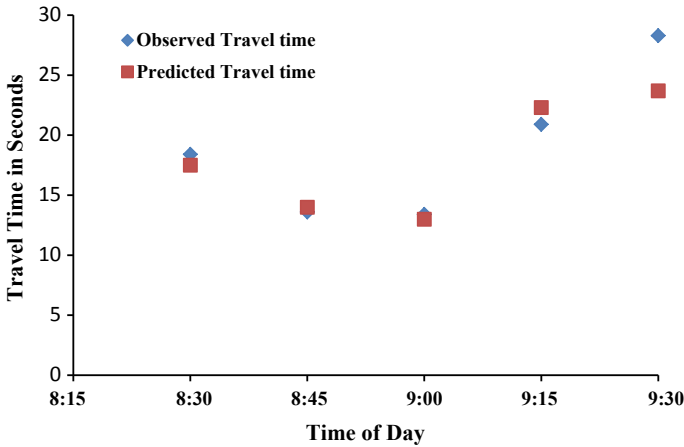


Fig. 2 Travel time response over time of day

Table 3 Error percentage between observed travel time and predicted travel time

Time of day	Observed travel time in seconds	Predicted travel time in seconds	Absolute error (%)
8.30 a.m.–8.45 a.m.	18.30	17.40	5
8.45 a.m.–9.00 a.m.	13.50	14.10	3
9.00 a.m.–9.15 a.m.	13.50	13.10	3
9.15 a.m.–9.30 a.m.	20.60	22.20	7

If error percentage between observed travel time and predicted travel time obtained from the model is less than 10%, model will fit for calculating travel time at future and from that we can predict the congestion level of the roadway. To check a model fit, error percentage between observed travel time and predicted travel time obtained from model was estimated. The error percentage was found to be less than 10%, so overall the obtained equations for travel time is a good fit and ensure statistical validation of the estimated model. In this study, R^2 statistic is found to be 0.89 for the travel time model, so overall the obtained equations for travel time are a good fit and ensure statistical validation of the estimated model.

6 Conclusions

Based on the studies observed in the selected urban road network in Bhubaneswar city,

1. Traffic congestion parameters which include volume count and travel time measurements were determined for the selected roads.

2. In India due to highly varying physical dimensions and speeds, vehicles could not follow lane discipline as any lateral position on the available road space is occupied by small-sized vehicles.
3. Different congestion indices such as buffer index, travel time index, and planning time index are evaluated for the selected roads in Bhubaneswar city.
4. From the results, we conclude that travel time and congestion indices are varied according to vehicle composition and lane distribution. Out of different congestion indices are evaluated, buffer index gives satisfactory results under Indian traffic conditions.
5. Travel time model was established, the error percentage was found to be less than 10%, so overall the obtained equations for travel time are a good fit and ensure statistical validation of the estimated model.

7 Recommendations

By reducing traffic congestion, city can play an important role in state, and at the same time, it can also bring relief and peace for the people by ensuring healthy environment free from noise and pollution. Here, some of the recommendations to reduce traffic congestion in Bhubaneswar city are as follows:

- By increasing the use of alternative transportation modes including parking, and bicycling/walking;
- By altering trip patterns through the application of measures such as land-use policies, alternative work-schedule arrangements, and pricing;
- By improving traffic flow through measures such as route guidance systems, traffic signal improvements, and incident management;
- The solution which may not necessarily need huge investment and mostly uses existing infrastructure.

References

1. De Palma A, Lindsey R (2011) Traffic congestion pricing methodologies and technologies. *Transp Res Part C Emerg Technol* 19(6):1377–1399
2. Mauray AK (2011) Comprehensive approach for modeling of traffic stream with no lane discipline. In: 2nd international conference on models and technologies for intelligent transportation system, Leuven, Belgium, 2011, pp 1–5
3. Padiath A, Vanajakshi L, Subramanian SC, Manda H (2009) Prediction of traffic density for congestion analysis under Indian traffic conditions. In: 12th international IEEE conference on IEEE intelligent transportation systems, ITSC'09, pp 1–6
4. Bigazzi, AY (2011) Traffic congestion mitigation as on emission reduction strategy, M.S Thesis in Civil Engineering Department, Portland State University
5. Chidambaram B, Zikos D (2012) Congestion mitigation measure in Hyderabad, A Midnight summer dream, South Asia chronicle. Sudasien Seminar Humboldt University, Berlin, pp 58–92

6. Tiwari G, Fazio J, Gaurav S (2007) Traffic planning for non homogeneous traffic. *Sadhana* 32(4):309–328
7. IRC SP-30 (2010) Manual on economic evaluation of highway projects in India. Indian Road Congress, New Delhi
8. Kobayashi K, Do M (2005) The informational impact of congestion tolls upon route traffic demand. *J Transp Res Part A* 39:651–670
9. Lyman K, Bertini RL (2008) Using travel time reliability measures to improve regional transportation planning and operation. *J Transp Res Board* 2046:1–10
10. Mahmud K, Chowdhury K, Gopeand SM (2012) Possible causes & solutions of traffic jam and their impact on the economy of Dhaka City. *J Manage Sustain* 2(2):112–135

Driver Behavior as Affected by Static Objects: A Naturalistic Driving Approach



Bhupali Dutta and Vinod Vasudevan

Abstract There are several studies in the literature on predicting and modeling driver behavior along longitudinal direction. However, drivers may also be influenced by objects, both static and dynamic, present laterally. Although a few works aimed at understanding the effect of static objects and features such as road geometric elements and roadside infrastructure on driver behavior have been carried out, there are certain limitations of these studies. Driver behavior studies are conducted with the purpose of identifying the effect of static objects that are not directly present on the path of travel. In most of these cases, microscopic models are developed to model driver behavior in the presence of static objects, but the results are validated through simulation. Also, majority of the reported work focused on macroscopic traffic flow modeling since macroscopic data can be collected easily using videographic method and vehicle detectors on the roadway section. In this study, an attempt is made to understand driver response to static obstacles present on the path of travel along the direction of movement. Naturalistic driving is used for the data collection on driver response. It is observed that the side of placement of obstruction and the pattern of restriction along the direction of movement influence driver behavior.

Keywords Driver behavior · Static obstacle · Side of presence · Obstruction pattern · Lateral gap · Lateral position

1 Introduction

Microscopic studies in traffic engineering predict and model individual driver's actions in different driving scenarios along the longitudinal direction. However, objects present laterally may equally influence the driver. There are several studies in the literature which examine the effect of geometric elements, roadside infras-

B. Dutta (✉)

Department of Civil Engineering, Indian Institute of Technology Kanpur, Kanpur 208016, India
e-mail: bhupali@iitk.ac.in

V. Vasudevan

Department of Civil Engineering, University of Alaska, Anchorage, AK 99508, USA
e-mail: vvasudevan@alaska.edu

© Springer Nature Singapore Pte Ltd. 2020

T. V. Mathew et al. (eds.), *Transportation Research*, Lecture Notes
in Civil Engineering 45, https://doi.org/10.1007/978-981-32-9042-6_54

685

tructure, and infrastructural changes on the driver. Nevertheless, there are certain limitations. Since data pertaining to microscopic studies are difficult to collect, most of the studies capture driver behavior either using driving simulator or microscopic parameters are derived from macroscopic data collected with the help of videography. Comprehensive microscopic models are developed, but these models are validated through simulation. The studies which are conducted for static objects basically deal with objects which are not directly present along the path of travel of the driver. The motivation behind this study is to understand driver reaction to obstacles present along the path of travel.

2 Literature Review

Several studies have been carried out to understand the effect of the presence of static objects on driver behavior. Michaels and Cozan [1] developed a model for the magnitude of lateral displacement in the presence of objects present laterally near the path of travel based on perception threshold. They defined 'perception' as the rate of change of angle of a cone made by the object with the driver's eyes. Chakraborty et al. [2] developed the only comprehensive driver behavior model based on potential field theory which analyzed driver behavior along both longitudinal and lateral directions. According to this theory, the lateral position on the road was a function of potential emanated by various objects present on the road. The potential field was a function of the properties of the objects.

Stamatiadis et al. [3, 4] found that vegetation type and density had a significant effect on driver discomfort and thus had the potential to influence operating speeds. A driving simulator study was carried out by Horst and Ridder [5] to understand the effect of trees and barriers had on driver's speeds and paths. It was found that when drivers initially approached the safety barriers, they tended to move away laterally from safety barriers and also reduced their speed. The type and size of a safety barrier had little impact; only its presence had an effect. Tay and Churchill [6] analyzed the influence of different types of median barriers on the comfort speed of drivers. Analyses showed that available shy distance influenced the amount of reduction in speed. In order to decrease their perceived risks, drivers compensated by lowering their speed when the desired shy distance was not available. A few studies in the available literature showed the impact of participants' age and obstacle direction on the minimum braking distance toward the obstacle. In a study conducted by Martin et al. [7], the authors found that older drivers maintained the greater lateral gap with the obstacle than younger drivers did. However, there was no significant difference in the minimum obstacle distance when the pedestrian (obstacle) appeared from the left or from the right. Bassat and Shinar [8] conducted a simulator study with the aim of analyzing the effect of shoulder width and guardrails on speed and lateral position on a simulated four-lane highway. Results showed that drivers were not influenced by the presence of either shoulder width or guardrails when they were considered individually. However, the presence of guardrail influenced the driving

speed when the influence of shoulder width was also taken into account. Bella [9] studied the impact of the availability of shoulder, in the presence of three roadside configurations: trees, trees and barriers, and trees and barriers that have undergone treatment on speed and lateral placement. Statistical analyses showed that speed and lateral placement were influenced by both geometric and roadside configurations. An instrumented vehicle study was conducted by Budhkar and Maurya [10] to evaluate the lateral clearance maintained by vehicles when they interacted with a single vehicle on the side versus when there were vehicles on both sides of the subject vehicle. From the study, they found that subject vehicle compromised with safety while interacting with vehicles on both sides; the lateral clearance maintained when vehicles were present on both sides was lesser than when the vehicle was present on only one side.

From the literature, it was observed that most of the studies on driver behavior on lateral objects were focused on the influence of road geometrics, roadside configurations, and infrastructure changes. Driver behavior was not observed for obstacles present directly on the path of travel. In the majority of the studies, data collection was carried through the driving simulator and videographic method.

3 Objective

The objective of this study was to understand driver response to obstacles present directly in the path of travel through naturalistic driving. Relevant questions in the context of driver response to static obstacles were as follows:

1. What was the influence of side of placement of the obstacle along the direction of travel on driving?
2. What was the influence of the pattern of obstruction along the direction of travel on the lateral positioning of the vehicle?

4 Method

To support the research, real data were collected through naturalistic driving. An instrumented vehicle was developed for the purpose of data collection by installing various sensors—LiDAR, video cameras, IMU-GPS unit, onboard diagnostic (OBD) scanner, and steering angle sensor on a vehicle. The data collection was carried out at a sampling frequency of 10 Hz. The experiments were conducted on a test track at the Indian Institute of Technology Kanpur, India. In India, drivers follow ‘keep left’ driving policy, where drivers have to drive on the left-hand side of the lane. The test track was a runway that was 900 m long and approximately 20 m wide. On this runway, two lanes of 3.5 m width each were created by placing traffic safety cones at an interval of 50 m along the length. The safety cones along the length represented the boundary of the lanes and served the purpose of lane markings. The

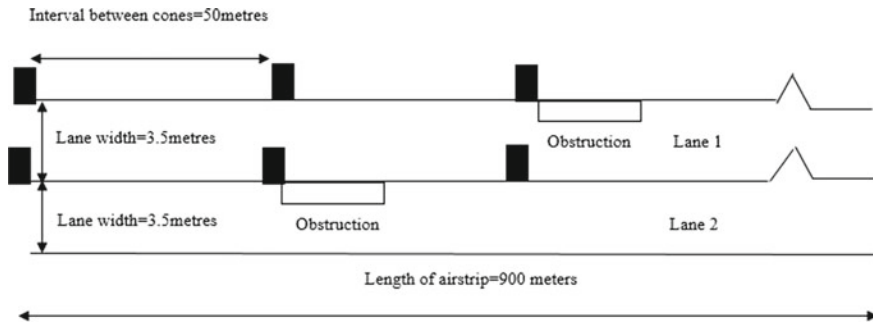


Fig. 1 Schematic diagram of prepared test track

total utilized length of the runway for the experiment was 800 m. Figure 1 shows the schematic diagram of the prepared test track for the experiments. The static obstruction introduced was a reduction in lane width from 3.5 m to 3 m and 3.5 m to 2.5 m, thus reducing the lane width by 0.5 m and 1 m, respectively. The length of the obstruction was 25 m and 100 m. The obstruction was introduced once along the left-hand side and once along the right-hand side of the lane along the direction of travel. The drivers drove at three different speed limits: 30, 40, and 50 kmph.

Five male drivers participated in the experiment. All the participants had at least five years of driving experience. They were instructed to drive as naturally as they could within the lane. None were told the purpose of the test. Each driver took a test run before the start of the experiment to be familiarized with the vehicle and the surrounding. The experiments were conducted in clear weather and dry pavement conditions.

5 Analysis

Two hypothesis tests at 95% significance level were performed to compare sample means. First hypothesis test was conducted to understand the influence of side of obstruction on the lateral gap. The obstruction was introduced once along the left-hand side and once along the right-hand side along the direction of travel. The mean lateral gap maintained from the obstruction was observed. Second hypothesis test analyzed the influence of the pattern of obstruction on lateral positioning of the vehicle. As mentioned, two lanes of 3.5 m width each were created by placing traffic safety cones along the width. The lateral boundary for lane 1 was marked by safety cones on one side, and the other side had a shoulder of 0.5 m width. The boundary for lane 2 was marked by traffic safety cones on both sides as shown in Fig. 2. The safety cones served the purpose of lane makings for both the lanes.

The lateral position was defined in terms of lateral position index (LPI). The LPI is defined in Eq. (1). Lateral position was estimated for the left wheel of the vehicle

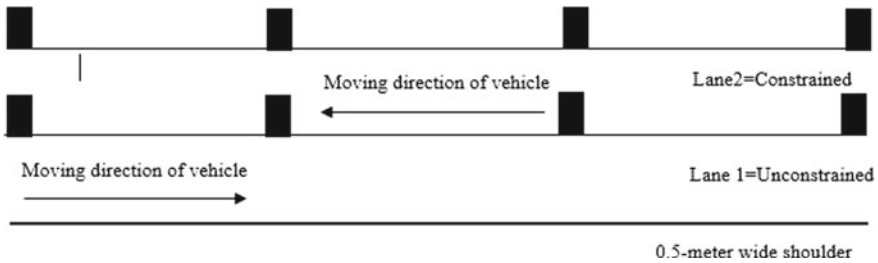


Fig. 2 Constrained and unconstrained conditions

in meters. LPI was calculated with respect to the lane markings on the left-hand side of the driver along the direction of travel. The LPI was studied for two conditions—unconstrained and constrained. In unconstrained condition, the lane marking was present along one side in the direction of travel, and the other side was free. In constrained condition, the lane marking was present along both sides in the direction of travel. Lanes 1 and 2 were in unconstrained and constrained condition, respectively

$$LPI = \frac{A}{B} \tag{1}$$

where A = Lateral position of the left wheel from left lane marking in meters, B = Available lane width in meters.

6 Results

6.1 Hypothesis 1

Null hypothesis was that mean lateral gaps when the obstacle was placed on left-hand side and right-hand side were equal (Eq. 2), and alternative hypothesis was that mean lateral gap from the obstacle when placed on the right-hand side was greater than the lateral gap when the obstacle was placed on the left-hand side (Eq. 3). Tables 1 and 2 show the descriptive statistics of the mean lateral gaps and the hypothesis test results for all the drivers for 25 and 100 m long obstruction, respectively.

$$H_0 : \mu_{\text{right}} = \mu_{\text{left}} \tag{2}$$

$$H_a : \mu_{\text{right}} > \mu_{\text{left}} \tag{3}$$

Based on the p -values it was observed that when the driving speed was less, for speeds of 30 and 40 kmph, the mean lateral gaps from the obstacle on the right-hand and left-hand side were equal. However, when the driving speed increased to around

Table 1 Descriptive statistics and hypothesis test results for 25-m long obstruction

Driver No.	Speed (kmph)	Lateral gap from obstruction on left-hand side		Lateral gap from obstruction on right-hand side		t-statistic	p-value	H ₀
		Mean (m)	SD (m)	Mean (m)	SD (m)			
<i>Lane width is reduced by 0.5 m</i>								
1	30	1.315	0.316	1.315	0.317	-2.733	0.974	Do not reject
	40	1.118	0.079	1.183	0.205	-0.589	0.705	Do not reject
	50	0.997	0.187	1.412	0.126	3.484	0.005	Reject
2	30	0.823	0.175	0.783	0.223	-3.641	0.989	Do not reject
	40	0.706	0.187	0.957	0.108	3.929	0.008	Reject
	50	0.869	0.207	1.204	0.224	6.687	0.001	Reject
3	30	0.891	0.200	0.838	0.096	-1.555	0.903	Do not reject
	40	0.956	0.126	1.024	0.172	3.133	0.017	Reject
	50	1.042	0.152	1.298	0.238	2.363	0.038	Reject
4	30	1.256	0.178	1.023	0.225	-0.112	0.542	Do not reject
	40	1.112	0.362	1.352	0.172	2.709	0.043	Reject
	50	0.976	0.152	1.158	0.285	2.167	0.047	Reject
5	30	1.413	0.280	1.244	0.242	-2.552	0.814	Do not reject
	40	1.364	0.237	1.405	0.159	-1.823	0.926	Do not reject
	50	1.110	0.275	1.308	0.169	2.592	0.035	Reject
<i>Lane width is reduced by 1 m</i>								
1	30	1.103	0.268	0.915	0.275	-5.427	0.997	Do not reject
	40	0.975	0.298	1.280	0.300	5.917	0.002	Reject
	50	1.067	0.350	1.268	0.219	4.855	0.009	Reject
2	30	1.130	0.245	0.955	0.376	-3.945	0.992	Do not reject
	40	1.088	0.301	0.869	0.279	-0.809	0.768	Do not reject
	50	0.898	0.344	1.107	0.163	2.647	0.032	Reject
3	30	0.865	0.255	0.857	0.215	-10.611	0.998	Do not reject

(continued)

Table 1 (continued)

Driver No.	Speed (kmph)	Lateral gap from obstruction on left-hand side		Lateral gap from obstruction on right-hand side		t-statistic	p-value	H ₀
		Mean (m)	SD (m)	Mean (m)	SD (m)			
	40	1.123	0.376	1.224	0.347	2.797	0.035	Reject
	50	1.142	0.270	0.935	0.124	-0.015	0.506	Do not reject
4	30	0.996	0.206	1.054	0.223	-1.321	0.872	Do not reject
	40	1.024	0.312	1.115	0.306	-0.405	0.649	Do not reject
	50	1.142	0.295	1.147	0.328	-1.206	0.550	Do not reject
5	30	1.197	0.307	1.104	0.287	-6.452	0.894	Do not reject
	40	1.123	0.252	1.310	0.487	2.302	0.045	Reject
	50	0.751	0.199	0.857	0.355	4.917	0.003	Reject

Note: SD standard deviation

50 kmph, the lateral gap from the obstacle on the right-hand side was greater than obstacle on the left-hand side. This behavior was more evident when the obstacle width was 0.5 m. There can be three possible reasons which are mentioned below:

1. When the driving speed was less, the driver could easily maintain a steady speed, irrespective of the side of obstacle placement. Hence, the driver was not influenced by the side of the obstacle. There was not much significant difference in the mean lateral gap from the obstruction when placed either on the right-hand side or left-hand side.
2. As the experiments were conducted in a region with a 'keep left' driving policy, it was the natural tendency of drivers to drive on the left-hand side of the lane. At high speed, it became difficult to maintain stable lane position and steady driving speed, particularly while encountering an obstruction. Hence, in order to maintain stability, steady state and to be on the safer side, the driver preferred to move away from the obstacle on the right and drive on the left-hand side of the lane. This resulted in an increase in the lateral gap from an obstacle on the right.
3. The original width of both the lanes was 3.5 m. When the lane width was reduced by 0.5 m, the lane width was reduced to 3 m. Based on perceived comfort lateral gap and steady speed, the driver could select a suitable lateral gap within the available 3 m width. However, when the lane width was reduced by 1 m, the available lane width was reduced from 3.5 m to 2.5 m. The lateral extent of obstruction of 1 m width was high; the drivers did not have the flexibility to vary the lateral gap much when encountering an obstruction. Hence, there was no

Table 2 Descriptive statistics and hypothesis test results for 100-m long obstruction

Driver No.	Speed (kmph)	Lateral gap from obstruction on left-hand side		Lateral gap from obstruction on right-hand side		t-statistic	p-value	H ₀
		Mean (m)	SD (m)	Mean (m)	SD (m)			
<i>Lane width is reduced by 0.5 m</i>								
1	30	0.567	0.244	1.009	0.236	1.813	0.036	Reject
	40	0.458	0.104	0.448	0.123	-2.639	0.987	Do not reject
	50	0.892	0.124	1.305	0.161	2.005	0.026	Reject
2	30	0.638	0.246	1.149	0.266	5.793	0.000	Reject
	40	1.146	0.229	0.874	0.235	-2.305	0.978	Do not reject
	50	0.765	0.150	1.024	0.293	2.418	0.018	Reject
3	30	0.963	0.147	0.935	0.244	-2.838	1.000	Do not reject
	40	1.012	0.266	1.317	0.169	3.041	0.006	Reject
	50	1.013	0.270	0.977	0.108	-5.928	0.999	Do not reject
4	30	1.064	0.372	1.115	0.178	-4.491	0.099	Do not reject
	40	1.064	0.224	0.975	0.129	-2.823	0.991	Do not reject
	50	1.079	0.238	1.359	0.200	2.193	0.042	Reject
5	30	1.151	0.299	1.008	0.297	-2.162	0.972	Do not reject
	40	1.165	0.209	1.076	0.147	-5.737	0.999	Do not reject
	50	1.154	0.232	1.402	0.179	2.962	0.017	Reject
<i>Lane width is reduced by 1 m</i>								
1	30	0.420	0.165	0.734	0.336	2.002	0.040	Reject
	40	0.745	0.083	0.683	0.086	-0.643	0.988	Do not reject
	50	1.042	0.222	0.769	0.047	-3.822	0.995	Do not reject
2	30	0.973	0.402	0.833	0.402	-3.828	1.000	Do not reject
	40	0.680	0.292	0.754	0.337	-3.041	0.976	Do not reject

(continued)

Table 2 (continued)

Driver No.	Speed (kmph)	Lateral gap from obstruction on left-hand side		Lateral gap from obstruction on right-hand side		t-statistic	p-value	H ₀
		Mean (m)	SD (m)	Mean (m)	SD (m)			
3	50	0.683	0.334	0.951	0.363	2.418	0.008	Reject
	30	0.692	0.476	0.676	0.287	-10.149	1.000	Do not reject
	40	0.783	0.332	0.805	0.256	-1.046	0.839	Do not reject
4	50	0.775	0.503	0.873	0.224	1.932	0.040	Reject
	30	0.785	0.347	0.754	0.256	0.452	0.209	Do not reject
	40	0.871	0.449	0.803	0.364	-0.113	0.642	Do not reject
5	50	0.852	0.268	0.814	0.227	0.336	0.371	Do not reject
	30	0.864	0.379	0.777	0.296	-3.173	0.995	Do not reject
	40	1.008	0.289	0.862	0.268	-0.786	0.775	Do not reject
	50	0.755	0.429	0.998	0.240	3.484	0.009	Reject

Note SD standard deviation

significant difference in the mean lateral gaps from the obstruction on the right-hand side and left-hand side when the lane width was reduced by 1 m.

6.2 Hypothesis 2

Null hypothesis was that LPI for unconstrained and constrained conditions was equal (Eq. 4), and the alternative hypothesis was that the LPI for the unconstrained condition was greater than the LPI for constrained condition (Eq. 5). Tables 3 and 4 show the descriptive statistics of the position profile values and hypothesis test results for all the drivers for 25 m and 100 m lengths of obstruction, respectively.

$$H_0 : \mu_{\text{unconstrained}} = \mu_{\text{constrained}} \tag{4}$$

$$H_a : \mu_{\text{unconstrained}} > \mu_{\text{constrained}} \tag{5}$$

Table 3 Descriptive statistics and hypothesis test results for 25-m long obstruction

Driver No.	Speed (kmph)	LPI-unconstrained condition		LPI-constrained condition		t-statistic	p-value	H ₀
		Mean	SD	Mean	SD			
<i>Lane width is reduced by 0.5 m</i>								
1	30	0.412	0.055	0.315	0.042	6.730	0.000	Reject
	40	0.387	0.069	0.379	0.036	0.787	0.215	Do not reject
	50	0.431	0.092	0.315	0.066	8.823	0.000	Reject
2	30	0.434	0.092	0.297	0.085	3.352	0.000	Reject
	40	0.420	0.069	0.459	0.060	-3.577	0.998	Do not reject
	50	0.436	0.061	0.383	0.054	2.195	0.016	Reject
3	30	0.355	0.078	0.221	0.046	4.553	0.000	Reject
	40	0.275	0.065	0.274	0.055	-3.842	0.999	Do not reject
	50	0.313	0.062	0.342	0.096	-6.487	1.000	Do not reject
4	30	0.361	0.062	0.367	0.041	-7.206	1.000	Do not reject
	40	0.442	0.035	0.440	0.026	-10.653	1.000	Do not reject
	50	0.453	0.062	0.304	0.055	3.834	0.000	Reject
5	30	0.345	0.067	0.370	0.098	-11.754	1.000	Do not reject
	40	0.453	0.063	0.387	0.071	8.471	0.000	Reject
	50	0.449	0.069	0.383	0.059	2.123	0.032	Reject
<i>Lane width is reduced by 1 m</i>								
1	30	0.398	0.048	0.265	0.062	8.326	0.000	Reject
	40	0.420	0.065	0.357	0.061	8.093	0.000	Reject
	50	0.405	0.055	0.427	0.058	-5.003	1.000	Do not reject
2	30	0.462	0.056	0.363	0.078	8.326	0.000	Reject
	40	0.424	0.076	0.387	0.055	8.093	0.000	Reject
	50	0.463	0.085	0.378	0.069	7.045	0.000	Reject
3	30	0.384	0.064	0.262	0.065	3.352	0.000	Reject
	40	0.334	0.092	0.329	0.064	-3.577	0.999	Do not reject
	50	0.317	0.065	0.343	0.071	-7.025	1.000	Do not reject

(continued)

Table 3 (continued)

Driver No.	Speed (kmph)	LPI-unconstrained condition		LPI-constrained condition		t-statistic	p-value	H ₀
		Mean	SD	Mean	SD			
4	30	0.421	0.056	0.335	0.072	8.263	0.000	Reject
	40	0.357	0.072	0.433	0.053	-9.117	1.000	Do not reject
	50	0.417	0.036	0.399	0.047	2.295	0.000	Reject
5	30	0.324	0.067	0.367	0.073	-6.687	1.000	Do not reject
	40	0.331	0.072	0.369	0.085	-8.614	1.000	Do not reject
	50	0.402	0.085	0.362	0.081	3.107	0.003	Reject

Note LPI (lateral position index) = (Lateral position of the left wheel of vehicle from left lane marking/lane width)

SD standard deviation

From descriptive statistics and p-values, it was observed that at low speeds of 30 and 40 kmph, the LPI for the unconstrained condition was greater than that for the constrained condition. However, as speed increased, the LPI for both the conditions merged and fell within a range of 0.4–0.5. There can be two possible reasons, which are explained as follows:

1. Drivers perceived the safety cones on the lane as obstacles. LPI for unconstrained condition ranged between 0.4 and 0.45. In lane 1, which was in unconstrained condition, the driver had the liberty to move away from the obstacle on the left-hand side toward the edge of the lane where the shoulder was available. The driver perceived the shoulder as an extra width to maneuver. As driver moved away from the obstacle toward the shoulder, there was an increase in LPI for unconstrained condition.
2. In lane 2, safety cones were present on both sides of the lane. The driver perceived these safety cones as obstacles on both sides. In the presence of obstacle along both sides of the lane, to be on the safer side, the drivers preferred to follow the driving policy ‘keep left’ on the lane. Hence, the value of LPI fell within 0.2 to 0.35, indicating that LPI was less in constrained condition.
3. At high speed, drivers preferred to drive in the middle of the lane, irrespective of the pattern of obstruction along the lane width. Hence, the value of the position profile for both unconstrained and constrained conditions was within 0.4 and 0.5.

Table 4 Descriptive statistics and hypothesis test results for 100-m long obstruction

Driver No.	Speed (kmph)	Position profile-unconstrained condition		Position profile-constrained condition		<i>t</i> -statistic	<i>p</i> -value	<i>H</i> ₀
		Mean	SD	Mean	SD			
<i>Lane width is reduced by 0.5 m</i>								
1	30	0.435	0.063	0.347	0.072	7.230	0.000	Reject
	40	0.442	0.079	0.418	0.064	-4.501	1.000	Do not reject
	50	0.434	0.037	0.434	0.045	-8.453	1.000	Do not reject
2	30	0.365	0.058	0.237	0.061	7.095	0.000	Reject
	40	0.294	0.084	0.361	0.044	-8.991	1.000	Do not reject
	50	0.279	0.071	0.343	0.062	-2.521	1.000	Do not reject
3	30	0.383	0.054	0.278	0.092	3.050	0.000	Reject
	40	0.298	0.119	0.307	0.067	-10.953	1.000	Do not reject
	50	0.372	0.096	0.331	0.063	2.661	0.000	Reject
4	30	0.362	0.096	0.348	0.059	3.241	1.000	Reject
	40	0.429	0.0678	0.349	0.066	2.145	0.005	Reject
	50	0.355	0.067	0.355	0.066	-2.412	1.000	Do not reject
5	30	0.449	0.071	0.379	0.117	6.723	0.000	Reject
	40	0.426	0.061	0.378	0.066	8.363	0.000	Reject
	50	0.411	0.069	0.391	0.072	-8.823	1.000	Do not reject
<i>Lane width is reduced by 1 m</i>								
1	30	0.429	0.036	0.292	0.075	2.753	0.000	Reject
	40	0.453	0.049	0.385	0.079	3.320	0.000	Reject
	50	0.464	0.073	0.466	0.042	-7.687	1.000	Do not reject
2	30	0.335	0.072	0.311	0.081	-3.742	1.000	Do not reject
	40	0.285	0.081	0.261	0.055	-2.473	1.000	Do not reject
	50	0.280	0.093	0.346	0.061	-3.405	1.000	Do not reject
3	30	0.271	0.099	0.249	0.079	-7.171	1.000	Do not reject

(continued)

Table 4 (continued)

Driver No.	Speed (kmph)	Position profile-unconstrained condition		Position profile-constrained condition		<i>t</i> -statistic	<i>p</i> -value	<i>H</i> ₀
		Mean	SD	Mean	SD			
4	40	0.332	0.055	0.215	0.032	3.552	0.000	Reject
	50	0.429	0.089	0.392	0.121	4.571	0.000	Reject
	30	0.305	0.084	0.231	0.073	4.425	0.000	Reject
	40	0.337	0.095	0.315	0.098	-7.216	1.000	Do not reject
	50	0.456	0.088	0.436	0.083	-5.023	1.000	Do not reject
5	30	0.380	0.078	0.304	0.085	8.839	0.000	Reject
	40	0.370	0.075	0.341	0.107	4.467	0.000	Reject
	50	0.338	0.091	0.389	0.076	-5.003	1.000	Do not reject

Note LPI (lateral position index) = (Lateral position of the left wheel of vehicle from left lane marking/lane width)

SD standard deviation

7 Conclusion

The motivation behind this study was to understand driver response to static obstacles present laterally along the path of travel. Data collection was done through naturalistic driving in an experimental test track for controlled sets of condition. The independent variables of interest were side and pattern of obstruction along the travel path, while the mean lateral gap and lateral position were the dependent variables. Literature showed that the drivers were not influenced by the side of the placement of obstruction. Contradictory to this observation, in the current study it was observed that the lateral gap maintained by the drivers was influenced by the side of the obstruction. From our findings, it was observed that at low speed, the driver was not affected by the side of placement of the obstruction. However, the impact of obstruction side along the direction of travel became more evident at higher speeds. Another interesting observation from the study was the influence of the pattern of roadside obstruction on the lateral positioning of the vehicle. Roadside obstruction can be in either constrained or unconstrained condition. Lateral position was defined in terms of LPI of the vehicle. It was observed that in the presence of obstruction on one side of the lane, the driver preferred to drive toward the unrestricted side of the lane. On the other hand, in the presence of obstruction along both sides of the lane, the driver preferred to follow the driving policy to be on the safer side. However, at higher driving speed, for both constrained and unconstrained condition, irrespective

of the pattern of roadside obstruction, the drivers preferred to drive in the middle of the lane.


The novelty of this study was in understanding of driver behavior in the presence of static objects directly along the path of travel. As expected, we found a significant effect of side and pattern of obstruction on driver behavior. One interesting observation was that side of obstruction influenced the lateral gap only at high vehicle speeds. Another significant contribution of the results was in the understanding of the influence of the pattern of obstruction on driving; the pattern of obstruction influenced drivers only at lower driving speeds. However, at higher speeds, the influence of obstruction pattern diminished and driver preferred to drive in the center of the lane in order to maintain a stable lane position and steady speed.

References

1. Michaels LM, Cozan LW (1963) Perceptual and field factors causing lateral displacement. U.S. Bureau of Public Roads, Washington D.C.
2. Chakroborty P, Agrawal S, Vasishtha K (2004) Microscopic modeling of driver behavior in uninterrupted traffic flow. *J Transp Eng* 130(4)
3. Stamatiadis N et al (2007) Use of context sensitive methods to influence operating speeds. *Transp Res Rec J Transp Res Board* 2025:90–97
4. Stamatiadis N, Bailey K, Grossardt T (2010) Evaluation of highway design parameters on influencing operator speeds through casewise visual evaluation. *Transp Res Rec J Transp Res Board* 2195:143–149
5. Horst RVD, Ridder SD (2007) Influence of roadside infrastructure on driving behavior driving simulator study. *Transp Res Rec J Transp Res Board* 2018:36–44
6. Tay R, Churchill A (2007) Effect of Different median barriers on traffic speed. *Can J Transp* 1(Part 1):56–66
7. Martin PL et al (2010) Comparison between younger and older drivers of the effect of obstacle direction on the minimum obstacle distance to brake and avoid a motor vehicle accident. *Accid Anal Prev* 42:1144–1150
8. Bassat TB, Shinar D (2011) Effect of shoulder width, guardrail and roadway geometry on driver perception and behavior. *Accid Anal Prev* 43:2142–2152
9. Bella F (2013) Driver perception of roadside configurations on two-lane rural roads: effects on speed and lateral placement. *Accid Anal Prev* 50:251–262
10. Budhakar AK, Maurya AK (2017) Characteristics of lateral vehicular interactions in heterogeneous traffic with weak lane discipline. *J Mod Transp*

Development of a Model for Heterogeneous Traffic Simulation



Amit Kumar Das , Manoj Kumar Biswal and Ujjal Chattaraj

Abstract Cellular automata (CA) being a simple and powerful analytical tool has been used in the present study for the analysis of heterogeneous traffic. Heterogeneous traffic comprises different types of vehicles having a wide range of static and dynamic characteristics. Moreover, the driving pattern in developing countries is without lane discipline. These factors added together make the analysis of heterogeneous traffic a cumbersome task. Hence, CA being a simple tool is used to analyse complex scenario. The concept of actual gap and perceived gap and movement according to perceived gap are proposed in the present study. It can be observed from the results that with the introduction of heterogeneity, the capacity value reduces drastically. Moreover, the introduction of slow moving vehicles reduces the stream speed to a great extent. The proposed model is validated using the flow and density data obtained from field.

Keywords Cellular automata · Time step · Heterogeneous traffic · Traffic behaviour · Lane discipline

1 Introduction

The development of infrastructure is one of the major factors for the development of a nation. Developing countries like India have considerably added to its road network in the recent past. As a result of increased communication facility, the number of vehicles has gone up by manifolds. Understanding the traffic behaviour under complex conditions of heterogeneous traffic added with movement without lane discipline becomes extremely necessary. Extensive research has been carried out to study the traffic flow characteristics in homogeneous traffic condition, but the

A. K. Das (✉) · M. K. Biswal · U. Chattaraj
National Institute of Technology, Rourkela 769008, Orissa, India
e-mail: amit76078@gmail.com

M. K. Biswal
e-mail: mbiswal25@gmail.com

U. Chattaraj
e-mail: ujjal.chattaraj@gmail.com

contribution towards the study of heterogeneous traffic is feeble. Moreover, the models developed earlier for heterogeneous traffic study were found to be computationally inefficient. Movement of a vehicle not only involves interaction with other vehicle but also with road elements. Different types of drivers and road conditions also act as a factor of consideration for the analysis procedure. Under such a wide range of variables, the analysis procedure becomes very complex. Hence, an attempt has been made in the present study to develop a model, which can mimic the real-world traffic scenario (under heterogeneous condition) with the minimal use of computational resources. The proposed model incorporates heterogeneous traffic characteristics, i.e. different types of vehicles, movement without lane discipline (movement in both longitudinal and lateral directions).

Nagel and Schreckenberg [1] were the first to propose one-dimensional cellular automata model for vehicular traffic. The model was capable to demonstrate phantom jams, i.e. jams out of no reason, as can be observed in real-world traffic [1]. Later, many modifications were proposed to the basic NaSch model. Takayasu and Takayasu [2] introduced the slow to accelerate concept in order to show the hysteresis effect as seen in real-world traffic. Benjamin et al. [3] introduced certain rules like acceleration rule, disorder rule and slow to start rule to incorporate the delay in human driving process. Slow to start rule can model the delay which a vehicle experiences while starting from stopped condition [3]. Barlovic et al. [4] brought certain changes to the slow to start rules to exhibit features like metastable states and hysteresis. A new concept known as velocity-dependent randomization (VDR) parameter was introduced into the model [4]. Brilon and Wu [5] proposed time-oriented CA model in which the interaction range of a vehicle was considered different from that of conventional CA models. Helbing and Schreckenberg [6] proposed a discrete optimal velocity model. The researchers brought certain changes to the acceleration and deceleration rules such that a vehicle cannot come to stop position from maximum velocity in a single time step [6].

Biham et al. [7] proposed two-dimensional cellular automata model, which separates low-density phase and high-density phase. The author suggests that vehicles move at maximum speeds at low density, whereas vehicles get stuck in a global traffic jam at high densities [7]. Rickert et al. [8] proposed lane-changing rules with “look back” phenomenon. The model was quite helpful to draw fundamental relations between macroscopic and microscopic measurements. Certain demerits such as ping-pong effect and tailgating dance while following a vehicle could be seen in the model [8]. Knospe et al. [9] proposed the brake light model in which the behaviour of a vehicle would depend on the brake light status of the preceding vehicle. Knospe et al. [10] proposed a lane-changing model with asymmetric lane-changing rules. This model could exhibit property like lane inversion [10]. Kerner et al. [11] proposed synchronization distance depending on which a vehicle following a preceding vehicle would adjust its speed.

Lan and Chang [12] proposed a two-dimensional cellular automata model for heterogeneous traffic comprising of cars and motorcycles. Different sizes of cells were used to represent different types of vehicles, whereas the basic updating rules were kept unchanged [12]. Mallikarjuna and Rao [13] used the Knospe’s brake

light model along with modified CA structure for the study of mixed traffic. Traffic comprising of cars and trucks were studied. Critical density conforming to maximum flow is high in case of mixed traffic when compared to only cars or only trucks [13]. Sreekumar and Maurya [14] proposed simulation model for heterogeneous traffic without lane discipline. The vehicular movements were divided into two parts, i.e. lateral control, which is achieved, by controlling the steering angle, and longitudinal control, which is achieved by controlling the speed [14]. Kong et al. [15] proposed a cellular automata model, which reflects the quantitative effect of trucks on passenger cars. This model depicts the behavioural changes of a car driver when near a truck. Road safety and traffic efficiency can be improved by using the results of this model [15].

From the study of literature, it can be concluded that for complex interactions between vehicles and road elements and heterogeneity of traffic, cellular automata can prove to be a very powerful tool to deal with such situations. The application of simple updating rules to mimic real-world traffic scenario cellular automata can prove to be useful.

2 The Proposed Model

2.1 Cell Size

In the present contribution, a road width of 7 m is simulated and the cells are divided into square-shaped cell of 0.1 m. This cell size helps to represent the road width as well as the vehicle size of each category. A road length of 1 km is considered for simulation with periodic boundary conditions. The time step (Δt) is taken to be 0.5 s. The value of time step is chosen according to the value of human reaction time [16]. Due to the discrete nature of space and time, it becomes easy to calculate velocity with respect to the length of each cell. A vehicle moving one single cell in a time step (0.5 s) acquires a velocity of 0.72 km/h. Vehicles travelling multiple cells would acquire speed in multiples of 0.72.

2.2 Actual Gap (G_a), Perceived Gap (G_p) and Buffer (B)

In real-world scenario, the movement of every vehicle depends on the space available in front of it. In order to mimic the real-life condition, three new terms have been proposed, i.e. actual gap, perceived gap and buffer space. Actual gap (G_a) refers to the physical separation between two consecutive vehicles, i.e. the distance between the front bumper of following vehicle and the rear bumper of leading vehicle. Buffer space (B) is the safe distance, which a vehicle reserves in front of it. In other words, it is a psychological space which a driver wants to reserve in order to utilise it in emergency condition. It is considered to be a function of speed.

Fig. 1 Schematic diagram depicting G_a , G_p and buffer

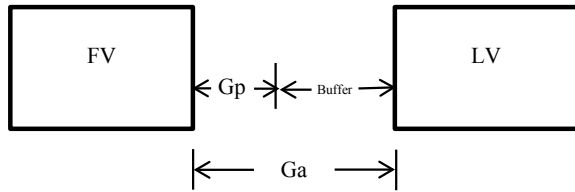


Table 1 Various vehicle sizes [16]

Type of vehicle	Length (m)	Width (m)
Car	4.2	1.7
Two-wheeler	1.8	0.6
Three-wheeler	2.6	1.4

$$B = C_1 + C_2v \tag{1}$$

where C_1 and C_2 are constants obtained from field data and v is speed in km/h.

Perceived gap is the distance, which a vehicle actually moves. It is the difference between actual gap and buffer space (Fig. 1; Table 1).

$$G_p = G_a - B \tag{2}$$

2.3 Updating Procedure

Simple rules were used for the movement of vehicles both in lateral and longitudinal direction. The lateral and longitudinal movements of vehicles occur simultaneously unlike the movement proposed by Kerner et al. [11] where the lateral and longitudinal movements of vehicles occur in two separate steps. Vehicles under homogeneous traffic condition and following lane discipline change lanes when the driver is not capable of achieving its desired speed and the space in the adjacent lane is sufficient and attractive enough for lane change to occur. Under heterogeneous traffic condition lane, changing keeps no meaning. Here, the driver makes the maximum use of the available space so as to move at his/her desired speed. It is assumed that a driver does not change his/her steering angle unless and until impeded by a static or dynamic obstacle. Static obstacle refers to road furniture and road elements, whereas dynamic obstacles refer to other vehicles. Steering angle change while meeting a static obstacle is to avoid collision, whereas steering angle change while meeting a dynamic obstacle is to avoid collision as well as move to a better place so as to achieve the desired speed. Basing upon the space available, the vehicle moves either to right or to the left. As in India, we follow overtaking from the right side; first preference is given to steering movement in right direction.

Step 1: Compute G_a

Step 2: Compute B

Step 3: If $(B > G_a)$ then

$v = v \times (G_a/B)^n$ (where n is an integer) (speed reduction)

Compute relative speed (RS)

if $(RS < 0$ and $x \pm 1 = 0)$ then

 change steering angle

 movement = $v/0.72$

move = round(movement)

$y = y - \text{move}$

else

$y = y - \text{move}$

Step 4: If $(B < G_a)$ then

$G_p = G_a - B$

Compute relative speed (RS)

if $(RS < 0$ and $x \pm 1 = 0)$ then

 change steering angle

 movement = $v/0.72$

move = round(movement)

$y = y - \text{move}$

else

$y = y - \text{move}$

Step 4: Update position

$y = y - \text{move}$

$x = x \pm 1$

3 Results

Various types of conditions were simulated using the above rules. First homogeneous traffic with all car condition was simulated. The legends at the top represent percentage cell occupancy. The flow values obtained in case of only cars situation are 9000–9500 veh/h (Fig. 2).

The second type of simulation carried was with a combination of 50% two-wheeler and 42% four-wheeler and 8% three-wheeler. The different percentages of vehicles presented above are same as those found in field condition. As the number of two-wheelers is more, their contribution towards the PCU values is more for the same cell occupancy. The values of PCU are adopted from IRC 106-1990 [17]. The number

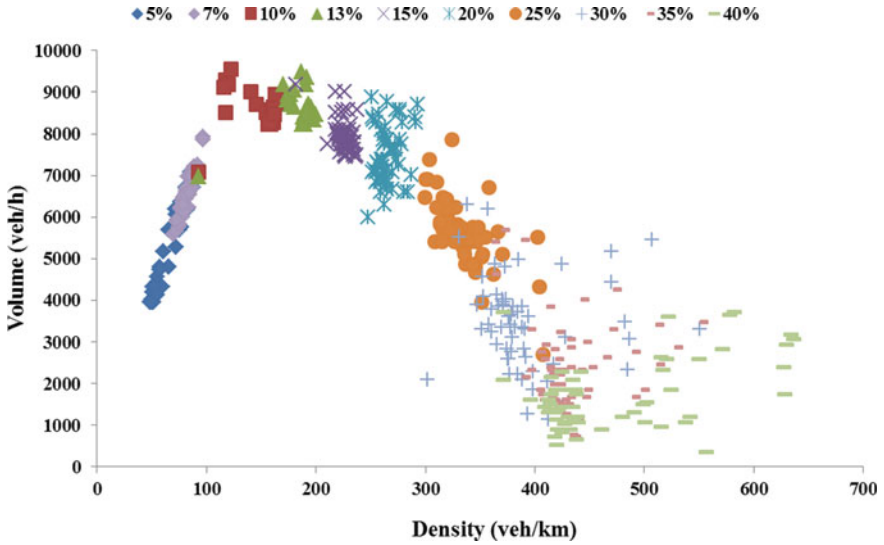


Fig. 2 Flow-density curves for all cars' condition

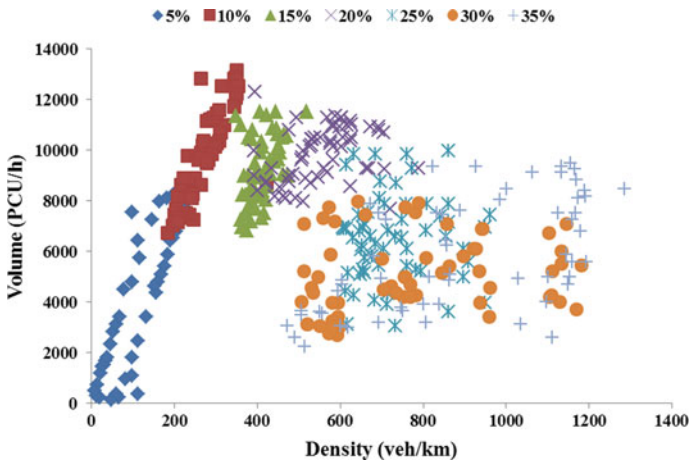


Fig. 3 50% two-wheeler and 42% four-wheeler and 8% three-wheeler

of two-wheelers required for the same cell occupancy is more when compared to a number of four-wheelers. Therefore, the contribution towards PCU is also more. Hence, the capacity values increase with the introduction of two-wheelers (Fig. 3).

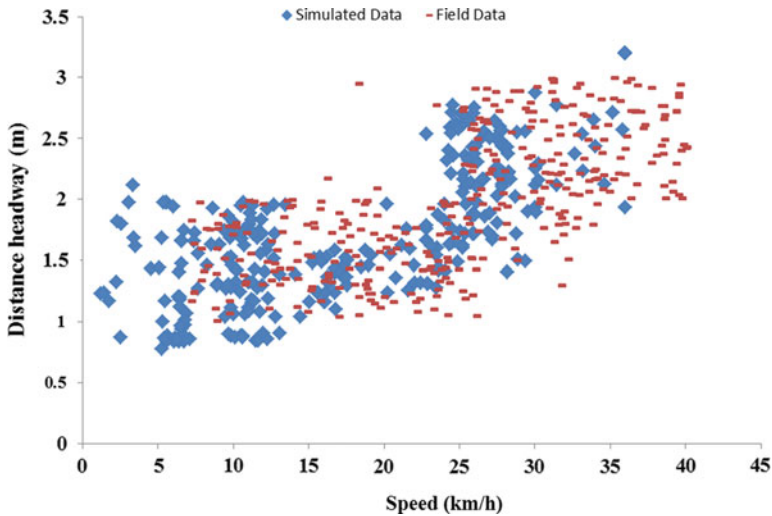


Fig. 4 Observed and simulated distance headway–speed relationship

4 Model Validation

The model is validated using the data collected in the urban roads of Bhubaneswar, Orissa. The urban traffic mainly comprises two-wheeler, three-wheeler and four-wheeler. As heavy vehicles are restricted during daytime within the city, there was no data obtained for heavy vehicles. The traffic composition was found to be 50% two-wheeler and 42% four-wheeler and 8% three-wheeler. The distance headway and speed curves for both simulated data and field data seem to have a close match, implying the validation of the simulation model (Fig. 4).

5 Conclusion

In the present contribution, a cellular automata model has been developed for simulating heterogeneous traffic. Characteristics of heterogeneous traffic such as different types of vehicles, movement without lane discipline have been introduced. Using the same rules for movement, homogeneous traffic is simulated to compare the capacity values. Three types of vehicles have been simulated, i.e. 2W, 3W and 4W. Flow—density relationship obtained from field data was compared with simulated data. It was found that the field data and simulated data match closely.

References

1. Nagel K, Schreckenberg M (1992) A cellular automaton model for freeway traffic. *J Phys I* 2(12):2221–2229
2. Takayasu M, Takayasu H (1993) $1/f$ noise in a traffic model. *Fractals* 1(04):860–866
3. Benjamin SC, Johnson NF, Hui PM (1996) Cellular automata models of traffic flow along a highway containing a junction. *J Phys A Math Gen* 29(12):3119
4. Barlovic R, Santen L, Schadschneider A, Schreckenberg M (1998) Metastable states in cellular automata for traffic flow. *Eur Phys J B Condens Matter Complex Syst* 5(3):793–800
5. Brilon W, Wu N (1999) Evaluation of cellular automata for traffic flow simulation on freeway and urban streets. In: *Traffic and mobility*. Springer, Berlin, Heidelberg, pp 163–180
6. Helbing D, Schreckenberg M (1999) Cellular automata simulating experimental properties of traffic flow. *Phys Rev E* 59(3):R2505
7. Biham O, Middleton AA, Levine D (1992) Self-organization and a dynamical transition in traffic-flow models. *Phys Rev A* 46(10):R6124
8. Rickert M, Nagel K, Schreckenberg M, Latour A (1996) Two lane traffic simulations using cellular automata. *Phys A Stat Mech Appl* 231(4):534–550
9. Knospe W, Santen L, Schadschneider A, Schreckenberg M (2000) Towards a realistic microscopic description of highway traffic. *J Phys A Math Gen* 33(48):L477
10. Knospe W, Santen L, Schadschneider A, Schreckenberg M (2002) A realistic two-lane traffic model for highway traffic. *J Phys A Math Gen* 35(15):3369
11. Kerner BS, Klenov SL, Wolf DE (2002) Cellular automata approach to three-phase traffic theory. *J Phys A Math Gen* 35(47):9971
12. Lan LW, Chang CW (2005) Inhomogeneous cellular automata modeling for mixed traffic with cars and motorcycles. *J Adv Transp* 39(3):323–349
13. Mallikarjuna C, Rao KR (2009) Cellular automata model for heterogeneous traffic. *J Adv Transp* 43(3):321–345
14. Sreekumar M, Maurya AK (2012) Need for a comprehensive traffic simulation model in Indian context. In: *IJCA proceedings on international conference on emerging frontiers in technology for rural area (EFITRA-2012)*, vol 5, pp 13–18
15. Kong D, Guo X, Yang B, Wu D (2016) Analyzing the impact of trucks on traffic flow based on an improved cellular automaton model. *Discret Dyn Nat Soc* 2016
16. Arasan VT, Koshy RZ (2005) Methodology for modeling highly heterogeneous traffic flow. *J Transp Eng* 131(7):544–551
17. IRC: 106-1990 (1990) Guidelines for capacity of urban roads in plain areas. The Indian Roads Congress, New Delhi

Highway Materials and Pavement

Resource Mapping of Highway Materials Along with Their Characteristic Properties and Desirability



P. N. Salini, B. G. Sreedevi and Sam Ebin

Abstract Highway construction materials are precious resources as the quantum of construction has been on the rise and there is a scarcity for these resources. There is also an urgent need to step up research and development efforts to enhance the use of locally available materials and create a database on their characteristic properties, performance and cost-effectiveness for adoption in road construction in a big way. This paper is oriented on resource mapping in order to map the resource locations with attributes such as physical characteristic properties, material availability, distance from the nearest primary road in geo-referenced map, thereby creating a scientific information on the availability and suitability of construction material in the southern districts of the Kerala state along with a scientific and comparative analysis on the engineering properties of the same. The resources available for construction works have a wide variation in their characteristic properties, and they are invariably required to be tested for all their physical characteristics. The findings of the study which include the comprehensive information regarding the occurrence, distribution, lead distance, quantum of materials, material properties and its suitability for various applications in construction works, accessibility, etc., are attached as attribute data on geo-referenced maps in GIS platform. The various findings of the study are useful for licensing authorities and execution departments and other stakeholders. The database with the quantum of materials available in each quarry and their desirability can be effectively used for optimum material planning.

Keywords Resource mapping · Fine and coarse aggregates · GIS mapping · Attribute data · Engineering properties · Optimum material planning · Desirability

P. N. Salini (✉) · B. G. Sreedevi · S. Ebin
National Transportation Planning and Research Centre (NATPAC), Thiruvananthapuram, Kerala,
India
e-mail: salini.jayaprakash@gmail.com

B. G. Sreedevi
e-mail: bgsreedevi@yahoo.com

S. Ebin
e-mail: ebin.natpac@gmail.com

1 Introduction

Highway materials are the inputs to road construction activity. Varied geographical regions with a wide range of soil types have diverse types of resources. Resources of highway materials are depleting, and the scarcity of highway materials poses difficulties for road construction which is quite cost intensive as well. Hence, stringent efforts are on to make use of the locally available resources. Materials alone cost more than 50–60% of the total construction cost. There are suitable checks and quality tests for judging the properties and performance of these localized materials. Improper selection of materials and resources will lead to problems in quality, delivery and timely availability of materials, cost overrun, etc. The location, exploitation and movement of large tonnages of aggregates have a considerable impact on the economy and environment. There is an urgent need to step up research and development efforts to enhance the use of locally available materials and create a database on their properties, performance and cost-effectiveness for adoption in road construction in a big way, thereby effecting optimum material planning.

The resources of coarse and fine aggregates available for construction works in Kerala have a wide variation in their characteristic properties. These aggregate materials are invariably required to be tested for all their properties, especially the shape indices expressed in terms of flakiness index (FI), elongation index (EI) and combined index (CI) before their use in any sort of construction works [1]. Flaky and elongated particles have larger specific surface area which results in higher demand of binder content to coat all aggregate surfaces adequately making the mix harsh and less durable [2]. The bitumen content required for mix sample with aggregates having high values of FI, EI and CI is likely to be higher than the optimum bitumen content designed for aggregates of particular size. However, high variation in proportions of such aggregates within permissible limit too can upset a well-designed mix and hence the quality of works. The bituminous mixes made with poor shape aggregates may result in poor compaction, high air void, insufficient voids filled with bitumen and poor stability and flow in finished work [2]. A comprehensive study needs to be done to determine the extents of variation of the shape indices of aggregates and other characteristic properties of aggregates like impact value, abrasion value, bulk density, specific gravity and water absorption. Flaky and elongated pieces of aggregates are more prone to break into smaller pieces due to impact or other forces. Hence, it is prudent to think of the possible effects of shape of aggregates on other properties of aggregates like aggregate impact value, Los Angeles abrasion value, bulk density and percentage air voids [3]. This paper orients in that direction making a comparative study and a scientific analysis on the various properties of coarse aggregates and their correlations if any [4].

2 Scope and Objectives

The scope of the study is limited to the resources of highway materials available within the southern districts of Thiruvananthapuram, Kollam and Pathanamthitta. The major objectives of the study involve the following:

1. Development of a spatial database, attribute database and scientific analysis and output modules.
2. Comparative study on the characteristic properties of the resources of coarse aggregates available from all the taluks in three districts of southern Kerala.
3. Preparation of geo-referenced maps in GIS platform with a comprehensive attribute data on resources.
4. Study on the influence of shape of aggregates in terms of FI, EI and CI on the other properties of aggregates.

3 Study Area

Aggregates were collected from different crushers/quarries situated in different taluks of three southern districts of Kerala state, i.e. Thiruvananthapuram, Kollam and Pathanamthitta. The southernmost district of Thiruvananthapuram situated between north latitudes $8^{\circ} 17'$ and $8^{\circ} 54'$ and east longitudes $76^{\circ} 41'$ and $77^{\circ} 17'$ is characterized by its undulating terrain of low coastal hills and busy commercial valleys. The district has four administrative subdivisions (taluks) and can be divided into three geographical regions: Highlands, Midlands and Lowlands. The geographical coordinates of Kollam district are $8^{\circ} 48' 00''N$ and $76^{\circ} 36' 00''E$. The district covers an area of $2,491 \text{ km}^2$ and ranks seventh in the state with respect to area. The district is immensely rich in mineral resources. Kollam district has five taluks, namely: Karunagappally, Kunnathur, Pathanapuram, Kottarakkara and Kollam. Pathanamthitta district is the youngest district located in the southern part of the state of Kerala. Pathanamthitta is a landlocked district, located at $9.05^{\circ}N$ and $76.9^{\circ}E$ spanning over an area of $2,637 \text{ km}^2$ ($1,018.15 \text{ m}^2$). The district is 10.03% urbanized. Pathanamthitta district has a reserve forest area which is approximately 50% of the total district area and is considered as industrially backwards. The Pathanamthitta district is divided into five taluks: Ranni, Kozhencherry, Adoor, Thiruvalla and Mallappally. The study area map is shown in Figs. 1, 2 and 3.



Fig. 1 Map of the study area—Thiruvananthapuram district



Fig. 2 Map of the study area—Kollam district

4 Methodology

4.1 Collection of Samples

Representative samples were taken from the stockpile of quarries for the purpose of testing. Such representative samples were collected from all the licensed quarries of the two districts. The production of aggregates is varying in sizes such as 1/2", 3/4", 1", 1 1/2" and rubble. Approximately, 40 kg of samples was collected from each quarry.



Fig. 3 Map of the study area—Pathanamthitta district

The geo-coordinates of sampling station were recorded with single-frequency Global Positioning System (GPS). The particulars of each quarry were also recorded in the data sheet, which was prepared for this study. It consisted of the details like location of the quarry including the village and taluk name, accessibility from the nearest junction, type of road availability, age of quarry, the quantum of material availability, method of production, available aggregate sizes and its operational period. Figure 4 shows two of the numbers of quarry locations from where the details and samples were collected.

The location and licence details of the quarries are obtained from the Taluk Office and Geological Survey Department. Details as per format are collected from local enquiry and samples collected from each location for laboratory distance from the nearest road/place and route, accessibility, age, whether the quarry is active, estimated quantity, method of production/collection and distribution (mechanical/manual), whether private or government, size of aggregates available, average annual production, operational period, geo-coordinates and any other formation available. The quantum of materials available is assessed by visual observation and measurement. Bitmaps showing the locations are prepared in AutoCAD as shown in Fig. 5.

Fig. 4 Two quarries in study area



4.2 Laboratory Tests

Aggregates are the components of a composite material used to resist compressive stress. The desirable properties of the aggregates were tested as given in Table 1 for judging the suitability of aggregates as per MoRTH specifications.

5 Analysis and Results

Quality and cost of highway material procurement are two attributes that are directly affected by the material supplier selection process. In order to maintain both of these attributes, supplier selection should be well defined, in a way that decreases project logistics and supply chain management costs. Hence, the spatial database and attribute database prepared by geo-referenced mapping and brought out in this paper are emphasized on these aspects. The facts inferred from the results of the tests conducted on the samples of coarse aggregates (CAs) collected from the districts in southern Kerala are summarized in Table 2. Desirability of respective aggregate resources for use in varied pavement layer types like stone matrix asphalt (SMA), bituminous concrete (BC), semi-dense bituminous concrete (SDBC), dense bituminous macadam (DBM), bituminous macadam (BM), close graded premix surfacing (CGPS), open graded premix surfacing (OGPS), surface dressing (SD), mastic

Fig. 5 Bitmap showing the location of two quarries

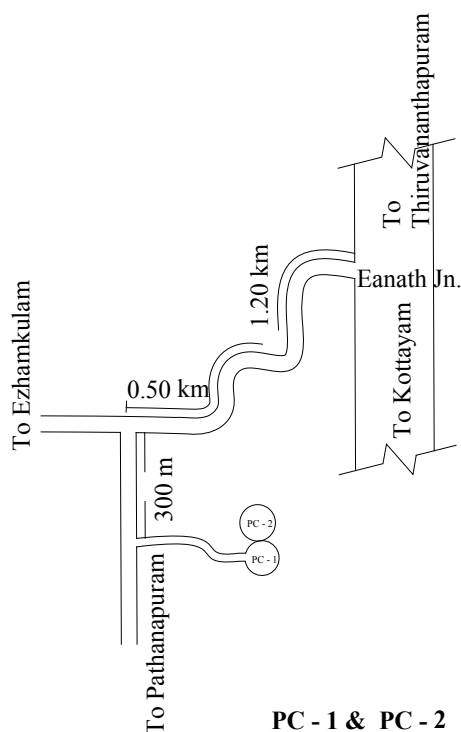


Table 1 Properties of aggregates

Sl. no.	Properties	Method of test
1	Shape test [FI (%), EI (%), CI (%)]	IS:2386 Part (I)-1963
2	Aggregate impact value (AIV) (%)	IS:2386 Part (IV)-1963
3	Los Angeles abrasion value (%)	IS:2386 Part (IV)-1963
4	Specific gravity and water absorption (%)	IS:2386 Part (III)-1963
5	Bulk density (kg/m^3) and percentage of voids	IS:383-1970

asphalt, BCM, water bound macadam (WBM), wet mix macadam (WMM), crusher run macadam (CRM) is investigated, and inferences are drawn on its possible applications. The suitability of aggregate resources in rural road construction is also examined and reported in Table 3. Total of 124 coarse aggregate samples were collected and tested from Thiruvananthapuram district, 53 samples from Kollam district and 100 samples from Pathanamthitta district. Hence altogether, 277 samples of available coarse aggregates were collected and tested from southern Kerala.

The specific gravity of all the samples of aggregates from the three districts comes under the limiting value between 2.6 and 2.8. Also, the water absorption values of all

Table 2 Summary of coarse aggregate properties and desirability of these resources in southern Kerala for the construction of highways

Property	Limiting value (%)	% samples of coarse aggregates in different districts falling within the limiting values			Recommended uses/suitability
		Thiruvananthapuram	Kollam	Pathanamthitta	
Flakiness index (FI)	<12	25.8	11.5	44	Suitable for stone matrix asphalt (SMA)
	<15	36.3	21.1	57	Suitable for BC, DBM
	<16	41.9	25	57	Suitable for BM, CGPS, OGPS, SD, mastic asphalt, BCM, lean BM
Elongation index (EI)	>16	58.1	75	43	Not suitable for pavement construction
	<18	25.0	1.9	31	Suitable for stone matrix asphalt (SMA)
	<20	26.6	1.9	34	Suitable for BC, DBM
	<24	38.7	1.9	48	Suitable for BM, CGPS, OGPS, SD, mastic asphalt, BCM, lean BM
Combined index (CI)	>24	61.3	98.1	52	Not suitable for pavement construction
	<30	15.3	23.1	31	For pavement construction in SDBC
	<40	32.3	40.4	51	For pavement construction in WBM, WMM, CRM
	<35	23.4	30.8	40	General construction purpose
	>40	67.7	59.6	49	Not desirable for pavement construction
Aggregate impact value (AIV)	<18	1.0	13.5	0	Suitable for stone matrix asphalt (SMA)
	<30	23.4	76.9	14	For BM, CGPS, OGPS, SD, mastic asphalt, BCM, lean BM, WBM, WMM, CRM
	<27	17.7	69.2	10	For DBM and SDBC
	<24	9.7	51.9	5	For BC

(continued)

Table 2 (continued)

Property	Limiting value (%)	% samples of coarse aggregates in different districts falling within the limiting values			Recommended uses/suitability
		Thiruvananthapuram	Kollam	Pathanamthitta	
Los Angeles abrasion	>30	76.6	23.1	86	Not desirable for pavement construction
	<25	43.5	0	13	Suitable for SMA
	<30	71	1.9	40	For BC
	<35	83.9	5.8	70	For DBM and SDBC
	<40	86.3	11.5	84	For BM, CGPS, OGFS, SD, mastic asphalt, BCM, lean BM, WBM, WMM, GRM
>40	13.7	88.5	16	Not desirable for pavement construction	

Table 3 Summary of aggregate properties and their desirability in rural road construction—resources from three districts of southern Kerala

Property	Limiting value (%)	% samples of coarse aggregates in different districts falling within the limiting values			Recommended uses
		Thiruvananthapuram	Kollam	Pathanamthitta	
Flakiness index (FI)	<30	78.2	69.2	97	Suitable for base course
	<40	90.3	76.9	100	Suitable for sub-base course
	>40	9.7	23.1	0	Not suitable for pavement construction
Combined index (CI)	<35	23.4	30.8	40	For bituminous course
	>35	76.4	69.2	60	Not suitable for pavement construction
Aggregate impact value (AIV)	<30	23.4	76.9	14	Suitable for bituminous course
	<40	36.3	78.8	36	Suitable for base course
	<50	41.1	78.8	37	Suitable for sub-base course
	>50	58.9	21.2	63	Not suitable for pavement construction
Los Angeles abrasion	<40	86.3	11.5	84	Suitable for bituminous course
	>40	13.7	88.5	16	May be used for base and sub-base course

the samples are less than 2%. The bulk density is less than 2.8 g/cc which is desirable. Hence with regard to specific gravity, water absorption and bulk density, they could be used for various bituminous courses, cement concrete works, RCC works and masonry works. It was also found from the results that the bulk density values of aggregates are decreasing with an increase in percentage of flaky aggregates.

There is negative effect of flaky particles on the strength properties of aggregates. The impact value of aggregates is increased with an increase in the percentage of flaky aggregates and with an increase in combined index values. This variation is shown in Figs. 6 and 7. It was found that with the increase in the percentage of flaky aggregates the bulk density of the aggregates is getting decreased resulting in high air voids. Hence, it is recommended that shape, size, grading and other properties of aggregates for various construction works have to be stringently monitored and ample attention to be given during the material selection.

The summary of the properties of fine aggregates available in southern Kerala and their suitability in construction purposes are also prepared and illustrated by GIS mapping. Total of 92 samples of fine aggregates were collected and tested comprising of 22 samples from Thiruvananthapuram district, 42 samples from Kollam district and 28 samples from Pathanamthitta district. Suitability of this fine aggregate resource for construction purposes is examined based on their engineering properties and is summarized in Table 4. The spatial and attribute databases of these fine aggregate resources are prepared in geo-referenced map (Figs. 8, 9 and 10).

Fig. 6 Variation of AIV with an increase in FI value

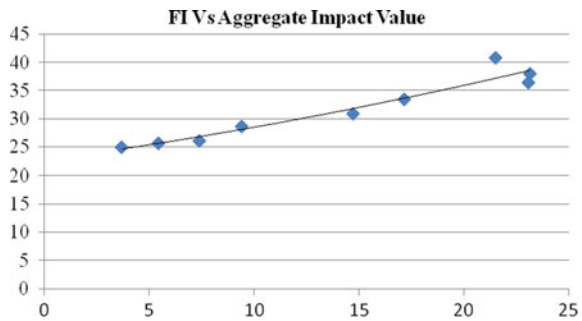


Fig. 7 Variation of AIV with an increase in CI value

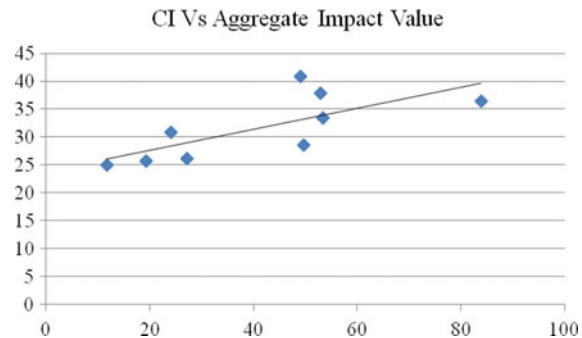


Table 4 Summary of fine aggregate properties and their desirability in construction—resources from three districts of southern Kerala

Property of fine aggregate	Limiting value	% of fine aggregate resources within the limiting value in different districts			Recommended uses/suitability
		Thiruvananthapuram	Kollam	Pathanamthitta	
Fineness modulus (FM)	<3.5	81.8	66.7	39.3	Suitable for concrete works
	>3.5	18.2	33.3	60.7	Not suitable for concrete works
Silt content	<3%	77.3	78.6	82.1	Suitable for concrete works
	>3%	22.7	21.4	17.9	Not suitable for concrete works
Bulk density	1.6–1.7	68.2	92.8	75	Suitable for construction
	<1.6 and >1.7	31.8	7.2	25	Not suitable for construction

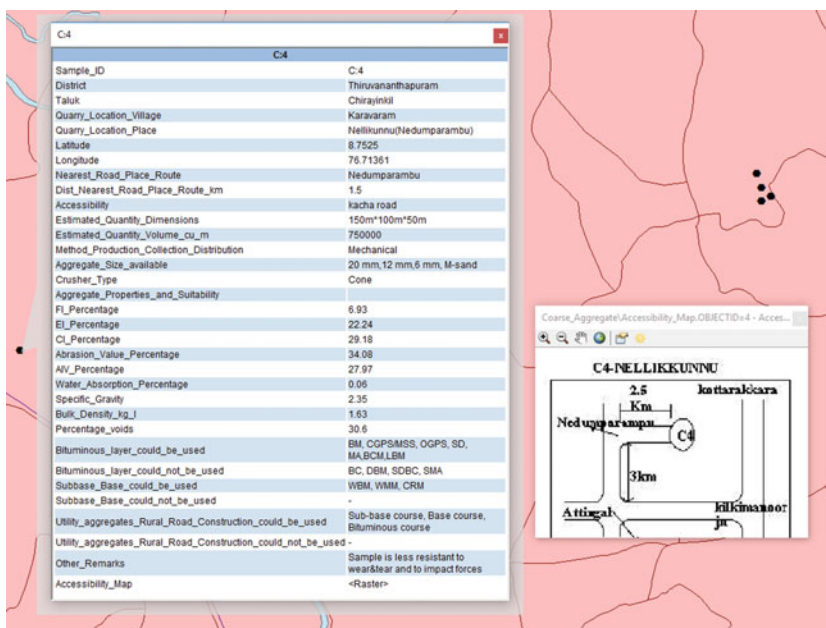


Fig. 8 Resource mapping for Thiruvananthapuram

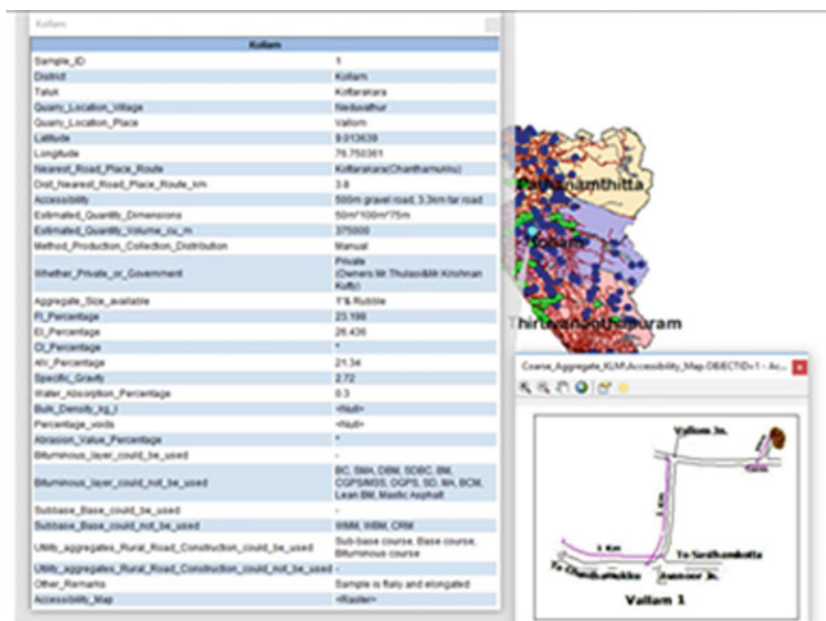


Fig. 9 Resource mapping for Kollam

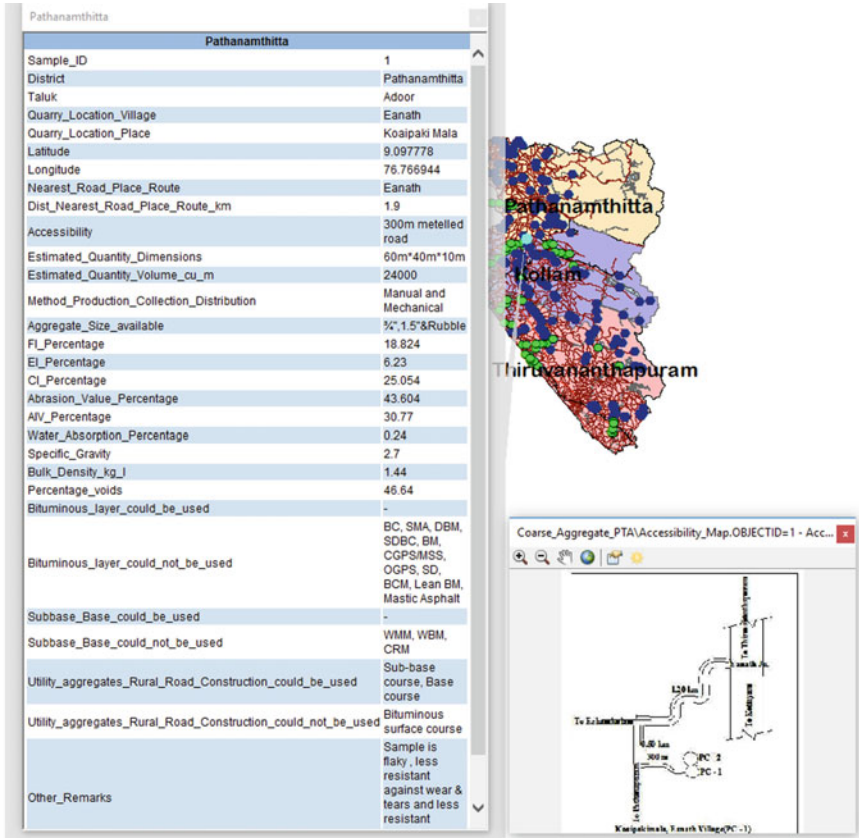


Fig. 10 Resource mapping for Pathanamthitta

6 Summary and Conclusions

Based on a scientific study and analysis, inferences are drawn on the suitability of available resources of fine and coarse aggregates for varied pavement construction purpose. It was found from the scientific analysis that the resources of fine aggregates available in southern Kerala have specific suitability to varied application in pavement construction. The geo-referenced spatial and attribute databases of these resources incorporating their properties and desirable application are prepared which will help in appropriate resource selection and optimal material planning. The findings are useful for licensing authorities and execution departments. The database with the quantum of materials available in each quarry can be used for material planning, and usefulness of the materials based on the engineering properties can be evaluated.

7 Scope for Further Research

The performance-related properties of these varied aggregates in bituminous mixes could be studied and reported. This will invariably contribute to progressive research on this area as the properties of aggregates have a significant role to play in the performance of mixes.

Acknowledgements The authors would like to acknowledge the support rendered by the scientists and technical assistants in carrying out the study. The authors would also like to express deep sense of gratitude to Kerala State Council for Science, Technology and Environment for the funding of this study.

References

1. Jha SN (2008) Necessity to monitor shape and size properties of aggregates. *Indian Highw* 36(3):49–58
2. Sengupta JB, Kumar S (2008) Effect of flakiness indices on the properties of aggregate and cement concrete. *Indian Highw* 36(4):57–62
3. Kumar S, Pokhriyal SP, Srivastava RK, Sharma BM (2009) Skid resistant aggregates in wearing courses. *Highw Res J* 2(2):13–21
4. Thakare PV, Mhaske SY (2014) GIS based material management and supplier selection in Thane city—a case study. *Int J Innovative Res Adv Eng (IJIRAE)* 1(5):13–21

Understanding Effects of Crushing Mechanism on Aggregate Morphology Using AIMS



Bharat Rajan, Dharamveer Singh, Saurabh Maheshwari and Gaurav Garg

Abstract The present study compared angularity, texture, sphericity and flat and elongation (F&E) ratio of three different sizes (P19-R12.5, P12.5-R9.5 and P9.5-R4.75) of coarse aggregate produced from two different types of crushing operations. The aggregates were collected from two different types of crushers (i) the first crusher had jaw, cone and vertical shaft impactor (VSI) as primary, secondary and tertiary crushers, respectively; and (ii) the second crusher had jaw, horizontal shaft impactor (HSI) primary and secondary crushing unit, respectively. The angularity, texture, sphericity and flat and elongation (F&E) of aggregates were measured using aggregate image measurement system (AIMS) in accordance with the AASHTO TP81 method. Further, laboratory tests like angle of repose (AoR) and VCA_{drc} were conducted to identify the influence of aggregate morphology on the performance of aggregates. The results showed that aggregates produced from JH series of crusher had higher F&E ratio, higher texture and lower sphericity as compared to aggregates from JCV series of crusher. However, both the crushers JH and JCV produced aggregates with similar angularity. The aggregates produced from JH series of crusher show better performance over JCV produced aggregates.

Keywords Angularity · Texture · Sphericity · Flat and elongation · AIMS

B. Rajan (✉) · D. Singh · S. Maheshwari · G. Garg
Department of Civil Engineering, Indian Institute of Technology Bombay, Powai, Mumbai
400076, India

e-mail: bharat.rajan08@gmail.com

D. Singh

e-mail: dvsingh@civil.iitb.ac.in

S. Maheshwari

e-mail: saurabhmaheshwari52@gmail.com

G. Garg

e-mail: ggarg0405@gmail.com

1 Introduction

Hot mix asphalt (HMA) primarily constitutes of coarse aggregate, fine aggregate and binder. Each component plays an important role in structural and functional stability of asphalt mixes. Like, coarse aggregates provide major load distribution network from the top of pavement surface to subsequent bottom layers, while fine aggregates fill the voids among coarse aggregates skeleton and help in producing denser mix. The binder provides glue action for aggregates to form a monolithic asphalt mix. The performance of new generation mixes, viz.: stone matrix asphalt (SMA) and open-graded friction courses (OGFC) mixes depend on stone-to-stone contact among coarse aggregates [1, 2]. The aggregate morphology such as angularity, texture and dimensional properties (e.g. sphericity, flakiness and elongation) can have high influence on the structural and functional performance of asphalt mixes [3]. Angularity indicates sharpness of corners, which affect interlocking of aggregates and consequently influence rut resistance behaviour of asphalt mixes [4–7]. Texture is a measure of aggregate surface irregularities, which can be directly associated with inter-aggregate surface friction and aggregate-asphalt bond strength. The dimensional properties (sphericity, flakiness and elongation) can influence aggregate breakage under dynamic loading.

The aggregate morphology is mainly governed by aggregate mineralogy, type of rock and crushing operation [8–10]. For given aggregate type, the associated crushing mechanism plays a decisive role in governing morphology of aggregates. The crushing of aggregates involves three prime mechanisms, namely abrasion, cleavage and impact [11]. The abrasion can only induce localised stress in a small fragment of total surface area and result in limited size reduction. Cleavage is the application of compressive stress on aggregate, which prompts a limited number of fractures plane and produce uniform size of coarse aggregates. The impact mechanism uses impact force for crushing of aggregates. Impact on the aggregates is generated by the collision of high-velocity aggregates either with aggregates or hard surface (i.e. anvil, hammer, etc.). Impact produces widest size range of aggregates (from fine to coarse) [11–13]. Hence, it is clear that all crushers have its unique type of crushing phenomena and that may play an imperative role in deciding the aggregate morphology.

In the present study, the effects of two different crushing operations (jaw-cone-vertical shaft impact (VSI): JCV and jaw-horizontal shaft impact (HSI): JH) on coarse aggregate morphology were studied. Angularity, texture, sphericity and F&E of three different sizes of coarse aggregates: passing a sieve of 19 mm and retaining a sieve of 12.5 mm (P19-R12.5), P12.5-R9.5 and P9.5-R4.75 were measured using aggregate image measurement system (AIMS). The AIMS works on the principle of digital imaging technique and enables rapid and impeccable measurement of aggregate morphology [1]. In addition, the packing and stability of coarse aggregates were studied using two different laboratory performance tests: angle of repose (AoR) and void in coarse aggregate in dry-rodged condition (VCA_{drc}).

2 Objective of Study

The objectives of the current study are outlined as:

- Study the morphology of three different sizes of coarse aggregates (P19-R12.5, P12.5-R9.5 and P9.5-R4.75) produced from JH and JCV type series of crushers.
- Performance analysis of aggregates by comparing the packing characteristics and stability using angle of repose (AoR) and VCA_{drc} test.

3 Materials and Methodology

The study uses basaltic aggregate produced from two different crushing mechanisms (i) jaw, cone and VSI (vertical shaft impactor) as primary, secondary and tertiary crushers, respectively (Jaw-Cone-VSI, denoted as JCV); and (ii) jaw and HSI (horizontal shaft impactor) primary and secondary crushing units, respectively (Jaw-HSI denoted as JH). Both the crushing mechanisms are extensively used for aggregate production.

3.1 Measurement of Aggregate Shapes Using Aims

Aggregate image measurement system (AIMS) is an automated device consists of a high-resolution camera with a variable magnification microscope, aggregate tray, backlighting and top-lighting systems [1]. AIMS enables the measurement of morphological characteristics for a wide range of aggregates (ranging from 37.5 to 0.075 mm) using digital image technique. Coarse aggregates (retaining on 4.75 mm) are analysed for angularity, sphericity, flat and elongated (F&E) and texture, while fine aggregate (passing 4.75–0.075 mm) is analysed for angularity and forms 2D. In addition, AIMS is capable to differentiate between different types of aggregates, crushing mechanism, etc. [6, 14, 15]. Figure 1 shows the sub-classification (i.e. low, medium, high and extreme) of angularity, texture and sphericity of coarse aggregates in AIMS [9].

3.2 Performance Tests

To understand the effect of aggregate shape on stability and packing behaviour, two widely used tests, namely VCA_{drc} and AoR were conducted on individual sizes of coarse aggregates.

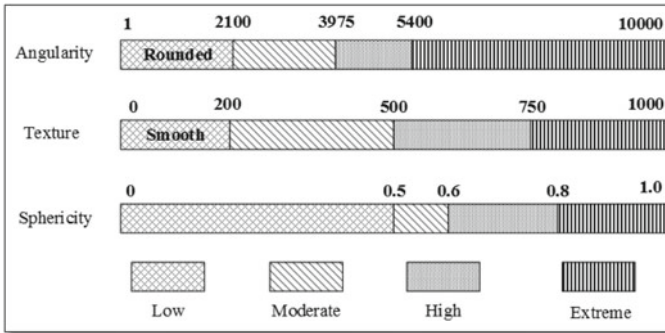


Fig. 1 Classification of aggregate morphology in AIMS

VCA_{drc}

The VCA_{drc} measures voids present in dry-rodded coarse aggregates. The test is useful to determine the particle packing behaviour of coarse aggregates. The aggregate with high texture and angularity may show higher VCA_{drc}. The VCA_{drc} is calculated using Eq. (1) in accordance with ASTM C29 [16].

$$VCA_{drc} = \frac{G_{CA}\gamma_w - \gamma_s}{G_{CA}\gamma_w} \times 100 \tag{1}$$

where G_{CA} —Bulk specific gravity of coarse aggregate; γ_s —Dry density of coarse aggregate; γ_w —Density of water (at measured temperature).

Angle of Repose (AoR)

Angle of repose (AoR) is a *measure* of aggregate packing behaviour and their structural stability. AoR is the maximum angle relative to horizon that an aggregate material can sustain naturally. The AoR is function of aggregate interlocking. A plane surface area was used as a test area [17, 18]. The aggregates were poured to from zero height in the form of heap by using 150-mm-hollow cylinder. The height and diameter of heave were measured with the help of two perpendicular cross-movable arms (Fig. 2). The height was measured from either side of heave (Fig. 2a), while diameter was measured at four different alignments with difference of 45° (Fig. 2b). The AoR (θ) was calculated using Eq. (2). The aggregates with better AoR show higher particle interlocking [18].

$$\text{Angle of Repose } (\theta) = \tan^{-1}\left(\frac{2h}{d}\right) \tag{2}$$

where θ —Angle of repose (in degree); h —Height of aggregate heave; d —Diameter of aggregate heave.

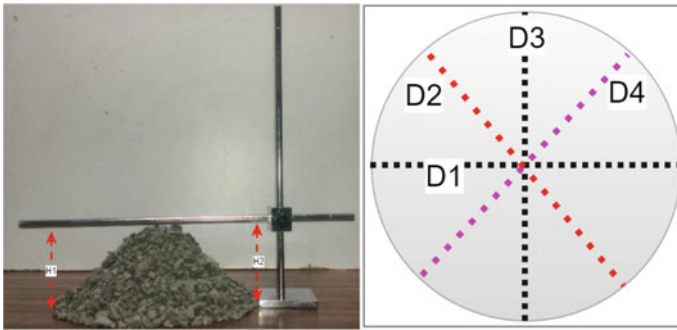


Fig. 2 Angle of repose **a** height measurement **b** diameter measurement

4 Results and Discussion

4.1 Aggregate Shape Properties

Figures 3, 4, 5 and 6 show the plot of mean values for angularity, texture, sphericity, and F&E of three different aggregate sizes (i.e. P19-R12.5, P12.5-R9.5 and P9.5-R4.75) of coarse aggregates produced from JH and JCV series of crushers. Further, the statistical analysis results are shown in Table 1.

Angularity

From Fig. 3, it can be seen that the mean angularity of coarse aggregates P19-R12.5 and P9.5-R4.75 produced from JH series of crusher is higher than aggregates obtained from JCV crusher, while P12.5-R9.5 aggregates show almost similar value (Fig. 3). Further, student’s *t*-test was conducted at 95% confidence level to compare

Fig. 3 Comparison of angularity of coarse aggregates

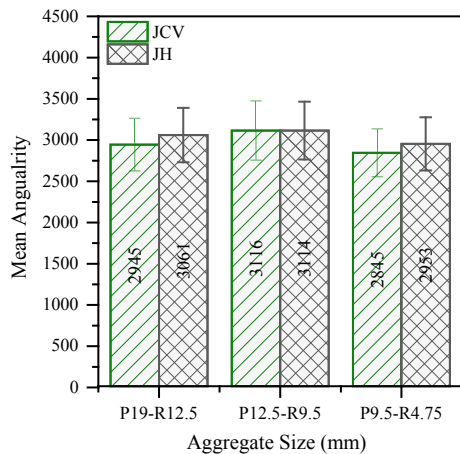


Fig. 4 Comparison of texture of coarse aggregates

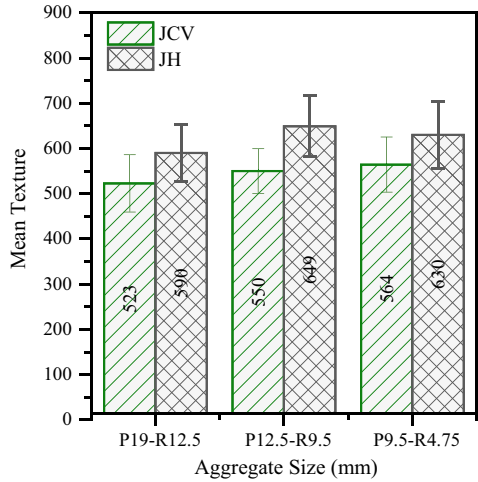
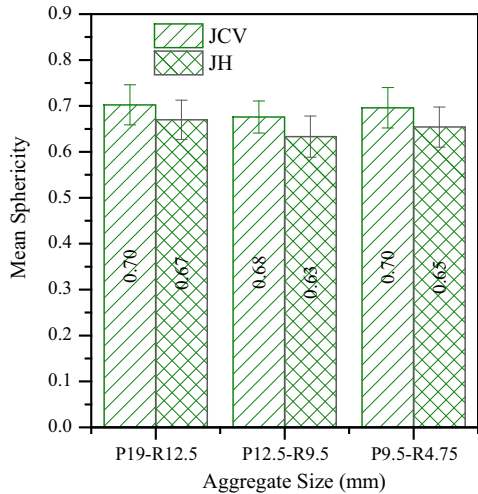


Fig. 5 Comparison of sphericity of coarse aggregates



differences in mean angularity of coarse aggregates produced from JH and JCV crushers. The summary of *t*-test is shown in Table 1. The result indicated that, for all aggregate sizes, *p*-value is higher than 0.05 ($p > 0.05$), showing that no significant difference in mean angularity for all sizes of aggregates produced from JH and JCV series of crushers. Thus, both the crushers produced aggregates with similar angularity.

Texture

Figure 4 shows that the mean texture for all sizes of coarse aggregates produced from JH was higher than JCV produced aggregates. Further, student's *t*-test, *p*-value for all sizes of coarse aggregate for both JH and JCV was found to be less than 0.05

Fig. 6 Comparison of F&E of coarse aggregates

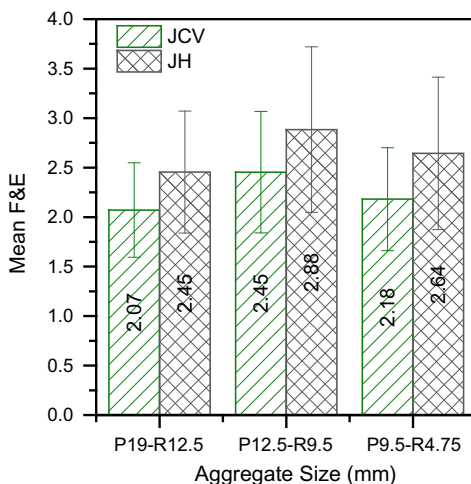


Table 1 Mean value, *t*-test and their significance

Aggregate size (mm)	Crusher type		<i>t</i> -test (<i>p</i> -value)	Significance (<i>t</i> -test)
	JCV	JH		
<i>Angularity</i>				
P19-R12.5	2945	3061	0.214	No
P12.5-R9.5	3116	3114	0.991	No
P9.5-R4.75	2845	2953	0.235	No
<i>Texture</i>				
P19-R12.5	523	590	0.048	Yes
P12.5-R9.5	550	649	0.000	Yes
P9.5-R4.75	564	630	0.000	Yes
<i>Sphericity</i>				
P19-R12.5	0.70	0.67	0.009	Yes
P12.5-R9.5	0.68	0.63	0.000	Yes
P9.5-R4.75	0.69	0.65	0.008	Yes
<i>Flatness and elongation (F&E)</i>				
P19-R12.5	2.07	2.454	0.000	Yes
P12.5-R9.5	2.454	2.884	0.000	Yes
P9.5-R4.75	2.181	2.644	0.016	Yes

Note 1. If ($p > 0.05$): the difference is not statically significant

2. If ($p < 0.05$): the difference is statically significant

($p < 0.05$; Table 1), showing significant difference in texture of aggregate produced from these crushers. It is expected that the aggregate to aggregate impact and higher interaction time period (abrasion with surrounding wall and aggregates) in JCV crushing mechanism may have resulted in decrease of texture.

Sphericity

Figure 5 shows mean sphericity of different sizes of coarse aggregates produced from JH and JCV series of crushers. It can be seen that aggregates produced from JCV crusher have higher sphericity as compared to aggregates from JH crusher. Thus, it can be concluded that JCV crusher produced more cubical aggregates compared to JH crusher. In addition, the statistical analysis result showed that the significant difference exists ($p < 0.05$) between mean sphericity of aggregate produced from JH and JCV series of crushers (Table 1).

Flatness and Elongation (F&E)

Figure 6 showed that JH aggregates had higher F&E (ratio of the longest dimension to the shortest dimension) compared to JCV aggregates. Statistical analysis showed that significant difference exists between mean F&E values of JH and JCV produced aggregates (Table 1). Additionally, Figs. 5 and 6 showed that the aggregates with higher mean sphericity had lower mean F&E value. It is believed that the additional tertiary crushing stage in JCV series of crushers, where the comminution is primarily controlled by rock to rock impact, might have resulted in breakage of aggregate sharp edges and hence, making aggregates more uniform along all three dimensions (higher sphericity and lower F&E).

4.2 Performance Analysis

Angle of Repose (AoR)

AoR is used to capture aggregate stability and packing behaviour. Generally, the higher AoR value indicates better interlocking of aggregates. Figure 7 shows AoR values for different sizes of aggregates produced from JH and JCV series of crushers. It can be seen that for all aggregate sizes, JH aggregates showed higher AoR value compared to JCV aggregates. This may be due to higher angularity and the texture aggregates produced from JH crusher. The *t*-test results showed that a significant difference exists in AoR values of P19-R12.5 and P9.5-R4.75 size of aggregates produced from JH and JCV series of crushers, while P12.5-R9.5 aggregates showed no significant difference (Table 2). However, this may be due to the comparable mean angularity of P12.5-R9.5 of JH and JCV aggregates (Fig. 3).

VCA_{arc}

VCA_{arc} is a measure of air voids of coarse aggregate in loose condition. Generally, the amount of air voids in the aggregate matrix is directly correlated to its packing

Fig. 7 Mean angle of repose value for coarse aggregates

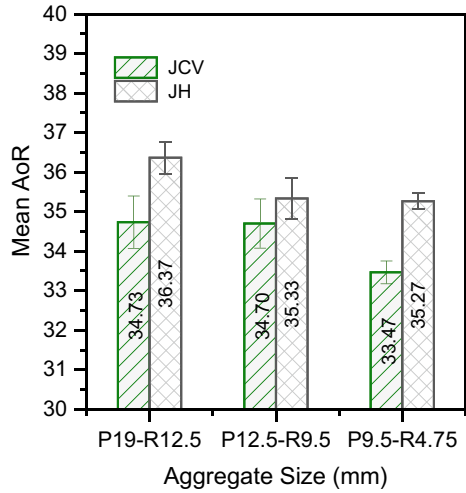


Table 2 *t*-test result of angle of repose (AoR) test

Aggregate size (mm)	Mean AoR		<i>t</i> -test (<i>p</i> -value)	Significance (<i>t</i> -test)
	JCV	JH		
P19-R12.5	34.73	36.36	0.022	Yes
P12.5-R9.5	34.70	35.33	0.246	No
P9.5-R4.75	33.46	35.27	0.005	Yes

Fig. 8 Mean VCA_{drc} value for coarse aggregates

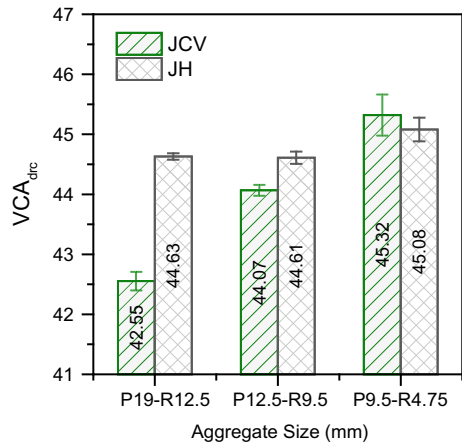


Table 3 *t*-test result of VCA_{drc} test

Aggregate size (mm)	Mean VCA_{drc}		<i>t</i> -test (<i>p</i> -value)	Significance (<i>t</i> -test)
	JCV	JH		
P19-R12.5	42.55	44.63	0.000	Yes
P12.5-R9.5	44.07	44.61	0.002	Yes
P9.5-R4.75	45.32	45.08	0.352	No

behaviour and angularity. Figure 8 shows that the JH aggregates had higher VCA_{drc} compared to JCV aggregates, except P9.5-R4.75 aggregates (Table 3). Though P9.5-R4.75 had higher VCA_{drc} for JCV aggregates, *t*-test results that there is no significance difference exists in mean VCA_{drc} . Overall, JH aggregates showed better interlocking and structural stability compared to JCV aggregates. Apparently, the VCA_{drc} value increases with decrease in aggregate size.

5 Conclusions

The current study compared the aggregate morphology (i.e. angularity, texture, sphericity and F&E) and associated laboratory performance test (i.e. VCA_{drc} and AoR) of three different sizes of coarse aggregate produced from JH and JCV series of crushers. The aggregates produced from JH series of crusher had higher texture, higher F&E and lower sphericity compared to JCV crusher. However, aggregates obtained from both JH and JCV crushers had similar angularity. The JH crushed aggregate showed better AoR and VCA_{drc} value compared to JCV produced aggregates. Overall, JH aggregates showed better interlocking and structural stability compared to JCV aggregates.

References

1. Masad EA, Luce A, Mahmoud E (2006) Implementation of AIMS in measuring aggregate resistance to polishing, abrasion and breakage (no. FHWA/TX-06/5-1707-03-1)
2. Reyes J (2007) Quantifying the role of coarse aggregate strength on resistance to load in HMA. ProQuest
3. Herndon DA, Xiao F, Amir Khanian S, Wang H (2016) Investigation of Los Angeles value and alternate aggregate gradations in OGFC mixtures. *Constr Build Mater* 110:278–285
4. Janoo V, Bayer JJ Jr, Benda CC (2004) Effect of aggregate angularity on base material properties. *J Mater Civ Eng* 16(6):614–622
5. Singh D, Zaman M, Commuri S (2012) Comparison of shape parameters for different types and sizes of coarse aggregates for pavement applications. In: Transportation research board 91st annual meeting (no. 12-0758)
6. Rajan B, Singh D (2017) Comparison of shape parameters and laboratory performance of coarse aggregates produced from different types of crushing operations. *J Mater Civ Eng* 29(7):04017044

7. Rajan B, Singh D (2017) Understanding influence of crushers on shape characteristics of fine aggregates based on digital image and conventional techniques. *Constr Build Mater* 150:833–843
8. Masad E, Button JW (2000) Unified imaging approach for measuring aggregate angularity and texture. *Comput Aided Civ Infrastruct Eng* 15(4):273–280
9. Pine Instrument Company (2013) Aggregate image measurement system, Grove City. Retrieved from <http://www.pineinst.com>
10. Singh D, Zaman M, Commuri S (2013) Effect of production and sample preparation methods on aggregate shape parameters. *Int J Pavement Eng* 14(2):154–175
11. Kelley EG, Spotiswood DJ (1982) *Introduction to mineral processing*. Wiley, New York
12. Nikolov S (2002) A performance model for impact crushers. *Miner Eng* 15(10):715–721
13. Gonçalves JP, Tavares LM, Toledo Filho RD, Fairbairn EMR, Cunha ER (2007) Comparison of natural and manufactured fine aggregates in cement mortars. *Cem Concr Res* 37(6):924–932
14. Fletcher T, Chandan C, Masad E, Sivakumar K (2003) Aggregate imaging system for characterizing the shape of fine and coarse aggregates. *Transp Res Rec J Transp Res Board* 1832:67–77
15. AASHTO TP81-10 (2010) Determining aggregate shape properties by means of digital image analysis. American Association of State Highway and Transportation Officials, Washington DC
16. ASTM International (2016) ASTM C29/C29M-16 standard test method for bulk density (“unit weight”) and voids in aggregate. Retrieved from http://dx.doi.org/10.1520/C0029_C0029M-16
17. Kumar A, Das A, Chakroborty P (2013) Effect of angle of repose of aggregates on asphalt indirect tensile strength value. *Proc Inst Civ Eng Constr Mater* 167(6):283–291
18. Nicks JE, Gebrenegus T, Adams MT (2015) Strength characterization of open-graded aggregates for structural backfills (no. FHWA-HRT-15-034)

Effect of Gradation of Fine Aggregates on Creep Deformation of Fine Aggregate Mix (FAM) and Asphalt Mix



Ambika Kuity and Animesh Das

Abstract In this work, the effect of gradation of aggregates of size 4.75 mm and below on the rutting response of asphalt mix is studied (while all other parameters are held constant). Four different gradations of fine aggregate are used. These gradations are identified as FA0, FA1, FA2, and FA3. The gradation FA0 contains sieve sizes 4.75P-2.36R (that is, passing through 4.75 mm sieve and retained on 2.36 mm sieve), 2.36P-1.18R, 1.18P-0.6R, 0.6P-0.3R, 0.3P-0.15R, 0.15P-0.075R, and 0.075P. In gradation FA1 and FA2, the sizes 2.36P-1.18R and 0.6P-0.3R are skipped, respectively. The gradation FA3 contains the same sizes as in FA0, but with different relative proportions. Using these gradations, two different types of samples are prepared, namely fine aggregate mix (FAM) samples and asphalt mix samples. The FAM samples are made up of asphalt binder and aggregates of size 4.75 mm and below (that is, 4.75P). Creep tests are performed on all the samples. From the creep test results, it is observed that deformation curves for the FAM samples almost follow the same trend as those of the corresponding asphalt mix samples.

Keywords Fine aggregates · Deformation · Creep test · Aggregate gradation

1 Introduction

Asphalt mix is composed of aggregates of various sizes and asphalt binder. The variation of size distribution of aggregate is captured through the aggregate gradation. The past researchers have found that the aggregate gradation affects stiffness [1], rutting [2, 3], indirect tensile strength [4], fatigue performance [5], permeability (for porous mixes) [6], etc. Typically in these studies, the entire range of aggregate gradation is varied to study the effect of aggregate gradation on the mechanical response of the asphalt mix. However, it seems that limited literature is available on the effect of variation of fine aggregate gradation on the mix, although some studies

A. Kuity · A. Das (✉)

Department of Civil Engineering, Indian Institute of Technology Kanpur, Kanpur 208016, India
e-mail: adas@iitk.ac.in

A. Kuity

e-mail: ambika.kuity86@gmail.com

© Springer Nature Singapore Pte Ltd. 2020

T. V. Mathew et al. (eds.), *Transportation Research*, Lecture Notes
in Civil Engineering 45, https://doi.org/10.1007/978-981-32-9042-6_58

are available (i) on the effect of shape of fine aggregates [7–9], and (ii) effect of filler gradation on asphalt mix [10–13]. Aggregates of size 4.75 mm and below are considered as fine aggregates [14, 15] in the present study, thus, the mix made using these aggregates is called as fine aggregate mix (FAM). The present work focuses on the effect of fine aggregate gradation on the creep behavior of the asphalt mix.

2 Experimental Studies

In this study, locally available aggregates and asphalt binder are used. The physical properties of these materials were tested in the laboratory in connection with other research works [10]. For aggregates, the values of impact test [16], flakiness index test [17], and elongation test [17] are obtained as 9, 20, and 35%, respectively [10]. For asphalt binder, the values of absolute viscosity at 60 °C [18], softening point [19], and penetration [20] are obtained as 2638 Poise, 47 °C and 65, respectively [10].

In the present study, the midpoint gradation of Bituminous Concrete grade II (i.e., BC grade II) as per MORTH guidelines [21] is adopted. Four different fine aggregate gradations (namely, FA0, FA1, FA2, and FA3) are chosen, the remaining part of the gradation is kept unchanged. The aggregate gradations are presented in Table 1, and Fig. 1 presents only the gradation of the fine aggregates. These gradations are used to prepare two kinds of samples, namely fine aggregate mixture (FAM) samples (which are prepared only with aggregates of size 4.75P, refer to Fig. 1) and asphalt mix samples (which are prepared with the entire size range, refer to Table 1). Sample preparation and test results are further discussed in the following.

Table 1 Aggregate gradations used for asphalt mix samples

Sieve size (mm)	Gradation of different asphalt mixes			
	Fine aggregate			
	FA0	FA1	FA2	FA3
19P-13.2R	5	5	5	5
13.2P-9.5R	16	16	16	16
9.5P-4.75R	17	17	17	17
4.75P-2.36R	12	14.1	14.1	10
2.36P-1.18R	9	–	10.5	9
1.18P-0.6R	9	10.5	10.5	7
0.6P-0.3R	9	10.5	–	6
0.3P-0.15R	7	8.2	8.2	7
0.15P-0.075R	9	10.5	10.5	14
0.075P-Pan	7	8.2	8.2	9

P Passing, R Retained

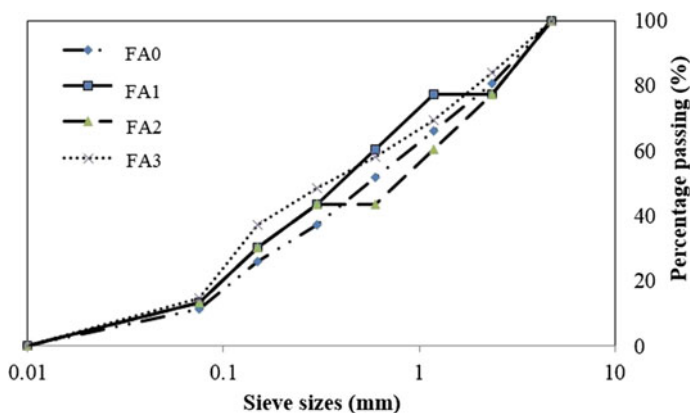


Fig. 1 Fine aggregate gradations used in the present study

2.1 Sample Preparation

For the preparation of FAM samples, the asphalt content is kept fixed at 10% by weight of (fine) aggregates. The fine aggregates and asphalt binder are heated separately at 110 and 160 °C [22], respectively. After mixing thoroughly, the samples are poured into the mold (of size 38-mm-diameter and 76-mm-height) and compacted by 10 blows in three layers. For asphalt mixes, asphalt content is kept fixed at 6% by the weight of aggregates, and the mold size is taken as 100-mm-diameter and 65-mm-height [22].

After 24 h, the samples are extruded and used for further study. Representative photographs of FAM samples and asphalt mix samples are shown in Fig. 2.

Before performing the creep test [23], the FAM and asphalt mix samples are conditioned for 3 h at 20 °C and subsequently, the test is conducted at the same temperature. During the creep test, a 500 N load is applied on the samples for total period of 120 s. The test results are discussed in the following.

The creep test results for FAM samples (average response of three replicate samples) are presented in Fig. 3a. From Fig. 3a, it is observed that the maximum deformation value for FA0 is lowest whereas FA2 is highest (which is almost 2.25 times more than FA0). The maximum deformation values for FA1 and FA3 are almost 1.68 times and 1.50 times more than FA0. Therefore, the present test results show that a well-graded distribution of fine aggregates (FA0) results in stiffer FAM.

The creep test results (average response of three replicate samples) of asphalt mixes are presented in Fig. 3b. From Fig. 3b, it is observed that the maximum deformation value for FA0 is lowest whereas FA2 is highest (which is almost 1.23 times more than FA0). This trend is similar to the test results of FAM samples (refer to Fig. 3a). The maximum creep deformations of FAM and asphalt mix samples are compared in Fig. 4.

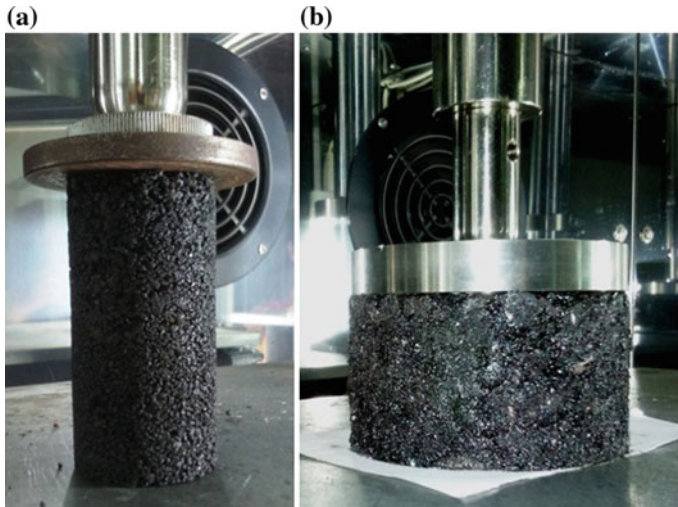


Fig. 2 Representative photographs of **a** FAM sample and **b** asphalt mix sample used in this study

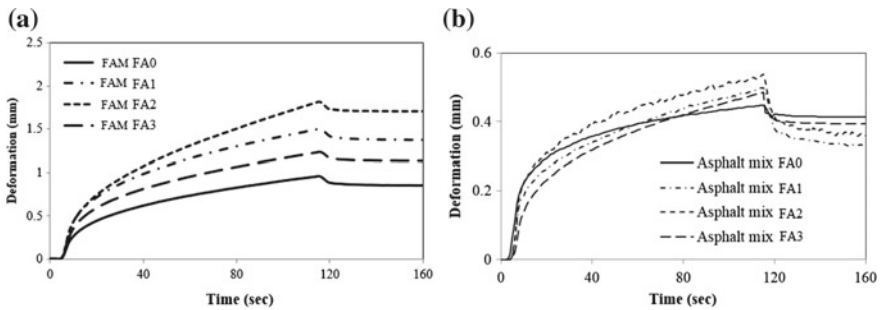


Fig. 3 Creep test results of **a** FAM samples **b** asphalt mix samples

As an effort to interpret the experimental results, internal arrangements of fine aggregates (of the FAM) are studied closely, following the method used by Kuity and Das [10] on aggregate particles smaller than 75μ (that is, filler particles).

Three replicate FAM samples are prepared for each of the four different gradations. Some portion of the sample from the top and bottom are removed, and the remaining portion is cut equally into four slices (for each of the samples). Grinding and polishing are done before capturing the images using a desktop scanner. Representative cross-sectional images of four different FAM samples are presented in Fig. 5. Aggregate boundaries are detected through image processing [24, 25]. Aggregate below 600μ is ignored for subsequent analysis because this is not clearly visible. A total of 10 images for each gradation type are used in the image analysis.

To study the homogeneity, overall centroid of the fine aggregates in each image is estimated [26, 27]. A superimposed diagram of all these overall centroids is presented

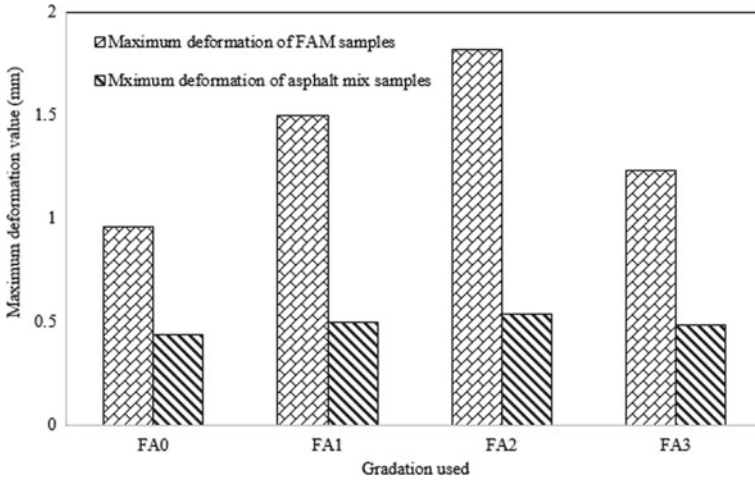


Fig. 4 Maximum deformation value of FAM and asphalt mix samples

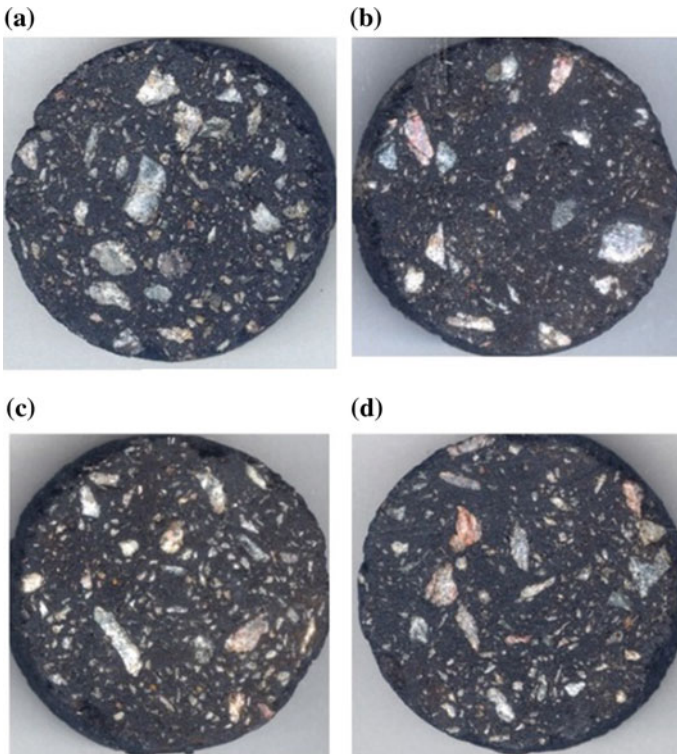


Fig. 5 Representative cross-sectional images of different FAM samples with gradation a FA0 b FA1 c FA2, and d FA3

in Fig. 6. The eccentricity of overall centroid is found to vary between 1205 and 2279 μ . The mean and standard deviation values of the radial distance are presented in Table 2. Considering that the radius of the image is 17.5 mm, it can be stated that the eccentricity is low and, thus, fine aggregates within FAM samples can be considered as homogeneously distributed.

Further, the minimum inter-aggregate distance is calculated by measuring distance (using image analysis) from the boundary of one irregular aggregate to the boundary of its nearest irregular aggregate following the method used by Kuity and Das [28].

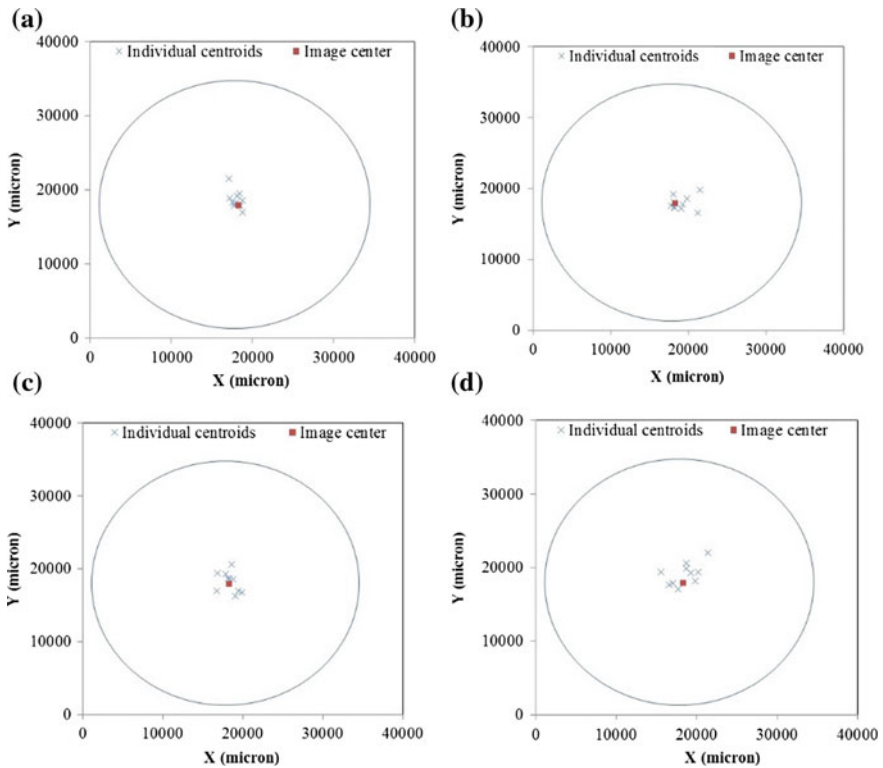


Fig. 6 Superposition of centroid of ten (10) FAM samples with gradation **a** FA0, **b** FA1, **c** FA2, and **d** FA3

Table 2 Mean and standard deviation of radial distance to the overall centroid for different FAM samples

FAMs	FA0	FA1	FA2	FA3
Mean (μ) ^a	1205	1399	1570	2279
Standard deviation (μ) ^a	1013	1147	644	1199

^aFor ten images

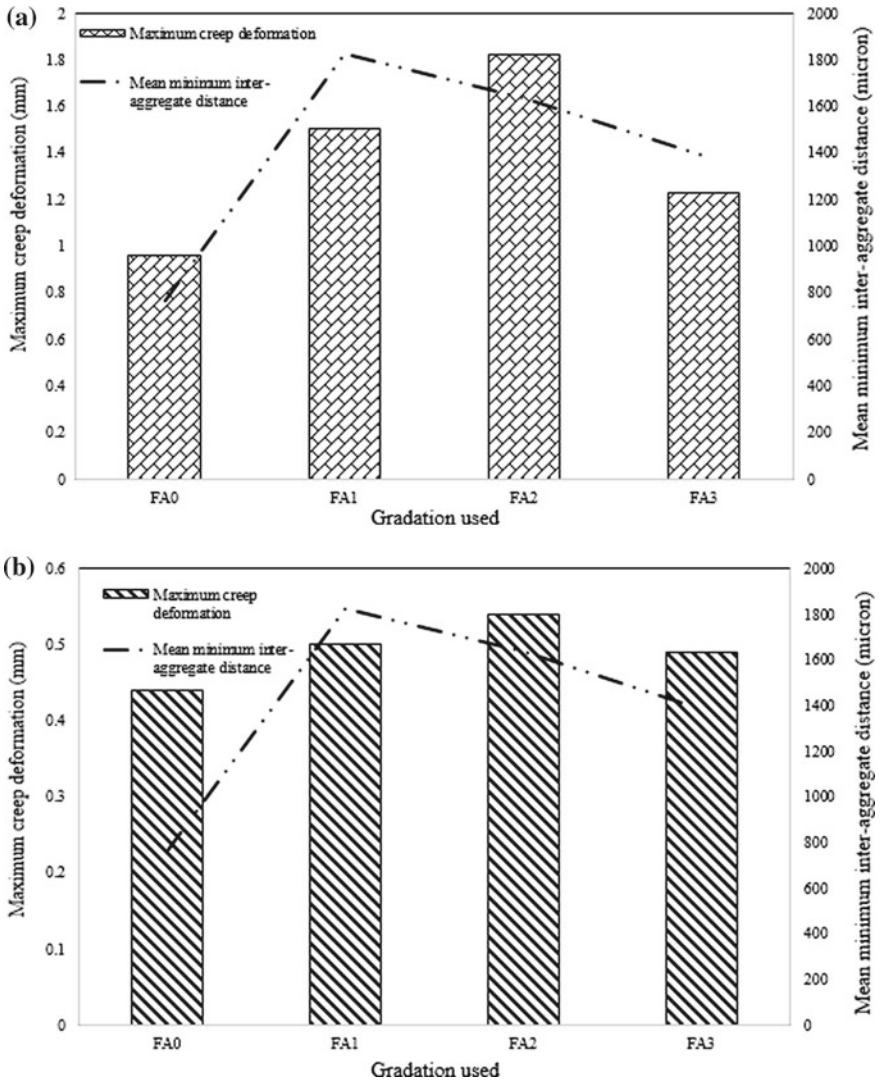


Fig. 7 Maximum deformation values of a FAM samples b asphalt mix samples with mean minimum inter-aggregate distance in FAM samples

Table 3 Mean and standard deviation of minimum inter-aggregate distance for FAM samples

FAMs	FA0	FA1	FA2	FA3
Mean (μ) ^a	762	1820	1634	1383
Standard deviation (μ) ^a	526	1270	1144	1194

^aFor ten images

The distribution of minimum inter-aggregate distance (for all the samples of a given gradation) is presented in Table 3. The mean minimum inter-aggregate distance is found to be minimum for FA0 mix.

In Fig. 7a, b, maximum creep deformation (of FAM samples and asphalt mix samples, respectively) and mean minimum inter-aggregate distance in FAM samples is compared. The trends seem to be almost matching.

3 Conclusions

The conclusions from the present study can be summarized as follows:

- Variation of fine aggregate (sieve size less than and equal to 4.75 mm) gradation affects the creep behavior of the FAM as well as the asphalt mix.
- Well-graded fine aggregates give rise to the stiffest mix.
- Mean minimum inter-aggregate distance (calculated only for FAM) for various mixes shows correspondence with the creep behavior of the respective mixes (for FAM and asphalt mix).

These above observations are in line with the observations made by Kuity and Das [10] on their study on aggregates of size $\leq 75 \mu$ (i.e., 0.075P).

Acknowledgements The authors thank the staff members of Transportation Engineering Laboratory of IIT Kanpur for their constant help and support during preparation of the samples and experiments.

References

1. Al-Mosawe H, Thom N, Airey G, Al-Bayati A (2015) Effect of aggregate gradation on the stiffness of asphalt mixtures. *Int J Pavement Eng Asphalt Technol* 16(2):39–49
2. Krutz NC, Sebaaly PE (1993) The effects of aggregate gradation on permanent deformation of asphalt concrete. *J Assoc Asphalt Paving Technol* 62
3. Kandhal P, Mallick R (2001) Effect of mix gradation on rutting potential of dense-graded asphalt mixtures. *Transp Res Rec* 1767:146–151
4. Elliott RP, Ford MC Jr, Ghanim M, Tu YF (1991) Effect of aggregate gradation variation on asphalt concrete mix properties. *Transp Res Rec* 317:52–60

5. Sousa J, Pais J, Prates M, Barros R, Langlois P, Leclerc AM (1998) Effect of aggregate gradation on fatigue life of asphalt concrete mixes. *Transp Res Rec* 1630:62–68
6. Mansour TN, Putman BJ (2012) Influence of aggregate gradation on the performance properties of porous asphalt mixtures. *Mater Civ Eng* 25(2):281–288
7. Masad E, Olcott D, White T, Tashman L (2001) Correlation of fine aggregate imaging shape indices with asphalt mixture performance. *Transp Res Rec* 1757:148–156
8. Lee C, White TD, West TR (1999) Effect of fine aggregate angularity on asphalt mixture performance, report# FHWA/IN/JTRP-98/20. Indiana Department of Transportation, Perdue University
9. Huber G, Jones J, Messersmith P, Jackson N (1998) Contribution of fine aggregate angularity and particle shape to superpave mixture performance. *Transp Res Rec* 1609:28–35
10. Kuity A, Das A (2017) Effect of filler gradation on creep response of asphalt mix. *Road Mater Pavement Des* 18(4):913–928
11. Huang B, Shu X, Chen X (2007) Effects of mineral fillers on hot-mix asphalt laboratory measured properties. *Int J Pavement Eng* 8(1):1–9
12. Tayebali AA, Malpan GA, Khosla NP (1998) Effect of mineral filler type and amount on design and performance of asphalt mixtures. *Transp Res Rec* 1609:36–43
13. Zulkati A, Diew WY, Delai DS (2012) Effects of fillers on properties of asphalt concrete mixture. *J Transp Eng* 138(7):902–910
14. ASTM C125 (2011) Standard terminology relating to concrete and concrete aggregates. ASTM International, West Conshohocken, Philadelphia
15. ASTM C33/C33M (2014) Standard specification for concrete aggregates. ASTM International, West Conshohocken, Philadelphia
16. IS 2386 (Part-IV) (2002) Aggregate impact value. Bureau of Indian Standard, New Delhi
17. IS 2386 (Part-I) (2002) Flakiness & elongation index test (shape test). Bureau of Indian Standard, New Delhi
18. ASTM D-2171 (2010) Standard test method for viscosity of asphalts by vacuum capillary viscometer. ASTM, West Conshohocken
19. IS 1205 (2004) Determination of softening point. Bureau of Indian Standard, New Delhi
20. IS 1203 (2004) Determination of penetration. Bureau of Indian Standard, New Delhi
21. Ministry of Road Transport and Highway (2013) Specifications for road and bridge works, 5th revision. Indian Roads Congress, New Delhi
22. ASTM D-6926 (2010) Standard practice for preparation of bituminous specimens using Marshall apparatus. ASTM, West Conshohocken
23. AASHTO T322 (2011) Standard method of test for determination the creep compliance and strength of hot mix asphalt (HMA) using the indirect tensile test device. AASHTO, Washington DC
24. ImageJ (2015) Image processing and analysis in java. <https://imagej.nih.gov/ij/>. Last accessed 20 June 2016
25. Matlab (2015) Matlab and image processing toolbox release 2015a. Math Works, Inc., Natick, Massachusetts, United States
26. Kuity A, Das A (2015) Homogeneity of filler distribution within asphalt mix—a microscopic study. *Constr Build Mater* 95:497–505
27. Peng Y, Sun LJ (2011) Towards an index of asphalt mix homogeneity. *Road Mater Pavement Des* 10(3):545–567
28. Kuity A, Das A (2019) In search of a possible size-demarcation between load bearing and suspended aggregates in asphalt mixture—an experimental approach. *Road Mater Pavement Des*. <https://www.tandfonline.com/doi/full/10.1080/14680629.2019.1604406>

Warm Mix Asphalt—A Comprehensive Case Study



Atasi Das  and Yash Pandey 

Abstract Warm Mix Asphalt (WMA) is a practiced technology that allows noteworthy benefits in terms of environment, material, as well as finance. WMA, in comparison to the conventional Hot Mix Asphalt (HMA), promises us various benefits like reducing asphalt usage, lowering mixing, and laying temperature, thus causing significant reduction in the carbon footprints by reducing the greenhouse gas emissions in the atmosphere. Although this technology has been in wide use around the world since the last two decades, and Guidelines for Warm Mix Asphalt has also been published by the Indian Roads Congress (IRC) as IRC: SP: 101-2014 [1], in India, there is still reservation regarding its adoption and utilization. There is a misconception that the bituminous mixture produced at lower temperature will not perform well, may not compact properly, may not meet moisture susceptibility, etc. There are a number of additives available in the market that proclaims to result in WMA mixes exhibiting the functions mentioned above. Of late, many of the additives claim to enhance the bituminous mixture properties like elastic modulus by reducing the air voids and behave as antistripping as well. Hence, there is confusion and lack in clarity with regard to the actual functions of the additives resulting in WMA. To streamline the functions of the additives available in the market, we embarked on studying the effects of multiple additives. In this study, five different additives from three leading manufacturers/suppliers have been used for the WMA production for which laboratory studies have been done. These additives used to modify the binder are based on amine and organosilane technology. In post-study, it was found that one additive has provided saving in the form of less binder consumption with some reduction in mixing and compaction temperature, while the second has provided benefit in form of enhanced temperature reduction with no effect on asphalt consumption and the other has provided benefit in both asphalt consumption reduction as well as mixing and compaction temperature reduction. The laboratory properties such as Marshall stability, indirect tensile strength (ITS), tensile strength ratio (TSR), moisture susceptibility, etc. with asphalt VG30 have been studied. Also,

A. Das (✉) · Y. Pandey (✉)
G R Infraprojects Limited, Gurugram 122015, India
e-mail: atasid@gmail.com

Y. Pandey
e-mail: yashpandey5@gmail.com

© Springer Nature Singapore Pte Ltd. 2020
T. V. Mathew et al. (eds.), *Transportation Research*, Lecture Notes
in Civil Engineering 45, https://doi.org/10.1007/978-981-32-9042-6_59

recycled asphalt pavement (RAP) material utilized in the bituminous mix production contributes partially to the carbon footprint reduction. The detailed paper targets to showcase some of the cost benefits involved in using WMA compared to hot mix for a typical project and provide guidance on the selection of the additive during usage.

Keywords Indirect tensile strength · Warm mix · Additive

1 Introduction

The flexible pavement construction industry is in continuous search of technological solutions that will boost up the materials performance with increase in construction efficacy, environmental degradation, and preserve resources. At the time of construction, the temperature should be adequate and conducive to confirm the workability of the mix. For slight or nil improvement in workability, increasing the bituminous mix temperature results in increased plant emissions and fumes at the construction site and binder aging. Around the world, efforts are being put forward to protect the environment. Nowadays, the focus is on reducing CO₂ emissions in view of minimizing the greenhouse effect. A number of new technologies are being developed to minimize the mixing and compaction temperatures of a hot bituminous mix without compromising the pavement quality, mainly WMA technologies were developed and now being used all over the world. It is a relatively new technology in India. These new processes and products use several chemical and mechanical methods to decrease the shear resistance of the bituminous mix at construction and compaction temperatures while sustaining or refining pavement performance.

1.1 Literature Survey of WMA

The reduction in mixing and compaction temperature achieved by WMA technologies brings many potential benefits in terms of economy, operation, and environmental effects. However, the specific benefits and their extent depend upon the specific WMA technology being used. Some of the major benefits of WMA are:

Fuel saving—WMA is manufactured at some low mixing and compaction temperatures compared to HMA which results in the reduction in the usage of fuels. The WMA additives reduce the viscosity of binder making it easy to mix with the aggregate at a lower temperature.

Longer Paving Season—since the production temperature of WMA is lower than HMA and also the compaction temperature is lower than HMA, it is possible to extend the time of paving from the time of its production and dispatch from plant and facilitating longer lead.

Better Workability and Compaction—energy conservation is eminent with lesser number of passes for compaction of bituminous layer surfacing. As already men-

tioned above since WMA facilitates better compaction at lower temperature and lesser number of passes, it becomes an obvious choice.

Reduced Plant Emissions of Greenhouse Gases—in asphalt plants, the burning of fuels generates heat needed to dry and heat aggregates so that they can be mixed and properly coated with asphalt. Then, the mix is stored at an elevated temperature in order to facilitate construction operations. Burning of fuels contributes to the production of several pollutants like carbon dioxide (CO₂), nitrogen oxide (NO_x), and sulfur dioxide (SO₂). By using the warm mix technology, it is possible to cut down the greenhouse gases emissions as the amount of fuel used in WMA is significantly less.

Improved Working Conditions—worker's exposure to fumes is less in WMA when compared to HMA. The reduction in the mixing temperature causes a visible reduction in the smoke and odor and thus, results in improved working conditions for the workers.

There are many ways available to prepare the WMA, i.e., by water-based technologies, using chemical additive, rheological modifiers, etc. In the present work, we have prepared WMA using chemical additives. There are a number of chemical additives available in the worldwide market; we have used five additives of three different companies which are in the approved list of the Indian Road Congress and Ministry's guidelines. These additives are based on amine based, which imparts bonding between aggregate and bitumen, and organosilane based, which imparts bonding between bitumen and bitumen.

2 Materials Used

Viscosity Grade-30 (VG-30) bitumen and limestone and sandstone type aggregates of different sizes were taken from the nearby local quarry and were used in this study. The asphalt was tested for physical properties as per IS (Indian Standards) code IS-73: 2013 [2] and the physical properties of aggregate were studied as per IS: 2386-1963 [3] and the specifications of Ministry of Road Transport and Highways (MORTH) [4] to determine its performance. The test results are given in Tables 1 and 2.

In addition to the aggregate and asphalt binder, five different types of additives were used which may be referred to as A1, A2, A3, A4, and A5 in the study in which A1, A2, A3, and A4 are amine based and A5 is organosilane-based additive. Also, 20% of milled material by weight of the aggregate has been added in preparing WMA.

Table 1 Properties of aggregates

Property	Test performed	Method of test	Specifications as per MORTH 2013	Test results
Cleanliness (dust)	Grain size analysis	IS:2386 part I	Max. 5% passing 0.075 mm sieve	0.96%
Particle shape	Combined flakiness and elongation test	IS:2386 part I	Max 35%	28%
Strength	Aggregate impact test	IS:2386 part IV	Max 27%	21%
Water absorption	Water absorption test	IS:2386 part III	Max 2%	0.57 (40 mm) 0.84 (20 mm) 0.98 (10 mm) 1.07 (6 mm) 1.40 (dust)
Specific gravity	Specific gravity test	IS:2386 part III	–	2.64 (40 mm) 2.64 (20 mm) 2.63 (10 mm) 2.62 (6 mm) 2.57 (dust)
Stripping	Coating and stripping of bitumen aggregate mix	IS:6241	Minimum retained coating 95%	98%

Table 2 Properties of VG-30

Property	Method of test	Requirement as per IS 73:2013 for VG-30	Test results
Penetration at 25 °C, mm	IS 1203	Min. 45	51
Softening point (R&B), °C	IS 1205	Min. 47	50.3
Absolute viscosity at 60 °C, Poise	IS 1206 (part 2)	Min. 2400	2945
Kinematic viscosity at 135 °C, cSt	IS 1206 (part 3)	Min. 350	490
Solubility in trichloroethylene, % by mass	IS 1216	Min. 99	99.5

3 Laboratory Work

The laboratory study is carried out on the Dense Bituminous Macadam (DBM) Grade 2 mix as per MORTH specifications. The aggregate gradation used is shown in Table 3 and gradation graph is shown in Fig. 1. The optimum binder content for the DBM mix was found to be 4.6% using Marshall’s method of mix design.

Table 3 Aggregate gradation for DBM Grade 2

IS sieve size (mm)	Average of actual % passing	Specified Limits as per MORTH-2013	
		Lower	Upper
45	100.00	100	100
37.5	97.81	95	100
26.5	76.96	63	93
13.2	63.51	55	75
4.75	45.02	38	54
2.36	33.31	28	42
0.300	13.32	7	21
0.075	4.48	2	8

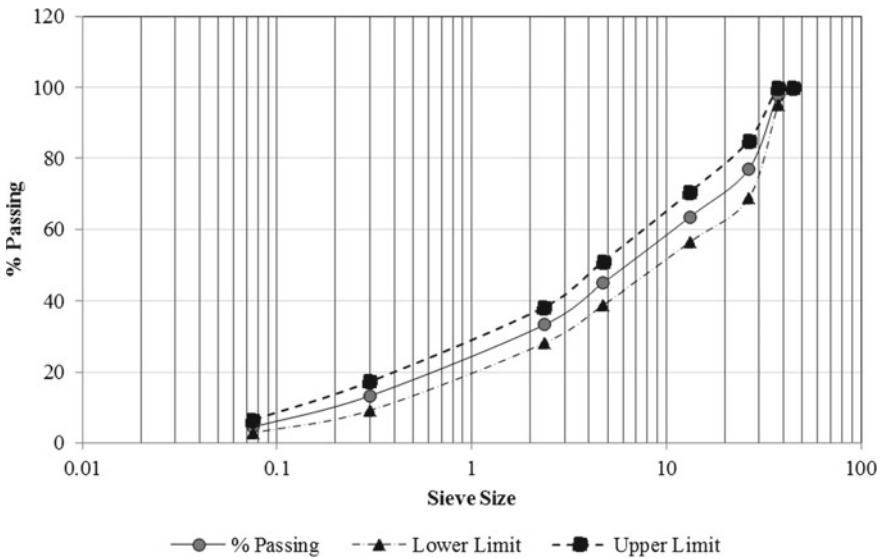


Fig. 1 Gradation curve for DBM Grade 2

Table 4 Aggregate gradation for DBM grade 2

Particular	Type of additive	Dosage, % of asphalt	Dry ITS, kPa	Wet ITS, kPa	TSR value, %
Without additive	–	–	820	520	63.4
With additive	A1	0.5	1275	899	70.5
		0.8	1196	965	80.7
	A2	0.3	1221	842	69.0
		0.5	809	748	92.5
	A3	0.4	826	799	96.7
		0.5	809	691	85.4
		0.7	779	641	82.3
	A4	0.5	1404	992	70.7
		0.8	1404	1150	81.9
	A5	0.08	1017	743	73.1
		0.12	1238	924	74.6
		0.14	1210	940	77.7
		0.16	1185	992	83.7

Bold signifies that these values meets the Indian specification

4 Indirect Tensile Strength

The ITS is used to determine the tensile properties of the asphalt mixture and thus can be related to the cracking properties of the pavement. The test provides information on tensile strength, fatigue characteristic, and permanent deformation characteristics of the pavement materials. Usually, a higher tensile strength corresponds to a stronger cracking resistance. Tensile strength is difficult to measure directly because of the secondary stresses induced while gripping a specimen during testing. Therefore, tensile stresses are typically measured indirectly by a splitting tensile test as per AASHTO T 283 [5].

Another aspect is the moisture damage in bituminous mixes which is the loss of serviceability due to the presence of moisture. The extent of moisture damage is called the moisture susceptibility.

The ITS test also evaluates the moisture susceptibility of a bituminous mixture. Tensile strength ratio (TSR) is a measure of water sensitivity. It is the ratio of the tensile strength of water conditioned specimen (ITS wet) to the tensile strength of unconditioned specimen (ITS dry) which is expressed as a percentage. The higher the TSR value, the lesser will be the strength reduction by the water soaking condition or the more water resistant, it will be and implies that the mixture will perform well with a good resistance to moisture damage.

As 20% of milled material has also been mixed, it is imperative to ensure the fatigue damage of the WMA. The ITS and TSR results of bituminous mix prepared without additive and with five different types of additives are tabulated in Table 4.

From the study, it is seen that the TSR of the normal HMA is found to be 63% which is appreciably lower than the minimum 80% criteria as specified in MORTH 2013 and thus requires the use of antistripping agent which serves for the warm mix additives. Five different types of warm mix additives are used as A1, A2, A3, A4, and A5, which are mixed in the asphalt in different dosages (as seen in Table 4). All the five types of additives are fulfilling the criteria for the minimum TSR of 80% at different dosages, but the cost-effectiveness of them is very much important which drives the overall project cost. The cost comparison [in Indian National Rupees (INR)] of the additive is mentioned in Table 5.

From the costing and the results as compared, in Fig. 2, it is clear that the different warm mix additives will be imparting a major implication in cost to the project. For the particular study done and among the additives used, the additive number A5 with 0.16% dosage was found to be cost-effective.

Table 5 Cost comparison of different types of additives

Particular	Type of additive	Dosage, % of asphalt	Per kg cost of additive, in INR	Extra cost of additive in per ton of asphalt, in INR
Without additive	A0	–	0	0
With additive	A1	0.5	200	1000
		0.8	200	1600
	A2	0.3	400	1200
		0.5	400	2000
	A3	0.4	600	2400
		0.5	600	3000
		0.7	600	4200
	A4	0.5	500	2500
		0.8	500	4000
	A5	0.08	835	668
		0.12	835	1002
		0.14	835	1169
		0.16	835	1336

Bold signifies that these values meets the Indian specification

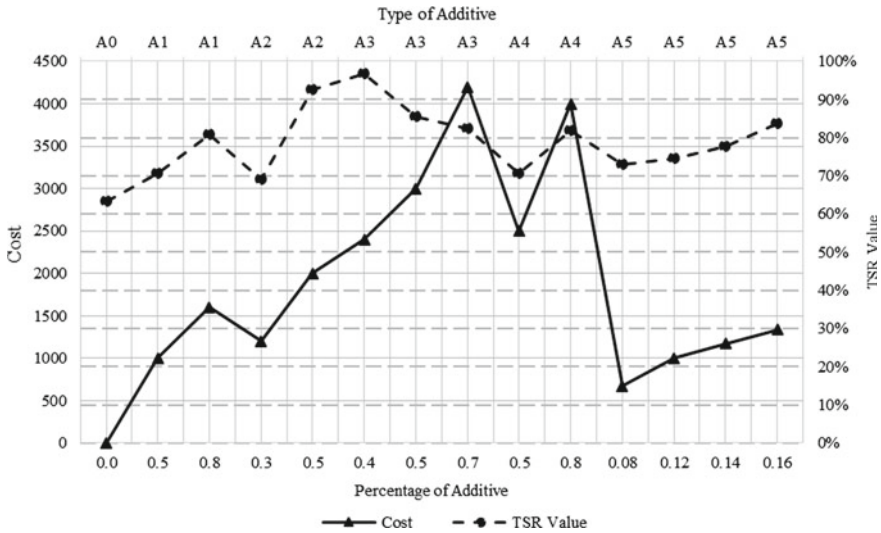


Fig. 2 Cost comparison of different types of additives

5 Conclusions

From the study, the following points have been concluded:

1. The ITS value varies on a large basis with respect to the type of admixture used, its dosage, and type of aggregate.
2. Before using any type of additive on any project, it is required to distinguish the rock type on basis of which the type of additive should be selected and used.
3. Although the dosage of all the types of additives used in the study varies a little, the rates of the same vary on a large scale which could add extra cost to the project on selecting a wrong additive.
4. A comprehensive laboratory study is very important to study about the effect of the costing of the project after selecting a type of additive on the basis of ITS, as almost all types of additives will fulfill our purpose but will differ in the cost.
5. The fatigue damage may also occur if a proper dosage of the additive is not used. So, it is important to study the fatigue behavior of the mix. However, this is subjected to field monitoring, which is out of scope of this paper.
6. On using the high dosage of the additive, i.e., more than the specified limits of the manufacturer, there is also need for study of the rheological properties of the bitumen.
7. There is a need for a comprehensive study of the technical as well as financial implication of the warm mix in laboratory and in field as well.

Acknowledgements The authors are thankful to the management team of M/s. G R Infraprojects Ltd., especially Mr. Ajendra Agarwal, Director (Technical) for guidance and providing all facilities in carrying out the reported work.

References

1. IRC SP (2014) Interim guidelines for warm mix asphalt, IRC SP no 101. Indian Roads Congress, New Delhi
2. IS:73 (2013) Paving bitumen—specifications, IS no 73. Bureau of Indian Standards, New Delhi
3. IS:2386 (1963) Methods of test for aggregates for concrete, part 1, 3 and 4, IS no 2386. Bureau of Indian Standards, New Delhi
4. Ministry of Road Transport and Highway (2013) Specifications for road and bridge works, 5th revision. Indian Road Congress, New Delhi
5. AASHTO (2007) Resistance of compacted hot mix asphalt to moisture induced damage, AASHTO, no 283. American Association of State Highway and Transport Officials, USA

The Effect of Using Acid-Modified Mixes on Performance of Asphalt Concrete



A. Ramesh , G. Abdul Khader and M. Kumar

Abstract Globalization has paved its path for an increase in commercial vehicular traffic. Conventional bitumen used in the preparation of hot mix asphalt (HMA) layers is unable to cope up with the increased traffic load characteristics. Alternatively, asphalt modification with additives has proven its role in improving binder characteristics. In the present study, an attempt is made to evaluate the performance characteristics of conventional and acid-modified mixes when prepared using polyphosphoric acid (PPA). Resilient modulus, stripping and rutting characteristics are used for evaluation of performance characteristics of above-modified mixes. PPA was added to conventional bitumen (VG-30) at regular intervals in the laboratory. Marshall parameters were improved with acid modification when added in a conventional binder. It is observed from the test results that tensile strength has increased for acid-modified mixes. Rutting and stripping properties were enhanced for acid-modified mixes than conventional mixes. The addition of acid to conventional mix has also improved the stiffness of modified mix and has resulted in enhancement resilient modulus value. 3% PPA was arrived as optimum content for modification in conventional binders.

Keywords Polyphosphoric acid · Bituminous concrete · Resilient modulus · Rut depth

A. Ramesh (✉) · G. Abdul Khader
Department of Civil Engineering, VNR Vignana Jyothi Institute of Engineering and Technology,
Hyderabad, Telangana, India
e-mail: ramesh_a@vnrvjiet.in

G. Abdul Khader
e-mail: gabdulkhader3@gmail.com

M. Kumar
Department of Civil Engineering, University College of Engineering, Osmania University,
Hyderabad, Telangana, India
e-mail: kumartrans@gmail.com

1 Introduction

Infrastructure facilities are provided for improving communication facilities to the commuters/road users and results in increasing the country's economy. Pavement construction provides a major contribution in improving the infrastructure facilities. These pavements shall be constructed as a long lasting durable structure which provides hard compacted surface so as to carry vehicular traffic. In our country, most of the pavements are built as flexible pavements as this provides ease in construction, operating and maintenance. These pavements are subjected to failures as functional and structural defects. Functional failure is observed because of the unsatisfactory levels by the road users. Structural defects in pavements are due to failure in engineering properties of pavement layers. These structural failures in hot mix asphalt (HMA) layers are observed as fatigue cracking and rutting as shown in Fig. 1. Fatigue failure is because of reparative load applications, and rutting is depression observed along the wheel path. Further, these are the most important distress (failure) mechanisms in bituminous pavements.

Fatigue and rutting in HMA layers depend on various factors such as aggregate gradation, shape and quality of aggregate, quantity and quality of binder, mix parameters such as the amount of air voids and Voids in Mineral Aggregates (VMA), temperature, construction practices and environmental conditions. Failures also occur due to the reduction in viscosity or stiffness in the asphalt due to high temperatures.

In order to improve the above distresses in asphalt mixtures which are related to viscoelastic behaviour, field engineers and researchers are attempting to modify the properties of asphalt binders and mixtures using different types of modifiers [3, 9, 18]. A good modifier shall improve the properties of asphalt binder by enhancing the performance characteristics of HMA layer. A number of proprietary products are available in the market with which asphalt can be modified. Polyphosphoric acid ($H_{n+2}P_nO_{3n+1}$) is a polymer of orthophosphoric acid (H_3PO_4). PPA's major applications are surfactant production, water treatment, pharmaceutical synthesis, pigment production, flameproofing, metals finishing and asphalt modification.



Fig. 1 Failures in pavements

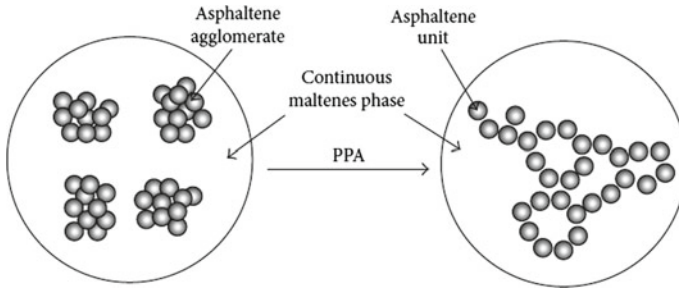


Fig. 2 PPA on the colloidal structure of bitumen. *Source* Adapted from Yadollahi and Sabbagh Mollahosseini [11]

1.1 Bitumen Modification with PPA

PPA interaction with bitumen compounds was studied by several authors. Figure 2 represents PPA on the colloidal structure [11]. The authors explain that PPA modification is carried using different methods depending on the chemical composition of bitumen and is largely influence by the source of crude oil. The reactivity of PPA increases with the polarity of the asphaltene fraction. This is because PPA boosts in dissociation disrupting the hydrogen bond network formed within the agglomerates of asphaltene micelles.

1.2 Objectives of the Present Study

Following are the objectives of the study

- (a) To determine the optimum acid content (PPA) when added at regular interval to conventional bitumen mixes.
- (b) To study the performance characteristics of conventional bituminous mix and modified bituminous mix when prepared with PPA.

2 Literature Review

Distresses of asphalt mixtures are associated with the viscoelastic behaviour of asphalt binders, researcher's and field engineers are continuously making efforts for modifying the properties of asphalt binders and mixtures using different additives [3–9] for improving the asphalt binder characteristics. A good modifier shall enhance the properties of asphalt binder by increasing its modulus at high temperatures and reducing the same parameter at low temperatures [2]. Asphalt mixtures

when modified with polymer-modified binders have yielded for improving the resistance towards rutting and fatigue properties [7, 8]. However, it is a known fact that polymer-modified binders are comparatively more expensive when compared with unmodified binders. In this context, it is required to find materials which are more cost-effective and environmentally friendly. These materials shall also improve the performance characteristics of the modified binder. Polymer modification when carried on different grades of bitumen exhibits the properties of fracture, brittle state and reversible ageing process. These properties were largely unaffected when modification of bitumen was carried using PPA [6, 20]. The role of PPA modification at different percentages in asphalt binders was well explained through dynamic shear rheometer, creep and recovery tests [4]. PPA effect on molecular structure behaviour during the ageing process is appraised through Fourier transform infrared (FTIR) spectroscopy, dynamic shear rheometer (DSR) and epifluorescence microscopy tests [12]. This modification has enhanced the binder ageing properties. Rheological studies for PPA-modified bitumen were primarily focused on its performance and stability. Giavarini et al. [5] presented that PPA-modified bitumen shows a higher penetration index (PI) and thus provides improvement in thermal susceptibility when compared with unmodified bitumen. The rheological studies with polymer-modified bitumen are proved that PPA changes the bitumen structure towards gel type, thus improving the stabilization interactions between the polymer and the bitumen components [1, 2, 10]. The present study is focused on performance characteristics of the bituminous concrete mix when modified with PPA at different dosages.

3 Methodology

A methodology is framed to evaluate the performance characteristics of asphalt mixes when modified using PPA at different percentages. Performance characteristics are evaluated from resilient and rutting test carried in the laboratory. Table 1 provides the sequential procedure for evaluation of the study.

Table 1 Methodology adopted for study

Stage	Description
1.	Literature survey and material collection
2.	Aggregate gradation arrived from mid-point process as specified in MoRTH 5th revision guidelines
3.	Estimation of Marshall parameters for different mix combinations and arriving for optimum content
4.	Performance characteristics of conventional and modified PPA mixes
5.	Inferences of above laboratory findings

4 Experimental Programme

In the present study, stability analysis was performed using Marshall tests and mix performance was evaluated for both conventional and modified bituminous concrete mixes using resilient and rutting characteristics.

4.1 Materials

Crushed aggregates, fine aggregates and stone dust were collected from the local quarry at Medchal District. Bitumen (VG-30) was provided by field engineers of Greater Hyderabad Municipal Corporation (GHMC), Hyderabad. PPA was purchased from online India mart. Aggregate gradation was carried through mid-point gradation as specified in Ministry of Road Transport and Highway (MoRTH) 5th revision for Bituminous Concrete grade-II [19].

4.2 Sample Mix Preparations

The asphalt binder was preheated to 135 °C, and PPA dosage was added at regular intervals. In order to achieve uniform mixing of PPA in asphalt, a mechanical stirrer is used and is operated at 450 rpm. Stirring was continued till 20 min duration while maintaining the binder temperature. Samples were immediately taken for measuring its asphalt properties after modification. Marshall specimens were prepared for arriving optimum binder content (OBC). This test is in accordance with ASTM 1559 (2013) and ASTM D5581-07a (2013) [13]. Samples were prepared in Marshall moulds giving 75 blows on each phase. Sample dia. is of 100 mm and 63.5 mm height [14]. A total of 84 specimens were prepared for both conventional and PPA-modified mixes. Figure 3 provides samples prepared for arriving Marshall parameters. A compressive load at a rate of 50.8 mm/min is applied on prepared Marshall samples and is monitored till its failure when tested at 60 °C. Peak load and flow in terms of mm or units (1 unit = 0.25 mm) are recorded.

Slabs were prepared using roller compactor as shown in Fig. 4. The slab has a volume of 6000 cc, and density of the mix was arrived from Marshall test and is used for the preparation of slabs. Compaction of the slab is achieved by applying hydraulic pressure in oscillatory motion. This compaction (no. of passes) is carried until the desired density is achieved.



Fig. 3 Marshal setup with specimens

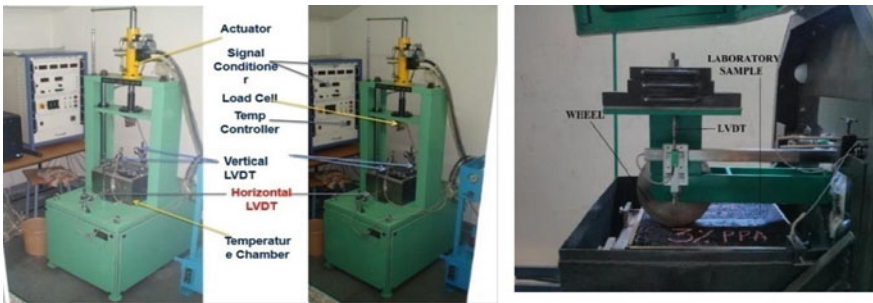


Fig. 4 Repeated load test setup and immersion-type wheel rutting apparatus

4.3 Indirect Tensile Test (IDT)

The IDT strength test is performed to assess the resistance of each mixture against cracking in accordance with ASTM D4123-82 [15]. The test temperature and loading rate were considered as 35 °C and 50 mm/min, respectively. The failure load was used to calculate the indirect tensile strength. The peak load from the IDT test was used as a prerequisite for the conduct of resilient modulus value. The tensile strength is calculated from Eq. (1)

$$\sigma_f = \frac{2P}{\pi dt} \tag{1}$$

where P is the failure load, d is the diameter of the specimen and t is the thickness of specimen.

4.4 Repeated Load Test

Resilient modulus is referred to as the elastic modulus for use with elastic theory. It is a well-known fact that most paving materials are inelastic but do experience in some permanent deformation after each load application. The deformation under each load repetition is nearly completely recoverable and proportional to the load and can thus be considered an elastic behaviour. The resilience modulus test is performed in accordance with ASTM D 4123 and is carried at the same temperature of IDT test, i.e. at 35 °C by applying a repetitive linear force along the diameter axis of the specimen. The total duration of loading and unloading is of 1 s. Figure 4 provides an experimental setup of repeated load test apparatus. Resilient modulus is calculated using Eq. (2)

$$M_R = \frac{P(\mu_{RI} + 0.27)}{t \Delta H_I} \quad (2)$$

where M_R is the instantaneous resilient modulus of elasticity, μ_{RI} is instantaneous resilient Poisson's ratio, ΔH_I is instantaneous recoverable horizontal deformation, ΔV_I is instantaneous recoverable horizontal deformation, P is the failure load and t is the thickness of the specimen.

4.5 Immersion-Type Wheel Rutting Test

Rutting and stripping characteristics were carried on immersion-type wheel tracking device as per AASHTO T 324 and BS-EN 12697-22 (2003) test guidelines [12, 16]. Rectangular slabs of dimensions of 6000 cc were prepared for conventional and PPA-modified mixes as per AASHTO T 283 and BS-EN 12697-33 (2007) using roller compactor [17]. A series of test specimens are prepared for conventional and modified PPA asphalt mixes. Initially, samples were preconditioned for arriving test temperature of 50 °C. The specimens were subjected to simulated trafficking with a simple harmonic motion with a wheel load of 710 N. A LVDT (linear variable differential transformer) is also provided to the side of the wheel for monitoring rut depth to a corresponding number of wheel passes and is shown in Fig. 4.

5 Experimental Results

Physical properties on aggregates were carried as per relevant IS specifications and are tabulated in Table 2. Consistency test on bitumen was performed, and results are presented in Table 3. For the present study, 1–6% at an interval of 1% was considered as the additive dosage of PPA. PPA was added into the molten bitumen

Table 2 Physical properties of aggregates

S. no.	Test property	Test results	MoRTH specifications	Test code
1.	Aggregate crushing value	19%	Max 30	IS:2386(IV)
2.	Aggregate impact value	17%	Max 30	IS:2386(IV)
3.	Combined elongation and flakiness indices	22%	<15	IS:2386(I)
4.	Water absorption	1.03	0.1–2	IS:2386(III)
5.	Specific gravity	2.704	2–3	IS:2386(III)
6.	Los Angeles abrasion value	22%	Max 30	IS:2386(IV)

Table 3 Physical properties of bitumen

PPA (%)	Penetration (1/10th of mm)	Softening (°C)	Ductility (cm)	Viscosity (poise at 60 °C)
^a 0	64	56	69	2565
1	64	57	71	2575
2	60	59	76	2584
3	57	61	78	2610
4	54	64	74	2616
5	51	64	71	2620
6	40	70	60	2625

^aAs per IS 73 2012 for viscosity grading

as per percentage to the weight of bitumen and stirred by a mechanical stirrer for homogeneity. Bituminous concrete of grade-II was selected and is shown in Fig. 5.

5.1 Marshall Properties

Marshall stability test was conducted on prepared conventional mixes and modified PPA mixes as per ASTM D 1559. Table 4 provides test results for different combination of mixes.

The above table of Marshal results implies that

- Maximum stability was obtained as 12.03 kN at 5.5% of bitumen content for conventional mixes, whereas modified mix with 3% PPA content provides stability value as 20.62 kN.
- Stability parameters decrease beyond 3% of PPA content in the modified mix; hence, 3% of PPA is considered as optimum acid content and is summarized in Table 3.

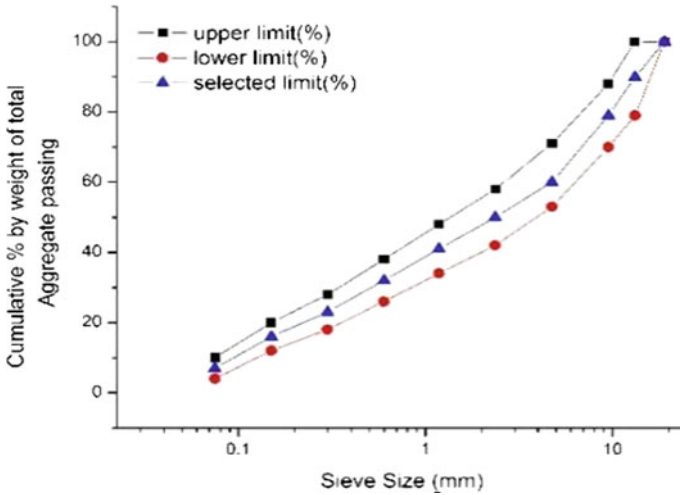


Fig. 5 Gradation of aggregates adopted as per MoRTH specifications

- (c) Further addition of PPA results in a reduction in stability properties as there is dissociation disrupting the hydrogen bond network formed within the agglomerates of asphaltene micelles.

5.2 Indirect Tensile Strength Properties

IDT was performed for both conventional and PPA-modified mixes. Figure 6 represents a comparison of tensile strength for conventional and modified mixes.

It is observed that tensile strength has reduced with an increase in binder content. Tensile strength has increased to 532.36 kPa for 3% PPA-modified bitumen and then decreased to 515.57 kPa with the increase in PPA content. This infers that at 3% PPA has better resistance to cracking than other mix combinations.

5.3 Resilient Modulus

Repeated load test was conducted on laboratory prepared conventional and PPA-modified specimens. Figure 7 provides a variation in resilient values for different mix combinations.

It was observed from the test results that resilient modulus for the conventional mix is 2712 MPa and was improved to 3371 MPa with the modification of 3% PPA content.

Table 4 Marshall test properties of conventional and PPA-modified mixes

Binder (%)	Bulk density (gm/cc)	Air voids (%)	VFB (%)	Flow (mm)	Stability (kN)
<i>PPA content—0%</i>					
4.5	2.31	8.28	57.3	3.53	9.67
5.0	2.36	5.34	68.62	3.97	10.81
5.5	2.37	4.06	72.51	4.09	12.03
6.0	2.35	2.84	88.23	4.38	7.82
<i>PPA content—1%</i>					
4.5	2.32	8.33	53.94	3.67	10.18
5.0	2.35	6.63	62.47	3.82	12.11
5.5	2.37	4.11	73	4.11	14.61
6.0	2.33	5.51	76.29	4.46	11.03
<i>PPA content—2%</i>					
4.5	2.31	7.69	65.05	3.45	10.43
5.0	2.33	5.79	67.14	4.25	13.11
5.5	2.35	4.18	69.38	4.73	15.38
6.0	2.32	4.52	76.55	4.97	11.56
<i>PPA content—3%</i>					
4.5	2.31	8.95	52.14	3.26	18.48
5.0	2.33	4.14	60.58	3.7	20.62
5.5	2.35	3.12	70.57	4.03	19.57
6.0	2.32	6.26	74.69	4.36	13.59
<i>PPA content—4%</i>					
4.5	2.34	7.43	57.2	3.7	13.5
5.0	2.36	6.06	64.7	4.19	15.1
5.5	2.37	4.22	72.89	4.47	11.64
6.0	2.35	5.08	76.36	4.7	9.66
<i>PPA content—5%</i>					
4.5	2.3	9.03	51.74	3.42	10.82
5	2.37	5.58	66.68	4.12	14.24
5.5	2.35	4.24	76.12	4.47	12.18
6	2.31	6.61	66.73	4.95	8.85
<i>PPA content—6%</i>					
4.5	2.32	8.17	54.55	3.55	11.88
5.0	2.35	6.43	63.24	4.22	13.28
5.5	2.33	4.23	77.14	5.03	11.15
6.0	2.31	5.59	81.48	5.27	9.78

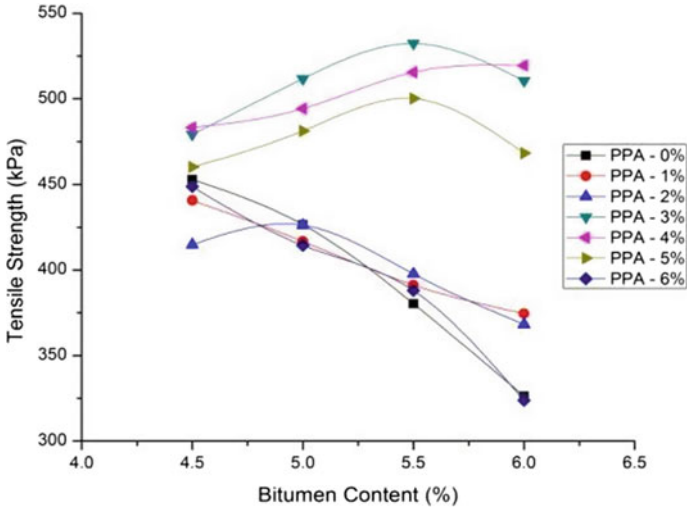


Fig. 6 Comparison of tensile properties for different mix combinations

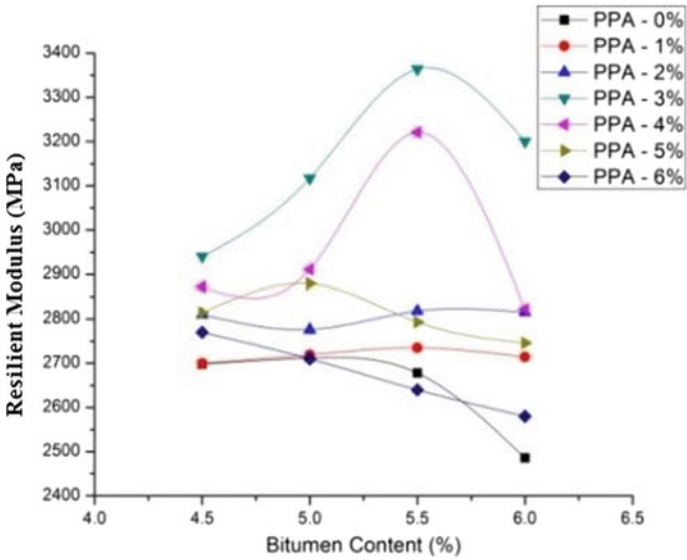


Fig. 7 Resilient modulus for different mix combinations

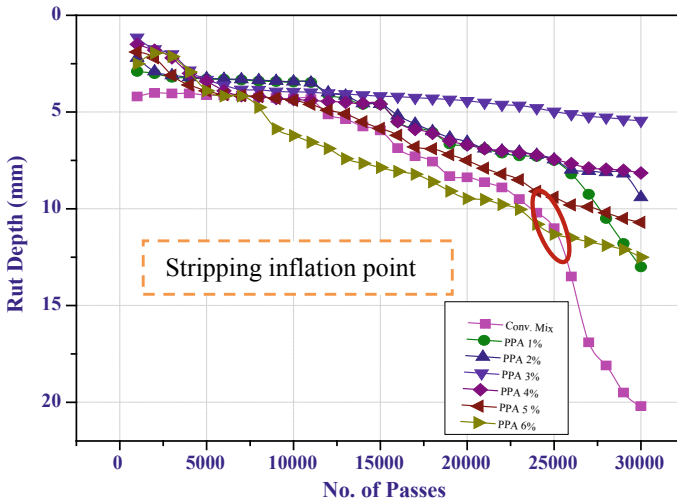


Fig. 8 Rutting and stripping properties for different mix combinations

5.4 Rutting Characteristics

Immersion wheel tracking instrument was used for evaluation of rutting performance of different mix combinations. Figure 8 provides rutting results for different mix combinations. Conventional mix has initiated stripping failure at 20,000 number of wheel passes and achieved 20 mm rut depth at 30,000 number of wheel passes. Modified mixes with 3% optimum content PPA have improved resistance. Figure 8 shows that rut depth for 3% PPA content is 5.5 mm and has improved when compared with conventional mixes for a same number of wheel passes.

6 Conclusion

The laboratory results explain conventional mixes and acid-modified mixes; the following conclusions are drawn.

- The Marshall stability value was improved for 3% PPA which shows that there is an increase in 21% stability value.
- It has been observed that tensile strength has reduced with an increase in bitumen content for conventional mixes whereas 3% PPA-modified mix exhibits better tensile properties. This infers that PPA has good resistance towards cracking.
- Resilient modulus values were slightly enhanced with the modification of bitumen. Further increase in PPA content has an effect in resilient properties. At 3% PPA, the modulus value is arrived as 3371 MPa.

- (d) Resistance towards rutting and stripping was improved for mixes prepared at optimum PPA content of asphalt mixes.

It is concluded that the modification of binder with 3% PPA increases stability and improves the performance characteristics of PPA-modified mixes. It is also observed that for PPA-modified mixes, the tensile properties are improved and good resilient characteristics. This results in achieving resistance for the formation of crack and rut depth. This will contribute success in improving serviceability in terms of performance characteristics.

References

Journals

1. Baldino N, Gabriele D, Lupi FR, Rossi CO, Caputo P, Falvo T (2013) Rheological effects on bitumen of polyphosphoric acid (PPA) addition. *J Constr Build Mater* 40:397–404
2. Behnood A, Olek J (2017) Rheological properties of asphalt binders modified with styrene-butadiene-styrene (SBS), ground tire rubber (GTR), or polyphosphoric acid (PPA). *J Constr Build Mater* 151:464–478
3. Dong F, Yu X, Liu S, Wei J (2016) Rheological behaviors and microstructure of SBS/CR composite modified hard asphalt. *J Constr Build Mater* 115:285–293
4. Fee D, Maldonado R, Reinke G, Romagosa H (2010) Polyphosphoric acid modification of asphalt. *J Transp Res Board* 2179-06:49–57
5. Giavarini C, Mastrofin D, Scarsella M, Barré L, Espinat (2000) Macrostructure and rheological properties of chemically modified residues and bitumen's. *J Energy Fuels* 14(2):495–502
6. Kodrat I, Sohn D, Hesp S (2007) Comparison of polyphosphoric acid modified asphalt binders with straight and polymer-modified materials. *J Transp Res Board* 1998-06:47–55
7. Kök B, Çolak H (2011) Laboratory comparison of the crumb-rubber and SBS modified bitumen and hot mix asphalt. *J Constr Build Mater* 25(8):3204–3212
8. Kök B, Yılmaz M, Geçkil A (2013) Evaluation of low-temperature and elastic properties of crumb rubber- and SBS-modified bitumen and mixtures. *J Mater Civ Eng* 25:257–265
9. Moghadas Nejad F, Azarhoosh A, Hamed GH, Roshani H (2014) Rutting performance prediction of warm mix asphalt containing reclaimed asphalt pavements. *J Road Mater Pavement Des* 15:207–219
10. Xia FS, Amirkhanian S, Wang H, Hao P (2014) Rheological property investigations for polymer and polyphosphoric acid modified asphalt binders at high temperatures. *Constr Build Mater* 64:316–323
11. Yadollahi G, Sabbagh Mollahosseini H (2011) Improving the performance of crumb rubber bitumen by means of poly phosphoric acid (PPA) and Vestenamer additives. *J Constr Build Mater* 25(7):3108–3116

Thesis and Codes

12. AASTHO T 324 (2017) Standard method of test for Hamburg wheel-track testing of compacted hot-mix asphalt

13. ASTM D5581-07a (2013) Standard test method for resistance to plastic flow of bituminous mixtures using Marshall apparatus (6 inch-diameter specimen)
14. ASTM D 6926-04 (2010) Standard practice for preparation of bituminous specimens using Marshall apparatus
15. ASTM D4123 (1995) Standard test method for indirect tension test for resilient modulus of bituminous mixtures
16. BS EN 12697-22 (2003) Standard test methods for hot mix asphalt bituminous mixtures—wheel tracking
17. BS EN 12697 33 (2007) Standard test methods for hot mix asphalt bituminous mixtures—specimen prepared by roller compactor
18. IRC: SP-53 (2010) Guidelines on use of modified bitumen in road construction, 2nd revision. Indian Roads Congress, New Delhi, India
19. Ministry of Road Transport and Highways (2013) MoRTH-2013, 5th revision, New Delhi
20. Ramasamy NB (2010) Effect of polyphosphoric acid on aging characteristics of PG 64-22 asphalt binder. A thesis submitted to University of North Texas for Master of Science

The Effect of Model Uncertainty on the Reliability of Asphalt Pavements



Abhishek Mittal and A. K. Swamy

Abstract Traditionally, fatigue and rutting have been the two most commonly adopted modes of failure for asphalt pavements. The design life of the pavement is considered to last till the fatigue cracking of bituminous surface or rutting in the pavement reaches its terminal value, whichever happens earlier. For both of these individual failure modes, the number of repetitions till failure is empirically correlated with certain mechanistic parameters of the pavement section, which is known as M-E transfer function. Traditionally, fatigue and rutting transfer functions are related to initial critical strain parameters. Horizontal tensile strain at the bottom of the bituminous layer and vertical compressive strain on the top of the subgrade are considered as critical parameters to limit fatigue and rutting of the pavement section. Such transfer functions are calibrated based on the field data and therefore possess uncertainty due to various factors such as material characteristics, loading conditions and climatic factors. So, this model uncertainty needs to be accounted for in the reliability analysis of pavements. The present study addresses this issue by applying model factors to the fatigue and rutting equations and examines the effect of uncertainty in the model factor on the reliability of the pavement design. This has been illustrated through examples of pavements designed as per Indian pavement design guidelines using IRC:37-2012.

Keywords Fatigue · Rutting · Model uncertainty · Simulation · Pavement design

1 Background

The structural design of pavement deals with determining the thicknesses of the various pavement layers. The design is done as per the mechanistic-empirical design procedure given in IRC:37-2012. The various input parameters such as pavement

A. Mittal (✉)

Flexible Pavement Division, CSIR-Central Road Research Institute, New Delhi, India
e-mail: mushimittal@gmail.com

A. K. Swamy

Civil Engineering Department, Indian Institute of Technology Delhi, New Delhi, India
e-mail: akswamy@civil.iitd.ac.in

© Springer Nature Singapore Pte Ltd. 2020

T. V. Mathew et al. (eds.), *Transportation Research*, Lecture Notes in Civil Engineering 45, https://doi.org/10.1007/978-981-32-9042-6_61

thickness, Poisson’s ratio, elastic modulus, commercial vehicles per day, tyre pressure, lane distribution factor (LDF), vehicle damage factor (VDF) and growth rate are considered as deterministic during the design process. However, in reality, none of these parameters is deterministic; in fact, they all are stochastic (probabilistic) [1, 2].

The current Indian pavement design guidelines [3] considers flexible pavement as an elastic multilayer structure. Stress and strains at critical locations are computed using a linear layered elastic model. IITPAVE software is used to compute stresses and strains in flexible pavements. Fatigue cracking and rutting are the two modes of failure that have been considered in the design guidelines. The horizontal tensile strain (ϵ_t) at the bottom of the bituminous layer and the vertical compressive strain (ϵ_v) on the top of the subgrade have been correlated with the fatigue and rutting failure of flexible pavements.

A schematic view of a three-layered pavement structure is shown in Fig. 1.

IRC:37-2012 also provides the fatigue and rutting models for 80 and 90% reliability levels. These models have been calibrated in the R-56 studies using the pavement performance data collected during the R-6 and R-19 studies sponsored by Ministry of Road Transport and Highways (MORTH). These models are given below:

Fatigue Model

$$N_f = 2.21 \times 10^{-4} \times \left(\frac{1}{\epsilon_t}\right)^{3.89} \times \left(\frac{1}{M_R}\right)^{0.854} \quad (80\% \text{ Reliability}) \quad (1)$$

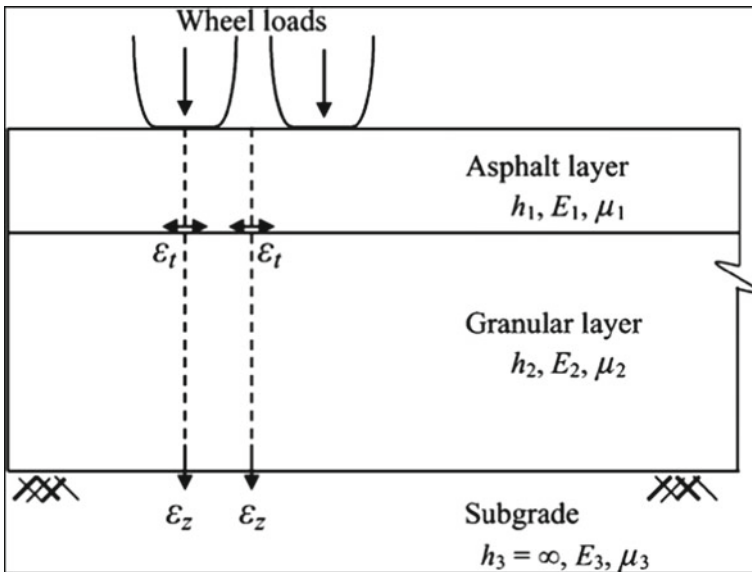


Fig. 1 Schematic diagram of a bituminous pavement structure

$$N_f = 0.711 \times 10^{-4} \times \left(\frac{1}{\varepsilon_t}\right)^{3.89} \times \left(\frac{1}{M_R}\right)^{0.854} \quad (90\% \text{ Reliability}) \quad (2)$$

Rutting Model

$$N_f = 4.1656 \times 10^{-8} \times \left(\frac{1}{\varepsilon_v}\right)^{4.5337} \quad (80\% \text{ Reliability}) \quad (3)$$

$$N_f = 1.41 \times 10^{-8} \times \left(\frac{1}{\varepsilon_v}\right)^{4.5337} \quad (90\% \text{ Reliability}) \quad (4)$$

Equations (1) and (3) are to be used when the design traffic is up to 30 million standard axle (msa) repetitions, and Eqs. (2) and (4) are to be used when the traffic is more than 30 msa.

2 Reliability Theory

Reliability is defined as ‘the probability that a component or system will perform a required function for a given period of time when used under stated operating conditions’ [4]. In simple words, it is defined as the probability of non-failure for a given period of time.

Mathematically, it can be written as,

$$R = 1 - P_f \quad (5)$$

where ‘ R ’ denotes reliability, and ‘ P_f ’ represents the probability of failure.

The reliability theory has been used in the design of structures to ensure their safety and their ability to fulfil their design requirements. However, the application of this theory for pavement structures has been limited and yet to be fully exploited.

For the application of reliability concepts to the pavement design problems, a limit state corresponding to each failure mode need to be identified. Since the current Indian guidelines consider only two failure modes, viz. fatigue and rutting, two limit-state equations need to be formulated. The limit-state equation for a flexible pavement can be expressed as the difference between the number of possible load applications a pavement can withstand before failing to meet a specified performance measure (either fatigue cracking or rutting), N_C (referred as the capacity of the pavement) and the actual number of load applications, N_D (referred as the demand on the pavement).

In simple mathematical terms, it can be expressed as:

$$g(x) = N_C - N_D \quad (6)$$

where $g(x)$ denotes a limit-state function in which x denotes a vector of n basic random design variables.



Fig. 2 Block diagram for failure modes in series system [5]

The probability of failure, P_f , is then given by:

$$P_f = P[g(x) \leq 0] \quad (7)$$

Equation (7) denotes the probability of failure for each failure mode. There are two failure modes for a pavement structure, viz. fatigue cracking and rutting, and they are assumed to be independent of each other. The fatigue and rutting component of a pavement system may be assumed to be operating in series as illustrated in Fig. 2.

In a series arrangement, the system fails when any one of the components fails. So, a pavement system is said to fail if either fatigue cracking or rutting failure occurs. Since they are assumed to be independent, the reliability of the pavement system, R_s will be the product of the reliabilities associated with each component [6]. Hence,

$$R_s = R_f \times R_r \quad (8)$$

and

$$P_{fs} = 1 - [(1 - P_{ff}) \times (1 - P_{fr})] \quad (9)$$

where

- R_s Overall reliability of pavement system
- R_f Reliability of pavement due to fatigue consideration
- R_r Reliability of pavement due to rutting consideration
- P_{fs} Overall probability of failure of pavement system
- P_{ff} Probability of failure due to fatigue consideration
- P_{fr} Probability of failure due to rutting consideration.

2.1 Monte Carlo Simulation Approach

In the present study, Monte Carlo simulation has been used [7]. Considering the variability of the pavement design input parameters, a random number is picked up from the distribution of each input, and then, the design procedure is run, which finally predicts a pavement performance. This constitutes one simulation. This process is repeated until the chosen number of simulations exhausted. Based on the defined performance criteria, the reliability of the design can be determined as the number of predicted performance passed the criteria out of the total number of simulations.

A MATLAB code has been written for the simulation purpose, and one million (10^6) simulations have been done for each reliability calculation.

2.2 Strain Transfer Functions

The two distress models for fatigue and rutting failure modes may be used easily for deterministic analysis as only the values of critical strains are needed. The use of the available pavement analysis software for the evaluation of these strains poses a challenge for the reliability analysis requiring an iterative evaluation of the distress models. This iterative process requires a considerable amount of computing power and calls for a more computationally efficient alternative. For this reason, the concept of response surface methodology can be used to establish an approximate functional relationship for critical strains through regression analysis. The following equations for strain transfer functions for horizontal tensile strain (ε_t) and vertical compressive strain (ε_z) are used in this work [8]:

$$\varepsilon_t = 364.9776 - 6.345h_1 - 0.9679h_2 - 0.01854E_1 - 0.09992E_2 - 0.09698E_3 \quad (10)$$

$$\varepsilon_z = 949.8377 - 14.9656h_1 - 7.44453h_2 - 0.02852E_1 - 0.11843E_2 - 1.19009E_3 \quad (11)$$

where h_1 and h_2 are the thicknesses of the asphalt layer and granular layer, respectively (in cm); E_1 , E_2 and E_3 are the elastic moduli of the asphalt layer, granular layer and subgrade, respectively (in MPa); ε_t and ε_z are in microstrain.

2.3 Model Uncertainty

In reliability analysis of flexible pavements, the probabilistic modelling of the calculation model (rutting and fatigue equations) is often ignored. As part of any reliability analysis, it is important to consider the uncertainty in the calculation model as well as the uncertainties in the various input parameters such as traffic loads and material properties. For example, while determining the allowable number of repetitions for rutting (or fatigue), there is some uncertainty in the equation itself since the equation has been developed based on the field performance data of selected test sections. The various input design parameters such as E_1 , E_2 , E_3 , h_1 and h_2 are uncertain and possess some variability. This leads to an uncertain prediction of N_f and N_r . Also, the use of approximate strain transfer functions developed through response surface methodology brings more uncertainty in the prediction of N_f and N_r . This issue has been addressed by applying a model factor, M , as a random variable with a mean value of unity to the calculation model, and examining what level of uncertainty in

the calculation model, represented by the coefficient of variation of M (COV_M), is necessary for this uncertainty to affect the reliability of the design [9]. This is carried out by increasing the value of COV_M , and observing the effect, this has on the component reliability values and on the system reliability. Thus, the empirical equations for the fatigue and rutting models become:

$$N_f = M \times k_1 \times \left(\frac{1}{\varepsilon_t}\right)^{k_2} \times \left(\frac{1}{M_R}\right)^{k_3} \quad (12)$$

$$N_r = M \times k_4 \times \left(\frac{1}{\varepsilon_v}\right)^{k_5} \quad (13)$$

Here, the values of coefficients k_1, k_2, k_3, k_4 and k_5 are as given in IRC:37-2012, depending on the reliability level adopted for design.

2.4 Details of Design Traffic and Pavement Sections

It has been decided to perform the reliability analysis for design traffic of 50 msa. The design traffic has been calculated in terms of million standard axles (msa) as per the following equation.

$$N = \frac{365 \times A \times D \times F \times ((1+r)^n - 1)}{r} \quad (14)$$

where

- N Cumulative number of standard axles for design, in msa
- A Initial traffic in terms of commercial vehicles per day (CVPD)
- D Lane distribution factor (LDF)
- F Vehicle damage factor (VDF)
- n Design life (in years)
- r Annual growth rate of commercial vehicles (in decimal)

To obtain the value of N as 50 msa, the following input parameters have been used in the above equation.

$$A = 1411, D = 1.0, F = 4.5, n = 15 \text{ and } r = 0.05.$$

Four different pavement sections were designed for 50 msa design traffic considering the different failure modes for asphalt pavements. The details of the pavement sections selected for analysis are given in Table 1.

For all the above sections, the values of actual and allowable strains have been calculated and are presented in Table 2.

Table 1 Details of selected pavement sections

Section No.	Bituminous layer thickness (mm)	Granular layer thickness (mm)	Nature of safety w.r.t. fatigue and rutting failure considerations
1	167	210	Just safe for both fatigue and rutting
2	161	249	Just safe for fatigue, oversafe for rutting
3	178	188	Just safe for rutting, oversafe for fatigue
4	180	250	Oversafe for both fatigue and rutting

Table 2 Strain calculations for the selected sections

Section No.	h_1 (mm)	h_2 (mm)	Tensile strain (ϵ_t) ($\times 10^{-6}$)		Compressive strain (ϵ_c) ($\times 10^{-6}$)	
			Actual	Allowable	Actual	Allowable
1	167	210	161.541	161.621	371.264	371.694
2	161	249	161.574	161.621	351.210	371.694
3	178	188	156.691	161.621	371.180	371.694
4	180	250	149.421	161.621	322.031	371.694

Note ' h_1 ' indicates bituminous layer thickness, and ' h_2 ' indicates granular layer thickness

2.5 Variability of Input Design Parameters

The values of failure probabilities for both the failure modes have been calculated for the design traffic of 50 msa. For these calculations, the values of coefficients k_1 , k_2 , k_3 , k_4 and k_5 have been adopted corresponding to 90% reliability level.

For the sake of simplicity, all the parameters in this study have been considered as uncorrelated normal random variables. Also, it has been assumed that the rutting and fatigue distress models uncertainty is represented by the model factor M , which has a mean value of 1.0. The design inputs adopted for this study are given in Table 3.

2.6 Calculation of Failure Probabilities

The values of COV_M have been varied from 0 to 50% to assess its effect on the failure probability of the pavement. Monte Carlo simulation (MCS) approach has been used to calculate the failure probability values for fatigue and rutting modes of failure. A MATLAB code employing the MCS approach has been specifically written for this purpose.

Table 3 Values for various input design parameters

S. No.	Parameter	Mean value adopted	COV (%)
1.	Bituminous layer thickness (h_1)	As per the section chosen	5
2.	Granular layer thickness (h_2)	As per the section chosen	10
3.	Elastic modulus for bituminous layer (E_1)	2500 MPa	15
4.	Elastic modulus for granular layer (E_2)	250 MPa	20
5.	Elastic modulus for subgrade (E_3)	60 MPa	20
6.	Commercial vehicles per day (CVPD)	1411	20
7.	Vehicle damage factor (VDF)	4.5	15
8.	Lane distribution factor (LDF)	1.0	10
9.	Growth rate	5%	10
10.	Design period	15 years	0 (Deterministic)

The failure probabilities for different COVs for factor M have been computed for all the four sections and presented in Tables 4, 5, 6 and 7.

Table 4 Variation of component failure probabilities and system failure probabilities for section 1

COV _M (%)	Probability of fatigue failure (%)	Probability of rutting failure (%)	Probability of system failure (%)
0	0.4481	0.4620	0.7031
10	0.4538	0.4672	0.7090
20	0.4674	0.4786	0.7223
30	0.4780	0.4893	0.7334
40	0.4868	0.4985	0.7426
50	0.4913	0.5027	0.7470

Table 5 Variation of component failure probabilities and system failure probabilities for section 2

COV _M (%)	Probability of fatigue failure (%)	Probability of rutting failure (%)	Probability of system failure (%)
0	0.4487	0.2606	0.5924
10	0.4546	0.2685	0.6010
20	0.4676	0.2908	0.6224
30	0.4793	0.3195	0.6457
40	0.4863	0.3462	0.6641
50	0.4911	0.3682	0.6785

Table 6 Variation of component failure probabilities and system failure probabilities for section 3

COV _M (%)	Probability of fatigue failure (%)	Probability of rutting failure (%)	Probability of system failure (%)
0	0.3138	0.4612	0.6303
10	0.3253	0.4655	0.6394
20	0.3526	0.4771	0.6615
30	0.3798	0.4895	0.6834
40	0.4009	0.4962	0.6982
50	0.4168	0.5027	0.7100

Table 7 Variation of component failure probabilities and system failure probabilities for section 4

COV _M (%)	Probability of fatigue failure (%)	Probability of rutting failure (%)	Probability of system failure (%)
0	0.1529	0.0755	0.2169
10	0.1666	0.0822	0.2351
20	0.2037	0.1023	0.2852
30	0.2475	0.1378	0.3512
40	0.2864	0.1780	0.4134
50	0.3171	0.2158	0.4645

3 Conclusions

Reliability analysis for four different sections corresponding to the design traffic of 50 msa has been carried out using the Monte Carlo simulation approach. The model uncertainty has been indicated by incorporating a model factor 'M', with a mean value of 1.0, in the fatigue and rutting models. The effect of model uncertainty on failure probabilities has been estimated by varying the COV for the model factor from 0 to 50%. The following conclusions have been drawn based on the results of the reliability analysis conducted for the four sections.

1. The effect of model uncertainty on the failure probability is quite significant for individual failure modes as well as for the overall failure of the system.
2. The percentage increase in the probability of failure for section 1, due to increased model uncertainty has been found to be 9.6, 8.8 and 6.3% for fatigue failure, rutting failure and system failure, respectively.
3. The percentage increase in the probability of failure for section 2, due to increased model uncertainty has been found to be 9.4, 41.3 and 14.5% for fatigue failure, rutting failure and system failure, respectively.
4. The percentage increase in the probability of failure for section 3, due to increased model uncertainty has been found to be 32.8, 9.0 and 12.6% for fatigue failure, rutting failure and system failure, respectively.

5. The percentage increase in the probability of failure for section 4, due to increased model uncertainty has been found to be 107.4, 185.8 and 114.2% for fatigue failure, rutting failure and system failure, respectively.
6. The study indicates that the effect of model uncertainty is more prominently observed for that failure mode for which the section was designed oversafe. It has been observed that the percentage increase in the probability of failure for section 2 (oversafe for rutting), section 3 (oversafe for fatigue) and section 4 (oversafe for fatigue and rutting both) was substantially high for rutting, fatigue and both failure modes, respectively, due to variation in model uncertainty.
7. The study also indicates that the deterministic design of pavement section could be quite misleading so far as the satisfactory performance of a pavement in its lifetime is concerned. Because almost all the input design variables have some uncertainty, it is desirable to adopt a reliability-based design for pavements for satisfactory performance.

Acknowledgements The authors would like to thank Prof. Satish Chandra, Director, CSIR-Central Road Research Institute (CSIR-CRRI), New Delhi, India, for his kind permission to publish this paper.

References

1. Hudson, WR (1975) State-of-the-art in predicting pavement reliability from input variability. Report No. FAA-RD-75-207, U.S. Army Waterways Experiment station, Vicksberg, Mississippi, US
2. Kalitha K, Rajbongshi P (2015) Variability characterisation of input parameters in pavement performance evaluation. *Road Mater Pavement Des* 16(1):172–185
3. IRC (2012) Guidelines for the design of flexible pavements. IRC No. 37, Indian Roads Congress, New Delhi
4. Ebeling CE (1997) Introduction to reliability and maintainability engineering. McGraw Hill Inc., New York
5. Ghosh I (2005) Reliability analysis of flexible pavements using mechanistic-empirical approach, Master's Thesis, Bengal Engineering and Science University, Shibpur
6. Harr ME (1987) Reliability based design in civil engineering. McGraw-Hill Inc., New York
7. Ayuub BM, McCuen RH (2011) Probability, statistics and reliability for engineering and scientists, 3rd edn. CRC Press, Taylor and Francis, FL
8. Dilip DM, Ravi P, Babu GLS (2013) Reliability design procedures for flexible pavements. *J Transp Eng* 139(10):1001–1009
9. Forrest WS, Orr TLL (2011) The effect of model uncertainty on the reliability of spread foundations. In: Proceedings of third international symposium on geotechnical safety and risk, Germany, pp 401–408

Investigation on Rutting Performance of Gap-Graded Asphalt Mixtures: Study on Aggregate Gradation



Veena Venudharan  and Krishna Prapoorna Biligiri 

Abstract The objective of this study was to investigate the rutting performance of gap-graded aggregate gradations in conjunction with the effect of asphalt binder. Two gap-graded aggregate gradations recommended by Arizona Department of Transportation (ADOT: gradation *A*), Texas DOT (gradation *B*), and one newly proposed gradation (gradation *C*) were considered in this study. Wheel-tracking test was performed at 60 °C on ten asphalt mixtures, and rut depth was statistically analyzed using 2³ factorial designs at 95% confidence interval. Main effect analysis showed that gradation *C* offered the highest rutting resistance followed by gradation *B* and *A*. Though the gradation *A* demonstrated a reduction in rutting resistance with increasing binder content, gradations *B* and *C* were less sensitive to variation in the binder content. Rutting characteristics estimated at different stages revealed that permanent deformation incurred in gradation *A* developed rapidly until 75% and then retarded to a stable rate. In the case of gradations *B* and *C*, there was a marginal difference in the permanent deformation at various stages. Further, gap-graded asphalt mixtures prepared with gradations *B* and *C* at both (OBC – 1) and OBC % showed better performance than conventional dense-graded (DG) asphalt mix. Overall, it was concluded that gap-graded mixture can be expected to outperform the DG mix when designed with appropriate mix parameters.

Keywords Gap aggregate gradation · Asphalt-rubber · Rutting · Wheel-tracking test · Statistical analysis · ANOVA

V. Venudharan (✉)
Indian Institute of Technology Kharagpur, Kharagpur, India
e-mail: veena.venudharan@gmail.com

K. P. Biligiri
Indian Institute of Technology Tirupati, Tirupati, India
e-mail: bkp@iittp.ac.in

1 Introduction

Rutting is a high-temperature distress of the flexible asphalt pavement, which occurs due to repetitive wheel loading. Owing to the heterogeneous mix-matrix, and nonlinear viscoelastic behavior of asphalt mixtures, the evaluation of rutting performance constitutes a challenging research facet that connects comprehensive rheological characteristics of asphalt mixtures on theoretical aspect with the real-time field performance simulation. Thus, a comprehensive understanding of materials behavior is of utmost importance toward the analysis, design, and evaluation of rutting performance of the flexible pavement.

In general, the study of rutting in asphalt mixtures can be categorized into two mainstreams: (a) analytical estimation of rutting, and (b) materials modification and performance characterization. The former employs numerical/analytical modeling based on the materials properties while the latter deals with the improvement of materials, including asphalt binder and aggregate through the modification techniques followed by characterization. Interestingly, the latter segment of research renders the necessary inputs to the former one, thus playing a very crucial role in the purview of large-scale rutting evaluation.

Although numerous studies [1–7] can be found in the literature that investigated rutting performance of asphalt mixtures in the line of two aforementioned domains, currently, material modification has been a major research focus in order to comply with the increasing traffic and wide variation of temperatures. In this direction, the utilization of gap-graded aggregate gradation over the conventional dense-graded (DG) one has been commonly adopted to improve the rutting performance of asphalt mixtures. Since gap-graded modified asphalt mixture outperforms the conventional dense-graded asphalt mix, various gap-graded aggregate gradations are adopted by different agencies across the world [8]. Thus, there is a need to understand the effect of different gap-graded aggregates and their relative performance assessment to mitigate rutting. Thus, the objective of this study was to investigate the rutting performance of gap-graded aggregate gradation in conjunction with the effect of asphalt binder. The scope of the work included (Fig. 1):

- Experimental investigation of rutting on three gap-graded aggregate gradations using wheel-tracking test
- Statistical assessment of the effect of aggregate gradation and binder content
- Performance analysis of rutting accounting for the effect of binder content
- Deformation history of different gap-graded mixture and estimate permanent deformation at various stages of rutting.

2 Materials and Experimental Program

Three gap-graded aggregate gradations were used in this study with commercially available crumb rubber modified, CRMB-60 binder. Three gap-gradations included:

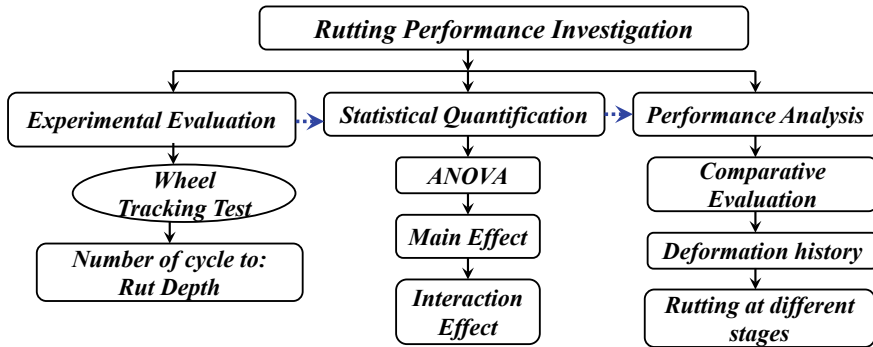


Fig. 1 Research outline

Arizona gap-gradation recommended by Arizona Department of Transportation (DOT) [9] designated as gradation A, Texas gap-gradation recommended by Texas DOT [10] designated as gradation B, and one newly proposed gradation designated as gradation C in this study. Figure 2 summarizes the details of aggregate gradations. At first, Superpave mix-design was employed to determine optimum binder content (OBC) for three aggregate gradations at $N_{des} = 125$ for 30 msa. The OBC of gradations A, B, and C was 7.8, 5.8, and 5.4%, respectively. Next, Superpave gyratory specimens were prepared at three binder contents: (OBC - 1), OBC, and (OBC + 1) %. Thus, a total of eighteen gyratory asphalt specimens were prepared for nine gap-graded asphalt mixtures at a rate of two specimens per mix type. Additionally, four DG mixes prepared with viscosity graded VG-40 binder were also included for comparison purposes.

All the Superpave specimens were cut using a water-cooled diamond cutter to evaluate rutting performance using wheel-tracking test as per EN 12697-22 [11]. Note

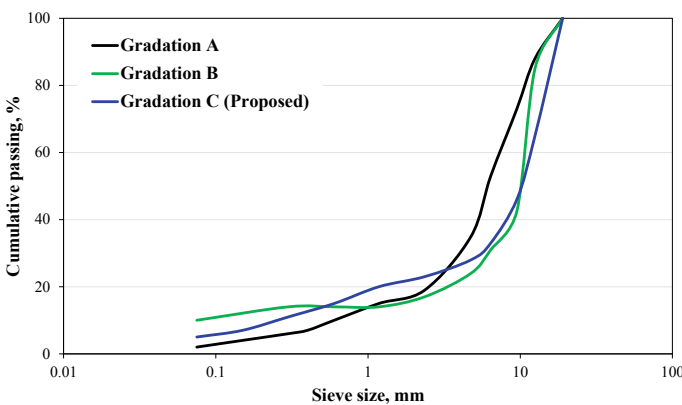


Fig. 2 Gap-graded aggregate gradations

Fig. 3 Experimental setup of wheel-tracking test



that each test employed assessment of rutting averaging across two specimens, thus a total of 40 specimens were utilized in this experimental program. The specimens were conditioned at 60 °C for four hours prior to the testing. Then, a wheel load of 70 ± 5 N was vertically placed on the specimen. The wheel was allowed to pass horizontally on the specimen at 20 rpm and surface deformation was measured at 27 points along the line of wheel passes on the specimen. The test termination criteria included a maximum of 25,000 wheel passes or an average rut depth of 10 mm, whichever occurred earlier. Figure 3 shows the wheel-tracking device used in this study.

3 Factorial Design—ANOVA

At 95% significant level, the null hypothesis can be rejected if the p -value of the factor shows a value less than 0.025. As observed in analysis of variance (ANOVA) results as shown in Table 1, both the factors produced p -value less than 0.025 indicating that the null hypothesis could be rejected. Hence, it can be concluded that both the

Table 1 ANOVA summary

Source	DF	SS _{adj}	MS _{adj}	F-value	p -value	Decision
Model	8	156.896	19.612	72.82	<0.025	–
Linear	4	140.34	5.0851	130.27	<0.025	
Gradation	2	122.943	61.471	228.25	<0.025	Significant
Binder content	2	17.397	8.698	32.30	<0.025	Significant
Interaction	4	16.555	4.138	15.37	<0.025	Significant
Grad * Binder	4	16.555	4.138	15.37	<0.05	Significant
Error	9	2.424	0.269	–		
Total	17	159.319	–			

factors aggregate gradation and binder content had a significant effect on *Rut depth* of all the mixtures. Further, the interaction between both the factors was also found to be significant. Thus, it can be anticipated that the interaction between these factors might result in differential response that would attribute to the dependent variable.

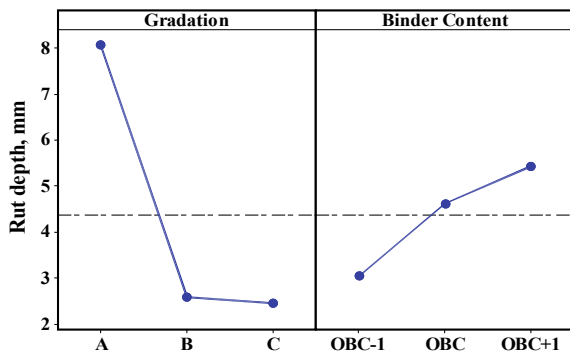
3.1 Main Effect

Main effect represents the influence of individual independent variables over the response variables by considering the change in mean across all the levels. Figure 4 shows the main effect of aggregate gradation and binder content. The reference mean of response variable: *Rut depth* used in this analysis is marked on the treatment response.

It is important to note that lower rut depth/rutting indicates higher rut resistance, and thereby essential for better pavement performance. As observed in Fig. 4, gradation *A* showed the highest rutting followed by gradations *B* and *C*. Since the working mechanism of aggregate gap-gradation against the rutting employs resistance developing from stone-to-stone contact, the aggregate particle distribution in gradation *B* and *C* plausibly formed a better stone-to-stone contact. Overall, the gradations illustrated a generalized trend on reference of mean response that can be expected when binder content remained constant.

On the other hand, rut depth increased with increasing binder content for all the gradations. The viscoelastic characteristics imparted by additional binder content in the mix-matrix attributed to the differential rutting properties. Since the gap-graded asphalt mixtures counter the rutting by the structural integrity of mix-matrix through stone-to-stone contact, the presence of additional binder content plausibly augments the viscous component of mix. Thus, additional binder content might be beneficial for other performances such as fatigue cracking and low-temperature fracture resistance but might lead to an adverse effect on rut resistance. It provided important information on the selection procedure of higher binder content in the design stage of gap-graded mixture. Further, the increase in *rut depth* was relatively less influential in the range

Fig. 4 Main effects of gradation and binder content on rutting performance



OBC – (OBC + 1) % than that of (OBC – 1) – OBC%. Much more information pertaining to the effect of binder content on different aggregate gradations can be better understood through interaction analysis as discussed next.

3.2 Interaction Effect

Since the ANOVA indicated significant influence on the interaction effect between two factors, interaction study was carried out to explore additional information on the behavioral change of materials toward rutting performance. Figure 5 shows the interaction relationship between the aggregate gradation and binder content.

The effect of binder content on three gradations can be found in the first row of Fig. 5. As observed, the *rut depth* of gradation A increased when binder content increased. But gradation B and C showed a marginal increment with increasing binder content. This is plausible because of the difference in OBC for three gradations. It is important to recall that gradation A had the highest OBC whereas gradations B and C showed a subtle difference in OBC. As a result, the presence of higher binder in gradation A perhaps counteracted against the stone-to-stone contact, and thereby facilitated aggregate movement under the shear force.

Concurrently, the effect of gradation on different binder contents is illustrated in the second row of Fig. 5. As observed, all the gradations produced a reduction in *rut depth* at all the levels of binder: (OBC – 1), OBC, and (OBC + 1) %. But gradation C resulted in the lowest rutting, followed by gradations B and C. Higher rate of improvement in rut resistance was reported for OBC, and (OBC + 1)% between

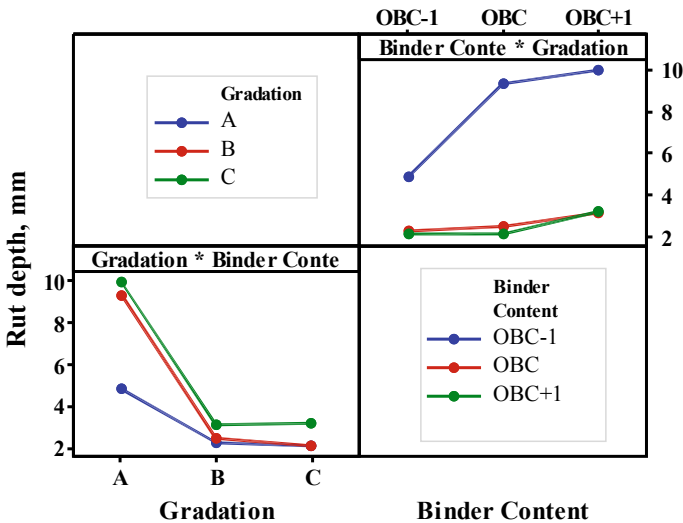


Fig. 5 Interaction effect

gradation *A* and other two gradations. Overall, it was found that the performance of gradation *C* was better than the other two gap-gradations, relatively.

4 Rutting Performance Analyzes

4.1 Comparative Evaluation of Rutting

Laboratory obtained rutting performance of nine gap-graded asphalt mixtures was compared with one conventional DG mix. Figure 6 presents the average *rut depth* of all the mixtures calculated from four replicate specimens. Note that X_{-1} , X , and X_{+1} indicate the gap-graded asphalt mixtures prepared with $(OBC - 1)$, OBC , and $(OBC + 1)$ %, respectively where “ X ” denotes the gradation type: *A*, *B*, and *C*. This part of analysis was based on the final permanent deformation at the end of the wheel-tracking test.

As expected from the main effect study, the gradation *A* showed the highest *rut depth* at all the binder contents. Further, this gradation showed the best performance in rutting at $(OBC - 1)$ % binder content, and rutting resistance decreased when binder content was further increased. Conversely, rutting performance of gradations *B* and *C* was relatively less sensitive in respect of binder content, especially in the range of $(OBC - 1) - OBC$. Thus, these two gradations offered a unique advantage to increase binder content without any compromise in rutting performance. With regard to the relative evaluation in the line of conventional DG mix, only four gap-graded asphalt mixtures: gradations *B* and *C* with both $(OBC - 1)$ and OBC % out of nine, exhibited better rutting performance than the conventional DG mixture. Hence,

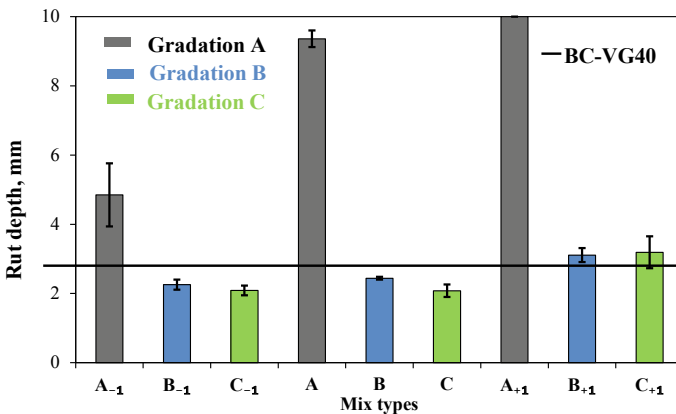


Fig. 6 Rutting performance of asphalt mixtures

it can be understood that the gap-graded mixtures can be expected to outperform the DG mix when designed with appropriate mix parameters.

4.2 Deformation History

Although the final *rut depth* provided important information on rutting performance, the study of deformation history throughout the rutting process is of utmost important to understand continuous progression of the distress. Note that the deformation history was recorded at an interval of five wheel passes totaling 5000 data points per test. For brevity purpose, deformation history was only analyzed at OBC for three gradations. Figure 7 illustrates the permanent strain accumulated for all gradations with progressive wheel passes.

As observed in Fig. 7, gradation *A* exhibited early deformation that rapidly increased with increasing wheel passes. In contrast, the deformation was relatively slower in the early stage of rutting for gradations *B* and *C*, which was entailed by a consistent increment for a very short span. After that, the mixtures prepared with these two gradations maintained a stable deformation rate until the test completion. Though gradations *B* and *C* showed a similar trend in deformation history analysis, a subtle increment can be noticed for gradation *B*, especially after the primary stage of rutting. It is noteworthy that the tertiary stage of rutting was not achieved for these two gradations, which required a longer duration of test runs. Nonetheless, the fundamental rutting properties of three gradations and associated effects of binder content were well-demonstrated by the test settings.

Fig. 7 Variation of rut depth at OBC

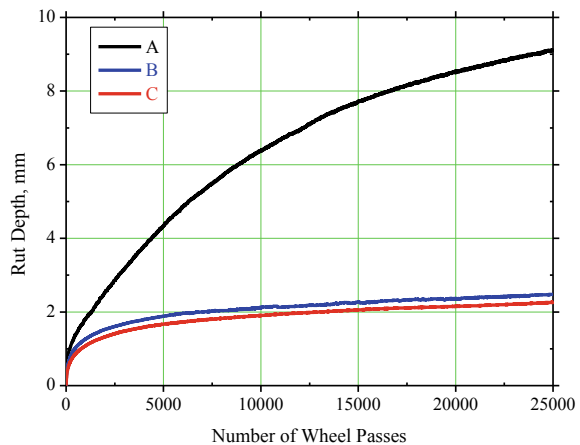
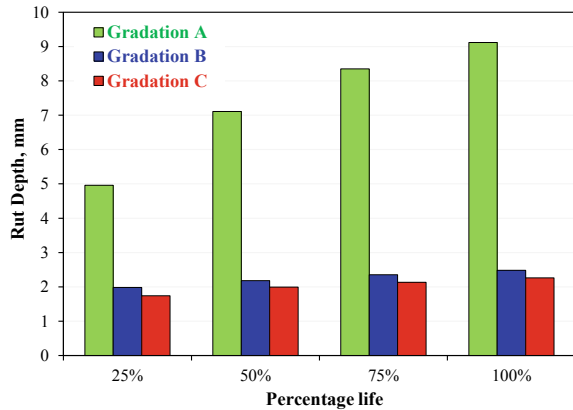


Fig. 8 Accumulated permanent deformation at different stages



4.3 Deformation at Various Stages

Though the deformation history provided primary information pertaining to the rutting mechanism, a better performance distinction calls for quantitative analysis at various stage of rutting. Since the three stages of rutting on the premise of mechanistic development (primary, secondary, and tertiary) are not very distinctive in this study, deformation was analyzed at four stages, namely 25, 50, 75, and 100% as shown in Fig. 8.

As observed, gradation A showed a consistent increment at all the stages of rutting. The growth rate at 50, 75, and 100% life included approximately 1.4, 1.7, and 1.8 times of 25%, respectively. It indicated that the permanent deformation incurred in gradation A developed very rapidly until 75% and then, retarded to a stable rate at the final term. On the other side, there was a marginal difference in permanent deformation at various stages of rutting. It reveals important information that the permanent strain for gradations B and C is expected to increase at a very slow rate, and probably obtains the tertiary stage of rutting after long time in comparison with gradation A. Though this analysis was based on three representative mixes from each gap-gradation at optimum level of binder content, a similar trend can be anticipated at other binder contents considered in this study.

5 Conclusions

The objective of this study was to investigate the rutting performance of gap-graded aggregate gradations in conjunction with the effect of asphalt binder. Nine crumb rubber-modified gap-graded mixtures were considered to evaluate the rutting characteristics and compared with one conventional DG mix. The major findings can be summarized under following heads:

- *Experimental investigation*: it was carried out on three aggregate gradations: gradation A, B, and C at 60 °C using wheel-tracking test method. Superpave mix-design method was adopted for mix-design, and gap-graded asphalt mixtures were prepared at OBC \pm 1%.
- *Statistical quantification*: ANOVA indicated that aggregate gradation and binder content had a significant influence on rutting performance. Main effect analyzes showed that gradation C offered the highest rutting resistance followed by gradation B and A. Though gradation A demonstrated a reduction in rutting resistance with increasing binder content, gradation B and C were less sensitive to variation in binder content.
- *Performance analysis*: gradation A exhibited early deformation that rapidly increased with increasing wheel passes. In contrast, the deformation was relatively slower in the early stage of rutting for gradations B and C, which was entailed by a consistent increment for a very short span. Rutting characteristics estimated at different stages revealed that permanent deformation incurred in gradation A developed rapidly until 75% and then, retarded to a stable rate. In the case of gradations B and C, there was a marginal difference in permanent deformation at various stages of rutting.
- *Performance comparison*: gap-graded asphalt mixtures prepared with gradation B and C at both (OBC – 1) and OBC% showed better performances than the conventional DG mix. Overall, it was concluded that gap-graded mixture can be expected to outperform the DG mix when designed with appropriate mix parameters.

Although the study investigated the rutting performance of three gap-graded aggregate gradations with one commercially available binder, a similar experimental methodology can be utilized for understanding the influence of other asphalt binders. In this direction, future study is certainly required to explore more information on the effect of aggregate particle distribution and associated stone-to-stone contact toward the rutting performance of asphalt mixtures.

Acknowledgements The authors gratefully acknowledge the Government of India Department of Science and Technology for their financial support vide Science and Engineering Research Board (SERB) research project grant number DST No: SERB/F/2670/2014-15 dated 17 July 2014.

References

1. Oliver JW (2000) Rutting and fatigue properties of crumbed rubber hot mix asphalts. *Road Mater Pavement Des* 1(2)
2. Xiao F, Amirkhanian S, Juang CH (2007) Rutting resistance of rubberized asphalt concrete pavements containing reclaimed asphalt pavement mixtures. *J Mater Civ Eng* 19(6):475–483
3. Fontes LP, Triches G, Pais JC, Pereira PA (2010) Evaluating permanent deformation in asphalt rubber mixtures. *Constr Build Mater* 24(7):1193–1200
4. Shirini B, Imaninasab R (2016) Performance evaluation of rubberized and SBS modified porous asphalt mixtures. *Constr Build Mater* 107:165–171

5. Imaninasab R, Bakhshi B, Shirini B (2016) Rutting performance of rubberized porous asphalt using Finite Element Method (FEM). *Constr Build Mater* 106:382–391
6. Topal A, Oner J, Sengoz B, Dokandari PA, Kaya D (2017) Evaluation of rutting performance of warm mix Asphalt. *Int J Civ Eng* 15(4):705–714
7. Venudharan V, Biligiri KP (2017) Effect of aggregate gradation on rutting performance of asphalt-rubber gap graded mixtures. In: International conference on advances in construction materials and systems, Indian Institute of Technology Madras, India, RILEM2017, 3–8 Sept 2017 (Conference Proceedings)
8. Venudharan V, Biligiri KP, Sousa JB, Way GB (2017) Asphalt-rubber gap-graded mixture design practices: a state-of-the-art research review and future perspective. *Road Mater Pavement Des* 18(3):730–752
9. Way GB, Kaloush KE, Biligiri KP (2012) Asphalt-rubber standard practice guide, 2nd edn. Prepared for the Rubber Pavements Association, USA
10. Stone Matrix Asphalt (2004) Item 346. Of Standard specifications for construction and maintenance, streets, and bridges. Texas Department of Transportation, pp 364–398
11. BS EN 12697-22 (2003) Bituminous mixtures. Test methods for hot mix asphalt. Wheel tracking, British Standards, UK

Performance Characteristic Evaluation of Asphalt Mixes with Plastic Coated Aggregates



Priyadarshini Saha Chowdhury, Sonu Kumar and Dipankar Sarkar

Abstract Construction and maintenance of a large number of road networks result in degradation of environment and depletion of natural resources chiefly: raw materials. As a mitigation strategy, sustainable and smart pavement technologies were developed and practiced with a view to balancing the performance criterion and need for utilization of waste materials. In this connection, the use of plastic waste in pavement construction has gained popularity. Despite the numerous studies available in the literature that evaluated the different performances of plastic modified asphalt mixtures, the effect of different levels of plastic inclusion and its associated performance improvement is a major research interest. Thus, the objective of the study was to utilize waste plastic in asphalt pavement construction and evaluate the effect of different levels of plastic inclusion. In this study, shredded waste plastics were added into mix starting from 2% by weight of asphalt binder to 12% with a successive increment of 2% through dry mix process. Different aggregate tests were performed to observe the effect of aggregate coating with plastic. After that, the Marshall test, retained stability, dry–wet and freeze–thaw indirect tensile strength tests were conducted upon modified and control asphalt mixes. Experimental results indicated that the physical properties of aggregate improved with the increment of the plastic content. It was possibly due to the improvement in adhesion between the aggregates with the presence of plastic. Also, ITS (dry, wet and freeze–thaw) increased due to plastic modification of mix. Further, an improvement in stability

P. Saha Chowdhury · S. Kumar (✉) · D. Sarkar

Department of Civil Engineering, National Institute of Technology Agartala, Agartala 799046, Tripura, India

e-mail: sonupremanshu@gmail.com

P. Saha Chowdhury

e-mail: bristy.sghs2@gmail.com

D. Sarkar

e-mail: dipankarnita@gmail.com

P. Saha Chowdhury

Department of Civil Engineering, Indian Institute of Technology Kharagpur, Kharagpur 721302, West Bengal, India

S. Kumar

L & T Construction, Gujarat 390019, India

© Springer Nature Singapore Pte Ltd. 2020

T. V. Mathew et al. (eds.), *Transportation Research*, Lecture Notes in Civil Engineering 45, https://doi.org/10.1007/978-981-32-9042-6_63

was observed due to plastic modification of mix. Thus, it can be also observed that the strength of the bond between the aggregate and the binder enhanced with the addition of plastic to the mix. Overall, it can be concluded that utilization of road plastic not only improved the environmental sustainability but also enhanced the pavement performance.

Keywords Plastic · Marshall mix design · Waste material · Retained stability · Indirect tensile test

1 Introduction

Rapid urbanization, increasing traffic load, higher traffic volume and insufficient maintenance lead to many severe distresses on road surfaces [1, 2]. Permanent deformation, *i.e.* rutting, thermal cracking and fatigue cracking, is frequent mode of distresses in asphalt pavements. Because of these failures during service time, there is a demand for higher performance of pavements and thus modifications of asphalt mixtures become essential in achieving required performance [3–5]. In order to improve the performance, studies have been performed on asphalt modification using polymers, waste materials such as crumb rubber, and various additives [6–10]. In addition to the above modifications, usage of waste plastic to improve the performance [11–13] has gained attention to reduce the ill-effects of plastic products on environment [14]. Approximately, 15,000 tonnes of plastic waste is generated every day in India as per Plastic Waste Management Rules, 2016, which is bound to increase in future [15]. Plastic being a non-biodegradable material has negative impacts on the human health and environment due to improper treatment and dumping. Critical issues are involved in disposal of plastic waste like choking of drains; reducing fertility of land; ingestion by cattle's leading to death; and emission of toxic gases [16, 17]. In order to mitigate the problem of waste plastic disposal and thereby reduce ill-effects on environment, several strategies have been implemented [18]. Among these strategies, usage of waste plastic in pavement materials has received growing attention owing to the material compatibility with asphalt and improved performance properties, making pavements more durable and eco-friendly [19–21]. Based on the literature survey and present need of the society, the research outline was developed which is given in Fig. 1.

The objective of the study was to utilize waste plastic in asphalt pavement construction and evaluate the effect of different levels of plastic inclusion. The major scope of the study included investigation of the effect of waste plastic on aggregate modification, performance characterization of plastic modified asphalt mixes through Marshall mix design and estimation of moisture performance using retained stability and indirect tensile strength.

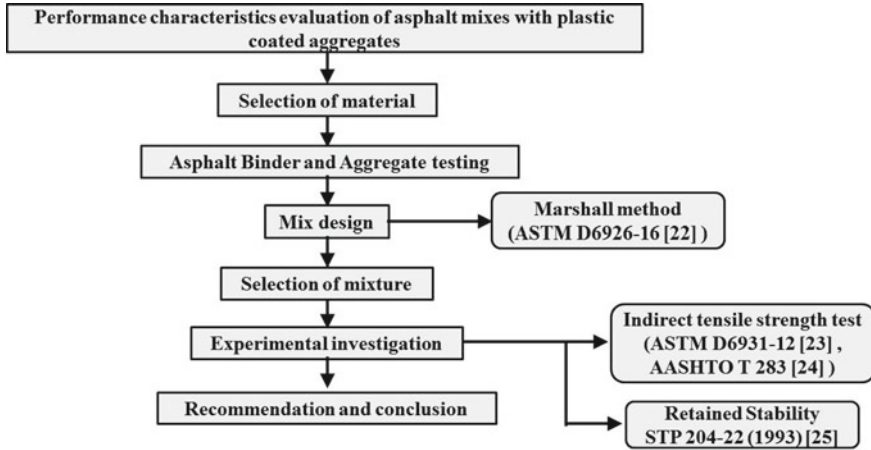


Fig. 1 Research outline

2 Materials and Sample Preparation

Asphalt mixture is a combination of asphalt binder and aggregates. Asphalt binder used in this study was viscosity grade asphalt binder, VG 30. Results of different tests conducted on the VG 30 binder are presented in Table 1. Those properties were compared with the IS 73 (2013) [26] paving grade asphalt binder specification.

Furthermore, the physical properties of aggregate were also evaluated. The physical properties of aggregates used in the study are given in Table 2. Bituminous con-

Table 1 Physical properties of asphalt binder

Properties of asphalt binder	Values	Specification	Relevant standard protocols
<i>Before ageing</i>			
Specific gravity	1.011	–	IS: 1202-1978 [27]
Penetration at 25 °C, 0.1 mm, 100 g, 5 s	46	Min. 45	IS: 1203-1978 [28]
Softening point (R&B) (°C)	52	Min. 47	IS: 1205-1978 [29]
Ductility at 27 °C (cm)	>100	Min. 75	IS: 1208-1978 [30]
Kinematic viscosity at 135 °C (cSt)	352	Min. 350	ASTM D4402/D4402M-15 [31]
<i>Rolling thin film test on residue (after ageing)</i>			
Loss in mass (%)	–0.14	–	ASTM D2872-12 [32]
Reduction of penetration at 25 °C	13	–	IS: 1203-1978 [28]
Increase in softening point (°C)	3	–	IS: 1205-1978 [29]

Table 2 Physical and mechanical properties of aggregate

Properties	Results	Specification	Standard for test method
Flakiness indices	24.2	Max. 25%	IS: 2386 (Part I)–1963 [34]
Elongation indices	21.3	–	IS: 2386 (Part I)–1963 [34]
Crushing strength test	29.9	Max. 30%	IS: 2386 (Part IV)–1963 [35]
Los Angeles abrasion value	28.9	Max. 30%	IS: 2386 (Part IV)–1963 [35]
Impact test	25.7	Max. 24%	IS: 2386 (Part IV)–1963 [35]

Table 3 Selected aggregate gradation BC-II (MoRTH: 2013 [33])

IS sieve (mm)	19	13.2	9.5	4.75	2.36	1.18	0.6	0.3	0.15	0.075
Cumulative % passing	100	95	79	62	50	41	32	23	16	7

crete–II (BC-II) specified by Ministry of Road Transport and Highways (MoRTH) [33] was selected for the study. The selected gradation with nominal maximum size of 13.2 mm is shown in Table 3.

In this present study, waste shredded plastic was used to enhance the properties of asphalt mix. Shredded plastic of size 2.36-mm sieve passing and retained on 600-micron sieve referring to IRC: SP: 098-2013 [36] was collected. Waste shredded plastic consists of polyethylene, polyester, LDPE, *etc.* The softening point of waste plastic was found to be varying from 100 to 135 °C. Shredded waste plastic was added to aggregate in various percentages by weight of asphalt binder through dry mix process at a temperature 160 °C. Six different levels of waste plastic addition, which included 2, 4, 6, 8, 10 and 12%, by weight of asphalt binder, were used to modify the mixture by adding the plastic on the heated coarse aggregates. The mixtures were designated as PM2, PM4, PM6, PM8, PM10 and PM12, where “PM” represents plastic modified mix and “X” indicates the percentage of plastic dosage. In addition, control mixture with VG 30 binder without any modification was prepared for comparison purposes. Marshall Mix Design [22] was adopted for preparation of asphalt mix.

3 Selection of Mixture

Selection of plastic dose was done based on strength, hardness, toughness and water absorption of aggregate, and stability and asphalt binder requirement of the mixture. Thus, the tests including crushing strength test, Los Angeles abrasion test, impact test, water absorption test were carried out for plastic coated aggregate and Marshall mix design was carried out for trial mixtures. The results of these tests are shown in Fig. 2. The red line in the figure shows the specified limits of each test as per MoRTH: 2013 [33].

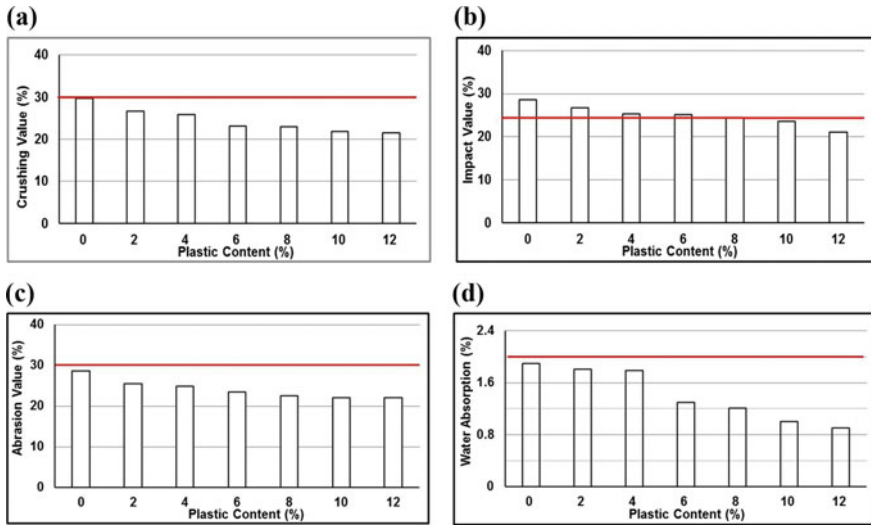


Fig. 2 Test results of a crushing, b impact, c abrasion and d water absorption of control and plastic coated aggregate

Figure 2a shows that there was up to 27% reduction from crushing value of virgin aggregate due to addition of plastic to virgin aggregate. This gain in strength was due to the fact that when the plastic was coated over the aggregate, initially it sticks to the aggregate surface and with the further addition of plastic, aggregate surface was covered with the very thin film of plastic. The molten plastic acted as glue, while the very thin layer of plastic on the surface of aggregate caused a binding effect, which led to better resistance against disintegration. From Fig. 2b, it was observed that toughness of aggregate increased due to the addition of plastic resulting in reduction up to 26.5% as compared to virgin aggregate in impact value. Further, Fig. 2c clearly demonstrates that the resistance to wear and tear also increased due to addition of plastic, which resulted in reduction up to 22.9% with respect to virgin aggregate in abrasion value. The reason behind toughness increment and abrasion reduction was again the glue effect and binding effect of aggregate surface due to plastic coating. There was very significant improvement in water absorption characteristics of aggregate because of addition of plastic as shown in Fig. 2d. Water absorption value decreased up to 52% against water absorption in virgin aggregate due to reduction in the voids and the presence of the air cavities in the aggregates. After analysing the above results, it could be stated that physical and mechanical properties of aggregates improved due to plastic coating. Hence, the aggregate properties improved with the increase in plastic dosages. The summary of optimum binder contents and stability values of all mixtures are shown in Table 4.

After analysing Table 4, it could be stated that PM8 showed lesser OBC requirement as well as more stability than other mixtures. There was no appreciable change in other parameters, and their values were within permissible range as mentioned

Table 4 Optimum binder contents and stability values of all mixtures

Type of mixtures	OBC	Stability
CM	5.1	14.0
PM2	4.6	15.1
PM4	4.5	15.9
PM6	4.5	17.1
PM8	4.5	18.3
PM10	4.6	16.9
PM12	4.5	16.5

in MoRTH: 2013 [33] specification. Therefore, 8% of plastic by weight of asphalt binder (PM8) was selected for performance evaluation in this study.

4 Experimental Investigation

4.1 Retained Stability

Retained Marshall stability is a measure of loss of strength due to the action of water on the mix. This test was carried out on unconditioned and conditioned samples as per STP 204-22 [25]. Unconditioned samples were kept in water bath for 30 min at 60 °C, and conditioned samples were kept in water bath for 24 h at 60 °C before Marshall testing. Retained Marshall stability is the ratio of average value of Marshall stability of conditioned sample to the unconditioned sample as given by Eq. (1). The results of this test are shown in Fig. 3. The red line indicates the limit of retained stability as 75%.

$$\text{Retained Stability (\%)} = \frac{\text{Stability after 24 h in water at } 60\text{ }^\circ\text{C}}{\text{Stability after 30 min in water at } 60\text{ }^\circ\text{C}} \times 100 \quad (1)$$

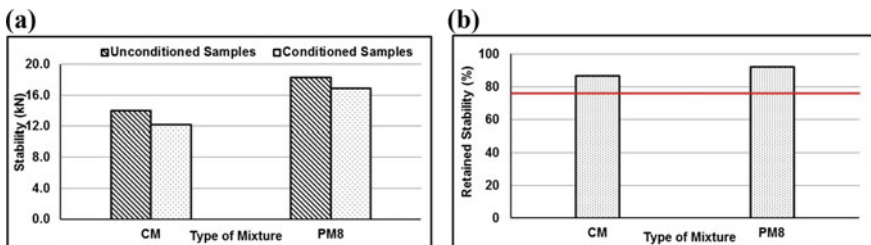


Fig. 3 Test results: **a** stability, and **b** retained stability of conditioned and unconditioned samples of retained marshall stability test

From Fig. 3a, it was stated that the conditioned as well as unconditioned samples of PM8 had higher strength than CM. Per cent stability retained followed the same trend as shown in Fig. 3b; *i.e.* it increased due to plastic modification of mixture. Based on these observations, it could be inferred that the bond between aggregate and binder became stronger with the addition of plastic to the mix.

4.2 Indirect Tensile Strength (ITS)

Moisture damage refers to the loss of strength and durability due to the presence of water in the bituminous mix. The extent or effect of moisture damage is known as moisture susceptibility, which depends on quality and type of materials used in bituminous mix along with other factors. In order to assess the moisture destruction, the current study adopted modified Lottman test, *i.e.* ITS test on conditioned and unconditioned samples. ITS tests were performed as per ASTM D6931 [23] and AASHTO T283 [24]. The dry group samples were tested with no special conditioning, and the wet group samples were tested after conditioning for 24 h at 60 °C. All the specimens were tested at 25 °C after soaking them in water bath at 25 °C for 2 h. Then, a compressive load was applied at a rate of 50 mm/min on a cylindrical specimen of approximately 101.6-mm diameter and 63.5-mm height (Marshall sample) along a vertical diametrical plane. The sample failed by splitting along the same vertical plane. The ITS value was calculated based on Eq. (2).

$$S = \frac{2000 * P}{\pi * D * t} \quad (2)$$

where

- S indirect tensile strength, kPa.
- P maximum load, N.
- t specimen height immediately before test, mm.
- D specimen diameter, mm.

Tensile strength ratio (TSR) was determined by comparing the wet indirect tensile strength (wet ITS) with dry indirect tensile strength (dry ITS) as shown in Eq. (3).

$$\text{TSR}_1 = \frac{\text{ITS wet}}{\text{ITS dry}} \quad (3)$$

where

- ITS dry average indirect tensile strength of dry group of samples, kPa.
- ITS wet average indirect tensile strength of wet group of samples, kPa.

The test results are shown in Fig. 4. The red line indicates the limiting value of TSR as 80% as per MoRTH: 2013 [33].

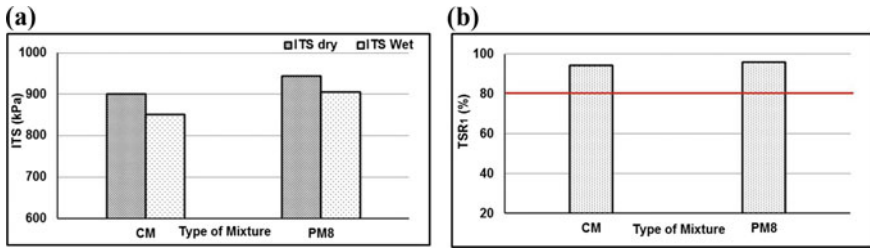


Fig. 4 Test results: **a** indirect tensile strength test (dry and wet) and **b** tensile strength ratio (dry/wet)

It was seen that the conditioned as well as unconditioned samples of PM8 samples had higher tensile strength corresponding to CM from Fig. 4a. The reason behind increase in ITS value due to plastic modification of mix was diffusion of plastic and asphalt binder at interphase, *i.e.* formation of three-dimensional internal cross-linked network structure between polymer molecules and asphalt binder constituents. Even PM samples had higher TSR value as compared to CM samples as shown in Fig. 4b. Therefore, it was understood that resistance to moisture susceptibility increased when plastic was added into the mixture.

Further, to know the effect of freeze–thaw cycle, the samples were tested after freeze cycle for 16 h at $-18 \pm 3 \text{ }^\circ\text{C}$ followed by thaw cycle for 24 h at $60 \text{ }^\circ\text{C}$. All other steps were same except conditioning of sample. TSR was determined by comparing the freeze–thaw indirect tensile strength (freeze–thaw ITS) with dry indirect tensile strength (dry ITS) shown in Eq. (4)

$$TSR_2 = \frac{ITS_{\text{freeze–thaw}}}{ITS_{\text{dry}}} \tag{4}$$

where

- ITS dry average indirect tensile strength of dry group of samples, kPa.
- ITS freeze–thaw average indirect tensile strength of frozen–thawed group of samples, kPa.

The test results are shown in Fig. 5. The red line indicates the limiting value of TSR as 80% which is the criteria or indication of resistance to moisture damage as mentioned in MoRTH: 2013 [33] specification.

ITS (freeze–thaw cycle) followed the same trend as ITS (dry–wet cycle); *i.e.* ITS increased due to plastic modification as shown in Fig. 5a. It is observed from Fig. 5b that CM had higher TSR value under freeze–thaw cycle corresponding to their PM8. So, it could be stated that resistance to moisture susceptibility under freeze–thaw cycle reduced due to addition of plastic to the mixture. The reason behind the change in behaviour of plastic additive might be the destruction of diffused layer of plastic and asphalt binder at extremely low temperature ($T < -16 \text{ }^\circ\text{C}$) for 24 h, which was followed by conditioning at intermediate temperature ($T = 60 \text{ }^\circ\text{C}$). Even PM8 had satisfied the criteria as shown in Fig. 5b.

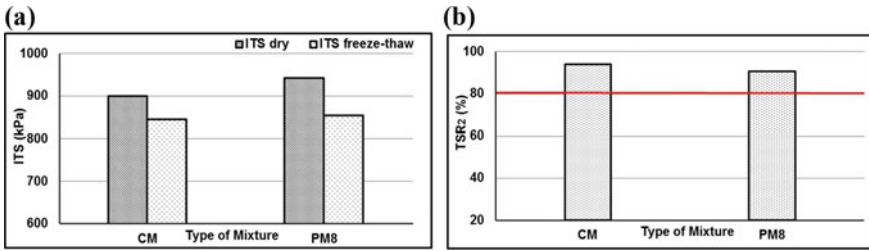


Fig. 5 Test results: **a** indirect tensile strength test (dry and freeze–thaw) and **b** tensile strength ratio (dry/freeze–thaw)

5 Conclusions

This research focused on a laboratory evaluation of the performance of asphalt pavement using waste plastic as an additive. This section summarizes the conclusions achieved through the research findings. The conclusions are presented as follows:

- The physical properties of aggregates improved significantly due to plastic coating. The reason behind this was glue effect, binding effect and very negligible smoothness of aggregate surface.
- Stability (normal as well as retained) increased due to plastic modification of mix. It can be stated that bond between the aggregate and the binder becomes stronger with the addition of plastic to the mix.
- ITS (dry, wet and freeze–thaw) increased due to plastic modification of mix. The reason behind increase in ITS value due to plastic modification of mix was diffusion of plastic and asphalt binder at interphase, *i.e.* formation of three-dimensional internal cross-linked network structure between polymer molecules and asphalt binder constituents. Resistance to moisture susceptibility under dry–wet cycle increases due to addition of plastic to the mix. Resistance to moisture susceptibility under freeze–thaw cycle reduces due to addition of plastic to the mix. The change in behaviour of plastic additive may be due to the destruction of diffused layer of plastic and asphalt binder during conditioning of the sample at extremely low temperature ($T < -16\text{ }^{\circ}\text{C}$) for 24 h followed by intermediate temperature ($T = 60\text{ }^{\circ}\text{C}$) for 24 h.

It was found that plastic not only improved the properties of aggregate but also acted as a secondary binder of mix. The recommended proportion of the plastic dose was 8% by the weight of asphalt binder content in all regions except cold region. During Marshall sample preparation, it was observed that CM samples required around 7–8 min for proper mixing while for PM samples needed about 10–12 min. So, it was recommended to devote little extra time for proper mixing of plastic modified mixtures. Rutting and fatigue analysis and analysis of test section can be carried out for further evaluation of mixes.

References

1. Dalhat MA, Al-Abdul Wahhab HI (2017) Performance of recycled plastic waste modified asphalt binder in Saudi Arabia. *Int J Pavement Eng* 18(4):349–357
2. Sikdar PK, Jain SS, Bose S, Kumar P (1999) Premature cracking of flexible pavements. *J Indian Roads Congr* 60(3):355–398
3. Ahmadinia E, Zargar M, Karim MR, Abdelaziz M, Ahmadinia E (2012) Performance evaluation of utilization of waste Polyethylene Terephthalate (PET) in stone mastic asphalt. *Constr Build Mater* 36:984–989
4. Costa LM, Hugo MR, Silva D, Oliveira JR, Fernandes SR (2013) Incorporation of waste plastic in asphalt binders to improve their performance in the pavement. *Int J Pavement Res Technol* 6(4):457–464
5. Saha Chowdhury P (2016) Use of natural rubber as a base material for flexible pavement—a laboratory study, Masters' Thesis (unpublished), Department of Civil Engineering, National Institute of Technology Agartala
6. Heitzman M (1992) Design and construction of asphalt paving materials with crumb rubber modifier. *Transp Res Rec* 1339
7. Isacson U, Lu X (1995) Testing and appraisal of polymer modified road bitumens—state of the art. *Mater Struct* 28(3):139–159
8. Panda M, Mazumdar M (2002) Utilization of reclaimed polyethylene in bituminous paving mixes. *J Mater Civ Eng* 14(6):527–530
9. Yildirim Y (2007) Polymer modified asphalt binders. *Constr Build Mater* 21(1):66–72
10. Punith VS, Veeraragavan A (2007) Behavior of asphalt concrete mixtures with reclaimed polyethylene as additive. *J Mater Civ Eng* 19(6):500–507
11. Kumar P, Garg R (2011) Rheology of waste plastic fibre-modified bitumen. *Int J Pavement Eng* 12(5):449–459
12. Kumar MV, Muralidharan R, Nair DJ (2013) Comparative study of wet and dry blending of plastic modified bituminous mix used in road pavements. *Indian Highw* 41(12)
13. Rahman WMNWA, Wahab AFA (2013) Green pavement using recycled polyethylene terephthalate (PET) as partial fine aggregate replacement in modified asphalt. *Procedia Eng* 53:124–128
14. Reddy MS, Reddy PS, Subbaiah GV, Subbaiah HV (2014) Effect of plastic pollution on environment. *J Chem Pharm Sci* 28–29
15. <http://pib.nic.in/newsite/PrintRelease.aspx?relid=138144>. Last accessed 18 Mar 2016
16. Silva JDAAE, Rodrigues JKG, de Carvalho MW, Lucena LCDFL, Cavalcante EH (2017) Mechanical performance of asphalt mixtures using polymer-micronized PET-modified binder. *Road Mater Pavement Des* 1–9
17. Moghaddam TB, Soltani M, Karim MR (2014) Evaluation of permanent deformation characteristics of unmodified and Polyethylene Terephthalate modified asphalt mixtures using dynamic creep test. *Mater Des* 53:317–324
18. Jafar JJ (2016) Utilisation of waste plastic in bituminous mix for improved performance of roads. *KSCE J Civ Eng* 20(1):243–249
19. Polacco G, Berlincioni S, Biondi D, Stastna J, Zanzotto L (2005) Asphalt modification with different polyethylene-based polymers. *Eur Polymer J* 41(12):2831–2844
20. Rongali U, Singh G, Chourasiya A, Jain PK (2013) Laboratory investigation on use of fly ash plastic waste composite in bituminous concrete mixtures. *Procedia-Soc Behav Sci* 104:89–98
21. Kumar S (2016) Waste plastic, a gateway to future roads, Masters' Thesis (unpublished), Masters' thesis, Department of Civil Engineering, National Institute of Technology Agartala
22. ASTM D6926 (2016) Standard Practice for Preparation of Asphalt Mixture Specimens Using Marshall Apparatus, ASTM D6926, ASTM International, West Conshohocken, PA
23. ASTM D6931 (2012) Standard test method for indirect tensile (IDT) strength of bituminous mixtures, ASTM D6931, ASTM International, West Conshohocken, PA

24. AASHTO T283 (2014) Standard method of test for resistance of compacted asphalt mixtures to moisture-induced damage, AASHTO T283, American Association of State Highway and Transportation Officials
25. STP 204-22 (1993) Standard test procedures manual-asphalt mixes: retained marshall stability, STP 204-22, Saskatchewan Highways and Transportation, Saskatoon, Canada
26. IS 73 (2013) Paving bitumen—Specification, IS 73, Bureau of Indian Standards, New Delhi
27. IS: 1202 (1978) Methods for testing tar and bituminous materials: determination of specific gravity, IS: 1202, Bureau of Indian Standards, New Delhi
28. IS: 1203 (1978) Methods for testing tar and bituminous materials: determination of penetration, IS: 1203, Bureau of Indian Standards, New Delhi
29. IS: 1205 (1978) Methods for testing tar and bituminous materials: determination of softening point, IS: 1205, Bureau of Indian Standards, New Delhi
30. IS: 1208 (1978) Methods for testing tar and bituminous materials: determination of ductility, IS: 1208, Bureau of Indian Standards, New Delhi
31. ASTM D4402/D4402M (2015) Standard test method for viscosity determination of asphalt at elevated temperatures using a rotational viscometer, ASTM D4402/D4402M, ASTM International, West Conshohocken, PA
32. ASTM D2872 (2012) Standard test method for effect of heat and air on a moving film of Asphalt (rolling thin-film oven test), ASTM D2872, ASTM International, West Conshohocken, PA
33. MoRT&H (2013) Specifications for road and bridge works, Ministry Of Road Transport and Highways, MoRT&H, Fifth Revision, The Indian Roads Congress, New Delhi
34. IS: 2386 (1963) Methods for aggregates of test for concrete-Part I particle size and shape, IS: 2386, Bureau of Indian Standards, New Delhi
35. IS: 2386 (1963) Methods for aggregates of test for concrete-Part IV mechanical properties, IS: 2386, Bureau of Indian Standards, New Delhi
36. IRC: SP: 98 (2013) Guidelines for the use of waste plastic in hot bituminous mixes (dry process) in wearing courses, IRC: SP: 98, Indian Road Congress, New Delhi

Effect of Non-uniform Soil Subgrade on Critical Stresses in Concrete Pavement



Rameshwar J. Vishwakarma and Ramakant K. Ingle

Abstract Rigid pavements are directly supported on foundation soil/sub-base, and hence, it is necessary to prepare uniform subgrade. The calculation of critical stresses given by various guidelines like PCA (1984) and IRC 58 (2015) are based on the assumption of uniform subgrade below the pavement slab. However, practically uniform compaction is hard to achieve in newly constructed roads as compared to old existing roads. Many times, widening of roads is done after few years, and it leads to non-uniformity in stiffness along width. Moreover, stiffness of the soil foundation shows variation along the length of the pavement. Recent guidelines do not suggest any solution for non-uniform stiffness of foundation. The study has been carried out by performing finite element (FE) analysis of slab with non-uniform soil stiffness. Portable falling weight deflectometer is used to study the variation of soil stiffness along the width and length of road. Realistic concrete slab is modeled and performed analysis for axle load, temperature load, and combined effect of axle and temperature to obtain critical stress. Stiffness of the spring is varied along the length as well as the width, and static load response is observed in several FE models. The paper compares various panel results with variation in subgrade stiffness.

Keywords Concrete pavement · Flexural stress · Edge stress · Slab thickness · Radius of relative stiffness · Simplified approach

1 Introduction

Rigid pavements are mostly preferred over flexible pavements due to their long fatigue life, very low maintenance, and good surface. Dekate and Pajgade [1] state that rigid pavements are better alternative to flexible pavement in case of high-density traffic corridors. In India, most of the new constructions are being made using

R. J. Vishwakarma (✉)

Department of Civil Engineering, Bajaj Institute of Technology, Wardha, Maharashtra, India
e-mail: rameshwarjv@gmail.com

R. K. Ingle

Department of Applied Mechanics, Visvesvaraya National Institute of Technology, Nagpur, India
e-mail: rkingle@apm.vnit.ac.in

© Springer Nature Singapore Pte Ltd. 2020

T. V. Mathew et al. (eds.), *Transportation Research*, Lecture Notes in Civil Engineering 45, https://doi.org/10.1007/978-981-32-9042-6_64

805

concrete roads. The thickness of jointed plain concrete pavement (JPCP) is mostly determined from fatigue ratio (ratio of flexural stress to flexural strength). Flexural stress depends on many factors like thickness of concrete slab, loading (axle and temperature), axle load location (edge, interior, or corner), and properties of supporting sub-base. Widely used guidelines suggest different methods or formulas to calculate critical edge stress developed due to application of axle load on concrete slab. There is difference in the obtained response (critical stress) because of different assumptions. Stress calculation as per IRC 58 [2] was given in the form of influence charts and close form equations based on fundamental concept of Westergaard and Picket & Ray's work. These equations predict approximate solution; however, availability of finite element tools has overcome many approximations. IRC 58 [3, 4] had given charts for the estimation of edge stress developed due to combined effect of temperature and axle load (single and tandem axle). These charts were prepared using finite element analysis of single slab panel size (3.5 m × 4.5 m). Portland Cement Association (PCA) [5] provided tables to determine equivalent flexural edge stress developed for axle load (single, tandem and tridem) with and without concrete shoulder. PCA [5] had not considered curling and warping of slab due to temperature variation. It is important to estimate flexural stress developed in pavement from realistic finite element models.

2 Critical Stresses in Concrete Pavement

Critical stress developed in JPCP is primarily due to vehicle and temperature loading. Plain concrete slab is the main structural element that provides bearing capacity to these loads. However, overall response of the concrete pavement depends on many factors like axle and temperature load, slab thickness, soil subgrade modulus, and elastic properties of concrete.

Maximum edge stress developed in the pavement due to vehicle axle load can be determined by using widely used guidelines like Portland Cement Association (PCA) [5], Indian Road Congress (IRC58) [3, 4], American Concrete Institute (ACI) [6], and American association of State Highway and Transportation Officials AASHTO [7].

These guidelines had given either charts or regression equations for the estimation of critical edge stress. Charts or graphs are represented for particular axle loads and modulus of subgrade reaction of foundation below concrete slab. Vishwakarma and Ingle [8] suggested a simple approach of analysis of concrete pavement using radius of relative stiffness (l). Table 1 gives regression equations provided by Vishwakarma and Ingle [8]. These equations can be used to determine critical edge stress developed in the concrete slab without shoulder [9].

$$\text{Maximum flexural tensile stress } S = \text{Stress Coefficient } (C) \times \frac{P}{1000 \times h^2} \quad (1)$$

Table 1 Regression equations to calculate stress coefficient from radius of relative stiffness (l)

Axle type	Stress coefficient (C)
Single	$C = -0.1052 \times l^3 - 0.0805 \times l^2 + 1.2292 \times l - 0.0296$
Tandem	$C = 0.1888 \times l^4 - 0.9629 \times l^3 + 1.5232 \times l^2 - 0.4627 \times l + 0.1828$
Tridem	$C = 0.1735 \times l^5 - 1.0117 \times l^4 + 2.1808 \times l^3 - 2.1755 \times l^2 + 1.1632 \times l - 0.1016$

Stress coefficient in Eq. (1) can be calculated from Table 1. P represents axle load (single, tandem, or tridem), and h represents thickness of concrete slab in Eq. (1).

All these above-mentioned methods have considered uniform subgrade stiffness below concrete slab. However, practically most of the times subgrade does not show uniform subgrade stiffness values below pavement. Variable soil type and its density after compaction may vary the stiffness of the subgrade soil.

Zokaei Ashtiani et al. [10] stated that magnitude of stress and deflection of concrete slab is controlled by the stiffness of underlying compacted subgrade or sub-base foundation. Maitra et al. [11] reported that slab on higher subgrade strength withstands higher peak load as well as higher crack length when compared to weaker subgrade. Support condition affects cracking performance of slab; Roesler et al. [12] conducted accelerated pavement full-scale testing on slab panels on different subgrade. It was observed by Roesler et al. [12] that for thin slab pavements, lower subgrade stiffness leads to large deformations. However, the effect of subgrade stiffness has less influence on the slabs with thicker sections. Delatte [13] stated that concrete pavements distribute loads more widely than asphalt pavements on subgrade foundation and thus the pressures on the subgrade are low. As a result, the bearing capacity of the underlying layers is less critical, and there is no need to use stiff base materials except for pavements which carry heavy loads. Analytically, it is observed that for uniform subgrade with low or high subgrade stiffness has less influence on critical edge stress. Vishwakarma and Ingle [14] reported that most of the concrete pavements are provided with thickness below 350 mm, and response of these pavements is greatly affected by the subgrade strength (K -value) of the soil foundation. Widely used guidelines recommend good and uniform compaction of subgrade. However, practically uniform compaction is hard to achieve. Stiffness of the soil foundation shows variation along length as well as width of the pavement. The study has been carried out by performing FE analysis of slab panels on non-uniform soil foundation. Realistic concrete slabs are modeled, and analysis is performed for axle load, temperature load, and combined effect of axel and temperature to obtain critical response.

3 Study of Variation in Subgrade Strength

Soil below concrete slab shows variation in stiffness. Artificial compaction is always done to achieve uniform compaction. However, 100% uniformity is very difficult to attain due to several reasons. It is therefore required to know the effect of non-uniform

soil stiffness on pavement response. The study has been carried out to determine the effect of non-uniform soil subgrade on critical stresses in concrete pavement. Figure 1 shows testing on soil foundation using portable lightweight deflectometer (LWD).

IRC 58 [4] expresses subgrade strength as a pressure per unit deflection of the foundation. It is determined by using plate load test. Strength of subgrade is also termed as K -value and determined from the pressure sustained at a deflection of 1.25 mm.

It is necessary to determine appropriate value of modulus of subgrade reaction of soil foundation so as to calculate flexural and temperature stresses more correctly. Asli [15] suggested use of portable falling weight deflectometer for the back calculation of elastic modulus of soil subgrade.

Portable lightweight deflectometer is used to determine deflection (δ), dynamic deformation modulus (E_{vd}), and degree of compaction of soil (S/V). Table 2 gives the observed readings from LWD. Ayyanchira [16] had given a relation between E_{vd} and CBR, which is used to determine the stiffness of subgrade. Table 3 represents the approximate relation between E_{vd} and CBR.

To estimate modulus of subgrade reaction for homogeneous soil subgrade from CBR data, IRC 58 [4] had given relation between K -value and CBR as given in Table 4.

IRC 58 [4] recommends frequency of one plate load test per km per lane, but the readings taken on lightweight deflectometer show a large variation of K -value along length as well as width.

Fig. 1 Testing of soil subgrade using lightweight deflectometer



Table 2 Readings observed on the output display of data acquisition system

	Chainage	Inner edge			Center			Outer/critical edge		
Deflection δ (mm)	8820 m	0.678	0.643	0.585						
Avg. δ (mm)			0.635							
S/V			3.172							
E_{vd} (MIN/m ²)			35.43							
Deflection δ (mm)	8830 m				0.456	0.418	0.408			
Avg. δ (mm)						0.427				
S/V						3.041				
E_{vd} (MIN/m ²)						52.69				
Deflection δ (mm)	8840 m	1.136	0.449	0.368				0.022	1.01	1.011
Avg. δ (mm)			0.651						0.681	
S/V			2.826						3.826	
E_{vd} (MIN/m ²)			34.56						33.04	
Deflection δ (mm)	8850 m				0.779	0.529	0.467			
Avg. δ (mm)						0.592				
S/V						2.913				
E_{vd} (MIN/m ²)						38.01				
Deflection δ (mm)	8860 m	0.297	0.259	0.24				0.963	0.9	0.924
Avg. δ (mm)			0.265						0.929	
S/V			2.392						3.77	
E_{vd} (MIN/m ²)			84.91						24.22	

Table 3 Relation between E_{vd} and CBR

E_{vd} (MN/m ²)	CBR %	E_{vd} (MN/m ²)	CBR %
5	2	55	34
10	4	60	37
15	6	65	42
20	10	70	46
25	13	75	50
30	17	80	55
35	19	85	60
40	23	90	65
45	25	95	70
50	30	100	80

Table 4 Relationship between K -value and CBR value for soil subgrade

Soaked CBR %	2	3	4	5	7	10	15	20	50	100
K -value (MPa/m)	21	28	35	42	48	55	62	69	140	220

4 Validation of FE Model

Finite element is powerful and versatile method used to analyze structure with complex geometry as well as loading configurations. Concrete pavements are simple slab structures with complex joint condition and loading configurations. There are many types of FE software available which can be used to analyze pavement slab for axle load and temperature load. However, SAP2000 is used for carrying out this study.

Comprehensive 3D models are prepared in SAP2000 by using shell as well as solid element as shown in Fig. 2 [8, 9], and finite element analysis is carried out for static axle loads first. Single axle load of 80 kN (18 kip) and tandem axle load of 160 kN (36 kip) are applied on mathematical model. Realistic FE model without concrete shoulder is prepared as per PCA document. Analysis results obtained from SAP2000 are compared with the results obtained from simplified approach by Vishwakarma and Ingle [8]. Model prepared is having slab length 4.572 m (180 in.), slab width 3.666 m (144 in.), slab modulus of elasticity 27,579 MPa (4 Mpsi), Poisson's ratio 0.15, constant wheel contact area $0.178 \times 0.254 \text{ m}^2$ ($7 \times 10 \text{ in.}^2$), wheel spacing 0.305 m (12 in.), axle spacing 1.273 m (50 in.), axle width 1.833 m (72 in.), and constant modulus of subgrade reaction 979.64 MPa/m. Soil stiffness is assigned as a spring below concrete slab at each node. Table 5 gives that the results obtained from FE analysis are in good agreement with simplified approach.

Same model is also validated for the edge stress developed due to temperature only loading. The results obtained from FE analysis are also compared with the method suggested by IRC 58 [2], *i.e.*, using Bradbury's warping stress coefficients for thermal stress computations. The comparison is given in Table 6.

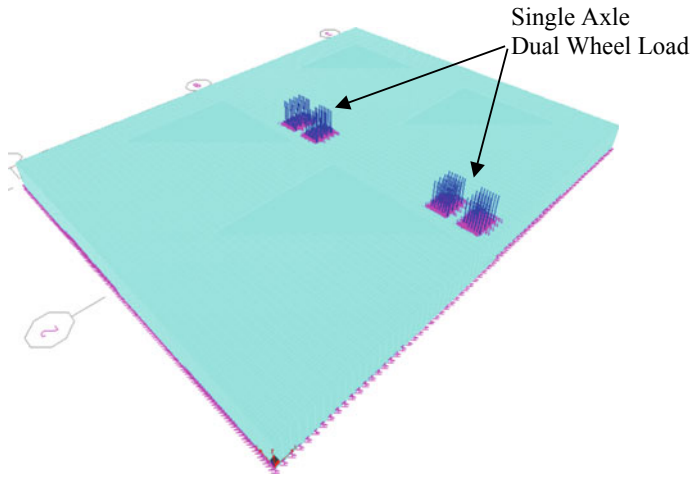


Fig. 2 Finite element model showing axle load placed at edge of slab

Table 5 Validation of the mathematical model

Axle type	Load (kN)	Thickness h (mm)	Stress S (MPa)		% difference
			FE analysis	Simplified approach	
Single	80	150	1.17	1.17	-0.1
Tandem	160		1.09	1.09	-0.1
Tridem	240		1.10	1.10	0.4

Temperature differential between the top and bottom of concrete pavement creates the slab to curl resulting in stresses. Maximum temperature difference is affected by geographical locations. IRC 58 [4] recommended maximum temperature differentials for concrete slabs according to the slab thickness. Temperature differences in India in some regions are very high, and hence, IRC 58 [4] guideline considers top-down and bottom-up cracking conditions while determining the pavement thickness. Flexural stresses for bottom-up cracking have been computed for nonlinear positive temperature difference; however, stresses for top-down cracking were computed for axle loads with linear negative temperature differential in the slab in nighttime.

In concrete pavement, critical stresses are developed due to the combined effect of wheel load and temperature differential leading to the initiation of cracks; these cracks propagate through the pavement which leads to the failure of slab. According to Maitra et al. [17], the pavement slab tries to bend due to the temperature variation along the depth, but it is arrested due to its self-weight which develops the curling stresses in the pavement. IRC 58 [2] follows Bradbury’s solutions for the calculations of curling stresses. This approach assumes the linear variation of temperature along the depth of the pavement, but actually, the temperature variation is nonlinear.

Table 6 Comparison of stresses in the slab panel for temperature loading

Temperature (°C)	Thickness h (mm)	Stress (MPa)							
		Interior		Long edge		Short edge		Corner	
		FE analysis	IRC 58-2002	FE analysis	IRC 58-2002	FE analysis	IRC 58-2002	FE analysis	IRC 58-2002
17.3	150	3.02	2.92	2.50	2.47	2.60	2.58	0.05	1.14
21	300	3.29	3.32	2.96	2.90	2.36	2.31	0.04	1.07

Slab size and other properties are considered as per PCA [5] for modeling concrete slab. Table 5 gives the results obtained for 150- and 300-mm-thick slab. Stresses are computed at interior, edge, and corner of the slab. The results computed using IRC 58 [2] and FE analysis are in good agreement for interior and edge locations. To study the effect of temperature and axle loading on non-uniform soil, FE models were prepared and analyzed.

5 Effect of Uniform and Non-uniform Subgrade

The analysis of pavement slab is done considering uniform as well as non-uniform soil stiffness. Table 7 gives the variation of critical edge stress developed in the panel for uniform subgrade stiffness for axle load only. Single, tandem, and tridem axle load is applied considering dual wheel for each axle. Soil stiffness is applied in the form of linear spring with stiffness only in vertical (normal to slab area) direction. Stiffness of the spring is calculated according to the mesh area of the slab.

Table 7 gives that with the increase in modulus of subgrade reaction, critical edge stress reduces. In this case, only axle load is considered and there is no temperature load. To model non-uniform subgrade, spring stiffness is varied along width in four layers. Different subgrade stiffness is assigned to the four equal layers as given in Table 8. In each layer, spring stiffness is uniform through layer.

Table 7 Critical edge stress (MPa) for different subgrade stiffness below slab

Axle type	Load (kN)	Thickness <i>h</i> (mm)	Modulus of subgrade reaction <i>K</i> (MPa/m)			
			40	80	150	300
Single	80	100	4.34	3.70	3.17	2.64
Tandem	160		3.54	3.11	2.80	2.47
Tridem	240		3.59	3.21	2.86	2.48
Single	80	150	2.54	2.16	1.88	1.60
Tandem	160		2.12	1.77	1.54	1.35
Tridem	240		1.90	1.72	1.57	1.39
Single	80	300	0.98	0.87	0.75	0.64
Tandem	160		0.93	0.79	0.66	0.54
Tridem	240		0.67	0.58	0.53	0.48

Table 8 Variation of subgrade stiffness along width from 150 to 300 MPa/m

Width inch (m)	0–36 (0–0.91)	36–72 (0.91–1.83)	72–108 (1.83–2.74)	108–144 (2.74–3.66)
<i>K</i> (MPa/m)	150	200	250	300

Edge stress from Table 9 for non-uniform subgrade stiffness is close to the stresses for the uniform subgrade stiffness 150 MPa/m from Table 7. If the stiffness of soil spring is assigned as per Table 10, the results are close to the stresses obtained for 300 MPa/m uniform subgrade stiffness from Table 7 and given in Table 11.

Higher subgrade strength is critical when temperature only load is considered. Table 12 gives edge stress in concrete slab for different load cases and combinations for uniform modulus of subgrade reaction 300 MPa/m. However, Table 13 represents same loading and load combinations with non-uniform soil subgrade. Variation of soil stiffness along width (K) ranges from 150 to 300 MPa/m).

Table 9 Critical edge stress for non-uniform soil stiffness along width from 150 to 300 MPa/m

Axle type	Load (kN)	Thickness h (mm)	Edge stress (MPa)
Single	80	100	3.17
Tandem	160		2.80
Tridem	240		2.86
Single	80	150	1.88
Tandem	160		1.54
Tridem	240		1.56
Single	80	300	0.74
Tandem	160		0.64
Tridem	240		0.52

Table 10 Variation of subgrade stiffness along width from 300 to 150 MPa/m

Width inch (m)	0–36 (0–0.91)	36–72 (0.91–1.83)	72–108 (1.83–2.74)	108–144 (2.74–3.66)
K (MPa/m)	300	250	200	150

Table 11 Critical edge stress obtained for non-uniform soil stiffness along width from 300 to 150 MPa/m

Axle type	Load (kN)	Thickness h (mm)	Edge stress (MPa)
Single	80	100	2.64
Tandem	160		2.47
Tridem	240		2.48
Single	80	150	1.60
Tandem	160		1.35
Tridem	240		1.40
Single	80	300	0.64
Tandem	160		0.54
Tridem	240		0.52

Table 12 Stresses in concrete slab for uniform modulus of subgrade reaction 300 MPa/m

Load type	K (MPa/m)	Thickness h (mm)	Stress at edge (MPa)
Single Axle	300	150	1.60
Tandem Axle			1.35
Tridem Axle			1.39
Temperature 17.3 °C		150	2.50
Single Axle + 17.3 °C		150	4.00
Tandem Axle + 17.3 °C			1.93
Tridem Axle + 17.3 °C			3.45

Table 13 Stresses in concrete slab for non-uniform modulus of subgrade reaction along width

Load type	K (MPa/m)	Thickness h (mm)	Stress at edge (MPa)
Single Axle	150–300	150	1.87
Tandem Axle			1.54
Tridem Axle			1.56
Temperature 17.3 °C		150	2.57
Single + 17.3 °C		150	4.38
Tandem + 17.3 °C			2.15
Tridem + 17.3 °C			3.58
Single Axle	300–150	150	1.60
Tandem Axle			1.35
Tridem Axle			1.40
Temperature 17.3 °C		150	2.50
Single + 17.3 °C		150	4.00
Tandem + 17.3 °C			1.93
Tridem + 17.3 °C			3.45

Uniform subgrade stiffness of 300 MPa/m is considered, and different loading and load combinations are considered. These results from Table 12 are compared with the results for non-uniform soil subgrade having similar loads and load combinations (Table 13).

Higher modulus of subgrade reaction with uniform stiffness below slab increases thermal stresses in the slab as it increases the restraint. However, from Tables 12 and 13, it can be seen that if the modulus of subgrade reaction is less but non-uniform, it may develop more stresses than the stress for highest uniform stiffness from non-uniform stiffness considered. Maximum stress obtained from Table 12 is 4.00 MPa with soil stiffness 300 MPa/m, while maximum for non-uniform stiffness (150–300 MPa/m) from Table 13 is 4.38 MPa.

6 Observations and Conclusions

Following are the significant observations and conclusions made from the study of effect of non-uniform soil subgrade on critical stresses in concrete pavement.

- Stresses in non-uniform subgrade are governed by the soil stiffness at the edge layer when only axle load is considered. It is recommended to do *K*-value test at the edge, when axle loads are only considered.
- Lower subgrade stiffness can be considered while analyzing for non-uniform subgrade, and it gives critical results for axle load only.
- When temperature loads are also included in the design of pavement, the analysis should be done by modeling non-uniform subgrade. Higher or lower uniform subgrade results in the underestimation of critical stresses.
- Guidelines are silent about the analysis of concrete pavement on non-uniform soil subgrade, and there is no solid method available. It is recommended to do FE analysis for such cases.

References

1. Dekate MN, Pajgade PS (2016) Bituminous versus cement concrete roads. *Indian Concr Inst* 17(2):38–41
2. IRC (2002) Guidelines for the design of plain jointed rigid pavements for highways. IRC 58, 2nd revision, Indian Road Congress, New Delhi, India
3. IRC (2011) Guidelines for the design of plain jointed rigid pavements for highways. IRC 58, 3rd revision, Indian Road Congress, New Delhi, India
4. IRC (2015) Guidelines for the design of plain jointed rigid pavements for highways. IRC 58, 4th revision, Indian Road Congress, New Delhi, India
5. PCA (1984) Thickness design for concrete highway and street pavements. PCA manual, Portland Cement Association, Skokie, Illinois
6. ACI 325.12R-02 (2002) ACI Committee 325. Guide for design of jointed concrete pavements for streets and local roads, ACI 325.12R-02, American concrete institute, Detroit, MI

7. AASHTO (1993) AASHTO guide for design of pavement structures, vol 1. American Association of State Highway & Transportation Officials
8. Vishwakarma RJ, Ingle RK (2017) Simplified approach for the evaluation of critical stresses in concrete pavement. *Struct Eng Mech* 61(3):389–396
9. Vishwakarma RJ, Ingle RK (2018) Effect of panel size and radius of relative stiffness on critical stresses in concrete pavement. *Arab J Sci Eng* 43(10):5677–5687
10. Zokaei-Ashtiani A, Tirado C, Carrasco C, Nazarian S (2015) Impact of different approaches to modelling rigid pavement base layers on slab curling stresses. *Int J Pavement Eng* 17(10):861–869
11. Maitra SR, Reddy KS, Ramachandra LS (2014) Numerical investigation of fatigue characteristics of concrete pavement. *Int J Fract* 189(2):181–193
12. Roesler JR, Cervantes VG, Amirkhanian AN (2012) Accelerated performance testing of concrete pavement with short slabs. *Int J Pavement Eng* 13(6):494–507
13. Delatte NJ (2014) Concrete pavement design, construction, and performance, 2nd edn. CRC Press, Taylor and Francis group
14. Vishwakarma RJ, Ingle RK (2017) Evaluation of subgrade strength of soil below concrete pavement using non-destructive method. In: Conference on numerical modeling in geomechanics. CoNMiG-2017, Roorkee, pp 21–26
15. Asli C, Feng ZQ, Porcher G, Rincen JJ (2012) Back-calculation of elastic modulus of soil and subgrade from portable falling weight deflectometer measurements. *Eng Struct* 34:1–7
16. Ayyanchira MM (2014) Introduction of light weight deflectometer. *Int J Eng Res Technol* 3(4):303–305
17. Maitra SR, Reddy KS, Ramachandra LS (2013) Estimation of critical stress in jointed concrete pavement. *Procedia Soc Behav Sci* 104:208–217

Comparative Study on Rheological Properties of Coir Fiber and Coir Powder Modified Bitumen



T. Sreelatha, Bino I. Koshy and Jithin Kurian Andrews

Abstract Rheology is a fundamental interdisciplinary science which deals with the study of the internal response of materials by the application of stresses. Bitumen rheology can be defined as the fundamental measurements associated with the flow and deformation characteristics of bitumen. The modified bitumen or asphalt reduces the amount and severity of pavement distresses and at the same time increases the service life of the pavement. The significance of this study is that the modifier used for binder modification is coir powder of size less than $75\ \mu$ and coir fiber of length 5 mm. Coir powder is used as a modifier because coir fiber takes advantage of a waste by-product, at the same time reducing environmental pollution. In this study, an attempt has been made to compare the rheological properties of coir fiber and coir powder modified VG30 bitumen. Here the coir powder and fiber in varying percentages of 0.4, 0.6, 0.8, 1 and 1.2% were mixed uniformly with VG30 bitumen. The bitumen–coir powder blend is prepared by mixing the two materials in a bitumen blending oven at 200 rpm, for a period of 30 min, and at a temperature of 145 °C. The mixing temperature is determined as per one of the methods suggested by Asphalt Pavement Environmental Council EC 101(2000), an industry guidance document. Based on EC 101(2000), the mixing temperature obtained is 145 °C. For determining the rutting susceptibility, the range of temperature variation corresponding to IS 15462:2004 was selected keeping angular frequency 10 rad/s and shear strain 10% constant. As per SHRP, when the value of $G^*/\sin\delta < 1$, the pavement become susceptible to rutting failure. The results showed that the coir powder modified bitumen can withstand a higher temperature than fiber modified bitumen. The coir powder modified bitumen showed better rheological properties through an increase in complex modulus value and decrease in phase angle value.

T. Sreelatha (✉) · B. I. Koshy (✉)
Civil Engineering, Rajiv Gandhi Institute of Technology, Kottayam, Kerala, India
e-mail: sreelatha@rit.ac.in

B. I. Koshy
e-mail: bino@rit.ac.in

J. K. Andrews (✉)
Civil Engineering, Saintgits College of Engineering, Kottayam, Kerala, India
e-mail: jithin2.kurian@gmail.com

Keywords Rheology · Bitumen · Coir powder · Rutting · Complex modulus · Phase angle

1 Introduction

Bituminous binders are predominantly used in surfacing the vast network of roads in India. In recent years, the increase in traffic loads and adverse climatic conditions created a situation for which modified binders with enhanced performance are needed [1]. Bitumen is a viscoelastic material, and the mechanical behavior depends on both temperature and loading time. At low temperature and short loading times, they behave as elastic solid and high temperatures and long times of loading they behave as viscous liquids [2]. The Strategic Highway Research Program (SHRP) developed the new specification for the rheological characterization of binders.

Considering the complexity of bitumen [3] and wide range of existing modifiers, the optimal condition of temperature, speed, and mixing time need to be determined in the laboratory to obtain a homogeneous binder for easy laying with high resistance of cracking and rutting. The concept of mixing fibers to improve the behavior of bitumen is not new. Natural fibers as a modifier in bituminous mixes have become a research focus for scientists and engineers.

By adding modifiers in bitumen, there is a reduction in the deformation produced by a given load and is shown by an increase in softening point, reduction in penetration, and increase in stiffness. This can reduce cost and improve the mechanical properties of the composite material [4]. The study focused on to evaluate the feasibility of using coir fiber, the agricultural waste in asphalt binder as an additive to reduce cost and improve the mechanical property of binder through which the service life of pavements has been extended.

In addition to that, there must exist a balance between disposal of waste material like coir fiber and at the same time incorporation of that material into the modification of bitumen. NCHRP report 648 [5] offered two methods for assessing the mixing and compaction temperature for modified binders. The first method is phase angle method, in which the mixing and compaction temperature are determined by constructing phase angle master curves at 80 °C. The second method is steady-shear viscosity method. Dynamic shear rheometer [6] is used for finding the viscosity at a shear stress of 500 Pa at different temperatures. But NCHRP-648 [5] recommended that mixing and compaction temperature determined by these methods should not be used to control plant production or pavement construction temperature. The paper describes and presents the results of laboratory investigations to assess the influence of coir powder and fiber on the rheological properties of the modified asphalt binder.



Fig. 1 Materials used **a** Coir powder **b** Coir fiber **c** Bitumen

2 Objective

The objective of this study is to compare the rheological properties of coir powder and coir fiber modified bitumen and corresponding variation in rutting resistance and in phase angle with temperature and the amount of additive used.

3 Materials and Methods

Materials used for the study is shown in Fig. 1. The binder used for the study was VG30 bitumen procured from Bharat Petroleum Corporation Limited (BPCL, Cochin). Fiber size affects the ease of mixing between asphalt and fiber. Smaller the fiber, easier the mixing process. The coir fibers of length 5 mm with differing percentages of 0.4, 0.6, 0.8, 1, and 1.2% were mixed with VG30 bitumen at a temperature of 145 °C by stirring for 30 min in bitumen blending oven at 200 rpm (Fig. 2a). Same percentage and mixing procedure were adopted for coir powder modified bitumen. Binder testing was carried out in dynamic shear rheometer (DSR) with temperature sweep of 35–85 °C and frequency sweep of 0.1–100 rad/s.

4 Results and Discussion

4.1 *Rheological Properties of Modified Binders*

Study about asphalt rheology helps in characterizing and quantifying the material properties through complex modulus and phase angle which determine the viscoelastic response of asphalt material, which is temperature susceptible. At low temperature, it shows elastic solid behavior and at high temperature behaves like a viscous liquid. DSR test is used to characterize the viscoelastic behavior of asphalt binders

at medium-to-high temperature. In this test, shearing action is created by placing the thin sample of asphalt between two circular plates of DSR (Fig. 2b).

The lower plate is fixed and upper plate oscillates back and forth across the sample at 10 rad/s of oscillation rate which simulates the shearing action corresponding to a traffic speed of 90 km/h. The complex shear modulus measures the materials overall resistance to deformation when repeatedly sheared and phase angle represents the elastic response or viscous response of the material under loading condition. If the phase angle ‘ δ ’ of the material becomes 90° , it is purely viscous, and if ‘ δ ’ is 0° , the material shows elastic solid properties. Table 1 shows the test results for complex modulus and phase angle values for different percentages of coir powder. Figures 3 and 4 illustrate the complex modulus and phase angle for different percentages of coir powder content. The coir powder modified bitumen exhibited slightly higher complex modulus throughout the temperature range compared to the original binder. The higher complex modulus indicated that binder strength has increased which can be correlated with higher rutting resistance. Higher values of phase angle indicate more viscous like behavior, while lower value indicates the elastic nature of the asphalt. In this study for different percentage of coir powder, 0.6% showed a lower phase angle value that indicates more elastic nature of the modified binder. Higher value

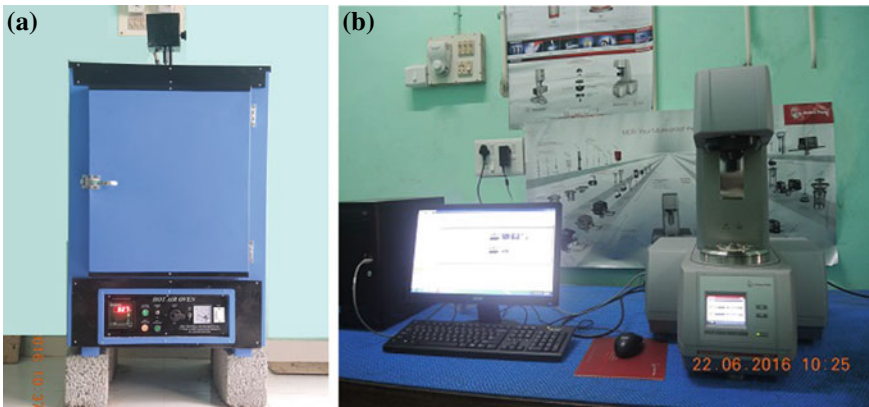


Fig. 2 Equipments used **a** Blending oven **b** Dyanamic Shear Rheometer (DSR)

Table 1 Variation of complex modulus and phase angle with different % coir powder modified binder

% binder	Phase angle (δ)	Complex modulus (G^*)
0	87.52375	5369.958
0.4	87.481	5436.536
0.6	86.72188	6653.669
0.8	87.17188	6023.848
1	87.0875	6069.494
1.2	86.7325	5834.217

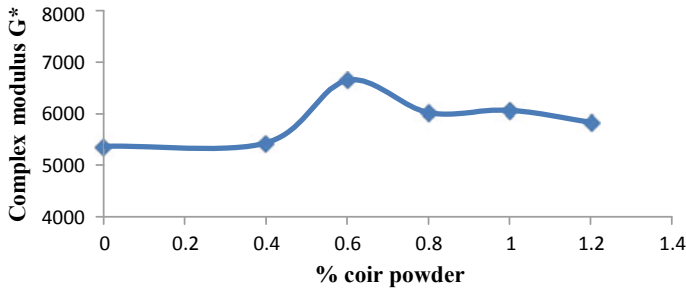


Fig. 3 Variation of complex modulus with % coir powder

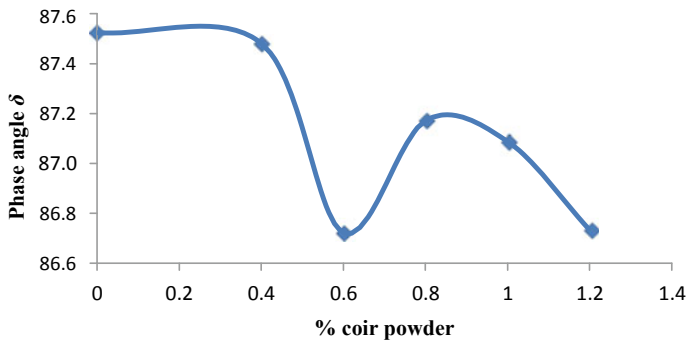


Fig. 4 Variation of phase angle with % coir powder

of complex modulus and lower value of phase angle are desirable for rut resistance. In addition to that, 0.6% coir powder modified bitumen showed better conventional rheological properties and volumetric properties. Hence, 0.6% was taken as optimum among other percentages of coir powder mentioned earlier in the study. As per Indian specification (IS: 15462:2004), the complex modulus is determined at 10 rad/s with a temperature variation which is from 35–85 °C.

Figure 4 shows that the phase angle for modified bitumen goes on decreasing compared to virgin bitumen as temperature increases. The reason is that the binder totally loses its elasticity (phase angle equal to 90°) and it becomes purely viscous.

Temperature sweep test is an oscillatory test for determining the rutting susceptibility of pavement. Temperature is varied from 35 to 85 °C, keeping angular frequency 10 rad/s and shear strain 10% constant. The temperature variation of 35–85 °C is taken because as per IS 15462:2004, and this particular temperature is suggested as the range for pavement temperature. According to SHRP when the value of $G^*/\sin\delta$, an indicator of binder stiffness to deformation at a specified temperature and load attains a value of 1, the pavement becomes susceptible to rutting failure. The temperature which corresponds to the $G^*/\sin\delta$ is equal to 1 kPa for 0, 0.4, 0.6, 0.8, 1, and 1.2% of coir powder and coir fiber are mentioned in Tables 2 and 3. Figure 5 gives

Table 2 Temperature sweep data for $G^*/\sin\delta$ for coir powder modified bitumen

Virgin		0.40%		0.60%		0.80%		1.00%		1.20%	
Temp.	$G^*/\sin\delta$	Temp.	$G^*/\sin\delta$	Temp.	$G^*/\sin\delta$	Temp.	$G^*/\sin\delta$	Temp.	$G^*/\sin\delta$	Temp.	$G^*/\sin\delta$
70.31	1.344	73.63	1.1856	76.08	1.147	75.37	1.0721	73.65	1.0907	73.76	1.0155
73.76	0.96149	75.37	0.98748	77.87	0.95819	77.10	0.89478	75.39	0.90043	74.04	0.93521

Table 3 Temperature sweep data for $G^*/\sin\delta$ for coir fiber modified bitumen

Virgin		0.40%		0.60%		0.80%		1.00%		1.20%	
Temp.	$G^*/\sin\delta$	Temp.	$C^*/\sin\delta$	Temp.	$C^*/\sin\delta$	Temp.	$C^*/\sin\delta$	Temp.	$G^*/\sin\delta$	Temp.	$G^*/\sin\delta$
70.31	1.344	74.24	1.0367	74.31	1.1819	73.64	1.1469	72.42	1.1409	70.46	1.0424
73.76	0.96149	76.00	0.88586	76.13	0.9841	75.39	0.94853	74.76	0.90836	73.78	0.9673

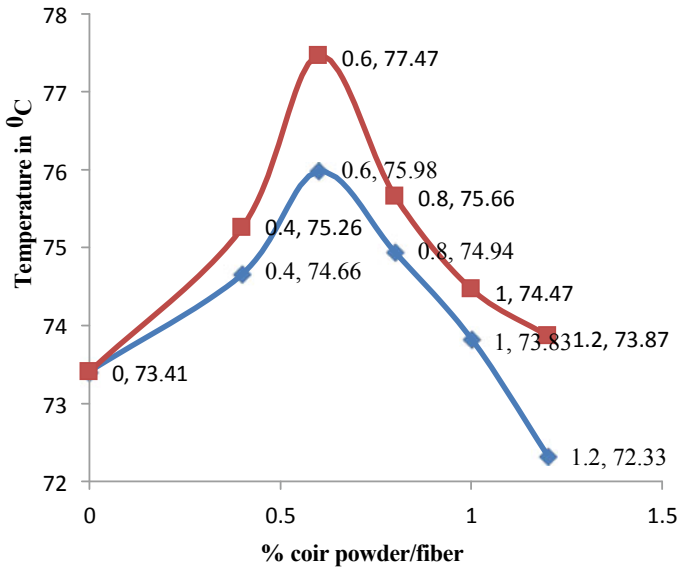


Fig. 5 Temperature at which $G^*/\sin\delta$ value approaches 1.0 kPa for varying % of coir fiber and coir powder

the temperature at which $G^*/\sin\delta = 1$ kPa, for varying percentages of coir powder and coir fiber content. From the graph, it is evident that the coir powder modified bitumen can withstand a higher temperature than coir fiber modified bitumen. From Table 2, it is evident that 0.6% coir powder modified bitumen possesses resistance to rutting up to temperature of 77.47 °C which is higher than for rest of the percentages of modified bitumen. From Table 3, the coir fiber modified bitumen can withstand only up to a temperature of 75.98 °C for 0.6% fiber modified bitumen.

From the two results, it is seen that the coir powder modified bitumen can withstand a higher temperature than coir fiber modified bitumen and neat bitumen which has temperature susceptibility of 73.41 °C. From the result, it is evident that coir powder modified bitumen can withstand a higher temperature compared to coir fiber modified bitumen and virgin bitumen.

The time-dependent behavior of a sample in the non-destructive deformation range can be determined through a frequency sweep test. High frequencies are used to simulate fast motion on a short timescale, while low frequencies simulate slow motion on a long timescale or at rest. In 2000, Asphalt Pavement Environmental Council published an industry guidance document EC 101 (2000), in which mixing temperature was determined by keeping temperature 80 °C, shear strain 10% constant and angular frequency varied from 0.1 to 100 rad/s. Since 0.6% coir powder modified bitumen showed better results compared to other percentages, frequency sweep data for 0.6% coir powder modified bitumen is taken for further analysis of ω for getting mixing temperature.

Table 4 Frequency sweep for 0.6% coir powder modified bitumen for 86° phase angle

Point No.	Angular frequency	Shear strain	Temperature	Phase shift angle	$G^*/\sin\delta$
	(rad/s)	(%)	(°C)	(δ°)	(kPa)
1	62.1	10	80	86.06	2.2299
2	65.6	10	80	85.91	2.3388

Under the above-mentioned conditions, the phase angle varied from 88.93° to 84.46° in decreasing order. For an angular frequency of 65.6 rad/s, there is a shift in phase angle value from 86.06° to 85.91°. From the frequency sweep test data given in Table 4, angular frequency, ω , is taken as 63.5 rad/s corresponding to 86° phase angle, which will decide the mixing temperature.

$$\text{Mixing temperature} = 310 \times \omega - 0.135 \text{ } ^\circ\text{F}$$

where ω is the angular frequency corresponding to 86° phase angle Mixing temperature = $310 \times \omega^{-0.135 \text{ } ^\circ\text{K}} = 310 \times 63.5^{-0.135 \text{ } ^\circ\text{K}} = 293 \text{ } ^\circ\text{F} = 145 \text{ } ^\circ\text{C}$

5 Conclusion

Results showed an improvement in viscoelastic properties for coir powder modified bitumen compared to coir fiber modified bitumen. The temperature corresponds to the rutting resistance of coir powder modified bitumen evaluated through $G^*/\sin\delta$ value showed an improvement in the same value compared to fiber modified bitumen. 0.6% coir powder modified bitumen possesses resistance to rutting up to temperature of 77.47 °C which is higher than for the rest of the percentages of coir powder modified bitumen. Maximum rutting resistance of bitumen is obtained for 0.6% coir powder modified bitumen, which is about 5.5% more as compared to unmodified bitumen. The coir fiber modified bitumen can withstand only up to a temperature of 75.98 °C for 0.6% fiber. From the frequency sweep test data, the mixing temperature has been obtained as 145 °C. The increase in complex modulus and decrease in phase angle for coir powder modified bitumen indicate an increase in stiffness, and consequently, there exists an increase in resistance to permanent deformation. From the results, it is evident that 0.6% coir powder modified bitumen shows better rheological properties compared to coir fiber modified bitumen. Coir powder modified bitumen can withstand a higher temperature than fiber modified bitumen and virgin bitumen.

References

1. Kandhal PS, Dhir MP (2011) Use of modified bituminous binders in India, Current imperatives. Indian Road Congr 72
2. Barnes HA, Hutton JF, Walters K (1989) An introduction to rheology. Elsevier Science Publishers B.V., Amsterdam
3. Lesueur D (2009) The colloidal structure of bitumen: consequences on the rheology and on the mechanism of bitumen modification. J Colloid Interface Sci 145
4. Putman BJ, Amirhanian SN (2004) Utilization of waste fibers in stone matrix asphalt mixtures. J Res Conserv Recycl 42
5. NCHRP-648 (2009) Mixing and compaction temperature of asphalt binders in Hot mix asphalt. Transportation Research Board, National Academies Press
6. ASTM D7175-15 Standard test method for determining the rheological properties of asphalt binder using dynamic shear rheometer

Calibration of M-E PDG Rutting Model for Indian Conditions



Bhanoj Dokku and J. Murali Krishnan

Abstract Within the context of the mechanistic-empirical pavement design guide, the rut depth transfer function used consists of local calibration and material-specific coefficients. The material-specific coefficients ensure that the material-specific creep and recovery data can be used within the context of simulation for quantification of rutting. In this work, material-specific coefficients of the mix with VG30 binder were developed using repeated creep and recovery test conducted at three different temperatures and for two different confinement conditions. The axle load and traffic data from ten national highways across India were chosen, and simulations were carried out for these highways. The results from M-E PDG simulations were analyzed, and the design life in terms of rutting was estimated. In addition, the adequacy of the pavement sections provided based on Indian pavement design code for a target rut depth was investigated.

Keywords Rutting · Mechanistic-empirical method · Traffic · Axle load · Calibration · Permanent deformation

1 Introduction

Rutting in the asphalt pavement is considered as a combination of two mechanisms, and they are densification and shear flow. Densification usually occurs in the early stages of pavement life due to volumetric changes in the mixture. Shear flow, however, starts when the aggregate structure of the mixture cannot withstand traffic loads, especially near high temperatures at which the stiffness of asphalt concrete mixtures drastically changes. In a pavement usually, shear flow causes more rutting when compared to densification [1]. While it is understood that the relative properties of the constituents of the material play a critical role in alleviating the rutting in bituminous

B. Dokku

Cube Highways and Transportation Assets Advisors (P) Limited, Noida, India
e-mail: Dokku.bhanoj@cubehighways.com

J. M. Krishnan (✉)

Department of Civil Engineering, IIT Madras, Madras, India
e-mail: jmk@iitm.ac.in

© Springer Nature Singapore Pte Ltd. 2020

T. V. Mathew et al. (eds.), *Transportation Research*, Lecture Notes
in Civil Engineering 45, https://doi.org/10.1007/978-981-32-9042-6_66

layers, the quantification of the same requires extensive laboratory experiments and structural simulations.

NCHRP [2] suggested that the permanent deformation test in the laboratory can be used to simulate rutting in the pavement. Here, the total rutting in the pavement is expressed as the sum of incremental permanent deformation in all the pavement layers and it is assumed to have the following power law form (Eq. 1).

$$\frac{\varepsilon_p}{\varepsilon_r} = a \times T^b \times N^c, \quad (1)$$

where ε_p —accumulated permanent strain in the pavement layers, ε_r —the resilient or elastic strain in the pavement layers, N —the number of axle load repetitions, T —mix or pavement temperature and a , b , c are regression constants.

The current M-E PDG field calibrated form of the laboratory-derived relationship from repeated load permanent deformation tests is given in Eq. (2).

$$\Delta_{p(\text{HMA})} = \varepsilon_{p(\text{HMA})} h_{\text{HMA}} = \beta_{1r} k_z \varepsilon_{r(\text{HMA})} 10^{k_{1r}} N^{k_{2r} \beta_{2r}} T^{k_{3r} \beta_{3r}}, \quad (2)$$

where $\Delta_{p(\text{HMA})}$ —accumulated permanent deformation in the Hot Mix Asphalt (HMA) layer/sublayer, in., $\varepsilon_{p(\text{HMA})}$ —accumulated permanent strain in the HMA layer/sublayer, $\varepsilon_{r(\text{HMA})}$ —the resilient or elastic strain calculated by the structural response model at the mid-depth of each HMA sublayer, in./in., h_{HMA} —the thickness of the HMA layer/sublayer, in., N —number of axle load repetitions, T —mix or pavement temperature, °F, k_{1r} , k_{2r} , and k_{3r} —global calibration parameters, β_{1r} , β_{2r} , and β_{3r} —local or mixture field calibration constants, and k_z —depth confinement factor (Eq. 3).

$$\begin{aligned} k_z &= (C_1 + C_2 D) 0.28196^D, \\ C_1 &= -0.1039(H_{\text{HMA}})^2 + 2.4868(H_{\text{HMA}}) - 17.342, \\ C_2 &= 0.0172(H_{\text{HMA}})^2 - 1.7331(H_{\text{HMA}}) + 27.428, \end{aligned} \quad (3)$$

where D —depth below the surface, in., H_{HMA} —total HMA thickness, in.

Many refinements were carried out on Eq. (1) before it reached the form as given in Eq. (2). One of the first works related to this was carried out by Leahy [3], and it was reported that the temperature was the most sensitive parameter related to permanent deformation. Using the data of Leahy [3], Aryes [4] developed an equation with only temperature and number of repetitions as the variables. Using Leahy's data and Superpave models resulting in a total database of 3476 samples, Kaloush and Witzczak [5] computed the present values suggested in M-EPDG [6] and they are $k_{1r} = -3.35412$, $k_{2r} = 1.5606$ and $k_{3r} = 0.4791$.

To determine the material-specific calibration coefficients, various investigations have been carried out at different test conditions. Such tests typically consist of repeated creep and recovery at various combinations of unconfined and confined conditions. For instance, Nelson et al. [7], NCHRP9-30A [8], and Kim et al. [9] carried out experimental investigations at deviatoric stress of 482 kPa and confinement

pressure of 69–138 kPa while the original investigation by Kaloush and Witczak [5] was carried out at unconfined test condition.

If the distress function in Eq. (2) has to be applied within the Indian context, it is necessary that material-specific calibration constants have to be estimated for simulation of asphalt pavement performance using M-E PDG. This investigation reports the experimental investigation carried out to determine such calibration constants. In this study, the calibration constants were found out following the procedure outlined in Kim et al. [9]. These calibration coefficients were then used for running simulations for rutting performance of ten National Highways (NH) in India. In the following, the M-E PDG rutting model is explained followed by the procedure for estimating the calibration coefficients. The experiments carried out are explained followed by rutting simulations using the newly determined coefficients.

2 Estimation of M-E PDG Calibration Coefficients

2.1 Identification of Secondary Stage

Kim et al. [9] estimated material-specific calibration coefficients from repeated creep and recovery experiment. As the permanent deformation model in M-E PDG is valid only for the secondary stage of the permanent deformation curve [1], it is necessary to identify the secondary stage of creep curve from the experimental data. Toward this end, the Francken model is used and it is given as follows [10]:

$$\varepsilon_p(t) = at^b + c[e^{dt} - 1]. \tag{4}$$

The above equation is used to find out the flow number by considering the rate of change of slope of irrecoverable deformation. The second derivative of the above equation with respect to the loading cycles is given as follows:

$$\frac{\partial^2(\varepsilon_p)}{\partial N^2} = ab(b - 1)N^{(b-2)} + cd^2e^{dN} \tag{5}$$

where ε_p is the permanent strain, $\frac{\partial^2(\varepsilon_p)}{\partial N^2}$ is the second derivative of the permanent strain, and a , b , c and d are the regression coefficients. The cycle number (N) at which there was a change in the sign was taken as the flow number value. It should be emphasized here that parameters a and b capture the primary stage, whereas the parameters c and d capture the onset of the tertiary stage. By carefully identifying these parameters, one can predict experimental data with all three stages assuming that the experimental data indeed display such three stages.

2.2 Experimental Investigations

Samples for the repeated creep and recovery experiment were fabricated using VG30 binder. The mid-gradation of wearing course, bituminous concrete, BC-grade II with the nominal maximum size of 13 mm from MORTH [11] was chosen for the experimental work. The experiments were carried out at three different temperatures and two confinement conditions. All the samples were subjected to 200 kPa deviatoric stress. The choice of the confinement pressure (200 kPa) was due to the limitations of the equipment. It should also be pointed out that higher confinement pressure than this will lead to a large time duration for testing. The test matrix is shown in Table 1.

All the experimental data were fitted using Francken model (see one sample plot in Fig. 1), and the flow number values were estimated. In the cases where the clear secondary stage was not obtained, the primary, secondary, and tertiary stages of creep curve were found out using Zhou et al. [12] approach. Once the end of the secondary stage is obtained (either through Francken model [10] or using Zhou et al. [12]), it is necessary to choose a range of loading cycles in which the response of the material shows steady-state behavior. Figure 2 shows a sample data used for determining the calibration constants. This dataset corresponds to 200 kPa deviator stress and 200 kPa confinement pressure at 50 °C.

Table 1 Test matrix

Description	Value
Test temperature (°C)	50, 55 and 60
Confinement pressure (kPa)	0 and 200
Loading waveform	Haversine
Loading and rest period, respectively	0.1 and 0.9 s

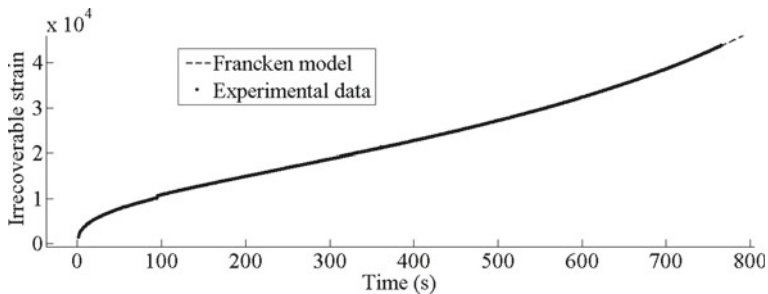
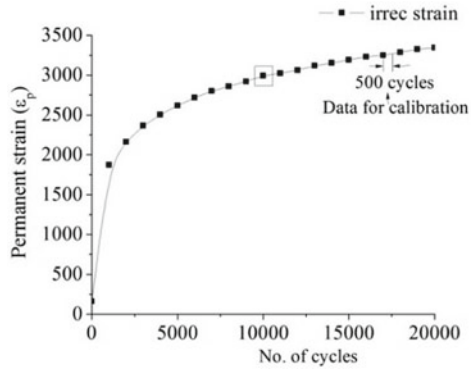


Fig. 1 Francken model fitting of unconfined data at 60 °C

Fig. 2 Variation of permanent strain (ϵ_p) for σ_d and $\sigma_c = 200$ kPa at 50°C



2.3 Estimation of Material-Specific Coefficients

Consider the permanent deformation equation of M-E PDG (2008), which is shown in Eq. (6).

$$\frac{\epsilon_p}{\epsilon_r} = \beta_{1r} \times k_z \times 10^{k_{1r}} \times T^{k_{2r}\beta_{2r}} \times N^{k_{3r}\beta_{3r}} \tag{6}$$

Let

$$K_1 = K_z \times \beta_{1r} \times 10^{k_{1r}}, K_2 = \beta_{2r} \times k_{2r}, K_3 = \beta_{3r} \times k_{3r} \tag{7}$$

Hence, Eq. (6) becomes

$$\frac{\epsilon_p}{\epsilon_r} = K_1 T^{K_2} N^{K_3} \tag{8}$$

Let

$$K_1 T^{K_2} = A \tag{9}$$

and hence Eq. (8) becomes

$$\frac{\epsilon_p}{\epsilon_r} = AN^{K_3} \tag{10}$$

Taking log on both sides of Eq. (9),

$$\log(A) = \log(K_1) + K_2 \log(T) \tag{11}$$

Also, taking log on both sides of Eq. (10),

Fig. 3 50 °C, unconfined

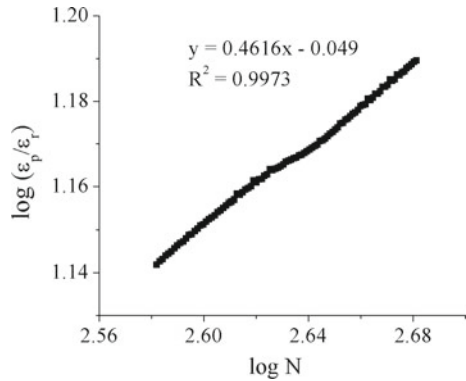
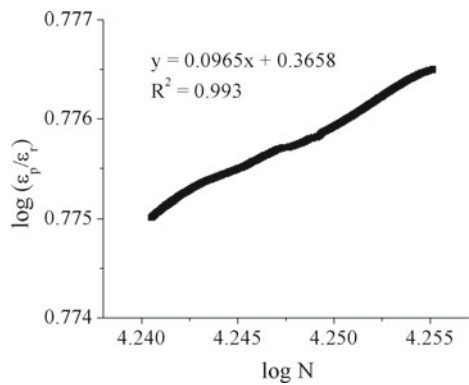


Fig. 4 60 °C, confined



$$\log\left(\frac{\epsilon_p}{\epsilon_r}\right) = \log(A) + K_3 \log(N) \tag{12}$$

Equations (11) and (12) both have the form of a straight line. Hence, the values of K_1 , K_2 and K_3 can all be obtained by plotting their straight line functions, as shown in Figs. 3, 4 and 5.

The calibration constants k_{1r} , k_{2r} and k_{3r} are obtained by substituting in Eq. (7) (Table 2).

2.4 M-E PDG Simulations

Using the above calibration coefficients, a total of 60 simulations were carried out in M-E PDG. These simulations were carried out for 10 different National Highway sections in India, namely NH 2, NH 3, NH 5BZA (NH 5 Vijayawada–Eluru section), NH 5CT (NH 5 Chennai–Tada section), NH 13, NH 15, NH 58, NH 69, NH 79, and NH 207, and the details are shown in Table 3.

Fig. 5 200 kPa deviator and 200 kPa confinement

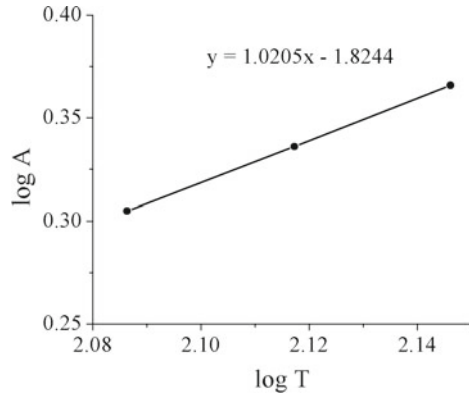


Table 2 Material-specific calibration coefficients

Coefficient	Default	Unconfined	200 kPa confinement
k_{1r}	-3.35412	-2.20472	-2.27332
k_{2r}	1.5606	0.8182	1.0206
k_{3r}	0.4791	0.46755	0.1

Table 3 Simulation details

National Highway section	Climatic location	Axle load collected
NH 2	New Delhi	Agra to Kanpur
NH 3	Jaipur	Agra to Gwalior
NH 5BZA	Visakhapatnam	Kallapuru toll plaza
NH 5CT	Chennai	Chennai to Tada
NH 13	Mangalore	318 km in the Hospet to Chitradurga stretch
NH 15	Amritsar	Southbound direction at 133rd km
NH 58	Lucknow	Sivaya toll plaza
NH 69	Bhopal	Obedullaganj
NH 79	Jaipur	189th km in the southbound direction
NH 207	Bangalore	126th km from Dobbaspeth

Traffic data: As part of DST project [13] executed at IIT Madras, traffic data was collected for all the 10 national highway sections. The collected data was used to develop pavement cross sections. The data was also used as an input to M-E PDG which requires complete axle load spectrum as an input. Hence, the collected data was analyzed to fit the format and used for simulations.

Climate data: As part of the DST project [13], climatic data was collected for 16 locations across India. The collected database was segregated into two parts, one was used to calculate average annual pavement temperature (AAPT) and another one was a two-year continuous hourly climatic database which consists of information

related to the sunshine, humidity, precipitation, temperature, wind speed, and water table depth. This database was used as an input in M-E PDG to run simulations. However, due to lack of climatic data for some of the locations where traffic data was collected, the most suited nearby climatic data among the available was chosen. The details are shown in Table 3.

Material properties: The dynamic modulus values for BC and DBM were obtained from [13], and the resilient modulus value of GB, GSB, and subgrade were obtained from IRC: 37-2012 [14].

Pavement cross section: Using the traffic database and the corresponding annual average pavement temperature (AAPT) of the mapped climatic location, pavement cross sections were designed following the guidelines stipulated in IRC: 37-2012 [14]. The pavement layers consisted of bituminous concrete, dense bituminous macadam, granular base, and granular subbase. In Table 4, the corresponding design thicknesses are shown.

Using the above data, simulations were carried out for three different calibration coefficients (default and the two calibrated coefficients) and for two speeds (40 and 80 kmph) to identify the influence of speed on rutting. Typical speeds of trucks in National Highways in India fall under this range.

3 Results and Discussions

Figure 6a, b shows the influence of calibration coefficients on total rutting for NH 15 and NH 207, respectively. Figure 7a, b shows the influence of calibration coefficients on asphalt concrete (AC) rutting for NH 15 and NH 207, respectively. Tables 4 and 5 show the total rutting and AC rutting for different national highways, respectively.

From the above Figs. 6, 7 and Tables 4, 5, it can be clearly seen that the pavements simulated with the default values are reaching the threshold value much quicker compared to the pavements simulated with calibrated coefficients (both at unconfined and confined conditions). This might be due to the values of the calibration coefficients because as one can notice that M-E PDG estimates rutting based on the permanent strain values (ϵ_p), where it will increase with the increase of these coefficients. Among the two calibrated values, the values calibrated from deviator stress of 200 kPa and unconfined condition showed a greater amount of rutting compared to the coefficients calibrated from deviator stress of 200 kPa and confinement pressure of 200 kPa. However, from the equation, one can understand that k_{3r} is more sensitive compared to other parameters toward rutting. Since k_{3r} is more for the unconfined condition, it can be understood that it shows more rutting compared to the confined one.

It is seen that the accumulation of rutting in the pavements is very less when using calibration factors corresponding to 200 kPa confinement pressure. Also, the rutting did not vary much when the simulation was carried for 40 and 80 kmph for the same case. But one expects a change in the rutting values due to the influence of speed. However, in this case, the sensitiveness of k_{3r} value dominates the effect of modulus

Table 4 Total rutting for different national highways

NH	ESAL (MSA)	Thickness	Total rutting in mm					
			Default		$\sigma_d = 200 \text{ kPa}, \sigma_c = 0 \text{ kPa}$		$\sigma_d = 200 \text{ kPa}, \sigma_c = 200 \text{ kPa}$	
			40 kmph	80 kmph	40 kmph	80 kmph	40 kmph	80 kmph
NH 2	15	30, 85, 250, 200	22.07 (6 years)	20.00 (10 years)	16.86	15.91	13.89	13.57
NH 3	18	30, 85, 250, 200	26.77 (2.5 years)	23.74 (4.5 years)	18.68	17.38	14.49	14.09
NH 5BZA	138	50, 165, 250, 200	29.28 (1.3 years)	26.63 (1.8 years)	21.42 (4 years)	20.16 (6.3 years)	16.65	16.23
NH 5CT	46	40, 120, 250, 200	33.29 (1.6 years)	29.84 (2 years)	23.17 (4 years)	21.63 (5.8 years)	17.82	17.32
NH 13	64	50, 110, 250, 200	27.93 (2 years)	26.07 (2.1 years)	22.78 (3.4 years)	21.81 (4.8 years)	19.48	19.08
NH 15	44	40, 105, 250, 200	37.47 (1.5 years)	33.01 (1.8 years)	25.24 (2.5 years)	23.35 (3.5 years)	19	18.45
NH 58	128	50, 165, 250, 200	23.36 (2.2 years)	22.57 (3.5 years)	17.76	17.39	14.55	14.36
NH 69	35	40, 120, 250, 200	22.67 (5 years)	21.05 (7 years)	18.52	17.7	15.99	15.63
NH 79	48	40, 120, 250, 200	35.22 (1.8 years)	30.28 (2.1 years)	20.46 (8.6 years)	18.49	12.9	12.49
NH 207	15	40, 80, 250, 200	24.04 (4 years)	22.22 (5.7 years)	19.4	18.5	16.79	16.39

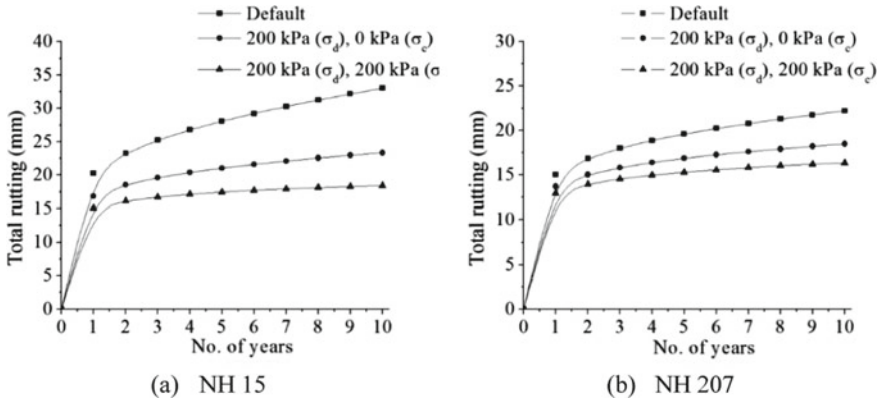


Fig. 6 Influence of calibration coefficients on total rutting

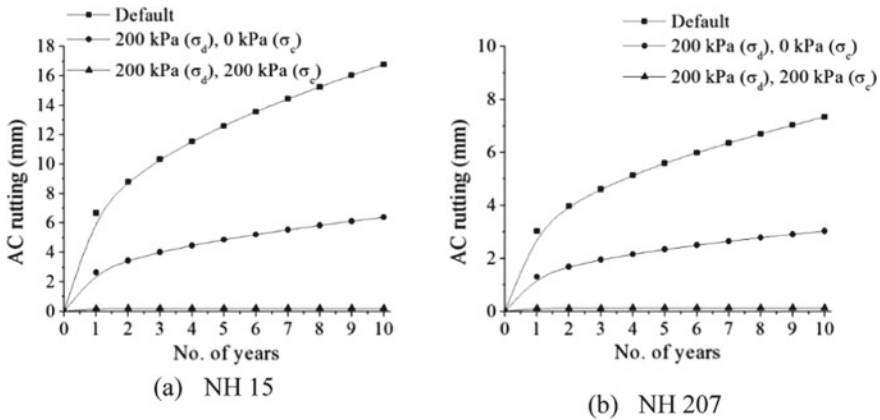


Fig. 7 Influence of calibration coefficients on AC rutting

value. One more interesting thing is that the increment in rutting due to speed was much high in granular layers compared to the asphalt layers.

The above graphs (Figs. 6 and 7) show that the pavements simulated with default values are reaching the threshold value of 20 mm even before the design life irrespective of the pavement thickness and the traffic anticipated. However, the pavements simulated with the calibrated coefficients derived from the deviator stress of 200 kPa and unconfined condition showed failure (reaching the threshold value) only in some cases. These cases correspond to high traffic levels as can be seen in the data presented in Tables 4 and 5.

Table 5 AC rutting for different national highways

NH	ESAL (MSA)	Thickness	AC rutting in mm					
			Default		$\sigma_d = 200 \text{ kPa}, \sigma_c = 0 \text{ kPa}$		$\sigma_d = 200 \text{ kPa}, \sigma_c = 200 \text{ kPa}$	
			40 kmph	80 kmph	40 kmph	80 kmph	40 kmph	80 kmph
NH 2	15	30, 85, 250, 200	9.83	7.93	4.05	3.29	0.15	0.13
NH 3	18	30, 85, 250, 200	14.23	11.43	5.53	4.46	0.22	0.18
NH 5BZA	138	50, 165, 250, 200	14.64	12.26	6.16	5.18	0.13	0.11
NH 5CT	46	40, 120, 250, 200	17.66	14.57	6.87	5.67	0.19	0.16
NH 13	64	50, 110, 250, 200	10.28	8.66	4.48	3.79	0.1	0.09
NH 15	44	40, 105, 250, 200	20.88	16.79	7.95	6.4	0.28	0.22
NH 58	128	50, 165, 250, 200	10.43	9.88	4.36	4.13	0.16	0.14
NH 69	35	40, 120, 250, 200	8.27	6.86	3.55	2.97	0.12	0.1
NH 79	48	40, 120, 250, 200	24.43	19.76	9.19	7.46	0.22	0.18
NH 207	15	40, 80, 250, 200	8.94	7.34	3.68	3.03	0.16	0.14

4 Conclusions

The first investigation corresponding to Indian highways in using material-specific calibration factors within the context of M-E PDG was presented here. From the investigation carried out, the influence of confinement condition and the magnitude of deviatoric stress on the simulated rut depth was documented for different scenarios. However, there is a need to collect field data and check for the veracity of such simulation studies.

Acknowledgements The authors thank the Department of Science and Technology for funding this investigation. The grant number is DST/TSG/STS/2011/46. The authors thank M/s V. R. Techniche, Delhi, and L&T IDPL, Chennai, for sharing the axle load data. The authors acknowledge the opportunity provided by the 4th Conference of the Transportation Research Group of India (4th CTRG) held at IIT Bombay, Mumbai, India, between December 17, 2017, and December 20, 2017, to present the work that forms the basis of this manuscript.

References

1. Kim RY, Jadoun FM, Hou T, Muthadi N (2011) Local calibration of the MEPDG for flexible pavement design. North Carolina Department of Transportation
2. NCHRP (2004) Appendix GG-1: calibration of permanent deformation models for flexible pavements. Technical report. http://onlinepubs.trb.org/onlinepubs/archive/mepdg/2appendices_GG.pdf, Accessed on 1st May 2017
3. Leahy RB (1989) Permanent deformation characteristics of asphalt concrete. Ph.D. thesis, University of Maryland, College Park
4. Aryes M Jr (2002) Unbound material rut model modification. Development of the 2002 Guide for the Design of New and Rehabilitated Pavement Structures. NCHRP 1-37A
5. Kaloush KE, Witzczak MW (2000) Development of a permanent to elastic strain ratio model for asphalt mixtures. In: Development of the 2002 guide for the design of new and rehabilitated pavement structures. NCHRP 1-37A
6. MEPDG (2008) Mechanistic-empirical pavement design guide: a manual practice. American Association of State Highway and Transportation Officials, Washington, D.C., USA
7. Nelson G, Kutay ME, Keramat D, Youtcheff J (2009) Multiaxial Strain response of asphalt concrete measured during flow number performance test. *J Assoc Asphalt Paving Technol* 78:25–63
8. NCHRP 9-30A (2010) Calibration of rutting models for HMA structural and mixture design. Transportation Research Board of the National Academies
9. Kim Y, Park HM, Aragao FT, Lutfi JES (2009) Effects of aggregate structure on hot-mix asphalt rutting performance in low traffic volume local pavements. *Constr Build Mater* 23:2177–2182
10. Francken L (1977) Pavement deformation law of bituminous road mixes in repeated load triaxial compression. In: Fourth international conference on the structural design of asphalt pavements, University of Michigan, Ann Arbor, USA, pp 483–496
11. MORTH (2013) Ministry of Road Transport & Highways: Manual for construction and supervision of flexible works. Indian Roads Congress, New Delhi, India
12. Zhou F, Scullion T, Sun L (2004) Verification and modeling of three-stage permanent deformation behavior of asphalt mixes. *J Transp Eng* 130(4):486–494

13. Krishnan JM, Veeraragavan A (2016) Development of warrants for the use of modified binders in Indian highways. Department of Science and Technology (India), Technical Report, Indian Institute of Technology Madras, Chennai, India
14. IRC: 37-2012 (2012) Guidelines for the design of flexible pavements. Indian Roads Congress, New Delhi, India

Development of Fatigue Model for Warm Mix Asphalt Based on Testing Frequency and Post-processing Method



K. Lakshmi Roja, A. Padmarekha and J. Murali Krishnan

Abstract Within the context of warm mix asphalt (WMA), there is a necessity to re-look at the distress mechanisms. Since the WMA undergoes reduced aging during mixing and compaction, one expects a reduction in the stiffness of the initial in-place material. Such reduced stiffness can lead to a widely varying mechanical response of the mixture during the performance and it will be interesting to bench-mark the same, especially, the fatigue behavior, when compared to hot mix asphalt (HMA) and this paper explores the same. In the current study, two types of WMA additives were used and they are Evotherm (chemical-based) and Sasobit (wax-based). To determine the fatigue life, four-point beam bending experiments were conducted at two different frequencies and the data was analyzed using two types of post-processing method. Using S-N plots, calibration factors for fatigue distress prediction model were determined for warm mix asphalt. It was found that the material calibration factors were dependent on the post-processing method used.

Keywords Warm mix asphalt · Four-point beam bending · Frequency · Post-processing · Material calibration

1 Introduction

While warm mix technologies are in the implementation stage world-over for pavement construction, a few important factors merit attention. These factors are related to the manner in which warm mix asphalt (WMA) layers exhibit the major mode

K. L. Roja · J. M. Krishnan (✉)
Department of Civil Engineering,
Indian Institute of Technology Madras, Chennai 600036, India
e-mail: jmk@iitm.ac.in

K. L. Roja
e-mail: lakshmiroja1988@gmail.com

A. Padmarekha
Department of Civil Engineering, SRM Institute of Science and Technology,
Kattankulathur, Chennai, India
e-mail: padmarea@srmist.edu.in

of distress such as fatigue cracking. Fatigue cracking in a bituminous pavement can manifest in the form of top-down or bottoms-up cracking, and such cracking develops when the pavement is subjected to repeated loading leading to accumulation of tensile strains.

It is well known that the temperatures used for the production of the bituminous mixture have a significant impact on the binder aging. Since WMA mixtures are produced at 20–30°C lower than HMA mixtures, they undergo less binder aging. While the environmental benefits of WMA mixtures are well recorded by many researchers, the influence of warm mix additive and reduced aging on the mechanical response of WMA mixtures is still not well quantified. Reduced aging is expected to reduce the rutting resistance; however, it can also enhance the fatigue resistance of the bituminous mixture. This paper focuses on the quantification of fatigue response of bituminous mixtures with two different WMA additives. In this investigation, the fatigue resistance of two types of WMA technologies is studied. One is chemical-based additive called Evotherm, and another is wax-based additive called Sasobit. These additives permit the reduction in mixing and compaction temperatures in a completely different manner. While chemical additives reduce the surface tension in Newtonian regime [1], wax-based additives reduce the viscosity [2].

Depending on the type of loading (constant load or constant displacement), mode of loading, frequency and temperature during loading, one can use different criteria to quantify fatigue life. Benedetto et al. [3] summarized the various modes of fatigue tests, and they are uniaxial tension/compression, two-point bending, three-point bending, four-point bending and indirect tension tests. Also, there exist different post-processing methods to quantify the fatigue life. For instance, AASHTO T 321–07 [4] assumes that the failure occurs when the reduction in stiffness is 50%. In cases where the experimental data is not enough to determine such 50% reduction, an exponential curve is fit to the collected data and the number of cycles corresponding to 50% stiffness is predicted. Alternate approaches based on normalized modulus [5], fitting ellipse [6] and energy ratio [7] are also used to determine the fatigue resistance of bituminous mixtures. Among all, the most commonly used methods are based on AASHTO T 321–07 [4] and ASTM D7460–10, [5].

Very limited test data is available in the literature as far as fatigue of WMA is concerned. It is also not clear whether the quantification of damage due to fatigue in WMA can be interpreted in the same manner as is followed for HMA. The fatigue resistance of the WMA mixture may vary with the type of WMA additive used, selected strain amplitude, the type of aggregate and binder used. Table 1 summarizes the relevant literature related to fatigue of WMA mixtures. In these literature, the strain-controlled tests were carried out using four-point beam bending equipment with sinusoidal loading and the experimental data was post-processed using AASHTO T 321–07 [4] method.

From Table 1, it is clear that the fatigue life of warm mix asphalt varies with the type of additive used. While some additives improve the fatigue response, few other additives reduce the fatigue life. While it is expected that reduced aging of the binder can lead to reduced stiffness thereby making the material less prone to fatigue

Table 1 Literature on fatigue of WMA mixtures

Author	Test details	Fatigue life
Xiao et al. [8]	500 $\mu\epsilon$, 10 Hz, 20 °C	$N_f(\text{Sasobit}) > N_f(\text{HMA}) > N_f(\text{Asphamin})$
Qin et al. [9]	150, 300 & 450 $\mu\epsilon$, 10 Hz, 20 °C	$N_f(\text{Sasobit}) > N_f(\text{HMA})$
Hasan et al. [10]	600 $\mu\epsilon$, 10 Hz, 25 °C	$N_f(\text{Sasobit}) > N_f(\text{HMA})$
Toraldo et al. [11]	400 $\mu\epsilon$, 10 Hz, 20 °C	$N_f(\text{Sasobit}) = N_f(\text{HMA})$

failure, it is possible that the material can exhibit different responses at different strain amplitudes and frequencies. In this paper, these issues are investigated.

This study reports the quantification of fatigue life of WMA using the 50% reduction in stiffness/exponential fitting method [4] and normalized modulus/Weibull fit method [5], and they are benchmarked with HMA. Using S-N curves, the material calibration factors are developed. Also, the influence of testing frequency and post-processing method on the fatigue life of WMA is reported.

2 Experimental Investigations

2.1 Materials

In this investigation, three types of bituminous mixtures were produced and they are Evotherm-treated mixture (WMA-Evotherm), Sasobit-treated mixture (WMA-Sasobit) in addition to the control bituminous mixture (HMA-VG30). For preparing mixtures, a base binder of VG30 was used meeting IS 73-2013 [12]. A binder content of 5% by mass of the total mix was selected. The details of dosage of additives, mixing and compaction temperatures of bituminous mixtures are given in Table 2. The selection of these temperatures is based on the relevant industry practice.

Aggregate gradation pertaining to bituminous concrete (grade II) grading as per the MoRTH [13], specification was used and beams of size 450 × 150 × 160 mm were fabricated using a shear compactor [14] and were sliced to the size of 380 × 63 × 50 mm for beam bending test. All the samples were tested at 4 ± 0.5% air voids.

2.2 Testing

Fatigue tests were carried out at five different strain levels 200, 400, 500, 600 and 800 $\mu\epsilon$ for both HMA and WMA beams. The selected frequency was 10 and 30 Hz with a sinusoidal loading waveform, and the testing temperature was 20 °C. The

Table 2 Details of dosage, mixing and compaction temperatures

Material	Dosage	Blending temperature (°C)	Mixing temperature (°C)	Compaction temperature (°C)	Short-term aging (°C)
HMA-VG30	–	–	165	150	135 °C for 4 h, 150 °C for 30 min
WMA-Evotherm	0.40%	145	135	117	117 °C for 4 h
WMA-Sasobit	1.50%	145	135	117	117 °C for 4 h

strain levels were selected as per AASHTO T 321–07 [4] and ASTM D7460–10 [5] to generate S-N plots. The initial stiffness was calculated at the 50th load cycle, and the test was terminated either at 80% reduction in stiffness or at 1×10^6 cycle, whichever occurs first.

3 Analysis of Fatigue Test Data

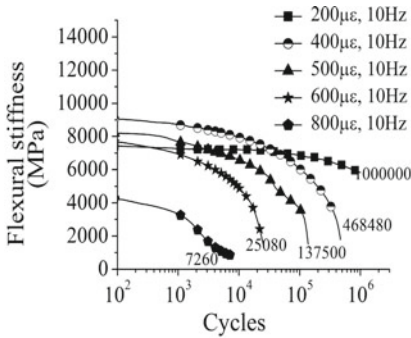
Figure 1 shows the variation of stiffness modulus with cycles as a function of strain for HMA-VG30, WMA-Evotherm and WMA-Sasobit samples. It was seen that the termination stiffness reached within the test duration at 400, 500, 600 and 800 $\mu\epsilon$ for both HMA and WMA samples. It was interesting to note that the WMA-Evotherm samples showed a large number of cycle to reach its 80% reduction in stiffness than HMA, followed by WMA-Sasobit at all strain levels for 10Hz frequency. When the frequency was increased to 30Hz, at 500, 600 and 800 $\mu\epsilon$ strain levels, WMA-Evotherm samples reached termination criteria earlier than WMA-Sasobit samples, followed by HMA (Table 3).

To understand the collected experimental data and interpret the results, two different post-processing methods were used and they are discussed in the following.

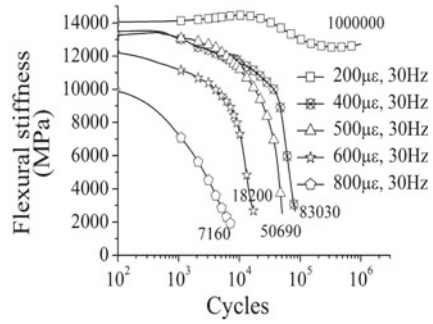
3.1 Determination of Fatigue Life

3.1.1 Exponential Fitting Method

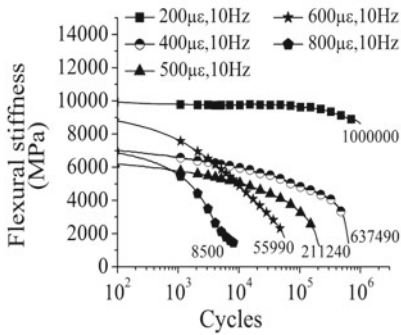
This method assumes that the fatigue failure initiates when the reduction in stiffness is 50% of the initial stiffness. Since it is possible that the collected experimental data (for instance, for 200 $\mu\epsilon$ in this case) may not reach the 50% reduction in stiffness



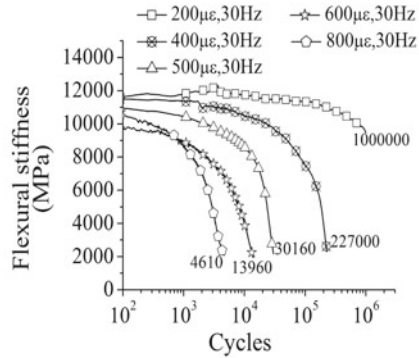
(a) HMA-VG30 at 10Hz



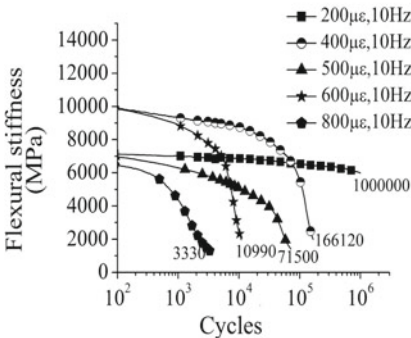
(b) HMA-VG30 at 30Hz



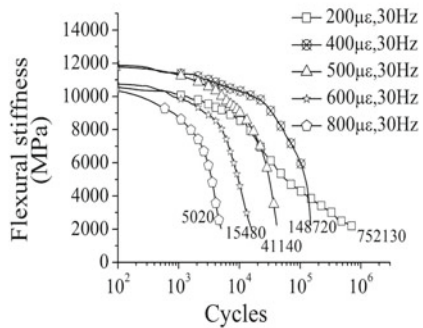
(c) WMA-Evotherm at 10Hz



(d) WMA-Evotherm at 30Hz



(e) WMA-Sasobit at 10Hz



(f) WMA-Sasobit at 30Hz

Fig. 1 Flexural stiffness at different strain amplitudes for different materials

Table 3 Number of cycles for termination

Sample	200 $\mu\epsilon$	400 $\mu\epsilon$	500 $\mu\epsilon$	600 $\mu\epsilon$	800 $\mu\epsilon$
10Hz					
HMA-VG30	1.00E+06	4.68E+05	1.37E+05	2.50E+04	7.26E+03
WMA-Evotherm	1.00E+06	6.37E+05	2.11E+05	5.59E+04	8.50E+03
WMA-Sasobit	1.00E+06	1.66E+05	7.15E+04	1.09E+04	3.33E+03
30Hz					
HMA-VG30	1.00E+06	8.30E+04	5.06E+04	1.82E+04	7.16E+03
WMA-Evotherm	1.00E+06	2.27E+05	3.01E+04	1.39E+04	4.61E+03
WMA-Sasobit	7.52E+05	1.48E+05	4.11E+04	1.54E+04	5.02E+03

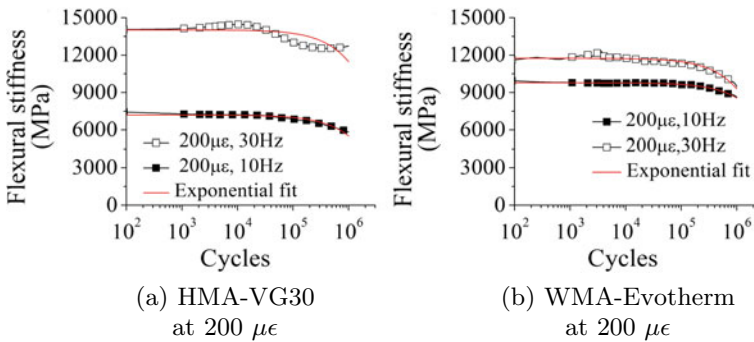


Fig. 2 Exponential fitting of different samples

within the duration of the experiment, an exponential function of the following form was fitted to the data [4]:

$$S = ae^{bx} \tag{1}$$

Here, S is the stiffness (MPa); x is the number of cycles; a and b are regression constants.

The initial stiffness was calculated at $x=50$, and the fatigue life for 50% reduction in stiffness was determined using exponential curve fitting.

It was found that all three mixtures did not reach the 50% reduction in stiffness criteria for 200 $\mu\epsilon$ at 10Hz frequency. Hence, an exponential fit was carried out for such data (Fig. 2). At 30Hz frequency, WMA-Sasobit reached termination criteria within the test duration for 200 $\mu\epsilon$. From the model parameters obtained, the fatigue life was determined and is summarized in Table 4.

It was observed that the WMA-Evotherm showed better fatigue life when compared to HMA samples, followed by WMA-Sasobit samples at 400, 500, 600 and 800 $\mu\epsilon$ strain levels for 10Hz frequency, whereas at 200 $\mu\epsilon$, WMA-Sasobit exhibited higher fatigue life than HMA-VG30. At 30Hz frequency, WMA-Evotherm exhibited better fatigue life than HMA-VG30 and WMA-Sasobit for 200 and 400 $\mu\epsilon$ (Table 4).

Table 4 Fatigue life using AASHTO T 321–07 [4]

Sample	200 $\mu\epsilon$	400 $\mu\epsilon$	500 $\mu\epsilon$	600 $\mu\epsilon$	800 $\mu\epsilon$
10Hz					
WMA-Evotherm	5.23E+06	4.48E+05	1.23E+05	2.29E+04	3.23E+03
HMA-VG30	2.63E+06	2.54E+05	8.04E+04	1.64E+04	2.62E+03
WMA-Sasobit	4.12E+06	1.17E+05	4.06E+04	6.78E+03	1.35E+03
30Hz					
WMA-Evotherm	3.85E+06	1.61E+05	2.38E+04	7.93E+03	2.35E+03
HMA-VG30	3.44E+06	6.38E+04	3.65E+04	1.18E+04	2.96E+03
WMA-Sasobit	1.20E+05	1.04E+05	2.67E+04	8.58E+03	2.89E+03

However, for all the other strain levels above 500 $\mu\epsilon$, better fatigue resistance was seen for HMA. At high strain levels such as 500, 600 and 800 $\mu\epsilon$, WMA-Evotherm samples failed earlier than WMA-Sasobit samples, followed by HMA for 30 Hz frequency.

3.1.2 Normalized Modulus/Weibull Fit Method

In this method, fatigue life was determined from normalized modulus approach. Normalized modulus approach is based on Miner's equation, and the peak of normalized modulus is considered as the fatigue failure initiation point. The normalized modulus was calculated using Eq. 2 [5],

$$NM_i = \frac{S_i}{S_o} \times \frac{N_i}{N_o} \quad (2)$$

where NM_i is the normalized modulus at the i th cycle, S_i is the flexural beam stiffness at cycle i (Pa), N_i is the i th cycle, S_o is the initial flexural beam stiffness at 50th cycle (Pa) and N_o is the number of cycles where the initial stiffness is estimated.

Figure 3a shows the normalized modulus versus number of cycles for WMA-Evotherm at 200 $\mu\epsilon$ and 10 Hz frequency. At low strain level (200 $\mu\epsilon$), the peak value was not attained and hence the peak value for the normalized modulus was determined by assuming Weibull distribution. In Weibull plot, the horizontal axis is the number of cycles to failure and the vertical axis is the cumulative distribution function, which describes the percentage of failure at a given number of cycle. In ASTM D7460–10 [5], Weibull distribution is used to extrapolate the fatigue failure point, especially at low strain levels, where the peak value of the 'normalized modulus' cannot be quantified within the test duration. In this procedure, the number of cycles to failure is calculated using the following equation:

$$\ln(-\ln(\text{SR})) = \gamma \times \ln(N) + \ln(A), \quad (3)$$

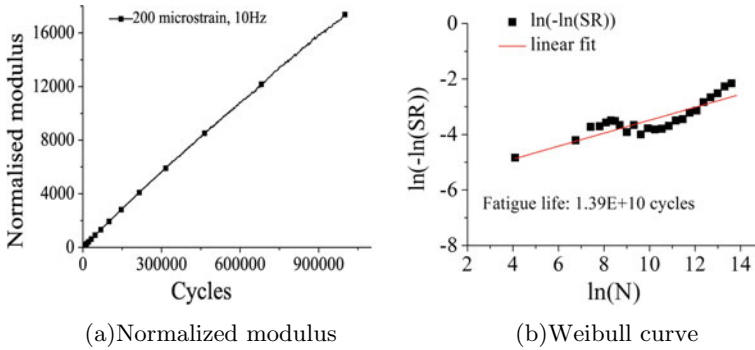
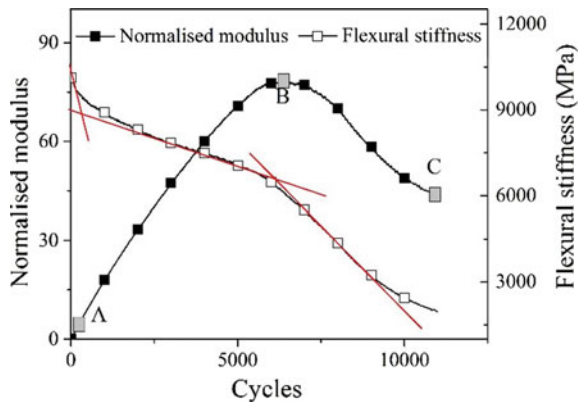


Fig. 3 Normalized modulus and Weibull curve for WMA-Evotherm at 200 $\mu\epsilon$, 10Hz

Fig. 4 Normalized modulus for WMA-Sasobit at 600 $\mu\epsilon$, 10Hz



where SR is the flexural beam stiffness ratio, N is the number of cycles, and γ and Λ are regression constants.

Figure 3b shows the Weibull curve for WMA-Evotherm at 200 $\mu\epsilon$ and 10Hz frequency. The failure point was estimated for the value of N where SR is equal to 0.5 for 50% reduction in stiffness criteria. It was observed that the normalized modulus curve attained the peak value at higher strain levels (400, 500, 600 and 800 $\mu\epsilon$) and the number of the cycles corresponding to the peak value was considered as fatigue life. Fig. 4 shows the normalized modulus curves for WMA-Sasobit at 600 $\mu\epsilon$.

In Fig. 4, initially the rapid decrement in the stiffness due to repetitive loading was seen; after some point, the rate of decrement of stiffness was constant till point 'B' and this point was considered as damage initiation point. In this analysis, for all the tests at 200 $\mu\epsilon$, Weibull distribution method was used to determine the fatigue life and for higher strain levels, normalized modulus method was used. The fatigue life values determined using normalized modulus/Weibull distribution are summarized in Table 5.

Table 5 Fatigue life using ASTM D7460-10 [5]

Sample	200 $\mu\epsilon$	400 $\mu\epsilon$	500 $\mu\epsilon$	600 $\mu\epsilon$	800 $\mu\epsilon$
10Hz					
WMA-Evotherm	1.39E+10	4.98E+05	1.55E+05	4.76E+04	2.99E+03
HMA-VG30	2.97E+07	3.60E+05	1.14E+05	1.73E+04	2.50E+03
WMA-Sasobit	1.63E+09	1.10E+05	4.09E+04	6.35E+03	1.39E+03
30Hz					
WMA-Evotherm	2.56E+07	1.67E+05	1.97E+04	8.77E+03	2.56E+03
HMA-VG30	1.27E+07	4.77E+04	3.74E+04	1.02E+04	3.98E+03
WMA-Sasobit	3.66E+05	1.14E+05	2.75E+04	8.98E+03	3.02E+03

From Table 5, WMA-Evotherm sample exhibited greater fatigue life than HMA-VG30, followed by WMA-Sasobit at 400, 500, 600 and 800 $\mu\epsilon$ for 10Hz frequency. At 200 $\mu\epsilon$, when fatigue life was determined using Weibull distribution, WMA-Sasobit exhibited better fatigue life than HMA-VG30 at 10Hz frequency. Also, from the experimental results (Fig. 1), one could observe the similar trend for the materials to reach their 80% reduction in stiffness at all strain levels above 400 $\mu\epsilon$ for 10Hz frequency. However, at 30Hz frequency, the trend of fatigue life completely changed at 500, 600 and 800 $\mu\epsilon$ and for such strain levels, HMA-VG30 exhibited better fatigue life than WMA-Sasobit, followed by WMA-Evotherm. At 200 and 400 $\mu\epsilon$, WMA-Evotherm has greater fatigue life for 30Hz frequency. An identical trend was observed for HMA and WMA mixtures when the fatigue lives were determined using exponential fitting method (Table 4).

3.2 S-N Plot

S-N plot is used to determine the fatigue life of a material at any strain level. As described earlier, the fatigue test was carried out at different strain levels (200, 400, 500, 600 and 800 $\mu\epsilon$) at the same temperature (20 °C) with two different frequencies 10 and 30Hz. The number of cycles to reach 50% reduction in stiffness against the corresponding strain amplitude is reported in Table 4. To develop the regression relation connecting the number of cycles and the strain level, linear fitting was carried out and S-N curve was plotted.

Figure 5a, b shows the S-N plots for WMA-Evotherm and WMA-Sasobit samples for the fatigue life determined by using the exponential fitting method. In Fig. 5a, the fatigue life of WMA-Evotherm samples was more than the control HMA samples at 10Hz frequency. At 30Hz frequency, the identical behavior of the HMA and WMA-Evotherm was seen. In Fig. 5b, the fatigue life of HMA and WMA-Sasobit samples was identical at low strain levels for 10Hz frequency. At 30Hz frequency, WMA-Sasobit was showing less fatigue life at low strain levels.

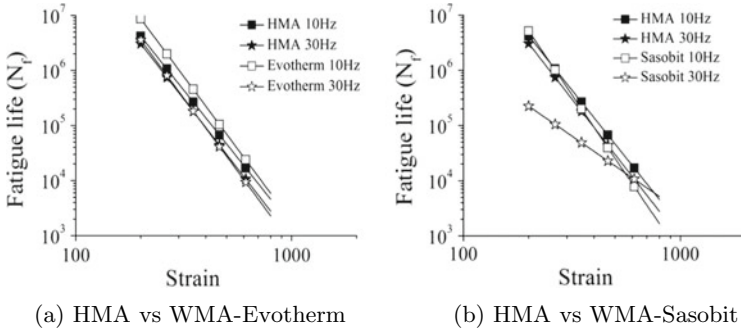


Fig. 5 S-N plot for HMA and WMA materials using exponential fitting method

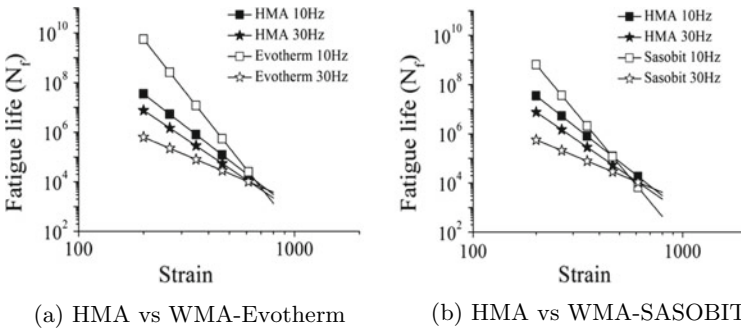


Fig. 6 S-N plot for HMA and WMA materials using normalized modulus/Weibull curve method

Figure 6a, b shows the S-N plots for WMA-Evotherm and WMA-Sasobit samples for the fatigue life determined by using normalized modulus/Weibull curve method. At low strain level ($200 \mu\epsilon$), it was observed that the fatigue life of WMA samples was more than the HMA samples at 10Hz frequency and it was less than HMA samples at 30Hz frequency.

3.3 Determination of Calibration Factors

M-E PDG [15] uses Eq. 4 to predict top-down and bottoms-up cracking in the bituminous mixture.

$$N_f = k_1 \beta_1 \left(\frac{1}{\epsilon_t} \right)^{k_2 \beta_2} \left(\frac{1}{E} \right)^{k_3 \beta_3} \tag{4}$$

Here N_f represents an allowable number of axle load applications for a flexible pavement, ϵ_t is strain (in/in), and E is the dynamic modulus of bituminous mix measured in compression (psi). k_1 , k_2 and k_3 are material calibration factors. β_1 , β_2

and β_3 are local or the field calibration factors. Here, in the absence of field distress data, β_1 , β_2 and β_3 were considered as 1 as suggested by M-E PDG [15].

S-N plot is a mere representation between N_f and ϵ_t , whereas Eq. 4 includes material calibration factors, local calibration factors as well as the modulus. For determining the calibration factors k_1 , k_2 and k_3 , the dynamic modulus (E) is required at 20°C for 10 and 30 Hz. The dynamic modulus values were determined using AASHTO TP 79-10 [16] and are given in Table 6.

The S-N plots for the fatigue life obtained using the exponential fitting method and normalized modulus/Weibull curve method (Figs. 5 and 6) were used for determining the calibration factors k_1 , k_2 and k_3 . Equation 4 is in the form of the power law, and it was used to fit the number of cycles to failure against strain levels by considering modulus parameter. The model calibration factors k_1 , k_2 and k_3 were determined for 10 and 30 Hz data using curve fit tool in MATLAB, and the model parameters are given in Table 7.

From the obtained material calibration factors for different frequencies based on two post-processing methods, the fatigue life was calculated using Eq. 4, for a tensile strain of 200 $\mu\epsilon$. When modulus parameter was considered for calculating fatigue life, at 10 Hz frequency, WMA-Evotherm has greater fatigue life than HMA-

Table 6 Dynamic modulus values at 10 and 30 Hz frequencies

Frequency (Hz)	WMA-Evotherm (psi)	HMA-VG30 (psi)	WMA-Sasobit (psi)
10	1,866,635	1,719,567	2,303,779
30	2,189,779	2,045,467	2,617,641

Table 7 Material calibration factors

Material and frequency	k_1	k_2	k_3	R^2	N_f ($\epsilon_t = 200 \mu\epsilon$)
<i>Exponential fitting method</i>					
HMA-VG30, 10 Hz	0.439	2.62	0.466	0.974	1.80E+12
WMA-Evotherm, 10 Hz	0.999	2.619	0.477	0.96	4.59E+12
WMA-Sasobit, 10 Hz	0.012	2.801	0.402	0.901	9.95E+10
HMA-VG30, 30 Hz	0.083	2.62	0.333	0.957	5.00E+10
WMA-Evotherm, 30 Hz	0.034	2.619	0.282	0.964	9.49E+09
WMA-Sasobit, 30 Hz	0.007	2.837	0.272	0.972	1.17E+10
<i>Normalized modulus/Weibull fit method</i>					
HMA-VG30, 10 Hz	0.225	2.715	0.308	0.959	2.12E+11
WMA-Evotherm, 10 Hz	0.077	3.358	0.575	0.903	7.82E+14
WMA-Sasobit, 10 Hz	0.088	2.985	0.123	0.973	5.87E+10
HMA-VG30, 30 Hz	0.043	2.715	0.252	0.958	1.81E+10
WMA-Evotherm, 30 Hz	0.040	1.961	0.046	0.912	1.39E+06
WMA-Sasobit, 30 Hz	0.009	2.239	0.109	0.974	8.51E+06

VG30, followed by WMA-Sasobit for both the post-processing methods. At 30 Hz frequency, HMA-VG30 showed superior performance when data was analyzed with both the post-processing methods. In WMA mixtures, WMA-Sasobit has better fatigue performance than WMA-Evotherm.

4 Conclusions

In this investigation, fatigue life was determined using two post-processing methods. From the overall analysis, it was understood that the fatigue life of WMA mixtures varied with the testing frequency and the post-processing method followed. From S-N curves, at 10 Hz frequency, WMA-Evotherm exhibited better fatigue life when compared to HMA and WMA-Sasobit, especially for lower strain levels. It was understood that the reduced stiffness of WMA-Evotherm due to less aging can help in improving fatigue life only at lower strain levels. When the testing frequency increased to 30 Hz, the order of ranking completely reversed and HMA exhibited better fatigue resistance at the lower strain level. The reduced stiffness of WMA-Evotherm may not be helpful in improving fatigue resistance at a higher frequency. However, it is not necessary that the material with higher stiffness can exhibit better fatigue performance at a higher frequency. At 30 Hz frequency, lower strain levels, the fatigue life of HMA is greater than WMA-Sasobit, followed by WMA-Evotherm.

When the influence of modulus is considered for calculating the fatigue life in terms of the M-E PDG fatigue distress prediction equation, at 10 Hz frequency and $200 \mu\epsilon$, the fatigue life of WMA-Evotherm is greater than HMA, followed by WMA-Sasobit. At 30 Hz frequency, the order of fatigue performance is identical as observed for S-N curves.

5 Limitations and Scope for Future Study

- Fatigue life of bituminous mixtures varies with various parameters, and they are frequency, temperature, rest period, strain amplitude. Temperature and rest period play a critical role in fatigue response of bituminous mixtures. Hence, the fatigue performance of bituminous mixtures may vary when the test conditions are different. One could characterize the fatigue response of WMA mixtures with rest period.
- Since different post-processing methods exist to determine the fatigue failure point of mixtures, the material calibration factors obtained from each post-processing method may differ with another method. Hence, one could derive the material calibration factors for the fatigue lives obtained from different other post-processing methods (for instance, fitting ellipse [6] and energy ratio [7]).

References

1. Bower N (2011) Laboratory evaluation of performance of warm mix asphalt in Washington State. Ph.D. thesis, Washington State University, Washington, USA
2. Jamshidi A, Hamzah MO, Aman MY (2012) Effects of sasobit content on the rheological characteristics of unaged and aged asphalt binders at high and intermediate temperatures. *Mater Res* 15(4):628–638
3. Benedetto DH, de La Roche C, Baaj H, Pronk A (2004) Fatigue of bituminous mixtures. *Mater Struct* 37:202–216
4. AASHTO T 321–07 (2007) Determining the fatigue life of compacted hot mix asphalt subjected to repeated flexural bending. American Association of State Highways and Transportation Officials, Washington, D.C., USA
5. ASTM D7460–10 (2010) Standard test method for determining fatigue failure of compacted asphalt concrete subjected to repeated flexural bending. ASTM International, West Conshohocken, Pennsylvania, USA
6. Al-Khateeb G, Shenoy A (2004) A simple quantitative method for identification of failure due to fatigue damage. *Int J Damage Mech* 20(1):321
7. Rowe G, Bouldin M (2000) Improved techniques to evaluate the fatigue resistance of asphalt mixtures, 2nd Eurasphalt and Eurobitume Congress., Barcelona
8. Xiao F, Zhao W, Amirkhanian S (2009) Fatigue behavior of rubberized asphalt concrete mixtures containing warm asphalt additives. *Constr Build Mater* 23:3144–3151
9. Qin Y, Wang S, Zeng W, Shi X, Xu J, Huang S (2012) The effect of asphalt binder aging on fatigue performance of evotherm WMA. *Adv Eng Mater* 14(12):1686–1692
10. Hasan Z, Hamid B, Amir I, Danial N (2012) Long term performance of warm mix asphalt versus hot mix asphalt. *J Cent South Univ* 20:256–266
11. Toraldo E, Brovelli C, Mariani E (2013) Laboratory investigation into the effects of working temperatures on wax-based warm mix asphalt. *Constr Build Mater* 44:774–780
12. IS 73-2013. Paving bitumen—specification, Bureau of Indian Standards. New Delhi, India (2013)
13. MoRTH (2013) Specification for road & bridge works, fifth revision. IRC publications, Ministry of Road Transport & Highways, New Delhi, India
14. ASTM D7981-15 (2015) Standard practice for compaction of prismatic asphalt specimens by means of the Shear box compactor. ASTM International, West Conshohocken, Pennsylvania, USA
15. M-E PDG (2008) Mechanistic empirical pavement design guide: a manual practice. American Association of State Highway and Transportation Officials, Washington, D.C, USA
16. AASHTO TP79-10 (2010) Determining the dynamic modulus and flow number for Hot Mix Asphalt (HMA) using the Asphalt Mixture Performance Tester (AMPT). American Association of State Highway and Transportation Officials, Washington D.C., USA

Influence of Aggregate Gradation on Laboratory Rutting Performance of Hot-Mix Asphalt Mixtures



B. S. Abhijith, Uma Chakkoth  and J. Murali Krishnan 

Abstract Distresses such as rutting in bituminous mixtures are known to be largely influenced by the aggregate skeleton. For a given optimum binder content, the challenge lies in making a choice of aggregate gradation which will lead to optimal performance in rutting and fatigue cracking. As a first step, the present work is focused on quantifying the rut resistance of two types of aggregate gradation. The two aggregate gradations are conventional dense gradation normally used in Indian highway and ternary blend derived from particle packing theory. Using these aggregate gradations, the bituminous concrete samples were prepared at two different air void level of $6 \pm 0.5\%$ and $4 \pm 0.5\%$. The samples were subjected to rut wheel testing for 5000 numbers of passes at 50°C . The rutting performance was captured in terms of rut depth, and it was found that the bituminous mixtures prepared using particle packing theory exhibited higher resistance to rutting when compared to the conventional dense-graded bituminous mixture.

Keywords Aggregate gradation · Bituminous mixtures · Optimal blend · Rutting

1 Introduction

Rutting is one of the primary distresses that occur when the bituminous material is subjected to repetitive mechanical loading at high pavement temperature [1]. Densification due to secondary compaction by traffic can be considered as a primary reason for rutting during initial years of service. It has been observed that most of the rutting occurs in the top layer of the bituminous mixture. The air void content and aggregate gradation are the parameters which are known to largely influence the

B. S. Abhijith · Uma Chakkoth · J. M. Krishnan (✉)

Department of Civil Engineering, Indian Institute of Technology Madras, Chennai 600036, India
e-mail: jmk@iitm.ac.in

B. S. Abhijith
e-mail: abi123bs@gmail.com

Uma Chakkoth
e-mail: umamenon88@gmail.com

rutting potential of these mixtures. Apart from the aggregate gradation and type, the maximum aggregate size is also believed to play a major role in resisting rutting [2].

It is understood that rutting of the bituminous mixtures can be minimized by using stiffer binders, larger aggregates, and less binder content. Some of the field studies have proven that the stone-matrix asphalt (SMA) which consists of a higher proportion of coarser particles and higher binder content (min. 5.8% as per MoRTH, 2001) has more resistance to rutting than the dense-graded bituminous mixtures [3–5]. In recent years, the balanced mixture design was proposed by some of the researchers [6]. In this method, the optimum binder content is computed by selecting an appropriate aggregate gradation which gives better resistance to both fatigue and rutting distresses. Therefore, obtaining an optimum packing of aggregates will play a significant role in balancing the distresses and also helps in relating closely the aggregate gradation to the rutting potential of the bituminous mixtures.

Various researchers have made an attempt to study the packing characteristics of the different components of the aggregate blends [7–11]. The first step toward providing a rational approach to combining the aggregates of mixed size and shape to obtain the desired void content for a two-component system was proposed by Furnas [7]. Substantial advancements have been made in aggregate gradation design for cement concrete. Here, two main types of interactions are observed, and they are the wall effect and the interference effect. The wall effect increases the void index (ratio of the volume of voids to the volume of solids) of the blend in a two constituent mix due to the disturbance of the arrangement of finer particles by the coarser particles at the wall interface. The loosening effect or the interference effect could be attributed to the spatial disturbances of the coarser particles by the finer particles which are present in the interstices. It is found that one can obtain the minimum possible void content by omitting certain intermediate sieve sizes. Also, the optimum proportions of finer and coarser particles in a two constituent mixture also change with the change in aggregate shape and compaction effort.

In the case of bituminous mixtures, the optimum binder content is related to the state of the aggregate packing at any given time. It is understood that the binder content selected to give maximum aggregate density with minimum air voids in the early stage of construction of pavements will not preserve the same state of packing after several years of service due to secondary compaction by traffic [9]. Hence, it is necessary that one designs a bituminous mixture in which not much substantial changes in aggregate skeleton has taken place over a large range of traffic load application. A traditional dense-graded gradation cannot satisfactorily do that, and hence, gradation appealing to particle packing models is required.

In the current study, the main objective was to compare the rutting potential of dense-graded bituminous mixtures and the bituminous mixtures designed using particle packing theory. The dense gradation adopted was the gradation specified in the Ministry of Road Transport and Highways [12]. Baron's approach for aggregate packing was used to obtain the optimum ternary aggregate blend [10]. In the following section, the preliminary literature associated with particle packing theories has been explained followed by the choice of aggregate gradation. Sample fabrication and rut wheel test procedure are outlined followed by the discussion of results.

2 Design of Aggregate Gradation Using Particle Packing

Two thresholds are defined here and they are ' P_x ' and ' P_t .' The threshold ' P_x ' corresponds to the maximum allowable coarse aggregate concentration that can be added to the larger proportion of fine aggregates without altering the fine aggregates arrangement. The threshold ' P_t ' corresponds to the maximum allowable fine aggregate concentration that can be added to the larger proportion of coarse aggregates without interfering the coarse aggregate layout. Three equations were defined by Olard and Perraton [10] depending on the desired percentage of finer aggregates in the overall mixture. When a higher percentage of fines is desired such that the proportion of coarser particles are lesser than the parameter ' P_x ,' the void ratio of the blend is given by,

$$e(x) = (1 - x)e_a + Dx. \quad (1)$$

Similarly, when the lower percentage of fines is desired such that the proportion of coarser particles is greater than the parameter ' P_t ,' the void ratio of the blend is given by,

$$e(x) = x(1 + e_b) - 1. \quad (2)$$

For the case when the medium percentage of fines is desired such that the proportion of coarser particles are in between the thresholds ' P_x ' and ' P_t ,' the void ratio of the blend is given by

$$e(x) = Ex. \quad (3)$$

Here, ' x ' is the volume fraction of coarse aggregates, ' e_a ' is the void ratio of 100% fine aggregates blend only and ' e_b ' is the void ratio of 100% coarse aggregates blend only, ' D ' is the coefficient of wall effect, and ' E ' is a coefficient without any physical significance.

In the following section, the details regarding the materials used and the determination of a blend with optimal particle packing as per the particle packing approach are explained.

3 Materials

The aggregates used were the crushed granite aggregates from Madurantakam located in Kanchipuram, India. The filler used was stone dust obtained from the same quarry. The gradation of coarse, fine, and filler aggregates used for preparing the optimal blend is given in Table 1. The specific gravity of the individual fractions was deter-

Table 1 Gradation of coarse, fine, and filler aggregates

Sieve size (mm)	Cumulative percentage passing		
	Coarse aggregate	Fine aggregate	Filler
26.5	100	100	100
19	90	100	100
13.2	–	–	–
9.5	45	100	100
4.75	0	100	100
2.36	0	50	100
1.18	–	–	–
0.6	–	–	–
0.3	–	–	–
0.15	–	–	–
0.075	0	0	100
Bulk specific gravity	2.834	2.815	2.674

Table 2 Properties of VG-30 binder as per IS 73:2013 [13]

Specification	Results	Limits
Penetration at 25 °C, 100 g, 5 s, 0.1 mm	43	45 min
Softening point (R & B), °C	52	47 min
Absolute viscosity at 60 °C (Poise)	3335	2400–3600
Kinematic viscosity at 135 °C (cSt)	534	350 min

mined in accordance with ASTM C127, C128, and C188. Viscosity graded VG-30 binder was used (see Table 2). A binder content of 5.0% was used.

4 Determination of Optimal Packing Blend

The aggregate mass was separated into three size fractions which were coarse, fine, and filler aggregates. The nominal maximum particle size of the coarse aggregates selected was 19.0 mm. The coarser particles constitute the macrostructure of the bituminous mixtures with stone-to-stone contact. In order to minimize the interparticle interactions, the size ratio of 0.20 was selected based on earlier research [7]. The aggregates sizes ranging from 26.5 to 4.75 mm was considered as coarse aggregates. The aggregates sizes ranging from 4.75 to 0.075 mm was considered as fine aggregates, and the particles passing 75 μm sieve size was considered as fillers.

The optimal blend was determined in two stages. Initially, the optimal blend of coarse and fine aggregates was obtained which was designated as Blend A (see Fig. 1) after which the optimal proportion of Blend A and fillers was determined (see Fig. 2). The step-by-step procedure followed to determine the optimum aggregate proportion is detailed below.

- (a) The blends of coarse and fine aggregates were prepared for different coarse aggregate proportions. The aggregate proportions were 100% coarse, 100% coarse + 5% fine aggregates, 100% coarse + 10% fine aggregates, and 100% coarse + 25% fine aggregates. Another set of blends were prepared with aggregate proportions, 100% fines and 100% fines + 66.7% coarse aggregates. Hence, a total of six blends was prepared.
- (b) The prepared blends (without adding binder) were compacted in two layers using the gyratory shear compactor by subjecting each layer to 10 gyrations. The volume of solids (V_s) was calculated using Eq. (4). The void ratio (e) was calculated using Eq. (5).

$$V_s = \frac{\text{Weight of aggregate blend}}{\text{Specific gravity of the blend}} \tag{4}$$

$$e = \frac{V}{V_s} - 1 \tag{5}$$

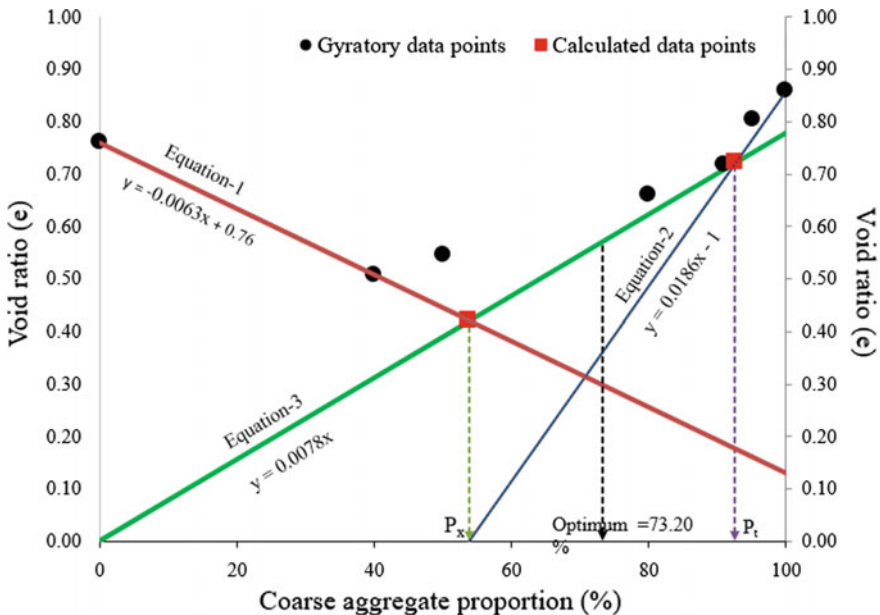


Fig. 1 Determination of P_x and P_t threshold of the coarse and fine aggregate mixture

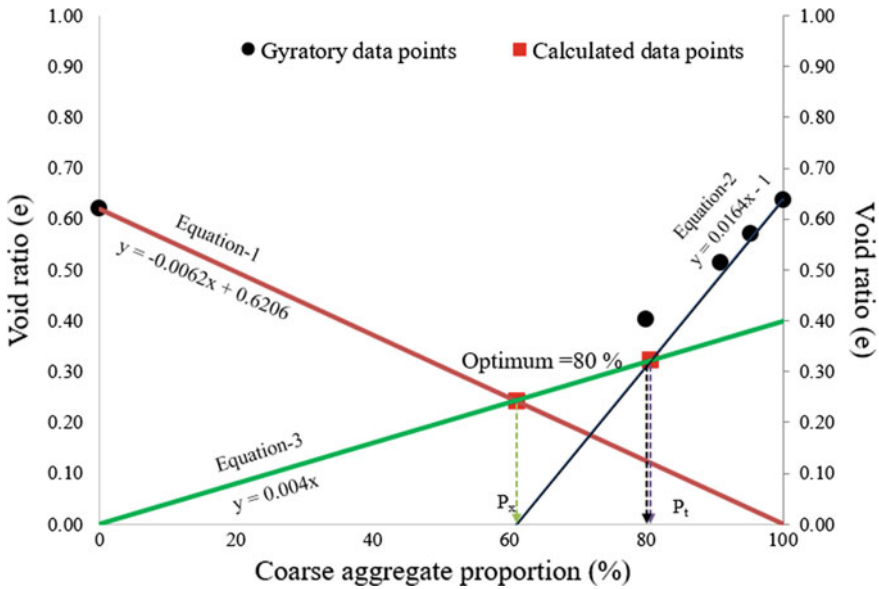


Fig. 2 Determination of P_x and P_t threshold of the Blend A and filler mixture

- (c) The line indicated by Eq. 1 in Fig. 1 shows the best fit line for the void ratio variation obtained by carrying out experiments using a different proportion of coarse aggregates when added to 100% fine aggregates. The line indicated by Eq. 2 in Fig. 1 shows the best fit line for the void ratio variation obtained by carrying out experiments using a different proportion of fine aggregates when added to 100% coarse aggregates.
- (d) The x -intercept of the line indicated by Eq. 2 in Fig. 1 is ' P_x .' The parameter ' P_t ' was obtained using Eq. 3. The mid-value of ' P_x ' and ' P_t ' was adopted as the optimized aggregate proportion for Blend A.
- (e) The ' P_x ' and ' P_t ' thresholds for various proportions of Blend A and fillers (75 μ m passing) were obtained following the same procedure as listed in steps a–d (Fig. 2).
- (f) The void ratio of fillers was obtained using the modified mini-compaction method as gyratory compaction is not suitable for void ratio determination of fillers. The sample mold was having 3.81 cm internal diameter and 10.0 cm height. The sample was compacted in three layers with each layer subjected to 36 blows with a 2.5 kg hammer [14].
- (g) The optimum proportion of Blend A and fillers were chosen near-threshold ' P_t ' to reduce the filler proportion (Fig. 2). The final proportion obtained was 58.6% coarse aggregates, 21.4% fine aggregates, and 20.0% fillers. The final optimal gradation is shown in Fig. 3.

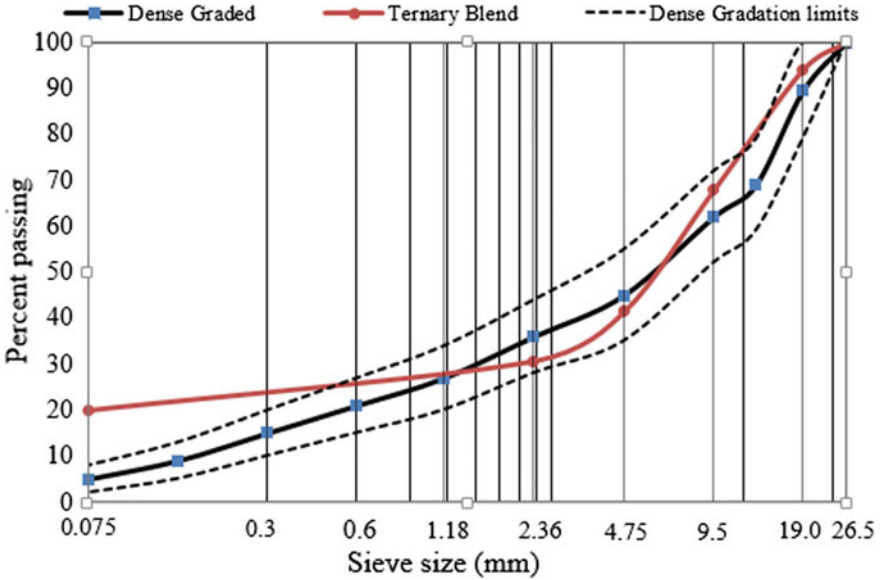


Fig. 3 Gradation curves for optimal blend and MoRTH specified blend

(h) It is observed that the aggregate size distribution of optimal blend is spread across both the coarser and finer sides when compared to the conventional dense gradation.

5 Results and Discussion

Bituminous mixes were prepared using the ternary blend and MoRTH specified blend. The resistance to rutting of both the mixes was evaluated.

5.1 Sample Preparation and Testing Methodology

The samples were compacted using a shear box compactor (ASTM D7981). The samples were compacted with two different air voids, and they were 6 ± 0.5 and $4 \pm 0.5\%$. The beam sample was sliced to get a rectangular slab of $300 \times 150 \times 50$ mm. A dry wheel tracker was used to determine the rut depth of the bituminous mixtures. In this test, a standard loaded wheel (700 N) moves forward and backward on top of the bituminous concrete sample at a speed of 26.5 rpm at a controlled temperature. The rut depth at each cycle is calculated using the mean of the rut depths measured at every 4 mm interval along the wheel path. The rut wheel samples were tested

at 50 °C. The number of passes for the current investigation was limited to 5000 numbers of passes.

5.2 Rut Wheel Test Results

The rut wheel test results at 50 °C are as shown in Fig. 4. There is a clear increase in the rut susceptibility of the bituminous mixtures prepared using conventional dense gradation (2.0 mm at $6 \pm 0.5\%$ air voids and 2.3 mm at $4 \pm 0.5\%$ air voids) when compared to the bituminous mixtures prepared with optimal aggregate packing (1.3 mm at $6 \pm 0.5\%$ air voids and 2.0 mm at $4 \pm 0.5\%$ air voids). It has been reported that the rutting of bituminous concrete mixtures could be due to the combined effect

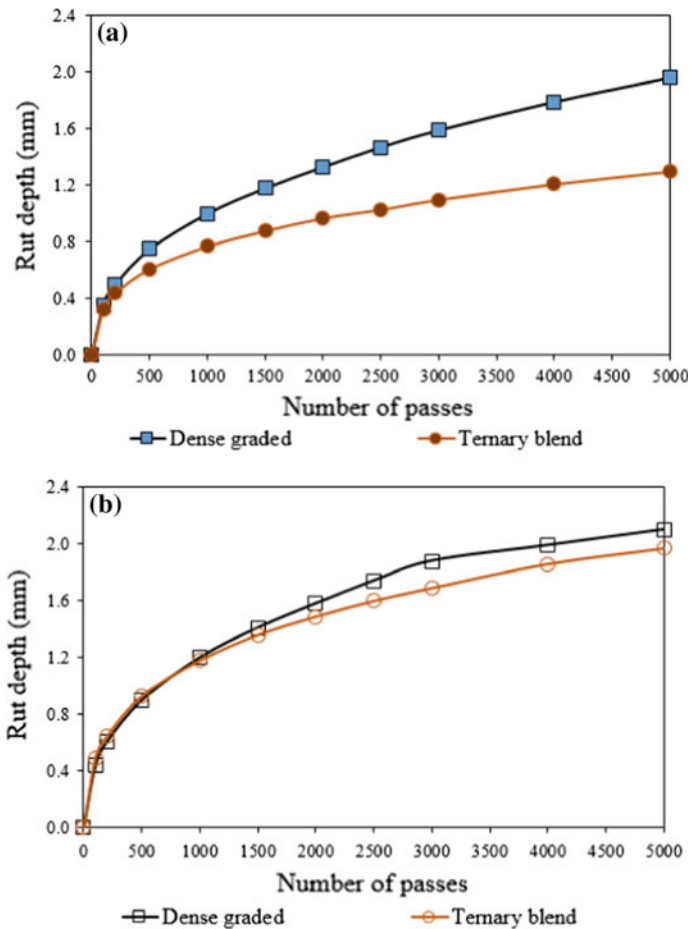


Fig. 4 Variation of rut depth at a $6 \pm 0.5\%$ air voids, b $4 \pm 0.5\%$ air voids

of densification and shear flow [15]. In the current investigation, the rut depth is observed to increase with a decrease in air voids. At 50 °C, for samples with 6% air voids, the mechanism of rutting can be attributed to densification only, while for samples with 4% air voids, the increased rut depth can be due to the shear flow [16]. The rate of rutting for both the bituminous mixtures was also quantified. It was observed that the rate of rutting for the ternary blend was lesser than conventional dense gradation (see Fig. 5).

The decrease in the rate of rutting for samples with $4 \pm 0.5\%$ air voids observed for the ternary blend (Fig. 5b) gives an indication of optimal packing through maximum densification.

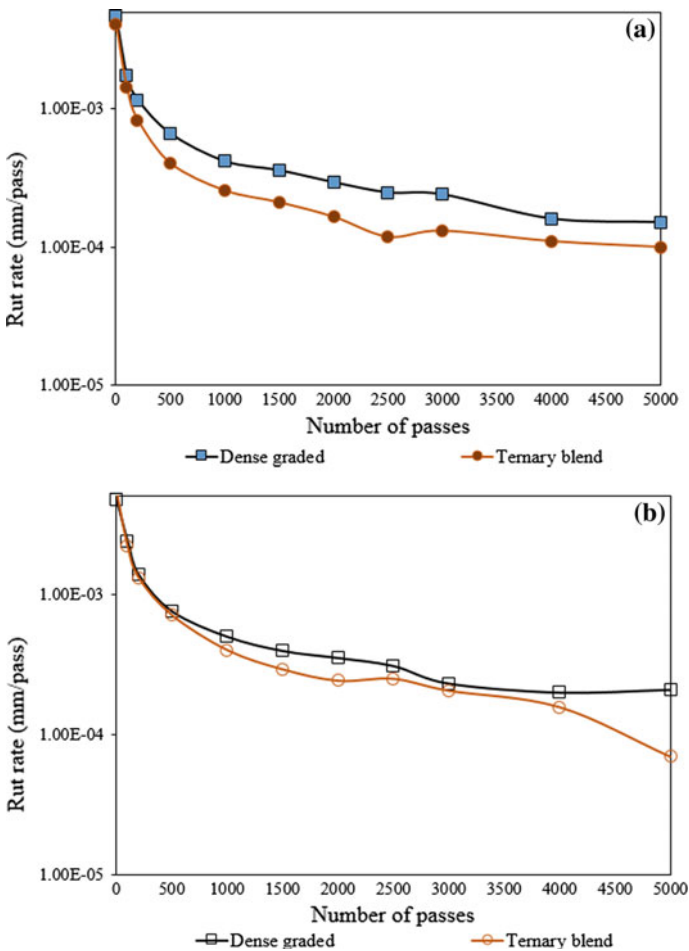


Fig. 5 Comparison of rate of rutting at a $6 \pm 0.5\%$ air voids, b $4 \pm 0.5\%$ air voids

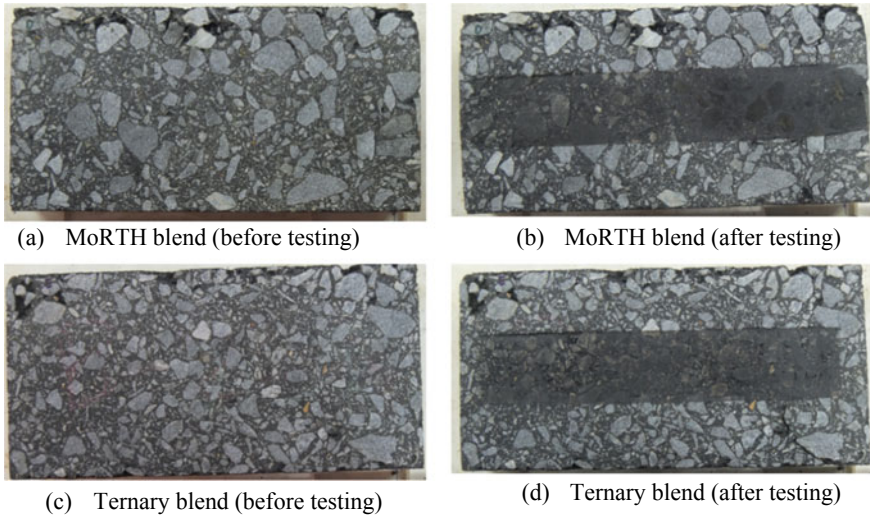


Fig. 6 Images of the bituminous mixtures captured before and after the rut wheel track testing

The images of the specimens were captured before and after the rut wheel tests as shown in Fig. 6. The distribution of coarser aggregates is larger in the bituminous mixtures prepared using optimal packing when compared to the conventional dense gradation.

6 Conclusion

The aim of this study was to investigate the influence of aggregate gradation on the rutting potential of hot-mix asphalt (HMA). Two different aggregate gradations were selected—optimal aggregate blend derived from particle packing theory and the conventional dense gradation. The rutting performance was captured in terms of rut depth, and it was found that the bituminous mixtures prepared using optimal aggregate packing theory had a higher resistance to rutting than the dense gradation. Also, the rut depth was found to increase with a further reduction in air voids.

As discussed earlier, the aggregate size distribution of optimal blend is spread across both the coarser and finer sides when compared to the dense gradation. This could be a reason that these samples exhibit better resistance to rutting. However, the segregation of aggregates in such mixtures should also be quantified. Hence, in order to obtain a comprehensive response of the bituminous mixtures to rutting, the variation in aggregate orientation and translation of aggregate particles during each repeated loading cycle should also be looked into.

Image processing (2D/3D) of the aggregate skeleton before and after rut wheel testing can provide additional information. This will help in understanding the rut-

ting behavior more closely and further in the aggregate gradation selection process. Currently, this work is being carried out by the authors.


Acknowledgements The authors acknowledge the opportunity provided by the 4th Conference of the Transportation Research Group of India (4th CTRG) held at IIT Bombay, Mumbai, India, between December 17, 2017, and December 20, 2017, to present the work that forms the basis of this manuscript.

References

1. Perraton D, Di Benedetto H, Sauzéat C, De La Roche C, Bankowski W, Partl M, Grenfell J (2011) Rutting of bituminous mixtures: wheel tracking tests campaign analysis. *Mater Struct* 44:969–986. <https://doi.org/10.1617/s11527-010-9680-y>
2. Brown ER, Cross SA (1989) A study of on-place rutting of asphalt pavements. *Proc Assoc Asphalt Paving Technol* 58:1–39. <https://trid.trb.org/view/367879>
3. Brown ER, Mallick R, Haddock J, Bukowski J (1997) Performance of stone matrix asphalt (SMA) mixtures in the United States. *J Assoc Asph Paving Technol* 66:426–457
4. Brown ER, Bassett CE (1990) Effects of maximum aggregate size on rutting potential and other properties of asphalt-aggregate mixtures. *Transp Res Rec* 1259:107–119
5. Xiao F, Amirkhanian S, Juang CH (2007) Rutting resistance of rubberized asphalt concrete pavements containing reclaimed asphalt pavement mixtures. *J Mater Civ Eng* 19:475–483. [https://doi.org/10.1061/\(asce\)0899-1561\(2007\)19:6\(475\)](https://doi.org/10.1061/(asce)0899-1561(2007)19:6(475))
6. Cooper S, Mohammad L, Kabir S, King W (2014) Balanced asphalt mixture design through specification modification. *Transp Res Rec J Transp Res Board* 2447:92–100. <https://doi.org/10.3141/2447-10>
7. Furnas CC (1928) The relations between specific volume, voids, and size composition in systems of broken solids of mixed sizes. US Department of Commerce, Bureau of Mines
8. De Larrard F (1999) Concrete mixture proportioning: a scientific approach. CRC Press, London
9. Lees G (1970) The rational design of aggregate gradings for dense asphaltic compositions. *Assoc Asph Paving Technol Proc* 39:60–97
10. Olard F, Perraton D (2010) On the optimization of the aggregate packing characteristics for the design of high-performance asphalt concretes. *Road Mater Pavement Des* 11:145–169. <https://doi.org/10.1080/14680629.2010.9690330>
11. Kumar SV, Santhanam M (2003) Particle packing theories and their application in concrete mixture proportioning: a review. *Indian Concr J* 77:1324–1331
12. MoRTH (2001) Specifications for road and bridge works, 4th revision. Ministry of Road Transport and Highways (MoRTH), Indian Roads Congress, New Delhi
13. IS73 (2013) Specifications for paving bitumen, Fourth revision. Bureau of Indian Standards, New Delhi
14. Sridharan A, Sivapullaiah PV (2005) Mini compaction test apparatus for fine grained soils. *Geotech Test J* 28:240–246. <https://doi.org/10.1520/GTJ12542>
15. Sousa JB, Deacon JA, Weissman S, Harvey JT, Monismith CL, Leahy RB, Paulsen G, Coplantz JS (1994) Permanent deformation response of asphalt-aggregate mixes. Report No. SHRP-A 415, pp 15–17. <http://onlinepubs.trb.org/onlinepubs/shrp/SHRP-A-415.pdf>. Last accessed on July 18, 2017
16. Roy N, Veeraragavan A, Krishnan JM (2016) Influence of confinement pressure and air voids on the repeated creep and recovery of asphalt concrete mixtures. *Int J Pavement Eng* 17:133–147. <https://doi.org/10.1080/10298436.2014.925622>

A Study on Permeability Characteristics of Asphalt Pavements



Rajan Choudhary , Vikramkumar R. Yadav, Abhinay Kumar 
and Anirudh Mathur

Abstract Ingress of moisture during early pavement life leads to undue deflection, increase of pore pressure under traffic, stripping of bitumen from aggregate and ultimately, reduction in strength. It is important to evaluate the sensitivity of asphalt mixes to the ingress of water, which can be quantified in terms of permeability (or hydraulic conductivity). The primary objective of the present study was to characterise permeability of a newly laid asphalt pavement through field-based and laboratory-based measurements. Field permeability of a newly laid pavement was measured at different sections in longitudinal as well as transverse directions. Cores were extracted from the locations where field permeability tests were conducted. Loose mixtures were also collected from plant and were compacted in laboratory to different air void contents through variable compactive effort. Permeability of field cores and laboratory compacted mixtures was determined in laboratory. Results indicated significant differences in field and laboratory permeability values. Field permeability showed a strong positive correlation with laboratory determined permeability of cores and compacted samples. Transverse variation of permeability was also found to be quite significant. All measured permeability values had a positive correlation with air voids. Statistical modelling of permeability–air void data was also attempted.

Keywords Asphalt mix permeability · Moisture damage · Air voids · Hyperbolic model

R. Choudhary (✉) · V. R. Yadav · A. Kumar · A. Mathur
Department of Civil Engineering, Indian Institute of Technology Guwahati, Assam, India
e-mail: rajandce@iitg.ac.in

V. R. Yadav
e-mail: er.vikramyadav178@gmail.com

A. Kumar
e-mail: abhinay.kumar@iitg.ac.in

A. Mathur
e-mail: ani.mat579@gmail.com

1 Introduction

Asphalt concrete (or bituminous concrete) is a widely used pavement construction material and plays an important role in the performance and durability of road transport infrastructure. About 98% of all highway pavements in India are surfaced with asphalt concrete. Moisture-induced damage is major distress observed on asphalt pavements in India. Intrusion of water is detrimental to pavement durability and can lead to an early onset of moisture-induced distresses such as stripping, cracking and reduction in load-bearing capacity [1–3]. The first step in addressing these distresses is to measure the receptiveness of an asphalt mixture to the ingress of water. This can be quantified in terms of its permeability (also termed hydraulic conductivity). Mathematically, permeability refers to the coefficient of permeability (k) defined by Darcy's law (Eq. 1):

$$Q = kiA \quad (1)$$

where Q = discharge flowing through the specimen; i = hydraulic gradient; and A = cross-sectional area of specimen perpendicular to the direction of flow. Equation 1 is based on the assumptions that the specimen is saturated and homogeneous, and that the flow is one-dimensional and laminar.

Water from precipitation entering a pavement surface would tend to flow in both vertical and horizontal directions since the flow is not confined. Under this perspective, evaluation of permeability of pavement in situ is preferred as it is more representative of the actual conditions. Field permeability determination is also advantageous as it is a non-destructive test and does not involve disfiguring a newly laid pavement surface through the extraction of cores. However, what is not known during field permeability measurement is whether the pavement layer is fully saturated and whether the flow of water is truly vertical, which are the two essential assumptions made in Darcy's law used for permeability calculations. Such limitations can be overcome if a core is extracted from the constructed pavement and evaluated for permeability in laboratory under controlled conditions of saturation and unidirectional flow. This approach has the advantage of the validity of Darcy's law, nevertheless does not simulate the actual flow regime encountered in the field. None of the aforementioned two approaches (permeability measurement on core or in field) would be beneficial for an asphalt mix designer since the testing is carried out after the mix has been placed and compacted. Consequently, laboratory permeability measurements can be made on asphalt mix specimens prepared in the laboratory to assess if the field permeability values correlate well with the laboratory permeability.

Several studies have focused individually on the evaluation of field permeability of asphalt pavements [4–6] or on laboratory permeability of field-recovered cores [7–9] or on laboratory permeability of specimens prepared in laboratory [1, 3, 10]. Other studies have attempted comparisons of permeability of cores and compacted specimens in the laboratory [11, 12] or comparisons of field and core

permeability [13, 14]. However, comparisons with all the three approaches for permeability determination have not been fully investigated.

2 Research Objectives

The primary objective of the present study is to understand general differences in magnitudes of permeability of a newly constructed asphalt pavement using the following three approaches:

- Field permeability (evaluated at the site itself), designated as ‘field’ permeability.
- Laboratory permeability of extracted cores, designated as ‘lab (core)’ permeability.
- Laboratory permeability of laboratory compacted mix, designated as ‘lab (compacted)’ permeability.

The specific objectives framed for this research are:

- To study the permeability of an ongoing paving project through field-based and laboratory-based testing. Laboratory-based evaluation consists of permeability measurement of field-recovered cores as well as compacted Marshall specimens in laboratory.
- To identify correlations between permeability values obtained through the three approaches.
- To study if field permeability varies significantly across the pavement width, i.e. transversely.
- To model permeability obtained from the three approaches as a function of air void content of the asphalt mix.

3 Methodology

In this study, an asphalt paving project was selected that involved construction of an asphalt course with an intermediate lane width of 5.5 m at the outskirts of Kishanganj city in the state of Bihar. Batch mix plant supplying the asphalt mix for the project was visited on the day of mix production. Loose mixtures were collected from the haul truck at hot-mix plant only before it departed for the paving site. The loose mixtures were then immediately brought to quality control lab (located at the hot-mix plant) in closed containers and compacted with varying blows of Marshall hammer. Some portion of the loose mix was kept separately for maximum specific gravity (G_{mm}) evaluation. On the following day, the paving site was visited for conducting field permeability testing and extraction of cores from the locations where the mix was actually laid and compacted. Overall methodological flow chart for the present study is shown in Fig. 1.

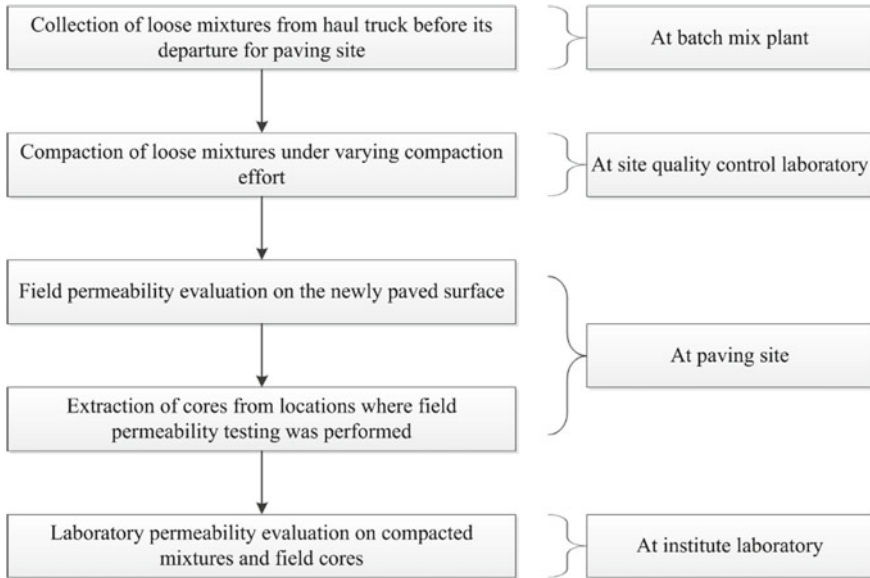


Fig. 1 Overall experimental flow chart

Figure 2 presents the locations on the constructed pavement where field permeability testing was performed. A total of 18 locations were selected at 6 chainages spaced at 30 m. At each chainage, permeability was evaluated at three transverse locations: near the right edge, centre and near the left edge. This was done to investigate the transverse variation of permeability. Cores were extracted from the same

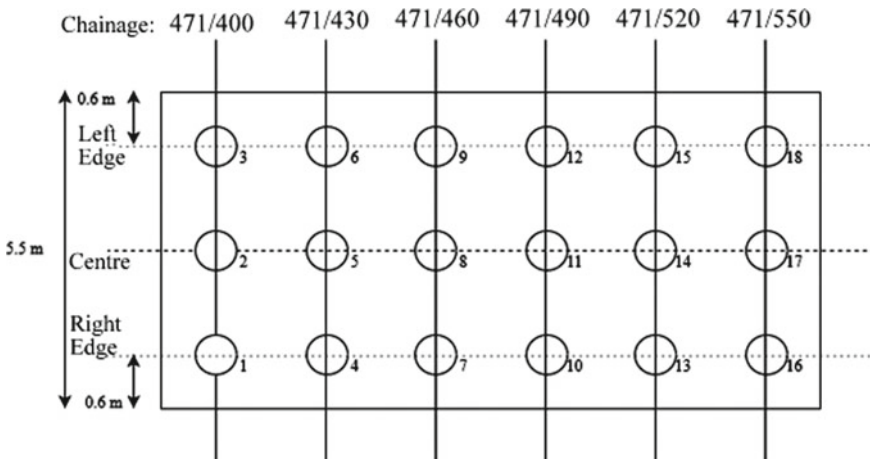


Fig. 2 Locations for field permeability testing

locations (shown in Fig. 2) chosen for field permeability evaluation, once the field permeability measurement was over.

3.1 Field Permeability Evaluation

National Center for Asphalt Technology (NCAT) developed a testing set-up to measure the permeability of asphalt mixes in the field. The NCAT asphalt field permeameter is based on the falling-head principle. Schematic diagram of a similar fabricated permeameter for field permeability measurement is shown in Fig. 3. This permeameter uses a four-tiered standpipe with decreasing inside diameters from bottom to top. For highly permeable surfaces, it would suffice to use the bottommost tier only. For low permeable surfaces (such as dense-graded asphalt layers), more tiers are included so that head fall can be accurately measured within a reasonable amount of time. It is important to ensure that there is no leakage between the base of the equipment and the pavement surface. Preliminary trials were conducted with plumber putty, silicone rubber and moulding clay to select an appropriate sealant material. Results of the trials showed that plumber putty took unreasonably longer time to set on the surface, while the silicone rubber was not effective in sealing the surface deformities and allowed leakage from above the pavement surface. Moulding clay was found to be the most effective measure in preventing water leakage and was selected for the study. Clay has also been used as a sealant for field permeability in a previous study [1].

As per the procedure developed by NCAT, equipment is placed on a cleaned pavement surface after application of the sealant. Counterweights are added to counteract

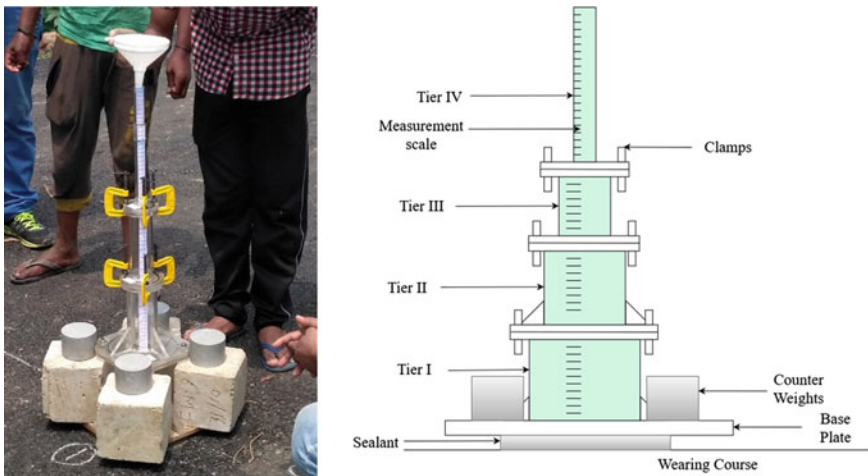


Fig. 3 Field permeameter: a photograph, and b schematics

the uplift pressure created at the base by the head of water. The water is added gradually from the top, and the rate of flow of water through the pavement is indicated by the time required for a suitable drop in head. Collected data are used to compute permeability based on the falling-head principle (Eq. 2):

$$k = \frac{aL}{At} \ln\left(\frac{h_1}{h_2}\right) \tag{2}$$

where k = permeability (cm/s); a = cross-sectional area of tier of standpipe used during measurement; A = cross-sectional area of pavement surface (area enclosed within the sealant); L = thickness of pavement layer (found from extracted core); and t = time (seconds) for head drop from h_1 (cm) to h_2 (cm). The test was repeated three times at each spot, and the average results were reported.

3.2 Laboratory Permeability Evaluation

A laboratory permeameter shown in Fig. 4, based on the falling-head principle, was fabricated for permeability measurement of field cores and the laboratory compacted mix samples. For determination of permeability, a specimen was saturated under water by application of 4 kPa vacuum pressure for 30 min. The saturated specimen was securely wrapped with thin plastic and placed in the sample holder of the permeameter. A thin annular ring of moulding clay was applied on the top circumference to prevent side leakage. Water was then filled in the standpipe above the specimen,

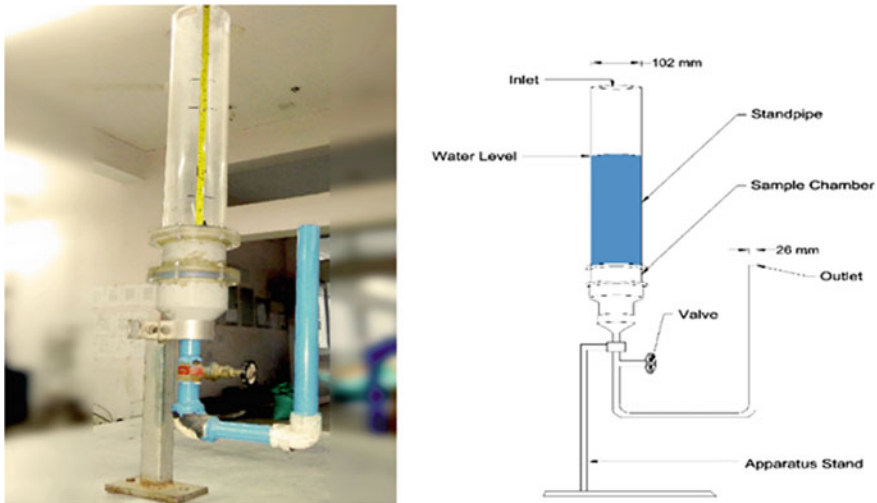


Fig. 4 Laboratory permeameter photograph and schematics

and the time (t) needed for the head to drop from initial value h_1 to the final value h_2 was recorded to compute permeability as per Eq. 2.

3.3 Evaluation of Air Voids

Air void content of laboratory compacted mix samples and field cores was obtained from the bulk density (G_{mb}) and theoretical maximum density (G_{mm}) measurements. Corelok vacuum-sealing device was used for G_{mb} and G_{mm} measurements as per ASTM D6857. Air void (AV) content was finally obtained as per Eq. 3:

$$AV = \frac{G_{mm} - G_{mb}}{G_{mm}} \quad (3)$$

It is to be noted that the same G_{mm} values were used for AV calculations of both field cores and laboratory compacted mix samples.

4 Results and Discussion

4.1 Transverse Variation of Field and Lab (Core) Permeability

Field permeability was determined at 18 locations of the paving project as per the layout shown in Fig. 2. Permeability testing was performed on each of the three transverse locations at the six chainages with three replicate measurements. Results of average field permeability at each location are shown in Fig. 5. Repeatability of the field permeameter used was assessed through the coefficient of variation (the ratio of the standard deviation to average, expressed as percentage) of multiple readings taken at the same location of testing. The coefficient of variation was less than 10% at all locations (with the exception of 15.4% at left edge of chainage 471/460). This showed that the permeameter used in the study produced acceptable repeatability. The data in Fig. 5 indicate that for most sections, the field permeability lied between 150×10^{-5} and 300×10^{-5} cm/s. The lowest permeability was observed at chainage 471/400, the starting chainage. This may be attributed to the fact that during compaction, this chainage received more roller passes compared to the following chainages.

The transverse variation of field permeability at any chainage can also be seen from Fig. 5. Permeability testing was performed at the centre of pavement as well at an offset of 0.6 m from the edges. The 'centre' permeability remains the minimum than at the edges. The results seem to indicate that the pavement edges offer higher permeability than the centre. This is likely as the centre of the pavement will be

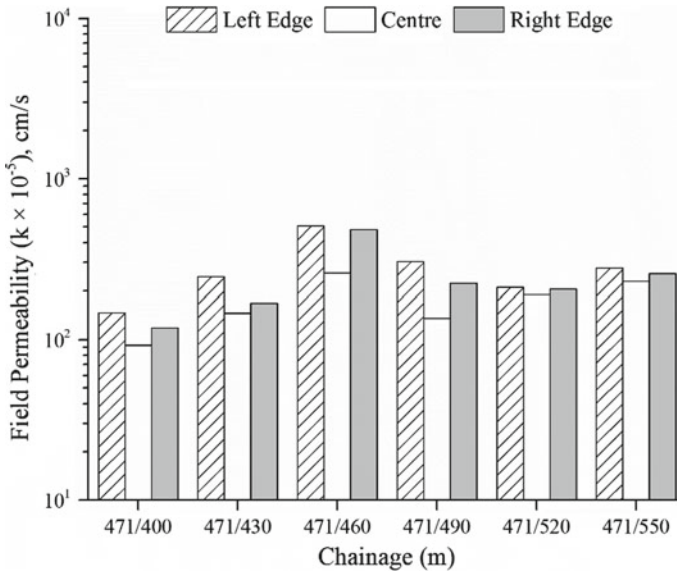


Fig. 5 Field permeability results

subjected to more overlaps during rolling operations and hence will be more densely compacted when compared to the edges.

Figure 6 shows the permeability of cored specimens extracted from the exact same location where field permeability testing was conducted. The cores were brought to the laboratory and evaluated for permeability. Hence, this permeability is designated as ‘lab (core)’ permeability. The figure is plotted to the same vertical scale as the field permeability (Fig. 5). A direct observation from Figs. 5 and 6 is that the lab (core) permeability is about an order of magnitude greater than the field permeability. The two permeabilities are compared in the next section of the paper. Further, it is observed that the transverse variation of lab (core) permeability is similar as in field permeability (permeability at the centre is lower than at the edges). It is to be noted that field and laboratory permeabilities were evaluated using different instruments under varying test conditions (sample saturation and unidirectional flow in case of laboratory permeability). In spite of that the lab (core) permeability values are able to capture the transverse variation of permeability occurring in the field.

To statistically examine the significance of differences shown by the two permeability tests, analysis of variance (ANOVA) followed by Tukey’s honest significance difference (HSD) comparisons (at 5% significance level) was performed separately on field and lab (core) permeability values. The influence of location (left, centre or right) on permeability was statistically analysed, and the results are shown in Table 1. Based on statistical analysis, permeability along the left edge is significantly higher than at the centre, suggesting that permeability can show significant variations across

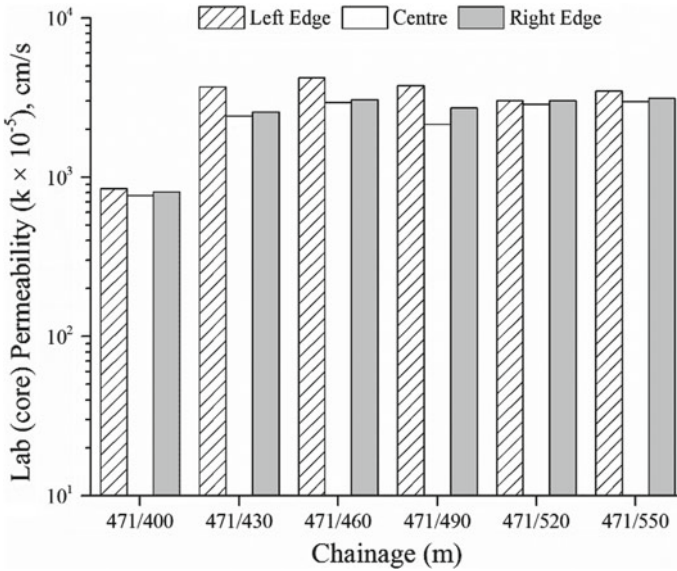


Fig. 6 Lab (core) permeability results

Table 1 Results of statistical analysis on field and lab (core) permeability

Comparison	Field permeability		Lab (core) permeability	
	p-value	Significant?	p-value	Significant?
Left versus centre	0.009	Yes	0.030	Yes
Right versus centre	0.139	No	0.791	No
Left versus right	0.494	No	0.131	No

the pavement width. This is likely due to non-uniform compaction achieved along the left edge compared to the centre of the section.

4.2 Field, Lab (Core) and Lab (Compacted) Permeability Comparisons

Laboratory permeability tests were conducted on loose mixtures collected from haul truck and compacted in the laboratory with varying blows of Marshall compactor. The information about the air void content of cores could only be obtained after extraction and testing of cores in laboratory. Consequently, prior information about sample air void content that will be achieved during compaction of loose mixtures was unavailable. For this reason, a 1200 g mass of loose mix was taken during compaction. Using varying compaction effort, a range of air voids was achieved. Five groups of

air voids were formed to categorise field, lab (core) and lab (compacted) permeability values so that they may be compared at similar air void contents. Figure 7 presents details of air voids along with the permeability values in each group.

Results indicate that the laboratory permeability is higher than the field permeability. Field results are expected to provide higher permeability based on the argument that the flow of water may occur in any direction during field testing, whereas the flow remains unidirectional in the laboratory permeameter. However, the results clearly deviate from what was anticipated. In general, the lab (core) permeability is found to be 8–16 times the field permeability. It has been widely accepted that asphalt pavements become undesirably permeable above in-place air voids of 8% [13, 15]. In the present case, air voids were always above this threshold. Therefore, it is undeniable that the pavement and the mixes considered in the study had high interconnected air voids. Cores as well as compacted samples have more interconnected voids which provide sufficient flow paths for water transmission. Moreover, the vertical flow may also get interrupted due to underlying tack coat/asphalt layer during field testing. Interconnected voids that extend through the sample thickness allow higher permeability values during laboratory evaluation as there is no interruption to the vertical flow. Similar findings were also reported in the study by Cooley et al. [16].

Figure 7 also illustrates the magnitudes of lab (core) and lab (compacted) permeability values. Compacted samples produce lower permeability than the cores. This is because of higher thickness of the compacted samples than the cores. Thickness of cores ranged from 20 to 40 mm, whereas thickness for compacted samples varied from 60 to 70 mm. A higher sample thickness offers more barriers to flow and hence reduces the propensity of the voids to become interconnected, thus decreasing the

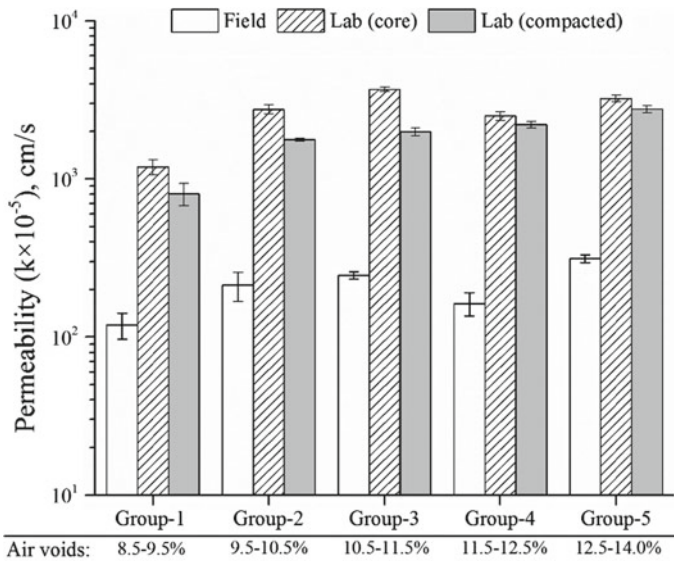


Fig. 7 Comparisons of field, lab (core) and lab (compacted) permeability

Table 2 Permeability correlations

Correlation	R-value
Field versus lab (core)	0.825
Field versus lab (compacted)	0.819
Lab (core) versus lab (compacted)	0.732

permeability. Lab (compacted) permeability values are, on an average, 30% lower than lab (core) permeability.

Correlation between field, lab (core) and lab (compacted) permeability values was determined using the Pearson correlation coefficient (*R*-value). Results obtained are presented in Table 2. Strong linear correlations ($R > 0.80$) exist between field permeability and laboratory permeability. A fairly good correlation is observed between the permeability of compacted samples and cores ($R = 0.732$).

4.3 Permeability–Air Voids Relationships

Air void content is the single most important factor affecting the permeability of asphalt mixes. Many studies in the past have attempted to model permeability solely as a function of air void content of the mix [1, 3, 17]. Figure 8 presents plots of permeability as a function of air voids for field, lab (core) and lab (compacted) permeability values. In all the three cases, the permeability appears to demonstrate an increasing trend with air voids. An important observation from Fig. 8 is that scatter in the plot is greater for field and lab (core) permeability than the lab (compacted) permeability. This is attributed to better control over air voids in the laboratory during compaction of loose mixes. On the other hand, variation in permeability–air void plot may be due to factors like localised segregation, non-uniform compaction, non-uniform lift thickness, etc.

An attempt was also made for developing regression models to capture the trend of permeability values with air void content. The models mostly reported by researchers to model permeability–air voids relationships were used, viz. linear, power law, exponential and hyperbolic models. Table 3 presents the details of each model, its mathematical form and statistical indicators of fit: coefficient of determination (R^2) and root-mean-square error (RMSE). The effect of scatter can be seen in terms of lower R^2 and higher RMSE for field and lab (core) data with linear, power and exponential models. Hyperbolic model performed the best with lowest RMSE and highest R^2 in all the cases.

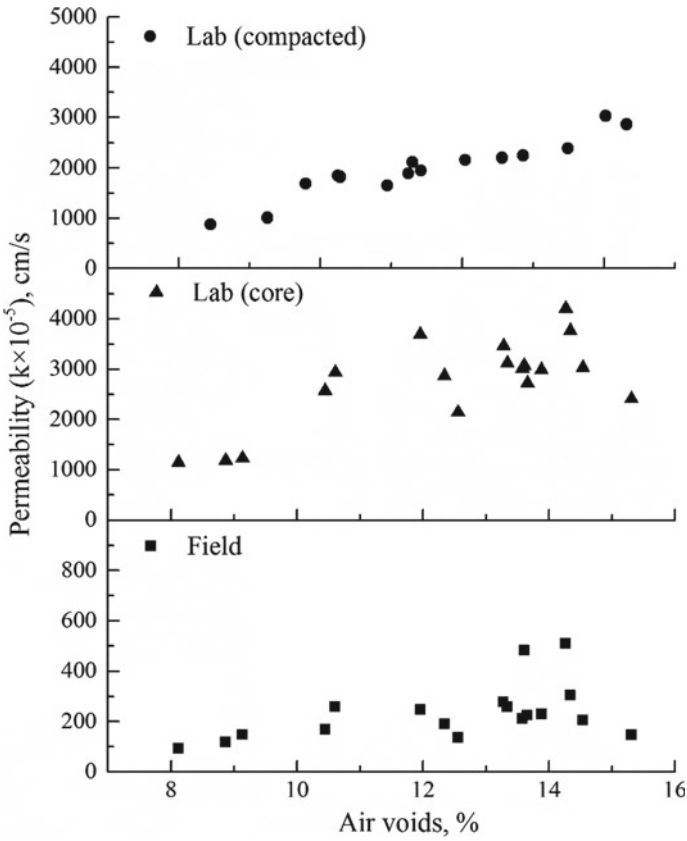


Fig. 8 Permeability–air void plots

Table 3 Results of statistical modelling of permeability–air voids data

Model	Form	Field		Lab (core)		Lab (compacted)	
		R ²	RMSE	R ²	RMSE	R ²	RMSE
Linear	$y = a + bx$	0.232	100.7	0.577	666.4	0.917	192.8
Power	$y = ax^b$	0.229	100.9	0.548	689.4	0.911	200.5
Exponential	$y = ae^{bx}$	0.199	102.8	0.500	724.8	0.897	215.5
Hyperbolic	$y = \frac{a}{(1/x)-b}$	0.919	2.144	0.886	231.4	0.921	9.896

Note y: permeability; x: air voids; a, b: model parameters; RMSE: root-mean-square error

5 Conclusions

Based on the results and analyses, the following conclusions are drawn:

- There was a significant difference in field and laboratory permeability values, even though both of them were measured using the falling-head principle. Laboratory permeability was found to be an order of magnitude greater than the field permeability.
- Field permeability showed strong positive correlations with laboratory determined permeability of cores and compacted samples.
- Field permeability significantly varies in the transverse direction with permeability at the centre lower than at the edges.
- Field, lab (core) and lab (compacted) permeability values had a positive correlation with air voids.
- Statistical modelling of permeability as a function of air voids indicated that hyperbolic model performed well with the lowest RMSE and highest R^2 in comparison with other models.

References

1. Kanitpong K, Benson C, Bahia H (2001) Hydraulic conductivity (permeability) of laboratory-compacted asphalt mixtures. *Transp Res Rec J Transp Res Board* 1767:25–32. <https://doi.org/10.3141/1767-04>
2. Vardanega PJ (2012) State of the art: permeability of asphalt concrete. *J Mater Civ Eng* 26(1):54–64. [https://doi.org/10.1061/\(ASCE\)MT.1943-5533.0000748](https://doi.org/10.1061/(ASCE)MT.1943-5533.0000748)
3. Choudhary R, Singh SK, Kumar A, Porwal SS (2016) Permeability characteristics of bituminous premix carpet and mix seal surfacing. *J Indian Roads Congress* 77(2):383–392
4. Cooley L, Brown E (2000) Selection and evaluation of field permeability device for asphalt pavements. *Transp Res Rec J Transp Res Board* 1723:73–82. <https://doi.org/10.3141/1723-10>
5. Cooley L Jr, Brown E, Maghsoodloo S (2001) Developing critical field permeability and pavement density values for coarse-graded Superpave pavements. *Transp Res Rec J Transp Res Board* 1761:41–49. <https://doi.org/10.3141/1761-06>
6. Li H, Kayhanian M, Harvey JT (2013) Comparative field permeability measurement of permeable pavements using ASTM C1701 and NCAT permeameter methods. *J Environ Manage* 118:144–152. <https://doi.org/10.1016/j.jenvman.2013.01.016>
7. Maupin G (2001) Asphalt permeability testing: specimen preparation and testing variability. *Transp Res Rec J Transp Res Board* 1767:33–39. <https://doi.org/10.3141/1767-05>
8. Mohammad L, Herath A, Huang B (1832) Evaluation of permeability of superpave® asphalt mixtures. *Transp Res Rec J Transp Res Board* 2003:50–58. <https://doi.org/10.3141/1832-07>
9. Tarefder RA, White L, Zaman M (2005) Neural network model for asphalt concrete permeability. *J Mater Civil Eng* 17(1):19–27. [https://doi.org/10.1061/\(asce\)0899-1561\(2005\)17:1\(19\)](https://doi.org/10.1061/(asce)0899-1561(2005)17:1(19))
10. Bhattacharjee S, Mallick RB (2002) An alternative approach for the determination of bulk specific gravity and permeability of hot mix asphalt (HMA). *Int J Pavement Eng* 3(3):143–152. <https://doi.org/10.1080/1029843021000067782>
11. Maupin G (2000) Asphalt permeability testing in Virginia. *Transp Res Rec J Transp Res Board* 1723:83–91. <https://doi.org/10.3141/1723-11>

12. Ahmad M, Tarefder RA (2017) Critical permeability values of asphalt concrete for field cores and laboratory-compacted samples. *J Transp Eng Part B: Pavements* 143(3):04017013:1–7. <https://doi.org/10.1061/jpeodx.0000016>
13. Mallick RB, Cooley LA, Teto M, Bradbury R (2001) Development of a simple test for evaluation of in-place permeability of asphalt mixes. *Int J Pavement Eng* 2(2):67–83. <https://doi.org/10.1080/10298430108901718>
14. Tarefder RA, Ahmad M (2014) Evaluating the relationship between permeability and moisture damage of asphalt concrete pavements. *J Mater Civil Eng* 27(5):04014172:1–10. [https://doi.org/10.1061/\(asce\)mt.1943-5533.0001129](https://doi.org/10.1061/(asce)mt.1943-5533.0001129)
15. Zube E (1962) Compaction studies of asphalt concrete pavement as related to the water permeability. In: Proceedings of the 41st annual meeting of the Highway Research Board, Washington DC, 1962, pp 12–31
16. Cooley LA, Prowell BD, Brown ER (2002) Issues pertaining to the permeability characteristics of coarse-graded Superpave mixes. NCAT Report No. 02-06, National Center for Asphalt Technology, Auburn
17. Nataatmadja A (2010) The use of hyperbolic function for predicting critical permeability of asphalt. In: Proceedings of 24th ARRB conference, ARRB Group, 2010, Melbourne, Australia

Characterization of Colloidal Stability of Blended Bitumen



Uma Chakkoth , K.R. Krishna, M. Ramkumar, P.V.C. Rao, Parag Ravindran and J. Murali Krishnan

Abstract Air blowing and propane deasphalting (PDA) blending are the two processes used by the refineries in India to produce paving grade bitumen. In the PDA blending process, the proportion of the constituents (PDA pitch and flux) used in producing bitumen is decided based on the grade of bitumen to be processed. One main issue in the production of bitumen through the blending process is the compatibility of the two constituents used. If the constituents do not exhibit blend stability and compatibility at the microstructural level, it is expected that the binder may not exhibit the required performance even if it meets the appropriate binder specifications such as penetration at 25 °C or viscosity at 60 °C. This study reports one such attempt to check for the compatibility of the blended material using automated flocculation titrimeter. The current investigation primarily focuses on characterizing the influence of proportion of PDA pitch and type of crude source on the colloidal stability of bitumen. The refinery streams processed from a crude oil mixture of Basrah Light (66%) and Murban (34%) was identified as the first crude source and a crude oil mixture of AXL (80%), Basrah (10%) and Iran Mix (10%) was identified as the

U. Chakkoth · J. Murali Krishnan (✉)
Department of Civil Engineering,
Indian Institute of Technology Madras, Chennai 600036, India
e-mail: jmk@iitm.ac.in

U. Chakkoth
e-mail: umamenon88@gmail.com

K. R. Krishna · M. Ramkumar · P. V. C. Rao
HP Green R&D Centre, KIADB Industrial Area,
Tarabahalli, Hoskote, Devanagundi, Bengaluru 560067, India
e-mail: krkrishna@hpcl.in

M. Ramkumar
e-mail: ramkumarm@hpcl.in

P. V. C. Rao
e-mail: drpvcr@hpcl.in

P. Ravindran
Department of Mechanical Engineering, Indian Institute of Technology Madras,
Chennai 600036, India
e-mail: paragr@iitm.ac.in

second crude source. Two different blend proportions of PDA pitch and flux from both the crude sources were made, and these were 75:25 and 80:20. These blend proportions were manufactured in a high shear rate blending facility. All the blends and the components were subjected to titrimetry at the unaged condition. It was seen that the compatibility of the material strongly depended on the proportion of the pitch as quantified by the asphalt state of peptization (P) value. The rheological properties of the blends were quantified by performance grading and frequency sweep tests. It was observed that blend samples with better compatibility also exhibited excellent rheological properties.

Keywords Component blending · Colloidal stability · Automated flocculation titrimer · Frequency sweep test

1 Introduction

Bitumen used for paving applications is processed from crude oil. Bitumen processing is completely different from any other civil engineering material in the sense that the manufacturer has no control over the raw material. The Indian refineries process crude from a wide variety of sources using at least two different processes. They are air blowing and component blending. This investigation is based on the characterization of component blended bitumen.

In the component blending process, the proportion of the constituents used in producing bitumen is decided based on the grade of bitumen to be processed. The blend components consist of flux or extract from solvent extraction unit and PDA pitch which is a mixture of asphaltenes and resins, obtained from propane deasphalting (PDA) process [1, 2]. The blending in the refinery is normally carried out by line blending, and adequate circulation is ensured in the bitumen storage tank before the delivery of the final product. The refineries which use component blending for the manufacture of paving bitumen use proportions such as 85:15 and 90:10 of PDA pitch and flux. The blend proportions of PDA pitch and flux are worked out in order to meet the required specification criteria. In India, the refineries use the blend proportion such as 86.8:13.2 of PDA pitch and flux to manufacture viscosity grade bitumen (VG30).

Various investigations have been carried out on different blending components of propane precipitated asphalt (PPA) considering the use of PPA blends in preparing bituminous mixtures [3, 4]. In a similar study on blended bitumen, the bitumen manufactured by two different processes (straight reduction to grade and component blending) was compared based on the viscosity of bitumen at 60 °C [4]. It is expected that if the constituents do not exhibit blend stability at the microstructural level, the binder may not exhibit the required performance even if it meets the appropriate binder specifications such as penetration at 25 °C or viscosity at 60 °C.

The chemical composition of bitumen is defined in terms of four generic fractions, widely known as Corbett fractions such as saturates, naphthene aromatics, polar

aromatics and isooctane insoluble asphaltenes [5]. The bitumen microstructure is normally assumed to follow a colloidal model, with asphaltenes forming the centres of the micelle and having a more pronounced aromatic nature. The asphaltenes are assumed to be surrounded by lighter constituents (resins) of less aromatic nature. The current understanding of ‘resins’ is more like that of a surfactant creating the solvation layer. In the case of the shortage of ‘resins’ (compounds in the immediate vicinity of asphaltenes), a mutual attraction of the micelles is facilitated resulting in an irregular open packing system which alters the stability of the bitumen leading to the formation of ‘flocs’. Hence, it will be desirable if one can check for the compatibility of the blends which should normally be made at the colloidal scale.

Colloidal stability of bitumen has been assessed indirectly using parameters such as the Gaestel index (ratio of the solubility based fractions) and by turbidimetric titration [6]. Other methods include Oliensis spot test which is a method for the evaluating the colloidal stability of bitumen wherein the compatibility is judged by the degree to which an oily ring develop surrounding the drop placed on a prepared surface [7].

The colloidal stability of asphaltene-containing residues has also been evaluated in terms of intrinsic stability (S-value) using optical methods. The colloidal stability of a system is related to the associated solubility parameters. While determining such solubility parameters are straight forward for most of the materials, for bitumen, one needs to use indirect methods and one such method uses turbidimetric titrations. The test method for automated titrimetry is detailed in the standard ASTM D6703, 2014 [8]. The principle of this method is to make a solution of bitumen in a solvent. Isooctane, which is the titrant is added at a fixed rate to the bitumen–solvent mixture until flocculation occurs. The formation of flocs is determined with a spectrophotometer by measuring the change in transmittance. Heithaus compatibility parameters are defined in terms of maximum flocculation ratio (FR_{max}) and minimum dilution concentration (C_{min}). Various investigations have been carried out to model bitumen colloidal and structural stability [9–11]. The starting point of the colloidal structure and the relation to the rheological properties is the influential article by Traxler and Romberg (1952) [12]. Redelius and Soenen (2005) determined the solubility parameters for a wide variety of bitumen and established preliminary correlations with the rheological properties of the same binders. Using statistical analysis, it was found that a good correlation existed between phase angle and solubility parameters [13]. The correlation of asphaltenes to the viscosity of the binder is also reported in the literature [14].

This investigation reports an attempt to check for the compatibility of the blended bitumen using automated flocculation titrimeter. The blends were prepared in the laboratory and the colloidal stability of the blends was quantified using Heithaus compatibility parameters. In order to evaluate the influence of blend compatibility on the binder performance, the rheological characterization of the blends was carried out by conducting performance grading and frequency sweep tests. The blends were tested at two ageing conditions, and the variation in the linear viscoelastic parameters was studied.

2 Experimental Investigation

The experimental investigation as part of the current study is divided into three main sections. The first is the blend preparation, and the second is the determination of the colloidal stability of the blends prepared using constituents obtained from two different crude sources. The third portion of this investigation is to quantify the influence of blend compatibility on the rheological properties of the blends.

2.1 Materials

The refinery streams processed from a crude oil mixture of Basrah Light (66%) and Murban (34%) was identified as the first crude source and a crude oil mixture of AXL (80%), Basrah (10%) and Iran mix (10%) was identified as second crude source. The properties of the constituents are given in Table 1.

2.2 Blend Preparation

The blending was carried out using the constituents, PDA pitch and flux. Different proportions were tried before the required specification compliance as per IS73, 2013 [15] was met. The required amount of the constituents was transferred to blending container and placed in an oven at 80°C for conditioning. An anchor stirrer was used for blending the constituents. The angular velocity of the stirrer for all the blending trials was kept constant at 500 rpm. The blending was carried out at a

Table 1 Properties of the blend constituents

Crude source	Material	Experiment	Measured value
Source-1 66% Basrah and 34% Murban	PDA pitch	Penetration at 25 °C, 0.1 mm, 100 g, 5 s	7
		Density at 15 °C (g/cm ³)	1.05
	Flux	Density at 15 °C (g/cm ³)	1.01
Source-2 80% AXL, 10% Basrah and 10% iran mix	PDA pitch	Penetration at 25 °C, 0.1 mm, 100 g, 5 s	12
		Density at 15 °C (g/cm ³)	1.058
	Flux	Density at 15 °C (g/cm ³)	0.98

Table 2 Details on blended bitumen

Crude source	Blend ID	Blend proportion (% of total weight of the blend)	Penetration at 25 °C	Absolute viscosity (Poise)	Grade (as per IS 73, 2013)
Source-1	Blend-1	75:25	148	827	VG10
	Blend-2	80:20	60	1810	VG20
Source-2	Blend-3	75:25	95	1104	VG10
	Blend-4	80:20	63	1779	VG20

constant temperature of 160 °C for a time duration of 90 min for all the blends. The penetration and viscosity measurements of blended bitumen were carried out as per the Indian standard specifications [15]. The results are presented in Table 2.

2.3 Turbidimetric Titration with Automated Flocculation Titrimeter

The automated flocculation titrimeter (AFT) model K47100 (Koehler Instruments) was used to carry out the experiments. The experimental parameters related to this test are shown in Table 3. The samples were transferred to the reaction vials and were dissolved in 4 ml of tetrahydrofuran (C₄H₈O). After a dissolution period of 5 hrs, each of the solutions (sample and solvent) was titrated with isooctane (C₈H₁₈). A titration loop is made by pumping titrant into the sample reaction vial at a constant flow rate using a low flow rate metering pump.

During titration, the output signal from spectrophotometer is recorded using a data acquisition system to record the change in percent transmittance (%T) of detected radiation at 740 nm as a function of time t , as the titrated solution passes through a quartz flow cell. The spectrophotometer output signal measures turbidity (change

Table 3 Experimental parameters

Parameters	Value
Weight of asphalt, W_a (g)	0.1, 0.2, 0.3
Volume of tetrahydrofuran (V_s) (ml)	4
Titration	Isooctane
Dissolution time (hr)	5
Flow rate (circulation pump) (ml/min)	1.058
Flow rate (titration pump) (v_t) (ml/min)	0.98
Temperature (°C)	45

in transmittance) of the sample solution as the titration experiment proceeds to a flocculation onset point or flocculation peak. The flocculation peak corresponds to the flocculating asphaltene phase separating from the solution.

Heithaus compatibility parameters

The raw data obtained by carrying out turbidimetric titration using AFT are the flocculation onset time denoted by t . This is the time required to obtain a flocculation peak. The volume of titrant (isooctane) V_T was computed using the following expression (Eq. 1) where v_t is the flow rate of titration pump and t is the flocculation peak time.

$$V_T = v_t \times t \quad (1)$$

$$FR = \frac{V_s}{V_s + V_T} \quad (2)$$

$$C = \frac{W_a}{V_s + V_T} \quad (3)$$

An experiment using AFT consists of three trials which correspond to flocculation onset time obtained for three different concentrations of bitumen in a solvent (see Table 4). Thus, for each experiment, three precipitation points are identified by calculating FR and C values. Two experiments (or six trials) for each blend samples were carried out. A linear trend line was fit through the three precipitation points and extrapolated to give the intersection with the FR-axis and the C-axis. The intersection with the FR-axis is denoted as FR_{max} , and the intersection with the C-axis is denoted as C_{min} . The Heithaus compatibility parameters are calculated based on the values for FR_{max} and C_{min} . The parameters are level of peptizability (p_a), solvency of the maltenes (p_o) and state of peptization (P), and they are given by Eqs. 4, 5 and 6.

$$p_a = 1 - FR_{max} \quad (4)$$

Table 4 Flocculation onset time of blend-2 of source-1

Trial No.	Binder weight (g)	Flocculation peak time (t) (s)	V_T (ml)	Dilution concentration (C) (g/ml)	Flocculation ratio (FR)	FR_{max}	C_{min}
1	0.1	1752.2	8.7610	0.0078	0.3135	0.3154	1.12
2	0.2	1777.55	8.8875	0.0155	0.3104		
3	0.3	1787.69	8.9385	0.0232	0.3092		
4	0.1	1739.01	8.6951	0.0079	0.3151	0.3182	0.701
5	0.2	1778.63	8.8932	0.0155	0.3102		
6	0.3	1752.2	8.7610	0.0231	0.3082		

$$p_o = FR_{\max} \left(\frac{1}{C_{\min}} + 1 \right) \quad (5)$$

$$P = \frac{p_o}{1 - p_a} \quad (6)$$

2.4 Rheological Characterization of Blends

The performance grading tests and frequency sweep tests were carried out on all the blends at two ageing conditions (unaged and short-term aged). Short-term ageing of the blends was carried out using a rolling thin film oven as per the test procedure specified in ASTM D2872 (1997) [16].

Performance grading

The performance grading of blends was carried out as per ASTM D6373, 2013 [17]. The grading practice specifies a parameter each considering rutting ($|G^*|/\sin\delta$) and fatigue failure ($|G^*| \sin\delta$). The temperatures at which the rutting and fatigue parameters achieve different values are used to determine the pass-fail temperature. In this investigation, only the rutting parameters are reported.

Frequency sweep tests

The frequency sweep test was performed on the unaged and short-term aged blend samples by varying the frequency from 50 to 1 Hz at the rate of 0.1 Hz per second. The test was performed at a constant temperature of 52 °C. The choice of test temperature was made based on performance grading test results. A strain amplitude of 0.07 % was used for the frequency sweep test. The frequency sweep experiment at a constant temperature was carried out to quantify the influence of colloidal stability on the change in rheological properties of the blends. The choice of temperature for the frequency sweep test was based on the performance grading test results. Each experiment was carried out twice to check for repeatability.

3 Results and Discussion

The data obtained by carrying out experiments using AFT were used to determine the Heithaus compatibility parameters of blended bitumen. The rheological properties of the blends were quantified using performance grading and frequency sweep test results. The variation of linear viscoelastic parameters with the binder ageing was evaluated.

3.1 Calculation of Compatibility Parameters

The flocculation peak plot for each dilution rate for the blend-2 sample of source-1 is shown in Fig. 1. The volume of titrant for each test condition specified in Table 3 was calculated using the time required for the onset of flocculation and titrant flow rate using Eq. 1. The FR and C values calculated using Eqs. 2 and 3 for all the experimental trials on blend-2 of source-1 are given in Table 4.

The inset plot (Fig. 2) indicates the three precipitation points. The three precipitation points correspond to the FR and C values calculated for each trial of an experiment. Figure 2 shows a sample plot of FR_{\max} as a function of C_{\min} plot for the first trial of an experiment carried out on blend-2 of source-1.

Figure 2 is an illustration of data postprocessing which involves the computation of FR_{\max} and C^{\min} . The other samples also follow the same trend. The FR_{\max} and C^{\min} values are given in Table 4. Similar plots were prepared for all the trials carried out using AFT.

The Heithaus compatibility parameters were calculated based on the values for FR_{\max} and C^{\min} . The parameters, namely level of peptizability (p_a), solvency of the maltenes (p_o) and state of peptization (P) was calculated for all the blends. The mean value of the parameters calculated from two experimental results is presented in Table 5.

The compatibility of a colloidal system is quantified in terms of the state of peptization, P. The value of P commonly varies between 2.5 and 10 for bitumen samples [8]. The materials calculated to have low values of P are designated as

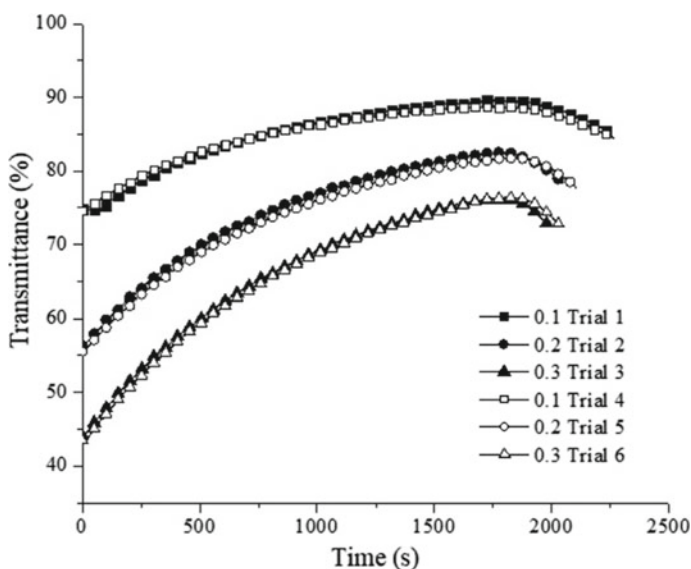


Fig. 1 Flocculation onset time for blend-2 of source-1

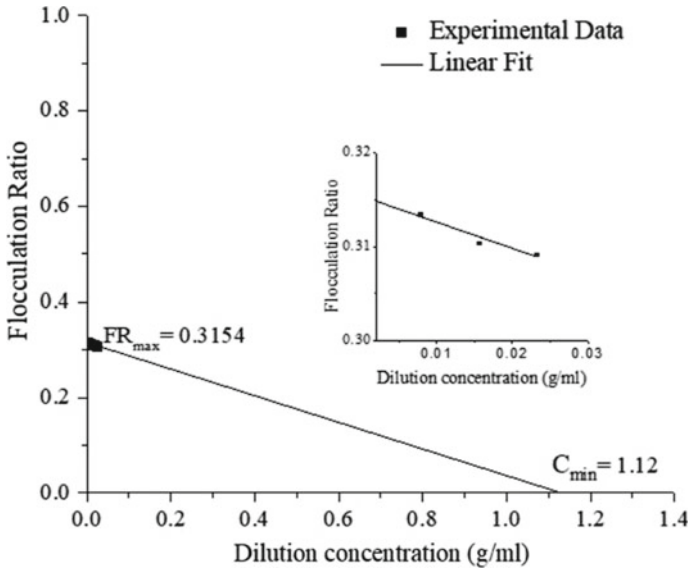


Fig. 2 Flocculation ratio versus dilution concentration for blend-2 of source-1 (Trial 1, 2 and 3)

Table 5 Compatibility parameters of the blends

Crude source	Blend ID	Asphaltene peptizability (p_a)	Maltene peptizing, power (p_o)	Asphalt state of peptization (P)
Source-1	Blend-1	0.682	1.093	3.440
	Blend-2	0.683	0.683	2.155
Source-2	Blend-3	0.703	0.691	2.329
	Blend-4	0.700	0.586	1.953

incompatible, whereas the materials calculated to have high P values are designated as compatible. It was observed that the samples prepared using source-1 exhibited better colloidal compatibility when compared to samples prepared using source-2. The performance grading tests were carried out on all the blends. The results are presented in Table 6. The performance grading test results of the blends indicate that pass/fail temperature of VG10 and VG20 samples from both the sources is in the same range. The dynamic modulus values obtained at 58 °C for all the blends at two ageing conditions are shown in Fig. 3. While comparing VG10 samples from both the sources (blend-1 and blend-3), the difference in dynamic modulus values observed between unaged and the aged sample was lesser for blend-1 (VG10 source-1) sample.

The linear viscoelastic parameters obtained from the frequency sweep tests for VG10 (blend-1 and blend-3) and VG20 (blend-2 and blend-4) samples were compared. The variation in these parameters of the blends with ageing was quantified in

Table 6 Comparison of blend properties

Crude source	VG Grade (as per IS 73,2013)	Blend ID	Asphalt state of peptization (P)	Pass/fail temperature (°C)		PG grade (as per ASTM D6373, 2014)
				Unaged	Short-term aged	
Source-1	VG10	Blend-1	3.440	59.1	57.1	PG 52-XX
	VG20	Blend-2	2.155	64.6	63.4	PG 58-XX
Source-2	VG10	Blend-3	2.329	61.4	58.8	PG 58-XX
	VG20	Blend-4	1.953	65.7	63.4	PG 58-XX

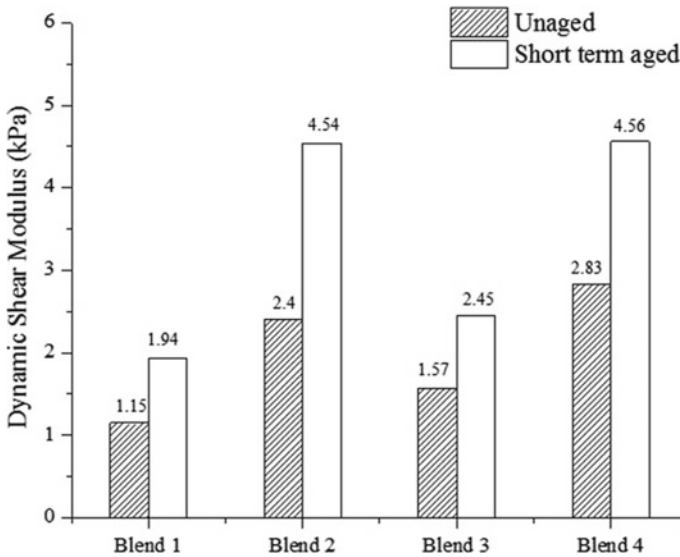


Fig. 3 Dynamic modulus of blends at two ageing conditions

terms of the change in phase angle as a function of the frequency. Figure 4a and b shows the variation of phase angle with frequency for VG10 and VG20 samples at two ageing conditions. Figure 5a and b shows the variation of dynamic shear modulus with frequency for VG10 and VG20 samples at two ageing conditions.

It was observed that for more compatible blends, on ageing, there is a lesser change in the phase angle. The phase angle as a function of frequency for source-1 VG10 (blend-1) sample was observed to show less variation with ageing when compared to the source-2 VG10 (blend-3) sample. However, an extensive experimental investigation over a wide temperature range should be carried out to capture the variation in rheological properties of the blends. The results reported here are the part of a preliminary study carried out towards this end.

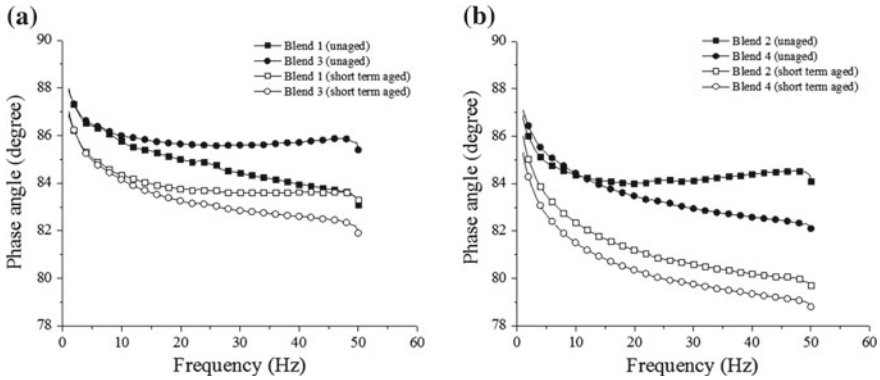


Fig. 4 Variation of phase angle with frequency

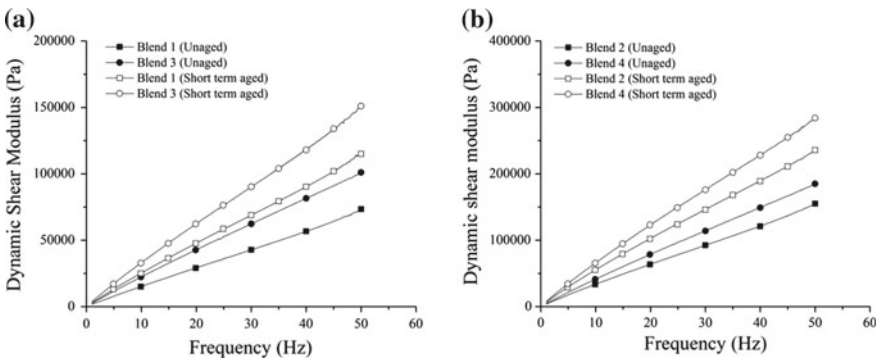


Fig. 5 Variation of dynamic shear modulus with frequency

4 Conclusion

This study aimed at characterizing the colloidal stability of blended bitumen. The experimental results indicate that the compatibility of the material as quantified by the state of peptization (P) value was influenced by the proportion of the pitch and type of crude source. The state of peptization value of the blends was observed to fall in the range of 2–3.44. The bitumen microstructure is normally assumed to follow a colloidal model, with asphaltenes forming the centres of the micelles which are dispersed in the maltenes. It is understood that the compatibility of the blend decreases with ageing. Hence, it is expected that the blends with better compatibility will have lesser changes in the rheological parameters obtained at two different ageing conditions. The results obtained in the current investigation are in agreement with the same. However, further investigation should be carried out to evaluate the influence of colloidal stability on rheological properties of blended bitumen. This study would help the refineries in producing bitumen of the required viscosity grade and will also provide guidelines on the choice of refinery streams to be used to produce a stable blend.

Acknowledgements The authors thank M/s HPCL Mumbai Refinery for providing materials for this investigation.

The grant number is RB/14-15/CIE/014/HPCL/JMUR.

The authors also acknowledge the opportunity provided by the 4th Conference of the Transportation Research Group of India (4th CTRG) held at IIT Bombay, Mumbai, India, between 17 December 2017 and 20 December 2017 to present the work that forms the basis of this manuscript.

References

1. Ishai I, Tuffour YA (1987) The use of propane precipitated asphalt (PPA) in bituminous paving mixtures. *J Assoc Asph Paving Technol* 56:599–631
2. Rakow M (2003) Petroleum oil refining. In: Totten G, Westbrook S, Shah R (eds) *Fuels and lubricants handbook: technology, properties, performance, and testing*. ASTM Manual Series, ASTM International, West Conshohocken, PA. <https://doi.org/10.1520/MNL37-EB>
3. Ishai I (1995) Long-term laboratory and field behaviour of PPA asphalt cement blends. *J Assoc Asph Paving Technol* 64:306–339
4. Ishai I, Yuval R (2002) Reformulation of asphalt cement for paving. *J Transp Eng* 128:111–122 (2002)
5. ASTM D4124 (2009) Standard test method for separation of asphalt into four fractions, American Society for Testing and Materials, West Conshohocken, Philadelphia, USA
6. Baginska K, Gawel I (2004) Effect of origin and technology on the chemical composition and colloidal stability of bitumens. *Fuel Process Technol* 85(13):1453–1462
7. ASTM D1370 (2012) Standard Test Method for Contact Compatibility Between Asphaltic Materials (Oliensis Test), American Society for Testing and Materials, West Conshohocken, Philadelphia, USA
8. ASTM D6703 (2014) Standard Test Method for Automated Heithaus Titrimetry, American Society for Testing and Materials, West Conshohocken, Philadelphia, USA
9. Karlsson R, Isacson U (2003) Bitumen structural stability characterisation using turbidimetric titration. *Energy & Fuels* 17:1407–1415
10. Li J, Huang X, Zhang Y, Xu M (2009) Bitumen colloidal and structural stability characterization. *Road Mater Pavement Des* 10:45–59
11. Andersen SI, Speight JG (1999) Thermodynamic models for asphaltene solubility and precipitation. *J Pet Sci Eng* 22:53–66
12. Traxler RN, Romberg JW (1952) Asphalt a Colloid material. *Ind Eng Chem* 44:155–158
13. Redelius PG, Soenen H (2005) Correlation between bitumen polarity and rheology. *Road Mater Pavement Des* 6(3):385–405
14. Petersen JC, Robertson RE, Branthaver JF, Harnsberger PM, Duvall J, Kim SS, Anderson DA, Christiansen DW, Bahia HU (1994) *Binder characterization and evaluation Vol. 1, SHRP-A-367; Vol. 2 – Chemistry, SHRP-A-368; Volume 3 – Physical Characterization, SHRP-A-369; and Volume 4 – Test Methods, SHRP-A-370, Strategic Highway Research Program, USA (1994)*
15. IS73 (2013) Specifications for paving bitumen, Fourth Revision, Bureau of Indian Standards, New Delhi
16. ASTM D2872 (1997) Standard test method for effect of heat and air on a moving film of asphalt (Rolling Thin-Film Oven Test), American Society for Testing and Materials, West Conshohocken, Philadelphia, USA
17. ASTM D6373 (2013) Standard specification for performance graded asphalt binder, American Society for Testing and Materials, West Conshohocken, Philadelphia, USA

An Investigation on Resilient Modulus of Bituminous Mixtures



S. Deepa and J. Murali Krishnan

Abstract IRC:37-2012 suggests to use resilient modulus as an input parameter in the design of bituminous pavements in India. IRC:37 specifies the values of resilient modulus at different temperatures for Bituminous Concrete (BC) and Dense Bituminous Macadam (DBM) mixes with various grades of unmodified and modified binders. However, IRC:37 recommends identical values of resilient modulus to be used for the mixes, irrespective of the type of modified binder used. At higher temperatures, it can be noticed that IRC:37 tabulated resilient modulus values for the mixes with unmodified binder are higher than those with modified binders. Also, the influence of Poisson's ratio is not incorporated since a constant value of 0.35 is used for all the mixes. In this investigation, BC mixtures with an unmodified (VG30) and three modified binders (CRMB, plastomer and elastomer) were tested at three different temperatures (25, 30 and 35°C) at 1 Hz frequency. Tests were conducted as per ASTM D7369-11. Samples of diameter 152.4 mm were used for the test. The sample was subjected to 200 cycles, and the last five cycles were used for the computation of Poisson's ratio and resilient modulus. Both instantaneous and total resilient modulus were computed, and these values were compared with the IRC:37 specified values. The possible reasons for the difference in the modulus values from the present study and IRC:37 are explored.

Keywords Resilient modulus · Elastomer · Plastomer · Pavement design

S. Deepa · J. Murali Krishnan (✉)
Department of Civil Engineering, Indian Institute of Technology Madras,
Chennai 600036, India
e-mail: jmk@iitm.ac.in

S. Deepa
e-mail: sdeepa8813@gmail.com

1 Introduction

Material characterization has a vital role in the design of bituminous pavements, and hence, substantial research has been carried out to decide on the material parameter to be used in the bituminous pavement design procedure. Different studies have adopted different modes of testing to characterize the bituminous mixtures. The most widely used test methods employ uniaxial compression, indirect tension and beam flexure for material characterization. The current Mechanistic-Empirical Pavement Design Guide (M-EPDG) developed by AASHTO [11] recommends dynamic modulus measured in uniaxial compression to be used in pavement design. However, an earlier version, AASHTO Design Guide [1], recommended the use of indirect tension mode to determine the material modulus, termed as resilient modulus. In 1982, the indirect tension test (IDT) was adopted by ASTM as a standard test method for measuring resilient modulus of bituminous mixtures [2]. After subsequent revisions, the test protocol was withdrawn in 2003 and finally standardized under ASTM D7369 [5]. Several studies have used the indirect tension mode of testing to characterize bituminous mixtures [10, 13, 14].

Pavement design in India is carried out as per IRC:37-2012 [7], wherein resilient modulus is used as the input parameter for bituminous materials in the stress analysis procedure. IRC:37-2012 tabulates the resilient modulus of BC and DBM mixes with modified and unmodified binders. IRC:37-2012 claims that the tests have been carried out following ASTM: D7369-09 [4]. However, it is clear from the experimental results that ASTM: D4123-82 [2] has been followed, and the resilient modulus values were calculated assuming a Poisson's ratio of 0.35. It can be observed from the IRC:37-2012 tabulated values that resilient modulus is the same for all the mixes irrespective of the type of modifier. Hence, the IRC:37-2012 tabulated values of resilient modulus do not distinguish between different types of modified binders. The influence of Poisson's ratio on resilient modulus is also not captured since a constant value of 0.35 is used for all the mixes.

ASTM: D7369-11 suggests three gauge lengths that can be used in the repeated load indirect tension test: one-fourth, one-half and full diameter of the sample [5]. The standard also states in Note 3 that "*The results obtained with gauge length of one-fourth of the diameter of the specimen have the best precision*". However, IRC:37-2012 [7] seems to have used the largest gauge length for all the tests. This will result in less precise results since the sample non-homogeneity exerts a greater influence when the gauge length is large. Small gauge lengths result in smaller measured deformations and hence lead to issues related to signal capture by the LVDTs. In the current investigation, tests were conducted following the ASTM: D7369-11 procedure adopting a gauge length of half the sample diameter [5]. A comparison of the experimental results with IRC:37-2012 [7] values and that computed following the ASTM: D4123-82 [2] post-processing has been carried out. The results are discussed in the further sections.

2 Experimental Investigations

2.1 Materials

Bituminous Concrete Grade 2 (BC-Grade 2) with nominal maximum aggregate size of 13.2 mm was employed in the current investigation. The gradation as per MoRTH has been adopted [12]. Four binders were used in this study, an unmodified bitumen and this base bitumen modified with three types of modifiers—elastomer, plastomer and crumb rubber. The base bitumen used is an air-blown bitumen of VG30 grade as per IS: 73-13 [9]. The plastomer, elastomer and crumb rubber modified bitumen used are PMB(P)40, PMB(E)40 and CRMB-60, respectively [8]. Further, the bituminous concrete mixes with VG30, plastomer, elastomer and CRMB will be referred to as BC-VG30, BC-PMB(P), BC-PMB(E) and BC-CRMB.

2.2 Sample Preparation

The bituminous mixtures were short-term aged for 4 hours at mixing temperature and half an hour at compaction temperature. The mixing temperature for the mix with unmodified binder was 165 °C, whereas 185 °C was adopted for mixes with modified binder. Compaction was carried out in the shear box compactor [6] by applying a constant vertical load of 600 kPa and a constant shear angle of 4°. The fabricated beam was 450 mm long and 150 mm wide, and the height was 169 mm, based on targeted air voids of $4 \pm 0.5\%$. Two cylinders, each of 150 mm diameter, were cored from the compacted beam. Further, each cylinder was sliced into two samples of 152.4 mm diameter and 63 ± 0.5 mm height. Thus, a total of four samples were obtained from a compacted beam as shown in Fig. 1.

2.3 Test Procedure

Prior to the conduct of the resilient modulus test (repeated load diametral indirect tension test), an indirect tension test [3] was carried out in order to estimate the failure load for each type of mix. The IDT was conducted on samples with 101.6 mm diameter and 63 mm thickness. The IDT samples were also cored and sliced from a beam compacted using the shear box compactor [6]. Since the sample diameter for the IDT test is small, three cylinders of 100 mm diameter could be cored from a compacted beam. Further, each cylinder was sliced into two samples, each of 101.6 mm diameter and 63 mm thickness. In the IDT test, the sample is loaded to failure and 10–20% of the failure load was used as the input load in the repeated load diametral indirect tension test.

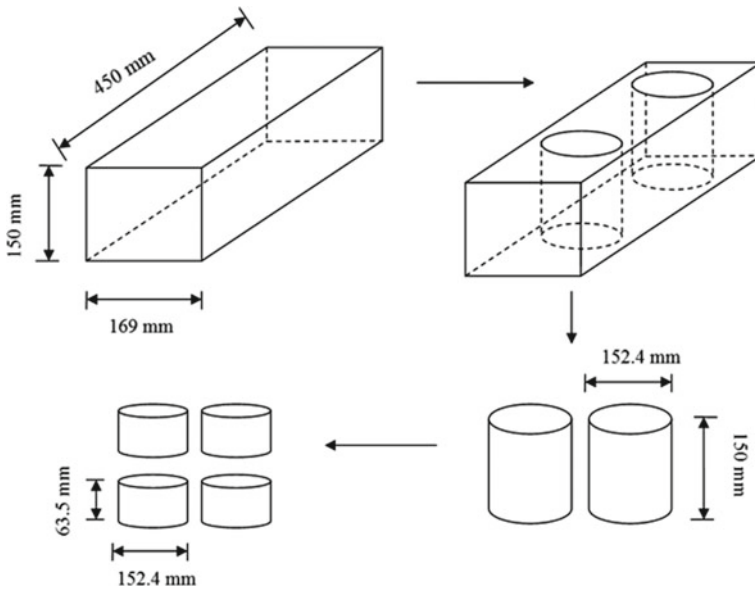


Fig. 1 Resilient modulus test samples cored and sliced from a compacted beam

Table 1 Input load levels

Temperature (°C)	P_{cyclic} (N) and (% loading)			
	BC-VG30	BC-CRMB	BC-PMB(E)	BC-PMB(P)
25	2354 (10)	1600 (10)	2170 (10)	2350 (10)
30	1330 (8)	1059 (9)	1458 (9)	1557 (9)
35	740 (6)	900 (9)	948 (9)	1205 (9)

After sample preparation, the next step involved was the fixing of LVDTs. The marking of the gauge positions, fixing of studs and mounting of LVDTs were carried out as per ASTM: D7369-11 [5]. Gauge length of one-half the sample diameter was used in the current investigation. Once the samples are mounted on the test setup, ASTM: D7369-11 suggests testing the sample in two orientations (0 and 90° rotation) and measure the deformations from both the planes of the sample. The load waveform is haversine compression with 0.1 s load duration followed by 0.9 s rest period. Table 1 shows the load levels used in the current study for repeated diametral indirect tension test.

In order to check the repeatability of results, the current investigation introduced slight modifications to the ASTM: D7369-11 procedure [5], and they are described further. The standard recommends applying 100 preconditioning cycles to the sample and using the last five cycles for modulus calculation. This is to ensure that the material response would attain a steady state for the purpose of modulus computation. However, there is no certainty on whether 100 cycles are sufficient to yield a steady

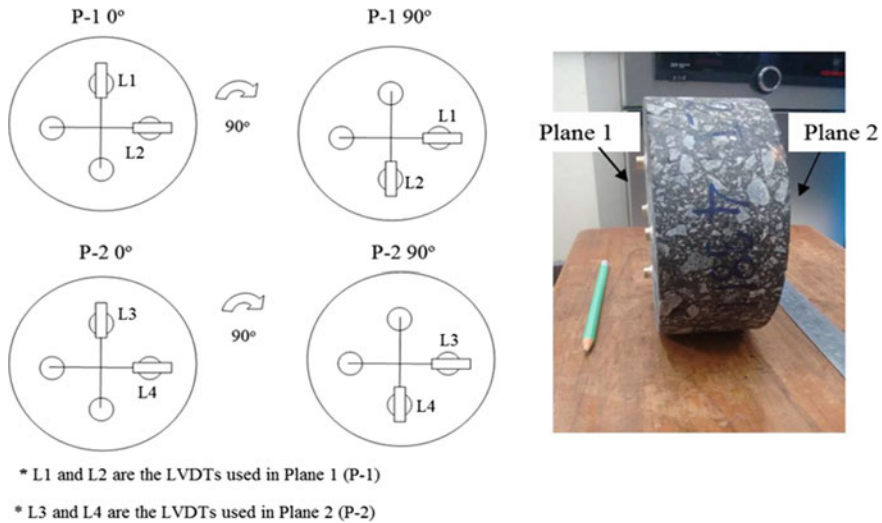


Fig. 2 Test procedure

state of response. Hence, in the current study, 200 cycles were applied to the sample, and the last five cycles were used for modulus determination.

The procedure adopted for the test in the current investigation is described briefly as follows. Initially, the sample was mounted with LVDTs on a single plane (Plane 1) and was subjected to 200 load cycles. The resulting deformations in the vertical and horizontal directions were measured using the LVDTs. This was followed by a rest period of 15 min after which a second trial was conducted. After a rest period of 15 min, the sample was rotated through 90° and the test was repeated. Further, LVDTs were mounted on Plane 2 of the sample, and the same procedure adopted for Plane 1 was repeated. Generally, as per ASTM: D7369-11, only one trial is performed in each orientation. However, this modification was introduced for the purpose of checking the repeatability between the trials. Also, since the applied loads are only a small percentage of the failure load (<10%), the sample is not damaged. The test procedure is schematically represented in Fig. 2.

2.4 Post-processing

Post-processing of the experimental data was conducted as per the ASTM: D7369-11 standard [5]. ASTM:D7369-11 suggests the calculation of two resilient modulus values based on the nature of recoverable deformation. First one is an instantaneous resilient modulus computed using the instantaneous recoverable deformation measured immediately after the load pulse, and the next is the total resilient modulus

computed using the total recoverable deformation measured at the end of a load-unload cycle. Poisson’s ratio (μ) and resilient modulus (MR) were determined using Eqs. 1 and 2.

$$\mu = \frac{I_4 - I_1(\frac{\delta_v}{\delta_h})}{I_3 - I_2(\frac{\delta_v}{\delta_h})} \tag{1}$$

$$MR = \frac{P_{cyc}(I_1 - I_2 \cdot \mu)}{\delta_h t} \tag{2}$$

where δ_v and δ_h are the recoverable deformations, t is the sample thickness, and P_{cyclic} is the cyclic load applied. The values of the constants are $I_4 = -1.0695$, $I_1 = 0.2339$, $I_2 = -0.7801$ and $I_3 = 0.3075$, and these have been specified in ASTM:D7369-11 [5] for the gauge length adopted in the current study. The computation of total and instantaneous recoverable deformations was carried out as per the regression procedure suggested by ASTM:D7369-11. Since the current investigation employed 200 cycles against 100 cycles specified in the standard, horizontal and vertical deformations for the last five cycles prior to both 100th and 200th cycles have been compared here. These deformations were used to compute the total and instantaneous resilient modulus corresponding to the 100th and 200th cycles. For demonstration, the instantaneous and total recoverable deformations and the corresponding Poisson’s ratio and resilient modulus for BC-VG30 (P-1 and 0° orientation) at 25 °C are shown in Tables 2 and 3.

Table 2 Instantaneous recoverable deformations for BC-VG30 at 25 °C

Deformation (μm)	Pulse 96		Pulse 97		Pulse 98		Pulse 99		Pulse 100		Mean
	H	V	H	V	H	V	H	V	H	V	
	1.968	-4.240	1.948	-4.201	1.965	-4.143	1.937	-4.225	1.96	-4.206	
Load (N)	2364		2354		2331		2344		2360		
μ	0.41		0.41		0.43		0.40		0.42		0.41
MR (MPa)	11061		11113		11218		10974		11144		11102

Table 3 Total recoverable deformations for BC-VG30 at 25 °C

Deformation (μm)	Pulse 96		Pulse 97		Pulse 98		Pulse 99		Pulse 100		Mean
	H	V	H	V	H	V	H	V	H	V	
	2.720	-5.953	2.683	-5.898	2.712	-5.876	2.68	-5.948	2.737	-5.943	
Load (N)	2364		2355		2333		2344		2360		
μ	0.40		0.39		0.41		0.39		0.41		0.40
MR (MPa)	7303		7339		7319		7230		7307		7300

3 Analysis of Experimental Data

The experimental data for all the four mixes was collected at 25, 30 and 35 °C. A total of eight resilient modulus values were computed for each mix at each temperature (two planes, two rotations and two recovery types) following ASTM: D7369-11 post-processing [5]. Resilient modulus was computed corresponding to each plane, rotation and mode of recovery for all the mixes used in the study.

3.1 Instantaneous Resilient Modulus

The instantaneous resilient modulus was computed using the instantaneous recoverable deformation measured immediately at the end of loading pulse. Since the time-dependent recovery is not captured, the instantaneous recoverable deformation is smaller compared to the total recoverable deformation measured at the end of the load–unload cycle. The average of the instantaneous resilient modulus over the last five cycles prior to the 100th and 200th cycles are shown in Table 4. From Table 4, it can be observed that the resilient modulus values do not vary more than 10% between the 100th and 200th cycles for any mix at any temperature.

3.2 Total Resilient Modulus

Total resilient modulus was calculated from the total recoverable deformations, and since the total recoverable deformation is larger than the instantaneous deformation, the corresponding modulus values are lower. The average of the instantaneous resilient modulus over the last five cycles prior to the 100th and 200th cycles is shown in Table 5.

From Table 5, it is clear that for mixes such as BC-VG30 and BC-PMB(P), there is as much as 30% reduction in total modulus compared to the instantaneous modulus at 25 °C. For BC-CRMB at 30 and 35 °C, the total modulus is less than the instantaneous modulus by more than 40%. This is true for all mixes at all the temperatures though the margin of variation is different.

Table 4 Instantaneous resilient modulus (MPa) as per ASTM: D7369-11

Temperature (°C)	BC-VG30		BC-CRMB		BC-PMB(E)		BC-PMB(P)	
	100th	200th	100th	200th	100th	200th	100th	200th
25	11102	11151	9277	9301	8678	8723	20572	21163
30	6193	6041	7643	7690	5455	5978	8374	8463
35	3952	3954	7279	7272	5263	5406	6113	6111

Table 5 Total resilient modulus (MPa) as per ASTM: D7369-11

Temperature (°C)	BC-VG30		BC-CRMB		BC-PMB(E)		BC-PMB(P)	
	100th	200th	100th	200th	100th	200th	100th	200th
25	7300	7344	6449	6417	5905	5868	15079	15641
30	5372	5366	4703	4725	4530	4472	5984	6055
35	2586	2551	3810	3805	3156	3231	3869	3898

Comparing the modulus calculated using ASTM D7369-11 [5], it can be observed that, at 25 and 30 °C, the mix with plastomer modified binder has the highest resilient modulus followed by BC-VG30, BC-CRMB and BC-PMB(E). At 35 °C, BC-VG30 has the least modulus followed by BC-PMB(E), BC-CRMB and BC-PMB(P).

3.3 Total Resilient Modulus Calculated Using an Assumed Poisson’s Ratio

Since IRC:37-2012 [7] has calculated the resilient modulus as per ASTM: D4123-82 [2], Poisson’s ratio of 0.35 was adopted for the calculation of resilient modulus. Since ASTM: D4123-82 [2] does not clearly mention as how to measure the instantaneous recoverable deformation, it is understood that IRC:37-2012 [7] used values of total recoverable deformations and computed total resilient modulus. For the purpose of comparing the results with that of IRC:37-2012 [7] tabulated data, the collected experimental data was further analysed using the post-processing method suggested in ASTM:D4123-82 [2], adopting a Poisson’s ratio of 0.35. Table 6 shows the total resilient modulus values computed as per ASTM: D4123-82 [2]. As observed from the Table 6, the resilient modulus computed as per ASTM: D7369-11 [5] is higher than that computed using ASTM: D4123-82 [2]. The difference is due to the fact that the actual Poisson’s ratio (computed using both horizontal and vertical deformations) of the material is greater than the assumed Poisson ratio of 0.35.

It can also be observed that when resilient modulus is calculated using ASTM: D4123-82 [2], assuming a Poisson’s ratio, the influence of the type binders on resilient

Table 6 Total resilient modulus (MPa) as per ASTM: 4123-82

Temperature (°C)	Instantaneous resilient modulus (MPa)							
	BC-VG30		BC-CRMB		BC-PMB(E)		BC-PMB(P)	
	100th	200th	100th	200th	100th	200th	100th	200th
25	6790	6825	5521	5649	5014	5041	10772	11019
30	3824	3738	3701	3681	3710	3779	5263	5251
35	1729	1839	2915	2880	2182	2146	3633	3489

modulus cannot be effectively captured. For instance, at 30 °C, BC-VG30, BC-PMB(E) and BC-CRMB are observed to have an average resilient modulus value of nearly 3700 MPa when a constant Poisson’s ratio is used for all the mixtures.

4 Comparison of Experimental Results with IRC:37-2012

The experimental data collected has been analysed using the post-processing methods suggested in ASTM D4123-82, and ASTM D7369-11 [2, 5]. Both instantaneous and total resilient modulus were calculated using ASTM D7369-11 [5]. Since ASTM D4123-82 [2] does not explain the regression procedure for finding instantaneous deformation, only total resilient modulus was computed assuming a Poisson’s ratio of 0.35. The next task is to compare these values with the IRC:37-2012 stipulated values. Table 7 shows the IRC:37-2012 stipulated values of resilient modulus for BC and DBM mixes with unmodified and modified binders. As observed from Table 7, IRC:37-2012 does not effectively distinguish between the resilient modulus of mixes with different modified binders. Also, IRC:37-2012 assigns lower resilient modulus to the mixes with modified binder at higher temperatures (30 and 35 °C) as compared with the ones with unmodified binder. Figure3 provides a comparison of the resilient modulus values specified by IRC:37-2012 and that determined by the current investigation.

The reason for the difference in the IRC:37-2012 tabulated values with the values calculated in the current study could be due to either the difference in the gauge length used or the sample dimensions. IRC:37-2012 results are based on the use of full sample diameter as the gauge length for measuring the horizontal deformations whereas the current study used a gauge length of half sample diameter. Since shorter gauge lengths give better precision, it is recommended to use short gauge lengths compared to full diameter gauge length.

5 Conclusions

To summarize, the current study compared the resilient modulus of bituminous mixtures listed by IRC:37-2012 and that computed using ASTM: D7369-11 and ASTM:

Table 7 Resilient modulus of bituminous mixes (MPa) as per IRC:37-2012

Mix type	Temperature (°C)				
	20	25	30	35	40
BC and DBM for VG30	3500	3000	2500	1700	1250
BC and DBM for modified bitumen	5700	3800	2400	1650	1300

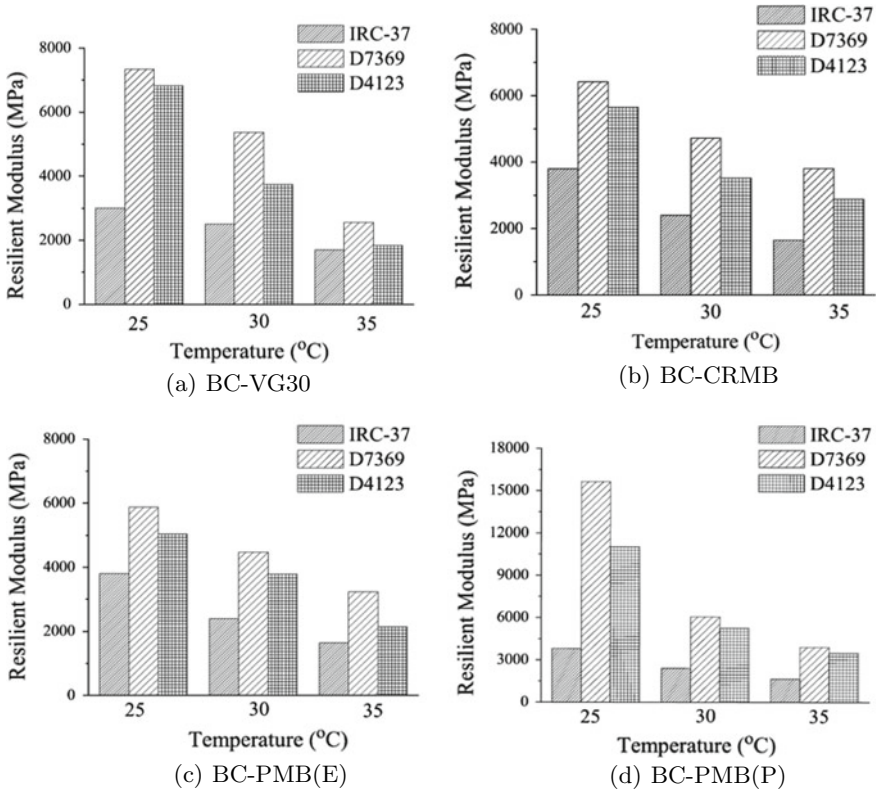


Fig. 3 Comparison of resilient modulus determined using different approaches

D4123-82 post-processing. It was observed that the use of a computed value for Poisson’s ratio rather than using an assumed value resulted in considerably higher values of resilient modulus for all the mixtures. It was also found that the modified binders have a significant influence on resilient modulus of the mixes, and hence, the same value should not be employed for all the mixes as suggested in IRC:37-2012. As per the experimental observations, at 25 and 30 °C, BC-VG30 had higher resilient modulus than BC-CRMB and BC-PMB(E). However, as test temperature was increased to 35 °C, all the mixes with modified binders had higher resilient modulus as compared to BC-VG30. On the other hand, IRC:37-2012 had reported lower modulus to the mixes with modified binders as compared to BC-VG30. It is observed that IRC:37-2012 reported values are too low as compared to those obtained from the experimental investigations. This could be either due to the difference in the gauge length used or the sample dimensions. The current study employed one-half sample diameter as the gauge length, while IRC:37-2012 values are based on full sample diameter as gauge length. Current study employed 150-mm-diameter samples, whereas the details on sample dimensions are not furnished by IRC:37-2012. To conclude,

the current study recommends using small gauge lengths for measuring deformation. It is also recommended to compute Poisson's ratio using measured horizontal and vertical deformations rather than assuming a value of 0.35.

Acknowledgements The authors thank Department of Science and Technology, Govt. of India, for funding this investigation. The grant number is DST/TSG/STS/2011/46. The authors acknowledge the technical assistance provided by M/s IPC Global, Australia, during the conduct of the experiments.

The authors acknowledge the opportunity provided by the 4th Conference of the Transportation Research Group of India (4th CTRG), held at IIT Bombay, Mumbai, India, between 17 December 2017 and 20 December 2017 to present the work that forms the basis of this manuscript.

References

1. AASHTO (1993) Guide for design of pavement structures. American Association of State Highway and Transportation Officials, Washington DC, USA
2. ASTM D4123-82 (1995) Standard test method for indirect tension test for resilient modulus of bituminous mixtures. ASTM International, West Conshohocken, Pennsylvania, USA
3. ASTM D6931-12 (2012) Standard test method for indirect tensile (IDT) strength of bituminous mixtures. ASTM International, West Conshohocken, Pennsylvania, USA
4. ASTM D7369-09 (2009) Standard test method for determining the resilient modulus of bituminous mixtures by indirect tension test. ASTM International, West Conshohocken, Pennsylvania, USA
5. ASTM D7369-11 (2011) Standard test method for determining the resilient modulus of bituminous mixtures by indirect tension test. ASTM International, West Conshohocken, Pennsylvania, USA
6. ASTM D7981-15 (2015) Standard practice for compaction of prismatic asphalt specimens by means of the shear box compactor. ASTM International, West Conshohocken, Pennsylvania, USA
7. IRC:37-2012 (2012) Guidelines for the design of flexible pavements. Indian Roads Congress, New Delhi, India
8. IS 15462-04 (2004) Indian standard specification for polymer and rubber modified bitumen. Bureau of Indian Standards, New Delhi, India
9. IS: 73-13 (2013) Specification for paving bitumen. Bureau of Indian Standards, New Delhi
10. Kim J, Lee HS, Kim N (2010) Determination of shear and bulk moduli of viscoelastic solids from the indirect tension creep test. *J Eng Mech* 136(9):1067–1075
11. M-E PDG (2008) Mechanistic empirical pavement design guide: a manual practice. American Association of State Highway and Transportation Officials, Washington, DC, USA
12. MoRTH (2013) Specification for road & bridge works, 5th rev. Ministry of Road Transport and Highways, Indian Roads Congress
13. Roque R, Buttlar W (1992) The development of a measurement and analysis system to accurately determine asphalt concrete properties using the indirect tensile mode. *J Assoc Asphalt Technol* 61:304–332
14. Von Quintus HL, Rauhut JB, Kennedy TW (1982) Comparisons of asphalt concrete stiffness as measured by various testing techniques. *J Assoc Asphalt Paving Technol* 51:35–52